Environmental Biotechnology and Engineering ISEBE Advances 2016

Candal, R.; Curutchet, G.; Domínguez-Montero, L.; Macarie, H.; Poggi-Varaldo, H.; Sastre, I. and Vázquez, S.

Environmental Biotechnology and Engineering

ISEBE Advances 2016

ISBN – 978-607-9023-51-5



Candal, R.; Curutchet, G.; Domínguez-Montero, L.; Macarie, H.; Poggi-Varaldo, H.; Sastre, I. and Vázquez, S.

Mexico City, Mexico, 2017.

Are property and responsibility of Authors.

All or any part of this publication may be reproduced or transmitted,
by any means, electronic or mechanical
(Including photocopying, recording or any
recovery system and storage), and must be included
with the corresponding citation of this compendious and their authors.

Environmental Biotechnology and Engineering
ISEBE Advances 2016

Editors
Héctor Poggi Varaldo
Lilian Edith Domínguez Montero
and others

D.R. © 1st Edition
Centro de Investigación y de Estudios Avanzados del I.P.N. Cinvestav, 2017.

Publisher
Cinvestav,
AV. I.P.N. 2508
07360, MÉXICO, D.F.

CD versión
200 copies
ISBN Vol. 2: 978-607-9023-51-5
ISBN Complete: 978-607-9023-44-7

November, 2017

Content

	Page
Content	*i*
How to cite an article of this book	*ii*
Preface	*iii*
Acknowledgements	*vii*
Section 1. Renewable and Alternative Energies and Biorefineries	1
Section 2. Climate Change / Risk Assessment and Environmental Impact / Sustainability and Environmental System Analysis	146
Section 3. Groundwater and Aquifer Remediation / Soil and Sediment Remediation	209
Section 4. Green Materials and Biomaterials	267
Section 5. Solid and Hazardous Waste Management and Treatment	363
Section 6. Microbial Ecology / Molecular Biology Applications to Environmental Problems	391
Section 7. Wastewater Treatment	428
Section 8. Control and Modelling of Environmental Processes	787
Section 9. Environmental Chemistry	819
Section 10. Environmental Education / Environmental Health / Environmental Toxicology	868
Section 11. Environmental Engineering	904
Section 12 Environmental Nanotechnology	976

How to cite an article of this book

For example, the chapter by J.C.G. Silva; J.L.F. Alves; W.V.A. Galdino; J.V. Scharf and H.J. José, entitled "**CHAPTER 1.1. COMBUSTION OF PISTACHIO SHELL: EVALUATION OF KINETIC AND THERMODYNAMIC PARAMETERS"** published in the pages 4 to 14 of this book, should be cited as follows:
Silva, J.C.G.; Alves, J.L.F.; Galdino, W.V.A.; Scharf, J.V. and José, H.J. ~~(2017).~~ Chapter 1.1. Combustion of pistachio shell: evaluation of kinetic and thermodynamic parameters. *In:* Candal, R.; Curutchet, G.; Domínguez-Montero, L.; Macarie, H.; Poggi-Varaldo, H.; Vázquez, S. and Sastre, I. (Editors): *Environmental Biotechnology and Engineering: ISEBE Advances 2016*, pages 4-14. Ed. Cinvestav, Mexico City, Mexico

Preface

This book compiles and organizes as chapters selected full contributions of the 5th International Symposium on Environmental Biotechnology and Engineering (5ISEBE) held in July 25th-29th, 2016, in the National University of San Martín, San Martín, Buenos Aires, Argentina.
This book aims at reaching a wide audience including researchers, practitioners, managers, and students who aspire to learn about or to create a deeper scientific foundation as well as technological applications of Environmental Engineering and Environmental Biotechnology that address creative and feasible solutions to environmental pollution and sustainable development.
The 5ISEBE accepted a total of 283 abstracts and 102 articles were selected and edited to be part of this book (**Table 1**) after a strict peer-reviewing process. These contributions were distributed among 12 subjects, from emerging and promising topics such as Renewable and alternative energies and biorefineries, and Green materials and biomaterials to more traditional, although very important subjects, such as Wastewater treatment.

TABLE 1. Distribution of articles per technical subject of the Symposium

Subject	No. of Abstracts	Proportion (%)
Renewable and Alternative Energies and Biorefineries	16	15.69
Climate Change / Risk Assessment and Environmental Impact / Sustainability and Environmental System Analysis	6	5.88
Groundwater and Aquifer Remediation / Soil and Sediment Remediation	6	5.88
Green Materials and Biomaterials	10	9.80
Solid and Hazardous Waste Management and Treatment	3	2.94
Microbial Ecology / Molecular Biology Applications to Environmental Problems	4	3.92
Wastewater Treatment	35	34.31
Control and Modelling of Environmental Processes	3	2.94
Environmental Chemistry	4	3.92
Environmental Education / Environmental Health / Environmental Toxicology	4	3.92
Environmental Engineering	7	6.86
Environmental Nanotechnology	4	3.92
Total	**102**	**100.00**

It is worth highlighting the high number of contributions classified under four emerging and increasingly important topics: Renewable and alternative energies and biorefineries, Sustainability and environmental system analysis, Climate change, Risk assessment and environmental impact, Environmental engineering, and Green materials and biomaterials that accounted for one third (38%) of the total abstracts and were close to the most classic and mature subjects constituted by Wastewater treatment and the two topics on Remediation (nearly 40%, **Table 1**).

Articles came from ten countries (**Table 2**) thus confirming the international repercussion of the 5ISEBE. There was a large contribution from countries in Latin America such as Argentina, Brazil, Mexico and Paraguay. European countries both from Western and Eastern Europe also submitted works to the Symposium. Interestingly, there is a noticeable presence of African countries represented by scientists from Algeria and Tunisia.

This striking feature of the articles distribution is consistent with the locomotive effect of the increasing interest on renewable energies and new materials that has permeated environmental applications in recent years. Moreover, it is an indication of the high degree of innovation that characterizes Environmental Biotechnology and Environmental Engineering R&D in the 21st century.

The synergistic interaction of Environmental Biotechnology and Environmental Engineering has a tremendous potential for making outstanding contributions to the sustainable development and sustainable management of resources in modern societies. To a great extent, we expect that these contributions will also positively impact on societies' organization and improve people's consciousness, education and habits. Sustainable development should become the basis for the life of future generations as opposed to over-exploitation of non-renewable energy and material resources.

On the one hand, there were several international and regional events dealing with Biotechnology but no other international event was devoted entirely to Environmental Biotechnology. At most, Environmental Biotechnology is the subject of one or two sessions in a Biotechnology Congress.

TABLE 2. Distribution of abstracts by country

Country	Proportion (%)
Argentina	24.51
Brazil	28.43
France	1.96
Mexico	36.27
Paraguay	1.96
Slovak Republic	2.94
Other (Algeria,Chile, Colombia,Tunisia)	3.92
Total	**100**

On the other hand, most regional Environmental Engineering events showed a strong commercial component that negatively competed with the exchange of advanced knowledge and the formation of research networks.
Moreover, Environmental Biotechnology and Environmental Engineering are two dynamic drives with a strong interaction, and the scientific community could obtain several advantages from their joint diffusion. In short, there was a need for an international event dedicated to both disciplines, with a strong vocation for serious dissemination of scientific and technological knowledge, as well as research networking.
The synthesis to this diagnostic was to launch a new event focused on both disciplines. In this way, the First International Meeting on Environmental Biotechnology and Engineering was born and held in Mexico City in 2004. This first event was co-organized by the Dept. of Biotechnology and Bioengineering at CINVESTAV of the IPN in Mexico, the IRD from France, the IMIA from Spain, the Mexican Polytechnic Institute (IPN) from Mexico, the National University of Mexico (UNAM, México), the University of Hidalgo (UAEH, México), among others. The event was backed-up by a diverse International Scientific Committee that had the contributions of outstanding scientists and professionals from Brazil, Italy, Spain, Scotland, France, and Mexico.
In 2008, we had the satisfaction to see that the 3rd International Meeting on Environmental Biotechnologya and Engineering held in Palma de Mallorca, Spain, had exponentially grown and matured. Its outreach was multiplied by a factor of 10 compared to that of the 1st IMEBE. The Organizing Committee led by Dr. Isabel Sastre-Conde has to be congratulated for the success and resonance of the third version of this event. This was a confirmation of the original diagnostic: the scientific community was avid of an international event with the characteristics of the IMEBE. At the same time, the success of the 3IMEBE in Palma de Mallorca led to a change of name and format, from Meeting to Symposium, in order to reflect the increases on both quantity and quality of our event.
Following its international vocation, now the 5ISEBE is held in Argentina, South America, led by a dynamic and committed group of outstanding Argentinian academicians headed by Dr. Gustavo Curutchet and Dr. Roberto Candal, accompanied by Dr. Susana Vázquez, as well as a group of international experts rooted in the IMEBE-ISEBE history, such as Dr. Isabel Sastre-Conde from Spain, Dr. Hervé Macarie from France, among others. With them, the ISEBE's dream goes on.
Therefore, this book intitle "Environmental Biotechnology and Engineering: ISEBE Advances 2016" offer a body of the current cutting-edge approaches and knowledge in crucial areas of environmental care, new energies, and sustainble development.
We look forward to meeting you at the 6th. International Symposium on Environmental Biotechnology and Engineering (6ISEBE) in 2018.

The Editors

Dr. Roberto Candal
Senior Researcher-Associated Professor
Instituto de Investigaciones e Ingeniería Ambiental 3IA, Escuela de Ciencia y Tecnología. Consejo Nacional de Investigaciones Científicas y Técnicas, Universidad Nacional de San Martín
Buenos Aires, Argentina

Dr. Gustavo Curutchet
Senior Researcher-Associated Professor
Intituto de Investigaciones e Ingeniería Ambiental 3IA, Escuela de Ciencia y Tecnología. Consejo Nacional de Investigaciones Científicas y Técnicas, Universidad Nacional de San Martín
Buenos Aires, Argentina

Lilian Edith Domínguez-Montero, Sc D
Research Associate, Environmental Biotechnology and
Renewable Energies R&D Group
Doctoral Program Society and Scientific and Technological Development
CINVESTAV del IPN, Mexico City, Mexico

Dr. Hervé Macarie
IRD Senior Researcher
Ecotechnology & Bioremediation Group
Aix Marseille Univ, Univ Avignon, CNRS, IRD, IMBE, Marseille, France

Professor Dr. Héctor M. Poggi-Varaldo
Group Leader, Environmental Biotechnology and
Renewable Energies R&D Group
Dept. of Biotechnology and Bioengineering
CINVESTAV del IPN, Mexico City, Mexico.

Dr. Isabel Sastre-Conde
Serveis de Millora Agraria i Pesquera, SEMILLA
Instituto de Investigaciones Agroambientales y de Economía del Agua, INAGEA
Islas Baleares. Spain.

Dr. Susana Vázquez
Instituto NANOBIOTEC
Universidad de Buenos Aires-CONICET
Buenos Aires, Argentina

Acknowledgements

The International Symposium on Environmental Biotechnology and Engineering and the Editors of this Book acknowledge the contribution of the following persons:

Ms. Catherine Giselle Mar-Pineda, Biotechnoly Eng., with the GBAER, CINVESTAV.
Mr. Orlando Flores-Ortíz with the GBAER, ENCB-IPN, CINVESTAV
Ms. Karla Viridiana Rivera-Flores, with the GBAER, LA SALLE, CINVESTAV

Also, the effort and participation of the Reviewers in the peer-review process of the Abstracts and selected Articles is gratefully acknowledged:

Areco María M. – 3iA UNSAM
Borbolla-Gaxiola Jaime – CINVESTAV-IPN
Candal Roberto – 3iA UNSAM
Cainzos Veronica – 3iA UNSAM
Carnelli Patricio – 3iA UNSAM
Cavalito Sebastián– CINDEFI UNLP
Cavello Ivana – CINDEFI UNLP
Curutchet Gustavo – 3iA UNSAM
Domínguez Montero Lilian E. – CINVESTAV-IPN
Fantoni Sofía – 3iA UNSAM
Fernández Niello Jorge – 3iA UNSAM
Flores-Ortíz Orlando – ENCB-IPN
Guz Lucas – FCEyN, UBA
Gortares Pablo – ITSON
Hernández Vera Rafael – CINVESTAV-IPN
López Loveira Elsa – 3iA UNSAM
Macarie Hervé – IRD-IMBE/AIX MARSEILLE UNIVERSITÉ
Mar-Pineda Catherine G. – CINVESTAV-IPN
Marco Brown Jose Luis – 3iA UNSAM
Martinez Heimann Diego – 3iA UNSAM
Medina Sara – 3iA UNSAM
Olivelli Melisa – 3iA UNSAM
Poggi-Varaldo Héctor M. – CINVESTAV-IPN
Porcionato Natalia – 3iA UNSAM
Rivera-Flores Karla Viridiana – LA SALLE
Sastre-Conde Isabel – SEMILLA
Sotelo-Novarro Pela X.– UAM- AZCAPOTZALCO
Tiscornia Gisela – 3iA UNSAM
Torres Sánchez Rosa – CETMIC CONICET
Tufo Ana – 3iA UNSAM
Vázquez Susana – NANOBIOTEC UBA-CONICET

Section 1.

Renewable and Alternative Energies and Biorefineries

ISEBE Advances 2016

Page

Chapter 1.1 Combustion of pistachio shell: evaluation of kinetic and thermodynamic parameters 4
J.C.G. Silva; J.L.F. Alves; W.V.A. Galdino; J.V. Scharf and H.J. José

Chapter 1.2 Producción de bioelectricidad en G*eobacter sulfurreducens* a través de la biosíntesis del pili 15
José Alberto Hernández-Eligio; Ángel Andrade; Maricela Olvera; Xadeni Burgos and Katy Juárez

Chapter 1.3 Bioeletrosintesis con productos de valor agregado y su integracion con biorrefinerias para el siglo XXI 27
E. Hernández-Correa and H. M. Poggi-Varaldo

Chapter 1.4 Series dark and photoheterotrophic fermentation of cheese whey 36
K.M. Muñoz Páez and H.M. Poggi-Varaldo

Chapter 1.5 Saccharification of a stream of pretreated intermediate solids from an h-m-z-s biorefinery 44
Leticia Romero-Cedillo; Héctor M. Poggi-Varaldo and M. Teresa Ponce-Noyola

Chapter 1.6 Pretreatment of intermediate solids from the enzyme stage in a biorefinery for further use 52
L. Romero Cedillo; H. M. Poggi-Varaldo and M. T. Ponce-Noyola

Chapter 1.7 Bio-hydrogen from pretreated intermediate solids and the organic fraction of municipal solid wastes in the context of an h-m-z-s biorefinery 59
L. Romero Cedillo; H. M. Poggi-Varaldo and M. T. Ponce-Noyola

Chapter 1.8 Effect of progressive organic loading rate over biobutanol production in anaerobic reactor using biodiesel waste as carbon source 64
R. Salles; C. Silva; J. Bassan; R. Monti; M. Zaiat; B. Varesche and G. Peixoto

Chapter 1.9 Evaluation of different inoculate for biobutanol production in anaerobic reactor using biodiesel waste as carbon source 75
C. Silva; R. Salles; J. Bassan; R. Monti; ZM. Zaiat; B. Varesche and G. Peixoto

Chapter 1.10 Extraction of cellulose from used disposable diapers for application in hydrogenogenic dark fermentation
Perla X. Sotelo-Navarro; Héctor M. Poggi-Varaldo; Sylvie J. Turpin-Marion; Rosa M. Espinosa Valdemar; Alethia Vázquez-Morillas; Mariana Nava-Ferreira and Jesús G. Méndez-Silva 86

Chapter 1.11 Ensayo de actividad metanogénica específica: una herramienta clave para evaluar la eficiencia en reactores anaeróbicos 91
P. Bres; M. E. Beily; S. Costa; J. L. Avila; R. Candal and D. Crespo

Chapter 1.12 Microbial fuel cells equipped with anion exchange membrane used for treating actual leachates 101
G. Hernández-Flores; H. M. Poggi-Varaldo; T. Romero Castañón and O. Solorza Feria

Chapter 1.13 Enrichement of microbial cultures for using in the cathodic and anodic chambers of a biocathode microbial fuel cell
J. E. Borbolla-Gaxiola; H. M. Poggi-Varaldo; M. T. Ponce-Noyola; O. Solorza-Feria and G. Hernández-Flores 113

Chapter 1.14 A Very low-cost method for monitoring electric potential in microbial fuel cells
J. E. Borbolla-Gaxiola; H. M. Poggi-Varaldo; M. T. Ponce-Noyola; O. Solorza-Feria and F. Esparza-García 122

Chapter 1.15 Sequential hydrogenogenic and methanogenic fermentation of waste disposable diapers
Perla X. Sotelo-Navarro; Héctor M. Poggi-Varaldo; Sylvie J. Turpin-Marion; Rosa M. Espinosa-Valdemar; Alethia Vázquez-Morillas and Margarita Beltrán-Villavicencio 130

Chapter 1.16 Biorefinery of lemon peel waste using cold adapted yeasts from antarctic and sub-antarctic regions
A. Albanesi; I. Cavello; D. Fratebianchi; A. Martinez; G. Garmendia; S. Vero and S. Cavalitto 136

CHAPTER 1.1 COMBUSTION OF PISTACHIO SHELL: EVALUATION OF KINETIC AND THERMODYNAMIC PARAMETERS

J.C.G. Silva *(1); J.L.F. Alves (2); W.V.A. Galdino (1); J.V. Scharf (2) and H.J. José (2)

(1) Federal University of Paraiba, Cidade Universitária, João Pessoa, Brazil.
(2) Federal University of Santa Catarina, Eng. Agronômico Andrei Cristian Ferreira St., Florianópolis, Brazil

ABSTRACT

The present concern with sustainable development has allowed research in the field of renewable energy to become essential in order to ensure a future in which the world primary energy is not only dependent of non-renewable sources. Among the renewable sources, biomass in form of waste, whether industrial, agricultural or urban, has shown great relevance because of its low cost and the several conversion routes.
Therefore, the present work had the objective to characterize the pistachio shell waste and evaluate the thermal and kinetic behavior of the combustion process. The pistachio shell was characterized through the proximate analysis, scanning electron microscopy with energy dispersive X-ray spectroscopy (SEM/EDS) and Fourier transform infrared spectroscopy (FTIR). The thermal and kinetic behavior were evaluated by a thermogravimetric analyzer under oxidant atmosphere in the temperature range of 30 ºC to 1000 ºC, where the process was performed in four different heating rates (10, 20, 30 e 40 ºC min^{-1}). Through the data were calculated activation energy (E_a), frequency factor (A) and the model of the reaction ($f(\alpha)$) by isoconversional method of Coats-Redfern. The thermodynamic parameters, enthalpy (ΔH), Gibbs free energy (ΔG) and entropy (ΔS) were determined by the results for E_a and A.
Based on thermogravimetric profiles of pistachio shell combustion, the presence of two distinct zones of mass loss were observed. The first zone is associated with volatilization that occurs between temperatures of 200 ºC and 375 ºC, with activation energy and frequency factor being 128.9 kJ mol^{-1} and $2.68x10^{10}$ min^{-1}, respectively. In this first zone, the reaction occurs through diffusional model, with thermodynamic parameters value of ΔH = 133.8 kJ min^{-1}, ΔG = 179.1 kJ min-1 and ΔS = -76.8 J min^{-1}. The second zone, on the other hand, occurs between temperatures of 400 ºC to 600 ºC, and refers to biochar oxidation, presenting E_a = 119.3 kJ min^{-1} and A = 5.55x107 min^{-1}. The values of enthalpy, Gibbs free energy and entropy for this zone were 125.2 kJ min^{-1}, 199.9 kJ min^{-1} and -126.3 J min^{-1}, respectively. Furthermore, it was observed that in this zone the reaction occurs under the Avrami–Erofe'ev model. The results demonstrate the applicability of the residue studied in combustion process, which may be used in development design and optimization reactors.

Keywords: Coats–Redfern method; combustion; pistachio shell; thermodynamic parameters

---

*Author for correspondence: jean.constantino@cear.ufpb.br

INTRODUCTION

The socio-economic and energetic development was led due to the exponential increase in the use of fossil fuels for decades[1]. However, this increased consumption has caused environmental problems on a global scale, due to the greenhouse gases emission, in many ways, from extraction to final use. Thus, several nations leaders have been meeting to discuss the limitation of greenhouse gas emissions and evaluate renewable energy alternatives.

Biomass is a renewable resource, defined as a non-fossil organic and biodegradable material originated from plants, animals and microorganisms, chemically composed of hydrocarbons[2]. Agro industrial waste has distinguished between different forms of biomass because of its low cost and does not compete with arable lands for food production[3,4].

Waste such as those generated by the cultivation of pistachios (*Pistacia vera* L.) may be a promising energy source, because the pistachio shell represents the majority of fruit weight, with an average of 64 %, which features a low moisture content and high energy potential, that can be applied to thermochemical processes such as pyrolysis, combustion and gasification.

In thermochemical processes besides the knowledge of the biomass characteristics, such as chemical composition and morphology, is very important knowledge and obtaining the kinetic and thermodynamic parameters of thermal decomposition. These parameters assist in understanding the behavior of biomass when subjected to temperature variation and are useful in the designer and efficiency of biomass conversion system for energy or other products.[6]. The kinetic parameters are usually obtained by the thermogravimetric analysis data using is conversional methods, among them, the most used are the methods Flynn-Wall-Ozawa, Friedman, Coats-Redfern and Vyazovkin[7].

Therefore, the goal of this study was to evaluate the oxidation process (combustion) by obtaining the kinetic and thermodynamic parameters of pistachio shell combustion in a thermogravimetric analyzer calculated by modified Coats-Redfern method. Furthermore, the biomass physicochemical characteristics were obtained through proximate analysis, Fourier transform infrared spectroscopy (FTIR) and scanning electron microscopy with energy dispersive X-ray spectroscopy (SEM/EDS).

MATERIALS AND METHODS

The samples of pistachio shell (*Pistacia vera* L.) provided by the LCA/UFPB were initially dried in an oven at 60 ºC for 24 h, subsequently ground in a ball mill.

Pistachio shell characterization was performed by proximate analysis, scanning electron microscopy with energy dispersive X-ray spectroscopy (SEM/EDS) and infrared Fourier transform spectroscopy (FTIR).

Proximate analysis was lead in a thermogravimetric analyzer DTG-60 Shimadzu following the ASTM E-1131 method[8].

The biomass surface morphology was obtained by scanning electron microscopy (SEM) on a JEOL JSM-6390LV Scanning Electron Microscope device and from a

secondary electron detector was possible to evaluate the qualitative and semi-quantitative sample composition by energy dispersive X-ray spectroscopy (EDS).

Fourier transform infrared spectroscopy (FTIR) was performed to obtain information about the chemical composition through the functional groups present in sample. The analysis was using a Shimadzu IRPrestige-21 though the KBr method.

The thermal behavior evaluation of samples was performed using a thermogravimetric analyzer DTG-60 Shimadzu under an oxidant (Synthetic air) and inert (99.995 % of N_2) atmosphere at heating rate of 20 ºC min^{-1} with a flow of 50 mL min^{-1}.

For the kinetic study of combustion an initial sample amount of ~10 mg were heated from room temperature to 1000 ºC under heating rates of 10, 20, 30 and 40 ºC min^{-1} with a gas flow of 50 ml min^{-1} (Synthetic air), where the data were calculated thought with a program developed in MS Excel.

The kinetic study of the oxidative decomposition at solid-state was based on single step described in Equation 1:

$$\frac{d\alpha}{dt} = k(T)\, f(\alpha) \tag{1}$$

where *k(T)* is the rate constant e *f(α)* is the reaction model. Equation 1 represents the conversion rate (α) of solid-state to gas-state as a function of time. The rate constant is based on the Arrhenius equation which relates the influence of temperature over reaction rate[9].

$$k(T) = Ae^{\frac{-E_a}{RT}} \tag{2}$$

where *A* is the frequency factor (min^{-1}), E_a is the activation energy (J mol^{-1}), *R* is the gas constant (8.314 J K^{-1} mol^{-1}) and *T* is the temperature (K). Therefore, based on the combination of Equations 1 and 2 has:

$$\frac{d\alpha}{dt} = Ae^{\frac{-E_a}{RT}} f(\alpha) \tag{3}$$

Equation 3 is not generally applied in thermogravimetric data this due the conversion processes are observed as a function of temperature and using several heating rate (*β*). The heating rate is given as a function of the temperature increases linearly with time ($dT = \beta dt$), thereby Equation 4 is obtained as:

$$\frac{d\alpha}{dT} = \frac{A}{\beta} e^{\frac{-E_a}{RT}} f(\alpha) \tag{4}$$

Equation 4 does not provide an analytical solution, therefore necessitating to use several models for the calculation of kinetic parameters. The isoconversional methods

("Free-model") are widely used for the determination of E_a without the prior knowledge of A and $f(\alpha)$. For this work the modified Coats-Redfern method[7,10] (Equation 5) was used.

$$\ln\left(\frac{\beta}{T_\alpha^{\,2}}\right) = \ln\left(-\frac{A_\alpha R}{E_{a,\alpha} g(\alpha)}\left(1-\frac{2RT_\alpha}{E_{a,\alpha}}\right)\right) - \frac{E_{a,\alpha}}{R}\frac{1}{T_\alpha} \quad (5)$$

Through obtaining the line plotting the term $ln(\beta/T_\alpha^2)$ against $1/T_\alpha$ at Equation 5, it is possible to obtain activation energy at each conversion value.

The isoconversional methods allow to calculate the E_a without the knowledge of $f(\alpha)$, thereby to obtain the frequency factor (A) becomes necessary the use of methods to estimate, among them the compensation method (Equation 6) is the most used for evaluate this parameter[11].

$$\ln\left(A_\alpha\right) = aE_{a,\alpha} + b \quad (6)$$

The compensation effect consists in using the model-fitting method for a single-heating by different models[12] $f_j(\alpha)$ to determine several lnA_j e Ea_j values, obtaining the compensation parameters a and b, where the term i indicates each reaction model, which can be found in several works[11–13]. The reaction model can be obtained through the curve $g(\alpha)$ using the parameters $E_{a,\alpha}$ and A_α calculated.

The thermodynamic parameters, Gibbs free energy (ΔG), enthalpy (ΔH) and entropy (ΔS) can be calculated based on the following equations[14,15]:

$$\Delta G = Ea + RT_m \ln\left(\frac{k_B T_m}{hA}\right) \quad (7)$$

$$\Delta H = E_a - RT \quad (8)$$

$$\Delta S = \frac{\Delta H - \Delta G}{T_m} \quad (9)$$

where k_B is the the Boltzmann constant, h the Plank constant and T_m is temperature where there is the greatest mass loss rate.

RESULTS AND DISCUSSION

Table 1 shows the result of the proximate analysis for pistachio shell waste made through the standard method.

The low moisture and ash content demonstrate the favorable applicability of these waste in combustion processes, due to the lower amount of energy required to eliminate the water in sample, as well as a less probability of fouling and slagging in equipment[16].

TABLE 1. Proximate Analysis results of pistachio shell

Proximate Analysis (wt%)			
Moisture[a]	Volatiles Matter[b]	Fixed Carbon[b]	Ash[b]
3.59 ± 0.21	82.97 ± 1.82	16.67 ± 1.46	0.36 ± 0.15

a: wet basis b: dry basis

The high volatile matter and fixed carbon content is proportional the reactivity of sample, where the material may have a low ignition temperature[17].

From the SEM/EDS was possible to identify some components present in biomass like carbon (C) and oxygen (O), in addition, sodium (Na), aluminum (Al) and potassium (K) are also in the sample.

TABLE 2. Composition obtained through SEM/EDS

C (%)	O (%)	Na (%)	Al (%)	K (%)
83.16 ± 1.67	16.32 ± 1.84	0.37 ± 0.10	0.06 ± 0.01	0.15 ± 0.04

The amount of K and Na, observed in **Table 2**, may reflect potential problems of fouling, where these alkalis in the presence of silica may form alkali silicates resulting in reducing the melting temperature and that may be dragged by the gases and condensing tubulations[16,18].

The microstructures of the pistachio shell, obtained by SEM, are shown in **Figure 1**. It is noted in **Figures 1a** and **1b** the surface and cross section of pistachio shell without any pores, demonstrating a dense surface with few cracks.

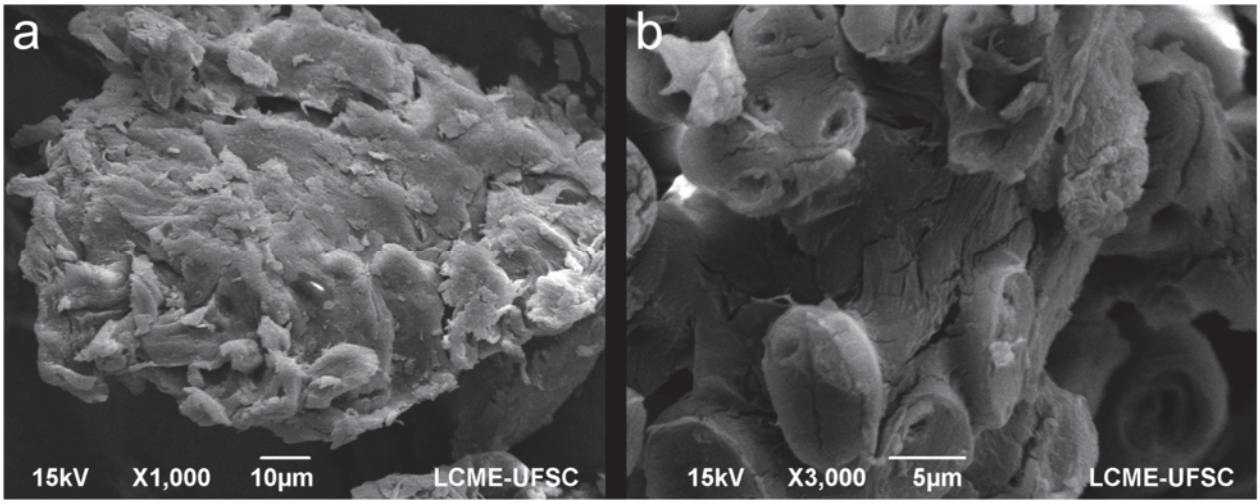


FIGURE 1. Scanning electron micrographs at a magnification ×1000 of pistachio Shell surface and magnification ×3000 of cross section

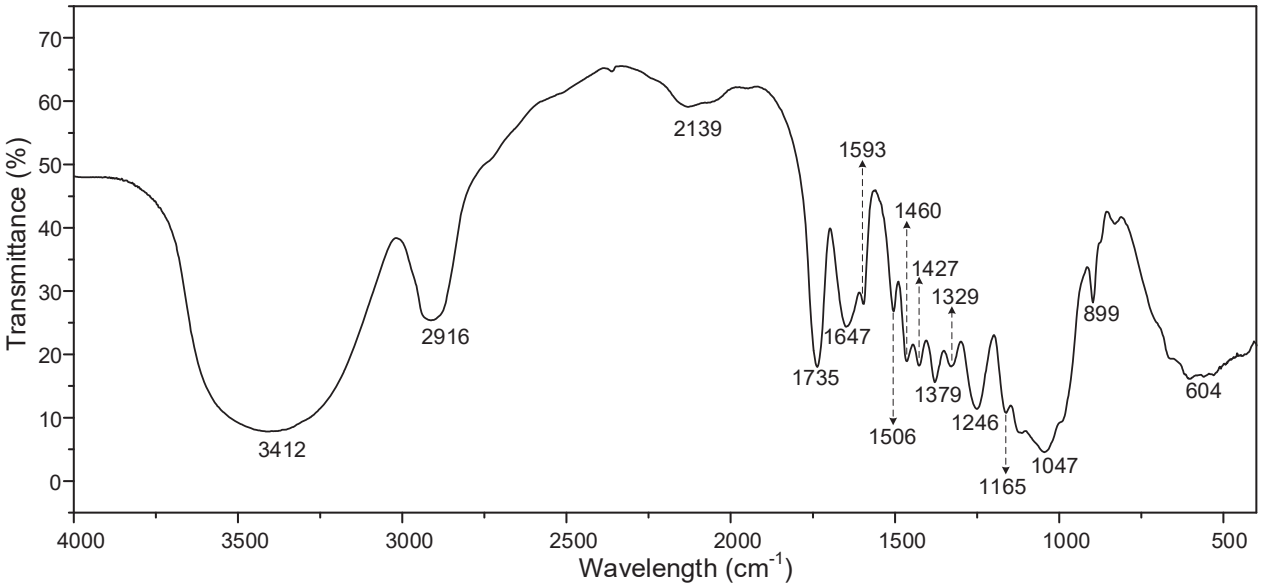


FIGURE 2. Fourier transform infrared spectroscopy spectrum of pistachio shell

The FTIR spectrum for the pistachio shell is shown in **Figure 2**. Note that the band at 3412 cm^{-1} corresponds vibrations of hydroxyl groups OH present in the sample, while the band at 2916 cm^{-1} is attributed to asymmetric C-H stretching of methylene groups. The band at 2139 cm^{-1} is attributed to alkyne groups stretching vibration of C≡C. The aliphatic aldehyde C=O stretching observed in the sample at wavelength 1735 cm^{-1}, while the C=C stretching in alkenes groups occurs in the band 1647 cm^{-1}. At the bands 1593 cm^{-1} and 1505 cm^{-1} occur the C=C vibrations in aromatic rings. The band at 1460 cm^{-1} is the corresponding C-H methylene scissoring while the band at 1379 cm^{-1} shows the symmetrical methyl C-H bending. The bands at 1427 cm^{-1} and 1246 cm^{-1} are attributed to C-O-H in-plane bending and C-O stretching, respectively, for carboxylic acids groups. The band at 1329 cm^{-1}, which has the first overtone of the C-H bending vibration, appears as a weak, broad band in the 1370-1220 cm^{-1} region. The band at 1165 cm^{-1} and 1047 cm^{-1} can be correlated with C-O stretching vibrations in alcohols and phenols that produce a strong band in the 1260-1000 cm^{-1} region of the spectrum. The band at 899 cm^{-1} can be attributed to third overtone C-H stretching (850-950 cm^{-1}), while the band at 604 cm^{-1} can be related with =C-H bending in alkynes (700-600 cm^{-1})[19,20].

For the kinetic study it is necessary to know the thermal behavior of the sample, thereby the **Figure 3** shows the TG and DTG curves for pistachio shell decomposition under an oxidant and inert atmosphere, which can be observed different decomposition stages for each atmosphere.

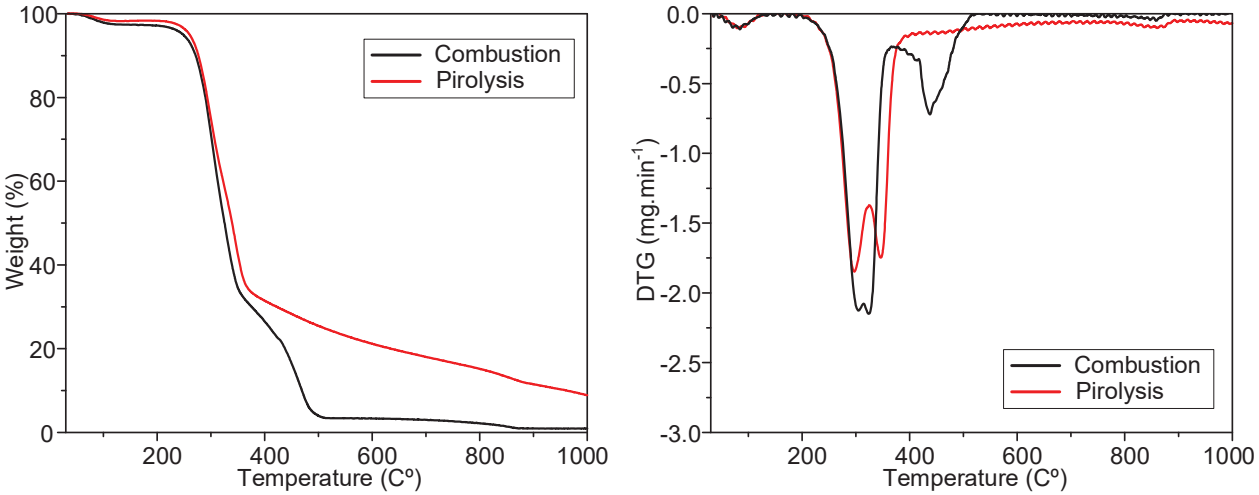


FIGURE 3. TG and DTG curves from (—) pyrolysis and (—) combustion process at 20 ºC min^{-1} heating rate

It is noted from **Figure 3** that when the sample is submitted to an inert atmosphere, at heating rate of 20 ºC min^{-1}, two decomposition zones, well defined, after the volatilization of moisture are observed. The majority decomposition of hemicellulose can be characterized by first region, between 200 and 325 ºC (mass loss of 40 %), due the chemical structure of hemicellulose, which presents low polymerization degree and various branches, making degradation easier at low temperatures[21], when compared with other lignocellulosic components. Subsequently, the second zone between 325 ºC and 400 ºC (mass loss of 27 %) can be attributed to quick cellulose decomposition, difference from hemicellulose, presents a high polymerization degree with intramolecular and intermolecular chemical interaction forces[21,22]. Lignin is complex structure formed of phenylpropane units, demonstrating a greater difficulty to break down, thus the lignin degraded over the whole experimental range as observed by Yang *et al.*[21].

In an oxidant atmosphere two decomposition zones are observed, however with different characteristics observed, when compared with inert atmosphere. The first zone in the temperature range of 200-360 ºC (mass loss of 65 %) can be characterized by hemicellulose and cellulose volatilization in sample and subsequently oxidized, resulting in a quick volatilization and shown a high peak, greater than observed in inert atmosphere. The subsequent region between 360 ºC and 520 ºC (mass loss of 29 %) is related with oxidation of residual biochar, i.e., the oxidation reaction occurs on the biochar surface, resulting in the formation of ash[16,24].

Based on these combustion zones, the kinetic study to evaluate the kinetic triplet (E_a, A, $f(\alpha)$) of this process can be performed. Thus, using the isoconversional method (modified Coats-Redfern method)[7,10] to evaluate the activation energy (Figure 4a) in volatilization (Zone 1) and oxidation of biochar (Zone 2) regions, being of the temperature ranges 200-375 ºC and 400-600 ºC, respectively for each zone with conversion range of $0.05 \leq \alpha \leq 0.95$.

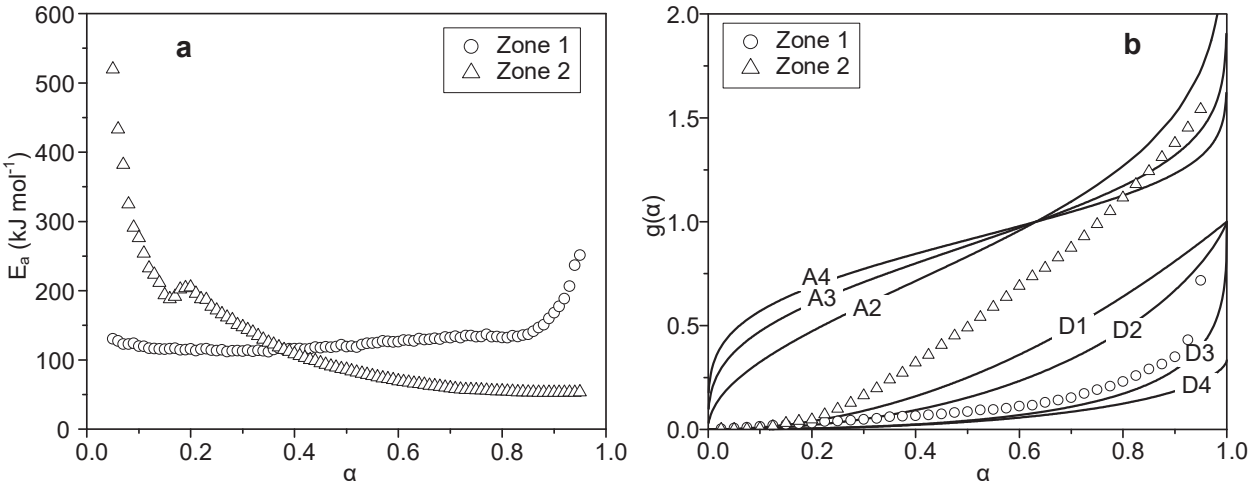


FIGURE 4. (a) Activation Energy results calculated by modified Coats-Redfern method and (b) Reaction model of each combustion zone

Figure 4a is shows the behavior of E_a *vs.* α in combustion process for each reaction zone. In Zone 1 shows that in a large conversion range $E_{a,\alpha}$ presents a small variation on its value, with an average ($E_{a,av}$) of 128.9 kJ mol^{-1}. This small variation may indicate that the process occurs by a single-step model[11], which is demonstrated in **Figure 4b**, shown that process follows a diffusional reaction model between D2 (Two-dimensional diffusion) and D3 (three-dimensional diffusion) in a wide conversion range. On the other hand, in Zone 2 is observed a wide variation of activation energy at beginning of the process ($\alpha \leq 0.50$), can be related to multiple-step reactions on the material surface in a diffusional model this due to quick biochar oxidation, however after it reaches the conversion of 0.5 is noted a small variation of activation energy that follows a Avrami-Erofe'ev model, which can be associated with nucleation reactions[25] between the inorganic compounds, result of biomass combustion. Zone 2 presented na $E_{a,av}$ of 119.3 kJ mol^{-1}.

For the determination of frequency factor (A) is necessary to use a method to estimate its value, among them the use of compensation effect is usually chosen[12]. Using the values obtained from Eq. 6 it is possible determine the A_α through $E_{a,\alpha}$ calculated by isoconversional method..

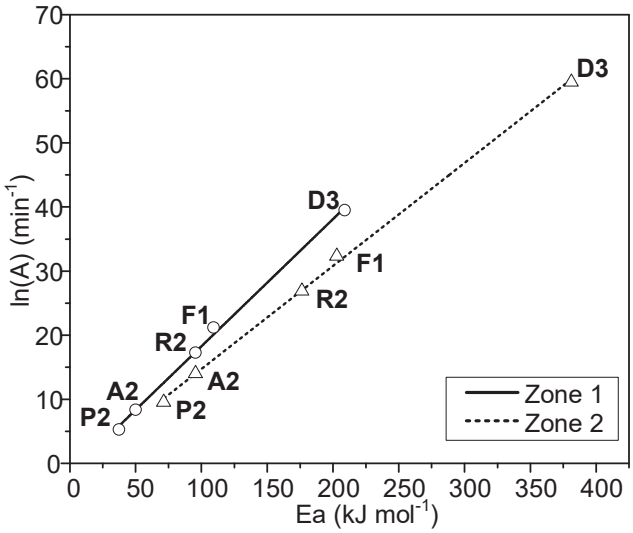


FIGURE 5. Compensation effect adjustment of each combustion zone

The straight line obtained from the compensation effect shown in **Figure 5** showed an adjustment of R^2 > 0.9977 to Eq. 6 for both Zones 1 and 2, being obtained the compensation parameter values of a_1 = 0.1984 and b_1 = -1.5716 for Zona 1, while Zone 2 showed a_2 = 0.1607 and b_2 = -1.3448. The average frequency factor value (A_{av}) were 2.68x10^{10} min^{-1} and 5.55x10^{7} min^{-1} for Zones 1 and 2, respectively.

Based on the values of $E_{a,\alpha}$ and A_α it is possible to evaluate the thermodynamic parameters ΔH, ΔG e ΔS by means of Equations 7, 8 e 9, its respective results are shown in **Table 3**.

TABLE 3. Thermodynamic Parameters

Zone	ΔH (kJ mol^{-1})	ΔG (kJ mol^{-1})	ΔS (J mol^{-1})
1	133.8 ± 13.8	179.1 ± 0.4	-76.8 ± 22.7
2	125.2 ± 62.9	199.9 ± 13.2	-126.3 ± 83.9

The ΔH value found reverts to the heat added to the system to make the oxidation reaction occur. Zone 1 has a higher ΔH than Zone 2, reverting to a greater amount of heat is required to break chemical bonds and to form of the activated complex[15]. The results for ΔG shows that there is a need of adding energy to the system for the reaction to occur[26]. The ΔG in Zone 2 presented a higher need of energy for formation of the activated complex, justified by Equation 7 which is directly related with E_a. The negative results observed of ΔS show that the disorder degree of the initial reactants are greater than its product [15], where Zone 2 showed lower disorder degree.

CONCLUSION

In this work it was observed that the pistachio shell presents a promising applicability in combustion processes, due to the low moisture and ash content observed through proximate analysis. On the other hand, some precautions should be made as to its due to the presence of K and Na identified from the SEM/EDS. It was identified through SEM

that the pistachio shell has a dense structure, which has many functional groups identified by FTIR.
Dynamic TG and DTG analysis used to evaluate the thermal behavior of the combustion process showed the presence of two zones decomposition at a heating rate of 20 ºC min^{-1}, related to volatilization of organic matter (200-360 ºC) and biochar oxidation (360-520 ºC).
From the different heating rates data, it become possible to evaluate the kinetic parameters by the modified Coats-Redfern method, using the decomposition (Zone 1) and oxidation (Zone 2) zones observed in DTG. The average activation energy obtained for Zones 1 and 2 were 128.9 kJ mol^{-1} and 119.3 kJ mol^{-1}, respectively, demonstrating that the Zone 1 requires a higher energy effectively occurrence of the reaction. Consecutively, from the result of the activation energy, it was possible to estimate the frequency factor for each zone through compensation effect with $R^2 > 0.9977$, which showed average values of 2.68x1010 min^{-1} (Zone 1) and $5.55x10^7$ min^{-1} (Zone 2). It was observed that each zone presented a different reaction model, while Zone 1 the process was mainly characterized by diffusion, Zone 2 initially showed a rapid diffusion process and converged to a Avrami–Erofe'ev model, which is related to nucleation of residues formed.
The data obtained from ΔH, ΔG and ΔS show thermodynamic characteristics for each reaction zone of samples, when subjected to an oxidation process, which can demonstrate the promising applicability of these waste in combustion processes.

ACKNOWLEDGMENTS

The authors gratefully acknowledge post graduation program in Renewable Energy at UFPB and the financial support from the CAPES with master's scholarship. Members of the Energy and Environment Laboratory (LEMA/UFSC) and Activated Carbon Laboratory (LCA/UFPB) by support and supply of biomass used in this study and Daniela Bresolin (LCP/UFSC) for assistance. Special thanks the support given by LCME/UFSC, which assisted in the research providing analysis of SEM/EDS.

REFERENCES

1. Huber M. T. Energizing historical materialism: Fossil fuels, space and the capitalist mode of production. Geoforum 40 (2009) 105–115.
2. UNFCCC. *Clarifications on definition of biomass and consideration of changes in carbon pools due to a CDM project activity*, EB-20, Report Annex. 8, 2005.
3. McKendry P. Energy production from biomass (part 1): Overview of biomass. Bioresour. Technol. 83 (2002) 37–46.
4. Ferreira-Leita V., Gottschalk L. M. F., Ferrara M. A., Nepomuceno A. L., Molinari H. B. C., Bon E. P. S. Biomass Residues in Brazil: Availability and Potential Uses. *Waste and Biomass Valorization* **1** (2010) 65–76.
5. Kashaninejad M., Mortazavi A., Safekordi A., Tabil L. G. Some physical properties of Pistachio (*Pistacia vera* L.) nut and its kernel. J. Food Eng. 72 (2006) 30–38.
6. Ounas A., Aboulkas A., El harfi K., Bacaoui A., Yaacoubi A. Pyrolysis of olive residue and sugar cane bagasse: Non-isothermal thermogravimetric kinetic analysis. Bioresour. Technol. 102 (2011) 11234–11238.

7. Brown M. E., Maciejewski M., Vyazovkin S., Nomen R., Sempere J., Burnham A. Computational aspects of kinetic analysis Part A: The ICTAC kinetics project-data , methods and results. Thermochim. Acta 355 (2000) 125–143.
8. ASTM Standard 1131-03. *Standard test method for composition analysis by thermogravimetry*, American Society for Testing and Materials (ASTM), (2003)
9. Laidler K. J. The Development of the Arrhenius Equation. J. Chem. Educ. 61 (1984) 494–498.
10. Burnham A. K.,Braun R. L. Global Kinetic Analysis of Complex Materials. Energy & Fuels 13 (1999) 1–22.
11. Vyazovkin S., Burnham A. K., Criado J. M., Pérez-maqueda L. A., Popescu C., Sbirrazzuoli N. Thermochimica Acta ICTAC Kinetics Committee recommendations for performing kinetic computations on thermal analysis data. Thermochim. Acta 520 (2011) 1–19.
12. Vyazovkin S., Isoconversional Kinetics of Thermally Stimulated, Springer International Publishing, (2015).
13. Khawam A., Flanagan, D. R. Solid-State Kinetic Models: Basics and Mathematical Fundamentals. J. Phys. Chem. B 110 (2006) 17315–17328.
14. Xu Y., Chen B. Investigation of thermodynamic parameters in the pyrolysis conversion of biomass and manure to biochars using thermogravimetric analysis. Bioresour. Technol. 146 (2013) 485–493.
15. Kim Y. S., Kim Y. S., Kim S. H. Investigation of thermodynamic parameters in the thermal decomposition of plastic waste-waste lube oil compounds. Environ. Sci. Technol. 44 (2010) 5313–5317.
16. Jenkins B. M., Baxter L. L., Miles T. R., Miles T. R. Combustion properties of biomass. Fuel Process. Technol. 54 (1998) 17–46.
17. García R., Pizarro C., Lavín A. G., Bueno J. L. Spanish biofuels heating value estimation. Part II: Proximate analysis data. Fuel 117 (2014) 1139–1147.
18. Baxter L. L. Ash deposition during biomass and coal combustion: A mechanistic approach. Biomass and Bioenergy 4 (1993) 85–102.
19. Stuart, B. H. Infrared Spectroscopy : Fundamentals and Applications, Wiley, (2004).
20. Silverstein R. M., Webster F. X., Kiemle D. J. Spectrometric Identification of Organic Compounds, Wiley, (2005).
21. Yang H., Yan R., Chen H., Lee D. H., Zheng C. Characteristics of hemicellulose, cellulose and lignin pyrolysis. Fuel 86 (2007) 1781–1788.
22. Rowell R. Handbook of Wood Chemistry and Wood Composites, CRC Press Taylor Fr. Gr., (2005).
23. Mohan D., Pittman C. U., Steele, P. H. Pyrolysis of Wood / Biomass for Bio-oil : A Critical Review. Energy & Fuesl 20 (2006) 848–889.
24. Gani A., Naruse I. Effect of cellulose and lignin content on pyrolysis and combustion characteristics for several types of biomass. Renew. Energy 32 (2007) 649–661.
25. Boström D., Skoglund N., Grimm A., Boman C., Öhman M., Broström M., Backman R. Ash Transformation Chemistry during Combustion of Biomass. Energy & Fuels 26 (2012) 85–93.
26. Ruvolo-Filho A., Curti P. S. Chemical kinetic model and thermodynamic compensation effect of alkaline hydrolysis of waste poly(ethylene terephthalate) in nonaqueous ethylene glycol solution. Ind. Eng. Chem. Res. 45 (2006) 7985–7996.

CHAPTER 1.2 PRODUCCIÓN DE BIOELECTRICIDAD EN *Geobacter sulfurreducens* A TRAVÉS DE LA BIOSÍNTESIS DEL PILI

José Alberto Hernández-Eligio (1,2); Ángel Andrade (1); Maricela Olvera (1); Xadeni Burgos (1) and Katy Juárez *(1)

(1) Departamento de Bioingeniería Celular y Biocatálisis, Instituto de Biotecnología UNAM, Av. Universidad No. 2001, Col. Chamilpa, Cuernavaca, Morelos, México.
(2) CONACyT Fellow Research, Consejo Nacional de Ciencia y Tecnología, Ciudad de México, Méx.

RESUMEN

La bacteria *Geobacter sulfurreducens* requiere de un filamento conductivo tipo pili para reducir óxidos de fierro y producir bioelectricidad. El pili está constituido por la proteína PilA y su gen (*pilA*) es regulado a nivel transcripcional por el factor σ^{54} y el sistema de dos componentes PilS/PilR. PilR activa directamente la transcripción de *pilA* y es un regulador tipo Enhancer Binding Protein (EBP). La activación transcripcional dependiente de reguladores EBP generalmente se ve favorecida por proteínas accesorias del tipo IHF que permiten la interacción de la holoenzima $E\sigma^{54}$ y dichos activadores. En este trabajo se determinó la participación del complejo IHF en la regulación transcripcional del gen *pilA*. Mutaciones en los genes que codifican para el complejo IHF muestran un fenotipo negativo en la transferencia de electrones, empleando fumarato, Fe(III) soluble y óxidos Fe(III) como aceptores de electrones. Mediante ensayos de inmunodetección, encontramos que las cepas mutantes son deficientes en producir la proteína estructural PilA. Usando el algoritmo "Virtual-Footprinting" logramos identificar tres posibles sitios de unión del complejo IHF en la región promotora de *pilA*. Con experimentos de reverso transcripción y PCR en tiempo real encontramos que las mutaciones en los genes *ihf* afectan a nivel transcripcional la expresión de *pilA*, y con experimentos de interacción ADN-proteína observamos que el complejo IHF se une específicamente a la región promotora de dicho gen. Con estos datos, proponemos un modelo de regulación donde el sistema de dos componentes PilS/PilR y el complejo IHF controlan la transferencia de electrones y con ello la producción de biolectricidad, al activar directamente la expresión del gen *pilA*.

Palabras claves: Integral host factor, pili, regulación transcripcional

INTRODUCCIÓN

Geobacter sulfurreducens en una delta proteobacteria, perteneciente a la familia *Geobacteraceae*. Esta familia de bacterias habita en el subsuelo donde tienen la capacidad de transferir electrones a diversos aceptores extracelulares como óxidos de Fe(III), Mn(IV), fumarato y sustancias húmicas[1]. Las especies de *Geobacter* han

---

*Author for correspondence: katy@ibt.unam.mx

cobrado gran importancia debido a que pueden ser usadas en gran variedad de aplicaciones, como en la biorremediación de ambientes contaminados con materia orgánica y metales en sedimentos acuosos y suelos subterráneos, y la producción de bioelectricidad en celdas microbianas de combustible (MFC)[2-3]. Para llevar a cabo estos procesos, *Geobacter* tiene la capacidad de transferir de manera extracelular los electrones que genera. La transferencia de electrones extracelular ha sido ampliamente estudiada en *Geobacter sulfurreducens*, debido a que se cuenta con la secuencia completa de su genoma[4-5]. El proceso de transferencia de electrones es complejo e involucra la participación de un filamento tipo pili y numerosos citocromos tipo *c*. Se ha determinado que el pili de *G. sulfurreducens* tiene propiedades conductivas y por tanto puede comportarse como un nanocable[6-7].

El pili de *G. sulfurreducens* está constituido por monómeros de una sola proteína denominada pilina o PilA y es codificada por el gen *pilA* cuya expresión esta estrictamente regulada. La regulación de la expresión del gen *pilA* ya ha sido estudiada y descrita en diversos microorganismos, por ejemplo en varias especies de *Pseudomonas*, *Moroxella*, *Dichelobacter*, *Myxococcus* y *Kingella*, la transcripción de *pilA* es dirigida principalmente por el factor σ^{54} (RpoN) y la proteína reguladora de respuesta PilR[8-13]. Se conoce que el factor σ^{54} requiere específicamente de los elementos conocidos como -12 y -24 dentro de la región promotora y de activadores transcripcionales tipo **EBP** (**E**nhancer **B**inding **P**rotein) para reconocer y activar sus genes blanco. PilR es un regulador tipo **EBP** y es miembro del sistema de dos componentes PilS/PilR. PilS es la cinasa detectora y PilR es el regulador de respuesta. Recientemente en *G. sulfurreducens*, describimos el mecanismo de regulación transcripcional de *pilA*, mediado por el sistema de dos componentes PilS/PilR. Encontramos que el regulador de respuesta PilR activa directamente la expresión de *pilA* al unirse en su región promotora; pero, a diferencia del mecanismo establecido para los sistemas de dos componentes, donde el regulador de respuesta fosforilado es la forma activa, en este sistema la forma no fosforilada de PilR es la que activa la transcripción de *pilA*[14].

Los activadores transcripcionales tipo **EBP** generalmente requieren de proteínas accesorias tipo **IHF** (**I**ntegration **H**ost **F**actor). Las proteínas **IHF** son nucleoproteínas tipo histonas que se unen al DNA en secuencias específicas donde promueven rearreglos en la estructura del DNA sitio especifica[15-17]. Las proteínas IHF son necesarias en la transcripción de genes regulados por σ^{54} y **EBP**, ya que usualmente las proteínas **EBP** se unen a secuencias de ADN río arriba del promotor dependiente de σ^{54} y por tanto es necesario la formación de una estructura secundaria o doblez en el DNA que permita la interacción de estos dos factores. La modificación de la estructura del DNA es inducida por la presencia de IHF y es un proceso que requiere energía[18]. La proteína IHF está constituida por dos subunidades (α y β); a pesar de que el heteródimero $\alpha\beta$ es la forma predominantemente activa, los homodímeros $\alpha\alpha$ y $\beta\beta$ podrían ser biológicamente activos. *G. sulfurreducens* posee 2 genes que codifican para la subunidad α (*ihf*α1 e *ihf*α2) y 2 genes que codifican para la subunidad β (*ih*β1 e *ihf*β2)[5]; sin embargo, en esta bacteria poco se conoce del mecanismo de regulación de IHF en la transcripción de sus gees blanco. Por lo tanto, el objetivo de este trabajo es determinar si el complejo IHF de *G. sulfurreducens* esta involucrado en la regulación

transcripcional del gen *pilA* y con ello en la participación en el mecanismo de transferencia extracelular de electrones.

MATERIALES Y MÉTODOS

Cepas y condiciones de cultivo. *Geobacter sulfurreducens* (PCA) y sus mutantes Δ*ihfA1*, Δ*ihfB1* y Δ*ihfB2*[19] fueron crecidas anaeróbicamente en medio NBAF, suplementado con acetato y fumarato. Para analizar la reducción de Fe(III) soluble e insoluble se usó medio citrato férrico y Iron Gel, suplementado con acetato y Fe(III). La cepa de *E. coli* ER fue crecida en medio LB con sus respectivos antibióticos.

Cuantificación de Fe(II). Para determinar la reducción de Fe(III) a Fe(II) se usó la técnica espectrofotométrica "Ferrozina". De los cultivos de *G. sulfurreducens* crecidas en citrato férrico y Iron Gel se tomaron 100 μL de muestra de cultivo a diferentes tiempos y se adicionó 900 μL de HCl 0.5 N. De la mezcla anterior, se tomaron 50 μL y se adicionó 2.45 mL de ferrozina (2 mM en 50 mM de HEPES), midiendo la absorbancia a 562 nm. Paralelamente se corrió una curva estándar de Fe(II).

Experimentos tipo "Western blot". Para los experimentos tipo "Western blot" se llevó a cabo la extracción de proteína total de *G. sulfurreducens* y sus mutantes crecidas en medio NBAF en fase exponencial. La extracción se llevó a cabo como sigue: las pastillas celulares fueron resuspendidas en 150 µl de "B-PER II Bacterial Protein extraction reagent" (Pierce) e incubadas por 15 min a temperatura ambiente. 1 µg de proteína total por muestra fue mezclada con buffer de carga y hervidas por 5 min, y separadas en una electroforesis SDS-PAGE al 15%. Después de la separación, las proteínas fueron transferidas a una membrana de nitrocelulosa usando un sistema semihúmedo (Hoefer SemiPhor). Para el análisis de inmunodetección, la membrana fue bloqueada con BSA al 3 % en buffer PBS por 12 h a 4°C seguido de la adición e incubación del primer anticuerpo anti-pilina preparado en una dilución 1/1,000 por 4 h. Después, la membrana fue lavada con buffer PBS 1X tres veces y se adicionó el segundo anticuerpo anti-conejo acoplado a la fosfatasa alcalina en una dilución 1/5,000, incubando la membrana por 3 h a temperatura ambiente. Finalmente, la pilina fue revelada con el reactivo 5-bromo-4-cloro-3-indolilfosfatasa "(BCIP)-Nitro Blue Tetrazolium" siguiendo las indicaciones del proveedor (Pierce).

Ensayos de retardo de la movilidad en gel. Fragmentos de la región regulatoria del gen *pilA* (F1-324, F2-204, F3-117) fueron amplificados a partir de ADN cromosomal de *G. sulfurreducens* por PCR con los oligonucleotidos "emsa1fw (AGCGGCGGTGTGAAAAG), emsa2rev (GTCTCCTTTCTTCTTTTTGCTG), pilASINfw (ATCGTCAGACACAAGTG) y emsa4rev (TAGCAAAAGCCGAACCAACT)" (Hernández-Eligio et al., 2016). Un fragmento que contiene parte de la región del gen *GSU303*, fue usado como control negativo en las reacciones de unión, y fue obtenido por PCR con los pares de oligonucleótidos IG_303F and IG_303R[14]. Los productos de PCR fueron purificados con el kit comercial "Purification PCR kit" (Roche). Las reacciones de unión fueron hechas mezclando 100 ng de cada fragmento de ADN con 100 ng del fragmento *GSU303* (control negativo) y diferentes concentraciones del complejo IHF, en un

volumen total de 20 µl de buffer de unión. El buffer de unión contiene: 40 mM HEPES, 8 mM $MgCl_2$, 50 mM KCl, 1 mM DTT, 0.05% Nonidet P-40 y 0.1 mg ml-1 BSA. Las reacciones de unión ADN-proteína fueron incubadas por 30 min a temperatura ambiente y separadas por electroforesis en geles de poliacrilamida nativos al 6% en 0.5X Tris-borato-EDTA buffer a temperatura ambiente. Los fragmentos de ADN fueron teñidos con bromuro de etidio y visualizados usando un fotodocumentador tipo "Gel Doc DZ imager" (Bio-rad).

Expresión y purificación del complejo IHF. Para expresar y purificar el complejo IHF, se uso el plásmido pET28-ihfβ1-ihfα1 previamente construido[19]. El plásmido pET28-ihfβ1-ihfα1 contiene los genes *ihfα*1 e *ihfβ*1 clonados en operón bajo el control del promotor lac y solo el gen *ihfβ*1 tiene clonada una secuencia que codifica para 6 histidinas. Dado que la proteína Ihfα1 interacciona con Ihfβ1, al purificar Ihfβ1 con etiqueta de histidinas, también copurifica Ihfα1. Por lo tanto, se indujo la expresión del complejo IHF (Ihfα1-Ihfβ1) en la cepa ER de *E. coli* por la adición de IPTG (0.1 mM). Después de 5 h de inducción, la purificación del complejo fue hecho a 4 °C bajo condiciones no desnaturalizantes usando la resina "Ni-nitrilotriacetic acid affinity chromatography" de Qiagen. El complejo purificado fue dializado contra un buffer (40 mM Tris-acetato pH 8.0, 4 mM $MgCl_2$ y 100 mM KCl) y concentrado usando el sistema de filtración "Ultracel 3K" de Amicon a 4 °C. El contenido de proteína fue estimado con el método de Bradford usando albúmina sérica de bovino como estándar (Biorad).

Reverso transcripción y PCR en tiempo real (RT-qPCR). Se extrajo ARN total de las cepas de *G. sulfurreducens* usando el "RNesasy Mini kit" (Qiagen) y su concentración fue estimada usando un NanoDrop 2000c. El ADN contaminante fue removido por la digestión con la enzima DNase I (RNase-free, Thermoscientific) acorde a las instrucciones del fabricante. La eliminación del ADN fue confirmada mediante una reacción de PCR usando una alícuota de ARN tratado con DNase I. Para la síntesis de ADNc se uso el kit "RevertAid H Minus First Strand cDNA Synthesis Kit" (Thermo scientific) y una mezcla específica de oligonucleótidos reversos (Andrade et al., 2016). El ADNc fue usado como molde para los ensayos de PCR en tiempo real.

Las reacciones de PCR en tiempo real se hicieron en un termociclador "Lightcycler II 480" (Roche) usando la mezcla "SYBR Green PCR Master Mix" (Themo scientific). Las condiciones de amplificación fueron las siguientes: 10 min a 95 °C, y un ciclo de dos pasos a 95 °C por 15 s y 60 °C por 60 s para un total de 40 ciclos. El tamaño de los amplicones fue de un rango de 100–120 pb. La concentración final de los oligonucleótidos fue de 2.5 pmol. Todas las reacciones de PCR en tiempo real fueron llevadas a cabo por triplicados de cada gen de cada cepa, obteniendo valores similares. Un control sin ADNc como control negativo fue incluido para cada gene. *recA* y *proC* fueron usados como controles internos para normalizar los resultados[19]. Para analizar los datos, se usó la técnica de cuantificación $2^{-\Delta,\Delta CT}$ [20]. La reproducibilidad del entero experimento fue confirmada por dos independientes repeticiones.

Análisis informático. Se utilizó el algoritmo "Virtual Footprinting" (http://www.prodoric.de/vfp/vfp_promoter.php) para localizar posibles sitios de unión de

IHF en la región promotora de *pilA*. El algoritmo usa la secuencia consenso de IHF para *E. coli*.

RESULTADOS Y DISCUSIÓN

Fenotipo de las cepas mutantes en el sistema IHF. *Geobacter sulfurreducens* tiene 4 genes que codifican para las diferentes subunidades del complejo IHF, 2 para la subunidad α (*ihfα*1 e *ihfα*2) y 2 para la subunidad β (*ihfβ*1 e *ihfβ*2). Los 4 genes están localizados en diferentes regiones del genoma, y sus proteínas presentan un alto grado de conservación. Ihfα1 e Ihfα2 de *G. sufurreducens* presentan 49 % y 47 % de identidad con Ihfα de *E. coli*, respectivamente; mientras que Ihfβ1 e ihfβ2 de *G. sulfurreducens* presentan 47 % y 48 % de identidad con Ihfβ de *E. coli*, respectivamente. Estudios previos de análisis de transcriptoma (comunicación personal), sugieren que bajo nuestras condiciones de cultivo (tanto en NBAF como en citrato férrico) solo los genes *ihfα*1, *ihfβ*1 e *ihfβ*2 tienen un buen nivel de expresión (comunicación personal); por tal razón, en este trabajo se descarto la caracterización de la mutante Δi*hfα*2. Un estudio reciente muestra que el complejo IHF esta involucrado en regular una gran cantidad de genes, incluyendo a varios citocromos tipo c (Andrade et al., 2016). Con la finalidad de observar si el complejo IHF está involucrado en los procesos de transferencia de electrones en *G. sulfurreducens*, se procedió a crecer a la cepa silvestre y mutantes Δ*ihfα1*, Δ*ihfβ1* e Δ*ihfβ2* con acetato como donador de electrones y diferentes aceptores de electrones. La **Figura 1** muestra el crecimiento de las cepas de *G. sulfurreducens* con acetato-fumarato (**Figura1a**), acetato-Fe(III) soluble (**Figura 1b**) y acetato-Fe(III) insoluble (**Figura 1c**).

Como se observa en la **Figura 1a** (línea negra con cuadros), la cepa silvestre de *G. sulfurreducens* presenta una curva de crecimiento clásica, con la fase lag en las primeras 6 horas, seguido de la fase exponencial hasta las 24 horas, continuando con la fase estacionaria hasta el final de la cinética. De manera interesante, observamos que las cepas Δ*ihfα*1 y Δ*ihfβ*2 presentan un retraso en el crecimiento en las primeras 42 horas de la cinética, alcanzando a la silvestre después de este tiempo; sin embargo, la cepa Δ*ihfβ*1 presenta un crecimiento similar a la cepa silvestre. En la **Figura 1b**, notamos que la cepa silvestre alcanza un máximo de reducción de Fe(III) a Fe(II) soluble (40 mM) en las primeras 36 horas de la cinética, manteniéndose estable hasta el final de la curva. Al igual que en la curva de crecimiento, las mutantes Δ*ihfα*1 y Δ*ihfβ*2 presentan una deficiencia en la reducción de Fe(III) a Fe(II), ya que la mutante Δ*ihfα*1 alcanza a reducir cantidades similares de Fe(III) que la silvestre hasta después de 60 horas, mientras que la mutante Δ*ihfβ*2 solo alcanza a reducir 10 mM de Fe(III) hasta el final de la cinética. La mutante Δ*ihfβ*1 presenta una cinética de reducción de Fe(III) soluble a Fe(II) similar a la silvestre. Finalmente, en la **Figura 1c** observamos, que la cepa silvestre alcanza un máximo de reducción de Fe(III) insoluble a Fe(II) hasta los 55 días de la cinética (22 mM de Fe(III) a Fe(II)); la mutante Δ*ihfβ*1 presenta una cinética de reducción similar a la cepa silvestre, mientras que la mutante Δ*ihfα*1 es deficiente en reducir Fe(III) insoluble, ya que solo alcanza a reducir 7.5 mM durante toda la cinética.

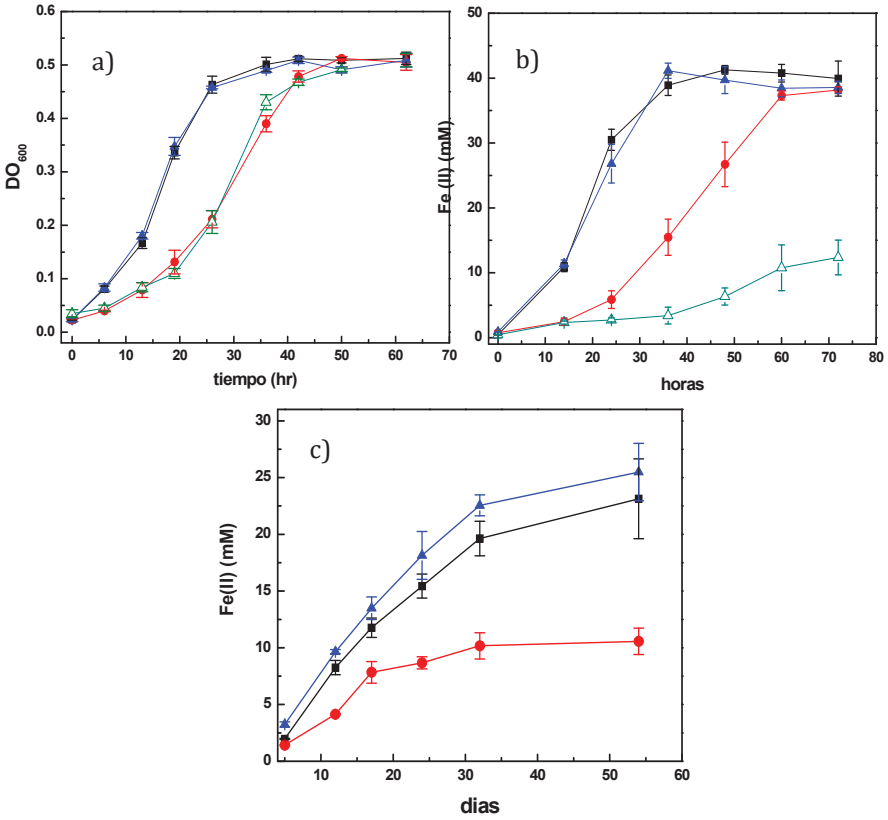


FIGURA 1. Fenotipo de las cepas de *G. sulfurreducens* con diferentes aceptores de electrones. 1a) Crecimiento con acetato-fumarato. 1b) Reducción de Fe(III) soluble a Fe(II). 1c) Reducción de Fe(III) insoluble a Fe(II). En las gráficas, la cepa silvestre corresponde a la línea negra con cuadros; Δ*ihfα*1 es línea roja con círculos; Δ*ihfβ*1 es línea azul con triángulos y Δ*ihfβ*2 es línea gris con triángulos vacíos.

La deficiencia en crecimiento y en la reducción de Fe(III) a Fe(II) en algunas de las mutantes *ihf*, sugiere que el producto de estos genes está participando en regular la transferencia de electrones de manera global. Las cepas Δ*ihfα*1 y Δ*ihfβ*2 presentan una deficiencia en el crecimiento acetato-fumarato, lo cual puede deberse a que en estas cepas se esta afectando el metabolismo de fumarato, ya sea a través de controlar el transporte de dicho aceptor de electrones o a las proteínas involucradas en la reducción de fumarato. De manera interesante, después de cierto tiempo de crecimiento, estas cepas, alcanzan un crecimiento similar a la silvestre, pudiendo deberse a que la falta de los genes *ihfα*1 e *ihfβ*2 es compensado con la expresión de las copias de estos genes (*ihfα*2 e *ihfβ*1). La deficiencia de reducción de Fe(III) soluble en las mutantes Δ*ihfα*1 y Δ*ihfβ*2 puede deberse a que IHF esta controlando la transcripción de genes que codifican a citocromos tipo-c relevantes en la transferencia de electrones a Fe(III) soluble; aunque el producto del gen *ihfβ*2 es importante para este proceso. Por último, la deficiencia en la reducción de Fe(III) insoluble en la mutante Δ*ihfα*1 puede deberse a que el producto de este gen controle la expresión de elementos importantes en la transferencia de electrones a óxidos metálicos o a electrodos como la producción de biopelículas conductivas o el pili.

IHF controla la producción de pilina a nivel transcripcional. Se ha reportado que el pili de *G. sulfurreducens* es un elemento importante en la reducción de metales como Fe(III), Mn(IV), U(VI) y en la generación de bioelectricidad[1,2,6]. Con la finalidad de investigar si algunas de las cepas mutantes en el complejo IHF son deficientes en la reducción de Fe(III) soluble e insoluble (**Figura 1b y 1c**) debido a la deficiencia de la producción de pili, se procedió a realizar un experimento tipo western blot para detectar a la proteína estructural PilA. La **Figura 2**, muestra el resultado de la inmunodetección de PilA en las distintas cepas de *G. sulfurreducens*.

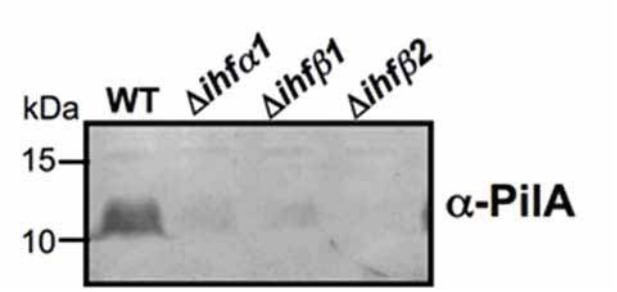


FIGURA 2. Inmunodetección de PilA en *G. sulfurreducens* y sus mutantes derivadas. WT significa cepa silvestre. Se muestra la posición de la proteína PilA.

Como se observa en la **Figura 2**, las cepas mutantes Δ*ihf* están alteradas en cuanto a producir pili, ya que todas presentan una drástica disminución de la proteína estructural PilA. De manera interesante, se observa que la mutante Δ*ihfβ2* es la más afectada en producir PilA, y aunque presenta un fenotipo mas drástico en cuanto a la reducción de Fe(III), el producto de los tres genes (*ihf*) están involucrados en el control de la producción de pili. Para saber si el complejo IHF de *G. sulfurreducens* controla la producción de PilA a nivel transcripcional, se procedió a cuantificar la expresión de su gen *pilA* por reverso transcripción y PCR en tiempo real en las diferentes mutantes (RT-qPCR). Las cepas fueron crecidas en medio NBAF (acetato-fumarato) y la extracción de ARN se llevo a cabo con las células cosechadas en fase exponencial. La **Figura 3**, muestra el resultado de la cuantificación.

En la **Figura 3**, se muestra que los niveles de expresión del gen *pilA* en las diferentes cepas mutantes Δ*ihf* están disminuidos drásticamente, semejante a lo observado en el experimento de inmunodetección. Lo anterior muestra que las proteínas del complejo IHF están controlando a nivel transcripcional la expresión de *pilA*, sugiriendo que los fenotipos en cuanto a la reducción de Fe(III) a Fe(II) pueden deberse principalmente a la ausencia del pili y a otras proteínas relevantes en la transferencia extracelular de electrones.

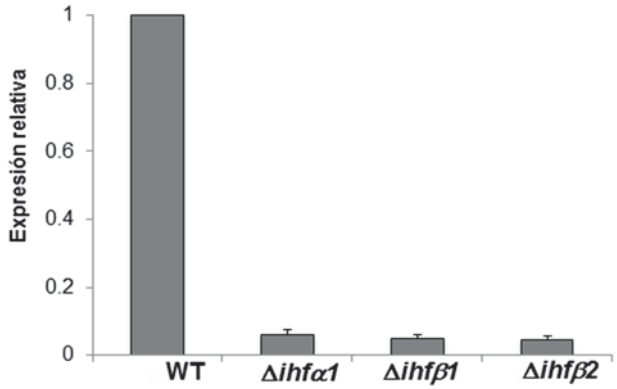


FIGURA 3. Expresión relativa del ARNm de *pilA* en las cepas de *G. sulfurreducens.* WT significa cepa silvestre, se muestran las barras de error. Para calcular los niveles de expresión, se usó los niveles de expresión de los genes *recA* y *proC* para normalizar los datos.

Búsqueda de sitios de unión IHF en la región promotora de pilA. En *E. coli*, ya se ha caracterizado el mecanismo de regulación del complejo IHF sobre varios de sus genes blanco[21-24]. Se conoce que IHF reconoce la secuencia consenso WATCARNNNNTTR (donde W es A o T, R es A o G y N puede ser A, T, G o C) en la región promotora y se une, formando una estructura secundaria tipo "loop". En un trabajo reciente, se demostró que en *Desulfovibrio vulgaris* -una bacteria relacionada filogenéticamente con *G. sulfurreducens*- el complejo IHF controla la transcripción del gen *orp* a través de unirse a dos secuencias consenso en la región promotora de dicho gen[17]. En ese trabajo, se observó que los sitios de unión de IHF en *D. vulgaris* están conservados con respecto a los sitios de unión de IHF en *E. coli*. Con la finalidad de localizar posibles sitios de unión de IHF en la región promotora de *pilA* de *G. sulfurreducens*, se analizó la región intergénica *pilR-pilA* con el algoritmo "Virtual Footprinting" que usa la secuencia consenso de IHF en *E. coli*. El análisis *in silico* resultó en la localización de 3 posibles sitios de unión a IHF en la región promotora de *pilA*. El primer sitio corresponde a la secuencia 5´-GTGTAACGTGCTG-3´ y esta localizado entre las posiciones -70 a -85, el segundo sitio tiene la secuencia 5´-GTTGAAGCGGTTG-3´ y esta localizado en las posiciones -87 a -102, y el tercer sitio comprende la secuencia 5´-GACGAAATAGGTG-3´, localizado en la posición -111 a -127. Los tres sitios están posicionados con respecto al codón de inicio de la traducción (**Figura 4**). Los tres posibles sitios están entre los sitios de unión del regulador PilR y el promotor dependiente de σ54 (**Figura 4**). Estos datos sugieren fuertemente que el gen *pilA* de *G. sulfurreducens* es regulado directamente a nivel transcripcional por el complejo IHF.

IHF se une de manera específica a la región promotora de pilA. Para demostrar que el complejo IHF de *G. sulfurreducens* regula de manera directa la transcripción del gen *pilA*, se procedió a llevar a cabo experimentos de interacción ADN-proteína. Para lo anterior, por un lado se amplificaron por PCR diferentes fragmentos de la región promotora de *pilA*, generando 3 fragmentos de diferente tamaño (**Figura 4**). El primer fragmento (F1 de 311 pb) comprende desde la región 3´ del gen *pilR*, hasta la región 5´ codificante de *pilA*. El fragmento 2 (F2 de 196 pb) comprende la región promotora de

pilA (región comprendida por las secuencias -24/-12 del promotor σ^{54} y los tres posibles sitios de unión de IHF), hasta la región 5´ codificante de *pilA*. El fragmento 3 (F3 de 109 pb) contiene los tres posibles sitios de unión a IHF (**Figura 4**). Por otro lado, se uso el plásmido pET28-ihfβ1-ihfα1 para expresar y purificar el complejo IHF de *G. sulfurreducens*.

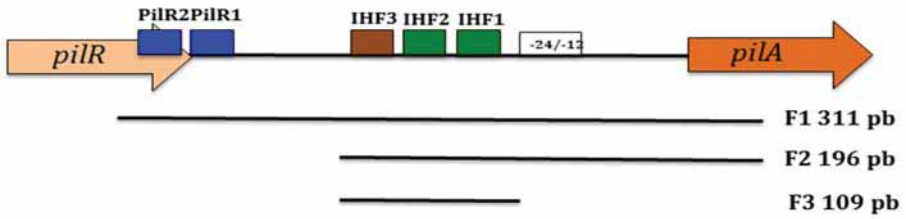


FIGURA 4. Representación esquemática de la región intergénica *pilR-pilA*. El recuadro blanco representa el promotor σ54 y las líneas negras muestran los tamaños de los fragmentos utilizados. Los cuadros sobre la línea muestran la posición de los sitios de unión a PilR y posibles sitios de unión a IHF.

Primero, determinamos si el complejo IHF se une a la región intergénica *pilR-pilA*; para esto, se usó el fragmento 1 (F1) y se mezcló con diferentes concentraciones del complejo IHF (40, 60, 80 y 100 nM) (**Figura 5a**).

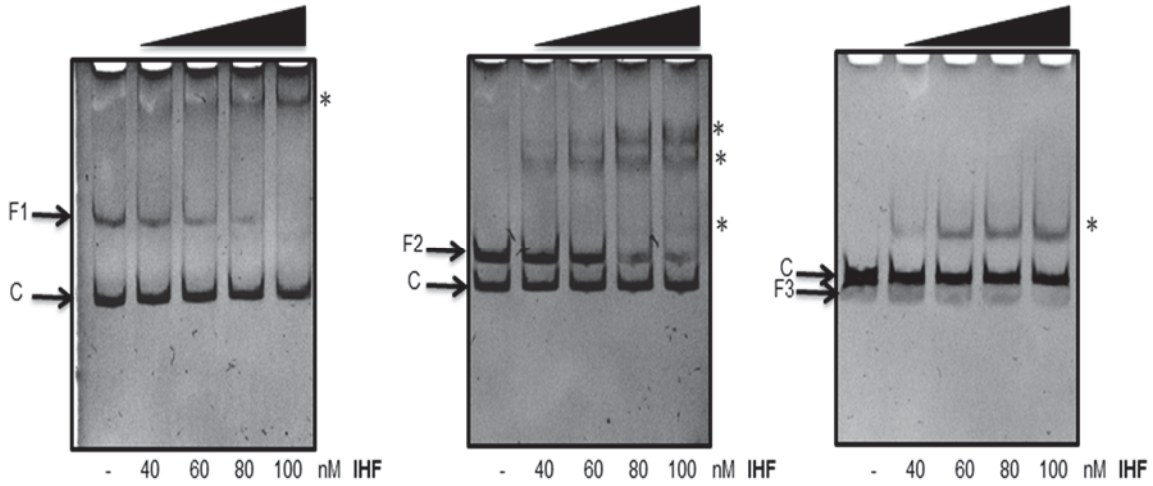


FIGURA 5. Ensayo de retardo de la movilidad en gel de la región promotora de *pilA*. En la parte inferior se muestra las cantidades de proteína utilizadas en la interacción y "-" significa sin proteína. Los asteriscos señalan los complejos ADN-proteína. Las flechas señalan la posición de los fragmentos libres. Se usó como control negativo ADN de la región intergénica *GSU303*. Se incubaron diferentes concentraciones de IHF con los fragmentos 1(a), 2(b) y 3(c).

Como se observa en la **Figura 5a**, el fragmento F1 retarda su migración en el gen. Este retardo en la migración es dependiente de la concentración del complejo IHF, ya que a mayor concentración del complejo IHF, mayor es el retardo en la movilidad. La unión

del complejo IHF a la región intergénica *pilR-pilA* es específica, ya que con el control negativo no retarda su migración en el gel (control). Para determinar si los 3 sitios de unión predichos en la región promotora de *pilA* son los reconocidos por IHF, se usaron los fragmentos F2 y F3 con concentraciones incrementadas del complejo IHF (**Figura 5b y 5c**). La figura 5b, muestra el resultado de la unión del fragmento 2 (F2) con el complejo IHF; la figura 5c muestra el resultado de la unión con el fragmento 3 (F3). Como se observa en la figura 5b y c, los 2 fragmentos usados en los experimentos de interacción (F2, F3) retardan su movilidad en el gel. El retardo en la movilidad de los fragmentos usados es dependiente de la concentración del complejo IHF, ya que a mayor concentración de IHF, mayor es el complejo retardado. La unión de IHF sobre el fragmento F3, sugiere que los sitios predichos con el algoritmo Virtual Footprinting son los sitios reconocidos de unión en la región promotora de *pilA*. Estos datos confirman que el complejo IHF regula de manera directa la transcripción del gen *pilA*.

CONCLUSIÓN

Con los resultados de este trabajo, proponemos el siguiente modelo de regulación, donde el complejo IHF participa en la activación transcripcional del gen *pilA*. El regulador de respuesta PilR (EBP) y la ARN polimerasa con el factor σ54 se unen a la región promotora de *pilA*; pero, para que exista una correcta activación de la transcripción, IHF se une entre el promotor y los sitios de unión de PilR. La unión de IHF en los sitios predichos, provoca la formación de una estructura secundaria en el ADN, favoreciendo la interacción entre PilR y la ARN polimerasa (σ54), activando la transcripción del gen *pilA*. Al transcribirse *pilA*, se produce pili, lo cual favorece la transferencia extracelular de electrones (**Figura 6**).

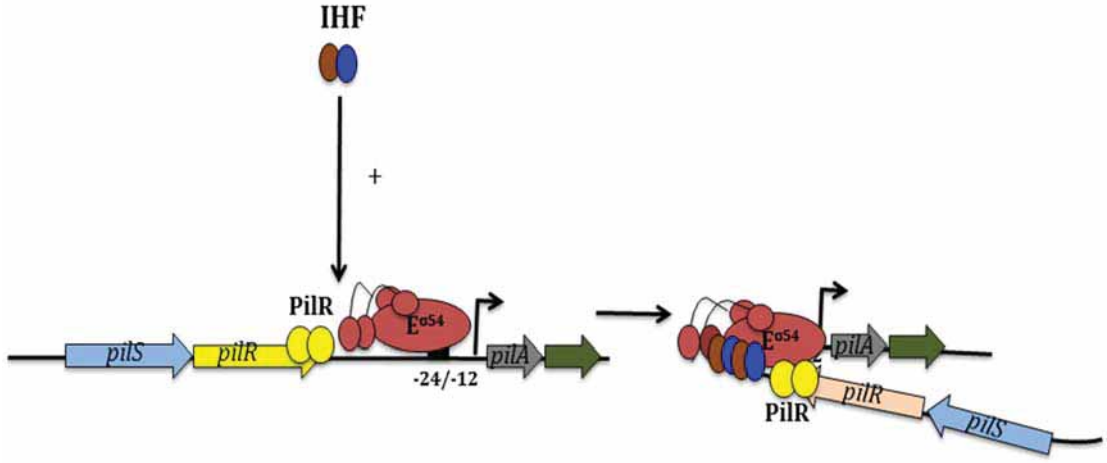


FIGURA 6. Modelo de regulación transcripcional del gen *pilA*, mediado por los reguladores PilR, σ54 e IHF en *Geobacter sulfurreducens*.

AGRADECIMIENTOS

Al CONACyT (CB-179684) por su financiamiento y a la “Cátedra 1433” otorgada al Dr. Hernández-Eligio.

REFERENCIAS

1. Lovley, D.R. (1997). Microbial Fe(III) reduction in subsurface environments. *FEMS Microbiol. Rev*. 20:305-315.
2. Lovley, D. (2006). Dissimilatory Fe (III)-and Mn (IV)-reducing prokaryotes. *Adv Microb Physiol*. 49:219-286.
3. Lovley, D. R., Ueki, T., Zhang, T., Malvankar, N. S., Shrestha, P. M., Flanagan, K. A., Aklujkar, M., Butler, J. E., Giloteaux, L., Rotaru, D. E. H., Franks, A. E., Orellana, R., Risso, C. and Nevin, K. P. (2011). *Geobacter*: the microbe electric’s physiology, ecology, and practical applications. *Adv Microb Physiol*. 59:1-100.
4. Coppi, M. V., Leang, C., Sandler, S. J. and Lovley, D. R. (2001). Development of a Genetic System for *Geobacter sulfurreducens*. *Appl Environ Microbiol.* 67(7):3180-3187.
5. Methe, B. A., Nelson, K. E., Eisen, J. A., Paulsen, I. T., Nelson, W., Heidelberg, J. F. and Fraser, C. M. (2003). Genome of *Geobacter sulfurreducens*: metal reduction in subsurface environments. *Science*. 302(5652):1967-1969.
6. Reguera, G., McCarthy, K. D., Mehta, T., Nicoll, J. S., Tuominen, M. T. and Lovley, D. R. (2005). Extracellular electron transfer via microbial nanowires. *Nature*. 435(7045):1098-1101.
7. Reguera, G., Nevin, K. P., Nicoll, J. S., Covalla, S. F., Woodard, T. L. and Lovley, D. R. (2006). Biofilm and nanowire production leads to increased current in *Geobacter sulfurreducens* fuel cells. *Appl Environ Microbiol.* 72(11):7345-7348.
8. Hobbs, M., Collie, E. S., Free, P. D., Livinston, S. P. and Mattick, J. S. (1993). PilS and PilR, a two-component transcripcional regulatory system controlling expression of type 4 fimbriae in *Pseudomonas aeruginosa*. *Mol Microbiol*. 7(5):669-682.
9. Ishimoto, K. S. and Lory, S. (1989). Formation of pilin in *Pseudomonas aeruginosa* requires the alternative sigma factor (RpoN) of RNA polymerase. *Proc Natl Acad Sci USA.* 86(6):1954-1957.
10. Ishimoto, K. S., Lory, S. (1992). Identification of pilR, wich encondes a transcripcional activator of the *Pseudomonas aeruginosa* pilin gene. *J Bacteriol.* 174:3514-3521.
11. Kehl-Fie, T. E., Porsch, E. A., Miller, S. E. and St Geme, J. W. (2009). Expression of *Kingella kingae* type IV pili is regulated by σ54, PilS, and PilR. *J. Bacteriol.* 191(15):4976-4986.
12. Mattick, J. S. (2002). Type IV pili and twitching motility. *Annu Rev Microbiol.* 56(1):289-314.
13. Wu, S. S. and Kaiser, D. (1997). Regulation of expression of the *pilA* gene in *Myxococcus xanthus*. *J Bacteriol*. 179(24):7748-7758.
14. Hernández-Eligio, A., Andrade, A., Soto, L., Morett, E. and Juárez, L. K. (2016). The un-phosphorylated form of the PilR two-component system regulates *pilA* gene expression in *Geobacter sulfurreducens*. *Environ Sci Pollut Res Int.* Feb.
15. Swinger, K. K. and Rice, P. A. (2004). IHF and HU: flexible architects of bent DNA. *Curr Opin Struct Biol.* 14(1):28-35.
16. Dorman, C. J. (2009). Nucleoid-associated proteins and bacterial physiology. *Adv Appl Microbiol.* 67:47-64.
17. Fiévet, A., Cascales, E., Valette, O., Dolla, A. and Aubert, C. (2014). IHF is required for the transcriptional regulation of the *Desulfovibrio vulgaris* Hildenborough orp operons. *PloS one.* 9(1): 86507.
18. Wigneshweraraj, S., Bose, D., Burrows, P. C., Joly, N., Schumacher, J., Rappas, M. and Buck, M. (2008). Modus operandi of the bacterial RNA polymerase containing the σ54 promoter-specificity factor. *Mol Microbiol*. 68(3):538-546.

19. Andrade Ángel, Hernández-Eligio J. A., Olvera M, Morett E., Juárez Katy. The IHF global regulator controls the electron transfers in *Geobacter sulfurreducens*. In preparation.
20. Livak, K. J. and Schmittgen, T. D. (2001). Analysis of relative genes expression data using real-time quantitative PCR and the 2(-Delta Delta C(T)) method. *Methods*. 25(4):402-408.
21. Werner, M. H.,Clore, G. M., Gronenborn, A. M. and Nash H. A. (1994). Symmetry and asymmetry in the fuction of Escherichia coli integration host factor: implications for target identification by DNA-binding proteins. *Curr Biol*. 4:447-487.
22. Zulianello, L., de la Gorgue de Rosny E., van Ulsen P., van de Putte, P. and Goosen, N. (1994). The himA and HimB subunits of integration host factor can specifically bind to DNA as homodimers. *EMBO J*. 13:1534-1540.
23. Zablewska, B. and Kur, J. (1995). Mutations in HU ans IHF affect bacteriophage T4 growth: HimD subunits of IHF appear to function as homodimers. *Gene*. 160:131-132.
24. Hiszczynska-Sawicka, E. and Ku, J. (1998). Effect of integration host factor of RNA II synthesis in replication of plasmid containing orip 15A. *Plas*

CHAPTER 1.3 BIOELETROSINTESIS CON PRODUCTOS DE VALOR AGREGADO Y SU INTEGRACION CON BIORREFINERIAS PARA EL SIGLO XXI

E. Hernández-Correa (1) and H. M. Poggi-Varaldo *(1)

(1) Environmental Biotechnology and Renewable Energies Group, Department of Biotechnology and Bioengineering, Centro de Investigación y Estudios Avanzados del IPN, P.O.Box 14-740, Ciudad de México D.F.,07000, México.

RESUMEN

La electrosíntesis microbiana (MES) es una nueva tecnología que requiere una fuente de energía eléctrica para la síntesis de compuestos químicos de valor agregado (CQVA), este proceso es realizado por biocatalizadores y puede ser acoplado a biorrefinerías.
Esta revisión presenta aspectos importantes y recientes (I) Celdas de electrolisis microbiana (MEC) y celdas de electrosíntesis (MES) para la producción química, (II) compuestos químicos de valor agregado, (III) consideraciones prácticas y metabólicas, (IV) Ruta eléctrica para la producción microbiana, (V) eficiencia energética y resistencia interna, (VI) nuevas aplicaciones y rendimiento de MES, (VII) Análisis de ciclo de vida (LCA) de las MES y (VIII) MES y biorrefinerías.
No existen muchos estudios que implementen una evaluación del rendimiento de las MES para determinar la eficiencia energética y el impacto ambiental, según a lo reportado en el presente trabajo, LCA es un método aceptado para determinar estos aspectos.
Aunque en los últimos años se han publicado algunos estudios, aún sigue faltando una investigación substancial en las MES para que pueden ser atractivas comercialmente. Las MES necesita superar grandes barreras como costos económicos, materiales de electrodos, membranas, microorganismos, etc. Hay pocos trabajos publicados en la producción de compuestos de valor agregado impulsados por energía eléctrica, se necesita un completo entendimiento del flujo de electrones entre el electrodo y el microorganismo a nivel molecular para desarrollar de una mejor manera las MES.

Palabras clave: análisis de ciclo de vida, biorrefinerías, celdas de electrosíntesis microbiana, compuestos de valor agregado.

INTRODUCCIÓN

***Sistemas bioelectroquímicos para la producción de compuestos químicos*.** Entre los sistemas bioelectroquímicos se encuentran las celdas de combustible microbiano y las celdas de electrólisis microbiana (MFC y MEC, por sus siglas en inglés, respectivamente), estos últimos a diferencia de MFC consumen energía eléctrica para

---

*Author for correspondence: r4cepe@yahoo.com

la producción de productos de valor agregado como H_2, metano, ácidos orgánicos, entre otros[1].

Sistemas de MEC para la producción de compuestos químicos. Las MEC son dispositivos a los que se les suministra un voltaje externo para la producción de H_2 en el cátodo, que es llevado a cabo mediante la reducción de protones[2]. La electrólisis del agua requiere un suministro de energía externo alrededor de 1.8 a 2 V, mientras que una MEC tan solo es necesario entre 0.6 a 1 V para la producción de H_2 [(3)]. Una celda de electrosíntesis típica se muestra en la **Figura 1**.

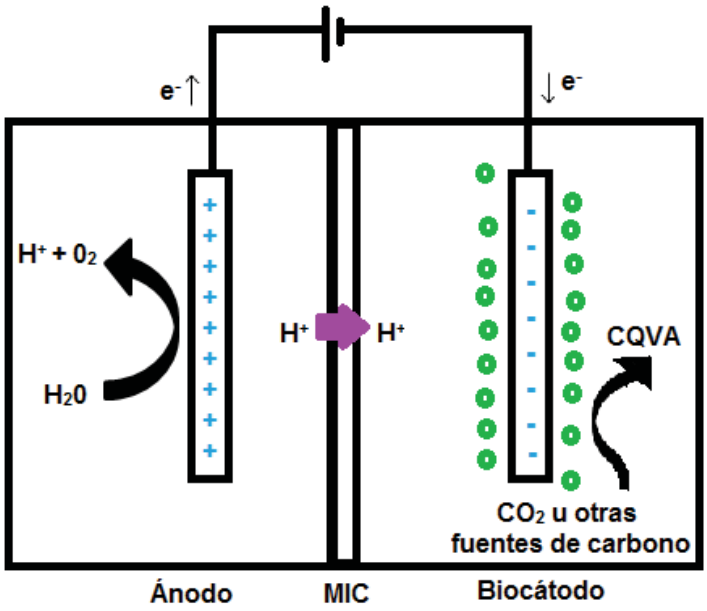


Figura 1. Celda de electrosíntesis típica

SISTEMAS BASADOS EN CELDAS DE ELECTRÓLISIS MICROBIANA PARA LA SÍNTESIS DE PRODUCTOS DE VALOR AGREGADO

Las celdas de electrosíntesis microbiana (MES, por sus siglas en inglés) son una nueva área de investigación, en la cual se busca la síntesis de compuestos químicos de valor agregado por medio de sistemas bioelectroquímicos en donde los microorganismos tienen la función de catalizadores, reduciendo el CO_2 a compuestos químicos de valor agregado, esta conversión del CO_2 es soportada por energía eléctrica[4].

Las MES proporcionan una vía para disminuir problemas como el calentamiento global al secuestrar el CO_2 atmosférico, el cual es materia prima para la producción de compuestos carbonados más elaborados. El potencial de las MES se multiplica al ser útiles para lidiar con problemas como el almacenamiento y cosecha de energía eléctrica en granjas solares, eólicas y exploraciones de gas natural, esto debido a que los microorganismos se encargan de fijar esta energía eléctrica en enlaces químicos carbono-carbono en los compuestos orgánicos producidos. Es especialmente importante en la energía solar ya que esta producción de energía eléctrica no siempre coincide con el pico de requerimiento de la demanda eléctrica [(5,6)].

Los estudios realizados en MES han sido intermitentes, dentro de los trabajos iniciales se ha demostrado la producción de succinato a partir de la reducción de fumarato en un reactor bioelectroquímico con un biocátodo dentro de la cámara catódica colonizada por *Actinobacillus succinogenes,* este proceso requiere la adición de mediadores como rojo neutro[7]; otro ejemplo es la utilización de electrones suministrado por el cátodo para la producción de acetato mediante la reducción de CO_2 por la biopelícula de *Sporomusa ovata*[8].

PRODUCCIÓN MICROBIANA DE PRODUCTOS DE VALOR AGREGADO IMPULSADA CON ELECTRICIDAD Y CO_2 Y OTRAS FUENTES DE CARBONO DE BAJO COSTO

Los compuestos orgánicos de valor agregado obtenidos mediante MES son producidos por microorganismos a partir de fuentes de carbono de bajo costo, principalmente CO_2 y esta síntesis es auxiliada por un suministro externo de energía eléctrica. Cuando la fuente de energía y carbono son el sol y el CO_2 respectivamente, se habla de una fotosíntesis artificial en donde los productos son compuestos orgánicos y oxígeno[9]. En la **Figura 2** se mencionan la ventajas y desventajas de esta reciente tecnología.

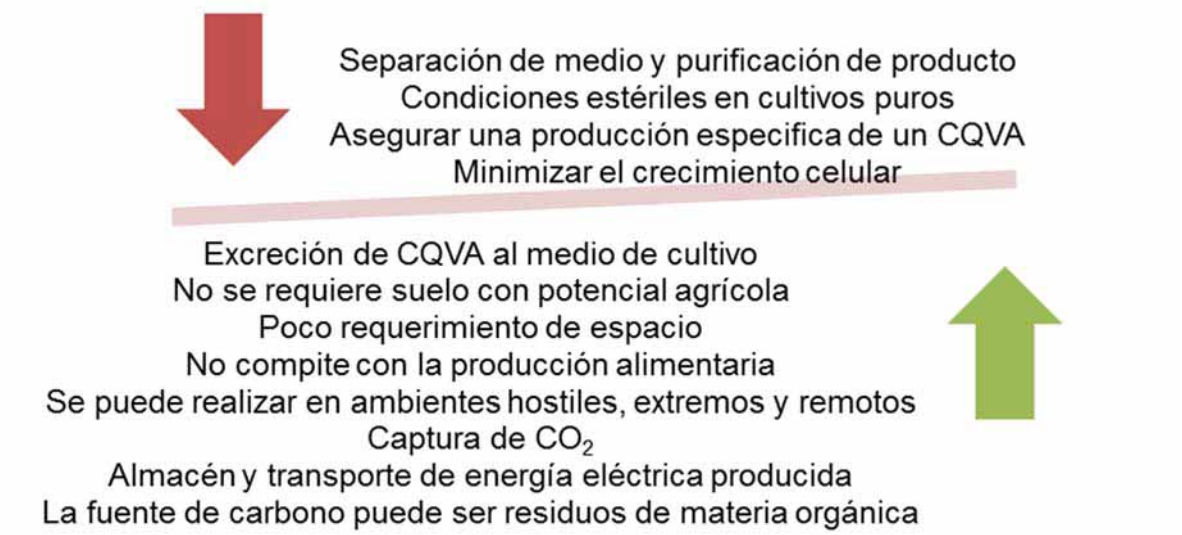


FIGURA 2. Tabla comparativa de la aplicación de celdas de electrosíntesis microbiana para la obtención de productos químicos de valor agregado ventajas y desventajas[9-11]

La biopelículas microbianas creciendo sobre el electrodo aceptan directamente los electrones provenientes del electrodo para llevar a cabo la reducción de CO_2 y la síntesis de productos de valor agregado estos últimos son excretados al medio[12]. Es importante reducir costos en el uso de MES, un importante factor es el material con el que se construye el electrodo, en el material empleado se ha utilizado carbono, grafito y acero inoxidable.

Flujo de electrones entre el cátodo y el microorganismo. Existen diferentes vías en que los microorganismos pueden aprovechar el flujo de electrones para la producción de productos de valor agregado, así como su crecimiento y el mantenimiento celular.

Los electrodos pueden transferir los electrones de manera directa o indirecta hacia los microorganismos, como lo reportan con bastante profundidad Rabaey y Rozendal (2010)[4]; sin embargo, esta relación electrodo-microorganismo es mucho mejor entendida en sistemas bioelectroquímicos con bioánodos a diferencia de los sistemas con biocátodos[13].

Transferencia indirecta de electrones por mediadores. En la transferencia de electrones indirecta se utilizan mediadores, como rojo neutro, aceptando electrones del cátodo y posteriormente donarlos a acarreadores de electrones en la célula, con las implicaciones que con lleva, como incrementar el costo del proceso, la toxicidad, la contaminación del producto[9].

Compuestos donadores de electrones. Es factible producir electroquímicamente compuestos como H_2, formato, amoniaco, sulfuro o Fe(II), los cuales pueden ser utilizados en el mantenimiento y crecimiento celular, así como en la producción de compuestos químicos de valor agregado[7,10,14,15]. El H_2 y el formato poseen el potencial redox lo suficientemente bajo para poder ser utilizados en la reducción del CO_2 a compuestos carbonados más elaborados[9].

Transferencia directa de electrones. Existen organismos capaces de tomar los electrones directamente del cátodo, estos organismos forman una biopelícula donde el soporte es el electrodo, ya sea ánodo o cátodo, este ultimo de gran importancia para el presente trabajo[8]. Las biopelículas agregadas en el electrodo enfrentan problemas típicos como limitaciones en la difusión externa e interna de nutrientes, CO_2, o altas concentraciones de productos inhibitorios en la capa más interna de la biopelícula, sin olvidar las ventajas del uso de biopelículas como la alta resistencia y estabilidad celular[3,11].

Se han descrito para algunos microorganismos como *Geobacter sulfurreducens* y *Shewanella oneidensis* una serie de complejos de la membrana externa y el espacio periplasmico que participan en la transferencia de electrones. Se ha propuesto que dicho fenómeno es ayudado por estructuras parecidas a pilis o apéndices membranales parecidos a pilus[4,16-18].

Microorganismos electrosíntetizadores de compuestos orgánicos de valor agregado. Se han publicado diversos trabajos acerca de microorganismos que impulsados por una corriente eléctrica con capaces de producir compuestos químicos de valor agregado, entre estos organismos se encuentran los metanogénicos a los cuales se les ha propuesto que podrían llevar una transferencia de electrones directa[19,20]. Las bacterias acetogenicas producen compuestos orgánicos de valor agregado mediante la ruta Wood-Ljungdahl y un suministro de H_2 y CO_2 en ambientes naturales[21]. Se han reportado trabajos donde se ha manipulado genéticamente a microorganismos del genero *Clostridium* para dirigir el metabolismo hacia el incremento en la producción de algún compuesto químico, como lo mencionan Lovley y Nevin de manera más detallada (2013)[9].

METABOLISMO HÍBRIDO Y CONSIDERACIONES PRÁCTICAS

Las fermentaciones podrían ser complementadas con un suministro de energía eléctrica, es decir una fermentación basada en heterotrofia auxiliada por una corriente eléctrica, lo cual incrementaría el poder reductor[7,22]. Rabaey *et al*. (2011)[11] realizan una comparación teórica entre fuentes de carbono para alimentar el sistema electroquímico evaluando CO_2 vs sustrato orgánico. La tabla 2 muestra algunos de los productos de valor agregado obtenidos por electrosíntesis, estos productos han sido hasta el momento de principal interés para la producción en MES; sin embargo, conforme avance la investigación en este campo la lista será más diversa.

TABLA 2. Tabla comparativa de los principales productos que se sintetizan en celdas de electro síntesis microbiana

Organismo	Producto	Tipo de transferencia de electrones	Sustrato	Producción*	Referencia
Actinobacillus succinogenes	Ácido succínico	Indirecta (Rojo neutro)	Hidrolizado de olote	0.256	Park *et al*., 2015[7]
Actinobacillus succinogenes	Ácido succínico	Indirecta (Rojo neutro)	Glucosa	0.523	Park *et al*., 2015[7]
Acetobacterium spp.	Acetato	Directa	CO_2	175 mM (10.5 gL^{-1})/20 d	Marshall *et al.*, 2013[18]
Sporomusa ovata	Acetato	Directa	CO_2		
Clostridium carboxidivorans y *C. ragsdalei*	Butirato	Directa	CO_2	15 mM (2.4 gL^{-1})/19 d	Ganigué *et al*., 2015[27]
Mixto	Etanol		Acetato	13.5 mM (0.62 g/L^{-1})/d	Steinbusch *et al*., 2009[28]

* Rendimiento ($g_{Prod.}/g_{Sustr.}$) y acumulación cuando la fuente de carbono es CO_2 en mM.

La producción de compuestos de valor agregado por microorganismos, incluyendo la MES, enfrentan una producción concominante, en donde además del compuesto químico de interés, se producen otros productos, por ejemplo en la producción de ácido succínico por *A. succinogenes* se genera además ácido acético; por lo cual se requiere la integración de un proceso de separación y purificación del producto[7,13]; otra manera de atacar este fenómeno es recurrir a la manipulación genética, donde se hacen cambios genéticos que favorecen el flujo metabólico hacia la producción del compuesto químico objetivo.

EFICIENCIA ENERGÉTICA Y RESISTENCIA INTERNA

Para que las MES se vuelva una tecnología aplicable se requiere que el valor de la producción obtenida del compuesto químico de valor agregado sea mayor al costo invertido en el proceso. Para lograr lo anterior es necesario minimizar costos y maximizar beneficios. Para lo cual es importante conocer parámetros de la MES como la eficiencia energética y la densidad de corriente eléctrica depende de la resistencia interna del sistema.

La eficiencia energética es un parámetro importante que refleja la energía suministrada al sistema (ya sea térmica, eléctrica o mecánica) y cuanta de esta energía es recuperada en el producto. La eficiencia energética depende de la eficiencia voltaica y la eficiencia coulómbica de la reacción en ambos electrodos, catódico y anódico[23]. La eficiencia coulómbica nos indica cuantos de los electrones suministrados al sistema mediante energía eléctrica y/o sustrato terminan en el producto.

La eficiencia voltaica (η) se define para una MEC como:

$$\eta = \frac{-E_{emf}}{-E_{app}} \qquad (1)$$

Dónde: E_{app} es el voltaje aplicado y Eemf es el voltaje termodinamico determinado por las reacciones de ambos electrodos a un mismo pH, esta eficiencia voltaica tendrá un valor negativo debido a la energía eléctrica suministrada para que la reacción en el cátodo tenga lugar[24].

Una MEC no se encuentra limitada para alcanzar la densidad de corriente máxima debido a la resistencia interna; es decir, el suministro de energía externa se puede incrementar hasta superar las barreras termodinámicas del sistema, sin embargo una alta resistencia interna en las MEC incluyendo las MES afectaría la eficiencia energética, ya que se requeriría un mayor suministro externo de energía para superar la alta resistencia interna del sistema[24].

ANÁLISIS DE CICLO DE VIDA EN CELDAS DE ELECTROSÍNTESIS MICROBIANA

El análisis de ciclo de vida (LCA, por sus siglas en inglés) es un método que permite determinar las consecuencias ambientales de un producto en particular, sobre todo en las nuevas tecnologías enfocadas a la producción bioenergía y la captura de CO_2, revelando los impactos ambientales negativos del proceso de producción completo y el verdadero potencial del producto sujeto a evaluación[13].

El implementar el LCA en las MES nos dará una idea de los beneficios y costos ambientales de la producción de compuestos químicos de valor agregado. Sin embargo, los principales impactos negativos en el ambiente de esta tecnología será el consumo de energía eléctrica, el transporte y manejo de las fuentes de sustrato, la adición de mediadores al medio de cultivo y la construcción de la celda electroquímica y el cultivos puros la necesidad de esterilizar el sustrato, los impactos ambientales positivos que presentan principalmente es dependiendo de la fuente de carbono la captura de CO_2 o la utilización de residuos orgánicos.

La factibilidad de producir un compuesto químico de valor agregado mediante un sistema bioelectroquímico dependerá del producto químico deseado, del organismo empleado y del diseño ingenieril del bioreactor, así como las condiciones del cultivo. Para una fermentación híbrida se podrían adaptar a los fermentadores actuales un bypass electroquímico que proporcione al fermentador una vía de poder reductor[11].

MES Y BIORREFINERÍAS

Una biorrefinería es una instalación con una conversión integrada, eficiente y flexible de biomasa renovable hacia múltiples productos de valor agregado, a través de una combinación de procesos físicos, químicos, bioquímicos y termoquímicos[25]. Las biorrefinerías y las MES se pueden integrar, las biorrefinerías generan desechos que son contaminantes descargados al ambiente, estos desechos pueden ser el sustrato de las MES y generar compuestos de valor agregado[26].

CONCLUSIÓN Y PERSPECTIVAS

Existen muy pocas publicaciones en este tema, se requiere más investigación para poder mitigar las incertidumbres acerca de la escalabilidad o comerciabilidad de esta nueva tecnología

Es necesario realizar más investigación en este campo para saber si es factible superar la producción de productos de valor agregado mediante producciones soportadas por energía eléctrica vs fermentaciones tradicionales o petroquímicas.

La MES tienen un gran potencial, sin duda esta tecnología se convertirá en el futuro, en uno de los procesos primarios para la producción de compuestos químicos de valor agregado; sin embargo, esta visión es poco realista y es necesario realizar más investigación para una aplicación práctica. La constante búsqueda de materiales cada vez más baratos y microorganismos más aptos desembocará en la implementación de una tecnología avanzada.

REFERENCIAS

1. Foley J.M., Rozendal R.A., Hertle C.K. Lant P.A. & Rabaey K. (2010) Life Cycle Assessment of High-Rate Anaerobic Treatment, Microbial Fuel Cells, and Microbial Electrolysis Cells. *Environ. Sci. & Technol.* 44(9):3629-3637.
2. Rozendal R.A., Hamelers H.V.M., Euverink G.J.W., Metz S.J. & Buismana C.J.N. (2006) Principle and perspectives of hydrogen production through biocatalyzed electrolysis. Int J Hydrogen Energy 2006;31:1632–40.
3. Logan B.E., Call D., Cheng S., Hamelers H.V.M., Sleutels T.H.J.A., Jeremiasse A.W. & Rozendal R.A. (2008). Microbial electrolysis cells for high yield hydrogen gas production from organic matter. Environ Sci Technol 2008;42:8630–40
4. Rabaey K. & Rozendal R.A. (2010). Microbial electrosynthesis—revisiting the electrical route for microbial production. Nature Reviews Microbiology, 8(10), 706-716
5. Lewis N.S., & Nocera D.G. (2006). Powering the planet: Chemical challenges in solar energy utilization. *Proceedings of the National Academy of Sciences*, *103*(43), 15729-15735.
6. Nevin K.P., Hensley S.A., Franks A.E., Summers Z. M., Ou J., Woodard T. L., Snoeyenbos-West O.L. & Lovley D. R. (2011). Electrosynthesis of organic compounds from carbon dioxide is catalyzed by a diversity of acetogenic microorganisms. *Applied and environmental microbiology*, *77*(9), 2882-2886.

7. Park D.H., Laivenieks M., Guettler M.V., Jain M.K., & Zeikus J.G. (1999). Microbial utilization of electrically reduced neutral red as the sole electron donor for growth and metabolite production. *Applied and environmental microbiology*, *65*(7), 2912-2917.
8. Nevin K.P., Woodard T.L., Franks A.E., Summers Z.M., & Lovley, D.R. (2010). Microbial electrosynthesis: feeding microbes electricity to convert carbon dioxide and water to multicarbon extracellular organic compounds. *MBio*, *1*(2), e00103-10.
9. Lovley D.R., & Nevin K.P. (2013). Electrobiocommodities: powering microbial production of fuels and commodity chemicals from carbon dioxide with electricity. *Current opinion in biotechnology*, *24*(3), 385-390.
10. Hawkins A.S., Han Y., Lian H., Loder A.J., Menon A.L., Iwuchukwu I.J., Keller M., Leuko T.T., Adams M.W.W. & Kelly R.M. (2011) Extremely thermophilic routes to microbial electrofuels. ACS Catal, 1:1043-1050.
11. Rabaey, K., Girguis, P., & Nielsen, L.K. (2011). Metabolic and practical considerations on microbial electrosynthesis. *Current opinion in biotechnology*, *22*(3), 371-377
12. Blankenship R.E., Tiede D.M., Barber J., Brudvig G.W., Fleming G., Ghirardi M., Gunner M.R., Junger W., Kramer D.M. Melis A., Moore T.A. Moser C.C., Nocera D.G., Nozik A.J., Ort D.R. Parson W.W. Prince R.C. & Sayre R.T. (2011). Comparing photosynthetic and photovoltaic efficiencies and recognizing the potential for improvement. *science*, *332*(6031), 805-809.
13. Sharma M., Bajracharya S., Gildemyn S., Patil S.A., Alvarez-Gallego Y., Pant D., Rabaey K. & Dominguez-Benetton, X. (2014). A critical revisit of the key parameters used to describe microbial electrochemical systems. *Electrochimica Acta*, *140*, 191-208.
14. Khunjar W.O., Sahin A., West A.C., Chandran K. & Banta S. (2012). Biomass production from electricity using ammonia as an electron carrier in a reverse microbial fuel cell. PLoS ONE. 7:e44846.
15. Li H., Opgenorth P.H., Wernick D.G., Rogers S., Wu T-Y, Higashide W., Malati P., Hou Y-X, Cho K.M. & Liao J.C. (2012) Integrated electromicrobiological conversion of CO2 to higher alcohols. Science, 335:1596.
16. Holmes D. E., Chaudhuri S. K., Nevin K. P., Mehta T., Methé B. A., Liu A., Ward J.E., Woodard T.L., Webster J. & Lovley D. R. (2006). Microarray and genetic analysis of electron transfer to electrodes in Geobacter sulfurreducens. *Environmental Microbiology*, *8*(10), 1805-1815.
17. Reguera G., McCarthy K. D., Mehta T., Nicoll J. S., Tuominen M. T., & Lovley, D. R. (2005). Extracellular electron transfer via microbial nanowires. *Nature*, *435*(7045), 1098-1101.
18. Hartshorne R.S., Reardon C.L., Ross D., Nuester J., Clarke T.A., Gates A.J., Mills P.C., Fredrickson J.K., Zachara J.M., Shi L., Beliaev A.S., Marshall M.J., Tien M., Brantley S., Butt J.N. & Richardson D.J. (2010) Characterization of an electron conduit between bacteria and the extracellular environment. *Proceedings of the National Academy of Sciences*, *106*(52), 22169-22174.
19. Morita M., Malvankar N.S., Franks A.E., Summers Z.M., Giloteaux L., Rotaru A.E. & Lovley D.R. (2011). Potential for direct interspecies electron transfer in methanogenic wastewater digester aggregates. *MBio*, *2*(4), e00159-11.
20. Kato S., Hashimoto K. & Watanabe K. (2012). Methanogenesis facilitated by electric syntrophy via (semi) conductive iron-oxide minerals. *Environmental microbiology*, *14*(7), 1646-1654.
21. Fast A.G. & Papoutsakis E.T. (2012). Stoichiometric and energetic analyses of non-photosynthetic CO 2-fixation pathways to support synthetic biology strategies for production of fuels and chemicals. *Current Opinion in Chemical Engineering*, *1*(4), 380-395.
22. Hongo M., & Iwahara M. (1979). Application of electro-energizing method to L-glutamic acid fermentation. *Agricultural and Biological Chemistry*, *43*(10), 2075-2081.
23. Hamelers H. V. M., Sleutels T.H.J.A., Jeremiasse A.W., Post J.W., Strik D.P.B.T.B. & Rozendal R.A. (2009) in Bioelectrochemical Systems: From Extracellular Electron Transfer to Biotechnological Application (Eds.: K. Rabaey, L. T. Angenent, U. Schrçder, J. Keller), IWA Publishing, London.
24. Sleutels, T. H., Ter Heijne, A., Buisman, C. J., & Hamelers, H. V. (2012). Bioelectrochemical systems: an outlook for practical applications. *ChemSusChem*, *5*(6), 1012-1019.
25. Sadhukhan, J., Ng, K. S., & Hernandez, E. M. (2014). Biorefineries and chemical processes: design, integration and sustainability analysis. John Wiley & Sons.

26. Sadhukhan, J., Lloyd, J. R., Scott, K., Premier, G. C., Eileen, H. Y., Curtis, T., & Head, I. M. (2016). A critical review of integration analysis of microbial electrosynthesis (MES) systems with waste biorefineries for the production of biofuel and chemical from reuse of CO 2. *Renewable and Sustainable Energy Reviews*, *56*, 116-132.
27. Ganigué, R., Puig, S., Batlle-Vilanova, P., Balaguer, M. D., & Colprim, J. (2015). Microbial electrosynthesis of butyrate from carbon dioxide. *Chemical Communications*, *51*(15), 3235-3238.
28. Steinbusch, K. J., Hamelers, H. V., Schaap, J. D., Kampman, C., & Buisman, C. J. (2009). Bioelectrochemical ethanol production through mediated acetate reduction by mixed cultures. *Environmental science & technology*, *44*(1), 513-517.

CHAPTER 1.4 SERIES DARK AND PHOTOHETEROTROPHIC FERMENTATION OF CHEESE WHEY

K.M. Muñoz Páez (1) and H.M. Poggi-Varaldo *(1)

(1) Department of Biotechnology and Bioengineering, Environmental Biotechnology and Renewable Energies Group, GBAER-EBRE, Centro de Investigación y Estudios Avanzados del IPN, P.O.BOX 14-740, Ciudad de México D.F., 07000, México

ABSTRACT

The dairy industry in Mexico produces several wastes that need to be treated in order to avoid pollution and comply with environmental regulations. One of these wastes is cheese whey (CW), which is originated by the milk coagulation in cheese manufacturing, and still contains around 80-90 % of the milk volume. The use of CW as substrate for biohydrogen production could help both to achieve an appropriate waste management and mitigate the actual energy crisis. In the biological hydrogen production from wastes, most of the studies were performed at temperatures in the mesophilic and thermophilic ranges. The H_2 production at ambient temperature could be interesting too, because it could help to reduce the energy expenditures (heating feedstock and reactors, among others). On the other hand, one tendency is the use of two H_2 production processes, such as dark (DF) and photoheterotrophic fermentation (PF) in order to obtain H_2 higher yields. Therefore, the main objectives of this work were (i) to evaluate H_2 production by dark fermentation using CW as substrate at ambient temperature, and (ii) to assess the PF of the dark fermentation effluents of CW. The DF was carried out in fluidized bed reactors using activated carbon as support. The reactors were operated at a hydraulic retention time of 1 day with an organic volumetric loading rates of 10 g CW/ L*day. The PF was carried out in batch reactors of 40 mL of operational volume, incubated at 32ºC and a light intensity of 3 klux. Either, it was used a mixed culture or *Rhodopseudomonas palustris* as inocula. PF reactors were fed with fermented CW from DF.

There was used sucrose as substrate for reactors start up, when the substrate was changed to CW de H_2 production diminished almost 10 fold. One alternative was the use of NaCl in order to reduce the effect of the lactic acid bacteriocin, increasing the H_2 yield almost 3 times, up to 1.4 mmol H_2/gTS. The H_2 production at ambient temperature was in the middle range of other studies using mesophilic and thermophilic temperature.

In the photoheterotrophic batch studies, when cultures of *Rhodopseudomonas palustris* were fed with fermented CW the cumulative H_2 production 4.7 mmol H_2/L_{LF}*day was nearly 22-fold of that with the mixed culture.

The H_2 production of cheese whey at ambient temperature showed results in the middle range of other studies at higher temperature and the PF of the effluents of DF of CW allowed to obtain two-fold the H_2 yield of that with only DF.

Keywords: biohydrogen, cheese whey, dark fermentation, photoheterotrophic fermentation.

---

*Author for correspondence: r4cepe@yahoo.com

INTRODUCTION

Cheese whey (CW) is one of the most important wastes of the dairy industry[1]. It consists of the milk nutrients that were not integrated during the casein coagulation, and could represents the 85-95 % of the milk volume[2-3]. The CW composition depends of several factors: *(i)* milk origin; *(ii)* milk quality; *(iii)* type of cheese manufacturing process; *(iv)* amount of yeast or acid used; and *(v)* type of cheese produced[4-5]. An average composition could be: 45-85 % lactose, 6-8 % protein, 5.6-8 % ash, 8.7 (g/kg) calcium; 23.5 (g/kg) potassium; 5.7 (g/kg) sodium; >50 % NaCl and KCl mineral salts; also urea, uric acid and B vitamins, among others[1, 3, 6-8].

The treatment of this wastewater (anaerobically) could be difficult due to the high content of organic matter (COD 70 g/L); low bicarbonate alkalinity (2.5 kg/m^3 as $CaCO_3$) and its tendency to be quickly acidified[2, 9-10]. So, it is necessary to find other ways to manage this waste. The use of CW to produce another products could help the management problem and is one step closer to the sustainability goal. There are several ways to re-use the CW, some of them are: *(i)* beverages with nutritive value; *(ii)* biofilms; and *(iii)* as culture medium for the enzyme, biomass, metabolites and biofuels production[4,10].

One of the biofuels that is considered competitive is biohydrogen[11]. It may be produced by biological fermentative processes such as dark fermentation and photoheterotrophic fermentation. The dark fermentation is a process light independent, where facultative and strict anaerobic bacteria transform complex substrates into H_2 and other products such as organic acids and alcohols[11]. The photoheterotrophic fermentation is the conversion, by the purple non sulfur bacteria (PNSB), of an organic substrate (such as organic acids) in H_2 and CO_2 [12].

As could be seen, there are the possibility to join two or more biological processes in order to improve the H_2 gain. For example, the dark fermentation effluents, rich on organic acids, could be used as fotoheterotrophic fermentation substrate[12-17]. The incubation/operation temperature is an important factor due to could affect: *(i)* metabolic activity of the microorganisms; *(ii)* growth rate; and *(iii)* substrate degradation[18-19]. The selection of the temperature may contemplate that the necessary energy to maintain temperatures in the mesophilic and thermophilic range could reduce the net gain of energy[20]. The H_2 production at ambient temperature is an interesting option. Therefore, the main objective of this work, was to evaluate the H_2 production using a dark fermentation-photoheterotrophic process at ambient temperature.

MATERIALS AND METHODS

Experimental design. The experimental design evaluate the H_2 production obtained with *Rhodopseudomonas palustris* and a mixed culture using fermented liquor (FL) of Cheese Whwy dark fermentation directly and with a dilution (1:2). Pfennig medium was used as control. The main response variables were: PH (mmol H_2/L, acids and solvents concentration (mg COD/L).

Dark fermentation. The dark fermentation was carried out in a fluidized bed bioreactor (FBR). The FBR consisted of a glass column with 3 L capacity. The medium support (1 L) was granular activated carbon (1-2 mm diameter). The reactor was incubated at ambient temperature (room without control temperature; average temperature 25°C). The hydraulic residence time (HRT) was 1 day on fluidized bed volume basis[21].

Photoheterotrophic fermentation. Glass vials of 60 mL were used as reactors with an operational volumen of 40 mL. The reactors were incubated at 32 °C and 3 klx. The inoculum (*Rhodopseudomonas palustris* or mixed culture) was added at 10 % (v/v) of the operational volume. The effluent of the dark fermentation of Cheese Whey (fermented liquor) was used as substrate. The liquid phase was operated in batch mode, whereas the gas phase in an intermittent mode: after the maximum production was detected, the reactor was flushed with argon and then, incubated again without inoculum or substrate[22].

Analyses. The H_2 and CH_4 concentration in biogas were determined in a Gow-Mac chromatograph (model 350), with a thermal conductivity detector and Molecular Sieve 5A packed column. The temperatures were: injector (25 °C), detector (100 °C) and column temperatures (25 ºC). The carrier gas used was Argon (21). The acids and solvents concentration were determined in the effluents after filtration through a glass-membrane filter in a chromatography Varian Star 3400 equipped with a flame ionization detector and a 50 m x 0.32 mm internal diameter fused silica capillary column coated with 0.2 mm CP-Wax 57 CB. The injector and detector temperatures were set at 250 ºC with N_2 as a carrier gas with a 20 mL/min flow rate. The oven temperature was programmed as follows: 60 ºC for 2 min, increasing to 140 ºC at 5 ºC/min, and then kept constant at 140 ºC for another 6 min.

RESULTS AND DISCUSSION

Initially, sucrose was used as substrate for reactors start up. After that, the substrate was changed to CW and it was observed a decrease of the H_2 production (almost 10-fold, **Table 1**). It was detected lactic acid in the effluent (data not shown), this could indicate the presence of lactic acid bacteria, and its presence is related with a loss of biohydrogen[23-24], as a combination of: hexoses are fermented to lactic acid and/or inhibitory effects of LAB on H_2-producing bacteria due to bacteriocins[23, 25]. One alternative was the NaCl addition (1 g/L) in the influent to reduce the effect of the lactic acid bacteriocin. The H_2 yield increase almost 3 times, up to 14 mmol H_2/L*day**.**

The effluent of the fermentation of CW without NaCL (fermented liquor, FL) was used for the photoheterotrophic fermentation in order to increase the H_2 production obtained. Pfennig medium (Pm) was used as control. It was observed higher cumulative H_2 production with *Rhodopseudomonas palustris* (Rp) than with the mixed culture (M; **Figure 1**).

TABLE 1. **Average performance of anaerobic fluidized bed reactor at ambient temperature using cheese whey as substrate**

Parameter	Sucrose	Cheese whey	
	10 $g/L_{bed}.day$	Without NaCl 10 $g/(L_{bed}.day)$	With NaCl 10 $g/(L_{bed}.day)$
H_2 concentration in biogas (%)	39.4 ± 8.5	11.8 ± 1.6	32.1 ± 6.9
H_2 productivity	42	4.5	14
($mmolH_2/(L*day)$	4.27 ±	4.31 ± 0.07	4.1 ± 0.2
pH	0.12		

Notes: Average results were obtained under steady-state conditions: S: day 8 to 22; CW: and CW-NaCl: day 15 to 22.

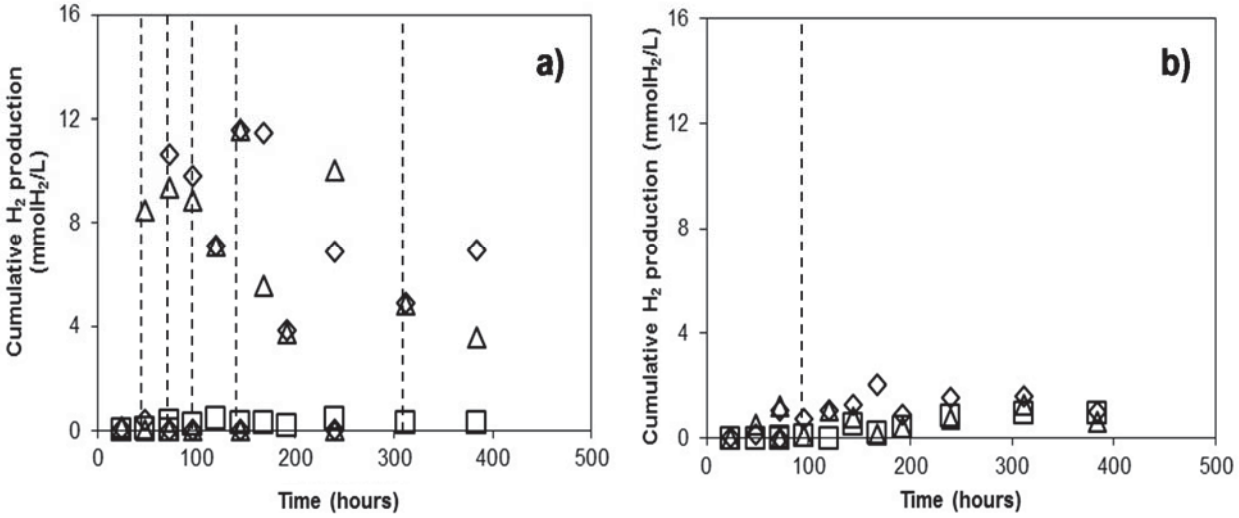


FIGURE 1. Photoheterotrophic H_2 production. a) *Rhodopseudomonas palustris* y b) Mixed culture. ◊ FL without dilution; Δ 1:2 FL-dilution; □ Pfennig medium. Dotted lines means gassed with argon.

The cumulative H_2 production with FL was 21.8 higher than with Pennig medium, despite both substrates had almost the same organic acid content, there could be other nutrients in the FL, remains from the CW, which helped to the PNSB's growth. It was observed that the trace elements in the fermentative medium had effect on the H_2 production and it also depends of the microorganisms used[26-27].

The FL was not sterilized, so it contained microorganisms from the dark fermentation. It was expected that Rp could be negatively affected for the introduction of microorganisms, but this did not happen.

The initial pH in all reactors was 7.03, whereas the final pH was near to 8 (**Table 2**), this could be due to the organic acids were consumed by the microorganisms to produce biomass or H_2.

TABLE 2. **Cumulative H_2 production and Final pH**

Reactor	P_H(mmol H_2/L)	Final pH
FL-M	2.01 ± 0.58	7.87 ± 0.28
FL-Rp	45.72 ± 7.93	8.43 ± 0.51
FL-1:2-M	1.86 ± 0.04	8.29 ± 0.08
FL-1:2-Rp	37.35 ± 11.84	7.89 ± 0.33
Rp	41.5 ± 5.9	8.2 ± 0.4
M	1.9 ± 0.1	8.1 ± 0.3
Pm-M	0.95 ±0.38	7.5 ± 0.3
Pm-Rp	0.64 ± 0.35	7.91 ± 0.53

Notes: FL-M: fermented liquor with mixed culture; FL-Rp: fermented liquor with *Rhodopseudomonas palustris*; FL-1:2-M: FL dilution 1:2 with mixed culture; FL-1:2- Rp: FL dilution 1:2 with *Rhodopseudomonas palustris.* Rp: average results with *Rhodopseudomonas palustris*; M: average results with mixed culture. Mp-M: Pfennig medium with mixed culture; Mp-Rp: Pfennig medium with *Rhodopseudomonas palustris*

It was observed high cumulative H_2 production both with the FL and with its dilution (1:2). With the dilution it was produced 1.7 fold higher cumulative H_2 production than with FL, 2.8 mmol H_2/L_{LF}*day and 4.7 mmol H_2/L_{LF}, respectively (considering the 16 days of photoheterotrophic fermentation). Interestingly, with both substrates was consumed almost all the organic acids (**Table 3**).

The H_2 productivity in the dark fermentation was 4.5 mmolH_2/L_{FL}*day (considering that the HRT was 1 day, bed volume=volume of CW fermented) and the production obtained with the photoheterotrophic fermentation was 4.7 mmolH_2/L_{FL}*day (with the 1:2 dilution); with both fermentations, the productivity is almost two fold that the obtained only with the dark fermentation.

CONCLUSION

- The H_2 productivity using CW was almost 10 fold lower than the obtained using sucrose.
- The use of CW-NaCl allowed the increase of H_2 productivity.
- The cumulative H_2 production with *Rhodopseudomonas palustris* was 22 fold higher than with the mixed culture.
- The H_2 production with the serial dark-phptoheterotrophic fermentation was two fold higher than with only the dark fermentation process.

TABLE 3. Microbial soluble products from the photoheterotrophic fermentation of fermented liquors.

Microbial soluble products (mg COD/L)	FL	Mp	FL-M	FL-Rp	FL-1:2-M	FL-1:2-Rp	Mp-M	Mp-Rp
Ácetic acid	302.8	618.8	ND	41.6 ± 29.6	24.0 ± 24.0	49.3 ± 12.0	66.5 ± ---	ND
Propionic acid	277.8	98.2	206.1 ± 57.7	ND	319.1 ± 64.3	250.6 ± 250.6	76.5 ± ---	ND
Butyric acid	581.1	108.2	158.4 ± 43.9	ND	309.9 ± 180.9	51 ± 15.9	118.7 ± ---	35.8 ± 23.1
Acetone	166.0	ND	43.2 ± 18.5	146.3 ± 109.2	10.3 ± 23.8	89.9 ± 89.9	ND	ND
Methanol	122.4	ND	150.8 ± 46.8	251.6 ± 291.3	116.4 ± 1.5	152.6 ± 152.6	ND	ND
Ethanol	22.4	ND	ND	ND	ND	32.1 ± 32.1	ND	ND
Butanol	12.6	ND	ND	ND	ND	ND	ND	ND
Ac/SMP (%)	11.2	ND	7.6 ± 1.0	40.0 ± 38.7	12.8 ± 1.7	22.1 ± 22.1	ND	ND
MetOH/SMP (%)	8.2	ND	27.0 ± 0.3	48.7 ± 48.7	14.0 ± 4.7	21.9 ± 10.2	ND	ND
EtOH/SMP (%)	1.5	ND	ND	ND	ND	3.8 ± 3.8	ND	ND
BuOH/SMP (%)	0.8	ND	ND	ND	ND	ND	ND	ND
HAc/SMP (%)	20.4	75	ND	11.3 ± 10.7	2.2 ± 2.2	9.5 ± 6.6	25.4 ± ---	ND
HPr/SMP (%)	18.7	11.9	37.0 ± 0.7	ND	37.2 ± 5.6	32.7 ± 29.8	29.2 ± ---	ND
HBu/SMP (%)	39.1	13	28.5 ± 0.6	ND	33.7 ± 8.9	10.0 ± 7.5	45.4 ± ---	100 ± 0.0
TVOA	1161.8	825.2	364.5 ± 101.6	41.6 ± 29.6	652.9 ± 279.1	350.9 ± 259.9	261.7 ± ---	35.8 ±23.1
PMS	1485.2	825.2	558.5 ± 166.9	439.5 ± 152.6	879.6 ± 304.5	625.5 ± 309.6	261.7 ± ---	---

Notes: Ac: acetone; MeOH: methanol; EtOH: ethanol; BuOH: butanol; HAc: acetate; HPr: propionate; HBu: butyrate; TVOA: total volatile organic acids= HAc+HPr+HBu; MSP: microbial soluble products=TVOA+Ac+MeOH+EtOH+BuOH. ND: not detected. FL-M: fermented liquor with mixed culture; FL-Rp: fermented liquor with *Rhodopseudomonas palustris*; FL-1:2-M: FL dilution 1:2 with mixed culture; FL-1:2- Rp: FL dilution 1:2 with *Rhodopseudomonas palustris.* Rp: average results with *Rhodopseudomonas palustris*; M: average results with mixed culture. Mp-M: Pfennig medium with mixed culture; Mp-Rp: Pfennig medium with *Rhodopseudomonas palustris*

ACKNOWLEDGMENTS

The authors wish to thank CINVESTAV-IPN and ICYTDF (now SECITI-GDF, Mexico) for financial support to this research (PICCO-10-27 and PICCO-10-28), CONACYT for the Infrastructure Project 188281 granted to HMP-V, and a graduate scholar¬ship to KMM-P. The authors appreciate the excellent technical help of Professor Elvira Ríos Leal, Mr Cirino Chávez-Rojas, Mr. Gustavo Medina as well as Mr. Rafael Hernández-Vera from the Biotechnology and Bioengineering Department.

REFERENCES

1. Ferchichi M., Crabbe E., Gil G.H., Hintz W., Almadidy A. Influence of initial pH on hydrogen production from cheese whey. J. Biotechnol. 120 (2005). 402–409
2. Mawson A.J. Bioconversion for whey utilisation and waste abatement. Bioresour. Technol. 47 (1994). 195–203.
3. Siso M.I.G. The biotechnological utilization of cheese whey: a review. Bioresour. Technol. 57 (1996) 1–11.
4. Cunningham A.E. Optimización De rendimientos de quesería. OEA 2000.
5. Kavacik B., Topaloglu B. Biogas production from co-digestion of a mixture of cheese whey and dairy manure. Biomass Bioenerg. 34 (9) (2010).1321-1329.
6. Panesar P.S., Kennedy J.F., Gandhi D.N, Bunko K. Bioutilisation of whey for lactic acid production. Food Chem. 105 (2007) 1–14
7. Suarez E., Lobo A., Alvarez S., Riera F.A., Alvarez R. Partial demineralization of whey and milk ultrafiltration permeate by nanofiltration at pilot-plant scale. Desalination.198 (2006) 274–281.
8. Yang P., Zhang R.H., MeGarvey J., Benernann J.R. Biohydrogen production from cheese processing wastewater by anaerobic fermentation using mixed microbial communities. Int. J. Hydrogen Energy. 32 (2007) 4761–71.
9. Malaspina F., Cellamare C.M., Stante L., Tilche, A. Anaerobic treatment of cheese whey with a downflow upflow hybrid reactor. Bioresour. Technol. 55 (1996). 131–9.
10. Valencia-Denicia E., Ramírez- Castillo M. L. La industria de la leche y la contaminación del agua. Elementos: Ciencia y cultura.16 (73) enero-marzo (2009). 27-31
11. Das D., Veziroglu N.T. Advances in biological hydrogen production processes. Int. J. Hydrogen Energy. 33 (2008) 6046-6057
12. Azwar M.Y., Hussain M.A., Abdul-Wahab A.K. Development of biohydrogen production by photobiological, fermentation and electrochemical processes: A review. Renew. Sust. Energ Rev. 31 (2014) 158–173
13. Argun H., Kargi F. Bio-hydrogen production by different operational modes of dark and photo-fermentation: An overview. Int. J. Hydrogen Energy. 36(2011) 7443-7459.
14. Basak N., Das D. The prospect of purple non-sulfur (PNS) photosynthetic bacteria for hydrogen production: the present state of the art. World J. Microbiol. Biotechnol. 23 (2007) 31–42
15. Laurinavichene T.V., Belokopytov B.F., Laurinavichius K.S., Khusnutdinova A.N., Seibert M., Tsygankov A.A. Towards the integration of dark- and photo-fermentative waste treatment. 4. Repeated batch sequential dark- and photofermentation using starch as substrate. Int. J. Hydrogen Energy. 37 (2012). 8800-8810.
16. Redwood M.D., Paterson-Beedl M., Macaskie, L.E. Integrating dark and light biohydrogen production strategies: towards the hydrogen economy. Rev. Environ. Sci. Biotechnol. 8(2) (2009) 149-185
17. Xia A., Cheng J., Lin R., Liu J., Zhou J., Cen K. Sequential generation of hydrogen and methane from glutamic acid through combined photo-fermentation and methanogenesis. Bioresour. Technol. 131 (2013). 146-151.
18. Lee K., Lin P., Chang J. Temperature effects on biohydrogen production in a granular sludge bed induced by activated carbon carriers. Int. J. Hydrogen Energy. 31(4) (2006). 465–472.

19. Mu Y., Zheng X.J., Yu H.Q., Zhu R.F. Biological hydrogen production by anaerobic sludge at various temperatures. Int J Hydrogen Energy. 31(6) (2006) 780–5
20. Perera K.R.J., Ketheesan B., Arudchelvam Y., Nirmalakhandan N. Fermentative biohydrogen production II: Net energy gain from organic wastes. Int. J. Hydrogen Energy. 37(1) (2012) 167–178.
21. Muñoz-Páez K.M., Ruiz-Ordáz N., García-Mena J., Ponce-Noyola M.T., Ramos-Valdivia A.C., Robles- González I.V., Villa- Tanaca L., Rinderknecht-Seijas N., Poggi-Varaldo H.P. Comparison of biohydrogen production in fluidized bed bioreactors at room temperature and 35°C. Int. J. Hydrogen Energy; 38 (2013) 12570-12579.
22. Acevedo-Benitez, J.A. Producción de hidrógeno con un Cultivo Mixto de Microorganismos Fotoheterótrofos, a partir de lixiviados acidogénicos. CINVESTAV, México. 2008.
23. Noike T., Takabatake H., Mizuno O; Ohba M., Inhibition of hydrogen fermentation of organic wastes by lactic acid bacteria. Int. J. Hydrogen Energy. 27(11-12) (2002) 1367-1371.
24. Escamilla-Alvarado C., Ríos-Leal E., Ponce-Noyola M.T., Poggi-Varaldo H.M. Gas biofuels from solid substrate hydrogenogenic–methanogenic fermentation of the organic fraction of municipal solid waste. Process. Biochem. 47(11) (2012) 1572–1587.
25. Daeschel MA. Antimicrobial substances from lactic acid bacteria for use as food preservatives. Food Technol. 43 (1989) 164–167.
26. Liu B.F., Ren N.Q., Ding J., Xie G.J., Guo W.Q. The effect of Ni2+ Fe2+ and Mg2+ concentration on photo-hydrogen production by *Rhodopseudomonas faecalis* RLD-53. Int. J. Hydrogen Energy. 34 (2009) 721-726.
27. Zhu H., Fang H.H.P., Zhang T., Beaudette L.A. Effect of ferrous ion on photo heterotrophic hydrogen production by *Rhodobacter sphaeroides*. Int. J Hydrogen Energy. 32(2007) 4112-4108.

CHAPTER 1.5 SACCHARIFICATION OF A STREAM OF PRETREATED INTERMEDIATE SOLIDS FROM AN H-M-Z-S BIOREFINERY

Leticia Romero-Cedillo (1); Héctor M. Poggi-Varaldo *(1,2) and
M. Teresa Ponce-Noyola *(3)

(1) Nanosciece and Nanotechnology Program, Centro de Investigación y de Estudios Avanzados del IPN.
(2) Environmental Biotechnology and Renewable Energies Group, Department of Biotechnology and Bioengineering, Centro de Investigación y Estudios Avanzados del IPN, P.O.Box 14-740, Ciudad de México D.F., 07000, México.
(3) Department of Biotechnology and Bioengineering, Microbial Genetics Group, Centro de Investigación y Estudios Avanzados del IPN, Av. Instituto Politécnico Nacional 2508, Ciudad de México, México.

ABSTRACT

Trichoderma reesei MCG 80 is filamentous fungi producing extracellular holocellulases and is capable to grow in mineral medium and fermented solids as a carbon source. The aim of this work was to improve the yields in reducing sugars production from the saccharification of pretreated solids X_z, derived from a biorefinery H-M-Z-S (Hydrogen, Methane, Enzymes, Saccharification).
The pretreated solids X_z were used as substrate in a saccharification process using concentrations of 1, 3 and 5 ($\%_{db}$). We considered three levels of enzyme concentration 3, 5 and 7 U/mL at each one, the saccharification was carried out at 55 °C for 48 h. For this experiment, we used holocellulases ultrafiltrate which were obtained from a previous stage in submerged cultures of the strain *Trichoderma reesei* MCG-80. Released sugars were determined by the absorbance at 550 nm, according to the Miller method. In general, the highest yield of reducing sugars in saccharification ($0.067_{g\ sugar/g\ holo}$) was observed in the tests that were containing 5 U/mL of enzyme and 1% of pretreated substrate (X_z); on the contrary when the substrate was increased the sugars performance decreases, for instance at level of 3% and 5% of substrate the yields were 0.049 $_{g\ sugar/g\ holo}$ and 0.043 $_{g\ sugar/g\ holo}$, respectively. Although the alkaline pretreatment successfully removed lignin which results in the increase of cellulose availability in the solids X_z, the reducing sugar yields were generally very low indicating that the pretreated substrate X_z is not suited for further reuse in the saccharification process. It is likely that the presence of inhibitors released after the thermochemical pretreatment, such as phenolic compounds caused from lignin degradation, could be linked to poor results.
We conclude that there is a limit of the principle of cascading regarding the use of the stream of solids X_z in saccharification for further obtaining reducing sugars, that in turn, could have been used for obtaining other value-added products. Yet, there is still a potential use for X_z in the form of soil fertilizer and amender.

Keywords: holocellulases, saccharification, *Trichoderma reesei* MCG 8

---

*Author for correspondence: r4cepe@yahoo.com; tponce@cinvestav.mx

INTRODUCTION

The use of renewable feedstocks for biofuels production is an alternative option due of its low cost. The composition of organic wastes is characterized by a large fraction of lignocellulose, which is an attractive substrate that can be used in biofuel production, for instance biohydrogen. Some natural and renewable sources for energy conversion are municipal wastes, forestry residues and agricultural[1]. Fort the efficient hydrolysis of lignocellulosic biomass it should be considered the degree of crystallinity, because the polymerization limit the accessibility of surface area and affect the interaction between enzyme and substrate, which reduces the conversion rate[2]. The complete hydrolysis of lignocellulosic material, is necessary an enzymatic complex integrated by cellulase, xylanase, pectinase among others[3]. The cellulolytic enzymes are produced by microorganisms such as *Cellulomonas fimi*, *Clostridium thermocellum*, *Bacillus subtilis, Penicillium funiculosum* and *Rhizopus oligosporus*[4].

Cellulolytic enzymes act in synergism breaking bonds type β-1.4 from the cellulose molecule, resulting in the release of glucose, cellobiose and oligosaccharides[5]. In order to improve the disruption of lignocellulosic wastes and hydrolysis of polymer, several pretreatment methods have been evaluated. The pretreatment alter the structure of cellulose and remove the lignin, this allows an increase of cellulose conversion into single sugars[6]. The removal of the lignin may be possible through physical, chemical or biological treatments or combining methods. The chemical pretreatment is frequently used through acid or alkaline hydrolysis[7].

Regarding this, Sartori *et* al.[8] pretreated corncob for 24 hours use as a substrate in fermentation processes by *Trichoderma viride*, the corncob was delignified by NaOH 0.25M using a mixture of 10%(w/v) and remaining at 121 °C for 1h at 110kPa. The delignified substrate was drying in an oven at 35 °C for 24 hours and resulted in 50% delignification[8].

In that study, they obtained the highest activity 26.78 U/mL using pretreated corncob as a substrate and the lowest activity resulted for the eucalyptus sawdust, 3.69 U/mL (90% lower specificity). The above could be because the action mode of enzyme may be affected as a result of the heterogeneity of many lignocellulosic substrates conventionally used in bioprocesses, for instance the variable composition of cellulose, hemicellulose and lignin in the organic fraction of the biomass[9]. Lignocellulosic biomass is degraded by several enzymes, for instance in filamentous fungi the cellulase complex consists of three major enzymes, an endo-1-4- β-glucanase (EC 3.2.1.4), a 1,4-β- D-cellobiohydrolase (EC 3.2.1.91), and a 1,4-β-glucosidase (EC 3.2.1.21), which act simultaneously in the various links of the polymer[10].

In other research about saccharification of cornstalk, Zhao *et* al. [11] found that 81.2% of substrate was converted by enzymatic saccharification process. The efficient conversion was obtained using 38.5 g/L of substrate and 35.7 IU/g for cellulases, at pH 5 and 49.7 °C; after saccharification, they used the liquor as substrate to dark fermentation and hydrogen production using *Thermoanabacterium thermosaccharolyticum* and resulted in 90.6 mLH_2/g cornstalk hydrolysate[11].

In previous works, Escamilla-Alvarado *et* al.[12] evaluated the holocellulases production from *Trichoderma reesei* MCG-80, using fermented solids wastes derived from hydrogenogenic stage in the H-M-Z-S biorefinery. They found higher cellulose activity when used fermented solids as substrate, comparing to the pure cellulose as substrate (Solka floc) 2140 FPU/L and 2100 FPU/L, respectively. Their results were attributed because in dark fermentation a partial degradation of the substrate is caused due the microbial activity causing hydrolysis of the polymers and alter the crystallinity of cellulose[12].

In order to increase the obtention of bio-products, the pretreatment of solid wastes in biorefinery could allow an increase in the saccharification process by using this pretreated wastes as a substrate. For the above, we evaluated the effect of alkaline pretreatment applied to X_z solids (generated after the holocellulases production) in order to determine the viability in the reuse of these wastes coupled to saccharification stage.

MATERIALS AND METHODS

Inoculum propagation. *Trichoderma reesei* MCG-80 was used to produce cellulases. The strain was spread from 200µL having concentration of spores $1*10^6$ spores/mL, this volume was seeded in agar plates supplemented with PDA and incubated at 30 °C for 5 days until observed a radial growth. For inoculation in flasks, were taken 3 cm^2 from mycelial growth using a sterile Pasteur pipette and then added to 500 mL Erlenmeyer flasks containing 150 mL of mineral medium Mandels and fermented organic wastes (FOW) (3%p/v). The complete composition of the medium (g/L) was: Urea 0.3, $(NH_4)_2SO_4$ 1.4, KH_2PO_4 (2), $CaCl_2 \cdot 2H_2O$ (0.3), $MgSO_4 \cdot 7H_2O$ (0.3), $FeSO_4 \cdot 7H_2O$ (0.005), $MnSO_4 \cdot 4H_2O$ (0.001), $ZnSO_4 \cdot 7H_2O$ (0.001), $CoCl_2$ (0.002), Peptone (1) and Tween-80 (1).

At the end of this period, new mineral medium (1L) was inoculated using 100 mL from the previous growth culture. Once inoculated, the Erlenmeyer flasks were incubated at 30 °C during five days at 150 rpm. The cellulolytic activity was monitored by quantification of reducing sugars according Miller method (1959) and then reported in paper filter units per unit volume (FPU/mL). After the holocellulases production, the remaining biomass was recovered by centrifugation at 7,000 rpm for 20 min; the enzymes present in the supernatant were concentrated by ultrafiltration using a 40 kDa membrane. The biomass was washed twice and then pretreated by further use as substrate in saccharification process.

Pretreatment of substrate. Once washed the residual biomass derived from holocellulases production stage, the solids (called X_z) were pretreated by alkaline solution NaOH 1M. The pretreatment consisted in a relation of 1:10 (wet mass-alkaline solution volume), mixed and heated at 60 °C for 1h. At the end of pretreatment, the separation of solids were at 7,000 rpm for 20 min and washed with distilled water. The pH was adjusted using HCl to eliminate traces of alkaline solution. Once the pH was neutralized, the solids X_z were dried in an oven at 100 °C and subsequently sieved with a mesh No. 40. Then the solids were stored at room temperature until further use.

Saccharification process. The reaction was carried out in 120 mL serum bottles with an operational volume of 20 mL consisted in a phosphate buffer citrates 0.05M at pH 4.8. The bottles were maintained at 50 °C, 150 rpm for 48 h. Every 24 h, 1mL of sample was taken and quantification of reducing sugars were analyzed according Miller method (1959).

Experimental design. Consisted in a factorial design 3^2, where the factors were enzyme and substrate concentrations. The levels for enzyme concentration were: 3 FPU, 5 FPU and 7 FPU (U/mg), whereas for substrate concentration the levels were: 1%, 3% and 5% (%w/v).

RESULTS AND DISCUSSION

In the present work the results obtained from holocellulases production showed the highest specific activity of cellulases at 72 h (0.56 IU/mg protein or 0.52 IU/mL) (**Figure 1**); compared to previous research using *T.reesei* MCG-80 and FOW (fermented organic wastes) as substrate, our results were lower (2.14 IU/mL cellulose activity[12], Escamilla-Alvarado *et* al. 2013). This could be due, because in the previous work used different operational conditions such as higher agitation (600 rpm) and stirred tank fermenters. Regarding the xylanolytic activity, the values obtained in the present work using *T. reesei* MCG-80 are nearby comparing to the results previously reported in *Cellulomonas flavigena* PR-22, (5.3 IU/mL and 8 IU/mL, respectively).

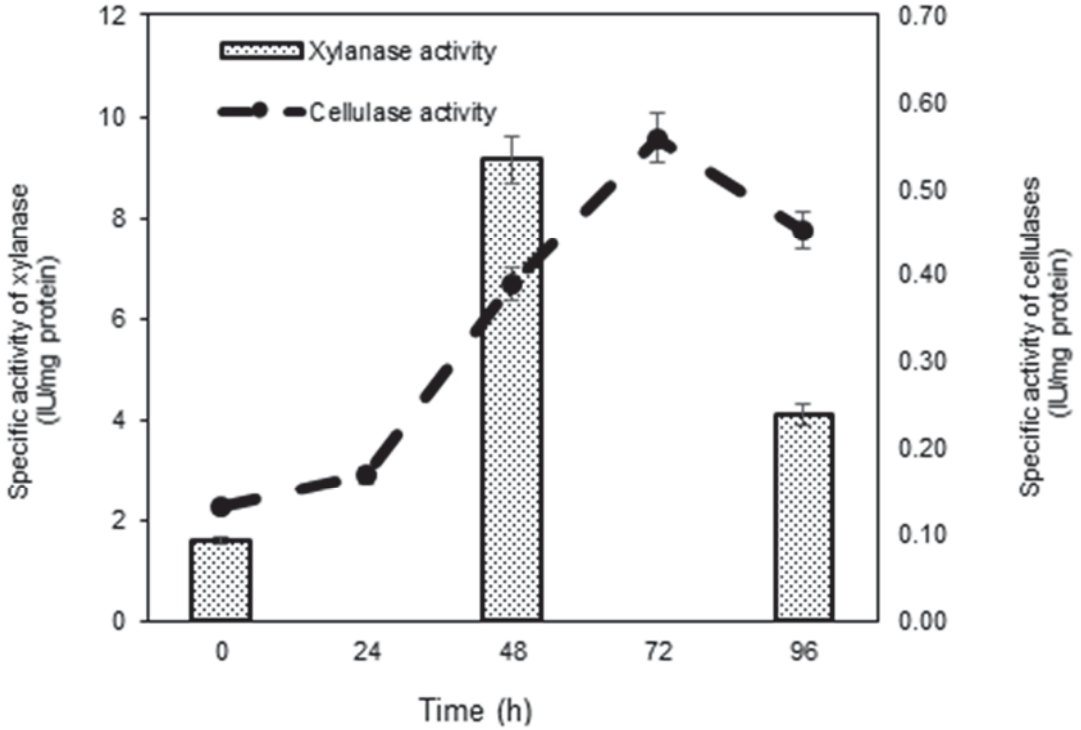


FIGURE 1. Specific activity of cellulases and xylanases from *T. reesei* MCG80 grown in FOW (fermented organic wastes)

It has also been reported that xyloligomers derived from xylan degradation play a crucial role in cellulase inhibition, and xylanases could reduce this inhibition by increasing the hydrolysis of xyloligomers to xylose[13].

The hydrolysis of lignocellulosic biomass can be significantly enhanced by addition of cellulase enzyme complexes with xylanases[14]. Due to the partial removal of the hemicellulose in the cell wall and further increased access to the enzymes, resulting in greater glucose yields.

Other research has been successfully reported, significant xylanolytic activity (60 IU/mL), using delignified steam-explosion pretreated sugar cane bagasse and the strain *Penicillium echinulatum*[15]. Regarding this, within the context of H-M-Z-S biorefinery, the pretreatment of several solid streams could improve the holocellulases production as long as there a significant cellulose content in the substrate, greater than 80%.

After the holocellulases production, the enzymatic complex was concentrated by ultrafiltration in order to get greater amount of enzyme. In **Figure 2**, after the saccharification of pretreated X_z it shows that 5 IU/mL had the best effect on the production of reducing sugars, even when lower amounts of substrate were used; for instance, when used 1% of pretreated X_z it was resulted in 0.4 g/L of reducing sugars, 0.9 g/L using 3% of substrate and 1.31 g/L at 5% concentration of substrate. This results, might suggest that there is a linear relationship between the concentration of enzyme and substrate, and apparently to increase the amount of both factors there would be a greater generation of reducing sugars. However, when the enzyme concentration was 7 IU/mL, there was a significant decrease of reducing sugars obtaining almost 50% (0.81 g/L).

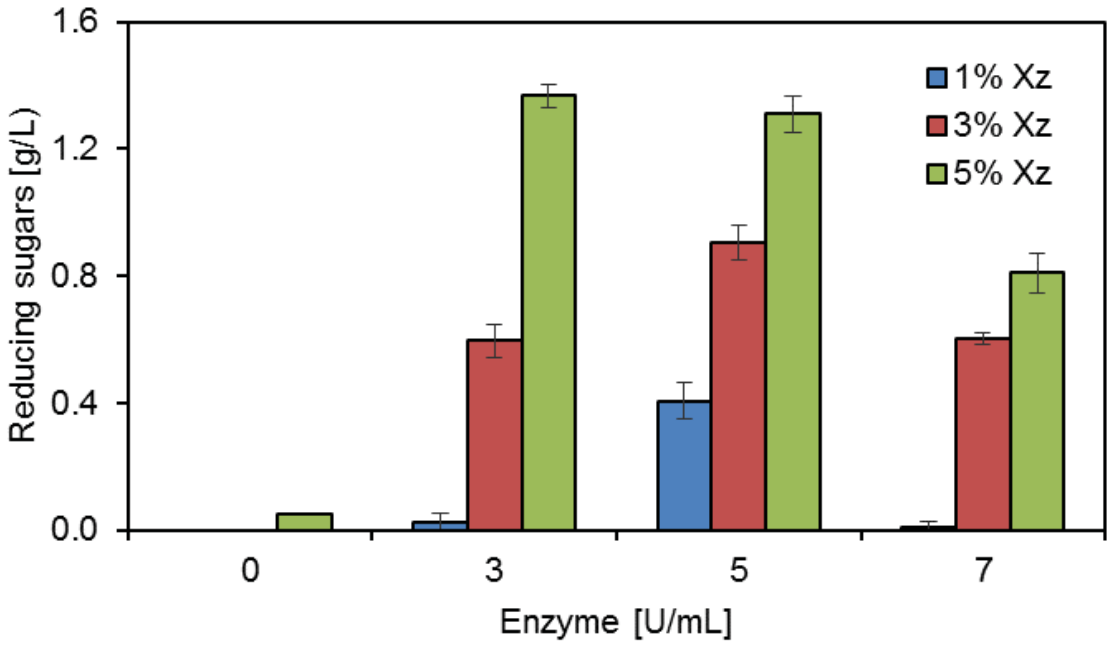


FIGURE 2. Production of reducing sugars

This trend in the decrease of reducing sugars increasing the concentration of enzyme, is similar to the reported by Escamilla-Alavarado *et* al.[12]. In that study, they obtained 10 g/L of reducing sugars by the addition of 40 FPU/gVS, and when increased the amount of enzyme until 120 FPU/gVS the production of sugars had no significant increase (11.6 g/L). The above results suggest that the enzyme-substrate ratio should be explored in order to determine the optimal conditions for saccharification process.

Comparing our results after the saccharification of pretreated X_z, in this work the highest amount of reducing sugars was only 1.4 g/L, using 3 IU/mL (FPase). In previous work, Escamilla-Alvarado *et* al.[12] used holocellulases from*Trichoderma reesei* MCG 80 at concentration of 60 FPU/g and obtained an efficiency of 72.7% (in basis holocellulose) and 13 g/L of reducing sugars (glucose and xylose).

Regarding the effciency, in the present study the most efficient conversion of the pretreated substrate was 6.72% (g sugar/g $holo_{db}$) (**Table 1**). It should be note that yields obtained may be result from the low concentration of enzyme (13 times lower than the reported un the previuous study).

If we extrapolating the 1.4 g/L of reducing sugars produced from 3 IU/mL and hypothetically add the 40 IU/mL of enzyme used in the saccharification of FOW, theoretically it could be obtain a production of reducing sugars of 16 g/L. The above estimated results are similiar to those reported by Escamilla-Alvarado *et* al. [12]. It should be note that this is an estimation based on the present results and it has to consider another factors such as phenolic compounds. During the pretreatment, the inhibitors derived from aromatic compounds are formed (furanes and phenols) under reactions at room and high tempreratures[16].

TABLE 1. Value obtained after the saccharification of Xz pretreated solids using holocellulases from Trichoderma reesei MCG-80

Enzyme[a] (IU/mL)	Substrate[b] (%w_{db}/v)	Holocellulose[c] (g_{db}/L)	Reducing sugars[d] (g/L)	Y' (%)[e] g sugar/g $holo_{db}$
0	1	6.04	0.00	0.00
3	1	6.04	0.02	0.40
5	1	6.04	0.41	6.72
7	1	6.04	0.01	0.15
0	3	18.14	0.00	0.00
3	3	18.14	0.60	3.29
5	3	18.14	0.90	4.98
7	3	18.14	0.60	3.32
0	5	30.23	0.05	0.16
3	5	30.23	1.37	4.52
5	5	30.23	1.31	4.33
7	5	30.23	0.81	2.68

Notes: [a]Enzyme FPase in IU/mL, [b]Substrate concentration of X_z solids in dry basis, [c]Holocellulose concentration in X_z in g/L, [d]Sugar concentration after 48h in g/L, [e]Yield of saccharification (%), in g sugar/g holocellulose.

CONCLUSION

Results from saccharification of pretreated X_z, were lower compared to the saccharification of FOW. However, it is to consider that pretreated X_z is a solid derived stream that comes from previous stages (holocellulases production) within the biorefinery H-M-Z-S and even when the alkaline pretreatment was applied, its composition is weak unlike other substrates that have suffered less degradation for instance the FOW. Also, it is necessary to evaluate a higher relation of enzyme in order to determine the technical feasibility for the saccharification of pretreated X_z.

ACKNOWLEDGMENTS

LRC is very grateful to CONACYT for the scolarship assigned for graduate studies.

REFERENCES

1. Han KJ., Pitman WD., Kim M., Day DF., Alison MW., Mccormick ME., Aita G (2012) Ethanol production potential of sweet sorghum assessed using forage fiber analysis procedures. GCB Bioenergy. 5 (2012) 358-366.
2. Fan LT., Lee YH., Gharpuray MM. The nature of lignocellulosics and their pretreatments for enzymatic hydrolysis. Advan Biochem Eng. 23 (1982)157-87.
3. Broda P., Birch PRJ., Brooks PR., Sims PFG. Lignocellulose degradation by Phanerochaete chrysosporium: gene families and gene expression for a complex process. *Mol Microbiol*. 19 (1996) 923-32.
4. Sukumaran RR, Mathew GM, Singghania RR, Pandey A. Cellulase production using biomass feed stock and its apllication in lignocellulose saccharification for bioetanol production. *Renewable Energy*. 34 (2009) 421-424.
5. Akhtar MS., Saleem M., and Akhtar MW. Saccharification of lignocellulosic materials by the cellulases of *Bacillus subtilis*. *International Journal of Agriculture & Biology*, vol. 3, no. 2, pp.199–202, 2001.
6. Weimer P., Weston W. Relationship between the fine structure of native cellulose and cellulose degradability by the cellulase complexes of *Trichoderma reesei* and *Clostridium thermocellum*. *Biotechnol Bioeng*. 27 (1985) 1540-7.
7. Ogeda TL and Petri DFS. Hidrólise Enzimática de biomassa. *Quimica Nova*. 33 (2010) 1549-1558.
8. Sartori T., Tibolla H., Prigol E., Colla LM., Vieira-Costa JA., Bertolin TE. Enzymatic Saccharification of Lignocellulosic residues by cellulases obtained from solid state fermentattion using Trichoderma viride. *BioMed Research International*. (2015) 1-9. DOI:10.1155/2015/342716.
9. Y. Sun and J.Cheng. Hydrolysis of lignocellulosicmaterials for ethanol production: a review. *Bioresource Technology*. 83 (2002) 1-11.
10. Xu F., Wang., J, Chen S. Strain improvement for enhanced production of cellulase in *Trichoderma viride*. *Applied Biochemistry and Microbiology*. 47 (2011) 53–58.
11. Zhao L., Cao GL., Wang AJ., Ren HY., Xu C., Ren NQ. Enzymatic saccharificationof cornstalk by onsite cellulases produced by Trichoderma viride for enhanced biohydrogen production. *GC Bioenergy*. 5 (2013) 591-598.

12. Escamilla-Alvarado C., Poggi-Varaldo HM, Ponce-Noyola MT. Use of organic waste for the production of added-value holocellulases with Cellulomonas flavigena PR-22 and Trichoderma reesei MCG-80. *Waste Management & Research.* 31(2013) 849-858.
13. Kumar R, Wyman CE (2009) Effect of enzyme supplementation at moderate cellulase loadings on initial glucose and xylose reléase from corn stover solid pretreated by leading technologies. *Biotechnol Bioeng* 102:457–467.
14. Berlin A, Gilkes N, Kilburn D, Bura R, Markov A, Skomarovsky A, Okunev O, Gusakov A, Greg D, Sinitsyn A, Saddler J (2005) Evaluation of novel fungal cellulase preparations for ability to hydrolyze softwood substrates—evidence for the role of accessory enzymes. *Enzyme Microb Technol* 37:175–184
15. Piovesan-Pereira BM., Alvarez TM., Da Silva-Delabona P., Pinheiro-Dillon AJ., Squina FM., Da Cruz-Pradella JG. (2013) Cellulase On-Site Production from Sugar Cane Bagasse using *Penicillium echinulatum*. *Bioenerg. Res*. 6: 1052-1062.
16. Klinke HB., Thomsen AB., Ahring BK. (2004). Inhibition of etanol-producing yeast and bacteria by degradation products produced during pre-treatment of biomass. *Appl Microbiol Biotechnol.* 66:10-26.

CHAPTER 1.6 PRETREATMENT OF INTERMEDIATE SOLIDS FROM THE ENZYME STAGE IN A BIOREFINERY FOR FURTHER USE

L. Romero Cedillo (1); H. M. Poggi-Varaldo (2) and M. T. Ponce-Noyola *(3)

(1) Environmental Biotechnology and Renewable Energies Group, Nanoscience and Nanotechnology Program, Centro de Investigación y Estudios Avanzados del IPN.
(2) Environmental Biotechnology and Renewable Energies Group, Department of Biotechnology and Bioengineering, Centro de Investigación y Estudios Avanzados del IPN, P.O.Box 14-740, Ciudad de México D.F., 07000, México.
(3) Department of Biotechnology and Bioengineering, Microbial Genetics Group, Centro de Investigación y Estudios Avanzados del IPN, Av. Instituto Politécnico Nacional 2508, Ciudad de México, México.

ABSTRACT

Stock pretreatments such as treatment with NaOH, KOH, Ca $(OH)_2$, and Mg $(OH)_2$ are effective for conditioning lignocellulosic wastes and improving yields of downstream processes such as anaerobic digestion or ethanol fermentation. Thus, the aim of this work was to evaluate selected pretreatments of solids derived from a stream of an OFMSW biorefinery. The residual solids (X_z) were recovered after growing cultures of *Trichoderma reesei* MCG 80 on fermented solids, which in turn, were originated in a previous dark fermentation process (hydrogenogenic). In order to obtain more added value products and reincorporate the solids in the H-M-Z-S biorefinery, recovery and pretreatment of X_z was targeted.
Three chemical pretreatments were evaluated: diluted acid with H_2SO_4 1.5% (v/v), NaOH 1M, and Na_2CO_3 1M. The pretreatment conditions consisted in a relation of 1:10 (w/v) and constant heating at 60 °C for periods of 1h.
Alkaline pretreatment using NaOH 1M exhibited the highest cellulose availability was 38.53% compared to the unpretreated solids (30.51%) whereas lignin content decreased from 16.7% to 7.41% after the pretreatment. No amorphous regions were revealed by scanning electron microscopy in samples pretreated with dilute acid; on the contrary, alkaline pretreatment using NaOH 1M led to typical zones characterized by damages in the structure and an irregular fiber structure. Due to the above results, pretreatment with NaOH 1M was selected to conditioning the X_z solids for further studies in biorefinery H-M-Z-S.

Key words: Alkaline, biorefinery, cellulose, dilute acid, pretreatment

INTRODUCTION

Recently, the research in biofuels and renewable energy has gained more attention in the context to explore a diversity of substrates and biomass composition, in order to evaluate sustainable process and obtain better yields in added value product generation. Other works, have been focused on improve the biomass accessibility through the pretreatment of raw materials and increase the degradation of lignocellulosic residues.

---

*Author for correspondence: tponce@cinvestav.mx

Some pretreatments are relatively effective to solubilize the wastes respect their efficiency; the best results have been obtained in pretreatments based on NaOH and KOH. However, high sodium concentration and potassium may affect further stages such as methanogenesis when occur anaerobic digestion[1]. Other studies have found that application of alkaline pretreatment on activated sludge, improve the solubilization of organic matter; Heo *et* al. (2003)[2] determined that the addition of 45 meq NaOH/L, improved methane production by 88% under mesophilic conditions. An interesting aspect of alkaline pretreatment, is the removal of uronic acid, which acts as enzyme inhibitor of cellulases in saccharification process; besides this, the increase in biodegradability of plant cell wall due to the brake down of lignin bounded to cellulose and hemicellulose[3]. However, an important disadvantage is an additional step for neutralization after the pretreatment, so it becomes more expensive.

It should be noted that there is a lot of substrates that have been studied to evaluate the effect on hydrolysis of several wastes such as food wastes[4,5], vegetable wastes[6], sewage sludge[7], pulp and paper sludge[8], corn stover[9], apple pomace[10], rice straw and spruce chips[11]. Several studies have been reported that dilute acid pretreatment hydrolyzed the hemicellulose up to 80-100% and sugars such as xylose, arabinose and galactose are obtained at the end of pretreatment[12,13]. However, some obstacles produced after dilute acid pretreatment are the formation of inhibitory compounds such as furanes, 5 HMF and and levulinic acid, causing damages in the structure of fermentative bacteria[14,15]. Thus, the dilute acid pretreatment allows to hydrolyze the cellulose and hemicellulose, to promote the release of sugars, organic acids and other soluble compounds and in turn reduce the time in the anaerobic digestion stage[16].

It has been reported that combined pretreatments have been successful because promotes cellulose decrystallization and also increases the surface accessibility of biomass by enzymes and microorganisms[17]. In this sense, the high carbohydrates content in wastes or substrates is related on better yields or enzyme activity which accelerates degradation of organic matter[18].

The purpose of this work, was to evaluate the effect of chemical pretreatments (alkaline and dilute acid) on removal of lignin from solid stream derived from an OFMSW biorefinery.

MATERIALS AND METHODS

The target material were solids derived from Z stage, these were recovered after the kinetics with *Trichoderma reesei* MCG 80 (the operational conditions were according Escamilla *et* al. 2013[19]); after that the residual biomass named X_z were subjected to alkaline and dilute acid pretreatment.

The pretreatments consisted in two separate alkali solutions NaOH 1M and Na_2CO_3 1M, for dilute acid used HCl 1.5% (%v/v); the solids were added for each of the three treatments at one relation of mass and volume (1:10), and heated for 1h at 60°C with constant stirring every 15 min.

At the end of pretreatment the samples were centrifuged at 7,000 rpm for 20 min, washed with distilled water and neutralized at pH of 7.0, then dried at 60°C for 24h until dehydration.

Subsequently dry samples ground using a mortar and stored in falcon tubes at room temperature until further studies in cellulose and lignin determinations, and for microscopic evaluation.

For cellulose determination, used 1g of pretreated sample (previously dried) which is placed in a flat-bottomed flask and then added 15 mL of acetic acid (80%) and 1.5 mL of nitric acid. The samples were refluxed for 20 min and then the residue is filtered using Gooch filters, and washed with concentrated ethanol. The samples were dried for 2h at 105 °C and constant weight is obtained. Then they are incinerated at 550 °C and weight is determined.

RESULTS AND DISCUSSION

Favorable results were observed in samples pretreated by alkali solutions which indicates an increase in the cellulose availability, respect to the control (X_z unpretreated). The greatest increase in cellulose presented in samples pretreated by NaOH 1M (29.75 to 39.7%), which represents almost 30% improvement. In this case, the cellulose availability is comparable to the cellulose content in the substrate used to produce holocellulases. In **Figure 1**, it shows the results after alkali or dilute acid pretreatment of different samples.

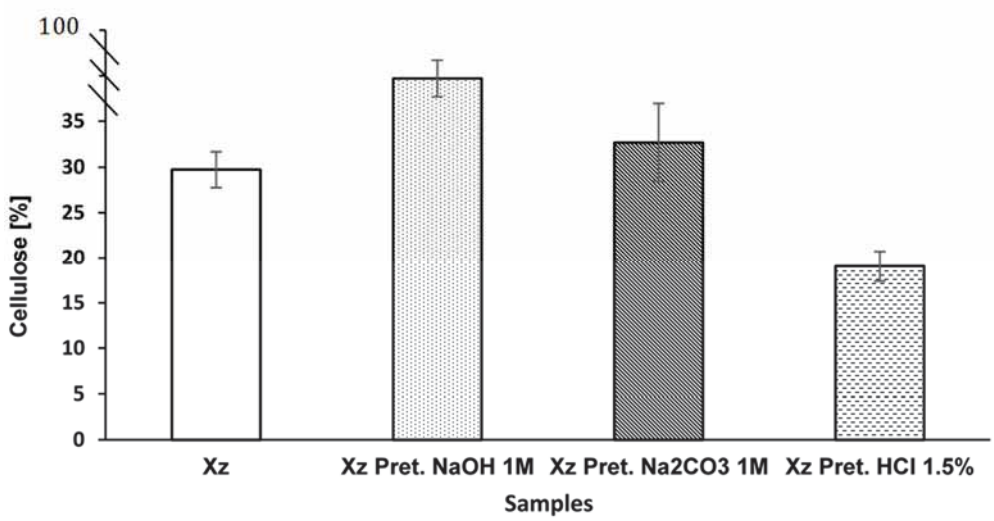


FIGURE 1. Comparative analysis of cellulose content in X_z samples subjected by alkali or dilute acid pretreatment

Most alkaline pretreatments are effective in removing lignin, unlike acid treatments in which hemicellulose is removed, thus lignin remain intact and apparently concentrated. In figure 2, it shows the effect of pretreatments on lignin content. The reduction of lignin is associated to the improved in the degradability of cellulose, due to the increase in availability of this polymer for cellulases activity and further degradation. The alkyl aryl bonds are ruptured under alkaline conditions at pH greater than 10 [(20)], this promote the increase in surface area reducing the stability of polymer, minimizing the crystallinity and the breakdown of linkages between lignin and carbohydrates, produce a disruption of the lignin structure[21].

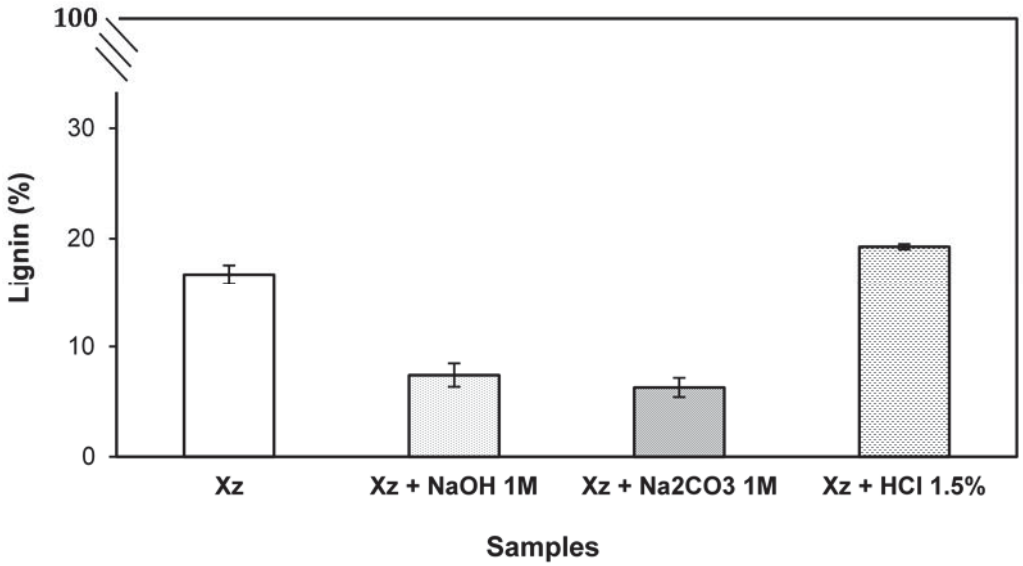


FIGURE 2. Comparative analysis of lignin content in X_z samples subjected by alkali or dilute acid pretreatment

The effect of each pretreatment on the X_z solids, was observed mainly on the compositional characteristics such as lignin and cellulose content. In table 1, we demonstrated that samples pretreated by dilute acid method with HCl 1.5%, did not shown an improved in cellulose degradability. On the contrary, when used alkaline treatment NaOH1M the results shown an increase in cellulose (38.53%) almost the same as the samples of OFMSW (39.63%).

TABLE 1. Characterization of different substrates derived from biorefinery stages

Parameter (% db)	OFMSW	FOW	Xz	Xz NaOH	Xz Na_2CO_3	Xz HCl
Holocellulose	74.52±0.78	69.84±0.66	60.19±0.89	60.47±0.41	48.86±0.98	62.94±0.78
Cellulose	39.69±0.84	46.13±0.54	30.51±1.12	38.53±0.89	35.01±0.46	19.75±0.51
Hemicellulose	19.21±0.37	6.41±0.35	6.57±0.43	ND	ND	25.39±0.35
Lignin	9.85±0.25	12.86±0.67	16.70±0.84	7.41±1.06	6.29±0.87	19.25±0.24
Ashes	15.63±0.35	17.3±0.48	23.11±0.7	32.13±0.43	44.85±0.6	17.81±0.54
VS	71.36±0.56	72.55±0.34	61.76±0.25	55.00±0.36	51.22±0.43	94.34±0.57

In **Figure 3**, the image *a* and image *d* did not change its topology, unlike alkaline pretreatments using NaOH 1M (image *b*) and sodium carbonate 1M (image *c*) in which can be observed fiber rupture and amorphous areas. These amorphous regions resulting from de breaking of the links of C-C and C-O groups, that are present in lignin. The above result in the release of smaller molecules and greater access to the cellulose giving an irregular structure.

After the dilute acid using HCl 1.5%, no breaking occurs in lignin polymer because there was only degradation of hemicellulose. The comparation between pretreatments by analyzing lignin removal, cellulose quantification and electronic microscopy, allowed the selection of best pretreatment resulting NaOH1M the most appropriate.

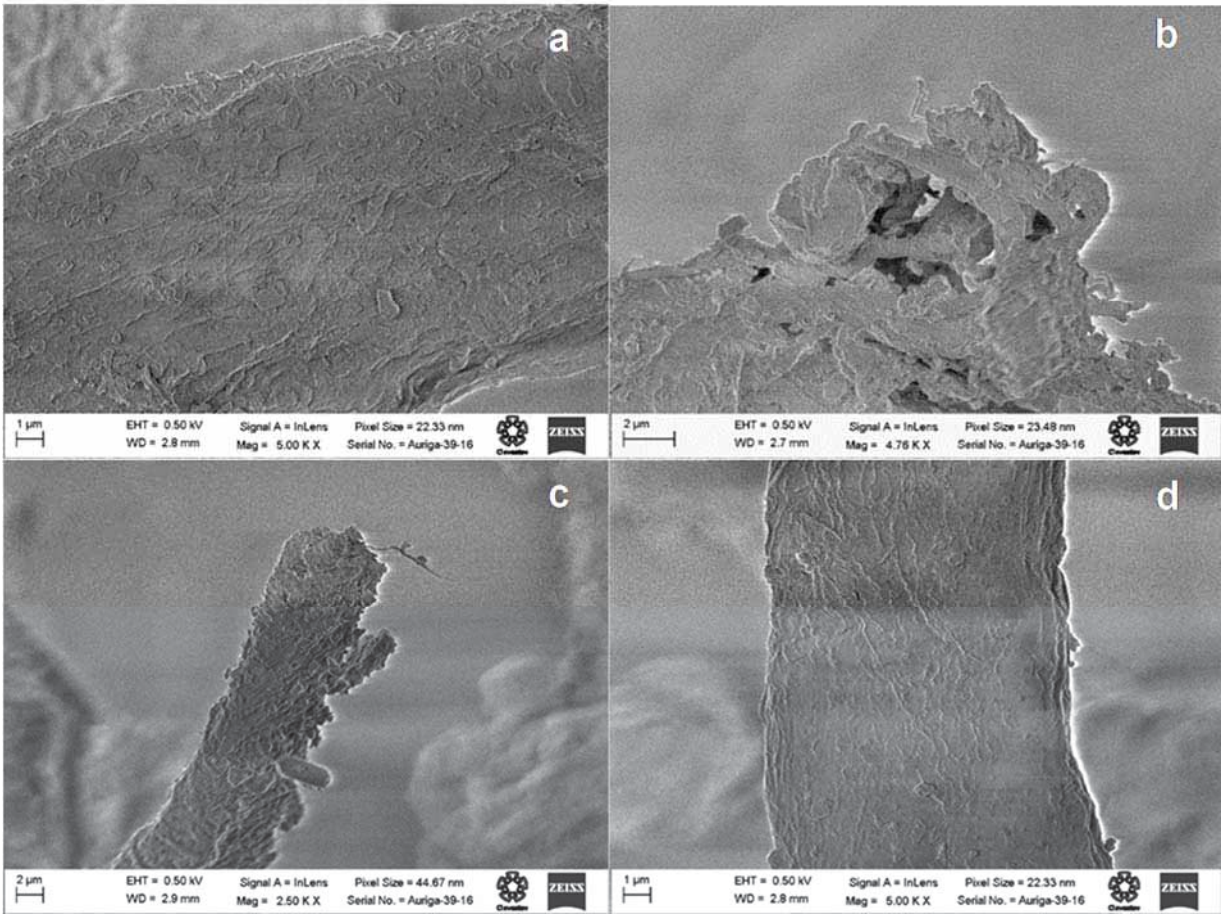


FIGURE 3. Scanning electron microcopy (SEM), of different samples: a) Xz unpretreated, b) pretreated by alkaline NaOH 1M, c) pretreated by Na_2CO_3 1M and d) X_z after pretreatment by HCl 1.5%

CONCLUSION

The increase in cellulose after alkaline pretreatment using NaOH 1M was obtained although the X_z waste has passed through previous degradations in other stages of the biorefinery (such as dark fermentation and cellulose production). Regarding the reduction of lignin is an indirect measure of crystallinity degree, we can infer that the X_z pretreated by alkaline method would be an easier substrate to degrade in further processes in biorefinery. Thus, the pretreatment of derived streams in H-M-Z-S biorefinery apparently can improve the production of value added products: hydrogen, methane and sugars. However, the incorporation of pretreatment depends on preliminary studies comparing yields of conventional processes to determine its viability.

ACKNOWLEDGMENTS

LRC are very grateful with CONACYT for the scholarship for graduate studies.

REFERENCES

1. Liu J, Cai Y, Liao X, Huang Q, Hao Z, Hu M, Zhang D (2012) Simultaneous laccase production and color removal by culturing fungus Pycnoporus sp. SYBCL3 in a textile wastewater effluent supplemented with a lignocellulosic waste *Phragmites australis*. Bull. Environ. Contam. Toxicol. 89, 269–273.
2. Heo NH, Park SC, Lee JS, Kang H (2003) solubilization of waste activated sludge by alkaline pretreatment and biochemical methane potential (BMP) tests for anaerobic co-digestion of municipal organic waste. Water Sci Technol 48(8): 211-219.
3. Gupta R, Khasa YP, Kuhad RCH (2011) Evaluation of pretreatment methods in improving the enzymatic saccharification of cellulosic materials. Carbohydrate polymers 84: 1103-1109.
4. Kim DH, Kim SH, Shin HS (2009) Hydrogen fermentation of food waste without inoculum addition. Enzyme and Microbial Technology 45:181-187.
5. Jang S, Kim DH, Yun YM, Lee MK, Moon C, Kang WS, Kwak SS, Kim MS, Hydrogen fermentation of food waste by alkali-shock pretreatment: Microbial community analysis and limitation of continuous operation. *Bioresource Technol* 186: 215-222 (2015).
6. Jia X, Li M, Xi B, Zhu C, Yang Y, Xia T, Song C, Pan H (2014) Integration of fermentative biohydrogen with methanogenesis from fruit vegetable-waste using different pre-treatments. Energ Convers Manage 88: 1219-1227.
7. Jung HK, Daekeun K, Tae JL, Hydrogen production and microbial diversity in sewage sludge fermentation preceded by heat and alkaline treatment. *Bioresource Technol* 109: 239-243 (2012).
8. Yunqin L, Dehan W, Shaoquan W, Chunmin W, Alkali pretreatment enhances biogas production in the anaerobic digestion of pulp and paper sludge. *J Hazard Mater* 170: 366-373 (2009).
9. Zhu J, Wan C, Li Y, Enhanced solid-state anaerobic digestion of corn stover by alkaline pretreatment. *Bioresource Technol* 101: 7523-7528 (2010).
10. Wang H, Wang J, Fang Z, Wang X, Bu H, Enhanced bio-hydrogen production by anaerobic fermentation of apple pomace with enzyme hydrolisis. *Int J Hydrogen Energ* 35: 8303-8309 (2010).
11. Teghammar A, Karimi K, Sárvári IH, Taherzadeh MJ, Enhanced biogas production from rice straw, triticale straw and softwood spruce by NMMO pretreatment. *Biomass Bioenerg* 36: 116-120 (2012).
12. Vasconcelos SM, Pinheiro-Santos AM, Moraes-Rocha GJ, Souto-Maior AM, Diluted phosphoric acid pretreatment for production of fermentable sugars in a sugarcane-based biorefinery. *Bioresource Technol* 135: 46-52 (2013).
13. Zheng Y, Kahnt J, Kwon IH, Mackie RI, Thauer RK (2014) Hydrogen formation and its regulation in Ruminococcus albus: involvement of an electron-bifurcating (Fe-Fe)-hydrogenase, of a non electron-bifurcating (FeFe)-hydrogenase and of a putative hydrogen-sensing (FeFe)-hydrogenase. *J. Bacteriol*. doi:10.1128/JB.02070-14.
14. Duarte LC, Silva-Fernandes T, Carvalheiro F, Gírio FM (2009) Dilute Acid Hydrolysis of Wheat Straw Oligosaccharides. Appl. Biochem Biotechnol, 15, 15: 116-126.
15. Lin R, Cheng J, Ding L, Song W, Zhou J, Cen K (2015) Inhibitory effects of furan derivatives and phenolic compounds on dark hydrogen fermentation. Bioresource Technology 196: 250-255.
16. Cheng J, Lin R, Ding L, Song W, Li Y, Zhou J, Cen K (2015) Fermentative hydrogen and methane cogeneration from cassava residues: Effect of pretreatment on structural characterization and fermentation performance. Bioresource Technology 179: 407-413.
17. Balan V, Bals B, Chundawat SP, Marshall D, Dale BE, Lignocellulosic biomass pretreatment using AFEX. *Methods Mol Biol* 581: 61-77 (2009).
18. Ren N, Guo W, Liu B, Cao G, Ding J (2011) Biological hydrogen production by dark fermentation: challenges and prospects towards scaled-up production. Curr Opin Biotechnol 22: 365–70.

19. Escamilla-Alvarado C., Poggi-Varaldo HM, Ponce-Noyola MT. Use of organic waste for the production of added-value holocellulases with Cellulomonas flavigena PR-22 and *Trichoderma reesei* MCG-80. *Waste Management & Research.* 31(2013) 849-858.
20. Park Y, Kim J (2012). Comparison of various alkaline pretreatment methods of lignocellulosic biomass. *Energy*, 47: 31-35.
21. Mosier N, Wyman C, Dale B, Elander R, Lee YY, Holtzapple M, Ladisch M (2005) Features of promising technologies for pretratment of lignocellulosic biomass. Bioresour Technol 96:673–686 28.

CHAPTER 1.7 BIO-HYDROGEN FROM PRETREATED INTERMEDIATE SOLIDS AND THE ORGANIC FRACTION OF MUNICIPAL SOLID WASTES IN THE CONTEXT OF AN H-M-Z-S BIOREFINERY

L. Romero Cedillo (1); H. M. Poggi-Varaldo *(2) and M. T. Ponce-Noyola (3)

(1) Environmental Biotechnology and Renewable Energies Group, Nanoscience and Nanotechnology Program, Centro de Investigación y Estudios Avanzados del IPN.
(2) Environmental Biotechnology and Renewable Energies Group, Department of Biotechnology and Bioengineering, Centro de Investigación y Estudios Avanzados del IPN, P.O.Box 14-740, Ciudad de México D.F., 07000, México.
(3) Department of Biotechnology and Bioengineering, Microbial Genetics Group, Centro de Investigación y Estudios Avanzados del IPN, Av. Instituto Politécnico Nacional 2508, Ciudad de México, México.

ABSTRACT

The principle of cascading is that it is contributes to sustainability of modern biorefineries. That principle fosters the use and recycling of biorefinery streams in order to obtain the most value-added products or energies. In the H-M-Z-S biorefinery, the stream X_z represents the solids that were used as substrate for enzyme production in the Z stage. The purpose of this study was to evaluate the effect of pretreatment of such stream of solids derived from an organic fraction of municipal solid waste (OFMSW) biorefinery on biohydrogen productivity. The biological hydrogen production was carried on in batch reactors using serum bottles at 35°C for a period of 38 days. The test was organized as a factorial experiment with type of substrate as the main factor: 100% OFMSW, 100% spent solids from the enzyme production stage of the biorefinery X_z, 100% pretreated X_z (with 1M NaOH), and selected mixtures 60% OFMSW/40% pretreated X_z and 60% OFMSW/40% X_z .
The order of cumulative H_2 production was 100%OFMSW > 60% OFMSW/40% pretreated X_z > 100% X_z > 60% OFMSW/40% X_z > 100% pretreated X_z. Part of these results were counterintuitive since the bioH_2 production was higher for the X_z stream than for the pretreated X_z stream. The highest cumulative yield was 2.2 mmolH_2/gTS using OFMSW as a substrate. In contrast, the lowest value 0.087 mmolH_2/gTS corresponded to pretreated solids.
There was a limit to the application of the principle of cascading to the stream of spent solids X_z for producing additional bioH_2 in the context of our biorefinery. According to this work, it is no worth pretreating the stream X_z for further obtaining H_2 in the biorefinery.

Key words: biohydrogen, biorefinery, OFMSW, pretreatment

---

*Author for correspondence: r4cepe@yahoo.com

INTRODUCTION

Bio-hydrogen is an attractive alternative to substitute fossil energies because its high-energy content does not generate any toxic byproducts. However, conventional technologies to generate H_2 are costly. The microbial H_2 production by algae, phototrophic bacteria or fermentative bacteria is an ecofriendly process, which in addition has managed to reduce production costs[1]. Thus to increase the efficiency of hydrolysis or degradation, lignocellulosic biomass must be conditioned so as to remove lignin and hemicellulose[2,3]. For more than 25 years it has been extensively studied the modification of acidogenesis route with the aim to promote the hydrolysis and increase the bio-hydrogen yields.

At initial reaction, carbohydrates such as glucose and sucrose used as the main source of feed, but actual organic wastes such as OFMSW, are commonly used for economic reasons. The use of these wastes is attractive by reducing waste through their integration into a biorefinery process option[4]. Kang *et* al. (2012)[5], reported a high solubilization of sewage sludge (85%) resulting in an increase of COD concentration, when used combined heat treatment and alkaline conditions (pH 13). After the pretreatment, fermentation of sewage sludge was 72.79 ml/L was observed at 175 mg/L ammonia concentration, showing the best hydrogen yield at lower ammonia concentrations[5].

MATERIALS AND METHODS

The biological hydrogen production was conducted in serum bottles containing different concentrations of OFMSW (organic fraction of municipal solid wastes) and residual solids from enzyme production X_z pretreated previously by alkaline method using NaOH 1M and X_z solids unpretreated. The total operational mass consisted of 40 g (wet weight) for each treatment and their respective controls. The relation of substrate and inoculum was 80% and 20% respectively; the inoculum was previously inhibited by heat shocked pretreatment at 95 °C for 1h to avoid methanogenic activity. Once inoculated, the head-space in reactors was gassed using nitrogen to maintain anoxic environment. The reactors were incubated at 35 °C for a period of 38 days.

Table 1 shows the composition of experimental units for each treatment used in the biological hydrogen production.

TABLE 1. Composition of reactor using different susbtrate and relation; the treatments were composed by OFMSW and pretreated solids X_z using NaOH 1M

Treatment	Composition
1	OFMSW 100%
2	Xz P 100%
3	Xz UP 100%
4	Xz P 40% + OFMSWF 60%
5	Xz P 40% + OFMSW 60%

*X_z: Residual solids from cellulase production; P: pretreated residual solids; UP: unpretreated residual solids

The hydrogen production was measured daily until the stationary phase was presented, the quantification was analyzed by gas chromatography using a GOW-MAC 350 chromatograph equipped with thermal conductivity detector. The temperature of injector, column and detector were 25, 25 and 100 °C respectively and argon was the carrier gas. A packed silica gel column of diameter 60/80 was used. Once the stationary phase was observed and there was not a substantial increase in hydrogen production, the reactors were subject by intermittent venting to stimulate a new cycle production. The intermittent venting was performed for 2 minutes and a water seal was used to avoid the release of gas in reactors and maintain the system closed.

RESULTS AND DISCUSSION

Before starting the fermentation, the five substrates were characterized in order to know the most elemental composition in respect to the content of volatile solids (VS) and ashes, mainly. In this sense, the substrates or treatment that presented the highest content of volatile solids were T1 and T4, (61% and 60.19%, respectively) and a content of ashes of 38.9% and 39.8%, respectively. The treatment T2 which contained 100% of pretreated solids X_z, presented the lowest values regarding volatile solids (42.5%) and a large amount of ashes (57.48%). The above could be due because there was most degradation of carbohydrates such as starch and other organic molecules during the pretreatment, and the remaining matter was in lower proportion (**Table 2**).

TABLE 2. Proximate analysis of the substrates used in each treatment for biological hydrogen production

Treatment	Total Solids	SD	Humidity	SD	Volatile Solids	SD	Ashes	SD
T1	23.59	±0.52	76.41	±0.52	61.02	±1.25	38.98	±1.25
T2	23.11	±0.23	76.89	±0.23	42.52	±0.97	57.48	±0.97
T3	23.35	±0.62	76.65	±0.62	52.33	±12.27	47.67	±12.27
T4	23.07	±0.85	76.93	±0.85	60.19	±1.33	39.81	±1.33
T5	22.82	±0.26	77.18	±0.26	57.60	±2.25	42.40	±2.25

The best yield of hydrogen production was presented in T1 and T4 treatments obtaining 2.19 mmolH_2/gTS and 1.11 mmolH_2/gTS, respectively. In **Figure 1** is showed the performance of the five treatments over the operation time. The first hydrogen production cycle was at initial time and was remained until the 10th day, at this stage intermittent venting was applied to start a new cycle of hydrogen production. The cycles 3, 4 and 5 started on days 16, 21 and 24 respectively.

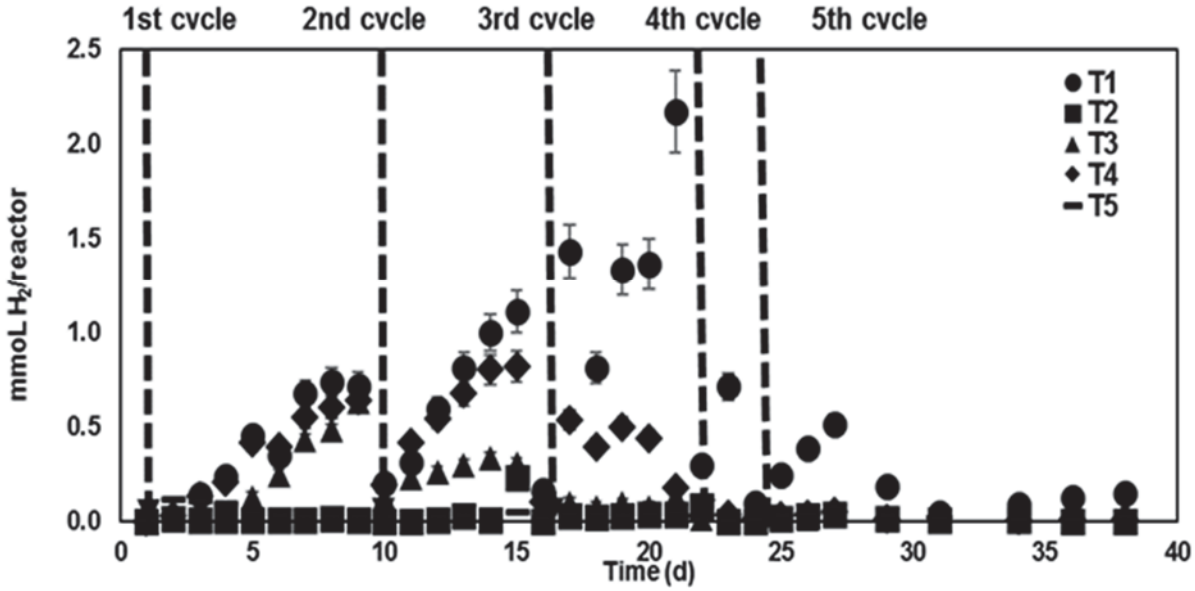


FIGURE 1. Performance of dark fermentation in batch reactors from different substrates and composition to evaluate the effect of alkaline pretreatment on the hydrogen yield

The lowest production of hydrogen was observed in T2, consisted in X_z pretreated. This could be due to the presence of inhibitors generated after the pretreatment. For instance, Reginatto *et* al. (2015)[6], obtained yields of 2.94 mmoL/H_2 gTS when used substrate previously pretreated by alkaline method, their results are lower than those obtained themselves that were not pretreated (4.54 mmoL/H_2 gTS). The composition and nature in the substrates was a determinat factor which affected the performance of different reactors. The results are shown in **Table 3**.

TABLE 3. Cumulative hydrogen production and yields obtained after 38 days of operation, corresponding to five treatments using different composition and substrate

Treatment	Composition	Σ*P*H_2 (mmoLH_2/reactor)	Σ Y' H_2 (mmoLH_2/gTS)
T1	OFMSW 100%	17.532	2.192
T2	X_zP 100%	0.699	0.087
T3	X_zUP 100%	4.209	0.526
T4	X_zP 40%, 60% OFMSW	8.882	1.110
T5	X_zUP 40%, 60%OFMSW	1.093	0.137

*X_z: Residual solids from cellulase production; P: pretreated residual solids; UP: unpretreated residual solids.

CONCLUSION

Despite a favorable performance occurs in one of the treatments containing a fraction of pretreated X_z (T4 treatment), the positive result was due to the presence of OFMSW in the mixture. This was observed in treatment T2, in which only pretreated solids were the substrate. The recalcitrance of this residue X_z, the low content of volatile solids and large amount of ashes is a result not only for the pretreatment, also is a waste that has gone through several previous degradation processes within the biorefinery H-M-Z-S.

ACKNOWLEDGMENTS

LRC is very grateful to CONACYT for the scolarship assigned for graduate studies.

References

1. Wang, H., Wang, J., Fang, Z., Wang, X., Bu, H. Enhanced bio-hydrogen production by anaerobic fermentation of apple pomace with enzyme hyrolysis. *Int J Hydrogen Energy* (2010); 35: 8303-8309.
2. Lissens G, Thomsen AB. Thermal wet oxidation improves anaerobic biodegradability of raw and digested biowaste. *Environ Sci Technol* (2004); 38:34182–241.
3. Datar R, Huang J, Maness PC, Mohagheghi A, Czernik S, Chornet E. Hydrogen production from the fermentation of corn stover biomass pretreated with a steam-explosion process. *Int J Hydrogen Energy* (2007); 32:932–939.
4. Jang, S., Kim, D-H., Yun, Y.M., Lee, M.K.., Moon, Ch., Kang, W.S., Kwak, S.S., Kim, M.S. Hydrogen fermentation of food waste by alkali shock pretreatment: Microbial community analysis and limitation of continuous operation. *Biores Technol* (2015); 186: 215-222.
5. Kang, J.H., Kim, D., Lee, T.J. Hydrogen production and microbial diversity in sewage sludge fermentation preceded by heat and alkaline treatment. Bioresource Technology (2012); 109: 239-243.
6. Reginatto V, Vasconcellos A. Fermentative hydrogen production from agroindustrial lignocellulosic substrates. *Brazilian Journal of Microbiology* (2015); 46: 323-335.

CHAPTER 1.8 EFFECT OF PROGRESSIVE ORGANIC LOADING RATE OVER BIOBUTANOL PRODUCTION IN ANAEROBIC REACTOR USING BIODIESEL WASTE AS CARBON SOURCE

R. Salles (1); C. Silva (1); J. Bassan (1); R. Monti (1); M. Zaiat (2); B. Varesche (2) and **G. Peixoto ***(1)

(1) Univ. Estadual Paulista (UNESP), Rodovia Araraquara-Jaú, Km 1, Araraquara, Brazil
(2) University of São Paulo (USP), Avenida João Dagnone, 1100, São Carlos, Brazil

ABSTRACT

Biobutanol is an alternative renewable fuel studied to work as an additive or replace gasoline because of similar energy density (29.2 MJ L^{-1}), octane number (87 %) and lower heating value (27.8 MJ L^{-1}). The attractive aspect of biobutanol production is that organic wastes can be used as raw materials for the anaerobic-solventogenic process. Glycerol derived from the transesterification process of biodiesel production is considered a promising carbon source for butanol generation due to large availability (10% w:w) and low cost. One of the most important control parameters in continuous bioprocesses is the organic loading rate (OLR), which translates by the amount of organic matter applied in terms of chemical oxygen demand (COD) per time (d) per unit of reactor volume (L). The variation of OLR can affect the immobilized bacterial strains driving the metabolic pathway to targeted products (butyric acid; butanol) or undesired metabolites (acetone; other volatile organic acids).
In this context, the aim of this study was to evaluate the performance of biobutanol production at the OLRs of 6.5, 13.0 and 26.0 g COD L^{-1} d^{-1}. For this purpose, a solution containing 30 g L^{-1} COD (glycerol) plus a simple nutritional medium was pumped at the flowrates of 9.0, 18.0 and 36.0 mL h^{-1}, which corresponded to the abovementioned OLRs. The bioprocess was conducted at 30ºC in a 2 L upflow anaerobic packed-bed reactor (UAPB) inoculated with sucrose auto-fermentation consortium. The application of 13.0 g COD L^{-1} d^{-1} yielded the highest production of butanol (0.44 g L^{-1}) detected in the experimental conditions evaluated. The operation performed at the OLR of 26.0 g COD L^{-1} d^{-1} resulted in the average generation of 0.23 g L^{-1}. In the experimental condition that evaluated the OLR of 6.5 g COD L^{-1} d^{-1} the metabolites profile suggests that low production of butanol occurred because organic matter concentration did not provided sufficient energy/nutrients for the bioprocess. On the other hand, the increase from 13.0 g COD L^{-1} d^{-1} to 26.0 g COD L^{-1} d^{-1} affected the consumption rate of butyric acid, which is the main precursor of butanol. The results indicated that OLR of 13.0 g COD L^{-1} d^{-1} was also suitable for other value added products, such as butyric, acetic and propionic acid. Thus, the improvement of butanol production through the optimization of OLR and the generation of valuable organic acids coupled with biodiesel fabrication could be an alternative to upgrade conventional plants into advanced biorefineries.

---

*Author for correspondence: peixotog@fcfar.unesp.br

Keywords: anaerobic digestion, biobutanol, glycerol, organic loading rate.

INTRODUCTION

ABE fermentation. In this fermentation, acetate and butyrate are primary produced (acidogenesis). Then, a shift in the metabolic pathway of bacteria drives the metabolism towards solvents production (solventogenesis) such as acetone, butanol and ethanol [1]. The increase in butyrate concentration and pH decrease to values under 5 are two critical factors that promote the shift from acidogenesis to solventogenesis.

Butanol is a valuable product because it has wide utilization in pharmaceutical and plastic industries. Moreover, the use as alternative to gasoline or fuel additive is another promising application since it has physico-chemical properties similar to conventional fuels, as demonstrated in **Table 1**.

TABLE 1. Physicochemical properties of common vehicle fuels

Properties / Fuels	Gasoline	Butanol	Ethanol
Air-Fuel Ratio	14.6	11.1	9.0
Energy Density (MJ L^{-1})	32	29.2	19.6
Research Octane Number (%)	91-99	96	107
Vehicle Octane Number (%)	81-89	78	89

Glycerol. It is also known as glycerin (commercial products with glycerol concentration above 95%), and represents the main byproduct of vegetal and animal oils subjected to transesterification for biodiesel production[2]. The expansion of biodiesel production also reflected in the increase of glycerol availability (10% v/v of biodiesel) and caused a hard decrease in the market price of this raw material. The ANP (National Agency of Petroleum, Natural Gas and Biofuels) pointed to the current production of 176 million of liters per year, which is only 17% of total volume predicted by Brazilian government in the next years. One possible solution to overcome the environmental problem of biodiesel wastes and restore market price of glycerol is to employ it in biotechnology industry as substrate for different bioproducts.

Glycerol is an interesting carbon source because it is a structural component of many lipids metabolized in same pathway of glucose, thus producing pyruvate and its subsequent products [3]. This characteristic allows the utilization of glycerol as carbon and energy source [2].

Butanol production from glycerol. The fermentation of glycerol for butanol production from pure cultures has already been extensive described in the literature. However, there are few studies reporting the utilization of mixed cultures.

Khanna et al. [4] employed *Clostridium pasteurianum* cells immobilized in Amberlite to process glycerol in 250 mL batch flasks at pH 7.5 and temperature of 30°C. The maximum production was 0.35 g butanol g^{-1} of glycerol (5 days fermentation) at initial concentration of 25 g L^{-1}.

Gallardo et al. [5] also evaluated the performance of *Clostridium pasteurianum* over the conversion of glycerol to butanol. In batch experiments the abovementioned authors obtained the maximum production of 0.30 g butanol g^{-1} of glycerol at 37°C with initial substrate concentration of 5 g L^{-1}.

Yadav et al. [6] studied butanol production from glycerol employing *Clostridium acetobutylicum* in 500 mL batch flasks with initial cell concentration of 30 g VSS L^{-1}. The optimum conditions found in this study were temperature of 37°C, pH 6,5, initial glycerol concentration of 35 g L^{-1}, 5% of yeast extract and medium supplementation with 6 g L^{-1} of Na_2CO_3.

In general, most of the researchers utilized pure cultures of *Klebsiella aerogenes*, *Clostridium butyricum* and *Clostridium pasteurianum*. As a consequence the costs of scalling up the processes would have great impact over butanol market price. Aiming to reduce the production costs new studies are required to develop non-sterile operations and to use pure or mixed cultures[3].

Kefir grains. These symbiotic conglomerates are formed by bacteria and fungi utilized in the fermentation of milk and other substrates. The microbiologic composition varies according to strain, cultivation methods and substrate. Witthuhn et al.[7] and Gulitz et al.[8] stated that milk and water-based kefir are majority composed by lactic acid bacteria, yeast and non-lactic bacteria. However, most of non-lactic bacteria are found in water-based kefir, in which it is possible to find bacteria of genus *Clostridium* and *Klebsiella,* recognized as butanol producers.

Heat-treated anaerobic sludge. Poultry slaughterhouse wastewaters are nutrient-rich substrates treated by biological process in many industries, thus resulting in large diversity of anaerobic microorganisms. Previous studies aiming to obtain bioproducts from wastewaters have successfully employed this inoculum source. Lazaro[9] in a study involving hydrogen production from vinasse characterized the inoculum after thermal treatment (90°C/10min) and found mostly bacteria from genus *Clostridium*. It is worth mentioning that this heat treated anaerobic sludge derived from poultry slaughterhouse wastewater that was previously utilized in the works by Penteado et al.[10] and Lucas et al.[11] generating butyrate, which is the main precursor of butanol.

Sucrose auto-fermentation consortium. Peixoto et al.[12] evaluated biological hydrogen production using mixed culture obtained from sucrose fermentation. In their study bacteria from genus *Clostridium* and *Klebsiella* were found. Fernandes et al.[13] also performed biomolecular analysis of this inoculum derived of hexose autofermentation and detected the presence of acidogenic bacteria from the genus *Clostridium*, which has the potential for hydrogen and butanol production from complex wastewaters including wastes from biodiesel production.

Effect of organic loading rate. Few studies have reported organic loading rates because the production of butanol is majority carried out in batch systems. Most of the works consisted in the utilization of cultivation flasks inoculated with *Clostridium pasteurianum*. In general, there was only one carbon source (glycerol) and organic matter concentration varied from 5 to 50 g L^{-1} of pure glycerol[14]. In the study by the

aforementioned authors the maximum yield was 0.2 g of butanol per gram of glycerol at the concentration of 35 g L^{-1}. A recent study conducted by Agnelli et al.[15] employed glycerol at the concentration of 30 g COD L^{-1} in a continuous reactor with hydraulic retention time (TDH) of 60h and detected butanol production. However, this study aimed hydrogen production instead of butanol.

MATERIALS AND METHODS

Reactor. An acrylic system with internal diameter of 82mm and total volume of 2L was utilized in the bioprocessing of glycerol. The bed zone (290mm in height) was filled with support material based in low density polyethylene and presented useful volume of 1L. The feeding of the system was performed by positive displacement pump installed in the bottom of the reactor, as shown in **Figure 1**.

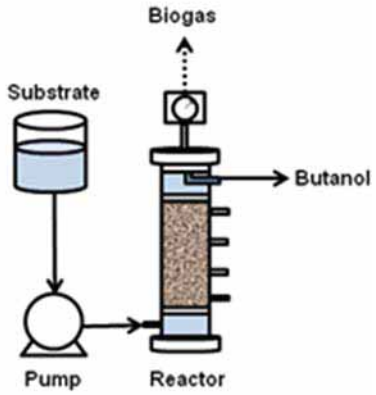


FIGURE 1. Experimental setup

Inoculation. Kefir grains were cultivated in medium containing sucrose solution with corresponding chemical oxygen demand (COD) of 30 g L^{-1}. The symbiotic conglomerates were incubated at 30°C for 24h, then the medium was completely replaced after solid fraction separation (biomass).

The consortium collected from the upflow anaerobic sludge blanket reactor (UASB) treating poultry slaughterhouse wastewater was subjected to thermal pretreatment. This treatment consisted in keeping the biomass at 90°C for 10 minutes with subsequent freezing in ice bath to eliminate the methanogenic archaea and selection of spore-forming bacteria.

The biomass derived from sucrose autofermentation was supplemented with the same medium utilized by Peixoto et al.[16]. Biomass from this inoculum source was cultivated till reaching more than 30 g of VSS.

Support material. Low density polyethylene was employed as support for biomass growth. The immobilization particles had approximately 5:5:6 mm. This type of support was chosen because it is preferentially colonized by acidogenic bacteria, including those from *Clostridia* species[17].

Substrate. Glycerol was used as the carbon source in the range of 30 g L^{-1} COD, which was a non-saturating concentration already utilized in the study by Peixoto et al. [16]. It was also utilized the same nutritional medium of the abovementioned authors to provide the minimum requirements of other macro and micronutrients for bacterial growth. The pH control was performed with sodium bicarbonate (500 mg L^{-1}) or hydrochloric acid (0.45 mL L^{-1}).

Organic Loading Rates. It is the amount of organic matter (mass) applied per day and per reactor volume, as presented in Equation 1.

$$OLR=(Q.S).V^{-1} \quad (1)$$

where:
OLR = organic loading rate (g COD L^{-1} d^{-1});
Q = flowrate (L d^{-1});
S = inlet substrate concentration (g DQO L^{-1});
V = useful reactor volume (L);

Analytical methods. Biogas flowrate was measured by a water displacement device similar to milligascounter (Ritter®). Volatile organic acids (VOA) and solvents were determined by gas chromatography (GC 2010 - Shimadzu®) equipped with Combi Pal headspace analyzer (AOC 5000) following the protocols described by Peixoto et al.[12].

Microscopic analysis of biomass was performed with a microscope Leica® DM LB coupled with a camera to execute frame capture for the software Image Pro Plus® versão 4.5.0.19.

Experimental procedure. The entire experiment was divided in 2 main stages. In the first step the bioreactors were individually operated and labeled as:

- R1-Sucrose autofermentation consortium;
- R2-Kefir grains consortium;
- R3-Heat-treated anaerobic consortium.

The operation length of bioreactors was approximately 42 days and it was preceded by inoculation with the respective consortium following the ratio of 130,46 mg SSV g^{-1} of support, which was previously employed by Peixoto et al.[16]. The temperature of all operations was maintained at 30°C by water jackets involving the reactors. The feed flowrate was 18 mL h^{-1}, resulting in a hydraulic retention time (HRT) of 60h and organic loading rate (OLR) of 13 g COD L^{-1} d^{-1}.

All reactors were fed with sucrose up to their 14th day of operation as a strategy to enhance the process of cell growth and attachment to the support material.

In the second step the biomass with higher performance was quantified and utilized for inoculation of a new reactor (R4). This reactor had periodic shifts in the flowrate (Q) aiming to increase the organic loading rate, as described in phases 1-3:

- Phase 1- 1st to 14th operation day – flowrate of 9.0 mL h^{-1} – OLR of 6.5 g COD L^{-1} d^{-1};

- Phase 2- 15th to 29th operation day – flowrate of 18.0 mL h^{-1} – OLR of 13.0 g COD L^{-1} d^{-1};
- Phase 3- 20th to 42nd operation day – flowrate of 36.0 mL h^{-1} – OLR of 26.0 g COD L^{-1} d^{-1}.

RESULTS AND DISCUSSION

Hydrodynamic characterization. Dourado et al. [18] executed assays with three different flowrates to assess the hydrodynamic pattern of the reactor. The parameters analyzed were real HRT, number of CSTR and dispersion number. The results are presented in **Table 2**.

TABLE 2. **Hydrodynamics characterization parameters**

Immobilization matrix	Bed porosity (%)	Flowrate (mL h^{-1})	Average HRT (h)	N (series of CSTR)	D.uL^{-1} (dispersion number)
polyethylene	50	17	69.38	141	0.004
polyethylene	50	34	33.03	276	0.002
polyethylene	50	68	16.01	428	0.001

According to **Table 2**, plugflow pattern was maintained in all flowrates (N>12; low dispersion). Regarding the flowrate employed in this study, the parameters obtained were 68h, N=141 and D/uL=0.004 for HRT, number of CSTR and dispersion number, respectively.

Butanol production with different inocula (1st step). The analysis of **Figure 2** indicated the absence of butanol production in reactor R1 up to the 16th day of operation, when sucrose was the carbon source.

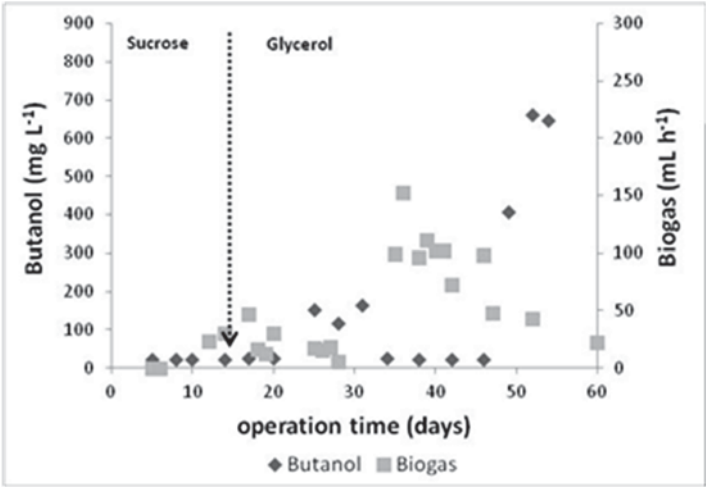


FIGURE 2. Butanol and biogas production in reactor R1

The begining of butanol production was reported after the introduction of glycerol as carbon source. As observed in **Figure 2**, it was detected 150 mg L^{-1} of butanol between the 25th and the 31st day of operation. In this stage the effluent pH was 3.2 because there was not addition of sodium bicarbonate. However, effluent pH set to 5.0 promoted the highest butanol production (660 mg L^{-1}) after the 45th day of operation.

According to Ramey et al.[1], 4.5 to 5.0 is the ideal range for butanol production because it promotes the shift from acidogenis to solventogenesis. It is likely that one of the factors influencing the yield of our process was the pH range.

Reactor R2 using kefir grains as inoculum also presented low butanol production (**Figure 3**) in the stage that sucrose was the carbon source and the medium have not prepared with the buffer composed of sodium bicarbonate.

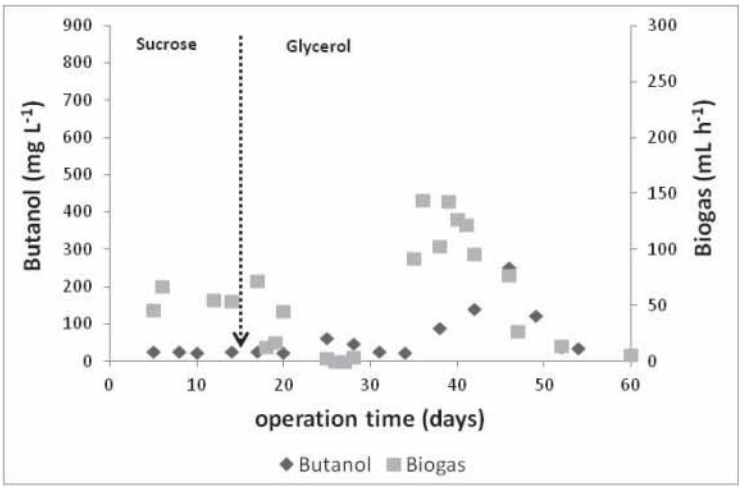


FIGURE 3. Butanol and biogas production in reactor R2

Butanol generation occurred at the 25th day of operation, reaching the maximum production of 250 mg L^{-1}, which was lower than that reported in reactor R1. Peixoto et al. (2015)[16] using kefir grains for hydrogen production from glycerol (30 g COD L^{-1}) detected butanol production of 271.5 mg L^{-1} at the end of reactor operation when hydrogen production collapsed. It is likely that inoculum based in kefir grains had similar limitations in this work and in the study by Peixoto et al. (2015)[16].

According to Figure 4, the reactor inoculated with heat-treated anaerobic consortium (R3) have not produced significant concentration of butanol despite one peak of 190 mg L^{-1} reported in the 21st day of operation when affluent and effluent pH were 6.8 and 4.1, respectively.

Overall, less butanol was produced at elevated biogas production (Figures 2-4). Otherwise, at lower biogas generation the butanol production tended to increase. A possible explanation is that most of the strict anaerobic microorganisms are unable to release molecular hydrogen from NADH, thus obligating its oxidation to NAD+ by means of metabolic products formation such as butyric acid, the main precursor of butanol (Braga et al., 2014)[19]. It is likely that hydrogen formation competes with butanol production by the oxidation of NADH to NAD+.

The highest butanol production achieved in this study was 0.6 g L^{-1} (R1), which is lower than those reported by Taconi et al. (2009)[20] and Ahn et al. (2011)[21]. However, in

the studies conducted by the abovementioned authors the fermentation for butanol production was performed at higher temperaratures (35-37°C) with pure culture (*C.*

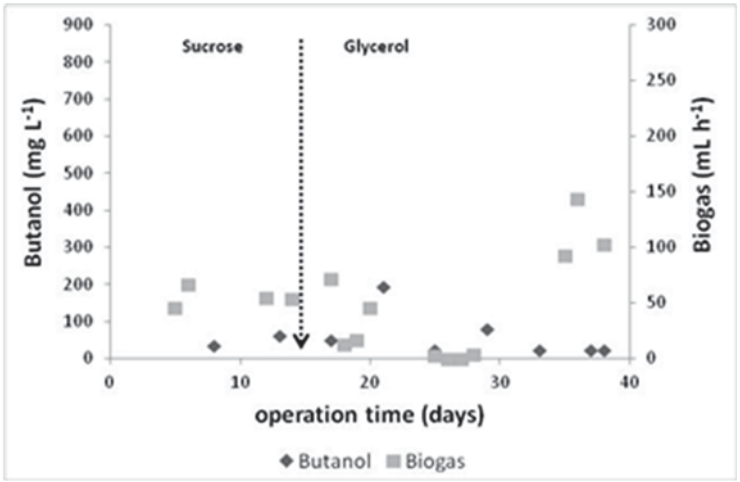


FIGURE 4. Butanol and biogas production in reactor R3

pasteurianum) in discontinuous operation. Moreover, in the study by Taconi et al. (2009)[20] nutritional supplementation was 40x higher ($FeSO_4$-$7H_2O$) than that utilized in this study.

Effect of different of OLR (2nd step). According to **Figure 5**, there was significant variation of butanol and biogas within the range of OLR evaluated.

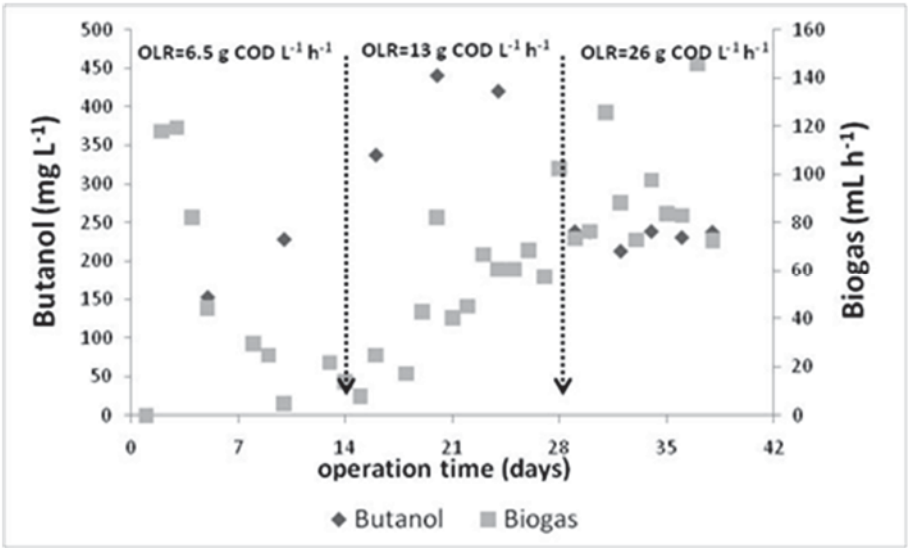


FIGURE 5. Butanol production at increasing OLR

In this reactor (R4) it was reported lower butanol production compared to R1 (**Figure 2**). Probably the absence of an “enrichment stage” with sucrose has influenced the result of R4. However, this system was inoculated with 20 g L^{-1} VSS from reactor R1.

According to the profiles of butanol and biogas in Figure 5, the increase in biogas production implied in the decrease of butanol production as observed for all previous operations (R1; R2; R3).

Figure 5 also depicts significant modification of butanol production profile between OLR of 6.5 to 26 g COD L^{-1} d^{-1}. Experimental data suggested that OLR of 13.0 g COD L^{-1} d^{-1} (HRT=60h) was more suitable for butanol production. A possible explanation involves the availability of butryric acid (data not shown). At OLR of 13.0 g COD L^{-1} d^{-1} it was observed the highest production of butyric acid while at the OLR of 6.5 g COD L^{-1} d^{-1} (HRT=120h) less than a half of butyrate concentration was detected. At the OLR of 26.0 g COD L^{-1} d^{-1} butyric acid generation likely decreased because excess of substrate. Possibly the biomass could not process all the organic matter and was inhibited.

Despite the relatively lower concentration of butanol, **Table 3** shows that other valuable metabolites were generated in R4 and could be used as raw material for chemical, pharmaceutical and food industries.

TABLE 3. Maximum concentrations of soluble metabolites generated in R4

Soluble metabolite	Concentration (mg L^{-1})
Acetic acid	499.0
Butyric acid	2090.9
Propionic acid	294.1
Acetone	270.0
Ethanol	3146.0

Acetate is employed as precursor of industrial polymers, especially vinyl acetate monomers, butyrate is utilized in industrial thermoplastics as cellulose acetate butyrate and propionate is used as food preservative.

CONCLUSION

Butanol was successfully produced from glycerol with mixed cultures. The inoculum source that presented the highest performance derived from sucrose auto-fermentation. Apparently, the continuous operation was useful to select butanol producing bacteria. Although the maximum yield achieved in this study was lower than those reported in the literature the innovative operation of continuous reactors with mixed culture figured as a promising alternative for butanol production. It was found an ideal range of organic loading rate for continuous bioreactors because significant differences in butanol production were observed with different OLR. The organic loading rate that enhanced the process was 13.0 g COD L^{-1} d^{-1}. Further optimization studies are necessary but the results of this work pointed to the feasibility of future process application in agro-industrial biorefineries because of the simultaneous production of other valuable metabolites.

ACKNOWLEDGMENTS

The authors thank PADC process 52/14 for supporting this research.

REFERENCES

1. Ramey, D.; Yang, S. Production of butyric acid and butanol from biomass. Final report to the US Department of Energy, Morgantown, 2004.
2. Da Silva, G.P.; Mack, M.; Contiero, J. Glycerol: A promising and abundant carbon source for industrial microbiology, Biotechnology Advances, v.27, p.30-39, 2009.
3. Temudo, M.F.; Poldermans, R.; Kleerebezem, R.; Van Loosdrecht, M.C.M, – Glycerol fermentation by (open) mixed cultures: A chemostat study. Biotechnology and Bioengineering 100(6), 1088-1098, 2008.
4. Khanna, S.; Goyal, A.; Moholkar, V. S. Production of n-butanol from biodiesel derived crude glycerol using *Clostridium pasteurianum* immobilized on Amberlite. Fuel. DOI:10.1016/j.fuel.2011.10.071.
5. Gallardo, R. A.; Rodrigues, L. R.; Alves, M. M. New strategies for the production of butanol. Abstracts Book of the 3rd MIT Portugal Conference - Excellence in Engineering for Innovation in Global Markets. Guimarães, Portugal, May 28-29, 22, 2012.
6. Yadav, S.; Rawat, G.; Tripathi, P.; Saxena, R.K. A novel aproach for biobutanol production by *Clostridium acetobutylicum* using glycerol: A low cost substrate. Renewable Energy. 71, 37-42, 2014.
7. Witthuhn, R.C.; Schoeman, T.; Britriz, T.J. – Characterization of the microbial population at different stages of kefir production and kefir grain mass cultivation. Intenational Dairy Journal, 15(4), 383-389, 2005.
8. Gulitz, A.; Stadie, J.; Wenning, M.; Ehrmann, M. A.; Vogel, R. F. The microbial diversity of water kefir. International Journal of Food Microbiology. 151:284-288, 2011.
9. Lazaro, Carolina Zampol. Influência da concentração de substrato e da temperatura na produção de hidrogênio a partir de vinhaça de cana-de-açúcar. 2012. Tese (Doutorado em Hidráulica e Saneamento) - Escola de Engenharia de São Carlos, Universidade de São Paulo, São Carlos, 2012. Disponível em: <http://www.teses.usp.br/teses/disponiveis/18/18138/tde-19102012-154700/>. Acesso em: 2016-01-31.
10. Penteado, E. D.; Lazaro, C. Z.; Sakamoto, I. K.; Zaiat, M. Influence of seed sludge and pretreatment method on hydrogen production in packed-bed anaerobic reactors. International Journal of Hydrogen Energy, 38, 6137-6145, 2013.
11. Lucas, S. D. M.; Peixoto, G.; Mockaitis, G.; Zaiat, M.; Gomes, S. D. Energy recovery from agro-industrial waste-waters through biohydrogen production: Kinect evaluation and technological feasibility. Renewable Energy. 75, 496-504,2015.
12. Peixoto, G.; Saavedra, N. K.; Varesche, M. B. A.; Zaiat, M. Hydrogen production from soft-drink wastewater in na upflow anaerobic packed bad reactor. International Journey of Hydrogen Energy. 36, 8953-8966, 2011.
13. Fernandes, B. S.; Peixoto, G.; Albrecht, F. R.; Saavedra, N. K.; Zaiat, M. Potencial to produce biohydrogen from various wastewaters. Energy for Sustainable Development. 14, 143-148, 2010.
14. Gallardo, R. Butanol Production By *Clostridium pasteurianum* using biodesel derived crude glycerol. 2011.
15. Agnelli, J. A. B.; Peixoto, G.; Barboza, M. ; Innocentini, M. D. M. ; Zaiat, M. Avaliação da produção de hidrogênio e produtos solúveis a partir de glicerol em reator em batelada e contínuo.II Seminário

do Projeto Temático FAPESP - Produção de bioenergia no tratamento de águas residuárias e adequação ambiental dos efluentes e resíduos, 2012.

16. Peixoto, G.; Agnelli, J.A.B.; Mockaitis, G.; Ferreira, F. V.; Zaiat, M. Biohydrogen production using glycerol: from batch to continuous reactor. 14th World Congress on Anaerobic Digestion, - Vina Del Mar, Chile 15-18 NOV 2015 - Congress Proceedings (4 pages - full paper).
17. Silva, A. J.; Hirasawa, J. S.; Varesche, M. B.; Foresti, E.; Zaiat, M. Evaluation of support materials for the immobilization of sulfate-reducing bacteria and methanogenic archea. Anaerobe. 12:93-98, 2006.
18. Dourado, C. P. Relatório parcial do Projeto, Caracterização hidrodinâmica de um reator de leito fixo utilizado para a produção de biobutanol a partir de resíduo da produção de biodiesel. Redigido em 31/07/2015.
19. Braga, Adriana Ferreira Maluf. Produção de hidrogênio em reatores anaeróbios termofílicos. 2014. Tese (Doutorado em Hidráulica e Saneamento) - Escola de Engenharia de São Carlos, University of São Paulo, São Carlos, 2014. Disponível em: <http://www.teses.usp.br/teses/disponiveis/18/18138/tde-26052015-144012/>. Acesso em: 2016-01-29.
20. Taconi, K. A.; Venkataramanan, K. P.; Johnson, D. T. Growth and solvent production by *Clostridium pasteurianum* ATCC®6013TM utilizing biodiesel-derived crude glycerol as the sole carbon source. Environmental Progress & Sustainable Energy. 28:100-110, 2009.
21. Ahn, J.; Sang, B.; Um, Y. Butanol production from thin stillage using *Clostridium pasteurianum*. Bioresourse Technology. 102:4934-4937, 2011.

CHAPTER 1.9 EVALUATION OF DIFFERENT INOCULA FOR BIOBUTANOL PRODUCTION IN ANAEROBIC REACTOR USING BIODIESEL WASTE AS CARBON SOURCE

C. Silva (1); R. Salles (1); J. Bassan (1); R. Monti (1); ZM. Zaiat (2); B. Varesche (2) and **G. Peixoto ***(1)

(1) Univ. Estadual Paulista (UNESP), Rodovia Araraquara-Jaú, Km 1, Araraquara, Brazil
(2) University of São Paulo (USP), Avenida João Dagnone, 1100, São Carlos, Brazil

ABSTRACT

The search for alternative and clean energy sources is subject of major concern because oil is not renewable and frequently associated to negative environmental impacts caused by the increase of greenhouse effect. Thus, the development and application of technologies for processing organic raw materials and wastes is critical to supply the growing need for renewable fuels. Biobutanol is an alternative renewable fuel studied to work as an additive or replace gasoline because of similar energy density (29.2 MJ L^{-1}), octane number (87 %) and lower heating value (27.8 MJ L^{-1}). The attractive aspect of biobutanol production is that organic wastes can be used as raw materials for the anaerobic-solventogenic process. Glycerol derived from the transesterification process of biodiesel production is considered a promising carbon source for butanol generation due to large availability (10% w:w) and low cost. Another important factor associated to the price of biobutanol is the inoculum source. In case of mixed culture, the costs tend to decrease. Moreover, microbial consortia generally present efficient adaptation to different carbon sources, which allow the use of complex substrates such as industrial wastes.

In this context, the aim of this study was to evaluate the effect of different inoculum sources over butanol production from glycerol. For this purpose inocula made of kefir grains, sucrose auto-fermentation consortium and heat-treated anaerobic sludge were incubated in 2 L sealed glass flasks at 30 ºC with the nutrient media and organic matter (glycerol) concentration of 30 g L^{-1}, in terms of chemical oxygen demand (COD). Each consortium was cultivated in batch operation to reach 30 g L^{-1} of volatile suspended solids (VSS) before the utilization in the upflow anaerobic packed-bed reactor (UAPB). The UAPB reactor had 1 L useful volume and all operations were performed at an average organic loading rate (OLR) of 12 g COD L^{-1} d^{-1}. Kefir grains, sucrose auto-fermentation consortium and heat-treated anaerobic sludge produced 21.6, 57.0 and 16.4 mg of butanol per gram of COD, respectively. Besides butanol production, significant amount of ethanol (249.6 mg g^{-1} COD), acetate (14.3 mg g^{-1} COD) and butyrate (139.5 mg g^{-1} COD) were generated in the bioprocessing of glycerol by sucrose auto-fermentation consortium. Thus, the improvement of butanol production

---

*Author for correspondence: peixotog@fcfar.unesp.br

with inoculum derived from sucrose auto-fermentation and the generation of valuable organic acids coupled with biodiesel fabrication could be an alternative to transform conventional plants into advanced biorefineries.

Keywords: anaerobic; biobutanol; glycerol; inoculum.

INTRODUCTION

ABE fermentation. In this fermentation, acetate and butyrate are primary produced (acidogenesis). Then, a shift in the metabolic pathway of bacteria drives the production towards solvents (solventogenesis) such as acetone, butanol and etanol (Ramey et al., 2004). The increase in butyrate concentration and pH decrease to values under 5 are two critical factors that promote the shift from acidogenesis to solventogenesis.

Butanol is a valuable product because its wide utilization in the pharmaceutical and plastic industries. Moreover, the use as alternative to gasoline or additive is another promising application since it has physico-chemical properties similar to convetional fuels, as demonstrated in **Table 1**.

TABLE 1. Physicochemical properties of common vehicle fuels

Properties / Fuels	Gasoline	Butanol	Ethanol
Air-Fuel Ratio	14.6	11.1	9.0
Energy Density (MJ L^{-1})	32	29.2	19.6
Research Octane Number (%)	91-99	96	107
Vehicle Octane Number (%)	81-89	78	89

Glycerol. It is also known as glycerin (commercial products with glycerol concentration above 95%), and represents the main byproduct of vegetal and animal oils subjected to transesterification for biodiesel production[1]. The expansion of biodiesel production also reflected in the increase of glycerol availability (10% v/v of biodiesel) and caused a hard decrease in the market price of this raw material. The ANP (National Agency of Petroleum, Natural Gas and Biofuels) pointed to the current production of 176 million of liters per year, which is only 17% of total volume predicted by Brazilian government in the next years. One possible solution to overcome the environmental problem of biodiesel wastes and restore market price of glycerol is to employ it in the biotechnology industry as substrate for different bioproducts.

Glycerol is an interesting carbon source because it is a structural component of many lipids metabolized in same pathway of glucose, thus producing piruvate and its subsequent products[2]. This characteristic allows the utilization of glycerol as sole carbon and energy source[1].

Butanol production from glycerol. The fermentation of glycerol for butanol production from pure cultures has already been extensively described in the literature. However, there are few studies reporting the utilization of mixed cultures.

Khanna et al.[3] employed *Clostridium pasteurianum* cells immobilized in Amberlite to process glycerol in 250 mL batch flasks at pH 7,5 and 30°C. The maximum production was 0.35 g butanol g^{-1} of glycerol (5 days fermentation) at initial concentration of 25 g L^{1}.

Gallardo et al. (2012) also evaluated the performance of Clostridium pasteurianum over the conversion of glycerol to butanol. In the batch experiments of the abovementioned authors, the maximum production of butanol was 0.30 g butanol g^{-1} of glycerol at 37°C and initial substrate concentration of 5 g L^{-1}.

Yadav et al.[4] studied butanol production from glycerol employing *Clostridium acetobutylicum* in 500 mL batch flasks with initial cell concentration of 30 g SSV L^{-1}. The optimun conditions found in this study were temperature of 37°C, pH 6,5, initial glycerol concentraton of 35 g L^{-1}, 5% of yeast extract and medium supplementation with 6 g L^{-1} of Na_2CO_3.

In general, most of the researchers utilized pure cultures of *Klebsiella aerogenes*, *Clostridium butyricum* and *Clostridium pasteurianum*. As a consequence, the costs of scalling up the processes would have great impact over butanol market price. Aiming to reduce the production costs new studies are required to develop non-sterile operations and to use pure or mixed cultures[2].

Kefir grains. These symbiotic conglomerates are formed by bacteria and fungi utilized in the fermentation of milk and other substrates. The microbiologic composite varies according to strain, cultivation methods and substrate. Witthuhn et al.[5] and Gulitz et al.[6] stated that milk and water-based kefir are majority composed by lactic acid bacteria, yeast and non-lactic bacteria. However, most of non-lactic bacteria are found in water-based kefir, in which it is possible to find bacteria of genus *Clostridium* and *Klebsiella* that are known butanol producers.

Heat-treated anaerobic sludge. Poultry slaughterhouse wastewaters are nutritent-rich substrates treated by biological process in many industries, thus resulting in large diversity of anaerobic microorganisms. Previous studies aiming to obtain bioproducts from wastewaters have successfully employed this inoculum source. Zampol Lazaro[7] in a study involving hydrogen production from vinasse characterized the inoculum after thermal pretreatment and found mostly bacteria from genus *Clostridium* that had already been associated to butanol production. It is worth mentioning that this heat treated anaerobic sludge derived from poultry slaughterhouse wastewater was previously utilized in the works by Penteado et al.[8] and Lucas et al.[9] generating
Butyrate, which is the main precursor of butanol.

Sucrose auto-fermentation consortium. Peixoto et al.[10] evaluated biological hydrogen production using mixed culture obtained from sucrose fermentation. In their study bactéria from genus *Clostridium* and *Klebsiella* were found. Fernandes et al.[11] also performed biomolecular analysis inoculum made of hexose autofermentation and detected the presence of acidogenic bacteria from the genus *Clostridium*, which has the potential for hydrogen and butanol production from complex wastewaters including wastes from biodiesel production.

MATERIALS AND METHODS

Reactor. Three acrylic systems with internal diameter of 82mm and total volume of 2L were utilized in the bioprocessing of glycerol. The bed zone (290mm in height) was filled with support material based in low density polyethylene and presented useful volume of 1L. The feeding of the systems was performed by positive displacement pumps installed in the bottom of the reactors, as shown in **Figure 1**.

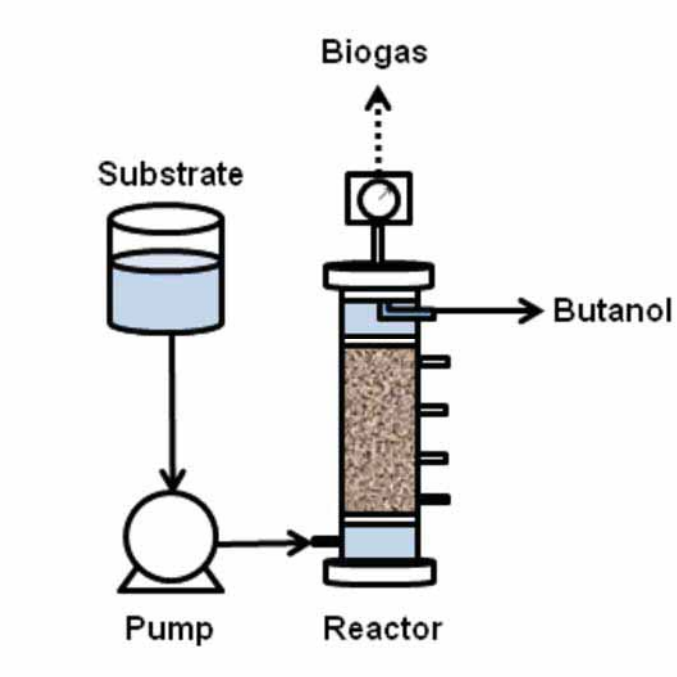


FIGURE 1. Experimental setup

Inoculation. Kefir grains were cultivated in medium containing sucrose solution with corresponding chemical oxygen demand (COD) of 30 g L^{-1}. The symbiotic conglomerates were incubated at 30°C for 24h, then the medium was completely replaced after solid fraction separation (biomass).

The consortium collected from the upflow anaerobic sludge blanket reactor (UASB) that was treating poultry slaughterhouse wastewater was subjected to thermal pretreatment. This treatment consisted in keeping the biomass at 90°C for 10 minutes with subsequent freezing in ice bath to eliminate the metanogenic archea and selection of spore-forming bactéria.

The biomass derived from sucrose autofermentation was supplemented with the same medium utilized by Peixoto et al.[10]. Biomass from this inoculum source was cultivated till reaching more than 30 g of VSS.

Support material. Low density polyethylene was employed as support for biomass growth. The immobilization particles had approximately 5:5:6 mm. This type of support was chosen because it is preferentially colonized by acidogenic bacteria, including those from *Clostridia* species.

Substrate. Glycerol was used as the carbon source in the range of 30 g L^{-1} COD, which was a non-saturating concentration already utilized in the study by Peixoto et al. (2015). It was also utilized the same nutritional medium of the abovementioned authors to provide the minimum requirements of other macro and micronutrients for bacterial growth. The pH control was made with sodium bicarbonate (500 mg L^{-1}) or hydrochloric acid (0.45 mL L^{-1}).

Analytical methods. Biogas flowrate was measured by a water displacement device similar to milligascounter (Ritter®). Volatile organic acids (VOA) and solvents were determined by gas chromatography (GC 2010 - Shimadzu®) equipped with Combi Pal headspace analyzer (AOC 5000) following the parameters described by Peixoto et al.[12].

Microscopic analysis of biomass was performed with a microscope Leica® DM LB coupled with a camera to execute frame capture for the software Image Pro Plus® versão 4.5.0.19.

Experimental procedure. The bioreactors were individually operated and labeled as:

- R1-Sucrose autofermentation consortium;
- R2-Kefir grains consortium;
- R3-Heat-treated anaerobic consortium.

The operation length of bioreactors was approximately 40 days and it was preceded by inoculation with the respective consortium following the ratio of 130,46 mg SSV g^{-1} of support, which was previously employed by Peixoto et al.[10]. The temperature of all operations was maintained at 30°C by water jackets involving the reactors. The feed flowrate was 18 mL h^{-1}, resulting in a hydraulic retention time (HRT) of 60h and organic loading rate (OLR) of 12 g COD L^{-1} d^{-1}.

All reactors were fed with sucrose up to their 14th day of operation as a strategy to enhance the process of cell growth and attachment to the support material.

RESULTS AND DISCUSSION

Hydrodynamic characterization. Dourado et al.[13] executed assays with three different flowrates to assess the hydrodynamic pattern of the reactor. The parameters analyzed were real HRT, number of CSTR and dispersion number. The results are presented in **Table 2**.

According to **Table 2**, plugflow pattern was maintained in all flowrates (N>12; low dispersion). Regarding the flowrate employed in this study, the parameters obtained were 68h, N=141 and D/uL=0.004 for HRT, number of CSTR and dispersion number, respectively.

TABLE 2. Hydrodynamics characterization parameters

Immobilization matrix	Bed porosity (%)	Flowrate (mL h^{-1})	Average HRT (h)	N (series of CSTR)	D.uL^{-1} (dispersion number)
polyethylene	50	17	69.38	141	0.004
polyethylene	50	34*	33.03	276	0.002
polyethylene	50	68	16.01	428	0.001

Butanol production with different inoculation. The analysis of Figure 2 indicated the absence of significant butanol production in reactor R1 up to the 16th day of operation, when sucrose was the carbon source.

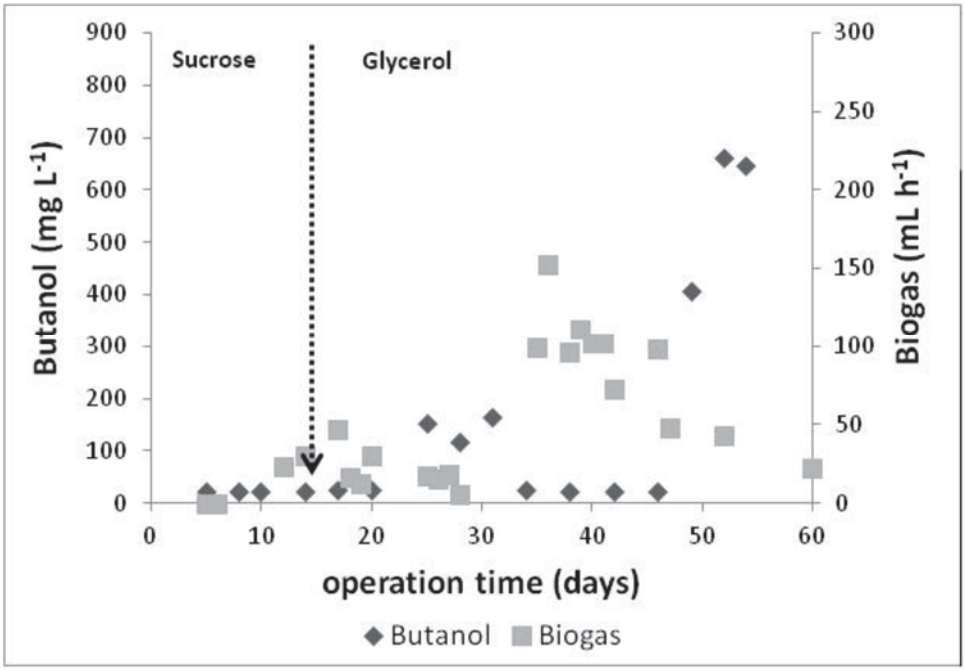


FIGURE 2. Butanol and biogas production in reactor R1

The beginning of butanol production was reported after the introduction of glycerol as carbon source. As observed in **Figure 2**, it was detected 150 mg L^{-1} of butanol from the 25th to the 31st day of operation. In this stage the effluent pH was 3.2 because there was not the addition of sodium bicarbonate. However, effluent pH set to 5.0 promoted the highest butanol production (660 mg L^{-1}) after the 45th day of operation.

According to Ramey et al.[14], 4.5 to 5.0 is the ideal range for butanol production because the shift from acidogenis to solventogenesis. It is likely that one of the factors influencing the yield of our process was also the pH range.

Reactor R2 using kefir grains as inoculum also presented low butanol production (**Figure 3**) in the stage that sucrose was the carbon source and the medium have not prepared with the buffer composed of sodium bicarbonate.

Butanol generation occurred at the 25th day of operation, reaching the maximum production of 250 mg L^{-1}, which was lower than that reported in reactor R1. Peixoto et al.[10] using kefir grains for hydrogen production from glycerol (30 g COD L^{-1}) detected butanol production of 271.5 mg L^{-1} at the end of reactor operation when hydrogen production collapsed. It is likely that inoculum based in kefir grains had similar limitations relative to the operational conditions in this work and in the study by Peixoto et al.[10].

According to **Figure 4**, the reactor inoculated with heat-treated anaerobic consortium (R3) have not produced significant concentration of butanol despite one peak of 190 mg L^{-1} reported in the 21st day of operation when affluent and effluent pH were 6.8 and 4.1, respectively.

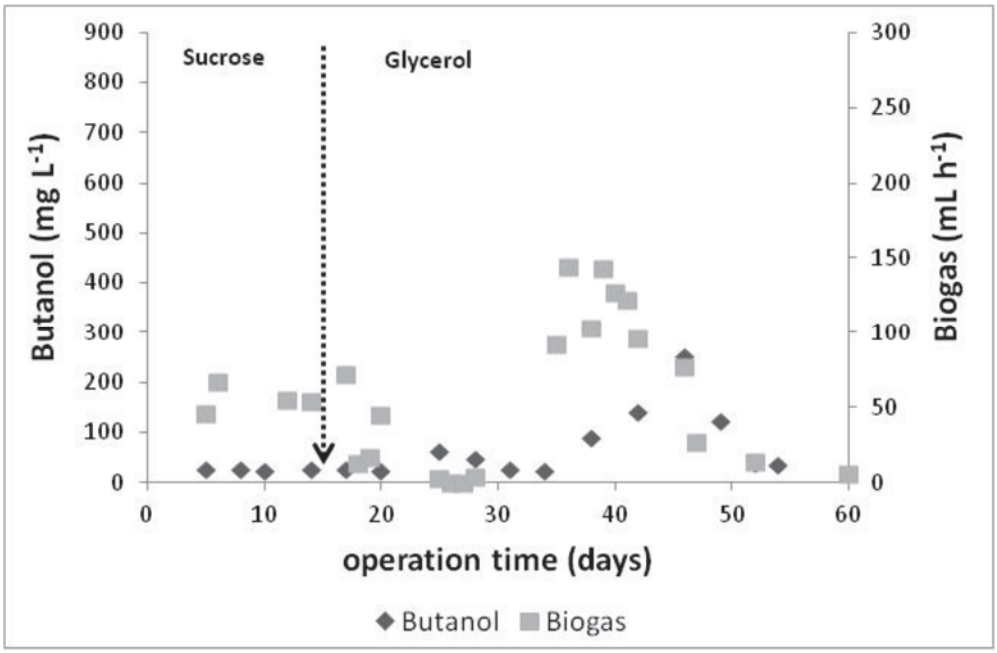


FIGURE 3. Butanol and biogas production in reactor R2

Overall, less butanol was produced at elevated biogas flowrate (Figures 2-4). Otherwise, at lower biogas flowrate the butanol production tended to increase. A possible explanation is that most of the strict anaerobic microorganisms are unable to release molecular hydrogen from NADH, thus it is necessary its oxidation to NAD+ by means of metabolic products formation such as butyric acid, the main precursor of butanol (Braga et al., 2014). It is likely that hydrogen formation competes with butanol production by the oxidation of NADH to NAD+.

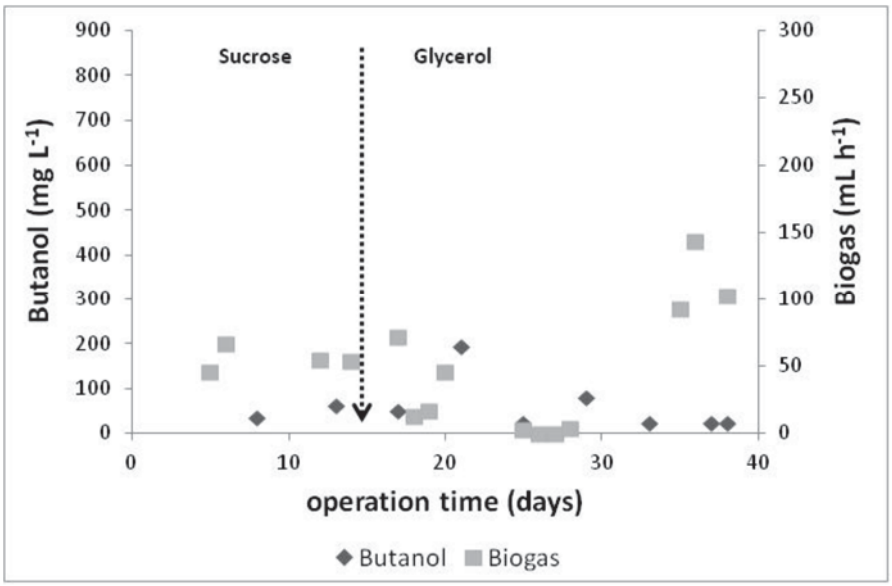


FIGURE 4. Butanol and biogas production in reactor R3

The highest butanol production achieved in this study was 0.6 g L^{-1} (R1), which is lower than those reported by Taconi et al.[15] and Ahn et al.[16]. However, in the studies conducted by the abovementioned authors the fermentation for butanol production was performed at higher temperaratures (35-37°C) with pure culture (*C. pasteurianum*) in discontinuous operation. Moreover, in the study by Taconi et al.[15] nutritional supplementation was 40x higher ($FeSO_4$-$7H_2O$) than that utilized in this study.

Despite the lower concentration of butanol, **Table 3** shows that other valuable metabolites were generated and could be used as raw material for chemical, pharmaceutical and energy industries.

TABLE 3. Maximum concentrations of soluble metabolites generated in the process

Soluble metabolite (mg L^{-1})	R1	R2	R3
Acetic acid	454,96	637,98	674,84
Butyric acid	2287,6	4468,92	2254,4
Propionic acid	46,32	1005,42	132,68
Acetone	27,1	12,06	25,26
Ethanol	3622,54	7547,38	977,24

The microscopic analysis of biomass at the end of the process suggests high diversity among the reactors, as shown in **Figure 5**.

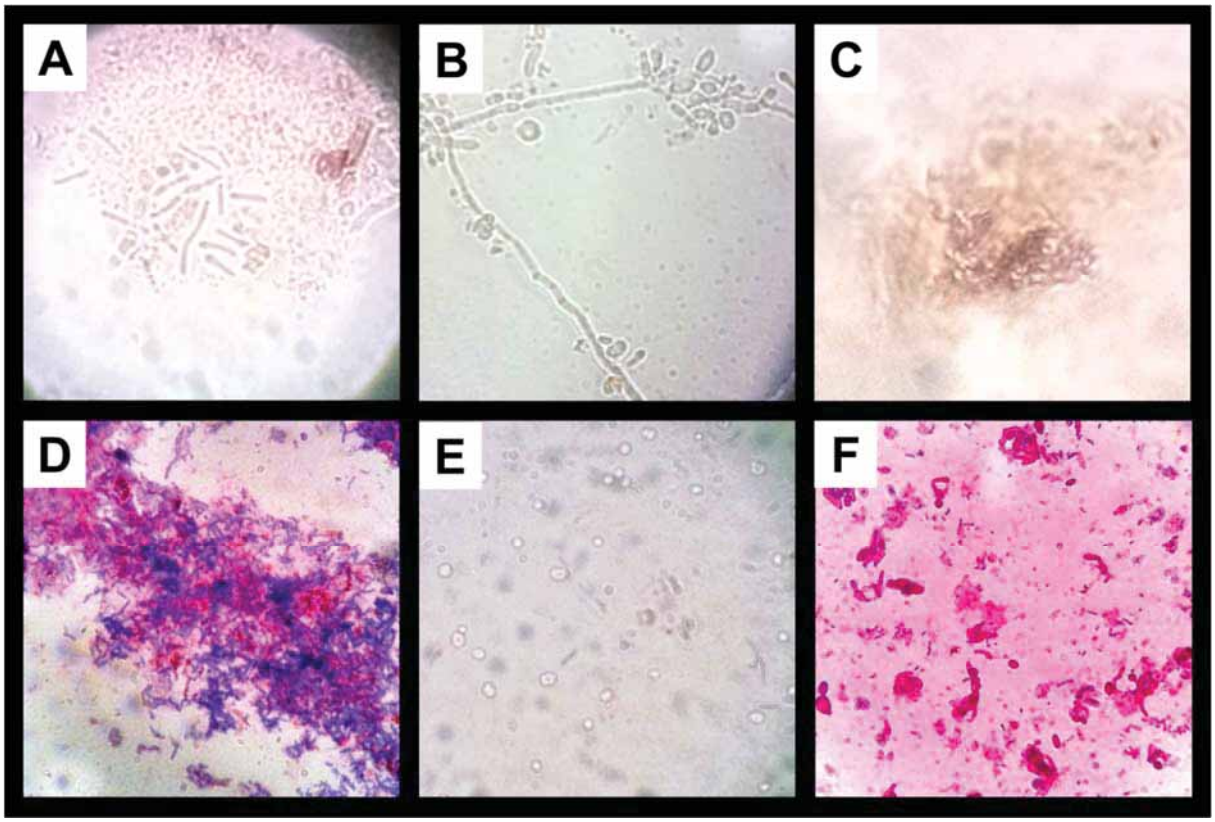


FIGURE 5. Microscopic analysis of biomass: (A) and (D) of reactor R1; (B) and (E) of reactor R2; (C) and (F) of reactor R3.

In reactor R1 (**Figure 5A**) it was mostly noticed bacillus morphologies. The presence of microorganisms related to butanol production was confirmed with the GRAM staining method. As seen in Figure 5B most of the bacillus morphologies were stained in violet blue, which indicates the plausible occurrence of GRAM positive bacteria from the genus *Clostridium.* This observation also supports the highest butanol production found in reactor R1.

The analysis of reactor R2 showed high diversity of morphologies. Some characteristics were typical of fugi and yeast, as demonstrated in Figures 5B and 5E. Possibly, yeast population have influenced the highest ethanol production among all systems, as reported in **Table 3**.

According to **Figure 5C**, bacillus shaped microorganisms were also found in reactor R3. However, GRAM staining did not reveal significant violet blue biomass, which would indicate the presence of some known butanol producers. Instead, morphologies similar to coccos were found in the observation of Figure 5F.

CONCLUSION

Butanol was successfully produced from glycerol with mixed cultures. The inoculum source that presented the highest performance derived from sucrose auto-fermentation. Apparently, the continuous operation was useful to select butanol producing bacteria. Although the maximum yield achieved in this study was lower than those reported in the

literature the innovative operation of continuous reactors with mixed culture figured as a promising alternative for butanol production. The utilization of mixed culture decreases the chance of contaminants predominance in the system, thus allowing the utilization of other wastewaters as carbon source for butanol production. Further optimization studies are necessary but the results of this work pointed to the feasibility of future process application in agro-industrial biorefineries.

ACKNOWLEDGMENTS

The authors thank PADC process 52/14 for supporting this research.

REFERENCES

1. Da Silva, G. P., Mack, M., Contiero, J. Glycerol: A promising and abundant carbon source for industrial microbiology. Biotechnol. Adv. 27 (2009) 30-39.
2. Temudo, M. F., Poldermans, R., Kleerebezem, R., Van Loosdrecht, M. C. M. Glycerol Fermentation by open mixed cultures: A chemostat study. Biotechnol. Bioeng. 100 (2008) 1088-1098.
3. Khanna, S., Goyal, A., Moholkar, V. S. Production of n-butanol from biodiesel derived crude glycerol using *Clostridium pasteurianum* immobilized on Amberlite. Fuel. 112 (2013) 557-561.
4. Yadav, S., Rawat, G., Tripathi, P., Saxena, R. K. A novel approach for biobutanol production by *Clostridium acetobutylicum* using glycerol: A low cost substrate. Renew. Energ. 71 (2014) 37-42.
5. Witthuhn, R. C., Schoeman, T., Britriz, T. J. Characterization of the microbial population at different stages of kefir production and kefir grain mass cultivation. Int. Dairy J. 15 (2005) 383-389.
6. Gulitz, A., Stadie, J., Wenning, M., Ehrmann, M. A., Vogel, R. F. The microbial diversity of water kefir. Int. J. Food Microbiol. 151 (2011) 284-288.
7. Zampol Lazaro C. Influência da concentração de substrato e da temperature na produção de hidrogênio a partir de vinhaça de cana-de-açucar. Escola de Engenharia de São Carlos, Universidade de São Paulo, 2012.
8. Penteado, E. D., Lazaro, C. Z., Sakamoto, I. K., Zaiat, M. Influence of seed sludge and pretreatment method on hydrogen production in packed-bed anaerobic reactors. Int. J. Hydrogen Energ. 28 (2013) 6137-6145.
9. Lucas, S. D. M., Peixoto, G., Gomes, S. D., Zaiat, M. Energy recovery from agro-industrial wastewaters through biohydrogen production: kinetic evaluation and technological feasibility. Renew. Energ. 75 (2015) 496-504.
10. Peixoto, G., Agnelli, J. A. B., Mockaitis, G., Ferreira, F. V., Zaiat, M. Biohydrogen production using glycerol: from batch to continuous reactor. Congress proceedings of 14th World Congress on Anaerobic Digestion (full paper), 2015.
11. Fernandes, B. S., Peixoto, G., Albrecht, F. R., Saavedra, N. K., Zaiat, M. Potential to produce biohydrogen from various wastewaters. Energ. Sustain. Develop. 14 (2010) 143-148.
12. Peixoto, G., Saavedra, N. K., Varesche, M. B. A., Zaiat, M. Hydrogen production from soft-drink wastewaters in an upflow anaerobic packed bed reactor. Int. J. Hydrogen Energ. 36 (2011) 8953-8966.
13. Dourado, C. P. Relatório parcial do Projeto: Caracterização hidrodinâmica de um reator de leito fixo utilizado para a produção de biobutanol a partir de resíduo da produção de biodiesel. Redigido em 31/07/2015.
14. Ramey D., Yang, S. Production of butyric acid and butanol from biomass. Department of Energy, Morgantown, Estados Unidos, 2004.

15. Taconi, K. A., Venkataramanan, K. P., Johnson, D. T. Growth and solvent production by *Clostridium pasteurianum* ATCC®6013™ utilizing biodiesel-derived crude glycerol as the sole carbon source. Environ. Prog. Sustain. Energ. 28 (2009) 100-110.
16. Ahn, J., Sang, B., Um, Y. Butanol production from thin stillage using *Clostridium pasteurianum.* Bioresource Technol. 102 (2011) 4934-4937.3
17. Ferreira Maluf Braga A. Produção de hidrogênio em reatores anaeróbios termofílicos, Escola de Engenharia de São Carlos, Universidade de São Paulo, 2014.
18. Gallardo, R. A., Rodrigues, L. R., Alves, M. M. New strategies for the production of butanol. Abstracts Book of the 3rd MIT Portugal Conference - Excellence in Engineering for Innovation in Global Markets. 22 (2012) 28-29.

CHAPTER 1.10 EXTRACTION OF CELLULOSE FROM USED DISPOSABLE DIAPERS FOR APPLICATION IN HYDROGENOGENIC DARK FERMENTATION

Perla X. Sotelo-Navarro (1); Héctor M. Poggi-Varaldo *(2); Sylvie J. Turpin-Marion (1); Rosa M. Espinosa Valdemar (1); Alethia Vázquez-Morillas (1); Mariana Nava-Ferreira (1) and Jesús G. Méndez-Silva (1)

(1) Department of Energy, Sustainable Technologies Area, UAM-A, Av. San Pablo #180 Col. Reynosa Tamaulipas, Ciudad de México, C. P. 02200, México
(2) Environmental Biotechnology and Renewable Energies Group GBAER-EBRE, Department of Biotechnology and Bioengineering, Centro de Investigación y Estudios Avanzados del IPN, P.O.Box 14-740, Ciudad de México, C. P. 07000, México.

ABSTRACT

The objective of this work was to extract the organic fraction (wood pulp cellulose) from used disposable diapers, which also contain super absorbent material (SAP), and plastics. It is believed that the presence of SAP and plastics can reduce the amount of biohydrogen produced in the dark fermentation process of a used diaper. Cellulose extraction was carried out by grinding the diapers, removal from the plastic and elastic parts, addition of water (1kg wet diapers: 10 L water) to the central portion (SAP-cellulose), and addition of $CaCl_2$ to reach a target concentration of 3000 mg/L of salt in the liquor were also carried out. The suspension was mixed for one day and filtered through a screen. The solids retained on the screen were composed by the calcium polymer (Ca-P) flocs and cellulose. These two fractions were manually separated, dried at 70 °C and stored.
The filtered solids consisted of 60% pulp and 40% of Ca-P (dry basis). The polymer can be reused in other processes such as water treatment, whereas the pulp can be fed to dark fermentation processes or another biological process. It can be concluded that this procedure is a feasible way for obtaining cellulose, which can be harnessed to the dark fermentation process with the subsequent production of biohydrogen. It is a significant step forward in the integration of waste disposable diapers management to modern biorefineries.

Keywords: calcium polymer, recycling, super absorbent, waste disposable diapers

INTRODUCTION

At the beginning of the new millennium, waste management has become a priority in many countries. One of the main problems today is to deal with an increasing amount of solid waste in an environmentally acceptable manner. Biowaste traditionally has been deposited in the disposal sites or even thrown into the sea, lakes or uncontrolled sites.

---

*Author for correspondence: r4cepe@yahoo.com

The treatment of organic waste by fermentation processes is an efficient way to convert it into useful, such as energy and fertilizer product, which allows the recycling of minerals and nutrients[1].

Among these wastes, disposable diapers represent a very important role because of its high generation. It is estimated that only in Mexico 7,517 tons of used diapers are discarded daily, corresponding to 6.52% of the total municipal solid waste (MSW)[2]. The design and composition of disposable diapers have changed considerably over the years. Its main components are cellulose, plastics (polyethylene and polypropylene) and a super absorbent polymer, sodium polyacrylate (SAP). There have been laboratory studies that led to various proposals for treatment and recovery of cellulose from used disposable diapers. Although the scale of the tests is small and most studies are focused on specific aspects, overall conclusions are positive.

For the production of H_2 is not recommended to use substrates with complex molecular structures because they are difficult to assimilate by microorganisms. However, a pretreatment of those complex substrates can improve its bioavailability H_2 producing bacteria[3].

The objective of this work was to extract the organic fraction (wood pulp cellulose) from used disposable diapers, which also contain superabsorbent material (SAP) and plastics, to make this waste a more readily degradable substrate in the dark fermentation process.

MATERIALS AND METHODS

To facilitate the separation of plastics a sample of disposable diapers was ground in a Vermeer BC 1000 grinder, and stored in a suitable container. The size of the diapers at the end of the process was approximately 5 cm x 5 cm.

Once the sample was ground, the plastic and elastic parts of the diapers were removed manually. Next, water was added to the central part, consisting mainly of cellulose pulp and SAP. $CaCl_2$ was incorporated to reach a target concentration of 3000 mg/L of salt in the liquor. The salt was used in order to dehydrate de SAP. In a 4 L beaker, 50 g of diaper were weighed and dispensed into the solution, which was stirred for 24 hours.

After 24 hours, the beaker solution was decanted and filtered. The solids (Ca-P flocs+ cellulose) were trapped in the filter, and their separation was performed manually. These two fractions were dried at 70 °C and stored. The test was run in triplicate.

According to differences between cellulose and Ca-P weights respect to the initial sample, it was obtained the percentage of recuperation of pulp cellulose (**Figure 1**).

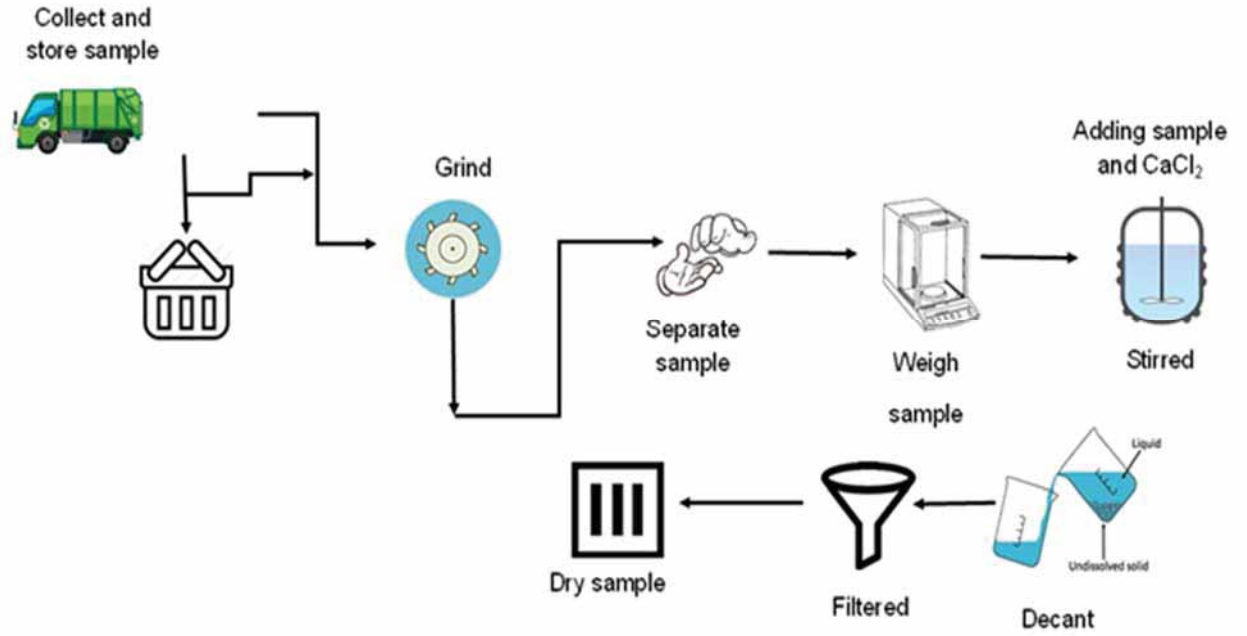


FIGURE 6. Diagram of the process

Subsequently the cellulose content in the separated wood pulp cellulose was measured. One gram of dried sample was mixed with 15 ml of 80% acetic acid and 1.5 ml of concentrated nitric acid. The mixture was kept on reflux for 20 min. Afterward, the solution was filtered, the residue was washed with ethanol, dried in oven at 100-105 ºC and weighed (A). Then it was incinerated at 540 ºC (B). Cellulose content was determined in accordance with van Soest and Wine (1967)[4].

$$\%\, Cellulose = \frac{(A - B)}{sample\ weight} * 100 \qquad (1)$$

RESULTS AND DISCUSSION

Figure 2 shows separately the components of used disposable diapers: the plastics, cellulose and Ca-P flocs formed by the reaction of sodium polyacrylate with $CaCl_2$. The efficiencies of recovery of wood pulp cellulose and Ca-P were 60 and 40% respectively, indicating that recovery wood pulp cellulose of used disposable diapers is feasible using this methodology.

It was found that contents of cellulose in the pulp were 85%, indicating that this substrate may be capable of being applied in the process of fermentation for the dark production of biohydrogen.



FIGURE 2. Disposable diaper separated by components (plastic, pulp cellulose and Ca-P)

CONCLUSION

Calcium chloride proved to be an efficient removal of SAP pulp salt, obtaining a dry basis recovery of 60%. In addition to the characteristics of the water used for the separation, it may be subjected to a process of anaerobic digestion to be treated, combined with the polymer-calcium (Ca-P) formed it can also be applied in the treatment of high nitrogen content wastewater.
The cellulose content in the pulp obtained recovered from used disposable diapers (85%), predicts that the pulp will function as a good substrate for hydrogen production by dark fermentation.

ACKNOWLEDGMENTS

The authors wish to thank the National Council of Science and Technology (CONACYT) for a graduate scholarship to PXS-N and support to CINVESTAV's infrastructure project 188221 of HMP-V. The excellent help of Professor Elvira Ríos Leal and Mr. Gustavo Medina (Central Analítica) as well as Mr. Rafael Hernández-Vera from the GBAER-EBRE Group, CINVESTAV del IPN, is gratefully acknowledged.

REFERENCES

1. Hajji A and Rhachi M. The Influence of Particle Size on the Performance of Anaerobic Digestion of Municipal Solid Waste. Energy Procedia 36 (2013) 515–520.
2. SEMARNAT, Secretaría de Medio Ambiente y Recursos Naturales Diagnóstico Básico para la Gestión Integral de los Residuos (2012), México, D. F.
3. Wang J. and Wan W. Factor influencing fermentative hydrogen production: A review. International Journal of Hydrogen Energy. 34:2 (2009) 799-811.
4. Van Soest, P.J., Wine, R.H. (1967). Use of detergents in the analysis of fibrous feed. IV. Determination on plant cell-wall constituents. *J. Assoc. Off. Anal. Chem.* 50:50-55.

CHAPTER 1.11 ENSAYO DE ACTIVIDAD METANOGÉNICA ESPECÍFICA: UNA HERRAMIENTA CLAVE PARA EVALUAR LA EFICIENCIA EN REACTORES ANAERÓBICOS

P. Bres *(1)**;** M. E. Beily (1); S. Costa (2); J. L. Avila (2); R. Candal (3) and D. Crespo (1)

(1) Instituto Nacional de Tecnología Agropecuaria, N. Repetto y de los Reseros S/N, Castelar, Pcia. Buenos Aires, Argentina.
(2) ALARALAB, Crisóstomo Álvarez 5515, Lugano, CABA, Pcia. Buenos Aires, Argentina
(3) Universidad Nacional de San Martin, CONICET, Instituto de Investigación e Ingeniería Ambiental, San Martin, Pcia. Buenos Aires, Argentina

RESUMEN

La actividad metanogénica específica (AME), evalúa la capacidad de un lodo en convertir un sustrato orgánico en metano. La eficiencia del tratamiento anaeróbico puede ser determinada mediante este tipo de *test*. El objetivo de este trabajo fue: a- evaluar la AME de lodos provenientes de diferentes fuentes; b- seleccionar y utilizar el lodo más activo como inóculo para el ensayo de potencial bioquímico metanogénico (PBM) de guano de aves ponedoras. A tal efecto, fue necesario como primera medida desarrollar el test, ajustando la metodología analítica y el procedimiento operativo a un diseño de reactores propio. Las muestras de lodos fueron recolectadas de diferentes fuentes de digestores anaeróbicos: residuos cítricos (RC), efluente porcino y residuos de forraje (PF), guano avícola (G1 y G2), efluente de la industria láctea (IL) y lodos de cervecería (PC1, PC2 y PC3). El volumen de biogás fue medido por método manométrico y su calidad (CH_4 y CO_2) por cromatografía gaseosa. Además, se determinaron variables fisicoquímicas al inicio y final del ensayo. Los resultados mostraron que los mayores valores de AME fueron encontrados en los lodos PC1, PC2 y PC3, (0,15, 0,10 y 0,10 gDQO/gSSV, respectivamente) y los % de remoción del carbono orgánico total (TOC) fueron superiores al 94% en promedio. El lodo PC1 presentó la mayor actividad de la biomasa, seleccionándose este lodo como inoculación para el tratamiento anaeróbico del guano de aves ponedoras.

Palabras clave: biogás, cervecería, lodos, metano

INTRODUCCIÓN

La cuantificación de la actividad de la biomasa, responsable de convertir el sustrato orgánico en CH_4, puede ser medida mediante el *test* de Actividad Metanogénica Específica (AME), donde se cuantifica la máxima velocidad de producción de metano bajo condiciones controladas[1, 2, 3, 4]. Esta herramienta es ampliamente utilizada para controlar y monitorear la capacidad metanogénica del reactor y consecuentemente para medir la eficiencia anaeróbica del sistema.

---

*Author for correspondence: bres.patricia@inta.gob.ar

Además, el *test* AME puede ser usado para evaluar la actividad de lodos durante diferentes tipos de operaciones de un sistema anaeróbico. Durante la etapa de arranque de un reactor, resulta relevante evaluar la evolución de la actividad del inóculo, y así determinar la máxima carga orgánica que puede ser aplicada al sistema[5,6,7]. Además, este test es ampliamente utilizado para estudiar los cambios morfológicos en la estructura granular del lodo y en la composición microbiana[7, 8, 9, 4].

Por otro lado, el monitoreo de la actividad metanogénica es utilizado para evaluar el comportamiento de lodos bajo el efecto de compuestos potencialmente tóxicos e inhibidores como ser sulfuro, metales, compuestos clorados, amoníaco, sodio y detergentes[10, 11, 12, 13, 14, 26]. Un cambio en la actividad del lodo determina una inhibición o acumulación de compuestos orgánicos de baja o nula biodegradabilidad[1].

Otras de las aplicaciones del *test* AME incluye la cuantificación de la afinidad de un grupo biológico a cierto tipo de sustrato y la determinación de parámetros operativos (temperatura, agitación) y cinéticos[15].

El *test* de biodegradabilidad anaeróbica o más conocido como potencial bioquímico metanogénico (PBM), mide la velocidad y el potencial de conversión de compuestos orgánicos a metano[1]. Para ello, un inóculo activo debe ser utilizado. La AME de este inóculo debe ser cuantificada y conocida antes del inicio del *test* PBM, asegurando así la optimización de la biodegradabilidad anaeróbica del compuesto orgánico. El volumen de inóculo a utilizar en el *test* PBM, está directamente relacionado con su actividad, demostrando así, la importancia de su cuantificación previa[27].

Numerosos trabajos han demostrado la aplicabilidad y la importancia del *test* AME. Sin embargo, no existe un protocolo estandarizado para su desarrollo. Los distintos protocolos varían en los procedimientos adoptados (tipo y concentración de sustrato, velocidad y tipo de agitación, temperatura, concentración de lodo, relación sustrato/lodo, tipo y concentración de nutrientes) y la metodología utilizada para cuantificar el biogás y el metano producido (método volumétrico, método manométrico, por cromatografía gaseosa, por sensor). La falta de consenso tanto en el procedimiento como en la metodología analítica dificulta la comparación entre los resultados[15, 16].

La propuesta de este trabajo fue evaluar la AME de lodos provenientes de diferentes fuentes. A tal efecto, fue necesario como primera medida desarrollar el test, ajustando la metodología analítica y el procedimiento operativo a un diseño de reactores propio. El lodo más activo será utilizado como inóculo en el *test* PBM de guano de aves ponedoras.

MATERIALES Y MÉTODOS

Lodos. Se recolectaron muestras de lodos, provenientes de digestores anaeróbicos, alimentados con distintos sustratos. Se realizaron 8 test AME, con los siguientes lodos:

RC: Reactor de mezcla completa, a 25 ºC, alimentado con residuos cítricos (escala industrial)

PF: Reactor de mezcla completa, a 35º C, alimentado en relación 3:1 con efluente porcino y residuos de forrajes (escala industrial).

G1: Reactor de polipropileno de mezcla completa, a 35ºC, alimentado 3 veces al día con guano de aves ponedoras (escala laboratorio, 20 l)

G2: Reactor en acero inoxidable de mezcla completa, a 35ºC, alimentado 3 veces al día con guano de aves ponedoras (escala laboratorio, 25 l).

IL: Primera laguna anaeróbica para el tratamiento de efluentes de la industria láctea (escala industrial).

PC1: Primer reactor de circulación interna (IC), a 35ºC, para la producción de cerveza (escala industrial).

PC2: Segundo reactor de IC, a 35ºC, para la producción de cerveza (escala industrial).

PC3: Segundo reactor de IC, a 35ºC, para la producción de cerveza (escala industrial).

Las muestras de lodos fueron caracterizadas inicialmente y luego almacenadas a 4ºC hasta su uso.

Diseño de los reactores. Los reactores fueron construidos con frascos de vidrios y tapas especiales, diseñadas para asegurar las condiciones anaeróbicas del sistema. Cada reactor consta de un frasco de vidrio borosilicato transparente de 560 ml, con inercia química entre el medio y el vidrio y resistente a altas temperaturas (hasta 135 ºC) y presiones (hasta 1,5 bar). La tapa fue construida de material polipropileno, a rosca con un *o-ring* interno para favorecer el cierre hermético. Cada tapa posee en el centro una llave de acero inoxidable con válvula esférica, acoplada a un conector neumático. La apertura de la válvula, permitirá cuantificar y analizar la calidad del biogás generado (**Figura 1**).

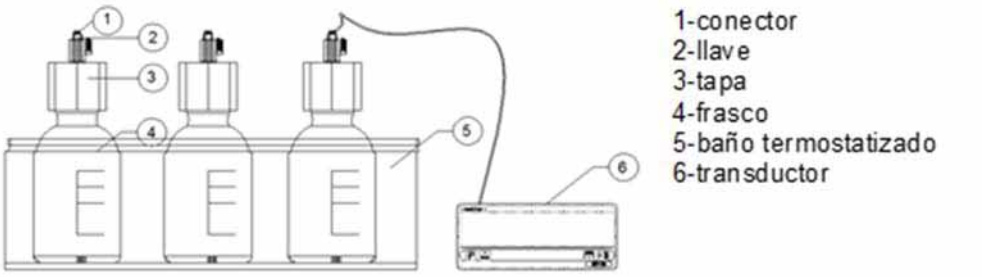


FIGURA 1. Sistema de reactores en Batch

Procedimiento experimental. Para el desarrollo del *test*, se fijó 20% de espacio de cabeza (*headspace)*, una concentración de 4 gSSV/L de lodo, un volumen efectivo de 448 mL y 2 g DQO/L de acetato de sodio como única fuente de carbono. Estas variables fueron ajustadas en función a metodologías descriptas por varios autores[17, 18, 15, 16] y el grupo BIOPROA de la Facultad de Ingeniería de la Universidad de la República del Uruguay (Uruguay).

Previamente al ensayo, las muestras de lodo fueron incubadas a 35ºC en un reactor de 2 L, con la llave abierta, durante 4 días. Este procedimiento se realizó para asegurar el consumo de la DQO residual del lodo.

Las muestras de lodo fueron diluidas con una solución stock de macro y micronutrientes hasta alcanzar 4g SSV/L (**Tabla 1**).

El volumen de lodo y de acetato de sodio se ajustaron a pH 7 con solución NaOH 6 N o solución 0,5 N HCl, según corresponda. Se agregó el volumen de lodo neutralizado a

cada reactor y luego la solución de acetato de sodio 2gDQO/L (57 mL). Se registró el pH final de la mezcla y se cerró inmediatamente. Luego, se barrió el O_2 presente en el reactor con una corriente de gas N_2 (25 psi de salida) hasta alcanzar 1 bar en su interior. El reactor presurizado fue sumergido en agua para comprobar la ausencia de pérdidas de gas. Asegurada la hermeticidad, se despresuriza hasta presión atmosférica y se repitió 3 veces este procedimiento. Los reactores fueron incubados a 35±1ºC mediante un baño termostático. La agitación se realizó manual, durante 1 minuto dos veces al día.

TABLA 1. **Solución stock de macro y micronutrientes**

Macro-nutrientes (10 mL/Ll)	**Concentración (g/L)**	**Micro-nutrientes (1 mL/L**	**Concentración (g/L)**
NH_4Cl	17	$FeCl_2.\ 4H_2O$	2,0
K_2HPO_4	3,70	H_3BO_3	0,05
$MgSO_4$	0,56	$ZnSO_4.H_2O$	0,07
$CaCl_2.2H_2O$	0,80	$CuCl_2.2H_2O$	0,04
		$MnCl_2.4H_2O$	0,05
		$(NH_4)_6Mo_7O_2.4H_2O$	0,05
		$CoCl_2.6H_2O$	0,05
		$NiCl_2.\ 6H_2O$	0,09
		EDTA	0,50
		HCl 36%	1 ml/L
		Na_2SeO_3	0,07
		Resazurina	0,50

Cada tratamiento fue realizado por triplicado. El blanco control se realizó con la muestra de lodo, sin el agregado del acetato de sodio y bajo las mismas condiciones que el tratamiento.

Determinaciones analíticas. Los lodos y las muestras del ensayo fueron caracterizados mediante la determinación de variables fisicoquímicas. Se analizaron las variables pH, sólidos suspendidos volátiles (SSV) y demanda química de oxígeno (DQO), según métodos normalizados[19]. Además, se determinó carbono orgánico total (TOC) en la muestra filtrada previamente con membrana de nitrocelulosa 0,45 µm. Se utilizó el equipo analizador *Shimadzu* (modelo TOC-L), el cual se basa en la oxidación catalítica a 680 °C donde todo el carbono orgánico presente en la muestra se oxida a CO_2. Este CO_2 es medido mediante un detector de infrarrojos no dispersivo (NDIR). La muestra se acidifica previamente en el equipo con ácido clorhídrico y se burbujea aire analítico libre de CO_2 para eliminar el carbono inorgánico.

El volumen de biogás se determinó mediante la presión generada en el *headspace* del reactor, utilizándose un transductor de presión (0-2,5 bares). Luego, la muestra de gas fue inyectada en el cromatógrafo de gases (Hewlett Packard 5890 GC) para determinar los porcentajes de CH_4, CO_2 y N_2, acorde a metodología estandarizada (ASTM D 1945). La inyección de la muestra en el equipo se realizó por conexión de la

válvula del reactor al LOOP de 0,25 m^3. Se utilizó la columna Tamiz Molecular 13 X, el detector de conductividad térmica TCD y gas Helio como *carrier* a una velocidad de flujo de 78 ml/min. Las temperaturas fueron de 90ºC, 130ºC y 250ºC para la columna, inyector y detector respectivamente.

Una vez medido el volumen de biogás y metano, el reactor fue despresurizado, llevándolo a presión atmosférica (P=1,013 bares).

Cálculos. El gas en el *headspace* es básicamente ocupado por tres gases: N_2, CO_2 y CH_4. El nitrógeno es el resultado del barrido para garantizar una atmósfera anaeróbica, mientras que el resto de los gases (CO_2, CH_4) representan la degradación anaeróbica del sustrato. Por lo tanto, la diferencia de presión es el volumen de biogás generado, donde el contenido de N_2 queda excluido de los cálculos. El volumen de biogás (NV_{biogas}) fue calculado acorde a la Ley de los Gases Ideales y corregido a condiciones normales de presión y temperatura (CNPT a 0ºC y 1 atm) mediante la siguiente fórmula:

$$\mathrm{NV_{biogas}} = \frac{(P1 + P2) \times Vg \times 273}{P1 \times (273 + T)} \quad (1)$$

Donde: P1= 1,013 bar, P2= presión (bar) medida por el transductor, Vg = volumen de la cámara de gas (112 ml), T= temperatura de trabajo en ºC, 273= temperatura a 0 ºC en unidad de Kelvin. El volumen de CH_4 producido (NV_{CH4}), se calculó multiplicando el volumen de biogás por el % de CH_4 obtenido por cromatografía gaseosa y normalizado.

La AME de cada lodo, se calculó mediante la siguiente fórmula:

$$\mathrm{AME\ (gDQO/\ gSSV.d)} = \frac{\mathrm{R}}{\mathrm{fc\ x\ SSV}} \quad (2)$$

Donde: R= la pendiente máxima de la curva de producción acumulada de metano en el tiempo y representa la velocidad de producción de metano por día (mlCH4/d), fc= equivalencia para transformar el volumen de metano en gDQO, considerando que 1gDQO = 350 ml de CH_4, en CNPT[20]; SSV= contenido de biomasa agregado al inicio del ensayo (gramos).

El análisis estadístico fue realizado por el programa INFOSTAT (Versión 2014). El test de Tukey fue utilizado para comparar los valores de AME entre los distintos lodos y para los valores fisicoquímicos obtenidos en cada lodo al inicio y al final del ensayo (nivel de confianza del 95%). Se calculó, además, el coeficiente de varianza y desvío estándar en los valores de AME para cada lodo.

RESULTADOS Y DISCUSIÓN

La caracterización inicial de los ocho lodos se muestra en la **Tabla 2**. En general, los lodos presentaron valores básicos de pH, exceptuando los de cervecería PC2 y PC3, con valores neutros, y los de la industria citrícola, con un valor inferior al neutro. El rango óptimo para las bacterias metanogénicas es de 6,5-7,5 [21]. Para favorecer la actividad de las metanogénicas y evitar la inhibición del proceso, será necesario ajustar el pH a neutro en los lodos al inicio del ensayo.

La concentración de sólidos suspendidos volátiles representa la biomasa en el lodo. El conocer esta variable es importante para definir la concentración inicial de biomasa en el test AME, ya que afectará la velocidad de degradación del sustrato disponible[16]. Para mantener iguales condiciones iniciales, los ocho lodos fueron diluidos hasta alcanzar los 4 gSSV/L.

Al final del ensayo se determinaron las variables pH, SSV y el porcentaje de remoción de TOC (%R TOC), mostradas en la **Tabla 3**. En cuanto al pH ninguno de los lodos evaluados mostró valores de pH ácidos, asegurando así que no hubo acidificación del sistema durante el proceso degradativo anaeróbico. Por el contrario, el pH se incrementó con respecto al valor inicial (pH neutro) en todos los casos. La alcalinización del sistema podría deberse al agotamiento del sustrato (acetato) y consecuentemente a la falta de alimentación para las bacterias metanogénicas[22].

TABLA 2. Caracterización fisicoquímica de lodos

Lodo	pH	SSV (g/L)	TOC (mg/L)	DQO (g/L)
RC	6,87 ± 0,04	23,4 ± 0,5	1100 ± 120	22,1 ± 1,1
PF	7,91 ± 0,01	10,5 ± 0,7	409,4 ± 0,5	8,6 ± 0,4
G1	8,34 ± 0,01	15,9 ± 0,7	275,9 ± 0,4	24,3 ± 1,5
G2	7,5 ± 0,01	8,6 ± 0,3	698,9 ± 14,4	
IL	7,71 ±0,01	8,5 ± 0,5	53,3 ± 0,0	13,3 ± 0,3
PC1	7,85 ± 0,07	57,9 ± 1,8	1017	25,6 ± 1,4
PC2	7 ± 0,0	49,1 ± 0,8	243,41	
PC3	7,1 ± 0,0	46,6 ± 4,4	287,61	

El valor medido de SSV al inicio del ensayo fue de 3,85 ± 1,10 g/L en promedio para todos los lodos evaluados. En general, los valores de SSV se mantuvieron constantes en todos los tratamientos. Sin embargo, G2 mostró diferencias significativas ($p<0,05$) entre el inicio y el final del ensayo (3,97 ± 0,14 gSSV/L Vs 1,47 ±0,20 gSSV/L). Esta caída de los SSV reflejó una disminución de la biomasa, mostrando el comienzo de la fase endogénica. James *et al*. (1990), también observó una leve disminución de la biomasa en sus 5 experiencias realizadas.

La conversión de la materia orgánica en CH_4 puede verse reflejada en la disminución del TOC al final del ensayo. Los mayores %R TOC fueron observados en los lodos de cervecería (PC1, PC2 y PC3), con valores superiores al 93 %. La elevada degradación del sustrato evidenció una alta actividad de los lodos.

TABLA 3. % de Remoción del TOC (%R), pH y SSV obtenidos en cada tratamiento al final del *test*

	pH	SSV (g/L)	%R TOC
RC	7,40 ± 0,09	4,49 ± 0,12	77,4
PF	7,37 ± 0,04	2,99 ± 0,23	61,8
IL	7,77 ± 0,12	4,1 ± 0,24	91,5
G1	7,39 ± 0,05	4,12 ± 0,24	89,0
PC1	7,70 ± 0,0	5,02 ± 2,41	93,3
PC2	7,90 ± 0,10	4,60 ± 1,42	94,9
PC3	7,76 ± 0,0	5,21 ± 0,74	94,5
G2	7,70 ± 0,0	1,47 ± 0,20	52,7

En la **Figura 1a** y **1b** se muestra la curva de producción de metano acumulada y la AME respectivamente, para los diferentes lodos evaluados.

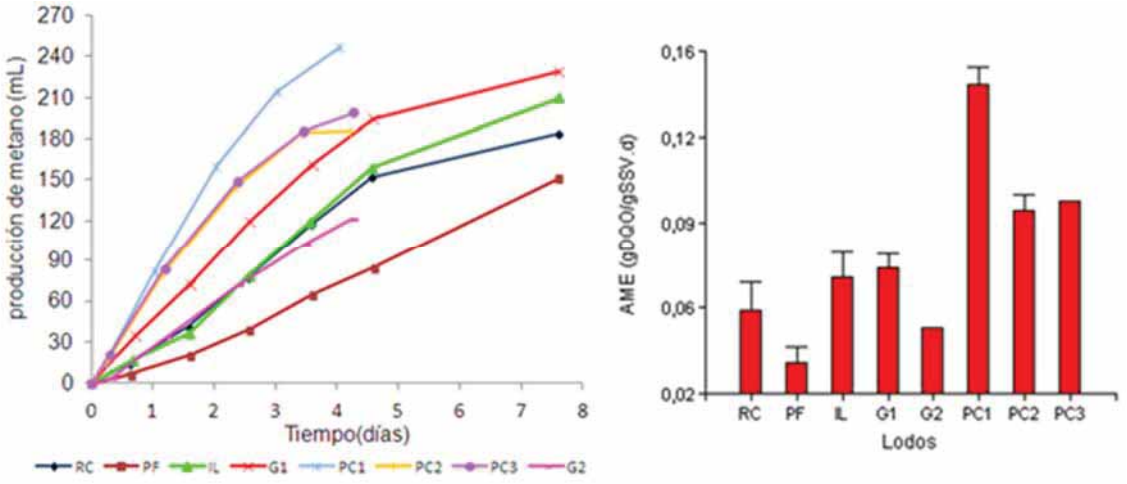


FIGURA 1. Producción de metano acumulada en el tiempo (a) y la AME en gDQO/gSSV.d (b) para los diferentes lodos evaluados

Los lodos de cervecería (PC1, PC2 y PC3), mostraron la mayor velocidad de producción (mayor pendiente) en el primer y segundo día del ensayo. Por otro lado, los lodos IL y PF presentaron una mayor fase lag, donde la mayor velocidad de producción se produjo entre los días 2 y 5 (**Figura 1a**). Estas diferencias en el tiempo de respuesta a la degradación del sustrato, podrían deberse a las distintas características del lodo.

Se calculó la AME, expresada como gDQO/gSSV.d, con los valores de la máxima pendiente obtenida (**Figura 1b**). Los coeficientes de varianza (CV) en los valores AME fueron bajos, siendo de 7,9% para G1, 0% para G2, 14,3% para IL, 4,9% para PC1, 6,0% para PC2, 0% para PC3, 0% para PF y 15,6% para RC. Los bajos valores obtenidos de CV reflejaron la buena reproducibilidad del *test*.

Los máximos valores fueron encontrados en PC1, PC2 y PC3 siendo 0,15, 0,10 y 0,10 gDQO/gSSV.d respectivamente. Estos valores fueron significativamente superiores que los

demás lodos evaluados ($p<0,05$). Estos lodos presentaron características de lodo granular. Varios trabajos han demostrado que existe una relación directa entre la formación de gránulos y la actividad. Los lodos granulares de mayor densidad y tamaño presentan mayor actividad de la biomasa, observándose valores altos de AME[8, 9, 23]. Shao y colaboradores (2008) utilizaron un reactor piloto discontínuo secuenciado (ASBR) para el tratamiento de las aguas residuales de cervecería. El reactor fue inoculado con un lodo floculento proveniente de un reactor UASB, donde el AME (acetato como sustrato) fue de 0,108 gDQO/gSSV.d durante la etapa de arranque del reactor. Luego de 60 días de operación, el AME fue de 0,721 gDQO/gSSV.d, asociando este valor alto a la granulación del lodo. Fang *et al* (1994) comparó la AME y la microestructura granular para tres tipos de lodos provenientes de reactores UASB. El lodo de cervecería presentó un valor de 0,49 gDQO/gSSV.d (acetato como sustrato). Los valores de AME para los lodos de cervecería encontrados en este trabajo, fueron inferiores a los reportados por Shao y Fang.

La comparación entre los resultados de AME para un mismo tipo y fuente de lodo resulta difícil, debido a la ausencia de un protocolo estandarizado y a los diversos factores que afectan el desarrollo del test (metodología de análisis y procedimiento aplicado). Además, existen otras variables como edad del lodo, densitometría y tamaño granular que influyen en la actividad de la biomasa. Sin embargo, debido a que en este trabajo el procedimiento y la metodología analítica aplicada para la determinación de la AME fue la misma en los 8 lodos, es factible la comparación entre los mismos.

Por otro lado, la máxima velocidad de producción (pendiente de la recta) y consecuentemente la AME podría estar subestimada en este tipo de lodos (PC1, PC2 y PC3), debido a la falta de mediciones de metano durante las primeras horas del *test*. En general, los lodos granulares o floculentos presentan la mayor actividad durante las primeras 4-10 horas del ensayo[17, 18].

Los menores valores de AME fueron 0,04 y 0,05 gDQO/ gSSV.d en el PF y G2 respectivamente. Los lodos de PF y G2 fueron recolectados a los 7 y 9 meses de funcionamiento del reactor, respectivamente. Estos valores bajos de actividad podrían estar asociados a que ambos lodos son jóvenes, encontrándose en la etapa de adaptación al sustrato. Por otro lado, PF y G2 provienen de reactores alimentados con compuestos ricos en nitrógeno (efluente porcino y guano de aves ponedoras respectivamente). Los compuestos nitrogenados podrían inhibir el proceso de digestión anaeróbica[24, 25]. Por lo tanto, la baja AME en PF y G2 podría deberse a una inhibición del sistema. Se requieren mayores estudios para determinar la causa de la baja actividad encontrada en estos lodos.

Por otro lado, se observó que la AME en G1 fue significativamente superior que G2 ($p<0,05$). Si bien ambos reactores fueron alimentados y mantenidos bajo las mismas condiciones ambientales y de operación, la edad del lodo fue diferente (2 años y 9 meses para G1 y G2, respectivamente). Además, la mayor actividad encontrada en G1, podría deberse a una adaptación de la biomasa a elevadas concentraciones de compuestos nitrogenados. Los valores de AME para este tipo de lodos fueron similares a los encontrados por Field (1987), quien describió que el valor de AME para estiércoles digeridos se encuentra entre 0,02 y 0,08 gDQO/gSSV.d.

CONCLUSIÓN

En cuanto al desarrollo del test, la buena reproducibilidad entre las réplicas demostró que se trabajó con un diseño de reactores hermético y con un sistema de medición del volumen y calidad del biogás altamente precisos. Sin embargo, para la optimización del test, dos modificaciones podrían ser incluidas en futuros ensayos: a) La agitación podría mejorarse utilizándose un sistema de agitación orbital y regulando la intensidad y el tiempo de la mezcla, ya que estas variables podrían afectar la actividad metanogénica de la biomasa. Souto *et al* 2010 recomienda la agitación orbital continua para el desarrollo del *test*; b) Aumentar el número de muestreos de volumen y calidad de biogás durante las primeras horas del ensayo, principalmente cuando se desee conocer el valor de la AME en lodos granulares o floculentos. Esto podría evitar una subestimación de la máxima pendiente encontrada en la producción de metano.
Por otro lado, los resultados mostraron que la máxima actividad metanogénica específica fue encontrada en los lodos de cervecería, principalmente en el PC1, con una rápida y eficiente remoción del sustrato. Debido a estas características, el lodo PC1 será el inóculo más óptimo para el tratamiento anaeróbico del guano de aves ponedoras.

REFERENCIAS

1. Hussain A., Dubey S.,K. Specific methanogenic activity test for anaerobic degradation of influents. Appl. Water Sci. (2015)
2. Soto M., Méndez R., Lema, J.M. Methanogenic and non- methanogenic activity test. Theoretical basis and experimental set up. Water Reserch. 27, 8 (1993) 1361 -1376.
3. Monteggia L. Proposta de metodología para avaliaçao do parámetro “actividade metanogenica específica”. In Proceeding: XIX Congreso de Engenheria Sanitária e ambiental. Foz do Iguaçu. (1997) 754-766.
4. Sorensen A. H., Ahring, B. K. Measurements of the specific methanogenic activity of anaerobic digestor biomass. Appl. Microbiol. Biotechonl 40 (1993) 427-431.
5. Chernicharo C. Princípios do tratamento biológico de águas residuárias: Reatores Anaeróbios. Belo Horizonte. *Departamento de Engenharia Sanitária e Ambiental (DESA/UFMG),* Vol. 5 245 p. 1997.
6. Ince O, Anderson GK, Kasapgil B. Use of the specific methanogenic activity test for controlling the stability and performance in anaerobic digestion of brewery wastewater. In: Proceedings of the 49th Purdue Industrial Waste Conference; 1994.
7. Jawed M., Tare V. Microbial composition assessment of anaerobic biomass through methanogenic activity test. Water S.A 25, 3 (1999) 345-350.
8. Jijai S., Srisuwan G., O-Thong S., Ismail N., Siripatana C. Specific Methanogenic Activities (AME) and biogas production of different granules size and substrates. In: Proceedings of the 1 st Environmental and natural Resources International Conference, 2014.
9. Fang H. H. P., Chui H. K., Li Y. Y. Microbial structure and activity of UASB granules treating different wastewaters. Water Science and Technology 30, 12 (1994) 87-96.
10. kouzeli-Katsirl A., Kartsonas N., Priftis A. Assessment of the toxicity of heavy metals to the anaerobic digestion of sewage sludge. Environ. Technol. Lett 9 (1988) 261-270.
11. Koster I. W. Rinzema A., De Vegt A. L., Lettinga G. Sulfide inhibition of the methanogenic activity of granular sludge at various pH-levels. Water Research 20, 12 (1986) 1561-1567.

12. Hickey R. F., Vanderwielen, J., Switzenbaum M. S. The effect of heavy metals on methane production and hydrogen and carbon monoxide level during batch anaerobic sludge digestion. Water Research 23 (1989) 207- 218.
13. Borja R., Sanchez E., Weiland P. Influence of ammonia concentration on thermophilic anaerobic digestion of cattle manure in upflow anaerobic sludge blanket (UASB) reactors. Process Biochemistry 31, 5 (1996) 477-483.
14. Cohen A. Effects of some industrial chemicals on methanogenic activity measured by sequential automated methanometry. In: Proceedings: VI international symposium on anaerobic digestion. São Paulo, 1–5 (1991)
15. Souto T., Aquino S., Silva S., Chernicharo C. Influence of incubation conditions on the specific methanogenic activity test. *Biodegradation,* 21 (2010) 411-424.
16. Aquino S, Chernicharo C., Foresti E., Dos Santos M., Moneteggia L. Metodologias para determinação da atividade metanogênicas específica (AME) em lodos anaeróbios. *Eng. Sanitária Ambiental*, 12, 2 (2007) 192-201.
17. James A., Chernicharo C. A. L., Campos, C. M. M. The development of a new methodology for the assessment of specific methanogenic activity. Water Research, 24, 7 (1990) 813-825.
18. Cho Y. T., Young J.C., Jordan J. A., Moon H. M. Factors affecting measurement of specific methanogenic activity. Water Sci Technol. 52, 1-2 (2005) 435-440.
19. APHA, AWWA, WPCF. Métodos Normalizados para el Análisis de Aguas Potables y Residuales. 17th Ed. (1992)
20. Speece R. E. Anaerobic biotechnology for industrial wastewaters. Nashville, TN: Archae Press (1996).
21. Don J., Zhao Y., Hong M., Zhang W. Influence of alkalinity on the stabilization of municipal solid waste in anaerobic simulated bioreactor. Journal of hazardous materials, 163, 2-3, (2009) 717-722.
22. Cendales Ladino E. Producción de biogás mediante la codigestión anaeróbica de la mezcla de residuos cítricos y estiércol bovino para su utilización como fuente de energía renovable. Universidad Nacional de Colombia, 2011.
23. Shao X., Peng D., Teng Z., Ju X. Treatment of brewery wastewater using anaerobic sequencing batch reactor (ASBR). Bioresource Technology 99 (2008) 3182–3186.
24. Salminen E., Rintala J. Anaerobic digestion of organic solid poultry slaughterhouse waste – a review. Bioresource Technology 83 (2002) 13-26.
25. Yenigun O., Demirel B. Ammonia inhibition in anaerobic digestion: A review. Process Biochemistry 48 (2013) 901 – 911
26. Colleran E., Concannon F., Golden T., Geochegan F., Crumlish B., Killilea E., Henry M., Coates J. Use of a methanogenic activity tests to characterize anaerobic biodegradability and determine toxicity thresholds against trophic groups and species. In: : Proceedings VI international symposium on anaerobic digestion, São Paulo, 15–20 (1991)
27. Angelidaki I., Alves M., Bolzonella, D., Borzacconi L., Campos J. L., Guwy A. J., Kalyuzhnyi S., Jenicek P., Van Lier J. B. Defining the biomethane potential (BMP) of solid organic wastes and energy crops: a proposed protocol for batch assays. Water Science & Technology 59, 5 (2009) 927- 934.

CHAPTER 1.12 MICROBIAL FUEL CELLS EQUIPPED WITH ANION EXCHANGE MEMBRANE USED FOR TREATING ACTUAL LEACHATES

G. Hernández-Flores (1); H. M. Poggi-Varaldo *(1); T. Romero Castañón (2) and O. Solorza Feria (3)

(1) Environmental Biotechnology and Renewable Energies R&D Group, Dept. of Biotechnology and Bioengineering, Centro de Investigación y de Estudios Avanzados del Instituto Politécnico Nacional. Av. Instituto Politécnico Nacional 2508, Col. San Pedro Zacatenco, Delegación Gustavo A. Madero, México D.F. Código Postal 07360 México, D.F. Tel: +52 (55) 5747 3800 ext 4321 & 4306
(2) Electric Research Institute. Reforma 113, Col. Palmira, C.P. 62490 Cuernavaca, Morelos, México. Tel: (777) 3623811 & 3623800
(3) Dept. of Chemistry, see entry [1]. Tel: +52 (55) 5747 3800 ext 3715 & 4473

ABSTRACT

Landfill leachates (*lea*) are concentrated effluents that typically contain several types of aggressive pollutants. In Mexico City, the sanitary landfill called “Bordo Poniente” (*BP*) generates significant amounts of alkaline leachates. Its presence could contaminate both the surface water and the aquifer. The goal of this work was to evaluate the performance of single chamber microbial fuel cells (*MFC*s) equipped with a Zirfon membrane (*ZF*) (an anion exchange membrane) with *lea* from *BP*, in terms of the volumetric power (P_V) delivered and chemical oxygen removal efficiency (η_{COD}). As reference, a proton exchange membrane Nafion 117 was used in another *MFC*. In period 1 of batch operation the *MFC*s was loaded with 30% *lea* + 70% sulphate reducing inoculum (*SR-I).* In the 2nd period, the spent liquor was replaced with 70% *lea* + 30% *SR-I.* Finally, in the 3rd period the cell was refilled with 50% *lea* + 50% *SR-I.*

In the first period, the *MFC* equipped with *ZF* exhibited P_V and η_{COD} of 4 260 mW m^{-3} and 63%, respectively. The *MFC* equipped with *NF* reached a P_V and η_{COD} of 70 mW m^{-3} and 68%, respectively. In the period II, the *MFC* fitted with *NF* increased up to 100 mW m^{-3}, and the η_{COD} was in the order of the previous period, 64%. However, the *MFC* fitted with *ZF* reached a very high value of P_V (8 050 mW m^{-3}), although the η_{COD} decreased to 36%. Finally, in the period III, again the *MFC equipped* with *ZF* showed encouraging power values, the P_V was up to 10 380 mW m^{-3} and the η_{COD} was 7%, whereas the *MFC* fitted with *NF* delivered a substantially lower P_V of 104 mW m^{-3} and higher η_{COD} of 48%.

In conclusion, the *MFC* equipped with *ZF* consistently exhibited the best performance. The membrane type (anionic or cationic) played a significant role according the substrate tested. Atypical alkaline pH of the *lea* could partially explain the better performance of *MFC*s equipped with *ZF* over those fitted with *NF* membranes, since according to the alkalinity of *lea* the charge balance is based on anion transport rather than cation transport. On the other hand, Nafion membrane is a proton (cation) exchange membrane, poorly suited to effect charge balance in alkaline solutions. Thus, in this work we have shown that *ZF* could be an attractive candidate membrane for treating alkaline leachates in *MFC*s.

---

*Author for correspondence: r4cepe@yahoo.com

Keywords: anion exchange membrane, landfill leachates, microbial fuel cells, proton exchange membrane

INTRODUCTION

Microbial fuel cells (*MFC*s) are important bioelectrochemical systems which offer the possibility of produce electrical energy from a wide range of substrates; simple and complex soluble organic or inorganic wastes including renewable biomass[1-5]. Furthermore, the *MFC*s are involved not only in the renewably energy production. It is a technology with interesting applications in wastewater treatment, bioremediation, removal of toxic compounds and also biomass synthesis or by-products, among others things [6-10]. Thus, the diversity of *MFC*s applications allow to incorporate them in different processes and contributing to sustainable development[11,12]. Nevertheless, the lower power densities and low removal efficiencies are the main challenge currently[2,5].

In *MFC*s, the microorganisms are the key. They are the biological catalysts which are known as electrochemically active bacterias (*EAB*) or electricigens and those converts biochemically the chemical energy of the compounds into electrical energy[1,2,13]. It is carried out oxidizing the simple or complex molecules to carbon dioxide and the *EAB* use the solid electrode as electron acceptor[13]. The *MFC*s must have at least two electrodes, a cathode and an anode. In the anodic section (oxidation section), the microorganisms in anoxic conditions oxidize the compounds and release electrons and protons (half reaction). Afterwards, the electrons are collected by the anode (the external electron acceptor) and conducted to the cathodic section (reduction section) towards an external circuit. On the other hand, the protons delivered travel trought a membrane or separator to the cathode. Finally, is in the cathode where the reaction is completed (the second half reaction) with the reduction of the *i.e*. molecular oxygen and water and electricity is produced[14-18].

The maximum theoretical potential difference in those bioelectrochemical devices, considering the oxygen as the terminal electron acceptor is 1.14 V (+0.820V and -0.320V; cathodic and anodic section, respectively), however under practical *MFC* conditions the real achievable potential is less than +0.51 V, it could be due by diverse factors included activation polarization losses[19,20].

The anode and cathode electrodes must be divided by a membrane or a separator in order to prevent the circuit short and to improve the *MFC*s performance among others features[10]. Nafion® 117 is the typical proton exchange membrane (*PEM*) used in *MFC*s[16,21-25]. Nevertheless the high cost of this membranes type is discouraging to scaling up the *MFC*s [1,26,27].

The presence/absence of *PEM* has an impact in *MFC*s performance; thus the type of membrane or separator must be considerate and chosen according the substrate characteristics[10,13].

On the other hand, in many countries around the world the landfills are the form of waste management [28]. These landfills produce aggressive leachates due to the biological and physicochemical processes. Currently, this type of effluents must be collected and treated before to discharge in any place[29].

Mexico City has a sanitary landfill (*SL*) called “Bordo Poniente” (*BP*) which the waste of the metropolitan area of Mexico was collected. Nowadays, this environmental passive is closed. However, significant amounts of leachates are generated with moderate-to-high organic matter concentration and moderate alkalinity levels. These leachates need to be collected and treated in order to avoid the infiltration into the ground, contaminating both the surface water and the aquifer [30,31].

Thus, according the leachates characteristics, the aim of this work was to evaluate the performance of single chamber microbial fuel cells (*SC-MFC*s) equipped with an anion exchange membrane, Zirfon membrane (*ZF*) with actual leachate (*lea*) as substrate.

MATERIALS AND METHODS

Experimental design. The experiment consisted of the operation in a batch process of the *SC-MFC*s divided in three periods (**Table 1**), evaluating the performance of the *SC-MFC*s equipped with an anion exchange membrane, Zirfon membrane (*ZF*) with actual leachate (*lea*) as substrate, in terms of the volumetric power (P_V) delivered and chemical oxygen removal efficiency (η_{COD}). Another *MFC* equipped with a protonic exchange membrane, Nafion 117 membrane (*NF*) was used as reference. The *SC-MFC*s were loaded with three different mixtures of *lea* with sulphate-reducing inocula (*SR-I*) as biocatalyst: 30% *lea* + 70% *SR-I* (period I); 70% *lea* + 30% *SR-I* (period II) and 50% *lea* + 50% *SR-I* (period III).

TABLE 1. Experimental design of the batch operation

Period	Membrane	*SR-I* (%) [a]	*Lea* (%) [b]
1	*ZF* [c] *NF* [d]	70	30
2	*ZF* *NF*	30	70
3	*ZF* *NF*	50	50

Notes: [a]sulphate-reducing inocula; [b]actual leachate; [c] Zirfon membrane; [d]Nafion 117 membrane.

In the period I, two characterizations were carried out at 0 and 8 d. In the period II and III the characterizations were carried out at the start the period.

Microbial fuel cell. The single chamber *MFC* consisted of a horizontal cylinder built in Plexiglas 80 mm long and 57 mm internal diameter (**Figure 1**). The anodic chamber was packed with graphite flakes. The cathode was a sandwich of circular layers (from inside to outside): *ZF* or *NF*, flexible carbon-cloth containing 0.5 mg cm^{-2} platinum catalyst (Pt 10 wt%/C-ETEK), and a perforated plate of stainless steel 1 mm thickness. The cathode was in direct contact with atmospheric air on the metallic plate side[10,12,14,27].

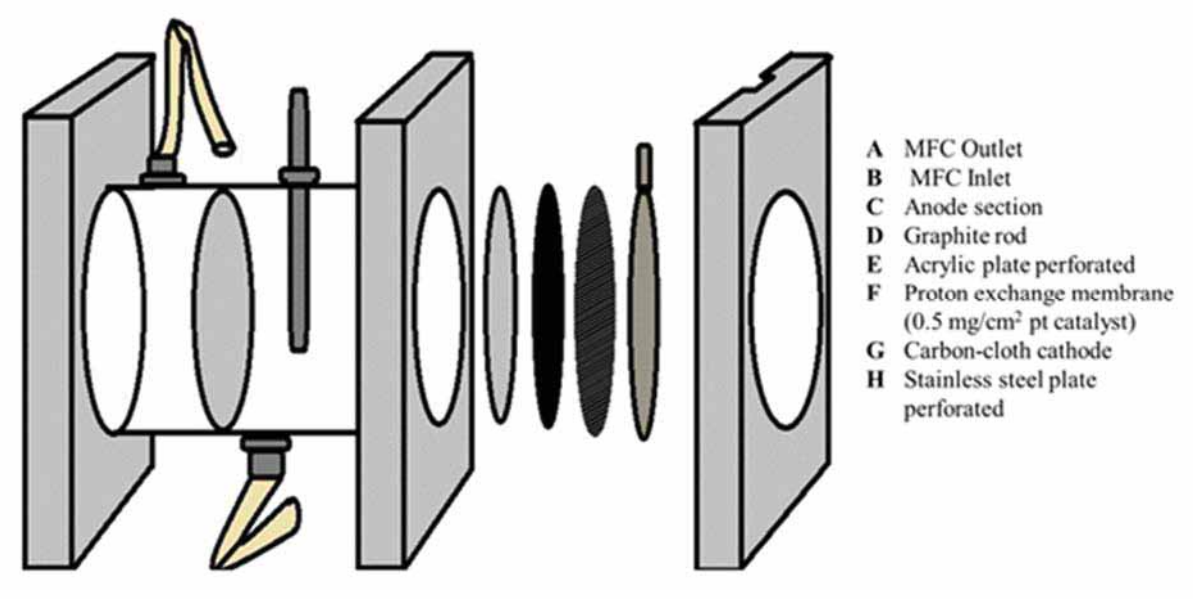


FIGURE 1. Microbial fuel cell configuration

Membranes pretreatment. The *NF* was pretreated to activate and to remove impurities before to use in the *MFC*. We describe a modified technique from Oh and Logan[32]. The membrane was soaked first in H_2O_2 (3% v/v), followed by soaking in deionized water. Afterwards, the membrane was immersed in 2 M H_2SO_4, followed by a last soaking in deionized water. Each stage lasted 1 h and was performed at 80 ˚C. On the other hand, the *ZF* was pretreated immersing the membrane 2 h in deionized water at 55 °C. Afterwards, the membrane was storage in deionized water at room temperature[5].

Finally, after the pretreatment and before to equipped in the cell, the protonic and anion exchange membranes (*NF* & *ZF*, respectively) were impregnated with 0.5 mg/cm2 platinum catalyst (Pt 10 wt%/C-ETEK).

Sulphate-reducing inoculum. The *MFC* was seeded with a *SR-In* sampled from a complete mix reactor. The reactor was operated at 37 °C in a constant temperature room. An influent containing mainly sucrose as carbon source was fed at a flow rate of 120 mL d^{-1} to the complete mix sulphate-reducing bioreactor. Its composition was (in g L^{-1}): sucrose (5.0), glacial acetic acid (1.5), $NaHCO_3$ (3.0), K_2HPO_4 (0.6), Na_2CO_3 (3.0), NH_4Cl (0.6), Na_2SO_4 (11.0) [4].

Leachates. The leachates were used as fuel in the cell. The leachates were sampled from Mexico City's *SL BP,* section 4 (*L-4*). Organic matter content of leachates was *ca.* 12 300 mg *COD* L^{-1} (Table 2). Furthermore, a high value of the ratio BOD_5 COD^{-1} was observed that suggests that leachates are biodegradable[33,34]. The pHs was alkaline, between 8 and 9.

Parameters of municipal wastewater and leachates were determined by Standard Methods[35].

TABLE 2. Characteristics of leachates

Parameter	*Leachates*
BOD_5 (mg L^{-1}) [a]	10 600 ± 200
COD (mg O_2 L^{-1}) [b]	12 300 ± 500
BOD_5/COD [c]	0.86
TSS (mg L^{-1}) [d]	324 ± 27
VSS (mg L^{-1}) [e]	270 ± 30
Nitrogen Kjeldahl (mg L^{-1})	2 900 ± 30
Sulphates (mg S L^{-1})	280 ± 10
Alkalinity (g L^{-1})	16.2 ± 1
pH	8.26 ± 0.02
Electrical conductivity (mS cm^{-1})	36.7 ± 0.1

Notes: [a]biological oxygen demand; [b]chemical oxygen demand; [c]biodegradability ratio; [d]total suspended solids; [e]volatile suspended solids

Determination of internal resistance of the cells. The R_{int} of the cell was determined using the polarization curve method, by varying the R_{ext} and monitoring both the voltage and the current intensity [15,16,36-38].

Briefly, the *MFC* was operated at open circuit; then the R_{ext} was varied from 10 Ω to 10 MΩ and viceversa. The voltage was measured and recorded with a Multimeter Escort 3146A. The current was calculated by the Ohm's law and the R_{int} was calculated as the slope of the linear section of the curve voltage versus the current intensity[15,21].

RESULTS AND DISCUSSION

Period I. The *SC-MFCs* were loaded with 30% *lea* + 70% *SR-I.* The initial and final conditions of the feed water are in the **Table 3**.

TABLE 3. Characteristics of the feed water and effluent of the *SC-MFCs*, period I

Parameters	Feed water (0 d)	Effluent	
		***SC-MFC/NF*[a] (at 15 d)**	***SC-MFC/ZF*[b] (at 15 d)**
COD [c] (mg L^{-1})	2685 ± 245	848 ± 245	989 ± 424
η_{COD} [d] (%)	NA [e]	68.42 ± 3.42	63.16 ± 3.16
Ph	7.9 ± 0.3	7.93 ± 0.3	7.83 ± 0.3
Electrical conductivity (mS cm^{-1})	23.25 ± 0.13	15.85 ± 0.05	16.3 ± 0.07
VSS [f] (mg L^{-1})	0.54 ± 0.18	ND [g]	ND
Temperature (°C)	22 ± 1	25 ± 1	25 ± 1

Notes: [a]single chamber microbial fuel cell equipped with Nafion 117 membrane; [b]single chamber microbial fuel cell equipped with Zirfon membrane; [c]chemical oxygen demand; [d]organic matter removal efficiency on *COD* basis; [e] No applicable; [f]volatile suspended solids; [g]No determinated.

On the other hand, the main values displayed by the cells in the electrochemical characterizations at 0 and 8 d are showed in **Table 4**.

TABLE 4. Electrochemical characterizations in Period I

Parameters	Time (d)			
	0 d		8 d	
	SC-MFC/ZF[a]	*SC-MFC/NF*[b]	*SC-MFC/ZF*	*SC-MFC/NF*
R_{int} [c] (Ω)	223 ± 93	2912 ± 215	43 ± 10	3205 ± 231
$Pv_{,max}$ (mW m^{-3})[d]	2015± 548	501 ± 31	1923 ± 248	1 ± 0.02
I_{MFC} (mA)[e]	0.82 ± 0.12	0.09 ± 0.01	2.12 ± 0.14	49.37 ± 0.76
P_{cat} (mW m^{-2})[f]	41 ± 11	10 ± 0.63	39 ± 5	0.03 ± 0.01
$V_{MFC,max}$ (mV)[g]	124 ± 18	292 ± 9	47 ± 3	92 ± 1
$V_{MFC,OC}$ (mV)[h]	330 ± 26	563 ± 19	254 ± 9	257 ± 12

Notes: [a]single chamber microbial fuel cell equipped with Zirfon membrane; [b]single chamber microbial fuel cell equipped with Nafion 117 membrane; [c]internal resistance; [d]maximum volumetric power; [e]current intensity value at the maximum power; [f]maximum power density based on surface area of electrode (cathode); [g]maximum potential at the maximum power; [h]Open circuit potential.

Thus, two external resistances (R_{ext}) with similar values as obtained in the electrochemical characterization were connected to the respective *SC-MFCs* (**Table 4**). The *SC-MFC* equipped with *NF* was connected to an R_{ext} of 3 300 Ω and the P_V and η_{COD} observed were 70 mW m^{-3} and 68% (**Table 3, Figure 2**), respectively. Regarding the *SC-MFC* fitted with *ZF* the obtained P_V and η_{COD} were 4 260 mW m^{-3} and 63% (**Table 3, Figure 3**), respectively, under an R_{ext} of 150 Ω.

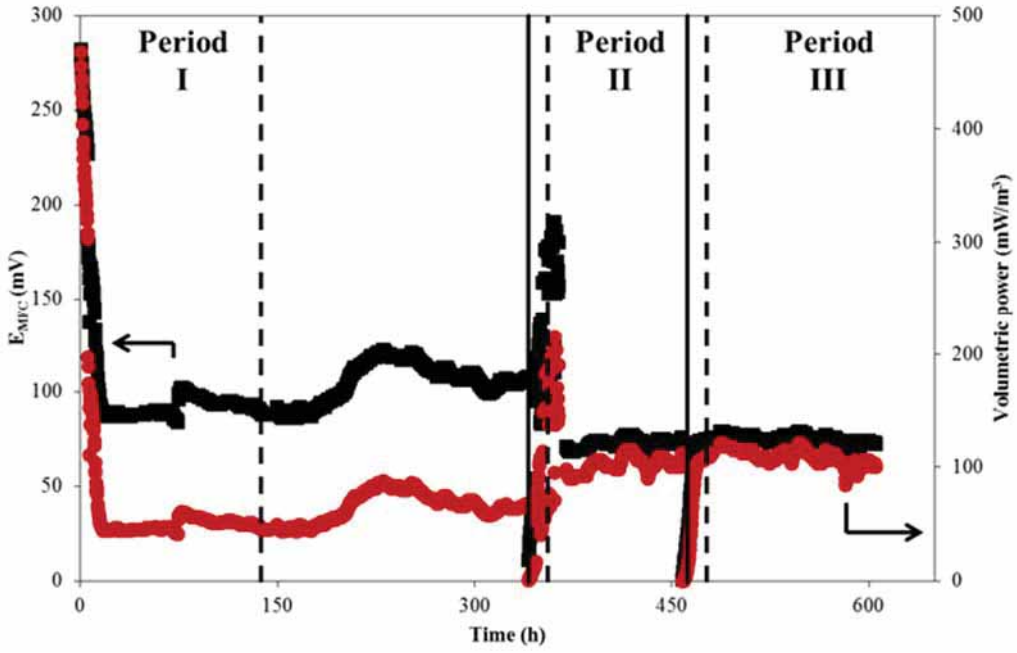


FIGURE 2. Batch operation of the single chamber microbial fuel cell equipped with Nafion 117 membrane

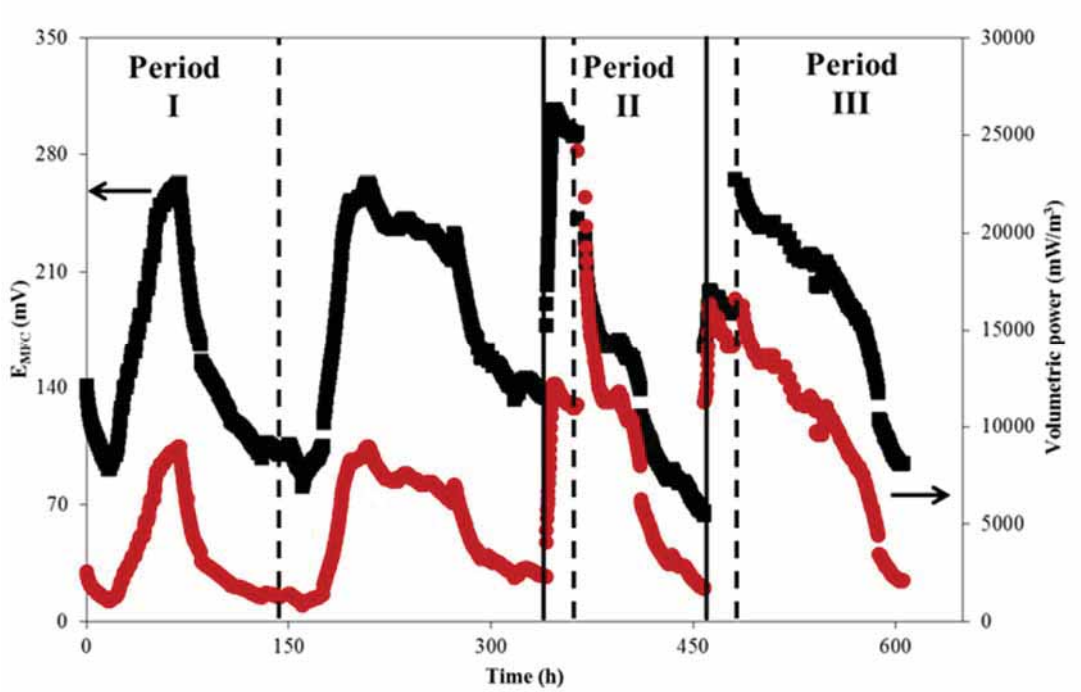


FIGURE 3. Batch operation of the single chamber microbial fuel cell equipped with Zirfon membrane

Period II. The *SC-MFCs* were refilled with a different concentration 70% *lea* + 30% *SR-I.* The initial and final conditions of the feed water are in the **Table 5**.

TABLE 5. Characteristics of the feed water and effluent of the *SC-MFCs*, period II

Parameters	Feed water (0 d)	Effluent	
		SC-MFC/NF[a] (at 5 d)	*SC-MFC/ZF*[b] (at 5 d)
COD[c] (mg L^{-1})	4410 ± 294	1584 ± 250	2827 ± 244
η_{COD}[d] (%)	NA[e]	64 ± 3.2	36 ± 1.8
pH	8.39 ± 0.3	8.17 ± 0.28	7.70 ± 0.33
Electrical conductivity (mS cm^{-1})	36.25 ± 0.05	29.7 ± 0.09	22.3 ± 0.08
VSS[f] (mg L^{-1})	0.33 ± 0.22	ND[g]	ND
Temperature (°C)	28 ± 1	25 ± 1	25 ± 1

Notes: [a]single chamber microbial fuel cell equipped with Nafion 117 membrane; [b]single chamber microbial fuel cell equipped with Zirfon membrane; [c]chemical oxygen demand; [d]organic matter removal efficiency on *COD* basis; [e] No applicable; [f]volatile suspended solids; [g]No determinated.

The electrochemical characterizations with these conditions are showed in **Table 6**.

Tabla 6. Electrochemical characterizations in Period II

Parameters	*SC-MFC/ZF*[a]	*SC-MFC/NF*[b]
R_{int} [c] (Ω)	33 ± 4	815 ± 12
$P_{V,max}$ (mW m^{-3})[d]	22655 ± 818	97 ± 2
I_{MFC} (mA)[e]	7.28 ± 0.13	0.071 ± 0 .001
P_{cat} (mW m^{-2})[f]	457 ± 17	2 ± 0.04
$V_{MFC,max}$ (mV)[g]	160 ± 3	71 ± 1
$V_{MFC,OC}$ (mV)[h]	525 ± 16	193 ± 9

Notes: [a]single chamber microbial fuel cell equipped with Zirfon membrane; [b]single chamber microbial fuel cell equipped with Nafion 117 membrane; [c]internal resistance; [d]maximum volumetric power; [e]current intensity value at the maximum power; [f]maximum power density based on surface area of electrode (cathode); [g]maximum potential at the maximum power; [h]Open circuit potential.

According the electrochemical characterization, the R_{ext} were readjusted. The *SC-MFC* fitted with *NF* and an R_{ext} of 1 000 Ω, the P_V increased up to 100 mW/m^3 and the η_{COD} was in the order of the previous period, 64% (**Table 5** and **3**, **Figure 2**). However, the *SC-MFC* fitted with *ZF* reached a very high value of P_V, 8 050 mW m^{-3} (**Figure 3**), although the η_{COD} decreased to 36% (**Table 6** and **5**, respectively).

Period III. Finally, in the last period (Period III), loaded with 50% *lea* + 50% *SR-I*. The initial and final conditions of the feed water are in the **Table 7**.

Table 7. Characteristics of the feed water and effluent of the *SC-MFCs*, period III

Parameters	Feed water (0 d)	Effluent	
		SC-MFC/NF[a] (at 8 d)	*SC-MFC/ZF*[b] (at 8 d)
COD [c] (mg L^{-1})	3053 ± 588	1584 ± 250	2827 ± 245
η_{COD} [d] (%)	NA [e]	48.11 ± 2.41	7.41 ± 0.37
pH	8.23 ± 0.25	8.10 ± 0.1	7.60 ± 0.33
Electrical conductivity (mS cm^{-1})	34 ± 0.1	30 ± 0.1	28 ± 0.1
VSS [f] (mg L^{-1})	0.42 ± 0.09	ND [g]	ND
Temperature (°C)	28.5 ± 1	25.5 ± 1	25.5 ± 1

Notes: [a]single chamber microbial fuel cell equipped with Nafion 117 membrane; [b]single chamber microbial fuel cell equipped with Zirfon membrane; [c]chemical oxygen demand; [d]organic matter removal efficiency on *COD* basis; [e] No applicable; [f]volatile suspended solids; [g]No determinated.

The electrochemical characterizations with these conditions are showed in **Table 8**.

TABLE 8. Electrochemical characterizations in Period III

Parameters	*SC-MFC/ZF*[a]	*SC-MFC/NF*[b]
R_{int} [c] (Ω)	62 ± 0.01	1119 ± 64.21
$Pv_{,max}$ (mW m^{-3})[d]	11411 ± 240	121 ± 1.29
I_{MFC} (mA)[e]	3.54 ± 0.04	0.08 ± 0.01
P_{cat} (mW m^{-2})[f]	230.34 ± 4.84	2.43 ± 0.03
$V_{MFC,max}$ (mV)[g]	166 ± 1.75	79 ± 0.42
$V_{MFC,OC}$ (mV)[h]	494 ± 23	217 ± 7

Notes: [a]single chamber microbial fuel cell equipped with Zirfon membrane; [b]single chamber microbial fuel cell equipped with Nafion 117 membrane; [c]internal resistance; [d]maximum volumetric power; [e]current intensity value at the maximum power; [f]maximum power density based on surface area of electrode (cathode); [g]maximum potential at the maximum power; [h]Open circuit potential.

In this last period (period III), again the *SC-MFC* fitted with *ZF* showed encouraging values (**Figure 3**), the P_V was up to 10 380 mW m^{-3} using an R_{ext} of 82 Ω and the η_{COD} was 7% **(Table 8**), whereas the *SC-MFC* fitted with *NF* delivered a substantially lower P_V of 104 mW m^{-3} () and higher η_{COD} of 48%.

At the end of the Period I (15 d), precipitation of salts appear in the cathode external surface of *MFC* equipped with *NF* and *ZF* (**Figure 4**). It could have impaired the reductive reaction of oxygen, and this, in turn, could have negatively affected its P_V. Salt precipitation apparently was not related to η_{COD}. Furthermore, the phenomenon of water evaporation was observed into the cells, however deionized water and sterilized was supply to keep full the cells and warrant the maximum surface area contact with the cathode.

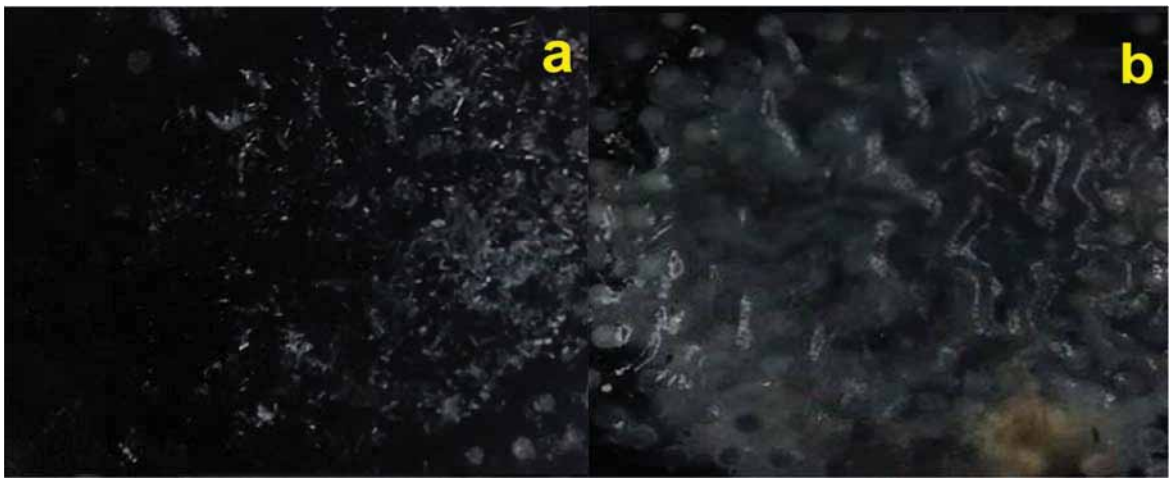


FIGURE 4. Precipitation of salts in the external side of cathode at 15 d of batch operation in *SC-MFC* equipped with a) Zirfon membrane and b) Nafion 117

CONCLUSION

In conclusion, membrane type played a significant role: the *SC-MFC* fitted with *ZF* in terms of P_V outperformed the *SC-MFC* fitted with *NF*, although the η_{COD} was lower, particularly in the last periods of operation. The proportion of *lea* and *SR-I* did not have a distinctive effect on *MFC* performance, whatever was the membrane type. Atypical high pH of the *lea* could partially explain the better performance of *MFC*s equipped with *ZF* over those fitted with *NF* membranes.

ACKNOWLEDGMENTS

The authors are also grateful to CINVESTAV-IPN and ICYTDF (now SECITI-GDF), Mexico, for financial support to this research (PICCO-10-27 and PICCO-10-28), and CONACYT for the Infrastructure Project 188281. Giovanni Hernández-Flores received a graduate scholarship from CONACYT, Mexico.
Also the authors thank Mr. Rafael Hernández-Vera, Mr. Alan C. Luna Monroy, Ms Sandra Canchola Alvizo, and technicians of the Environmental of Biotechnology and Renewable Energy R&D Group, CINVESTAV-IPN for their excellent technical help.

REFERENCES

1. Rozendal RA, Hamelers HVM, Rabaey K, Keller J, Buisman CJN. Towards practical implementation of bioelectrochemical wastewater treatment. Trends in Biotechnology 2008;26(8):450-459.
2. Lovley DR. The microbe electric: conversion of organic matter to electricity. Curr. Opin. Biotechnol. 2008;19:564-571.
3. Pant D, Bogaert GV, Diels L, Vanbroekhoven K. A review of the substrates used in microbial fuel cells (*MFC*s) for sustainable energy production. Bioresour. Technol. 2010;101:1533-1543.
4. Poggi-Varaldo HM, Carmona-Martínez A, Vázquez-Larios AL, Solorza-Feria O. Effect of inoculum type on the performance of a microbial fuel cell fed with spent organic extracts from hydrogenogenic fermentation of organic solid wastes. J. New Mater. Electrochem. Syst. 2009;12:49-54.
5. Pant D, Bogaert GV, Smet MD, Diels L, Vanbroekhoven K. Use of novel permeable membrane and air cathodes in acetate microbial fuel cells. Electrochimica Acta 2010;55:7710-7716.
6. Hsu L, Chadwick B, Kagan J, Thacher R, Wotawa-Bergen A. Richter K. Scale up considerations for sediment microbial fuel Cells. RSC Advances 2013;*3*:15947-15954.
7. Camacho-Pérez B, Ríos-Leal E, Solorza-Feria O, Vazquez-Landaverde PA, Barrera-Cortés J, Ponce-Noyola MT, Garcia-Mena J, Rinderknecht-Seijas N, Poggi-Varaldo HM. Preformance of an electrobiochemical slurry reactor for the treatment of a soil contaminated with lindane. J. New Mat. Electrochem. Systems 2013;16:217-228.
8. Logan BE, Rabaey K. Conversion of wastes into bioelectricity and chemicals by using microbial electrochemical technologies. Science 2012;337:686-690.
9. Vázquez-Larios AL, Solorza-Feria O, Poggi-Varaldo HM, González-Huerta RG, Ponce-Noyola MT, Ríos-Leal E, Rinderknecht-Seijas N. Bioelectricity production from municipal leachate in a microbial fuel cell: effect of two cathodic catalysts. Int. J. Hydrogen Energy 2014;39:16667-16675.
10. Hernández-Flores G, Poggi-Varaldo HM, Solorza-Feria O, Romero-Castañón T, Ríos-Leal E, Galíndez-Mayer J and Esparza-García F. Batch operation of a microbial fuel cell equipped with alternative proton exchange membrane. Int J Hydrogen Energy. 2015;40:17323-17331. DOI http://dx.doi.org/10.1016/j.ijhydene.2015.06.057.

11. Poggi-Varaldo HM, Munoz-Paez KM, Escamilla-Alvarado C, Robledo-Narváez PN, Ponce-Noyola MT, Calva-Calva G, Ríos-Leal E, Galíndez-Mayer J, Estrada-Vázquez C, Ortega-Clemente A, Rinderknecht-Seijas N. Biohydrogen, biomethane and bioelectricity as crucial components of biorefinery of organic wastes: a review. Waste Management Research 2014;32:353-365, doi: 10.1177/0734242X14529178.
12. Hernández-Flores G, Poggi-Varaldo HM, Solorza-Feria O, Ponce Noyola MT, Romero-Castañón T, Rinderknecht-Seijas N. Improvement of microbial fuel cell performance by selection of anodic materials and enrichment of inoculum. J. New Mat. Electrochem. Systems 2015;18:121-129.
13. Fornero JJ, Rosenbaum M, Angenent LT. Electric power generation from municipal, food, and animal wastewaters using microbial fuel cells. Electroanalysis 2010;22(7-8): 832-843.
14. Hernández-Flores G, Poggi-Varaldo HM, Solorza-Feria O, Ponce Noyola MT, Romero-Castañón T, Rinderknecht-Seijas N. Tafel equation based model for the performance of a microbial fuel cell. Int J Hydrogen Energy 2015;40:17421-17432. DOI http://dx.doi.org/10.1016/j.ijhydene.2015.06.119.
15. Vazquez-Larios AL, Solorza-Feria O, Vazquez-Huerta G, Esparza-Garcia FJ, Rios-Leal E, Rinderknecht-Seijas N, Poggi-Varaldo HM. A new design improves performance of a single chamber microbial fuel cell. J. New Mater. Electrochem. Syst. 2010;13:219-226.
16. Logan BE. Microbial Fuel Cells. John Wiley-Interscience. New Jersey, USA, 2007.
17. Escamilla-Alvarado C, Ponce-Noyola T, Ríos-Leal E, Poggi-Varaldo HM. A multivariable evaluation of biohydrogen production by solid substrate fermentation of organic municipal wastes in semi-continuous and batch operation. Int J Hydrogen Energy 2013;38:12527-12538.
18. Escamilla-Alvarado C, Ríos-Leal E, Ponce-Noyola T, Poggi-Varaldo HM. Gas biofuels from solid substrate hydrogenogenic–methanogenic fermentation of the organic fraction of municipal solid waste. Process Biochemistry 2012;47:1572-1587.
19. Modin O, Gustavsson DJ. Opportunities for microbial electrochemistry in municipal wastewater treatment–an overview. Water Sci. Technol. 2014;69(7):1359-1372.
20. Schröder U. anodic electron transfer mechanisms in microbial fuel cells and their energy efficiency. Physical Chemistry Chemical Physics 2007;(9):2619-2629.
21. Logan BE, Hamelers B, Rozendal R, Schröder U, Keller J, Freguia S, Aelterman P, Verstraete W, Rabaey K. Microbial fuel cells: Methodology and technology. Environ. Sci. Technol. 2006;40: 5181-5192.
22. Pant D, Bogaert GV, Smet MD, Diels L, Vanbroekhoven K. Use of novel permeable membrane and air cathodes in acetate microbial fuel cells. Electrochimica Acta 2010;55:7710-7716.
23. Rabaey K, Verstraete W. Microbial fuel cells: novel biotechnology for energy generation. Trends Biotechnol. 2005;23: 291–298.
24. Narayanaswamy VP, Sangeetha D. Characterization and performance study of sulfonated poly ether ether ketone/Fe3O4nano composite membrane as electrolyte for microbial fuel cell. Chemical Engineering Journal 2014;243:564-571.
25. Kim Y, Shin SH, Chang IS, Moon SH. Characterization of uncharged and sulfonated porous poly(vinylidene fluoride) membranes and their performance in microbial fuel cells. Journal of Membrane Science 2014;463:205-214.
26. Sivasankaran A, Sangeetha D. Development of *MFC* using sulphonated polyether ether ketone (SPEEK) membrane for electricity generation from waste water. Bioresour. Technol. 2011;102(24):11167-11171.
27. Hernández-Flores G, Poggi-Varaldo HM, Solorza-Feria O, Ponce-Noyola MT, Romero-Castañón T, Rinderknecht-Seijas N, Galíndez-Mayer J. Characteristics of a single chamber microbial fuel cell equipped with a low cost membrane. Int J Hydrogen Energy 2015;40:17380-17387. DOI http://dx.doi.org/10.1016/j.ijhydene.2015.10.024.

28. Damiano L, Jambeck JR, Ringelberg DB. Municipal Solid Waste Landfill Leachate Treatment and Electricity Production Using Microbial Fuel Cells. Appl. Biochem. Biotechnol. 2014;173:472-485.
29. Tchobanoglous G, Kreith F. Handbook of solid waste management McGraw-Hill, 2nd edition, 2002.
30. Domínguez-Montero LE, Poggi-Varaldo HM, Pérez-Angón MA, Jiménez-Cisneros BE, Cañizares-Villanueva RO, Caffarel-Méndez S, Frixione-Garduño E. Instrumentos tecnológicos patentados en México para tratar aguas residuales. Rev. Int. Contam. Ambie. 2016; In Press.
31. Belmonte-Jiménez SI, Bortolotti-Villalobos A, Campos-Enríquez JO, Pérez-Flores MA, Delgado-Rodríguez O, Ladrón de Guevara-Torres MA. Electromagnetic methods application for characterizing a site contaminated by leachates. Rev. Int. Contam. Ambie. 2014; 30(3):317-329.
32. Oh SE, Logan BE. Proton exchange membrane and electrode surface areas as factors that affect power generation in microbial fuel cells. Appl Microbiol Biotechnol 2006;70:162-169.
33. Poggi-Varaldo HM, Rinderknecht-Seijas N. A differential availability enhancement factor for the evaluation of pollutant availability in soil treatments. Acta Biotechnologica (Engineering in Life Sciences, Ed John Wiley) 2003;23:271-280.
34. Singh SK, Tang WZ. Statistical analysis of optimum Fenton oxidation conditions for landfill leachate treatment. Waste Management 2013;33(1):81-88.
35. APHA, AWWA and WPCF. Standard Methods for the Examination of water and Wastewater. 21st ed. American Public Health Association, American Water Works Assotiation and Water Environment Federation, Washington, 2005;874 pp.
36. Watson VJ, Logan BE. Analysis of polarization methods for elimination of power overshoot in microbial fuel cells. Electrochemistry Communications 2011;13:54-56.
37. Xia X, Tokash JC, Zhang F, Liang P, Huang X, Logan BE. Oxygen-reducing biocathodes operating with passive oxygen transfer in microbial fuel cells. Environmental Science & Technology 2013;47(4):2085-2091.
38. Martínez-Santacruz CY, Herrera-López D, Gutiérrez-Hernández RF, Bello-Mendoza R. Tratamiento de agua residual doméstica mediante un reactor rafa y una celda microbiana de combustible. Rev. Int. Contam. Ambie. *2016;32(3):267-279.* DOI: http://dx.doi.org/10.20937/RICA.2016.32.03.02.

NOTATION

BP	bordo poniente
CE	coulombic efficiency
COD	chemical oxygen demand
$E_{MFC,max}$	maximum potential of the cell
$E_{MFC,OC}$	open circuit potential of the cell
L-4	leachate from section 4 of the sanitary landfill
SC-MFC	single chamber microbial fuel cell
P_{cath}	power density per unit area of electrode
P_v	average volumetric power
$P_{v,max}$	maximum volumetric power
R_{ext}	external resistance
R_{int}	internal resistance
SR-In	sulphate-reducing inoculum
SL	sanitary landfill

GREEK CHARACTERS

η_{COD}	organic matter removal efficiency on *COD* basis

CHAPTER 1.13 ENRICHEMENT OF MICROBIAL CULTURES FOR USING IN THE CATHODIC AND ANODIC CHAMBERS OF A BIOCATHODE MICROBIAL FUEL CELL

J. E. Borbolla-Gaxiola (1); H. M. Poggi-Varaldo *(1); M. T. Ponce-Noyola (2); O. Solorza-Feria (3) and G. Hernández-Flores (1)

(1) CINVESTAV, Centro de Investigación y Estudios Avanzados, Dept. Biotechnology and Bioengineering, Environmental Biotechnology and Renewable Energies Group GABER-EBRE, P.O.Box 14-740, Mexico City DF, 07000, Mexico.
(2) CINVESTAV, Centro de Investigación y Estudios Avanzados, Dept. Biotechnology and Bioengineering, Microbial Genetics Group
(3) CINVESTAV, Centro de Investigación y Estudios Avanzados, Dept. Chemistry, Hydrogen and Fuel Cells Group

ABSTRACT

The microbial fuel cell (MFC) is a promising technology for simultaneous power generation and pollution abatement, which can be obtained via microbial metabolism. The performance of the MFC is highly related to the microbial activity, thus, a specialized culture could improve the metabolic rates of the reactions and electric current generation. The electrochemically active bacteria (EAB) enrichment is a technique used to exert selective pressures on microbial cultures in order to work with a solid electrode, adapting them to the extracellular electron transfer. While there are several examples of bioanode enrichments, studies of EAB enrichment of the biocathode cultures to improve cell's performance are limited. The objective of this work was to develop two enrichments based on mixed cultures subjected to selective pressures, in order to be used in a biocathode MFC, i.e., one enrichment for the anodic chamber, and one enrichment for the biocathode. The culture for the anode was a sulphur-reducing consortium that was further enriched with Fe^{+3} as the electron acceptor and acetate as C source. On the other hand, the culture for the biocathode was initially a denitrifying culture enriched with Fe^{+2} as a non-soluble source of electrons supplemented with acetate bicarbonate as carbon source. The enrichment monitoring was based on determination of appearing (anodic enrichment) or disappearing (cathodic enrichment) of Fe^{+2}. Maximum enrichment index (ε) of 5.51 mM Fe^{+2} d^{-1} in the second cycle for the biocathode enrichment, similar to ε values reported in literature using similar culture conditions (i.e. 3.61 and 1.95 mM Fe^{+2} d^{-1}) was obtained. For the bioanode enrichment the maximum ε was 24.83 mM Fe^{+2} d^{-1} in the fifth cycle, in previous studies of the work group the ε ranged from 6.5 to 38 mM Fe^{+2} d^{-1} for bioanode enrichment.
Even though the cultures showed adaptability to the non-soluble electron source/acceptor of the EAB enrichment, a bioelectrochemical test is undergoing to confirm the electrochemical activity of these consortia and the advantage of using specialized cultures in biocathode cells.

---

*Author for correspondence: r4cepe@yahoo.com

Keywords: anode, biocathode, microbial enrichments, MFC

INTRODUCTION

The microbial fuel cells are a relatively new technology that utilizes microbial cultures as catalyst to transform the chemical energy in organic matter directly into electricity[1]. The technology has as advantage that it can use wastewater or other low-grade biomass to produce bioelectricity, which is hardly utilized by other technologies[2]. The typical functioning of the microbial fuel cell starts at the anodic chamber, where the microbes oxidize the organic matter in a dissimilative process, producing electrons and protons, the electrons are transferred to the anode where they are later transported to the cathode. Meanwhile, the produced protons migrate to the cathode through a proton exchange membrane (PEM). Both electrons and protons meet at the cathode, where a metallic catalyst catalyze the oxygen reduction to form water[3]. One important implementation in a MFC is the biocathode, which utilizes a microbial culture to also catalyze a reduction reaction. Among the most important advantages of the biocathode are the decrease of the construction and maintenance cost of the cell, avoiding the expensive metallic catalyst, and the capability to take advantage of the microbial metabolism to remove a wide variety of oxidized compounds that could serve as electron acceptors, providing the MFC with a reductive treatment capacity, increasing its applications options and sustainability[4].

A two-chamber MFC utilizing both bioanode and biocathode can be used to treat a wastewater contaminated with oxidized and reduced compounds, or two different effluents depending on the necessity. A MFC relies on the microbial activity to perform properly, thus, in a cell with both bioanode and biocathode it is fundamental the use of an optimum inoculum on both chambers; it has been mentioned that a pre-inoculation enrichment of the culture increases the cell performance[5]. The electrochemical enrichment could be carried out in-cell[6] or ex-cell. One reported bioanode enrichment technique consists of an ex-cell serial inoculation of flasks containing an insoluble electron acceptor Fe^{+3}, this technique has shown great improvement on cell performance as applies a selective pressure on the culture, beneficiating electrochemically active bacteria[7-9].

Although the bioanode enrichment has been tested in typical MFC, there are no studies where a two-chamber MFC has its bioelectrodes enriched by this technique. Also, enriched biocathode studies are limited. Gregoire et al. (2014)[10] proposed a similar enrichment technique for biocathode, achieving the maximum current density reported so far for a biocathode working on microbial electrolysis cell mode (MEC) using nitrate as electron acceptor. Nitrate is one of the most studied electron acceptors for biocathodes[11-12]; however, electrochemical results have been low.

In this work was tested, for the first time to our knowledge, a two-chamber MFC with both bioanode and biocathode previously enriched. It is also the first biocathode enrichment with this technique for MFC operation.

METHODOLOGY

***Electrochemically active bacteria enrichment*.** Both anodic and cathodic enrichment cultures parted from previously adapted cultures. The inoculum for the anodic enrichment was taken from a sulfate-reducing reactor, and the cathodic culture from a denitrifying reactor. The anodic enrichment used the technique described by Lovley and Phillips[13-14], where serum bottles containing an insoluble electron acceptor, FeOOH, were inoculated with sulfate reducing culture and the appearance of Fe^{+2}, as Fe^{+3} is reduced, was monitored with a spectrophotometric technique using FerroZine as indicator[15]. The cathodic enrichment used was proposed by Gregoire et al.[10]. This technique, analogously, uses sequential serum bottles incubation, and utilizes an insoluble electron donor, in this case, $FeCO_3$. 12 mL of the denitrifying culture was inoculated into a serum bottle for a final volume of 75 mL, the composition of the medium was (in g/L): $NaHCO_3$ 2.52, NH_4Cl $7H_2O$ 0.3, $MgCl_2$ $6H_2O$ 0.4, KH_2PO_4 0.6, $CaCl_2$ $2H_2O$ 0.1. Fe^{+2} ion was added from a stock solution of $FeCl_2$ for a final concentration of 6 mM, and KNO_3 0.606 g as electron acceptor for a final concentration of NO^{-3} of 10 mM. The cathodic enrichment was also monitored with the FerroZine technique, but the Fe^{+2} disappears as the microorganisms oxidize the Fe^{+2} to Fe^{+3}. The enrichment was evaluated using the enrichment index, calculated with the formula:

$$\varepsilon = \frac{\Delta[Fe^{+2}]}{t_{lag}} \quad (1)$$

Where ε is the enrichment index, t_{lag} the time before the activity starts and the concentration difference was taken at the initial concentration and when the plateau starts. Every new inoculation into a fresh serum bottle is denominated as pass.

Cell Setup. To evaluate the enrichment on the cell performance, three cells were inoculated with different inoculum; the configurations are shown in **Table 1**. The cells used were two-chamber cells, divided by a Nafion 117 membrane with an area of 9 cm^2. Graphite granules were used as solid electrode for increasing the electrode area, and a graphite rod as electron collector, each chamber had a volume of 27 cm^3 and the graphite granules occupied 8 cm^3, leaving an active volume of 19 cm^3. After inoculation, the cells were given two weeks of adaptation to the cell with decreasing external resistance, called stages.

TABLE 1. Configurations used for the cell performance experiment. Being BA: enriched bioanode culture; BC: enriched biocathode culture; SR: non-enriched sulfate-reducing culture; DN: non-enriched denitrifying culture

Cell	Inoculum	
	Bioanode	Biocathode
1	BA	DN
2	BA	BC
3	SR	DN

The biomass load for each culture was reported as volatile soluble solids. For the first inoculation, the cell was left overnight at OCV, stage I started the next day closing the circuit with a 5600 Ω resistor. After a week, stage II started with 1000 Ω. The cells were refilled with new medium at the beginning of each stage, the medium composition was (in g/L): $(NH_4)_2HPO_4$ 0.6, KH_2PO_4 0.6, $NaHCO_3$ 0.2, $MgCl_2$ 0.2, 5 g of sodium acetate for the anolyte and 7.5 g of KNO_3 for the catholyte, plus 10 %v/v of mineral solution and 5 %v/v of vitamin solution. For the main run (stage III), the cell characterization was carried out after refilling, the characterization techniques used were polarization curve and electrochemical impedance spectroscopy (EIS) with a potenciostat (PARSTAT® 2273) for the internal resistance of the cells; and power curve for finding the external resistance for higher power generation was made with a multimeter (Escort® 3136) . The voltage monitoring started after the cell characterization with an Arduino UNO board.

***Data analysis*.** The cell performance was evaluated with different parameters, for the electrochemical performance was calculated the maximum volumetric power (P_{max}), maximum current density (j_{max}), power generated (P_{gen}) and coulumbic efficiencies for DQO consumption for anode and Nitrate reduction for the cathode.

$$Pv_{max} = \frac{(IE)}{V_{cell}} \quad (2)$$

Where *I* is current intensity, *E* cell potential and V_{cell} active volume of the cell. Current density calculation was evaluated with eq. 3, where *A* corresponds to the specific area of the solid electrode of the cell.

$$j_{max} = \frac{I}{A} \quad (3)$$

The total power generated was calculated integrating all power results with the trapezium technique.

$$P_{gen} = \int_{t0}^{t} P\, dt \quad (4)$$

RESULTS AND DISCUSSION

***Electrochemical Enrichment*.** In **Figure 1** is shown the summary of the enrichment passes. The anodic enrichment behave increasing the Fe^{+2} concentration and reducing the time within each pass, reaching its maximum enrichment index with 24.83 mm Fe^{+2} d^{-1} at pass 5, and maintaining a high activity afterwards. In the other hand, the cathodic enrichment showed different behavior when incubated with carbon source against the incubation without it. In the enrichment with no carbon source, the Fe^{+2} disappearance decreased with each pass; in contrast, the bottles with carbon source showed a slight decrease of the enrichment index in the first pass, but maintained an steady index afterwards, reaching its maximum at pass 1 with a enrichment index of 5.51 mM Fe^{+2} d^{-1}.

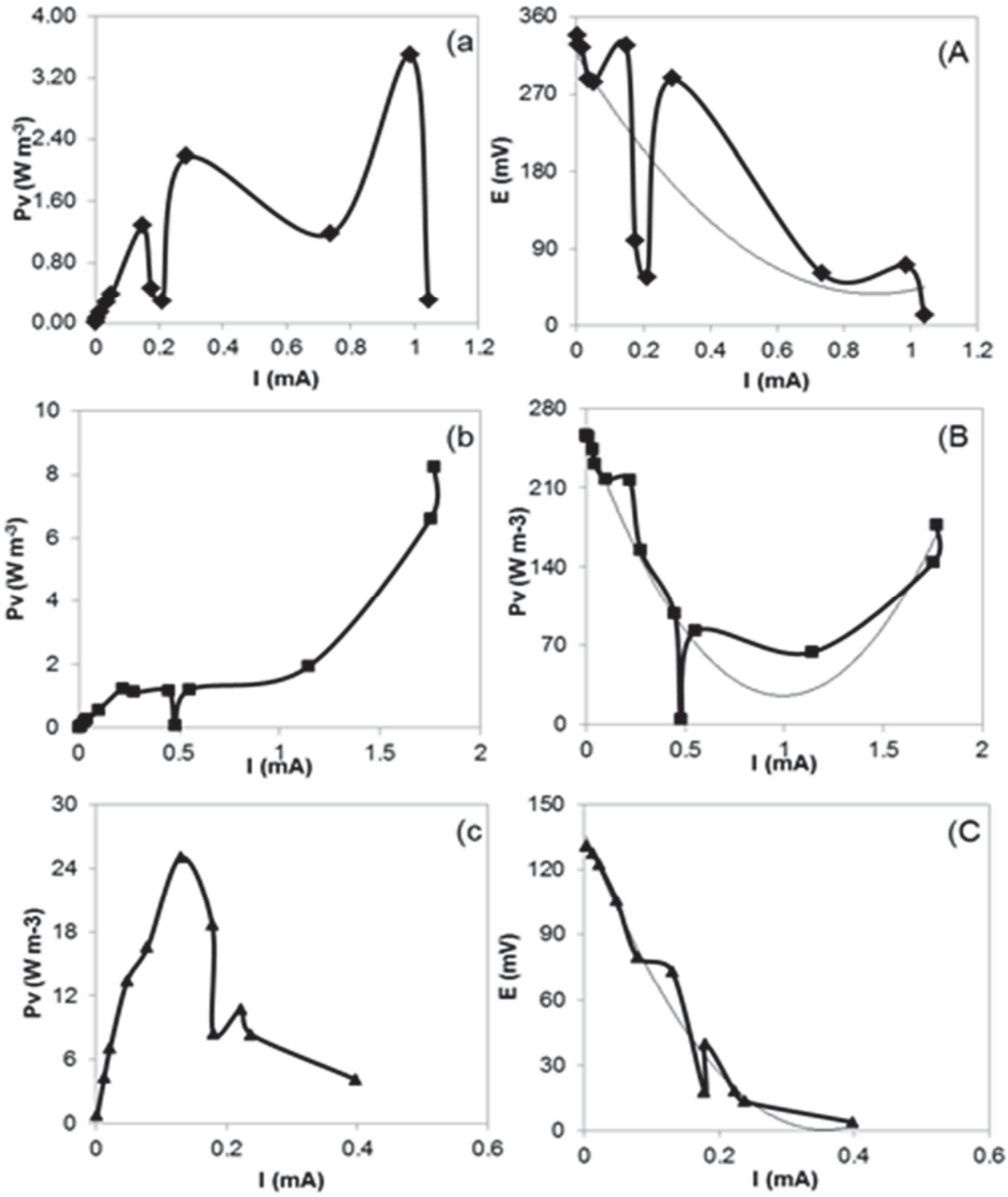


FIGURE 1. Cells electrochemical characterization with R_{ext} variation: Power curve (a, b and c) and polarization curve (A, B and C) for cells 1, 2 and 3 respectively

This behavior in the cathodic enrichment could possibly be due to the maintenance of the biomass, the chemolithoautotrophic could not produce enough biomass in the incubation time to counter the biomass wash with each pass, while the bottles with carbon source, the heterotrophic metabolism of the acetate consumption could maintain the biomass after passes. In **Table 2** is summarized the enrichment index of each pass for both anodic and cathodic culture.

TABLE 2. Enrichment index in each pass for both cathodic and anodic enrichment

	ε (mM Fe^{+2} d^{-1})				
	Pass 0	Pass 1	Pass 2	Pass 3	Pass 4
BC	0.19	6.44	2.69	0.25	0.15
BC+FC	0.02	5.51	4.47	4.62	4.85

	ε (mM $Fe^{+2}d^{-1}$)						
	Pass 0	Pass 1	Pass 2	Pass 3	Pass 4	Pass 5	Pass 6
BA	1.29	0.79	0.38	8.28	24.11	24.83	10.99

***In-cell experiment*.** The cell operation had 13 days adaptation previous the experiment, corresponding to stage I and II. After the adaptation period, a cell characterization was carried out with different techniques. On Figure 1 are shown the polarization curves and power curves of the three cells. Based on the power curves, the chosen external resistances were 100 Ω for cells 1 and 2, while cell 3 a 560 Ω resistance.

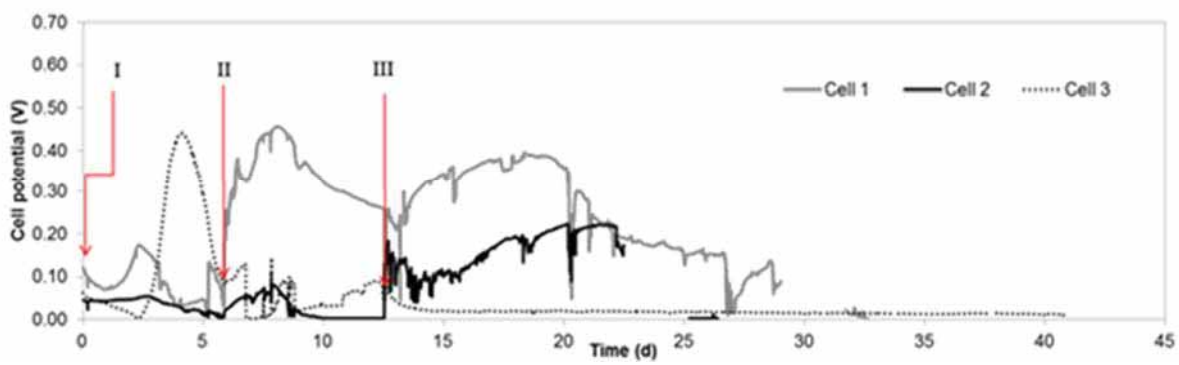


FIGURE 2. Cell potential during the complete experiment

The voltage behavior of the cells during the three stages is shown in **Figure 2**. It is observed that the cell 1 showed the higher cell potential at stage I with the higher external resistance, decreasing as the external resistance decreased. Inversely, cells 1 and 2 increased their potential as resistance decreased. This could be attributed to the enrichment of the cultures, cells 1 and 2. Both had an enriched bioanode, while in cell 3 neither of the cultures was enriched, preventing the cell to work with high current intensities present with lower external resistances.

The summary of the cells performance is reported in **Table 3**. It is noticeable how the electrochemical parameters such as volumetric power, current densities and power generation increased in every stage. The results of both cell 1 and 2 are remarkable for MFC with working biocathode. The maximum volumetric power achieved by the cell 1 was the highest, with 41.13 W m^{-3}, followed by the cell 2 with 13.1 W m^{-3}, and cell 3 reaching only 4.78 W m^{-3}. Oon et al.[16] working with a double-chamber cell with 1000 Ω R_{ext} and nitrate as electron acceptor achieved 669 mW m^{-3} and 3.48 A m^{-3}. Comparing them to our result in stage II with equal R_{ext} is observed that cell 1 reached higher results, with 5.48 W m^{-3} and 12.01 A m^{-3}. However, cell 2 and 3 fell behind in

performance. Zhang et al.[17] reported 99 W m^{-3} working with an aerobic biocathode utilizing a R_{ext} of 100 Ω, the electrode used was a combination of graphite fiber brush and graphite granules, when graphite granules was used as the only electrode material, as the current work, they reported a lower power of 72.84 W m^{-3}.

TABLE 3. Electrochemical characteristics of the cells during stage III

Stage	E_{av}	Pv_{max} (mW m^{-3})	j_{max} (mA m^{-2})	jv_{max} (mA m^{-3})	Power generated (mW h)
I					
Cell 1	0.09	141.51	0.80	815.46	0.24
Cell 2	0.04	13.68	0.25	253.52	0.04
Cell 3	0.16	914.16	2.04	2072.65	1.24
II					
Cell 1	0.34	5486.89	11.83	12016.32	19.28
Cell 2	0.02	191.84	2.21	2246.84	0.20
Cell 3	0.05	540.39	3.71	3771.05	0.63
III					
Cell 1	0.23	41132.01	104.04	105682.20	284.89
Cell 2	0.16	13104.19	57.80	58714.56	67.04
Cell 3	0.02	478.80	4.67	4742.68	0.31

The internal resistance analysis was done with electrochemical impedance spectroscopy, the summary of the resistances in stages III per component is shown in **Table 4**. The non-enriched inoculated chambers showed the lowest resistance, this could indicate that a polarization took place. However, the Rint of the three cells are similar, so the internal resistance cannot fully explain by itself the big difference in the performance of the cells. Another factor that could explain the behavior of the cells is the biomass load. The biomass load for each culture was (in mg/L): BA 125, BC 110, SR 450, and DN 1035. Based on these results, BA-inoculated cells showed a better performance than the SR, even if the biomass load is 260 % higher for SR inoculum, this confirm the benefits of the bioanode enrichment improving the culture efficiency. In the case of the biocathode, inoculum in cell 1 was non-enriched and resulted in higher power generation than cell 2, which had enriched biocathode. This indicates that the denitrifying culture is able, to some point, to handle the current generated with the enriched bioanode. The power generation during the experiment was in cell 1 was and 284 W h and 18.41W m^{-3} for average volumetric power. This is more than four times the power generated in cell 2 with 67 W h and more than double the average volumetric power (7.36 W m^{-3}). However, the biomass load at inoculation time was almost ten times greater in cell 1 than the one in cell 2. This non-proportionality between power generation and biomass load could indicate a higher activity by the enriched inoculum.

TABLE 4. Internal resistance by component for the three cells at stage III, Ran: anode resitance, Rcat: cathode reistance, Rw: whole cell resitance. Measured by electrochemical impedance spectroscopy and analyzed with the software Zview®

Cell	R_{an} (Ω)	R_{cat} (Ω)	R_W (Ω)
1	211.44	27.45	372.92
2	147.24	63.15	377.08
3	103.22	33.44	280.15

CONCLUSION

The electrochemical enrichment of the cultures showed an improvement of the electrochemical performance. The cells with enriched cultures (1 and 2) showed higher values for P_{max}, j_{max} and energy generated, than the cell with non-enriched cultures, confirming the bioanode enrichment and its implementation in double chamber *MFC* with biocathode. However, cell 1 (with enriched bioanode and non-enriched biocathode), was the cell with best performance, and not cell 2 (with both bioanode and biocathode enriched) as expected. The power generation by cell 2 was acceptable for *MFC* with anaerobic biocathodes even with a biomass inoculum ten times lower than cell 1, this could indicate that the biocathode enrichment possibly increased the microbial activity. Nevertheless, this experiment could not confirm the benefits of biocathode enrichment with the technique used in this work, more studies considering factors like biomass load are needed to confirm if the technique used contributes to the improvement of MFC performance with enriched biocathode.

REFERENCES

1. Logan, B. E. (2007). Microbial Fuel Cells. Microbial fuel cells. Hoboken, New Jersey: John Wiley & Sons, Inc. http://doi.org/10.1016/B978-0-444-53199-5.00098-1
2. Zhou, M., Wang, H., Hassett, D. J., & Gu, T. (2013). Recent advances in microbial fuel cells (MFCs) and microbial electrolysis cells (MECs) for wastewater treatment, bioenergy and bioproducts. Journal of Chemical Technology and Biotechnology, 88(4), 508–518. http://doi.org/10.1002/jctb.4004
3. Du, Z., Li, H., & Gu, T. (2007). A state of the art review on microbial fuel cells: A promising technology for wastewater treatment and bioenergy. Biotechnology Advances, 25(5), 464–482. http://doi.org/10.1016/j.biotechadv.2007.05.004
4. He, Z., & Angenent, L. T. (2006). Application of bacterial biocathodes in microbial fuel cells. Electroanalysis, 18(19-20), 2009–2015. http://doi.org/10.1002/elan.200603628
5. Poggi-Varaldo, H. M., Ortega-Martínez, A., Vázquez-Larios, A. L., Rindernknecht-Seijas, N., Vazquez Vazquez, G., & Solorza-Feria, O. (2009). Application of biocathodes and enrichment strategies as promising alternative for enhanced bioelectricity generation in microbial fuel cells. New Biotechnology, 25S(September), S252. http://doi.org/10.1016/j.nbt.2009.06.561
6. Doyle, L. E., & Marsili, E. (2015). Methods for enrichment of novel electrochemically-active microorganisms. Bioresource Technology, 195, 273–282. http://doi.org/10.1016/j.biortech.2015.07.025

7. Hernandez-flores, G., Solorza-feria, O., & Ponce-noyola, M. T. (2013). Improvement of Microbial Fuel Cell Characteristics by Inoculum Enrichment and Selection of Anodic Materials, 129, 121–129.
8. Sathish-Kumar, K., Solorza-Feria, O., Tapia-Ramírez, J., Rinderkenecht-Seijas, N., & Poggi-Varaldo, H. M. (2013). Electrochemical and chemical enrichment methods of a sodic-saline inoculum for microbial fuel cells. International Journal of Hydrogen Energy, 38(28), 12600–12609. http://doi.org/10.1016/j.ijhydene.2012.11.147
9. Vázquez-Larios, A. L., Poggi-Varaldo, H. M., Solorza-Feria, O., & Rinderknecht-Seijas, N. (2015). Effect of type of inoculum on microbial fuel cell performance that used RuxMoySez as cathodic catalyst. International Journal of Hydrogen Energy, 40(48), 17402–17412. http://doi.org/10.1016/j.ijhydene.2015.09.143
10. Gregoire, K. P., Glaven, S. M., Hervey, J., Lin, B., & Tender, L. M. (2014). Enrichment of a High-Current Density Denitrifying Microbial Biocathode. Journal of The Electrochemical Society, 161(13), H3049–H3057. http://doi.org/10.1149/2.0101413jes
11. Ghafari, S., Hasan, M., & Aroua, M. K. (2008). Bio-electrochemical removal of nitrate from water and wastewater — A review, 99, 3965–3974. http://doi.org/10.1016/j.biortech.2007.05.026
12. Mousavi, S., Ibrahim, S., Aroua, M. K., & Ghafari, S. (2012). Development of nitrate elimination by autohydrogenotrophic bacteria in bio-electrochemical reactors - A review. Biochemical Engineering Journal, 67, 251–264. http://doi.org/10.1016/j.bej.2012.04.016
13. Lovley, D. R., & Phillips, E. J. P. (1986). Organic matter mineralization with reduction of ferric iron in anaerobic sediments. Applied and Environmental Microbiology, 51(4), 683–689. http://doi.org/10.1080/01490458709385975
14. Lovley, D. R., & Phillips, E. J. P. (1987). Rapid assay for microbially reducible ferric iron in aquatic sediments. Applied and Environmental Microbiology, 53(7), 1536–1540. http://doi.org/10.1007/BF01611203
15. Stookey, L. L. (1970). Ferrozine-A New Spectrophotometric Reagent for Iron, 42(7), 779–781.
16. Oon, Y.-S., Ong, S.-A., Ho, L.-N., Wong, Y.-S., Oon, Y.-L., Lehl, H. K., & Thung, W.-E. (2016). Long-term operation of double chambered microbial fuel cell for bio-electro denitrification. Bioprocess and Biosystems Engineering, 39(6), 893–900. http://doi.org/10.1007/s00449-016-1568-y
17. Zhang, G. D., Zhao, Q. L., Jiao, Y., Zhang, J. N., Jiang, J. Q., Ren, N., & Kim, B. H. (2011). Improved performance of microbial fuel cell using combination biocathode of graphite fiber brush and graphite granules. Journal of Power Sources, 196(15), 6036–6041. http://doi.org/10.1016/j.jpowsour.2011.03.096

CHAPTER 1.14 A VERY LOW-COST METHOD FOR MONITORING ELECTRIC POTENTIAL IN MICROBIAL FUEL CELLS

J. E. Borbolla-Gaxiola (1); H. M. Poggi-Varaldo *(1); M. T. Ponce-Noyola (1); O. Solorza-Feria (1) and F. Esparza-García (1)

(1) CINVESTAV, Centro de Investigación y Estudios Avanzados, Dept. Biotechnology and Bioengineering, Environmental Biotechnology and Renewable Energies Group GABER-EBRE, P.O.Box 14-740, Mexico City DF, 07000, Mexico.
(2) CINVESTAV, Centro de Investigación y Estudios Avanzados, Dept. Biotechnology and Bioengineering, Microbial Genetics Group
(3) CINVESTAV, Centro de Investigación y Estudios Avanzados, Dept. Chemistry, Hydrogen and Fuel Cells Group

ABSTRACT

The Microbial Fuel Cell (MFC) is a versatile technology which uses the metabolism of microbial cultures for the generation of electric power and pollution control. The electric current (*I*) generated in MFCs tends to be low, so its direct measurement for monitoring cell performance is not practical. Instead, the electrical potential is the variable of choice for monitoring MFCs. However, a major problem of voltage monitoring is the high cost of instruments, either potentiostats (price range 100 000 to 500 000 USD) or multimeters (price range 1500 to 5000 USD). Arduino UNO is a very low-cost microcontroller, with a price around $ 21 USD in the Mexican market. This microcontroller allows an easy programming for reading conditions and data acquisition. Even if the Arduino UNO microcontroller is easily programmable for voltage reading, there are no antecedents of its use and its accuracy in the monitoring of the electric potential of MFCs.
The aim of this research was to determine the feasibility of using Arduino UNO as an instrument for electric potential monitoring of MFC. We operated a two-chamber (bioanodic and biocathodic) MFC, and the voltage was monitored with both the Arduino UNO and a commercial multimeter (Escort® 3146A) simultaneously. The Arduino UNO, with just minor coding adaptation, achieved an average absolute error of 0.75 mV with a standard deviation of ± 0.66 mV with respect to the error. The norm of the absolute error was 357 mV^2. Since the monitoring was performed in an extended timespan with varying potentials, the standard deviation based on the norm was ca. 1 mV.
With these results, Arduino UNO readings can achieve an absolute error well below 1 mV and a relative error assuming the multimeter as true value ranged between 1% to 2% for the high (20 to 80 mV) and lower potentials (0 to 20 mV) respectively. Then, its accuracy is very satisfactory and can be used in systems were the voltage is relatively high, i.e. in the range of 80 to 1000 mV, with an investment cost of 0.5% of the cost of a multimeter or 0.0067% of the cost of a potentiostat.

Keywords: arduino, low-cost, MFC, potential monitoring

---

*Author for correspondence: r4cepe@yahoo.com

INTRODUCTION

Microbial fuel Cells (*MFC*) are a relatively recent technology which generates an electric current due to the electric potential difference between a pair of electrodes (*E*), where at least one of them must be bio-catalyzed. In order to a bioelectrochemical system to be considered as a *MFC*, there must be a current generation and the bioelectrochemical reactions be self-driven, in cases where a potential is applied on the cell to accelerate microbial metabolism it is known as microbial electrolysis cell (*MEC*)[1-3]. In typical *MFC*, the electron acceptor of choice is the oxygen, due to the high abundance and high reduction potential (0.82 V), the oxygen reduction reaction is catalyzed by a metallic catalyst, such as platinum. As an alternative, the *MFC* implemented with biocathode, utilize a microbial culture to catalyze the cathodic reaction. The biocathode reduction capacity is used in the treatment of wastewaters with oxidized contaminants. Although, the MFC with biocathode has more remediation advantages, the power generated is still lower that the generated in a typical *MFC*[4].

The first approach when studying an electric system is the voltage measurements. The maximum voltage is the open circuit voltage (*OCV*) where the resistance is infinite and the current is zero, and as the resistance decreases, the voltage decreases also according to Ohm's Law, where the equation states the voltage is directly proportional to the resistance. While the voltage decreases along with the resistance, the current increases when the resistances drop. Being the current produced in *MFC* too low to measure, it is calculated with the equation $I = E / R_{ext}$, using a fixed external resistance and only measuring voltage[5].

Bioelectrochemical systems studies are sometimes limited by the instruments used for monitoring. One aspect is the price of accurate instruments with automatic data acquisition and sometimes their incapability to take readings from more than one device at the same time.

Arduino is an open-source platform, able to receive and send information to multiple devices, this allows the use of Arduino board in the construction, programming and controlling of electronic devices. Among its features is the user-friendly language (simplified C++) of its compiler, easy to load the code via USB cable, multiple analog ports for multiple voltage readings simultaneously, and the low cost of the board (pricing around 21 $USD in the Mexican market)[6].

The Arduino board is reported to be used in different occasions for voltage monitoring for different energy-related electronic devices [7]–[10]; however, the veracity of the Arduino board voltage measurements versus a voltage monitoring instrument such as a multimeter was not found. In the case of *MFC*, as their voltage range is low, even small deviations could result in high relative error. In this work is evaluated the accuracy of the Arduino board in voltage monitoring of an operating double-chamber *MFC* against a multimeter, in order to evaluate if the Arduino board could be considered as an option for a low-cost voltage monitoring of bioelectrochemical systems.

METHODOLOGY

Cell setup. A double chamber *MFC* was inoculated with mixed cultures. Each chamber volume was 27 cm^3, and contained 8 cm^3 of graphite granules for a specific area of the electrode of 193 cm^2. The external resistance used in the test was a 1000 Ω resistor. The chambers were separated with a Nafion® 117 PEM. The anode chamber was inoculated with sulfur-reducing enriched culture and the cathode chamber was inoculated with a denitrifying enriched culture. The medium used in the anode chamber contained the follow composition, in g/L: $(NH_4)_2HPO_4$ 0.6, KH_2PO_4 0.6, $NaHCO_3$ 0.2, $MgCl_2$ 2 and sodium acetate 6. The cathodic chamber had a similar composition, but, instead sodium acetate it contained $NaNO_3$ 11.6 g/L. The medium initial pH was 6.91 and 6.73 respectively.

The cell voltage was monitored with both an Arduino UNO and a multimeter (ESCORT 4631A), the readings were set every 15 min. In order to improve the accuracy of the Arduino UNO, it is needed to improve the resolution of the Arduino board and to decrease the noise. Arduino UNO has ADC of 10 bits and a voltage reference of 5 V by default, with this combination the every analog unit represents 4.88 mV being a low resolution. To approach this aspect it was set a voltage reference of 0.83 V to improve the ADC resolution. This needed a constant DC power source, it was used a AA battery as a DC source and was implemented a voltage divider with a 33 kΩ resistor and the internal resistance of 32 kΩ of the Arduino board. According to the voltage divider equation Vf = Vi * 32 / (32+33), the final voltage should be around 0.73 mV, but after reading it with a multimeter, the true voltage (0.83 mV) was added to the code.

The code was also written to take readings every 100 milliseconds, do an average every 20 readings, and print only the results every 15 min. Based on previous tests was added an adjustment factor for better fitting at low voltages, the printing command of the code was modified to work with the public interface PLX-DAQ in Microsoft Excel . The final code is shown as follows:

```
const int NUM_LEC = 20;
const int NUM_PRINT = 450;
float voltage0 = 0;
float voltagePrint0 = 0;
float voltageAV0 = 0;
float voltage01 = 0;
float TOTAL_LEC = 0;
int Lec = 0;
int i;
int j = 0;
int Index = 0;
float totalLecturas = 0;
float promedioLecturas = 0;
int Index2 = 0;
int inputPin0 = A0;
void setup() {
```

```
  Serial.begin(9600);
  analogReference(EXTERNAL);
  Serial.println("CLEARDATA");
  Serial.println("LABEL,TIME,CELL 1 (V)");
  analogReference(EXTERNAL);
}
void loop() {
  while (j < NUM_PRINT){
          //las iteraciones se programan para una lectura cada 100 ms y
un promedio cada 2 s
          for (int i = 0; i < NUM_LEC; i++){
          Lec = analogRead(inputPin0);
          float voltageLEC0 = Lec * (0.83 / 1023.000);
          totalLecturas = totalLecturas + voltageLEC0;
          delay(100);
           }
          TOTAL_LEC = totalLecturas;
          totalLecturas = 0;
      i = 0;
      j++;
  }
      voltageAV0 = TOTAL_LEC/NUM_LEC;
      if (voltageAV0 <= 0.100){
      voltagePrint0 = voltageAV0 + 0.00245;}
      else if (voltageAV0 > 0.100){
      voltagePrint0 = voltageAV0 + 0.0018;}
      Serial.print("DATA,TIME");
      Serial.print(",");Serial.print(voltagePrint0,5);
Serial.print(",");
      Serial.println("ROW,SET,2");
      TOTAL_LEC = 0;
      voltageAV0 = 0;
      voltagePrint0= 0;
      j = 0;
      voltage01 = 0;
}
```

Data analysis. The collected data during the operation of the cell was evaluated with different statistical parameters.

Absolute error:

$$e_{Abs} = V_{mult} - V_{Arduino} \quad (1)$$

Relative Error:

$$e_{Abs} = \frac{(V_{mult} - V_{Arduino})}{V_{mult}} \quad (2)$$

Where V_{mult} is the voltage reading of the multimeter at any specific time and $V_{Arduino}$ is the potential reading with the Arduino UNO at the same time. For the average absolute error was used the following equation:

Absolute error average:

$$\bar{e}_{Abs} = \frac{1}{N}\sum(V_{mult} - V_{Arduino}) \quad (3)$$

Average voltage:

$$\bar{V} = \frac{1}{N}\sum V_{Arduino} \quad (4)$$

Norm:

$$Norm = \sum(E_{mult} - E_{Arduino})^2 \quad (5)$$

Being N the total number of readings. The norm was calculated according to eq. 5 and, for the error variance, standard deviation and variation coefficient were calculated as follows:

Variance

$$\sigma_e^2 = \frac{1}{N-1}\sum(E_{mult} - E_{Arduino})^2 \quad (6)$$

Standard deviation

$$\sigma_e = \sqrt{\sigma_e^2} \quad (7)$$

Variation coefficient:

$$C_e = \left(\frac{\sigma}{\bar{V}}\right) x\ 100 \quad (8)$$

RESULTS AND DISCUSSION

After 4 days of monitoring, the voltage dropped at 96.5 hours. **Figure 1** shows the behavior of the voltage during the operation, with both the Arduino and the multimeter. An analysis of the results showed an average error between the both systems of 0.75 mV with a standard deviation of ±0.66 mV, and an average relative error of 2.86 %.

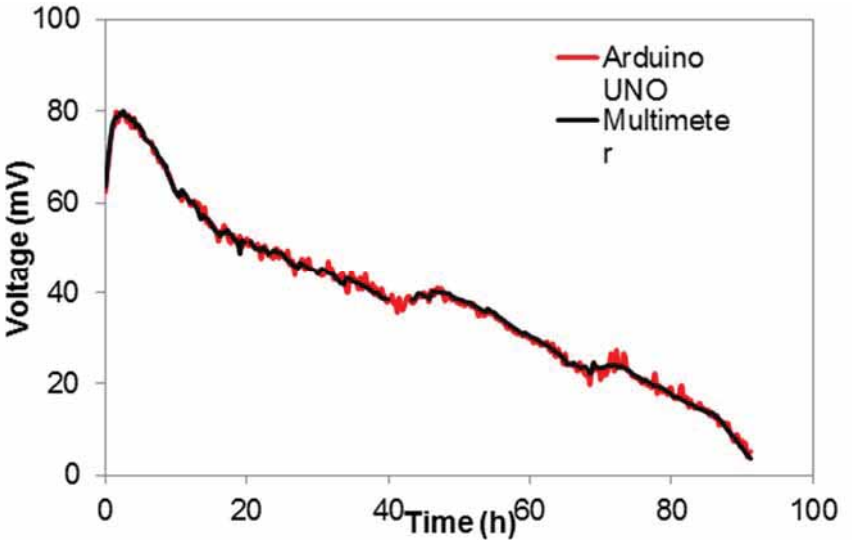


FIGURE 1. Voltage measuring test with Arduino UNO against the multimeter during the whole run

Even though the absolute error was constant the whole operation, the relative error was still high, this was due to the fact that the reference value keep lowering. With the absolute error being constant at different voltages, we can predict the error based on the operation voltage of the MFC at the moment. A list of predicted relative error according to the operation voltage is shown in **Table 1**. According to **Table 1**, with a cell voltage over 80 mV, the low-cost system can be used with a relative error less than 1%, achieving 0.375% at 200 mV and reaching less than 0.15% operating over 500 mV.

TABLE 1. Predicted relative error at different cell voltages using Arduino, considering a constant average error

Voltage (V)	Relative Error (%)	Voltage (V)	Relative Error (%)
0.5	0.150	0.07	1.071
0.4	0.188	0.06	1.250
0.3	0.250	0.05	1.500
0.2	0.375	0.04	1.875
0.1	0.750	0.03	2.500
0.09	0.833	0.02	3.750
0.08	0.938	0.01	7.500

Even if the average absolute error was lower than 1 mV, a few points on the Arduino line were evidently not fitting vs the multimeter line, a post-operation mathematical arrangement could be done for smoothing the line and achieve a better fitting. In this case, a running average of three values was used; the modified line is shown at the **Figure 2**. With this running average, the average absolute error decrease to 0.62 mV, and the average relative error to 2.45 %. The fact that the behavior in this experiment was a constant slope decreased the possible improvement to the fitting by the mathematical method.

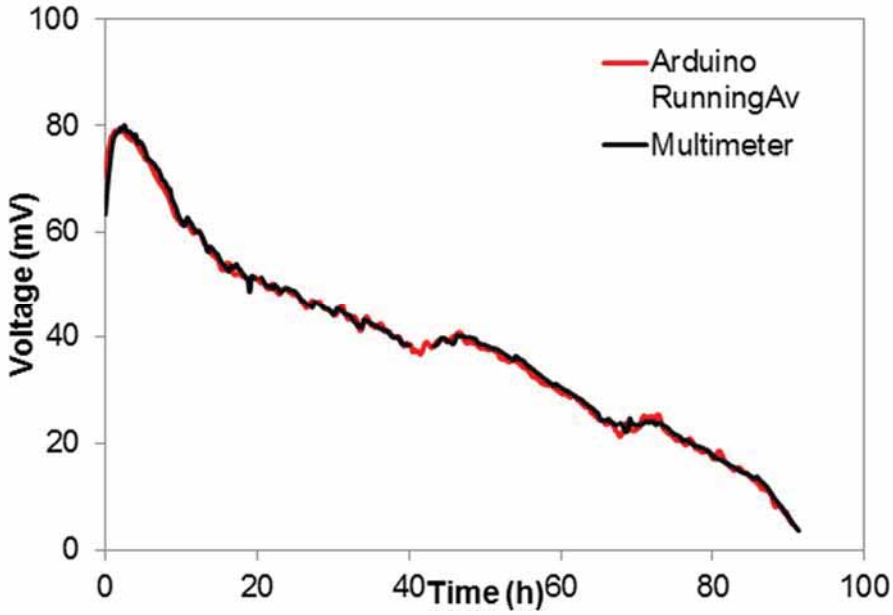


FIGURE 2. Voltage measuring test after mathematical smoothing using running average method

CONCLUSION

The low-cost system performed with high fidelity when tested against the multimeter. Even if the low-cost system has its flaws, it showed under 1 % relative error with cell voltages over 80 mV and with relative error over 2% only under 40 mV, which are voltages easily surpassed by MFC, and often present only in decay stage. The conditions of the test were the most adverse for it to operate, a never-steady slope and very low voltages, so a better performance is expected with more promising behavior. The system could keep improving to obtain even better results.

REFERENCES

1. B. E. Logan, Microbial Fuel Cells. Hoboken, New Jersey: John Wiley & Sons, Inc., 2007.
2. A. E. Franks and K. P. Nevin, “Microbial fuel cells, a current review,” Energies, vol. 3, no. 5, pp. 899–919, 2010.
3. M. Zhou, H. Wang, D. J. Hassett, and T. Gu, “Recent advances in microbial fuel cells (MFCs) and microbial electrolysis cells (MECs) for wastewater treatment, bioenergy and bioproducts,” J. Chem. Technol. Biotechnol., vol. 88, no. 4, pp. 508–518, 2013.

4. Z. He and L. T. Angenent, “Application of bacterial biocathodes in microbial fuel cells,” Electroanalysis, vol. 18, no. 19–20, pp. 2009–2015, 2006.
5. B. E. Logan, B. Hamelers, R. Rozendal, U. Schröder, J. Keller, S. Freguia, P. Aelterman, W. Verstraete, and K. Rabaey, “Microbial fuel cells: Methodology and technology,” Environ. Sci. Technol., vol. 40, no. 17, pp. 5181–5192, 2006.
6. Y. A. Badamasi, “The working principle of an Arduino,” Proc. 11th Int. Conf. Electron. Comput. Comput. ICECCO 2014, 2014.
7. A. Sattar, “Solar Power Remote Monitoring and ControllingUsing Arduino , LabVIEW and Web browser,” Power Gener. Syst. Renew. Energy Technol., pp. 1–4, 2015.
8. R. W. Fransiska, E. M. P. Septia, W. K. Vessabhu, W. Frans, W. Abednego, and Hendro, “Electrical power measurement using Arduino Uno microcontroller and LabVIEW,” Proc. 2013 3rd Int. Conf. Instrumentation, Commun. Inf. Technol., Biomed. Eng. Sci. Technol. Improv. Heal. Safety, Environ., ICICI-BME 2013, pp. 226–229, 2013.
9. A. Jamaluddin, L. Sihombing, A. Supriyanto, A. Purwanto, and M. Nizam, “Design real time battery monitoring system using LabVIEW Interface for Arduino (LIFA),” Proc. 2013 Jt. Int. Conf. Rural Inf. Commun. Technol. Electr. Technol. rICT ICEV-T 2013, pp. 5–8, 2013.
10. M. Armendariz, M. Chenine, L. Nordström, and A. Al-Hammouri, “A co-simulation platform for medium/low voltage monitoring and control applications,” 2014 IEEE PES Innov. Smart Grid Technol. Conf. ISGT 2014, 2014.

CHAPTER 1.15 SEQUENTIAL HYDROGENOGENIC AND METHANOGENIC FERMENTATION OF WASTE DISPOSABLE DIAPERS

Perla X. Sotelo-Navarro (1); Héctor M. Poggi-Varaldo *(2); Sylvie J. Turpin-Marion (1); Rosa M. Espinosa-Valdemar (1); Alethia Vázquez-Morillas (1) and Margarita Beltrán-Villavicencio (1)

(1) Department of Energy, Sustainable Technologies Area, UAM-A, México, D. F. Av. San Pablo #180 Col. Reynosa Tamaulipas,Ciudad de México, México. C. P. 02200.
(2) Environmental Biotechnology and Renewable Energies Group, Department of Biotechnology and Bioengineering, Centro de Investigación y Estudios Avanzados del IPN, P.O.Box 14-740, Ciudad de México, C. P. 07000.

ABSTRACT

The aim of this research was to evaluate the series hydrogenogenic-methanogenic fermentation of waste disposable diapers (dd) improving the yields compared to a one-phase process.
The batch bioreactors of the first stage (the hydrogen producing or H-stage) were loaded with used disposable diapers (DD) at 25% total solids and heat-shocked inoculum, and incubated at 35 and 55°C. Reactors were operated with intermittent venting and flushing (SSAHF-VI). The fermented solids coming out from H bioreactors were fed individually to methane producing bioreactors in the second stage of the experimental design (M-stage). M-stage bioreactors were operated at the same temperature of their feed in the batch process. The factors tested were the feed source and temperature of operation.
In the H-stage of our series process, the thermophilic temperature had a positive significant effect on higher hydrogen productivities compared to mesophilic operation. Methane production was similar in all cases; there was no difference by substrate condition, or by temperature. The energy potential of CH_4 in the M stage was significantly higher than the energy potential of H_2 harvested in the H stage. We conclude that this experiment is a significant beach-head for integrating waste DD treatment to modern biorefineries.

Keywords: biofuel, digestion, hydrogen, methane

INTRODUCTION

Fossil fuels have traditionally been used for power generation. However, these are scarce and non-renewable, so the study of new forms of energy is required. Among these is the use of biomass as a source of energy[1].

The transformation of biomass into fuel products, such as hydrogen and methane is carried out mainly by biological processes such as dark fermentation and anaerobic digestion[2-5].

---

*Author for correspondence: r4cepe@yahoo.com

Generally, biotechnological processes are based on the production of a single product, but because of the constant need for different products in series, a change of approach, from biotechnology to biorefineries, is needed[6]. In recent years the study and development of processes of biorefining waste has increased, in order to contribute to its energy recovery and reduce environmental impacts due to its poor disposal and treatment[7].

Within the principle of biorefinery, dark fermentation contributes to the degradation of biomass and the production of secondary metabolites, capable of being used in a second phase, such as the hydrogenesis-methanogenesis sequence[8,9].

The aim of this study was to use disposable diapers waste to investigate the two-stage process, combining hydrogen and methane production.

MATERIALS AND METHODS

A two-stage process for the sequential production of hydrogen and methane (H–M process, **Figure 1**) was implemented. The batch bioreactors of the first stage (H-stage), were fed (25% TS) with disposable diapers in three different conditions (whole diapers with feces, urine and plastics, WD; diapers without plastic components, with urine and feces, DWP; diapers without feces and plastic, MSD). The H-stage performance was evaluated at mesophilic (35 ± 0.5 ◦C) and thermophilic (55 ± 0.5 ◦C) regimes.

The fermented solids coming out from each of the different hydrogenogenic bioreactors were fed individually to methane producing bioreactors in the second stage of the experimental design (M-stage). M-stage bioreactors were operated at the same temperature of their feed in the batch process. The tested factors were the feed source and temperature of operation.

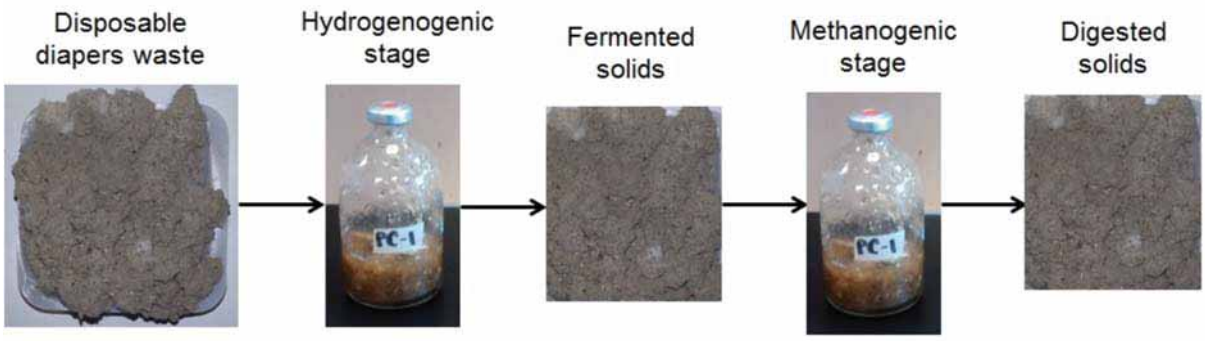


FIGURE 7. Two-stage experimental set-up for solid substrate fermentation.

Bioreactors for H and M stages were seeded with digests from solid substrate methanogenic, lab scale, and anaerobic digesters. The digesters were either mesophilic (35 ± 0.5 ◦C) or thermophilic (55 ± 0.5 ◦C). Methanogenic digests were previously subjected to heat-shock at 90 ºC for 1 h for de H-stage. After inoculation, the bioreactors headspace was flushed with N_2 in order to maintain anoxic conditions. Then, the bioreactors were incubated at the corresponding temperature.

According to the experimental design, H-stage fermented solids were fed to M-stage bioreactors. Neither pH adjustment nor washing of the solids was performed. The

operational period of hydrogenogenic bioreactors (H first stage) was around 79 days, whereas that of the methanogenic bioreactors was ca. 43 days. All treatments were run in triplicate.

Both stages were operated based on the solid substrate anaerobic hydrogen fermentation with intermittent venting and headspace flushing method (SSAHF-IV), that is, when a maximum H_2 or CH_4 cumulative was observed, the headspace of the bioreactors was gassed-out with N_2 to expel the accumulated H_2 or CH_4. Afterward, the bioreactors were reincubated, for another cycle of production and repeated until no more H_2 or CH_4 was harvested in the cycle.

H_2 and CH_4 contents were determined by gas chromatography in a GOW-MAC chromatograph model 350 fitted with TCD and a Molecular Sieve 5A packed column (injector, detector, and column temperatures were 37, 100 and 70◦C, respectively). Argon was used as carrier gas.

The energy analysis of H-M system (E_{HM}) was performed by summing the energy potential of the methanogenic hydrogenic processes (Eq. 1). The potential (Eq. 2) energy is directly proportional to the hydrogen production (QH_2) or methane (QCH_4) for a time t of operation, combustion enthalpy (ΔHc). In the case of batch operation equation 2, is amended by the cumulative production of H_2 or CH_4 respectively (Eq. 3).

$$E_{HM} = E_{H_2} + E_{CH_4} \quad (1)$$

$$E_{H_2}[KJ] = \int_0^t Q_{H_2\,[NL/d]}\,dt * \frac{1\ mol}{22.4\ NL} * \Delta Hc_{H_2}\,[KJ/mol] \quad (2)$$

$$E_{H_2}[KJ/Kg_{db}] = \frac{Vol._{H_2\ cumulative}\ [mol]}{TS_{dry\ basis}} * \Delta Hc_{H_2}\,[KJ/mol] \quad (3)$$

RESULTS AND DISCUSSION

The H-stage with intermittent venting (SSAHF-IV) of disposable diapers allowed three cycles of hydrogen generation with no addition of new substrate or inoculum between cycles (**Figure 2A** and **2B**), A fourth cycle was attempted, but no noticeable hydrogen generation was found. In the case of M-stage two cycles were set up (**Figure 2C** and **2D**). Cumulative P_{H2} (production of H_2) and P_{CH4} (production of CH_4) in subsequent incubation cycles in our work were lower than those obtained in the first cycle for both cases (**Table 1),** as expected.

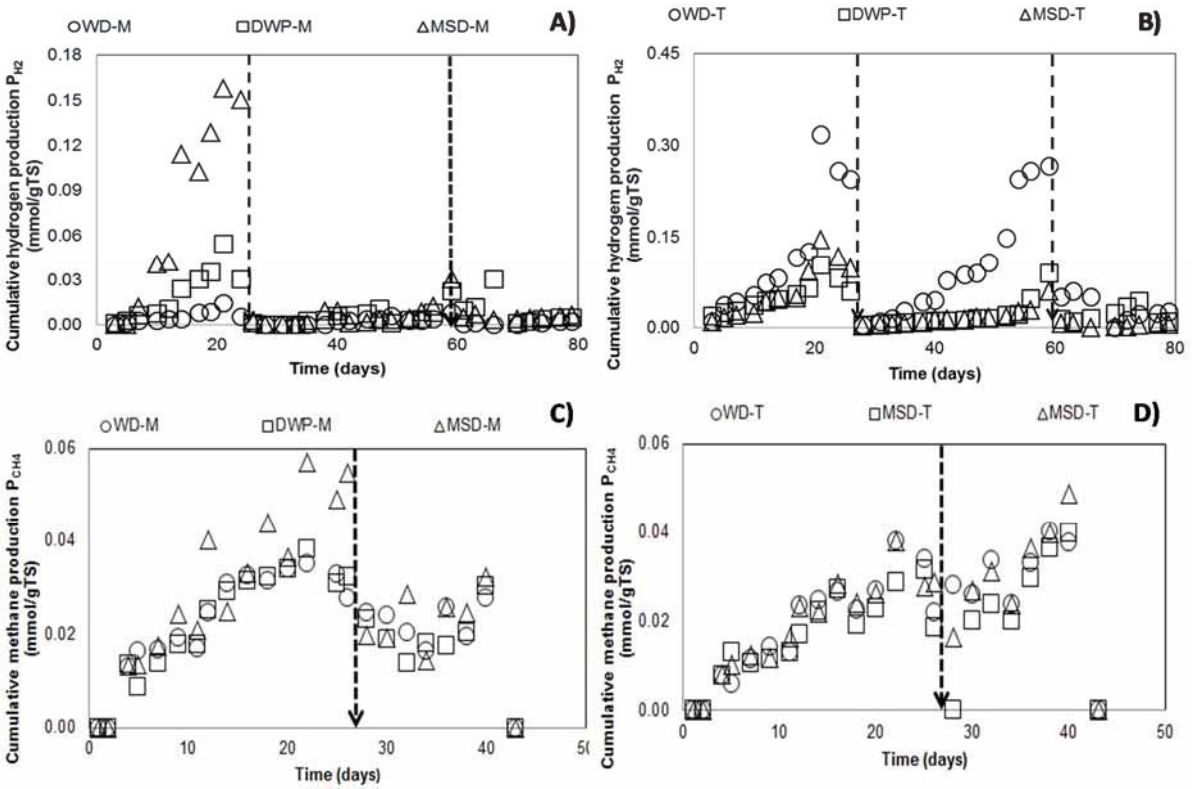


FIGURE 8. Hydrogen and methane stage dynamics: A) H-stage mesophilic, B) H-stage thermophilic, C) M-stage mesophilic and D) M-stage thermophilic; Keys: vertical arrows indicate flushing of bioreactor headspace with N_2.

Table 1 shows the cumulative production of H_2 and CH_4 obtained at different stages. We can see that the increased production of H_2 was obtained in the thermophilic range for the three conditions was substrate, especially the production of whole diapers with feces, urine and plastics (WD), almost three times greater than the other two wing same temperature. Methane production in methanogenic stage showed similarities in all cases.

TABLE 4. H_2 and CH_4 from used disposable diapers in each incubation cycle and total hydrogen and methane production

Factor		P_{H2} [a] per incubation cycle			Total P_H ($\Sigma_1^3 P_H$)[b]	P_{CH4} [c] per incubatiom cycle		Total P_{CH4} ($\Sigma_1^2 P_H$)[d]
Condition	Temperature	1	2	3		1	2	
WD	M	0.014±0.002	0.008±0.001	0.002±0.001	0.024±0.001	0.035±0.001	0.030±0.005	0.063±0.007
DWP	M	0.054±0.003	0.022±0.009	0.004±0.000	0.081±0.004	0.034±0.009	0.025±0.004	0.059±0.006
MSD	M	0.158±0.025	0.030±0.005	0.000±0.000	0.188±0.01	0.044±0.014	0.032±0.007	0.075±0.022
WD	T	0.317±0.016	0.266±0.033	0.026±0.002	0.609±0.017	0.038±0.006	0.040±0.007	0.078±0.001
DWP	T	0.102±0.005	0.089±0.001	0.008±0.001	0.200±0.014	0.032±0.001	0.040±0.001	0.072±0.002
MSD	T	0.145±0.007	0.060±0.000	0.005±0.000	0.210±0.002	0.038±0.012	0.049±0.028	0.087±0.040

[a]Net H_2 production average in each incubation cycle (mmoles H_2/g_{TS}), [b] Cumulative sum of H_2 produced in the three incubation cycles, (mmoles H_2

[c]Net CH_4 production average in each incubation cycle (mmoles CH_4/gTS), d Cumulative sum of CH_4 produced in the two incubation cycles, (mmoles CH_4/gTS)

Some studies have found that hydrogen energy production processes in series are not competitive with methane[10-12]; however, the synergy that exists between these two processes improves the net potential energy of the system (**Table 2**). It can be seen that despite having a low yield of methane, the energy potential of the sequential method increases remarkably compared with the hydrogen to most cases. The energy value of CH_4 in the M stage was significantly higher than the energy value of H_2 harvested.

TABLE 2. Potential energy production by hydrogen and methane.

Factor		Hydrogen		Methane		H-M system
Condition	Temperature	Cumumulative H_2 (mol/Kg)	E_{H2} (KJ/Kg_{db})	Cumumulative CH_4 (mol/Kg)	E_{CH4} (KJ/Kg_{db})	E_{HM} (KJ/Kg_{db})
WD	M	0.024	6.860	0.063	56.095	62.955
DWP	M	0.081	23.153	0.059	52.534	75.687
MSD	M	0.188	53.738	0.075	66.780	120.518
WD	T	0.609	174.077	0.078	69.451	243.528
DWP	T	0.200	57.168	0.072	64.109	121.277
MSD	T	0.210	60.026	0.087	77.465	137.491

CONCLUSION

This work shows that a two-stage process combining hydrogen and methane production from disposable diapers waste can work successfully. This process produces 0.609 mmolH_2/g_{TS}, and 0.078 mmolCH_4/g_{TS} when applied to WD.
The use of solids fermented in a H-stage for the production of methane is feasible, since the serial connection of these processes is perfectly complementary; however, the net production of methane from the solids fermented was low.
The energy value of CH_4 in the M stage was significantly higher than the energy value of H_2 harvested in the H stage. We conclude that this experiment is a significant beach-head for integrating waste DD treatment to modern biorefineries.

ACKNOWLEDGMENTS

The authors wish to thank the National Council of Science and Technology (CONACYT) for a graduate scholarship to PXS-N and support to CINVESTAV's infrastructure project 188221 of HMP-V. The excellent help of Professor Elvira Ríos Leal and Mr. Gustavo Medina (Central Analítica) as well as Mr. Rafael Hernández-Vera from the GBAER-EBRE Group, CINVESTAV del IPN, is gratefully acknowledged.

REFERENCES

1. Bridgwater, T. (2006). Biomass for energy. Journal of the Science of Food and Agriculture, 86(12); 1755-1768.
2. Madigan MT, Martinko JM, Stahl DA y Clark DP. (2012). Brock. Biology of Microorganism. 13ª edición. Pearson.

3. Hallenbeck, P. C. and Benemann, J. R. (2002). Biological hydrogen production; fundamentals and limiting process. International Journal of Hydrogen Energy, 27, 1185-1193.
4. Levin, D.B., Pitt, L. y Love, M., (2004). Biohydrogen production: prospects and limitations to practical application. International Journal of Hydrogen Energy, 29, pp.173–185.
5. Angement, L. T., Karim, M. H.., Al-Dahhan, B. A. Wrenn and Dominguez-Espinosa. (2004). Production of bioenergy and biochemicals from industrial and agricultural wastewater, Trends Biotechnol, 22(9):477-485.
6. Kamm, B. and Kamm, M. (2004). Principles of biorefineries, Applied Microbiology and Biotechnology, 64(2):137-145.
7. Ragauskas, A. J., Beckham, G. T., Biddy, M. J., Chandra, R., Chen, F., Davis, M. F., Davison, B. H., Dixon, R. A., Gilna, P., Keller, M., Langan, P., Naskar, A. K., Saddler, J. N., Tshaplinski, T. J., Tuskan, G. A. and Wyman, C. E. (2014). Lignin valorization: improving lignin processing in the biorefinery, Science, 344.
8. Liu, D., Zunge, R. J. and Angelidaki, I. (2006). Hydrogen and methane production from household solid waste in the two-stage fermentation process. Water Research, 40(11):2230-2236.
9. Escamilla-Alvarado, C., Ponce-Noyola, M. T., Poggi-Varaldo, H. M., Ríos-Leal, E., García-Mena, J., Rinderknecht-Seijas, N. (2014). Energy analysis of in-series biohydrogen and methane production from organic wastes. International Journal of Hydrogen Energy, 39:16587-16594.
10. Venkata-Mohan, S., Mohanakrishna, G. and Sarma, P. N. (2008). Integration of acidogenic and methanogenic processes for simultaneous production of biohydrogen and methane from wastewater treatment. International Journal of Hydrogen Energy, 33(9): 2156-2166.
11. Zhu H, Stadnyk A, Beland M, Seto P.(2008) Co-production of hydrogen and methane from potato waste using a two-stage anaerobic digestion process. Bioresour Technol; 99(11):5074-5085.
12. Cooney, M., Maynard, M., Cannizzaro, C. and Benemann, J. (2007). Two-phase anaerobic digestion for production of hydrogen–methane mixtures. Bioresource Technology; 98(14): 2641-2651.
13. Cavinato, C., Bolzonella, D., Fatone, F., Giuliano, A. and Pavan, P. (2011). Two-phase thermophilic anaerobic digestion process for biohythane production treating biowaste: preliminary results. Water Science and Technology; 64(3): 715-721.

CHAPTER 1.16 BIOREFINERY OF LEMON PEEL WASTE USING COLD ADAPTED YEASTS FROM ANTARCTIC AND SUB-ANTARCTIC REGIONS

A. Albanesi (1); **I. Cavello** *(1); D. Fratebianchi (1); A. Martinez (2); G. Garmendia (2); S. Vero (2) and S. Cavalitto (1)

(1) CINDEFI, UNLP, CONICET. Calle 47 y 115. (B1900ASH) La Plata. Argentina
(2) Cátedra de Microbiología, Departamento de Biociencias, Facultad de Química, UdelaR, Montevideo, Uruguay.

ABSTRACT

Cold adapted yeasts from soil samples from King George Island and Tierra del Fuego province were evaluated for their potential to produce extracellular pectinases. Pectinolytic yeasts were previously identified by 26S rDNA (D1/D2 domain) sequencing and phylogenetic analyses. Among 103 isolates, only eight showed pectinolytic activity at 20ºC, and only four -strains e9.2, 4.6, 5.9 and 8E- were capable to produce pectinolytic activity at 8ºC. Strain 8E identified as *Guehomyces pullulans* and the strains e9.2 and 5.9 identified as *Cystofilobasidium infirmominiatum* and *Cryptoccocus adeliensis* were selected for enzyme production under submerged fermentation.

All the strains were capable to grow in presence of lemon peel. *C. adeliensis* 5.9 produced the highest enzyme activity at 24 h (4.8 U/ml) while *C*. *infirmominiatum* e9.2 and *G*. *pullulans* 8E showed considerable activity at 45 h (3.9 U/ml and 2.83 U/ml, respectively). It could be seen that at 10ºC enzyme/s remained active. Besides polygalacturonase (PGase), presence of other pectin-degrading enzymes in the culture supernatants was investigated. None of the strains produce neither pectin or pectate lyase activity nor rhamnogalacturonan hydrolase activity. Regarding pectin esterase activity, it was only produced by *G*. *pullulans* (0.022 U/ml). All the strains produced enzymatic pools that showed higher activity against highly esterified pectin than against pectin with 63% methoxyl. This behavior could be attributed to the presence of polymethylgalacturonase activity (PMGase) in its supernatant. β-glucosidase activity was detected in all supernatants.

This is the first report on the capacity of these species to produce pectinases. Inulinase activity was detected in *G*. *pullulans* and *C. infirmominiatum* supernatants, while xylanase and cellulase activities were only detected in *G*. *pullulans* supernatants.

Keywords: agro-industrial wastes, cold adapted enzymes, lemon peel.

---

*Author for correspondence: icavello@biotec.quimica.unlp.edu.ar

INTRODUCTION

Twenty-two per cent of the global fruit market corresponds to citrus production. Within this group, oranges represent 66%, while tangerine and lemon represent 21% and 7% respectively, being 28% of citrus production industrialized. The most important producing countries are Brazil (orange), China (grapefruit and tangerine) and the US. Argentina is the eighth largest producer of citrus and world's largest producer of lemon and has been exporting fresh lemon fruits, juices and essential oils since 1970. The basic structure of the citrus activity in Argentina consists of 5,300 primary producers, which have a cultivable area of 147,466 ha with citrus, with a production of 2.7 million tons of fruit per year. There are 16 industries for juices and derivatives and 529 packaging plants that provides direct employment to about 120,000 people and generates a value of U$S 528 million annually, 64% of which are due the exportation of fresh fruit, juice concentrates and other derivatives. Production is mainly destined to industry (47%) and domestic consumption (32%), being the rest exported. Argentina's production covers a period of ten months from March to December and consist of lemons (49%), oranges (27%), tangerines (18%) and grapefruit (6%). 92% of fruit exports is conducted between May and September and the main destination is the European Union.

The main solid waste of the citrus industry is composed of peels, seeds, pulp and skins. The volumes that these industries handle makes this waste a true ecological problem, which is usually solved by disposing it in dumpsites or sometimes throwing it in river banks and margins and river courses, producing great contamination. Lemon peel is a by-product of the citrus industry that is mainly used as raw material for pectin extraction. Today the fall of this market makes necessary the study of other alternatives for the use of this waste. It is estimated that the lemon peel represents 19.8% of the dry weight of the fruit. Thus, an annual production of 1.5 million lemons generates approximately 148,000 tons of this waste.

Pectinolytic enzymes or pectinases are depolimerizing enzymes that degrade pectic susbtances present in cell walls of plant tissue[1,2]. This enzymes have wide-spread applications in the food industry for clarification of fruit juices, wines, coffee and tea fermentations[3]. Today, the main source of pectinases used in these industries is from fungi, mainly *Aspergillus niger*, since it produces high amounts of these enzymes and is a GRAS microorganism[4] . Yeasts declared as GRAS microorganisms, and which produce high levels of pectinases might be an interesting alternative source of pectinase for these industries.

Interest in cold-active enzymes has been growing in recent years due to the possibility to use them in mild conditions. For example, cold-active pectinases are attractive for it usage in fruit juice industry, as colder temperatures hamper spoilage and favor milder conditions that avoid changes in organoleptic and nutritional properties[2].

This work reports on three cold-adapted, pectinase producing yeast species isolated in Antarctica and Tierra del Fuego province, and presents a preliminar characterization of polygalacturonase activities produced by them. Production of other enzymes such as inulinase, celullase, xylanase and β-glucosidase was also investigated.

MATERIALS AND METHODS

Microorganisms. A collection of 103 yeast strains previously isolated and identified from soil samples from King George Island and Tierra del Fuego province were used in this study. The culture collection is maintained by cryopreservation (-80ºC in 10% glycerol) at Research and Development Center for Industrial Fermentations (CINDEFI-Argentina).

Screening and selection of pectinolytic yeasts. In order to detect pectinolytic enzymes, a selective medium containing 10 g/l citrus pectin (Sigma-Aldrich), 1.4 g/l $(NH_4)_2SO_4$, 2.0 g/l K_2HPO_4, 0.2 g/l $MgSO_4.7H_2O$, 1 ml sol. A (5 mg/l $FeSO_4.H_2O$, 1.6 mg/l $MnSO_4.H_20$, 2 mg/l $CoCl_2$) and 20 g/l agar was used. Isolates were point-inoculated and incubated at 8 ºC and 20ºC for 72 h. Yeasts producing pectinases were selected by the formation of a clear halo around the colonies after flooding the solid media plates with Lugol´s iodine solution[5]. Those yeasts which produced the largest halo diameter/colony diameter (Dh/Dc) were selected to continue with production studies.

Enzyme production. Submerged fermentation was carried out in 250 ml Erlenmeyer flask containing 50 ml of culture medium (10 g/l lemon peel, 1.4 g/l $(NH_4)_2SO_4$, 2.0 g/l K_2HPO_4, 0.2 g/l $MgSO_4.7H_2O$, 5 mg/l $FeSO_4.H_2O$, 1.6 mg/l $MnSO_4.H_20$, 2 mg/l $CoCl_2$, 5 g/l yeast extract and 2 g/l peptone, pH 5.0) and inoculated with 1 ml of yeast inoculums (DO 0.4). Flasks were incubated at room temperature (20ºC) and samples were with draw at different intervals of time and assayed for polygalacturonase activity.

Lemon peels were thoroughly washed with tap water to remove soluble sugars and dried in a hot air oven at 60ºC. Then the peels were milled (Mesh 35) and used as source of pectin.

Enzymatic assays. Polygalacturonase activity (PGase) was determined using polygalacturonic acid (Sigma Aldrich) as substrate. The reaction mixture containing 180 μl of 0.20 % polygalacturonic acid dissolved in citrate - phosphate buffer solution (CPB, 12.5 mM; 6.25 mM, pH 5.0) and 20 μl of the crude extract was incubated at 20 ºC for 30 min (Haggag et al., 2006). The release of reducing sugars was quantified by the Nelson-Somogyi method, using galacturonic acid as standard. One unit of enzyme activity was defined as the amount of enzyme that catalyzed the release of one micromole of galacturonic acid per minute under the given assay conditions. PGase activity was additionally measured at 10º C.

Pectinolityc activity was assayed by quatifying the reducing sugars released from a pectin solution dissolved in CPB (12.5 mM; 6.25 mM, pH 5.0), after incubation with 20 μl of the crude extract at 20 ºC for 15 min. Reducing sugars were measured using the Nelson-Somogyi method; galacturonic acid was used as standard. One unit of pectinolytic activity was defined as the amount of enzyme required to release one micromole of reducing sugars per minute under the given assay conditions. High and low methoxyl pectin were used for this assay, i.e., pectin esterified from citrus fruits (> 86 % methoxyl, Sigma) and pectin from citrus fruits (63 % methoxyl, Sigma), respectively.

Pectin esterase (PE) activity was measured by a titration method. To 10 ml of 0.5% w/v of citric pectin in 0.2 M NaCl, 250 μl of crude enzyme was added. The pH was adjusted to 5.50 with 0.1M HCl and the admixture was incubated for 5 min at 20ºC. PE activity was measured by determining the carboxyl groups released by titration with 0.0026 N NaOH. One unit of PE was defined as the amount of enzyme releasing one milliequivalent of ester hydrolyzed (carboxyl group) per minute.

Lyases. Pectin-lyase and pectate-lyase activities were estimated by measuring the increased in absorbance, due to the formation of unsaturated products.

In the case of pectin-lyase, 180 μl of citric pectin (Sigma Aldrich) 0.2% w/v in CPB (12.5 mM citric acid and 6.25 Mm Na_2HPO_3, pH 5.0) and 20 μl of the crude extract were incubated at 20º C for 15 min. Absorbance at 235 nm was monitored during the incubation time against a blank, in which the heat inactivated enzyme extract was used. One unit was defined as the increase in absorbance at 235 nm of 1.0 in the reaction mixture per minute under the given assay conditions.

For pectate-lyase activity, determinations were performed as stated immediately above, except for the fact that polygalacturonic acid was used as substrate and 1mM $CaCl_2$ was added to the reaction mixture.

Rhamnogalacturonan hydrolase activity was determined using rhamnogalacturonan (Sigma Aldrich) as substrate. The reaction mixture containing 180 μl of 0.20 % rhamnogalacturonan dissolved in CPB (12.5 mM; 6.25 mM, pH 5.0) and 20 μl of the crude extract was incubated at 20º C for 30 min. The release of reducing sugars was quantified by using the Nelson-Somogyi method; rhamnose was used as standard. One unit of enzyme activity was defined as the amount of enzyme that catalyzed the release of one micromole of rhamnose per minute under the given assay conditions.

Inulinase activity was determined using inulin (Difco) as substrate. The reaction mixture containing 180 μl of 0.20 % inulin dissolved in CPB (12.5 mM; 6.25 mM, pH 5.0) and 20 μl of the crude extract was incubated at 20º C for 30 min. The release of reducing sugars was quantified by the Nelson-Somogyi method, using fructose as standard. One unit of enzyme activity was defined as the amount of enzyme that catalyzed the release of one micromole of fructose per minute under the given assay conditions. Activity against sacarose was additionally measured.

β-glucosidase activity was detected by zymogram using 4-methylumbelliferyl beta-glucoside (MUG).

All enzyme assays were carried out in triplicate.

Zymogram analysis of pectin degrading enzymes and β-glucosidase detection. Zymograms were performed in conjunction with SDS-PAGE according to the method of García-Carreño et al.[6]. with slight modifications. SDS-PAGE was performed as described by Laemmli, using 5% (w/v) stacking gel and 12% (w/v) separating gel. For zymograms, after electrophoresis, the gel was submerged in CPB (12.5/ 6.25 mM, pH 5.0) containing 2.5% Triton X-100 for 60 min, with constant agitation in order to remove SDS. Triton X-100 was then removed by washing the gel three times with buffer. The gel was later incubated with PGA solution 0.2% (w/v) in buffer at 20ºC for 20 min. Finally, gels were stained with ruthenium red solution for zymographic analysis. The

development of clear zones on the pink background of the gels indicated the presence of pectinolytic activity. The development of clear zones on a pink background indicated the presence of pectinolytic activity. The molecular mass marker used was PageRuler™ prestained protein ladder, 10 to 180 kDa.

For β-glucosidase detection the gel was incubated with a 0.5mM MUG solution in sodium acetate buffer pH 4.5. After incubating the gels at 20° C for 15 min β-glucosidase activity was visualized as clear bands under UV light (λ=365 nm).

Thin-Layer chromatography (TLC). The endo- or exo-mode of action of the pectinolytic pools was studied by performing a TLC analysis of the final enzymatic degradation products.

For TLC analysis of PGA degradation products, heat inactivated samples were spotted (2 µL) on aluminium sheets (silica gel 60 F254, Merck) and the chromatography performed by using the ascending method with n-butanol : acetic acid : water (9 : 4 : 7, v/v/v) as the solvent system. Detection was accomplished by spraying the dried plate with 3% (w/v) phosphomolybdic acid dissolved in 10% (v/v) sulfuric acid in ethanol followed by heating at 105°C for 5 min. Tri galacturonic acid (TGA, Sigma) and galacturonic Acid (GA, Sigma) were used as standard.

An endo-PG is characterized by the production mainly of oligomers, whereas an exo-PG produces mostly monomers or dimmers.

RESULTS AND DISCUSSION

Screening of pectinolytic activity for yeast selection. One hundred and three yeasts isolated from soil samples from King George Island and Tierra del Fuego province were evaluated for their potential to produce extracellular pectinases. Among them, only eight isolates showed pectinolytic activity on plate at 20ºC. These strains were pre-selected and subjected to a secondary screening to study their capacity to grow and produce cold active pectinases (8 ºC). It could be seen that although all of them showed well developed colonies, only strains LP e9.2, LP 4.6, LP 5.9 and 8E were capable to produce pectinolytic enzymes (**Figure 1**).

Table 1 shows the ratio between clarification halo size and colony size (Dh/Dc) at 8 and 20º C. This relation was the first criteria used to select pectinolytic strains. According to these results, the isolate identified as *G*. *pullulans* 8E from King George Island, which showed the highest Dh/Dc ratio among the Antarctic isolates, and the two pectinolytic yeasts isolated from Tierra del Fuego province (*C*. *infirmominiatum* e9.2, *C*. *adeliensis* 5.9) were selected to continue with pectinase production studies. The strain 4.6 was not selected to continue with production studies because it was identified as *G*. *pullulans* and, although it developed a great halo, the strain 8E displayed the largest Dh/Dc relation.

The 26S rRNA gene partial sequences of all the three strains were deposited in Genbank database available at NCBI with the following accession numbers: KU 659491, KU 659577 and KU 659556 corresponding to *G. pullulans* 8E, *C. infirmominiatum* e9.2 and *C. adelienses* 5.9, respectively.



FIGURE 1. Screening of cold adapted yeasts in solid medium containing pectin after addition of lugol´s solution. a) plates incubated at 8 ºC and b) plates incubated at 20º C. A clear halo around the colonies indicates the production of pectinolytic enzymes.

TABLE 1. Halo diameter/colony diameter relation (Dh/Dc) for the pectinolytic strains at 8 and 20º C resulting from screening cultures in solid media containing pectin. Strains selected for production studies are indicated in bold.

Strain	Identity	Dh (mm)	Dc (mm)	Dh/Dc
8ºC				
LPe 9.2		70	50	1.4
8E		130	35	3.7
LP 4.6		125	55	2.3
LP 5.9		50	30	1.7
20ºC				
LP 1.1	*Cryptococcus antarticus*	90	50	1.8
LPe 9.2	*Cystofilobasidium infirmominiatum*	100	50	2.0
8E	*Guehomyces pullulans*	200	50	4.0
7BE	*Candida davisiana*	70	60	1.2
LP 4.6	*Guehomyces pullulans*	180	70	2.6
10E	*Cryptococcus victoriae*	50	40	1.3
37E	*Metschnikowia australis*	100	40	2.5
LP 5.9	*Cryptococcus adeliensis*	100	30	3.3

Production of pectinases by selected yeasts under submerged fermentation. PGase activity was evaluated during the culture time course as is shown in **Figure 2**. *Cryptoccocus adeliensis* 5.9 showed the highest enzyme production with a maximum at 24 h of cultivation (4.8 U/ml), followed by *Cystofilobasidium infirmominiatum* (3.9 U/ml) and *Guehomyces pullulans* (2.9U/ml). Enzyme activity was evaluated at 10ºC and it could be seen that at this temperature PGAse activity remains active. *C*. *infirmominiatum* supernatant retained 46% of its activity and *G*. *pullulans* supernatant 44%, while the activity of *C*. *adeliensis* supernatant increased to 150% which could be attribute to the instability of the enzymes at 20ºC.

Pectinase production from cold adapted yeasts is a field that is still relatively unexplored and, to our knowledge there are no reports on pectinases from any *Guehomyces pullulans*, *Cystofilobasidium infirmominiatum* or *Cryptoccocus adeliensis.*

Furthermore, there are only two reports on polygalacturonases from cold-adapted *Cystofilobasidium* strains. Nakagawa et al. (2002, 2004) [2,8] and Birginson et al [7] isolated yeasts with pectinolytic activity belonging to the order Cystofilobasidiales which is a group of psychrophilic basidiomycetes[9]. *Cystofilobasidium capitatum* strains PPY-1, PPY-5 and PPY-6 were isolated from soil samples from Hokkaido, Japan[8] while *C*. *larimarini* S3B and *C*. *capitatum* S5 were isolated by Birginson et al (2003)[7] from frozen soils, leaves and branches from the south-west of Iceland.

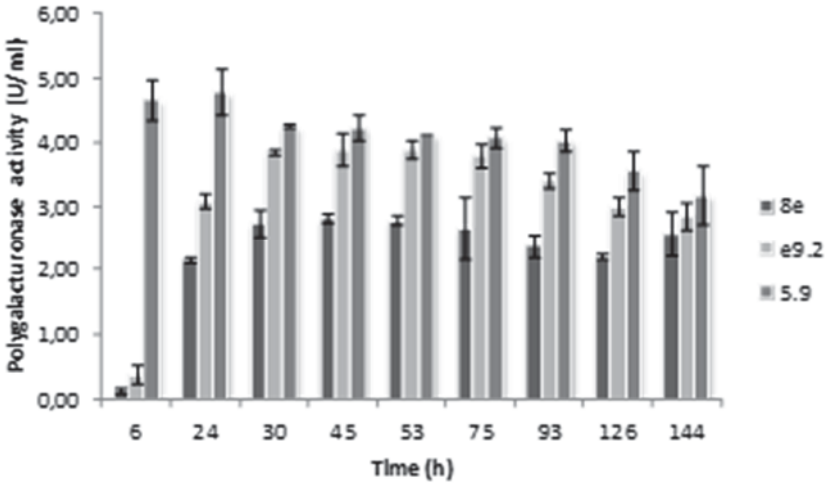


FIGURE 2. Time course of PGAse production by cold adapted yeast under submerged fermentation using cheap row material (lemon peels) as substrate.

Besides PGase, presence of other pectin-degrading enzymes in the culture supernatant of all three isolates was investigated. None of the strains produced neither pectin or pectate lyase activities nor rhamnogalacturonan hydrolase activity. Regarding pectin esterase activity, it was only produced in lower amounts by *G*. *pullulans* (0.022 U/ml). Differences were observed among the isolates when different pectins were used. All strains produced enzymatic pools that showed higher activity against highly esterified pectin compared with that measured when pectin with 63% methoxyl degree was used. This behavior could be attributed to the presence of polymethylgalacturonase activity (PMGase) in their supernatants. β-glucosidase activity was detected in all the

supernatants (**Figure 3**). Inulinase activity was detected in *G*. *pullulans* and *C. infirmominiatum* supernatants, while xylanase and cellulase activities were only detected in *G*. *pullulans* supernatants.

Zymogram analysis of pectin degrading enzymes and β-glucosidase detection. Zymogram analyses of pectinolytic enzymes in culture supernatants of the selected strains were performed. As can be seen in **Figure 3** *C*. *adeliensis 5.9* produces at least two active pectinases against PGA (180 kD and 40 kDa). *C*. *infimominiatum e9.2* produces a pectinase whose molecular weight is close to 70 KDa, whereas *G*. *pullulans 8E* produces at least 3 pectinases whose molecular weights are close to 55 KDa. Comparing with previously reports on pectinases characterization, the ones presented here have higher molecular weight; *Kluyveromyces marxianus* NCYC 578 produces four isoenzymes whose molecular weight ranges between 46 to 49 KDa[10] while *Saccharomyces pastorianus* produces a 43 KDa PGase and *Cryptococcus albidus* produces a polygalacturonase whose molecular weight is 41 KDa[11]. Nakagawa et al. (2005)[2] reported the production of five active pectinases for *Cystofilobasidium capitatum* PPY-6.

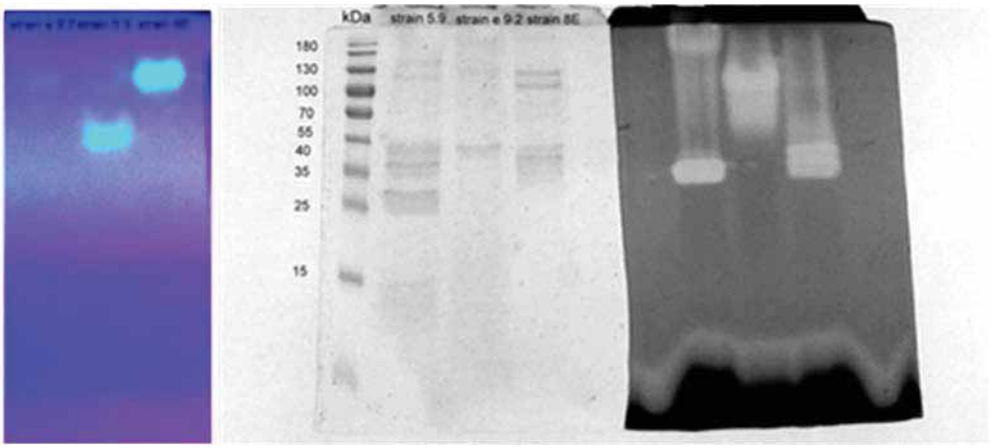


FIGURE 3. Zymogram analyses of pectinolytic enzymes and detection of b-glucosidase enzymes in culture supernatants of cold adapted yeast.

Thin-Layer chromatography TLC. TLC analysis of the products of PGA hydrolysis indicates that di-, and tri-galacturonates,as well as higher oligosaccharides were produced from the initial stages of the hydrolysis, and accumulated throughout the incubation period. PGases present in cold adapted yeasts supernatants did not seem to be able to attack dimers and trimers as these products were accumulated throughout the incubation period (**Figure 4**). From these results, it can be deduced that they act by an endo-splitting mechanism, and so they are endo-PGases (EC 3.2.1.15).

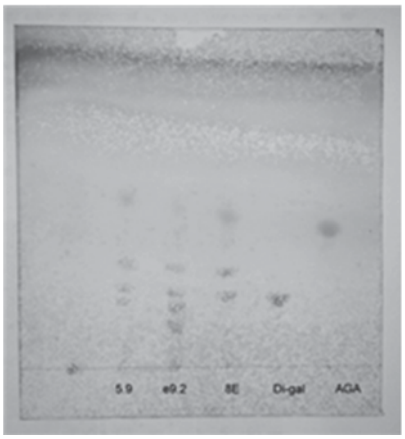


FIGURE 4. Thin-layer chromatography of the degradation products during enzymatic digestion of PGA with culture supernatants of pectinolytic yeasts.

CONCLUSION

The present study emphasized on cold active enzyme production and the capability of the yeasts to use lemon peels as a low cost raw pectin source for pectinolytic production at room temperature. This is commercially very important as the use of cheaper raw materials reduces the production costs significantly. Since the pectinolytic systems remain active at 10ºC they can be applied in fruit juice clarification. Fruit juices are cold stored to prevent spoilage and to increase its shelf life. Clarification at low temperature by these enzymes is cost effective since the temperature of the juice does not need to be raised so as to allow mesophilic enzymes work.

ACKNOWLEDGMENTS

This work was supported by grants from Consejo Nacional de Investigaciones Científicas y Técnicas (CONICET, PIP 112-201101-00662) and Agencia Nacional de Promoción Científica y Tecnológica (PICT 2014-1655).

REFERENCES

1. Naga Padma P, Anuradha K, Reddy G. Pectinolytic yeast isolates for cold-active polygalacturonase production. Innov Food Sci & Emerg Technol 12 (2011) 178-181.
2. Nakawa T, Nagaoka T, Miyaji T, Tomizuka N. Cold-Active Polygalacturonase from Psychrophilic-Basidiomycetous Yeast *Cystofilobasidium capitatum* Strain PPY-1. Biosc Biotechnol Biochem 69 (2005) 419-421.
3. Whitaker JR. Pectic substances, pectic enzymes and haze formation in fruit juices. Enz Microbial Technol 6 (1984) 341-349.
4. Alkorta I, Garbisu C, Llama MaJ, Serra JL. Industrial applications of pectic enzymes: a review. Process Biochem 33 (1998) 21-28.
5. Buzzini P, Martini A. Extracellular enzymatic activity profiles in yeast and yeast-like strains isolated from tropical environments. J Appl Microbiol 93 (2002) 1020-1025.

6. García-Carreño FL, Dimes LE, Haard NF. Substrate-gel electrophoresis for composition and molecular weight of proteinases or proteinaceous proteinase inhibitors. Anal Biochem 214 (1993) 65-69.
7. Birgisson H, Delgado O, Garciaa Arroyo L, Hatti-Kaul R, Mattiasson B. Cold-adapted yeasts as producers of cold-active polygalacturonases. Extremophiles 7 (2003) 185-193.
8. Nakagawa T, Kaichiro Y, Tatsuro M, Noboru T. Cold-active pectinolytic activity of psychrophilic-basidiomycetous yeast *Cystofilobasidium capitatum* strain PPY-1. J Biosc Bioeng 94 (2002) 175-177.
9. DePriest T, Ivanova N, Fahselt D, Alstrup V, Gargas V. Sequences of psychrophilic fungi amplified from glacier-preserved ascolichens. Can J Bot 78 (2002) 1450-1459.
10. Barnby FM, Morpeth FF, Pyle DL. Endopolygalacturonase production from *Kluyveromyces marxianus*. I. Resolution, purification, and partial characterisation of the enzyme. Enz Microbial Technol 12 (1990) 891-897.
11. Blanco P, Sieiro C, Villa TG. Production of pectic enzymes in yeasts. FEMS Microbiol Lett 175 (1999) 1-9.

Section 2.

Sustainability and Environmental System Analysis, Climate Change and Risk Assessment and Environmental Impact

Page

Chapter 2.1 Diseño sustentable de la cadena de suministro forestal considerando aspectos económicos y ambientales 148
Sandra Campanella; Gabriela Corsano and Jorge M. Montagna

Chapter 2.2 Environmental management as a tool for organizational development and business competitiveness: case study in Brazil 159
J. M. P. Filho; T. H. S. dos Santos; M. D. Alencar and M. O. B. C. de Melo

Chapter 2.3 Stress tolerance based on osmotic adjustment and yield of barley (*Hordeum Vulgare L.*) submitted to progressive drought and subsequent recovery 167
A. Thameur; K. Hessini; S. Ferchichi and C. Abdelly

Chapter 2.4 Análisis de tendencia de las precipitaciones en el interior del estado de Paraíba (Brasil) 182
S.E.L. Medeiros; R. Abrahão; I. García-Garizábal; I.M.B.M Peixoto and L. P. Silva

Chapter 2.5 The oasis system: a model of adaptation to the climatic changes 191
A. Boulassel; B. Mouhouche; D. Smadhi and L. Saidi

Chapter 2.6 Anionic surfactant quantification in Ipojuca River and textile laundry wastewater in the Caruaru City, Northeastern Brazil 200
J. L. Costa; I. F. B. Vieira; M. A. P. Kelm; E. A. Pastich; S. Gavazza and L.F. C. Souza

CHAPTER 2.1 DISEÑO SUSTENTABLE DE LA CADENA DE SUMINISTRO FORESTAL CONSIDERANDO ASPECTOS ECONÓMICOS Y AMBIENTALES

Sandra Campanella *(1); Gabriela Corsano(1,2) and Jorge M. Montagna(1)

(1) Instituto de Desarrollo y Diseño (INGAR, CONICET-UTN), Avellaneda 3657, Santa Fe, Argentina.
(2) Facultad de Ingeniería Química (UNL), Santiago del Estero 2829, Santa Fe, Argentina.

RESUMEN

La Cadena de Suministros (CS) forestal comprende desde las plantaciones de los árboles, materia prima fundamental para la mayoría de los productos, hasta la distribución de los productos a los clientes. A lo largo de la CS se generan diversos residuos (de las plantaciones) o subproductos (chips, aserrín, etc.) en los aserraderos a partir de la producción de madera. Un uso adecuado de estos materiales permitiría un desarrollo sustentable de estas industrias y agregaría valor a la cadena de producción. En este trabajo se propone una herramienta para evaluar alternativas de usos de los residuos y subproductos como materia prima para otros productos o como fuente de energía. De esta forma se enfatiza la importancia de reusar y reciclar material que, anteriormente, no tenía valor o el mismo era reducido. Por otro lado, más allá de los resultados económicos que se alcancen, es preciso considerar el impacto ambiental de las distintas alternativas. La herramienta propuesta está basada en un programa matemático mixto entero lineal, (MILP) en el que se evalúan tanto aspectos económicos como ambientales. En este último caso se utiliza como indicador las emisiones de gases de efecto invernadero (GEI) generados por el sistema. Debido a que existen diversos compromisos entre aspectos económicos y ambientales en los sistemas productivos, se recurre a la metodología ε-constraint, la cual permite confrontar estas perspectivas en la CS forestal. Los resultados muestran la importancia de tener en cuenta el punto de vista ambiental respecto a la configuración de sistemas productivos forestales y el impacto de considerar diversos tipos de unidades de producción y distintos tipos de calderas para el diseño sustentable de la CS.

Palabras claves: Cadena de suministro forestal, criterios ambientales, optimización multiobjetivo, sustentabilidad.

INTRODUCCIÓN

Las exigencias del mercado y los gobiernos en la protección del ambiente se ven reflejadas por las industrias e instituciones en sus intenciones en mantener sus acciones en el marco de una gestión ambiental[1]. En este contexto el diseño sustentable de la CS juega un rol importante, campo que está adquiriendo creciente interés entre investigadores y profesionales dedicados a la operación y gestión de la CS[2].

---

*Author for correspondence: campanellasr@santafe-conicet.gov.ar

Muchos trabajos han abordado la industria forestal desde la CS utilizando la programación matemática como una herramienta eficaz para su análisis y planeamiento. D'Amours y otros[3], presentan un modelo general del flujo de la madera dentro de la industria forestal. Utilizan la modelación matemática como herramienta para su diseño en función de resolver diferentes problemas de planeamiento. Danserau y otros[4], proponen una herramienta para tomar decisiones sobre políticas, basadas en las variaciones de mercado aplicada a la CS de biorefinerías que utilizan material forestal como combustible para su producción. Si bien la mayoría de los trabajos se enfocan en analizar la CS desde una perspectiva económica, existen otros autores que consideran la variable ambiental como un elemento importante. En este contexto, el uso de emisiones de Gases de Efecto Invernadero (GEI) y el análisis de ciclo de vida son herramientas frecuentemente utilizadas. Por ejemplo, Mälkki y otros[5] utilizan el análisis de ciclo de vida para contabilizar las emisiones de CO_2 producidas por la gestión de residuos de la madera, provenientes de plantaciones y aserraderos, para ser utilizados en la producción de energía. Se puede notar qué, a diferencia de la mayor parte de otras industrias, las forestales tienen la ventaja de poder utilizar sus residuos para contribuir a cubrir sus necesidades energéticas[6].

El trabajo que se propone a continuación tiene como objetivo presentar un análisis sobre la CS forestal, su configuración teniendo en cuenta criterios económicos y ambientales y los compromisos que se generan al considerar ambas perspectivas simultáneamente. Dadas las condiciones actuales en Argentina, se hace hincapié entre las alternativas de configuración de la CS, del uso de los residuos y subproductos como combustible y/o materia prima para otros productos.

En cuanto al aspecto ambiental, se utiliza como indicador las emisiones de GEI. Es importante destacar que existe un debate sobre cómo considerar las emisiones de la producción de energía a partir de combustibles biomásicos. Por un lado, es muy común asignarles un valor neutro, ya que el dióxido de carbono que se libera forma parte de la atmósfera actual (es el que absorben y emiten continuamente las plantas). Sin embargo, esta postura está siendo actualmente bastante discutida. Incluso, el comité científico de la Agencia Europea de Medio Ambiente (AEMA)[7] lo considera como un concepto erróneo. Los mismos sostienen que: "la combustión de biomasa aumenta la cantidad de carbono presente en el aire (al igual que la combustión de carbón, petróleo y gasolina), y la extracción de biomasa reduce la cantidad de carbono almacenada en plantas y terrenos de cultivo o reduce la continua captura y almacenamiento de carbono." Por este motivo en este trabajo se realiza un análisis del efecto de considerar o no estas emisiones sobre la generación de energía a partir de combustibles de biomasa vegetal. En esta controversia, influye además el tipo de tecnología utilizada para la generación de energía, ya sea con combustibles fósiles o a partir de biomasa, aspecto que será tenido en cuenta en esta propuesta.

Planteamiento del problema. Actualmente en Argentina existe un uso deficiente de residuos y subproductos de la industria forestal. Estos materiales pueden ser reutilizados con el fin de generar una producción más sustentable ambientalmente y a la vez, lograr mayor rentabilidad en este sistema productivo.

En este contexto, en este trabajo se presenta un análisis del diseño de la CS forestal considerando aspectos económicos y ambientales. La CS asumida considera varias

opciones de producción y el uso de residuos y subproductos como materia prima para otros productos, y como combustible para la generación de energía.

La misma consiste en tres niveles: sitios de obtención de materia prima, plantas de producción y áreas de clientes. Los sitios de materia prima proveen a las diferentes industrias de troncos y residuos, estos últimos generados a partir del crecimiento y cosecha de los árboles. Del árbol que se obtiene para ser usado como materia prima, el 38% corresponde a residuos de poda (ramas, hojas, etc.). En este trabajo se asume que, de este total, el 60% puede ser utilizado con diferentes fines mientras que el 40% restante debe quedar en los bosques para mantener las propiedades del suelo.

Se consideran cuatro tipos de unidades de producción: aserraderos, destilerías de etanol, tableros de partículas y pellets. Entre éstas pueden existir diversos flujos de materiales que se observan en la **Figura 1**. Los troncos pueden ser utilizados como materia prima para los diferentes productos contemplados, mientras que los residuos sólo pueden ser destinados a la producción de etanol y pellets. Los aserraderos, a lo largo de su tren de producción, generan diferentes subproductos: chip proceso, chip leña, corteza y aserrín y virutas, los cuales pueden ser usados como materia prima para la producción de etanol, pellets y/o tableros. Además, pueden ser vendidos a terceros o utilizados como combustible en las calderas de biomasa.

Para los diferentes procesos productivos se requiere energía térmica. Para esto se considera la posibilidad de instalar calderas, las cuales pueden usar como combustible fuel oil o biomasa vegetal. Las calderas de biomasa pueden ser hornos de incineración o calderas de cogeneración. En este último caso la energía extra que no se utiliza en los procesos puede ser vendida a la red. Tanto los subproductos de los aserraderos como los pellets pueden ser utilizados como combustible para este tipo de calderas.

Los productos generados en las diferentes plantas deben ser enviados a los clientes para abastecer una demanda mínima establecida, existiendo además un tope para cada producto y área de clientes.

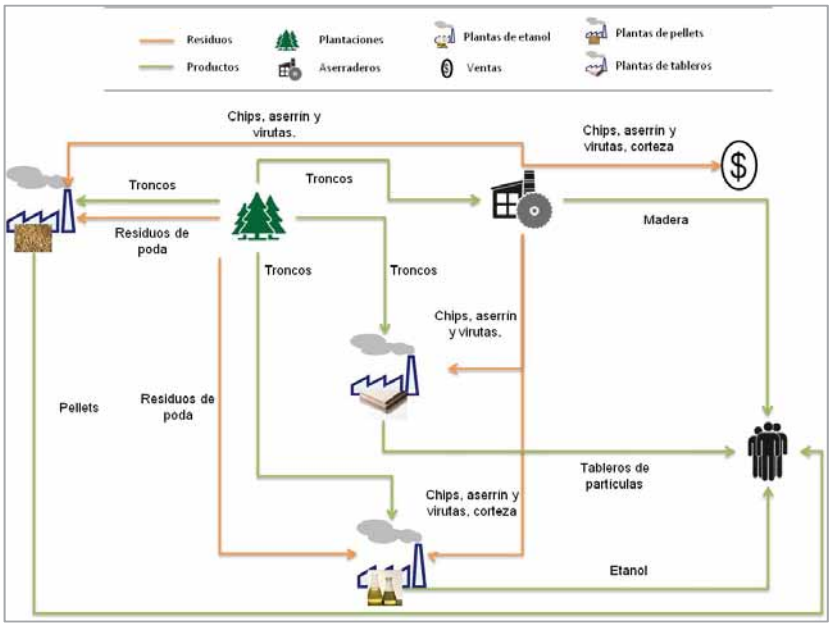


FIGURA 1. Flujos entre plantas de producción

MATERIALES Y METODO

Para el diseño y análisis del problema de la CS forestal presentado en el punto anterior se utiliza un modelo matemático. Se genera un MILP en el cuál se describen las diferentes relaciones y balances de materiales mencionadas mediante restricciones. A fin de considerar la performance de este sistema, el modelo considera el beneficio económico y las emisiones de GEI. Para el modelado de este problema se utiliza el software GAMS y para la resolución CPLEX.

Como se mencionó anteriormente, se busca analizar el diseño de la CS forestal considerando criterios económicos y ambientales. Para esto se utiliza la metodología "ε-constraint" tomando como restricciones las emisiones producidas por el sistema analizado y como función objetivo la rentabilidad de la CS. Esto significa que se acotan las emisiones de GEI a un valor máximo, y con esta cota propuesta, se maximiza el beneficio económico de la CS. A medida que se varía el máximo valor admitido para las emisiones, se obtiene una configuración diferente de la CS. De algún modo, esto permite determinar si realmente las restricciones ambientales impactan sobre la CS. Como resultado, se obtiene la curva de Pareto que muestra la relación entre los resultados económicos y ambientales y, en función de estos resultados, hacer un análisis sobre el comportamiento de la CS forestal.

Consideraciones ambientales: emisiones de GEI y límites del sistema. Para estimar las emisiones de GEI se siguieron los principios de “The International Council of Forest and Paper associations” (ICFPA)[8]. Tres tipos de gases son considerados en este tipo de industrias: el dióxido de carbono (CO_2), metano (CH_4) y óxido nitroso (N_2O), los cuales son llevados a CO_2 equivalente.

Las emisiones generadas por un sistema productivo generalmente son divididas en dos tipos: emisiones directas y emisiones indirectas. Las emisiones directas corresponden a fuentes que son controladas o que son propiedad de la empresa. Las emisiones indirectas son aquellas que son consecuencias de las actividades de la empresa, pero que son emitidas desde fuentes que no son controladas o que no son propiedad de la misma. En este trabajo se contabilizan sólo las emisiones directas producidas por la CS considerada.

Las estimaciones de este tipo de industrias, según el informe base que se toma como referencia[8], provienen de: emisiones de CO_2 de la combustión estacionaria de fuel, emisiones de CH_4 y N_2O de calderas de fuel y biomasa, emisiones de CO_2, CH_4 y N_2O provenientes del transporte, emisiones de CH_4 que se pueden atribuir al tratamiento de residuos provenientes de las plantas, emisiones de GEI relacionados con la importación y exportación de energía y vapor. En este caso también se analizan las emisiones de CO_2 provenientes de las calderas de biomasa.

En la **Figura 2** se puede observar los límites que se consideraron en el sistema bajo estudio. No se tiene en cuenta el tratamiento de los residuos líquidos y sólidos producidos a lo largo de los diferentes procesos productivos, por lo tanto, tampoco las emisiones producidas en el mismo. Las emisiones por importación de energía, al ser emisiones indirectas, no son tenidas en cuenta. Por lo tanto, sólo se consideran, finalmente, las emisiones producidas por el transporte y las calderas.

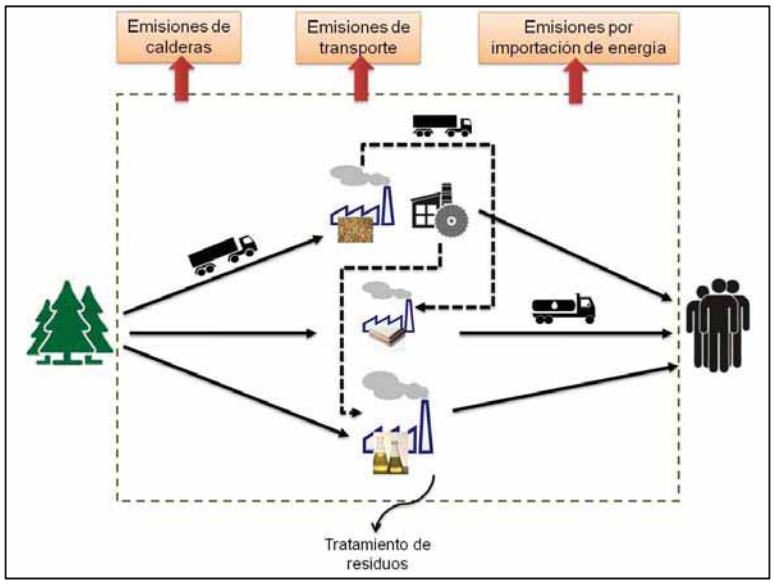


FIGURA 2. Límites para el análisis de emisiones de GEI

Consideraciones económicas. Dentro del sistema analizado se consideran tanto los costos como los ingresos. Entre los primeros se encuentran los costos de: adquisición de troncos, producción, adquisición de fuel oil para las calderas de fuel, instalación de plantas de producción, instalación de calderas, transporte de materiales entre los nodos considerados (materia prima, productos, residuos y subproductos). En este punto cabe aclarar que la adquisición de pellets o subproductos para la generación de energía no tiene ningún costo solamente el de transportarlos a su destino.

Los ingresos vienen determinados por la venta de productos, subproductos y energía a la red, en caso de que existiera. El beneficio económico del sistema viene determinado por la diferencia entre la totalidad de los ingresos menos la totalidad de los costos.

Caso de estudio. El enfoque propuesto en este trabajo se aplica a un caso de estudio basado en parámetros de Argentina. La CS propuesta involucra la región noreste y central del país. La primera de éstas se caracteriza por comprender la mayor cantidad de plantaciones del país en el área forestal, mientras que los principales consumidores se encuentran en la región central. Los parámetros utilizados en el modelo son propios de la industria forestal en Argentina, pero pueden ser fácilmente modificados y actualizados.

Las características del caso de estudio analizado son las siguientes:

- Se consideran cuatro sitios de materia prima (I1, I3, I4, I5) y cuatro de clientes (I8, I9, I10, I11).
- Las plantas de producción pueden instalarse en doce lugares diferentes: cuatro de ellos son sitios de materia prima, cuatro son de clientes y los restantes son puntos intermedios (I2, I6, I7, I12).
- Para cada planta de producción existen tres posibles capacidades con la cual puede instalarse. No puede haber más de una planta de cada tipo en un sitio. Plantas de

distinto tipo pueden instalarse en el mismo sitio, permitiendo disminuir costos de transporte y mejorando la interacción entre ellas.

- Las calderas pueden ser de diversas capacidades de producción seleccionadas entre un conjunto discreto de alternativas y pueden instalarse varias en un mismo sitio. La energía generada puede ser compartida entre las diferentes unidades de producción del sitio donde se encuentran instaladas.
- El transporte de los diferentes materiales se realiza mediante camiones, cuyo costo varía de acuerdo al material transportado.

RESULTADOS Y DISCUSION

El primer aspecto que se analiza es la influencia que tiene el tipo de caldera que se utiliza para la generación de la energía necesaria en las unidades de producción en la cantidad de emisiones de GEI. Para esto se consideran cuatro posibilidades en la solución óptima de máximo beneficio: 1) solo existe la posibilidad de generar energía a partir de calderas de fuel, 2) solo existe la posibilidad de generar energía a través de calderas de biomasa considerando sus emisiones, 3) existe la posibilidad de generar energía con ambas calderas considerando ambas emisiones, y 4) existe la posibilidad de generar energía con ambas calderas pero las emisiones de CO_2 de las calderas de biomasa se consideran neutras.

La distribución de troncos usados como materia prima varía notablemente en cada uno de los casos analizados. En la **Figura 3** se puede observar que en el caso 1 se destina una mayor cantidad a la producción de etanol. El caso 2 es el que mayor variación presenta frente a los otros. En primer lugar, es el caso en el que se destina mayor cantidad de troncos a la producción de madera. Esto se debe a la necesidad de generar mayor cantidad de subproductos para usarlos como combustible en las calderas y poder cubrir los requerimientos de energía. También se puede observar que, con este mismo objetivo, se destina mayor cantidad de troncos a la producción de pellets en comparación con otros casos, por más que la producción total de pellets no varíe significativamente. Esto se debe a que, en los otros casos, utiliza subproductos para generarlos y en este los utiliza como combustible para calderas. El destino de troncos a etanol se ve disminuido, dado que se destina una cantidad considerable a la producción de maderas, tableros y pellets. En los cuatro casos la materia prima es usada en su totalidad. Lo mismo sucede con los residuos generados en las zonas de materia prima, los cuales en los cuatro casos son destinados a la producción de etanol.

De la **Figura 4** se puede observar que la producción varía cuando se consideran las diferentes posibilidades. La producción de madera aumenta en el segundo caso, mientras que la producción de tableros disminuye debido a que no se utilizan subproductos para su elaboración. La producción de etanol también se ve reducida en este caso debido a que se destina menor cantidad de materia prima. La producción de pellets se mantiene en cantidades muy similares en los cuatro casos analizados. Si comparamos el caso 1 con el caso 3 y 4 podemos observar que la producción de tableros disminuye levemente y la de etanol aumenta.

El destino de los subproductos generados en los aserraderos se configura de manera muy diferente en cada caso, según muestra la **Figura 5**. En el caso 1 se destina en su

totalidad a la producción de tableros mientras que en el 2do caso a las calderas de biomasa. En el caso 3 y 4 se distribuyen entre la producción de tableros y generación de energía en las calderas.

En el primer caso, la energía total generada por las calderas de fuel es de 4,05E+9 Mj/año, mientras que en el segundo caso se genera 1,76E+9 Mj/año energía a partir de hornos de incineración. En el caso 3 y 4 se generan 3,94 E+9 Mj/año con ambos tipos de caldera, el 88% se genera con calderas de fuel y el porcentaje restante con hornos de incineración. Estas diferencias de generación de energía se deben a los requerimientos específicos para cada tipo de proceso productivo. En ningún caso los pellets son destinados como combustibles de las calderas y, al no instalarse calderas de cogeneración, se puede concluir que tampoco se vende energía a la red esto se debe a que el precio al que se compra no es atractivo frente a los costos de las mismas.

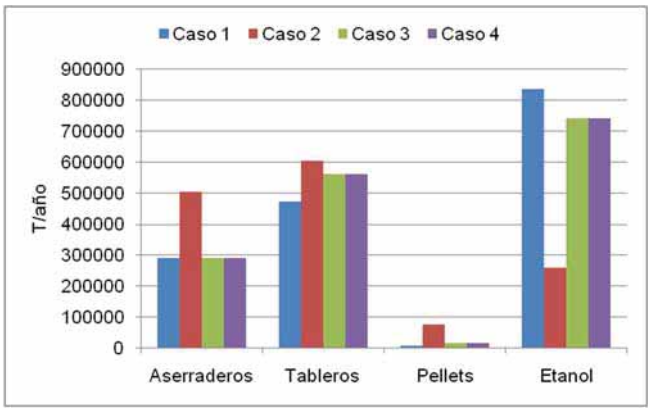


FIGURA 3. Destino de troncos

De la **Figura 6** se puede determinar que el beneficio económico (Bf) también se ve afectado de acuerdo a la configuración de la CS. En el caso 1 es solamente un 4% menor al del caso 3 y 4, mientras que al sólo considerar la posibilidad de instalar calderas de biomasa el beneficio disminuye más de un 50 % respecto a estos últimos.

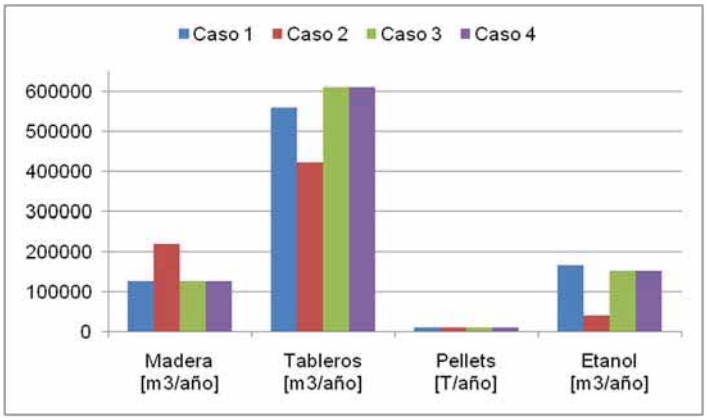


FIGURA 4. Producción en cada caso

Las emisiones de transporte (Etransp) varían de acuerdo a los diferentes casos (Fig. 6). En el caso 2 es donde existe menor emisión dado que no se transportan tantos

productos a clientes porque la producción se ve disminuida. Mientras que, en el tercer y cuarto caso, al darse la situación contraria, las emisiones presentan el mayor valor. En cuanto a las emisiones de las calderas (Ecald) existe una notable diferencia en cada caso.

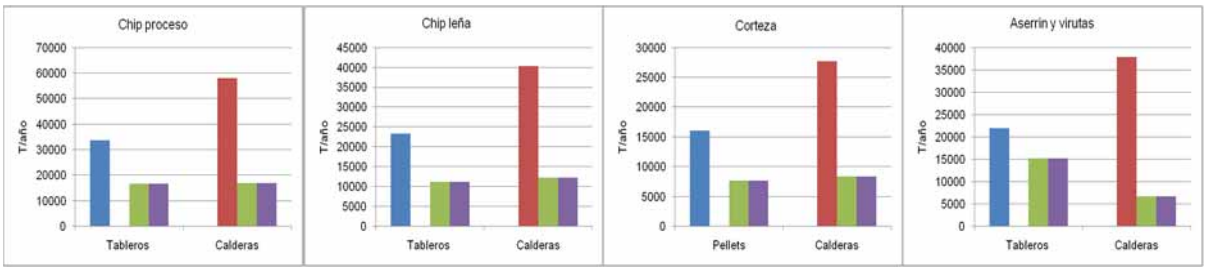


FIGURA 5. Destino de subproductos.

La mayor cantidad de GEI emitido a la atmósfera por esta fuente se da en el caso 2 dónde solo se genera energía a partir de calderas de biomasa. Si comparamos el caso 3 y el 4 vemos que el hecho de considerar neutras las emisiones de CO_2 provenientes de la energía de biomasa, en este caso de estudio, no es significativo ya que las emisiones de caldera disminuyen sólo en un 3%. Esto se debe a qué, la generación de energía por parte de las calderas de biomasa (4,66E+8 Mj/año) es un orden de magnitud menor a la cantidad producida por las calderas de fuel (3,46E+9 Mj/año).

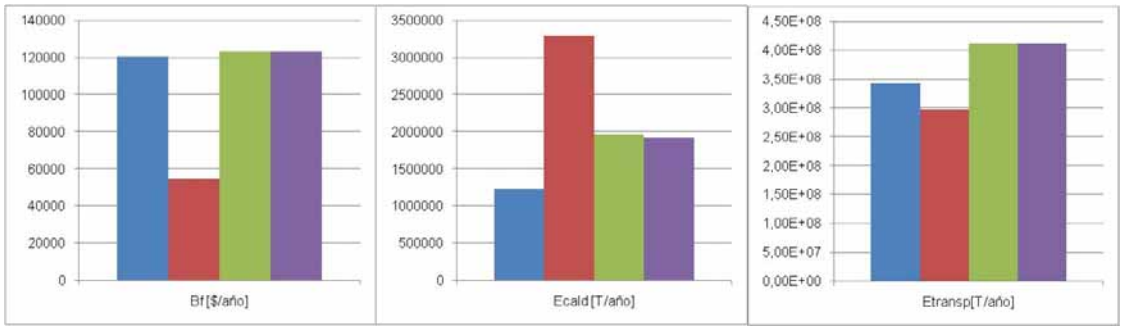


FIGURA 1. Resultados de los casos de estudio.

En el segundo aspecto se estudian los trade-offs existentes entre los resultados desde la perspectiva económica y considerando el punto de vista ambiental. Mediante la metodología ε-constraint se analizan diferentes puntos a lo largo de la CS; maximizando el beneficio y tomando como epsilon/restricciones valores de emisiones de las calderas y del transporte en forma discriminada.

En las **Figuras 7** y **8** se pueden observar las curvas de Pareto para cada uno de los casos. Si observamos ambas figuras vemos que no existen diferencias notables, dado que las emisiones de CO_2 por partes de las calderas de biomasa en este caso no son significativas.

En la **Tabla 1** y **2** se presentan diferentes valores y resultados para 4 puntos de la curva de Pareto para cada caso. Partiendo desde el punto de menor beneficio, se presenta el punto 1, 4, 6 y 11; es importante aclarar que el punto 11 representa el punto de máximo beneficio posible de la CS.

TABLA 1. Configuraciones del caso 3

	Punto 1		*Punto 4*		*Punto 6*		*Punto 11*	
Bf [$/año]	2.87E+04		8.40E+04		1.11E+05		1.23E+05	
Ecald [T/año]	4.23E+05		8.86E+05		1.19E+06		1.97E+06	
Etransp [T/año]	7.80E+07		1.78E+08		2.45E+08		4.11E+08	
Cald. Fuel [Mj/año]	1.40E+09		2.93E+09		3.93E+09		3.46E+09	
Cald. Biom.[Mj/año]							4.66E+08	
Producción		Sitios		Sitios		Sitios		Sitios
As.[m3/año]	127500	*I4 I5 I9 I10*	127500	*I3 I4 I5 I9*	127500	*I1 I4 I5 I9*	127500	*I2 I4 I8 I9 I10*
Tab.[m3/año]	146407	*I4 I5 I9*	370590	*I3 I4 I5 I8 I10*	392631	*I3 I4 I5 I8 I9*	610000	*I1 I2 I3 I4 I5 I8 I9 I10*
Pell.[T/año]	9500	*I5 I9*	10000	*I5 I8*	9450	*I8 I9*	9788	*I4 I8*
Et.[m3/año]	59022	*I4 I5*	122632	*I3 I4 I5*	181917	*I1 I3 I4 I5*	152282	*I1 I3 I4 I5*

En ambos casos existe una tendencia a aumentar la producción tanto de tableros como de etanol a medida que se permite emitir mayor cantidad de GEI; esto no ocurre con la producción de madera y de pellets, las cuales permanecen casi constantes. Se puede observar que, entre el punto 6 y el 11, la producción de etanol disminuye y la de tableros aumenta notablemente. En el punto 6, en los sitios donde se producen tableros, se instalan plantas con la mayor capacidad, el límite de las emisiones no permite que esta producción se expanda a otros sitios, por lo tanto, se decide producir mayor cantidad de etanol. En el punto 11, no existen restricciones acotadas de emisiones, esto permite expandir la producción de tableros a otros sitios por su mayor rentabilidad, y en compensación a esto, disminuye la producción de etanol.

TABLA 2. Configuraciones del caso 4

	Punto 1		*Punto 4*		*Punto 6*		*Punto 11*	
Bf [$/año]	2.86E+04		8.24E+04		1.10E+05		1.23E+05	
Ecald [T/año]	4.19E+05		8.70E+05		1.16E+06		1.97E+06	
Etransp [T/año]	7.79E+07		1.78E+08		2.45E+08		4.11E+08	
Cald. Fuel [Mj/año]	1.38E+09		2.87E+09		3.84E+09		3.46E+09	
Cald. Biom.[Mj/año]							4.66E+08	
Producción		Sitios		Sitios		Sitios		Sitios
As.[m3/año]	127500	*I4 I5 I9 I10*	127500	*I1 I2 I3 I4 I5 I6*	127500	*I1 I2 I3 I4 I5 I9*	127500	*I2 I4 I8 I9 I10*
Tab.[m3/año]	156568	*I4 I5 I9*	240000	*I4 I5 I8*	457282	*I3 I4 I5 I8 I9 I10*	610000	*I1 I2 I3 I4 I5 I8 I9 I10*
Pell.[T/año]	9500	*I5 I9*	9557	*I5 I8*	9478	*I8 I9*	9788	*I4 I8*
Et.[m3/año]	56843	*I4 I5*	137124	*I4 I5*	167001	*I3 I4 I5*	152282	*I1 I3 I4 I5*

Las plantas se sitúan en los primeros tres puntos mostrados en la **Tabla 2**, en sitios de materia prima o en los sitios donde se encuentran localizados los clientes, esto permite disminuir las emisiones provocadas por el transporte. Tanto en el punto 1 como en el 4 se instalan una unidad de cada planta en el sitio I5, sitio de materia prima, generando un polo productivo. En general, a lo largo de todos los puntos, existe una tendencia en localizar las plantas en un mismo sitio; desde un punto económico esto disminuye el costo de transporte y disminuye el costo de instalación y funcionamiento de las calderas. Si analizamos esta perspectiva desde un punto de vista ambiental, el hecho de que se localicen conjuntamente disminuye las emisiones provocadas por el transporte.

En cuanto a la energía generada por las calderas, puede observarse que existe una preferencia de instalar calderas de fuel en ambos casos. Esto se debe qué las emisiones por parte de las calderas de fuel son menores que las de biomasa, incluso considerando neutras las emisiones de CO_2. En el punto 11 no existen restricciones

para las emisiones, es por esto que decide instalar ambos tipos de calderas. De esta forma se da un mejor aprovechamiento, de manera más integral, de los subproductos de los aserraderos.

Si observamos las curvas de Pareto presentadas en las **Figura 7** y **8**, podemos ver que existe una pendiente más pronunciada en los primeros puntos de la curva respecto a los últimos cinco. Esto quiere decir que al mismo "costo ambiental", en los primeros puntos, el beneficio mejora notablemente mientras que en los últimos esto no es tan pronunciado.

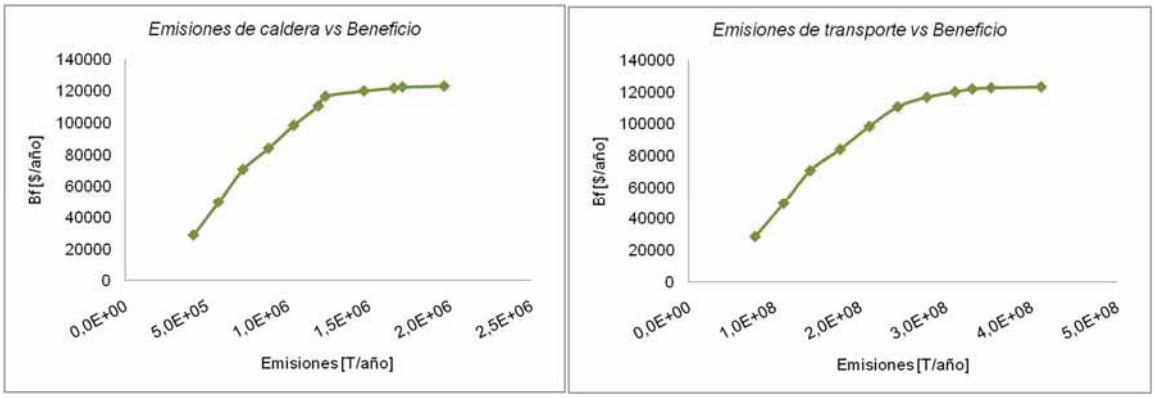


FIGURA 7. Gráficos de Pareto para el caso 3

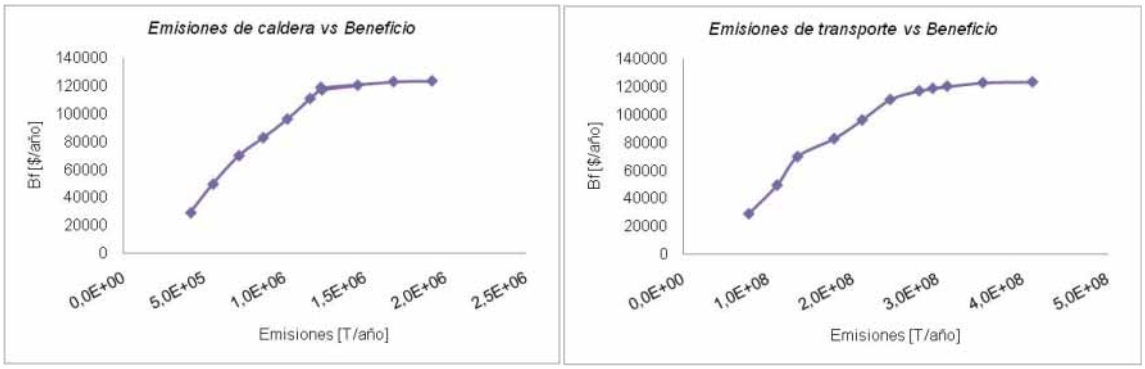


FIGURA 8. Gráficos de Pareto para el caso 4

CONCLUSIÓN

En este trabajo se desarrolló un modelo para el diseño óptimo sustentable de una CS forestal, donde se busca maximizar el beneficio económico considerando el impacto de las emisiones de GEI.

A partir de los resultados mostrados en la sección anterior se puede observar que considerar de manera integral la CS, teniendo en cuenta diversas alternativas de producción y de generación de energía, permiten evaluar el impacto de la sustentabilidad sobre los beneficios económicos alcanzados. Es importante destacar que, en todos los casos, existe una tendencia en utilizar todos los residuos y subproductos como materia prima de otros productos y como fuente de energía.

Considerar el indicador ambiental en el caso de estudio permite analizar qué costo ambiental tiene el beneficio económico a partir de las emisiones que genera el sistema.

En cuanto a considerar las emisiones de CO_2 de las calderas de biomasa como neutras, vemos que en este caso, no presenta diferencias significativas.
La herramienta propuesta permite analizar diferentes escenarios de este tipo de industria, poniendo en valor materiales qué, en varios casos, no tienen un destino específico. Por otro lado, el modelo permite estudiar escenarios dónde se analice como influye en la CS la variación del precio del fuel oil y el valor de venta de energía a la red, dado que, en el presente caso, con los valores considerados, no es rentable.
El instrumento presentado en este trabajo puede ser aplicado para lograr diseños sustentables de sistemas forestales, y ser utilizado a la hora de una evaluación ambiental considerando los compromisos con aspectos económicos.

AGRADECIMIENTOS

Los autores agradecen el soporte financiero de CONICET, ANPCyT y UTN para desarrollar las actividades de investigación mediante sus proyectos PIP 0688, PIP 0682, PICT-2012-2484, PID 25/O152 y EIUTIFE0003974TC.

REFERENCIAS

1. Zhu, Q., Cote, R. Integrating green supply chain management into an embryonic eco-industrial development: a case study of the Guitang Group. Journal of Cleaner Production 12 (2004) 1025–1035.
2. Srivastava, S. Green supply-chain management: A state-of-the-art literature review. International Journal of Management Reviews 9 (2007) 53-80.
3. Stephen J.D., Mabee W.E., Saddler J.N. Lignocellulosic ethanol production from woody biomass. The impact of facility siting on competitiveness. Energy Policy 59 (2013) 329-340.
4. Dansereau L.P., El-Halwagi M., Mansoornejad B., Stuart P. Framework for margins-based planning: Forest biorefinery case study. Comput Chem Eng 63 (2014) 34–50.
5. Mälkki H., Virtanen Y. Selected emissions and efficiencies of energy systemas based on logging and sawmill residues. Biomass and Bioenergy 24 (2003) 321-327.
6. Organización de las Naciones Unidas para la Agricultura y la Alimentación (FAO). *Conservación de la energía en las industrias mecánicas forestales*, Roma, Italia,1991.
7. http://www.eea.europa.eu/.
8. Climate change working group of ICFPA. *Calculation tools for estimating greenhouse gas emissions from wood products facilities, NC, USA,* 2005.

CHAPTER 2.2 ENVIRONMENTAL MANAGEMENT AS A TOOL FOR ORGANIZATIONAL DEVELOPMENT AND BUSINESS COMPETITIVENESS: CASE STUDY IN BRAZIL

J. M. P. Filho (1); **T. H. S. dos Santos ***(1); M. D. Alencar (1) and M. O. B. C. de Melo (1)

(1) AssociaçãoCaruaruense de Ensino Superior e Técnico – ASCES, Av. Portugal, Nº 584, Caruaru - PE, Brazil.

ABSTRACT

In organizational development, environmental management plays a decisive role for the betterment of the institution. Some companies resort to this tool of sustainable development as administrative strategy: competitive advantage and cost reduction[1]. From the assertion that the waste is everything that does not assign value to the product or service, the cleaner production proposes that there is no waste generation. Thus, this work has a qualitative nature, characterized as exploratory and descriptive research that through a case study, aimed to analyze the environmental management in a manufacturing company of alcoholic beverages (mill) in Pernambuco through cleaner production as well as the implication of this form of environmental management while competitiveness factor. Therefore, investing in environmental management strategically adds value to the product, service and image of the institution and, thus, what would be the cost once more, becomes a competitive strategy that produces economic growth cleanly, i.e. without assaulting the environment.

Keywords: Cleaner production, competitiveness, environmental management, sustainable development.

INTRODUCTION

The idea that economic development and environmental management are not associated prevailed for a long time. Today, it is understood that these concepts are not antagonistic; on the contrary, the environmental management creates new business opportunities and in the current market scenario is seen as a factor of competitive advantage[2].

In organizational development, environmental management plays a decisive role for the betterment of the institution. Some companies resort to this tool of sustainable development as administrative strategy: competitive advantage and cost reduction[1]. Therefore, this paper intends by means of a case study to analyze the environmental management in a plant of Pernambuco through cleaner production as well as the implication of this form of environmental management while competitiveness factor.

---

*Author for correspondence: thiiiagohss@hotmail.com

MATERIALS AND METHODS

In line with the objective of the present research, which have qualitative nature, we can classify it as exploratory and descriptive. According to Gil (2010)[3] a descriptive research refers to the description of the characteristics of a specific population or phenomenon, or the establishment of relationships between variables.

As regards the technical procedures, this research is characterized as being case study, whose primary purpose is to analyze the environmental management in a manufacturing company of alcoholic beverages (engenho) in Pernambuco through cleaner production as well as the implication of this form of environmental management while competitiveness factor.

The data were collected by means of on-the-spot observations and interviews to owners of the company. For Yin (2005)[4], the interviews are one of the most important sources of information for a case study. Also was the literature review from the query on articles, books, websites and journals, which contributed to the theoretical basis of the study and provided information to the analysis of the results.

Theoretical foundation.

Environmental management (EM). The EM can be conceptualized as a group of actions, programs and policies carried out by companies or institutions for the promotion of health and safety of people and environment preservation, so that its strategic planning and operations do not undermine the quality of life of individuals as well as the environmental impacts are mitigated or cancelled[5,6]. In addition, the EM intends to establish, recover or maintain the balance between nature and man[7].

Today, it is understood that natural resources are finite and that the world is experiencing a time of environmental crisis. Much is heard about greenhouse effect, global warming and ozone layer degradation. However, once these matters were handled by a specific audience, restricting a few. The opposite occurs in the present day. The 21ST century man participates in the dialogue on environmental issues and has science social crises that involves[8]. With that, the companies producing goods and services are urged to contribute to the preservation of the environment and with the mitigation of social problems, not as an action of corporate philanthropy, but as a way to meet the requirement of your client[9,10].

Sustainable Development proposes the improvement of production systems through practices that contribute not only to reduce costs but to preserve the environment. These practices are listed in the following table, where you can also verify the importance of disclosure of these actions. With this, it is understood that the EM efficient has been a key issue for the development of enterprises and society.

Environmental management as a factor of competitiveness. Second Porter in the page 5 of 1989 "the failure of the strategies of many companies is due to the inability to translate a competitive strategy in specific action steps necessary to obtain competitive advantage*".* From there, it is no use having a good idea or broad strategy if there is no gradual decision-making process, that is, to respect the EM, it is necessary to perform

differentiated and innovative actions so that the overall objective is achieved as well as the company prevail to the detriment of competition.

It is known that the EM is crucial for maintaining business and competitiveness in the market. According to Mello (2010)[11], besides the legal obligation that fits the institutions, the EM is critical for influencing directly the success of international trade as, for example, on the accession of international certificates issued by the International Organization for Standardization - ISO, that without them the company has difficulties in reaching foreign trades. Another relevant factor of importance is the fact that EM has become a form of imposition placed by society to entrepreneurs in support of socially responsible policies. According to Mello (2010)[11], the EM should not be seen as an ' extra ' cost, but as a great opportunity to add value to the image of the institution.

For Porter and Van der Linde (1999)[2] the need of environmental adequacy (legal enforcement and market requirement) should not be seen as an impediment to business growth and as an opportunity that generates innovation and competitiveness. However, according to the authors, this is only possible from the moment that the EM is conducted strategically within the Organization and the environmental impacts are intrinsically linked to the company's productivity.

Cleaner production (P+L). The P + L is the continuous application of an integrated preventive environmental strategy to processes, products and services to increase overall efficiency and reduce risks to people and the environment ", a concept given by the United Nations Environmental Program-UNEP in 1988. The P + L has as its main function the pursuit of reducing the waste of raw materials, namely, try to make the most of every material used in the production, minimize environmental impacts from the more efficient use of natural resources in order to not generate waste or pollution.

One of the approaches of the P + L is the choice of a productive *layout* that favors the use of local relief and also provides the least amount of movement possible, thus generating security and reduction of productive activity. To this end, the P + L allows the company to operate in a way that is environmentally safe and responsible.

Search results

Organizational context. The company analyzed is a company of family economics and operates in the manufacture of alcoholic beverages in the State of Pernambuco. For this segment, according to the Ministry of agriculture, livestock and food supply, 4,124 brands of cachaça vying for market in Brazil, where 70% of brazilian production is industrial or column cachaça and 30% of alembic cachaça. According to the aforementioned source, the State of Pernambuco is the second largest consumer of the country and in 2015 was in fourth place in the ranking of exportation national cachaça, besides, it currently has 130 registered trademarks**.**

Founded in 2006, the company studied is a pioneer in the field of production of rum from sugar cane and uses renewable solar photovoltaic energy in your manufacturing process. Their products are organic, without chemical additives, flavourings, fermentation accelerators, and all stages of the process emerges products for reuse of the inputs.

TABLE 1. Details of the production steps and action of P + L

STEPS	ACTIVITY/PROCESS	SUSTAINABLE ACTION AND (P + L)
1	**Cut sugar cane** · The timeout between the cutting and processing of raw material is 12:00 am · Two tons of sugarcane per day during the period of harvest are cut	The cane is planted in the lands of ingenuity and cultivated without chemicals. Even in property is maintained a vegetable garden where food produced are only for personal use. The company has invested in agroflorestment: agroforestry planting search produce food in native forest environment. In partnership with the SNE-Northeastern Society of Ecology, forest carbon and the factory annually produces, and accompanies the growth of hundreds of fruit trees and seedlings native to the Atlantic forest.
2	**Grinding** · Sugarcaneextract	About 1/3 of all of the pulp produced is used as fuel in the boiler. The remaining 2/3 are watered down with vinasse and when plus organic materials, including the ashes from boiler, form an excellent compost, returning to the plantation as a natural fertilizer.
3	**Preparation of the broth** · Water is added to the broth · 12% sucrose · Maximum duration period of 12:00 am, being overseen every 2 hours. · Use of 15 to 20 1000 liters of water per day in the production period	Use of water from a well crafted that meets the need of the local water supply.
4	**Fermentation process** · Add the yeast to the transformation of sugar into alcohol	Using natural yeast: in stainless steel barrels with yeast developed and multiplied naturally. During fermentation, the yeast "work" instrumental music of quality. This action is the result of scientific research proving the benefits of classical music, and instrumental music soft also provide to living beings.
5	**Distillation process** · Steam power · Separation of water and alcohol (heating at 90 degrees Celsius) · Change from liquid to gas (boil)	The steam produced by the boiler energy is originated from sugar cane bagasse and copper pot stills are used in order to minimize the emission of chemical substances in the process. In addition, the Copper Alembic still provides special features of aroma and flavor.
6	**Condensationprocess** · Cooling jacket · Alcohol passes from the gaseous to the liquid	For the use of the water that is thrown into a tank and that will be pumped by a windmill to supply homes. All the water used for cooling in the production of cachaça is reused thus providing a savings of over 50%.
7	**Generation and separation** **Three types of products**: · 10%-Rum (low quality and high concentration of alcohol) · 80%-Rum of heart (main product will be commercialized after aging) · 10%-Rum syrup (composition similar to the cachaça of head)	The cachaça of syrup and head are not sold, but are used to that from a new process of distillation generate a compound formed by more than 95% of alcohol to be used as fuel for domestic use.
8	**Aging process** · The cachaça of heart is stored in three types of wooden barrels: Freijó, oak and Umburana	The machine plant on your property trees that make available the timbers to the aging process.
9	**Marketing**	

The company's flagship is the organic cachaça. This product corresponds to 85% of the company's revenue, generating an output of 16 1000 liters of cachaça by vintage (period from October to February). There is also the production of brown sugar did, brown sugar, liqueurs, candies and jelly of cachaça.

The production plan of the organization is based on the principles of cleaner production and sustainability. In addition, the company presents a broadcast culture of environmental education and the preservation of nature by the local community.

Sustainable Layout. As seen in the study of Sarkar et al (2015), the company analyzed resorted to a *Layout* in order to take advantage of gravity in the productive process, thus, eliminating the use of pumps or turbines. This kind of decision favored the use of devices and technologies that would require investments and would directly in fixed costs of the organization. In addition, this *layout* reduces the need for sustainable use of natural resources from the time using a law of nature serving efficiently the production process of the product.

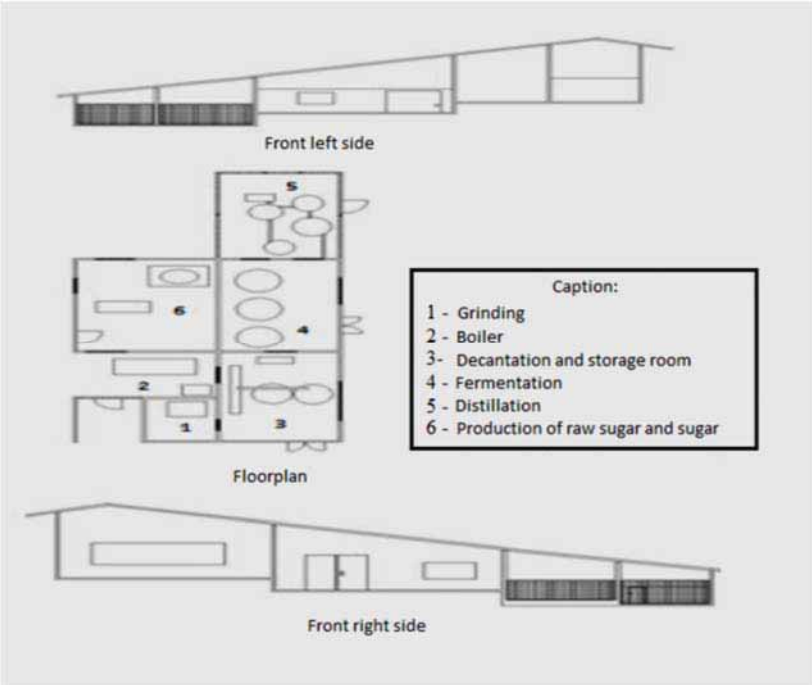


FIGURE 1. Mill's Layout
Source: Silva et al (2015)[12]

The deployment of photovoltaic power system. At the end of the year of 2015, the company takes a bold decision, but that would consolidate all a business strategy based on GA, the implementation of a photovoltaic power system. This system made the mill started producing electricity by means of solar power through photovoltaic panels. This innovation would generate the machine the primacy, in the liquor industry, to have a productive process totally dependent on a renewable source: sunlight.

The system chosen was the *ON-Grid*, i.e. is a type of shared and system that interacts with the electric grid. Moreover, even being interactive, the *ON-Grid* system

replaces the source of electrical distribution, so the function of single power generator on site.

RESULTS AND DISCUSSION

The discussion of this work was built on the basis of the theories covered in his theoretical framework and the actions cited in the case study.

For Porter (1989)[13] the differentiation is a competitiveness strategy and that is identified as an advantage over the competition. Thus, technological innovation is important to be able to allow the cost is reduced and the increased differentiation simultaneously. The company must always seek to blunt form the best opportunities to the point of permitting the reduction of costs and you don't sacrifice the differentiation[13].

For Monks (1987)[14] "*production Activities are the basis of the economic system of a nation, since they are responsible for the transformation of capital resources, human and material goods and services of higher value.*" From this understanding, in the productive process of the company studied, a point of importance of GA under enterprise is the cost factor, which is directly related to waste reduction and minimization of expenses[15]. Decreasing the waste and economics of inputs in the processing activities, increase profit, which Romm (1996)[16], by reducing the use of raw material, in addition to helping in the conservation of the environment, cause an impact on productivity far beyond what one might expect. With it, you can see that with the economy only of material and an efficient control of losses can be reduced considerably the waste and thus maximize profit.

In the company, there is the use the most productive inputs to generate waste and pollution to the environment. It is understood that this type of policy has contributed to cost reduction and environmental preservation.

Regarding the sustentable *Layout*, this initiative is the result of a study of topography, which for Doubek (1989)[17] that science "has the objective of the study of the instruments and methods used to obtain the graphical representation of a portion of the land on a flat surface." This study allows the good use of local relief and choice for improving the process to the point to assign construction opportunities in a smart way, for example, the reduction of time and movement attributed to production. That way, you know that the layout of the physical structure and the location of the equipment used in the production process will influence directly in the movement and flow of materials since the entry of the raw material to the finished product output and, of course, throughout the process of transformation.

The company stands out nationally for being the only device to produce organic products in a sustainable way and through a clean energy generation system. In addition, in line with the ideas of Porter (1989)[13], after the investment of this technology, the implementation of a photovoltaic system, reduction of cost and differentiation factor was consolidated. These actions can be identified as a result of a GA efficient. With this, it is understood that the competitive differential part of a singular strategy or even the bold actions planning that can add value to the final product and the institutional image.

CONCLUSION

From the study, it is understood that the strategy adopted by the company analyzed is structured in an integrated EM actions that gave the sustainability cause for existence of the organization. Therefore, to Porter (1989)[13] this kind of posture strengthens the administration strategy to the point of determining its organizational development and, of course, remain on the market and to excel regarding to the competition.
It is appropriate to highlight the importance of EM as a successful strategy for organizations. Therefore, this assertive meets a paradigm once imposed there was how to reconcile economic development with the maintenance of the environment. In addition, invest in a EM strategically adds value to the product, service and image of the institution and, thus, what would be the cost once more, becomes a competitive strategy that produces economic growth cleanly, i.e. without harm the environment.

REFERENCES

1. BANKUTI, Sandra Mara Schiavi; BANKUTI, FerencIstvan. Gestão ambiental e estratégia empresarial: umestudoemuma empresa de cosméticos no Brasil. **Gest. Prod**., São Carlos, v. 21, n. 1, p. 171-184, Mar.2014.
2. PORTER, M.; VAN DER LINDE, C. Verde e competitivo: acabando com o impasse. In: PORTER, M. **Competição**: estratégias competitivas essenciais. Rio de Janeiro: Campus, 1999.
3. GIL, Antonio Carlos. **Como elaborar projetos de pesquisa**. 5. ed. São Paulo: Atlas, 2010. 184p
4. YIN, Robert K.**Estudo de Caso:** planejamento e métodos. Tradução de Daniel Grassi. 3. Ed. Porto Alegre: Bookman, 2005.
5. MOURA, LuizAntônioAbdalla de. **Qualidade e Gestão Ambiental**. 5 ed. São Paulo. Editora Juarez de Oliveira. 2008.
6. QUEZADA, Raymundo, PIERRE, Carla V. **Gestão Ambiental Empresarial**, 1º, 2º, 3º e 4º módulos. SEBRAE/RJ, CidadeUniversitária, UFRJ, Rio de Janeiro, nov. 1998.
7. PHILIPPI JR, Arlindo; ROMÉRO, Marcelo de Andrade; BRUNA, Gilda Collet. **Curso de Gestão Ambiental**. Barueri, SP: Manole, 2004
8. BARBIERI, J. C. **Gestão ambiental empresarial**. São Paulo: Saraiva, 2007.
9. BACKER, de Paul. **Gestão Ambiental**: A Administração Verde. Rio de Janeiro: Qualitymark, 2002.
10. WEBER, P. S. A Gestão Ambiental na Empresa. **Revista Sanare**, v. 12, 1999. Disponívelem: <http://www. ambientebrasil.com.br>. Acessoem: 22 maio 2012.
11. MELLO, V. S. **Vantagens Competitiva da Gestão Ambiental**. 2010. 20p. Trabalho de Conclusão (GraduaçãoCiênciasEconômicas). Faculdade de CiênciasEconômicas. Universidade Federal do Rio Grande do Sul, Porto Alegre, 2010.
12. SILVA, W; et al. LayoutSustentável: o caso da cachaçariae a proposição de um modelo de planejamento. In V CONGRESSO BRASILEIRO DE ENGENHARIA DE PRODUÇÃO, 2015, **Anais...** Paraná: Universidade Tecnológica Federal do Paraná, 2015.
13. PORTER, Michael. **Vantagem competitiva**: criando e sustentando umdesempenho superior. 15. ed. Rio de Janeiro: Campus, 1989.
14. MONKS, J. G. **Administração da produção**. São Paulo: MCGraw-Hill, 1987
15. WERNKE, R. CustosAmbientais: umaabordagem teórica comênfase na obtenção de vantagem competitiva. **Revista Brasileira de contabilidade do Conselho Regional de São Paulo**. São Paulo – SP: ano 5, nª 15, p.40-49, mar. 2001.

16. ROMM, Joseph J. **Umpassoalém da qualidade:** como aumentar seus lucros e produtividadeatravés de umaadministração ecológica. São Paulo: Futura, 1996.
17. DOUBECK, A. **Topografia**. Curitiba: Universidade Federal do Paraná, 1989.

CHAPTER 2.3 STRESS TOLERANCE BASED ON OSMOTIC ADJUSTMENT AND YIELD OF BARLEY (*Hordeum Vulgare* L.) SUBMITTED TO PROGRESSIVE DROUGHT AND SUBSEQUENT RECOVERY

A. Thameur *(1); K. Hessini (2); S. Ferchichi (2) and C. Abdelly (2)

(1) Regional Center of Agricultural Research, B.P 357 Road Gafsa Km 6, Sidi Bouzid 9100, Tunisia
(2) Laboratoire d'Adaptation des Plantes aux Stress Abiotiques, BP 901, Centre de Biotechnologie, Technopole de Borj Cédria, Hammam-Lif 2050, Tunisia

ABSTRACT

Dry areas of the Mediterranean region are characterized by low rainfall with high fluctuations in precipitation due to climate change. In Tunisia, water scarcity is no longer limited to arid areas but spread in all the country. This study aims to determine the physiological effects of progressive drought and subsequent recovery on the behavior of two barley genotypes (*Hordeum vulgare* L.) "Ardhaoui" (A) and "Manel" (M). A greenhouse experiment with different irrigation regimes was carried out in four replications. Progressive drought (7, 14 and 21 days of water withholding) and subsequent recovery during 7 days were applied. Mild drought (7 days of water withholding) decreased significantly ($P<0.05$) the stomatal conductance (gs) and the transpiration rate (E). Green leaf number was less reduced (23%) in "Manel" compared to "Ardhaoui" (47%) under moderate drought. Plants grown under mild water stress showed lower (Ψ_{md}) than in control plants with values that averaged −1.7 and −2.2 MPa respectively for "Ardhaoui" and "Manel". After 7 days of water withholding, "Ardhaoui" showed a greater increase in proline (3.50 µmol/g DW) compared to "Manel". Under mild drought, A and gs decreased in both genotypes thus increasing significantly ($P<0.01$) intrinsic water use efficiency ($WUE_{A/gs}$) in "Ardhaoui" (1.8-fold). Under moderate drought, total soluble carbohydrates increased significantly in Ardhaoui (2.2-fold). Under drought conditions, "Ardhaoui" showed precocity and the highest grain yield and its component, exceeding the control, were recorded under mild drought followed by a recovery phase. On the contrary, "Manel" was not very responsive to re-watering. It is clear that the photosynthetic apparatus was significantly affected after 21 days of withholding water. Results showed that a recovery phase after mild drought was beneficial to enhance yield in "Ardhaoui". Eventually, "Ardhaoui" was the most efficient genotype by increasing water use efficiency and reducing effectively water loss by transpiration, suggesting it presents the most favorable traits to enhance plant productivity especially when subjected to mild drought followed by a recovery phase which possibly trigger the expression of genes involved in drought tolerance.

Keywords: Drought, gas exchange, *Hordeum vulgare* L., water potential,

---

*Author for correspondence: afwa_thameur@yahoo.fr

INTRODUCTION

Barley (*Hordeum vulgare* L.), the most drought tolerant of the small grain cereals and a major crop in the Mediterranean region. Agricultural drought occurs when there is not enough soil moisture to support average crop production on farms[1]. Limited water availability impairs plant growth and is one of the main issues of future climate changes[2]. More than fifty percent of the food consumed in the Middle East and North Africa (MENA) region is imported, making it the largest food importing region in the world[3]. Achieving zero hunger is a primary goal tackled by the Sustainable Development Goals (SDGs) set by the United Nations. In order to achieve food security, the development of drought tolerant cultivars is essential for maintaining yields under climate change conditions[4]. Barley is considered as a model to study and understand the genetic basis and mechanisms of drought tolerance[5]. Plants have developed a wide diversity of morphological and physiological mechanisms to tolerate drought[6]. Drought will limit plant growth[7] especially leaf area[8]. The reduction of leaf area expansion[9] is an adaptive strategy to reduce water loss by transpiration. Osmotic adjustment (OA) has been considered as an important physiological adaptation key factor associated with drought tolerance and it has drawn much attention during the last years. OA involves the net accumulation of solutes in a cell in response to reductions in water potential of the cell's environment. As a consequence, the cell's osmotic potential is diminished which in turn attracts water into the cell by tending to maintain turgor pressure[6,10]. Drought stress causes decline of photosynthesis[11]. Particularly, when stomatal conductance drops below a certain threshold (<50 mmol H_2O m^{-2} s^{-1}) limitations of non-stomatal processes become more important[12,13]. Water use efficiency (WUE) is considered as relevant criteria to determine the relationship between plant productivity and water use in plants[14]. Drought tolerance is the ability of a plant to survive, grow, and produce a harvestable yield with limited water supply or under periodic conditions of water deficit[15]. In the present study we aim to better understand the physiological mechanisms affecting yield and WUE by comparing two barley Mediterranean genotypes. The local barley (*Hordeum vulgare* L.) genotype Ardhaoui (the unique in southern Tunisia) and Manel genotype. We hypothesize that barley genotypes with different origins show different WUE and that the degree of drought stress followed by a recovery phase may modify the response to drought and probably trigger plant potentialities under constraining conditions.

MATERIALS AND METHODS

Plant material. Two barley (*Hordeum vulgare* L.) genotypes differing for yield potential and drought tolerance were used in this study. (1) Ardhaoui: is the unique local barley genotype of the south of Tunisia. Six-rowed barley, resistant to drought; (2) Manel: from ICARDA, recommended especially in humid and subhumid climates[16].

Experimental conditions. The field experiment was carried out at the Experimental Station of Tunis Biotechnology Centre during the winter-summer season. The experimental station is found near the Mediterranean Sea shore, 35km south-east of Tunis (10°10'E, 36°48'N; 10m of altitude) with a mean temperature and an annual

rainfall of 19.4°C and 456mm respectively. Germinated seeds were sown in pots filled with a mixture of sandy soil and organic matter. After one month of growth under non-limiting conditions, plants were submitted to drought treatments (7, 14 and 21 days) followed by a re-watering period of 7 days.

***Soil water content*.** Soil moisture content of the soil was measured gravimetrically for both well-watered and water stressed pots. Fresh weight of the soil samples were determined and then these samples were oven-dried at 105 °C for 72^h. Gravimetric water content was calculated as defined by the following expression:

$$\theta\ (\%) = (WW - DW)/WW \times 100 \quad (1)$$

where WW is the wet weight and DW is dry weight of the soil sample.

Growth parameters. Roots of the plant were cut from the stem, dried moisture free in a hot air oven at 80ºC for 48 hours (till attaining constant weight), weighed and recorded in gram. The shoot dry weight was recorded separately after drying the shoot portion. Root volume was determined in 'cc' using water displacement method Musick et al. (1965).

Physiological measurements

Leaf water potential. Leaf water potential (Ψ_w) was measured at 10:00 a.m and 05:00 am for (Ψ_{md}) and (Ψ_{pd}) respectively on five fully expanded leaves per treatment. Leaf water potential (Ψ_w) was measured using a pressure chamber (Soil Moisture Equipments Corp., Santa Barbara, CA, USA) [17].

Gas exchange measurements. Gas exchange measurements were taken between 09:30 and 11:30 in daylight hours. The gas exchange was measured on a well developed flag leaf of the control and stressed plants using the portable photosynthesis system (Li-Cor 6200, Li-Cor Nebraska, USA). Three replicates were measured per treatment.

Water use efficiency. In order to compare water use efficiency (WUE) at the leaf level, water use efficiency of photosynthesis was analyzed ($WUE_{A/E}$). $WUE_{A/E}$ was analyzed as the relationship between net CO_2 exchange and transpiration from measurements of leaf gas exchange. Intrinsic water use efficiency was also measured $WUE_{A/gs}$ as the relationship between net CO_2 exchange and stomatal conductance. Measurements were done at 7, 14 and 21 days of treatment, for both control and drought treatments, and after subsequent recovery.

Proline and soluble carbohydrates content. Free proline was specifically quantified from 1 g fresh weight of leaf samples according to Bates et al. (1973)[18]. Total soluble carbohydrates were extracted in 80% ethanol from 1 g of leaf fresh tissue and quantified by the classical anthrone method[19] using a spectrophotometer (Sherwood Scientific Ltd., model 259, Cambridge,UK).

Osmotic adjustment. Osmotic potential was measured using a vapor pressure osmometer (Losel, Germany) according to Hummel et al. (2010)[20]. Then osmotic adjustment (OA) was calculated as the difference in Ψ_s^{100} between the control (Ψ_{sc}^{100}) and the stressed plants (Ψ_{ss}^{100}) [21].

$$OA = \Psi_{sc}^{100} - \Psi_{ss}^{100} \quad (2)$$

Agronomical traits. Grain yield was recorded at maturity. Yield components which are the number of ear per plant, kernel number (no ear $^{-1}$) and thousand kernel weight (g) were determined.

Statistical analysis. Statistical analysis was performed using SPSS Version 16.0 software. The data were subjected to ANOVA, and differences between means were determined using the Duncan's test at 5%.

RESULTS AND DISCUSSION

Soil water content. During the development of water stress, soil water content (SWC, %) decreased progressively and similarly in pots of the two genotypes (**Figure 1**). At the end of the experiments, SWC of the stressed plants was on average about 0.03 % after 21 days of water withholding, as compared to 20% in control plants. Under moderate drought, Ardhaoui seems to be more water-saving genotype (5%) compared to Manel (2%).

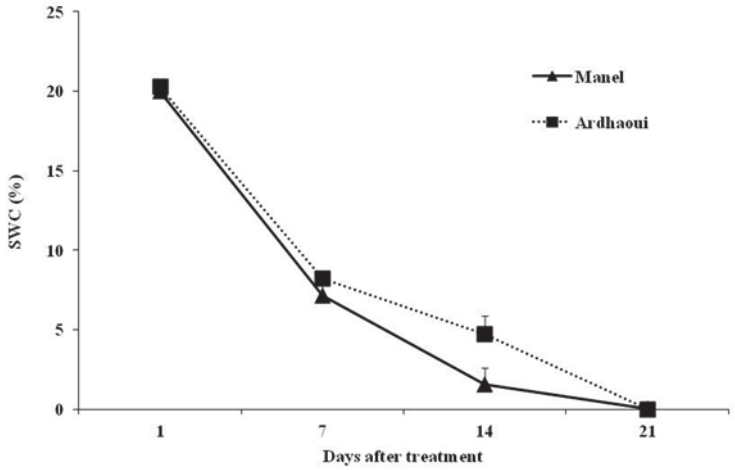


FIGURE 1. Variation of soil water content (SWC, %) in pots of studied genotypes; Ardhaoui and Manel submitted to water withholding during 7, 14 and 21 days.

Plant growth. Results showed that treatment did not affect significantly the plant height under mild drought (1 and 7 % reduction respectively for A and M). Afterwards, genotypes decreased their height by 23 and 27 % for Manel and Ardhaoui respectively under moderate drought (**Figure 2**). The effect of the treatment was very highly significant ($P<0.001$). The effect of the genotype was highly significant under mild and moderate drought ($P<0.01$). The interaction GXT was not significant. For the green leaf

number, Ardhaoui was not very sensitive to mild drought and reduction was only 8 %. On the other hand Manel decreased by 24% the number of green leaf.

Under moderate drought, Ardhaoui decreased drastically the leaf number by 47% while Manel kept reducing its leaf number by 23% (**Figure 2**). It's only under severe drought that the latest decrease notably the leaf number by 88%. Similar reduction was observed in Ardhaoui (81%). Under moderate drought recovery was more important in Manel (2-fold against 1-fold in Ardhaoui). Under severe drought, the recovery phase did not enhance the plant growth in Manel. The effect of the treatment was very highly significant ($P<0.001$). The effect of the genotype was significant under mild and moderate drought ($P<0.05$). The interaction GXT was significant ($P<0.05$).

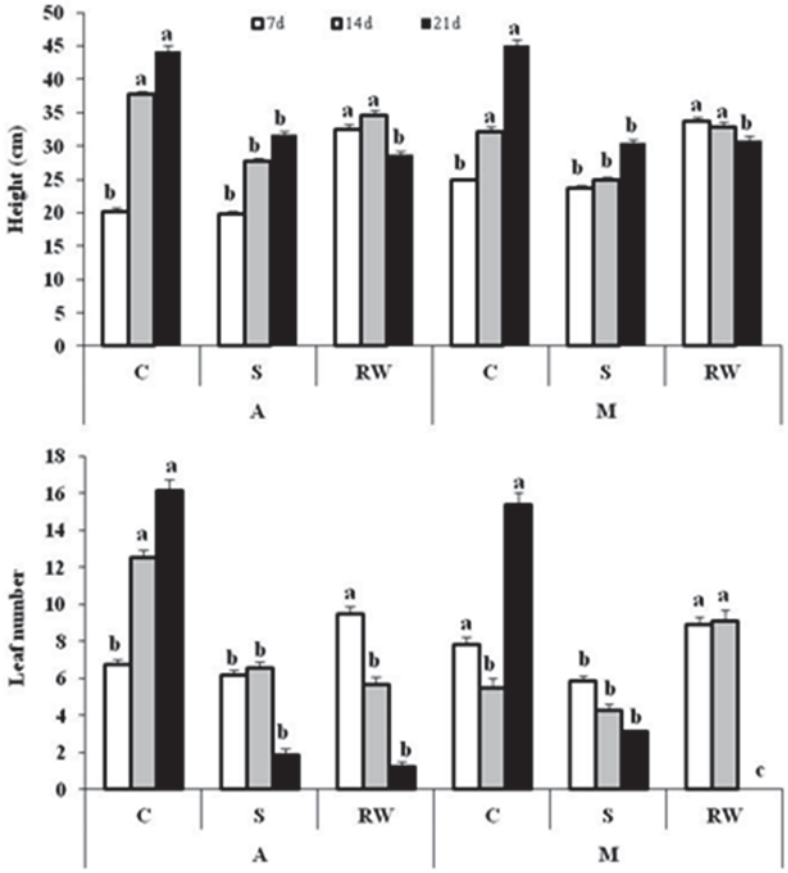


FIGURE 2. Effect of different water treatment (7, 14 and 21 days of water withholding) and subsequent recovery (+7 days under well-watered conditions) on height and leaf number in two barley genotypes (A: Ardhaoui and M: Manel). Different letters indicate a significant difference between treatments. Values represent means ± S.E.; n=5.

Under mild drought, we noticed that root volume did not vary significantly for both genotypes. Under moderate, A did not reduce the root volume while Manel recorded a reduction by 58%. Under severe treatment, we noticed that a pronounced reduction was observed in Manel (70%) compared to Ardhaoui (33%). The effect of the recovery was similar in both studied genotypes. A clear adaptive strategy is showed in Ardhaoui to

maintain root growth to absorb water in the deepest profiles of the soil under drought conditions (**Figure 3**).
The effect of the treatment and genotype were very highly significant (P<0.001) under moderate and severe drought. The interaction GXT was also very significant (P<0.001).

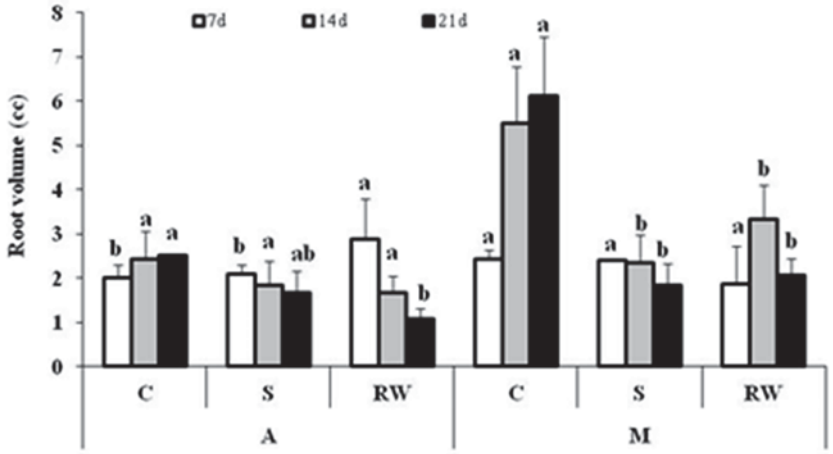


FIGURE 3. Effect of different water treatment (7, 14 and 21 of water withholding) and subsequent recovery (+7 days under well-watered conditions) on root volume (cc) in two barley genotypes (A: Ardhaoui and M: Manel). Different letters indicate a significant difference between treatments. Values represent means ± S.E.; n=5.

Under mild drought, the shoot dry weight diminished by effect of water stress in Ardhaoui (85%) compared to 76% in Manel. Under moderate, less reduction was recorded in both genotypes (30 and 45% respectively for A and M). Highest reductions were observed in Manel 80 % against 57% in A under severe drought. The recovery was more pronounced for Ardhaoui under mild and moderate drought (6-fold under both treatments). The recovery for Manel was less important (2-fold increase) with respect to stressed plants (**Figure 4**). Under severe drought, very slight recovery was observed in both genotypes (1-fold). The root dry weight increased significantly under mild and moderate drought (5 and 6-fold respectively) in Ardhaoui while a reduction of 78% was observed in Manel under mild drought. While under moderate drought, Manel increased slightly root growth (1-fold). Under severe drought, both genotypes decreased root dry weights by 52 and 63 % in A and M.
The effect of the treatment and genotype were very highly significant (P<0.001) on shoot and root dry weights. The interaction GXT was also very significant (P<0.001).

Leaf water potential. Results showed that in response to the water stress treatment, the predawn leaf water potential (Ψ_{pd}) was significantly reduced (**Figure 5**, P<0.05). At the end of the water stress period, the decrease was marked under the severe water stress treatment (21 days of water withholding) than the mild drought (7 days of water withholding) with a reduction of 78% and 61% respectively for Manel. The reductions were less pronounced for Ardhaoui genotype (4 and 50% respectively for mild and severe drought). The same trend of variation was observed under mild drought for Ψ_{md} 45% of reduction in Ardhaoui against 61% in Manel. Values recorded were about -2.2 MPa and -1.7 MPa respectively for Manel and Ardhaoui.

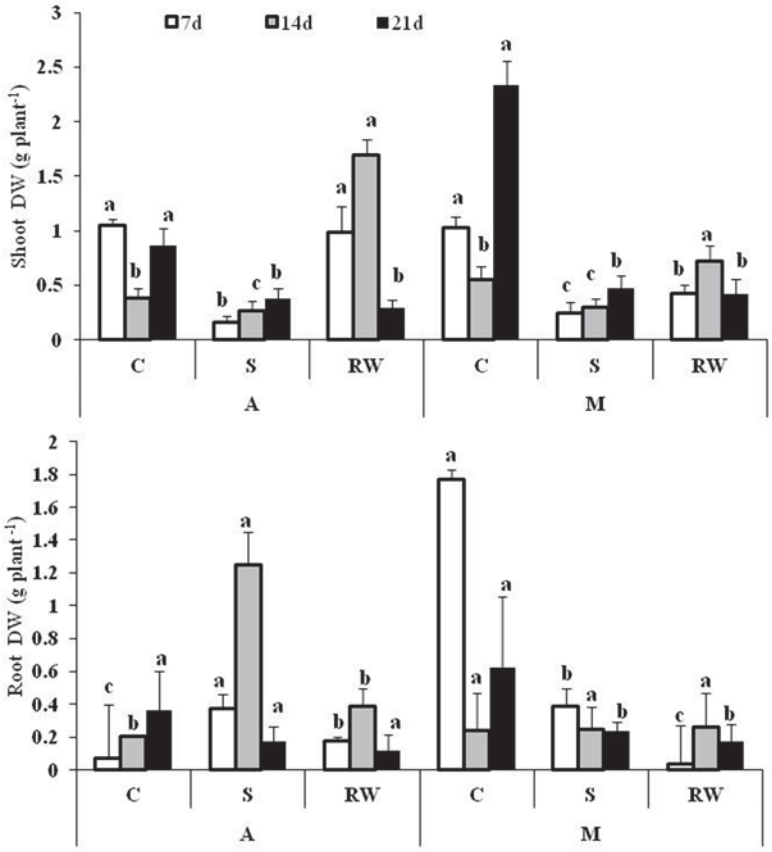


FIGURE 4. Effect of different water treatment (7, 14 and 21 of water withholding) and subsequent recovery (+7 days under well-watered conditions) on shoot and root dry weights in two barley genotypes (A: Ardhaoui and M: Manel). Different letters indicate a significant difference between treatments. Values represent means ± S.E.; n=5.

Gas exchange measurements. Results showed that drought decrease net photosynthetic rate (A) since the onset of mild drought. Under severe drought, the reduction was about 73% for Manel against 29% for Ardhaoui. Values of about 3 and 10 µmol CO_2 m^{-2} s^{-1} were recorded respectively for Manel and Ardhaoui. During the recovery phase, we noticed that the an increase of A observed particularly for Ardhaoui that reached 8.60 µmol CO_2 m^{-2} s^{-1} against 3 µmol CO_2 m^{-2} s^{-1} for Manel). The same pattern of variation was observed under mild and moderate drought. The effect of treatment was highly significant P<0,001. The effect of the genotype and the interaction TXG was significant (**Figure 6**, P<0.05).

For the stomatal conductance, data showed that Ardhaoui tend to close stomata under mild drought and the reduction was about 71% which was not the case for Manel where only 45% of reduction was observed. The recovery was clear for A (4-fold increase against 2-fold for Manel). In the same way, under moderate drought the decrease was important in A (72% against 61% Manel) suggesting that Ardhaoui reduces water loss by evaporation to maintain relatively high net photosynthetic rate. The effect of treatment was highly significant P<0,001 (Figure 6).

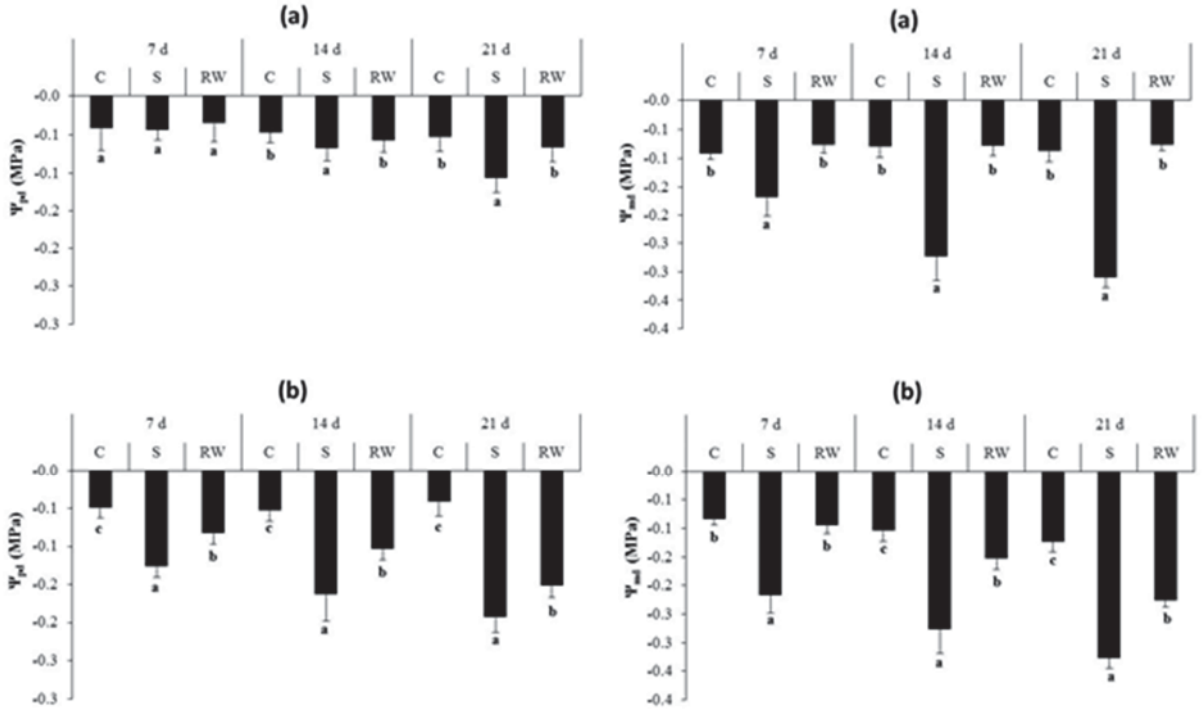


FIGURE 5. Effect of different water treatment (7, 14 and 21 of water withholding) and subsequent recovery (+7 days under well-watered conditions) on predawn (Ψ_{pd}) and midday (Ψ_{md}) leaf water potentials in two barley genotypes (A: Ardhaoui (a) and M: Manel (b)). Different letters indicate a significant difference between treatments. Values represent means ± S.E.; n=5.

The effect of the genotype was highly significant under mild and moderate drought ($P<0.001$) and the interaction TXG was significant ($P<0.05$) under moderate drought and highly significant under mild and severe drought (**Figure 6**).

Transpiration was most reduced under severe drought 96% in Manel and 76% for Ardhaoui confirming previous results found for stomatal conductance. A recovery phase, after moderate drought, increased transpiration rate especially in Ardhaoui (2-fold compared to Manel 0.5-fold).

An important decrease in Ci was observed in Ardhaoui under mild drought which explains that the photosynthetic apparatus is being functional (**Figure 6**). On the other hand, we noticed a slight decrease in it for the genotype Manel. Under moderate drought the decrease was about 18% in Ardhaoui and only 5 % in Manel. The recovery phase was more important under moderate drought (2-fold Ardhaoui against 1-fold in Manel).

Water use efficiency. After 14 days of water withholding, no differences between genotypes were shown for $WUE_{A/E}$ (**Figure 7**) in control plants (**Figure 7**). Under severe drought, $WUE_{A/E}$ increased in all genotypes which had the highest $WUE_{A/E}$ (**Figure 7**) with Ardhaoui having the greatest increase, which was 1.9-fold greater than the control (**Figure 7**). After mild drought, $WUE_{A/E}$ increased in A and M by 1.9 and 1.8-fold.

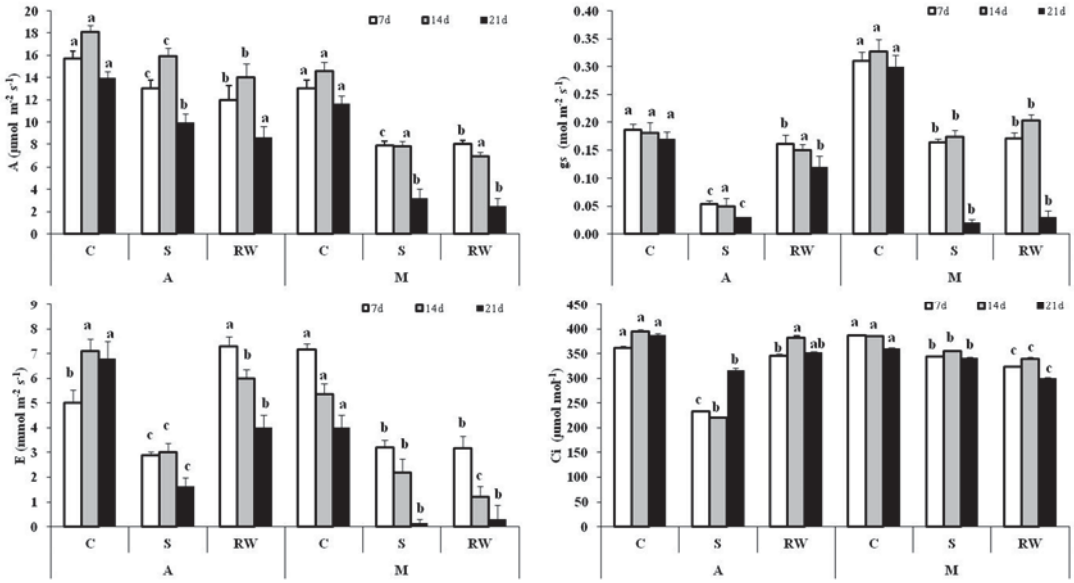


FIGURE 6. Effect of different water treatment (7, 14 and 21 days of water withholding) and subsequent recovery (+7 days under well-watered conditions) on leaf gas exchange parameters in two barley genotypes (A: Ardhaoui and M: Manel). Different letters indicate a significant difference between treatments. Values represent means ± S.E.; n=5.

After 21 days of treatment, irrespective of the genotypes, WUE $_{A/gs}$ was modified by water stress and the recovery period (**Figure 7**). WUE $_{A/gs}$ was increased particularly in Manel by 2.5-fold. Nervetheless, the highest value was recorded in Ardhaoui (122 µmol mol^{-1}). Under mild drought, Ardhaoui increased most its WUE by 1.8-fold (**Figure 7**). Nevertheless, Manel genotype achieved the increase of this parameter only under severe stress (98 µmol mol^{-1}), the WUE $_{A/gs}$, unlike for Ardhaoui, increased after recovery in Manel (**Figure 7**).

Proline and total soluble carbohydrates contents. At the end of the experimental period, proline concentration strongly increased in response to water stress conditions ($P<0.05$) of about 4.8-fold in Ardhaoui. An increase was observed in Manel (4.1-fold) under severe drought. Under mild drought, Ardhaoui recorded 3.50 µmol/g DW (1.5-fold of increase) and Manel 1.61 µmol/g DW (3.2-fold of increase). The recovery was clear in Ardhaoui which decreased proline content. However, Manel was not responsive and similar values were observed under moderate (mean average of 5 µmol/g DW) and severe drought (mean average of 7 µmol/g DW) and their respective re-watered plants (**Figure 8**).

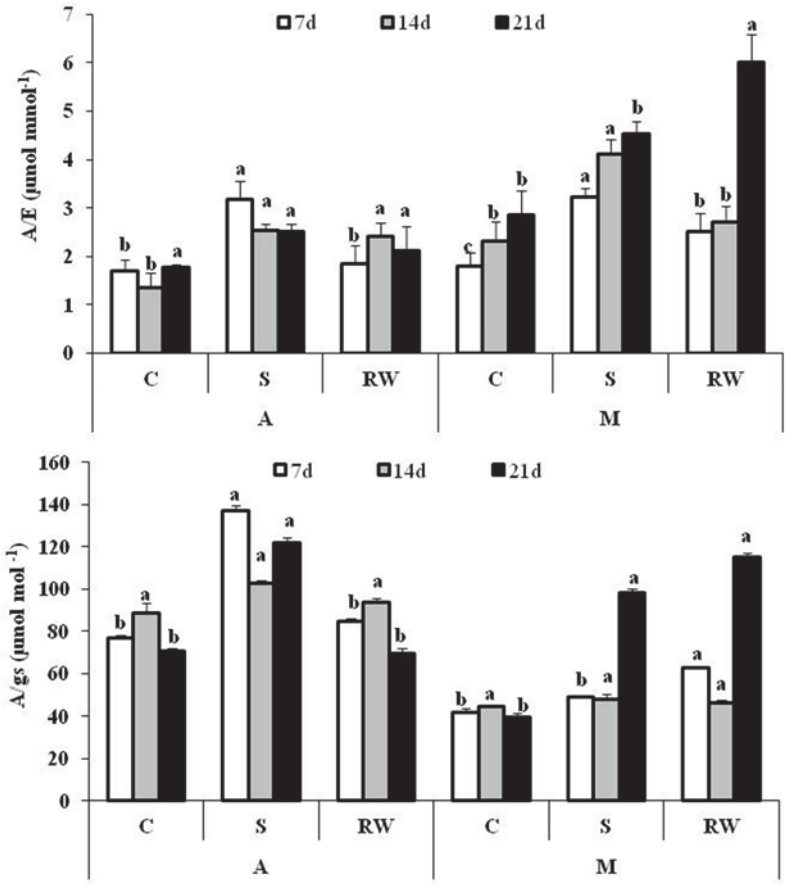


FIGURE 7. Effect of different water treatment (7, 14 and 21 of water withholding) and subsequent recovery (+7 days under well-watered conditions) on instantaneous (A/E) and intrinsic (A/gs) water use efficiency in two barley genotypes (A: Ardhaoui and M: Manel). Different letters indicate a significant difference between treatments. Values represent means ± S.E.; n=5.

After 14 days of water withholding, Ardhaoui was very responsive and, total soluble carbohydrates concentrations augment significantly in response to water stress ($P<0.05$; Figure 8) with mean values from 4.4 mg/g DW in the control treatment to 9.4 mg/g DW (2.2-fold increase). Values reached 8 mg/g DW after re-watering (**Figure 8**). Unlikely, Manel increased notably soluble carbohydrates content under mild drought (5.1 fold). A slight increase was observed under moderate and severe drought (1.9 and 1.3-fold respectively).

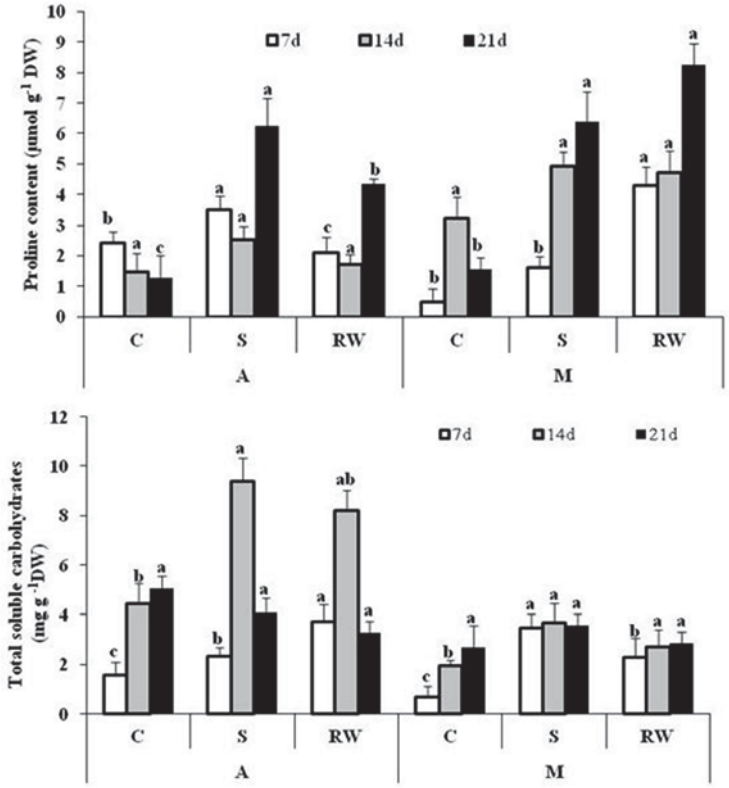


FIGURE 8. Effect of different water treatment (7, 14 and 21 of water withholding) and subsequent recovery (+7 days under well-watered conditions) on proline and total soluble carbohydrates in two barley genotypes (A: Ardhaoui and M: Manel). Different letters indicate a significant difference between treatments. Values represent means ± S.E.; n=5.

The enhancement of osmotic adjustment was about 94 % under severe drought in Ardhaoui compared to 62% in Manel. OA was similar under moderate drought in both genotypes. Under mild drought the OA was enhanced by 20% in Ardhaoui compared to 10% in Manel (**Figure 9**).

Yield and yield components. The number of kernel per spike and 1000 kernel weight was greater in watered conditions than under water stress for all genotypes. Under mild drought, Ardhaoui recorded the highest kernel number per spike (48 g). For Ardhaoui, control and mild drought ranked in the same group by Duncan's test for the 1000 kernel weight (**Table 1**).

Ardhaoui had both higher grain yield and water potential. Manel had the lowest grain yield under severe drought (24g) compared to Ardhaoui (37 g).

Osmotic adjustment

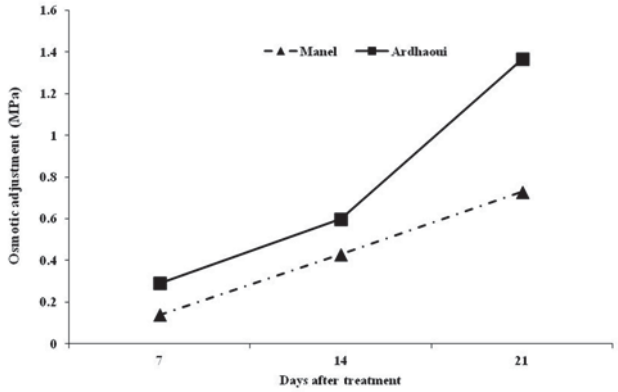


FIGURE 9. Osmotic adjustment (OA) in two barley genotypes (A: Ardhaoui and M: Manel) under different water treatment (7, 14 and 21 of water withholding).

The water stress showed great impact in plant water relations under conditions of water shortage, since the plants showed different responses under drought compared with the control plants (**Figure 5**). These different responses could be due to the fact that barley has certain tolerance mechanisms, such as stomatal closure to maintain their water status during soil water deficit[22] in order to keep leaf turgor, since it underwent a loss in all genotypes. Drought-stress reduced gs, as water potential decreased in both genotypes (**Figure 5**). In other plant species, reduction of gs under drought stress was a mechanism of water conservation, limiting the loss of water in order to maintain leaf turgor[23]. Leaf water potential (Ψ_w) was good indicator of water status in plants[24]. This study showed that the leaf Ψ_w was significantly reduced (**Figure 5**). There was a decrease in the gas exchange parameters with drought stress (**Figure 6**). Stomatal closure was partially responsible for the reduction in $A_{CO2,}$ because, with drought stress, there is a decrease of intercellular CO_2 concentration (Ci) that could be more important

TABLE 1. Ear/plant, Kernel number (N° ear^{-1}), kernel weight (g ear^{-1}) and thousand kernel weight (g) determined in control and water stressed barley genotypes (A: Ardhaoui; M: Manel). Stressed plants were subjected to a treatment of 21 days of water withholding

Genotype	Treatment	Ear/plant	Kernel number	Kernel weight	Thousand kernel weight
A	C	1.7±0.3a	34.2±1.3a	1.5±0.3a	43±0.7a
	mild	2.1±0.2a	39.3±1.2b	1.9±0.3b	48±0.7a
	moderate	1.5±0.2a	23.9±1.1c	1.1±0.2c	45±0.7b
	severe	1.4±0.3a	17.8±1.2c	0.7±0.2c	37±0.6c
M	C	5.1±0.4a	49.0±1.3a	2.2±0.3ab	44±0.7b
	mild	2.5±0.2b	26.4±0.6a	1.2±0.1a	44±0.5a
	moderate	1.8±0.3bc	9.0±0.7b	0.3±0.1bc	37±0.7ab
	severe	1.0±0.0c	6.3±0.4b	0.2±0.1c	24±0.4c

Means in the same column with the same letters (a–c) are not significantly different by Duncan's multiple range test (DMRT) (at $p < 0.05$).

in A_{CO2} limitation than non-stomatal factors. The increased intrinsic gas-exchange efficiency (A/gs) in drought stressed leaves indicates a greater reduction of gs than of A_{CO2}, thus increasing water use efficiency (**Figure 7**). Thus, increasing WUE, rather than gs reduction, could have been a mechanism of adaptation to drought. The genotype Ardhaoui shows a clear behaviour of water-saving. Similar results were obtained focusing on transpiration efficiency[25]. Improved water use efficiency, biomass accumulation and root weight occurred among water stressed transgenic wheat lines expressing the barley (*Hordeum vulgare* L.) gene, *HVA1*, encoding for some late embryogenesis abundant proteins that work as osmo-protectants[26]. Although A_{CO2} was affected by drought in all genotypes but the recovery phase was more important in Ardhaoui. According to our observations, Ardhaoui manages to keep a high net photosynthetic rate in conditions of water stress. On the contrary, Manel is the most sensitive. The other work carried out by Alves and Setter (2000)[27] indicates that under drought plant close their stomata and decrease the surface of their leaves. The reduction of the green leaf number is accompanied by the reduction of the solar radiation intercepted by the canopy which leads to the decrease of CO_2 assimilation. Aase (1971)[28] showed that the pale colour of the leaves is a passive adaptation to the strong light intensity. Kameli and Losel (1996)[29] found similar decrease in relative water content in wheat approximately 10 days after stress treatment. However, they reported that it was a reversible decrease which recovered quickly after re-watering. Siddique et al (2000)[24] reported that there was a positive relation between leaf water status and photosynthetic rate. The capacity to maintain high water potential values under drought was observed in Ardhaoui and could be explained by their capacity to accumulate great quantities of proline and other osmotic active compounds, which participate in osmotic adjustment. The relation between osmotic potential decrease and osmotic adjustment has already been observed by Teulat et al (1997)[30] in barley and wheat and by Rodrigues et al (1993)[12] in grapevine. In the same way, leaf full turgor (Ψ_{s100}) and osmotic potential at turgor loss point (Ψ_{s0}) declined consistently in response to water stress at the end of the experimental period, but the enhancement of osmotic adjustment was larger under severe water stress by 94 % in Ardhaoui compared to 62% in Manel. Yield components such as kernel number and thousand kernel weight were also affected by drought in these genotypes but at a lesser extent in genotype Ardhaoui. Yield benefits from biochemical accumulations should be considered in breeding programs because osmotic adjustment seems to use energy to accumulate photo-assimilates in other plant organs to ensure survival at the expense of grain yield[31].

CONCLUSION

According to our results, the genotype Ardhaoui is considered as drought tolerant compared to Manel which would be classified as a susceptible genotype to drought. The tolerant genotype was able to maintain the physiological parameters (photosynthesis, transpiration and water relations), by reducing growth (number of leaves, biomass accumulation). Moreover, the osmotic adjustment was a key factor in the resistance to water stress in this genotype. The susceptibility of Manel genotype would be explained by the marked decrease of physiological parameters leading to notable decrease in yield and yield components.

REFERENCES

1. Wilhite D.A., Glantz M.H. Understanding the drought phenomenon: the role of definitions. Water Int. 10 (1985) 111–120.
2. Loreto F., Centritto M. Leaf carbon assimilation in a water limited world. Plant Biosystems. 142 (2008) 154–161.
3. World Bank. The World Bank Annual Report. 2008.
4. Tubiello F.N., Jean-Francois S., Howden S.M. Crop and pasture response to climate change, Proc. Natl. Acad. Sci. USA 104. 2007.
5. S. Ceccarelli, S. Grando, Drought as a challenge for the plant breeder, Plant Growth. Regul. 20 (1996) 149–155.
6. Blum A., Munns R., Passioura J.B., Turner N.C., Sharp R.E., Boyer J.S., Nguyen H.T., Hsiao T.C. Letters to the editor. Genetically engineered plants resistant to soil drying and salt stress: how to interpret osmotic relations? Plant Physiol. 110 (1996) 1051–1053.
7. Thameur A., Ferchichi A., López-Carbonell M. Involvement of abscisic acid metabolites and the oxidative status of barley genotypes in response to drought. Can. J. Plant Science. 94 (2014) 1481–1490.
8. Mahajan S., Tuteja N. Cold, salinity and drought stresses: an overview. Arch. Biochem. Biophys. 444 (2005) 139–158.
9. Boyer J.S. Leaf enlargement and metabolic rates in corn, soybean, and sunflower at various leaf water potentials. Plant Physiol. 46 (1970) 233–235.
10. Hessini K., Martínez J.P., Gandour M., Albouchi A., Soltani A., Abdelly C. Effect of water stress on growth, osmotic adjustment, cell wall elasticity and water-use efficiency in *Spartina alterniflora.* Env. Exp. Bot. 67 (2009) 312–319
11. Arnau G., Monneveux P., This D., Alegre L. Photosynthesis of six barley genotypes as affected by water stress. Photosynthetica 34 (1997) 67–76.
12. Rodrigues M.L., Chaves M.M., Wendler R., David M.M., Quick W.P., Leegood R.C., Stitt M., Pereira J.S. Osmotic adjustment in water stressed grapevine leaves in relation to carbon assimilation. Aust. J. Plant. Physiol. 20 (1993) 309–321.
13. Flexas J., Bota J., Galmes J., Medrano H., Ribas-Carbo M. Keeping a positive carbon balance under adverse conditions: responses of photosynthesis and respiration to water stress. Physiol. Plant. 127 (2007) 343–352.
14. Saranga Y., Flash I., Paterson A.H., Yakir D. Carbon isotope ratio in cotton varies with growth stage and plant organ. Plant. Sci. 142 (1999) 47–56.
15. Turner N.C. Drought resistance and adaptation to water deficits in crop plants, in: H. Mussell, C.R. Staples (Eds.), Stress physiology in crop plants, John Wiley & Sons, New York, 1979.
16. Musick G.J., Fairchild M.L., Ferguson V.L., Zuber M.S. J. Crop Science. 5 (1965) 601.
17. Scholander P., Hammel H., Bradstreet E.Y., Hemmingsen E. Sap pressure in vascular plants. Science.148 (1965) 339–346.
18. Bates L.S., Waldren R.P., Teare D. Rapid determination of free proline for water stress studies. Plant Soil. 39 (1973) 205–207.
19. Staub A.M. Extraction, identification et dosages des glucides dans les extraits d'organes et les corps bactériens, in: Masson et Compagnie (Eds.), Techniques de laboratoire, Tome 1 et 2, Paris. 1963.
20. Hummel I., Pantin F., Sulpice R., Piques M., Rolland G., Dauzat M., et al. Arabidopsis plants acclimate to water deficit at low cost through changes of carbon usage: an integrated perspective using growth, metabolite, enzyme, and gene expression analysis. Plant. Physiol. 154 (2010) 357–372.

21. Zhang J., Nguyen H.T., Blum A. Genetic analysis of osmotic adjustment in crop plants. J. Exp. Bot. 50 (1999) 291–302.
22. Monneveux P., Belhassen E. The diversity of drought adaptation in the wide. Plant. Growth. Regul. 20 (1996) 85–92.
23. De Herralde F., Biel C., Savé R., Morales M.A., Torreciallas A., Alarcon J.J., Sanchez Blanco M.J. Effect of water and salt stresses on the growth, gas exchange and water relations in *Argyranthemum coronopifolium* plants. Plant and Soil. 139 (1998) 9–17.
24. Siddique M.R.B., Hamid A., Islam M.S. Drought stress effects on water relations of wheat. Bot. Bull. Acad. Sin. 41 (2000) 35–39.
25. Vadez V., Kholová J., Medina S., Kakkera A., Anderberg H. Transpiration efficiency: new insights into an old story. J. Exp. Bot. 64 (2014) 6141–6153.
26. Sivamani E., Bahieldin A., Wraith J.M., Al-Niemi T., Dyer W.E., Ho T.H.D., Qu R. Improved biomass productivity and water use efficiency under water deficit conditions in transgenic wheat constitutively expressing the barley *HVA1* gene. Plant Science. 155 (2000) 1–9.
27. Alves A.C.C., Setter T.L. Response of cassava to water deficit: leaf area growth and abscissic acid. Crop. Sci. 40 (2000) 131–137.
28. Aase J.K. Growth, water use, and energy balance comparisons between isogenic lines of barley. Agr. J. 63 (1971) 425–28.
29. Kameli A., Losel D. M. Growth and sugar accumulation in durum wheat plants under water stress. New. Phytol. 132 (1996) 57–62.
30. Teulat B., Monneveux P., Wery J., Borries C., Souyris I., Charrier A., This D. Relationships between relative water content and growth parameters under water stress in barley: a QTL study. New. Phytol. 137 (1997) 99–107.
31. Mwadzingeni L., Shimelis H., Ernest Dube E., Laing MD., Tsilo T.J. Breeding wheat for drought tolerance: Progress and technologies. J. Integ. Agr. 15 (2016) 935–943.
32. Deghais M., Kouki M., Gharbi M.S., El Falah M. Les variétés de céréales cultivées en Tunisie. 2007.

CHAPTER 2.4 ANÁLISIS DE TENDENCIA DE LAS PRECIPITACIONES EN EL INTERIOR DEL ESTADO DE PARAÍBA (BRASIL)

S.E.L. Medeiros *(1); R. Abrahão (1); I. García-Garizábal (2,3); I.M.B.M Peixoto (1) and L. P. Silva (1)

(1) Universidade Federal da Paraíba (UFPB), Centro de Energias Alternativas e Renováveis, Cidade Universitária, João Pessoa, Brasil.
(2) Escuela Superior Politécnica del Litoral (ESPOL), Facultad de Ingeniería en Ciencias de la Tierra, Campus Gustavo Galindo, Guayaquil, Ecuador.
(3) Secretaría Nacional de Educación Superior, Ciencia, Tecnología e Innovación (SENESCYT)

RESUMEN

El estado de Paraíba, perteneciente a la región Nordeste de Brasil, contiene 223 municipios distribuidos en un área de 56.469 m^2, y se divide en cuatro grandes regiones: Zona de la Mata, Agreste, Borborema y el Sertão Paraibano. Para este estudio, se eligió la mesorregión Sertão Paraibano, con la finalidad de comprender la vulnerabilidad al cambio climático, dada la importancia socioeconómica de la región para abastecimiento hídrico y energético.
Para ello, se utilizó la prueba no-paramétrica de Mann-Kendall con el propósito de evaluar las tendencias de las series históricas de datos de precipitación mensual, trimestral, semestral y anual. Las series empleadas correspondieron al periodo 1912-2012 y fueron construidas a partir de datos proporcionados por cinco estaciones meteorológicas distribuidas por la mesorregión y mantenidas por la *Superintendência do Desenvolvimento do Nordeste* (SUDENE), por la *Agência Executiva de Gestão das Águas* (AESA) y por el *Instituto Nacional de Meteorologia* (INMET).
Los resultados indican que hay una tendencia de incremento en la precipitación de la mesorregión, principalmente en el trimestre diciembre-enero-febrero, con pendientes anuales entre 2,99 mm/año y 5,98 mm/año. Este trabajo evidencia la necesidad de profundizar en los estudios de influencia de cambio climático en la mesorregión Sertão Paraibano, con el intento de mitigar sus efectos o, al menos, promover prontas medidas de adaptación.

Palabras clave: análisis de tendencia, cambio climático, precipitación, test de Mann-Kendall.

INTRODUCCIÓN

El cambio climático puede definirse como el conjunto de variaciones estadísticas de un estado medio del clima o de su variabilidad (atribuido directa o indirectamente a la actividad humana), variaciones que persisten durante largos períodos de tiempo y que pueden ser detectados y analizados a través de series históricas de variables meteorológicas[1]. Además, se entiende que la tendencia climática se caracteriza por un cambio (aumento o disminución) suave y monótona en los valores medios de una serie

---

*Author for correspondence: susane.eterna@cear.ufpb.br

meteorológica. A través de las tendencias de series temporales se puede confirmar la ocurrencia de cambio climático para una determinada región[2].

El estado de Paraíba, al nordeste de Brasil, presenta un clima semiárido en la mayor parte de su territorio, y por lo tanto una baja disponibilidad de recursos hídricos[3]. La región cuenta con el complejo hídrico Coremas-Mãe D'água, perteneciente a la cuenca del rio Piranhas[4]. El complejo de Coremas-Mãe D'água almacena un total de 1.358 millones de m^3, y representa el 34,8% del agua utilizada en el estado. La zona cuenta con una pequeña planta de generación hidroeléctrica desde 1957, la cual se abastece de los embalses Estevam Marinho y Coremas-Mãe D'água[5]. La planta dispone de 2 unidades con potencia de generación de 1.760 kW cada, abasteciendo un total de 3.520 kW.

Lucena[6] et al. (2009) indican que el cambio climático afectará a los recursos naturales relacionados a las fuentes de energía renovable, pronosticando una disminución de la productividad en todos los sectores de energía en Brasil, principalmente en la región Nordeste. Alteraciones en los patrones de precipitación y temperatura también pueden originar y acentuar deficiencias hídricas y problemas de calidad del agua en el área[7].

Debido a la importancia de esta área para los suministros de agua y energía del estado de Paraíba, y el impacto potencial del cambio en la disponibilidad de los recursos hídricos en la matriz de producción de energía hidroeléctrica, el presente estudio tiene como objetivo comprender el comportamiento de posibles tendencias en las precipitaciones del área cercana al complejo hídrico Coremas-Mãe D'água, en la mesorregión Sertão Paraibano.

MATERIALES Y MÉTODOS

***Caracterización del área de estudio, identificación de las estaciones meteorológicas y organización de los datos*.** El Nordeste de Brasil abarca el estado de Paraíba. La región presenta tres tipos de clima (húmedo del litoral, tropical y semiárido)[8], con un régimen anual muy variable de precipitaciones que oscilan entre los 300 mm – 2000 mm [9]. Más concretamente, la zona de estudio se localiza en el estado de Paraíba, el cual está dividido en cuatro mesorregiones: Litoral, Agreste, Borborema y Sertão Paraibano, siendo esta última la elegida para el estudio (**Figura 1**).

Para los análisis de la variabilidad y tendencias de la precipitación se generaron series temporales con información pluviométrica entre 1912 y 2012. Dicha información fue proporcionada por las redes de seguimiento de la Superintendencia do Desarrollo del Nordeste de Brasil (SUDENE), la Agencia Ejecutiva de Gestión del Agua (AESA), el Instituto Nacional de Meteorología (INMET) y el Departamento Nacional de Obras contra la Sequía (DNOCS).

De acuerdo con Becker et al. (2011) [11], la red pluviométrica del estado de Paraíba es estandarizada. Cuenta con 265 estaciones equipadas con pluviómetros Ville de París, y sigue los criterios y normas de funcionamiento de la Organización Meteorológica Mundial (OMM) [11]. Para este estudio, se consideraron cinco estaciones de las más de

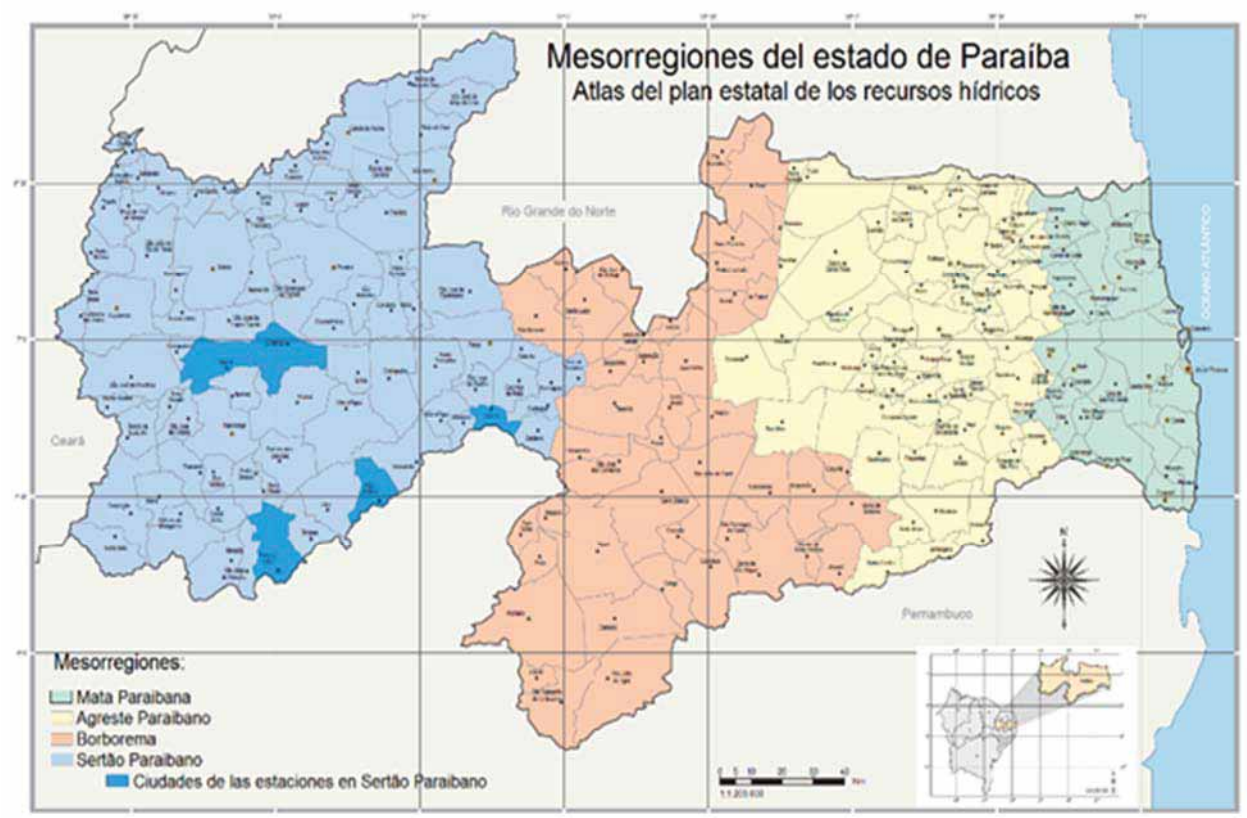


FIGURA 1. Localización geográfica de las mesorregiones del estado de Paraíba y identificación de las ciudades con las estaciones elegidas (Adaptado de AESA, 2009)[10].

cuarenta que hay en la mesorregión Sertão Paraibano, estaciones seleccionadas por la proximidad al complejo hídrico Coremas-Mãe D'água y la calidad de sus datos (mayor número de años disponibles con menos interrupciones en las series). La información pluviométrica se organizó en series temporales discretas siguiéndose criterios de identificación y evaluación de los valores atípicos, llamados *outliers*, y de tal manera que todos los años analizados contienen todos los meses de enero a diciembre sin faltas (**Tabla 1**).

Métodos estadísticos para el análisis de tendencias. Para describir el comportamiento de las series temporales y verificar la existencia de tendencias, se aplicó el método de regresión lineal y la prueba estadística no paramétrica de Mann-Kendall, de acuerdo con la metodología propuesta por Sneyers (1992)[12].

Para los análisis de tendencia de las precipitaciones de las series anuales, semestrales (Enero a Junio: E-J; Julio a Diciembre: J-D), trimestrales (Diciembre-Enero Febrero: DEF; Marzo-Abril-Mayo: MAM; Junio-Julio-Agosto: JJA; Septiembre-Octubre-Noviembre: SON) y mensuales se utilizó el programa Makesens[13], programa que aplica la prueba de Mann-Kendall basada en la suposición de estabilidad de una serie temporal, es decir, la distribución de probabilidad es constante y la sucesión de valores ocurre de forma independiente[14,15].

TABLA 1. Estaciones pluviométricas utilizadas en el estudio.

Número de la estación	Operadora	Municipios	Intervalo da serie (año)	Lat.	Lon.	Período (años)
737022	AESA	Água Branca	1936 – 1991	-7,51	-37,62	72
	AESA		1994 - 2012	-7,51	-37,64	
738025	DNOCS	Aguiar	1935 – 1991	-7,08	-38,18	71
	AESA		1994 – 2012	-7,09	-38,17	
737019	DNOCS	Coremas	1934 – 1985	-7,02	-37,97	64
	AESA		1994 – 2012	-7,03	-37, 94	
738013	DNOCS	Princesa Isabel	1912 – 1991	-7,73	-38,02	97
	AESA		1994 – 2012	- 7,73	-37,99	
737002	DNOCS	Teixeira	1926 – 1991	-7,22	-37,27	78
	AESA		1994 - 2011	-7,22	-37,25	

El programa Makesens utiliza la prueba no paramétrica de Mann-Kendall para detectar la tendencia monótona de series temporales, empleando la pendiente de Sen como cuantificador de la tendencia.

RESULTADOS Y DISCUSIÓN

Se detectaron aumentos en los valores de tendencia de la precipitación de carácter significativo para todas las estaciones seleccionadas a nivel anual, semestral, trimestral y mensual (**Tabla 2**).

Para la precipitación anual, a excepción de la estación Princesa Isabel, todas las estaciones arrojaron valores de tendencia positivos significativos, de entre 2,99 y 5,98 mm/año (**Tabla 2**).

En los intervalos semestrales, mientras que entre E-J todos los valores de la pendiente resultaron positivos, en el periodo J-D dos de ellos son de carácter negativos, si bien no significativos. De esta manera, los valores de tendencia oscilaron entre 0,77 mm/año de la estación Teixera en J-D, y 4,34 mm/año de la estación Água Branca. Así mismo, las pendientes en el semestre E-J fueron siempre superiores a los de J-D (**Tabla 2**).

Trimestralmente, a excepción del periodo SON, en el que no se detectan tendencias significativas, se encuentran aumentos de la precipitación los trimestres DEF, MAM y JJA de entre 1,09 mm/año y 2,67 mm/año. DEF resulta el periodo con mayores aumentos en la precipitación, al encontrarse cambios significativos en 4 de las 5 estaciones analizadas. Un 20% de los valores de pendiente fueron negativos, si bien todos carentes de significancia estadística (**Tabla 2**).

TABLA 2. Tendencias de precipitación para el periodo 1912-2012 para las estaciones del estado de Paraíba: Água Branca, Aguiar, Coremas, Princesa Isabel e Teixeira.

	Precipitación (mm/año)				
Periodo	Água Branca	Aguiar	Coremas	Princesa Isabel	Teixeira
Anual	5,98 ***	2,99 +	4,20 *	0,63 ns	5,26 **
Ene-Jun	4,34 **	3,83 +	3,82 +	0,94 ns	3,92 **
Jul-Dic	1,32 ***	-0,21 ns	0,22 ns	-0,12 ns	0,77 ***
Dic/Ene/Feb	2,67 ***	1,87 *	2,12 *	-0,25 ns	2,12 **
Mar/Abr/May	1,20 ns	0,96 ns	-0,27 ns	1,14 +	1,64 ns
Jun/Jul/Ago	1,09 ***	-0,14 ns	0,13 ns	0,29 ns	-
Sept/Oct/Nov	0,06 ns	-0,08 ns	0,00 ns	-0,20 ns	-
Enero	0,96 ***	0,91 +	1,04 *	0,33 ns	0,64 **
Febrero	0,91 *	0,75 ns	0,46 ns	-0,19 ns	0,50 ns
Marzo	0,19 ns	-0,50 ns	-0,93 ns	0,25 ns	0,08 ns
Abril	-0,01 ns	0,59 ns	0,20 ns	0,50 ns	0,83 ns
Mayo	0,91 *	0,52 ns	0,24 ns	0,29 ns	0,33 ns
Junio	0,36 +	-0,09 ns	0,00 ns	0,01 ns	-
Julio	0,33 *	-0,01 ns	0,04 ns	0,14 ns	-
Agosto	-	-	-	-	-
Septiembre	-	-	-	-	-
Octubre	-	-	-	-	-
Noviembre	-	-	-	-	-
Diciembre	-	-	0,041 ns	-0,01 ns	-

ns: no significativo; + p < 0,10; * p < 0,05; ** p < 0,01; *** p < 0,001
- : datos no concluyentes

A escala mensual, los principales cambios en la precipitación se encuentran entre enero y julio, y aunque hay un predominio de valores de tendencia positivos, solo la cuarta parte de los mismos presentan significancia estadística. El mes de enero resulta el más afectado de todos al presentar cuatro de las cinco estaciones tendencias significativas de entre 0,64 mm/año y 1,04 mm/año. De igual manera, la estación Água Branca presenta el mayor número de meses afectado por tendencias de carácter significativo, que se sitúan entre los 0,33 mm/año de julio y los 0,96 mm/año de enero.

No fue posible obtener resultados concluyentes entre los meses de agosto y diciembre debido a la aparición de eventos de sequía en los que no ocurrieron precipitaciones. En esas condiciones, la prueba de Mann-Kendall se muestra limitada, poniendo de manifiesto la necesidad de aplicar junto a los análisis de tendencia otros métodos estadísticos para la comprensión de los cambios climáticos mensuales[16].

El Núcleo de Asuntos Estratégicos de la Presidencia de Brasil[17, 18] indica que el Nordeste de Brasil es una de las regiones más vulnerables al cambio climático debido a

la unión de factores climáticos (entorno semiárido), sociales y económicos, por lo que el complejo Coremas-Mãe D'água de Paraíba es una infraestructura clave para abastecimiento de la población y generación de electricidad. De esta manera, estudios que incluyen análisis de variabilidad climática de la región de Paraíba son necesarios para abordar de manera temprana la problemática del cambio climático y su incidencia ambiental, económica y social. Aunque las proyecciones del IPCC indican aumento de

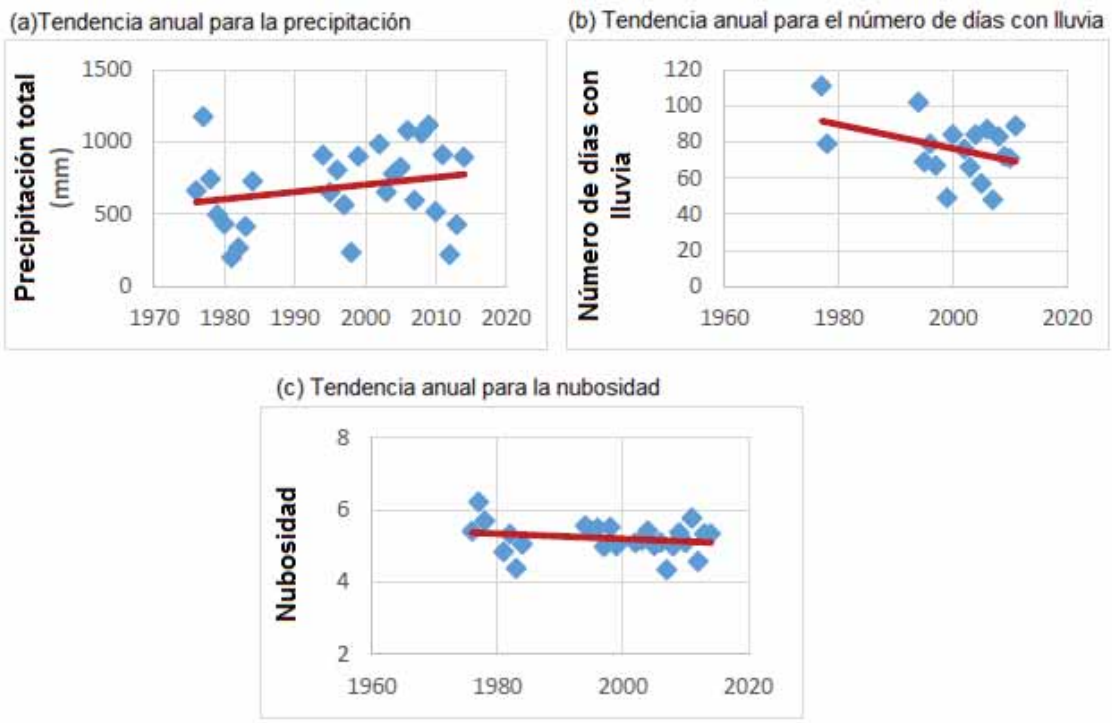


FIGURA 2. Tendencias anuales para la precipitación (a), número de días con lluvia (b), y nubosidad (c) para la estación de Patos-PB, en la mesorregión del Sertão Paraibano (Adaptado de Peixoto y Abrahão, 2015)[20].

las temperaturas en todo el territorio de Brasil, los análisis de precipitación no arrojan resultados concluyentes[1], lo que manifiesta la necesidad de seguir desarrollando estudios pluviométricos que analicen la dinámica y evolución de esta componente climática.

En el presente estudio, se observa una tendencia de aumento en el total anual de las precipitaciones, resultados que complementan los encontrados por Peixoto y Abrahão (2015) para los municipios de Patos y São Gonçalo, en la mesorregión del Sertão Paraibano, que detectaron descensos en la nubosidad y en el número de días con lluvia (**Figuras 2 y 3**)[19], así como aumentos en la frecuencia de días secos consecutivos[1].

Estos cambios en los regímenes de lluvia, tendrán importantes consecuencias en las prácticas agrícolas y ambientales, así como mayores riesgos de inundaciones e incidencia de enfermedades (como el dengue), además de los problemas de disponibilidad de agua para el abastecimiento de la población o para la generación de energía eléctrica. De acuerdo con la Agencia Nacional del Agua de Brasil (ANA), la mayoría de las poblaciones con más de cinco mil habitantes del nordeste semiárido de

Brasil, tendrá dificultades para el abastecimiento de agua para el consumo humano, debido al crecimiento de la población y el aumento de la demanda por agua[20].

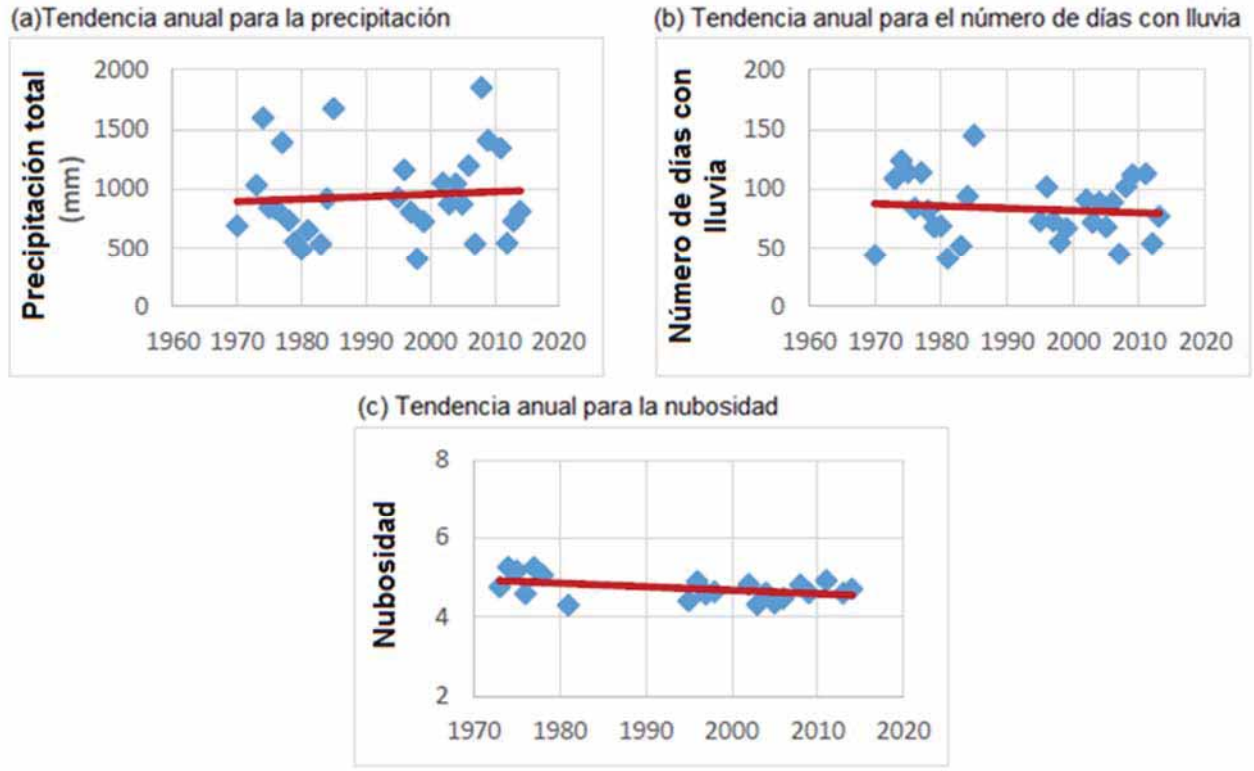


FIGURA 3. Tendencias anuales para a precipitación (a), número de días con lluvia (b), y nubosidad (c) para la estación de São Gonçalo-PB, en la mesorregión del Sertão Paraibano. (Adaptado de PEIXOTO; ABRAHÃO, 2015) [20]

Es importante recordar que Brasil tiene su matriz energética basada en fuentes renovables, y aunque para el estado de Paraíba la producción en centrales hidroeléctricas representó solamente el 0,7% de la capacidad instalada[21], la electricidad generada mediante centrales hidroeléctricas en el Nordeste de Brasil representó el 49,1% de su capacidad total de generación de electricidad, si bien a nivel del país ascendió al 68,6% del total[22]. De esta manera, la composición de una matriz energética basada en hidroelectricidad implica la necesidad de seguir elaborando estudios que determinen la ocurrencia y distribución de las precipitaciones de cara a elaborar adecuados planes de gestión de recursos hídricos y energéticos.

CONCLUSIÓN

Los análisis de tendencia de las series de precipitación detectaron pendientes positivas de carácter significativo en cuatro de las cinco estaciones estudiadas para los intervalos temporales anuales en la mesorregión Sertão Paraibano.

Los valores de tendencia obtenidos en las distintas estaciones e intervalos temporales analizados son heterogéneos, si bien cuatro de las cinco estaciones presentaron similares comportamientos en la evolución de la precipitación, con valores positivos de

pendiente a escala anual, de entre 2,99 mm/año y 5,98 mm/año, y semestral (E-J), de entre 3,82 mm/año y 4,34 mm/año.
Aunque en la escala mensual hay un predominio de valores de pendiente de la precipitación positivos, debido a una habitual ausencia de lluvias entre los meses de agosto y diciembre, los análisis de tendencia mensuales no resultaron concluyentes, siendo recomendable aplicar nuevos análisis estadísticos y de series temporales que complementen a los actuales.
Este trabajo ha supuesto un importante avance para comprender la dinámica de evolución climática de la mesorregión de Sertão Paraibano, información que puede ser aplicada en el desarrollo de medidas ambientales y de gestión de recursos hídricos en esta región semiárida.

AGRADECIMIENTOS

Este trabajo fue realizado con el apoio de AESA (Agência Executiva de Gestão das Águas) y del proyecto CNPq 305419/2015-3.

REFERENCIAS

1. IPCC. International Panel on Climate Change. Climate change 2007: Climate change impacts, adaptation and vulnerability, IPCC Working Group II, 4th Assessment Report.Sumary for Policymakers. Houghton, 2007.
2. Blain, G. C. Tendências e variações climáticas em séries anuais de precipitação pluvial do Estado de São Paulo. Bragantia, vol. 69, nº. 3, Campinas, 2010.
3. Pedroza, I. C. B. Estimativa da Climatologia Diária da Precipitação e Investigação de Possíveis Influências das Fases da Lua nas Chuvas no Estado da Paraíba. Campina Grande, 2009.
4. AESA. Agência Executiva de Gestão das Águas do Estado da Paraíba. Plano Estadual de Recursos Hídricos – Relatório final. João Pessoa, 2009. Disponible en: http://www.aesa.pb.gov.br/perh/. Acceso en: 27 de enero de 2016.
5. CHESF. Companhia Hidroelétrica do São Francisco. Curemas. Recife, 2016. Disponible en: https://www.chesf.gov.br/SistemaChesf/Pages/SistemaGeracao/Curemas.aspx. Acceso en: 12 de enero de 2016.
6. Lucena, A. F. P.; Szklo, A. S.; Schaeffer, R.; Souza, R. R.; Borba, B .S. M. C.; Costa, I. V. L.; Amaro Júnior, O. P.; Cunha, S. H. F. The vulnerability of renewable energy to climate change in Brazil. Energy Policy, vol. 37, p. 879–889, 2009.
7. Benito, Y. 2013. Energia e Mudança Climática. Programa de Capacitação em Energias Renováveis. Observatório de Energias Renováveis para a América Latina e o Caribe.
8. IBGE. Instituto Brasileiro de Geografia e Estatística. Atlas geográfico brasileiro. 2002. Disponible em: http://atlasescolar.ibge.gov.br/images/atlas/mapas_brasil/brasil_clima.pdf. Acceso em: 04 de febrero de 2016.
9. Cavalcanti, Iracema F. A.; Ferreira, Nelson J.; Dias, M. Assunção F. da Silva; Silva, M. Gertrudes A. Justi da. Tempo e clima no Brasil. São Paulo: Oficina de textos, 2009.
10. AESA. Agência Executiva de Gestão das Águas do Estado da Paraíba. Mapa das mesorregiões do Estado da Paraíba. João Pessoa, 2009. Disponible en: http://www.aesa.pb.gov.br/perh/. Acceso en: 27 de diciembre de 2015.

11. Becker, C. T.; Melo, M. M. M. S.; Costa, M. N. M.; Ribeiro, R. E. P. Caracterização Climática das Regiões Pluviometricamente Homogêneas do Estado da Paraíba. Revista Brasileira de Geografia Física. Vol. 4, n.º 2, p. 286-299. 2011.
12. SNEYERS, R. On the use of Statistical Analysis for the Objective Determination of Climatic Change. Meteorol. Zeitschrift. V.1: p. 247–256. 1992
13. SALMI, T. et al. detecting trends of annual values of atmospheric polluants by the Mann-Kendall test and Sen's slope estimates: The excel template application Makesens. Helsinki, Publications on Air Quality, n.º 31, 2002.
14. Mann, H. B. Nonparametric tests against trend. Econometrica. The econometric society, v.13, n.3, p. 245-259. 1945.
15. Kendall, M. G. Rank Correlation Methods. London: Charles Griffin, p.120. 1975.
16. ABRAHÃO, R. Compreensão de mudanças climáticas regionais atraves da aplicação de tres métodos estatísticos. V Congresso Brasileiro de Energia Solar, Recife, 2014.
17. NAE. Núcleo de Assuntos Estratégicos da Presidência da República. Mudança de clima, v. 1: Negociações internacionais sobre a mudança de clima: vulnerabilidade, impactos e adaptação à mudança de clima. Cadernos NAE. Brasília: NAE-SECOM, 2005.
18. NAE. Núcleo de Assuntos Estratégicos da Presidência da República. Mudança de clima, v. 2: Mercardo de carbono. Cadernos NAE. Brasília: NAE-SECOM, 2005.
19. PEIXOTO, I. M. B. M.; ABRAHÃO, R. Mudanças climáticas e seus impactos no Nordeste brasileiro. Relatório final. Programa de iniciação científica e tecnológica (PIBIC). 2015.
20. ANA. Agência Nacional das Águas. Caderno de Recursos Hídricos. Disponibilidade e demanda de recursos hídricos no Brasil, p. 134, 2005.
21. NOGUEIRA, G. M. F.; GIRARD, O. R. S.; PAVAN, R. C.; SOARES, L. C. R. Eixos integrados de desenvolvimento da Paraíba: Uma visão estratégica para o Estado. João Pessoa: SEPLAG, 2014.
22. EPE. Empresa de Pesquisa Energética: Anuário Estatístico de Energia Elétrica 2014 – ano base 2013. Disponible en: http://www.epe.gov.br/AnuarioEstatisticodeEnergiaEletrica/20130909_1.pdf. Acceso en: 12 de agosto de 2015.

CHAPTER 2.5 THE OASIS SYSTEM: A MODEL OF ADAPTATION TO THE CLIMATIC CHANGES

A. Boulassel *(1,2); B. Mouhouche (2); D. Smadhi (3) and L. Saidi (4)

(1) Institut National de la Recherche Agronomique d'Algérie (INRAA), Centre Régional d'Oued Ghir, 06017 Béjaia, Algérie
(2) Département Génie Rural, Laboratoire de Maîtrise de l'eau en Agriculture, Ecole Nationale Supérieure Agronomique (ENSA), Avenue Hacène Badi, BP 182, El Harrach, 16200 Alger, Algérie
(3) Institut National de la Recherche Agronomique d'Algérie, Division de Bioclimatologie et Hydraulique Agricole, Alger.
(4) Institut Technique des Grandes Cultures, El Harrach, 16200 Alger, Algérie

ABSTRACT

The oasis is a living space of life, a model of integrated development combining socio-economic and environmental dimensions and not only a farming system.
The oasis system has proven somehow over time, as a sustainable system, and, under extremophilic conditions at Saharan environment.
Today, per hour of the climatic changes, the research of the strategies of attenuation and adaptation is recommended. The oasis system which proved somehow over time remains a model of adaptation to the most hostile conditions of the environment.
The system works like a real ecosystem in the biophysical sense and at the same time as a socio-economic and cultural organization highly diversified across the arid regions especially in the Sahara. It is an old system based on the rational management of water and soil resources which is associated "the date palm". It is accordingly that our paper fits.

Keywords: adaptation, climatic change, oasis model.

INTRODUCTION

Since its existence, Algerian Sahara, which represents more of 80% of the national territory, was occupied by small human establishments called "Oasis" strewed here and there if the water, the symbol of the life, exists[1-4].

The Algerian oasis are largely located in the North of Sahara where weather conditions seem to be more favorable for the blooming of the culture of the date palm[5]. This oasis covered 63000 ha adding up 6626000 date palm located for 60 % in the northeast of Sahara (Ziban, Oued Righ, El Oued and Ouargla) and 40 % on the West (Mzab, Touat, Gourara, Tidikelt)[6]. The Algerian oasis which represent a very varied mosaic, knew a remarkable evolution these last decades to reach a surface of 93000 ha and more than 10 million palm trees that is 11 % of the world total. Who oasis is isolated, of size more at least moderated as the oasis of Ouargla, which counts to her

---

*Author for correspondence: boulassel_ma@yahoo.fr; b.abdelmadjid.@gmail.com

alone more than a million palm trees, sometimes grouped as those of Oued Righ where 47 oasis are spread out over 150 km with 1,7 million palm trees: the agricultural surface of oasis is mainly occupied by the palm tree. In Adrar, the palm tree dominates all of the surface; in Ouargla the occupation rate of the palm tree is 80 %, it is around 50-60 % for the rest of oasis[7].

Generally, the importance of oasis is dependent in the agricultural activities, but it remains so connected to the strategic and geopolitical positions (as the oasis of Djanet, Tamanrasset, Tindouf), their industrial potential (Hassi Messaoud, Hoggar, Béchar), businesses and services (Ghardaïa, Biskra, Ouargla), their tourist assets (Taghit, Beni Abbès, Timimoun, M'zab, etc.).

If, in the appearance all the oasis is alike; in reality, they are quite different between them due to the constants of the environment and the management of the conditions of the environment necessary for the preservation and/or the development of the local economy. Indeed, the oasis of Souf postpone from those of Wadi Righ and those Ziban are different the previous ones. In the same ecosystem, this oasis can present differences predisposing them to a system of production rather than to another one (**Figure 1**).

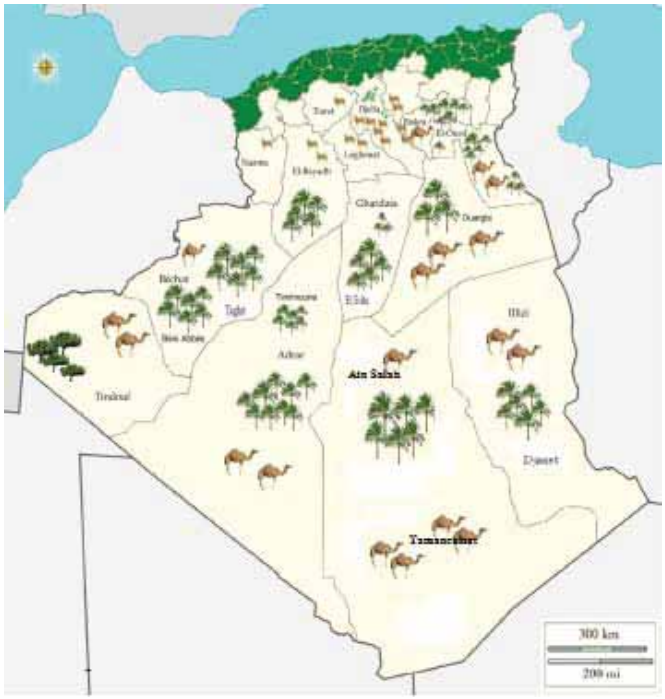


FIGURE 1. The oasis of Algeria

METHODOLOGY

The continuous observation of the oasis model for more than twenty years, allowed us to notice that the system works as a real ecosystem in the sense biophysics of the term and at the same time as a socioeconomic and cultural organization very (highly) diversified through all Sahara[8].

It is thousand-year old inheritance of these material and immaterial heritage that it is necessary to us to promote at all costs and to protect, through its principles of bases, its way of functioning except all the anthropological natural hazards which make of the oasis one of the most model of sustainable development.
To demonstrate the relevance of the study, we have proceeded to a territorial diagnostic analysis, based essentially on semi-direct interviews with resources people, primary and secondary data and observations on the ground to understand better the system of functioning of the "Oasis system".

RESULTS AND DISCUSSION

Basic principle of an Oasis and a functioning of the "oasis system". The oasis is a human creation. it is defined as a water source in a desert environment (dry) all-around of which developed human activities essentially around the date palm, generator of places of life and income. For that purpose, the oasis bases on the sharing and the mode of use of the water resource. The way of sharing the water has a social and economic dimension which differs from an oasis to another one. According to the type of harnessing, storage, routing and distribution (casting) of the water, we distinguish:

- Oasis of Touat-Gourara de la Saoura et du Tidikelt (south west) : are based on the foggara system (**Figure 2**)
- Oasis of Souf : System based on the Ghouts, ingenious system to irrigate Palm without using pumps, segias and others, and, is a way to combat silting (**Figure 3**).

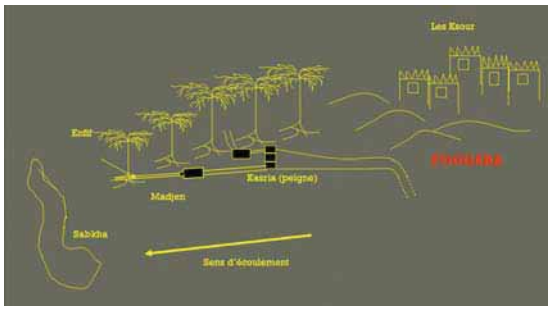
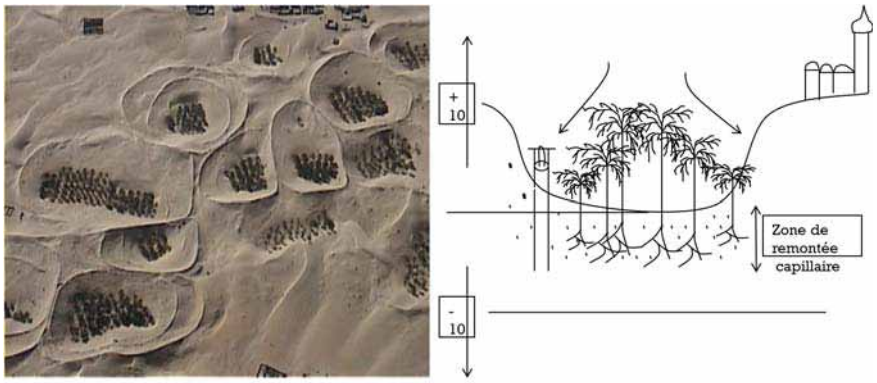


FIGURE 2. Organization of an Oasis of south west

- Oasis of piedmont : exploitation of surface and/or ground waters (**Figure 4**)
- Oasis de l'Oued Righ: Management of salt (**Figure 5**)
- Oasis of M'zab : Exploitation of the flood waters and foggara (**Figure 6**)



FIGUIRE 3. The Ghout system (to the left an aerial view of a "Polynesia" of Ghouts and to the right principle of functioning of Ghout)



FIGURE 4. The oasis of Roufi



FIGURE 5. Oasis of Oued Righ

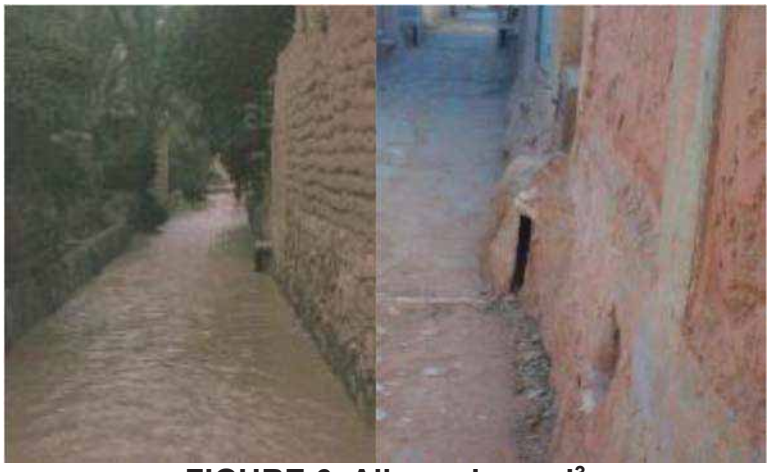


FIGURE 6. Alleys channel[3]

We also distinguish, other types of oasis, in particular in northern Sahara, it is about palm trees *Bour* (without irrigation), Tlou'e system (irrigation by excavation) and the Djali system (Boulassel and Lakhdari, 2013) (**Figures 7 - 9**)

This oasis are located right in the Saharan desert environment marked by the climatic aridity (less of 100mm of rain/year), an extreme ETP (> 2000 mm/year on average) and scorching temperatures (50-55°C) in summer season. It is also windy and endorheic areas where the agricultural grounds are quasi-non-existent with the exception of some niches (dayas, alluvial river).



FIGURE 7 . Palm grove *Bour*

The ingenuity of the system lies in the judicious choice of the implantation site allying the presence of an accessible subterranean water resource and a ground capable of the irrigation-drainage and the putting in culture.

The ingenuity of the system still lies in the meticulous choice of an adapted species "the date palm" allowing an agricultural practice in these extremophilic conditions.

It tolerates the various typical of thermal, hydric and salt stress[9], the date palm remains the fruit species cultivated by the man, the best adapted to the agro-pedo-climatic conditions which reign in Sahara. Its high tolerance in the salinity allowing it to support until 20000 microhms (Lakhdari, 2014).



Figure 8. Palm grove Thlou'e

It is clear that the practice of the phoeniciculture allowed a diversification of the cultures led on behalf under the cover of the going palm tree of the fruits trees (vine, pomegranate tree, apricot tree, fig tree), herbaceous cultures, up to the condiment and aromatic plants where from the name of intercalary cultures or still oasis system in three floors (the most dominant model).

The introduction of forage crops allowed a diversification of the caprine, ovine breeding and the poultry farming. This allowed a food reassurance, in particular in animal-derived proteins. The camelin which values the big desert areas remains the protein archetypal source for oasis population[10].



Figure 9. Palm grove Djali

We also noticed that all the by-products of the culture of the palm tree find use in the Oasis:

-The Downgraded dates and pits as livestock feed,

-The Biomass depending on its condition, it is directed to crafts (basketry), the structures at the palm grove as fences, wind breezes and / or to protect young plants (djebbar) (**Figure 10**).



FIGURE 10. Fence with the by-products of the date palm.

There is good reason to note that the oasis system is at the origin of a preservation of a biodiversity of the local and/or acclimatized species in the conditions of the environment, like valley of Oued Righ[9]; one of the oldest cultivated and saltier areas in the lower Sahara. Besides the domesticated botanical and animal species, the Oasis also shelters a floral and spontaneous biodiversity rich and diversified faunistique[1]. She also insures the relay role for migratory birds in search of feeder and clement niche in winter season[11-13].

With its original concept based on integrated management of space, natural resources, its own productions and their derivatives, Oasis generates practically no waste. Everything is used and/or is recycled between the palm grove, breeding and habitat and / or flow outside the Oasis through trade and exchanges: it functions as a selfregulating system, while being very open to the world

Oasis & Climatic change. Along its history, the Oasis has capitalized on a tangible and intangible heritage in terms specific know-how of the arid and hot environments in all areas of human life (hydraulic, dryland, built, environment, cultural handicrafts) which increases its interest takes on another dimension at the time of the climate threats.

The Oasis model with three floors is recommended today as a basic model for adaptation, mitigation of climate change while maintaining food security and the environmental dimension (smart climate agriculture)[14].

CONCLUSION

Although it is human design at least on the base, the whole works as an ecosystem in the sense biophysics of the term but also as a social, economic and cultural organization with an economic basis around the date.
What makes of the Oasis a shape of adaptation for the extreme conditions of the desert, a model of sustainable development, a place of archetypal life allying the environmental and socioeconomic dimension.

REFERENCES

1. Boulassel A., Lakhdari K., La diversité dattière de deux écosystèmes oasiens: cas des oasis de Goug et d'El Alia, Sahara Septentrional, Algérie. Communication orale au colloque international «la biodiversité et les populations dans le contexte du changement climatique»; Antananarivo, Madagascar, 10-11 décembre 2013.
2. Boulassel A., Lakhdari K., Dakhia N., Le palmier thlou'e :on « cosystème oasien original du Sahara Septentrional Algérien. Communication au Meeting international: Ressources phytogénétiques du palmier dattier: Etat, caractérisation et défis de gestion, Djerba 15-17 Avril 2013.
3. Boulassel A., Mouhouche B., Boucherit H., Management and Conservation Water Techniques for and by Farmers: when the water management is a risk shared by the community. Case of fragile ecosystems in Algeria. International Journal of Engineering Research & Science (IJOER) ISSN: [2395-6992] [Vol-2, Issue-5 May- 2016], 22-27.
4. Dubost, D., Ecologie, Aménagement et développement agricole des oasis Algériennes. Ed. CRSTRA, BISKRA (2002), 423p.
5. Khengani, M.A., Caractérisation des sols alluviaux et de la nappe alluviale de l'oasis de Guerrara. Thèse Magister en science Agronomiques, option Science du sol, université Kasdi Merbah, Ouargla, (2010) 78p.
6. Bouzaher A., - Création d'oasis en Algérie. Option méditerranéenne série A/N°11, 1990.
7. Zella L. et Smadhi D., Gestion de l'eau dans le milieu désertique : cas des oasis Algériennes. Laryhss journal de l'université de Biskra, (2006) 5p.
8. Lakhdari F., l'Agriculture Saharienne hier, aujourd'hui et demain? Conférence plénière, Salon National de Valorisation et de la Recherche MESRS-DGRSDTOran, 7-9 Avril 2014
9. Lakhdari, K., Kherfi Y., et Boulassel, A., Atlas des semences locales et/ou acclimatées dans les oasis de l'Oued Righ. Ed. CRSTRA, Biskra, (2010) 78p.
10. Lakhdari K., Boulassel A., Belhamra M., L'élevage camelin en Algérie : une contribution dans la sécurité alimentaire de la population oasienne (cas d'Ouargla). VIIème Séminaire International de la Médecine Vétérinaire, Constantine, Algérie 11-12 Avril 2015
11. Doumandji-Mitiche B., Doumandji S., Kadi A., Kara F., et Sahraoui L., Orthpterological fauna of some Algerian oasis (Béchar, Adrar and Tamanrasset) Med. Fac. Landboww, Univ. Gent, 64/3a,(1999) 149-153
12. Idder M. A., Lutte biologique en Palmeraie à Ouargla ; cas de la cochenille blanche Parlatoria blanchardi, de la pyrale des dattes Ectomyelois ceratoniae et du BOUFAROUA Oligonychus afrasiaticus. Thèse de Doctorat en sciences agronomiques, Ecole. Nat. Sup. Agro., El-Harrach, (2011) 152p.
13. Farhi Y., Structure et Dynamique de l'Avifaune Steppique Présahariens et Phoenicicole des Ziban. Thèses Doctorat en Sciences Agronomiques Université de Biskra,(2014) 384p.

14. CIRAD Ciel, ma terre ! Agriculture et dérèglement climatique. (2015), 12p. http://www.cirad.fr/content/download/9630/110082/version/2/file/SIA15-Brochure+FR-xlight.pdf
15. Lakhdari, K., Boulassel, A., Dakhia, N., Etude comparative de deux écosystèmes oasiens: Cas des oasis de Goug et d'El Alia. Communication orale au 1er Colloque International REZAS'12 "Les Ressources en Eaux dans les Zones Arides et Semi-arides REZAS12", Beni Mellal, Maroc,

CHAPTER 2.6 ANIONIC SURFACTANT QUANTIFICATION IN IPOJUCA RIVER AND TEXTILE LAUNDRY WASTEWATER IN THE CARUARU CITY, NORTHEASTERN BRAZIL

J. L. Costa (1); I. F. B. Vieira (2); **M. A. P. Kelm** (2); E. A. Pastich (1); S. Gavazza (3) and L.F. C. Souza *(1)

(1) Laboratory of Environmental Engineering, Academic Center of Agreste, Federal University of Pernambuco, Rodovia BR-104, Km 62, Nova Caruaru, Caruaru-PE, CEP: 55002-970, Brazil
(2) Caruaruense Association of Higher Education - ASCES, Caruaru-PE, Brazil.
(3) Laboratory of Environmental Sanitation, Department of Civil Engineering, Federal University of Pernambuco, Recife-PE, Brazil

ABSTRACT

Discharge of untreated effluents into water bodies is an ancient practice that still persists in Brazil. In northeastern of Brazil, the consequences of this practice are intensified due to long periods of drought, low rainfall and, sometimes, intermittent river regimen that reduce the auto depuration capacity. Caruaru city in Pernambuco state centralizes an important textile pole, specialized in jeans washing (laundries). Some laundries in the region release their effluents in the crossing rivers without proper treatment. Surfactants in textile effluents are versatile due to the ability of interacting and reacting with different types of molecules. The linear alkyl benzene sulfonate (LAS) is a widely used synthetic anionic surfactant, to produce cleaning agents such as soaps and detergents. High concentrations of LAS in water bodies can cause significant environmental, social and economic problems, although its known aerobic biodegradability. In this work, the LAS concentration was analyzed in different sections of the Ipojuca river and in the textile effluents, and it was measured as total anionic surfactant (TAS). Samples from six jeans laundries effluents were monthly collected and analyzed, between July and September of 2014. The sampling of Ipojuca river water was performed in the five points: two in rural area, one before and one after the river reach Caruaru city (named P1 and P5) and three points in the city urban area (named P2, P3, P4) where the laundries are located. The water river samples were monthly collected, from October of 2014 to October of 2015. Independently of the laundry size, similar TAS concentration was detected, around 2 ± 1 mg MBAS (Methylene Blue Active Substances). L^{-1} in samples from laundries effluents. The TAS concentration in laundries effluents was lower than the found in the average in water from the river (around 3 ± 3 mg MBAS.L^{-1}). This finding indicates that possibly domestic sewage may also have contributed to the found TAS concentration in the river. The lowest TAS concentration was 1.3 ± 0.7 mg MBAS.L^{-1} and 2 ± 1 mg MBAS.L in P1 (rural area) and P2 (industrial center) sampling points, respectively. In P3 and P4, both in the urban center, the highest concentrations were found, 5 ± 3 mg MBAS.L^{-1} and 4 ± 2 mg MBAS.L^{-1}, respectively. Finally, in point P5, the TAS concentration decreased again to 2 ± 2 mg MBAS.L^{-1}, showing the Ipojuca river

---

*Author for correspondence: luizas@gmail.com

ability in partially depurating the pollution discharges. Considering this parameter, we noted that, in terms of LAS concentration in the Ipojuca river, domestic sewage may have contributed more than textile wastewater. Besides that, the concentration decreased when leaving the urban center showing the auto depuration river ability.

Keywords: auto depuration, domestic sewage, surfactants, textile effluent;

INTRODUCTION

Surfactants are fundamental components in detergents and cleaners to remove dirty. From the four groups of surfactants, anionic deserve mention for its large utilization. Among them, the Linear Alkylbenzene Sulfonate (LAS) is the anionic surfactant of higher production and consumption due to efficient power of detergency. A sulfonated aromatic ing attached to a linear carbon chain forms the LAS, but your products used commercially are a mixture of homologues and isomers, distinguished by the carbon number of the linear chain of 10 to 13 and the aromatic ring connecting position, respectively[1]. The large increase in production is initiated by the fact that the LAS is biodegradable in aerobic conditions, replacing, for environmental reasons, the Alkylbenzene Sulfonate (ABS), which was not easily degradable[2].

Despite its biodegradability, uncontrolled release of LAS in ecosystems generate environmental impacts, such as the decrease of dissolved oxygen concentration because of the reduction of the surface tension between water and air, the impossibility of passage of light because of the excessive presence of foams, increased turbidity and facilitating of solubilization of xenobiotic substances[3].

This study aimed to evaluate the contribution of textile effluents generated in the city of Caruaru in the concentration of LAS in the Ipojuca river, Brazil. The Ipojuca river is an important source of water for the Agreste region of Pernambuco. In its path of 323.9 km, crosses 24 cities that make use of the river water for public supply, industrial use and irrigation, besides being receiver of household, industrial and agroindustrial effluents[4].

Among the cities bathed by the river the city of Caruaru stands out for its economy, dimensions (approximately 921 km²) and population (approximately 314,000 inhabitants)[5]. The city along with two others, Santa Cruz do Capibaribe and Toritama, are part of the Productive Local Arrangement of Clothing Industry of Agreste of Pernambuco. Only in Caruaru there are approximately 4,530 production units of this market[6] with a production that ranges on average from 12,000 to 250,000 peaces of clothing per month. In addition to the productive textile sector there is also the processing sector, which are the laundries. The clothes produced are subjected to a wash step to produce various aesthetic effects. In this step occurs elevated consumption of detergents, softeners (surfactants in general) and water, generating consequently a high flow of effluents[7]. In the region concerned, these wastes are generally not treated properly before being released in the Ipojuca river and its tributaries, a fact that is aggravated at certain periods of the year when the river flow is reduced due to local climatic conditions.

MATERIALS AND METHODS

The Ipojuca river is located in a region classified as BSh in the Köppen rating scale. The highest temperatures are usually in the months of November and February, reaching 30°C, and the lowest in June and July, around 17°C. The annual rainfall is 764 millimeters (mm), concentrated between March and July[8].

LAS analyzes were performed in the effluent of six textile laundries (L1, L2, L3, L4, L5 and L6) located in Caruaru city in the period from July to September 2014, being held three sample collection totalizing 18 samples. The laundries studied were chosen according to their availability and support on the research and they were classified according to their effluent flow as small, medium or large sizes. Were classified as small laundries those with smaller effluent flow than 1000 $L.h^{-1}$, medium size with effluent flow between 1000 and 3000 $L.h^{-1}$ and large size with a higher effluent flow than 3000 $L.h^{-1}$. **Table 1** shows the laundries classification, however the laundries L5 and L6 could not be classified due the lack of availability of necessary information for classification.

TABLE 5. Laundries classification

Laundries	Effluent flow ($L.h^{-1}$)	Classification
L1	935	Small
L2	1750	Medium
L3	4000	Large
L4	4500	Large
L5	Information not available	-
L6	Information not available	-

Anionic surfactants concentration in the Ipojuca river were analyzed in five sample points located along the city of Caruaru, as shown in **Figure 1**, and these samples were taken monthly from October 2014 to October 2015. The selection and distribution of the sample points aimed evaluate the behavior river in relation to the anionic surfactants concentration along its path. The points P1 and P5 were located in rural areas, being upstream and downstream from the urban center, respectively. The point P2 is in the industrial area of Caruaru. The points P3 and P4 are, following the river path, at the beginning and end of the urban center, respectively, since this trade area generates a high population concentration (**Table 2**).



FIGURE 2. Localization of the city of Caruaru and the sample points

Source: The brazilian map and the map with the location of the sample points were generated from <https://www.google.com.br/> and Caburé System available in <http://www.cabure.cprh.pe.gov.br>, respectively

TABLE 6. Description of the localization and the geographic coordinates of the sample points

Sample points	Description of the localization	Geographic Coordinates
P1	Upstream of the city (about 10 km from the urban area)	Long.: -036° 05’ 44.4’’ Lat.: -08°19’15.0’’
P2	Located in industrial area	Long.: -036° 00’ 38.4’’ Lat.: -08° 18’ 09.8’’
P3	Located at the beginning of an area with high population concentration	Long.: -035° 59’ 05.5’’ Lat.: -08° 17’ 27.2’’
P4	Located at the end of an area with high population concentration	Long.: -035° 56’ 22.8’’ Lat.: -08° 16’ 49.2’’
P5	Downstream of the city (about 3.5 km from the urban area)	Long.: -035° 54’ 24.7’’ Lat.: -08° 15’ 57.2’’

Anionic surfactants concentration in textile laundries effluent and the Ipojuca river waters were determined as Total Anionic Surfactants (TAS) according to the MBAS method (5540 C) present in the Standard Methods for the Examination of Water and Wastewater[10].

For a better analysis of the river behavior during rainy or dry periods were collected monthly rainfall data from a rainfall station in the city of Caruaru (station 211). These information are from the Agência Pernambucana de Águas e Clima (APAC)[11].

RESULTS AND DISCUSSION

The TAS concentrations observed in the Ipojuca river (**Figure 2**) had a large dispersion resulting in high standard deviation. This dispersion occurred for several reasons, being they natural as the rainfall, or by human influence as the periods in which the city is receiving large number of tourists because of cultural festivals. On some holidays, such as June Festivities (June), Christmas and New Year's Eve (December), an increase in the people circulation in the city of Caruaru and region have been occurred, mainly because of its famous fairs, in which it is commercialized several products, in special articles of clothing and jeans. This increase of tourists leads to a greater production of domestic sewage.

Anionic surfactant concentration in October and November 2014, at the beginning of the experiment, as shown in Figure 2, remained low, not exceeding 2 mg MBAS.L^{-1}. Over the next four months (December 2014 and January, February and March 2015), an increase in the concentrations at the sample points P3 and P4 (urban center) was observed, which began to excel values. This increase is probably due to intense production in the laundries and the movement of people in the city because of the holidays. In April 2015 there was a marked decrease in the results of all points. In the last four months of sample collection (July, August, September and October 2015), the TAS concentrations increased in sample points P3 and P4 (urban center) reaching values above 5 mg MBAS.L^{-1}. After the rainy season (June and July), a greater water availability in the region occurred, reaching thus higher flow in the network of water distribution, which in turn generates increased sewage production.

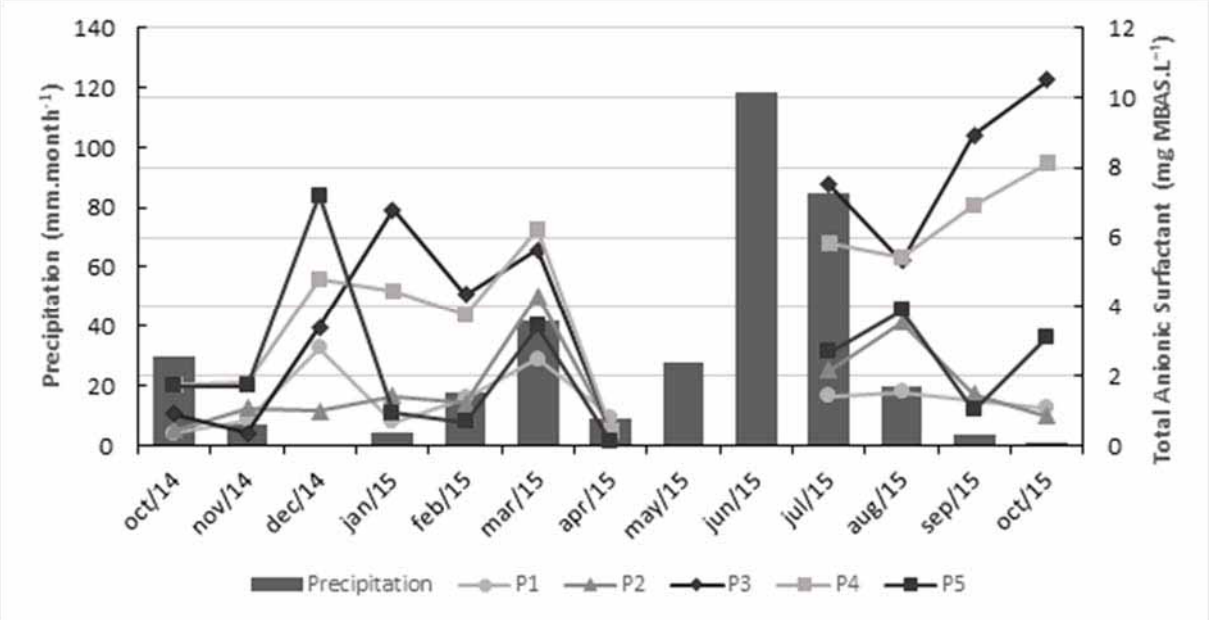


FIGURE 2. TAS concentrations in the sample points of the Ipojuca river and monthly rainfall during the sample collection

Figure 3 shows the behavior of results over the path of the Ipojuca river. A gradual increase in the TAS concentration from the sample point P1 to P3, and then a gradual decrease from the sample point P3 to P5 were observed. This behavior demonstrates urban center contribution on TAS concentration in Ipojuca river, and after the sample point P3 depuration trend of the river.

The sample point P1, which is located upstream of Caruaru city, characterized by having the lowest TAS concentrations during the analysis period (average of 1.3 ± 0.7 mg MBAS.L^{-1}). This point is located on the border with the city of São Caitano.

The sample point P2 was also characterized by having low concentration (average of 2 ± 1 mg MBAS.L^{-1}). This point was located in the industrial center, with some laundries worked, and after a residential area (Alto do Moura neighborhood), the domestic sewage contribution is much lower than that found in the urban center. Thus, probably TAS concentration is within the river's carrying capacity.

The biggest problem of TAS average concentrations was found at the sample points P3 and P4, 5 ± 3 mg MBAS.L^{-1} and 4 ± 2 mg MBAS.L^{-1}, respectively. Domestic sewage discharge in these points contributed more with TAS concentration increase than in P1 and P2.

At the samples point P5 lower concentrations were observed (average of 2 ± 2 mg MBAS.L^{-1}) than the results found in the points P3 and P5. This can be explained by the distance from de point P5 to the city center (3.5 km), which reduces the contribution of domestic sewage, allowing the river to be able to partially purify the load from LAS.

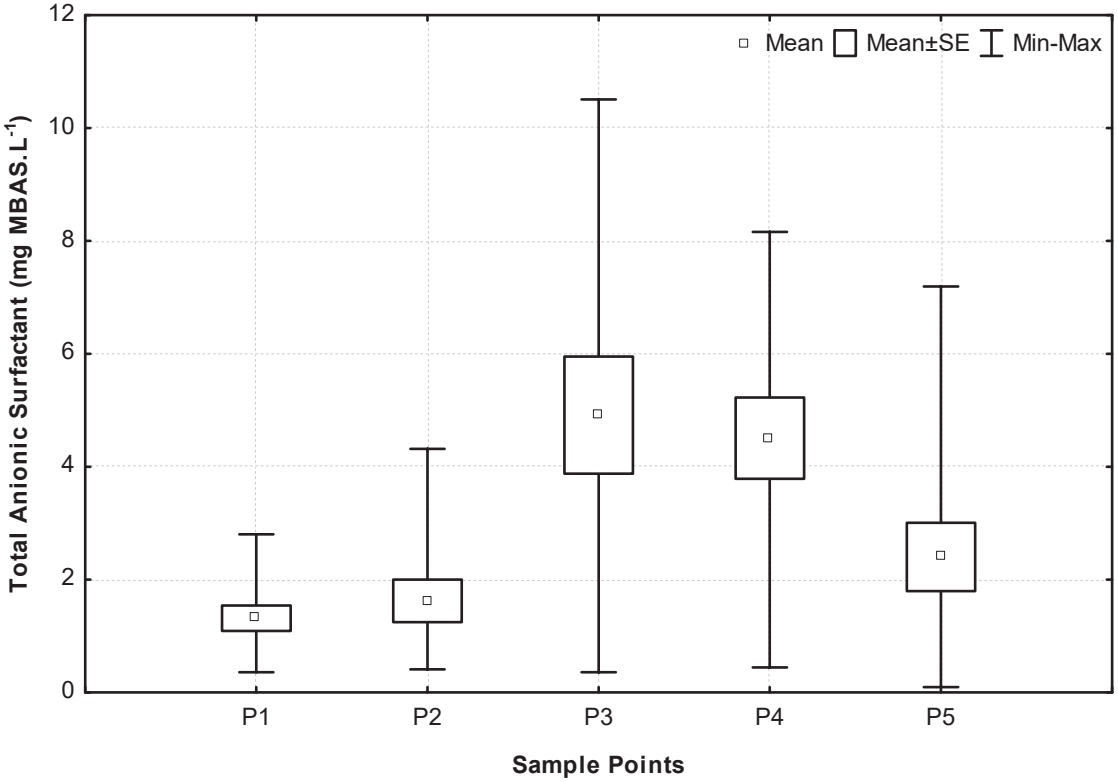


FIGURE 3. TAS concentrations in the sample points of the Ipojuca river

In Brazil, the Conselho Nacional do Meio Ambiente (CONAMA) is responsible for establishing standards and technical criteria related to environmental management. According to CONAMA resolution 357/05, regardless of the water body classification regarding its use, being fresh water, the maximum concentration of surfactant substances reacting with methylene blue (anionic surfactants) must be equal or lower than 0.5 mg MBAS.L^{-1}. The concentrations observed in this study, at all sample points are much higher than those allowed in that legislation[12].

Eichhorn et al. (2002) determined the concentration of LAS (the anionic surfactant more industrially produced) in various parts of the Macacu river, located in the Brazil Southeastern. As the Ipojuca river, analyzed in this study, LAS data were also linked to population density and the consequent contribution of domestic sewage. The results in the Macacu river ranged between 0.014 and 0.155 mg.L^{-1} [13].

McAvoy et tal. (1993) evaluated the presence and the LAS behavior in various types of sewage treatment in multiple rivers of the United States. The LAS concentrations found were generally lower than 0.05 mg.L^{-1} [14]. These low values found in the United States must come from an effective treatment performed in its sewage while in Brazil only 40% of sewage is treated[15]. What reinforces the importance of treatment of domestic sewage before its release aiming to ensure the water quality of receiving bo, dies.

Besides damaging activities such as irrigation and public supply, aquatic ecosystems also suffer from high concentration of anionic surfactant in water. The accumulation of foam on the surface of the water body prevents the passage of light and this makes it impossible to perform photosynthesis by photosynthetic organisms present in the ecosystem.

According to Helenius and Simons (1975), the surfactants act with its toxic capacity in some microorganisms disrupting its cell membrane[16]. In addition, Venhuis and Mehrvar (2004) reported that LAS concentrations between 0.02 and 1.00 mg.L^{-1} cause physiological problems on fishes, such as damage to breath because of the malfunction of fishes' gill due the action of surfactants[17].

Figure 4 shows the results found in textile laundries effluents. The TAS concentrations in the textile effluents are smaller than those found in the river. This shows that the contribution of laundries in the TAS concentration in the Ipojuca river is small. The fundamental reason for this result is the possible use by laundries of products that do not have anionic surfactants in their composition, but have equivalent washing effect as those products that have anionic surfactants. The use of detergent in the laundries is intended to remove excess dye of the clothes but not to removing dirty, such as its residential use.

The laundries effluents samples showed a variation in TAS concentration between the sampling months, once the effluents are related to factors that interfering in its composition such as changing brands and types of cleaners used, the amount and types of clothes produced and the quality of water used for washing the clothes.

Regardless of the size of the laundry, the behavior in relation to TAS concentrations in the effluents was similar. The laundry L1, classified as small, showed an average concentration of 1 ± 1 mg MBAS.L^{-1}. The laundry L2, even being classified as medium size, had the highest average in the TAS concentration (2.4 ± 0.9 mg MBAS.L^{-1}). The laundries L3 and L4, both classified as big, had averages 1.3 ± 0.5 mg MBAS.L^{-1} and 2

± 1 mg MBAS.L^{-1}, respectively. The laundries L5 and L6, that for lack of information has not been classified according to their size, showed average of TAS concentration of 1.3 ± 0.8 mg MBAS.L^{-1} and 1 ± 1 mg MBAS.L^{-1}.

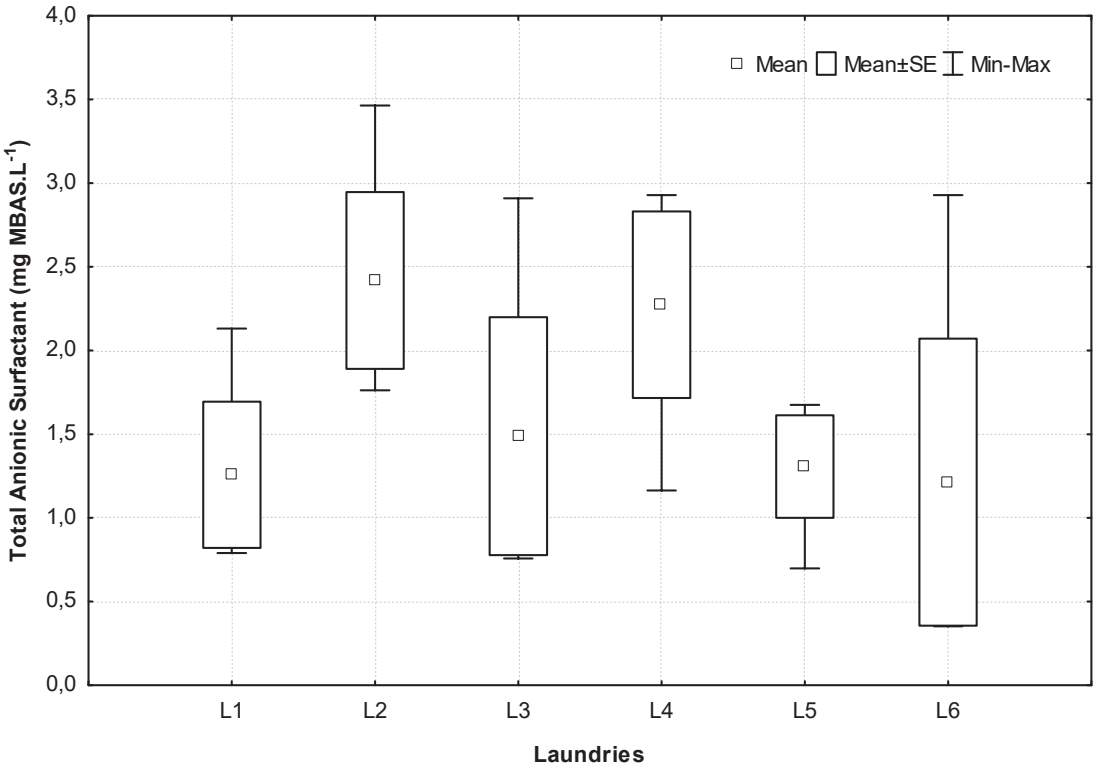


FIGURE 4. TAS concentrations in the studied laundries

CONCLUSION

From the observed results, it was concluded that the high level of pollution of the Ipojuca river may be a consequence of the lack of sewage treatment in the cities bordering the river, especially Caruaru. The concentration of LAS was associated with periods of popular festivities and rainfall that increase or decrease the self-purification capacity of the river. The concentration of LAS observed in the river is much higher than allowed by the environmental legislation in Brazil, which can cause significant environmental impacts on the Ipojuca river. Besides that, it was noted that the domestic sewage could be contributing more to the current situation of the river than the industrial sewage.

ACKNOWLEDGMENTS

The authors would like to thank the following: the Laboratory of Environmental Engineering (LEA) in the Federal University of Pernambuco and the brazilian agencies Cnpq, Finepe and Facepe, for providing support to the LEA-UFPE via grants and scholarships.

REFERENCES

1. HERA, Linear Alkylbenze Sulphonates (LAS), 2013.
2. Zago Neto O. G., Del Pino J. C. Working Chemical Soaps, Chemical Institute, Federal University of Rio Grande do Sul. Rio Grande do Sul, Brazil.
3. Haigh S. D. A review of interaction of surfactants with organic contaminants in soil. The Sci. of the Total Envir. 185 (1996) 161-170.
4. CONDEPE/FIDEM The Ipojuca River watershed, Recife, Brazil, 2015.
5. IBGE. Available in: <http://www.ibge.gov.br>. Access: May, 23rd, 2016.
6. SEBRAE Economic Study of the Textile Local Productive Arrangement of Agreste of Pernambuco, Recife, Brazil, 2013.
7. Silva Filho A. R. A. Development of simplified environmental management system applied to micro and small jeans processing companies, Technology and Geosciences Center, Federal University of Pernambuco, Recife, Brazil. 2013.
8. APAC. Available in: <http://www.apac.pe.gov.br/>. Access: February, 3th, 2016.
9. CPRH System of Geo-environmental Information of Pernambuco. Available in: <http://www.cabure.cprh.pe.gov.br/>. Access: January, 10th, 2016.
10. APHA, Standard Methods for the examination of water and wastewater, 22nd edition, (2012).
11. APAC. Available in: <http://www.apac.pe.gov.br/>. Access: February, 3th, 2016.
12. CONAMA Resolution 357/05: Determining the classification of freshwater, brackish and saline waters in Brazil, Brasília, Brazil. 2005.
13. Eichhorn P., Rodrigues S. V., Baumann, W., Knepper, T. P. Incomplete degradation of linear alkylbenzene sulfonate surfactants in Brazilian surface Waters and pursuit of their polar metabolites in drinking waters. The Sci. of the Total Envir. 284 (2002) 123-134.
14. Mcavoy D.C., Eckhoff W. S., Rapaport R. A. Fate of linear alkylbenzene sulfonate in the environment. Envir. Toxic. and Chem. 12 (1993) 977-987.
15. SNIS Diagnosis of Water Services and Sewage 2014. Available in: <http://www.snis.gov.br/>. Access: May, 30th, 2016.
16. Helenius A., Simons K. Solubilization of membranes by detergents. Bioch. et Bioph. Acta. 415 (1975) 29-79.
17. Venhuis S. H., Mehrvar, M. Health effects, environmental impacts, and photochemical degradation of selected surfactants in water. Intern. Journal of Photo. 6 (2004) 115-125.

Section 3.
Soil and Sediment Remediation and Groundwater and Aquifer Remediation

Page

Chapter 3.1 Biodegradación de la benzofenona-3 en suelos agrícolas enmendados con compost procedentes de edar urbanas
Julio César Benítez-Villalba; Alberto Zafra-Gómez; M. José Belén Juárez-Jiménez; Noemí Dorival-García; Francisco Paulo Ferreira-Benítez and J.L. Vílchez 211

Chapter 3.2 Residuos de palma africana para el tratamiento de suelo contaminado con hidrocarburos
M. C. Cuevas-Díaz; O. Guzmán-López; P. Pavón-Orozco; A. Ortega-Martínez; M. Ríos Enríquez and G. Fuentes-Algarín 224

Chapter 3.3 Analysis and evaluation of heavy metals pollution in sediments from Coatzacoalcos River in Veracruz, Mexico
L. J. Mota Vázquez; M. R. Gutiérrez Lara; M. C. Cuevas Díaz; O. Guzmán-López; A. C. Ortega-Martínez and G. de Jesús-Antonio 231

Chapter 3.4 Diseño de un biorreactor para lodos residuales de centros de lavado
J. Pérez Vargas, G. Zafra Jiménez; S. E. Vigueras Carmona and G. Calva Calva 241

Chapter 3.5 Efectos del grado de contaminación y de la remediación por biolixiviación en la composición mineral y textural de sedimentos contaminados del Río Reconquista
A. Tufo; N. Porzionato and G. Curutchet 249

Chapter 3.6 Manganeso geogénico en agua subterránea: caso de estudio en Hidalgo, México
D. A. Rivera-Rodríguez; R. I. Beltrán-Hernández; C. Coronel-Olivares; M. Villanueva-Ibáñez; C. A. Lucho-Constantino and G. Vázquez-Rodríguez 260

CHAPTER 3.1 BIODEGRADACIÓN DE LA BENZOFENONA-3 EN SUELOS AGRÍCOLAS ENMENDADOS CON COMPOST PROCEDENTES DE EDAR URBANAS

Julio César Benítez-Villalba *(1); Alberto Zafra-Gómez (2); M. José Belén Juárez-Jiménez (2); Noemí Dorival-García (2); Francisco Paulo Ferreira-Benítez (1) and J.L. Vílchez (2)

(1) Facultad de Ciencias Exactas y Naturales, Universidad Nacional de Asunción, Campus Universitario, San Lorenzo, Paraguay.
(2) Grupo de Investigación de Química Analítica y Ciencias de la Vida, Departamento de Química Analítica, Campus de Fuentenueva, Universidad de Granada, E-18071 Granada, España.

RESUMEN

En este trabajo se realizó un estudio de la biodegradación de la Benzofenona-3 (BP3) en suelos agrícolas enmendados con compost y no enmendados con compost procedentes de lodos de depuradoras urbanas EDARs (estación depuradora de aguas residuales). Para ello se ha desarrollado y validado una metodología analítica que ha permitido la identificación y cuantificación de este contaminante en las matrices seleccionadas (suelo agrícola y suelo agrícola contaminado con compost). Se realizó un estudio del comportamiento de la microbiota en los suelos tratados. Primeramente, se realizó el recuento de la microbiota cultivable en dichos suelos, mediante la técnica de siembra en placa. Se caracterizó bioquímicamente microorganismos seleccionados a partir de los suelos tratados empleado kits donde se concluyó que cada microorganismo los metabolizaba de forma diferente y nos permitió discriminar los microorganismos estudiados y seleccionar aquellos que eran diferentes desde el punto de vista metabólico. Posteriormente se estudió la cinética de crecimiento de los microorganismos seleccionados y el estudio de degradación de la BP3 en presencia de estos microorganismos. Demostrando la habilidad de crecimiento de los microorganismos en presencia de este compuesto como fuente de carbono y energía (C/E).

Palabras clave: Benzofenona-3, biorremediación, compost, enmendados.

INTRODUCCIÓN

La sociedad actual depende en gran medida de numerosas sustancias químicas, empleadas en las múltiples actividades de la vida cotidiana. Sin embargo, su uso masivo y a veces descontrolado, se está convirtiendo en una gran preocupación para los diferentes estamentos sociales, debido a su posible impacto medioambiental, ya que, en la actualidad, no existe una legislación clara y específica para muchos de estos compuestos, especialmente en relación a las concentraciones presentes en el medio ambiente[1-4]. Dentro de este grupo de contaminantes, que en la actualidad han sido

---

*Author for correspondence: julio81benitez@gmail.com

denominados “emergentes”, se incluye una vasta variedad de productos farmacéuticos, antimicrobianos y numerosos compuestos químicos con actividad como disruptores endocrinos[5-8].

Los disruptures endocrinos son sustancias químicas capaces de alterar el sistema hormonal, tantos en seres humanos como en animales, responsable de múltiples funciones vitales como el crecimiento o el desarrollo hormonal[9-10]. Muchos de estos compuestos pueden tener como destino final las aguas residuales urbanas e industriales, pudiendo ser degradados y eliminados durante el tratamiento de las mismas la EDAR. Sin embargo, está demostrado que los procedimientos de depuración no son completamente efectivos, ya que estas sustancias permanecen en los efluentes tratados, pudiendo reingresar al medio ambiente convirtiéndose en un serio peligro para los ecosistemas[11-13].

En la actualidad se piensa, aunque no se cuenta aún con evidencia suficiente, que la presencia de estas sustancias en este tipo de ambientes puede representar un riesgo para la salud humana y los ecosistemas, ya que al encontrarse adsorbidos, los microorganismos del suelo no pueden biodegradarlos satisfactoriamente, convirtiéndose en bioacumulables, persistentes y tóxicos; existiendo la posibilidad de ser transferidos a las cosechas, y de ingresar en la cadena alimentaria de los seres vivos[14-16].

Generalmente, los lodos de depuradoras son sometidos a tratamientos de compostaje, ya que es un tratamiento de bajo costo que presenta numerosas ventajas tales como la desinfección de los fangos, la eliminación por vía microbiana de algunos contaminantes, y la obtención de un sustrato rico en materia orgánica y nutrientes, apto para el enmendado de suelos agrícolas. Además, se trata de un proceso ambientalmente más favorable en comparación con otros como la incineración o la acumulación en vertederos. Actualmente, se conoce muy poco acerca de la capacidad que tiene este proceso en la eliminación definitiva de estos contaminantes emergentes. Tampoco se tienen evidencias de que parámetros o factores favorecen la degradación de estas sustancias durante este proceso. Por otro lado, se desconoce de manera exacta del efecto que produce el enmendado de los suelos con fango o compost sobre los contaminantes presentes, así como el riesgo real al que están expuestos los seres humanos, ya que estas sustancias pueden transferirse, por ejemplo, a las aguas subterráneas[17,18].

El compuesto seleccionado para este estudio es la Benzofenona-3 (BP3), es una sustancia blanca y cristalina, insoluble en agua y con un color rosa. Actúa como filtro para las radiaciones UV ya que es capaz de absorberla (promoviendo sus electrones a un estado excitado) y disiparla en forma de calor. Esto es posible debido a que la benzofenona posee sus estados de singlete y triplete energéticamente muy próximo entre sí. La BP-3 se utilizan en productos tales como perfumes y jabones para evitar que la luz ultravioleta degrade el olor y el color de estos productos. También se utilizan como componente de protectores solares y se pueden añadir en los plásticos de embalaje para que estos bloqueen los rayos UV protegiendo el producto[19-21].

En este trabajo se ha llevado a cabo un estudio de la biodegradación de la Benzofenona-3 (BP-3) en presencia de microorganismos aislados de suelos agrícolas enemendados con compost procedentes de una planta de depuración de aguas residuales EDAR, se caracterizó los microorganismos aislados de los suelos y se realizó un estudio químico de degradación del compuesto y la cinética crecimiento de la

misma en presencia de los microorganismos. Esto nos permitió estudiar y avaluar este contaminante en suelos agrícolas enmendados y no enmendados con compost procedente de lodos de depuradoras urbanas.

MATERIALES Y MÉTODOS

Productos químicos y reactivos. Se utilizaron reactivos de grado analítico. El patrón de Benzofenona-3 y el patrón interno Benzofenona-d_{10} fueron suministradas por la casa comercial Sigma-Aldrich (St. Louis, MO). La solución del BP3 (200 $mg.mL^{-1}$) se prepararon en metanol mensualmente y se almacenaban a -20 °C. Las soluciones estándar, mezclas de este compuesto junto con el patrón interno se prepararon en metanol o en la fase móvil inmediatamente antes de su uso. Estos estándares se almacenaban a 4°C y se preparaban semanalmente. Todas las soluciones se almacenaron en botellas de vidrio oscuro. El agua y metanol que se utilizaron para la preparación de la fase móvil fueron de grado LC-MS suministradas por Fluka (St. Louis, MO, EE.UU.). El amoníaco (> 25%), acetonitrilo, y acetato de etilo se adquirieron de Merck (Darmstadt, Alemania). El agua (18,2 MΩ cm) se purificó por un sistema Millipore Milli-Q (Bedford, MA, ESTADOS UNIDOS). Para el estudio de la cinética de crecimiento de microorganismos se utilizó el medio de cultivo base diluido 1/10 con 5 $mg.L^{-1}$ del compuesto.

Instrumentación y software. Para la recolección de las muestras de compost se emplearon palas convencionales y para las muestras de suelos un muestreador de calado (superficiales) y una barrena helicoidal para mayores profundidades. La temperatura y humedad del suelo fueron controladas a las diferentes profundidades del suelo estudiadas, de forma continua, mediante una sonda AquaCheck. El trabajo experimental se desarrolló utilizando una sonda de ultrasonidos Digital Sonifier S450D (BRANSON) provista de: Convertidor tipo 102, resonador estándar de 12.7 mm de diámetro, punta enroscable de 12.7 mm de diámetro, sonda de temperatura, Micropunta enroscable de diametro final 3 mm. Un cromatógrafo Waters Acquity UPLC™ acoplado a espectrómetro de masas triple cuadrupolo Waters H-Class-Xevo TQS™. Provisto de: Bomba: Quaternary Solvent Manager. Acquity UPLC H Class. (Waters); Inyector: Sample Manager-FTN. Acquity UPLC. Waters; Detector: Xevo TQ-S. (Waters). La separación de los compuestos se obtuvo con una columna ACQUITY UPLC BEH™ C_{18} (1,7 µm; 2,1 mm × 50 mm) (Waters). Una fuente de ionización ionización por electroespray Z-spray™ ESI para la detección del analitos. El software utilizado para la detección e integración de los picos fue el MassLynx V.4.1 SCN.803 programa de gestión y tratamiento de los datos obtenidos por el cromatógrafo Waters Acquity UPLC™ H-Class - Xevo TQS™. Un Vortex (Yellow line, Wilmington, NC, USA), una centrifuga Hettich Zentrifugen, universal 32 (Tuttlingen, Alemania). En la cinética de crecimiento los resultados se expresaron de acuerdo a la relación densidad óptica/recuento UFC mL^{-1} a través de un espectrofotómetro (UNICAM UV/VIS 5821) a 600 nm. Por último, se emplearon los equipos (balanzas, estufas, agitadores, incubadoras, etc.) y el material de vidrio habituales de un laboratorio de química analítica y de microbiología. Para el tratamiento estadístico se utilizó un software

Statgraphics Plus versión 5.0 (Manugistics, Rockville, MD, EE.UU., 2000). Paquetes Microsoft® Office: Word®, Excel® y PowerPoint® 2007.

Desarrollo Experimental

Estudio de campo BP3. El estudio de campo se llevó a cabo en una parcela experimental que está situada en la Huerta de Santa María en la Vega de Granada – España. En el suelo agrícola no se ha utilizado ningún tipo de pesticida, herbicida o insecticida en los últimos 10 años con el objetivo de no alterar la microbiota del suelo[22,23]. Las muestras de compost fabricado a partir de lodos de depuradora que fueron utilizados para este ensayo, fueron recolectadas en la empresa compostadora "Biomasa del Guadalquivir" situada en Santa Fe (Granada).

Con el fin de determinar la influencia de este contaminante químico objeto de estudio sobre la microbiota cultivable presente en el suelo agrícola se adicionó dicho compuesto al suelo de la parcela experimental, dividida en este caso en subparcelas de 1 m^2 siendo la cantidad de compuesto añadida de 1 $g.L^{-1}$, en un volumen de agua de pozo de 120 $L.m^{-2}$ para que la disposición del compuesto fuera homogénea en la zona de aplicación. Cada subparcelas estaba separado por tasquibas de 30 centímetros de espesor. Previamente se realizó una limpieza de la vegetación existente para evitar posibles interferencias de los mecanismos de adsorción-desorción, la degradación de los compuestos en estudio, o la interferencia sobre alguna variable general como el índice de evaporación del agua. Se fijaron dos condiciones diferentes: Parcela 1 (P1) suelo contaminado con el BP-3 aplicado directamente al suelo, Parcela 2 (P2) suelo enmendado con compost y contaminado con BP-3. Para este estudio se tomaron tres muestras de cada subparcelas a lo largo de tiempo (0, 15 y 30 días) y a tres profundidades (superficie, 30 y 60 cm). Las muestras se trasladaron al laboratorio y se secaron a temperatura ambiente en un desecador durante 24 h, con el objeto de eliminar resto de humedad. A continuación, se homogeneizaron y tamizaron utilizando un tamiz estéril de 1 mm de diámetro de poro.

Recuento de la microbiota cultivable. Mediante la técnica de siembra en placa. Todas las siembras, así como el procesamiento de las muestras (preparación de diluciones), se llevaron a cabo en una campana de flujo laminar. A partir de 1 g de cada muestra se realizaron diluciones seriadas (1/10) en solución salina (NaCl, 0.9 %, p/v), sembrándose 0.1 mL de cada dilución en medio solido TSA (Agar Tripticasa Soja, Oxoid) mediante método de siembra de la gota. De cada dilución se realizaron tres replicas. Posteriormente, las placas se incubaron en aerobiosis durante 24/48 h en la estufa a 28-30°C.

Los resultados se expresaron como logaritmo de Unidades Formadoras de Colonias de microorganismos heterótrofos cultivables por gramo de suelo (log UFC $g\ suelo^{-1}$).

Caracterización morfológica de los microorganismos aislados y seleccionados a partir de las diferentes parcelas estudiadas. Una vez realizado el recuento de la microbiota cultivable en las diferentes parcelas tratadas con la BP-3 objeto de estudio, se procedió a realizar los aislamientos y selección de los microorganismos dependientes de cultivo presentes en los diferentes suelos, en medio solido en placa (TSA). De cada tipo de

suelo se realizaron 20-25 aislamientos. La selección de los microorganismos se realizó en función de criterios morfológicos de las colonias (forma, elevación, borde, tamaño y coloración) así como de criterios microscópicos (Gram, morfología, y agrupación). Con objeto de poder obtener una información inicial acerca de los microorganismos presentes en lo suelos de estudio, se realizó la tinción de Gram de los microorganismos seleccionados. Dicha tinción generó información acerca del tipo de pared celular así como de la morfología y tipo de agrupación celular. La posterior observación al microscopio permitió averiguar cuáles eran las características morfológicas básicas de los microorganismos de trabajo.

Cinéticas de crecimiento de microorganismos y estudios de degradación de los compuestos. Se seleccionó una batería de microorganismos procedentes de las muestras de suelo tratadas con los diferentes compuestos y compostadas (codificados con las iniciales del compuesto adicionado a esa parcela y un número consecutivo). La selección se realizó en base a criterios morfológicos de las colonias. Además, se utilizaron 10 de los microorganismos para los ensayos de cinética de crecimiento y degradación. Para la cinética se utilizó medio de cultivo base diluido 1/10 con 5 mg L^{-1} del compuesto en estudio y se incubó a 30 ºC durante cinco días.

Tras el estudio de recuentos microbianos obtenidos a partir de las muestras de las parcelas tratadas y no tratadas con compost y el microcontaminante objeto de estudio, se procedió a realizar aislamientos con objeto de seleccionar aquellos microorganismos capaces de crecer y degradar los diferentes compuestos.

Los aislamientos se realizaron en placa con medio de cultivo TSA. La selección de microorganismos se realizó en base a criterios morfológicos de las colonias aisladas. De todos los microorganismos aislados finalmente se realizó una selección de 10 microorganismos para los ensayos de cinética crecimiento y degradación de cada analito.

Los ensayos se llevaron a cabo en frascos fondo cónico tubo de centrifuga estériles de acuerdo a la **Tabla 1.** El analito utilizado como fuente de C/E se realizaron 20 cultivos + 1 frasco sin microorganismo sometido al mismo proceso de incubación (control químico).

TABLA 1. Descripción de los ensayos (10 microorganismos por analito)

Ensayo	Muestras	Tipo de Análisis
Medio TSB1/10 + Microorganismo + analito	10	Microbiológico / Químico
Medio TSB1/10 + Microorganismo	10	Microbiológico (Controles)
Medio TSB1/10 + analito	1	Químico (Control)

Medio de cultivo e inoculo. 15 mL TSB diluido 1/10 suplementado con 50 mg L^{-1} del compuesto en estudio. Se utilizó TSB diluido de acuerdo con los ensayos realizados Valkova[24]. Los inóculos se prepararon en medio TSB diluido 1/10. Inoculo inicial/ensayo = 105 UFC mL^{-1}.

Incubación, toma de muestra y lectura de resultados. Todos los tubos se incubaron en un agitador orbital (New Brunswick E25R) a 100 r.p.m. a 30°C durante 5 días.

Análisis microbiológicos. Se realizó la medida de densidad óptica en un espectrofotómetro (UNICAM UV/VIS 5821) a 600 nm. Las lecturas se realizaron a las 0 h, 24 h, 48 h, 72 h y 96 h. Los resultados de UFC mL^{-1} se obtuvieron de acuerdo a las diferentes curvas de calibración (relación D.O./recuento UFC mL^{-1}).

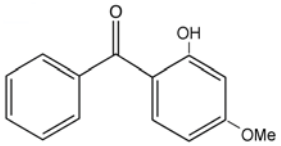


FIGURA 1. Estructura Química de la Benzofenona 3

Análisis químicos mediante UPLC-MS/MS. La determinación de la cantidad de compuesto degradado se realizó mediante la técnica de UPLC-MS/MS, empleando las condiciones descritas en la **Tabla 2**. Tras la toma de muestra se centrifugó a 13.000 r.p.m. para la retirada de células. Las medidas se realizaron a tiempo inicial y final de ensayo (0 horas y 96 horas).

La **tabla 3** muestran los parámetros optimizados para la separación cromatográfica y la detección mediante espectrometría de masas. Una vez optimizadas estas variables se seleccionaron las dos transiciones en el espectrómetro (cuantificación e identificación identificación) óptimas para la determinación inequívoca de la molécula.

TABLA 2. Valores óptimos de las condiciones cromatográficas

Fase estacionaria	ACQUITY UPLC® BEH C18 (2.1 x 100 mm) 1.7µm		
Fase móvil	A: Agua (0.025 % amoniaco) B: Metanol (0.025 % amoniaco)		
Modalidad: Gradiente	Tiempo (min)	A %	B %
	0.0	40	60
	6.0	0	100
	6.5	0	100
	6.6	40	60
	10.0	40	60
Flujo	0.3 mL min^{-1}		
Volumen de inyección	4 µL		
Temperatura del horno	40°C		
Detección	ESI-MS/MS		

TABLA 3. Parámetros del espectrómetro de masas para la BP-3

Analito	Transición	CV / CE	Transición	CV / CE	Modo
BP-3	229.0→ 150.8	4/20	229.0→ 104.9	4/18	ESI(+)
BP-d_{10}	193.1→ 109.8	18/16	193.1→ 81.8	18/30	ESI(+)

CV: Voltaje del cono; CE: Energía de colisión

Caracterización Bioquímica de los Microorganismos. Con objeto de determinar el comportamiento de los microorganismos en relación a su capacidad de usar diferentes sustratos como fuente de carbono y energía (C/E), así como a su capacidad enzimatica, se realizaron ensayos de API 50 CH (estudio del metabolismo de carbohidratos) y API ZYM (estudio de la actividad enzimática).

El sistema API 50 CH es un sistema estandarizado que está compuesto por 50 ensayos bioquímicos destinados al estudio del metabolismo de los carbohidratos (CH) en los microorganismos. El API 50 CH se utiliza en combinación con el API 50 CHB/E Medium para la identificación de: Lactobacillus y microorganismos proximos, de Bacillus y microorganismos próximos y de las Enterobacteriaceae y Vibronaceae.

La galería API 50 CH está compuesta por microtubos y permite el estudio de la utilización de sustratos perteneciente a la familia de los hidratos de carbono y derivados (heterosidos, polialcoholes, ácidos uronicos). Los ensayos de fermentación se inoculan en API 50 CHB/E Medium que rehidrata los sustratos. Durante el periodo de incubación, la utilización de HC se traduce en un cambio de color en el microtubo, debido a una producción de ácidos en anaerobiosis (fermentación) y en aerobiosis (oxidación) revelada por el indicador de pH del medio elegido. El primer microtubo, sin principio activo, sirve como testigo negativo.

De los microorganismos seleccionados se realizaron estudios tanto de oxidación como de fermentación ya que esta galería permite estudiar ambas vías. La oxidación se investigó en microtubos no sellados, y la fermentación en microtubos sellados con parafina liquida. El envase de los test consta de 10 galerías API 50 CH, 10 cámaras de inoculación, 10 hojas de resultados y una ficha técnica.

Para el ensayo se empleó medio de inoculación (API 50 CHL Medium), aceite de parafina, escala McFarland Standard y agua destilada. Las galerías se conservaron a 2-8°C hasta la fecha de su utilización.

El microorganismos para realizar el test de carbohidratos fue aquel capaz de degradar altos porcentajes del contaminante, concretamente el microorganismo codificado como BP3-5. De igual modo, se seleccionaron para el ensayo de las actividades enzimáticas los más representativos del grupo de muestras, es decir BP3-5, BP3-7, BP3-10, BP3-14, BP3-16.

RESULTADOS Y DISCUSIÓN

Estudio microbiológico

Influencia de la presencia del BP-3 y del compost en el recuento de la microbiota del suelo. Los resultados porcentuales de log UFC/g de suelo obtenidos en suelos sin

tratamiento con compost **(Figura 2a)** fueron diferentes a las muestras superficiales (100%), siendo el descenso de microorganismos observado de un 8,1 % y de un 21,8 % para las muestras recolectadas a 30 y 60 cm, respectivamente. En los suelos enmendados con compost y contaminados con BP-3 **(Figura 2)** fue decreciente, observándose una reducción de 0,5 log en el recuento de UFC suelo/g a lo largo del tiempo de ensayo. Si comparamos ambas figuras, se observa una tendencia descendente del recuento al aumentar la profundidad del suelo; este comportamiento se repite en todos los ensayos realizados a lo largo del tiempo (0, 15 y 30 días).

En los recuentos tanto de las muestras de la parcela control como de las tratadas con el BP-3 no se observaron variaciones significativas en el recuento en superficie (2 centímetros), lo cual indica que los niveles poblacionales se mantuvieron cuantitativamente constantes a lo largo del tiempo. De igual modo, tanto los recuentos realizados a 30 como a 60 centímetros de profundidad indicaron que no existían variaciones significativas en el tiempo en relación a la cantidad de bacterias presentes en las muestras de suelo control como en las tratadas, obteniéndose valores muy similares en el número de microorganismos en las muestras recogidas a 30 centímetros así como los de 60 centímetros de profundidad. De acuerdo a los resultados obtenidos se observó un aumento del número absoluto de microorganismos en presencia de compost respecto al suelo no enmendado, ya que el material compostado no sólo aporta nutrientes químicos, sino que también aumenta la riqueza microbiana. Por tanto, hay un mayor desarrollo microbiano en las parcelas enmendadas. Este hecho sería muy aprovechable a la hora de potenciar una mejora en las características del compost, aislando los microorganismos de mayor interés y suplementando el material con ellos.

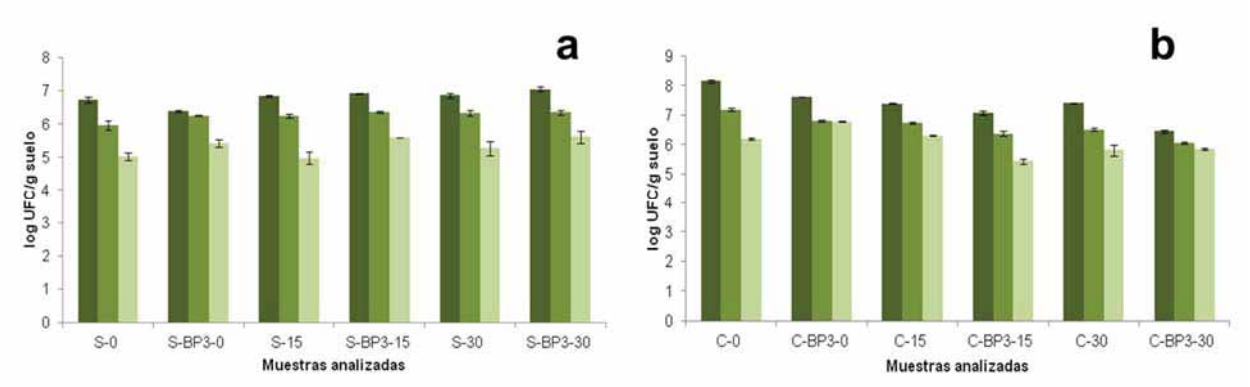


FIGURA 2. Ejemplo de recuento de microorganismos (Log UFC/g suelo) en muestras de suelo tratado y no tratado con BP-3 a diferentes profundidades, a tiempo inicial de ensayo (0 días), a 15 y 30 días. (a) Control de suelo sin compost (S) y contaminado con el compuesto (S-BP-3). (b) Control de suelo + compost (C) y suelo + compost contaminado (C-BP-3). Superficie (■); a 30 cm (■) ; a 60 cm (■).

Caracterización Morfológica de los Microorganismos Aislados de las parcelas estudiadas. De los 20 a 25 microorganismos aislados de la parcela tratada con BP-3 se seleccionaron 10 y se realizaron sus caracterizaciones morfológicas de las colonias y sus criterios morfológicos. Los microorganismos observados en los suelos tratados con

BP-3 se aislaron cinco bacilos Gram positivos, dos bacilos Gram negativos y tres cocos Gram positivos.

TABLA 4. Características morfológicas de los microorganismos aislados en los suelos tratados con los diferentes compuestos

BP-3			
Identificación	**Gram**	**Morfología**	**Agrupación**
BP-3-1	+	Bacilo	Aislado
BP-3-5	+	Bacilo	En cadena
BP-3-7	+	Coco	En cadena
BP-3-10	+	Coco	En cadena
BP-3-11	+	Bacilo	Aislado
BP-3-14	+	Bacilo	En cadena
BP-3-16	+	Coco	en cadena
BP-3-18	-	Bacilo	Aislado
BP-3-20	-	Bacilo	Aislado
BP-3-21	+	Bacilo	aislado

Caracterización bioquímica de los microorganismos seleccionados. El empleo de los kits API 50 CH para el metabolismo de carbohidratos y API ZYM para la actividad enzimática permitió caracterizar numerosos microorganismos.

A partir de los resultados obtenidos en los procesos de oxidación y fermentación de carbohidratos, se concluyó que cada microorganismo los metabolizaba de forma diferente. Este dato, sumado a los resultados de actividad enzimática, que informa sobre la presencia o ausencia de una determinada actividad de una enzima, grupo de ellas o de una determinada vía metabólica, nos permitió discriminar los microorganismos estudiados y seleccionar aquellos que eran diferentes desde el punto de vista metabólico.

Cinética de crecimiento en presencia de BP-3 como fuente de C/E. Degradación de los compuestos. La **Figuras 3 (a) y (b)** muestra un ejemplo de cinética de crecimiento de diferentes microorganismos en presencia del contaminante estudiado.

Los resultados mostraron que los microorganismos seleccionados fueron capaces de crecer en presencia del contaminante y que este crecimiento fue superior al obtenido en el medio base en ausencia del compuesto (control).

Como resultado de las cinéticas de crecimiento de los diferentes microorganismos seleccionados, en la **Tabla 4** se expone la diferencia de crecimiento (log UFC mL^{-1}) entre los cultivos en presencia de BP-3 y los cultivos control sin compuesto tras 48 h de ensayo. La mayor diferencia de crecimiento entre ambos cultivos se observó en el caso del ensayo con el microorganismo BP-3-7, siendo este de 10.0 %.

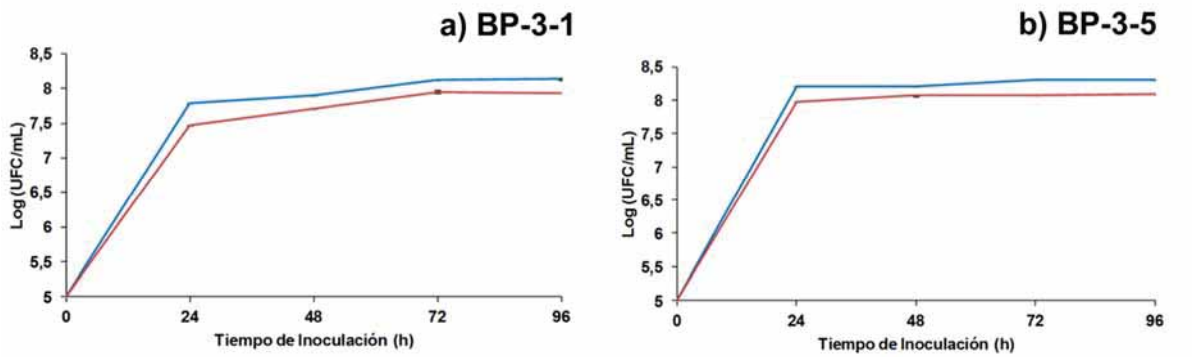


FIGURA 3. Ejemplos cinética de crecimiento del microorganismo codificados como BP-3-1, BP-3-5 en un medio de cultivo conteniendo 5 ppm de BP-3. Línea azul: crecimiento del microorganismo en medio TSB 1/10 suplementado con BP-3. Línea roja: control, crecimiento del microorganismo en medio TSB 1/10.

TABLA 4. Relación entre los cultivos de los diferentes microorganismos en presencia y ausencia de BP-3 a las 48 h de incubación

Microorganismo	A – B (log UFC mL^{-1})	Microorganismo	A – B (log UFC mL^{-1})
BP-3-1	0.19	BP-3-14	0.41
BP-3-5	0.14	BP-3-16	0.33
BP-3-7	**0.76**	BP-3-18	0.21
BP-3-10	0.26	BP-3-20	0.33
BP-3-11	0.31	BP-3-21	0.16

A: Cultivo en presencia de compuesto. B: Cultivo en ausencia de compuesto. Resultados expresados como log UFC mL^{-1}

Degradación de BP-3 en Presencia de Diferentes Microorganismos. La cantidad del compuesto degradada en presencia de los diferentes microorganismos fue similar en todos los ensayos realizados. En la **Tabla 5** se observa que, tras 96 h de cultivo, todos los microorganismos ensayados degradaron el compuesto en una concentración superior al 75 %, siendo casi total la degradación en el caso del microorganismo BP-3-1 (99.3 %) y BP-3-14 (99.9 %). Los microorganismos que degradaron el compuesto en menor porcentaje fueron BP-3-7 (78.0 %) y BP-3-11 (76.3%).

TABLA 5. Concentración final de BP-3 (ppm) determinada mediante LC-MS/MS

Microorganismo	A (ppm)	B (ppm)
BP-3-1	0.03	4.05
BP-3-5	0.43	3.65
BP-3-7	0.89	3.18
BP-3-10	0.36	3.72
BP-3-11	0.96	3.12
BP-3-14	$1.0 \cdot 10^{-3}$	4.08
BP-3-16	0.59	3.48
BP-3-18	0.53	3.55
BP-3-20	0.27	3.81
BP-3-21	0.68	3.39
CONTROL	**4.08**	

Concentración inicial 5 ppm. A: Concentración final (ppm) de BP-3 detectada tras 96 h de cultivo con diferentes microorganismos aislados de suelos tratados con MPB. B: Concentración de BP-3 degradada (ppm) tras finalizar el ensayo

CONCLUSIÓN

El recuento de la microbiota heterótrofa cultivable de los suelos tratados con la BP-3 y de los suelos enmendados con compost y tratados con este contaminante demostró que, al aumentar la profundidad en el suelo, se produce un descenso progresivo del número de microorganismos viables. Por otro lado, se pudo observar que el mayor desarrollo microbiano ocurría en las parcelas enmendadas con compost.

El estudio de las características morfológicas y tintoriales de los microorganismos aislados de los suelos tratados con la benzofenona 3 demostró una mayor proporción de bacilos Gram (+) y Gram (-).

El compuesto aislado fue degradado en mayor o menor proporción por los microorganismops seleccionados, siendo los porcentajes de degradación superiores a 70% en todos los casos.

Los compuestos estudiados fueron degradados en mayor o menor medida por los microorganismos seleccionados, siendo los porcentajes de degradación superiores al 70 por ciento en todos los casos. Los resultados obtenidos demuestran la habilidad de crecimiento de los microorganismos seleccionados en presencia de este compuesto como fuente de C/E. Por tanto, estos microorganismos podrían ser utilizados en procesos de biorremediación de ambientes contaminados con benzofenona 3.

REFERENCIAS

1. Cunningham, V.L., Buzby, M., Hutchinson T., Mastrocco F., Parke N., Roden, N. Effects of human pharmaceuticals on aquatic life: next steps. *Environmental Science and Tecnology* 40 (2006) 3456-3465.
2. Calamari, D. Assessment of persistence and bioaccumulating chemicals in the aquatic Environment. *Journal of Pharmacy and Pharmacology* 37 (1995) 1-12.
3. Richardson, M.L., Bowron, J.M. The fate of pharmaceutical chemical in the aquatic *environment. Journal of Pharmacy and Pharmacology* 37 (1985) 1-12.
4. Doughton, C.G., Ternes, T.A. Pharmaceuticals and personal care products in the Environment: Agents of subtle change. *Environmental Health Perspectives* 107 (1999) 907-938.
5. Cunningham, V.L., Buzby, M., Hutchinson T., Mastrocco F., Parke N., Roden, N. Effects of human pharmaceuticals on aquatic life: next steps. *Environmental Science and Tecnology* 40 (2006) 3456-3465.
6. Calamari, D. Assessment of persistence and bioaccumulating chemicals in the aquatic Environment. *Journal of Pharmacy and Pharmacology* 37 (1995) 1-12.
7. Richardson, M.L., Bowron, J.M. The fate of pharmaceutical chemical in the aquatic *environment. Journal of Pharmacy and Pharmacology* 37 (1985) 1-12.
8. Doughton, C.G., Ternes, T.A. Pharmaceuticals and personal care products in the Environment: Agents of subtle change. *Environmental Health Perspectives* 107 (1999) 907-938.
9. Frang, H., Tong, W.D., Shi, L.M., Blair, R., Perkins, R., Branham, W., Hass, B.S, Xie, Q., Dial, S.L., Moland, C.L., Sheehan, D.M. Structure-activity relationships for a large diverse set of natural, synthetic, and environmental estrogens. *Chemical Research in Toxicology* 14 (2001) 280-294.
10. King, K.A., Zaun, B.J., Schotborgh, H.M., Hurt, C. DDE-induced eggshell thinning in white-faced ibis: A continuing problem in the western United States. *Southwestern Naturalist* 48 (2003) 356-364.
11. Petrovic, M., Hernando, M.D., Díaz-Cruz, M.S., Barceló, D. Liquid chromatography-tandem mass spectrometry for the analysis of pharmaceutical residues in environmental samples: A Review. *Journal of Chromatography A* 1067 (2005) 1-14.
12. Díaz-Cruz, M.S., Barceló, D. Determination of antimicrobial residues and metabolites in the aquatic environment by liquid chromatography tandem mass spectrometry. *Analytical and Bioanalytical Chemistry* 386 (2006) 973-985.
13. Temes, T., Joss, A. Human pharmaceuticals, hormones and fragrances: the micropollutant challenge for urban water management. *Water* 21 (2006) 121-148.
14. Drewes, J.L., Heberer, T., Rauch, T., Reddersen, K. Fate of pharmaceuticals during ground water recharge. *Ground Water Monitoring and Remediation* 23 (2003) 64-72.
15. Kummerer, K. Significance of antibiotics in the environment. *Journal of Antimicrobial Chemotherapy* 52 (2003) 5-7.
16. Khetan, S.K., Collins, T.J. Human pharmaceuticals in the aquatic environment: A challenge to green chemistry. *Chemical Reviews* 107 (2007) 2319-2364.
17. Spellman, F.R. Handbook of water and wastewater plant operations. *CRC Press, 2nd Ed., Boca Raton* (2009) 825-826.
18. Cheremisinoff, N.P. Handbook of water and wastewater technologies. *Butterworth-Heinemann, Boston* (2002) 645-654.
19. Jeon, H.K., Chung, Y., Ryu, J.C, Simultaneous determination of benzophenone – type UV filters in water and soil by gas chromatograohy-mass spectrometry. *J Chromatogr A* (2006) 192-202.
20. Sánchez-Brunete C., Miguel, E., Alberto, B., Tadeo, J.L. Analysis of salicylate and benzophenone-type UV filters en soil and sediments by simultaneous extraction cleanuo and chromatography-mass spectrometry. *J Chromatogr A* (2011) 4291-4298

21. Zhang, Z., Ren, N., Li, Y., Kunisue, T., Gao, D., Kannan, K. Determination of benzotriazole and benzophenone UV Filters in sediment and sewage sludge. *Environ Sci Technol* (2011) 3909-3916.
22. Araujo, A., Monteiro, R., Abarkeli, R. Effect of glyphosate on microbial activity of two Brazilian soils. *Chemosphere, Oxford* 52 (2003) 799-804.
23. Haney, R., Senseman, S., Hons, F., Zuberer, D. Effect of glyphosate on soil microbial activity and biomass. *Weed Science* 48 (2000) 89-93.
24. Valkova, N., Lépine, F., Valeanu, L., Dupont, M., Labrie, L., Labrie, L., Bisaillon, J.G., Beaudet, R., Shareck, F., Villemur, R. Hydrolysis of 4-hydroxybenzoic acid esters (Parabens) and their aerobic transformation into phenol by the resistant enterobacter cloacae strain EM. *Applied and Environmental Microbiology* (2001) 2404-2409.

CHAPTER 3.2 RESIDUOS DE PALMA AFRICANA PARA EL TRATAMIENTO DE SUELO CONTAMINADO CON HIDROCARBUROS

M. C. Cuevas-Díaz *(1); O. Guzmán-López (1); P. Pavón-Orozco (1); A. Ortega-Martínez (1); M. Ríos Enríquez (1) and G. Fuentes-Algarín (1)

(1) Universidad Veracruzana, Facultad de Ciencias Químicas, Av Universidad Km 7.5 Col Santa Isabel, Coatzacoalcos, Veracruz, México.

RESUMEN

Existen varios tipos de tratamientos de suelos contaminados con hidrocarburos pero se siguen buscando nuevas alternativas, en este trabajo se propone un tratamiento de remoción secuencial utilizando primero un proceso de oxidación avanzada como es el Fenton y posteriormente uno biológico, para el cual se utiliza el composteo adicionando los residuos que se generan del proceso de obtención de aceite de palma africana (*Eleais guineensis*) en proporción 98:2, con la finalidad de servir de acondicionador del suelo aportando nutrientes así como una mayor densidad del suelo, se incrementa también la porosidad y la difusión de oxígeno; se ajustó previamente la relación C:N:P a 100:10:1. El suelo contaminado tuvo textura arenosa con una concentración inicial de HTP fracción pesada de 95 368 mg Kg^{-1}. El tratamiento Fenton fue de 72 h y se pudo remover el 22.9 % mientras que en el biológico se removió el 24.7% a los 30 días. Con este estudio se plantea una aplicación más para los residuos de palma africana lo que puede reducir el impacto ambiental al ser desechado usualmente a suelo abierto.

Keywords: Biorremediación, fenton, hidrocarburos, palma africana

INTRODUCCIÓN

La contaminación por hidrocarburos de suelo y agua proviene de fuentes diversas, ya sea accidentales o intencionales, siendo producto de las actividades industriales del hombre. En particular, el suelo contaminado representa un riesgo al ambiente, que debe ser minimizado. La biorremediación es un proceso que utiliza a los microorganismos para metabolizar sustancias orgánicas como los hidrocarburos del petróleo. La biorremediación se puede realizar entre otras tecnologías, mediante la adición de nutrientes (bioestimulación) y la adición de residuos agroindustriales como bagazo y cachaza de caña de azúcar, mazorca de maíz, entre otros los que sirven como soporte, mejoran la aireación y aportan de microorganismos en el sistema [1,2]. El procesamiento para la obtención del aceite de palma africana (*Eleais guineensis*) genera varias toneladas de residuos (bagazo y raquis) por hora, los cuales no son aprovechados originando problemas ambientales, por lo que resulta una alternativa para su uso en biorremediación.

---

*Author for correspondence: ccuevas@uv.mx

Generalmente, las concentraciones por arriba de 50 000 ppm de hidrocarburos del petróleo en suelo contaminado, hacen ineficiente los tratamientos biológicos, siendo recomendable un tratamiento previo como el tratamiento químico. Dentro de los tratamientos químicos el de Fenton tiene como ventaja su capacidad una mejor disolución por la oxidación de los productos de escasa solubilidad [3]. El tratamiento mediante el reactivo de Fenton consiste en la dosificación de H_2O_2 y Fe^{+3} o Fe^{+2}, generando radicales OH^- que oxidan a los compuestos químicos complejos en menor tiempo que la biorremediación [3,4].

Se han realizado tratamientos con oxidación química con reactivo de Fenton, seguido de nutrientes o de inóculos microbianos, sin embargo, la adición de residuos y nutrientes son escasos, pero se puede mencionar el uso de cáscara de cacahuate en el tratamiento de suelos contaminados con hidrocarburos [5]. La necesidad de encontrar alternativas para la remediación de suelos contaminados con hidrocarburos pueden ser más eficientes al realizar tratamiento secuencial mediante el reactivo de Fenton con el que se pueden degradar compuestos más complejos que en la biorremediación [6], seguido de la adición de los residuos como el bagazo de palma africana y nutrientes.

Por lo anterior, en este trabajo se tuvo como objetivo evaluar el efecto de dos tratamientos secuenciales de suelo contaminado con hidrocarburos utilizando el reactivo de Fenton seguido del tratamiento biológico adicionando bagazo de palma africana.

MATERIALES Y MÉTODOS

El suelo contaminado con hidrocarburos fue tomado de un sitio a donde se llevó para su tratamiento, ubicado en el Municipio de Cosoleacaque, Veracruz. Para caracterizar el suelo se trituró, homogeneizó y tamizó (malla #10, diámetro de poro de 2 mm). Se realizó la determinación de parámetros: pH, la humedad, la textura, la materia orgánica, el nitrógeno total, el fósforo total según la NOM-021-SEMARNAT-2000 y los hidrocarburos fracción pesada con la NMX-AA-134-SCFI-2006, utilizándose para su extracción la técnica de microsoxhlet con una mezcla de diclorometano y hexano 1:1 [2,7].

Tratamiento con reactivo de Fenton. En la primera etapa del tratamiento se utilizó un método químico con la finalidad de disminuir la concentración de los hidrocarburos. Para ello se emplearon 100 g de suelo contaminado con hidrocarburos para el tratamiento con reactivo de Fenton, en las condiciones: 0.0456 M y 1 M para el $FeSO_4 \cdot 7H_2O$ y H_2O_2 respectivamente [8], con tres réplicas, con duración de 72 h. Como suelo control se utilizó suelo contaminado sin tratamiento. Al término del tratamiento se determinaron los hidrocarburos totales de petróleo fracción pesada (HTPp), materia orgánica, pH y cuenta heterorófica de bacterias con agar nutritivo y cuenta total de hongos con agar dextrosa papa [9].

Tratamiento biológico. En la segunda etapa correspondiente al tratamiento biológico, se procedió al ajuste de nutrimentos a una relación de C:N:P de 100:10:1 usando como fuente de nitrógeno al NH_4NO_3 y de fósforo KH_2PO_4, dejando en reposo durante siete días con la finalidad de regenerar en tiempo mínimo la flora microbiana [5, 10], seguido de la adición de bagazo de palma de aceite en una relación 98:2 en peso, ajustándose la

humedad a capacidad de campo e incubándose a 28 °C; como control se utilizó el suelo contaminado esterilizado en auto-clave [11]. Las variables de respuesta fueron los HTPp, pH, materia orgánica, así como cuenta total bacteriana y cuenta total de hongos

La media y la desviación estándar de los parámetros químicos se calcularon para las tres réplicas de los tratamientos. Después de comprobar la homogeneidad de varianza y la normalidad de los datos se realizó el análisis de una vía de ANDEVA, los límites significativos considerados como $p < 0.05$ para la diferencia entre los tratamientos. Se utilizó el software de prueba Minitab 15.

RESULTADOS Y DISCUSIÓN

El suelo inicial de textura arenosa, se caracterizó (**Tabla 1**) antes de iniciar el tratamiento secuencial.

TABLA 1. Caracterización del suelo

Parámetro	Valor
pH	5.66
Capacidad de campo (%)	28.78
Materia orgánica (%)	21.65
Carbono orgánico (%)	12.56
Nitrógeno total (%)	0.028
Fósforo soluble (mg kg^{-1})	1.0331
HTP fracción pesada (mg kg^{-1})	95 368.4

La cantidad elevada de material orgánica en suelo tipo arenoso se debe a la alta concentración del hidrocarburo de petróleo, asimismo el suelo se encontró deficiente de fósforo y nitrógeno.

Tratamiento con reactivo de Fenton. En la primera etapa correspondiente al tratamiento con el reactivo de Fenton, el pH de 5.7 después de 72 h, no sufrió variación, este efecto puede deberse a la generación de OH^- y a la producción de CO_2, debido a la mineralización de compuestos orgánicos [12,13]. La materia orgánica total disminuyó 13.85% y el nitrógeno disminuyó 8.1 % después de haber sido sometido al tratamiento con reactivo de Fenton, al igual que en estudios previos en que se reportan disminución en los nutrientes del sistema y puede deberse a reacciones de óxido-reducción; en el caso del nitrógeno pudo haber sufrido volatilización por transformación en amoniaco [8]. Los resultados de HTP se presentan en la **Figura 1**.

La remoción de hidrocarburos del petróleo en este trabajo con el reactivo de Fenton fué significativa ($p = 0.007$) y 22.9 % mayor al presentado en otros trabajos en los que para una sola dosis en 72 h la remoción por Fenton corresponden a 8 % [11].

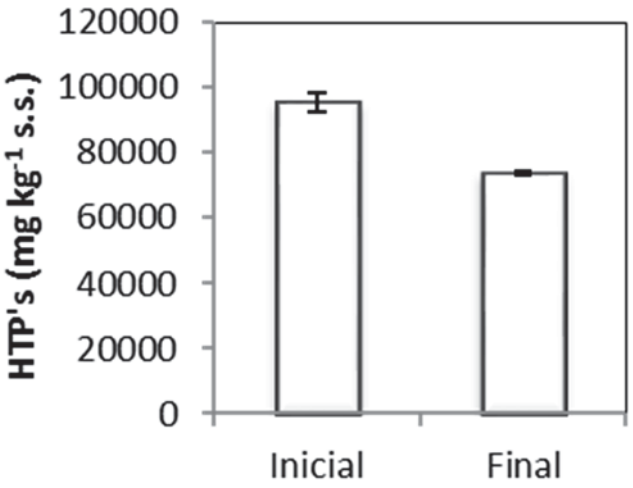


FIGURA 1. HTP fracción pesada en el tratamiento con reactivo de Fenton (n=3)

Tratamiento biológico con bagazo de palma africana. La aplicación del reactivo de Fenton seguida de la adición de NH_4NO_3 y KH_2PO_4 y el bagazo de palma africana permitió que la actividad generada por los microorganismos disminuyera la materia orgánica en relación a su contenido inicial (**Figura 2**).

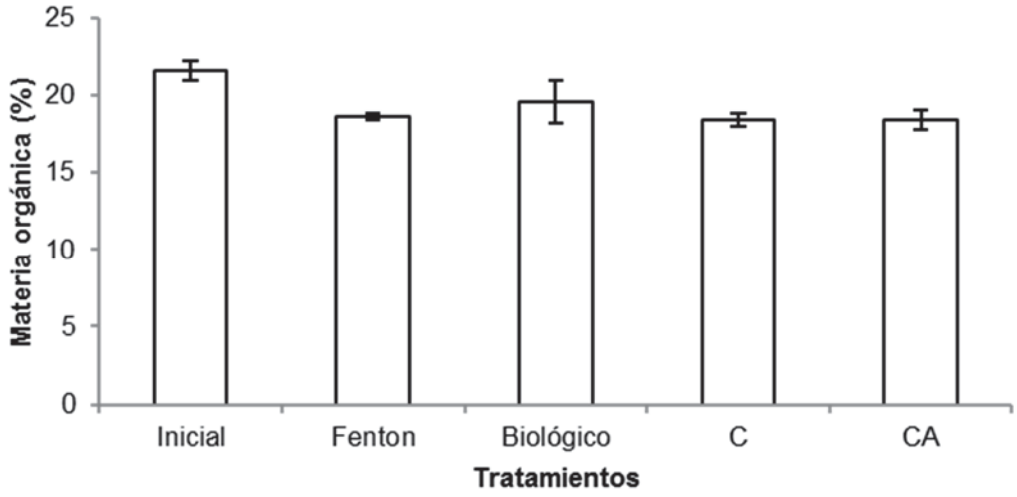


FIGURA 2. Comportamiento de la materia orgánica en los tratamientos (n = 3)
C = control sin tratamiento CA = control abiótico

La cuenta para los microorganismos demuestra cierta actividad después del día 7, pero casi no hay actividad microbiana al inicio del experimento (**Tabla 2**), disminuyendo al finalizar el tratamiento Fenton, debido a que el peróxido de hidrógeno y los radicales libres pueden causar lisis de la pared celular.

TABLA 2. Cuenta microbiana en los tratamientos

Tipo	Suelo inicial	Fenton	Bagazo de palma africana + nutrimentos (7 d)
Bacterias heterotróficas (UFC g^{-1} suelo seco)	2.3 E+04	1.2 E+03	6.1 E+07
Hongos (UFC g^{-1} suelo seco)	S/D	2.3 E+03	2.2 E+06

S/D = sin determinar

Los resultados para los HTP (**Figura 3**) fueron significativos para los tratamientos p = 0.00 y la diferencia de medias por Tukey indicó que ambos tratamientos son diferentes y a su vez difieren del control de suelo sin tratamiento. La remoción de HTPp por adición de bagazo de palma y nutrientes a los siete días fue de 19.7% y a los 30 días 24.7%, esto indica que la actividad de los microorganismos disminuyó después de siete días, debido probablemente a la formación de algún metabolito tóxico o a la disminución de los nutrimentos necesarios para su desarrollo [14]. A menudo un aumento de la degradación biológica se ha atribuido a las condiciones aerobias creadas por oxidación química y a la adición temprana de nutrimentos [15,16]. Para el tratamiento secuencial la remoción final de HTP fue de 41.9 %.

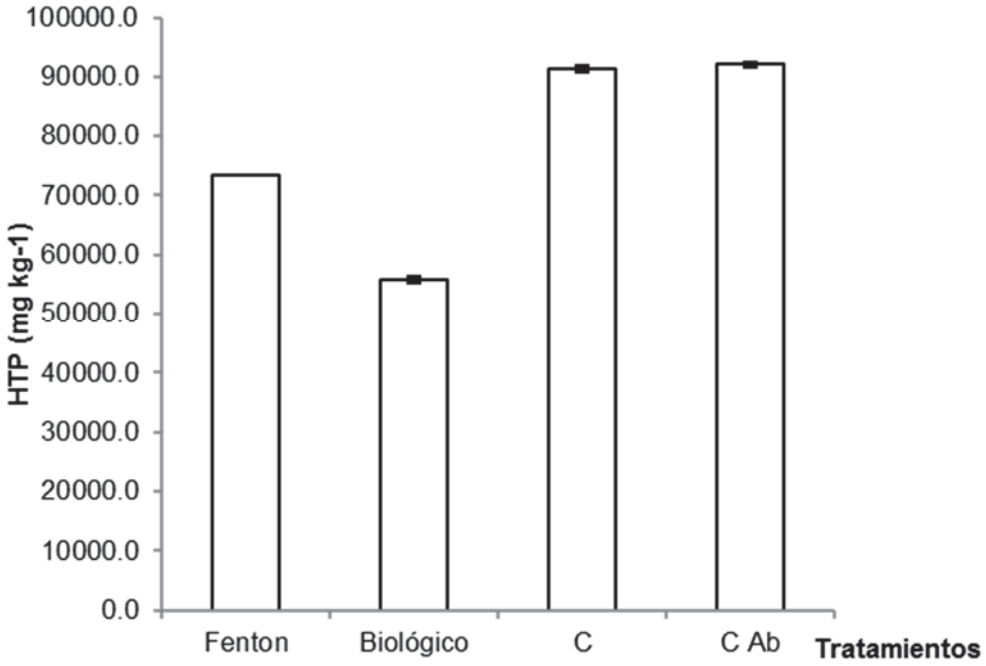


FIGURA 3. Hidrocarburos totales del petróleo en tratamientos y control (n=3). F = Tratamiento con Fenton B = Tratamiento biológico C = Control suelo sin tratamiento Cab = Control Abiótico

CONCLUSIÓN

Los residuos de bagazo de palma africana utilizados en el tratamiento biológico resultan una alternativa para su aprovechamiento, esto puede disminuir el impacto ambiental generado cuando se desecha en grandes cantidades. Por otra parte, los tratamientos secuenciales con Fenton y el biológico permitieron remover los HTP de la fracción pesada hasta en un 41.9 % en suelos altamente contaminados, se puede profundizar más adelante en el estudio de la fisiología, adición de nutrientes, bioaumentación, remoción a mayor escala, así como en los parámetros cinéticos. Finalmente, el tipo de tratamientos utilizado ayudaría a resolver la problemática causada por la contaminación de los suelos con hidrocarburos la cual es usual en lugares donde es almacenado o transportado

AGRADECIMIENTOS

CEISA S.A. de C.V., Recursos PIFI y PRODEP

REFERENCIAS

1. Molina-Barahona L., Rodríguez-Vázquez R., Hernández-Velazco M., Vega-Jarquín C., Zapata - Pérez O., Mendoza-Cantú A. y Albores A. (2004). Diesel removal from contaminated soils by bioestimulation and supplementation with crop residues. Appl Soil Ecol. 27 (2004) 165-175.
2. García-Torres R., Ríos-Leal E., Martínez-Toledo Á., Ramos-Morales F. R., Cruz-Sánchez J. S. y Cuevas-Díaz M. C. 2011. Uso de cachaza y bagazo de caña de azúcar en la remoción de hidrocarburos en suelo contaminado. Rev. Int. Contam. Ambient. 27 (2011) 31-39.
3. Sirguey C., Silva P., Schwartz C. y Simonnot M. O. Impact of chemical oxidation on soil quality. Chemosphere 72 (2008) 282–289.
4. Yap C.L., Gan S., Ng H.K. Fenton based remediation of polycyclic aromatic hydrocarbons-contaminated soils. Chemosphere. 83 (2011) 1414-1430.
5. Cheng M., Zeng G., Huang D. Lai C., Xu P., Zhang C., Liu Y. Hydroxyl radicals based advanced oxidation processes (AOPs) for remediation of soils contaminated with organic compounds: A review. Chem. Eng J. 284 (2016) 582-598.
6. Lee B. D. y Hosomi M. Ethanol washing of PAH-contaminated soil and fenton oxidation of washing solution. J. Mater. Cycles Waste Manag. 2 (2000) 24–30.
7. Arce O. J.M., Rodríguez V. R., Rojas A. N.G. Identification of recalcitrant hydrocarbons present in a drilling waste-polluted soil. J. Environ. Sci. & Health Part A, 39 (2004) 1535-1545.
8. Reyes-Bonifant J.A. Degradación de hidrocarburos aromáticos policíclicos en suelo contaminado mediante oxidación avanzada (reactivo de fenton). Universidad Veracruzana, Facultad de Ciencias Químicas campus Coatzacoalcos. *Tesis de Licenciatura*. 2013.
9. Clark, E. Agar plate method for total microbial count. In page: A.L. Miller, R.H. Keeney, D.R. (Eds). *Methods of Soil Analysis*, Part 2. American Society of Agronomy. Madison, WI. Pp 1460-1466. (1982).
10. US EPA. Field applications of in situ remediation technologies: chemical oxidation. In: *Solid waste and emergency responses*. EPA, Washington, DC, 37. (1998).
11. Sutton N. B., Grotenhuis J., Tim C., Langenhoff-Alette A. M. y Rijnaarts-Huub H. M. (2011). Efforts to improve coupled in situ chemical oxidation with bioremediation: A review of optimization strategies. J. Soils Sediments. 11 (2011) 129–140.

12. Pignatello J. J., Oliveros E. and MacKay A. Advanced Oxidation Processes for Organic Contaminant Destruction Based on the Fenton Reaction and Related Chemistry. Critical Reviews in Environ. Sci. Technol. 36 (2006) 1-84.
13. Pardo F., Rosas J.M., Santos A., Romero A. Remediation of a biodiesel blend- contaminated soil by using a modified Fenton process, Environ. Sci. Pollut.Res. 21 (2014) 12198–12207
14. Gong X.B. Remediation of weathered petroleum oil-contaminated soil using a combination of biostimulation and modified Fenton oxidation. Inter. Biodeter. Biodegr. 70 (2012) 89-95.
15. Kulik N., Goi A., Trapido M. y Tuhkanen T. Degradation of polycyclic aromatic hydrocarbons by combined chemical pre-oxidation and bioremediation in creosote contaminated soil. J. Environ. Manage. 78 (2006) 382–391.
16. Palmroth M. R. T., Langwaldt J. H., Aunola T. A., Goi A., Puhakka J. A. y Tuhkanen T. A. Treatment of PAH-contaminated soil by combination of Fenton's reaction and biodegradation. J. Chem. Technol. Biotechnol. 81 (2006) 598–607.

CHAPTER 3.3 ANALYSIS AND EVALUATION OF HEAVY METALS POLLUTION IN SEDIMENTS FROM COATZACOALCOS RIVER IN VERACRUZ, MEXICO

L. J. Mota Vázquez (1); M. R. Gutiérrez Lara (2); **M. C. Cuevas Díaz** *(3); O. Guzmán-López (3); A. C. Ortega-Martínez (3) and G. de Jesús-Antonio (3)

(1) LIPATA, Instituto de Ingeniería, Universidad Nacional Autónoma de México, Blvd. Juriquilla 3001, 76230 Qro., Mexico.
(2) Facultad de Química, Universidad Nacional Autónoma de México, México.
(3) Facultad de Ciencias Químicas, Universidad Veracruzana campus Coatzacoalcos, Av. Universidad Km 7.5, Col Santa Isabel, 96538, Veracruz, México.

ABSTRACT

Sediments provide a useful guide to solve problems in comprehensive environmental reviews, studying sediments from the point of geological, chemical or environmental perspective. It allows the processes understanding of contaminants in the environment. It is appropriate to use this complex matrix as environmental control parameter in the analysis of heavy metals in the study area, considering the high density of oil facilities housing; the diversity of ecosystems that presents including wetlands and mangroves, economic activities that take place in it and their complex socioeconomic dynamics, derived from petrochemical development.
Samples from 14 sampling stations along the Coatzacoalcos River were assessed by atomic absorption spectrometry for two times in a year, having solid and wet samples of the same sites. The results expressed in intervals of low to high concentration in mg/kg of sediment: chromium 0.6 - 6.8, copper 0.1 - 8.1, manganese 0.08 - 8.81, mercury 0.12 - 0.80, nickel 0.8 - 3.5, lead 0.3 to 8, vanadium 0.12 - 0.44. The predominant soil type in the river was the sands, and to a lesser extent clay and silt, which indicates a dynamic medium and influenced by the lithology of the region. Different methods and tools to analyze the results obtained were used, the most demonstrative; the correlation coefficient Pearson and Registry of Emissions and Pollutant Transfer (RETC) which allowed us to relate the data of industrial emissions of heavy metals (government data) with the experimental values, determining the influence of various pollution sources on the Coatzacoalcos river. This environmental scientific research with social commitment; it represents a contribution to the analysis of the impact on the environment and ecological problems of industrialization in the study area; the total concentration of Cr, Cu, Hg, Mn, Ni, Pb and V is satisfactorily determined; with which it is intended to contribute to the development of social, environmental and scientific knowledge in the Coatzacoalcos river; although it is wise that contaminants in sediments depend on many parameters but not evaluated (the geology of the area, erosion, diagenesis, metamorphism, etc.).

Keywords: Atomic absorption spectrometry (AAS), heavy metals, sediments.

---

*Author for correspondence: marycarm81@hotmail.com

INTRODUCTION

Mexico is one of the largest producers and exporters of oil. The average oil production is 2.576 million barrels per day[1]; this activity is a significant source of pollution that can cause significant damage to the environment. This industry, including its vast infrastructure, has an extensive network of pipelines (4,767 km) and pipelines (7,526 km) to the distribution and transmission of oil products distributed throughout the country and through major urban, industrial areas, agricultural and natural[1]. As a result of the activities resulting from the exploitation, refining, transportation and storage of oil and its derivatives, as well as failures in the maintenance, operation of pipelines and illegal connections; there are reports of 203 accidents between spills and leaks[2], especially in southeastern of Mexico where most oil production is concentrated. In 2010, Petroleos Mexicanos spilled 27,971 tons of oil[1]. The state of Veracruz was the most affected[3], with 117 incidents, followed by the states of Tamaulipas (75), Oaxaca (69), Hidalgo (54) and Puebla (50). These five states accounted for almost 50% of emergencies that occurred between 2003 and 2006.

The Coatzacoalcos River in Veracruz State is the most important tributary of the entity, and one of the most polluted in the world due to discharges it receives from the industries in the region[4].

By the territorial extension that forms the basin; productive activities that develop around them generate a high content of hazardous waste, whose final destination is the river which in 2009 was downloaded 86,876 million m^3 of wastewater, with a total load of 3540 ton of pollutants[2]. It has been considered that the activities have impacted in the area with a high degree of pollution are the constant traffic of oil tankers and their loading and unloading, petrochemical complexes, dredging continuous, local agriculture and wastewater from human activities[5]. These activities are causing changes on aquatic fauna and physicochemical characteristics of the area (water, vegetation and sediment), plus high emissions of inorganic and organic products that go into the atmosphere are generated, producing acid rain and high rates of erosion[6].

Elemental analysis of solid samples (soils, sediments and sludge digestion from plants water treatment) is of great importance, since they are involved in adsorption, transportation and disposal of contaminants in the environment as a result of the action biological, physical and / or chemical soil [Rodríguez, 2001] agents. Thus the nutritional chain is affected because the plants accumulate trace metals via the root or by direct deposit on the leaves of airborne particles. Therefore, the living organism that consumes this plant reflects the damage caused by trace metal bioaccumulation if concentration levels exceeding normal. For the above stated, and in order to protect public health, it is necessary to have highly selective and sensitive analytical methodologies for the determination of metals accurately, quickly and economically, at the level of 10% of the maximum permissible limit (as official rules of each country)[7]. Based on the characterization of metals such as chromium (Cr), copper (Cu), nickel (Ni), lead (Pb) and vanadium (V) in sediment samples from the basin of the Coatzacoalcos River. This paper aims to expose the physical, socio-economic risks, but especially chemicals; defining the vulnerability of this region to past and future environmental emergencies.

Studies at the international level of heavy metals from the start of industrial development have always been of environmental concern, however, documented studies and published studies[8-12] starting from that was discovered disaster generated in Japan during 1956, which was documented human poisoning with methylmercury due to intake of fish and shellfish contaminated by waste dumped into Minamata bay[13]. In the case of Mexico, the main studies on the behavior of heavy metals in river sediments were as follows: [14-18].

Based on the above information internationally and in Mexico, it is suitable to use river sediments as environmental control parameters in the analysis of heavy metals, so this complex matrix was used in the characterization of the study area. Concern about the risk caused by pollution in this region has its earliest antecedents in the sixties, with the development of the petrochemical industry in Mexico, also the first investigations in the basin of the Coatzacoalcos River to assess the ecological effects of industrial development date from that time, but until 1989 coordinated by the Center for Ecological Development, CECODES project[19] where key issues such as the characterization, levels of the major toxic substances, and the effect is addressed by pollution heavy metals and hydrocarbons in the local population. In later work[6] is analyzed and the presence of certain metals (Pb, Cr, Cu, Ni, Zn) is shown in sediments and organisms of the Coatzacoalcos River, as revealed concentrations exceeding by far the natural levels affecting the geochemical balance of these elements in unpolluted coastal areas, according to the authors. The same region was selected in this study, considering the high density of oil installations housing, diversity of ecosystems presents, including wetlands and mangroves, recognized as conservation priority in the policies of the federal government[20] the variety of economic activities taking place in it and their complex socioeconomic dynamics, derived from petrochemical development and other specific characteristics of that region.

MATERIALS AND METHODS

The use of wet samples was obtained to preserve the redox conditions of the medium and reducing potential physical interactions as is recommend[21]

Fourteen sampling stations along the Coatzacoalcos River (**Figure 1**) were selected in November 2010 between 10:00 and 14:00 h. Having solid and wet samples of the same sites; also liquid samples of the Coatzacoalcos River. The points sampling were the same of the National Program for Monitoring and Evaluation of Toxic Persistent (PRONAME). An Auger equipment was used, taking the sediment up 15 cm (EPA-823, 2001). Sediment samples collected (1 kg per sample) were stored in polyethylene bottles wide mouth and conditioned in plastic bags, following recommendations; samples were preserved at 4°C once came to the laboratory.

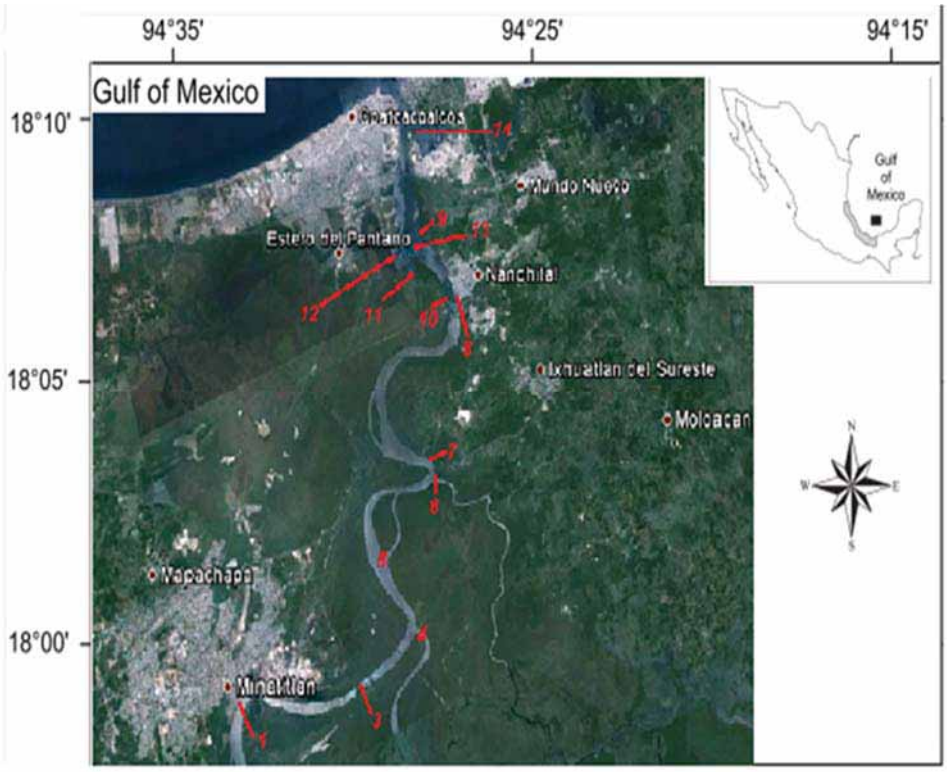


FIGURE 1. Sampling sites in the study area. [Google Earth. 2013 DigitalGlobe-Google-INEGI-GeoEye-Cnes/SpotImage]

Sediment samples from Coatzacoalcos River, were identified for work in the laboratory, from the sample, Cz1 to Cz14, in the case of dry samples; in agreement to the number of the sampling station (**Table 1**).

TABLE 1. Identification of samples tested

#	ID	Latitudes	Longitudes
1	Cz1	17°58'36"N	94°32'45"O
3	Cz3	17°57'49"N	94°30'4"O
4	Cz4	17°58'4"N	94°28'22"O
5	Cz5	17°59'41"N	94°28'42"O
6	Cz6	18°00'38"N	94°26'51"O
7	Cz7	18°00'51"N	94°26'50"O
8	Cz8	18°03'55"N	94°24'48"O
9	Cz9	18°05'52"N	94°25'14"O
10	Cz10	18°04'1"N	94°25'5"O
11	Cz11	18°08'56"N	94°23'43"O
12	Cz12	18°05'44"N	94°25'11"O
13	Cz13	18°05'30"N	94°25'44"O
14	Cz14	18°08'16"N	94°24'22"O

Excess water from the polyethylene bottles are physically and directly decanted and the samples (Cz1 to Cz14) were dried at room temperature up to 36 h using glass material to constant weight previously washed and rinsed in HNO_3 3%.

The first process before the digestion of the sample is the homogenization, which is unavoidable to volatilize organic components of the matrix, leaving the analyte in a less complex matrix evaluate; during this step, the Cz1 to Cz14 dehydrated samples were mixed with a plastic spatula equipped for this experimentation; they thereby controlling the probable physical interactions, dried to constant weight in a drying oven Felisa®, with a gradual increase in temperature every 4 hours to 105°C, below the temperature at which could result in decreased analyte.

TABLE 2. Features in the quantification of metals analyzed

Analyte	Method	λ (nm)	Reference	AAS equipment
Cr	FAAS C_2H_2-air	357.9	NMX-AA-044-SCFI-2001	PerkinElmer AAnalyst™ 700
Cu	FAAS C_2H_2-air	324.8	NMX-AA-051-SCFI-2001	PerkinElmer AAnalyst™ 700
Ni	GFAAS	232		GBC AAvanta Σ932/933
Pb	GFAAS	217		GBC AAvanta Σ932/933
V	GFAAS	318.5		GBC AAvanta Σ932/933

Generally sediments of environmental interest are those that remain in the surface layers and are finely divided (<200μm); therefore after drying of the samples they were removed undesirable materials such as rocks, branches, leaves, etc. And larger particles were discarded, (using a 2mm sieve opening) because they are unreactive, and tend to avoid the homogeneity of the sediment. This procedure is applicable both in soils and sediments.

For measurement of the total concentration of metals in sediment; it requires a mineralization of the sample to remove the organic matter in sediments. The most frequently used method is digestion with oxidizing agents. It was performed to the samples under study, a total acid digestion, using the EPA-3050B method (Acid digestion of sediments, sludges, and soils) and ASTM_D-4698 (Standard Practice for Total Digestion of Sediment Samples for Chemical Analysis) method. Three replicates were performed for each sample, having a reagent blank each time it is digested.

Quantification of the metals analyzed in sediment was conducted, considering the regulations applicable in the country; by atomic absorption spectrophotometry, atomic absorption spectrophotometer PerkinElmer brand, model 700 with software AAnalystTM WinLab32 and atomic absorption spectrophotometer GBC Avanta brand, Σ932 / 933 model version 1.33, as summarized in **Table 2** was used.

RESULTS AND DISCUSSION

The predominant soil type in the river, based on the literature and information analysis[22]; it was the sands, and to a lesser extent clay and silt, which indicates a dynamic medium and influenced by the lithology of the region.

The total content of the metals analyzed (Cr, Cu, Ni, Pb, and V) from the sediments, are summarized in **Table 3**.

The % recovery was calculated to verify the accuracy of the analytical method and have the support reliability of results; it would be greater to have a certified reference material and quality control.

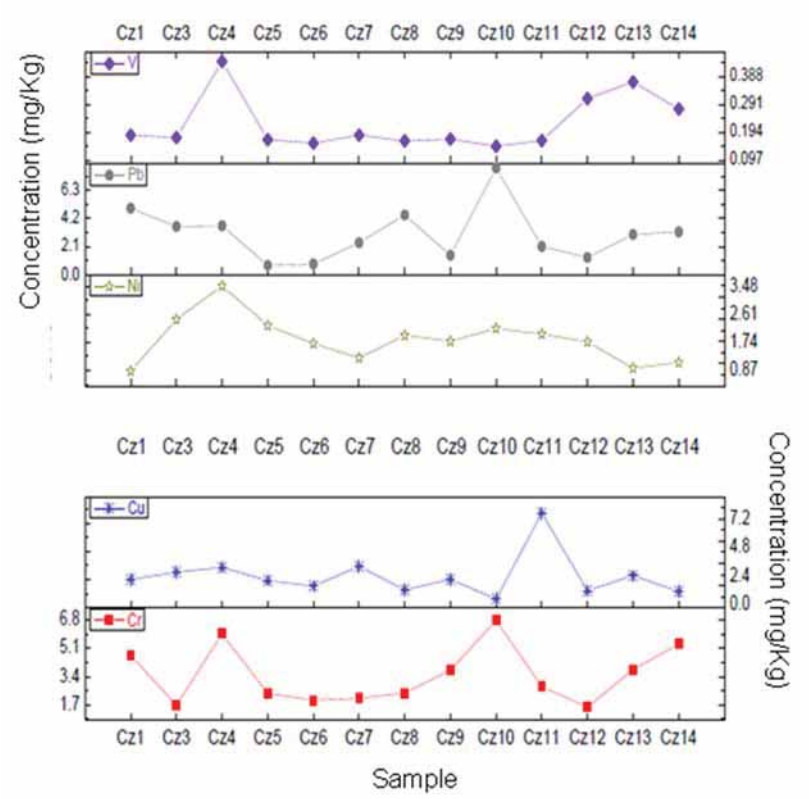


FIGURE 2. Interrelationship total concentration of dried samples obtained.

The % recovery was calculated for each analyzed metal, adding to a sample of each group, a known amount of analyte of interest. The addition was between 5 and 50 times the method detection limit, always looking for the midpoint in the calibration curve, i.e., 25 times the LDM. Metal recovery added for all cases was between 85% and 98%, reflecting reliable analytical results in the methods used. The next part of the analysis, data management was performed with dry samples obtained values; in the case of heavy metals; which they are comparable and the analysis of results, it is more practical (**Figure 2**).

TABLE 3. Total metal content (mg/Kg) in samples of the Coatzacoalcos River

ID sample	Cr	Cu	Ni	Pb	V
Cz1	4.68	2.43	0.85	4.96	0.18
Cz3	1.67	3.05	2.46	3.60	0.17
Cz4	5.98	3.45	3.50	3.65	0.44
Cz5	2.37	2.33	2.27	0.70	0.17
Cz6	1.97	1.88	1.71	0.80	0.16
Cz7	2.07	3.53	1.26	2.39	0.18
Cz8	2.41	1.55	1.96	4.45	0.16
Cz9	3.78	2.43	1.78	1.45	0.17
Cz10	6.79	0.78	2.18	7.96	0.15
Cz11	2.79	8.05	2.00	2.11	0.17
Cz12	1.55	1.48	1.76	1.29	0.31
Cz13	3.81	2.75	0.94	3.00	0.37
Cz14	5.37	1.40	1.12	3.19	0.28
CzL1	1.41	0.53	0.80	0.48	0.17
CzL3	0.63	0.24	1.44	0.42	0.16
CzL4	2.84	0.22	0.84	0.88	0.27
CzL5	0.98	0.31	0.95	0.60	0.16
CzL6	1.11	0.18	0.97	1.55	0.17
CzL7	1.34	0.36	0.91	1.83	0.16
CzL8	1.42	0.12	1.34	0.29	0.15
CzL9	1.61	0.21	1.59	0.59	0.16
CzL10	0.82	0.10	0.78	1.34	0.12
CzL11	1.72	0.40	0.78	1.31	0.19
CzL12	0.58	0.06	1.59	1.82	0.18
CzL13	0.97	0.17	0.94	1.50	0.26
CzL14	3.45	0.15	1.10	0.53	0.17
Min.	0.58	0.06	0.78	0.29	0.12
Max.	6.79	8.05	3.50	8.0	0.44
Average	2.47	1.47	1.45	2.027	0.20
SD	1.66	1.74	0.65	1.74	0.07
% Recovery	93	98	95	85	88

Cz2 = Undeterminated

Different methods and tools to analyze the results obtained were used, and then presented the most demonstrative: analysis of metals using Pearson correlation and analysis of heavy metals using the RETC.

The values of total concentration obtained for each metal, evaluated statistically using Pearson correlations, considering a 95% confidence level, with a value of Pearson

product-moment correlation coefficient 0.178, which allows observing two groups of metals with a significant positive correlation for the number of samples analyzed Cu, Ni and V are attributed to another source emission common.

A directly proportional correlation was also found between the concentrations of Ni and Pb; this feature can be attributed to particle size in the sediment samples, according to various authors, because while smaller particle sizes are the concentrations of Cu and Cr are greater than those of Pb.

Metal concentrations observed in the Coatzacoalcos River are mostly comparable and are within the ranges reported in the literature for other coastal systems Mexico considered moderately or slightly polluted concentration (Table 4), according to the criteria given by the authorities environmental.

TABLE 4. Permissible limits for metals in sediments established by Canada (CEQG, 2001) and reference background levels for United States (NOAA, 1999).

References		Cr (mg Kg^{-1})	Cu (mg Kg^{-1})	Ni (mg Kg^{-1})	Pb (mg Kg^{-1})	V (mg Kg^{-1})
CEQG	ISQG	37.3	35.7	-	35	-
	PEL	90	197	-	91.3	-
NOAA		7-13	10-25	9.9	4-17	50

CEQG: Canadian Environmental Quality Guidelines for sediments.Sediment Quality Guidelines for the Protection of Aquatic Life Freshwater and Marine ISQG/PEL.
ISQG: Interim Sediment Quality Guideline PEL: Probable Effect Level.
NOAA: National Oceanic and Atmospheric Administration; background levels (Screening Quick Reference Table for Inorganics in Freshwater Sediment).

The highest concentrations of Pb (8 mg kg^{-1}) and Cr (6.79 mg kg^{-1}) reported in this work in the rainy season are within background values of NOAA, it being lower than those founded by Botello y Paez (1986) with concentration of 43.53 mg kg^{-1} and 71.80 mg kg^{-1} for Pb y Cr, respectively.

CONCLUSION

According to the results we cannot demonstrate that a site is the most polluted of all, just that; chromium and lead to higher values found in the sample Cz10, for copper the highest values were found in the Cz11 sample and for nickel and vanadium in the Cz4 sample.

As to whether or not they meet the regulations, unfortunately it must say yes, because although apparently are high and harmful to living beings concentrations comply with the law, in the absence of any form of regulating the sediments and this harms the population including in food chains.

The influence of various pollution sources on the Coatzacoalcos River based on the RECT, something truly useful and very rarely performed, taking into account that official figures are caused by federal agencies was determined.

By measuring heavy metals it was found that it is very feasible to use metal analysis, as an environmental indicator to determine the existence of oil pollution and pay more

attention or mark those routes or routes as weak or susceptible to greater environmental impacts.

The determination of the total concentration of metals provides an assessment of the level of contamination, but a chemical speciation is necessary to have information regarding the bioavailability in the area and to assess environmental risks in living in the region.

The Registry of Emissions and Pollutant Transfer (RETC) is a national database with information from a list of 104 pollutants emitted into the ambient air, water, soil and subsoil or are transferred in the wastewater and / or the Dangerous residues. This record stems from Article 109a of the LGEEPA and integrates information from different emission sources of competition of the three orders of government.

The information contained in the RETC allows propose effective policies to preserve and protect the environment, in addition to supporting the evaluation of international agreements. In addition to the information available pollutant emissions are generated national territory can be known with greater certainty the environmental infrastructure that the country needs. Emission sources can assess their performance and identify sites for reducing releases and transfers.

By locating the companies that emissions report to air, soil and water for chromium, nickel and lead, within the area of study, it was found that companies close to the station 14 are most emit chromium water with a total of 7753.2 kg/year and down with 5.041kg / year. Likewise, the company that a nickel compounds emission to air is reported PEMEX, Refinería General Lázaro Cárdenas with 763.52 Kg/year. The above data are the highest values for emissions in each environmental sphere that the RECT evidence; these companies and the remaining area 25 of the federal competition emissions were located in industrialized Coatzacoalcos-Minatitlan area. This is consistent with the highest concentrations found corresponding to the sampling stations Tepache lagoon, south arm end portion of the Calzadas River and Tepeyac, left bank, 6 m before the confluence with the Coatzacoalcos river stream.

ACKNOWLEDGMENTS

We gratefully acknowledge financial support from PRODEP.

REFERENCES

1. Petróleos Mexicanos PEMEX. *Anuario Estadístico* (2011); Download from: http://www.ri.pemex.com/index.cfm?action=content&sectionID=134&catID=12202
2. PEMEX. *Informe de Responsabilidad Social; Apéndice Estadístico. Fugas y derrames de hidrocarburos*. (2010). Descargado de: http://www.pemex.com/informes/descargables/index.html
3. Blanno M. y U. Ruiz Saucedo. *Anexo 1: Análisis estadístico de las emergencias ambientales en suelos mexicanos durante el periodo 2003-2006*. Proyecto Gtz-SEMARNAT: Residuos peligrosos y sitios contaminados. Informe final. México, 2007.
4. Comisión Nacional del Agua CONAGUA. *Consejo de cuenca del río Coatzacoalcos*, 2012. http://www.cuencacoatza.org/index.php; consultado en línea el 25/01/2013

5. Morales De la Garza E., Ortiz Zamora, Carranza Edwards. *Estudio Sedimentológico ambiental de Sedimentos del río Coatzacoalcos, Veracruz, México*. Instituto Nacional de Geoquímica, A. C., Actas INAGEQ Vol.4 (1998) No.1, 33-41.
6. Vázquez Botello A. *El problema Crucial: La Contaminación. Serie Medio Ambiente en Coatzacoalcos* Centro de Ecodesarrollo. Vol 1. 180 pp. México, D. F., 1995.
7. Rodríguez-Salazar M.T.J. *Evaluación de metodologías analíticas para la determinación de arsénico en muestras sólidas ambientales.* Tesis de Maestría en Ciencias Químicas (Química Analítica). Facultad de Química, Universidad Nacional Autónoma de México, 2001.
8. Axtmann E.V.,Louma S.N. 1997. Effect of tributary inflows on the distribution of trace metal in fine-grained bed sediments and benthic insects of the Clark Fork River Montana. Environ. Sci. Technol. 31 (1997) 750-758.
9. Murray K.S., Cauvet D., Lybeer M. Particle size and chemical control of heavy metal in bed sediment from the Rogue River, southeast Michigan. Environ. Sci. Tenchnol. 33 (1999) 987-992.
10. Luque C.J. *Tipificación, cartografía y contenido en metales pesados de comunidades vegetales de las Marismas del Odiel. Dinámica poblacional del género Spergularia.* Tesis Doctoral. Universidad de Sevilla, 1996.
11. Lozano S., Borrego J., López G., Carro B. Características geoquímicas y factores de enriquecimiento (FE) de los sedimentos estuarios de la Costa de Huelva, España, Geogaceta 38 (2005) 147 -150.
12. Kaushik A., Kansal A., Santosh, Meena, Kumari. Heavy metal contamination of river Yamuna, Haryana, India assessment by metal enrichment factor of the sediments. J. Hazard Mater. 164 (2009) 265-270.
13. McCurry J. Japan remembers Minamata. The Lancet 367 (2006) 99-100.
14. Gutiérrez E., Flores E., Villaescusa y González J. Metales pesados en tejido y en biodepósitos sedimentarios del ostión *Crossostrea gigas* en la zona de cultivo de Bahía San Quintín, Baja California, México. Inv. Mar. CICIMAR 6(1), (1991) 175-186.
15. Rosales Hoz L., Cundy A., Bahena Manjarrez J. Heavy metals in sediment cores from a tropical estuary affected by anthropogenic discharges: Coatzacoalcos estuary, Mexico. Estuarine, Coastal and Shelf Science 58 (2003)117–126.
16. Ayala Rodríguez L. Metales pesados en agua y sedimentos del Río Sinaloa. Tesis de Maestría en Recursos naturales y Medio Ambiente. IPN. CIIDIR. Sinaloa. México, 2010.
17. Ávila P., Frías H., Zarazúa G. y Rodríguez S. Caracterización elemental de los sedimentos de la Presa J. A. Álzate. Instituto Nacional de Investigaciones Nucleares, Gerencia de Ciencias Ambientales, Departamento de Estudios del Ambiente 18- 1027. México D.F., 1996.
18. Leal Acosta M. L. Caracterización geoquímica de los sedimentos del sistema lagunar Ohuira-Topolobampo-Santa María. CIIDIR-SIN, IPN. 80 (2008) 7236 p.
19. Toledo A., Vázquez A., Herzig, P. La Contaminación en la región del río Coatzacoalcos. Ciencia y Desarrollo. Vol. XV, (1989) 86.
20. SEMARNAT. *Reglamento de la Ley General del Equilibrio y Protección al Ambiente en materia de Registro de Emisiones y Transferencia de Contaminantes*. Publicado en el Diario Oficial de la Federación el 3 de Junio del 2004.
21. Duarte G., Teixeira M.C., Ciminelli V.S.T. Arsenite immobilization onto a modified thiol chelating resin: pH dependence evidenced by XAS In: VII Meeting of the Southern Hemisphere on mineral Technology / XXII Encontro Nacional de Tratamiento de Minérios y Metalurgia Extrativa, Oro Preto. 2. (2007).
22. Mota Vázquez L.J. *Análisis y evaluación de la contaminación por metales pesados en sedimentos del río Coatzacoalcos, Veracruz, México*. Aplicando EAA. Tesis de licenciatura en Ingeniería Química. Facultad de Química. UNAM, 2013.

CHAPTER 3.4 DISEÑO DE UN BIORREACTOR PARA LODOS RESIDUALES DE CENTROS DE LAVADO

J. Pérez Vargas*(1), G. Zafra Jiménez (1); S. E. Vigueras Carmona (1) and G. Calva Calva*(2)

(1) Tecnológico de Estudios Superiores de Ecatepec, Av. Tecnológico S/N, Estado de México, México
(2) CINVESTAV-IPN, Av. IPN 2508, Ciudad de México, México

RESUMEN

El desarrollo de pequeñas industrias como los servicios de autolavado generan miles de metros cúbicos de agua contaminada por algunos derivados del petróleo como gasolina, aceite automotriz, limpiadores, líquidos refrigerantes, líquidos de frenos, anticongelantes, disolventes de limpieza de piezas, diesel, gasolina, desengrasantes, aceites y grasas lubricantes, champú, siliconas o ceras entre otros, como resultado del lavado de carrocerías y motores. Estos centros de lavado producen una gran cantidad de lodos residuales que contienen grasas, aceites e hidrocarburos y no pueden disponerse libremente debido a que requieren de un tratamiento antes de ser eliminados. El objetivo de este trabajo fue establecer un bioproceso basado en biorreactores y utilizar bacterias de vida libre fijadoras de nitrógeno atmosférico (BFNA) para el tratamiento de estos lodos. Se presentan los resultados con cultivos de el tratamiento del lodo en un biorreactor de columna de burbujeo utilizando BFNA que se ha comprobado pueden utilizar hidrocarburos como fuente de carbono, se han obtenido resultados interesante en donde en 48 horas los lodos residuales pierden totalmente el color negro inicial, además del olor a hidrocarburo no se percibe y la cantidad de sólidos totales se ve disminuida hasta en 80% y de una concentración inicial de 60g/L de hidrocarburos totales se llega a un 75% de reducción.

Keywords: biorreactor, BFNA, Hidrocarburos, lodos residuales

INTRODUCCIÓN

Tratamiento de aguas residuales en los servicios de autolavado. Generalmente el agua residual de los servicios de autolavado contienen en promedio 1100 mg/L de aceites y grasas, 4500 mg/L de DQO y 3500 mg/L de sólidos suspendidos totales[1]. Para remover estos contaminantes se utilizan separadores convencionales de aceites y grasas, como una trampa de sólidos y un separador de aceites, lo que permite reducir la carga contaminante con una eficiencia del 80%, pero no siempre esta reducción es eficiente para obtener un efluente con los límites permisibles para ser enviados al drenaje de acuerdo a la NOM-002-SEMARNAT-1996[2]. Está norma al igual que la NOM-003 establece los límites máximos permisibles de contaminantes en las descargas de aguas residuales a los sistemas de alcantarillado urbano o municipal, para el caso de

---

*Author for correspondence: gcalva@cinvestav.mx; djperezvargas@hotmail.com

grasas y aceites su concentración no debe ser mayor de 50 ppm.

Las características físicas, químicas y biológicas del agua residual de estos servicios de autolavado, son muy diferentes de un servicio a otro ya que depende de su procedencia y del tratamiento llevado a cabo.

Fall et al. (2007)[1] realizó una comparación entre los contaminantes reportados en aguas residuales de un servicio de autolavado de camiones comerciales de los Estados Unidos en el 2004 con un servicio de autolavado en México. Reportó características de los efluentes muy diferentes, ya que depende del servicio que se requiera y del lugar donde se encuentre el establecimiento.

En estos servicios de autolavado las grasas y aceites son compuestos orgánicos constituidos principalmente por ácidos grasos de origen animal, así como aceites y grasas lubricantes de los hidrocarburos del petróleo. Las principales fuentes aportadoras de grasas y aceites son de uso doméstico (baños y servicios) y del lavado de motores y carrocerías[3].

Se lleva a cabo el tratamiento de los lodos residuales para cumplir con la NOM-004-SEMARNAT-2002[4], generalmente el tipo de lodo que se obtienen en un servicio de autolavado después de un tratamiento, es primario ya que el lodo obtenido se encuentra en el fondo del tanque primario de sedimentación. La composición del lodo depende de las características del proceso realizado, generalmente contiene gran cantidad de materia orgánica y se caracteriza por ser un fluido denso con un porcentaje de agua que varía entre 93% y 97%.

La importancia de tratar estos lodos, es la reducción de sustancias orgánicas contaminantes, sólidos totales, microorganismos patógenos y la eliminación de olores desagradables, con el fin de mejorar sus propiedades para que los lodos puedan ser utilizados posteriormente.

Sin embargo han proliferado los centros de lavado como nuevas microempresas en las cuales no se consideran sistemas de tratamiento y esta agua va directamente al drenaje, parte del trabajo es convencer a los propietarios de tratar el agua, por lo que se les ha propuesto sistemas simples de tratamiento y los lodos residuales obtenidos deben aún ser dispuestos por lo que para ayudar a concientizar al propietario del centro de lavado se le propuso un sistema final de tratamiento de los lodos residuales generados a través de un sistema de columna de burbujeo que tuviera un mínimo de manipulación para que un estudiante de licenciatura pudiera llevar a cabo su servicio social o sus residencias profesionales, lo que permitiría al alumno adquirir experiencia en el tratamiento de los lodos y resolver cualquier problema técnico que resultara debido a la naturaleza de los lodos que se están obteniendo de manera cotidiana, esto ha reforzado al mismo tiempo el nuevo programa institucional de adquisición de competencias profesionales.

En México es obligatorio que los lodos residuales obtenidos de algún sistema de tratamiento de agua residual de un servicio de autolavado sean tratados para disminuir sus contaminantes y puedan ser vertidos al drenaje, lo que puede considerarse un gran problema a corto plazo si no se generaliza, pues la demanda de los servicios de autolavado tienden a aumentar, ya que el 70 % de los automóviles de la ciudad de México son lavados una vez por semana.

La importancia de tratar estos lodos, es la reducción de sustancias orgánicas contaminantes, sólidos totales, microorganismos patógenos y la eliminación de olores

desagradables, con el fin de mejorar sus propiedades para que los lodos puedan ser utilizados posteriormente.

El empleo de microorganismos para estabilizar estos lodos residuales es una alternativa para eliminar las grasas y aceites de hidrocarburos presentes, obteniendo lodos que contaminen menos al medio ambiente, para ello es importante conocer la eficiencia de remoción de estos contaminantes por la BFNA.

Se ha estudiado la posibilidad de encontrar microorganismos que utilizan compuestos contaminantes como fuente de carbono y energía en donde el producto final sea la producción de CO_2, asegurando la eliminación del compuesto contaminante, entre los géneros de microorganismos degradadores de hidrocarburos se encuentran las bacterias, las algas, las levaduras y los hongos filamentosos[5 y 6].

De acuerdo a lo reportado se ha propuesto un sistema de biorreactor airlift para determinar si el reactor junto con las BFNA elimina los contaminantes presentes en los lodos y obtener un residuo que puede ser dispuesto sin ningún otro tratamiento debido a que no tiene compuestos contaminantes del ambiente.

MATERIALES Y MÉTODOS

Microorganismo. Se utilizó un cultivo de BFNA, aislado de un suelo contaminado con hidrocarburos del estado de Tabasco. Se inocularon en medio líquido mineral usando los lodos residuales como única fuente de carbono, en cultivo en lote, a 27°C, 180 rpm en un agitador orbital por tres días. El cultivo obtenido fue centrifugado a 5000 rpm por 15 minutos, el paquete celular fue resuspendido en 30 ml de solución salina isotónica, este fue el inóculo utilizado en los experimentos.

Muestra de lodo residual. De un tren de tratamiento de diez ciclos de la planta de tratamiento del servicio de autolavado, ubicado en Av. Anillo Periférico. Blud. Adolfo López Cortines 40000- Bis. Álvaro Obregón. Col. Jardines del Pedregal (Toyota). Se muestrearon 20 L de lodos residuales de un reactor de sedimentación que se encuentra al final del proceso fisicoquímico. Los recipientes de plástico utilizados para el muestreo fueron lavados previamente, la muestra fue colectada directamente del vertedor del tanque de almacenamiento de los lodos y se identificó de acuerdo a los procedimientos de muestreo de la norma (NMX-AA- 003 -1980). El lodo fue consolidado por sedimentación libre y almacenado a 4°C durante 48 horas.

Determinación de pH. Se determinó de acuerdo a la norma NMX-AA-008-SCFI-2000[7].

Determinación de sólidos suspendidos. Se cuantificó el porcentaje de sólidos totales de acuerdo a la norma NMX-AA-034-SCFI-2001[8].

Determinación de grasa y aceite automotriz.

Método de extracción líquido-líquido. La extracción de se realizó tomando 50 ml de la muestra de hidrocarburos totales se adicionaron 70 ml de diclorometano, y otras dos extracciones de 30 ml del solvente, los extractos recuperados fueron evaporados en un

rotavapor el residuo se llevó a peso constante y se cuantificó la cantidad de grasas y aceites de acuerdo al Método EPA 3540C[9].

Método de extracción por Soxhlet. Se tomaron 50 ml de la muestra, se centrifugaron y el sedimento se pasa a un dedal de celulosa y se coloca en un equipo Soxhlet se utilizan 150 ml de diclorometano y perlas de ebullición suficientes para evitar la proyección del solvente al calentarse, se mantuvo el reflujo en estas condiciones durante 8 horas, de tal manera que se efectuaron de 6 y 8 reflujos por hora. Terminada la extracción se colocó en un rotavapor para concentrar el extracto orgánico se llevo a peso constante y se determinó la concentración de grasas y aceites recuperables, de acuerdo a la norma, NMX-AA-005-SCFI-2000[10].

Cuantificación de grasas y aceites de hidrocarburos por cromatografía de gases. Una vez obtenido el extracto orgánico, se suspendió en 40 ml de hexano, el cual se dejó reposar durante 12 a 24 horas para precipitar los asfáltenos. Las muestras diluidas se pasaron a viales para el cromatógrafo. Se inyectó 1 μl de la muestra en el cromatógrafo de gases equipado con una columna capilar AT-5 y un detector de ionización de flama. Se determinó la concentración de hidrocarburos en la muestra, considerando el área bajo la curva de los picos resueltos y extrapolando dicho valor en la curva de calibración (Método 8015B).

RESULTADOS

El agua residual muestreada del centro de lavado era de color negro y lechoso en la superficie del agua podía observarse un aspecto aceitoso, debido a l gran cantidad de hidrocarburos que provenían de los autos camionetas e incluso camiones a los que da mantenimiento la planta de Toyota y antes de entregar los lava. El muestreo realizado de acuerdo a la norma NMX-AA-003-SCFI-1980[12], fue guardado en refrigeración para consolidar y permitir que sedimentara la mayor cantidad de sólidos. Se tomaron las muestras para realizar la determinación de microorganismos totales así como patógenos, hongos, levaduras y BFNA, encontrando crecimiento en cada uno de los medios encontrados. Este fue un resultado que llamo la atención porque era muy abundante y se determinó primero saber que estaba pasando en la planta de tratamiento. Se encontró que era un problema humano por la falta de conocimiento y se realizaron nuevamente los muestreos de agua encontrándose la disminución notable de la carga microbiana en general.

Se realizaron las determinaciones fisicoquímicas correspondientes a las aguas residuales (**Tabla 1).** Como puede observarse en la **Tabla 1,** la cantidad de sólidos totales se ve disminuida hasta los límites que la norma correspondiente indica, esto se atribuye a que al estar dentro de la columna de burbujeo airlift este produce que haya una mejor dispersión de los compuestos que hacen que formen flóculos más grandes y produciendo que se vayan al fondo, al mismo tiempo al estar aireando se permite que la bacterias presentes en el agua tratada junto con el inóculo de BFNA en el sistema eliminen muchos de los compuestos que corresponden a hidrocarburos totales. Es notable como el olor se ve eliminado, así como la apariencia negra del agua, lo que tiene un impacto a la vista. Esto tiene un beneficio hacia el usuario, es decir, las

personas que laboran en el centro de lavado porque pueden reutilizarla ya que ellos ven como principal problema que el agua tratada se ve negra.

TABLA 1. Determinación de parámetros fisicoquímicos del agua del centro de lavado automotriz

*

Parámetros	Características Del agua tratada	Características del agua tratada después del tratamiento en la columna	Límites normativos de aguas de reuso *
Sólidos totales (ppm)	2966	500	500
pH	6.5	6.5	6 – 7
Conductividad (µS)	1357	1245	Na
Temperatura	18 -25°C	20^0C	18- 25°C
Hidrocarburos totales	600000	150000	
Grasas y aceites (ppm)	2850	2500	
Color	Negro lechosa	Sin color	Sin color
Olor	Aceite, aguas negras	Sin olor	Na

NOM- 003-SCFI-1980[13]

En la **Figura 1** se puede observar como el cultivo de BFNA utiliza los hidrocarburos como fuente de carbono, debido a que el reactor solo es alimentado con el agua residual, hay que hacer notar que también los microorganismos que contiene el agua y que no son eliminados por lo que pueden hacer sinergia con el cultivo y eliminar una mayor cantidad de compuestos estos datos no son presentados. En la curva puede observarse que aproximadamente a las 50 horas el cultivo empieza a disminuir su crecimiento, esto puede deberse a que la cantidad de hidrocarburos que puede utilizar como fuente de carbono no son asimilables para el cultivo.

En la **Figura 2,** se presentan los resultados obtenidos para los estudios de remoción para la determinación de los hidrocarburos remanentes de acuerdo al método 8015B. Se pudo observar que el agua tratada posee una gran cantidad de hidrocarburos y estos son producto del servicio que se da a todos los autos camiones y camiones de carga, es muy interesante ver que aun cuando en el medio hay hidrocarburos estos no son utilizados como fuente de carbono para el microorganismo, esto puede deberse a la naturaleza de los compuestos y también que pueden producirse productos de desecho que pueden también ser tóxicos para el microorganismo por lo que no son asimilables aun cuando las concentraciones remanentes son altas aun.

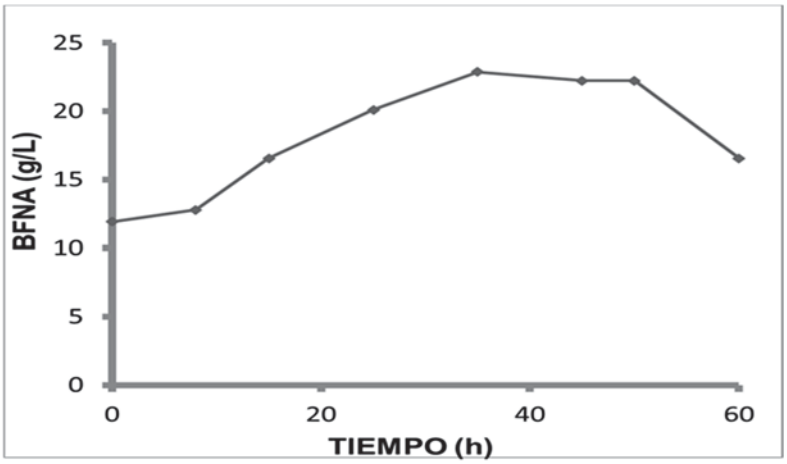


FIGURA 1. Curva de crecimiento para el cultivo BFNA utilizando como fuente de carbono los hidrocarburos del agua tratada proveniente de un centro de lavado automotriz.

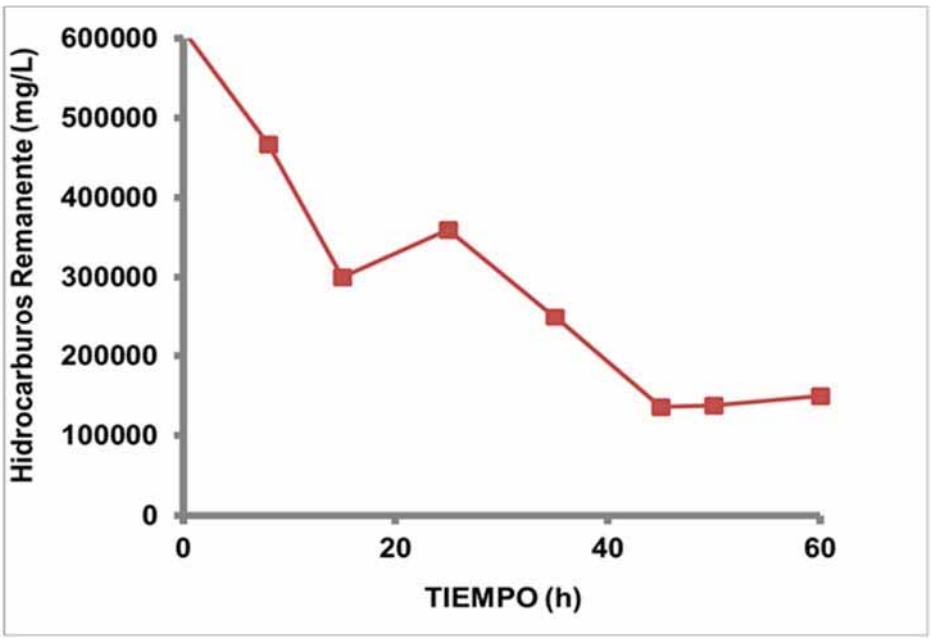


FIGURA 2. Curva de remoción de hidrocarburos totales por BFNA en un agua tratada proveniente de un centro de lavado automotriz.

En la **Figura 3a** podemos observar el perfil cromatográfico presentado para los hidrocarburos y en el tiempo cero pueden verse que hay una gran variedad de compuestos; en la **Figura 3b** puede verse que la variabilidad de compuestos se ve disminuida y algunos de los compuestos iniciales desaparecen y pudiera ser que los compuestos remanentes no pueden soportar el crecimiento del cultivo de BFNA. Al determinar la eficiencia de la remoción se encuentra que es del 75% lo que es un gran aporte al trabajo ya que la eliminación de los compuestos lo hacen en un periodo máximo de 60 horas.

CONCLUSIÓN

Es posible la eliminación de hidrocarburos en aguas residuales provenientes de centros de lavado automotriz utilizando BFNA en un reactor de columna de burbujeo con una eficiencia del 75% en 60 horas de tratamiento.

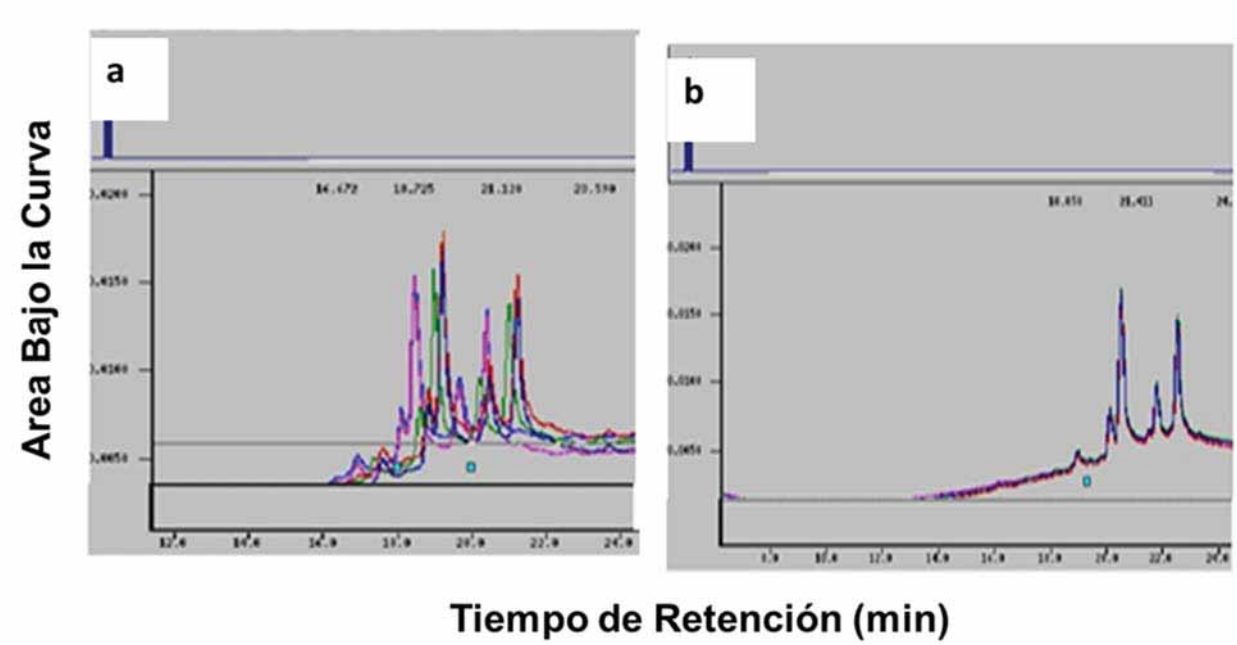


FIGURE 3. Perfil cromatográfico de los hidrocarburos remanentes de los lodos residuales tratados por la columna de burbujeo. a) Tiempo cero; b) al final de las 60 horas de tratamiento

AGRADECIMIENTOS

Se agradece el apoyo recibido por El Tecnológico Nacional del México a través del proyecto 366.15-PD para la realización del proyecto.

REFERENCES

1. Fall, C., Lopez. V.M., Jiménez . M. K., Díaz. D.C García. P.D Y Chavez L.M. (2007), *Carwash wastewaters: Characteristics, Volúmen And Treatability by Gravity oil Separation,* Revista Mexicana de Ingeniería Química, 6(2), 175-184UNESCO *water for people, water for life,* Executive Summary of the UN World, Water Development Report, Paris, France, 2003.
2. NOM-002-ECOL-1996. Que establece los límites máximos permisibles de contaminantes en las descargas de aguas residuales a los sistemas de alcantarillado urbano o municipal http://200.77.231.100/work/normas/noms/1998/002-ecol.pdf
3. Arce. V. A. (2000). Serie autodidáctica de medición de la calidad del agua. Guía: *Muestreo y preservación de grasas y aceites y determinación en cambio de pH, temperatura y materia flotante.* Subdirección general de administración del agua. México. http://www.conagua.gob.mx/CONAGUA07/Noticias/Fundamentos_Tecnicos.pdf

4. NOM-004-SEMARNAT-2002. Protección ambiental, lodos y biosólidos. Especificaciones y límites máximos permisibles de contaminantes para su aprovechamiento y disposición final.http://www.profepa.gob.mx/innovaportal/file/1342/1/nom-004-semarnat-2002.pdf
5. Pérez V. J y García E. G. (2013). *Biorremediación de Suelos y Aguas Contaminadas con compuestos orgánicos e inorgánicos*. Ed. Trillas. México. Cap 2: 32-38.
6. Pérez. V. J., Poggi. V. A., Calva. C. G., Ríos. L. E., Rodríguez. V.R., Ferrera. C. R. y García. E.F. (2000). *Nitrogen fixing bacteria capable of utilising kerosene hydrocarbons as a sole carbon source.* Water. Science and Technology. 42(5-6): 407 -410
7. NMX-AA-008-SCFI-2000 Análisis de agua determinación del pH. http://anfacal.org/media/Biblioteca_Digital/Usos_Ecologicos/Tratamiento_de_Aguas/ANALISIS_DE_AGUA_DETERMINACION_DEL_pH.pdf
8. NMX-AA-034-SCFI-2001 Análisis de agua - determinación de sólidos y sales disueltas en aguas naturales, residuales y residuales tratadas.http://www.conagua.gob.mx/conagua07/noticias/nmx-aa-034-scfi-2001.pdf
9. Method EPA 8015 C, "Characterization of C_6 to C_{35} Petroleum hydrocarbons in environmental samples: Total petroleum hydrocarbons, Aliphatic Hydrocarbons, Aromatic Hydrocarbons, Aproximate Boiling Point/carbon number distribution", Julio 2002. http://www.epa.gov/osw/hazard/testmethods/sw846/pdfs/8015c.pdf
10. NMX-AA-005-SCFI-2000. Determinación de grasas y aceites recuperables en aguas naturales, residuales y residuales tratadas. http://www.conagua.gob.mx/conagua07/noticias/nmx-aa-005-scfi-2000.pdf
11. NOM-138-SEMARNAT/SS-2003. Límites máximos permisibles de hidrocarburos en suelos y las especificaciones para su caracterización y remediación.http://www.respyn.uanl.mx/xiii/3/contexto/Mexico_-_NOM-138.pdf.
12. NMX-AA-003-SCFI-1980 Secretaria de comercio y fomento industrial norma mexicana aguas residuales muestreo. http://www.conagua.gob.mx/CONAGUA07/Noticias/NMX-AA-003-1980.pdf.
13. NOM-003-ECOL-1997. Límites máximos permisibles de contaminantes para las aguas residuales tratadas que se reúsen en servicios al público y residuales tratadas. http://www.profepa.gob.mx/innovaportal/file/3297/1/nom-003-semarnat-1997.pdf.

CHAPTER 3.5 EFECTOS DEL GRADO DE CONTAMINACIÓN Y DE LA REMEDIACIÓN POR BIOLIXIVIACIÓN EN LA COMPOSICIÓN MINERAL Y TEXTURAL DE SEDIMENTOS CONTAMINADOS DEL RÍO RECONQUISTA

A. Tufo *(1); N. Porzionato (1) and G. Curutchet (1)

(1) 3iA, UNSAM, Av. 25 de Mayo y Francia, San Martín, Buenos Aires, Argentina

RESUMEN

La cuenca del río Reconquista atraviesa las periferias de la Región Metropolitana de Buenos Aires, recibiendo un fuerte aporte de efluentes contaminados. En consecuencia, es posible encontrar altos niveles de metales en sus sedimentos anaeróbicos. Estos pueden ser re-movilizados hacia la columna de agua por eventos como la lluvia y el dragado, que provocan cambios en las condiciones redox. En general, esto ocurre mediante reacciones biocatalizadas de oxidación de compuestos del azufre presentes en el sedimento. En el 4ISEBE hemos mostrado que la biolixiviación constituye una posible estrategia de remediación y que además su eficiencia mejora por el agregado de azufre elemental en cuanto a la lixiviación del Zn y el Cu[1]. La gran disminución del nivel de metales por este tipo de tratamiento permitiría la disposición segura de los sedimentos. Sin embargo, para determinar el uso futuro y destino de los sedimentos remediados es necesario conocer los cambios que dicho proceso de remediación provoca en la composición mineral y textural de los mismos. Es por esto que el objetivo de este trabajo fue la caracterización de los sedimentos descontaminados y particularmente de su fracción arcillosa. Se estudiaron sedimentos de una zona muy contaminada del río Reconquista antes y después del tratamiento por biolixiviación en biopilas mostrado en el 4ISEBE. La composición mineral se estimó por difracción de rayos X y se determinó el área superficial por el método de BET. Los resultados de DRX del sedimento indicaron al cuarzo como mineral 1^{rio} en todos los casos y que existen diferentes tipos de tectosilicatos y arcillas entre los minerales secundarios. En las fracciones arcillosas de las muestras sin tratar y con bajo grado de tratamiento, se determinó la presencia de $CaSO_4$ (que difiere entre ambas solo por la intensidad de sus reflexiones) y de arcillas del tipo inter-estratificadas de Illita-Montmorrillonita. La fracción arcillosa de la muestra tratada con azufre también se encontró $CaSO_4$, pero con reflexiones de gran intensidad y una baja proporción de arcillas inter-estratificadas y simples de Illita, Montmorrillonita, Clorita y Haloisita. La diferencia en intensidad para la fase de $CaSO_4$ se correlacionó con los valores de sulfato encontrados en los sedimentos[1]. Asimismo, está de acuerdo con los valores área superficial obtenidos (sin tratar (23) < con bajo grado de tratamiento (27) >> tratada con azufre (3 $m^2\ g^{-1}$)). Por lo tanto, estos resultados muestran que además de disminuir el nivel de metales, el proceso de biolixiviación con el agregado de azufre provoca un aumento en la concentración de sulfatos y cambios en la estructura mineralógica y superficial de los sedimentos descontaminados.

---

*Author for correspondence: anaetufo@gmail.com

Palabras claves: Biolixiviación; composición mineral; metales; sedimentos.

INTRODUCCIÓN

El río Reconquista es reconocido en todo el mundo como un símbolo de los problemas ambientales de la Argentina[2,3]. Se localiza en el norte de la provincia de Buenos Aires y en su recorrido de 82 Km recibe el aporte de varios afluentes. En la cuenca media-baja, es un sistema acuático muy deteriorado tanto en lo relacionado con la química de sus aguas como en sus aspectos biológicos y ecológicos. Además, debido a que su curso atraviesa 18 partidos del conurbano bonaerense, una importante población establecida en sus alrededores está expuesta a los posibles efectos negativos sobre la salud[4]. La contaminación es, principalmente, de origen antropógenico, debido a la descarga en sus aguas de contaminantes domiciliarios, municipales e industriales. La gran mayoría de las industrias descargan sus efluentes sin tratar al río (metales, productos sintéticos, hidrocarburos, fertilizantes, plaguicidas, aguas servidas y residuos sólidos), lo que conduce a la acumulación de metales y sustancias orgánicas en los sedimentos[5-7]. Por esta razón, para evaluar el alcance de la contaminación la posibilidad de remediación no debe limitarse el análisis solo a las aguas superficiales sino que también deben ser tenidos en cuenta los sedimentos que reciben desde hace décadas el aporte de desechos que contienen varios contaminantes. Dentro de la gran variedad de estos, los metales reciben especial interés debido a su persistencia en el ambiente. Estos pueden ser retenidos superficialmente en los sedimentos, precipitar en la forma de óxidos o sulfuros (según el tipo de metal y el potencial redox del sedimento) o bien quedar ocluidos en la estructura de los minerales en formación. Es importante resaltar que la interacción entre los sedimentos y los metales por cualquiera de los procesos mencionados deriva en la inmovilización natural de estos contaminantes, limitando así su bio-accesibilidad[8]. Es posible generalizar que los sedimentos pueden comportarse como sumideros de metales, sin olvidar que asimismo estos pueden actuar como fuentes secundarias de contaminación[9], si ocurren procesos de removilización de los mismos[1;10,11]. Estos procesos, a su vez, dependen de varios parámetros fisicoquímicos tales como pH, disponibilidad de oxígeno, actividad microbiológica, materia orgánica y otros compuestos complejantes. Además, las características de los sedimentos pueden condicionar la biodisponibilidad, el tiempo de vida media y la permanencia de estos contaminantes en el ambiente.

Las reacciones biocatalizadas de oxidación de compuestos del azufre provocan la acidificación de los sedimentos y por lo tanto generan cambios en las condiciones redox que derivan en reacciones que re-movilizan los contaminantes, es decir favorecen la re-liberación de los metales hacia el cuerpo de agua[6;12-14]. La eliminación de estos contaminantes desde los sedimentos contaminados por lo tanto resulta de prioridad para la recuperación, gestión y disposición segura de los mismos. Porzionato y col. estudiaron como posible estrategia de remediación de los sedimentos contaminados del río Reconquista utilizar el proceso de biolixiviación en biopilas basado en la oxidación biocatalizada de las fases del sedimento que contienen diferentes compuestos de azufre. Se demostró que en este proceso se logra una gran eficiencia utilizando agregado de azufre elemental en cuanto a la lixiviación del Zn (71%) y el Cu (45%)[1; 15.] La gran disminución del nivel de metales por este tipo de tratamiento indica un buen

grado de descontaminación de los sedimentos. Sin embargo, para determinar el destino y potencial uso futuro de los sedimentos remediados es necesario conocer la calidad de los mismos y posiblemente los cambios que dicho proceso ha provocado en la composición mineral y textural.

A pesar de que existen antecedentes sobre la relación entre las diferentes características de los sedimentos y el mecanismo de biolixiviación, el tema aún no está claro[16-18]. De la misma manera es escasa la bibliografía acerca de cuáles son los cambios que sufren los sedimentos una vez que han sido remediados y como esto afecta su calidad final. Es por esto que el objetivo de este trabajo fue la caracterización estructural y textural de los sedimentos descontaminados y particularmente de su fracción arcillosa.

MATERIALES Y MÉTODOS

El sitio de estudio elegido para este trabajo se muestra en la **Figura 1**. El mismo se encuentra ubicado en el Canal José León Suárez, a 4,5 Km. de su desembocadura sobre el río Reconquista. Es en este punto donde dicho canal sale a cielo abierto luego de atravesar una gran parte del Partido de General San Martin en forma de canal entubado. A lo largo de su recorrido recibe el aporte de efluentes industriales clandestinos y domiciliaros (cloacales), ambos contaminantes que, debido a los procesos antes mencionados, se acumulan en los sedimentos.



FIGURA 1. Ubicación del sitio de muestreo (34° 31′ 19.4″ S, 58° 35′ 28.0″ W). Imagen satelital de distrito de J. L. Suárez en la provincia de Buenos Aires, Argentina.

Se estudió como posible tratamiento de los sedimentos superficiales, la biolixiviación en biopilas durante tres meses[15]. Para llevar a cabo este tratamiento, los sedimentos fueron previamente acondicionados con el agregado de perlita que mejora su drenaje y aireación. Posteriormente estos fueron empaquetados en una columna de PET y se saturaron con una suspensión en medio 0K[19] de mezcla de cultivos de *Acidithiobacillus ferrooxidans* (DSM 11477) y *Acidithiobacillus thiooxidans* (DSM 11478). Durante el proceso, los lisímetros se regaron periódicamente para permitir el pasaje del oxígeno y nutrientes al interior de la biopila, y se recirculó el lixiviado hasta que el mismo alcanzó los

parámetros adecuados para recuperar los metales presentes. Con el objetivo de optimizar el desarrollo de la flora azufre oxidante responsable de la biocatálisis, se estudió el agregado en diferentes concentraciones de azufre elemental como suplemento (1 %, 2 % y 5 % p/p). Se reportó que el proceso de biolixiviación alcanza su máxima eficiencia cuando se suplementa un 5% p/p de azufre[18].

A partir de estos sedimentos remediados se estudiaron las muestras: sin tratar, con bajo grado de tratamiento (sin azufre) y tratada con 5% de azufre.

La composición mineralógica se estimó por Difracción de Rayos-X de polvos (DRX) utilizando un difractómetro Siemens D5000, con tubo de Cu-Kα. Los diagramas de DRX fueron medidos en el intervalo 2θ= 10–70°, utilizando pasos de 0,02° y un tiempo de lectura de 3 segundos por paso. Se utilizó un voltaje de 40 kV y un amperaje de 35 mA. El análisis se realizó mediante la indexación de las reflexiones utilizando un Software—XRD, JADE[20]. Se difractaron los sedimentos de las tres muestras húmedas cubierta con film, es decir en las condiciones finales del proceso de lixiviación. Posteriormente, las muestras fueron secadas a 40°C y se homogeneizaron por molienda y tamizado. Sobre estos sedimentos secos se repitió la medición de DRX para evaluar si aparecían o desaparecían fases por efecto del secado. Sobre estos últimos sólidos se determinó el área superficial específica a través de las isotermas de adsorción-desorción de N_2 a 77K aplicando el método de BET[21]. Fue necesario realizar una etapa previa de desgasado suave a 60°C por 15 hs para evitar cambios de fase del sólido.

Por otro lado, desde los sedimentos remediados se extrajo la fracción arcillosa (partículas menores a 2-4 μm), aplicando el Método de Atterberg en base a la ley de Stoke[22]. Para esto, los sólidos secos se re-suspendieron en agua bidestilada, se dispersaron por ultrasonido y se filtraron mediante una malla de 120μm. Las partículas o granos más gruesos que se retuvieron se dejaron secar a 40°C. El resto de la suspensión tamizada se colocó en un tubo de Atterberg y se completó hasta los 25 cm de altura con agua bidestilada, dejándose en un ambiente termostatizado a 23°C. La suspensión se dejó decantar durante 18 hs, se retiró el sobrenadante y se lo dejo evaporar a 40°C hasta reducir el volumen en un 90%. Finalmente, se realizaron tres tipos de preparados: de arcillas orientadas preferencialmente (denominadas “directas”); de arcillas orientadas preferencialmente expuestas a una atmosfera de etilenglicol durante 12 hs (denominadas “glicoladas”); de arcillas orientadas preferencialmente calcinadas a 500°C durante 1 hs (denominadas “calcinadas”). El análisis conjunto de los patrones de difracción de estos tres preparados permite la diferenciación entre arcillas expandibles y no expandibles.

RESULTADOS Y DISCUSIÓN

Análisis de los sedimentos. Durante los procesos de biorremediación, como el utilizado por Porzionato y col., se hace uso de las características nutricionales de microorganismos especializados nativos del curso de agua en estudio, con el fin de remover los metales desde sedimentos contaminados. Sin embargo, estos procesos pueden derivar en el deterioro de los minerales que componen los sedimentos o bien pueden brindar ciertas características que resultan en un sedimento recuperado que puede ser utilizado para otros fines[23-26].

Estimación mineral por DRX de los sedimentos: Los diagramas de difracción de las muestras tanto con su humedad natural (“húmedas”) como previamente desecadas (“secas”) no presentaron diferencias significativas. Por esta razón, se prosiguió únicamente con el análisis de las muestras “secas”. Se determinó que tanto para los sedimentos sin tratar y para los tratados con y sin agregado de azufre, el mineral mayoritario es el cuarzo (SiO_2). La intensidad de los picos correspondientes a la fase de SiO_2 dificultó la identificación de minerales minoritarios, por lo tanto, se retiraron las reflexiones de esta fase y se pudieron visualizarlas reflexiones de menor intensidad. En la **Figura 2**, se muestran los difractogramas pertenecientes a los sedimentos tratados con 5% de azufre y sin tratar (se indican las diferencias entre ambos (*)). Se pudo identificar en ambos patrones la presencia de feldespato, silicatos y varias arcillas. Las reflexiones que sólo aparecen en los sedimentos tratados con 5% azufre, sugieren la presencia de óxidos de hierro y sulfatos de calcio y/o de hierro.

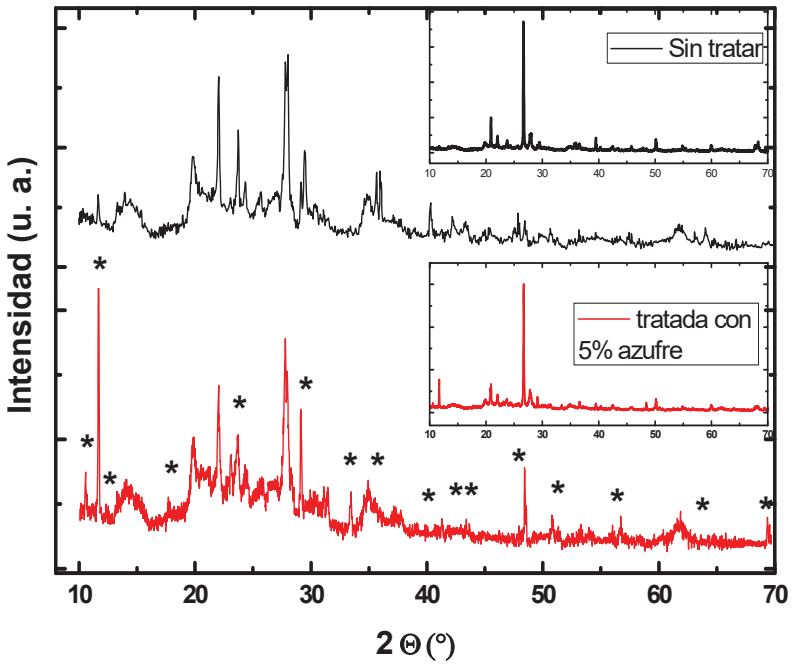


FIGURA 2. Patrones de difracción de las muestras sedimentos sin tratar y tratadas con 5% de azufre. En el *inset* se observa el patrón completo.

Caracterización superficial y textural de los sedimentos: Los valores de área superficial específica indicaron diferencias entre las muestras por el tipo de tratamiento de biolixiviación, ya que se obtuvieron valores similares para los sedimentos sin tratar y con bajo grado de tratamiento (27 y 23 $m^2\ g^{-1}$ respectivamente). Sin embargo, el sedimento tratado con 5% de azufre presento un valor de 3 $m^2\ g^{-1}$, es decir que el área superficial disminuyo en ~ 88%. Este hecho se relaciona directamente con un cambio en la composición de mineral de los sedimentos por efecto del tratamiento. A partir de las isotermas de adsorción-desorción de N_2 (ver **Figura 3**) se encontraron diferencias a nivel textural entre los sedimentos. Las isotermas de las muestras sin tratar y bajo grado de tratamiento, son similares entre si y corresponden a isotermas del tipo IV, con un ciclo de histéresis del tipo H3 (clasificación IUPAC)[27]. Se observó un aumento brusco

en la adsorción de N_2 cercano a p/p^0 > 0,8 revelando la presencia de grandes mesoporos y/o macroporos formados por espacios entre partículas agregadas. Además, la isoterma de desorción cae en p/p^0 ~ 0,45, que se asocia a la cavitación inducida por evaporación (o formación de burbujas de vapor) indicando la presencia de una red de mesoporos con tamaños < 5 nm. Esta clasificación presume la existencia de partículas con una estructura de poro en formas de placasen paralelo, típicamente encontrado en las arcillas pilareadas. Esta particularidad está de acuerdo con la composición mineral estimada por DRX.

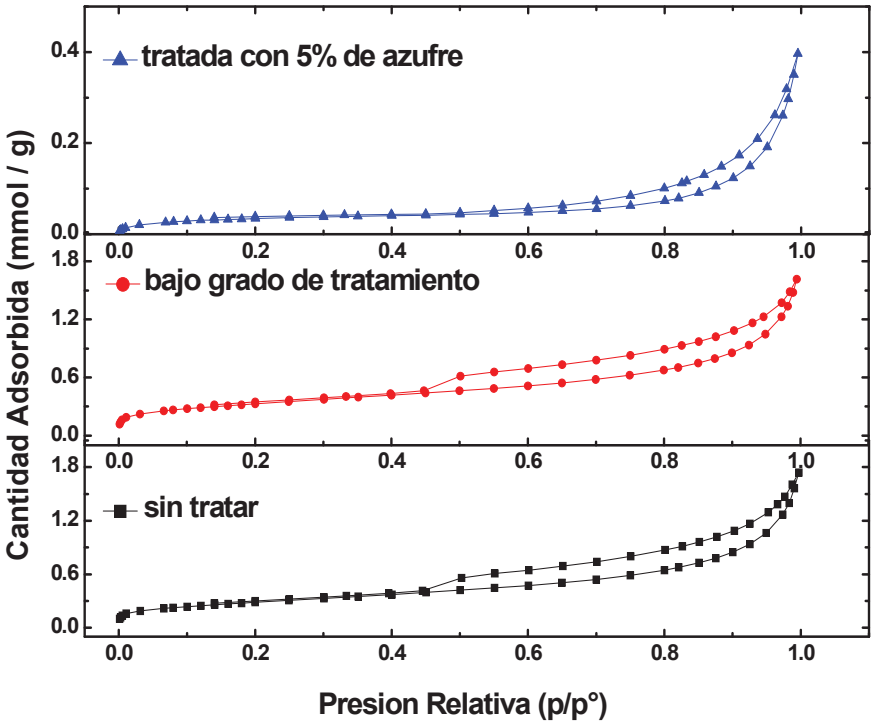


FIGURA 3. Isotermas de adsorción-desorción de N_2

En la muestra tratada con 5% de azufre, la isoterma es similar a las de tipo II, con un estrecho ciclo de histéresis H3 sugiriendo la presencia de un material no poroso o macroporoso. El ciclo de histéresis indica que existe condensación capilar entre las partículas (normalmente dentro de un agregado que no es rígido).

Esto indica que los poros se localizan en los intersticios de las partículas constituyentes, y esto nuevamente está de acuerdo a lo estimado por DRX, ya que los óxidos de hierro y sulfatos son estructuras compactas poco porosas (macroporosas). Además, estos resultados se correlacionan con los valores de sulfato encontrados en los sedimentos descontaminados: tratada sin azufre (5400±900 mg kg^{-1}) <<< tratada con 5% azufre (19500±500 mg kg^{-1}).

El conjunto de resultados indicó que solo con el tratamiento más enérgico (5% de azufre) ocurren modificaciones significativas en los sedimentos, como la disminución del área superficial y el posible cambio en la porosidad de los mismos ya que se vuelven un material compacto no poroso o macroporoso.

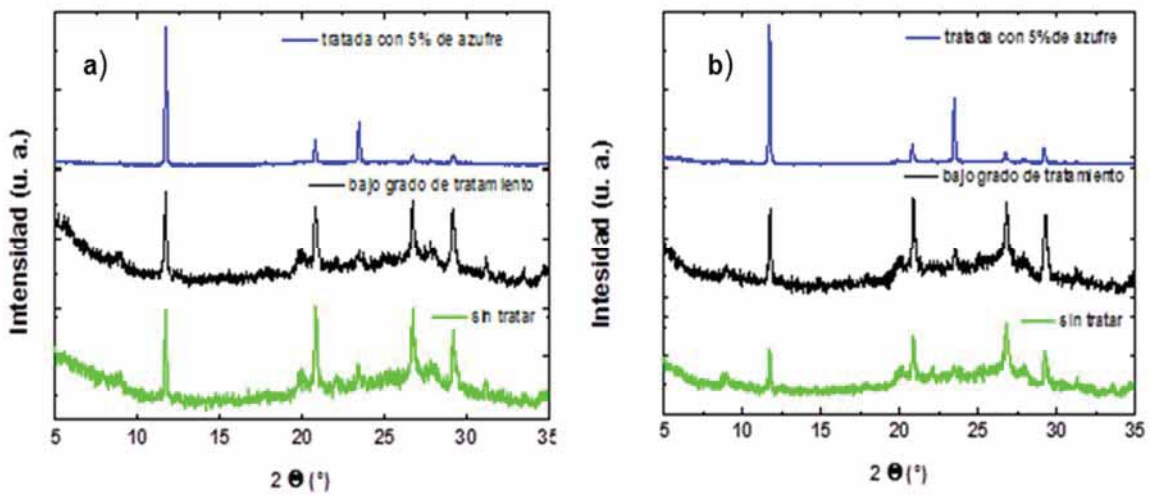


FIGURA 4. Análisis de patrones de DRX: fracción arcillosa de todas las muestras. a) En el preparado directo; b) En el preparado glicolado.

Análisis de la fracción arcillosa. En la bibliografía se reporta la importancia del rol de los microorganismos durante el proceso de biolixiviación, particularmente por su interacción con las arcillas. Esta interacción puede resultar en la disolución, precipitación y transformación de las mismas modificando drásticamente sus propiedades físicas y químicas**¡Error! Marcador no definido.**. Por esta razón y sumado al hecho que se encontraron que varios tipos de arcillas forman parte de los sedimentos remediados, se evaluaron los cambios a nivel de la fracción arcillosa extraída por DRX, SEM y EDS. Generalmente esta fracción corresponde a las partículas menores a 2 o 4 µm, pudiéndose encontrar también minerales, que no pertenecen a la familia de los filosilicatos, como los carbonatos, feldespatos, cuarzo e hidróxidos de Fe y Al (minerales accesorios o asociados). Estos últimos, están íntimamente relacionados y pueden interferir en la identificación de las arcillas[28].

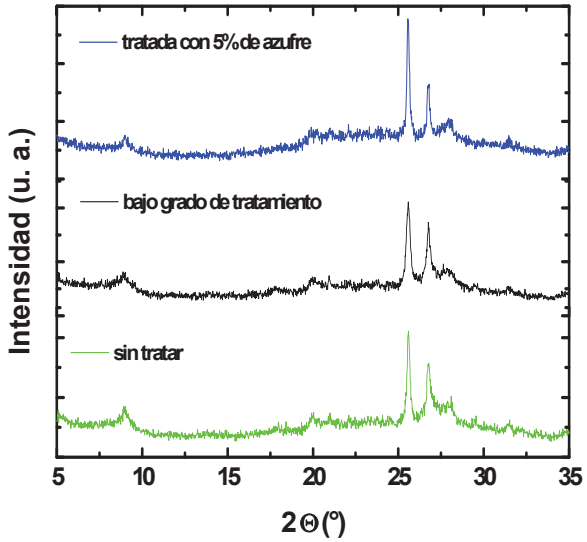


FIGURA 5. Patrones de difracción de las muestras sin tratar, con bajo grado de tratamiento y tratadas con 5% de azufre, para las partículas orientadas calcinadas.

Estimación mineral por DRX de las fracciones arcillosas: En los diagramas de difracción de las muestras sin tratar y con bajo grado de tratamiento, cuando estas son orientadas preferencialmente (**Figura 4a**), se encontraron reflexiones que se condicen con la presencia de sulfato de calcio hidratado ($CaSO_4.2H_2O$), arcillas inter-estratificadas de Illita-Montmorrillonita y posiblemente las fases individuales de cada una. En cambio, la muestra tratada con 5% de azufre, presento un patrón de gran intensidad que también se corresponde con $CaSO_4.2H_2O$ y nuevamente reflexiones (de baja intensidad) de arcillas inter-estratificadas y simples de Illita, Montmorrillonita, Clorita y Haloisita. En los diagramas de las muestras "glicoladas" (**Figura 4b**) se pudo observar que la banda que aparece a $2\theta < 7°$ indica la presencia de minerales pertenecientes a la familia de las smectitas y que esta aumenta en intensidad con respecto al preparado "directo". El resto de las reflexiones no presentan cambios significativos. En la **Figura 5** se muestran los difractogramas de las muestras "calcinadas", donde se observa que la banda a $2\theta < 7°$ colapso y que el pico a ~ 9° se ensancho, indicando la presencia de arcillas inter-estratificadas de Illita-Montmorillonita que derivan en Illitas de diferentes tipos. Además, en ambas muestras se observan los picos correspondientes a $CaSO_4$ deshidratado, presentando variaciones en la intensidad de los picos y por ende indica variaciones en la concentración de este compuesto. Este resultado está de acuerdo a las concentraciones de sulfatos determinadas en las muestras. Análisis morfológico de la fracción arcillosa por SEM: En la **Figura 6** se pueden observar las micrografías de las tres muestras de diferentes zonas y con distintos aumentos, de forma tal que sean representativas de la totalidad de las muestras.

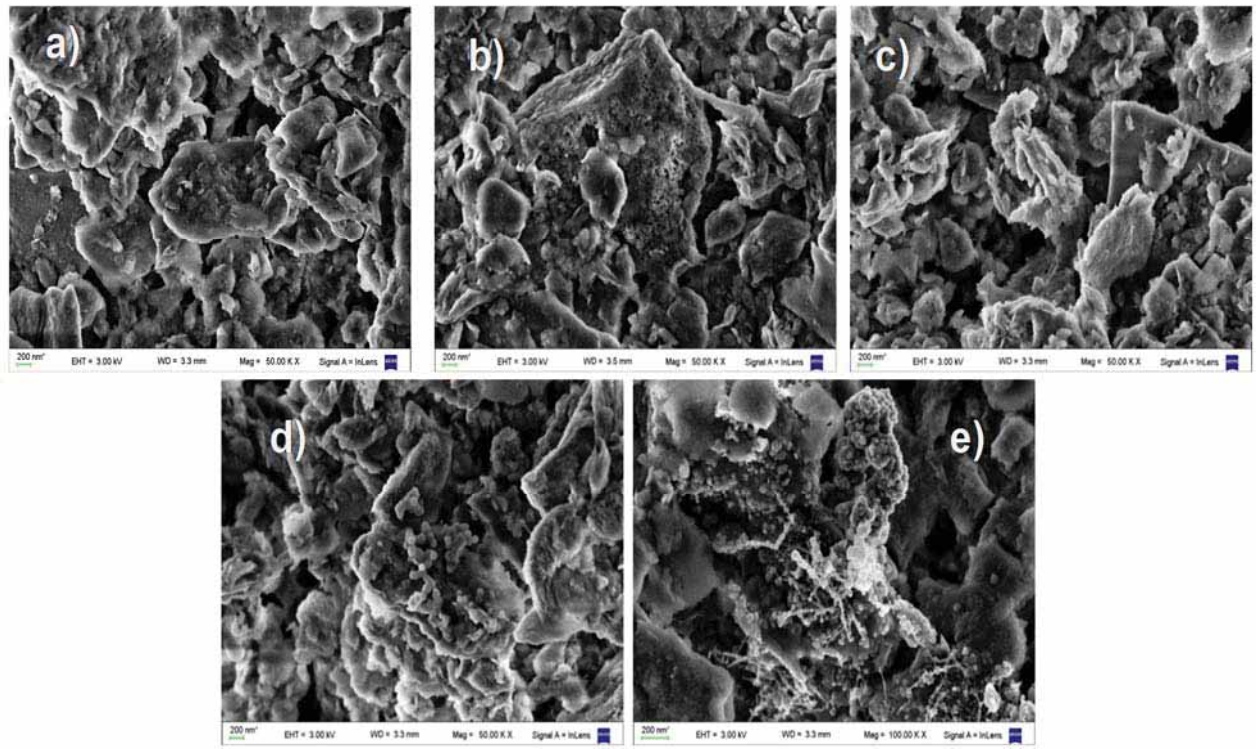


FIGURA 6. Micrografías SEM de la fracción arcillosa extraída desde los sedimentos. a) sin tratar; b) con bajo grado de tratamiento; c), d) y e) tratada con 5% de azufre.

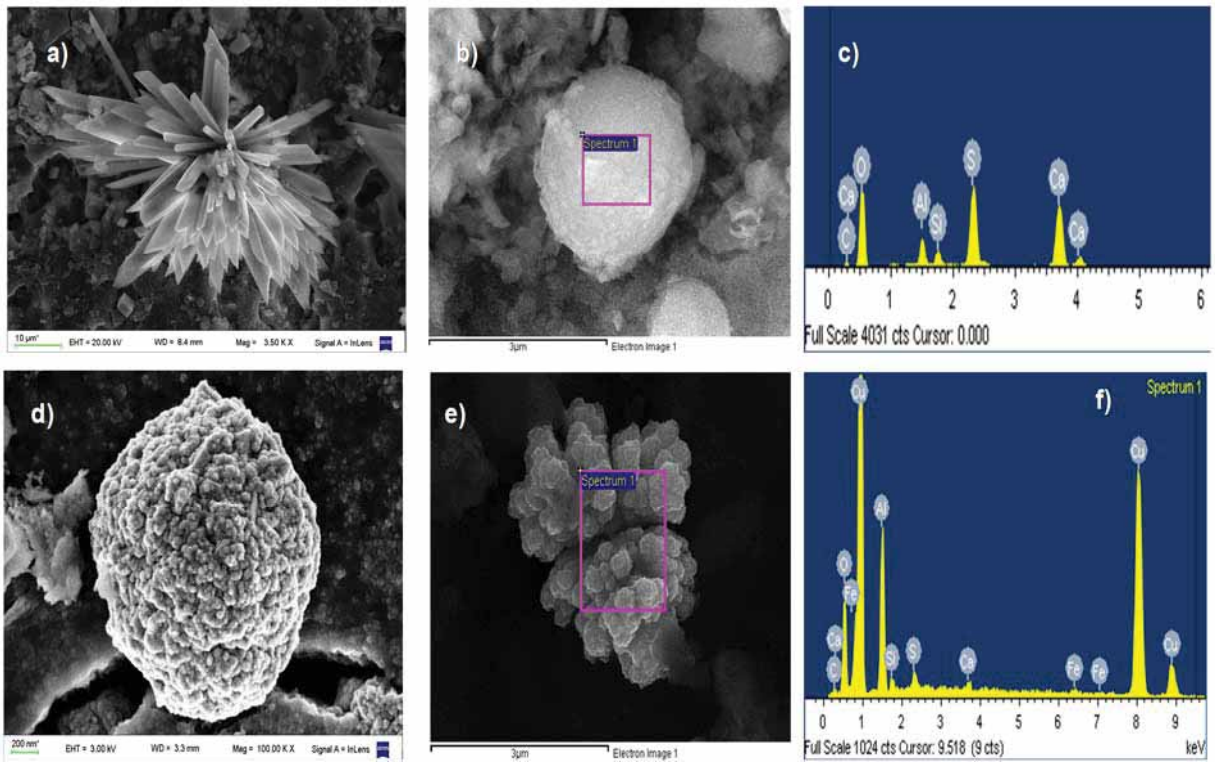


FIGURA 7. Micrografías SEM y espectros de EDS de la fracción arcillosa de la muestra tratada con azufre. a) Cristales de sulfato de Ca; b) EDS: esfera lisa; c) Espectro de EDS; d) Nano-esfera rugosa; e) EDS: superficie analizada y f) Espectro de EDS.

Se observó la morfología típica de las arcillas como partículas en forma de placas y porosidad variable (**Figura 6b**).

La muestra tratada con 5% de azufre presento una morfología muy heterogénea, ya que se observaron partículas tipo placas compactas, placas abiertas similares a estructuras “cavernosas” y nanopartículas con diversas morfologías (esféricas, hexagonales y cubicas) retenidas en la superficie de las placas (**Figuras 6d y 6e**). Se observó que las placas de partículas más compactas presentan bordes y superficies irregulares posiblemente como resultado del ataque químico generado por el bajo pH que se alcanza en consecuencia del ácido sulfúrico que se genera por el tratamiento. La espectroscopia de dispersión de energía de rayos-X (EDS) sobre las nanopartículas y los cristales observados indico que están compuesto por S, Ca y O (sobre placa de Si). Este resultado está de acuerdo a lo estimado por DRX, es decir la presencia de sulfato de calcio (**Figura 7a, 7b y 7d**). El EDS sobre algunas partículas esféricas estimo que la composición está dada por S, Ca, O, Cu, Al y Fe (**Figura 7d, 7e y 7f**). Este tipo de partículas no pudieron ser identificadas por DRX.

CONCLUSIÓN

El proceso de biolixiviación estudiado en un trabajo anterior generó una disminución apreciable en el contenido de metales del sedimento mostrando potencialidad para la remediación.

Los resultados obtenidos en este trabajo demuestran que además de la mencionada disminución de metales, el aumento en la concentración de sulfatos, cambios en pH y oxidación de sulfuros obtenidos conducen a modificaciones en la composición mineralógica y en las características superficiales y texturales del sedimento y en particular de su fracción arcillosa.

Se determinó la aparición y desaparición de minerales y sobre sus características superficiales, que derivan en un material formado por el agregado de partículas compactas macroporosas o no porosas. Estas características indican la generación de un sedimento de menor porosidad, aunque los agregados de mayor tamaño determinan características texturales más similares a un "suelo". Si bien son necesarios estudios complementarios como el análisis del cambio del volumen de poros para asegurar si existió una mejora en su permeabilidad, los cambios texturales y las observaciones en el comportamiento de las columnas de biolixiviación muestran esta tendencia, resultado que añade una potencial ventaja más al uso de biolixiviación en la remediación de este tipo de sistemas.

REFERENCIAS

1. Porzionato, N., Candal, R., Curutchet, G. Biolixiviación de metales de sedimentos anaeróbicos del Río Reconquista (Argentina) como estrategia potencial de remediación. In Proceedings 4th International Symposium on Environmental Biotechnologhy and Engenieering, (2014).
2. Castañé, P. M., Rovedatti, M. G., Topalián, M. L., Salibián, A. Spatial and temporal trends of physicochemical parameters in the water of the Reconquista River (Buenos Aires, Argentina). Environ. Monit. Assess. 117 (2006) (1-3), 135-144.
3. Defensoría del Pueblo 2007.
4. INDEC (Instituto Nacional de Estadística y Censos) (2010) Censo Poblacional Nacional. http://www.censo2010.indec.gov.ar/cuadrosDefinitivos/analisiscuarta_publicacion.pdf.
5. Di Nanno, M. P., Curutchet, G., Ratto, S. E.. S, Zn, Cr, Cu and Fe changes during fluvial sediments oxidation. Ciencia del Suelo 27 (2009) (2).
6. Di Nanno, M. P., Curutchet, G., Ratto, S. Anaerobic sediment potential acidification and metal release risk assessment by chemical characterization and batch re-suspension experiences. J. Soils Sediments 7 (2007) (3) 187-194.
7. Gutierrez, R., Grinberg, S., Curutchet, G. Participación Social en el Monitoreo y Remediación de la Contaminación Ambiental. Ambiente & Sociedade 15 (2012) (2),173-194.
8. Yin, H., Zhu, J. In situ remediation of metal contaminated lake sediment using naturally occurring, calcium-rich clay mineral-based low-cost amendment. Chem. Eng. J. (2016) 285, 112–120.
9. Jakomin, L. M., Marban, L., Grondona, S., GlokGalli, M., Martínez, D. E. Mobility of Heavy Metals (Pb, Cd, Zn) in the Pampeano and Puelche Aquifers, Argentina: Partition and Retardation Coefficients. Bull Environ. Contam. Toxicol. (2015).
10. Lombardo, R. J., O'Farrell, I., dos Santos Afonso, M. Spatial and Temporal Ion Dynamics on a Complex Hydrological System: The Lower Luján River (Bs. As., Argentina) Aquat. Geochem. 16 (2010) 293-309.
11. Teuchies, J., Bervoets, L., Cox, T., Meire, P., De Deckere, E. J. Soils Sediments 11 (2011) 364-372.
12. Förstner U. Traceability of sediment analysis. Trends in Analytical Chemistry 23 (2004) (3) 217-236.
13. Seidel H., Wennrich R., Hoffmann P., Löser C. Effect of different types of elemental sulfur on bioleaching of heavy metals from contaminated sediments. Chemosphere 62 (2006) (9) 1444-1453.
14. Cappuyns V., SwennenR., Vandamme A., Niclaes M. Environmental impact of the former Pb–Zn mining and smelting in East Belgium. J. Geochem. Explor. 88 (2006) (1) 6-9.

15. Porzionato N., Tufo A., Candal R., Curutchet G. Metal bioleaching from anaerobic sediments from Reconquista River basin (Argentina) as a potential remediation strategy. Environ. Sci. Pollut. R. (2016) 1-10.
16. Calmano W., Hong J., Förstner U. Binding and mobilization of heavy metals in contaminated sediments affected by pH and redox potential. Water Sci. Technol. 28 (1993) (8-9) 223-235.
17. Löser C., Zehnsdorf A., Hoffmann P., Seidel H. Remediation of heavy metal polluted sediment by suspension and solid-bed leaching: estimate of metal removal efficiency. Chemosphere 66 (2007) (9) 1699-1705.
18. Zehnsdorf A., Seidel H., Hoffmann P., Schlenker U., Müller R. A. Conditioning of sediment polluted with heavy metals using plants as a preliminary stage of the bioremediation process: a large-scale study. J. Soils Sediments 13 (2013) (6) 1106-1112.
19. Silverman M. P., Lundgren D. G. Studies on the chemoautotrophic iron bacterium Ferrobacillus ferrooxidans: I. An improved medium and a harvesting procedure for securing high cell yields. J. Bacteriol. 77 (1959) (5) 642.
20. JADE Version 7 Software-XRD Processing Identification and Quantification, Materials Data, Inc., (2004).
21. Brunauer S., Emmett P. H., Teller E. Adsorption of gases in multimolecular layers. J. Am. Chem. Soc. 60 (1938) 2, 309-319.
22. Delgado Calvo-Flores R., Delgado Calvo-Flores G., González Martínez D., Barahona Fernández E. (1996) Patente: Procedimiento para la extracción y extractor, automáticos de arcilla en suspensión, para muestreo rápido.
23. Gadd G. M. Metals, minerals and microbes: geomicrobiology and bioremediation. Microbiology 156 (2010) (3) 609-643.
24. Jaisi D. P., Eberl D. D., Dong H., Kim J. The formation of illite from nontronite by mesophilic and thermophilic bacterial reaction. Clay Clay Miner. 59 (2011) (1) 21-33.
25. Dong H. Clay–microbe interactions and implications for environmental mitigation. Elements 8 (2012) (2) 113-118.
26. Favre F., Stucki J. W., Boivin P. Redox properties of structural Fe in ferruginous smectite. A discussion of the standard potential and its environmental implications. Clay Clay Miner. 54 (2006) (4) 466-472.
27. Rouquerol J., Rouquerol F., Llewellyn P., Maurin G., Sing K. S. Adsorption by powders and porous solids: principles, methodology and applications. Academic Press (2013).
28. Heller-Kallai L., Bergaya F., Theng B. K. G., Lagaly G. Handbook of Clay Science. Developments in Clay Science (2006).

CHAPTER 3.6 MANGANESO GEOGÉNICO EN AGUA SUBTERRÁNEA: CASO DE ESTUDIO EN HIDALGO, MÉXICO

D. A. Rivera-Rodríguez (1); R. I. Beltrán-Hernández (1); C. Coronel-Olivares (1); M. Villanueva-Ibáñez (2); C. A. Lucho-Constantino (1) and **G. Vázquez-Rodríguez ***(1)

(1) Área Académica de Química, Universidad Autónoma del Estado de Hidalgo, Carr. Pachuca-Tulancingo km. 4.5. Mineral de la Reforma, Hidalgo, México.
(2) Universidad Politécnica de Pachuca, Ex-Hacienda de Santa Bárbara, Carr. Pachuca-Cd.Sahagún km 20. Zempoala, Hidalgo, México.

RESUMEN

En México el agua subterránea es un recurso de enorme trascendencia, debido a que representa el 60% del agua consumida por la población y la industria. Sin embargo, la información relativa a su calidad es escasa. Existen reportes de que en la localidad de Santa Cruz (Apan, Hidalgo, México) se abastece agua subterránea con características compatibles con la presencia excesiva de Mn. Por tal razón, el objetivo de este trabajo fue evaluar la calidad fisicoquímica y microbiológica del agua de esta localidad. Según los resultados obtenidos, el agua subterránea del sitio tiene una concentración de sales reducida (con rangos de CE de 454-515 μS/cm y de STD de 139-258 mg/L, respectivamente) y está escasamente mineralizada. Los contenidos de materia orgánica y de contaminantes nitrogenados fueron bajos y cumplieron con lo establecido por la normatividad mexicana vigente. Se detectó también la presencia de ciertos indicadores microbiológicos, en particular de *Escherichia coli*, que señalaron contaminación del acuífero, posiblemente debida a la percolación de excretas animales desde la superficie, o bien a fugas de aguas residuales. Sin embargo, el mayor obstáculo para el consumo del agua es la concentración de Mn encontrada, que en promedio es de 5.6±0.35 mg/L y es muy probablemente geogénica. Debido a hallazgos recientes que relacionan la ingesta de Mn con desórdenes neurológicos, principalmente en niños, la normatividad mexicana y la Organización Mundial de la Salud establecen valores máximos de Mn en agua potable de 0.15 y 0.4 mg/L, respectivamente. Por lo tanto, es necesario proporcionar alternativas de remoción de Fe, Mn, Pb y *E. coli* del agua de este pozo que permitan su consumo seguro.

Palabras claves: Acuífero, contaminación geogénica, potabilización

INTRODUCCIÓN

El manganeso (Mn) es un metal traza ubicuo en la naturaleza. En la corteza terrestre se encuentra en forma de óxidos, carbonatos y silicatos, tanto en rocas como en suelos, y es parte de la familia del hierro, al que se encuentra asociado en procesos geoquímicos[1]. El Mn es el décimo elemento más abundante en la corteza terrestre y el

---

*Author for correspondence: g.a.vazquezr@gmail.com

segundo metal pesado más común después del hierro[2]. Puede existir en varios estados de oxidación, pero las formas más comunes en el medio ambiente son Mn(II) y Mn(IV), que son respectivamente soluble e insoluble. Es un elemento traza esencial para la mayoría de los seres vivos, en particular para plantas y otros organismos fotosintéticos, ya que es crucial para el funcionamiento del complejo de evolución del oxígeno. Asimismo, a bajas concentraciones, es indispensable para la salud humana[1].

El Mn se encuentra comúnmente en fuentes de abastecimiento de agua potable, tales como aguas subterráneas; ahí, es frecuente la forma reducida Mn(II), que es soluble, a concentraciones que pueden variar entre menos de 1 μg/L a 550 μg/L[3]. A concentraciones excesivas, el Mn aporta un sabor metálico al agua, tiñe ropa y superficies y, una vez oxidado, forma depósitos en la infraestructura de distribución del agua. Además, recientemente se han reportado relaciones significativas entre la exposición al Mn (vía el consumo de agua potable) y efectos neurotóxicos en niños, como deficiencias intelectuales alteraciones motoras e hiperactividad[4]. Por tales motivos, la Organización Mundial de la Salud ha fijado un límite máximo permisible de 0.4 mg/L para agua potable[5]; en México, este límite es de 0.15 mg/L[6].

Aunque el Mn puede estar presente en acuíferos debido a factores antrópicos tales como la minería o el uso de pesticidas (*i.e.*, fungicidas ditiocarbámicos como el mancozeb), una gran parte de los estudios señala causas geogénicas[7]. Entre estas se encuentran la geoquímica de las rocas y la química del agua[1]. Por ejemplo, las rocas máficas y ultramáficas, las lutitas, las grauvacas y la piedra caliza tienen contenidos elevados de Mn, que por procesos de intemperismo conducen a concentraciones altas de Mn en aguas subterráneas[1]. Otros factores, como el pH, el potencial redox (Eh) y las concentraciones de oxígeno y de carbono orgánico disueltos, gobiernan la especiación y la movilidad del Mn en medio acuoso. Así, a pH 7 y a un Eh máximo de 800 mV, el manganeso se encuentra como Mn^{2+}.

Aunque en México el agua subterránea es la principal fuente de abastecimiento para la población y la industria (60%), la sustentabilidad de su manejo está en riesgo por la constante inducción de agua de baja calidad[8]. Asimismo, la información acerca de su calidad es escasa, y se refiere principalmente a los acuíferos afectados por intrusión salina. En consecuencia, la población de numerosas regiones de México se abastece con agua cuya calidad no ha sido evaluada, lo que en el pasado ha resultado en serios efectos a largo plazo[9]. Existen reportes de que en la localidad de Santa Cruz (Apan, Hidalgo, México) se suministra agua subterránea con características compatibles con la presencia excesiva de Mn. Por tal razón, el objetivo de este trabajo fue evaluar la calidad fisicoquímica y microbiológica del agua de esta localidad.

MATERIALES Y MÉTODOS

Área de estudio. La localidad de Santa Cruz se encuentra en el municipio de Apan, en Hidalgo, México (**Figura 1**). La localidad se ubica entre los paralelos 19° 36’ y 19° 52’ de latitud norte y los meridianos 98°17’ y 98° 34’ de longitud oeste, a una altitud de 2570 msnm.



FIGURA 1. Ubicación de la zona de estudio.
Fuente: http://apan.blogia.com/pagina/8/

Toma y análisis de muestras. Se tomaron cinco muestras a intervalos mensuales en el pozo de la localidad, las cuales se analizaron *in situ* mediante un analizador Hanna Instruments® en términos de temperatura, pH, conductividad eléctrica (CE), potencial redox (Eh), sólidos totales disueltos (STD), salinidad y oxígeno disuelto. Las concentraciones de Fe, Mn, Na, Pb y Na se midieron por absorción atómica en un espectrofotómetro Perkin-Elmer ICP-OES (E.U.A.). Las muestras también se analizaron para determinar $N\text{-}NH_4^+$, $N\text{-}NO_2^-$, $N\text{-}NO_3^-$ y DQO según métodos estándar[10]. Otra parte de las muestras, destinada a los análisis microbiológicos, se recogió en bolsas Whirl Pak®, y se mantuvo a 4°C hasta su análisis; posteriormente se filtraron alícuotas de 100 mL en membranas de nitrocelulosa de 0.45 μm de tamaño de poro, que luego se sembraron en un agar no selectivo para la cuantificación de heterótrofos en placa y en agares selectivos para el análisis de estafilococos, *Enterococcus* sp., *Pseudomonas* sp., hongos y levaduras, *Clostridium* sp., *Escherichia coli*, *Salmonella enteriditis*, *Shigella flexneri* y *Enterobacter aerogenes*.

RESULTADOS Y DISCUSIÓN

Análisis in situ. La **Tabla 1** concentra los valores encontrados *in situ* luego de los distintos muestreos. Según estos, el agua subterránea del sitio tiene una concentración de sales reducida (con rangos de CE de 454-515 μS/cm y de STD de 139-258 mg/L, respectivamente) y está escasamente mineralizada. Nuestros valores son inferiores a los que reportan Huizar-Álvarez et al.[11] para un extenso muestreo realizado en la subcuenca Apan-Tochac, a la que pertenece el acuífero de Santa Cruz. En el citado estudio, se reporta en promedio 7.7, 274 μS/cm y 312.4 PSU para el pH, la CE y los STD, respectivamente. Este estudio asocia los menores valores de sólidos y sales a los pozos situados en las zonas más altas y que corresponden a los sitios de recarga de los acuíferos, lo cual probablemente sea el caso para el pozo de Santa Cruz.

Análisis fisicoquímicos. Las concentraciones de Fe, Mn, Pb y Na determinadas se muestran en la **Figura 2**. Los valores medios corresponden a 0.54, 5.67, 0.033 y 24.05 ppm, respectivamente. No se encontró As en las muestras analizadas. La bibliografía señala que, por lo general, las altas concentraciones de Mn se acompañan de altas concentraciones de Fe[12], pero en nuestro caso estas fueron en promedio diez veces

TABLA 1. Características del agua subterránea medidas *in situ*

Parámetro	Valor*
Temperatura	19.74±1.60
pH	6.74±0.20
Conductividad eléctrica [μS/cm]	473±27
Potencial redox [mV]	-13.5±8.06
Sólidos totales disueltos [ppm]	236.67±13.43
Salinidad (PSU)	0.23±0.01
Oxígeno disuelto [ppm]	3.83±0.53

* Valor medio±desviación estándar (n =5)

menores a las de Mn. Dado que los límites máximos permisibles por la modificación a la NOM-127-SSA1-1994 para el Fe, Mn, Pb y Na son 0.3, 0.15, 0.01 y 200, se constató que el agua del pozo debe recibir un tratamiento para que los niveles de Fe, Mn y Pb cumplan con la normatividad vigente. En el estudio anteriormente citado de Huizar-Álvarez et al.[11] no se analizaron las concentraciones de Fe, Mn o Pb; en cambio, sí se cuantificó el Na, que se reportó con un valor promedio muy similar (*i.e.*, 24.9 ppm) al encontrado en nuestro estudio (24.0 ppm).

Las concentraciones de Mn encontradas en Santa Cruz, Hidalgo, sobrepasan todos los datos que pudimos recopilar para acuíferos en México. Piña y Ramírez[13] mencionan que el agua de abastecimiento de la ciudad de Guaymas, Sonora, presenta 0.5 ppm, y que en su fuente (*i.e.*, los pozos del Río Yaqui) pueden determinarse concentraciones comprendidas entre 0.1 y 1.5 ppm. En el mismo trabajo, se refieren niveles de Mn en agua subterránea de 0.39-0.54 en Veracuz, Veracruz; de 0.4-0.5 en Culiacán, Sinaloa, y de 1.3 ppm en Navojoa, Sonora. La mayor concentración que reporta este estudio es el límite superior del rango de 0.16-4.61 ppm que se encontró en los pozos profundos que suministran agua potable a la zona norte de Ciudad Nezahualcoyotl, Estado de México[13].

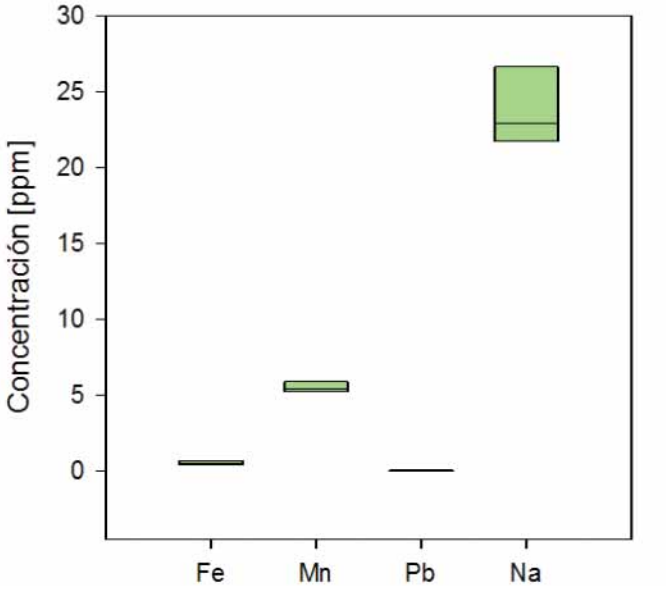


FIGURA 2. Concentraciones de metales determinadas en el agua subterránea

Las concentraciones de contaminantes nitrogenados se muestran en la **Figura 3**. En promedio, se determinaron 0.081, 0.015 y 0.053 ppm de $N\text{-}NH_4^+$, $N\text{-}NO_2^-$ y $N\text{-}NO_3^-$. Estas concentraciones cumplen con los límites máximos establecidos por la NOM-127-SSA1-1994, a saber, 0.5, 0.1 y 10 ppm, respectivamente. Asimismo, el contenido promedio de DQO fue de 9.8 ppm. Aunque este último parámetro no está contemplado por la NOM-127-SSA1-1994, el valor obtenido puede considerarse adecuado para agua potable ya que está justo por debajo del valor guía establecido por la OMS (10 ppm)[5].

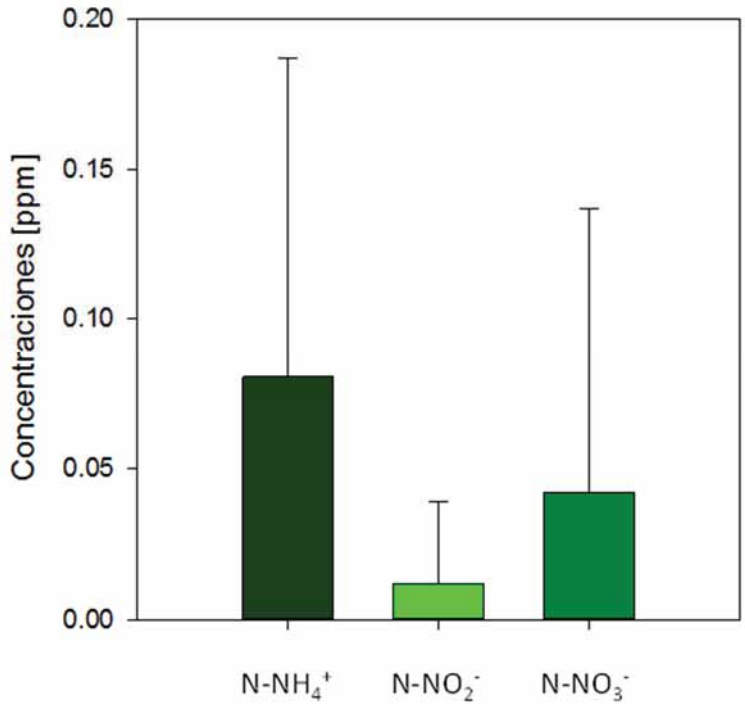


FIGURA 3. Contaminantes nitrogenados presentes en el agua subterránea

Análisis microbiológicos. *Enterobacter aerogenes* y *Enterococcus* sp. no fueron encontrados en ninguna de las muestras analizadas (n=5), mientras que *Salmonella enteriditis* y *Shigella flexneri* solo fueron detectados en una de las muestras (a razón de 1 y 2 UFC/100 mL, respectivamente). Las densidades de los microorganismos detectados se presentan en la **Figura 4**. Se destaca la presencia de *Escherichia coli* (con un promedio de 2.5 UFC/100 mL), ya que la NOM-127-SSA1-1994 estipula que debe estar ausente en agua destinada a abastecimiento público. Esta contaminación probablemente se debe a la percolación de excretas animales desde la superficie, o bien a fugas de aguas residuales.

En otros estudios realizados en acuíferos del estado de Hidalgo también se ha reportado contaminación microbiológica, por lo general debida a infiltraciones de aguas residuales desde la superficie o a fugas en el sistema de drenaje. En pozos localizados en el Valle del Mezquital, específicamente en Teocalco y Tezontepec de Aldama, se han determinado concentraciones de coliformes fecales de 1.3 y 4.2 NMP/100 mL, respectivamente[14]. En esta zona se utiliza desde principios del siglo XX el agua residual doméstica proveniente del Valle de México para riego, con la cual los acuíferos se

recargan de modo artificial[14]. En otro acuífero del estado de Hidalgo, el de Cuautitlán-Pachuca, se encontró contaminación por amibas en los seis pozos analizados[15]. Así, al igual que el agua de estos pozos, el agua de Santa Cruz deberá recibir una desinfección adecuada antes de abastecer a la población.

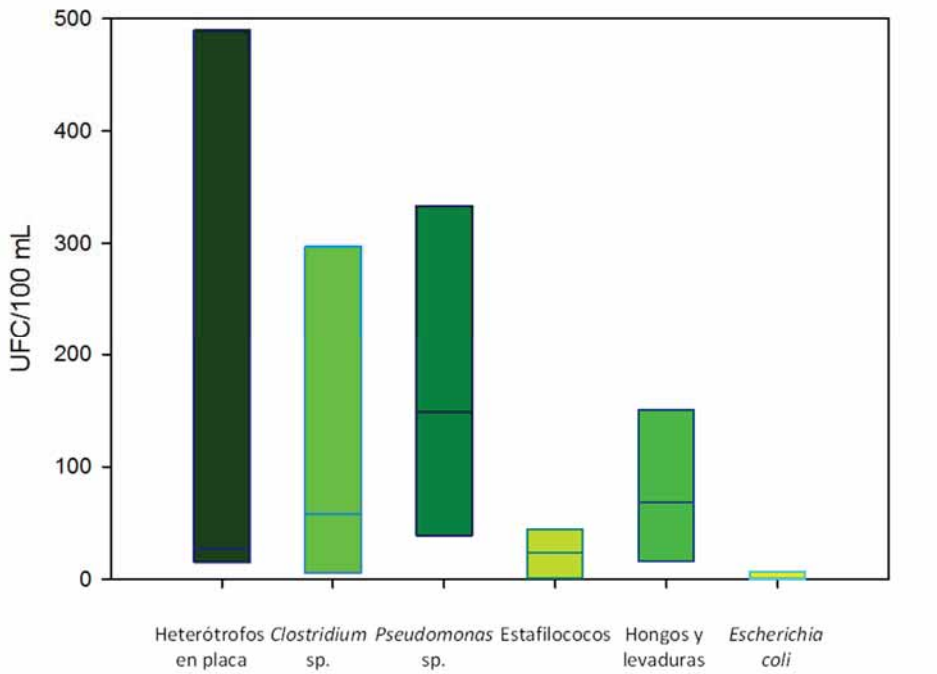


FIGURA 4. Contaminantes microbiológicos encontrados en el agua subterránea. Se presentan la mediana y los rangos entre percentiles 10-90

CONCLUSIÓN

Los análisis realizados permitieron establecer que el agua subterránea de la comunidad de Santa Cruz es de escasa salinidad y mineralización. Sin embargo, presenta concentraciones de Fe, Mn, Pb y *E. coli* que sobrepasan los límites establecidos por la normatividad vigente. En particular, el contenido de Mn encontrado en este pozo sobrepasa todos los datos que pudimos recopilar para acuíferos en México. En consecuencia, es necesario proporcionar alternativas de remoción de Fe, Mn, Pb y *E. coli* del agua de este pozo que permitan su consumo seguro.

AGRADECIMIENTOS

Los autores agradecen el financiamiento proporcionado por el proyecto de la Red Temática de Ingeniería de Procesos Avanzados de Sistemas Ambientales SEP/PRODEP.

REFERENCIAS

1. Homoncik S.C., MacDonald A.M., Heal K.V., Dochartaigh B.É.Ó., Ngwenya B.T. Manganese concentrations in Scottish groundwater. Sci. Total Env. 408 (2010) 2467-2473.
2. Post J.E. Manganese oxide minerals: Crystal structures and economic and environmental significance. Proc. Natl. Acad. Sci. USA 96 (1999) 3447-3454.
3. Kabata-Pendias A., Mukherjee A.B. Trace elements of group 7. En *Trace elements from soil to human*, Springer (2007) 193-208.
4. Bouchard M.F., Sauvé S., Barbeau B., Legrand M., Brodeur M.È., Bouffard T., Limoges E., Bellinger D.C., Mergler D. Intellectual impairment in school-age children exposed to manganese from drinking water. Environ. Health Perspect. 119 (2011) 138-143.
5. WHO Guidelines for Drinking-water Quality, 4th edition, World Health Organization (2011).
6. Modificación a la Norma Oficial Mexicana NOM-127-SSA1-1997, Salud ambiental. Agua para uso y consumo humano. Límites permisibles de calidad y tratamiento a que debe someterse el agua para su potabilización (2000).
7. de Joode B.V., Barbeau B., Bouchard M.F., Mora A.M., Skytt Å., Córdoba L., Quesada R., Lundh T., Lindh C.H., Mergler D. Manganese concentrations in drinking water from villages near banana plantations with aerial mancozeb spraying in Costa Rica: Results from the Infants' Environmental Health Study (ISA). Environ. Pollut. 215 (2016) 247-257.
8. Domínguez J.S., Carrillo-Rivera J.J. El agua subterránea como elemento de debate en la historia de México. En *México en tres momentos*: *1810-1910-2010*, Universidad Nacional Autónoma de México (2007).
9. Carrillo-Rivera J.J., Cardona A., Huizar-Alvarez R., Graniel E. Response of the interaction between groundwater and other components of the environment in Mexico. Environ. Geol. 55 (2008) 303-19.
10. APHA. Standard methods for the examination of water and wastewater, 22nd edition, American Public Health Association/American Water Works Association/Water Environment Federation (2012).
11. Huizar-Alvarez R., Méndez-García T., Madrid-Ríos R. Hidrogeoquímica del agua subterránea de la subcuenca de Apan-Tochac, Hidalgo, México. Rev. Mex. Cienc. Geol. 16 (1999) 89-96.
12. Davraz A. Studies of Geogenic Groundwater Contamination in Southwestern Anatolia, Turkey. Procedia Earth Planetary Sci. 15 (2015) 435-441.
13. Piña M., Ramírez A. Remoción de Hierro y Manganeso en Fuentes de Agua Subterránea para Abastecimiento Público. En Agua potable para comunidades rurales, reuso y tratamientos avanzados de aguas residuales domésticas, Red Iberoamericana de Potabilización y Depuración del Agua y Centro Interamericano de Recursos del Agua, Facultad de Ingeniería de la Universidad Autónoma del Estado de México (2003). http://tierra.rediris.es/hidrored/ebooks/ripda/index.html#
14. Pérez R., Jiménez R., Jiménez B.E., Chávez A. ¿El agua del valle del Mezquital, fuente de abastecimiento para el Valle de México? Documento de trabajo. http://www.bvsde.paho.org/bvsaidis/saneab/mexicona. 2009.
15. Ramírez Flores E., Valderrama E.R., Patiño R.A., Rodríguez B.M. Calidad amebológica del agua de pozos utilizados para suministro de agua potable en el Estado de Hidalgo. Ingeniería FI-UADY 16 (2012) 219-228.

Section 4.
Green Materials and Biomaterials

Page

Chapter 4.1 Development of green hygienic coating based on essential oil microcapsules 269
S. Bogdan; M. C. Deyá; R. Romagnoli and M. V. Revuelta

Chapter 4.2 Nuevas fuentes de taninos que pueden ser utilizados como agentes curtientes en reemplazo de las sales de cromo 280
A. Bonfranceschi Barros*; G. Mazzilli; J.A. Markán; L.M.I. López, L.M.I. and J.E. Martegani

Chapter 4.3 Improved strength and durability of concrete through metabolic activity of ureolytic bacteria 285
N. Balagurusamy; M.J. Castro Alonso; C.E. López Ortiz; S.O. Garcia Perez; R. Narayanasamy; G.J. Fajardo San Miguel and H. Herrera Hernández

Chapter 4.4 Evaluación de la producción de biogás de biomasas no convencionales 295
F. Cerutti; V. Córdoba and E. Santalla

Chapter 4.5 Proteolytic extracts of three bromeliaceae species as eco-compatible tools for leather industry 307
M. E. Errasti; N. O. Caffini and L. M. I. Lopez

Chapter 4.6 Estudio de nanocompuestos de almidón termoplástico reforzados con bentonita modificada obtenidos mediante extrusión reactiva 318
M. P. Guarás; L. N. Ludueña and V. A. Alvarez

Chapter 4.7 Experimental study and mathematical modeling for lead removal via a photosynthetic consortia using evolutionary optimization approach 326
B. Camacho Pérez; D. J. Hernández Melchor; P. A. López Pérez; A. Alberto Murrieta; S. Carrillo Vargas and E. González Gómez

Chapter 4.8 Optimization of a method of feather biodegradation of chicken 338
M. E. Pahua-Ramos; D. J. Hernández-Melchor; B. Camacho-Pérez; G.I. Cerón-Montes and M. Quezada Cruz*

Chapter 4.9 Vermicomposteo de lodos residuales del reciclado de papel mezclados con residuos sólidos orgánicos de manejo especial 348
I. J. Rodríguez Meléndez; F. Robles Martínez and M.O. Franco Hernández

Chapter 4.10 Nanoaptasensor para la detección de escherichia coli en agua potable: modificación de ntcs para alta sensibilidad 353
E. K. Velazquez; I. Morales-Reyes; F. Ramírez-Vives; A. Abad-Sánchez; M. Picquart; O. Monroy-Hermosillo and N. Batina

CHAPTER 4.1 DEVELOPMENT OF GREEN HYGIENIC COATING BASED ON ESSENTIAL OIL MICROCAPSULES

S. Bogdan *(1); M. C. Deyá (2); R. Romagnoli (1,3) and M. V. Revuelta (1,3)

(1) CIDEPINT (Centro de Investigación y Desarrollo en Tecnología de Pinturas) (CONICET-CIC), Av. 52 entre 121 y 122 (B1900AYB), La Plata, Argentina.
(2) Facultad de Ingeniería, Universidad Nacional de La Plata, 1900, La Plata, Argentina.
(3) Facultad de Ciencias Exactas, Universidad Nacional de La Plata, 1900, La Plata, Argentina.

ABSTRACT

The challenges for developing new materials are accomplishing more functionality with less material due to the increasing efficiencies of the smart approaches. In this sense, the coating technology based on the incorporation of microcapsules has emerged recently as a strategy in the advance of protective and functional materials, promising an environmentally friendly approach. Microbial colonization of painted surfaces is a major concern because it shortened the useful life of the coating by discoloration and degradation. Besides there is a great concern about the indoor microbial colonization especially in places that should have high standards of environmental hygiene as in the food industry and those related to human health-care. The aim of this work is to develop a novel green antifungal water-borne paint formulated with melamine-formaldehyde (MF) microcapsules containing essentials oil as biocide agent. The microcapsules were synthesized by interfacial polymerization. Melamine-formaldehyde resin was used for the microcapsule shell wall, and two different essential oils (EOs) as core materials. The EOs studied were Tea Tree and Lavandin Abrialis. Microcapsule morphology was examined by Field-Emission Scanning Electron Microscopy (FE-SEM), while their size distributions were determined by light diffraction (LD). Microcapsule composition (shell and core) was analyzed by FTIR-ATR spectroscopy. Preparation of acrylic water-borne paint was done in a high speed disperser. The microcapsules (MF-Tea tree and MF-Lavandin) were incorporated into the original paint just before used, at 6% by weight of the total paint composition. As negative control a paint without biocide was used. The effectiveness of these microcapsules on paint film was evaluated by plaque inhibition assay. Commercial gypsum boards were used as substrate. Each painted panel was inoculated with 100 µl of the spore suspension of *Aspergillus sp*. and kept in a culture chamber at 86% relative humidity for 4 weeks. The fungal growth was estimated as a percentage of coverage onto the surface and scored according to ASTM D5590 standard specification. The results obtained in antifungal assay on paint film were promising. According to ASTM D5590, the score obtained by MF-lavandin paint was 1, which indicate just a trace growth onto the painted surface (<10%). On the other hand, the control and MF-Tea tree paints obtained the same score: 4 points, the highest qualification (fungal growth >70%). Comparing those results, it can be seen that

---

*Author for correspondence: m.revuelta@cidepint.gov.ar

Aspergillus sp. growth reduction was significant when MF-lavandin paint was used, suggesting that those microcapsules had an inhibitive activity on the dry film whereas MF-Tea tree had not such activity.

Keywords: antifungal paint; essential oil; Lavandin Abrialis; microencapsulation

INTRODUCTION

Microbial colonization of painted surfaces is a mayor concern because it shortened the useful life of the coating by discoloration and degradation. Besides there is a great concern about the indoor microbial colonization especially in places that should have high standards of environmental hygiene, as in the food industry and those related to human health-care. Among the most deleterious organisms are fungi, a very large and diverse group which is found in practically every ecological niche. The genera most frequently isolated inside buildings are *Penicillium*, *Aspergillus*, *Cladosporium* and *Alternaria*[1-4].

The antimicrobial coatings can supply an extra line of defense for maintaining hygiene standards. The most important property of hygienic coatings is its antimicrobial activity (against bacteria, viruses, fungi and spores) but they also need to be non-toxic and non-allergic to humans while, at same time, they must be non odorous, durable and cost effective [5]. The water-borne paints are complex mixtures of polymers, pigments and functional additives. In these paints the vehicles is an emulsion of resin in water, and have been created as alternative to solvent borne paint because of the volatile organic compound (VOC) content in these paints is significantly lower, thereby reducing VOC emissions. Waterborne paints dry by evaporation of the water. The coalescing solvents allow the resin particles to fuse together (coalesce) as the water evaporates to form a continuous coating. The disadvantage of these paints is the high content of additives required for its formulation, all susceptible to biodeterioration[6-8].

Conventional additives used as biocides in paints and coatings are often toxic, causing environmental pollution and health problems [9,10]. An eco-friendly alternative for replacement could be the use of natural products, such as essential oils.

Essential oils (EOs) are known for their antiseptic, i.e. bactericidal, and fungicidal, and medicinal properties so; they are commonly used in pharmaceutical, cosmetic and food industries. Generally, EOs are volatile substances sensitive to oxygen, light, moisture, and heat, characterized by a strong odour. They are formed by aromatic plants as secondary metabolites[11,12]. These reported special characteristics could impair their applicability.

The coating technology based on the incorporation of microcapsules has emerged recently as a strategy in the advance of protective and functional materials, promising an environmentally friendly approach. The challenges for developing new materials are to accomplish more functionality with less material due to the increasing efficiencies of the smart approaches

Microencapsulation provides many benefits for coatings containing biocides. The microcapsule protects the biocide from degradation and allows the proper control of the release process, prolonging thereby the duration of the biocidal effect and reducing the

waste of biocides. In this sense, essential oils had been reported more effective when they are microencapsulated, thus improving their long-term function and durability [13]. There are several chemical methods for the microencapsulation of essential oils such as in situ polymerization, coacervation, and interfacial polymerization [14]. The in situ polymerization relies on prepolymers formed in a continuous phase. Urea and melamine, along with formaldehyde, have usually been used for the synthesis, and the characteristics of microcapsules, such as morphology and particle size distribution, rely on the preparation conditions including the rate of shear, the shearing period, the kind of emulsifier used, and the viscosity of the core material.

The aim of this work is to develop a novel green antifungal water-borne paint formulated with melamine-formaldehyde (MF) microcapsules containing essentials oil as biocide agent.

MATERIALS AND METHODS

Materials. Poly (ethylene-alt-maleic anhydride) (Poly (E-MA)), formic acid and Tea Tree (*Melaleuca alternifolia*) oil were purchased from Sigma Aldrich (Argentina). The commercial melamine-formaldehyde (MF) prepolymer Beetle® PT312 (73% solids content and 0.2% to 0.3% free formaldehyde) was purchased from BIP Limited (Oldbury, UK). The essential oil Lavandin (*Lavandula hybrid var. Abrialis)* was purchased from Indukern (Brazil). Agar-agar was supplied by Parafarm (Argentina) and proteose peptone was purchased from Oxoid (Tecnolab, Argentina). All materials were used as received without further purification.

Preparation of the MF microcapsules by in situ polymerization. The MF microcapsules were prepared using a modified *in situ* polymerization procedure[15]. MF resin was used for the microcapsule shell wall and two essential oils (EO) as core materials. The biocide agents studied were the essential oil of Tea Tree (TTO) and Lavandin (LVO). Experimentally, 2.55 g of MF resin was first dissolved (in a 250 mL beaker) in 30 g of water containing the surfactant Poly (E-MA) (3.3% w/w) and sodium hydroxide (1.4% w/w). Then, 17 g of essential oil was added slowly to the aqueous continuous phase under stirring to form the emulsion. The resulting mixture was stirred at 1000 rpm for 1 hour. After this time, the pH of the reaction mixture was adjusted to 5 using formic acid, and the temperature of the reaction was raised up to 70 ºC and maintained for 3 hours under stirring. After 3 hours, the synthesized MF microcapsules were cooled down to room temperature, cleaned with methanol/water and resuspended in water.

Characterization of the microcapsules

Scanning electron microscope (SEM). The morphology of MF-Essential oil microcapsules was examined by Field-Emission Scanning Electron Microscopy (FE-SEM) on a FEI Quanta 650 microscope using aluminium tape as support. Before imagining, the samples were coated by Au-Pd.

Particle size distribution. The average diameter of the MF-Essential oil microcapsule and its size distributions were determined by light diffraction (LD) on a Mastersizer 2000 (Malvern Instruments). The particle size was expressed as the equivalent volume

diameter and three replicates were performed for each batch of microcapsules, in order to reduce error, an average curve was calculated and analyzed. Microcapsules were dispersed in water in a sonicator before testing.

Fourier transform infrared (FT-IR) spectroscopy. The infrared spectra of the MF-Essential oil microcapsules and that of paint film containing MF-EO microcapsules, as KBr pellets, were obtained by a FT-IR (Spectrum, Perkin Elmer, USA) spectrometer according to diamond ATR method, in order to identify their chemical structure. The FT-IR spectra were recorded in the 4000 to 400 cm^{-1} range and scanned with background correction at 60 scans with 4 cm^{-1} resolutions.

Fungal strain and culture. *Aspergillus sp*, isolated from contaminated interior paints, was used in the study. The main reasons for choosing *Aspergillus* was that this fungus is a primary colonizer of building materials because its low water activity request, fast growth, easy viewing and major resistance to biocides[1,16].

The fungus was cultured in agarized media (MCA: 1.5g agar-agar, 1.0g dextrose, 0.5 g protease peptone, 0.1g KH_2PO_4, 0.05g $MgSO_4$ and distilled water up to 100 mL) and incubated at 28º C for 7 days. The spore suspension was prepared from a MCA culture and incubated in the conditions before mentioned. The spores were removed from the plate and placed in a test-tube with 5 mL of NaCl 0.85% (w/v) and 0.005% (w/v) of Tween-20. The spore concentration was adjusted to 10^6 spores /mL employing a Neubauer chamber.

Paint formulation. Acrylic water-borne paint was formulated without any kind of biocide; the composition is shown in **Table 1**. Paint preparation was done in a high speed disperser. In the first step water was mixed with dispersing, antifoaming and thickener additives. Then, the pigments (titanium dioxide, calcium carbonate) were added and finally the resin (an acrylic styrene) together with the co-solvents. After preparation, the paint was filtered and kept in a closed jar under laboratory conditions until use.

The microcapsules (MF-Tea tree and MF-Lavandin) were incorporated into the original paint just before used, at 6% (w/w) by weight of the total paint composition. As negative control, paint without biocide was used.

TABLE 1. Paint composition

Component	% (w/w)
Water	25.20
Antifoaming	0.30
Cellulose Thickener	0.50
Dispering agent	0.45
Wetting agent	0.15
Pigments	64.3
Resin	7.20
Mineral spirit	1.30
Butylglycol	0.60

Antifungal assay on paint film. Commercial gypsum boards, cut into test pieces (2.5 cm x 2.5 cm) and sterilized at 121 ºC for 20 min, were used as substrate. The panels were painted with two coats of the formulated paints and were kept under laboratory conditions for 15 days to cure the paint. Afterward, the panels were irradiated with U.V-light for 20 minutes, for providing a superficial sterilization and, then, placed into Petri dishes containing filter paper moistened with 1 mL of sterile water. Each panel was inoculated with 100 µL of the spore suspension of *Aspergillus* and kept in a culture chamber at 86% RH for 4 weeks. Four replicates were used for each paint. The fungal growth was estimated as a percentage of surface coverage. The panels were scored according to ASTM D5590 standard specification (**Table 2**)[17]. Additionally, observations by scanning electron microscopy (SEM) were made. The selected samples for further studies were those that presented better result and the control. The panels were prepared as follows: small sections of the panels surfaces were cut and fixed in 2.5% v/v gluteraldehyde (24h) and dehydrated in graded series of ethanol solution from 20% v/v at 100% v/v. Finally, they were dried with the critical point and coated with gold. The coated samples were examined by Scanning Electron Microscopy (FE-SEM) on a FEI, Quanta 200 microscope at high vacuum.

TABLE 2. Fungal growth qualification over the surface (ASTM D 5590)

Growth observation	Qualification
None	0
Trace of growth (<10%)	1
Light growth (10-30%)	2
Moderate growth (30-70%)	3
Heavy growth (>70%)	4

RESULTS AND DISCUSSION

Characterization. SEM photographs of microcapsules morphologies obtained by the *in situ* polymerization method, containing the essential oils, are shown in **Figure 1A and 1B**. As can be seen, microcapsules have spherical shape and a smooth surface. The melamine-formaldehyde microcapsules revealed sizes of around 15 μm for the Lavandin oil (**Figure 1A**) and sizes of more than 20 μm for the Tea Tree oil, (**Figure 1B**). The average size of these microcapsules was subsequently confirmed by laser diffraction measurements (**Figure 2**).

The graphical distribution of the mean diameters for the different microcapsules is indicated in **Figure 2A and 2B**. Both microcapsules had narrow particle size distribution. The mean particle sizes showed changes depending on the essential oil employed. The average particle size diameter was 15 µm in the case of Lavandin microcapsules while those Tea Tree size microcapsules reached 22 µm. Thus, the prepared microcapsules in this study seemed to be adequate for incorporation in a paint, due to them monodisperse size distribution. In addition, the greatest mean particle sizes of MF- Tea tree can be attributed to the viscosity of the core material used for microencapsulation, which is an important factor affecting the particle size of the MF microcapsules [14].

A) B)

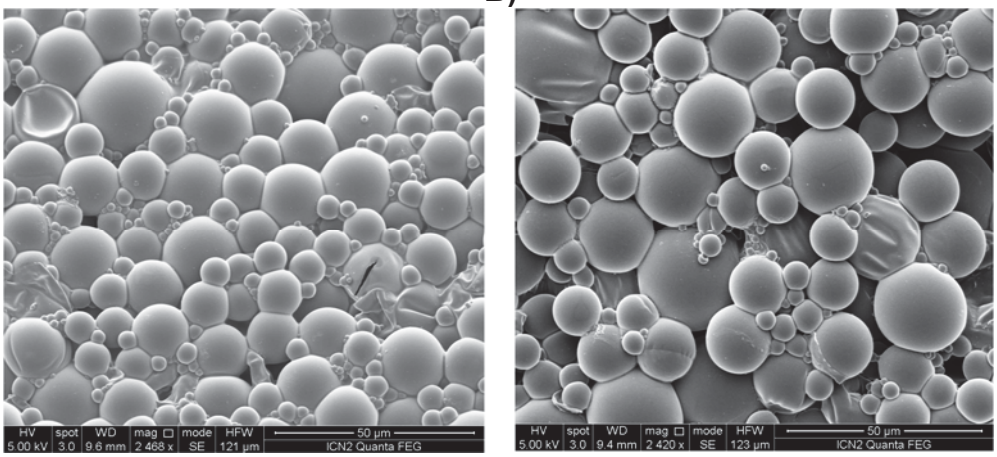
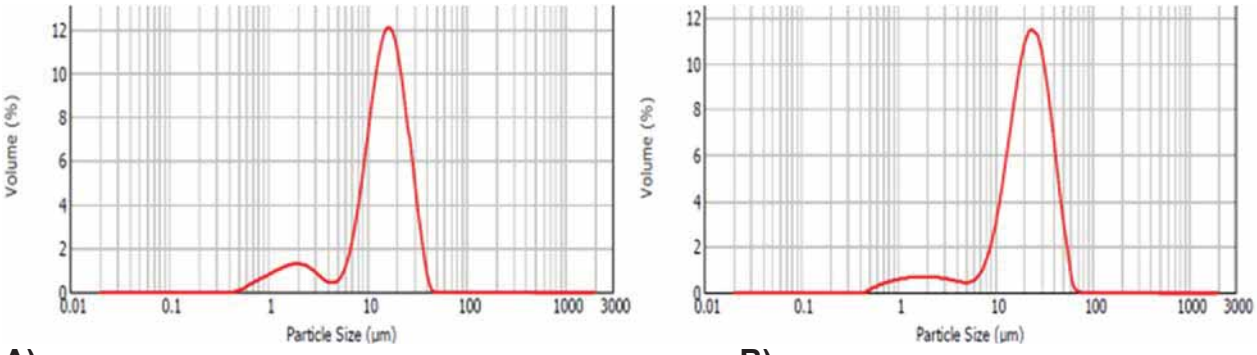


FIGURE 1. SEM micrographs of melamine-formaldehyde microcapsules containing A) Lavandin oil and B) Tea Tree oil, at 2400x magnifications

FTIR studies were conducted to confirm whether the EO-microcapsules were prepared successfully or not. **Figure 3A** and **3B** depict chemical components of microcapsules containing LVO or TTO as core material and melamine-formaldehyde as the wall respectively.

First of all, melamine-formaldehyde resin can be assumed to constitute in the capsule walls because the secondary amine group N-H stretching vibration was observed at 3393 cm^{-1} and 3349 cm^{-1} in the respective spectrum **(Figure 3 A-b** and **3B-b**). This result is supported by a previous investigation[18] of melamine-formaldehyde prepolymer prior to encapsulate core material which showed N-H vibration at 3300 cm^{-1}. The C-N stretching vibration was shown at 1339 -1336 cm^{-1}. These findings partially matched those reported in a previous study [18,19] dealing with melamine formaldehyde as wall material of microcapsule. In addition, strong adsorption peaks located at 2967-2963 cm^{-1} are associated with the C-H stretching vibration which was frequently encountered in organic compounds like natural essential oil.



A) B)

FIGURE 2. Particle-size distribution for A) the MF-Lavandin microcapsules and B) the MF-Tea Tree microcapsules, as measured by laser diffraction

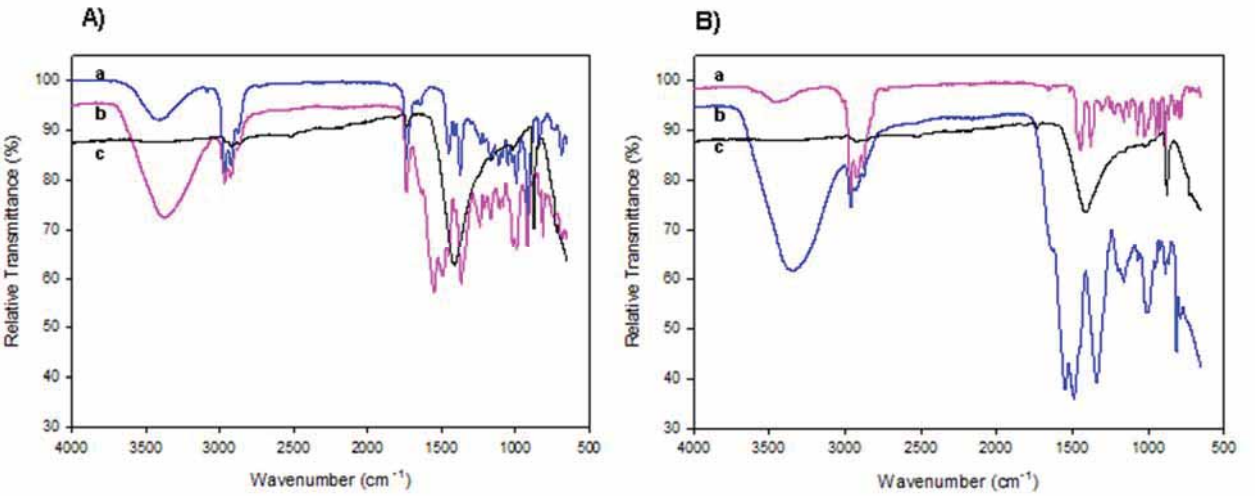


FIGURE 3. FT-IR spectra: (A) a) Lavandin oil, b) MF-Lavandin microcapsules and c) paint film containing MF-Lavandin microcapsules. (B) a) Tea tree oil, b) MF-Tea tree microcapsules and c) paint film containing MF-Tea tree microcapsules.

Figure 3A-a shows FTIR spectra corresponding to Lavandin oil. The basic components of the LVO are linalool, linalyl acetate, lavandulol, and citronellol [20]. These components have characteristic molecule groups such as –COOR and C=O. In **Figure 3A-a** the strong absorption peak of the LVO due to carbonyl was found at 1741 cm^{-1}. Besides, other notable peaks appeared at 2970 cm^{-1}, 1460 cm^{-1}, 1371 cm^{-1}, and 1000 cm^{-1}, which are due to C–H stretching vibration, CH_2 asymmetric deformation, CH_2 symmetric deformation [21].

Figure 3B-a shows FTIR spectra corresponding to Tea Tree oil. The TTO spectrum shows characteristic bands corresponding to its major components such as 1-terpinen-4-ol, γ-terpinene, 1,8-cineole and α-terpinene, among others, in published reports [22]. It shows characteristic peaks corresponding to the vibrations OH around 3400 cm^{-1}, alkyl C-H stretching vibration between 2960 and 2854 cm^{-1}. The band corresponds to C=O vibration bond was found at 1744 cm^{-1}. Between 1464 and 1385 cm^{-1} the C-H bending vibration was observed. Characteristic absorption band of vibration C-O-C aromatic rings appeared at 881 cm^{-1}.

In summary, FT-IR spectroscopic data showed that essential oils were successfully encapsulated by melamine-formaldehyde as wall.

In order to chemically characterize the paints film with MF-essential oil were performed spectra FTIR, **Figure 3A-c and 3B-c**. The spectra show the bands due to $CaCO_3$ (1726 cm^{-1}, 1415 cm^{-1}) and talc (1015 cm^{-1}) as well as the typical one for the acrylic resin at 1720 cm^{-1}. $CaCO_3$ and talc are one of the pigments used in latex paints. These results are consistent with studies reported [23]. The bands due to the MF-essential oil did not appear, showing the optimal encapsulation of essential oil in the microcapsules.

Antifungal assay on paint film. Figure 4 shows in detail the antifungal effects of microcapsules in paint by quadruplicate, compared with the respective control (paint without microcapsules) after 4 weeks.

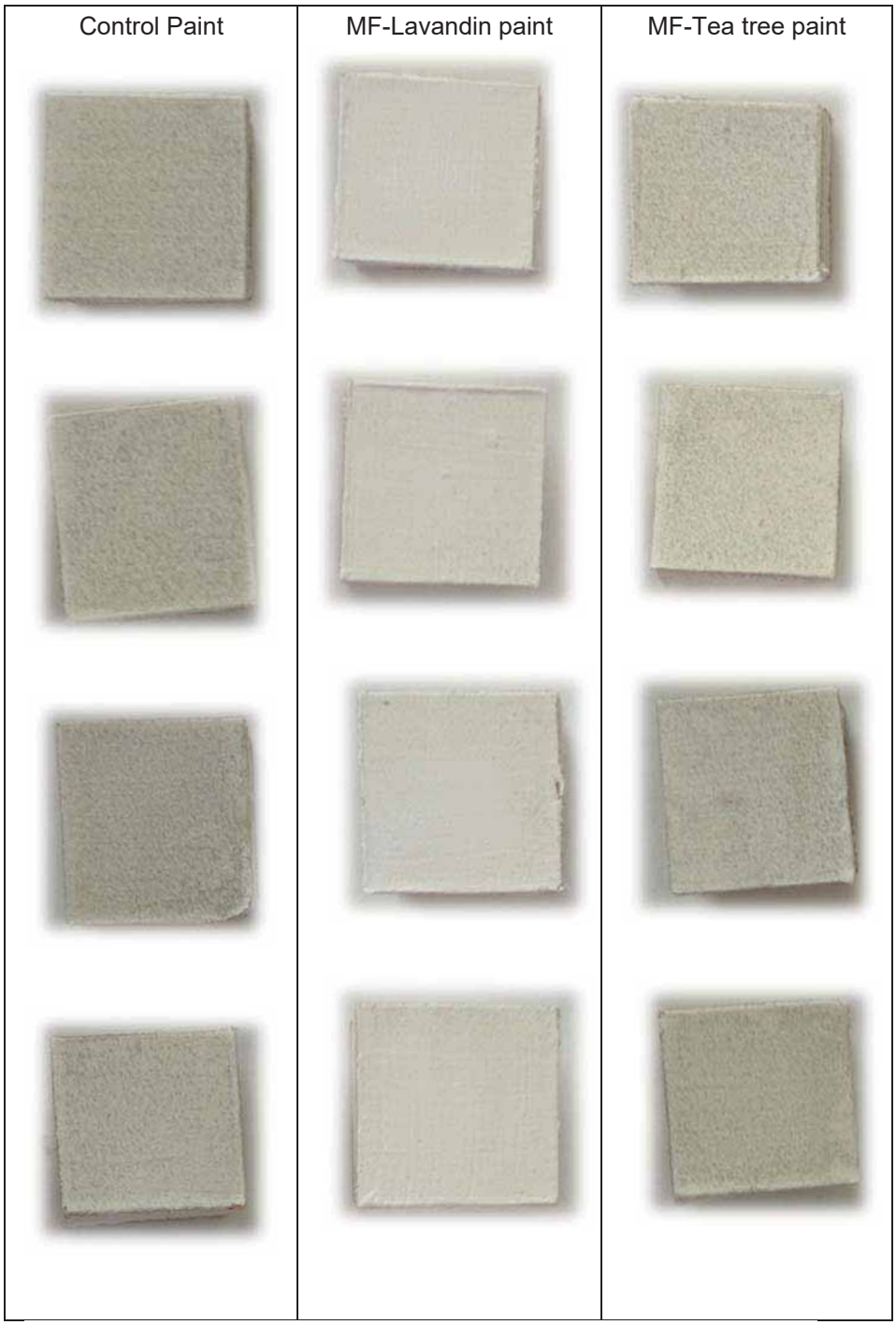


FIGURE 4. Antifungal assay on paint film containing MF-EO exposed to *Aspergillus sp.* after 4 weeks (quadruplicate)

Evaluation of the fungi growth degree on paints by ASTM D5590 (4th week) is shown in **Table 3**.

TABLE 3. **Fungal growth qualification over the paint surface**

Paint	Qualification
Control	4
MF-Lavandin	1
MF-Tea tree	4

According to standard specification, the score obtained by MF-lavandin paint was 1, which indicate just a trace growth onto the painted surface to naked eye (<10%). On the other hand, the control and MF-Tea tree paints obtained the same score: 4 points, the highest qualification. This score corresponds to degree of coverage by the fungal growth higher than 70%. Comparing the results, it can be seen that *Aspergillus sp*. growth reduction was significant when MF-Lavandin paint was employed, suggesting that these microcapsules has fungal growth inhibition activity on the dry film whereas MF-Tea tree did not affect the growth.

Observation of paint film by scanning electron microscope (SEM). Macroscopic observation was confirmed by SEM. The **Figure 5** shows the micrographs of the fungal film of the control paint and paint with MF-Lavandin microcapsules.

As shown in **Figure 5A**, the fungal colonization is abundant, with a wide mycelial development covering all control paint surface together with many spores. The spores are dark pigmented and lead to an aesthetic damage in the paint. Moreover, it is well documented that spores are the principal source of fungal bioaerosol that cause irritative disorders (i.e. allergy and asthma) [4,24]. On the other hand, in **Figure 5B** it can be seen a poor mycelial development and a few spores, also it is possible to distinguish the microcapsules immersed into the paint.

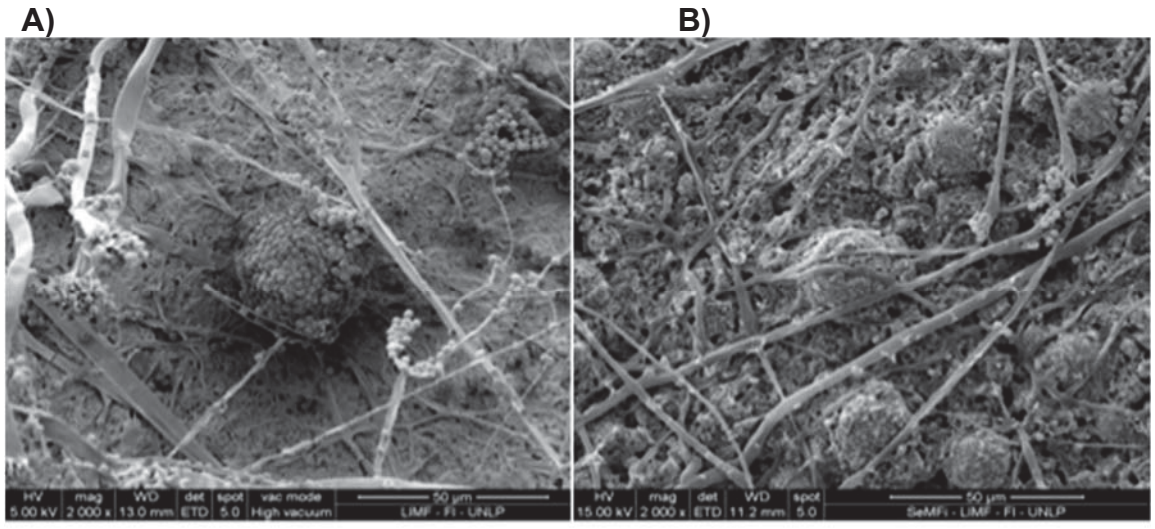


FIGURE 5. SEM micrographs: a) control paint and b) MF-Lavandin paint, exposed to *Aspergillus sp.* after 4 weeks, at 2000x magnifications.

CONCLUSION

This work has proposed the use of melamine-formaldehyde resin microcapsules containing two different essential oils as a natural biocide, for the development of a green hygienic coating. The microcapsules containing LVO and TTO, obtained by in situ polymerization, were evaluated with regard to their morphologies, size distribution, and chemical structure. The formation of MF-EO microcapsules has evidenced smooth surface morphologies and the mean particle sizes have reached values around 15 and 22 μm. These microcapsules resulted adequate to be incorporated in a paint, due to them monodisperse size distribution. FTIR studies have demonstrated that the essential oils were successfully encapsulated by melamine-formaldehyde as wall and the microcapsules were effectively incorporated in the paint.
It is important to keep in mind that a paint is a complex system and, at the same time, essential oil is a volatile compound. For this reason, it is important to achieve a good system of encapsulation to reduce the loss of essential oil and decrease the possible interaction with others paint components, thus, the oil will be available exclusively as biocide. In this sense, the results obtained in the antifungal assay on paint film were promising. It can see that the growth reduction against *Aspergillus sp* was significant when MF-Lavandin were incorporated in the paint, suggesting that these microcapsules have fungal growth inhibition activity on the dry film.
This kind of coatings has a good potential, given that the essential oil is a natural resource, renewable and eco-friendly. An inconvenience, in this time, is the cost of raw materials. When the process is considered for mass production, cost can be high, but may be acceptable if they are considered for special applications, those cases where conventional technology fails or when restrictions to traditional biocides would be implemented. Further experimental investigations are needed and work together with companies to make feasible the selection of ideas, technologies and eco-friendly compounds for the generation of commercial products.

ACKNOWLEDGMENTS

The authors are grateful to Consejo Nacional de Investigaciones Científicas y Técnicas (CONICET), Comisión de Investigaciones Científicas de la Provincia de Buenos Aires (CICPBA), and Universidad Nacional de La Plata (UNLP). This research is supported by Grant 813/13 named ‘Recubrimientos antimicrobianos con extractos de vegetales', from Comisión de Investigaciones Científicas de la Provincia de Buenos Aires (CICPBA).

REFERENCES

1. Li D., Yang C.S. Fungal contamination as a major contributor to sick building syndrome, Adv. Apllied Microb., 55 (2004) 31-96.
2. Verdier T., Coutand M., Bertron A., Roques C. A review of indoor microbial growth across building materials and sampling and analysis methods, Building and Environment, 80 (2014) 136-149.
3. Negrin M., Del Panno M.T., Ronco A.E. Study of bioaerosols and site influence in the La Plata area (Argentina) using conventional and DNA (fingerprint) based methods, Aerobiologia, 23 (2007) 249-258.

4. Alexopoulos C. J., Mims C. W., Blackwell M., Introductory Mycology, 4th edition (1996).
5. Sontakke T.K., Jagtap R.N., Arvind Singh, Kothari D.C. Nano ZnO grafted on MAA/BA/MMA copolymer: An additive for hygienic coating, Progress in Organic Coatings 74 (2012) 582– 588.
6. Guiamet P.S., Videla H.A. Microbiological spoilage of aqueous based surface coatings, Corrosion Reviews 14 (1996) 47-58.
7. Rhoades A. M., Douglas A. W., Bruhaspathy M., Williamson J. Interactions of an antimicrobial peptide (Ac-RRWWRF-NH2) and surfactants: Towards antimicrobial peptide additives for coatings applications, Progress in Organic Coatigs 58 (2007) 209-216.
8. Houghton D. R., Smith R. N., Eggins H. O. W. (Eds.), Biodeterioration 7, (1988).
9. Hare C. Microbiologically-influenced attack of coatings, JPCL, (2000), 51-65.
10. Johns K., Hygienic coatings: the next generation, Surface Coatings International, 86 (2003) 101-110.
11. Bakkali F., Averbeck S., Averbeck D., Idaomar M., Biological effects of essential oils - A review, Food and Chemical Toxicology 46 (2008) p. 446–475
12. El Asbahani A., Miladi K., Badri W., Sala M., Aït Addi E.H, Casabianca H., El Mousadik A., Hartmann D., Jilale A., Renaud F.N.R., Elaissari A. Essential oils: From extraction to encapsulation, International Journal of Pharmaceutics, 483 (2015) 220–243.
13. Ashraf M.A., Ullah S., Ahmad I., Qureshi A.K.,Balkhairf K.S., Abdur Rehmang M. Green biocides, a promising technology: current and future applications to industry and industrial processes. J Sci Food Agric, 94:3 (2014) 388-403.
14. Hwang J.S., KimJ.N., Wee Y.J., Jang H.G., Kim S.H., Ryu H.W. Factors affecting the characteristics of melamine resin microcapsules containing fragrant oils. Biotechnology and Bioprocess Engineering, 11 (2006) 391-395.
15. García-Jimeno S., Cano-Sarabia M., Mejias N., Navarro V., Frances A., Maspoch D. Healing damaged coatings using friction-sensitive hybrid. J. Mater. Chem. A, 3 (2015) 17966-17970.
16. Nielsen K.F., Mould growth on building materials. Secondary metabolites mycotoxins and biomarkers, PhD Thesis, 2002.
17. ASTM D5590-00. Standard Test Method for Determining the Resistance of Paint films and Related Coatings to Fungal Defacement by Accelerated Four-Week Agar Plate Assay (2010).
18. Lee A. R., Han C.H.,Yi E. Preparation and Characterization of Melamine-formaldehyde Microcapsules Containing *Citrus unshiu* Essential Oil. Fibers and Polymers 15:1 (2014) 35-40.
19. Hwang J.S., Kim J.N., Wee Y.J., Yun J.S., Jan H.G., Kim S.H., Ryu H.W. Preparation and characterization of melamine-formaldehyde resin microcapsules containing fragrant oil. Biotechnology and Bioprocess Engineering 11: 4 (2006) 332-336.
20. Varona S., Rodriguez Rojo S., Martin A., Cocero MJ., Serra AT., Crespo T., Duarte C. Antimicrobial activity of lavandin essential oil formulations against three pathogenic food-borne bacteria. Industrial Crops and Products 42 (2013) 243– 250.
21. Zuobing X., Wanlong L., Guangyong Z., Rujun Z. Yunwei N. Production and characterization of multinuclear microcapsules encapsulating lavender oil by complex coacervation. Flavour Fragr. J. 29 (2014) 166–172.
22. Perez M.A., Paya´ F.J., Arán F., Orgilés C. Effect of the shell-forming polymer ratio on the encapsulation of tea tree oil by complex coacervation as a natural biocide. J Microencapsul, 31:2 (2014)176–183.
23. Bellotti N., Salvatorea L., Deyá C, Del Panno M., Del Amo B., Romagnoli R. The application of bioactive compounds from the food industry to control mold growth in indoor waterborne coatings. Colloids and Surfaces B: Biointerfaces 104 (2013) 140–144.
24. Denning D.W., O'Driscoll B.R., Hogaboam C.M., Bowyer P., Niven R.M. The link between fungi and severe asthma: a summary of the evidence, Eur Respir J, 27 (2006) 615–626.

CHAPTER 4.2 NUEVAS FUENTES DE TANINOS QUE PUEDEN SER UTILIZADOS COMO AGENTES CURTIENTES EN REEMPLAZO DE LAS SALES DE CROMO

A. Bonfranceschi Barros*; G. Mazzilli; J.A. Markán; L.M.I. López, L.M.I. and J.E. Martegani

Centro de Investigación y Tecnología del Cuero (CITEC), Camino Parque Centenario entre 505 y 508. Manuel B. Gonnet

RESUMEN

El objetivo del trabajo fue obtener y caracterizar diversos extractos vegetales en cuanto a su contenido en taninos y poder curtiente. Los materiales vegetales fueron seleccionados debido a su alta disponibilidad. Se utilizaron vainas sin semillas de *Gleditsia triacanth*os (acacia), exocarpio de frutos de *Juglans regia* (nogal) un subproducto en la cosecha de la nuez; ramas, hojas y flores de *Larrea tridentata* (jarilla) y acículas de *Araucaria auracana* (araucaria). En una primera etapa se optimizó el método de extracción de taninos testeando diversos tiempos y temperaturas, los mejores resultados fueron obtenidos realizando el tratamiento del material pulverizado (tamaño de partícula: diámetro máximo promedio de 3mm) al 1% (p/v) en agua durante 60 minutos a ebullición. Los extractos obtenidos fueron caracterizados en cuanto al contenido de sólidos totales disueltos y la capacidad curtiente. Para determinar la capacidad curtiente se siguió un procedimiento desarrollado en el CITEC, de acuerdo al cual la fracción de sólidos retenida por el polvo de piel representa las sustancias polifenólicas (taninos) capaces de unirse al colágeno presente en dicho material. Los resultados fueron expresados como gramos de taninos/Kg de material vegetal seco. El mejor rendimiento se obtuvo para el exocarpio del nogal (192 g/Kg), seguido por las vainas de acacia (158 g/Kg), jarilla (77g/Kg) y araucaria (72g/Kg). Por otra parte cabe consignar que los taninos representaron el 56% de los STD en el caso de araucaria, el 47% para nogal, el 42% para acacia y el 39% para la jarilla. Los extractos tánicos fueron ensayados en la planta experimental de curtiduría del CITEC como agentes curtientes de pieles de cabra. Los cueros obtenidos serán evaluados en cuanto a su temperatura de contracción y la solidez del color al UV. El extracto tánico obtenido a partir de un producto de desecho en la obtención de la nuez resultó ser muy promisorio como fuente de taninos ya que fue el que tuvo el mayor rendimiento en gramos de taninos por Kg de material vegetal seco y permitió desarrollar un proceso de curtido de piel de cabra que generó un cuero con buena temperatura de contracción y un óptimo índice de resistencia al UV.

Palabras claves: curtiembre; curtientes; taninos

---

*Author for correspondence: alfon1274@hotmail.com

INTRODUCCIÓN

A pesar de su contribución significativa a la economía de los países, la industria del curtido provoca una grave contaminación del medio ambiente debido a la utilización de sustancias químicas nocivas y a la liberación de una variedad de materiales de desecho perjudiciales. En particular las curtiembres que utilizan sales de cromo como parte del proceso de curtido, forman parte de las industrias más contaminantes para el medioambiente dado que el cromo es un metal pesado con un riesgo potencial para la salud humana[1]. Por ello el empleo de taninos como agentes curtientes, en reemplazo de las sales de cromo, implica una disminución importante en la toxicidad de los efluentes generados. Por otra parte diversos diseñadores de vanguardia están demandando artículos de cuero sostenibles y no los consideran así cuando los cueros se han curtido al cromo o al vegetal utilizando extractos naturales provenientes de árboles cultivados y cortados, como son todos los usados hoy por las curtiembres[2]. Los taninos son polifenoles de origen vegetal. Su principal característica es que se unen a las proteínas y están presentes en plantas comestibles y no comestibles[3] (Mañach et al., 2004). El objetivo del trabajo fue obtener y caracterizar diversos extractos obtenidos a partir de materiales vegetales que fueron seleccionados por ser de fácil acceso, que no impliquen la tala de árboles o ser productos de desecho de otras industrias, para evaluar su contenido en taninos y poder curtiente.

MATERIALES Y MÉTODOS

Material vegetal. Se utilizaron vainas sin semillas de *Gleditsia triacanthos* (acacia), exocarpio de frutos de *Juglans regia* (nogal) un subproducto en la cosecha de la nuez; ramas, hojas y flores de *Larrea tridentata* (jarilla) y acículas de *Araucaria auracana* (araucaria).

Extracción. Para maximizar el rendimiento del proceso de extracción se procedió inicialmente a moler el material vegetal, utilizando un molino a cuchilla, hasta que el tamaño de partícula máximo fuese de aproximadamente 3mm. El material pulverizado fue tratado con agua (1% p/v) durante 60 minutos a ebullición, filtrado y secado en estufa a 60°C durante 24 hs.

Caracterización de los extractos vegetales. Los extractos obtenidos fueron caracterizados en cuanto al contenido de sólidos totales disueltos (STD, Standard methods for the examination of water and wastewater, 12nd edition) y la capacidad curtiente. Para determinar la capacidad curtiente se siguió un procedimiento desarrollado en el CITEC (basado en las normas ISO/DIS 14088 y IULTCS/UC 32). La fracción de sólidos retenida por el polvo de piel representa las sustancias polifenólicas (taninos) capaces de unirse al colágeno presente en dicho material. Los ensayos se realizaron por duplicado.

Empleo de las soluciones de taninos como agentes curtientes de piel de cabra
Proceso de curtido (*)
Remojo : las pieles de cabra conservadas por secado fueron sumergidas durante 10hs a 25^{o}C en un baño que contenía H2O (400%), Na2CO3 (0,3%), bactericida (Baicide 0,2 %); detergente (Azymol 6SE 0,4%); Desengrasante (Isogras OVN 0,2%); pH 9,0. Estático.
Descarnado: se llevó a cabo empleando una máquina descarnadora de rodillo
Depilado: se llevó a cabo empleando una serie de tratamientos secuenciales: Na2S (0,5%) durante 15 minutos; CaO (1,5%) durante 60 minutos; Na2S (1,8 %) durante 60 minutos; CaO (3,5%) durante 60 minutos y Thiolime Open DC (1 %) durante 60 minutos.
Lavado: CaO (3%); H2O (100%) durante 60 minutos.
Desencalado: $Na_2S_2O_5$ (0,5%), $(NH_4)2SO4$ (0,3%); H2O (100%) durante 50 minutos (pH 8,0).
Purga: Neozym P (0,12%) 40 minutos.
Piquelado: H2O (50%), ácido fórmico (1,5%), ácido sulfúrico (0,8%); pH 3,8.

Una vez finalizada la etapa de piquelado la piel fue fraccionada en 4 partes equivalentes y el proceso se siguió con cada una de ellas por separado para evidenciar la acción curtiente de cada extracto vegetal.

Curtido: se llevó a cabo en baño de piquelado (10%) con el agregado de los taninos obtenidos partir de cada uno de los 4 extractos vegetales al 1%.

(*) Todos los porcentajes indicados fueron calculados sobre masa de piel seca

Análisis de los cueros obtenidos. Solidez del color a la luz UV. La metodología empleada está basad en la norma IRAM 8568. El tiempo de exposición fue de 7 y 12 horas. La evaluación se realizó con las escalas de grises (ISO 105-A02: 1993; BS EN 20105-A02: 1995; ISO 105-A3:1993), el valor 1 de la escala es el de mayor contraste y 5 el de menor contraste.

La temperatura de contracción (Tc) está relacionada con la calidad del curtido logrado. La determinación se llevó a cabo según protocolo elaborado en el CITEC: sujetando un trozo de cuero de 1,5cm x 7,0cm desde los extremos más angostos, se lo pliega parcialmente y se sumerge en agua de grifo a temperatura ambiente. Con agitación magnética, se eleva la temperatura del baño a razón de 5^{o}C/min y se registra visualmente el momento en que las fibras de colágeno se desnaturalizan y la piel doblada se estira.

RESULTADOS Y DISCUSIÓN

Los resultados fueron expresados como gramos de sólidos totales disueltos (STD) por Kg de material vegetal seco, porcentaje de taninos en los STD y taninos/Kg de material vegetal seco. El mejor rendimiento en cuanto a la cantidad de taninos obtenidos por Kg de material vegetal seco se obtuvo para el exocarpio del nogal (192 g/Kg), seguido por las vainas de acacia (158 g/Kg), jarilla (76,8 g/Kg) y araucaria (72,1 g/Kg).

TABLA 1. Extracción de taninos a partir de diferentes fuentes vegetales

Vegetal	Temperatura de contracción (ºC)	Indice de solidez al UV (7 horas)	Indice de solidez al UV (12 horas)
Acacia *Gleditsia triacanthos*	62	4/5	4/5
Jarilla *Larrea tridentata*	55	4/5	4/5
Nogal *Juglans regia*	61	5	5
Araucaria *Araucaria auracana*	60	4/5	4/3

Por otra parte cabe consignar que los taninos representaron el 56,3 % de los STD en el caso de araucaria, el 47,3 % para nogal, el 41,5% para acacia y el 38,6% para la jarilla (**Tabla 1**).

TABLA 2. Caracterización de los productos curtidos con taninos

Vegetal	pH final	STD (g) /Kg vegetal seco	Taninos/STD (%)	Taninos (g) /Kg vegetal seco
Acacia *Gleditsia triacanthos*	5,57	381	41,5	158
Jarilla *Larrea tridentata*	5,54	199	38,6	76,8
Nogal *Juglans regia*	6,03	405	47,3	192
Araucaria *Araucaria auracana*	5,11	128	56,3	72,1

Los cuatro extractos (**Figura 1**) fueron evaluados como agentes curtientes en un ensayo a escala piloto en la Planta Experimental de Curtido del CITEC. Los datos de la temperatura de contracción permiten prácticamente descartar el extracto obtenido a partir de la jarilla (*L. tridentata*) por ser demasiado bajo lo que implica un proceso de curtición deficiente. En tanto que de los otros 3 extractivos se destaca el obtenido a partir del nogal (*J.regia*) porque mantuvo el índice más alto de resistencia al UV (**Tabla** 2).



FIGURA 1. Material vegetal triturado y extracto acuoso obtenido a partir de los cuatro materiales vegetales examinados.

CONCLUSIÓN

El extracto tánico obtenido a partir de un producto de desecho en la obtención de la nuez resulta ser muy promisorio para la obtención de taninos ya que es el que resultó tener el mayor rendimiento en gramos de taninos por Kg de material vegetal seco y permitió desarrollar un proceso de curtido de piel de cabra que generó un cuero con buena temperatura de contracción y un óptimo índice de resistencia al UV. Dicho material fue seleccionado para continuar los estudios.

AGRADECIMIENTOS

Comisión de Investigaciones Científicas de la Provincia de Buenos Aires, CONICET (PIP 0297), INTI.

REFERENCIAS

1. Shanker A.K., Venkateswarlu B. Chromium: Environmental Pollution, Health Effects and Mode of Action. Encyclopedia of Environmental Health (2011) 650-659.
2. Salvador R., Bacardit, a., Font,J., Ollé, L. Comparación de las características de pieles vacunas curtidas con extracto de semilla de uva, versus otros extractos vegetales convencionales. 61º Congreso de la Asociación Química Española de la Industria del Cuero
3. Manach, C., Scalbert, A., Morand, C., Rémésy, C., Jiménez, L. Polyphenols: foodsources and bioavailability. Am. J. Clin. Nutr. 79 (2004) 727–747.

CHAPTER 4.3 IMPROVED STRENGTH AND DURABILITY OF CONCRETE THROUGH METABOLIC ACTIVITY OF UREOLYTIC BACTERIA

N. Balagurusamy*(1); M.J. Castro Alonso (1); C.E. López Ortiz (1); S.O. Garcia Perez (1); R. Narayanasamy (2); G.J. Fajardo San Miguel (3) and H. Herrera Hernández (4)

(1) Laboratorio de Biorremediación, Facultad de Ciencias Biológicas, Universidad Autónoma de Coahuila, Carretera Torreón-Matamoros Km 7.5, Torreón, México.
(2) Facultad de Ingeniería, Ciencias y Arquitectura de la Universidad Juárez del Estado de Durango.
(3) Universidad Autónoma de Nuevo León, Facultad de Ingeniería Civil, Av. Universidad S/N, Ciudad Universitaria, Nuevo León, , México.
(4) Centro Universitario, Universidad Autónoma del Estado de México.

ABSTRACT

Concrete is the most used construction material because of its strength, durability and low cost compared with other materials. However, it is vulnerable to weathering due to physical, chemical and biological factors. As a consequence of increase in porosity, formation of microcracks, both durability and structural capacity of concrete are reduced. The deterioration of this material requires an expensive maintenance and repair. Repair cost has been estimated to about $147/m^3 of concrete[1], despite the fact that concrete production cost ranges between $65 and $80/m^3. In recent years, biomineralization has been successful in development of bioconcrete or bio influenced self-healing concrete, which has emerged as an effective method for controlling the formation of cracks, reducing permeability and increasing durability of concrete. Bioconcrete is a product result of biomineralization induced by microbial processes resulting in calcium carbonate precipitation[2].

In this study, 24 different ureolytic strains of bacteria were isolated from the soils of the Laguna Region of Mexico. Subsequently, the 6 strains out of 24 strains showing higher urease activity than other isolates were selected for further study. Selected ureolytic strains were grown in Urea - $CaCl_2$ medium for 48 hours and the following concentrations of the strains, viz., 10^5, 10^6 and 10^7 per mL were used for the preparation of the mortar mix. Cement and sand were properly mixed at a ratio of 1:2.75 by weight and a water-cement ratio was maintained at 0.485 according to ASTM C 109 / C 109 M-07. Physico-mechanical properties like compressive strength, electrical resistivity, and resistance to penetration of chloride ions of the biomaterials were analyzed. Further, deposition of calcite in bioconcrete was visualized with scanning electron microscopy. The mortars prepared with the bacterial strains showed a significant increase in compressive strength after 36 days of curing. Similarly, a significant increase in resistivity was observed after 65 days. In addition, bioconcrete mortars showed a low permeability after 36 days of curing. It is clearly observed from this study that the durability of biomortars were increased significantly due to addition of bacterial strains.

---

*Author for correspondence: bnagamani@uadec.edu.mx

Keywords: Bioconcrete; biomineralization; durability; ureolytic bacteria

INTRODUCTION

Concrete is widely used as construction material around the world due to its resistance, durability and low cost in comparison with other construction materials[2,3]. However, it is susceptible to undergo deteriorations due to diverse physico-chemical and biological factors[4,5]. These factors induce formation of cracks in internal structure of concrete causing irreversible damage. It has been estimated that the cost of repair and maintenance is around $147/m^3$ of concrete, despite the fact that cost of concrete production ranges between $65 and $80/m^3$ [6]. Cement is the most important component of the concrete since it provides properties of compaction, and with growth of modernization and industrialization demand for cement has been increasing. The demand for cement in 2006 was about 2540 million tons (Mt), which is predicted to increase between 3680 (low estimate) and 4380 Mt (high estimate) in 2050. This increase in activity of the construction industry has generated a negative impact on the environment. Concrete industry emits about 0.73 – 0.99 t CO_2/ t of cement produced, which accounts for about 5-7% of global CO_2 emission[7]. In addition, the durability of concrete structures is extremely complex, since various external agents can provoke the onset and spread of the different types of deterioration, both in reinforced concrete and steel structures[8]. Permeability of the concrete is the property, which has a direct impact on the mechanisms of deterioration of concrete structures reinforced. This permeability is generated by the porous nature of concrete, which permits passage to aggressive (such as CO_2, Cl^-, and SO_4) agents, which can accelerate the deterioration of reinforced concrete structures[9]. Of late various procedures and techniques are proposed to minimise and recover from structural damages such as cracking and others. Most of these techniques either require large investment or involve complex procedures. Biological treatment offers the sustainable and more economic method. Different bacterial strains are employed to facilitate Biomineralization process, which generate compounds compatible with the material of origin, are formed due to bacterial metabolic process resulting in the formation of solid inorganic compounds or minerals, commonly referred as bioconcrete[1,4].

As mentioned, biomineralization process involves the formation of calcium carbonate by metabolic activity of microorganisms, where urease enzyme plays a vital role[10,11]. Existing biological principles and the advances on the process of the microbial induced precipitation of carbonate (MICP) offer opportunities to use stable natural system to meet these challenges. The carbonate precipitation is resultant product of the urease enzyme activity produced by ureolytic bacteria. This enzyme catalyzes the hydrolysis of urea into CO_2 and ammonia, resulting in an increase of the pH and the concentration of carbonate in the bacterial environment[12]. The application of ureolytic bacteria as a healing agent to the concrete mixture is an environmental friendly technology and also minimises the cost[13]. It has been reported to improve the resistance to compression, tension, elasticity and other structural characteristics of concrete[14,15]. However, there are few studies on MICP on cement matrices and hence the objectives of the current study

are to assess the effect of the ureolytic bacteria on resistance to compression, permeability and electrical resistivity of cementitious matrices.

MATERIALS AND METHODS

Isolation and selection of Ureolytic bacteria: Ureolytic bacterial strains were isolated from semi-arid, alkaline soils of *Comarca Lagunera* of North=East Mexico by employing Urea-$CaCl_2$ agar medium[16]. Twenty-four bacterial strains were isolated and evaluated for their growth characteristics and urease activity. Strains were grown on Urea-$CaCl_2$ broth and growth was determined in terms of optical density (A_{600}) measurements and cellular protein. One milliliter of bacterial culture was periodically drawn, centrifuged (10,000 rpm; 20 min), cell pellet was washed twice in sterile distilled water and hydrolyzed with 0.1 mL of 1N NaOH. Cell hydrolysates and the supernatants collected after the first centrifugation were determined for cellular and extra-cellular protein respectively by following dye-binding assay[17]. Based on the obtained growth data, different growth kinetics data were determined.

Moreover, collected cell pellet samples were sonicated (Cole Palmer, USA, 20 kHz; 30 min) to release cell protein and evaluated for intracellular urease activity along with extracellular fraction by using phenol-hypochlorite method[18]. Effect of different nickel concentrations (5, 8 & 10 mM) as a co-factor on urease activity was also determined. In addition, optimum conditions for the maximum urease activity by the selected bacterial isolates were determined at different urea concentrations (40, 60, 80, 100, 120 & 140 mM), pH (6.5, 7, 7.5, 8, 8.5 & 9) and temperatures (25, 40, 60 & 80°C). Enzyme kinetic parameters, *viz*., Km and Vmax were determined.

Based on the results, two bacterial strains, *viz*., ACRN 3, and ACRN 5 were selected for this study.

Description of materials used for bio-mortar preparation: Ordinary Portland cement called CPO 40 (in accordance with NMX C 414), standard silica sand, which complies with ASTM C 778 and distilled water were used for the preparation of cementitious mixtures. The proportions of the materials used were according to the ASTM C 109 and ASTM C 305.

Preparation of Bio-mortar specimens: A total of 18 cubes of mortar with dimensions of 50 x 50 x 50 mm and 10 cylinders of 50 mm of diameter with a height of 13 cm were fabricated. ACRN 3 and ACRN 5 bacterial cells grown on Urea – $CaCl_2$ broth were added to the cement and sand mixture at different cell concentrations, *viz*., 10^5, 10^6 and 10^7 per mL of water. Cement and sand were mixed in a proportion of 1:2.75 by weight and with a ratio of water and cement was 0.485 as per the ASTM C 109 / C 109 M-07. Control mortar samples were prepared by using distilled water to mix cement and sand. After casting, all of samples were placed in the curing chamber for 24 ± 2 hours and after that the molds were taken off to continue with curing of bio-mortar specimens. In the case of cylinder specimens, they were cut into two parts after three days of casting in order to perform various tests of durability. After curing period, all bio-mortar and cylinder specimens were withdrawn from the curing chamber, dried thoroughly and subjected to tests. Compression tests for all the bio-mortar specimens were carried out at 7, 21, 28, 36, 56 and 90 days according to ASTM C 109 / C 109 M - 07.

Determination of the electrical resistivity: Electrical resistivity measurements were determined in a cell composed of three electrodes (work electrode, auxiliary electrode and Calomel electrode), controlled by a potentiostat/ galvanostat VoltaLab PGZ-301. The response of the bio-mortars was registered in the range of 1-100 kHz frequency by means of electrochemical impedance spectroscopy technique. A polarization of 10 mV peak-to-peak starting from the potential of corrosion Ecorr was applied. The obtained data were processed using the VoltaLab R31 V.003 program to get the results on electrical resistivity of mortars.

RESULTS AND DISCUSSION

Results on growth kinetics of the two selected bacterial strains and their urease activity are presented in **Table 1** and **Figure 1**. It was observed that ACRN5 showed higher urease activity than ACRN3. In the case on the effect of nickel concentrations, it was observed that 10 and 8 mM of nickel sulfate significantly (increased the intracellular and extracellular urease activity of ACRN5 (**Figure 2**) and were in accordance with earlier[19, 20].

TABLE 1. **Growth kinetics of ACRN3 and ACRN5 bacterial isolates**

Strains	N	μ ($g*h^{-1}$)	g(h)	K (h^{-1})
ACRN 3	2.6346	0.0875	3.7837	0.1884
ACRN 5	2.4889	0.0832	3.6159	0.1916

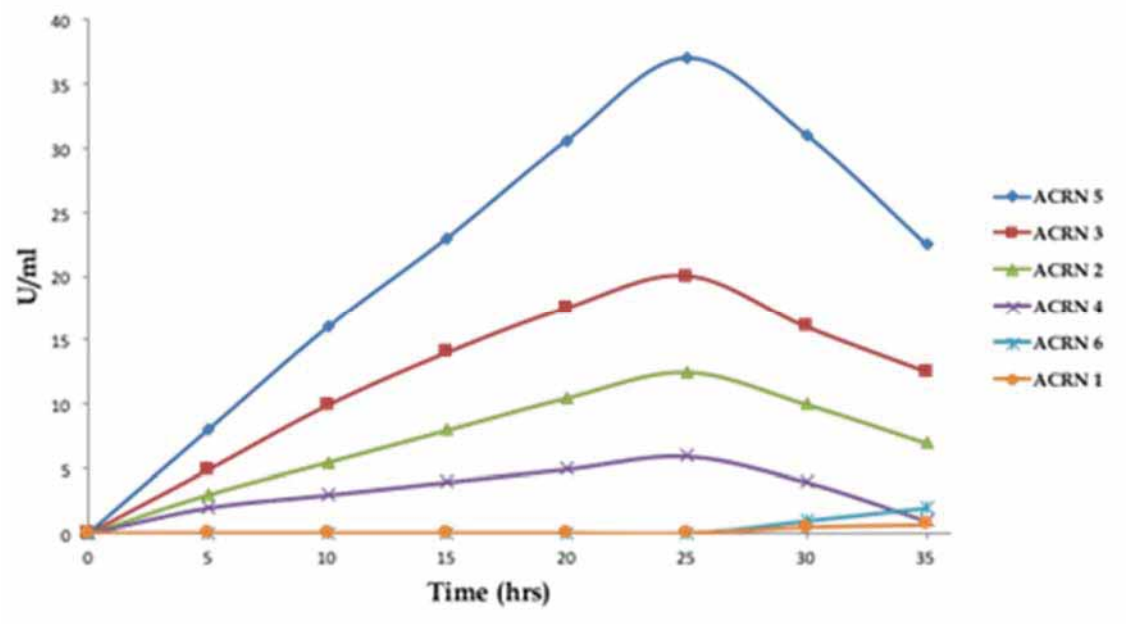


FIGURE 1. Urease activity of different uratolytic bacterial strains

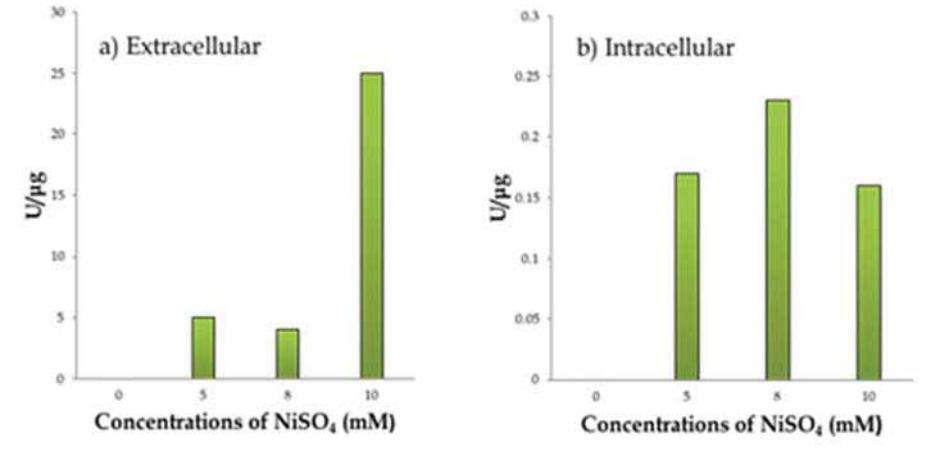


FIGURE 2. Effect of nickel on urease activity of ACRN 5

It was observed that the optimum substrate concentration, pH and temperature was 120 mM (**Figure 3**), pH 8 (**Figure 4**) and 25°C (**Figure 5**) respectively. Similar optimum conditions for pH and temperature have been reported earlier[21,22]. Further, Km and Vmax of urease activity of ACRN5 was found to be 21.38 mM and 0.212 mM.min^{-1} respectively.

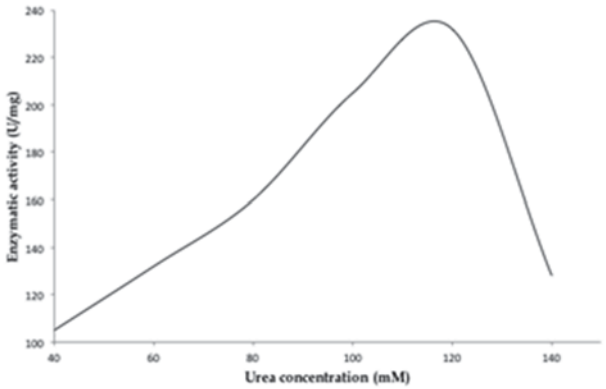


FIGURE 3. Urease activity of ACRN 5 at different urea concentrations

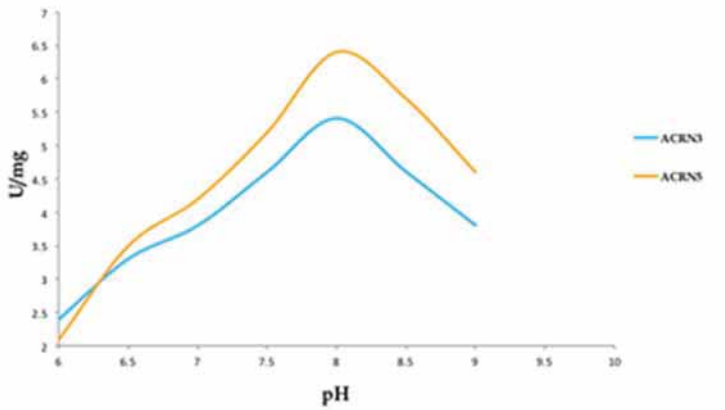


FIGURE 4. Urease activity of ACRN 3 and ACRN 5 at different pH

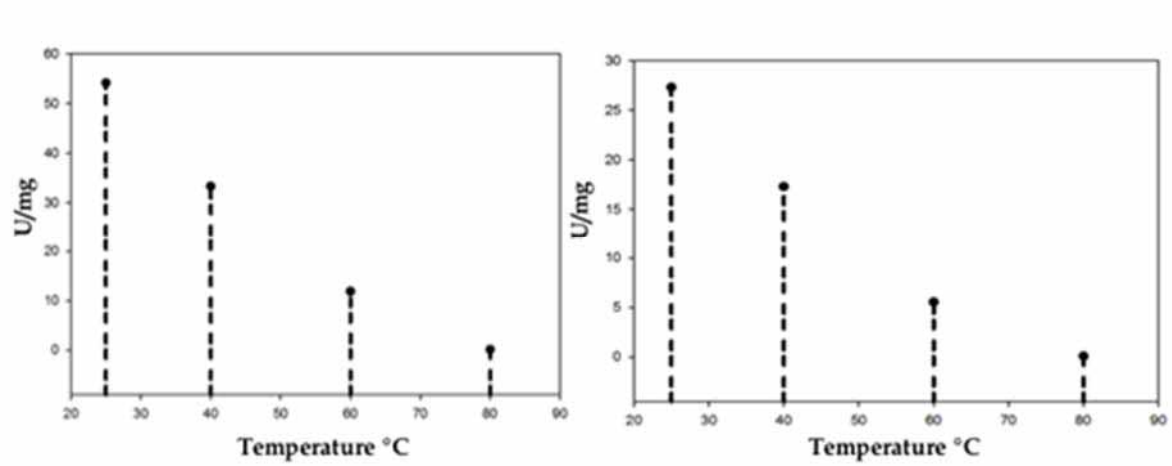


FIGURE 5. Specific urease activity of ACRN 3 and ACRN 5 at different temperatures

Results on the compressive strength of cement bio-mortar cubes prepared with two bacterial strains ACRN 3 and 5 at different cell concentrations of 10^5, 10^6 and 10^7 per mL of water are presented in Table 2. The results showed that there is an increase in the compressive strengths of bio-mortar in comparison to the control mortars without bacteria.

TABLE 2. Effect of the addition of bacterial strains ACRN 3 & ACRN 5 at different cell concentrations on the resistance of mortar cubes

Concentration of bacteria per mL of water	Average of compressive strength of specimens (kgf/cm^2)											
	7 days		21 days		28 days		36 days		56 days		90 days	
		Increase (%)		Increase (%)		Increase (%)		Increase (%)		Increase (%)		Increase (%)
Control	392.5	-	420.2	-	473	-	419.6	-	482.4		505.7	
ACRN3												
1 x 10^5	395.5	0.76	421.5	0.31	462.3	-2.26	449.4	7.1	456.3	-5.41	515.2	1.88
1 x 10^6	366.2	-6.7	394.5	-6.12	434.4	-8.16	449.4	7.1				
1 x 10^7	369.1	-5.96	409.5	-2.55	436.6	-7.70	436.7	4.08	444.4	-7.88	526.5	4.11
ACRN5												
1 x 10^5	430.6	9.71	483.4	15.04	432.0	-8.67	482.3	14.94	450.6	-6.59	487.9	-3.52
1 x 10^6	411.4	4.82	439.4	4.57	476.1	0.66	429.8	2.43	493.5	2.30	557.8	10.3
1 x 10^7	389.5	-0.76	396.9	-5.54	452.6	-4.31	420.7	0.26	495.8	2.78	500.1	-1.11

Compressive strength of bio-mortars for different curing periods is given in Figure 6. It is observed that the mortars made with ACRN 3 at a concentration of $1x10^5$ per mL of water showed a slight increase (7.1%) in compressive strength after 36 days of curing. However, ACRN 5 at a concentration of $1x10^5$ and $1x10^6$ per mL of water showed a more noticeable increase of 14.94% and 10.3% after and 36 days of curing respectively. The observed tendency of increase in compressive strength is similar to other previous reports[14,15,23].

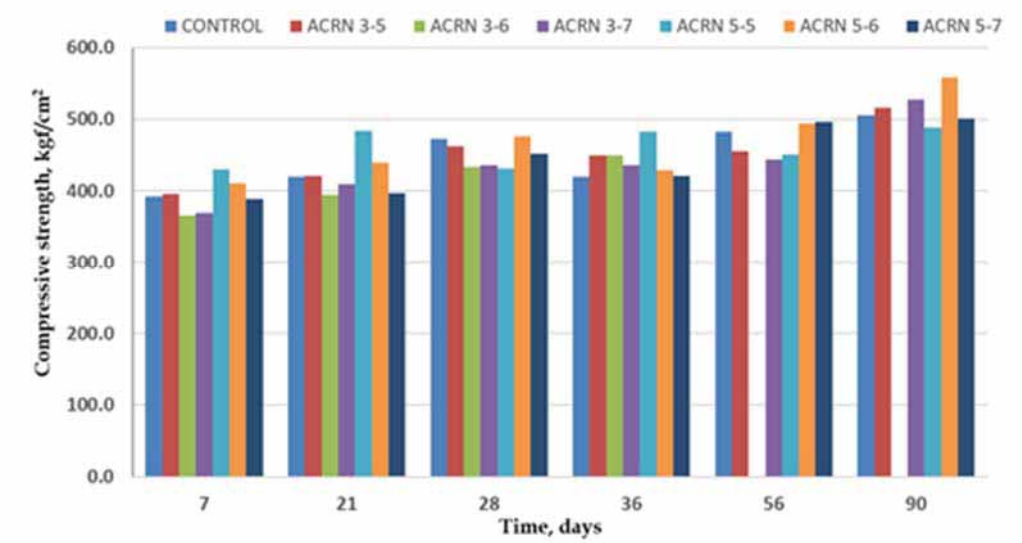


FIGURE 6. Compressive strength of bio-mortars at different bacterial concentrations and at different curing periods.

Results on electrical resistivity at different curing periods is shown in **Figure 7**. In general, the bio-mortars prepared with the ACRN 3 strain at a concentration of $1x10^7$ per mL of water showed a slight increase in resistivity after 65 days of curing. Mortars containing the ACRN 5 strain at a concentration of $1x10^5$ and $1x10^6$ per mL of water showed an increase in resistivity after 65 and 97 days of curing respectively.

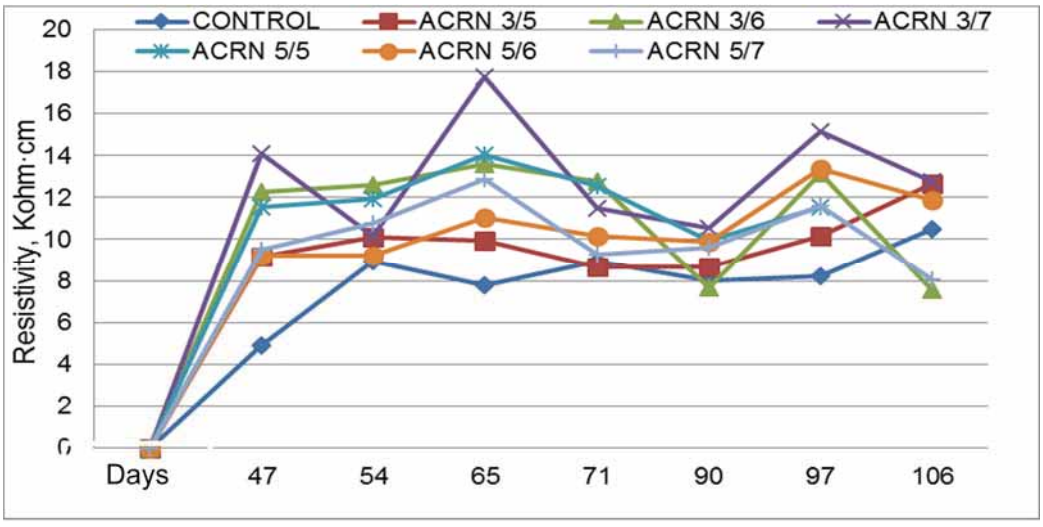


FIGURE 7. Resistivity of bio-mortars at different cell concentrations and at different curing periods.

Results of the rapid test on the permeability of chloride ions by bio-mortars at the end of the curing period is presented in **Figure 8**. It can be observed that all bio-mortar specimens recorded a low to moderate permeability. This is in agreement with previous studies, where such results yielded improvements in the durability of concrete structures[13,24-26].

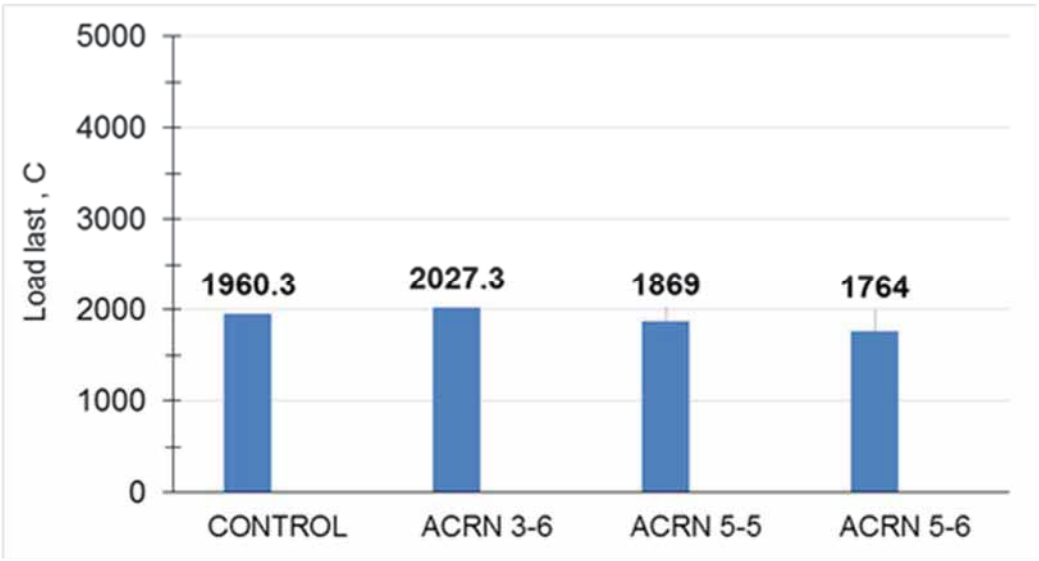


FIGURE 8. Permeability of bio-mortars at different cell concentrations at the end of curing period.

Bio-mortar specimens were also analyzed by scanning electron microscopy and energy dispersive X-ray diffraction spectrometry. The formation of calcite was observed in bio-mortar specimens confirmed the role of ureolytic microorganisms, their metabolic activity in formation of calcite and the consequent improvement in the strength and durability of concrete.

CONCLUSION

It can be concluded from the results of the study that addition of bacterial strains improved the compressive strength, resistivity and reduced the permeability of bio-mortar specimens. This study demonstrated that the physico-mechanical and structural characteristics of bio-mortar, such as resistance and durability increased with addition of the bacterial strain ACRN 5 due to biomineralization. Between the strains tested, ACRN 5 recorded better compressive strength than ACRN 3. Based on the results, it can be suggested that the addition of bacterial strains with urease activity can improve the features and performance of the concrete.

ACKNOWLEDGMENTS

Authors thank Alejandra Alvarado, Claudia Obregon, Sara Hernandez, students of Ciencias Biologicas of UAdeC, Torreon for their assistance in microbiological experiments.

REFERENCES

1. Achal V. & Mukherjee A. A review of microbial precipitation for sustainable construction. Constr Build Mater. 93 (2015) 1224-1235.
2. Khaliq W. & Ehsan M., B. Crack healing in concrete using various bio influenced self-healing techniques. Constr Build Mater. 102 (2016) 349-357.
3. Siddique R., Nanda V., Kadri E. H., Khan M. I., Singh M., & Rajor A. Influence of bacteria on compressive strength and permeation properties of concrete made with cement bag house filter dust. Constr Build Mater. 106 (2016) 461-469.
4. Achal V., Pan X., & Özyurt N. Characterization of Urease and Carbonic Anhydrase Producing Bacteria and Their Role in Calcite Precipitation. Ecol Eng. 37 (2011) 554-559.
5. Al-Salloum Y., Abbas H., Sheikh Q. I., Hadi S., Alsayed S., & Almusallam T. Effect of some biotic factors on microbially induced calcite precipitation in cement mortar. Saudi J Biol Sci. (2016). In press, DOI: 10.1016/j.sjbs.2016.01.016
6. Seifan M., Samani A. K., & Berenjian A. Bioconcrete: next generation of self-healing concrete. Appl Microbiol Biotechnol. 100 (2016) 2591-2602.
7. Hasanbeigi A., Price L., & Lin E. Emerging energy-efficiencyandCO_2 emission-reduction technologies for cementand concrete production: A technical review. Renew Sustainable Energy Rev. 16 (2012) 6220-6238.
8. Fajardo G., Valdez P. & Pacheco J. Corrosion of Steel rebar embedded in natural pozzolan based mortars exposed to chlorides. Const Build Mat. 23 (2009) 768-774.
9. Sánchez I., Nóvoa X.R., De Vera G. & Climent M. A. Microstructural modifications in Portland cement concrete due to forced ionic migration tests. Study by impedance spectroscopy. Cem Conc Res. 38 (2008) 1015-1025.
10. Achal V., Mukherjee A., Kumari D., & Zhang Q. Biomineralization for sustainable construction: A review of processes and applications. Earth-Sci. Rev. 148 (2015) 1–17.
11. Kim I. G., Jo B. H., Kang D. G., Kim C. S., Choi Y. S., & Cha H. J. Chemosphere. Biomineralization-based conversion of carbon dioxide to calcium carbonate using recombinant carbonic anhydrase. 87 (2012) 1091-1096.
12. Narayanasamy R., Villegas-Flores N., Betancourt-Silva F., Betancourt-Hernandez J. & Balagurusamy N. Application of bacteria in repairing the concrete cracks – a review Concrete under severe conditions. Environment and Loading, CRC Press, Taylor & Francis Group, London, UK. (2010) 1237-1244
13. De Muynck W., Verbeken K., De Belie N. & Verstraete W. Influence of temperature on the effectiveness of a biogenic carbonate surface treatment for limestone conservation. Appl Microbiol Biotechnol. 97 (2013) 1335-1347.
14. Ghosh S., Biswas M., Chattopadhyay B. D., & Mandal S. Microbial activity on the microstructure of bacteria modified mortar. Cement concrete comp. 31 (2009) 93–98.
15. Biswas M., Majumdar S., Chowdhury T., Chattopadhyay B., Mandal S., Halder U. & Yamasaki S. Bioremediase a unique protein from a novel bacterium *BKH1*, ushering a new hope in concrete technology. Enzyme and Micro Technol. 46 (2010) 581- 587.

16. Stocks-Fischer S., Galinat J.K. & Bang S.S. Microbiological precipitation of $CaCO_3$. J Soil Biol and Biochem. 31 (1999) 1563–1571.
17. Bradford M. M. A rapid and sensitive method for the quantitation of microgram quantities of protein utilizing the principle of protein-dye binding. Anal Biochem. 72 (1976) 248-254.Natarajan K. R. Kinetic study of the enzyme urease from *Dolichos biflorus*. J Chem Educ. 72 (1995) 556-557.
18. Bachmeier K. L., Williams A. E., Warmington J. R., & Bang S. S. J. Urease activity in microbiologically-induced calcite precipitation. Biotechnol. 93 (2002) 171-181.
19. Mulrooney S. B., Ward S. K., & Hausinger R. P. Purification and properties of the *Klebsiella aerogenes* UreE metal-binding domain, a functional metallochaperone of urease. J Bacteriol. 187 (2005) 3581-3585.
20. Achal V., Pan X. & Ozyurt N. Improved strength and durability of fly ash-amended concrete by microbial calcite precipitation. Ecol Eng. 37 (2010) 554-559.
21. Cheng I. & Cord-Ruwish R. *In situ* soil cementation with ureolytic bacteria by surface percolation. Ecol Eng. 42 (2012) 64-72.
22. Ghosh P., Mandal S., Chattopadhyay B.D. & Pal S. Use of microorganism to improve the strength of cement mortar. Cem Concr Res. 35 (2005) 1980-1983.
23. Ramachandran S.K., Ramakrishnan V. & Bang S.S. Remediation of concrete using microorganisms. ACI Materials Journal. 98 (2001) 3–9.
24. Van Tittelboom K., De Muynck W., De Belie N. & Verstraete W. In 1st WTA International PhD Symposium: Building materials and building technology to preserve the built heritage International Association for Science and Technology of Building Maintenance and the Preservation of Monuments (WTA) 33 (2009) 439-457.
25. Khan A., Hashim J., Arshad N., Khan I., Siddiqui N., Wadood A. & Choudhary M I. Dihydropyrimidine based hydrazine dihydrochloride derivatives as potent urease inhibitors. Bioorg Chem. 64 (2016) 85-96.

CHAPTER 4.4 EVALUACIÓN DE LA PRODUCCIÓN DE BIOGÁS DE BIOMASAS NO CONVENCIONALES

F. Cerutti *(1,2); V. Córdoba (1) and E. Santalla (1)

(1) Laboratorio de Bioenergía, Centro de Tecnologías Ambientales y Energía. INTELYMEC. Facultad de Ingeniería, UNICEN, Av. Del Valle 5737. B7400JWI Olavarría, Argentina

RESUMEN

Se evaluó la producción de biogás y de metano de tres biomasas lignocelulósicas como son sorgo silero (SS), sorgo biosilero (SB) y el residuo agotado (SA) de aserrín de álamo luego de la producción del hongo *Gymnopilus pampeanus*. La experiencia se realizó en bioreactores de tipo batch a escala laboratorio, en régimen mesofílico (35°C), utilizando como inóculo lodos de depuradora. Con la finalidad de evaluar la influencia de la cantidad de inóculo sobre la producción de metano se estudiaron relaciones sustrato/inóculo S/I (expresadas en unidades de sólidos volátiles) variables entre 0,5/1 y 16/1. La producción promedio de metano alcanzó 210,0 ± 18,4, 185,5 ± 6,4 y 116,4 ± 9,9 mL/g SV para SB, SS y SA respectivamente. La mayor capacidad de producción de metano se observó en SB para la menor relación S/I; en todos los ensayos se pudo observar que una mayor proporción de inóculo promovió mayor concentración de metano en el biogás aunque se detectaron diferencias relacionadas con la naturaleza del sustrato. La baja producción de metano obtenida en SA fue explicada tanto por su baja biodegradabilidad, verificada en una exigua remoción de materia orgánica (9,3% respecto al rango de 19-50% observado para los silajes de sorgo) como por la baja concentración de inóculo utilizada. El modelo de Gompertz ajustó adecuadamente los datos experimentales (R^2>0.98) y permitió obtener los parámetros cinéticos del proceso. Para los sustratos SS y SA no se detectaron influencias significativas de la relación S/I sobre los valores ajustados de los parámetros cinéticos; en SB la relación S/I influyó sobre el potencial de metano y en el tiempo de retardo obteniendo diferencias significativas entre los valores obtenidos lo que reveló que esta variedad presenta un potencial de metano promisorio para la producción de bioenergía.

Palabras claves: biomasa; digestión anaeróbica; metano; sorgo silero

INTRODUCCIÓN

En la continua búsqueda de nuevos recursos energéticos que reduzcan el uso de los combustibles fósiles y los impactos desfavorables sobre el medio ambiente, las múltiples fuentes de residuos y efluentes orgánicos conjuntamente con las biomasas provenientes de cultivos energéticos celulósicos representan una oportunidad sustancial para los futuros sistemas de energía, especialmente en el marco de una política climática global que contribuya a estabilizar la concentración de CO_2 en niveles bajos[1].

---

*Author for correspondence: vcordoba@fio.unicen.edu.ar

Argentina, por su característica de país agrícola ganadero, cuenta con una amplia variedad de climas y suelos que le permiten disponer de una superficie agrícola apta para el desarrollo de cultivos no convencionales que aporten biomasa para la producción de energía. La producción de metano a partir de la digestión anaeróbica (DA) de biomasas agrícolas ha sido implementada en varios países desarrollados aunque en Argentina la experiencia es aún incipiente. Ante el acentuado incremento de la población mundial y la demanda de alimentos, es posible imaginar una competencia entre la producción de biomasas para alimentación y para usos industriales o para la producción de energía, pero el biogás tiene la ventaja de que puede producirse tanto a partir de cultivos no convencionales que pueden cultivarse en áreas marginales como de una gran variedad de residuos y efluentes industriales. Muchos de los cultivos se utilizan directamente en la DA para producir metano aunque existen factores como la cosecha retardada que se asocian a mayor contenido de celulosa lo que provoca biodegradaciones más lentas y menor producción de metano[2]. El silaje, como un método de preservación de cultivos, ha demostrado mejorar la producción de metano en diversos cultivos como remolacha azucarera[3], maíz y arroz[4]. El sorgo pertenece a la familia *Poaceae* de fotosíntesis C_4 y constituye a nivel mundial uno de los cinco cultivos más importantes junto con el maíz, arroz, trigo y cebada. En Argentina existe amplia experiencia en el desarrollo de cultivos sileros pero son muy pocos los estudios relacionados al uso de estos materiales como fuentes de biomasa para la producción de bioenergía. Durante los últimos años se ha producido el desarrollo agronómico de nuevas variedades de sorgos sileros con mayor producción de biomasa por hectárea y de rendimiento de forraje digestible. El INTA ha evaluado nuevas variedades de sorgos sileros como el INTA Pemán que además de sus características morfológicas de alto contenido de azúcar en tallo y jugosidad (18º Brix en quinto entrenudo) presenta como características tecnológicas un alto potencial de productividad de biomasa (60 a 180 t/ha de materia volátil) por lo que es recomendado para bioenergía[43]. Los materiales ligno-celulósicos son reticentes a la conversión en biogás debido fundamentalmente a la cantidad de lignina presente. Si bien algunos pre-tratamientos químicos han demostrado reducir el contenido de lignina acelerando la etapa hidrólisis durante la DA[5,6] en general se consideran poco atractivos dado los altos costos que implican y los impactos ambientales asociados[7]. Por el contrario, los pre-tratamientos biológicos han mostrado ventajas en relación a menor requerimiento de energía y ser ambientalmente más sustentables[8] como es el caso de la acción favorable de determinadas enzimas sobre la biodegradabilidad de compuestos lignocelulósicos para mejorar la producción de biogás[9,10,11]. Ciertos microorganismos tales como la podredumbre blanda de hongos pueden ser utilizados como tratamientos biológicos para atacar materiales a través de la acción de sus enzimas[12,13], entre ellos se encuentra el hongo del género *Gymnopilus pampeanus*, como una especie comestible que se lo ha comenzado a cultivar con fines de consumo humano[14]. En la producción de este hongo se utiliza con frecuencia aserrín de *Populus* y de *Eucalypus*[15,16], materiales ambos ampliamente utilizados en Argentina en la industria maderera y para envases. Como resultado de la producción de hongos, se genera un residuo conocido como sustrato agotado, material de muy baja densidad que provoca un alto requerimiento de espacio y problemas para su disposición final.

La energía neta que se produce en un proceso anaeróbico es una tarea compleja que depende de una gran variedad de factores que afectan directamente la producción

de metano[17]. Uno de los parámetros claves en la DA de sustratos sólidos es la relación entre la cantidades de sustrato (S) y de inóculo (I) aplicadas, expresadas en términos de la cantidad de sólidos volátiles (SV) agregados al reactor, siendo este parámetro uno de los más importantes del proceso ya que representa la fuente de materia orgánica disponible para la producción de metano[18]. La cantidad de inóculo añadido al proceso representa una fuente variada de organismos promotores de la acción metanogénica que influye no solamente durante la puesta en marcha del proceso sino también sobre la velocidad de producción de metano y en el rendimiento final del proceso[19,20,21]. El efecto del tipo y cantidad de inóculo sobre la producción de metano de diversos sustratos ha sido estudiado por varios autores. Se ha reportado que relaciones S/I entre 1:1 y 1:3 son favorables para la producción de metano aunque el valor óptimo depende fuertemente del tipo de sustrato[22]. Para el caso de sustratos recalcitrantes se han sugerido relaciones S/I entre 1:1 y 1:2[23,24]. También se ha reportado la importancia de determinar la relación óptima para sustratos desconocidos con el objetivo de minimizar el requerimiento de inóculo activo durante la etapa de puesta en marcha de un digestor[21].

El objetivo del presente trabajo es estudiar el comportamiento de dos biomasas lignocelulósicas como son el silaje de sorgo y el residuo agotado de la producción de hongos bajo digestión anaeróbica con la finalidad de evaluar su potencial de producción de metano, la influencia de la relación sustrato/inóculo y la cinética del proceso a partir de la determinación y el análisis de los parámetros cinéticos obtenidos al aplicar el modelo de Gompertz.

MATERIALES Y MÉTODOS

Sustratos utilizados. Se utilizaron dos variedades de sorgo INTA-Pemán y el sustrato agotado de la producción de *Gymnopilus pampeanus* (SA). Los sorgos de tipo silero (SS) y biosilero (SB) fueron sembrados ambos ad-hoc con control de malezas, de insectos y fertilización. Para el ensilado de ambos cultivos se procedió a realizar el picado de planta entera con un tamaño de 20 mm aproximadamente seguido por inoculación con bacterias lácticas específicas. Los rendimientos en materia verde resultaron 50 y 70 t/ha con 28,19 y 25,37% de materia seca (MS) y una DIVMS (digestibilidad in vitro de materia seca) de 55,73 y 58,12% % para silero y biosilero respectivamente. Estos sustratos se conservaron refrigerados a 5°C hasta el comienzo del ensayo. Como blanco se utilizaron muestras de ambos sorgos sin inocular. El SA corresponde a aserrín de *Populus sp* con ajuste previo de humedad (70%), esterilizado (autoclave, 2 h, 120 °C, 120 psi), inoculado al 5% p/p en flujo laminar con *G. pampeanus*, fermentado durante 75 días en condiciones controladas (25 °C, 60% humedad y oscuridad), acondicionado del sustrato colonizado para la producción (18-20 °C, 80-90% humedad y fotoperíodo de 9/15 luz/oscuridad). Una vez realizada la cosecha se obtuvo el sustrato agotado el cual fue almacenado a -20 °C antes de su uso[14]. Como blanco se utilizó sustrato sin fermentar ni colonizar (SSF).

Inóculo. Se utilizó lodo de depuradora de la planta de tratamiento de aguas residuales de Olavarría. Con el objetivo de asegurar la degradación de la materia orgánica

fácilmente degradable que pudiera estar presente en el inóculo (I), se mantuvo el mismo en reactores batch en condiciones mesofílicas (35°C ±1) hasta su uso[28].

Diseño experimental. Se desarrolló un diseño experimental utilizando diferentes relaciones sustrato/inóculo (S/I). Se realizaron ensayos por duplicado incluyendo como blancos cada uno de los sustratos y el inóculo. Se utilizaron bioreactores batch de 1 L de capacidad en régimen mesofílico (35°C)[25]. Con el fin de tener en cada bioreactor un contenido de sólidos totales inferior al 10%, tal que asegure la degradación de la materia orgánica bajo DA de tipo húmeda[26] se agregó a cada bioreactor la cantidad necesaria de agua destilada. El experimento fue monitoreado diariamente y se detuvo cuando la diferencia diaria de la producción acumulada de metano resultó inferior a 0,2%. La **Tabla 1** describe las condiciones de cada ensayo.

TABLA 3. Diseño experimental

Biomasa	**SS**			**SB**				**SA**		**SSF**	**I**
S/I (g SV S/g SV I)	0,5/1	1/1	blanco	0,5/1	1/1	2/1	blanco	3/1	16/1	blanco	
Sustrato (g)	53,8	53,8	53,8	66,1	66,1	66,1	66,1	200	200	200	-
Inóculo (g)	801	400		801	400	200		300	50		300
Volumen de agua (mL)	22	71	120	9	58	83	107	300	300	300	-

Caracterización física y química de los sustratos y del inóculo. Los parámetros analizados fueron porcentaje de sólidos totales (ST), de sólidos volátiles (SV) y cenizas. Para el inóculo se determinó además la demanda química de oxígeno (DQO, mg/L), el contenido de nitrógeno total (NT, mg/L), pH y alcalinidad total (AT, mg/L), todos de acuerdo a los métodos APHA[27]. Además, se determinó %SV al inicio y al final de cada ensayo.

Análisis de biogás. El volumen de biogás se determinó por desplazamiento de agua[25]. La calidad del biogás se evaluó según la concentración de metano a través de mediciones periódicas (al menos diariamente) utilizando un medidor portátil (Landgem GA2000) provisto de celdas infrarrojas para la medición de metano y dióxido de carbono (máximo error ±0.5%) y celdas electroquímicas para la medición de oxígeno (máximo error ±1.0%). La calibración de las celdas se realizó con una mezcla de gases certificados patrón (CH_4-CO_2, AGA Certificado N° 165342). La producción de metano de cada ensayo se refirió como producción neta del sustrato utilizado, para lo cual se restó la producción de metano producida por el inóculo[28].

Cinética de la producción de metano. Los modelos que representan la cinética de la producción de metano bajo DA proveen información útil para el diseño y operación del proceso[29,30]. Los de cinética de primer orden resultan los más simples para estudiar la DA de sustratos complejos, ya que permiten comparar el desempeño del proceso

estacionario en condiciones prácticas. La producción acumulada de metano durante una DA batch de sustratos con alto contenido de sólidos se puede describir a través de la ecuación de Gompertz[31,32] (Ec. 1) la cual representa una regresión no lineal que ha sido utilizada en la simulación de la producción de metano e hidrógeno de lodos granulares[29,33], en la co-digestión de purín de cerdo y residuos alimenticios[34] y en la co-digestión de residuos orgánicos con cenizas[35], entre otros.

$$M(t)= P\,exp[-exp(R/P)(\lambda-t)e+1)] \quad (1)$$

donde M es la producción acumulada de metano (mL/g SV) en el tiempo t (días); λ es el tiempo de retardo (días); P es la producción potencial máxima de metano (mL/g SV); R es la velocidad máxima de producción de metano (mL/g SV/d) y e es la constante matemática. Los datos experimentales de la producción acumulada de metano se ajustaron a la ecuación de Gompertz utilizando Statgraphics Centurion XVI (v.16.2.04).

Análisis estadístico. Para el análisis estadístico de los resultados se utilizó t-Student a un nivel de confianza de 95.0 %. Los datos experimentales se expresaron como valores medios ± el desvío estándar de los duplicados. Se aplicó el test ANOVA para determinar la diferencia significativa mínima de Fisher (LSD) para una tasa de error individual α=0.05. Para la determinación de los parámetros estadísticos se utilizó Statgraphics Centurion XVI (v.16.2.04).

RESULTADOS Y DISCUSIÓN

Caracterización física y química de los sustratos y del inóculo. La **Tabla 2** muestra los resultados de la caracterización de los sustratos y del inóculo. El menor porcentaje de ST observado en I indica una composición con mayor contenido en agua. La cantidad de SV es un parámetro importante para el análisis del proceso anaeróbico ya que representa la fuente de materia orgánica a partir de la cual el biogás es producido[18]; el sustrato SS supera en 4,8 y 12,6% el contenido de este parámetro respecto a SB y SA respectivamente.

La mayoría de las bacterias anaeróbicas, incluyendo las metanogénicas, se desempeñan satisfactoriamente en un rango de pH de 6,8 a 7,2; valores de pH por debajo de 6 o superiores a 8 pueden resultar tóxicos para la formación de estas bacterias[40]. Como puede observarse, el pH del SB está dentro de este rango óptimo, mientras que el del inóculo y el del SS son levemente superiores, aunque por debajo del valor restrictivo, por lo que no se consideró necesario realizó ningún acondicionamiento de la biomasa del reactor tendiente a regular este parámetro. Para mantener el pH estable durante el proceso, se requiere un alto grado de alcalinidad[36], valores mayores a 3000 mg/L aseguran la estabilidad del proceso[23,37]. El valor de AT en el inóculo es indicador de una adecuada capacidad amortiguadora del sistema mientras que su contenido en NT revela una baja relación DQO/NT (123/5) comparada con el rango recomendado (entre 350/5 y 1000/5) para asegurar un crecimiento adecuado de los microorganismos[37].

TABLA 4. Caracterización física y química de los sustratos y del inóculo

Parámetro	SS	SB	SA	I
ST (%)	28,43 ± 2,64[a]	23,07 ± 1,04[b]	15,06 ± 0,53[c]	5,01 ± 0,07[d]
SV (%)	26,02 ± 2,70[a]	21,19 ± 1,37[b]	13,40 ± 0,57[c]	3,32 ± 0,11[d]
Cenizas (%)	2,40 ± 0,46[a]	1,88 ± 0,35[b]	1,66 ± 0,10[b]	1,69 ± 0,04[b]
pH	7,87	7,13	-	7,92
AT (mg/L)	1044±22[a]	843±33[b]	-	6109 ± 90[c]
NT (mg/L)	-	-	-	1825 ± 120
DQO (mg/L)	-	-	-	44750 ± 2616
Lignina (%)		5,78[a]	11,28[b]	

Los valores obtenidos son el promedio de duplicados ± desvío estándar. Valores con la misma letra, en una misma fila, indican que no tienen diferencias significativas (p>0.05). Los porcentajes expresados son en base húmeda. [a] http://www.peman.com.ar/silero.html [b] Ref[14]

Efecto de la relación S/I sobre el potencial metano génico. La **Figura 1** muestra la producción de metano y de biogás obtenida para cada uno de los sustratos estudiados con diferentes proporciones de inóculo. En SS la producción acumulada promedio de biogás disminuyó 13% al duplicar la cantidad de inóculo, aunque la generación de metano no presentó diferencias significativas obteniendo 185±6 mL/g SV y 182±15 mL/g SV para S/I 1/1 y 0,5/1 respectivamente.

La producción de biogás para SB no mostró diferencias significativas entre las distintas relaciones S/I analizadas alcanzando un promedio de 345±21 mL/g SV. La mayor producción acumulada de metano para este sustrato se obtuvo para la relación S/I de 0,5/1 y resultó 210±18 mL/g SV, disminuyendo 9% y 25% la capacidad metanogénica al aumentar la relación S/I a 1 y a 2 respectivamente (diferencias estadísticamente no significativas). Un comportamiento similar fue observado en SA, donde la mayor producción de metano (116±10 mL/g SV) se observó para la relación S/I 3/1 disminuyendo 38% al aumentar la relación a 16 (diferencias significativas); para el mismo sustrato, la producción de biogás resultó 201±2 mL/g SV para la relación 3/1 y disminuyó 27% al incrementar la relación S/I a 16/1 (diferencia significativa).

En todos los casos la utilización de mayor proporción de inóculo propició una mejor calidad de biogás en términos de contenido de metano, tal como se observa en la **Figura 1**. Varios autores[38,39] afirman que existe una relación S/I óptima, de manera tal que no produzca la sobrecarga del proceso, pero que sea lo suficientemente alta como para inducir las enzimas necesarias para la biodegradación del sustrato y que favorezcan la producción de metano. De los resultados obtenidos se observa que el mismo inóculo puede tener un efecto específico diferente según las características del sustrato y que el potencial de metano no siempre está directamente ligado a la cantidad de inóculo utilizado.

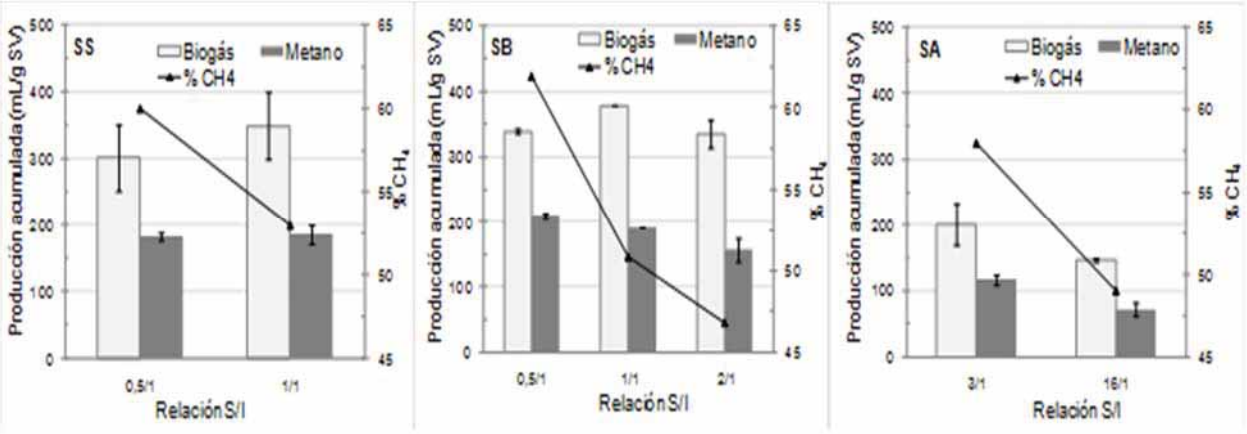


FIGURA 3. Variación de la producción acumulada de biogás y metano con la relación S/I

La remoción de materia orgánica en términos de SV para las diferentes relaciones S/I ensayadas, se mantuvo en el rango de 19 a 38% para SS , entre 25 y 50% para SB, y sólo 5,5 (S/I 16) y 9,3% (S/I 3) para SA. La baja de remoción de materia orgánica mostrada por SA durante la DA reveló que la degradación biológica sufrida por el aserrín durante la producción del hongo no resultó suficiente para destruir su estructura lignocelulósica y facilitar el acceso a las bacterias metanogénicas, como demostraron Colavolpe y Albertó[14] al reportar un remanente final de lignina luego de la acción fúngica de 11,28%.

Los resultados observados de producción de metano en función de la relación S/I para los sustratos estudiados mostraron similar tendencia a los reportados por otras biomasas diversas como tallos de algodón[21], el residuo de la producción de vinagre[40], la vinaza[41], residuos del desmote de algodón o del orujo de aceitunas[42], tal como muestra la Figura 2. Como tendencia general se observa que a medida que la concentración de inóculo disminuye también lo hace la producción de metano; esta tendencia resulta más acentuada para relaciones S/I bajas, en donde al aumentar la relación S/I de 0,5 a 2, la producción de metano se reduce en un 25,2% para el SB comparable a las reducciones alcanzadas por los residuos de desmote de algodón (31,3%) y por el orujo de aceituna (41,6%). Cuando la relación supera el valor de 2, la incidencia de la cantidad de inóculo utilizada es menos significativa, tal como se ve en la producción de metano a partir de tallos de algodón y de residuos de la producción de vinagre donde al aumentar la relación de 2 a 6 la reducción fue del orden de 39,6% y 10,1% respectivamente, similar a la observada en el presente trabajo para SA, donde el incremento de la relación de 3 a 16 redujo la producción de metano 38%.

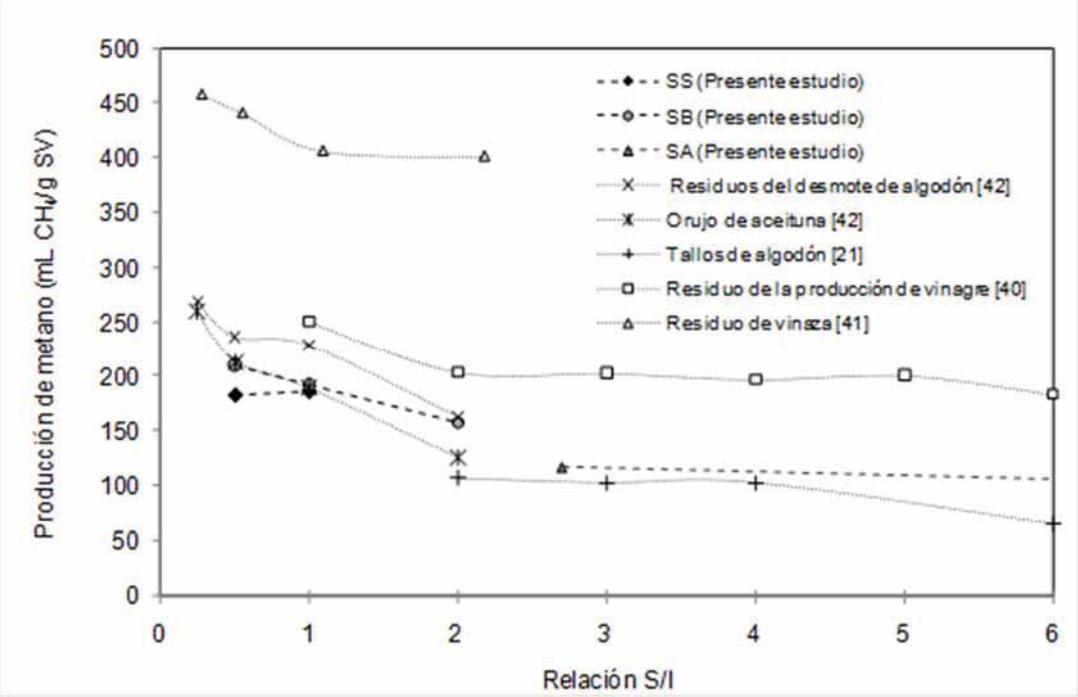


FIGURA 4. Variación de la producción de metano con la relación S/I para diversas biomasas.

Análisis cinético de producción de metano. Los datos experimentales de producción de metano fueron ajustados al modelo de Gompertz (Ec. 1). La **Tabla 3** detalla los parámetros cinéticos obtenidos y sus estadísticos. Los datos experimentales ajustaron adecuadamente al modelo mostrando un coeficiente de determinación superior a 98%. La **Figura 3** muestra los datos experimentales de producción acumulada de metano (rótulos) y los resultados del ajuste (líneas) del modelo de Gompertz para cada uno de los sustratos analizados.

TABLA 5. Parámetros cinéticos de la producción de metano de las tres biomasas estudiadas con diferente relación S/I y su ajuste a la ecuación de Gompertz

Ensayo	Potencial de CH_4 P		Dif.	R	λ	R^2
	Experimental	Ajustado				
	mL CH_4/g SV		%	mL CH_4/g SVd	d	
SS 0,5/1	182,5 ± 14,8^a	185,4 ± 23,3^a	1,6	7,4 ± 0,2^a	1,4 ± 1,9^a	99,46
SS 1/1	185,5 ± 6,4^a	188,3 ± 4,5^a	1,5	7,7 ± 0,3^a	1,1 ± 0,1^a	99,59
SB 0,5/1	210,0 ± 18,4^a	219,1 ± 8,2^c	4,3	7,7 ± 0,3^a	-0,3 ± 0,3^a	99,06
SB 1/1	192,0 ± 0,0^a	194,1 ± 0^b	1,1	7,7 ± 0,4^a	1,5 ± 0,3^b	99,57
SB 2/1	157,0 ± 4,2^a	157,8 ± 2,8^a	0,5	7,4 ± 0,2^a	3,5 ± 0,5^c	99,70
SA 3/1	116,4 ± 9,9^b	149,3 ±12,3^a	28,3	1,7 ± 0,1^a	32,2 ± 2,6^a	98,36
SA 16/1	71,7 ± 7,3^a	98,3 ±3,1^a	37,1	1,7 ± 0,0^a	58,0 ± 0,4^b	99,96

Los valores obtenidos son el promedio de duplicados ± desvío estándar. Para el mismo sustrato, valores con las mismas letras indican diferencias no significativas (p>0.05).

El potencial de metano experimental resultó en todos los casos inferior al valor predicho por el modelo, aunque las diferencias fueron inferiores al 5% para ambos sorgos sileros. Para el caso del SA la mayor diferencia observada entre los valores medidos y los reportados por el modelo se explica en el hecho de que el tiempo total del ensayo se determinó con el criterio de que cuando la diferencia diaria de la producción acumulada de metano fuera inferior a 0,2% se consideraba concluido, lo que pudo generar una subestimación del valor total acumulado. El sustrato SA presentó en ambos ensayos una velocidad máxima de producción de metano (R) significativamente inferior (entre 76 y 77%) a las obtenidas para SS y SB mientras que la fase de letargo (λ) resultó sensiblemente superior a los ensilados de sorgo, acentuada a mayor concentración de sustrato (**Figura 3**).

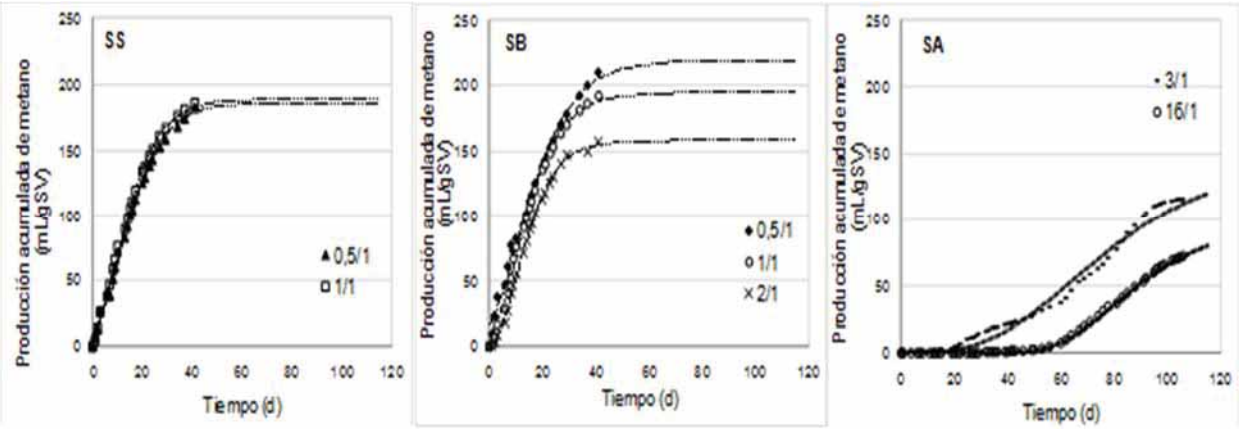


FIGURA 5. Ajuste del modelo de Gompertz a los datos experimentales de producción acumulada de metano de los tres sustratos estudiados.

Para los sustratos SS y SA no se detectaron influencias significativas de la relación S/I sobre los valores ajustados de los parámetros cinéticos obtenidos. En SB la relación S/I influyó sobre el potencial de metano y en el tiempo de retardo obteniendo diferencias significativas entre los valores obtenidos para cada S/I. Del análisis de estos parámetros se evidencia que la naturaleza del sustrato tiene un efecto significativo sobre la cinética de la producción de metano; mientras SA es una biomasa de baja biodegradabilidad con un contenido de lignina comparativamente alto para la cual el proceso de fermentación provocado por el metabolismo del hongo no resultó suficiente para degradar la estructura lignocelulósica, los sorgos ensilados mostraron aptitud para la producción de metano.

CONCLUSIÓN

Se estudió el comportamiento bajo digestión anaeróbica de tres sustratos de tipo lignocelulosicos (sorgo silero, sorgo biosilero y aserrín de álamo degradado biológicamente) evaluando la producción y calidad del biogás generado al utilizar diferentes concentraciones de inóculo. Los resultados mostraron que mayor concentración de inóculo mejora la calidad del biogás en términos de concentración de

metano, aunque se observaron diferencias relacionadas con la naturaleza del sustrato. Entre los sorgos ensilados, la variedad biosilero mostró mayor capacidad de producción de metano. El metabolismo del hongo no resultó suficiente como proceso de fermentación para degradar la estructura lignocelulósica de un sustrato de alto contenido de lignina como es el aserrín de álamo y habilitarlo para la acción posterior de las bacterias metanogénicas, lo cual se verificó en términos de una baja remoción de materia orgánica, baja productividad de metano y mayor fase de letargo. El modelo de Gompertz ajustó adecuadamente los datos experimentales de producción de metano y permitió obtener los parámetros cinéticos para las biomasas estudiadas con un ajuste superior a 98%.

AGRADECIMIENTOS

Los autores agradecen a la Comisión de Investigaciones Científicas de la Provincia de Buenos Aires por la beca de entrenamiento otorgada a la alumna Florencia Cerutti como así también a la Cooperativa Eléctrica de Olavarría (Coopelectric), al Ing. Elbio Woeffray y al Dr. Edgardo Albertó (IIB-INTECH) por el suministro respectivo de lodos, sorgos y sustrato agotado de la producción de hongos, utilizados para el desarrollo del trabajo.

REFERENCIAS

1. Popp A., J, P, Dietrich, H, Lotze-Campen, D. Klein, N. Bauer, M. Krause, T. Beringer, D. Gerten, and O. E. The economic potential of bioenergy for climate change mitigation with special attention given to implications for the land system. Environ. Res. Lett. 6, 34–44 (2011).
2. Braun, R., Weiland, P. & Wellinger, A. Biogas from energy crop digestion. IEA Bioenergy Task (2008).
3. Weissbach, F. Gas production potential of fresh and ensiled sugar beets in biogas production. Landtechnik 6, 394–397 (2009).
4. Herrmann, C., Heiermann, M. & Idler, C. Effects of ensiling, silage additives and storage period on methane formation of biogas crops. Bioresour. Technol. 102, 5153–5161 (2011).
5. Sambusiti, C., Ficara, E., Malpei, F., Steyer, J. P. & Carrère, H. Effect of sodium hydroxide pretreatment on physical, chemical characteristics and methane production of five varieties of sorghum. Energy 55, 449–456 (2013).
6. Sambusiti, C., Ficara, E., Malpei, F., Steyer, J. P. & Carrère, H. Influence of alkaline pre-treatment conditions on structural features and methane production from ensiled sorghum forage. Chem. Eng. J. 211-212, 488–492 (2012).
7. Costa, J. C., Barbosa, S. G., Alves, M. M. & Sousa, D. Z. Thermochemical pre- and biological co-treatments to improve hydrolysis and methane production from poultry litter. Bioresour. Technol. 111, 141–147 (2012).
8. Sun, Y. & Cheng, J. Hydrolysis of lignocellulosic materials for ethanol production : a review q. Bioresour. Technol. 83, 1–11 (2002).
9. Bruni, E., Jensen, A. P. & Angelidaki, I. Comparative study of mechanical, hydrothermal, chemical and enzymatic treatments of digested biofibers to improve biogas production. Bioresour. Technol. 101, 8713–8717 (2010).
10. Fernandes, T. V., Klaasse Bos, G. J., Zeeman, G., Sanders, J. P. M. & van Lier, J. B. Effects of thermo-chemical pre-treatment on anaerobic biodegradability and hydrolysis of lignocellulosic

biomass. Bioresour. Technol. 100, 2575–2579 (2009).
11. Pakarinen, A. et al. Evaluation of preservation methods for improving biogas production and enzymatic conversion yields of annual crops. Biotechnol. Biofuels 4, 20 (2011).
12. Zhong, W. et al. Effect of biological pretreatments in enhancing corn straw biogas production. Bioresour. Technol. 102, 11177–11182 (2011).
13. Colavolpe, B. et al. comestibles como co-digestor para obtener biogás. AVERMA 16, 01–01 – 01–06 (2012).
14. Colavolpe, M. B. & Alberto, E. Cultivation requirements and substrate degradation of the edible mushroom Gymnopilus pampeanus-A novel species for mushroom cultivation. Sci. Hortic. (Amsterdam). 180, 161–166 (2014).
15. D.G. Pire, J.E. Wright, E. A. Cultivation of shiitake using sawdust from Widely available local woods in Argentina. Micol. Apl. Int. 13, (2001).
16. Omarini, A., Lechner, B. E. & Albertó, E. Polyporus tenuiculus: A new naturally occurring mushroom that can be industrially cultivated on agricultural waste. J. Ind. Microbiol. Biotechnol. 36, 635–642 (2009).
17. Mateescu, C. & Constantinescu, I. Comparative analysis of inoculum biomass for biogas potential in the anaerobic digestion. UPB Sci. Bull. Ser. B Chem. Mater. Sci. 73, 99–104 (2011).
18. Drosg, B. Process monitoring in biogas plants. (IEA Bioenergy, 2013).
19. Neves, L., Oliveira, R. & Alves, M. M. Influence of inoculum activity on the bio-methanization of a kitchen waste under different waste/inoculum ratios. Process Biochem. 39, 2019–2024 (2004).
20. M.F. Demirbas, M. B. Progress and Recent Trends in Biogas Processing. Int. J. Green Energy 117–142 (2009).
21. Cheng, X. & Zhong, C. Effects of Feed to Inoculum Ratio, Co-digestion, and Pretreatment on Biogas Production from Anaerobic Digestion of Cotton Stalk. Energy & Fuels 28, 3157–3166 (2014).
22. Lesteur, M. et al. Alternative methods for determining anaerobic biodegradability: A review. Process Biochem. 45, 431–440 (2010).
23. Chynoweth, D. P., Turick, C. E., Owens, J. M., Jerger, D. E. & Peck, M. W. Biochemical methane potential of biomass and waste feedstocks. Biomass and Bioenergy 5, 95–111 (1993).
24. Owens, J. M., Legrand, R. & Chynoweth, D. P. Renewable methane from anaerobic digestion of biomass. Renew. Energy 1–8 (2001).
25. Córdoba, V., Fernández, M. & Santalla, E. The effect of different inoculums on anaerobic digestion of swine wastewater. J. Environ. Chem. Eng. 4, 115–122 (2016).
26. Pakarinen, A. et al. Evaluation of preservation methods for improving biogas production and enzymatic conversion yields of annual crops. Biotechnol. Biofuels 4, 20 (2011).
27. APHA. APHA: Standard Methods for the Examination of Water and Wastewater. 20th ed. Washington, DC. (American Public Health Association, 1999).
28. Hansen, T. L. et al. Method for determination of methane potentials of solid organic waste. Waste Manag. 24, 393–400 (2004).
29. Mu, Y., Wang, G. & Yu, H.-Q. Kinetic modeling of batch hydrogen production process by mixed anaerobic cultures. Bioresour. Technol. 97, 1302–7 (2006).
30. Angelidaki, I., Ellegaard, L. & Ahring, B. K. A Mathematical Model for Dynamic Simulation of Anaerobic Digestion of Complex Substrates: Focusing on Ammonia Inhibition. Biotechnol. Bioeng. 42, 159–166 (1993).
31. Lay, J., Li, Y., Noike, T., Endo, J. & Ishimoto, S. Analysis of environmental factors affecting methane production from high-solids organic waste. Water Sci. Technol. 36, 493–500 (1997).
32. Lay, J., Li, Y. & Noike, T. Influences of pH and moisture content on the methane production in high-solids sludge digestion. Water Res. 31, 1518–1524 (1997).

33. Lin, C. & Shei, S. Heavy metal effects on fermentative hydrogen production using natural mixed microflora. Int. J. Hydrogen Energy 33, 587–593 (2008).
34. Shin, J. et al. Predicting Methane Production Potential of Anaerobic Co-digestion of Swine Manure and Food Waste. Environ. Eng. Resour. 13, 93–97 (2008).
35. Lo, H. M. et al. Modeling biogas production from organic fraction of MSW co-digested with MSWI ashes in anaerobic bioreactors. Bioresour. Technol. 101, 6329–6335 (2010).
36. Gerardi, M. H. The microbiology of anaerobic digesters. (John Wiley & Sons, Inc., Hoboken, New Jersey, 2003).
37. Ghasimi, S. M. D., Idris, a, Chuah, T. G. & Tey, B. T. The Effect of C:N:P ratio, volatile fatty acids and Na+ levels on the performance of an anaerobic treatment of fresh leachate from municipal solid waste transfer station. African J. Biotechnol. 8, 4572–4581 (2009).
38. Elbeshbishy E1, Nakhla G, H. H. Biochemical methane potential (BMP) of food waste and primary sludge: influence of inoculum pre-incubation and inoculum sourceNo Title. Bioresour Technol. (2012). DOI: 10.1016/j.biortech.2012.01.025.
39. Zhou, Y. et al. Influence of substrate-to-inoculum ratio on the batch anaerobic digestion of bean curd refuse-okara under mesophilic conditions. Biomass and Bioenergy 35, 3251–3256 (2011).
40. Feng, L. et al. Biochemical methane potential (BMP) of vinegar residue and the influence of feed to inoculum ratios on biogas production. BioResources 8, 2487–2498 (2013).
41. Eskicioglu, C. & Ghorbani, M. Effect of inoculum/substrate ratio on mesophilic anaerobic digestion of bioethanol plant whole stillage in batch mode. Process Biochem. 46, 1682–1687 (2011).
42. Pellera, F. & Gidarakos, E. Effect of substrate to inoculum ratio and inoculum type on the biochemical methane potential of solid agroindustrial waste. J. Environ. Chem. Eng. (2016). DOI: 10.1016/j.jece.2016.05.026
43. INTA. Evaluación de sorgos para silajes - Grupo Producción Ganadera - Área de Producción Animal. Ing. Agr. Marcelo De León / Ing. Agr. Rubén Giménez. http://www.peman.com.ar/silero.html

CHAPTER 4.5 PROTEOLYTIC EXTRACTS OF THREE BROMELIACEAE SPECIES AS ECO-COMPATIBLE TOOLS FOR LEATHER INDUSTRY

M. E. Errasti *(1); N. O. Caffini (1) and L. M. I. Lopez (2)

(1) CIProVe, FCE, UNLP, Calle 47 & 115, La Plata, Argentina
(2) Centro de Investigación y Tecnología del Cuero (CITEC), CIC-INTI. Camino Parque Centenario e/ 505 & 508. Manuel B. Gonnet, Argentina

ABSTRACT

In addition to the large quantities of solid waste rich in protein, most tanneries use high proportions of Na_2S and CaO during the dehairing step, resulting in effluents of high alkalinity and large amounts of suspended solid, besides the risk of liberating the toxic hydrogen sulphide. The current worldwide legislation on environmental requires tanneries to reduce pollution and to replace conventional processes by greener technologies.

Enzymes are a technological tool of interest for industry because are able to achieve a high reaction rate under soft pH, temperature, and pressure conditions, besides a high specificity of reaction, biodegradability, non-toxic nature and non-polluting effluent generation. In leather industry enzymes are principally used in pre-tanning operations (soaking, dehairing, bating, and degreasing) and waste treatment. Particularly, proteases have been chosen as a promising eco-friendly alternative to lime and sodium sulphide dehairing.

Extracts rich in cysteine proteases with high proteolytic activity (CU) have been obtained from fruits of Bromeliaceae species: *Bromelia balansae* (Bb), *B. hieronymi* (Bh), and *Pseudananas macrodontes* (Pm). In this work, Bb, Bh, and Pm have been studied for application in leather industry compared with commercial enzyme, focusing in their dehairing properties. Enzymatic activities against representative substrates of skin proteins were spectrophotometrically measured at 25, 35, and 55ºC (Tris-HCl, 0.1 M, pH 8, Cys 20 mM). Keratin Azure (KA), Elastin-Congo Red (E), epidermis substrate (EP), and Hide Powder Azure (HPA) were used as representative substrates of keratin, elastin, epidermis, and collagen, respectively. Ability to dehairing was evaluated by incubating soaked cow skins with different concentrations of extracts at 25ºC and pH 8 during 24 h. Grain surface and cross section of skins were observed by scanning electron microscopy.

Extracts were able to degrade representative substrates of skin proteins and when compared to the same CU showed similar activity on collagen and epidermis; however, Bh and Pm were the most actives against keratin, while Bh was the only active against elastin. Extracts showing different proteolytic activity (Bb required 1 CU/ml, Bh 1.5 CU/ml, and Pm 0.5 CU/ml) were able to depilate cow skin after a gentle scraping. Although depilated skins with Bb, Bh, and Pm showed different surface aspects, desirable characteristics of dehairing were observed for all extracts since hair pores did

---

*Author for correspondence: eerrasti@gmail.com

not show residual hair, grain surface were clean and intact, and collagen fiber bundles of dermis were not damaged.
In conclusion, results here presented show that proteolytic extracts of Bromeliaceae species are promising eco-compatible tools for leather industry, principally in treatment of their waste and dehairing process.

Keywords: Bromeliaceae; dehairing; leather; plant proteases

INTRODUCTION

Leather has played a key role in the development of human civilization and leather industry has had an important contribution in economy of many countries, with a rising worldwide market for the coming years[1,2]. Despite those benefits, it has a negative image in society due to the use of toxic chemicals for human health and their wastes (solid, liquid and gaseous) which it means a source of environmental pollution. Accordingly, the current worldwide legislation on environmental requires tanneries to reduce pollution and to replace conventional processes by greener technologies[3].
The goal of leather manufacture is transform unstable skins or hides in leather, but only 15-25 % of hide weight is converted into leather and the rest are solid wastes, mainly constituted by proteins[4,5]. Leather processing involves a series of unit operations that can be classified into three groups: (i) pre-tanning or beamhouse operations, which clean the hides or skins; (ii) tanning, which permanently stabilizes the skin or hide matrix; and (iii) post-tanning and finishing operations, where aesthetic value is added[6]. Among the pre-tanning operations, dehairing is an important step in which hair along with epidermis, non collagenous proteins and other cementing substances are removed from the skin[7].
The conventional dehairing process employs lime (calcium oxide) and sodium sulphide, contributing to most of pollution generated in pre-tanning operations[2,3,5,6]. Due to the low solubility of the commercial grade of used lime, its use has the disadvantage of generating large quantities of solid waste which requires being disposed safely[8], besides of subsequent acid treatment of the resulting alkaline effluent[9]. Use of sodium sulphide has the risk of liberating hydrogen sulphide, a toxic gas which is a health hazard to the tannery workers and sewer men[10]. On the other hand, during this process the hair is largely disintegrated by hydrolysis of keratin, contributing to the biochemical oxygen demand (BOD) and chemical oxygen demand (COD) of the wastewater[6,8,11]. Consequently, conventional dehairing processes generates 83 % of BOD, 73 % of COD, 60 % of suspended solids, and 76 % of the total polluting charge produced during the manufacturing process of hides[5].
Thereby, finding a cleaner alternative to lime-sulphide dehairing constitutes an efficient strategy for reducing the negative impact of tanneries on environment. Enzymes are a technological tool of interest for industry because are able to achieve a high reaction rate under soft pH, temperature, and pressure conditions, besides a high specificity of reaction, biodegradability, non toxic nature and non polluting effluent generation[12]. In leather industry enzymes are principally used in pre-tanning operations (soaking, dehairing, bating, and degreasing)[3,6,12,13] and waste treatment[12,14]. Among those enzymes, proteases are highlighted because skin is mostly constituted by different

proteins which are the targets in the various steps of leather processing. Moreover, proteases have been chosen as a promising alternative to lime and sodium sulphide dehairing. Several works have shown the efficacy and environmental benefits of enzyme-based dehairing, such as reduction in effluent pollution, reduction of solid waste and lime sludge, reduction of total solids and neutral pH of effluents. In addition, due to poor keratinolytic activity of used enzymes, the hair is removed intact, leading to low BOD and COD in the effluent and allowing its use as raw material for other industries.
However, there is yet some reticence in industry to apply this technology, among other reasons, because of the risk of collagen degradation, protein that form the basic skin structure. As leather quality is closely related to state and quantity of skin proteins[11,13,15] is essential to know the enzyme specificity on representative substrates of skin to improve efficiency[8,13,16].
Several cysteine proteases have been isolated and characterized in our research group from plant species belonging to the family Bromeliaceae. Particularly, proteolytic extracts with suitable properties for industrial applications, such as high thermal stability and neutral or slightly alkaline (6-10) optimum pH range, have been obtained from fruits of *Bromelia balansae* (Bb)[17], *B. hieronymi* (Bh)[18,19,20], and *Pseudananas macrodontes* (Pm)[21,22,23]. In this work, proteolytic extracts rich in cysteine proteases (Bb, Bh, and Pm) have been studied for application in leather industry, focusing in their dehairing properties. To understand enzyme action on skin, proteolytic activity on representative substrates of skin protein was measured at 25, 35, and 55ºC and pH 8. Additionally, to evaluate dehairing action, assays were carried out by employing pieces of cow skin.

MATERIAL AND METHODS

Chemicals. Casein (from bovine milk), Coomassie brilliant blue G-250, cysteine, bovine serum albumin, Elastin-Congo Red, Hide Powder Azure, Keratin Azure, and Tris were purchased from Sigma-Aldrich (St. Louis, Missouri, USA). Ethylenediaminetetraacetic acid was purchased from Invitrogen (Carlsbad, California, USA), sodium phosphate (98%) from Carlo Erba (Rodano, MI, Italy), detergent Azymol 6SE from Pellital (Victoria, BA, Argentina). All other chemicals were of analytical grade.

Plant material.

Bromelia hieronymi. Mez fruits were collected by Prof. Lucas Roic in Santiago del Estero, Argentina. A voucher specimen (Leg. Venturi, LP7050) was deposited at the herbarium of the Vascular Plant Division, Faculty of Natural Sciences and Museum, National University of La Plata, Argentina. Infructescences of *B. balansae* Mez and *Pseudananas macrodontes* (Morr.) Harms fruits were collected by Dr. Aníbal Amat (National University of Misiones) in Santa Ana, Province of Misiones, Argentina. Voucher specimens (Leg. Amat, No. 1596-7) were deposited at the herbarium of the Faculty of Exacts, Chemical and Natural Sciences of the National University of Misiones, Posadas, Argentina. Fruits were washed with distilled water, dried, and stored at -20°C until extraction.

Enzymatic preparations. Each plant extract was obtained by chopping and homogenizing frozen unripe fruits with 0.1 M sodium phosphate buffer containing ethylenediaminetetraacetic acid and cysteine as protective agents[17,18,21]. The homogenate was filtered and centrifuged. Then, supernatant was collected, lyophilized, and stored at -20ºC. For all assays, samples of proteolytic extracts were prepared by dissolving the lyophilized powder in reaction buffer (Tris-HCl 0.1 M, pH 8.0, containing cysteine 20 mM).
In order to comparing dehairing action with a commercial dehairing enzyme, New1875 from CERGEN LLC was used.

Determination of proteolytic activity and protein content. Caseinolytic activity assays were carried out to determine the proteolytic activity by using casein as substrate (1% w/v in reaction buffer) at 37ºC. An arbitrary enzyme unit (caseinolytic unit, CU) was used to express proteolytic activity[21].
Protein content was determined by the Bradford[24] method, using bovine serum albumin as standard.

Proteolytic assays on representative substrates of skin proteins

Hide Powder Azure (HPA) substrate[25]. Sample (100 µl) was incubated with HPA (5 mg in 1.9 ml of reaction buffer) under magnetic stirring during 5, 10, and 15 min. Subsequently, dispersion was centrifuged and absorbance of the supernatant was measured at 595 nm (Abs595). Blank determination was made replacing sample by reaction buffer. The unit of activity on HPA (U_{HPA}) was defined as the enzyme amount per ml that increases 0.001 units of Abs595 per min.

Elastin-Congo Red (E) substrate[25]. Sample (250 µl) was incubated with E (5 mg in 1.75 ml of reaction buffer) under magnetic stirring during 15, 30, 60, 90, and 120 min. Subsequently, dispersion was centrifuged and absorbance of the supernatant was measured at 495 nm (Abs495). Blank determination was performed. Elastinolytic activity unit (U_E) was defined as the enzyme amount per ml that increases 0.001 units of Abs495 per min.

Keratin Azure (KA) substrate[25]. Sample (100 µl) was incubated with KA (3 mg in 1 ml of reaction buffer) during 24 h. Abs595 of reaction liquid was measured at 0.5, 1, 2, 4, and 24 h. Blank determination was performed. Keratinolytic activity unit (U_{KA}) was defined as the amount of enzyme per ml that increases 0.001 units of Abs595 per min.

Epidermis (EP) substrate. Sample (100 µl) was incubated with epidermis substrate[25] (20 mg in 1.9 ml of reaction buffer) under magnetic stirring during 20, 40, and 60 min. Reaction was stopped by addition of 1.5 ml of TCA (5%). Then, dispersion was centrifuged and absorbance of supernatant measured at 280 nm (Abs280). Blank determination was performed. The unit of activity on epidermis (U_{EP}) was defined as the amount of enzyme per ml that increases 0.001 unit of Abs280 per min.

Dehairing experiments. Pieces of 4g were cut from wet-salted cow hide. Prior to dehairing, soaking was carried out by incubating pieces in 20 ml of soaking bath (0.2 % of bactericide, 0.3 % of detergent, and 0.13 % of Na_2CO_3) at 25 °C during 24 h. Dehairing assay was performed by immersing each piece into 20 ml of reaction buffer containing different concentrations (CU/ml) of proteolytic extract. After 24 h at 25 °C with orbital stirring (ω = 75 rpm), pieces were withdrawn from baths and hair was removed by a standardized gentle scraping. Samples were cut from depilated pelts, washed and fixed in formal saline.

Microscopy analyses. Samples of fixed pelts were cut with uniform thickness, washed, dehydrated with a graded ethanol series, and then coated with gold. The micrographs of the grain surface and cross section were obtained by operating the Scanning Electron Microscopy (FEI, Quanta 200) from the Service Electronics Microscopy and Microanalysis (SEM-LIMF) of Faculty of Engineering of UNLP (Argentina), with an accelerating voltage of 20 KV in different lower and higher magnification levels.

Data analyses. Results of activity assays were obtained from three independent experiments done in duplicate and data expressed as mean ± SD. Previously the linear range of enzymatic reaction for each assay was determined. The data were analyzed with One Way ANOVA followed by Tukey Multiple Comparison test.

RESULTS AND DISCUSSION

Extracts obtained from fruits of *Bromelia balansae* (Bb), *B. hieronymi* (Bh), and *Pseudananas macrodontes* showed proteolytic activity per expected[17,18,21] (**Table 1**). Bh was the extract with the highest activity per mg of preparation, but if the protein content is considered, Bb had the highest specific activity (CU/μg protein) with a value of 0.012, like that of the commercial product New 1875, which was 0.015.

TABLE 1. Caseinolytic activity (CU) and protein content (μgpro) per mg of preparation. CU, caseinolytic units (pH 8). Mean ± SD

Sample	Caseinolytic activity (CU/mg)	Protein (μgpro/mg)
Bb	0.04 ± 0.01	3.38 ± 0.06
Bh	0.17 ±0.02	22 ± 3
Pm	0.09 ± 0.02	15 ± 4
New1875	0.09 ± 0.01	6 ± 1

Casein is an adequate substrate to measure total proteolytic activity due to that mimics closely the natural substrates of proteolytic enzymes[26], but it is a non specific substrate. The goal of this work is to study the extracts as a possible technology for the skin treatments used during leather manufacture, for which it is suitable to know their activities on skin proteins. Keratin Azure (KA), elastin-Congo Red (E), and HPA were used as representative substrates of keratin, elastin and collagen, respectively. Epidermis substrate (EP) is epidermis layer, hair follicle, and hair removed from skin[25].

Because keratin is the main protein of epidermis layer and hair, epidermis substrate is also representative of keratin.
In **Figure 1** are shown activities on KA, HPA, E and EP at 25, 35, and 55ºC. Except elastinolytic activities of Bb and Pm, activities increased with temperature. Therefore, temperature is a variable that could be operated to regulate the activities according to the desired effect. It has reported that the three proteolytic preparations keep the activity between 50-90% after 2 h at 55ºC[17,18,23], thus this temperature could be chosen if they are wanted to use for high protein waste treatment.

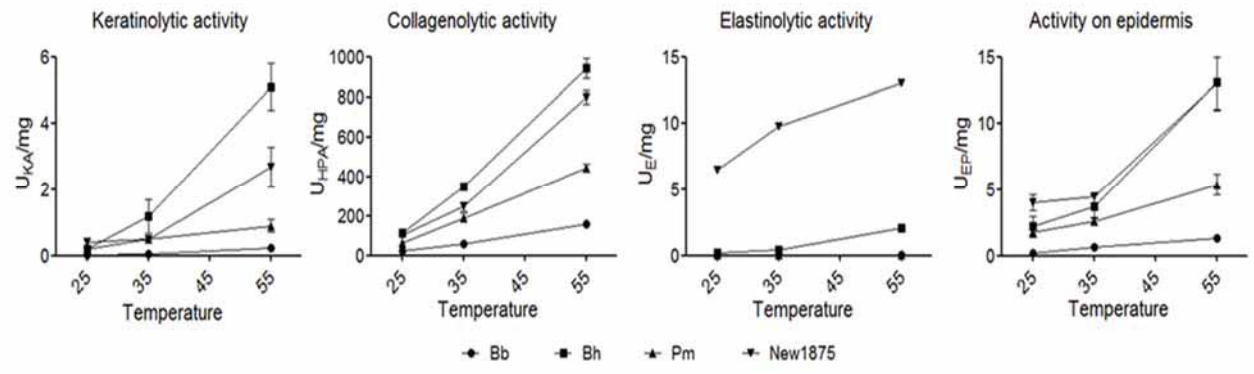


FIGURE 1. Activity on representative substrates of skin proteins as a function of temperature. Mean ± SD

Bh was the plant extract most active on all substrates; however, it could be due to major proteolytic activity per mg (CU/mg) of Bh, per **Table 1**. To compare extracts regardless of their total proteolytic activity, activities on each substrate were normalized to the same caseinolytic unit (1 CU), which are shown for 35ºC in **Table 2**.

TABLE 2. Normalized activity on representative substrates of skin proteins at 35ºC

Sample	U_{KA}/CU	U_{HPA}/CU	U_E/CU	U_{EP}/CU
Bb	$1^{a} \pm 0.3$	$1840^{a} \pm 93$	$1.1^{a} \pm 0.2$	$17^{a} \pm 5$
Bh	$7^{b} \pm 3$	$2052^{ab} \pm 75$	$2.5^{b} \pm 0.3$	$22^{ab} \pm 5$
Pm	$5^{b} \pm 1$	$2305^{b} \pm 255$	$0.46^{a} \pm 0.04$	$29^{b} \pm 3$
New1875	$5^{b} \pm 2$	$2468^{b} \pm 235$	$98^{c} \pm 2$	$45^{c} \pm 2$

Keratinolytic activity, activity on HPA, elastinolytic activity, and activity on epidermis were expressed as activity units per caseinolytic unit (U_{KA}/CU, U_{HPA}/CU, U_E/CU, and U_{EP}/CU, respectively). Tukey's test: the means with one common superscript letter are not significantly different at $p< 0.05$. Mean ± SD

Bh and Pm showed similar effect on collagen and keratin than those of the New1875 while Bb was slightly lower. Collagen is a protein arranged in fiber bundles which form the basic skin structure and, due to that is closely related with quality of leather, its degradation must be minimized during the leather manufacture[11,13,15]. However, high collagenolytic activity is desirable if enzyme is used to degrade waste solid from tannery. Among plant extracts, Bh was the most active against elastin.
The major differences between plant extracts and the commercial enzyme were found in elastinolytic activity and activity on epidermis substrate. High elastinolytic activity has been reported for enzymes used in soaking and bating[13], two steps of pre-taining

process in which undesirable proteins are removed. During soaking, previous to dehairing, fats and non collagenous proteins present between collagen fibers are removed, leading to opening up of theses fibres facilitating rehydration of the skin[6] necessary to diffusion of chemical agents during making of leather[26]. Bating is the subsequent step to dehairing, which cause physicochemical changes in the skin[6]. During this process continues the opening up of collagen fibers and the hide structure is softened[13], making the leather soft and easier to dye[1]. Removal of elastin has been associated to softness and flexibility of the final leather[25,28] and it has been suggested having some effect in loosening proteins around the base of the hair follicles[13].
Even when some keratinases can act as an excellent eco-friendly dehairing system[16,29], also it has been found that keratinase activity, measured from the KA assay, is not important for good removal of hair[13]. Because the dehairing process consists mainly in removal of epidermal layer and hair, activity on epidermis substrate could be a better measurement of dehairing action.

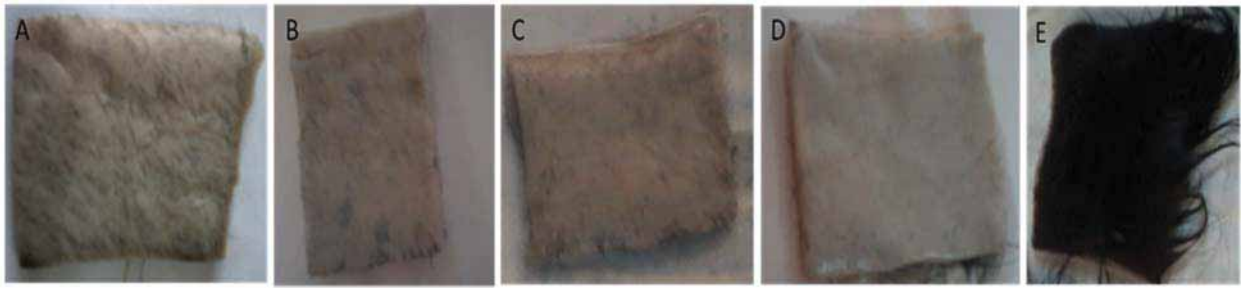


FIGURE 2. Images of cow skins after treatment with: (A) 1 CU/ml of Bb; (B) 1.5 CU/ml of Bh; (C) 0.5 CU/ml of Pm; (D) 0.2 CU/ml of New1875; (E) reaction buffer (Control).

Ability to dehairing was evaluated by incubating soaked cow skins with different proteolytic activities (CU/ml) of extracts. Due to the activity on collagen greatly increases with temperature (**Figure 1**), 25ºC was chosen as incubation temeperature, to diminish collagen degradation. For each enzymatic sample, it was determined the minor concentration of CU capable of uniformly removing hair from entire skin area by a gentle scraping: 0.2 CU/ml of New1875, 0.5 CU/ml of Pm, 1 CU/ml of Bb, and 1.5 CU/ml of Bh (**Figure 2**). In **Figure 3** are shown the percentage relative activity on substrates (considering 100% to the highest activity) for concentration of each enzymatic preparation used to depilate during the dehairing assay.

Although the values of keratinolytic activity and activity on epidermis were the most similar between the samples used at different concentrations to depilate, no activity on substrate could be considered completely representative of the dehairing action. However, it could conclude that elastolytic activity is not essential to depilate, which is in accordance with Foroughi *et al* (2006)[13]. In view of skin complexity, it is probably that other target skin proteins of the dehairing agent had been degraded.
On the other hand, it is remarkable that the dehairing action of Bb and Pm coexisted with lower collagenolytic activity than that of Bh, although higher than that of New1875, which also had the highest elastinolytic activity.

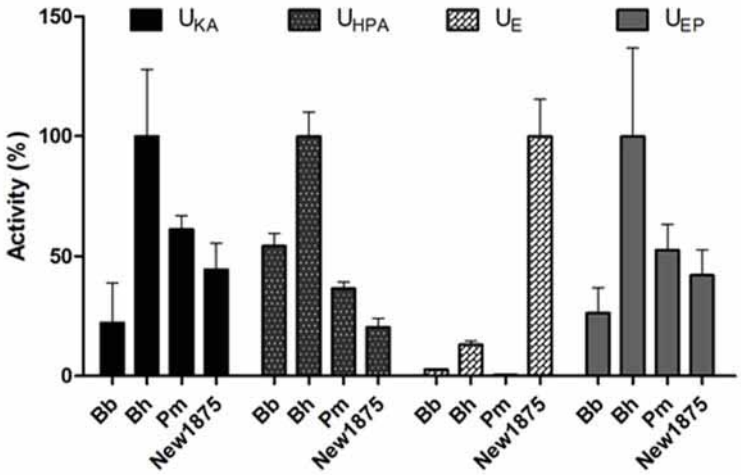


FIGURE 3. Percentage relative activity on substrates used in the dehairing experiment. U_{KA}, keratinolytic activity unit; U_{HPA}, activity unit on HPA; U_E, elastinolytic activity unit; U_{EP}, activity unit on epidermis. Mean ± SD.

Surfaces of cow skins were observed by scanning electron microscopy (**Figure 4**). Comparing micrographs of the proteolytically treated and untreated skins confirms the dehairing action of the proteolytic samples, since hair and epidermis were completely removed from treated skins. Additionally, the clean hair pores would indicate removal of the hair from root without damaging hair (in fact it was observed intact hair into the incubating baths). The surface of depilated skins is the grain surface (upper dermis) and its structure is related with properties of final leather[11]. The dehaired skins display clean grain structures and although there are differences between their surfaces, no damage is observed.

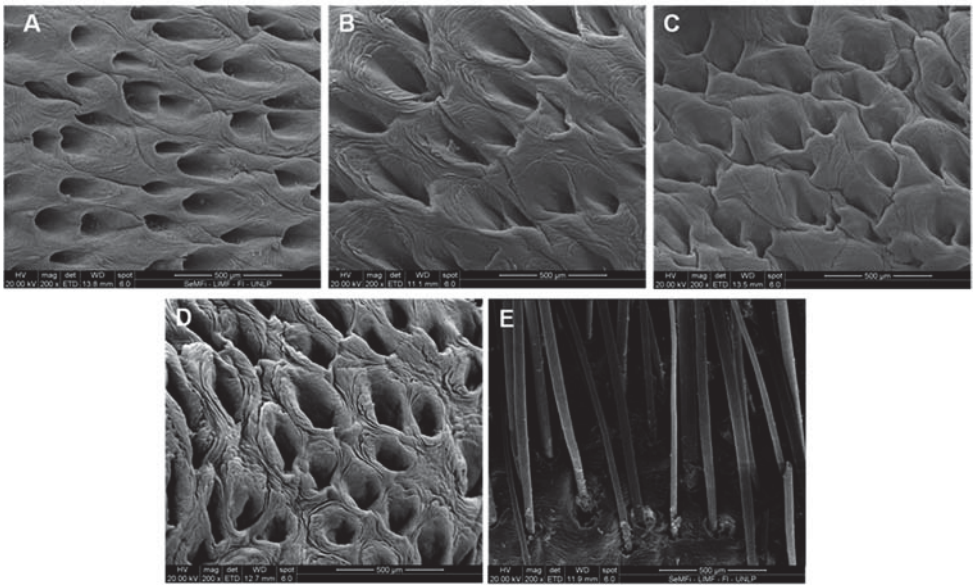


FIGURE 4. Scanning electron micrographs (200 X) of grain surface of cow skins after treatment with: (A) 1 CU/ml of Bb; (B) 1.5 CU/ml of Bh; (C) 0.5 CU/ml of Pm; (D) 0.2 CU/ml of New1875; (E) reaction buffer (Control)

Analysis by scanning electron microscopy of cross section of cow skins (**Figure 5**) showed no difference respect to disposal of the collagen fiber bundles between dehaired and control skins. Observations at higher magnifications did not show damage of collagen, while skins treated with Bb and Pm showed better opening of fiber bundles (data not shown).

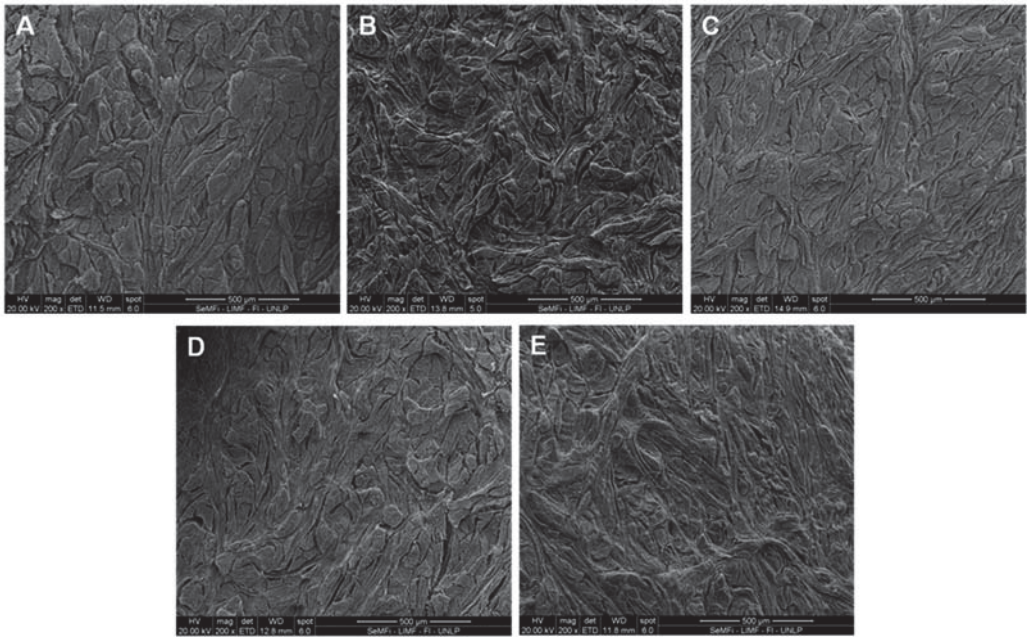


FIGURE 5. Scanning electron micrographs (200 X) of cross section of cow skins after treatment with: (A) 1 CU/ml of Bb; (B) 1.5 CU/ml of Bh; (C) 0.5 CU/ml of Pm; (D) 0.2 CU/ml of New1875; (E) reaction buffer (Control)

CONCLUSION

Proteolytic extracts from fruits of *Bromelia balansae* (Bb), *B. hieronymi* (Bh), and *Pseudananas macrodontes* (Pm) showed activities against representative substrates of skin, as keratin, collagen, elastin and epidermis. In view of these activities it could be expected different applications in leather industry. So, Bh could be proposed as a suitable soaking and bating enzyme due to its elastinolytic activity; all extracts could act like dehairing enzymes due to their activities against epidermis, while due to activities against the main skin proteins they could be used for treatment of waste from tanneries. On the other hand, Bb, Bh, and Pm could depilate cow skin after incubating 24 h at 25ºC and pH8. Furthermore, desirable characteristics of dehairing were observed since that hair pores did not show residual hair, grain surface of depilated skins were clean and intact, and collagen fiber bundles of dermis were not damaged. These findings, coupled with low keratinolytic activity showed, provide evidence that Bb, Bh, and Pm would be secure and eco-friendly dehairing agents suitable to leather process. Besides, due to observed differences in grain surface and opening of collagen fibers achieved by the different extracts, it is expected that Bb, Bh, and Pm will produce different types of leather. However, more studies are necessary to adapt these proteolytic extracts to

entire leather processing as well as evaluate pollution parameters of process and physical mechanical properties of the final leather.

ACKNOWLEDGMENTS

Errasti, ME is CONICET fellow. Lopez, MIL is member of the CONICET Researcher Career. The present work was supported by grant from CONICET (PIP 00297). Authors want to thank to Germán Mazzill from technical staff of the CITEC (CIC-INTI), who performed the soaking process.

REFERENCES

1. Madhavi J., Srilakshmi J., Rao M.R., Rao, K.R.S.S. Efficient leather dehairing by bacterial thermostable protease. Int. J. Biosci. Biotechnol. 3 (2011) 11-26.
2. Saran S., Mahajan R.V., Kaushik R., Isar J., Saxena R.K. Enzyme mediated beam house operations of leather industry: a needed step towards greener technology. J. Clean. Prod. 54 (2013) 315-322.
3. Dixit S., Yadav A., Dwivedi P.D., Das M. Toxic hazards of leather industry and technologies to combat threat: a review. J. Clean. Prod. 87 (2015) 39-49.
4. Kanagaraj J., Velappan K.C., Chandra Babu N.K., Sadulla S. Solid wastes generation in the leather industry and its utilization for cleaner environment-A review. *J. Sci. Ind. Res.* 65 (2006) 541-548.
5. Dettmer A., Cavalli É., Ayub M.A., Gutterres M. Optimization of the unhairing leather processing with enzymes and the evaluation of inter-fibrillary proteins removal: an environment-friendly alternative. Bioprocess Biosyst. Eng. 35 (2012) 1317-1324.
6. Thanikaivelan P., Rao J.R., Nair B.U., Ramasami T. Progress and recent trends in biotechnological methods for leather processing. Trends Biotechnol. 22 (2004) 181-188.
7. Ramasami T., Rao J.R., Chandrababu N.K., Parthasarathi K., Rao P.G., Saravanan P., Gayathri R., Sreeram K.J. Beamhouse and tanning operations: process chemistry revisited. J. Soc. Leath. Tech. Ch. 83 (1999) 39-45.
8. Saravanan P., Renitha T.S., Gowthaman M.K., Kamini N.R. Understanding the chemical free enzyme based cleaner unhairing process in leather manufacturing. J. Clean. Prod. 79 (2014) 258-264.
9. Sivasubramanian S., Manohar B.M., Rajaram A., Puvanakrishnan R. Ecofriendly lime and sulfide free enzymatic dehairing of skins and hides using a bacterial alkaline protease. Chemosphere 70 (2008) 1015-1024.
10. Arunachalam C., Saritha K. Protease enzyme: an eco-friendly alternative for leather industry. Indian J. Sci. Technol. 2 (2009) 29-32.
11. George N., Chauhan P.S., Kumar V., Puri N., Gupta N. Approach to ecofriendly leather: characterization and application of an alkaline protease for chemical free dehairing of skins and hides at pilot scale. J. Clean. Prod. 79 (2014) 249-257.
12. Choudhary R.B., Jana A.K., Jha M.K. Enzyme technology applications in leather processing. Indian J. Chem. Technol. 11 (2004) 659-671.
13. Foroughi F., Keshavarz T., Evans C.S. Specificities of proteases for use in leather manufacture. J. Chem. Technol. Biotechnol. 81 (2006) 257-261.
14. Aftab M.N., Hameed A., Haq I.-u., Chen R.-s. Biodegradation of Leather Waste by Enzymatic Treatment. Chin. J. Proc. Engin. 6 (2006) 462-465.

15. Valeika V., Beleška K., Valeikienė V., Kolodzeiskis V. An approach to cleaner production: from hair burning to hair saving using a lime-free unhairing system. J. Clean. Prod. 17 (2009) 214-221.
16. Dettmer A., Ayub M.A., Gutterres M. Hide unhairing and characterization of commercial enzymes used in leather manufacture. Braz. J. Chem. Eng. 28 (2011) 373-380.
17. Pardo M.F., López L.M., Canals F., Avilés F.X., Natalucci C.L., Caffini N.O. Purification of balansain I, an endopeptidase from unripe fruits of Bromelia balansae Mez (Bromeliaceae). J. Agric. Food Chem. 48 (2000) 3795–3800.
18. Bruno M.A., Pardo M.F., Caffini N.O., López L.M.I. Hieronymain I. a new cysteine peptidase isolated from unripe fruits of *Bromelia hieronymi* Mez (Bromeliaceae). J. Protein Chem. 22 (2003) 127-134.
19. Bruno M.A., Trejo S.A., Avilés X.F., Caffini N.O., López L.M.I. Isolation and characterization of hieronymain II, another peptidase isolated from fruits of *Bromelia hieronymi* Mez. Protein J. 25 (2006) 224-231.
20. Bruno M.A., Trejo S., Caffini N.O., López LMI. Purification and characterization of hieronymain III. Comparison with other proteases previously isolated from *Bromelia hieronymi* Mez. Protein J. 27 (2008) 426-433.
21. López L.M., Sequeiros C., Natalucci C.L., Caffini N.O., Brullo A., Maras B., Barra D. Purification and characterization of macrodontain I, a cysteine peptidase from unripe fruits of Pseudananas macrodontes (Morr.) Harms (Bromeliaceae) Protein Expres. Purif.18 (2000) 133-140.
22. López L.M., Sequeiros C., Trejo S.A., Pardo M.F., Caffini N.O., Natalucci C.L. Comparison of two cysteine endopeptidases from *Pseudananas macrodontes* (Morr.) Harms (Bromeliaceae). Biol. Chem. 382 (2001) 875-878.
23. Brullo A. (2003), Aislamiento, purificación y caracterización de las endopeptidasas cisteínicas presentes en frutos de *Pseudananas macrodontes* (Morr.) Harms (Bromeliaceae). Ph. D. Thesis. National University of La Plata, Argentina. Available at http://sedici.unlp.edu.ar/bitstream/handle/10915/2246/Documento_ completo__.pdf?sequence=23.
24. Bradford MM. A rapid and sensitive method for the quantitation of microgram quantities of protein utilizing the principle of protein-dye binding. Anal Biochem. 72 (1976) 248-254.
25. Cantera C.S., Goya L., Galarza B., Garro M.L., Lopez L.M.I. Hair saving unhairing process. Part 5 Characterisation of enzymatic preparations applied in soaking and unhairing processes. J. Soc. Leath. Tech. Chem. 87 (2003) 69-77.
26. Thompson V.F., Saldaña S., Cong J., Goll D.E. A BODIPY fluorescent microplate assay for measuring activity of calpains and other proteases. Anal. Biochem. 279 (2000) 170-178.
27. Cantera C.S., Angelinetti A.R., Altobelli G., Gaita G. Hair saving enzyme assisted unhairing: influence of enzymatic products upon final leather quality. J. Soc. Leath. Tech. Chem. 80 (1996) 83-86.
28. Sivasubramanian S., Manohar B.M., Puvanakrishnan R. Mechanism of enzymatic dehairing of skins using a bacterial alkaline protease. Chemosphere 70 (2008) 1025-1034
29. Jaouadi N.Z., Jaouadi B., Hlim H B., Reki H., Belhou M., Hmidi M., Bejar S. Probing the crucial role of Leu31 and Thr33 of the *Bacillus pumilus* CBS alkaline protease in substrate recognition and enzymatic depilation of animal hide. PloS one, 9(9) (2014) e108367.

CHAPTER 4.6 ESTUDIO DE NANOCOMPUESTOS DE ALMIDÓN TERMOPLÁSTICO REFORZADOS CON BENTONITA MODIFICADA OBTENIDOS MEDIANTE EXTRUSIÓN REACTIVA

M. P. Guarás *(1); L. N. Ludueña (1) and V. A. Alvarez (1)

(1) Grupo de Materiales Compuestos (CoMP) - Instituto de Investigaciones en Ciencia y Tecnología de Materiales (INTEMA) - Facultad de Ingeniería – Universidad Nacional de Mar del Plata – Solís 7575 - (B7608FDQ) Mar del Plata - Argentina.

RESUMEN

Con el fin de reducir la acumulación de residuos de corta vida útil y la consecuente contaminación del medio ambiente, la investigación de polímeros biodegradables de origen natural ha sido un campo de investigación muy activo. El almidón es un recurso abundante, económico y biodegradable. Su estructura debe ser modificada de modo de facilitar su procesamiento. Puede adquirir carácter termoplástico (TPS), mediante la desestructuración del gránulo y procesándolo con un plastificante adecuado a una determinada temperatura. Sin embargo, el TPS, no es apto para su utilización como material de envases, debido a sus pobres propiedades mecánicas y su elevada hidrofilicidad. Se han desarrollado numerosos métodos de modificación fisicoquímicos de modo de mejorar dichos aspectos. La derivatización del almidón es un tipo de modificación química mediante el cual se sustituyen los grupos hidroxilos del mismo, por otros grupos con la funcionalidad deseada. En el presente trabajo la derivatización se realizó con anhídrido maleico, una vez modificado se procesó en presencia de un plastificante en una extrusora de doble tornillo. A su vez se incorporaron nanorefuerzos con el objetivo de mejorar las propiedades mecánicas y de barrera del material. Para ello se utilizaron nanoarcillas (bentonita) nativa y modificada en un 3%. Se estudiarán las propiedades térmicas por calorimetría diferencial de barrido (DSC) y termogravimetría (TGA), las propiedades mecánicas, la efectividad de la modificación química mediante espectroscopía FTIR, de absorción de humedad y las propiedades morfológicas mediante difractometría de rayos X (DRX).

Palabras claves: almidón termoplástico, derivatización, nanorefuerzos

INTRODUCCIÓN

Los polímeros convencionales derivados de combustibles fósiles no son sólo recursos no renovables y finitos, sino que también causan problemas en el procesamiento post-consumo, ya que son en gran medida inertes al ataque microbiano. El uso de polímeros capaces de ser degradados por la acción de microorganismos y / o enzimas sin causar efectos nocivos es una estrategia en la gestión de los residuos. El almidón es un biopolímero natural, abundante y de bajo costo obtenido a partir de recursos renovables. Sin embargo, la estructura del almidón nativo debe ser modificada, ya que -

---

*Author for correspondence: paula.guaras@fi.mdp.edu.ar

su temperatura de degradación es inferior a la de fusión, además de no poseer características termoplásticas. Por esta razón el almidón natural no puede ser procesado por métodos habituales de procesamiento de polímeros sin ser modificado. Dicha modificación se realiza a partir de la descomposición del gránulo de almidón procesándolo en presencia de una cantidad específica de plastificante, bajo ciertas condiciones de extrusión[1]. El proceso de desestructuración, consiste en la transformación de los gránulos semicristalinos en una matriz homogénea de polímero amorfo.

El almidón puede ser modificado químicamente con el fin de mejorar sus propiedades, tales como propiedades mecánicas, cristalinidad y absorción de humedad, ya que es muy frágil y sensible a la humedad debido a su naturaleza hidrofílica. La derivatización del almidón desempeña un papel de plastificación interna y reduce el grado de cristalinidad del almidón, de modo que la molécula de plastificante puede penetrar de una mejor manera en la molécula de almidón para la posterior plastificación. Por otro lado, el grupo éster puede mejorar la hidrófobicidad de materiales de base almidón. El anhídrido maleico (MAH) tiene alta reactividad en la preparación de almidón esterificado[2].

Con el objetivo de mejorar la competitividad de este material con una alta relación eficiencia / costo se incorporaron nanocargas a las mezclas. La adición de nanocargas a polímeros ha demostrado ser una forma eficaz de mejorar tanto las propiedades mecánicas como las de barrera. Las nanoarcillas han sido ampliamente estudiadas, debido a su gran disponibilidad y su bajo costo. La bentonita es una arcilla compuesta principalmente de aluminosilicatos en capas, que por sustituciones requieren cationes. Debido a su estructura, las arcillas son capaces de alojar una gran variedad de moléculas en sus espacios interlaminares. Para realizar su compatibilización con diferentes matrices se substituyen los cationes presentes en las interlaminas de la arcilla por cationes de ciertos modificadores, a esta técnica se la conoce como intercambio catiónico. Los modificadores pueden cambiar tanto propiedades físicas como químicas, tales como la hidrofilicidad, el espaciado interlaminar y la resistencia térmica entre otras, permitiendo mejorar la compatibilidad con diferentes polímeros[3].

El objetivo de este trabajo fue preparar, nanocompuestos biodegradables que resulten rentables a su vez, preparados mediante intercalación en fundido utilizando extrusión reactiva. Se reforzó la matriz de TPS y de TPS modificada mediante derivatización. Fue utilizada una nanoarcilla comercial (bentonita natural) y la misma modificada mediante cloruro de benzalconio como refuerzo de la matriz de almidón termoplástico. Se estudió el efecto de la modificación de la arcilla en la morfología (Difractómetro de rayos X, DRX), pro/piedades /térmicas (calorimetría diferencial de barrido, DSC, y termogravimetría, TGA), absorción de /agua y en las propiedades mecánicas.

MATERIALES Y MÉTODOS

El almidón de maíz se utilizó en forma de polvo provisto por "Distribiudora Dos Hermanos". El plastificante utilizado fue glicerol (EG, JT Baker). Se utilizó ácido esteárico (AE Shuchardt Merck OHG) como un lubricante para el procesamiento. El anhídrido maleico (MAH, Anedra de grado analítico) se utilizo para la modificación

química del almidón. La bentonita natural comercial fue provista por Minarmco. El cloruro de benzalconio (DEM, 80% pureza) es una sal de amonio cuaternaria utilizada para modificar la bentonita natural.

Preparación de almidón termoplástico. En primer lugar, se realizó una pre-mezcla a mano en la cual se introdujeron el almidón nativo (69,5%p/p), los plastificantes utilizados (30%p/p), los cuales fueron glicerol y agua (en una proporción de 90%p/p y 10%p/p con respecto a la cantidad total de plastificante) y el ácido esteárico (%0,5p/p). Luego se introdujo la mezcla en una extrusora de doble tornillo de D = 18 mm y L / D = 25D con velocidad de 50 rpm y un perfil de temperaturas: 80/90/100/110/100°C. Estas proporciones utilizadas y las condiciones de extrusión resultaron de trabajos previos realizados. Al almidón termoplástico lo llamaremos TPS3.

Modificación química del almidón. El almidón (400g) fui introducido en un reactor que contenía una solución de anhídrido maleico (4%p/almidón) con acetona (4lt) a 25°C durante 24 hs. Luego fue centrifugado y lavado varias veces con agua destilada, y por último secado en estufa a 50°C. Luego se proceso de la misma manera y en las mismas proporciones que el TPS sin modificar. Al almidón termoplástico modificado lo llamaremos MTPS3.

Modificación química de la bentonita y preparación de nanocompuestos. Se llevó a cabo la modificación de la bentonita natural en un reactor, en el cual se introdujeron agua destilada (5lt), bentonita (150g) y se calculó la masa de modificador (cloruro de benzalconio, CBK)) de modo de obtener una fracción de CEC de 0,75. Se mantuvo agitando dicha solución a 150 rpm y a una temperatura de 80°C durante 30min. Luego se retiró la solución, se filtro y se secó en estufa a 100°C.

Se realizaron cuatro mezclas por extrusión de TPS3 y MTPS3 en las mismas proporciones y condiciones de procesamiento descriptas anteriormente, con un 3% de bentonita y con 3% de CBK. Las mismas se llamaran TPS3-3BENT, TPS3-3CBK, MTPS3-3BENT y MTPS3-3CBK.

Una vez extraídas todas las mezclas de la extrusora, fueron pelletizadas y conformadas mediante moldeo por compresión en films de 0.07 cm de espesor, 15 cm de ancho y 20 cm de largo, durante 10 minutos a 120 ºC de temperatura sin presión, luego 10 minutos a 120 ºC y una presión de 50 kg/cm2, y por último los moldes de la prensa se enfriaron con agua hasta 30 ºC y los films obtenidos fueron retirados de la misma.

Caracterización de las mezclas. La caracterización térmica se llevó a cabo mediante el uso de un calorímetro diferencial de barrido TA Instrument Q2000. Se utilizó una cápsula de aluminio vacía como referencia. Se pesaron 4 mg de cada muestra y se colocaron en cápsulas de aluminios cerradas de forma hermética. Las muestras se enfriaron a -60 º C, y luego se calentaron hasta 200 ºC a una velocidad de barrido de 10 º C / min º. Finalmente, se enfriaron hasta temperatura ambiente.

Se realizaron pruebas de termogravimetría mediante un Instruments TGA HI-Res™500. Las muestras se calentaron a velocidad constante, 10 º C / min desde temperatura ambiente hasta 600 º C º, en atmósfera de nitrógeno.

Los ensayos de tracción se realizaron en una máquina Instron 4467 utilizando una celda de carga de 100N y a una velocidad de traversa de 1 mm / min. Antes de llevar a cabo el ensayo, las muestras fueron acondicionadas a 65% de humedad relativa durante 48 horas a temperatura ambiente.

La dispersión de la arcilla fue analizada mediante Difracción de rayos X. Los patrones de DRX fueron obtenidos mediante un equipo Analytical Expert Instrument (K∞Cu=1.54 Å) desde 2θ = 2 º a 60 º (2 º/minuto) a temperatura ambiente. El voltaje generado fue de 40kV y la corriente de 40mA. El espaciado interlaminar de las arcilla fue calculado antes y después de realizadas las mezclas mediante la Ley de Bragg. Dichos valores fueron llamados d_{001}.

Se llevaron a cabo ensayos de absorción de humedad en muestras de 20 mm^2 de superficie en forma de cuadrados. Previo a las mediciones de absorción de humedad, las muestras se secaron en una estufa de vacío a 30-35 º C durante 48 h. Las muestras se acondicionaron en recipientes herméticos a temperatura ambiente con 90% de humedad relativa, usando una solución de glicerina y agua. La cantidad de agua absorbida por las muestras fue determinada pesando periódicamente, hasta que se alcanzó un peso constante. La absorción de agua (W) fue dada por la siguiente ecuación:

$$W(\%) = \frac{M_t - M_0}{M_0} \times 100 \qquad (1)$$

Donde M_t es la masa al tiempo t y M_0 es la masa inicial.

RESULTADOS Y DISCUSIÓN

Absorción de humedad. Uno de los objetivos principales de la modificación de almidón es la mejora de las propiedades en cuanto a la susceptibilidad que presenta el TPS frente a la humedad. El agregado de refuerzos, y en especial modificados con agentes higroscópicos debería producir un efecto favorable en la matriz. Se estudiaron estas propiedades de modo de observar si realmente se produjo una mejora en el material. Los resultados pueden observarse en la **Tabla 1**.

Se puede observa claramente una disminución de un 8% en la absorción del almidón modificado. Por otro lado, al agregarle el nanorefuerzo modificado con CBK la disminución en la absorción es aún mayor.

TABLA 1. Absorción de humedad de las mezclas de almidón termoplástico

Muestra	% Absorción de Humedad
TPS3	29.74 ± 1.47
MTPS3	21.88 ± 0.94
TPS3-3BENT	20.78 ± 0.55
TPS3-3CBK	19.49 ± 0.49
MTPS3-3BENT	21.63 ± 0.08
MTPS3-3CBK	16.15 ± 0.38

Una de las mayores dificultades en el uso del almidón termoplástico es su gran afinidad con el agua y su poca estabilidad frente a cambios de humedad. EL TPS es hidrofílico debido a que contiene numerosos grupos hidroxilo en su estructura. El anhídrido maleico contiene enlaces ester hidrofóbicos (C=O). Cuando se lleva a cabo la derivatización del TPS, parte de los grupos hidroxilos del almidón se sustituyen por enlaces ester. Esto facilita la disminución en la absorción del almidón, mejorando la resistencia a la absorción de agua del TPS[1].

Propiedades Mecánicas. Las propiedades de tracción tales como módulo de Young (E), Tensión de fluencia (σ_y) y elongación a la rotura (ε_b) se evaluaron a partir de las curvas tensión-deformación. En la **Tabla 2** pueden observarse los resultados obtenidos.

En primer lugar la modificación del almidón produjo un aumento muy considerable en cuanto a la elongación a la rotura, a expensas de una perdida de resistencia en el material. Es posible observar también, que el agregado de bentonita natural no mejoró la resistencia del TPS3, por el contrario disminuyó su módulo de manera apreciable. El efecto contrario se produjo al reforzar el MTPS3, aumento el módulo disminuyendo su elongación, lo cual es resultado esperable al reforzar las matrices de polímero. Dicho efecto se observó de manera mayormente apreciable al reforzar el MTPS3 con CBK, se incremento aún más el módulo, y disminuyó su elongación.

TABLA 2. Propiedades mecánicas de las mezclas de almidón termoplástico

Muestra	E (MPa)	σf (MPa)	εb(%)	T_g (°C)
TPS3	12.62 ± 1.12	1.08 ± 0.079	16.3 ± 1.5	46.5
MTPS3	2.02 ± 0.48	0.17 ± 0.02	93.5 ± 12.1	26.4
TPS3-3BENT	2.71 ± 0.42	1.12 ± 0.08	91.5 ± 7.8	43.0
TPS3-3CBK	6.63 ± 0.93	1.07 ± 0.08	60.4 ± 4.1	40.4
MTPS3-3BENT	8.39 ± 1.17	0.77 ±0.04	50.5 ± 3.4	30.7
MTPS3-3CBK	14.25 ± 1.32	1.52 ± 0.08	22.8 ± 0.9	31.4

Propiedades térmicas. Se realizaron ensayos de DSC de las mezclas realizadas, los resultados pueden observarse en la **Tabla 2**. Las curvas de flujo de calor, presentan un cambio de capacidad calorífica. Este descenso en temperatura se atribuye a la transición vítrea del material. Autores tales como A.L. Da Róz, 2006[1]; han reportado valores de Tg similares al obtenido para la misma formulación de TPS de este trabajo. En los termogramas no se observa temperatura de fusión, esto es debido a que en la presencia de plastificante y determinadas condiciones de temperatura y corte, el granulo de almidón nativo se desestructura, rompiendo los enlaces de hidrogeno dando como resultado la destrucción de la naturaleza cristalina del almidón. La Tg del almidón es extremadamente sensible a la humedad. Las interacciones intermoleculares y los enlaces de hidrógeno presentan un rol muy significativo en la plastificación del material[5]. El MTPS3 presenta una gran disminución en la Tg, lo cual evidencia un aumento en el volumen libre del material debido a los grupos funcionales que se enlazan a la cadena principal.

Las curvas de TGA de las mezclas de almidón se muestran en la **Figura 1**. En un principio entre 100-150°C de temperatura se observa la perdida de agua del material. No se observan diferencias grandes en descomposición de los componentes de las mezclas, y las misma se produce en dos etapas. Es posible observar en primer lugar la descomposición del plastificante, en el caso del almidón modificado la descomposición del anhídrido maleico; y en las mezclas reforzadas con CBK la descomposición del modificador. Luego se alcanza la descomposición del almidón.

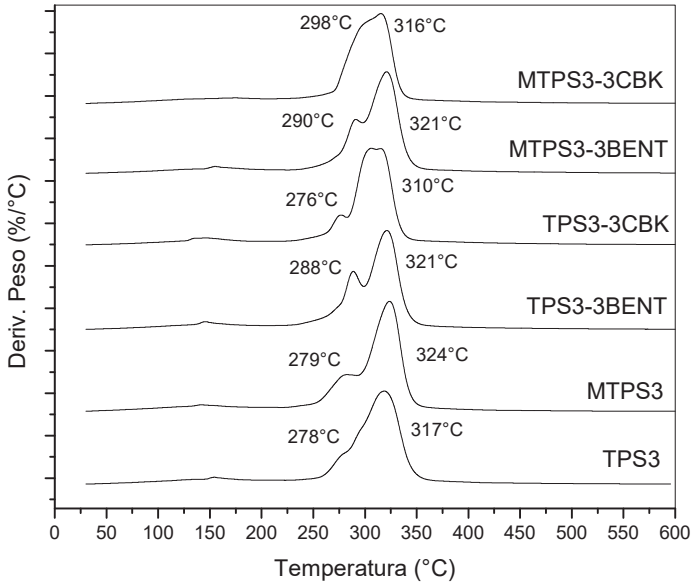


FIGURA 1. Derivada del peso de las mezclas de almidón termoplástico

Difracción de rayos X. El almidón es un biopolímero semicristalino compuesto por dos estructuras polímericas diferentes: la amilosa y la amilopectina. Las moléculas de amilopectina son significativamente más grandes que las moléculas de amilosa. Una de las propiedades más importantes del almidón natural es su semicristalinidad donde la amilopectina es el componente dominante para la cristalización y la parte amorfa está formada por regiones ramificadas de amilopectina y amilosa4. El método de DRX puede utilizarse para determinar el cambio de cristalinidad del almidón. En la **Figura 2** pueden observarse los patrones de DRX de las mezclas realizadas. El almidón nativo exhibe un patrón tipo-A, con picos 2θ en 15°, 18° y 23°. Al procesar el almidón con un plastificante, el carácter cristalino cambia y el grado de cristalinidad disminuye. El TPS presenta un patrón de difracción tipo-V y al mismo tipo exhibe un patrón tipo-B[2]. El MTPS3 presenta el mismo patrón que el TPS3, por lo que se puede concluir que la modificación del almidón no cambia el tipo de cristalinidad del TPS3. Esto es una evidencia de que la reacción de derivatización ocurre preferentemente en la parte amorfa del almidón. La modificación del almidón disminuye la cristalinidad, mejorando al TPS aumentando las regiones amorfas en el material.

Luego en los nanocompuestos podemos observar los picos característicos de la bentonita. A partir del pico principal ubicado en 6.3° podemos calcular el espaciado interlaminar de la arcilla mediante la Ley de Bragg. Este parámetro es de gran

importancia debido a que se espera que d_{001} incremente, mediante la modificación química de las arcillas, de modo que las cadenas de polímero tengan mayor espacio para intercalarse y así obtener un nanocompuesto con una buena dispersión. En la **Figura 2b** podemos observar que mediante la modificación de la bentonita con CBK el pico principal se corrió hacia un ángulo menor 5°, aumentando de esa manera el espaciado interlaminar de la arcilla. Sin embargo, vemos que las mezclas que contienen bentonita, muestran que este aumento su d_{001}, evidenciando que las cadenas de polímero se intercalaron dentro del refuerzo, mientras que las que contienen arcilla modificada no variaron su d_{001}. Este efecto no significa que no se encuentren intercaladas las cadenas de polímero, sino que vemos que se intercalaron más en la bentonita debido a que da alguna forma presentan mayor afinidad con la misma. La bentonita presenta un carácter mayormente hidrofílico, mientras que el CBK es una sal mayormente hidrofóbica, esta puede ser la causa a partir de la cual el TPS se intercala de forma más eficiente cuando utilizamos bentonita como refuerzo. Es así como anteriormente observamos que las mezclas que contienen CBK presentaron mejor porcentaje de absorción de agua.

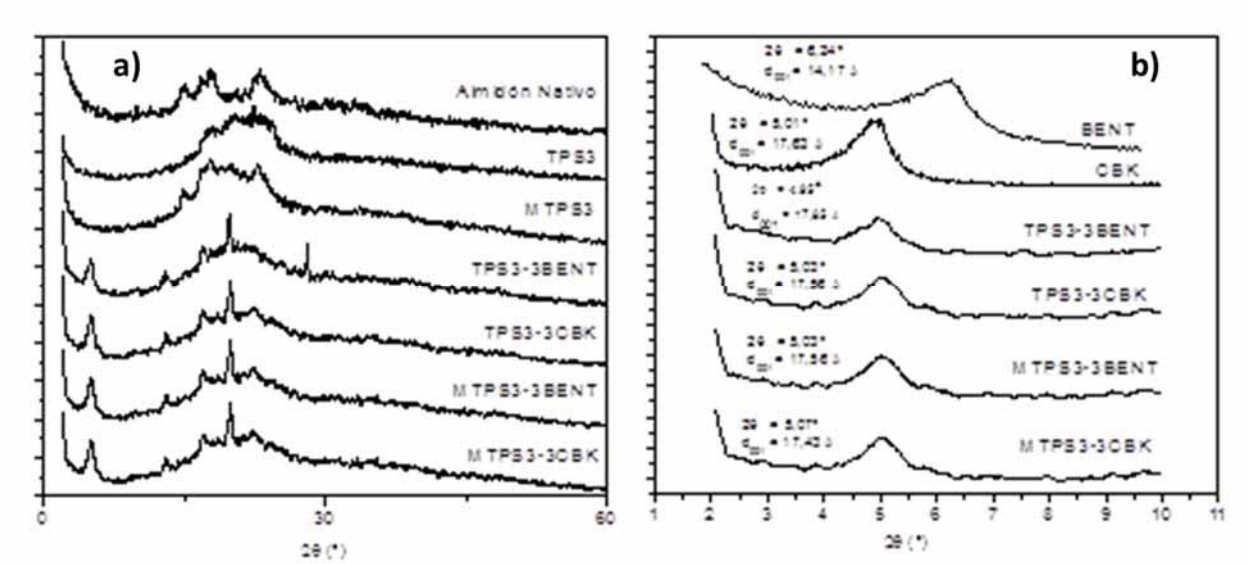


FIGURA 2. Patrón de DRX de las mezclas de almidón termoplástico y almidón nativo. a) Análisis del cambio de cristalinidad, b) Análisis del cambio en espaciado interlaminar de las arcillas y de las arcillas en las mezclas.

CONCLUSIÓN

Resumidamente, fue posible modificar TPS mediante reacción química en un reactor y luego procesarlo mediante extrusión. Además, fue posible modificar químicamente bentonita y utilizarla como nanorefuerzo en las mezclas de TPS3 y MTPS3. Las propiedades mecánicas mostraron que la modificación del TPS generó una perdida en la resistencia del material, sin embargo, la elongación a la rotura incremento de forma apreciable. Este resultado se condice con la disminución en la temperatura de transición vítrea del material. Por otro lado, la arcilla modificada con CBK favoreció el incremento

del módulo en la matriz modificada. Este resultado cumple con el objetivo del nanorefuerzo, mediante el cual se espera que aumente la resistencia del material a expensas de una disminución en la elongación a la rotura. En cuanto a la absorción de humedad, se observó una mejora notable. Los grupos funcionales hidrofóbos introducidos con la adición de anhídrido maleico facilitaron la disminución de la absorción del almidón. Por lo tanto, la reacción de derivatización mejoró significativamente la resistencia al agua del TPS, tal como se esperaba. Las propiedades térmicas de los materiales mostraron diferencias claras entre el TPS modificado y sin modificar en cuanto a que la modificación disminuyo de manera notable la Tg del material. Este hecho muestra una nueva evidencia de que el proceso de modificación mediante derivatización del TPS fue logrado. No se observó un aumento significativo en la estabilidad térmica del TPS. Mediante DRX fue posible constatar que el procesamiento del almidón logró romper en su mayor parte su estructura cristalina, mostrando así un material en su mayor parte amorfo. Se observó una mayor interacción entre la matriz y la bentonita, ya que el aumento el espaciado interlaminar de la misma. La bentonita modificada con CBK no mostró este comportamiento. Esto puede deberse a que el CBK es mayormente hidrofóbico, mientras que la matriz de TPS presenta un carácter hidrofílico.

REFERENCIAS

1. Róz, A.L.D., et al. Carbohydrate Polymers, 2006. 63(3): p. 417-424.
2. Zuo, Y., et al. Journal of thermoplastic composite materials, 2004. p. 1-13
3. Ray, S. S.; Okamoto, M. Prog Polym Sci 2003, 28, 1539.
4. Diaz Cajiao, D.F. (2012). Plan de negocios diseño, fabricación y comercialización de bolsas biodegradables,
5. Universidad EAN Facultad de Posgrados especialización en gerencia de proyectos Bogotá.
6. Cyras, V.P., et al. Journal of Applied Polymer Science, 2006. 101: p. 4313-4319.

CHAPTER 4.7 EXPERIMENTAL STUDY AND MATHEMATICAL MODELING FOR LEAD REMOVAL VIA A PHOTOSYNTHETIC CONSORTIA USING EVOLUTIONARY OPTIMIZATION APPROACH

B. Camacho Pérez* (1); D. J. Hernández Melchor (1); P. A. López Pérez (2); A. Alberto Murrieta (1); S. Carrillo Vargas (1) and E. González Gómez (3)

(1) Universidad Tecnológica de Tecámac, Carretera Federal México - Pachuca Km 37.5, Estado de México, México
(2) Universidad Autónoma del Estado de Hidalgo, Escuela Superior Apan, Carretera Apan-Calpulalpan Km.8, Hidalgo, México
(3) Centro Interdisciplinario de Investigaciones y Estudios sobre Medio Ambiente y Desarrollo, Calle 30 de Junio de 1520 s/n, Ciudad de México, México

ABSTRACT

This work presents an experimental-theoretical strategy for a batch process for lead removal by consortia (algae) under photosynthetic oxygenation, whose capacity for removing heavy metals are being studied. Photosynthetic consortia isolated from a treatment plant wastewater of Tecámac (México) was used as inoculum in photobioreactors column type bubble to evaluate the kinetics of lead removal at different initial concentrations (15, 30, 40, 50 and 60 mg/L), carried out in batch culture with hydraulic residence time of 14 days using Bold's basal mineral medium. The operating conditions of the photobioreactor were: aeration of 0.5 vvm, a quantity of light of 80 mol photons m^{-2} s^{-1} and a photoperiod light: dark 12:12. After determining the best growth kinetics of biomass and metal removal they were tested using these conditions wastewater at different ratios (30 and 60%) from the culture medium, in addition, it was quantified the biomass growth, nitrogen consumption, chemical oxygen demand and metal removal. Therefore, lead removal amounted to more than 96.4%, when the initial cadmium concentration was of up to 50 mg/L using 60% of wastewater. A mathematical model, unstructured-type was developed to simulate lead removal. Numerical experiments clearly illustrated the successful implementation the proposed model. The parameters of the model are optimized by two methods: using the Levenberg–Marquardt optimization approach and Genetic Algorithms. The optimization parameters via genetic algorithms showed the best results. The mathematical model developed can be used for optimization and control purposes.

Keywords: Dynamic model, kinetics, photobioreactor, wastewater.

---

*Author for correspondence: beni.camacho@gmail.com

INTRODUCTION

Environmental pollution with toxic metals result of human activities for more than 10,000 years in different areas has brought consequences in the atmosphere, soil and water[1-3]. Lead was classified by the US Environmental Protection Agency (EPA) as a probablehuman carcinogen. Substances and exposures that can lead to cancer are called carcinogens (Lead compounds, inorganic). Some carcinogens do not affect DNA directly, but lead to cancer in other ways. For example, they may cause cells to divide at a faster than normal rate, which could increase the chances that DNA changes will occur[4]. Between the most toxic metals affecting the population is lead, because that can affect almost all organs and body systems, the system is more susceptible nervous system, both in children and adults[5-7]. Globally there have been different irremediable events lead contaminated sites. Recently in Michigan (USA) they reported 10 deaths from contaminated with lead waters[7]. In Shanghai poisoning of 49 children due to industrial pollution, three companies were involved (A battery plant, one of auto parts and recycling plant) was reported[8]. On the other hand, in Mexico there have been various studies, yielding a high proportion of children with blood lead level above those recommended by the Mexican regulatory limits, the study sites were Avalos (Chihuahua) Morales, Cedral (San Luis Potosi) and Trinidad (Tlaxcala)[5]. Several industrial applications utilize lead in their process, such as electroplating, petrochemical processes, battery manufacturing, printing pigments, fuels, photographic materials [9-11].

Chemical and physical methods, such as chemical precipitation, chemical-oxidation or reduction, electrochemical treatment, evaporative recovery, filtration, ion exchange, and membrane technologies have been widely used to remove heavy metal ions from industrial wastewater[12]. These processes may be ineffective or expensive, especially when the heavy metal ions are in solutions, containing in the order of 1–100 mg/L dissolved[12].

Compared to the other organisms used for biosorption processes, namely fungi, cyanobacteria, and bacteria, algal cells have higher heavy metal biosorption capacities which relates to the different structure and composition of their cell wall[13, 14]. Cell walls of different microorganisms have different functional groups which are involved in metal ion binding, such as amino, amide, carbonyl, carboxyl, hydroxyl, imidazole, phosphate, sulfate, sulfhydryl, and phenol moieties [15]. Depending on the variations in the cell wall composition, there will also be differences in the metal ion binding mechanisms and affinities [16].

The goal of the recently emerging interest in modelling of biological processes is to understand and describe quantitatively the dynamics of living cells. To attain this purpose, new experimental procedures and modelling techniques are needed to generate and analyze relevant biological data. The kinetic modeling is an important aim in the bio-chemical reaction engineering to design, optimize, operate and control bio-chemical reactors. However, the develop of accurate kinetic models is still a challenging issue, due to the lack of knowledge to identify the main phenomena related to proceed and identify the corresponding parameters of the kinetic models actually employed[17].

Parameter estimation has also been accomplished using a variety of nonlinear procedures. Most of these techniques are calculus-based search algorithms that use the

gradient of the response surface to search for a minimum in the residual sum of squares[18]. In general, a genetic algorithm (GA) can be described as a calculus-free, heuristic optimization tool[19]. Its principal strength is that it obtains parameters that satisfy the optimization problem even for poorly behaved functions. Gas have been widely used for optimization problems in biotechnology and bioengineering[20,21]. Chen et al. [22] introduced the use of GA for identifying the unknown parameters of seventh-order nonlinear model of fed-batch culture of hybridoma cells on-line and to optimize feed rate control profiles for glucose and glutamine. Therefore, there is a models and procedures development demand that describe the process in such way optimization, control and improved operation techniques may be used[23, 24].

This paper proposes an experimental-theoretical strategy for a batch process for lead removal by consortia (algae) under photosynthetic oxygenation. It is necessary to develop strategies to treat contaminated by biological processes which do not impact the environment for long-term exposure sites so the aim of this study was to evaluate the removal of lead by a consortium photosynthetic microbial. The isolation consortium has the capacity to grow with wastewater which means low operating costs, tends to decrease the concentrations of nitrogen, phosphorus and COD, decreases the concentration of lead, also can be evaluated in operation semi-continuous for increasing its performance for large-scale applications (Dynamic model), its disadvantage is the metal adsorption time regarding immobilized cells, however it should be noted that these methods require more technology. Nevertheless, this problem can be overcome by using our consortium in this type of operation. In addition, a mathematical model, unstructured-type was developed to simulate lead removal. Numerical experiments clearly illustrated the successful implementation the proposed model. The parameters of the model are optimized by two methods: using the Levenberg–Marquardt optimization approach and Genetic Algorithms. The optimization parameters via genetic algorithms showed the best results. Plus, the proposed model can be used as virtual plant to regulate the concentration of the metal under a control law.

MATERIALS AND METHODS

The methodology of this study was divided into 4 stages described below.

Step 1. Isolation and propagation of a photosynthetic microbial consortium from Tecámac. Sampling was conducted at the plant wastewater treatment "Sierra Hermosa" by the Decentralized Agency of Water and Wastewater (ODAPAS) of Tecámac. The sample was taken from two different stages of the treatment system of wastewater, which were activated sludge and primary treatment. Samples were collected in sterile plastic containers and stored in 4°C until use. Subsequently a homogeneous mixture of different samples collected and used as inoculum for the growth of photosynthetic microorganisms in the laboratory was conducted. Growth thereof was conducted using a selective medium reported for cultivation of microalgae in photobioreactors in 250 mL batch culture. The culture medium used was the Basal Bolds (0.25 gL^{-1} $NaNO_3$, K_2HPO_4 gL^{-1} · $3H_2O$, 0.175 gL^{-1} KH_2PO_4, 0.075 gL^{-1} $MgSO_4$ · $7H_2O$, 0.084 gL^{-1} $CaCl_2$ · $2H_2O$, 0.00498 gL^{-1} $FeSO_4$ · $7H_2O$, 0.05 gL^{-1} EDTA 2Na-Mg, 0.025 gL^{-1} NaCl, 0.031 gL^{-1} KOH, 11.42 μgL^{-1} H_3BO_4, 1.44 μgL^{-1} $MnCl_2$ · $4H_2O$, 8.82 μgL^{-1} $ZnSO_4$ · $7H_2O$, 1.57 mgL^{-1}

$CuSO_4 \cdot 5H_2O$, 0.49 μgL^{-1} Co $(NO_3)_2 \cdot 6H_2O$, 0.71 MoO_3)[26]. The operating conditions of the photobioreactor were: aeration of 0.5 vvm, a quantity of light of 80 mol photons m^{-2} s^{-1} and a photoperiod light: dark 12:12. The hydraulic residence time was batch cultivation of 14 days.

Step 2. Evaluation of the lead removal and biomass growth of photosynthetic microbial culture. The operating conditions of the bioreactors were mentioned in step 1. The reactors were inoculated with 10% of the consortium obtained in step 1 using the basal culture medium of Bolds. Quantification of biomass over time was performed by absorbance spectrophotometer at 750 nm. Lead concentrations tested were 15, 30, 40, 50 and 60 mg/L. To quantify the concentration of residual lead in the culture medium 15 mL aliquots of the suspension culture were taken and centrifuged at 3500 rpm for 20 min, to subsequently carry out the digestion of the supernatant and quantitated in atomic absorption spectrophotometer (Perkin Elmer, model analyst 100) in laboratory analysis and environmental monitoring CIIEMAD-National Polytechnic Institute. Assays for quantification of biomass and for lead removal were performed in triplicate.

Step 3. Evaluation of the lead removal in wastewater from a tertiary treatment plant wastewater treatment Tecamac, Edo. Mex. At this stage the lead removal with two concentrations of wastewater (30 and 60%), water was artificially contaminated with 50 mg/L of lead was evaluated, this concentration was chosen because in the Stage 2 showed higher biomass growth. The operating conditions of the bioreactors were mentioned in step 1. The reactors were inoculated with the consortium (10%) obtained in step 2 using the basal culture medium of Bolds [26]. Quantification of biomass and Pb were carried out as in stage 2.

Step 4. The parameters of the model are optimized by two methods: using the Levenberg–Marquardt optimization approach and Genetic Algorithms.

Levenberg–Marquardt optimization approach (L-M). Biological systems have been traditionally fit using graphical-based techniques, in which parameter estimation is converted to a linear regression problem[25]. However, the applicability of this approach is related to the functionality of the model. Furthermore, graphical methods have been shown to produce inferior parameter estimates than those generated using nonlinear regression techniques. Nonlinear regression was used based on the Levenberg-Marquardt least squares minimization algorithm, which is a hybrid of the Gauss-Newton and the steepest descent methods.

The performance of the proposed mathematical model was statistically evaluated using the dimensionless coefficient of efficiency (Π)[27].

$$\Pi = 1 - \frac{\sum_{i=1}^{N}\left[\left|Y - Y^*\right|\right]}{\sum_{i=1}^{N}\left|Y^* - \overline{Y}\right|} \qquad (1)$$

Where Y is the simulated value of the variable at time t_i, Y^* is the observed value of the same variable at time, and $\bar{Y}$ is the mean value of the observed variable. Π varies between (-∞, 1]. A positive value of Π represents an acceptable simulation whereas Π > 0.5 represents a good simulation

Based on a genetic algorithm (GA). For this work, a GA was used to estimate the model parameters from sets of experimental data. This was accomplished using the genetic algorithm package developed by Matlab™ R2009 library "gatool". As with most GAs, were incorporated three basic genetic operators: selection, crossover, and mutation (**Fig. 1**).

To implement the genetic algorithms, the model's parameters should be presented in terms of chromosomes. Decimal numbers for the parameter values have been used to represent this principle instead of a binary profile. Each chromosome corresponds to one different objective function value. In the literature, the most often used optimization criterion is defined as a modelling error, i.e. the mean square deviation between the model output and the corresponding data obtained during the fermentation. The optimization criteria are presented as follows:

$$\lambda_Y = \sum \left(Y - Y^*\right)^2 \rightarrow min \qquad (2)$$

Where Y is the simulated value of the variable at time t_i and Y* is simulated values (experimental), respectively for Nitrogen (NI), Chemical Oxygen Demand (C), Biomass (X), and Lead removal (L).

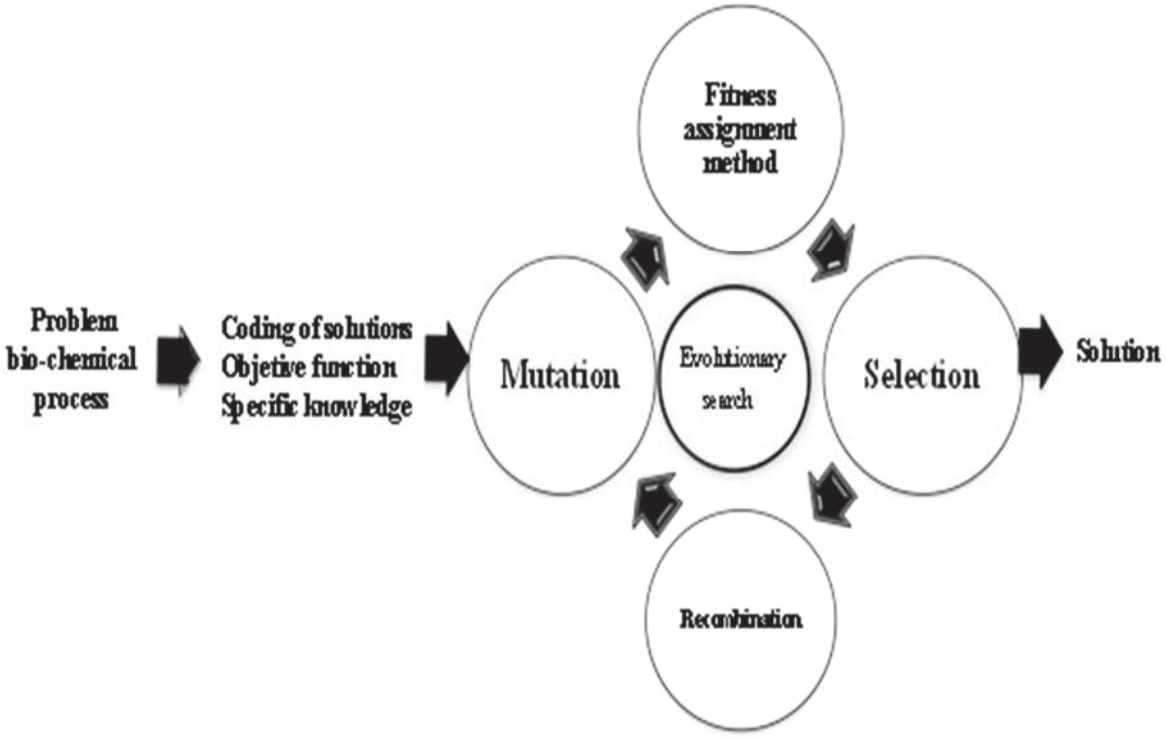


FIGURE 1. Evolutionary algorithms

The initial values of other algorithm's parameters and functions are:

Population:

- Population type: Double vector
- Population zize: 350

Fitness scaling

- Scaling function: Proportional
- Selection: Stochastic uniform

Reproduction

- Elite count: 180
- Crossover fraction: 0.9
- Crossover : Single point

Mutation

- Mutation function: Adaptive feasible

RESULTS AND DISCUSSION

Experimental studies. Minimum inhibitory concentration (MIC) was tested for the resistance to lead in varying concentration from 15 to 60 mg/L. In overall, the consortium isolated showed the maximum resistance to Pb at 50 mg/L and the least resistance to 60 mg/L (**Fig. 2** and **Fig 3**). According to that reported in literature it can be potentially considered as a bioadsorbent for the removal of heavy metals[28]. Deng et al. [29] reported the use of *Cladophora fascicularis* to remove lead from wastewater by biosorption mechanism. The ability of any bio-adsorbent is mainly influenced by the characteristics of the biomass, physicochemical properties of the metal in question and the microenvironments of the solution (pH, temperature and interactions with other ions)[30]. In this study reported that C. *fascicularis* is a bio-sorbent efficient for the removal of lead from the wastewater material. The maximum absorption capacity was 198.5 mg g^{-1} at 298 K and a pH of 5. Therefore, removal Pb was evaluated at 50 mg/L (**Fig. 3**).

Figure 3 shows the removal of lead is observed, finding that a concentration of 50 mg/L showed the greater removal of lead (96.4%). This is probably due to the high concentration of biomass present in the photobioreactor, which has a greater number of sites available on the cell wall for the adsorption of metal, this has been reported in literature [30-32].

Sulaymon et al. [31] measured the percentage removal (50 mg/L) from microalgae culture using different biomass concentrations (0.5-3 g) as adsorbents, showing approximately 90% removal of the element regardless of the biomass concentration used as the factors involved more in the process is the pH (3-5). Depending on the variations in the cell wall composition, there will also be differences in the metal ion binding mechanisms and affinities. The bio-chemical characteristics of the functional

adsorbent (i.e., functional groups, polarity, and solubility) are responsible for determining the binding mechanism and the nature of the adsorption process[33].

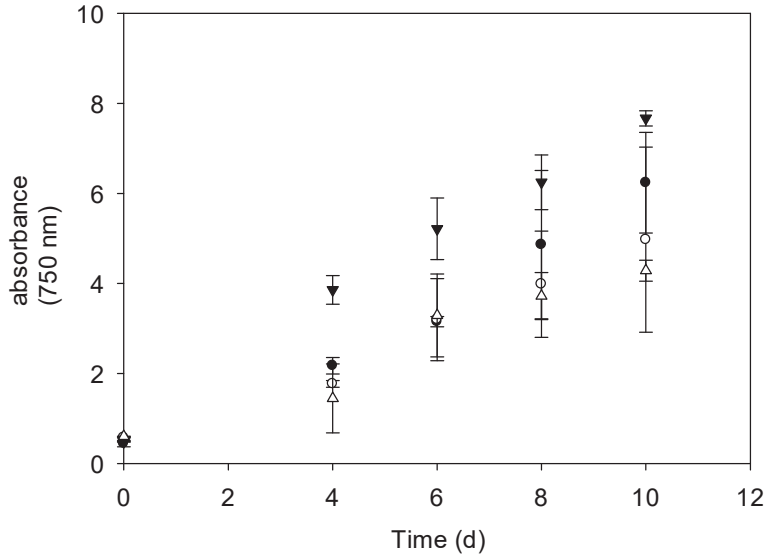


FIGURE 2. Minimal inhibitory concentration determination for consortia isolated from a treatment plant wastewater

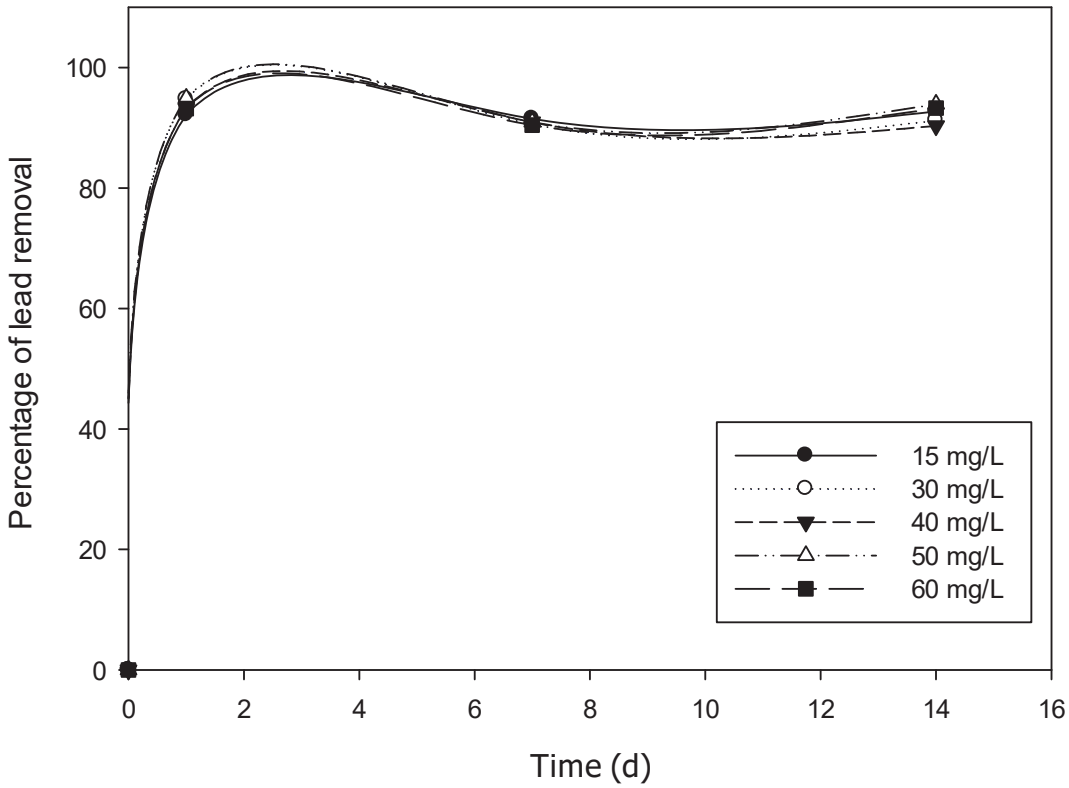


FIGURE 3. Lead removal (MIC)

After determining the best growth kinetics of biomass and metal removal they were tested using these conditions wastewater at different ratios (30 and 60%) from the culture medium, in addition, it was quantified the biomass growth, nitrogen consumption, chemical oxygen demand and metal removal. Therefore, lead removal amounted to more than 97.4%, when the initial cadmium concentration was of up to 50 mg/L using 60% of wastewater (see **Fig.4**).

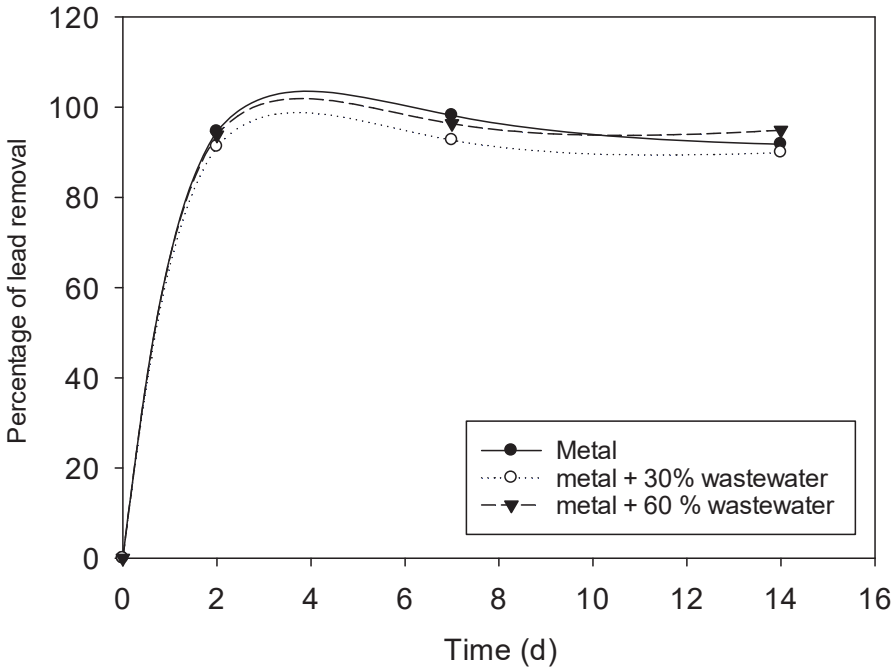


FIGURE 4. Lead removal to different concentrations of wastewater

Kinetic model. The macroscopic models, i.e. phenomenological models describing the dynamic evolution of a few macroscopic components (e.g. main substrates, biomass, products of interest), are now routinely used in bioprocess engineering for optimization, monitoring and control purposes. As macroscopic models involve fewer components, and therefore less parameter, they have better identifiability properties, and offer the possibility to study the dynamics of a cell culture, which is useful for process optimization and control[34]. The classical growth with Lead removal is described by Equations (3)-(8) in a batch bioreactor.

Assumptions of the model were as follows:

1) The photobioreactor is completely mixed;
2) The specific growth rate of algae is related to the nitrogen;
4) Temperature, air (CO_2) and pH are constant in the culture;

Limitations to the model are listed as follows:

1) Kinetic parameters were obtained from initial conditions

2) Nutrient inhibition is considered in the proposed expression for the specific growth rate;

3) Since the proposed model was derived based on the Monod and Luong model, it will have the same limitations of the unstructured-type.

The advantages of the proposed model are:

1) Effect of the initial concentration of nitrogen;
2) Many parameters

Kinetic terms:

$$\gamma_1 = \left(1 - \frac{NI}{k_{NI}}\right)^{\alpha} \left[\frac{C}{k_C + C}\right]\left[\frac{X}{k_X + X}\right] \tag{3}$$

$$\gamma_2 = \left(1 - \frac{NI}{k_{NI}}\right)^{\beta} \left[\frac{C}{k_C + C}\right]\left[\frac{L}{k_L + L}\right] \tag{4}$$

Nitrogen mass balance (NI):

$$\frac{dL}{dt} = \frac{\mu_{max_L}}{Y_P}\gamma_2 L \tag{5}$$

Biomass balance (X):

$$\frac{dX}{dt} = \mu_{max}\gamma_1 L - k_d\ X \tag{6}$$

Chemical Oxygen Demand (COD), (C):

$$\frac{dC}{dt} = \frac{\mu_{max}}{Y}\gamma_1 L \tag{7}$$

Lead removal (L):

$$\frac{dL}{dt} = \frac{\mu_{max_L}}{Y_P}\gamma_2 L \tag{8}$$

Genetic algorithm gives the better results, which are in good agreement with the experimental data, when compared to simulations conducted with optimized parameters obtained by method of Levenberg–Marquardt.

TABLE 1. Model efficiency coefficients for the mathematical model

Variable (Π)	GA	L-M
NI	0.99	0.98
L	0.966	0.997
C	0.973	0.95
X	0.988	0.976
Global	0.97925	0.97575

CONCLUSION

Batch cultures of consortia isolated from a treatment plant wastewater were conducted in media containing different initial lead concentrations. Consortia isolated were grown in batch process which were able to remove nearly all lead (97.4%) when the initial concentration was less than 50 mg/L. A proposed mathematical model closely fitted the experimental data in particular at lead concentration under 50 mg/L. The mathematical model developed can be used for optimization and control purposes. Also worth mentioning that the consortium was able to lower the concentration of COD, nitrates and lead, with a medium composition at 60% of wastewater for an initial concentration of 50 mg/L therefore emerges as a biotechnologically sustainable alternative.

ACKNOWLEDGMENTS

López-Pérez, P.A. is grateful for the support of “Apoyo a la Incorporación de Nuevos PTC 2015, F-PROMEP-39/Rev-04, DSA/103.5/15/7001”1, DSA/103.5/15/7001, CIIEMAD-Instituto Politécnico Nacional, Universidad Tecnológica de Tecámac.

REFERENCES

1. Cañizares-Villanueva R.O. Biosorción de metales pesados mediante el uso de biomasa microbiana. Revista Latinoamericana de Microbiología. 42 (2000) 131-143.
2. Maldonado A., Luque C., Urquizo D. Biosorción de plomo de aguas contaminadas utilizando Pennisetum clandestinum Hochst (kikuyo). Revista Latinoamericana de Metalurgia y Materiales. S4 (2012) 52-57.
3. Deng L., Su Y., Su H., Wang X., Zhu X. Sorption and desorption of lead (II) from wastewater by green algae Cladophora fascicularis. Journal of Hazardous Materials 143: 2007220–225.
4. UNEP. "Lead Exposure and Human Health." UNEP- United Nations Environment Programme. 2013. http://www.chem.unep.ch/pops/pdf/lead/leadexp.pdf

5. Flores-Ramírez R., Rico-Escobar E., Núñez-Monreal J.E., García-Nieto E., Carrizales L., Ilizaliturri-Hernández C., Díaz-Barriga F. Exposición infantil al plomo en sitios contaminados. Salud Pública de México, 54 (2012) 383-392.
6. Sánchez-Alarcón J., Gómez Olivares J.L., Waliszewki Stefan M., Montiel González J.M.R., Valencia-Quintana R. Elaboración de un listado preliminar de sitios potencialmente contaminados con plomo (Pb) en el estado de Tlaxcala. Ra Ximhai, 8 (2012) 165-174
7. http://es.sott.net/article/11867-Contaminacion-industrial-causa-intoxicacion-por-plomo-de-49-ninos-en-Shanghai
8. http://es.sott.net/article/43708-10-muertos-en-Michigan-por-aguas-contaminadas-con-plomo-en-EEUU
9. Mehta S.K., Gaur J.P. Removal of Ni and Cu from single and binary metal solutions by free and immobilized Chlorella vulgaris. European J. Protistology. 37 (2001) 261-271.
10. Sarma P.J., Kumar R., Pakshirajan K. "Batch and Continuous Removal of Copper and Lead from Aqueous Solution using Cheaply Available Agricultural Waste Materials." Int. J. Environ. Res. 9 (2015) 635-648.
11. Jeyakumar R., Suresh P., Chandrasekaran V. "Adsorption of lead(II) ions by activated carbons prepared from marine green algae: Equilibrium and kinetics studies." International Journal of Industrial Chemistry (Springer) 5, no. 2 (2014).
12. Das N., Vimala R., Kartika P. Biosorption of heavy metals-An overview. Indian J. Biotechnol 7 (2008) 159-169.
13. Bayramoğlu G., Tuzun I., Celik G, Yilmaz M, Arica M.Y. Biosorption of mercury(II), cadmium(II) and lead(II) ions from aqueous system by microalgae Chlamydomonas reinhardtii immobilized in alginate beads. Int. J. Miner. Process 81 (2006) 35–43.
14. López-Pérez Pablo A., Neria-González Isabel., Aguilar-López R., A biotechnological alternative in the cadmium removal at high concentration: desulfovibrio alaskensis 6sr., International Journal of Environmental Science and Technology. 12 (2015) 1975-1986.
15. Schiewer S., Volesky B. Biosorption processes for heavy metal removal. In: Lovley DR (ed) Environmental microbe–metal interactions. ASM Press, Washington DC, (2000) pp 329–362.
16. Godlewska-Żyłkiewicz B. Biosorption of platinum and palladium for their separation/ preconcentration prior to graphite furnace atomic absorption spectrometric determination. Spectrochim Acta B. 58 (2003) 1531–1540
17. Resat H., Petzold L., Pettigrew M.F. Kinetic Modeling of Biological Systems Methods, Mol. Biol. 541 (2009) 311–335.
18. Roubos J., van Straten G., van Boxtel A. An evolutionary strategy for fedbatch bioreactor optimization: Concepts and performance. J. Biotechnol, 67 (1999) 173–187.
19. Chen L., Nguang S., Chen X., Li X. Modelling and optimization of fedbatch fermentation processes using dynamic neural networks and genetic algorithms. Biochem. Eng. J. 22 (2004) 51–61.
20. Patil K., Rocha I., Forster J., Nielsen J. Evolutionary programming as a platform for in silico metabolic engineering. BMC Bioinformatics. 6 (2005) 1–12.
21. Sarkar D., Modak J. Optimisation of fed-batch bioreactors using genetic algorithms. Chem. Eng. Sci. 58 (2003) 2283–2296.
22. Chen L.Z., Nguang S.K., Chen X.D. On-line identification and optimization of feed rate profiles for high productivity fed-batch culture of hybridoma cells using genetic algorithms. ISA Trans. 41 (2002) 409-419.
23. Andrade R.R., Rivera E.C., Atala D.I.P., Maciel Filho R., Maugeri Filho F., Costa A.C. Study of kinetic parameters in a mechanistic model for bioethanol production through a screening technique and optimization. Bioprocess Biosyst. Eng. 32 (2009) 673-680.

24. Almquista J., Cvijovicc M., Hatzimanikatise V., Nielsen J., Jirstrand M. Kinetic models in industrial biotechnology – Improving cell factory performance. Metab. Eng. 24 (2014) 38–60.
25. Vasanth Kumar K. Linear and non-linear regression analysis for the sorption kinetics of methylene blue onto activated carbon. J. Hazard. Mater. B137 (2006) 1538–1544.
26. Richmond A., Hu Q. Handbook of Microalgal Culture: Applied Phycology and Biotechnology, 2nd Edition. Wiley-Blackwell: Great Britain, (2013) 545 pp.
27. López-Pérez P.A., Neria-González I., Aguilar-López R. A mathematical model for cadmium removal using a sulfate reducing bacterium: desulfovibrio alaskensis 6sr. International Journal of Environmental Research. 7 (2013) 501-512.
28. Sheng P.X., Ting Y.P., Chen J.P., Hong L. Sorption of lead, copper, cadmium, zinc and nickel by marine algal biomass: characterization of biosorptive capacity and investigation of mechanisms. J. Colloid. Interface Science. 275 (2004) 131-141.
29. Deng L., Su Y., Su H., Wang X., Zhu X. Sorption and desorption of lead (II) from wastewater by green algae Cladophora fascicularis. Journal of Hazardous Materials. 143 (2007) 220–225.
30. Masoumi F., Khadivinia E., Alidoust L., Mansourinejad Z., Shahryari S., Safaei M., Mousavi A., Salmanian A-H., Zahiri H.S., Vali H., Noghabi K. A. Nickel and lead biosorption by Curtobacterium sp. FM01, an indigenous bacterium isolated from farmland soils of northeast Iran. Journal of Environmental Chemical Engineering. 4 (2016) 950-957.
31. Sulaymon A.H., Mohammed A.A., Al-Musawi T.J. Competitive biosorption of lead, cadmium, copper, and arsenic ions using algae. Environ. Sci. Pollut. Res. 20 (2013) 3011–3023.
32. Robalds A., Naja G.M., Klavins M. Highlighting inconsistencies regarding metal biosorption. Journal of Hazardous Materials. 304 (2016) 553-556.
33. Aksu Z. Biosorption of reactive dyes by dried activated sludge. Equilibrium and kinetic modeling. Biochem. Eng. J. 7 (2001) 79–84.
34. Dochain D. State and parameter estimation in chemical and biochemical processes: a tutorial. Journal of Process Control. 13 (2003) 801-818.

CHAPTER 4.8 OPTIMIZATION OF A METHOD OF FEATHER BIODEGRADATION OF CHICKEN

M. E. Pahua-Ramos; D. J. Hernández-Melchor; B. Camacho-Pérez; G.I. Cerón-Montes and **M. Quezada Cruz***

(1) Laboratorio de Biotecnología Ambiental, Universidad Tecnológica de Tecámac. Km. 37.5 Carretera Federal México – Pachuca, Tecámac, Edo. de México.

ABSTRACT

According to the FAO, 108.7 million tons of poultry meat were consumed worldwide in 2014[1], generating millions of tons of feathers as waste, which affects public health and the environment. It is estimated that total poultry consumption in Mexico will reach 3274 million tons by 2018, generating about 163.7 to 327.4 million tons of feathers[2]. The most widely used processes for the degradation of feathers use pure strains of bacteria; however, in Mexico there are few studies on this issue. The aim of this research is to standardize the optimum laboratory conditions for the biodegradation of chicken feathers.

The study was conducted in one liter flasks with a consortium of bacteria isolated from a chicken processing plant. The culture conditions included stirring at 120 rpm and a pH of 6.8-7.2 for 14 days. In the first stage, an experimental design 2^3 was used to evaluate the following factors: temperature (25, 32 and 37 °C) and carbon source (whey, nutrient broth Luria Bertani broth). The degradation of the feathers and microbial growth were evaluated by measuring absorbance at 620 nm. The best results obtained in the first stage (temperature and carbon source) informed the second stage, which consisted in the evaluation of the degradation of feathers using different concentrations of nutrient broth (25, 50 and 100%). The concentration of protein was quantified according to Bradford (1976)[3], and the presence of aromatic amino acids in the soluble fraction left after the degradation of the feathers was determined by UV spectrophotometry.

The results showed that the proposed method can achieve total degradation of feathers (including the rachis) in 14 days. In the first stage, the best operating conditions were using a nutrient broth and a temperature of 32 °C. In the second stage, total degradation of feathers was achieved using nutrient broth at 50% and 32 to °C. The bacteria formed round or elliptical structures around the rachis of the feathers during the degradation process; this allowed them to achieve total degradation of the feathers. The maximum concentration of protein in the soluble fraction obtained after the degradation process at 32 °C and with nutrient broth at 25, 50 and 100%, was 12.60±0.1, 14.60±0.02 and 18.60±0.01 µg/ml, respectively. Some of the amino acids in the soluble fraction included tryptophan and tyrosine. This study shows a promising biotechnology for reducing pollution by feathers. The amino acids obtained at the end of the degradation process have great industrial potential.

Keywords: amino acids; biodegradation; feathers

---

*Author for correspondence: mabelqz@yahoo.com.mx

INTRODUCTION

One of the first methods used to reduce the impact of the pollution generated by chicken feathers was to incorporate them into animal feed supplements, since 95% of their dry weight is protein, of which 88% is keratin[4].However, the disulfide bridges, hydrogen bonds and hydrophobic interactions of keratin make it insoluble and very difficult to digest[5]. Several studies have tried to increase its solubility by subjecting it to a process with high pressure and temperature; however, this process has serious disadvantages, including its high cost and the destruction of some thermolabile amino acids such as histidine, methionine and tryptophan[5].

Kornillowicz-Kawalska and Bohacz (2010)[10] mention that these problems have led to a radical change in the methods used to dispose of feathers. The new methods studied in recent years involve the biodegradation of feathers through fermentation using microorganisms or enzymes; these processes are economical and also allow the development of new products. Recent studies have evaluated the degradation of feathers by microorganisms such as bacteria of the following genera: *Bacillus*[7-13], *Chryseobacterium*[14], *Kocuria*[4,5,15], *Xanthomonas*[16,17], *Pseudomonas*[18-20], *Leuconostoc*[18], *Scopulariopsis*[21], *Stenotrophomonas*[22], *Fervidobacterium*[23]; actinomycetes such as *Actinomadura*[24]; fungi such as *Coprinopsis* and *Aspergillus*[25,26], consortia of bacteria[27] and consortia de actinomycetes[28]. Moreover, some authors have made genetic modifications to strains of *Escherichia coli*, *BreviBacillus sp*. and *Bacillus subtilis* in order to accelerate the degradation of chicken feathers[29-31]. In Mexico, there are few studies on the degradation of poultry waste. The objective of this research was to standardize the optimum laboratory conditions for the biodegradation of chicken feathers.

MATERIALS AND METHODS

Microorganisms. We used a consortium of bacteria isolated from the chicken processing plant "Las Rosas", located in the municipality of Tizayuca, in the state of Hidalgo, Mexico. The bacteria were grown in nutrient broth for 48 hours at 37 °C and 121 rpm.

Preparation of the feathers. The feathers were washed with tap water and allowed to dry for 24 hours at 60 °C. Five grams were weighed and washed 2 times in boiling water for 5 minutes before being placed in the flask.

Conditions of the degradation process. The study was conducted in one liter flasks with a working volume of 500 mL. One hundred ml of the consortium of bacteria previously grown in nutrient broth were added to the flasks. The culture conditions were: stirring at 120 rpm and pH 6.8-7.2 for 14 days. In the first stage, an experimental design 3^2 was used to evaluate the following factors: temperature (25, 32 and 37 °C) and carbon source (whey, nutrient broth Luria Bertani broth). In the second stage, the degradation of the feathers was evaluated with different concentrations of nutrient broth (25, 50 and 100%).

Degradation of the feathers. The degradation of the feathers and the growth of bacteria were evaluated by measuring absorbance at 620 nm according to previous reports [32,5]. After the degradation process, the samples were filtered through Whatman glass fiber paper (GF/A paper, 22-mm diameter) to quantify the concentration of protein in the soluble fraction and detect some amino acids. The concentration of soluble protein was determined according to the method of Bradford (1976)[3]; to build the calibration curve, we used bovine albumin (SPINREACT, S.A./S.A.U.*).* The presence of some aromatic amino acids (tryptophan and tyrosine) was detected by UV spectrophotometry using a Jenway spectrophotometer, 6715-8 UV-Vis[33].

Scanning Electron Microscopy*.* The samples of the structure (spherical and elliptical) formed during the degradation of the rachis of the feathers were fixed in glutaraldehyde (3.0%) in phosphate buffer (0.1 M; pH 7.2) for 24 hours at room temperature. They were rinsed 2 times with deionized water and allowed to stand in deionized water for 40 min. Post-fixation was performed in osmium tetroxide (1%) for one hour and then the samples were rinsed with phosphate buffer. After post-fixation, the samples were dehydrated in a series of alcohols at different concentrations and dried to a critical point. They were then coated with a thin layer of gold-palladium for 60 seconds using a Jeol, JFC-1100 fine coat ion sputter. The samples were observed in a scanning electron microscope JEOL JSM 6390 at 5,000 and 10,000x.

Statistical analysis. The influence of the factors studied (temperature and carbon source) on the degradation of feathers was determined by ANOVA analysis was performed using Minitab statistical software with a significance level (α) of 0.05.

RESULTS AND DISCUSSION

Figures 1a, 1b and **1c** show the results of the degradation of feathers; in all cases, the absorbance increases with the growth of bacteria, indicating the degradation of feathers [10].

Chaturvedi et al. (2014)[20] conducted a study on the degradation of feathers under similar conditions. They placed 5 grams of feathers in a 250-ml flask at 30 °C, with pH 7.5 and 125 rpm. They observed an increased growth of cells during the degradation of feathers.

Some authors have observed that, in the absence of feathers, and with a carbon source, *Bacillus megaterium* produces almost no keratinolytic enzyme. The presence of feathers greatly increases the production of this enzyme compared to the medium without feathers. Furthermore, it has been observed that the combination of feathers and some carbon source (glucose, fructose, galactose, mannitol, soluble starch, etc.) causes a high production of the keratinolytic enzyme[10].

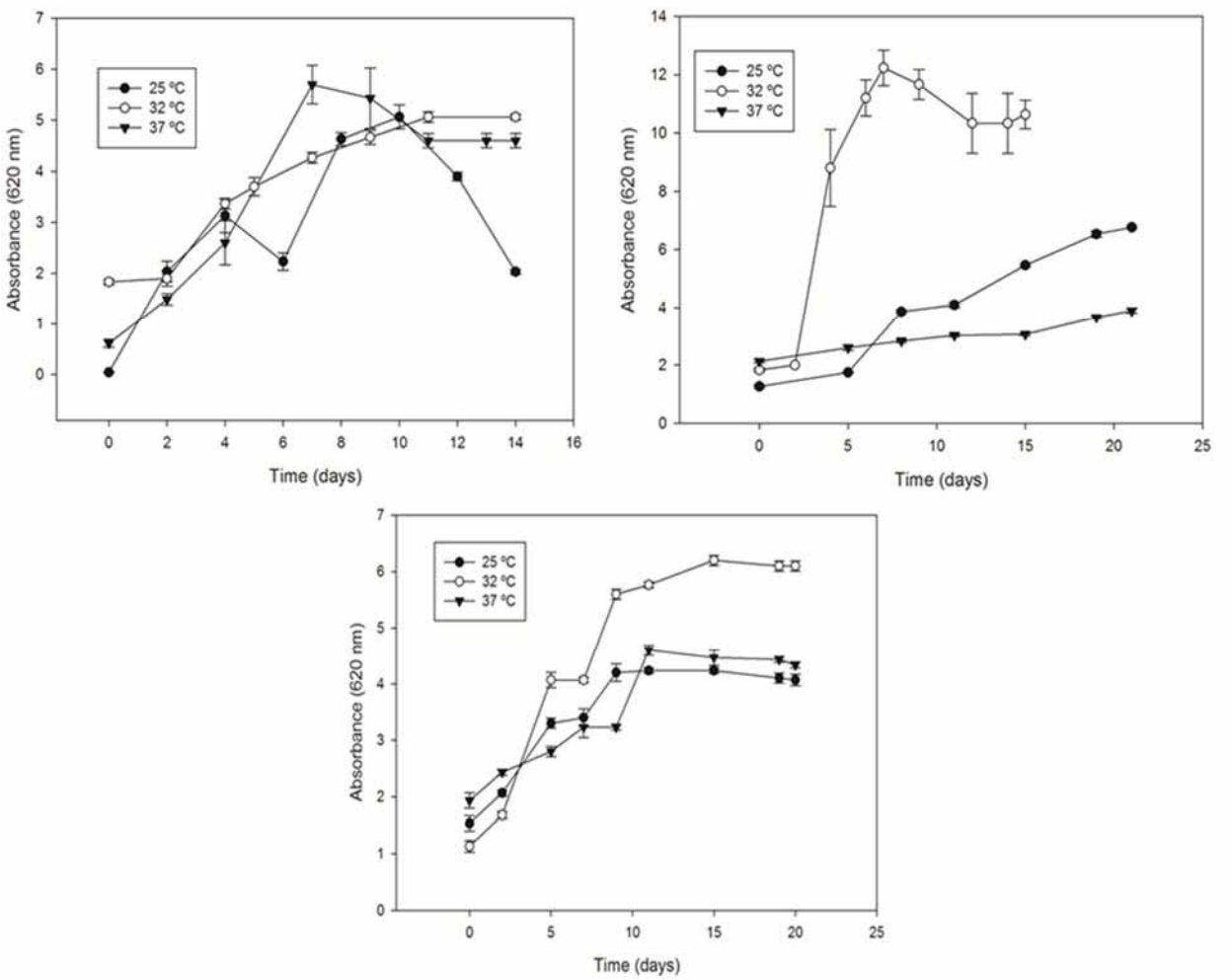


FIGURE 1. Growth and degradation of feathers: a) with nutrient broth, b) with whey, c) with Luria-Bertani broth.

Figure 2 shows the degradation of chicken feathers obtained with each treatment. As mentioned above, the absorbance is related to the degradation of chicken feathers. The highest absorbance was observed at 32 °C, using whey as carbon source. The ANOVA analysis showed that the factors under study had a significant on the degradation of chicken feathers. The average absorbance for temperature was (**Figure 3**) 4.60, 7.06 and 4.08 for 25, 32 and 37 °C, respectively. The average absorbance for the carbon sources (**Figure 4**) was 5.82, 4.91 and 4.87 for whey, nutrient broth and Luria Bertani broth, respectively.

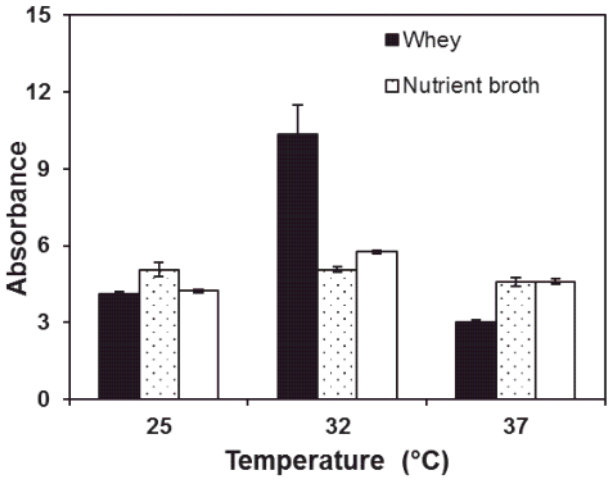


FIGURE 2. Degradation of chicken feathers at 11 days of treatment.

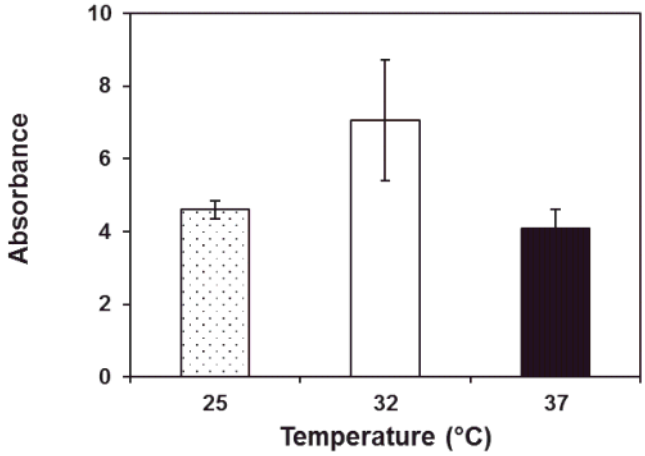


FIGURE 3. Effect of temperature on the degradation of chicken feathers at 11 days of treatment.

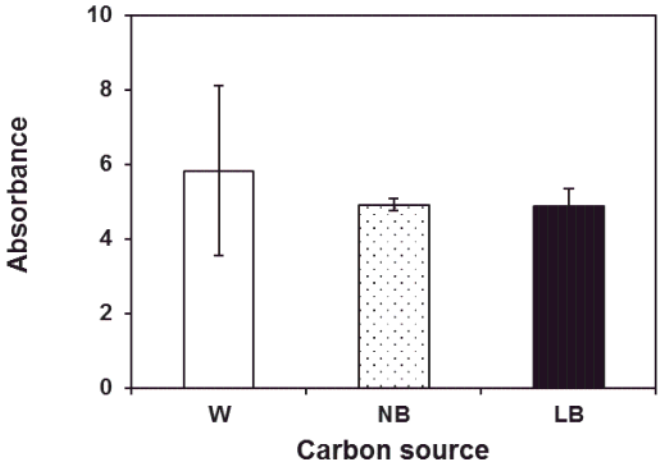


FIGURE 4. Effect of carbon source on the degradation of chicken feathers at 11 days of treatment.

Three different concentrations of the nutrient broth were used to determine its influence on the degradation of feathers. The results showed that the concentration of soluble protein (**Figure 5**) increased with increasing concentrations of nutrient broth (25, 50 and 100%): 12.60±0.1, 14.60±0.02 and 18.60±0.01 µg/ml, respectively. The highest concentration of soluble protein (18.6 µg/L) was obtained by using nutrient broth at 100% in the fermentation process, which promoted the growth of the microbial consortium. These results are similar to those obtained by Jeong et al. (2010)[16], who used different carbon sources (glucose, mannitol, soluble starch, etc.) with *Stenotrophomonas maltophilia* to degrade feathers and obtained a concentration of soluble protein of 11.2±0.8-19.7±2.6 µg/ml. They observed that the maximum production activity of the keratinolytic enzyme (29.5±0.5 U/ml), and the maximum values of cell growth and concentration of soluble protein, were obtained by adding glucose at 2%.

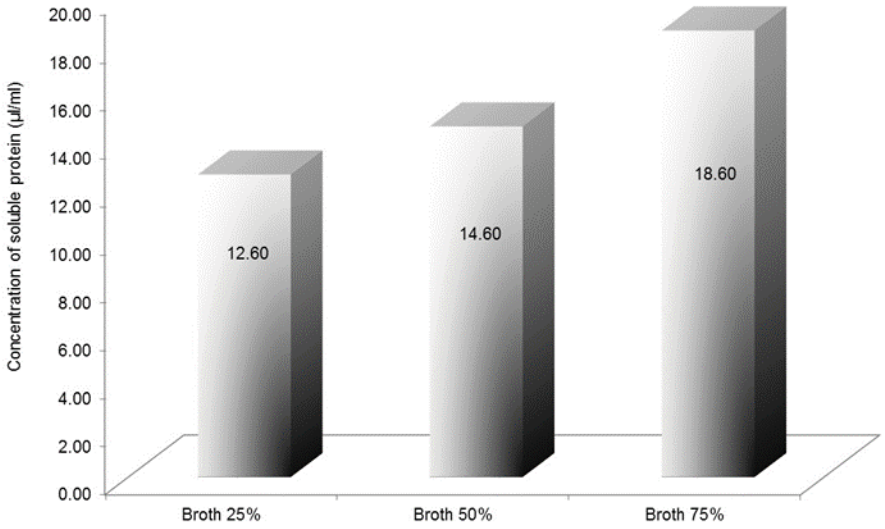


FIGURE 5. Concentration of soluble protein in the degradation with nutrient broth.

In this study, we detected tryptophan and tyrosine by ultraviolet spectrophotometry after 14 days of the degradation process. Nam et al. (2002)[23], who conducted a study on the degradation of feathers in thermophilic conditions with *Fervidobacterium islandicum* AW-1, found that the amino acids produced after degradation were alanine, serine, cysteine (belonging to the feathers). They also found essential amino acids such as methionine, lysine and tryptophan (not belonging to the feathers).

The electron microscopy study showed that, in a first stage, the bacteria degraded the barbules of the feathers (during 9 days); in a second stage, the bacteria formed round and elliptical structures (**Figure 6**) around the rachis in order to degrade it. The study of these structures revealed the presence of bacteria in the form of bacilli on the fibrils of the rachis during the degradation process, and a large amount of bacteria in the sediment formed after degradation (**Figure 7**).



FIGURE 6. **Round and elliptical structures in rachis.**

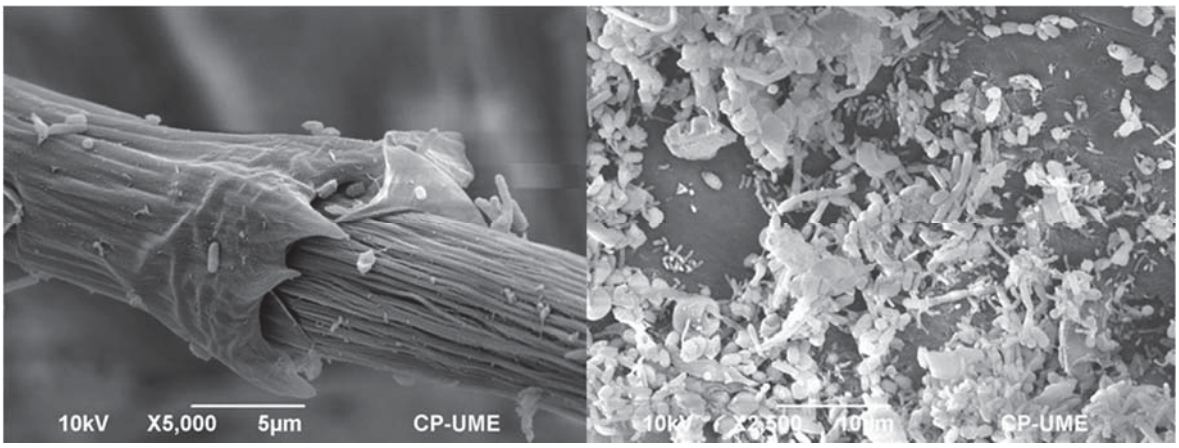


FIGURE 7. Micrography of degradation of feathers: a) round and elliptical structures. b) bacteria in a fibril rachis feather. c) bacteria in the sediment after feathers degradation.

Algunos investigadores han realizado observaciones en microscopía electrónica de barrido para verificar el proceso de degradación de la pluma[16,25,20]. Jeong et al. (2010)[22] estudiaron el proceso de degradación de plumas de pollo utilizando la cepa *Stenotrophomonas maltophilia* R13, realizando observaciones mediante microscopia electrónica de barrido para verificar el proceso de degradación. En estas observaciones reportan la degradación de las bárbulas a los 2 días de incubación, la degradación del eje de las plumas a los 4 días de incubación y finalmente mencionan un agregado de bacterias con una matriz extracelular adherida a la superficie de degradación.

Some studies have used scanning electron microscopy to verify the degradation of the feathers[16,25,20]. Jeong et al. (2010)[22] studied the degradation of chicken feathers using *Stenotrophomonas maltophilia* R13, and verified the degradation by scanning electron microscopy. They reported that the barbules were degraded at 2 days of incubation and the feather axis at 4 days of incubation; they also reported an aggregate of bacteria embedded in an extracellular matrix adhering to the degradation surface.

CONCLUSION

The consortium of bacteria used in this study showed a high potential for use in the total degradation of feathers (including the rachis). The formation of round or elliptical structures around the rachis allows the bacteria to degrade it completely. The ANOVA analysis showed that the temperature and the carbon source had a significantly influence on the degradation of chicken feathers. A temperature of 32 °C and the addition of a carbon source such as nutrient broth at 100% allowed us to obtain the highest values of bacterial growth and production of soluble protein (18.60±0.01 µg/ml).

ACKNOWLEDGEMENTS

We thank the technical support of Valencia Ramirez Valentín (TSU), of Victoria Enciso Tenorio (IBT) and Dr. Porfirio Raul Garcia of the Universidad Tecnológica de Tecámac. We thank Dra. Hilda Zavaleta Mancera, from the Colegio de Postgraduados for providing technical and financial support in the use of scanning electron microscopy.

REFERENCES

1. FAO Food and Agriculture Organization of the United Nations. Producción y sanidad animal. Consumo de carne. Departamentode Agricultura y protección del consumidor, 2014. http://www.fao.org/ag/againfo/themes/es/meat/background.html
2. SAGARPA Secretaria de agricultura, ganadería, desarrollo rural, pesca y alimentación Escenario base: Proyecciones para el sector Agropecuario de México. México, D.F. pp 51 – 53, 2009.
3. Bradfor M. M. A rapid and sensitive method for the quantitation of microgram quantities of protein utilizing the principle of protein-dye binding. Anal Biochem. 72 (1976) 248–254.
4. Costa J.C., Barbosa S.G., Sousa D.Z. Effects of pre-treatment and bioaugmentation strategies on the anaerobic digestion of chicken feathers. Bioresour Technol. 120 (2012) 114-119.
5. Coello N., Vidal L., Bretaña A. Aislamiento de una cepa de Kocuria rosea degradadora de plumas de aves de corral. Rev C FCV-Luz. 10(2) (2000) 107-113.
6. Kornilłowicz-Kowalska T., Bohacz J. Dynamics of growth and succession of bacterial and fungal communities during composting of feather waste. Bioresour Technol.101(4) (2010) 1268-1276.
7. Liu Q., Zhang T., Song N., Li Q., Wang Z., Zhang X., Lu X., Fang J., Chen J. Purification and characterization of four key enzymes from a feather-degrading Bacillus subtilis from the gut of tarantula Chilobrachys guangxiensis. Int Biodeter Biodegr.96 (2014) 26-32.
8. Fakhfakh N., Ktari N., Haddar A., Mnif I.H., Dahmen I., Nasri M. Total solubilisation of the chicken feathers by fermentation with a keratinolytic bacterium, Bacillus pumilus A1, and the production of protein hydrolysate with high antioxidative activity. Process Biochem. 46(9) (2011) 1731-1737.
9. Kumar E.V., Srijana M., Chaitanya K., Reddy Y.H.K., Reddy G. Biodegradation of poultry feathers by a novel bacterial isolate Bacillus altitudinis GVC11.Indian J. Biotechno . 10 (2011) 502-507.
10. Park G.T., Son H.J. Keratinolytic activity of Bacillus megaterium F7-1, a feather-degrading mesophilic bacterium.Microbiol Res . 164(4) (2009) 478-485.
11. Forgács G., Alinezhad S., Mirabdollah A., Feuk-Lagerstedt E., Horváth I.S. Biological treatment of chicken feather waste for improved biogas production. J Environ Sci. 23(10) (2011) 1747-1753.
12. Tiwary E., Gupta R. Medium optimization for a novel 58 kDa dimeric keratinase from Bacillus licheniformis ER-15: Biochemical characterization and application in feather degradation and dehairing of hides. Bioresour. Technol. 101(15) (2010) 6103-6110.

13. Lo W.H., Too J.R., Wu J.Y. Production of keratinolytic enzyme by an indigenous feather–degrading strain Bacillus cereus Wu2. J Biosci Bioeng. 114(6) (2012) 640-647.
14. Fontoura R., Daroit D.J., Correa A.P.F., Meira S.M.M., Mosquera M., Brandelli A. Production of feather hydrolysates with antioxidant, angiotensin-I converting enzyme- and dipeptidyl peptidase-IV-inhibitory activities. N. Biotechno. 31(5) (2014) 506-513.
15. Bertsch A., Álvarez R., Nereida C. Evaluación de la calidad nutricional de la harina de plumas fermentadas por kocuria rosea como fuente alternativa de proteínas en la alimentación de aves. Rev C FCV-LUZ. 13(2) (2003) 139-145.
16. Jeong J.H., Park K.H., Oh D.J., Hwang D.Y., Kim H.S., Lee C.Y., Son H.J. Keratinolytic enzyme-mediated biodegradation of recalcitrant feather by a newly isolated Xanthomonas sp. P5. Polym Degrad Stab. 95(10) (2010) 1969-1977.
17. DeToni C.H., Richter M.F., Chagas J.R., Henriques J.A., Termignoni C. Purification and characterization of an alkaline serine endopeptidase from a feather-degrading Xanthomonas maltophilia strain. Can J Microbiol. 48(4) (2002) 342-348.
18. Tamil Kani P. S.K., Madhanraj P., Senthilkumar G., Panneerselvam A. Degradation of chicken feathers by Leuconostoc sp. and Pseudomonas microphilus. Eur J Exp Biol. 2(2) (2012) 358-362.
19. Chaturvedi V., Bhange K., Bhatt R., Verma P. Biodetoxification of high amounts of malachite green by a multifunctional strain of Pseudomonas mendocina and its ability to metabolize dye adsorbed chicken feathers. J Environ Chem Eng. 1(4) (2013) 1205-1213.
20. Chaturvedi V., Bhange K., Bhatt R., Verma P. Production of kertinases using chicken feathers as substrate by a novel multifunctional strain of Pseudomonas stutzeri and its dehairing application. Biocatal Agric Biotechnol. 3(2) (2014) 167-174.
21. Sharaf E.F., Khalil N.M. Keratinolytic activity of purified alkaline keratinase produced by Scopulariopsis brevicaulis (Sacc.) and its amino acids profile Saudi J Biol Sci. 18(2)(2011) 117-121.
22. Jeong J.H., Lee O.M., Jeon Y.D., Kim J.D., Lee N.R., Lee C.Y., Son H.J. Production of keratinolytic enzyme by a newly isolated feather-degrading Stenotrophomonas maltophilia that produces plant growth-promoting activity. Process Biochem. 45(10) (2010) 1738-1745.
23. Nam G.W., Lee D.W., Lee H.S., Lee N.J., Kim B.C., Choe E.A., Hwang J.K., Suhartono M.T., Pyun Y.R. Native-feather degradation by Fervidobacterium islandicum AW-1, a newly isolated keratinase-producing thermophilic anaerobe. Arch Microbiol. 178(6) (2002) 538-547.
24. Habbeche A., Saoudi B., Jaouadi B., Haberra S., Kerouaz B., Boudelaa M., Badis A., Ladjama A. Purification and biochemical characterization of a detergent-stable keratinase from a newly thermophilic actinomycete Actinomadura keratinilytica strain Cpt29 isolated from poultry compost. J Biosci Bioeng. 117(4) (2014) 413-421.
25. Al-Musallam A.A., Al-Gharabally D.H., Vadakkancheril N. Biodegradation of keratin in mineral-based feather medium by thermophilic strains of a new Coprinopsis sp. Int Biodeter Biodegr. 79 (2013) 42-48.
26. Mazotto A.M., Couri S., Damaso M.C.T., Vermelho A.B. Degradation of feather waste by Aspergillus niger keratinases: Comparison of submerged and solid-state fermentation. Int Biodeter Biodegr. 85 (2013) 189-195.
27. Xia Y., Massé D.I., McAllister T.A., Beaulieu C., Ungerfeld E. Anaerobic digestion of chicken feather with swine manure or slaughterhouse sludge for biogas production. Waste Manage. 32(3) (2012) 404-409.
28. Vasileva-Tonkova E., Gousterova A., Neshev G. Ecologically safe method for improved feather wastes biodegradation. Int Biodeter Biodegr. 63(8) (2009) 1008-1012.
29. Mukherjee A.K., Rai S.K., Bordoloi N.K. Biodegradation of waste chicken-feathers by an alkaline β-keratinase (Mukartinase) purified from a mutant Brevibacillus sp. strain AS-S10-II. Int Biodeter Biodegr.65(8) (2011) 1229-1237.

30. Zaghloul T. I., Embaby A.M., Elmahdy A.R. Biodegradation of chicken feathers waste directed by Bacillus subtilis recombinant cells: Scaling up in a laboratory scale fermentor. Bioresour Technol. 102(3) (2011) 2387-2393.
31. Sharma R., Verma V.V., Gupta R. Functional characterization of an extracellular keratinolytic protease, Ker AP from Pseudomonas aeruginosa KS-1: A putative aminopeptidase with PA domain,J Mol Catal B Enzym. . 91 (2013) 8-16.
32. Agrahari S. and Wadhwa N. Degradation of Chicken Feather a Poultry Waste Product by Keratinolytic Bacteria Isolated from Dumping Site at Ghazipur Poultry Processing Plant.Int. J. Poult. Sci . 9(5) (2010) 482-489.
33. Baranowska I., Kozlowska M. TLC separation and derivative spectrophotometry of some amino acids. Talanta. 42 (1995)1553-1557.

CHAPTER 4.9 VERMICOMPOSTEO DE LODOS RESIDUALES DEL RECICLADO DE PAPEL MEZCLADOS CON RESIDUOS SÓLIDOS ORGÁNICOS DE MANEJO ESPECIAL

I. J. Rodríguez Meléndez*(1); F. Robles Martínez (1) and M.O. Franco Hernández (1)

(1) Unidad Profesional Interdisciplinaria de Biotecnología - IPN, Av. Acueducto, S/N, Ciudad de México. México.

RESUMEN

Actualmente la inadecuada gestión de los residuos de manejo especial en México supone un derroche de energía y recursos; produce contaminación de las aguas subterráneas, emisión de gases de efecto invernadero, malos olores, etc.
El vermicomposteo es una técnica de tratamiento aplicada a los Residuos Sólidos Orgánicos (RSO) mediante la utilización de lombrices de algunas especies. En este bioproceso se tienen efectos benéficos, físicos, químicos y biológicos sobre los suelos, además de incrementar el crecimiento de la planta y el rendimiento al aplicarlo en cultivos.
El objetivo del trabajo fue establecer un proceso para la producción de un fertilizante orgánico mediante el uso de la lombriz roja Californiana (*Eisenia foetida)* y su aplicación a 5 mezclas de diferentes sustratos como lodo residual de reciclado de papel, RSO, estiércol de vaca y mulch. Se determinó el aporte de C, N, Relación C/N, mismas que para las pilas P_1 a P_5 fueron: 8.35, 7.76, 4.15, 4.49 y 1.86 respectivamente. Para P en cada mezcla tuvo un aumento considerable en todos los casos, además se determinó la producción de fertilizante que fue mayor en la P_2 (28.478 kg), y la biomasa de cada pila. Se concluyó que el lodo residual de reciclado de papel presente en mayor cantidad en la P_1, es adecuado para la producción de humus de lombriz de calidad.

Palabras claves: *Eisenia foetida*; lodo de proceso; sustratos orgánicos.

INTRODUCCIÓN

Aunque la aplicación de RSO, lodos de aguas negras, residuos agrícolas y agroindustriales, a la tierra puede beneficiar la calidad del suelo debido a la incorporación de elementos nutritivos y materia orgánica (MO), éstos pueden contener productos tóxicos, incluyendo metales pesados, compuestos orgánicos y organismos patógenos, los cuales son nocivos para la calidad del suelo y pueden persistir durante largos períodos de tiempo.
Las problemáticas relacionadas a la generación de residuos de manejo especial en México son diversas. En el caso del estiércol no existe un control adecuado en el almacenamiento, transporte o aplicación en terrenos de cultivo. Además, se da una

---

*Author for correspondence: ijrmelendez@gmail.com

emisión de gases de efecto invernadero y contaminación de cuerpos de agua superficiales y subterráneos.Por otra parte, la inadecuada gestión de los lodos residuales de producción de papel supone, por un lado un derroche de energía y recursos insostenible; además, constituye una fuente de problemas ambientales entre los que se encuentran: la contaminación de las aguas subterráneas, la emisión de gases al aire, humos y malos olores.

Los residuos sólidos orgánicos generados en las centrales de abasto del país, no son la excepción, en la actualidad, en las centrales de abasto del país se producen diariamente miles de toneladas de desechos orgánicos y alrededor de 80 por ciento de estos desperdicios son productos hortícolas. En la mayoría de los casos, estos desechos no reciben tratamiento alguno y su destino final es un sitio de disposición final, donde su degradación anaerobia ocasiona problemas de contaminación[1].

Hoy en día existen diversas evidencias de que las lombrices de tierra provocan diferentes efectos benéficos, físicos, químicos y biológicos, sobre los suelos y diversos investigadores han demostrado que estos efectos pueden incrementar el crecimiento de la planta y el rendimiento de los cultivos tanto en ecosistemas naturales como en los ecosistemas manejados[2]. Ésta avanza excavando en el terreno a medida que come, depositando sus deyecciones y convirtiendo este terreno en uno mucho más fértil, ya que los excrementos de la lombriz contienen 5 veces más nitrógeno, 7 veces más fósforo, 5 veces más potasio y 2 veces más calcio, que una composta estándar; puede vivir a temperaturas que oscilan de 20-30 °C, una humedad entre 75-85%, y pH de 5-8[3]. El objetivo del trabajo fue establecer un proceso para la producción de un fertilizante orgánico mediante el uso de la lombriz roja Californiana (*Eisenia foetida)* y su aplicación a 5 mezclas de diferentes sustratos como lodo residual de reciclado de papel, RSO, estiércol de vaca y mulch.

MATERIALES Y MÉTODOS

Se realizaron cinco tratamientos (pilas de 150 kg) con mezclas porcentuales de cuatro sustratos: lodos residuales del reciclado de papel, estiércol de vaca, residuos sólidos orgánicos (RSO); (naranja, papaya, plátano, piña, lechuga y jitomate) y mulch a diferentes proporciones, manteniendo la última constante a 15%. P1: L_{70}-E_5-R_{10}, P2: L_{50}-E_{15}-R_{25}, P3: L_{30}-E_{15}-R_{40}, P4: L_{10}-E_{20}-R_{55} y P5: L_0-E_{25}-R_{60} (**Tabla 1**).

TABLA 1. Composición de mezclas propuestas para los experimentos

MEZCLA	LODOS RESIDUALES (%)	ESTIÉRCOL DE VACA (%)	RESIDUOS ORGÁNICOS (%)	MATERIAL ESTRUCTURANTE (%)
1	70	5	10	15
2	50	10	25	15
3	30	15	40	15
4	10	20	55	15
5	0	25	60	15

La determinación de los tipos de residuos a incorporar en cada pila se definió de acuerdo a los residuos mayormente generados en la central de abastos de la Ciudad de México, según lo reportado por Robles-Martínez et al. (2010)[4].

Previo a la incorporación de las lombrices se compostaron las pilas por 24 días y se monitoreó la temperatura de todas ellas. En la primera etapa se redujo la actividad proteolítica de los RSO para garantizar la sobrevivencia y reproducción de la lombriz. Posteriormente cuando se alcanzaron temperaturas de 21°C en las pilas, se incorporaron 200 lombrices adultas de entre 5 y 7 cm en cada pila, mismas que fueron pesadas antes de hacerlo. Después de 90 días se evaluó el aporte de carbono (C), nitrógeno (N), relación C/N y fósforo (P) en cada pila, así como la producción de biomasa y fertilizante.

RESULTADOS Y DISCUSIÓN

En la **Figura 1**, se muestra el resultado de las tomas de temperatura en el monitoreo de las pilas durante su acondicionamiento hasta los 24 días y posterior a ello al incorporar las lombrices durante los 90 días subsecuentes.

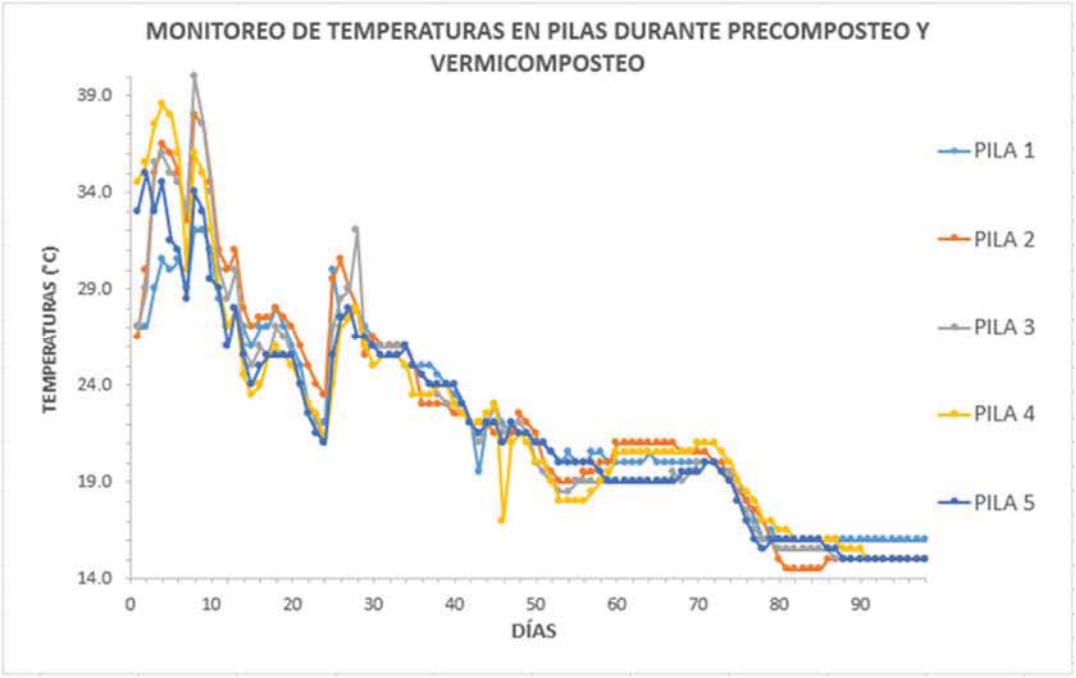


FIGURA 1. Monitoreo de temperatura en etapa de acondicionamiento y vermicomposteo

Se observó que al inicio del proceso, así como a los días 8 y 13 hubo un aumento de temperatura, esto debido al volteo que se dio para airear cada pila y propiciar el precomposteo de la materia orgánica, dando como resultado al día 24 una disminución en todas ellas, llegando hasta 21°C, momento en el cual se incorporaron las lombrices garantizando así su sobrevivencia y reproducción en las pilas. Se procedió a elegir solamente lombrices adultas con clitelo, mismas que fueron pesadas.

Además, se monitoreó el pH en las pilas (**Figura 2**), donde se observó que el pH inicial fue de entre 7.4 y 8.2, mismo que al tercer día disminuyó debido a la producción de ácidos orgánicos debido a la degradación por los microorganismos. Posteriormente aumentó hasta 9, pero fue decreciendo paulatinamente por la misma razón hasta el final del proceso, mismo que quedó estable en 7.2 en los 5 tratamientos.

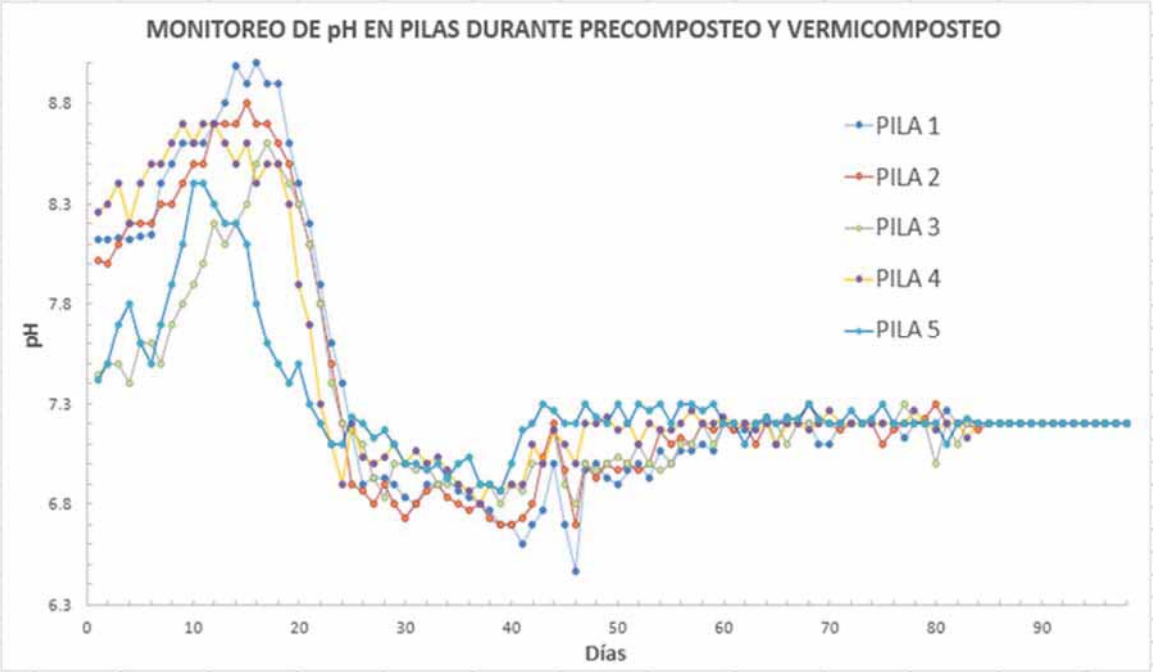


FIGURA 2. Monitoreo de pH durante en etapa de acondicionamiento y vermicomposteo

Se determinaron al inicio C, N, Relación C/N, P y Biomasa y al final los mismos parámetros junto con la producción de fertilizante, mostrados en la **Tabla 2**.

TABLA 2. Resultados obtenidos al final del proceso de vermicompostaje

PILA	C.O.T. (%)	N_T (%)	RELACIÓN C/N	P ($mgPO_4^{3-}/kg$)	PRODUCCIÓN DE FERTILIZANTE (kg)	BIOMASA (g)
1	27.67 ± 1.53	3.31 ± 0.03	8.35 ± 0.39	144.54 ± 26.84	21.899	278.61
2	30.09 ± 3.67	3.87 ± 0.10	7.76 ± 0.73	277.67 ± 5.22	28.478	379.00
3	21.27 ± 1.09	5.12 ± 0.12	4.15 ± 0.22	532.44 ± 15.18	12.858	283.95
4	29.5 ± 2.84	6.56 ± 0.37	4.49 ± 0.36	588.49 ± 87.35	20.458	186.35
5	19.89 ± 1.75	10.69 ± 0.53	1.86 ± 0.18	702.34 ± 125.56	15.000	121.43

Se observó una disminución en la cantidad de carbono orgánico al final del proceso de vermicomposteo con respecto al inicio en cada una de las pilas. En el caso de nitrógeno total los resultados fueron mayores al final con respecto al inicio mostrando que tanto el carbono como el nitrógeno se mineralizaron adecuadamente, por lo que la relación C/N después del vermicomposteo en cada caso fue de: P_1: 8.35, P_2: 7.76, P_3: 4.15, P_4: 4.49 y P_5: 1.86. Se observó que las mejores relaciones se obtuvieron en la pila 1 y 2, que aunque fueron las pilas que más lodo residual tenían, el aporte de nutrientes de estiércol y RSO fue adecuado para dar a las lombrices mayor capacidad de reproducción.

Para el fósforo se observó un aumento considerable de concentración con respecto al resultado inicial en cada tratamiento, P_1: 5.1 veces, P_2: 9.4 veces, P_3: 11.9 veces, P_4: 13.2 veces y P_5: 15.5 veces, lo que está relacionado con la producción directa de fertilizante, obteniendo mayor rendimiento en la pila 1 (21.899 kg) y en la pila 2 (28.478 kg), mismas que se relacionan con una alta producción de biomasa total obtenida 278.6 g. y 379.0 g. respectivamente. El pH final fue de 7.2 en los dos casos, que es cercano a la neutralidad e idóneo para la reproducción de la lombriz.

CONCLUSIÓN

Las mejores proporciones de residuos para la producción de vermicomposta fueron los tratamientos 1 y 2, ya que tuvieron la mayor relación C/N, y mejores rendimientos de producción de fertilizante y biomasa, lo que demuestra que además de las proporciones de estiércol de vaca y residuos orgánicos, el lodo residual del proceso de reciclado de papel puede ser utilizado para la obtención de un fertilizante de calidad que puede ser aplicado como mejorador de suelo y usado en los cultivos vegetales para mejorar las características nutrimentales de los mismos.

AGRADECIMIENTOS

Se agradece a la Secretaría de Investigación y Posgrado (SIP) del Instituto Politécnico Nacional por financiar el proyecto con número de registro 20161464. También se agradece al la Unidad profesional Interdisciplinaria de Biotecnología (UPIBI-IPN), por las facilidades para la realización del mismo.

REFERENCIAS

1. Robles-Martínez, F., Durán-Páramo E., Sánchez-Núñez J.M., (2003) *Como aprovechar desechos sólidos en centrales de abasto*. Revista Industrial del campo 2000 AGRO. 21, 86-88.
2. Atiyeh, R. M., Lee, S., Edwards, C. A., Arancon, N. Q., & Metzger, J. D. *"The influence of humic acids derived from earthworm-processed organic wastes on plant growth"*, Biores. Technol. 2002, 84: 7-14.
3. Pineda, J. 2006. *Lombricultura*. Primera edición. Tegucigalpa-Honduras (Ed. Instituto Hondureño del Café) (1), 38.
4. Robles-Martínez F., Ramírez-Sánchez I.M., Piña-Guzmán A.B. y Colomer-Mendoza F.J. (2010). *Efecto de la adición de agentes estructurantes a residuos hortícolas en tratamientos aerobios.* Ingeniería Agrícola y Biosistemas, 2(1), 45-51.

CHAPTER 4.10 NANOAPTASENSOR PARA LA DETECCIÓN DE *ESCHERICHIA COLI* EN AGUA POTABLE: MODIFICACIÓN DE NTCS PARA ALTA SENSIBILIDAD

E. K. Velazquez *(1); I. Morales-Reyes (1); F. Ramírez-Vives (1); A. Abad-Sánchez (2); M. Picquart (1); O. Monroy-Hermosillo (1) and N. Batina (1)

(1) UAM-I, Av. San Rafael Atlixco 189, Ciudad de México, México.
(2) UAM-AZC, Av. San Pablo Xalpa 180, Ciudad de México, México.

RESUMEN

Se desarrolló una aptasensor que permite conocer la calidad microbiológica del agua en tiempo real mediante mediciones de conductividad con electrodos de oro modificados con nanotubos de carbono (NTC) y un aptámero específico (A_{E10}) para detectar *E. coli.* Las bacterias en suspensión son atrapadas por el aptámero en la superficie del electrodo modificando la lectura de conductividad. La diferencia entre la conductividad del agua y la modificada se relaciona con la concentración de bacterias en suspensión. La modificación de la superficie del NTC con aptámero se caracteriza por AFM (Atomic force microscopy), SEM (Scanning electron microscope) por sus siglas en inglés y espectroscopia Raman. La concentración de bacterias se mide por citometría de flujo y se correlaciona con unidades formadoras de colonias (UFC). Los resultados claramente señalan un cambio en la superficie del electrodo por NTC y el aptámero inmovilizado pudiendo detectar concentraciones de 0 UFC/100 mL (10^5/100 mL cuentas viables). Este cambio en la superficie influyó en la detección de *E. coli* tanto en la sensibilidad y afinidad del sistema como en el tiempo de respuesta.

Keywords: aptámero; aptasensor; nanotubos de carbono

INTRODUCCIÓN

Los indicadores de calidad de agua que se usan mundialmente a nivel normativo son los microorganismos fecales, coliformes totales[1], utilizando técnicas dependientes de cultivo que presentan dificultades, como la baja sensibilidad y la presencia de bacterias viables pero no cultivables. Las técnicas que utilizan el ADN, como la reacción en cadena de la polimerasa (PCR por sus siglas en inglés) desarrollada[2], la PCR en tiempo real y el ELISA (siglas en inglés de ensayo por inmuno absorción ligado a enzimas) han revolucionado la identificación de microorganismos permitiendo una rápida cuantificación[3]. Los aptámeros, (del latín *aptus*que significa “fijar” y del griego *meros* que significa “partícula”) se les considera anticuerpos sintéticos construidos con moléculas funcionales derivadas de los ácidos nucleicos de cadena sencilla (ssDNA, RNA) con una estructura tridimensional específica que permite unirse con alta afinidad a la molécula objetivo. Diseñados con método de evolución sistemática de ligandos por

---

*Author for correspondence: bani@xanum.uam.mx

enriquecimiento exponencial (SELEX por sus siglas en inglés)[4], permiten identificar moléculas muy variadas desde iones metálicos, proteínas, péptidos hasta microorganismos. Debido a estas propiedades, los aptámeros pueden ser utilizados en un amplio rango, como agentes diagnósticos, en análisis cromatográfico, electroforesis y en biosensores[5].

Los aptasensores, son biosensores que utilizan aptámeros como elemento de reconocimiento[6,7] pueden estar unidos a nanomateriales como soporte, entre ellos los NTC (nanotubos de carbono) que proporcionan características de alta conductividad, elevada superficie de contacto, características químicas únicas y proporcionar estabilidad al ssDNA (al poderse unir a los NTC mediante enlace covalente) al quedar anclados. Los aptámeros son una herramienta analítica para detectar con alta sensibilidad y especificidad, biomoléculas objetivo[3].

Esta tecnología se ha usado para la detección de microorganismos patógenos o indicadores de calidad en alimentos y agua[8], Se han reportado diversos aptasensores electroquímicos capaces de detectar microorganismos (desde virus hasta bacterias) utilizando como transductor la superficie del electrodo con nanomateriales y midiendo la señal electroquímica; existe en la literatura el reporte de un aptasensor para detectar *E. coli*, usando NTC de pared sencilla[9], en otros trabajos diseñaron un aptasensor utilizando nanopartículas de oro y aptámeros específicos para detectar cepas enteropatógenas (*E .coli* O157:H7 y *Salmonella typhimurium*)[10], midiendo una respuesta colorimétrica con un nivel de detección menor a 10^5 UFC/mL en 20 min y especificidad del 100%[11]; el reporte de un aptasensor para detectar a *Salmonella typhi*, inmovilizando el aptámero a los NTC y midiendo una señal electroquímica (logrando una sensibilidad de 5 UFC/mL en 20 min), otros autores reportaron un aptasensor potenciométrico[12], donde inmovilizan covalentemente un aptámero modificado a NTC de pared sencilla para la determinación rápida (60s) y sensibilidad 0.2 UFC/mL en PBS (1UFC/5mL) de *Salmonela typhi.* Otros autores diseñaron un aptasensor potenciométrico para detectar *E. coli* obteniendo una sensibilidad de 6 UFC/mL en una muestra de leche y 26 CFU/mL en jugo de manzana[13]. El objetivo de este trabajo fue desarrollar un novedoso aptasensor ultra sensible con límite de detección de >1 CFU/100 mL equivalente a 10^6 UFC/100 mL de bacterias viables detectadas por citometría de flujo CFU/100 mL que fue fabricado con base en NTC de multi paredes carboxilados, fijados a un electrodo de oro formando una matriz altamente conductiva donde se inmovilizó un aptámero específico para *E. coli* (modificado con un grupo funcional amino)[7]; esta modificación se caracterizó por espectrometría Raman (que es una técnica fotónica de alta resolución química) y AFM (que permite analizar los cambios estructurales a nivel nanométrico).

MATERIALES Y MÉTODOS

Medios de cultivo. Medio de Conservación y propagación para *E coli:* Medio Agar Soya y tripticaseina sólido en tubo inclinado para stock de trabajo conservadas a 4ºC y medio líquido caldo de soya y tripticaceina para propagar y Agar eosina y azul de metileno (Bioxon) para el crecimiento en placa de *E. coli.*

Microorganismos. Cepa de *E. coli* ATCC 25922. Preparación de la muestra para la cuantificación en agua potable. Se tomó un volumen de 1 mL del cultivo de *E. coli* y se centrifugó a 12000 g por 15 min, el sobrenadante se descartó y el pellet fue resuspendido en 0.5 mL de agua estéril destilada, posteriormente se midió la densidad óptica de la suspensión a 540 nm en un espectrómetro UV-VIS Hach. Se realizaron diluciones seriadas en frascos de dilución de 100 mL y agua potable. Se cuantificaron los coliformes viables como unidades formadoras de colonias (UFC) mediante la técnica de filtración en membrana[1]. Para las mediciones por citometría de flujo (FASCcalibur marca BectonDickinson), se usó un láser de excitación a 488 nm y el detector FL1 para la fluorescencia SyberGreen y FL3 para el yoduro de propidio. La adquisición de los datos fue con el software del equipo CellQuest™ y el análisis fue realizado con un Flowing software 2.5.1. Para el efecto, de las muestras se homogenizó la muestra, se tomó 1 mL de suspensión bacteriana, se adiciono 10 μL de SayGergreen y 10μL de yoduro de propidio, se mezclaron y se dejaron reposar por 30 min en la obscuridad. La cuantificación de células viables se realizó midiendo el volumen de inyección y relacionandolo a 100 mL

Aptámero. El aptámero SSDNA (E10) aislado[7], fue utilizado en este estudio para construir el aptasensor. La secuencia del aptámero es la siguiente: 5'GCAATGGTACGGTACTTCCGTTGCACTGTGCGGCCGAGCTGCCCCCTGGTTTGT GAATACCCTGGGCAAAAGTGCACGCTACTTTGCTAA3', modificado con (NH_2) en el extremo 3' sintetizado por Sigma-Aldrich Inc., USA. El aptámero fue disuelto en agua MilliQ a una concentración de (114 μM), la concentración se determinó por espectrometría UV (Biochrom modelo BioDrop).

Funcionalización de NTCs. Los NTC multipared con 3.86 Wt%-COOH y < 1.5wt% de cenizas y 10–50μm de longitud y 8-15 nm fueron adquiridos en Cheaptubes Inc. Cambridgeport, VT, USA.

Se pesó 20 mg de NTC y mediante un tratamiento con una mezcla de ácido sulfúrico y ácido nítrico en una relación 3:1 y sonificando por 2 h, posteriormente se centrifugó a 12 000 g por 20 min y se lavó dos veces con agua bidestilada de acuerdo con el protocolo[14]. Posteriormente se resuspendieron en SDS (dodecilsulfato sódico) y sonificando por 15 min en un baño de agua. La suspensión fue centrifugada a 12000 g por 30 min y lavada dos veces con agua bidestilada. Los NTC se usaron para la construcción del aptasensor.

Todos los reactivos utilizados en este estudio fueron grado reactivo (>99%) y fueron adquiridos por Sigma – Aldrich Inc., México.

Espectrometria Raman y UV para determinar la unión de A_{E10} a los NTC por enlace covalente y afinidad. En este ensayo se prepararon muestras en tubos de microcentrífuga de 2 mL, los cuales contenían soluciones de A_{E10} (50,100, 250, 500, 2500, 5000 nM) y 1.5 mg/mL de NTC y los reactivos de acoplamiento para la reacción de imidación: 1-etil-3-(3-dimetilaminopropil) carbodiimida (EDC), N-Hidroxisuccinimida (NHS) en concentraciones (0.4 M /0.1 M) en relación 1:1 vol., se mezclaron por sonicación durante 10 min, se dejaron incubar 12 h, se centrifugaron a 12000 g por 20 min.

Para determinar la curva de saturación del NTC-A_{E10} se tomó un volumen de 1.5 µL del sobrenadante de la muestra y se leyó la absorbancia a DO 260 nm para determinar las concentraciones de $A_{E10,}$ se calcularon con el factor de conversión de 1 DO 260 nM = 40 µg/mL de SSDNA, la diferencia entre el valor de A_{E10} en equilibrio y el valor de la concentración inicial da los valores del complejo A_{E10}-NTC. La fase sólida (NTC-COO-A_{E10}), se utilizó para analizarla por espectrometría Raman. (Micro-Raman (Horiba Johin Yvon, T64000), se realizó a temperatura ambiente con un laser 532.1 nm y 20mW a la salida y objetivo 100 X. Se realizaron 10 acumulaciones de 1 min por espectro.

La caracterización de la superficie de NTC en una superficie de Au por AFM. Se realizó a temperatura ambiente con un AFM IV (Veeco, USA), usando una velocidad de escáner de 0.4-0.7 Hz en la muestra en modo pulsos (tapping).

El análisis SEM de los electrodos de Au-NTC y Au-NTC-A_{E10}. Mediante un microscopio (SEM Hitachi S-570), se analizaron la superficie de Au sin A_{E10} y con NTC-$A_{E10,}$ después de estar en presencia de *E. coli* (10^3 CFU/mL), posteriormente, se realizaron lavados sucesivos para eliminar las bacterias en la superficie, los electrodos se incubaron 48 h en medio selectivo para *E. coli* (Eosina y azul de metileno).

Fabricación del aptasensor. El desarrolló del aptasensor para la detección de *E. coli* se fabricó primero: preparando los electrodos de trabajo (superficie del electrodo de Au de 4 mm de diámetro), los cuales se recubrieron con NTC previamente funcionalizados (con grupos carboxilos), seguido de la: inmovilización del A_{E10} mediante enlace covalente, el procedimiento consistió en mezclar 15µL (EDC 0.4 M) y 16µL (NHS 0.01M) con 300 µL de A_{E10} (114 µM) y se aplicó15 µL de A_{E10} a cada electrodo.

Ensamblado del aptasensor. Se prepararon dos juegos de electrodos (Au y Au-NTC-A_{E10}) y se acoplaron en soportes de plástico y los soportes con los electrodos se posicionaron a una distancia fija de 3 mm entre cada soporte conectados a un conductímetro comercial.

Medición de la conductividad. Se realizó utilizando un conductímetro (Modelo H I98312, Hanna Instruments Inc., USA), conectado a un sistema de dos electrodos de Au y dos de Au-NTC-A_{E10}, estos juegos de electrodos van a medir el cambio de conductividad de la solución estándar de KCl 2.5 mM con bacterias y sin bacterias. Los electrodos se sumergieron por 3 min, tiempo en el cual se estabiliza la medición (datos no mostrados) en la solución de KCl sin *E. coli,* posteriormente se midió la conductividad con el par de electrodos Au sin modificar (C_{Au}) y se midió la conductividad con los electrodos modificados ($C_{Au\text{-}NTC\text{-}AE10}$), la diferencia de ambas mediciones es ΔC (Ecuación 1), los experimentos se realizaron por triplicado.

$$\Delta C = (C_{Au\text{-}NTC\text{-}AE10}) - (C_{Au}) \qquad (1)$$

RESULTADOS Y DISCUSIÓN

Detección de E. coli con el aptasensor. Para determinar la funcionalidad del aptasensor en muestras de agua potable, primero se determinó la correlación entre UFC y citometría de flujo, como se puede observar en la **Figura 1**, donde existe una correlación lineal (UFC = 3 x10^{-6} CV - 0.4), R^2= 0.9811.

Para valores de cero UFC/100 mL, se obtienen valores de células viables de (1, 2,3 E+05), lo que indica que existen bacterias viables aún que no se tenga valores de UFC/100 mL. Para 2 UFC/100 mL se obtiene 6 E+05 de células viables y para 8UFC/100 mL, 2 E+06. Los valores de la curva de cero UFC/100 mL son los de más relevancia porque nos permite correlacionar las lecturas del aptasensor con los valores de cero UFC/100mL y detectar los cambios de conductividad a estos niveles de bacterias y determinar si se detectan en las muestras de agua.

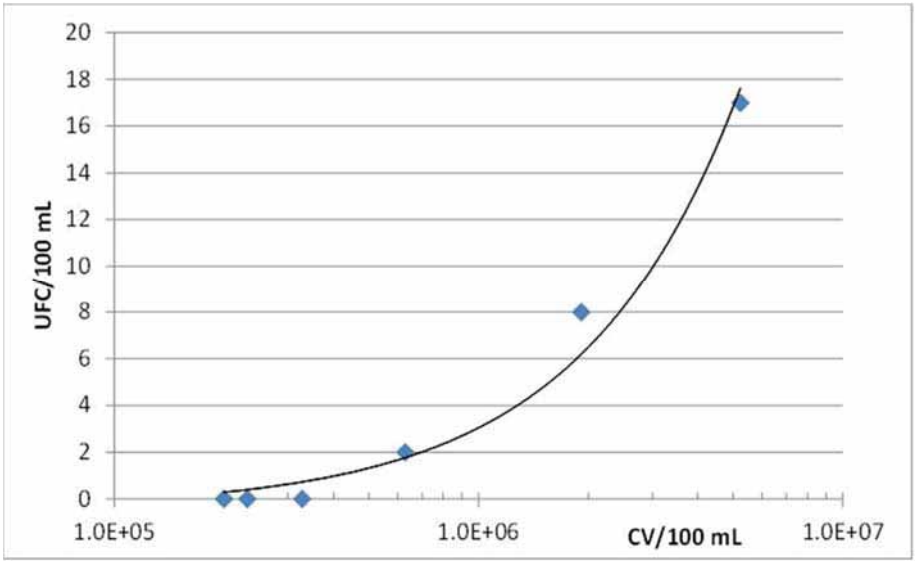


FIGURA 1. **Correlación entre células viables y UFC/100mL**

Las mediciones con el aptasensor se realizaron con diferentes concentraciones de bacterias, se compararon con las lecturas obtenidas con el citómetro de flujo. Los valores del aptasensor (ΔC) para 10^5 cv/100mL (0 UFC/100mL) fue de 100±10 µS/cm. Este valor es la respuesta por células de *E. coli* vivas que son reconocidas por A_{E10}. Para 4x10^5 cv/100mL (1 CFU/100mL) se observó un decremento en la señal del aptasensor (90 µS/cm). A partir de esta concentración, no hay cambios en la señal conductimétrica. Al aumentar hasta 20 UFC/100mL se obtiene un valor de (71 µS/cm) en la señal del aptasensor. La señal se debe al incremento de las células vivas presentes en la muestra. Mediante esta técnica se demostró que la respuesta del aptasensor es función de la concentración de células vivas en la muestra.

Este cambio en la conductividad nos está indicando que la superficie del electrodo está cubierta con *E. coli* y que los iones más ligeros no pueden migrar al electrodo que detecta la conductividad. De acuerdo al principio básico del diseño del aptasensor: la interacción de aptámeros fijados en superficie de electrodo y la presencia de *E. coli* en

solución. a través de los cuales se hace circular una corriente eléctrica alternante este cambio de conductividad electrolítica de la muestra va a depender de la concentración de *E. coli* en la muestra, donde a mayor número de bacterias aumenta el valor de ΔC.

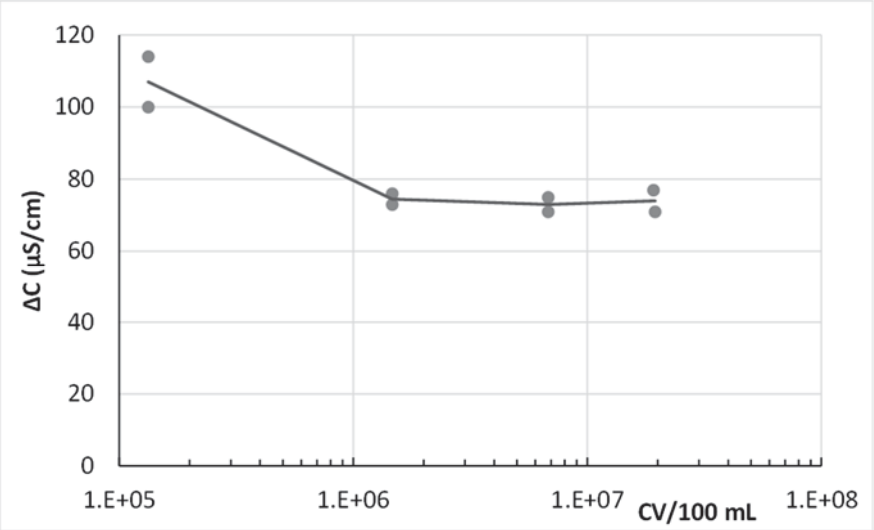


FIGURA 2. **Detección de *E. coli* en agua potable**

La afinidad de los NTC con A_{E10}. A los NTC funcionalizados con carboxilos se les midió su afinidad por el A_{E10}. La **Figura 3** muestra el equilibrio de Langmuir con la constante de afinidad (K_{E10}) igual a 19 µg/mL y la saturación máxima de (S_{max}) 22 µg/mg NTC. Algunos autores[15] encuentran que por adsorción física la S_{max} = 116 µg/mg de NTC de pared sencilla. Los valores obtenidos de saturación pueden variar dependiendo del tipo de nanotubo, de los métodos de funcionalización (reacción química de acoplamiento o adsorción física); por lo que para cada electrodo modificado se tiene que determinar la concentración de saturación.

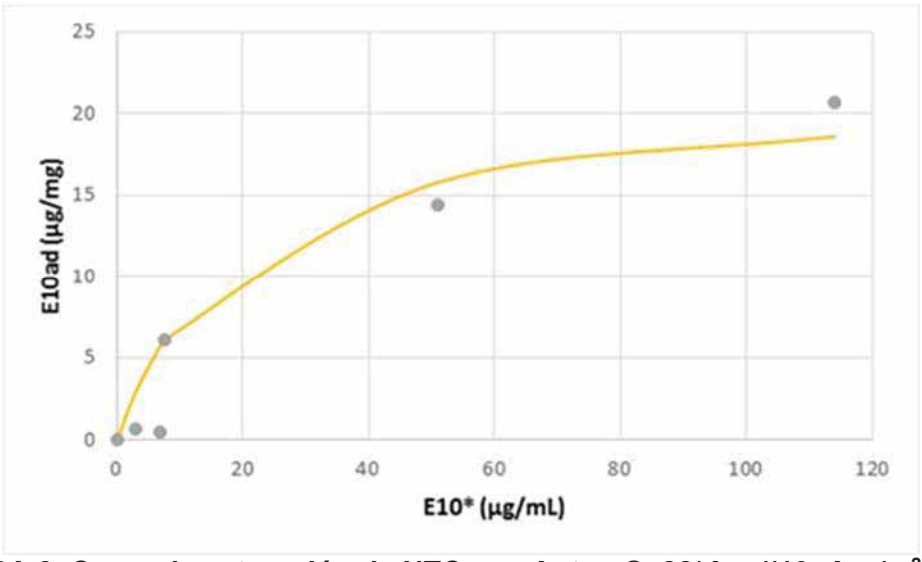


FIGURA 3. **Curva de saturación de NTC con Apt_{e10}. $S=22*A_{E10}/(19+A_{E10})$ $r^2= 0.99$**

La caracterización de la funcionalización de los NTC carboxilados con A_{E10} mediante espectroscopía Raman. Esta afinidad de A_{E10}-NTC se explica por la carboxilación previa demostrada mediante espectroscopia Raman, que muestra el tipo de unión al NTC. La caracterización de los NTC se muestra en la **Figura 4A** donde se presenta el espectro (a) de los NTC carboxilados, donde se observan dos bandas intensas en 1342 y 1577 cm^{-1}, en la región de alta frecuencia. El pico D está relacionado con la existencia de carbono amorfo, es decir, la estructura grafítica no cristalina en una nanoestructura de carbono. El pico G es atribuido a la vibración longitudinal C – C de las capas de grafito e indica el grado de grafitización en las nanoestructuras de carbono. En los espectros (b) y (c), se observan los picos típicos D y G de los nanotubos funcionalizados con COOH y con la modificación con A_{E10} en concentraciones crecientes (250 y 5000 mM), donde se observa aumento en la intensidad Raman, lo que indica que hay más desorden estructural en la muestra funcionalizada con mayor concentración de A_{E10}.

En la **Figura 4B** se muestra el espectro Raman de una muestra de nanotubos de carbono en presencia de *E. coli*. Se pueden observar los picos D y G de los NTC típicos y picos características. de *E. coli*, en la región de alta frecuencia de 1000 -1300 (cm^{-1}) y los picos de baja frecuencia de 400-800 (cm^{-1}).

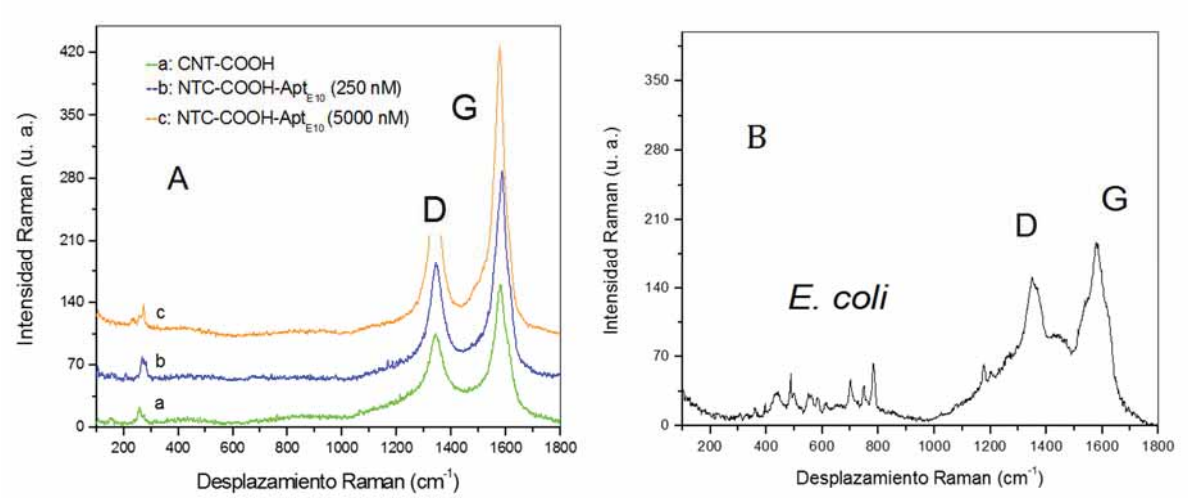


FIGURA 4. Espectro Raman de NTC A) funcionalizados con grupos carboxilo (—), modificados con A_{E10}, 250 mM (—) y 5000 mM (—) y B) *E. coli* fijada en el NTC-A_{E10}

Análisis de la superficie del electrodo de Au modificado con NTC y aptámero por AFM. El análisis de AFM consistió en monitorear la superficie y obtener la topología del electrodo modificado con NTC sin A_{E10} y NTCA_{E10}. En la **Figura 5** se muestra la superficie de 500 nm de NTC sin A_{E10} en un electrodo de oro A) y los diámetros de los NTC caroxilados de 34 nm en la **Figura 5B**, la superficie tridimensional de NTC sin A_{E10} del electrodo de oro en la **Figura 5C**. Las imágenes de los NTC en la superficie de electrodo de oro (600 nm) funcionalizados con A_{E10} (**Figura 6D**), se observa un cambio de diámetros de (61 nm) E), en la imagen tridimensional (**Figura 5F**) se puede apreciar más claramente el cambio en la superficie. Si comparamos los diámetros con y sin A_{E10} observamos que es aproximadamente de dos veces mayor con A_{E10} que sin el con este

análisis se demuestra que sí existe un cambio en la estructura del NTC producto de su modificación con A_{E10} confirmando los datos de espectrometría Raman.

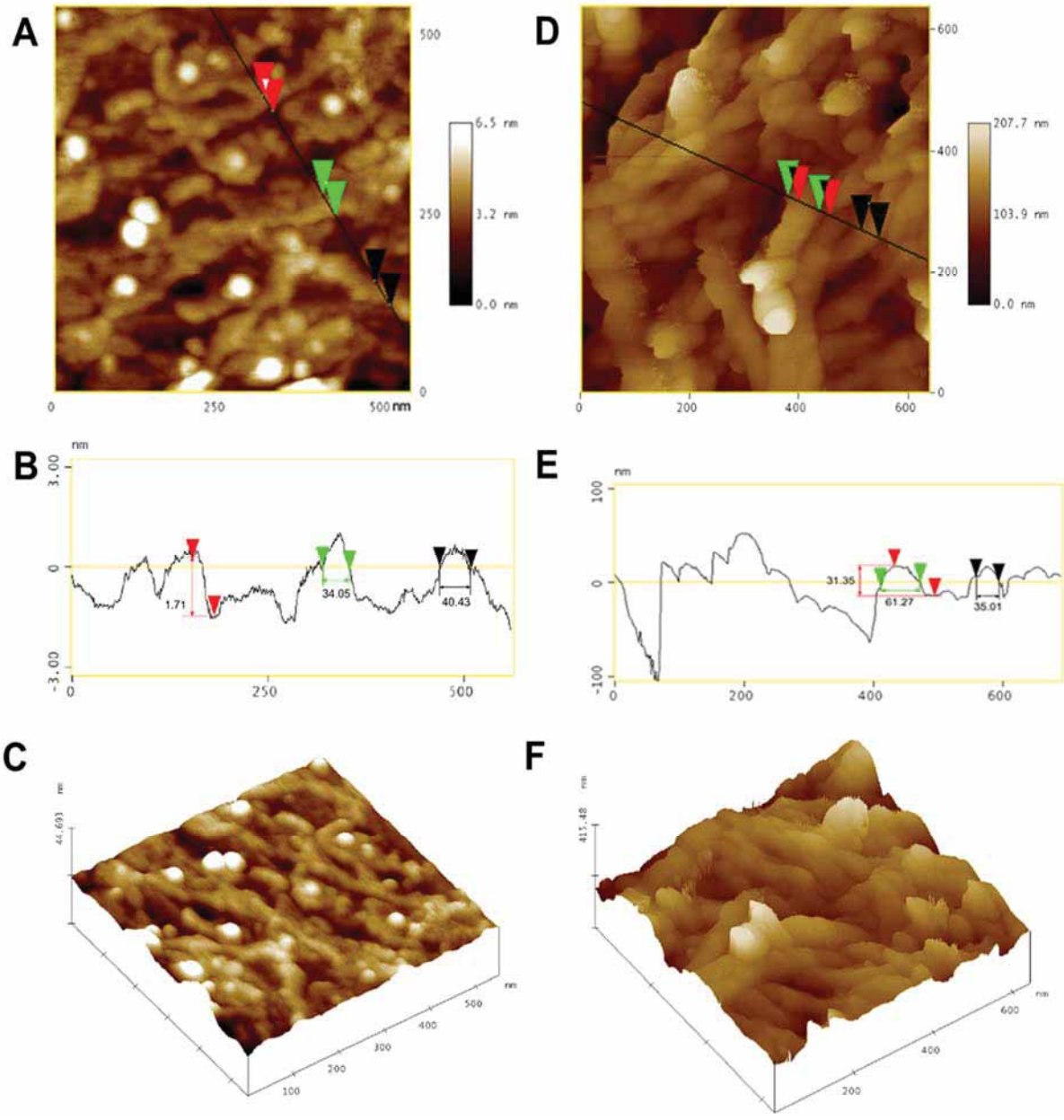


FIGURA 5. **Imágenes de la topografía AFM de NTC (A) sin A_{E10}, (B) NTC - A_{E10}, diámetros de NTC sin modificar y NTC modificado y Imágenes 3D de NTC: (C) sin A_{E10} (F) NTC - A_{E10}**

Afinidad de E. coli por el aptámero. La afinidad de A_{E10} por *E. coli* se confirmó por SEM y los resultados de las micrografías se observan en la (**Figura 6A** y **6B**) que muestran un electrodo Au - NTC y otro Au-NTC-A_{E10} ambos en contacto con *E. coli*. Se puede apreciar que en la primera no hay presencia de *E. coli* y que su presencia en **Figura 6B** se debe a la afinidad del aptámero como se observó por espectrometría Raman.

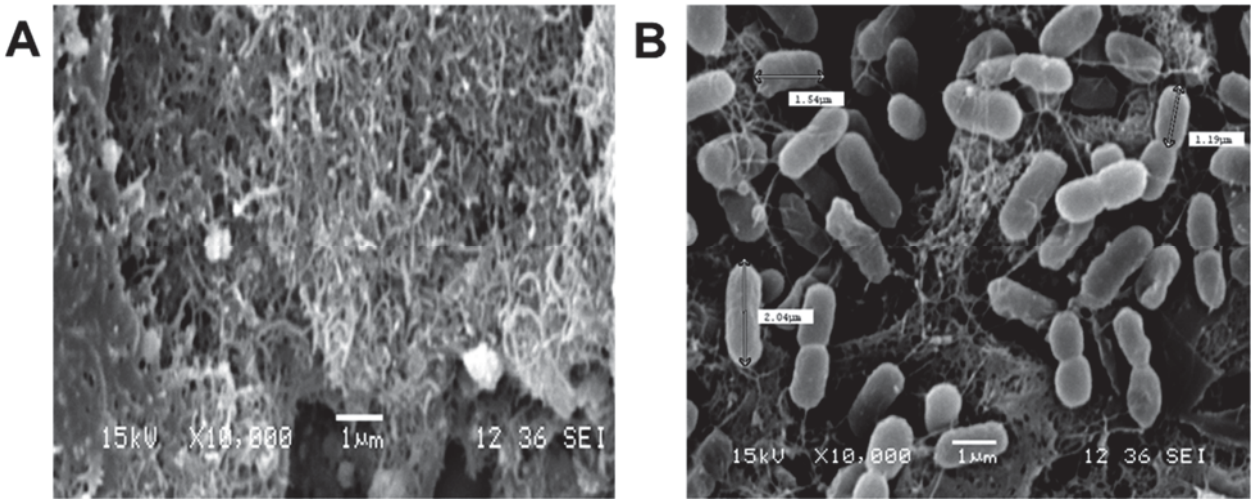


FIGURA 6. Micrografías SEM de electrodos de oro modificados con NTC sin aptámero expuestos a *E.coli* (A) y electrodo de oro modificado con NTC$^-$ funcionalizados con A $_{E10}$ en presencia de *E.coli* (B).

CONCLUSIÓN

En este trabajo se desarrolló un aptasensor con electrodos de Au modificados con NTC carboxilados y aptámero funcionalizado capaz de detectar *E. coli* en niveles de 0 UFC/100 /mL (10^5 células viables) de forma rápida, y sencilla. Al analizar la superficie del aptasensor anivel nanométrico por AFM y por espectrometría Raman se pudo constatar que los aptámeros se unieron a los NTC formando el transductor con una superficie de contacto amplia que va a permitir tener una gran área de contacto y aumentar la sensibilidad en la detección de *E. coli* provocando un cambio en la respuesta de conductividad detectada como se pudo constatar en la muestras inoculadas con bajas concentraciones de bacterias. Este aptasensor tiene el potencial de ser utilizado como una herramienta para la aplicación en el área de agua potable, para la detección rápida de la calidad microbiana del agua en hogares, red de distribución y durante el proceso de potabilización.

AGRADECIMIENTOS

Los autores agradecen a: Dr. José Sepúlveda y MC. Cristina Acosta por la ayuda con las micrografías SEM; Dra. Edith Cortés Barberena y Dra. Rocío Ortiz, por su apoyo con el citómetro de flujo, al SECITI del GDF por el financiamiento (SECITI054/2013); al CONACyT (EKVM) y UAM (beca 317298 y posgrado en Biotecnología 001466).

REFERENCIAS

1. APHA, American Public Health Association American Water Works Association, Water Pollution Control 1Federation. *Standard Methods for the Examination of Water and Wastewater.* Washington, D.C.22 *Edition*. (1995).
2. Bej, A.K.,J.L.Haff ,R.M.Atlas. Detection of Escherichia and Shigella spp.in water by using the Polymerase Chain Reaction and Gene Probes for uid.App.Environ.Microbiol. 57(1991) 1013—1017.

3. Lazcka O., Del Campo F. Muñoz X. Phatogen detection: A perspective of traditional methods and biosensors. Rew 22(2007) 1205—1217.
4. Ellington D.A and Szoztak W.J.In vitro selection of RNA molecules that bind specific ligands. Nature 346(1990)218—222
5. Song S., Wang L., Li J., Zhao J., Fan C. Aptamer-based biosensors. Trends in Analytical Chemistry.27,2(2008)111—117.
6. Yang L., Zhang X.,Ye M.,Jiang J., Yang R., Fu T., Chen Y., Wang K., Liu Ch., Tan W., Aptamer-conjugated nanomaterials and Their applications. Advanced Drug Delivery Reviews. 63 (2011) 1361—1370.
7. Kim Y.S,Chung J.,Song M.Y.,Jurng J.,Byoung.). Aptamer cocktails: Enhancement of sensing signals compared to single use of aptamers for detection of bacteria. Biosensors and Bioelectronics.54 (2014)195-198.
8. Hayat A. and Marty J.L.Aptamer base electrochemical sensors for emerging environmental pollutants.Frontiers in Chemistry.Rew.2 (2014) 41,1—9.
9. Song S., Wang L., Li J., Zhao J., Fan C. Aptamer-based biosensors. Trends in Analytical Chemistry. 27(2008) 2, 111—117.
10. Wu W., Li M., Wang Y., Ouyang H., Wang L.,Li C., Cao Y., Qing-he M, Lu J. Aptasensors for rapid detection of Escherichia coli O157:H7 and Salmonella typhimurium.Nanoscale Research Letters. 7 (2012) 658—665.
11. García-Aljaro C.,Cella N.L., Shirele J.D.,Park M.,Muñoz F.J.,Yates V.M.,Mulchandani A. Carbon nanotubes-based chemiresistive biosensors for detection of microorganisms. Biosensors and Bioelectronics. 26(2010)1437—1441.
12. Zelada-Guillén GA.,Blondeau P.,Rius X.,Riu J.Carbonotube-based aptasensors for the rapid and ultrasensitive detection of bacteria. Methods. 63(2013)233—238.
13. Le V. T. Ngo C. L., Le Q.T., Ngo T.T., Nguyen N.N. and Vu M.T.Surface modification and functionalization of carbon nanotube with some organic compounds. Adv. Nat. Sci.: Nanosci. Nanotechnol. 4 (2013) 3 1—5.
14. Evtugyn G., Porfireva A.,Ryabova M.,Hianik T. Aptasensor for Thrombin Based on Carbon Nanotubes-Methylene Blue Composites. Electroanalysis. 21(2008)2310—2316.
15. Yang M., Peng Z.,Ning Y., Chen, Y., Zhou Q. and Deng L.Highly specific and Cost-Efficient Detection of Salmonella Paratyphi A Combinig Aptamers with Single-Walled Carbon Nanotubes. Sensors. (2013) 13 6866—6881.

Section 5.
Solid and Hazardous Waste Management and Treatment

Page

Chapter 5.1 Study of the spent ion exchange resins pyrolysis treatment and plasma conditioning of the off-gas 365
H. A. Castro; V. Luca and H. L. Bianchi

Chapter 5.2 Characterization of cashew production solid waste and its energetic potential evaluation for thermal conversion processes 376
P.T. Tavares; J. C. G. Silva; T. S. E. Pereira; B. F. M. L. Gomes and S. L. F. Andersen

Chapter 5.3 Microbial and parasitic risks related to application of animal wastes to soil 386
J. Venglovsky; N. Sasakova; F. Toth; I. Papajova; G. Gregova and R. Hromada

CHAPTER 5.1. STUDY OF THE SPENT ION EXCHANGE RESINS PYROLYSIS TREATMENT AND PLASMA CONDITIONING OF THE OFF-GAS

H. A. Castro (1,2); V. Luca (1) and H. L. Bianchi *(1,2)

(1) CNEA, Centro Atómico Constituyentes, Av. General Paz 1499, 1650 San Martín, Argentina
(2) Universidad Nacional de General San Martín, Campus Miguelete, Martín de Irigoyen 3100, 1650 San Martín, Argentina

ABSTRACT

Polystyrene divinylbenzene-based ion exchange resins are employed extensively within nuclear power plants (NPPs) and research nuclear reactors for chemical control of the cooling water system. To maintain the highest possible water quality the resins are regularly replaced as they become contaminated with a range of isotopes derived from compromised fuel elements as well as corrosion and activation products including ^{14}C, ^{60}Co, ^{90}Sr, ^{129}I and ^{137}Cs. Such spent resins constitute a major proportion (in volume terms) of the solid radioactive waste generated by the nuclear industry.
Several treatment and conditioning techniques have been developed with a view toward reducing the spent resin volume and generating a stable waste product suitable for long-term storage and disposal. Pyrolysis is one of the most effective thermal methods and is characterized as a low temperature flameless process (compared with high temperature thermal methods, e.g. incineration) in which the organic material is heated in a reducing atmosphere to leave a carbonaceous product or char. Several successful commercial applications in the nuclear industry, such as THORsm in USA, were conducted and the Pettersson *et al.* leading experience is the reference of actually developed processes. Another major advantage of pyrolysis is that a large part of radioactive inventory is confined within the product. This simplifies the treatment of the flue gases since little or no radioactivity is expected to be present.
In the present work, we discuss results relating to the pyrolysis of simulated spent resins and the treatment of the off-gas generated during the process.
A stable and chemically inert waste product was obtained for pyrolysis treatment at temperatures between 300 and 350°C. The samples showed a significant volume reduction (>50%) and a high retention of the semi-volatile radionuclides in the matrix. As part of the present investigation the process off-gas was thoroughly characterized.
Additionally, the application of plasma technology for the treatment of the off-gas current was studied as an alternative to conventional processes (e.g. post-combustion chamber). A laboratory scale flow reactor, using inductively coupled plasma, operating under sub-atmospheric conditions was developed. Fundamental experiments using model compounds have been performed demonstrating a high destruction and removal ratio (>99,99%) for different reaction medias, at low reactor temperatures and moderate power consumption. The role of H_2O as an important participant of the oxidation mechanisms in plasma conditions was established.

---

*Author for correspondence: bianchi@cnea.gov.ar

The combination of both processes could represent a simple, safe and effective alternative for treating spent resins with a large reduction of generated gaseous byproducts.

Keywords: off-gas treatment, plasma, pyrolysis, spent ion exchange resins

INTRODUCTION

Polymeric ion exchange resins are indispensable materials across a broad spectrum of industries[1], including the nuclear industry. Within nuclear power plants (NPPs) and nuclear research reactors, polystyrene divinylbenzene-based ion exchange resins are extensively employed at the cooling water systems to control chemistry quality in order to minimize corrosion or the degradation of system components and to remove radioactive contaminants derived from activation and compromised fuel elements. Once exhausted, however, these materials become one of the most important operational waste streams (in volume terms) generated by the nuclear industry.

The treatment and conditioning of spent ion exchange resins is a complex process encompassing a detailed consideration of their physical and chemical characteristics and their compatibility with the various processing, storage and/or disposal options.

Basically, there are two main strategies for the treatment of this kind of materials: (1) the degradation of the organic materials with the objective of reducing the spent resin volume and producing an inorganic intermediate product, that may or may not be further conditioned, suitable for long-term storage and/or disposal and (2) direct immobilization in a matrix such as cement, bitumen and polymers. Within the first group we can find a wide list of developed processes such as thermal, chemical, thermo chemical and biochemical[2].

Pyrolysis is one of the most effective thermal methods and is characterized as a low temperature flameless process (compared with high temperature thermal methods, e.g. incineration) in which the organic material is heated in a reducing atmosphere to leave a carbonaceous product or char. This process is being increasingly implemented at industrial scale for the treatment of municipal and industrial organic wastes including biomass[3], waste plastics[4] and tyres[5].

Being a flameless technology, pyrolysis has the advantage of lower operational temperature and, of critical importance in a nuclear context, an enhanced safety profile. Thus, pyrolysis features as an innovative technology in a recent IAEA report on thermal processing of radioactive wastes[6], being considered, and even practiced, as a method for the treatment and conditioning of radioactive organic wastes such as solvents, oils and especially spent ion exchange resins derived from the operation of nuclear facilities.

In this field the Pettersson *et al*.[7] leading experience is a reference for the developed industrial scale processes, and we can find several successful commercial applications likes of Nukem[8] and Belgoprocess[9].

Another interesting example is the Thermal Organic Reduction (THORsm)[10] process carried out at the Studsvik plant (Energy Solutions Inc.) in Erwin, Tennessee, where approximately half of the spent resin generated by the US power reactors has been treated until 2014.

Another major advantage of pyrolysis is that a large part of radioactive inventory is confined within the product. This simplifies the treatment of the flue gases since little or no radioactivity is expected to be present.

An important issue to consider is that thermal decomposition of this kind of wastes can lead to the formation of complex gas streams, formed by compounds of diverse nature and toxicity, which should be processed in a safe and efficient way (generally through a post-combustion stage) in order to satisfy air emission regulations both from the environmental viewpoint as radiological aspects.

In the recent years, the plasma technology emerged as a novel process for environmental applications such as the treatment of different waste streams due to its high chemical reactivity[11]. This attribute added to the possibility of having control on the reaction products and avoiding the emissions dilution associated with the incorporation of additional fuels and air, positions the plasma technology as a novel alternative for substitution of conventional high temperature processes at post-combustion systems for the elimination of diverse complex compounds, including the dioxins.

In the present work we discuss results relating to the pyrolysis of spent resins, the process off-gas characteristics and studies of removal of model compounds associated with the latter using an inductively coupled plasma laboratory scale flow reactor operating under sub-atmospheric conditions.

MATERIALS AND METHODS

Low temperature pyrolysis of ion exchange resins and characterization of the off-gas. The resins used throughout this study were cross-linked polystyrene gel beads Lewatit Monoplus M500 with quaternary amine functional groups and Lewatit Monoplus S100 with sulfonic acid functional groups.

Thermal analyses were conducted in flowing argon using a TA Instruments Q600 system. A gas mass spectrometer (Pfeiffer, Omnistar GSD 320) attached was used to characterize the composition of the off-gas streams generated.

Plasma chemical decomposition of model compounds. The experimental system used in this work consists on an inductively coupled plasma laboratory scale flow reactor operating under sub-atmospheric conditions (**Figure 1**).

The power was supplied to the plasma reactor by a 6-turn induction cooper coil (coupling antenna) from a radiofrequency (RF) generator (Advance Energy, AE CESAR 1330 400V) operating at an oscillator high frequency of 13,56 MHz, with a power rating of 3 kW, which was adjusted by a matching network (Advance Energy, AE VarioMatch Match Network, VM 5000 Platform).

The plasma was confined into a cylindrical quartz tube reactor (1050 mm in length, 40 mm at outer diameter and 36 mm at inner diameter) which was located inside a confinement chamber.

High purity argon and oxygen were used as plasma and carrier gases. The flow rate and composition of the gas streams were adjusted by a set of mass flow controllers (Horiba, SEC-Z500 series).

The system was maintained under slight negative pressure by a chemical resistant vacuum pump (Vacuumbrand, PC 3004 VARIO).

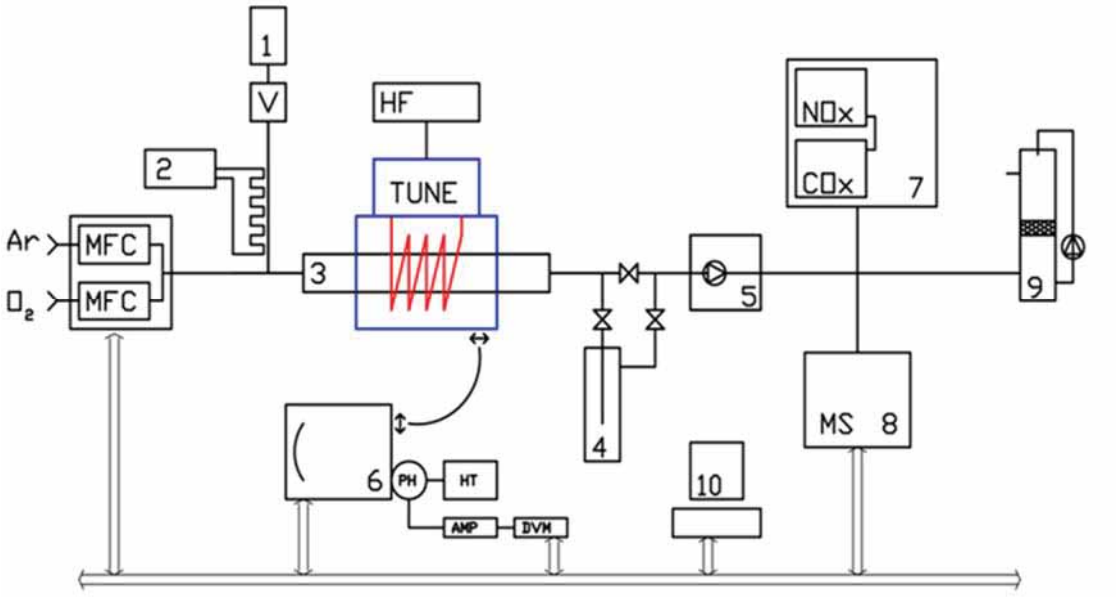


FIGURE 1. Scheme of the experimental arrangement.
1. Sample, 2. Injection heater, 3. Quartz reactor, 4. Cold trap, 5. Chemical resistant vacuum pump, 6. High resolution spectrometer, 7. Multi-gas analyzer, 8. Gas mass spectrometer, 9. Scrubber, 10. PC, MFC: Mass Flow Controllers, HF y Tune: RF generator and matching network.

As a final conditioning stage, the gas stream passed through a wet scrubber before being released to the atmosphere.

A high-resolution spectrometer (Sciencetech 9490SD) was used to determine diagnostic parameters (Electron density and Electron temperature) of the reaction medium through optical emission spectroscopy (OES) by studying the hydrogen Balmer lines[12,13]. The measurements indicated that the plasma, at the chosen experimental conditions, had an Electron density of $10^{19} m^{-3}$ and the Electron temperature exceeded 7000°C.

The samples treated in this work were solutions of different concentrations of model compounds: butylamine (99,5%, Sigma-Aldrich), propylamine (98%, Sigma-Aldrich), acetonitrile (98%, AnalytiCals) and ethylenediamine (98%, Biopack). These solutions were in a graduated glass tube and introduced into a camera in a controlled form via a needle valve. Both the injection system and the camera were heated by a simple electrical control. Inside them the solutions vaporize and mixed well with the carrier and plasma gases before enter into the reactor. The injection flow rate of the samples was 0,20 cm^3/min.

The experiments were carried on with a supplied plasma power of 400 W ± 5 W and an operating pressure of 50 mbar. The plasma and carrier gases flow rates were 950-1000 sccm for argon and 0-50 sccm for oxygen. The total flow rate was the same for all the experiments.

The determination of the efficiency of our system for the abatement of the model compounds was done since the calculation of the destruction and removal efficiency (DRE). The treated streams were captured downstream the reactor in a liquid nitrogen cooled trap. The concentrations of the model compounds in the samples collected were

measured by Electrospray Ionization-Mass Spectrometry (MS-ESI) with a single quadrupole mass spectrometer of LCMS2020 (Shimadzu).

The gas byproducts analysis was done with a multi-gas analyzer system (Horiba, PG-250) for NO_x, CO, CO_2 and O_2 and a gas mass spectrometer (Pfeiffer, Omnistar GSD 320) for H_2.

RESULTS AND DISCUSSION

Low temperature pyrolysis of ion exchange resins and characterization of the off-gas stream. TGA-DTA analyses of the resins are shown in **Figure 2**. These analyses suggest that the degradation of both types of resins can be separated into three basic stages. The weight loss between 25 and 150°C is ascribed to dehydration. From 150 to 250°C and from 250 to 350°C for anionic and cationic resins, respectively, the major part of weight loss results from the decomposition of the functional groups. The last stage (temperatures above 400°C) is associated with the degradation of the organic matrix and its subsequent mineralization. As can be seen, the degradation process presents considerable differences between the cationic and the anionic resins.

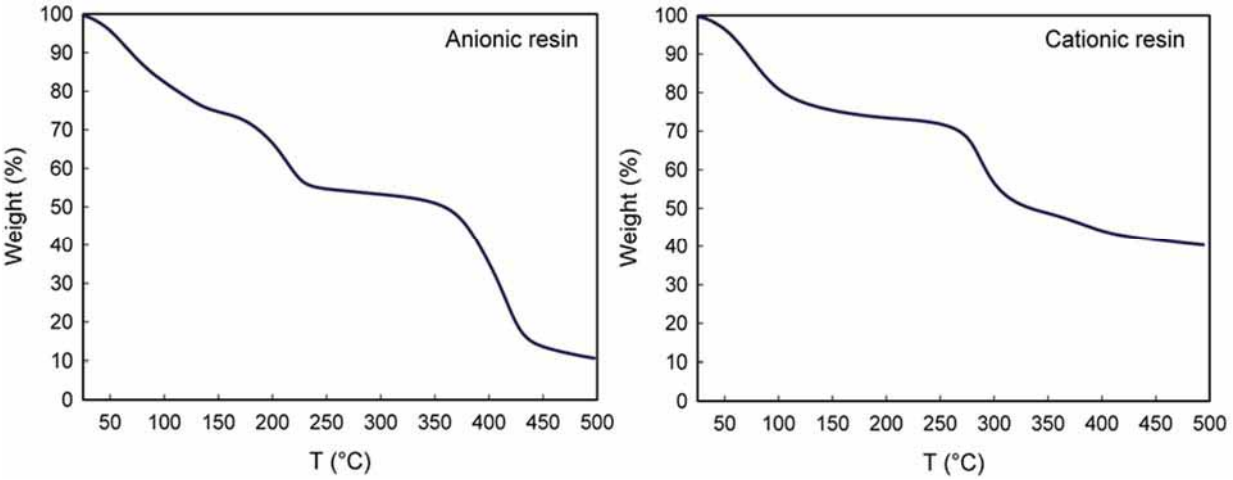


FIGURE 2. TGA-DTA analysis of samples of ionic resins.

Figure 3 shows the gas mass spectrums of gases pyrolysis byproducts in argon atmosphere in function of the temperature for both types of resins. As seen in **Figure 2**, we can clearly observe the emission of compounds associated with the decomposition of the functional groups and the degradation of the organic matrix at the mentioned temperatures ranges.

The anionic resin is characterized by releasing a greater amount of volatile degradation byproducts as amines (methylamine and trimethylamine were the principal amino-compounds detected), while the cationic resin mainly emits SO_2. These results agree with the observations of Matsuda *et al.*[14].The lower mass reduction of the cationic resins is due to stabilization processes of the residual matrix associated with the formation of sulphur structures[15].

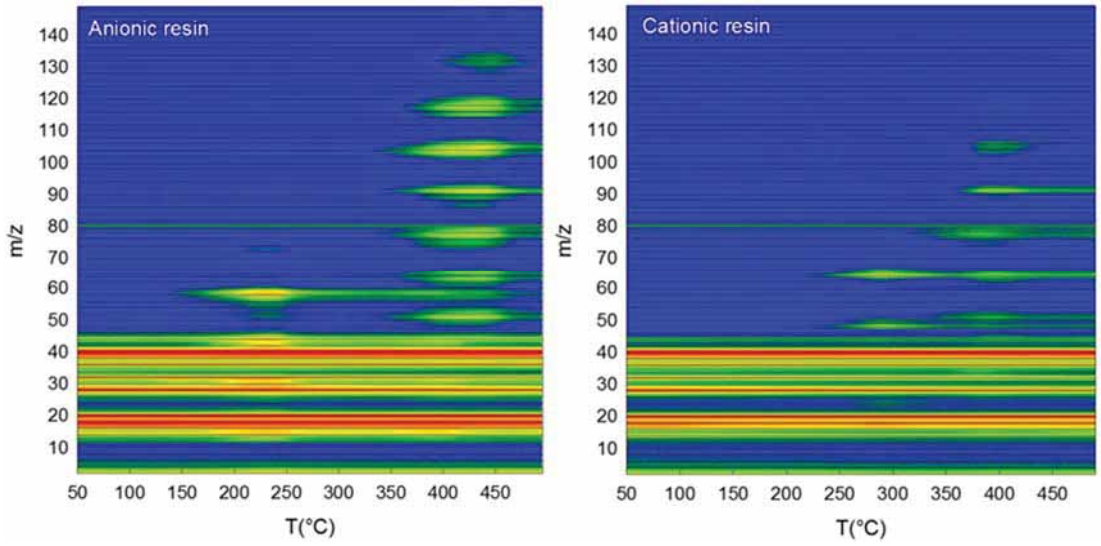


FIGURE 3. GAS mass spectrums of gases pyrolysis byproducts in argon atmosphere for both types of resins in function of the temperature. The colours indicate the signal intensity for each m/z ratio where blue is low intensity and red high intensity.

The pyrolysis treatment of the resins at temperatures between 300 and 350°C resulted in a stable and chemically inert waste product with a significant volume reduction (>50%).

Studies with simulating spent ion exchange resins of nuclear power plants loaded close to their exchange capacity with a selection of cations (Cs^+, Sr^{2+}, Co^{2+}, Ni^{2+})[16] and anions (I^-, Cl^-, CO_3^{2-})[17] were carried out. A significant fraction of the initial carbonate inventory was volatilized at temperatures in the range 200-300°C. However, at 300°C most of the semi-volatile elements remained within the pyropolymer product. Besides, the leaching and water reabsorption tests threw good results for the product obtained. These characteristics are suitable for its long-term storage and disposal.

Due to the complexity and hazardous importance of the gases byproducts originated during the thermal degradation of the anionic resins compared with the cationic ones, we decided to dump our efforts in a first instance to the study of plasma chemical decomposition of model compounds associated with anionic resins.

Plasma chemical decomposition of model compounds. The performance of our plasma system in the abatement of the model compounds is described in terms of the destruction and removal efficiency (DRE):

$$\mathrm{DRE}\ (\%) = \frac{C_{in} - C_{out}}{C_{in}} \mathrm{x}\ 100 \qquad (1)$$

Where C_{in} and C_{out} are the concentration of the compounds before and after the plasma treatment, respectively.

The concentration of the different model compounds was estimated from the MS-ESI spectrums obtained. For each compound the m/z peak of its protonated species was tracked: 74 (butylamine-H^+), 60 (propylamine-H^+), 61 (ethylenediamine-H^+).

The DRE values were 99,99% for butylamine and propylamine and 99,92% for ethylenediamine. The value for acetonitrile was not calculated because it cannot be detected by MS-ESI technique. An important point is that this high DRE values were observed for reactor temperatures low enough (60-100°C) compared to conventional thermal processes.

The DRE for butylamine was also analysed as function of the energy density or specific energy (P_W/Q), which is a parameter widely used in the field of nonthermal plasma processes, in presence and absence of O_2 in the reaction medium (**Figure 4**).

DRE values did not vary significantly for the energy densities range studied and the incorporation of O_2 in the reaction medium did not generate any influence on the DRE trend.

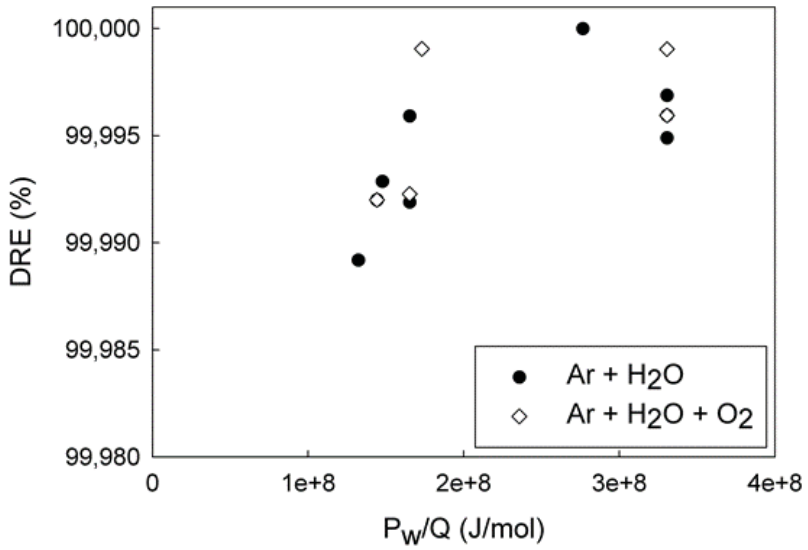


FIGURE 4. Evaluation of DRE for butylamine as function of the energy density (P_W/Q) in presence and absence of O_2 in the reaction medium.

Study of the composition of the treated gas stream. The influence of water in the reaction medium on the main products (CO, CO_2, NO_x and H_2) at the post plasma treatment gas stream was studied.

The selectivity formation of each product was calculated through formulas (2) - (5).

$$S_{CO} = \frac{[CO]}{[CO] + [CO_2]} \quad (2)$$

$$S_{CO_2} = \frac{[CO_2]}{[CO] + [CO_2]} \quad (3)$$

$$S_{NO_x} = \frac{\text{moles of } NO_x \text{ produced}}{\text{moles N in the inlet}} \quad (4)$$

$$S_{H_2} = \frac{\text{moles of } H_2 \text{ produced}}{2 * \text{moles of H in the inlet}} \quad (5)$$

Table 1 resumes the moles of the model compounds and water used in each experiment and the results obtained.

TABLE 1. Composition of the inlet mixture and selectivity formation of CO, CO_2, NO_x and H_2

Sample		Moles compound	Moles water	$R_{O/C}$	$R_{O/N}$	S_{CO}	S_{CO2}	S_{NOx}	S_{H2}
ethylenediamine (%w/w)	4,1	0,07	5,32	39	39	0,18	0,82	0,12	0,08
	10,0	0,17	4,99	15	15	0,39	0,61	0,08	0,09
	62,5	1,04	2,08	1	1	0,94	0,06	0,00	0,10
acetonitrile (%w/w)	5,6	0,14	5,24	19	38	0,18	0,82	0,21	0,06
	10,0	0,24	4,99	11	22	0,26	0,74	0,11	0,06
	53,0	1,29	2,61	1	2	0,86	0,14	0,00	0,19
propylamine (%w/w)	4,0	0,07	5,33	27	81	0,18	0,82	0,25	0,05
	8,1	0,14	5,10	13	39	0,30	0,70	0,14	0,20
	52,0	0,88	2,66	1	3	0,90	0,10	0,00	0,26
butylamine (%w/w)	5,0	0,07	5,27	20	80	0,19	0,81	0,22	0,08
	10,0	0,14	4,99	9	36	0,33	0,67	0,09	0,06
	50,0	0,68	2,77	1	4	0,89	0,11	0,00	0,27

$R_{A/B}$: ratio between the moles of A and the moles of B in the inlet mixture.

The results indicate a growth of the oxidized species formation (CO_2 and NO_x) as the ratio between moles of O and moles of C or N is incremented. This responds to an increase in the moles of water in relation with the moles of model compound in the inlet sample and remark the role of the solvent as an important participant of the oxidation mechanisms in the reaction medium. The plasmolysis of water generates O_2 and reactive oxidative species as O and OH radicals[18] that reacts with the compounds under treatment (contributing to a high DRE) leading to the formation of oxidized products as mentioned.

Meanwhile, it is observed that as the initial mixture is enriched in model compounds, and consequently decreases the O/H ratio, the selectivity in the formation of H_2 increases. **Figure 5** indicates this behaviour and shows the selectivity in the formation of H_2 for various initial mixture compositions for the different studied compounds.

While the selectivity towards the formation of H_2 increases with decreasing water content (or in other words the O%) in the inlet mixture, it is clear that the concentrations of H_2 in the final gaseous mixtures obtained were always in values significantly lower than those corresponding to the flammability limits for mixtures of these features (**Figure 6**).

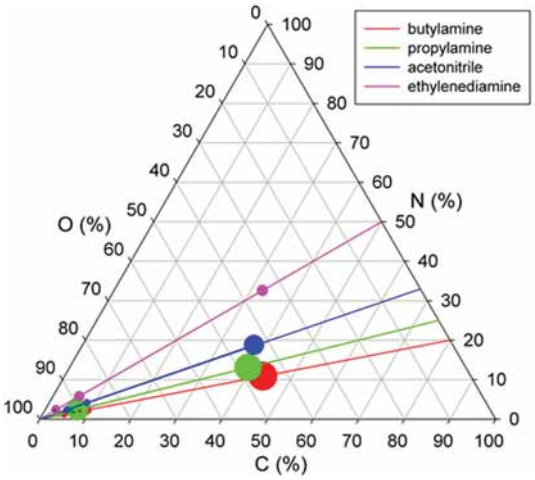


FIGURE 5. Selectivity of H_2 formation depending on the composition of the initial mixture for the compounds studied. The size between the bubbles is proportional to the differences between the values of selectivity.

On the other hand, the influence of O_2 incorporation as plasma and carrier gas was studied for the butylamine abatement. The O_2 was aggregated in two ways: in balance ratio and in excess. In the balance case, the moles of O_2 required were calculated based on the stoichiometric reaction with the butylamine and taking into account that the sample was fully vaporized at the heated camera.

As can be observed, O_2 affects the reaction products promoting the production of the oxidized species of C and N, thus obtaining a CO_2 selectivity near 1,0 and being the most relevant point the significant decrease of the selectivity of formation of H_2, as was also observed in **Figure 6**.

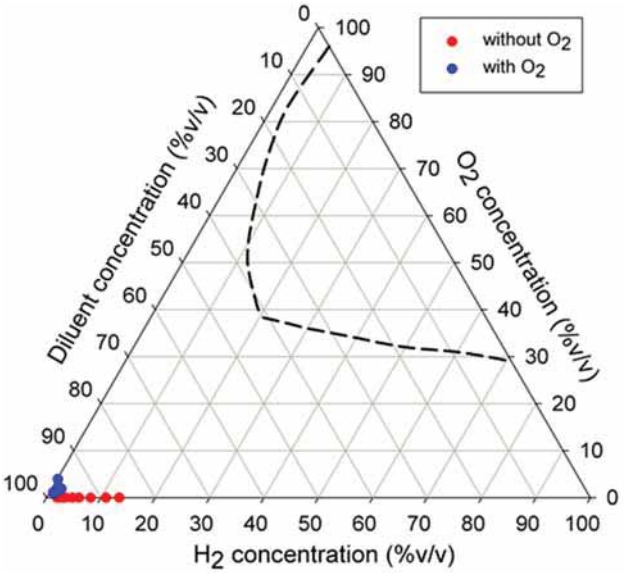


FIGURE 6. Diagram of concentration (%v/v) of H_2 in the resulting gas mixture considering the O_2 concentration and other components (Ar, H_2O and model compound) in the inlet mixture. (The dotted line encloses the flammability region for H_2 in air at 1013 mbar with water at 422 K)

Figure 7 shows the evolution in the selectivity of formation of NO_x, CO, CO_2 and H_2 for experiments with butylamine 10%w/w solutions without adding O_2 to the reaction medium and adding it in stoichiometric and excess amounts.

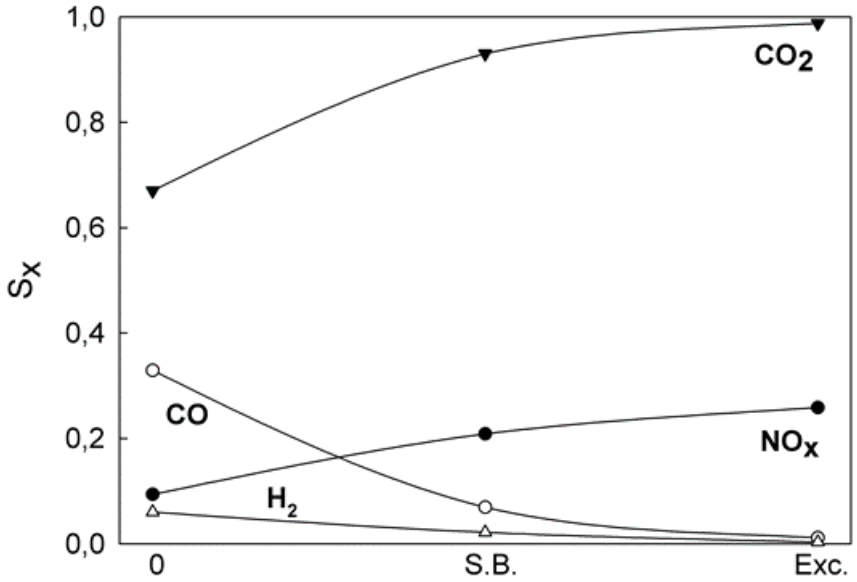


FIGURE 7. Influence of the incorporation of O_2 in the reaction medium on the selectivity of formation of CO, CO_2, NO_x and H_2 for the treatment of a butylamine 10%w/w solution. (0: no added O_2, S.B.: O_2 added at stoichiometric balance; Exc.: O_2 in excess).

CONCLUSION

The present study together with previous work of our group[16,17] suggests that low temperature pyrolysis (~ 300°C) could be used to convert spent anionic and cationic resins to chemically stable pyropolymer products, with a great volume reduction (>50%), and in which a large proportion of the initial radionuclide inventory could be retained.
The characteristics of the final product are suitable for its long-term storage and disposal.
The results of the plasma chemical decomposition of model compounds showed the high destruction and removal efficiency (>99,9%) of our arrangement in a variety of working conditions for considerably low reactor temperatures and with moderate power consumption. We could obtain a good control of the reaction products and the influence of H_2O and O_2 over them was established.
These first results are promising regarding the use of this technology in the treatment of the off-gases stream generated by the pyrolytic process.
The combination of both low temperature and flameless processes could represent a novel alternative for treating spent resins and any gaseous byproducts generated in a simple, safe and effective way fulfilling low environmental impact principles.

REFERENCES

1. Alexandratos, S. D., Ion-Exchange Resins: A Restrospective form Industrial and Engineering Chemistry Research, Ind. Eng. Chem. Res. 48 (2009) 388–398.
2. Application of Ion Exchange Processes for the Treatment of Radioactive Waste and Management of Spent Ion Exchangers, Technical Reports Serie N°408, IAEA (2002).
3. Bridgwater, A.V., Review of fast pyrolysis of biomass and product upgrading, Biomass and Bioenergy 38 (2012) 68-94.
4. Kaminsky, W., Thermal recycling of polymers, J. Anal. Appl. Pyrolysis 8 (1985) 439-448.
5. Quek, A., Balasubramanian, R., J. Anal. Appl. Pyrolysis 101 (2013) 1-16.
6. 6-Innovative waste treatmet and conditioning technologies at nuclear power plants, TECDOC 1504, IAEA (2006).
7. Pettersson, S., Kemmler, G., Experience on Resin Pyrolysis, Waste Management '84, Proceedings of the Symposium: Waste Isolation in the US Technical Programs and Public Education; Tucson, AZ, USA; Code 6533 (1984).
8. Brähler, G., Slametschka, R., Pyrolysis of Spent Ion Exchange Resins, Waste Manage Conference, USA (2012).
9. Luycx, P., Deckers, J., Pebble bed pyrolysis for the processing of alpha contaminated organic effluents. Waste Manage Conference, USA (1999).
10. THORsm Steam Reforming Process For Hazardous and Radioactive Wastes – Technology Report (TR-SR02-1, Rev. 1)
11. Mollah, M.Y.A., Schennach, R., Patscheider, J., Promreuk, S., Cocke, D.L., Plasma chemistry as a tool for green chemistry, environmental analysis and waste management, Journal of Hazardous Materials B79, (2000) 301–320.
12. Konjevic, N., Ivkovic, M., Sakan, N., Hydrogen Balmer lines for low electron number density plasma diagnostics, Spectrochimica Acta Part B 76 (2012) 16-26.
13. Da-Zhi, J., Zhong-Hai, Y., Ping-Ying, T., Kun-xiang, X., Jing-yi, D., Hydrogen plasma diagnosis in penning ion source by optical emission spectroscopy, Vacuum 83 (2009) 451-453.
14. Matsuda, M., Funabashi, K., Nishi, T., Yusa, H., Decomposition of Ion Exchange Resins by Pyrolysis, Nuclear Technology, Vol. 75 (1986) 187-192.
15. Matsuda, M., Funabashi, K., Yusa, H., Kikuchi, M., Influence of Functional Sulfonic Acid Group on Pyrolysis Characteristics for Cation Exchange Resin, Journal of Nuclear Science and Technology, 24:2 (1987) 124-128.
16. Luca, V., Bianchi, H. L., Manzini, A. C., Cation immobilization in pyrolyzed simulated spent ion exchange resins, Journal of Nuclear Materials 424 (2012) 1–11.
17. Luca, V., Bianchi, H. L., Allevatto, F., Vaccaro, J. O., Alvarado, A., Low Temperature Pyrolysis of Simulated Spent Anion Exchange Resins. (To be published)
18. Rehman, F., Lozano-Parada, J. H., Zimmerman, W. B., A kinetic model for H_2 production by plasmolysis of water vapours at atmospheric pressure in a dielectric barrier discharge microchannel reactor, International Journal of Hydrogen Energy, Vol. 37, I. 23 (2012) 17678-17690.

CHAPTER 5.2 CHARACTERIZATION OF CASHEW PRODUCTION SOLID WASTE AND ITS ENERGETIC POTENTIAL EVALUATION FOR THERMAL CONVERSION PROCESSES

P.T. Tavares *(1); J. C. G. Silva (1); T. S. E. Pereira (1); B. F. M. L. Gomes (1) and S. L. F. Andersen (1)

(1) Universidade Federal da Paraíba, Cidade Universitária, João Pessoa, Brazil

ABSTRACT

The exponential increase in energy demand requires diversification of energy sources. Biomass has stood out due to its low cost, fast growth rate and the possibility of production of a high quality solid fuel, with low ash content and high calorific value, and may be considered as the energy source of the future.
Brazil has ranged from the fifth, eighth and tenth in the world for cashew production between 2008 and 2012. Its cultivation and beneficiation generated, in 2015, between 1.4 and 1.5 million tons of cashew nut shell (CNS) and between 4.2 and 5.0 million tons of cashew apple bagasse (CAB). Therefore, the use of waste for energy purposes would reduce disposal issues of these and could substitute fuels.
The objective of this study is to verify the possibility of using solid waste from cashew culture (CNS and CAB) as an alternative and renewable energy source in thermal conversion processes, characterizing them physical-chemically (immediate analysis, calculation of calorific value, SEM and XRF), and verifying the probability of ash melt. Furthermore, the thermal behavior of the residues was evaluated by thermogravimetric analysis carried out in inert and oxidizing atmosphere in order to analyze the processes of pyrolysis and combustion, respectively.
The CAB and the CNS showed a high volatile matter content and low ignition temperature, 167 ºC and 199 ºC respectively, as well as low ash content, 3.55 and 2.16% for CAB and CNS, respectively. The pyrolysis curve showed that there were three major peaks for CNS, relating to the degradation of hemicellulose, cellulose and lignin fraction, respectively; while for CAB it was observed the presence of a well defined peak at 300 ºC, representing the superposition of simultaneous degradation of lignocellulosic components. During the combustion, there are three peaks for CNS, which indicates loss of hemicellulose, cellulose and lignin, predominantly, and for CAB there were two predominant peaks, corresponding to the loss of the hemicellulose and cellulose to the oxidation of the cellulose. In conclusion, it was found that the solid wastes in question have potential to be used as an alternative and renewable energy source and may collaborate with energy diversification, giving a sustainable disposal for cashew cultivation residues.

Keywords: Biomass; cashew nut shell; renewable energy; solid waste

---

*Author for correspondence: priscilla.tavares@cear.ufpb.br

INTRODUCTION

The oil shortages, climate instabilities, the exponential increase of energy demand and the need for energy independence from other countries, bring a need for diversification of energy resources.

Due to its rapid growth rate, endurance and possibility of solid fuel production with low ash content, high calorific value and low alkalis index, biomass is one of the energy sources that can fulfill the requirements[1]. Biomass refers to the biodegradable organic material chemically composed of hydrocarbons, which are originated from plants, animals and micro-organisms, comprising residues from the industries, municipal and agroindustrial[2] activities.

The waste generated by several crops can be a promising energy source because it does not compete with protected lands or arable lands and its energy use is an environmentally appropriate way of end disposal[3].

Cashew is a plant belonging to the *Anacardiaceae* family, originated in tropical America and includes trees and tropical and subtropical shrubs, located between 27 ºN and 28 ºS, between Southeast Florida and South Africa, and the main economically significant products are the nut and cashew nut shell liquid (CNSL). The Brazilian cashew crop and processing has produced an average of 126,691 million tons of cashew nuts in the last five years. Comparing the 2015 harvest with previous ones, it is seen that in 2015 the cashew crop occupied a smaller land amongst the four previous years, while its production was the fourth highest recorded among the five years. This processing of the cashew generated between 1.4 and 1.5 million tons of cashew nut shell and between 4.2 and 5.0 million tons of cashew bagasse in Brazil during 2015.

Thus, the waste from the cashew culture demonstrate to be an alternative energy source because the great generation of waste materials. In addition, the use of solid waste of the cashew cultivation for energy production can reduce the problem of disposal of this waste and could replace part of the firewood used in industry. Among the biomass conversion processes, thermochemical presents good applicability in energy production, where several studies demonstrate the use of cashew waste in thermochemical processes, showing excellent results when applied mainly in gasification systems[4–6].

Processes such as the use of biomass directly in furnaces (combustion) or gas production to be used in diesel engines (gasification) require a prior study of the physicochemical properties of the biomass[7].

Therefore, the objective of this study is to characterize physicochemically the solid waste from cashew processing (nut shell and peduncle bagasse) evaluating the energy potential to apply this biomass in thermochemical systems for energetic purposes.

MATERIALS AND METHODS

The solid wastes (biomass) selected for this study were the cashew bagasse (CAB) and cashew nut shells (CNS). The cashew bagasse was obtained from a juice industry located in the city of João Pessoa-PB, Brazil, while samples of cashew nut shell were obtained in a cashew nut industry in Natal-RN, Brazil. CAB sample was pre-dried in air

for about 24 hours, and then dried in an oven with recirculating air at 100 ºC ± 5 ºC for 24 hours to ensure that the whole mass was dried. The CNS sample was dried in an oven under the same conditions of CAB. The CAB samples were milled in a knife mill, while the CNS sample was milled in a ball mill. For the physicochemical characterization, samples were sieved (particle diameter <100 μm) for uniform particle size.

Physicochemical characterization. The physicochemical characterization of the solid waste was conducted by means of proximate analysis, thermogravimetric analysis (TGA), calorific value calculation and scanning electron microscopy (SEM). The biomass ashes were analyzed in terms of morphology and chemical composition: SEM for morphology and X-ray fluorescence (XRF) to obtain the elemental composition of inorganic compounds and to evaluate the potential of the ash melt. The proximate analyses were performed in duplicate in accordance with the methodologies described by ASTM E1755[7] and ASTM E872[8], for the ash (A) and volatile matter (VM), while the moisture (M) was obtained using a moisture analyzer, MF-50, AND. The fixed carbon (FC) of the solid wastes, on a dry basis, was determined by difference according to Eq. 1.

$$FC(\%) = 100 - VM(\%) + A(\%) \quad (1)$$

Thermogravimetric analyses were performed using a thermogravimetric analyzer, Shimadzu, Model DTG-60H, under inert atmosphere (N_2 99.995%) and oxidant (synthetic air) in order to evaluate the pyrolysis and combustion processes, respectively. 10 mg of samples were submitted to a heating rate of 10 ºC.min^{-1} from room temperature to 900 ºC under a flow of 50 mL min^{-1}.

The high heating value (HHV) was calculated based on an empirical equation using the data of proximate analysis[9], where the equation (2) is a function of fixed carbon and volatile matter.

$$HHV\left(MJ.kg^{-1}\right) = 0.312\left[FC(\%)\right] + 1.1535\left[VM(\%)\right] \quad (2)$$

SEM analyses were performed to observe the morphology of the samples and their respective ash. The equipment used was the Electronic Microscope LEO brand Scan, LEO 1430.

To obtain the chemical composition of the ash, it was used the X-ray fluorescence technique (XRF). The diffractometer used was Shimadzu XRF 1800 model, using the elements method with opening diameter of 10 mm mask. Based on the data obtained from the XRF it was possible to predict the possibility of ashes melt through the Equation 3[10,11].

$$R_{A/B} = \frac{Fe_2O_3 + CaO + MgO + Na_2O + K_2O + P_2O_5}{SiO_2 + Al_2O_3 + TiO_2} \quad (3)$$

Where weight concentration is required of each component in the ashes for use in the equation. The base-to-acid ratio ($R_{A/B}$) has often been used as a measure of the fouling tendency of a fuel ash, and its results can be related to the melting temperature of these ashes[11].

RESULTS AND DISCUSSION

Physicochemical characterization

The results of proximate analysis, theoretical HHV and ash composition of CAB and CNS samples are shown in **Table 1**.

TABLE 1. **Proximate analysis, HHV and ash composition of CAB and CNS**

	CAB	**CNS**
Moisture*	69.91 (±0.73)	6.16 (±0.21)
Volatile Matter*, a	74.88 (±0.57)	84.08 (±0.13)
Fixed Carbon*, a	21.57	13.76
Ash*, a	3.55 (±0.12)	2.16 (±0.07)
HHV ($MJ.kg^{-1}$)b	18.22	17.89
Ash composition*		
K_2O	61.29	50.57
P_2O_5	19.03	15.50
MgO	5.75	10.29
CaO	3.81	6.37
SO_3	3.55	2.39
Na_2O	2.00	5.88
SiO_2	1.24	2.39
Cl	0.78	0.59
Fe_2O_3	0.76	2.65
Al_2O_3	0.60	1.48
MnO	0.29	0.71
Rb_2O	0.27	0.30
ZnO	0.27	0.16
Cr_2O_3	0.15	0.24
CuO	0.13	0.27
SrO	0.08	0.20
$R_{A/B}$	50.35	23.58

*wt%, adry basis, bcalculated (Equation 2).

CNS and CAB presented a moisture content of approximately 6.16% and 69.91%, respectively, this result interferes directly in thermochemical processes such as pyrolysis and combustion, because when there is a high content of water there is a greater need for energy to eliminate it, thus it reduces the energetic density, becoming an important parameter that must be taken into consideration because of the necessity of preheating[5]. It was also observed a high volatile matter and low ash content for the CNS

when compared to CAB, however the CAB samples showed a high HHV compared to CNS.

The results of the calorific value shows that when dried the materials present a high HHV when compared to the results obtained by Demirbaş[9] which analyzed 16 different biomass presenting values ranging from 15.0 to 20.5 MJ kg^{-1}.

The volatile matter content found in this study for the CNS (84.08%) differed by approximately 2% to CNS studied by Tsamba *et al.*[12] (2006) (81.80%), and the CNS studied by Das and Ganesh (2003) (69.31%) showed a difference of more than 14 and 12%. This volatile matter content is related to the amount of fuel gases that can be released from the heating of these biomasses when properly dried, in addition, this value is directly related to the low ignition temperatures and flame stability[5,13].

Table 1 shows that the elements K, P, Ca and Mg are in highest concentration in the ashes of CAB and CNS, where K is predominant concentration, when compared with the other elements. This high concentration of K can increase the probability of the same to react with Si to form an alkali silicate[11], which can be seen from the results of the $R_{A/B}$. A high value of the ratio acid base ($R_{A/B}$ > 0.75) is observed for both the CAB ($R_{A/B}$ = 50.35) and CNS ($R_{A/B}$ = 23.58), which predict a low ash melting temperature and can contribute to the slagging and fouling formation[11,14].

The result of SEM analyses of CAB and CNS samples and its ashes are shown in **Figure 1**.

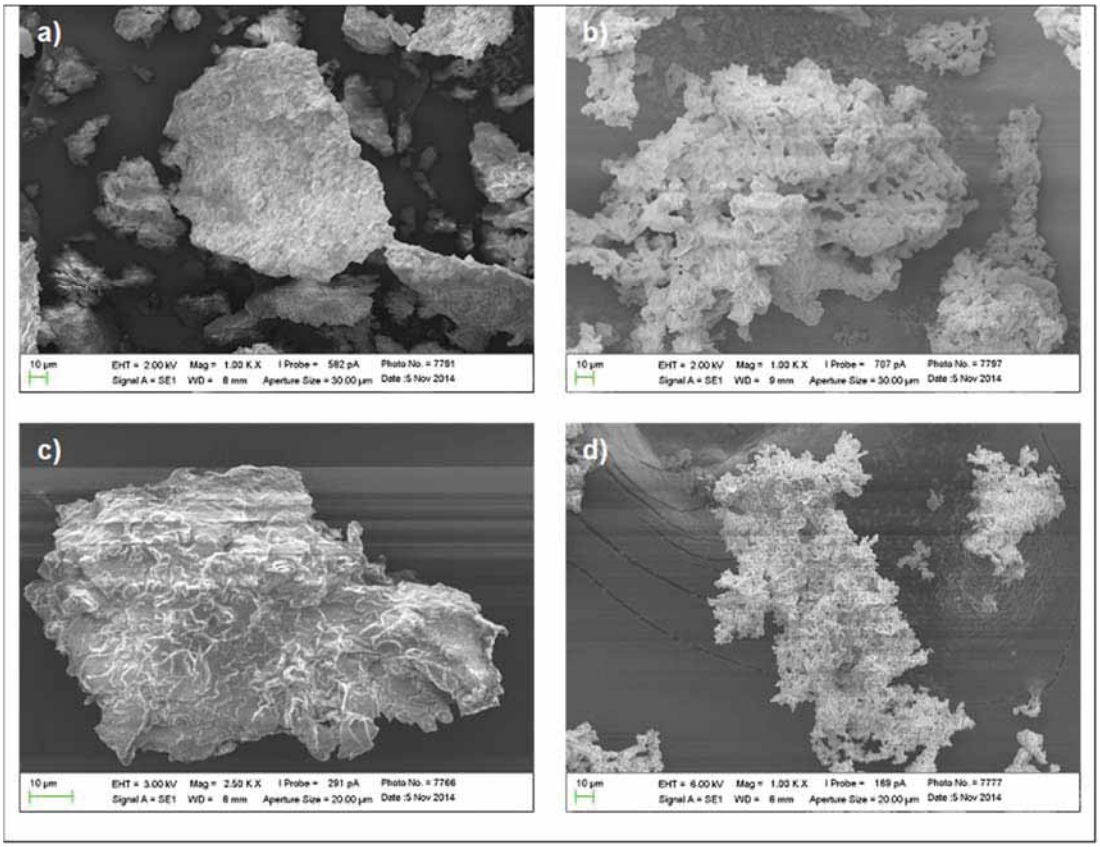


FIGURE 1. Scanning electron images: ×1000 of (a) CAB, (b) CAB ash, (c) CNS, (d) CNS ash

The CAB morphology (**Figure 1a**) consists in laminar grains, irregular and dense, with few pores, different from its ashes that have several pores (**Figure 1b**). The CNS is similar to CAB showing few pores between the particles (**Figure 1c**), while its ashes are more porous (**Figure 1d**) than CAB.

This difference in the amount of pores between the sample in natura and ash occurs because the chemical bonds that composes the volatile material are weaker, which burn at lower temperatures releasing gases and promoting combustion[15].

Thermogravimetric analysis. **Figure 2** shows the results of thermogravimetric analysis (TG and DTG) of CAB under inert and oxidant atmospheres.

Initially it can be seen that the moisture loss under inert and oxidizing atmospheres occurs between 30-140 ºC with mass loss 4.6% and 3.9%, respectively. After the drying process of CAB there is a small amount of water weight in the sample. After this initial drying process, it is observed a change in the curves for the two atmospheres.

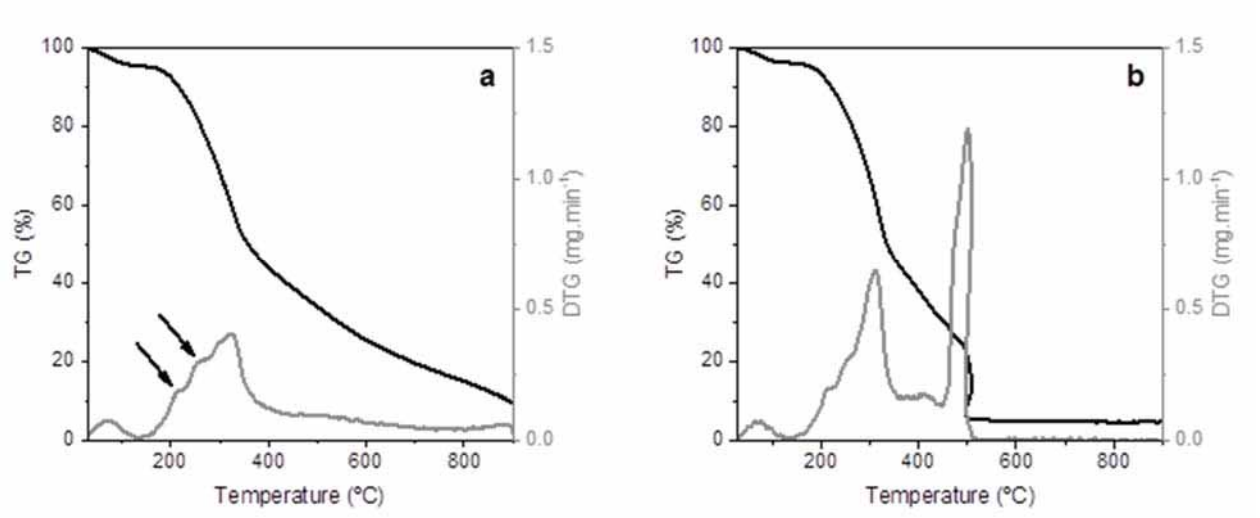


FIGURE 2. TG (—) and DTG (—) curves for CAB in: (a) inert (N_2) (b) oxidant (Air) atmosphere

Under inert atmosphere (**Figure 2a**) it refers to the pyrolysis of material, which has a thermal decomposition of lignocellulose, starting at about 140 ºC and finishing at 375 ºC. This region is observed in the presence of a DTG peak, which presents two "shoulders" (indicated by arrows in Figure 2a), showing the decomposition of different components of biomass overlaid. The first "shoulder" between the temperatures of 140 ºC and 225 ºC, having mass loss of 6.9%, can be related to the onset of hemicellulose and lignin decomposition along with the release of other gases which refers to the thermal decomposition of organic extracts as waxes, carboxylic acids, fats, etc. which are present in large quantities in the material[16].

The second “shoulder” (mass loss of 12.2%) occurs between 225-275 ºC and it can be related, according to some authors[17–19], to the thermal decomposition of hemicellulose, by the fact that the hemicellulose constitute a smaller chemical chain

compared to lignin and it is decomposed more easily, requiring a lower temperature than cellulose. The cellulose can be represented by the decomposition temperature ranging between 275-375 ºC which has the highest decomposition rate under inert atmosphere at 313 ºC (0.40 mg min^{-1}) with a mass loss of 28.9%.

After the cellulose and hemicellulose decomposition, it occurs only a slow lignin decomposition at the whole experimental temperature range, due to the complex chemical structure of lignin[18]. According to some authors[18,20,21] the lignin is decomposed slowly in a large experimental range, starting at temperatures about 170 ºC, and may also present several decomposition stages. At the end of the process under inert atmosphere, there is still 9.4% of residual mass, being comprised by the ashes, determined in the proximate analysis, and lignin that was not degraded.

Under oxidant atmosphere, it is possible to observe a different behavior of the curve shown in Figure 2b. There are two regions of mass loss rate. The first region with a mass loss of 34.8% (160-450 ºC) is related to the lignocellulose decomposition, similar as occurred under inert atmosphere, however the oxidant gas promotes the combustion of volatiles released[22], which has ignition temperature of 167 ºC obtained by overlapping the TG curves of oxidant and inert atmosphere, where the burning temperature (onset) is when the temperature profile in an oxidant atmosphere change with respect to an inert atmosphere[23]. The ignition observed in Figure 2b resulted an increase in mass loss rate in DTG curve, which coincides with the end of the moisture loss in the TG curve.

There is, in this first region, a higher mass loss rate (0.65 mg min^{-1}), compared to the inert atmosphere. This increase in rate should be taken into consideration due to a possible turbulence generated by the quick material volatilization, and requires, when developing equipment, more burn stages in order to prevent the formation and release of pollutants such PAHs and fuel gases from incomplete oxidation[11].

The biochar burning region occurs quickly between temperatures of 450 ºC and 505 ºC having mass loss of 12.1%. At 500 ºC the sample had a mass loss rate of 1.21 mg min^{-1}, being this rate promoted by the high concentration of oxidizing gas on the sample[24].

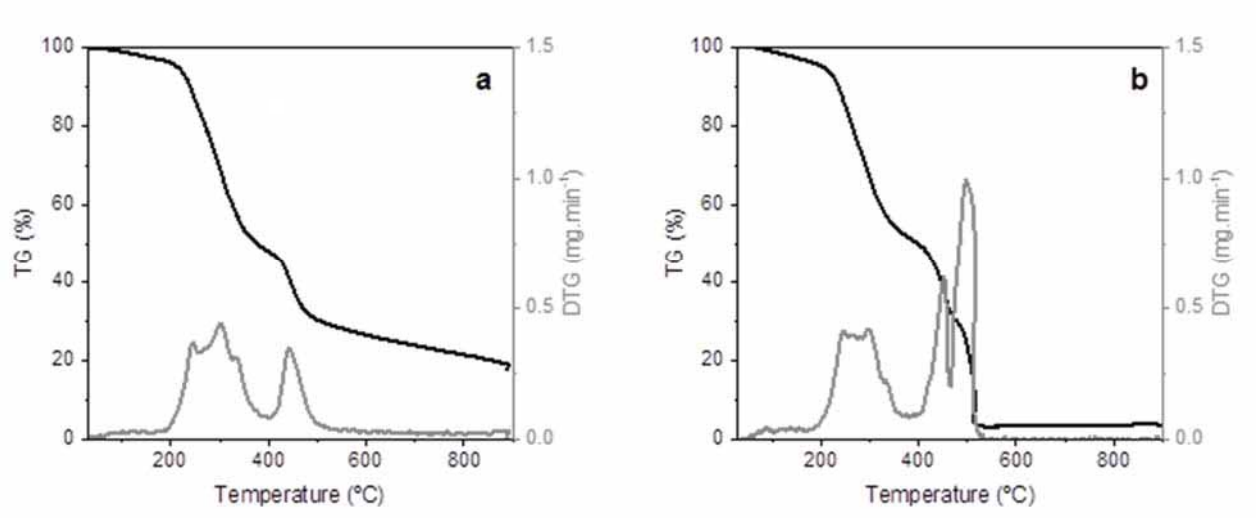


FIGURE 3. **TG (—) and DTG (—) curves for CNS in: (a) inert (N_2) (b) oxidant (Air) atmosphere.**

Figure 3 shows the results of thermogravimetric analysis (TG and DTG) of CNS under inert and oxidant atmospheres.

In **Figure 3**, it is possible to note that moisture is initially released at temperatures between 30 ºC and 190 ºC. The DTG curve show that the moisture loss occurs slowly in both atmospheres. After this process, pyrolysis process begins.

In inert atmosphere showed in Figure 3a there is a different behavior in the CNS mass loss, when compared to the CAB (Figure 2a). There is a higher pyrolysis region (190 ºC to 500 ºC) with a mass loss of 66.2%. In the CNS pyrolysis region it is observed the presence of three peaks at temperatures of 243 ºC, 302 ºC and 441 ºC, that indicate different components in material, which are decomposed in close ranges, thereby promoting an overlap of the curves.

The first peak in the region of 190 ºC and 260 ºC can be related to the hemicellulose degradation with mass loss of 13.1% and having a maximum decomposition rate of 0.37 mg min^{-1}. In addition, this region can present the decomposition of organic extracts (in lower amount), which may have resulted in the absence of the shoulders as observed for the CAB[12,19].

Subsequently, the region between 260 ºC and 325 ºC can be related to the cellulose decomposition, and a small amount of hemicellulose and lignin, representing a mass loss of 22.9% and a maximum decomposition rate of 0.44 mg min^{-1}. This mass loss rate is approximately similar to that found for the CAB under inert atmosphere.

Within the temperature range of 390 to 500 ºC it can be observed a peak with a mass loss of 18.5%, which was not observed for the CAB. This peak was also observed by Gangil[25] who studied waste cashew nut shell under the same conditions of this study, and it was observed a maximum mass loss rate at 446.7 ºC which was similar to that found for CNS (442 ºC).

In the end of the process, it remains a residue, which is 18.9% of the initial mass of the sample, possibly being 16.2% of ash and 16.74% of lignin still present in the sample, which is degraded at higher temperatures.

Under oxidant atmosphere (Figure 3b), it is observed that the region between 190 ºC to 465 ºC shows a similar behavior to that observed under inert atmosphere, with mass loss of 63.7%. However, unlike the behavior under inert atmosphere, a small variation in mass loss rate was observed between 245 ºC and 300 ºC, being approximately 0.41 ± 0.02 mg min^{-1} with a mass loss of 20.0%. It is observed that the ignition temperature for the CNS occurred at 199 °C.

The biochar oxidation (28.7%) occurs between 465 ºC and 520 ºC and show a mass loss rate of 0.99 mg min^{-1}, this rate can be related to the gas contact area with the surface of the sample, which provides a rapid oxidation of the biochar[24].

CONCLUSION

In this work, residues from cashew beneficiation (cashew bagasse and cashew nut shell) were characterized phisicochemically to evaluate its energetic potential. The analyses performed were: proximate analysis, thermogravimetric analysis, scanning electron microscopy and X-ray fluorescence of the ashes.

It was observed that for the CAB application in thermal processes it is necessary a preliminary drying process to remove the large amount of moisture present in this

material, which can directly affect the calorific value. In the other hand, the high percentage of volatile matter resulted in low ignition temperatures: 167 ºC (CAB) and 199 ºC (CNS).

The beginning of release and oxidation of both biomasses occurred at approximately 200 ºC, where the CNS showed three well defined peaks of degradation under both atmospheres, however the CAB showed two degradation peaks under inert atmosphere and under oxidizing atmosphere. Both biomasses were not completely degraded up to 900 ºC under an inert atmosphere. A residue of 9.4% (CAB) and 17.5% (CNS) remained at the end of the process, being constituted by ash and residual lignin that was not degraded, while for oxidant atmosphere the lignin in the sample oxidizes at temperatures about 500 ºC for both the samples.

Finally, it is verified that the cashew bagasse and cashew nut shell have potential for its use as an alternative and renewable source of energy in thermal conversion processes.

REFERENCES

1. Bada S. O., Falcon R. M. S., Falcon L. M. Investigation of combustion and co-combustion characteristics of raw and thermal treated bamboo with thermal gravimetric analysis. Thermochim. Acta 589 (2014) 207–214.
2. UNFCCC. *Clarifications on definition of biomass and consideration of changes in carbon pools due to a CDM project activity*, EB-20, Report Annex. 8, 2005.
3. Ferreira-Leita V., Gottschalk L. M. F., Ferrara M. A., Nepomuceno A. L., Molinari H. B. C., Bon E. P. S. Biomass Residues in Brazil: Availability and Potential Uses. Waste and Biomass Valorization 1 (2010) 65–76.
4. Tippayawong N., Chaichana C., Promwangkwa A., Rerkkriangkrai P. Gasification of cashew nut shells for thermal application in local food processing factory. Energy Sustain. Dev. 15 (2011) 69–72.
5. García R., Pizarro C., Lavín A. G., Bueno J. L. Characterization of Spanish biomass wastes for energy use. Bioresour. Technol. 103 (2012) 249–258.
6. Singh R. N., Jena U., Patel J. B., Sharma, A. M. Feasibility study of cashew nut shells as an open core gasifier feedstock. Renew. Energy 31 (2006) 481–487.
7. 7.ASTM Standard E1755-01. *Standard Test Method for Ash in Biomass*, American Society for Testing and Materials (ASTM), (2003).
8. ASTM Standard E872-98. *Standard Test Method for Volatile Matter in the Analysis Sample of Coal and Coke*, American Society for Testing and Materials (ASTM), (2003).
9. Demirbaş, A. Calculation of higher heating values of biomass fuels. Fuel 76 (1997) 431–434.
10. Demirbaş, A. Biomass resource facilities and biomass conversion processing for fuels and chemicals. Energy Convers. Manag. 42 (2001) 1357–1378.
11. Jenkins B. M., Baxter L. L., Miles T. R., Miles T. R. Combustion properties of biomass. Fuel Process. Technol. 54 (1998) 17–46.
12. Tsamba A. J., Yang W., Blasiak W. Pyrolysis characteristics and global kinetics of coconut and cashew nut shells. Fuel Process. Technol. 87 (2006) 523–530.
13. Williams A., Pourkashanian M., Jones J. M. Combustion of pulverised coal and biomass. Prog. Energy Combust. Sci. 27 (2001) 587–610.
14. Khan A. A., Jong W., Jansens P. J., Spliethoff H. Biomass combustion in fluidized bed boilers: Potential problems and remedies. Fuel Process. Technol. 90 (2009) 21–50.
15. Fang X., Jia L., Yin L. A weighted average global process model based on two−stage kinetic scheme for biomass combustion. Biomass and Bioenergy 48 (2013) 43–50.
16. Mészáros E., Jakab E., Várhegyi G. TG/MS, Py-GC/MS and THM-GC/MS study of the composition and thermal behavior of extractive components of *Robinia pseudoacacia*. J. Anal. Appl. Pyrolysis 79 (2007) 61–70.

17. Varhegyi G., Antal M. J., Szekely T., Szabo P. Kinetics of the thermal decomposition of cellulose, hemicellulose, and sugarcane bagasse. Energy & Fuels 3 (1989) 329–335.
18. Yang H., Yan R., Chen H., Lee D. H., Zheng C. Characteristics of hemicellulose, cellulose and lignin pyrolysis. Fuel 86 (2007) 1781–1788.
19. Mohan D., Pittman C. U., Steele P. H. Pyrolysis of Wood / Biomass for Bio-oil: A Critical Review. Energy & Fuels 20 (2006) 848–889.
20. Gani A., Naruse I. Effect of cellulose and lignin content on pyrolysis and combustion characteristics for several types of biomass. Renew. Energy 32 (2007) 649–661.
21. Burhenne L., Messmer J., Aicher T., Laborie M. P. The effect of the biomass components lignin, cellulose and hemicellulose on TGA and fixed bed pyrolysis. J. Anal. Appl. Pyrolysis 101 (2013) 177–184.
22. Blasi C. Di. Modeling and Simulation of Combustion Processes of Charring and Non-Charring Solid Fuels. Prog. Energy Combust. Sci. 19 (1993) 71–104.
23. Norton G. A. A review of the derivative thermogravimetric technique (burning profile) for fuel combustion studies. Thermochim. Acta 214 (1993) 171–182.
24. Fang, M. X., Shen D. K., Li Y. X., Yu C. J., Luo Z. Y., Cen K. F. Kinetic study on pyrolysis and combustion of wood under different oxygen concentrations by using TG-FTIR analysis. J. Anal. Appl. Pyrolysis 77 (2006) 22–27.
25. Gangil S. Dominant thermogravimetric signatures of lignin in cashew shell as compared to cashew shell cake. Bioresour. Technol. 155 (2014) 15–20.

CHAPTER 5.3 MICROBIAL AND PARASITIC RISKS RELATED TO APPLICATION OF ANIMAL WASTES TO SOIL

J. Venglovsky *(1); N. Sasakova (1); F. Toth (2); I. Papajova (2); G. Gregova (1) and R. Hromada (1)

(1) University of Veterinary Medicine and Pharmacy in Kosice, Komenského 73, Košice, The Slovak Republic
(2) Institute of Parasitology of the Slovak Academy of Sciences, Hlinkova 3, Košice, The Slovak Republic

ABSTRACT

The study investigated viability *Salmonella typhimurium* and *Ascaris suum* eggs in raw pig slurry stored at 4º, 20º and 42ºC in order to asses the microbial and parasitic risks related to application of animal wastes to soil. *S. typhimurium* culture and carriers with *A. suum* eggs were introduced into the slurry. *A. suum* eggs stored in distilled water at the respective temperatures served as a control. Plate counts of *S. typhimurium* and the number of devitalised non-embryonated model *Ascaris suum* eggs were determined on days 0, 7, 12, 22, 32, 40, 55, 90 and 115 of storage.
S. typhimurium survived in the slurry for less than 115 days at 4ºC and for less than 90 days at 20ºC and 42ºC. Devitalization of *A. suum* eggs was affected by temperature and the time of storage but complete devitalization was not achieved even after 115 days at 42ºC.
Our investigations confirmed that there exists potential microbial and parasitic risk related to application of pig slurry to soil even after 115 days of storage. This risk can be reduced by relevant preventive hygiene measures and strict observation of legislative provisions.

Key words: animal wastes; Ascaris suum; risks; Salmonella typhimurium

INTRODUCTION

Animal manure is applied to soil with the aim to supply important nutrients to plants and to improve the soil structure. However, if not handled and processed properly, such disposal of animal manure, particularly pig slurry, can be associated with significant microbial and parasitic risks.

With regard to animal wastes we are concerned particularly with representatives of the family *Enterobacteriacea*, the majority of which have zoonotic character, such as *Salmonella* sp., *Escherichia coli, Mycobacterium* sp., *Enterococcus* sp., *Streptococcus* sp., *Staphylococcus* sp. and similar, which are a threat to both farm animals and man.

Excrements of farm animals are also a source of endoparasites (cysts, eggs, larvae of genera *Ascaris* sp., *Oesophagostomum* sp., *Trichuris* sp., *Strongyloides* sp., *Isospora* sp., *Eimeria* sp., *Giardia* sp., *Balantidium* sp., and others) that may cause massive parasitic infections in both specific hosts and non-specific ones, such as man. An

---

*Author for correspondence: priscilla.tavares@cear.ufpb.br

important factor in spreading of endoparasitoses is high tenacity of some propagative stages of parasites (Papajová and Juriš[1]).

According to Reissbrodt[2], salmonella species are important food-borne pathogens that represent a significant and increasing public health problem in industrialized countries. There are more than 2000 different salmonella serotypes. The most common pathogens *S. enteritidis* and *S. thyphimurium* are responsible for nearly half of all illnesses. The persistence of these bacteria in the environment (e.g. in soil, water, sewage, etc.) depends on the long-term survival of heavily stressed cells, particularly the so-called viable- but-nonculturable (VNC) organisms, that cannot grow on conventional laboratory plating media but may revive in vivo and cause diseases (Brandl[3]).

The aim of the study was to investigate the viability of *S. typhimurium* and *Ascaris suum* eggs in raw pig slurry stored at different temperatures in order to asses the microbial and parasitic risks related to application of animal wastes to soil.

MATERIALS AND METHODS

The experiment was carried out on raw pig slurry obtained from a pig farm. The slurry was stored for 115 days in closed plastic containers of volume 5 litres as follows:

1. in a refrigerator at 4°C;
2. in a thermostat at 20°C,
3. in a thermostat at 42°C.

Before storage, lyophilised strain *S. typhimurium* SK 14/39 (SZÚ Prague, CR) was inoculated into the investigated slurry (initial count of *S. typhimurium* 3.6×10^9 CFU.ml^{-1}). Also special polyurethane containers, each containing 1500 *A. suum* eggs, obtained by dissection of distal ends of the uterus of *A. suum* females were introduced into the slurry.

Plate counts of *S. typhimurium* were determined at days 0, 7, 12, 22, 32, 40, 55, 90 and 115 of storage. At the same intervals devitalisation of *A.suum* eggs was observed in comparison with *A.suum* eggs stored in distilled water at the same temperatures.

The following changes in physical and chemical properties of the slurry were monitored as they may affect devitalisation of pathogens: pH, dry mater (DM), chemical oxygen demand (COD_{Cr}), and ammonium ions (NH_4^+). Results were published elsewhere.

The number of damaged *A. suum* eggs was expressed as mean ± standard deviation ($\overline{X} \pm SD$). Significance of differences between experimental and control groups of parasites were determined using Student t-test, ANOVA and Dunnet Multiple Comparison test at the levels of significance 0.05; 0.01 and 0.001 (Statistica 6.0).

RESULTS AND DISCUSSION

It is generally known that some eggs, infectious larvae (L3), oocysts or sporocysts can survive for considerable time, frequently for several years, even under unfavourable environmental conditions. The most dangerous are highly resistant eggs of some parasitic nematodes, e.g. *Ascaris* spp., *Trichuris* spp. and coccidial oocysts (Juriš[4]).

Although the possibility of survival of Salmonella in soil for more than 900 days was known earlier, there were questions about its pathogenicity for roots and other plant parts.

In 2008 Vienna Plant Molecular Biology Laboratory, in collaboration with French laboratories concluded that Salmonella is able to actively penetrate the soil to the root hairs, and so behave like a typical plant pathogen. Therefore, the risk to public health arising from application of insufficiently treated animal manure to soil may be higher than detected by common methods. At 4° C the initial concentration of the tested *S. typhimurium* strain decreased by three orders of magnitude by day 90 and on day 115 of storage the test strain was no more recovered. At 20°C a marked decrease by 7 orders of magnitude was observed on day 32 and from this day the test strain was investigated only qualitatively. The most marked decrease in plate counts of test bacteria was recorded in pig slurry stored at 42°C.

Arrus[5] observed influence of temperature on *S. typhimurium* and concluded that while Salmonella did not grow in hog manure, storage reservoir temperatures would facilitate. Salmonella survival over winter enabling contamination of fields at spring application (Reissbrodt[6]).

Key to controlling salmonella is to follow the general rules that have been successfully applied to other infectious diseases (Plym Forshell and Wierup[7]).

Parasite survival in animal manures may also be related to temperature, but the trends are not as pronounced as those reported for bacterial pathogens. This is likely due to their ability to form cysts and oocysts for protection from environmental pressures. Olson[7] noted that *A. suum* eggs are highly resistant to inactivation in faeces, potentially remaining infectious for years. A direct contact with infected animal, but also contaminated environment, or contaminated food chain (water, vegetables) are considered as a potential risk factor (Papajová and Juriš[1]).

Our study showed that higher temperatures supported devitalisation of *A. suum* eggs (**Table 1**).

TABLE 1. Survival of non-embryonated model *A. suum* eggs in raw pig slurry stored at three different temperatures

Exposure time (days)	Devitalized eggs of *A. suum* ($\overline{X}$ % ± SD)		
	4ºC	20ºC	42ºC
0	15.55 ± 2.52	10.13 ± 3.17	14.90 ± 4.06
7	16.86 ± 2.39	16.72 ± 1.38	74.30 ± 0.82***
12	20.33 ± 9.31	17.17 ± 5.74	92.39 ± 4.95**
20	17.04 ± 11.25	16.86 ± 3.64	99.23 ± 1.09***
32	21.54 ± 16.67	26.90 ± 4.38	92.85 ± 10.10**
40	22.87 ± 4.06	21.85 ± 10.69	96.15 ± 5.44**
55	24.90 ± 1.28*	23.81 ± 13.46	98.24 ± 2.48***
90	25.87 ± 5.84	36.28 ± 10.91	95.83 ± 5.89**
115	26.97 ± 5.14	37.65 ± 8.34	99.65 ± 1.34***
Control	14.14 ± 0.82	15.14 ± 0.92	14.14 ± 0.22

*P<0.05; ** P<0.01; *** P<0.001

Besides temperature and the time of storage the survival of pathogens in the slurry may well depend on factors other than temperature and duration of heat treatment, e.g. moisture content, free ammonia concentration, pH, the presence of other micro-organisms and other physico-chemical properties (Venglovský[9]).

For this reason the stored pig slurry was subjected also to physico-chemical examination. Changes in physico-chemical parameters were related to decomposition processes, however, some variations were observed which require further study and prevented us to from drawing relevant conclusions regarding their potential influence on devitalisation of *S. typhimurium* and *A. suum* eggs.

CONCLUSION

There are significant microbiological risks related to animal wastes spread onto land subsequently used for crop production or livestock grazing. Animal slurries are of particular concern, as the temperature in these substrates during their storage and some ways of common processing does not ensure complete devitalisation of potential bacterial and viral pathogens and eggs of parasites, as indicated by our observation of devitalisation of *S. typhimurium* and *A. suum* eggs at 4°, 20° and 42°C during 115 days of storage.

In advanced countries, relevant legislative regulations require acceptable procedures for the disposal, processing and application of animal manures. However, there are still aspects that may raise some risk for safety of human food chain and require further investigations.

The best way is to put stress on preventive actions and measures that may eliminate any known or suspected danger resulting from pathogens present in animal manures applied to the soil that is used for animal grazing or growing of crops for human consumption.

ACKNOWLEDGEMENTS

The study was supported by Ministry of culture and education grant agency N. 003UVLF-4/2016.

REFERENCES

1. Papajová, I., Juriš, P. The sanitation of animal waste using anaerobic stabilisation. In: Kumar, S., Bharti, A. (Eds.) *Management of organic waste*. Rijeka: InTech, 2012, 49-68.
2. Reissbrodt, R., Heier, H., Tschäpe, H., Kingsley, R. A., Williams, P. H. Resuscitation by ferrioxamine E of stressed *Salmonella enterica* serovar *typhimurium* from soil and water microcosms. Appl. Environ. Microbiol., 66 (9), 2000, 4128-4130.
3. Brandl, M.T. Fitness of human enteric pathogens on plants and implications for food safety. Annual Review of Phytopathology, 44, 2006, 367-392.
4. Juriš, P., Rataj, D., Ondrašovič, M., Sokol, J., Novák, P. *Sanitary and ecological requirements on recycling of organic wastes in agriculture*. Vyd. Michala Vaška, Prešov, 2000, 178 pp. (in Slovak).

5. Arrus, K. M., Holley, R. A., Ominski, K. H., Tenuta, M., Blank, G. Influence of temperature on *Salmonella* survival in hog manure slurry and seasonal temperature profiles in farm manure storage reservoirs. *Livestock Science,* 102, 2006, 226-236.
6. Reissbrodt, R., Heier, H., Tschäpe, H., Kingsley, R. A., Williams, P. H. Resuscitation by ferrioxamine E of stressed *Salmonella enterica* serovar *typhimurium* from soil and water microcosms. Appl. Environ. Microbiol., 66 (9), 2000, 4128-4130.
7. Plym Forshell, L., Wierup, M. Salmonella contamination: a significant challenge to the global marketing of animal food products. Rev. sci. tech. Off. int. Epiz., 25 (2), 2006, 541 - 554.
8. Olson, M. (2003) Human and animal pathogens in manure. http://www.gov.mb.ca/agriculture/livestock/livestockpt/papers/olson.pdf (accessed 08.01.05.).
9. Venglovský, J., Martinez, J., Plachá, I. Hygienic and ecological risks connected with utilization of animal manures and biosolids in agriculture. Livestock Science, 102 (3), 2006, 197 – 203.

Section 6.
Microbial Ecology and Molecular Biology Applications to Environmental Problems

Page

Chapter 6.1 Influence of as (v) on the diversity of biofilms formed on different substrata 393
S.E. Rastelli and M.R. Viera

Chapter 6.2 Efecto cometabólico en la biotransformación de fenantreno por tres zigomicetos 402
J. C. Antonio Huerta; M. T. Rodríguez Casasola; C. Cruz Mondragón; E. Ríos Leal and F. J. Esparza García*

Chapter 6.3 Identification of iron-reducing bacteria from river sediments by 16S RRNA 412
A. M. Hernández Núñez; K. Juárez López; P. Pavón Orozco and A. C. Ortega Martínez

Chapter 6.4 Evaluation of biocides in oilfield environments using fluorescent *in-situ* hybridization 418
M. R. Viera; C. Terada; R. E. Madrid; J. C. Felice and M. T. Del Panno

CHAPTER 6.1 INFLUENCE OF AS (V) ON THE DIVERSITY OF BIOFILMS FORMED ON DIFFERENT SUBSTRATA

S.E. Rastelli (1,2) and **M.R. Viera *(1,3)**

(1) Centro de Investigación y Desarrollo en Tecnología de Pinturas (CIDEPINT; CICPBA-CONICET) Calle 52 entre 121 y 122 (1900) La Plata, Argentina.
(2) Facultad de Ciencias Naturales y Museo (UNLP). Av. 60 y 122. (1900) La Plata, Argentina.
(3) Facultad de Ciencias Exactas (UNLP), calle 47 y 115. (1900) La Plata, Argentina

ABSTRACT

Microorganisms, including bacteria, present in natural and artificial aquatic environments, tend to attach to and grow on immersed surfaces developing a biofilm. Many problems in drinking water networks such as corrosion, persistence of pathogenic species and increased resistance to biocides are due to the presence of biofilms. Arsenic is a contaminant widely distributed in the Argentinean underground water. Despite arsenic's toxicity, a number of microorganisms are capable of growing in arsenic environments playing an important role in the process of arsenic mobilization. The aim of this work was to study the influence of As (V) on the bacterial planktonic community and biofilms structures grown on different drinking water distribution materials.
To simulate a water distribution system, two tanks with a closed loop of polypropylene (PP) tubes were built and filled with drinking water. As(V) (5 mg L^{-1}) was added in one of the tanks. Coupons of four materials were place in the loops for biofilm formation: commercial iron (Fe), commercial zinc (Zn), copper (Cu) and PP. Bacterial planktonic and sessile communities were analysed by culture (heterotrophic plate counts) and molecular (DNA extraction, PCR, sequencing, DGGE) techniques.
Bacterial counts on Fe and Zn were higher than those obtained on Cu and PP and, except for Cu, they were higher in the presence of 5mg.L^{-1} of As(V). Culturable As-tolerant bacteria able to grow in the presence of high As(V) concentration (up to 1g.L^{-1}) were obtained from all the biofilms except Cu-biofilms, which grew in the presence of up to 300mg.L^{-1} As(V). It was possible to isolate and identify 60 colonies corresponding: 40% to the Class Bacilli, 40% α-Proteobacteria (both Classes were found in all the biofilms), 10% Actinobacteria (detected in biofilms formed on Fe in the absence of As, Cu and PP in the presence of As), 8% β-Proteobacteria (found on Fe, Zn and PP biofilms in the presence of As) and 2% γ-Proteobacteria (detected only in biofilms formed on Zn in the absence of As). The DGGE profiles of the planktonic bacterial communities were qualitative and quantitative affected by the presence of arsenic. In general, the planktonic community developed in the water without As showed higher richness and diversity indices, indicating that the presence of a toxic element induced a selection of the species in the water with Arsenic. In the case of the sessile communities, the trends were not so clear. The clustering analysis of the sessile communities showed that the nature of the substrata was a more important factor for the establishment of the community than the presence of arsenic in water.

---

*Author for correspondence: m.viera@cidepint.gov.ar

Keywords: arsenic, biodiversity, biofilms, drinking water, distribution materials.

INTRODUCTION

Microorganisms, including bacteria, present in natural and artificial aquatic environments, tend to attach to and grow on immersed surfaces developing a biofilm[1]. Many problems in drinking water networks such as corrosion, persistence of pathogenic species and increased resistance to biocides are due to the presence of biofilms[2]. The presence of bacterial biofilms on the inner surface of water distribution pipes could lead to a deterioration of the water quality and its subsequent impact in public health.

Another problem related with water quality is the presence of chemical contaminants of diverse origin. Amongst them, arsenic (As) is being increasingly detected in distribution water services, which generate serious sanitary and social problems impacting large urban areas throughout the Planet. In Argentina, As is of great concern due to its natural occurrence in high concentrations in groundwater in large areas of the country[3]. Despite As toxicity, a number of microorganisms are capable of growing in arsenic environments. These microorganisms could be involved in arsenic mobilization and may play a role in arsenic removal[4]. The presence of toxic agent as arsenic in the water phase could induce changes in the bacterial planktonic and sessile communities[5,6]. The aim of this work was to study the influence of As on biofilm formation in water distribution systems. The structures of the planktonic and the sessile communities were analyzed. The presence of Arsenic tolerant-microorganisms was assayed.

MATERIALS AND METHODS

Experimental setup. Two laboratory simulated water distribution circuits consisting each in a 50 L polyethylene storage tank and a closed loop of polypropylene tubes (inner diameter: 2.32 cm; length: 200 cm) with a removable 20 cm acrylic cell were used. La Plata City drinking water was pumped from the tank through the loop at a laminar flux with 30/60 minutes work/stop periods along the day and no flow at night to simulate domestic network operating cycles. To study the settlement of bacteria on different water distribution network materials, coupons of 1 cm x 1 cm x 0.02 cm of commercial low carbon steel (Fe), zinc (Zn), copper alloy (Cu) and polypropylene (PP) were placed in the acrylic cell. To study the influence of arsenic, 5 mg L^{-1} As(V) were added in one of the circuits.

Bacterial community characterization. After circulation time (45 days), 4 coupons of each material were withdrawn from each circuit, and replaced by new coupons. Biofilms were scrapped and poured in 1mL physiological solution for enumeration. Arsenic-resistant sessile bacteria was evaluated by culturing in nutritive broth with 50 to 1,000 $mg.L^{-1}$ As(V) by dilution to extinction technique.

To analyze the microbial communities, total DNA of the planktonic and sessile microorganisms was collected. Planktonic DNA was obtained by filtering 1 L water from each tank through a 0.22 µm sterile membrane. For total sessile DNA extraction, the

material scraped from the coupons was centrifuged at 13,000 g for 15 min and the supernatant discarded. Culturable sessile DNA was obtained from 1mL nutritive broth culture of 1/10 dilution. In all the cases, DNA was extracted using a commercial kit (E.Z.N.A. Soil DNA kit) following the manufacturer's instructions. The 16S rRNA gene sequence was amplified by PCR using the universal primers for eubacteria: 341F (with a GC clamp) and 907R[7]. Negative controls (without DNA) were run in all the amplifications and the presence of PCR product was confirmed by 1.2% w/v agarose gel electrophoresis and Sybr® Gold staining. DGGE was performed in a 6% (w/v) polyacrylamide gel with a 30–70% denaturant gradient (100% denaturant is 7 M urea and 40% v/v formamide) loaded with the PCR products (10–15 µL). Electrophoresis was performed in TAE buffer for 16 h at 100 V. The gels were stained, observed and photographed in a UV transillumination. For statistical evaluation, the gels were analyzed using the Gel Compare II software. The band-based Dice coefficient was used to calculate the similarity matrix with a position tolerance of 1%[8]. The unweighted pair group method with arithmetic mean (UPGMA) was applied for clustering. Richness and diversity statistics were calculated from the DGGE profiles of the planktonic and sessile communities by using the number and intensity of the bands in each profile. Phylotype richness (***S***) was calculated as the total number of distinct bands in a DGGE profile. The Shannon-Weiner diversity index (***H***) was calculated considering the proportion of an individual band intensity relative to the sum of all band intensities. Simpson´s index of diversity was calculated from the equation $\boldsymbol{D} = 1 - \Sigma (p_i)^2$ (where pi is the relative intensity of band *i*)[9].

Identification of bacteria. DNA from isolated colonies formed on nutrient agar plates was extracted by suspending, with the aid of an inoculating loop, a colony in 1 mL of sterile distilled water and boiling for 10 min., centrifuged at 13,000 g for 5 min and the supernatant was transferred to a new tube. PCR amplification of almost the whole 16S rRNA gene sequence was carried out using the primers 27F and 1541R. The PCR product was purified and sequenced by MACROGEN (Korea). Sequence data were compared for initial identification, with the closest relatives represented by the retrieved sequences obtained from homology searches using the Blast algorithm at the NCBI (http://www.ncbi.nlm.nih.gov/blast/).

RESULTS AND DISCUSSION

Sessile total and arsenic-resistant bacterial counts. Bacterial biofilms developed on all the tested materials in the presence and in the absence of As (**Figure 1**). However, two features can be pointed out. On one side, the influence of the substrate nature: biofilms developed on Fe and Zn exhibited the highest counts, while biofilms on Cu and PP were one or two orders of magnitude lower. These results are in agreement with the observations made by other authors who found that the number of bacteria attached to iron or steel was higher than that on plastic or copper pipes[9]. On the other side, the influence of the As: higher bacterial counts were found in biofilms developed in the As-containing water except in the case of Cu. Biofilm formation allows microorganisms to survive in the presence of contaminants. In the present case, this hypothesis seems to be confirmed by the higher bacterial counts in those coupons exposed to arsenic-

containing water, except in the case of Cu. Furthermore, the low counts obtained on Cu in both systems could be related to the release of toxic copper ions.

Culturable As-tolerant bacteria were obtained from all the biofilms. These bacteria were able to grow in the presence of up to 1gL^{-1} of As(V) except bacteria from Cu-biofilms which could grow up to 300 mgL^{-1} . Arsenic-resistant bacteria have been isolated from both, arsenic rich environments and arsenic-free ones[10]. In our case, we found arsenic resistant bacteria in both systems, with a higher number in the biofilms formed in the arsenic-containing water, indicating a degree of adaptation.

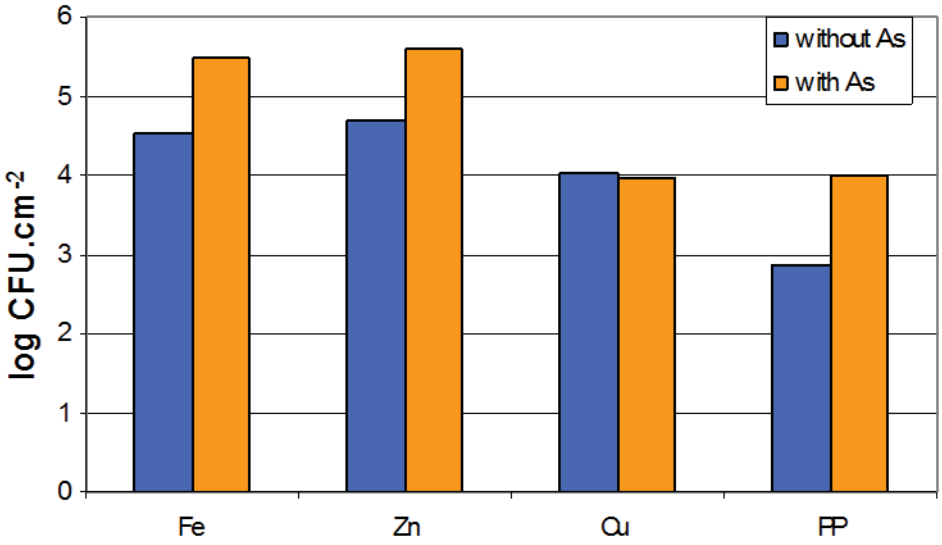


FIGURE 1. Heterotrophic sessile bacteria counts (Log CFU cm^{-2}) of the biofilms formed on the four substrata (Fe, Zn, Cu and PP) in water, with or without 5 mg L^{-1} As(V).

Bacterial community characterization. Direct PCR-DGGE based on the 16S rRNA gene of the planktonic and sessile DNA allowed a description of the structure of microbial communities developed in the water and in the biofilms, respectively. **Figure 2** illustrates the DGGE band patterns corresponding to the planktonic communities presented in both circuits at the end of 7 independent experiments. It can be seen that each sample produced a distinctive DGGE profile, with different number of bands with diverse position and intensity. At the beginning of each experiment, both circuits were filled with the same water source, then As(V) was supplemented in one of them, thus the same populations were originally present in both circuits. The different profiles at the end of each experiment indicated that the presence of arsenic induced qualitative (band position) and quantitative (band intensity) changes in the microbial community.

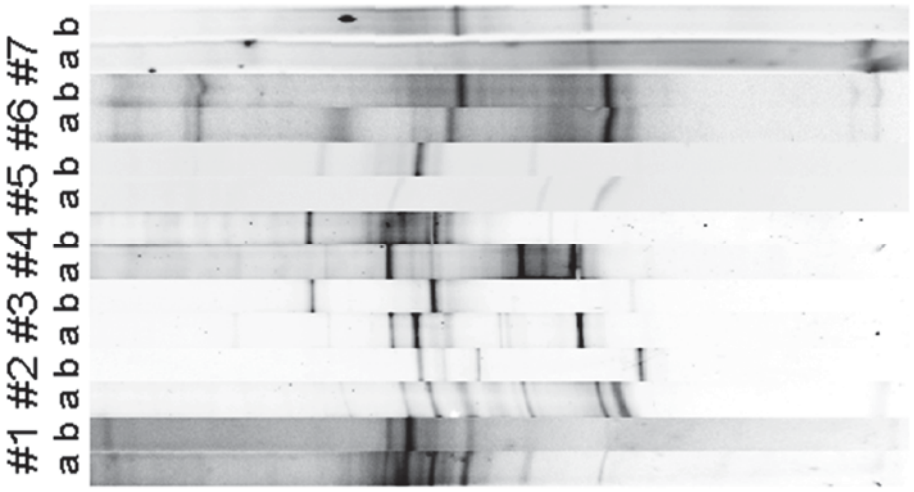


FIGURE 2. DGGE profiles of amplified bacterial 16S rDNA fragments from the planktonic communities in: (a) the circuit without As(V); and (b) with 5 mg/L As(V) in 7 independent experiments.

The DGGE profiles of the biofilms formed on the four materials assayed in the presence and in the absence of As in several independent experiments are shown in Figure 3. All the samples generated a different profile, but several bands were detected in most of the biofilms **(Figure 3**, green arrows), while others were detected in one simple only (blue arrows).

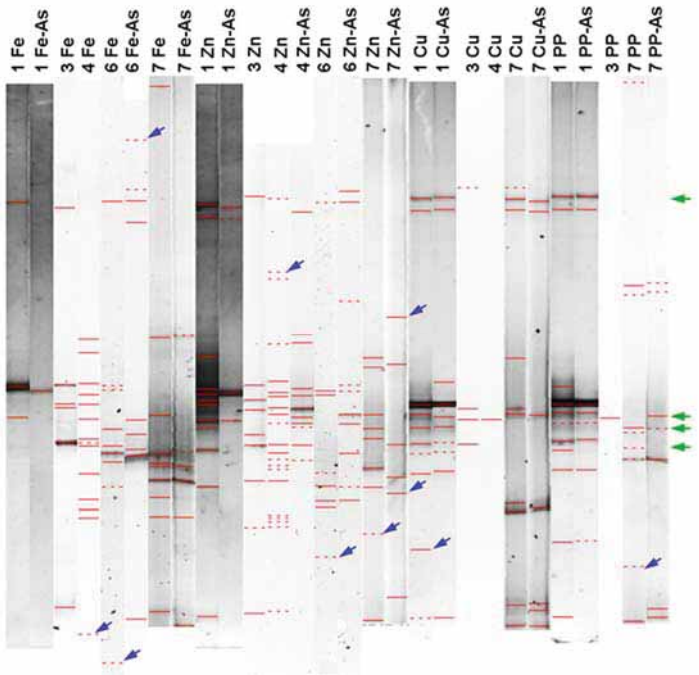


FIGURE 3. DGGE profiles of biofilms growth in presence and absence of As(V) on Fe, Zn, Cu and PP. in seven independent experiments. Green arrows: bands present in all the communities; blue arrows: bands present in one community.

As can be noticed in **Figure 3**, it was not possible to obtain DNA from all the biofilms in all the experiments. Only in experiments 1 and 7 all the profiles could be obtained. The clustering analysis of the 8 profiles in these two experiments was performed (Figure 4). The result shows a clear trend for biofilms formed on a particular material to cluster together with a high similarity regardless the presence of arsenic in the liquid phase. This finding indicated that the nature of the substrata was a more important factor for the establishment of the sessile community than the presence of arsenic. It has been reported that surface properties affected biofilm community composition[11]. Certain materials can release different compounds that can influence biofilm development[12]. In our case, the community profile developed on different materials differed as well as the magnitude of the attack produced on the substrata[13]. A high similitude amongst the established community on the materials less susceptible to bacterial attack (PP and Cu) was observed. These results suggested that a relationship could exist amongst the established community and its deterioration effect on the substratum.

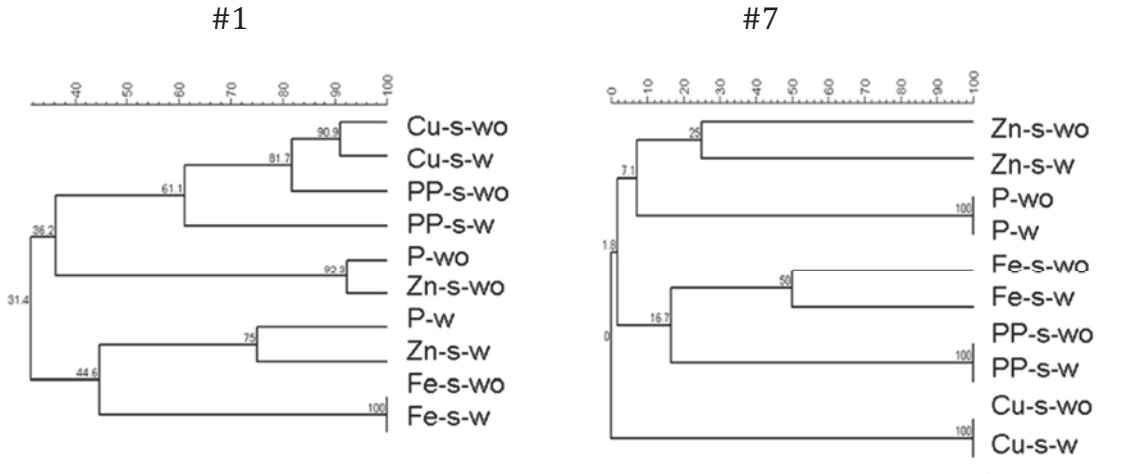


Figure 4. Clustering analysis of the Planktonic (P) and Sessile (s) communities formed on the four materials assayed (Fe, Zn, Cu and PP) in both circuits: with As (w) or without As (wo) in experiments 1 and 7.

DGGE provides an indication but not an absolute measure of the degree of biodiversity in a bacterial community. However, based on the number and intensity of the bands and using of appropriate software, it was possible to obtain richness (S) and diversity (H, D) indices of all the samples (**Table 1**). In general, the planktonic community developed in the water without As showed higher richness and diversity indices, indicating that the presence of a toxic element induced a selection of the species in the water with Arsenic. In the case of the sessile communities, the trends were not so clear. Most of the biofilms gave H and D indices between 2 and 3, values normally found for biofilms formed in water[9], however biofilms with high (H>3 and D close to Dmax), and very low diversity (S=1 and D= 0, only one band) were found.

TABLE 1. Richness (S) and Diversity (H, D) indices for planktonic and sessile communities in different experiments

Planktonic Samples				
Experiment	Richness (S)	Shannon-Weiner Diversity (H)	Simpson diversity (D)	D_{max}
1	10	2.9	0.8	0.9
1-As	5	1.9	0.6	0.8
2	11	3.0	0.8	0.9
2-As	6	2.0	0.7	0.8
3	10	2.5	0.7	0.9
3-As	4	1.4	0.5	0.7
4-As	17	3.6	0.9	0.9
5	18	3.7	0.9	0.9
5-As	5	1.0	0.3	0.8
6	13	3.3	0.8	0.9
6-As	11	3.1	0.8	0.9
7	9	2.8	0.8	0.8
7-As	4	1.5	0.6	0.7
Biofilm Samples				
Experiment	Richness (S)	Shannon-Weiner Diversity (H)	Simpson diversity (D)	D_{max}
1-Fe	3	0.8	0.2	0.6
1-Zn	12	3.5	0.9	0.9
1-Cu	10	2.9	0.8	0.9
1-PP	11	2.9	0.8	0.9
1-Fe-As	1	0	0	0
1-Zn-As	4	1.0	0.3	0.7
1-Cu-As	10	2.5	0.7	0.9
1-PP-As	8	2.2	0.6	0.8
2-Fe	6	2.0	0.6	0.8
2-Zn	9	2.7	0.8	0.8
2-Cu	4	1.5	0.6	0.7
2-PP	1	0	0	0
3-Fe	14	3.5	0.9	0.9
3-Zn	22	3.6	0.8	0.9
3-Cu	1	0	0	0
3-Zn-As	11	2.9	0.8	0.9
5-Fe	9	2.7	0.8	0.8
5-Zn	8	2.8	0.8	0.8
5-Fe-As	9	2.5	0.7	0.8
5-Zn-As	10	2.7	0.7	0.9
7-Fe	9	2.9	0.8	0.8
7-Zn	9	2.7	0.8	0.8
7-Cu	10	3.1	0.8	0.9
7-PP	9	2.6	0.7	0.8
7-Fe-As	6	2.3	0.7	0.8
7-Zn-As	6	2.4	0.8	0.8
7-Cu-As	7	2.7	0.8	0.8
7-PP-As	7	2.4	0.7	0.8

Regarding the nature of the surface, biofilms formed on Zn had the highest diversity indices. Thus this substrate gave the biofilms with the highest number of bacteria and the highest number of bacterial species. However, there is not direct correlation between bacterial counts and diversity. For instance, biofilms formed on Cu and PP gave low bacterial counts and their diversity indices were similar to that found in the others surfaces.

Identification of bacteria. Among all the colonies obtained in nutrient agar plates seeded with the scrapped biofilm, 60 isolates could be identified through the amplification on the 16SrRNA gene (34 of them were already included in the GeneBank under the accession numbers KM349185- KM349219). The bacteria identified belong to genus normally found in water distribution systems[14]. Bacteria belonging to the Class Bacilli (genus *Bacillus, Paenibacillus* y *Staphylococcus)* and α-Proteobacteria (*Brevundimonas*, *Sphingomonas*) were found in all the biofilms, Actinobacteria (*Kokuria, Micrococcus, Janibacter*) were found in biofilms formed on Cu and PP without As, β-Proteobacteria (*Delftia*, *Acidovorax)* were found in biofilms in the As containing water and γ-Proteobacteria (*Acinetobacter*) detected only in biofilms formed on Zn in the absence of As (**Figure 5**).

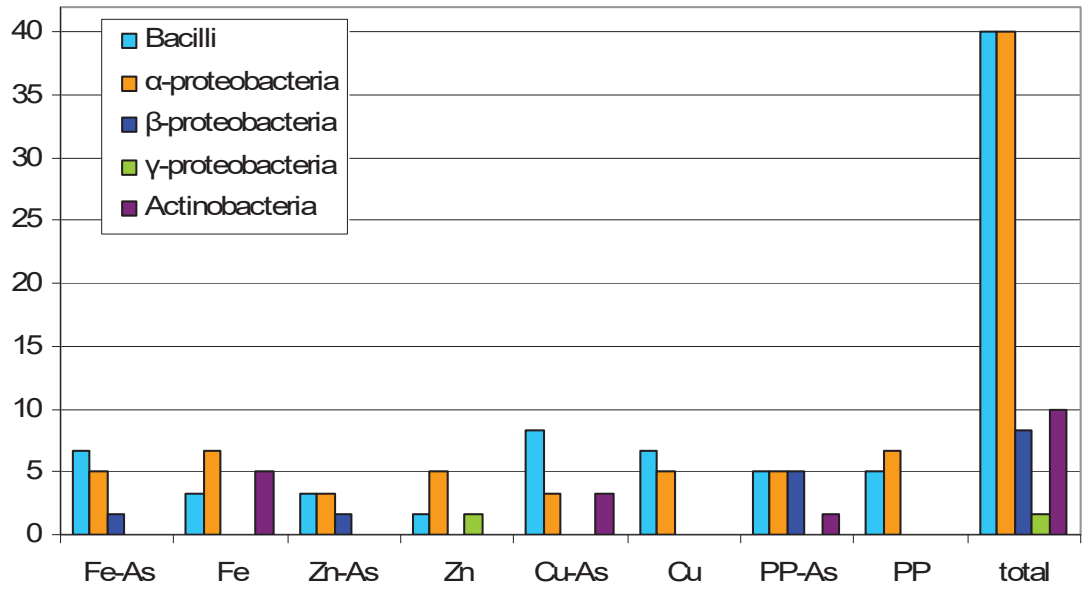


FIGURE 5. Abundance (in percentage) of the different bacterial Classes found on all the materials assayed (Fe, Zn, Cu and PP) in absence or presence of 5 mg.L^{-1}As(V) in the water

CONCLUSION

Bacteria could form biofilms on all the materials tested. The number of bacteria attached to Fe and Zn were higher than those found on Cu and PP. Slightly higher values were found for biofilms developed in the As-containing water, except in the case of biofilms formed on Cu. Culturable As-tolerant bacteria were obtained from most of the biofilms originated in both circuits.

The presence of As(V) in the water induced qualitative and quantitative changes in the planktonic bacterial community. In general, the planktonic community developed in the water without As showed higher richness and diversity indices, indicating that the presence of a toxic element induced a selection of the species. However, for the establishment of the sessile community, the nature of the substrata resulted in a more important factor than the presence of arsenic.

ACKNOWLEDGMENTS

Financial support for this work from the governmental Agencia Nacional de Promoción Científico-Tecnológica, PICT 38380, is gratefully acknowledged.

REFERENCES

1. Dexter S. Microbiologically Influenced Corrosion. In Cramer S., Covino Jr. B, Handbook. Corrosion: Fundamentals, Testing and Protection (2003)
2. Berry D., Xi C., Raskin, L. Microbial ecology of drinking water distribution systems. Curr. Opin. Biotech. 17 (2006) 297-302.
3. Pérez Carrera A., Fernández Cirelli A. Arsenic concentration in water and bovine milk in Cordoba, Argentina. Preliminary results. J. Dairy Res. 72 (2005) 122-124.
4. Takeuchi M., Kawahata H., Gupta L., Kita N., Morishita Y., Ono Y., Komai, T. Arsenic resistance and removal was evaluated in nine bacterial strains of marine and non-marine origins. J. Biotechnol. 127 (2007) 434-442.
5. Rasmussen L., Sörensen S. Effects of mercury contamination on the culturable heterotrophic, functional and genetic diversity of the bacterial community in soil. FEMS Microbiol. Ecol. 36 (2001) 1-9.
6. Li Z., Xu J., Tang C., Wu J., Muhammad A., Wang H. Application of 16S rDNA-PCR amplification and DGGE fingerprinting for detection of shift in microbial community diversity in Cu-, Zn-, and Cd-contaminated paddy soils. Chemosphere 62 (2006) 1374-1380.
7. Green S., Leigh M., Neufeld, J. Denaturing gradient gel electrophoresis (DGGE) for microbial community analysis. In: Timmis K., Microbiology of Hydrocarbons, Oils, Lipids, and Derived Compounds (2009)
8. Roeder R., Lenz J., Tarne P., Gebel J., Exner M., Szewzyk U. Long-term effects of disinfectants on the community composition of drinking water biofilms. Int. J. Hyg. Envir Heal. 213 (2010) 183-189.
9. Yu J., Kim D., Lee T. Microbial diversity in biofilms on water distribution pipes of different materials. Wat. Sci. Technol. 61 (2010) 163-171.
10. Drewniak L., Styczek A., Majder-Lopatka M., Sklodowska A. Bacteria, hypertolerant to arsenic in the rocks of an ancient gold mine, and their potential role in dissemination of arsenic pollution. Environ. Pollut. 156 (2008) 1069–1074.
11. Iasur-Kruh L., Hadar Y., Milstein D., Gasith A., Minz D. Microbial Population and Activity in Wetland Microcosms Constructed for Improving Treated Municipal Wastewater. Microbial Ecol. 59 (2010) 700-709.
12. Lehtola M., Miettinen I., Keinänen M., Kekki T., Laine O., Hirvonen A., Vartiainen T., Martikainen P. Microbiology, chemistry and biofilm development in a pilot drinking water distribution system with copper and plastic pipes. Water Res. 38 (2004) 3769-3779.
13. Rastelli S., Rosales B., Viera M., Elsner C. Bacterial biofilms formed in arsenic-containing water: Biodeterioration of water network materials. J. Water Supply Res. Technol. AQUA 64 (2015) 738-748.
14. Liu R., Zhu J., Yu Z., Joshi D., Zang H. Molecular analysis of long-term biofilm formation on PVC and cast iron surfaces in drinking wáter distribution system. J. Environ. Sci. 26 (2014) 865-874.

CHAPTER 6.2 EFECTO COMETABÓLICO EN LA BIOTRANSFORMACIÓN DE FENANTRENO POR TRES ZIGOMICETOS

J. C. Antonio Huerta; M. T. Rodríguez Casasola; C. Cruz Mondragón; E. Ríos Leal and F. J. Esparza García*

Centro de Investigación y Estudios Avanzados del Instituto Politécnico Nacional, Av. Instituto Politécnico Nacional núm. 2508, col. San Pedro Zacatenco, Delegación Gustavo A. Madero, México. Ciudad de México: código postal 07360. Tel (55) 57473800 ext. 4330.

RESUMEN

Se estudió la capacidad de biotransformación del fenantreno en compuestos más polares y en el efecto de detoxificación cometabólica por los hongos *Cunninghamela blakesleeana var. Elegans* CDBB-H-256, *Mucor hiemalis* CDBB-H-286, *Mucor rouxii* CDBB-H-288. Se realizaron experimentos en cultivo líquido a diferentes tiempos de incubación, se determinó biomasa en base seca, se analizaron por cromatografía en capa delgada el fenantreno residual y los productos formados más polares. Se determinaron los subproductos encontrados en la biotransformación como el 9-fenantrol mediante HPLC-DAD y CGMS.

Palabras claves: biotransformación, cometabolismo, fenantreno

INTRODUCCIÓN

Los hidrocarburos aromáticos policíclicos (HAP) son compuestos que están formados por átomos de carbono e hidrogeno, agrupados en anillos aromáticos de 5 o 6 átomos de carbono. Los HAP son generados durante la combustión incompleta del carbón, aceites, madera, residuos domésticos y en general de sustancias de origen orgánico. Se encuentran de forma natural en el petróleo, carbón, alquitrán y como productos de la utilización de combustibles. El interés de estos compuestos es debido a que algunos de estos han sido identificados como mutagénicos. Además, sus características lipofílicas permiten la bioacumulación en mamíferos.

El fenantreno (**Figura 1**) es un HAP tricíclico, cristalino, incoloro, con olor débil. Se usa en la fabricación de pinturas, explosivos, drogas y en la investigación biológica. Es el más simple de los HAP que contienen las regiones K y bahía de estructura.

La región de bahía se forma entre los carbonos 4 y5, mientras que la región K se forma entre los carbonos 9 y 10. La importancia de estas regiones estriba en el hecho de que el ataque microbiológico es específico en alguna de ellas dependiendo del microorganismo y de la enzima producida[1].

---

*Author for correspondence: fesparza@cinvestav.mx

Su presencia en mamíferos no es mutagénica, pero su exposición provoca irritación en la piel, ojos, y vías respiratorias[2]. El fenantreno está clasificado por la International Agency for Research on Cancer (IARC) en el grupo 2B como un compuesto posiblemente cancerígeno para los seres humanos[2].

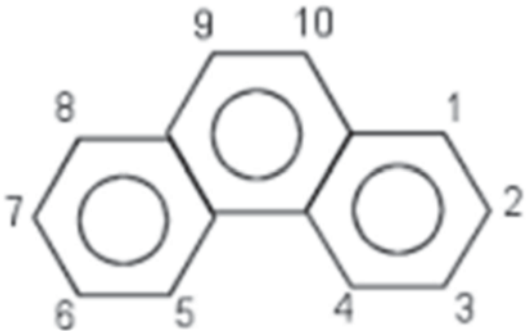


FIGURA 6. Estructura del fenantreno

Los microorganismos que metabolizan hidrocarburos producen por inducción una o varias enzimas con las que degradan o rompen algún enlace molecular de los compuestos hidrocarbonados y en algunos casos pueden utilizarlos como fuente de carbono[3]. En particular, en la biotransformación de hidrocarburos aromáticos policiclicos que es catalizada por monooxigenasas, se incluyen la eliminación de hidrógeno e inserciones de oxígeno, lo cual puede inducir posteriormente a la apertura de los anillos aromáticos[4]. Los HAP y otros contaminantes ambientales tóxicos se han transformado exitosamente por monooxigenasas y epóxidohidrolasas que se han aislado de hongos, bacterias y células vegetales en ensayos realizados bajo condiciones de laboratorio controladas[5].

Los hongos zigomicetos *Cunninghamella* (**Figura 2**) y *Mucor* (**Figura 3 y 4**) son típicamente saprobios, presentan reproducción asexual (esporangiosporas o conidiosporas) y sexual (fusión de gametangios). La formación de micelio es profusa y se constituye por numerosas hifas sin septas[6]. En el ápice del túbulo germinal se lleva a cabo la síntesis de nuevo material celular y en ocasiones, se forman estructuras esféricas llamadas esporangios, las cuales en su interior contienen esporangiosporas que después en su madurez son liberadas[7, 8, 9].

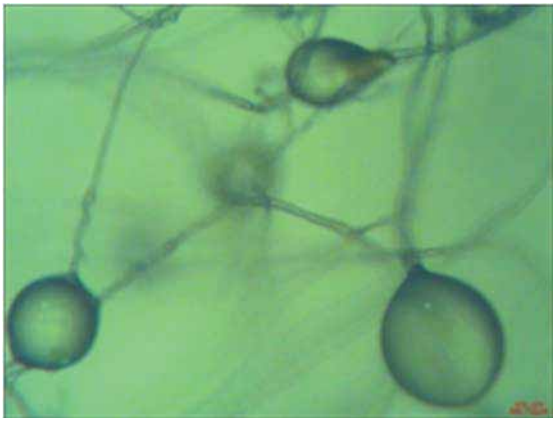


FIGURA 7. *Cunninghamella blakesleeana var. elegans* CDBB-H- 256

En la **Figura 2** se observa el hongo *Cunninghamella blakesleeana*, que presenta hifas cenocíticas con esporangios con conidios esféricos sobre pedicelos cortos, implantados sobre vesículas globosas terminales, se originan en el extremo de un conidióforo.

En la **Figura 3** se observa a *Mucor hiemalis* que presenta hifas cenocíticas delgadas con esporangioforos sencillos con aplanósporas que se presentan en cualquier sitio del micelio.

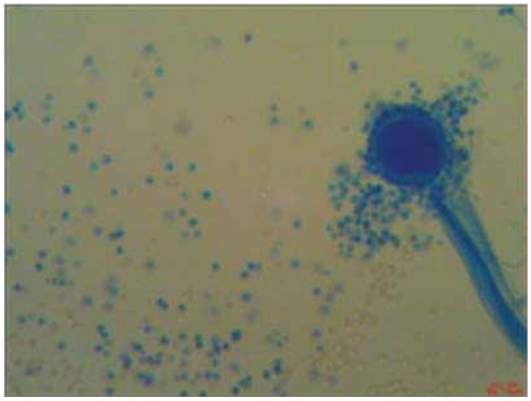


FIGURA 3. *Mucor hiemalis* CDBB-H- 286

La **Figura 4** muestra a *Mucor rouxii* que presenta también hifas cenocíticas delgadas con esporangioforos sencillos con aplanósporas que se presentan en cualquier sitio del micelio.

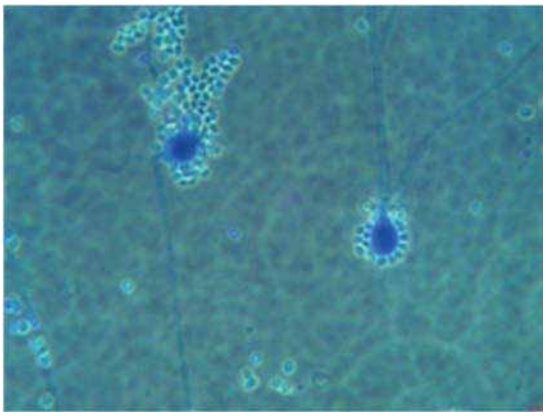


FIGURA 4. *Mucor rouxii* CDBB-H- 288

MATERIALES Y MÉTODOS

Concentración del contaminante. Se preparó una solución de fenantreno al 10% en etanol, de esta solución se añadieron las diferentes alícuotas a matraces con medio de cultivo para obtener una concentración de 200 mg/L de fenantreno[10].

Suspensión de esporas. Se preparó un "stock" de esporas de un cultivo en botella de 1L de donde fueron separadas las esporas con la ayuda de un "scraper" estéril, agregando 30 mL de agua destilada estéril. Se realizo la cuenta de esporas en cámara

de Neubauer obteniendo: 8 * 10^7 esporas/mL de *Mucor hiemalis*, 4.5 * 10^7 esporas/mL de *Mucor rouxii* y 8.75 * 10^7 esporas/mL de *Cunninghamella blakesleeana* (Ramírez, 2000).

Cultivo liquido de los tres zigomicetos. Se inoculo con 0.5 mL de la suspensión de esporas de *Mucor hiemalis*, *Mucor rouxii* y *Cunninghamella blakesleeana* en matraces de 125 mL con 25 mL de medio liquido YPG modificado (extracto de levadura, 3g; peptona de carne, 10g; glucosa, 20g, en 1 litro de agua destilada) Se dejaron incubar durante 24 horas a una temperatura de 30 °C con agitación de 150 rpm, posteriormente se adiciono fenantreno disuelto en etanol a una concentración final de 200 mg/L; además se utilizaron testigos sin fenantreno. Finalmente fueron incubados a 0, 24, 48 y 72 horas a las mismas condiciones previas[10].

Cultivo liquido de Cunninghamella blakesleeana y cinética de crecimiento. Se inoculo con 0.375 mL de la suspensión de esporas de *Cunninghamella blakesleeana* en matraces de 125 mL con 25 mL de medio liquido YPG modificado (extracto de levadura, 3g; peptona de carne, 10g; glucosa, 20g, en 1 litro de agua destilada) Se dejaron incubar durante 24 horas a una temperatura de 30 °C con agitación de 150 rpm, Posteriormente se adiciono fenantreno disuelto en etanol a una concentración final de 200 mg/L; además se utilizaron testigos sin fenantreno. Finalmente fueron incubados a 0, 8, 24, 48, 72, 96 y 120 horas a una temperatura a las mismas condiciones previas[10].

Para la determinación del crecimiento de los hongos, se midió biomasa en base seca en filtros de nailon Millipore de 0.45 µm de diámetro de poro[11]. También se efectuó una extracción liquido-liquido para obtener el fenantreno y sus subproductos del caldo de cultivo utilizando 50 mL de cloroformo 99.9% puro (J.T. BAKER).

Cromatografía de gases acoplada a espectrómetro de masas (GC-MS). Se analizaron las muestras y los blancos obtenidos por la extracción liquido-liquido por GC-MS, además de los estándares de fenantreno (Sigma-Aldrich) y 9-fenantrol (Sigma-Aldrich).

Los extractos obtenidos del caldo de cultivo se llevaron a sequedad y el residuo se resuspendió con 5 mL de cloroformo. Para el análisis en (GC-MS) se concentraron en 100 µL de cloroformo, en las siguientes condiciones de operación:

TABLA 1 Condiciones de operación (GC – MS)

Cromatografía de gases	Espectrómetro de masas
Temp. Inyector: 250 °C Programa Temp: 120 °C – 3 min – 8 °C/min – 280 °C – 5 min Flujo He: 0.8 mL/min	Inlet Temp: 200 °C Source Temp: 180 °C Solvent Delay: 3 min MS SCAN: 30 – 500 (m/z)

Utilizando una columna Perkin Elmer Elite – 5MS 30 x 0.32 x 0.25

RESULTADOS Y DISCUSIÓN

Los resultados de las cinéticas de crecimientos fueron los siguientes:

La **Figura 5** muestra el crecimiento de los tres hongos zigomicetos; durante un periodo de 72 horas, temperatura de incubación de 30 °C, agitación de 150 rpm y sin la adición de fenantreno.

En la cual se observa el crecimiento normal de los tres hongos, teniendo como el punto de mayor cantidad de biomasa a las 48 horas, también se puede apreciar que a las 72 horas los tres hongos entran en la fase de muerte, al ver una disminución en la cantidad de biomasa debido al posible lisamiento del micelio.

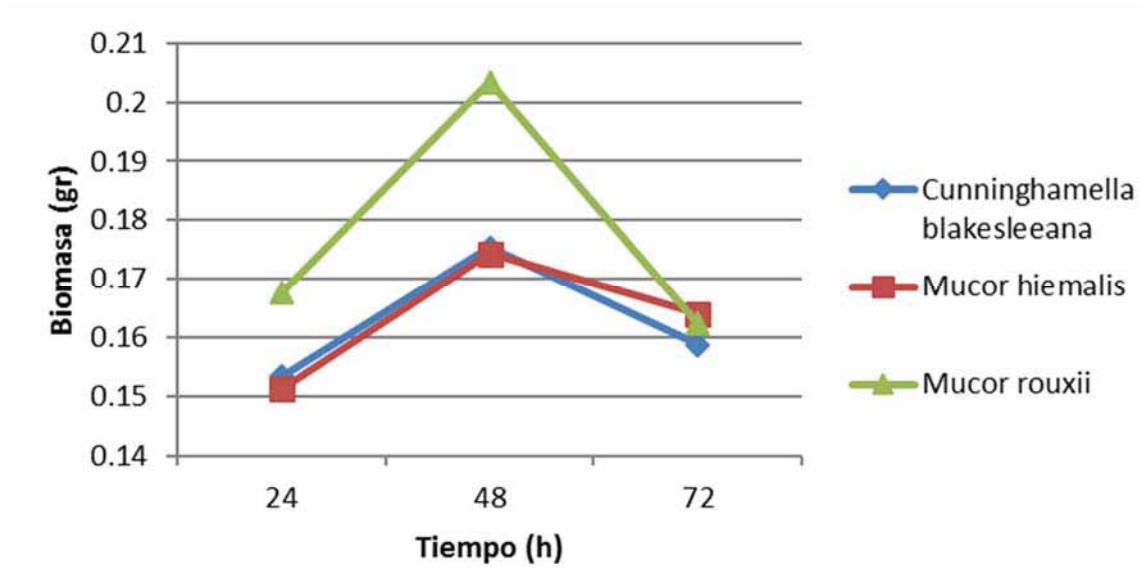


FIGURA 5. Cinética de crecimiento de tres hongos, en medio de cultivo YPG con una duración de 72 horas a las condiciones de 30 °C, agitación de 150 rpm, sin adición de fenantreno

En la **Figura 6** se muestra el crecimiento de los tres hongos zigomicetos; durante un periodo de 72 horas, temperatura de incubación de 30 °C, agitación de 150 rpm con la adición de fenantreno disuelto en etanol.

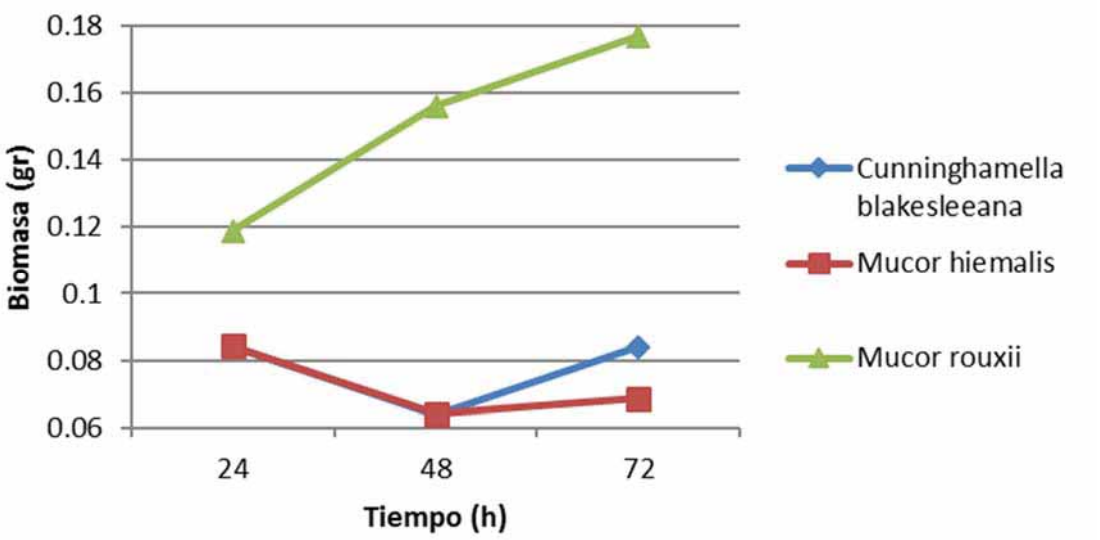


FIGURA 6. Cinética de crecimiento de tres hongos, en medio de cultivo YPG con una duración de 72 horas a las condiciones de 30 °C, agitación de 150 rpm, con adición de fenantreno

Se observa que la adición de fenantreno disuelto en etanol, provoca una inhibición en el crecimiento de los tres hongos (**Tabla 2**).

El fenantreno es el causante principal de la inhibición de crecimiento para el hongo *Cunninghamella blakesleeana*, mientras que para *Mucor hiemalis* y *Mucor rouxii* a pesar de que el fenantreno también causa inhibición en el crecimiento, para estos hongos la principal causa de la inhibición es el etanol[13].

TABLA 2. Porcentajes de inhibición en crecimiento para los tres hongos

Cunninghamella blakesleeana	***Mucor hiemalis***	***Mucor rouxii 48 hrs***
47 %	58.1%	23.3 %

También se puede apreciar que después de 48 horas, los hongos *Cunninghamella blakesleeana* y *Mucor hiemalis* tienen una recuperación en su crecimiento debido a la detoxificación que realizan al fenantreno. En el caso de Mucor rouxii se sabe que también realiza la detoxificación pero que esta la empieza a realizar en un tiempo aproximado de 2 horas[13].

La **Figura 7** muestra la cinética de crecimiento de *Cunninghamella blakesleeana* en medio YPG con un tiempo de incubación de 120 horas, 30 °C, 150 rpm, con y sin adición de fenantreno. Donde se aprecia una inhibición en el crecimiento cuando se adicionó el fenantreno.

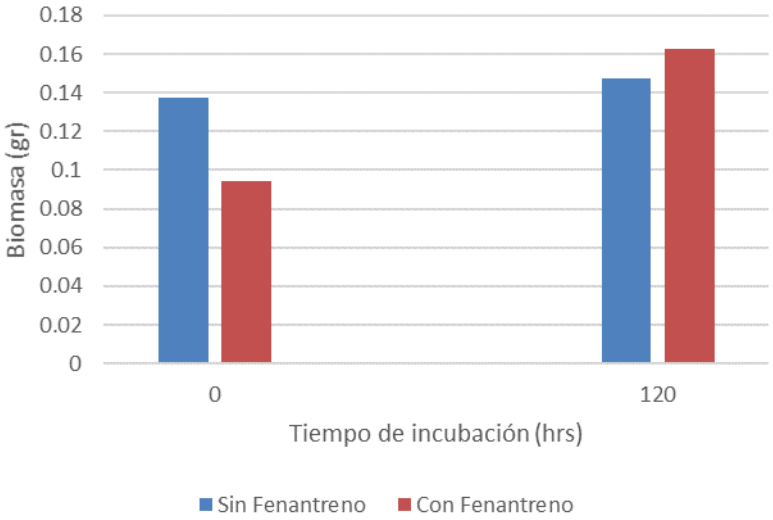


FIGURA 7. Valores de cinética de crecimiento de *Cunninghamella blakesleeana*, en medio de cultivo YPG, en los tiempos de 0 y 120 horas a las condiciones de 30 °C, agitación de 150 rpm, con y sin adición de fenantreno.

Los resultados de la cromatografía de gases acoplada a espectrómetro de masas (GC-MS) fueron los siguientes:

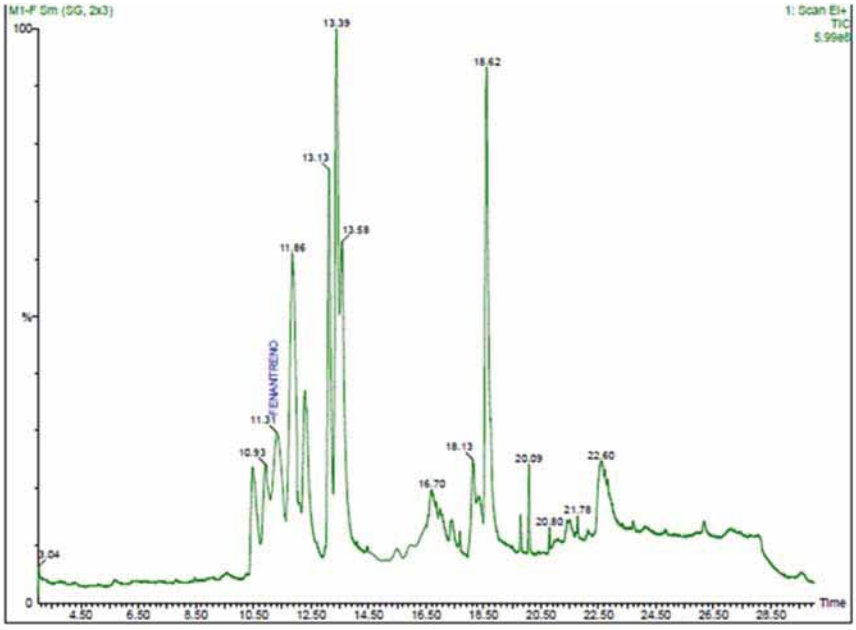


FIGURA 9. Cromatograma de muestra con fenantreno a las 0 horas

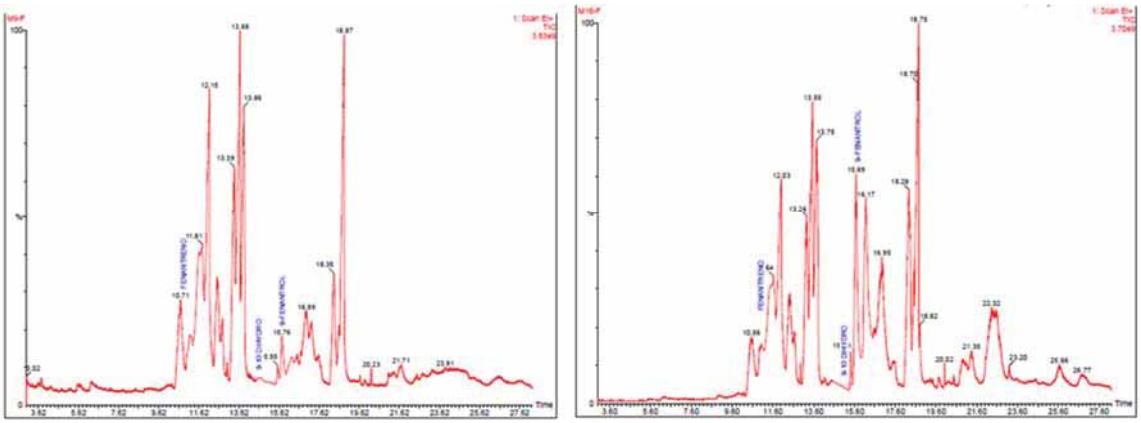


FIGURA 10. Cromatogramas de muestra con fenantreno a las 48 y 120 horas respectivamente

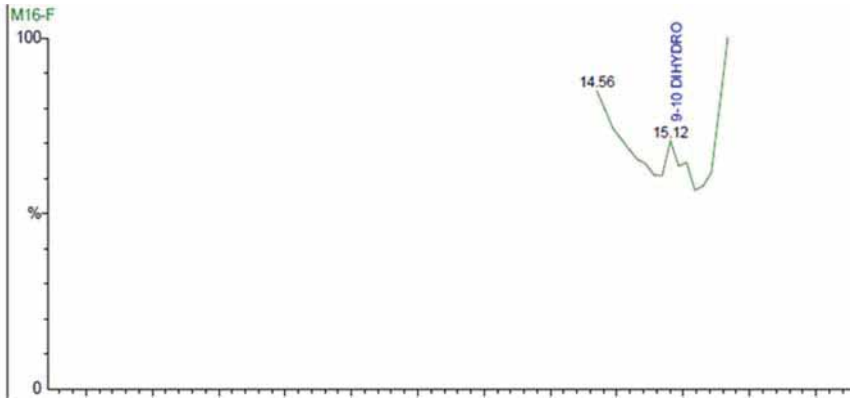


FIGURA 11. Segmento SIR que describe el compuesto 9-10 Dihidroxy Fenantreno al tiempo de 120 horas

En la **Figura 9** se observa el cromatograma de la muestra al tiempo de 0 horas, en el cual se aprecia solamente la presencia de fenantreno. Para el cromatograma a las 48 horas (**Figura 10**) se observa la aparición de 9 – Fenantrol y del 9 – 10 Dihidroxy Fenantreno, apareciendo este último en una cantidad mínima. Por último, el cromatograma de las 120 horas muestra un aumento significativo de 9 – Fenantrol paralelamente de una disminución del Fenantreno inicial, corroborando así la capacidad de biotransformación del fenantreno por *Cunninghamella blakesleeana.*

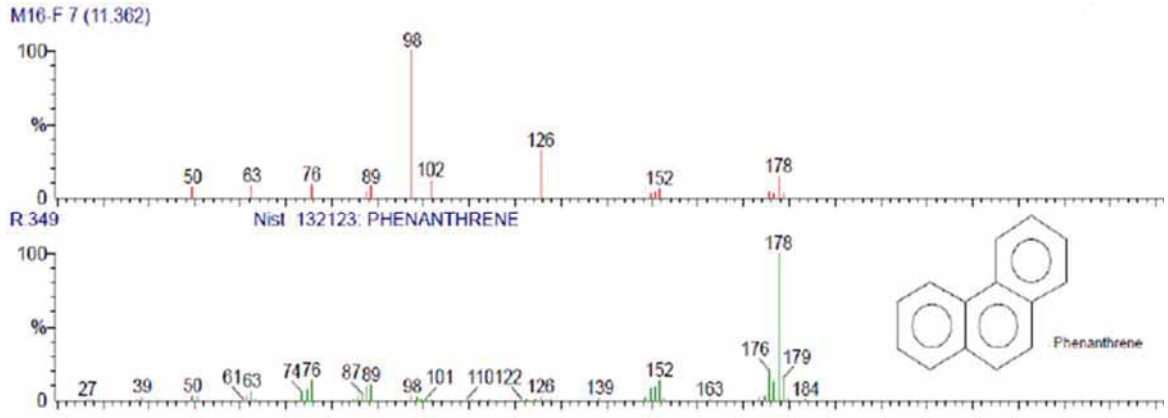


FIGURA 12. Espectro de masas de fenantreno a las 120 horas

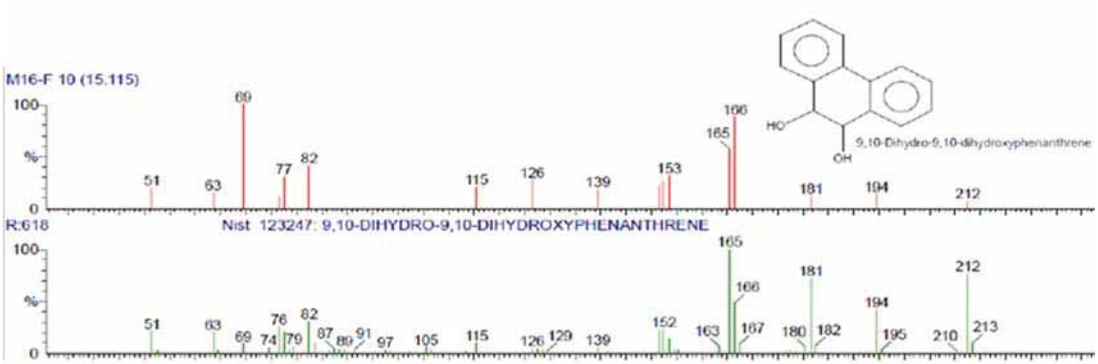


FIGURA 13. Espectro de masas de 9-10 Dihidroxy Fenantreno a las 120 horas

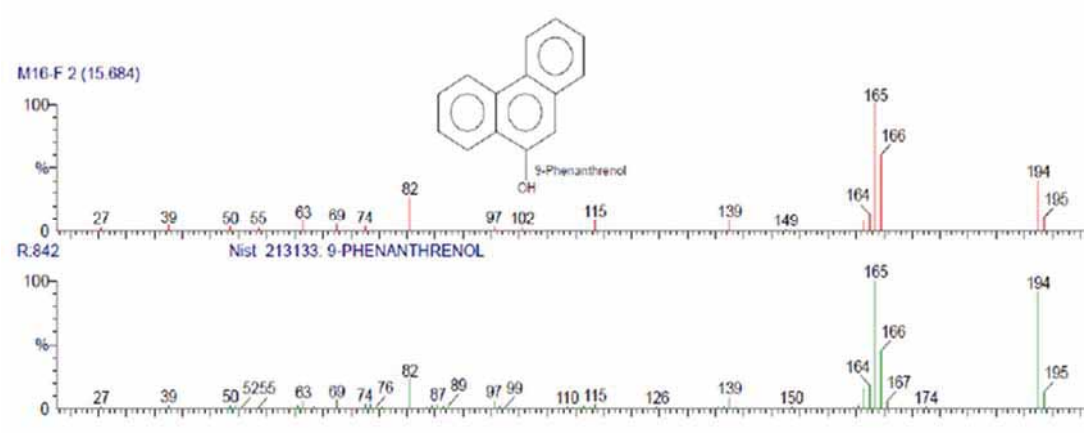


FIGURA 14. Espectro de masas de 9- Fenantrol a las 120 horas

El segmento SIR (**Figura 11**) corrobora la presencia de 9 – 10 Dihidroxy Fenantreno, en la muestra de 120 horas. Recordando que este compuesto puede ser un intermediario en la ruta de hidroxilación del fenantreno a través de la formación del epóxido[12].

Los espectros de masas (**Figuras 12, 13** y **14**) validan los subproductos de la biotransformación: 9 – Fenantrol y 9 – 10 Dihidroxy Fenantreno.

CONCLUSIÓN

En base a la investigación presentada, la molécula de fenantreno penetra al micelio de *Cunninghamella blakesleeana* para ser biotransformada según se muestra en los ensayos de biotransformación por medio de las células miceliares de *Cunninghamella blakesleeana,* esta biotransformación es realizada como una detoxificación del fenantreno para obtener subproductos más polares que son menos tóxicos para el microorganismo.

Dichos subproductos son excretados al caldo de cultivo; los productos de la biotransformación 9 –Fenantrol y 9 – 10 Dihidroxy Fenantreno, así como el Fenantreno residual (sustrato sin biotransformar) permanecen en el caldo de cultivo como se

demostró en los análisis cromatográficos por cromatografía de gases acoplada a espectrómetro de masas.
Los espectros de los subproductos validan las estructuras de los mismos comprobando que el hongo *Cunninghamella blakesleeana* tiene un cometabolismo con la capacidad enzimática de biotransformar el fenantreno y su detoxificación a las condiciones de incubación ensayadas.

AGRADECIMIENTOS

Al I.Q.I. Gustavo Gerardo Medina Mendoza, por su apoyo técnico en la técnica de cromatografía. A la Ing. Sara Vera G y a la Ing. Adriana Vázquez M. por su apoyo técnico durante la elaboración del experimento.

REFERENCIAS

1. Ortiz A. Biodegradacion de hidrocarburos en suelos: Efecto de la adicion de cosubstratos gaseosos. Tesis que para obtener el grdo de Doctor en Ciencias, Universidad Autonoma Metropolitana-Iztapalapa. Divisionde Ciencias Basicas e Ingenieria, México 2004, págs. 34,36.
2. Federación de la Industria (2010). *Los hidrocarburos aromaticos policiclicos (HAP). Acercamiento a su problemática como riesgo laboral*. España: Antonio Agudo
3. Bollag W., Bollag J. Biodegradation. *Enciclopedia of microbiology*. Chapter 1, 1992 págs. 269-385.
4. Zazueta R. Oxigenasas paso inicial en la Biodegradación de Hidrocarburos por la cepa YR-¡ de *Mucor circinelloide*. Ide@s CONCYTEG año 3 Núm. 37, 2008, págs. 38,39
5. Guerrero A. Efecto de la Presencia de Fenantreno sobre la Expresion de Proteinas y la Actividad Enzimatica Radical de *Cyperus hermaphroditus*. Polibotanica núm. 27, 2009 pág. 105.
6. Garcia C., Vera (2004). *Introducción a la microbiologia*. UENED. 2° edición. Costa Rica, 55-57. Guión y coordinación: Secretaría de Salus Laboral y Medio Ambiente, MCA-UGT.
7. Ulloa, M. (1978). *Atlas de microbiologia basica* 1° edición. México: Editorial Concepto, S.A.,45.
8. Pernia, Beatriz (2012). “Biodiversidad y potencial hidrocarbonoclástico de hongos aislados de crudo y sus derivados: un metaanálisis”. *Rev. Latinoam. Biotecnol. Amb. Algal*.,3(1),1-39.
9. Herrera Teofilo (2004). Reno de los hongos. Microbiología básica y aplicada. 2° edición. México: Fondo de Cultura Economica. 143-150. Disponible en: http://toxamb.pharmacy.arizona.edu(cl-2-6.html
10. Sánchez M., Rosalina (2011). “Analisis cromatografico de la biotrnsformacion del fenantreno por *Mucor rouxii* IM-80”. Tesis. México: Centro de Investigaciones y Estudios Avanzados del Instituto Politecnico Nacional.
11. Ramirez Gama. R. M. et al. (2000). *Manual de practicas de microbiologia general*. 1° edición. México: editora R. M. Ramirez Gama, 90-100.
12. Ouyang J., Phenanthrene Pathway Map. UM-BDD compunds ans reactions page for the Phenanthrene pathway. University of Minnesota.
13. Lopez R., Jorge Arturo (2013). “Efecto toxico del fenantreno y su detoxificación en cepas de hongos de los generos Mucor y Cunninghamella”. Tesis. México: Centro de Investigaciones y Estudios Avanzados del Instituto Politecnico Nacional.

CHAPTER 6.3 IDENTIFICATION OF IRON-REDUCING BACTERIA FROM RIVER SEDIMENTS BY 16S RRNA

A. M. Hernández Núñez (1); K. Juárez López (2); P. Pavón Orozco (1) and **A. C. Ortega Martínez** *(1)

(1) Facultad de Ciencias Químicas, Universidad Veracruzana, Av. Universidad km. 7.5. Col. Paraíso, Coatzacoalcos, Veracruz 96538, México.
(2) Departamento de Ingeniería Celular y Biocatálisis, Instituto de Biotecnología, Universidad Nacional Autónoma de México, Av. Universidad 2001. Col. Chamilpa, Cuernavaca, Morelos 62210, México.

ABSTRACT

Iron-reducing bacteria are microorganisms that utilize iron oxides or hidroxides as electron acceptors. Coatzacoalcos River is a high-polluted river located in southeast Mexico next to the main Latin-American oil industries. This river receives slurries as: organic matter, suspended solids, heavy metals (*e.g.* Fe^{+2}, Cu^{+2}, $Pb^{2+,4+}$) and organic compounds. In this work the bacteria species, from the C river sediments, were enriched and iron-selected for their molecular identification. The aim of this work is to identify the endogenous iron-reducing bacterial species present in the Coatzacoalcos River.

Keywords: 16S rRNA, bacteria, Coatzacoalcos, identification.

INTRODUCTION

Iron is the one of the most abundant elements in the Earth's crust, making up by mass up to 5.1%. In the environment, it is found in the trilavent (Fe^{3+}) and divalent (Fe^{2+}) state[1]. The change between Fe^{3+} and Fe^{2+} plays an important role in the redox processes in anoxic soils and sediments. Dissimilatory iron-reducing bacteria gain energy by coupling the oxidation of organic compounds or hydrogen and enzymatically catalyzing the reduction of iron oxides or hidroxides[2, 3]. The first system described was the aerobic acidophilic bacteria *Thiobacillus ferrooxidans*, which can grow in media with a pH of 1-2 in which ferric and ferrous iron exist as dissolved ions[4]. *Geobacter metallireducens* and *Shewanella putrefaciens* are too bacterial genuses that oxidize fatty acids, sugars, amino acids and aromatic compounds with iron as the electron acceptor[5]. Soil is considered as a complex environment, it is a big reservoir of microbial genetic diversity, sediments and soils can contain iron minerals at quantities in the range of several 10 mmol per kg dry matter, and ferric iron is by mass the most important electron acceptor in such environments. Only in marine sediments, the high sulfate content (28 mM in seawater) counterbalances the dominance of ferric iron as electron acceptor[6]. Coatzacoalcos River is located in southeast Mexico, a large-scale industrial development area, it receives slurries from different industries, which contain: heavy metals, suspended solids, organic compounds and organic matter; besides, in December 2011, a spill was reported; therefore, it is a high-polluted area. 16S rRNA is a

---

*Author for correspondence: areortega@uv.mx

1,550-nucleotide protein found in the bacterial ribosome's small subunit, it is known for its highly conserved regions[7]. In the past decade, applications of molecular biological methods for microbial identification have provided unique insights into the uncultured microbial communities of soil avoiding biases, as in traditional culture-based microbiological methods[11]. Molecular methods are increasingly being used to explore the microbial diversity of environmental systems without needing to isolate microorganisms from their natural environment, especially because many relevant organisms have proven difficult to isolate from their environmental sources. Recently, there has been an increase in the number of studies using a metagenomic approach to investigate the diversity, metabolic pathways and catalytic potential of uncultured microorganisms[10]. This work will help in the future understanding of microbial dynamics in this environment and its application to bioremediation techniques and its use in electrical cells.

MATERIALS AND METHODS

Culture conditions. Two sediment samples were withdrawal from Coatzacoalcos River, close to an oil-pipeline where a spill in 2011 was reported (18°03'45.3''N, 94°25'07.6''W). Sediment samples Cf1 and Cf2 were cultured in medium with 50 mM $FeH_5C_6O_7$ as electron acceptor and 20 mM CH_3COONa as electron donor. Bacteria were grown at 30°C under dark and anaerobic conditions in an 80% CO_2 - 20% N_2 atmosphere.

Nucleic acid preparation. Genomic DNA extraction was carried out by using standard methods[8]. Preparation of genomic DNA -from two serum bottles- consisted of resuspending a sample in 60 µl of 20% SDS solution for cell lysis and centrifuging it at 10,000 x g for 30 s. The supernatant was transferred to a new tube, and 250 µl of a high-concentration salt buffer was added for DNA precipitation. The precipitated was loaded in a spin column with a silica-based membrane and ethanol washed for DNA purification at 10,000 x g for 1 min. DNA was recovered with MilliQ water.

PCR amplification and purification of product. 4.5 µg of genomic DNA was amplified in a 300-µl reaction by using the Taq DNA polymerase kit. 16S rRNA was amplified using the 27F and 1492R primers[9]. Conditions consisted in 30 cycles of 94°C (1:30 min), 50°C (1:30 min) and 72°C (1:30 min), plus one additional cycle with a final 10-min chain elongation. Amplification was performed in a Bio-Rad T-100 thermal cycler. The amplicons were purified on a spin column with a silica-based membrane (ThermoScientific®) by following the specifications of the manufacturer.

Cloning. Cloning of purified PCR products was followed by using standard molecular biology protocols[8]. Amplicons were cleaved with a blunting enzyme at the appropriate termini, and ligated into pJET1.2 vector (ThermoScientific®). Plasmid was transformed by electroporation on *E. coli* MC1061 strain, plated on LB (Luria-Bertani) medium supplemented with 200 µg/ml ampicillin, and incubated at 37°C for 8 hours. Plasmid preparation was performed by the alkaline lysis method[12] and digestion was carried out with *XbaI* restriction endonuclease.

Sequencing and bacterial identification. Sequencing was carried out by Sanger dye-terminator method[13] at the Unit for DNA Sequence and Synthesis of Instituto de Biotecnología, UNAM. Chromatograms were exported to BioEdit[14] to get the consensus sequences. Analysis sequences were performed by blast on GenBank database (www.ncbi.nlm.nih.gov) and phylogenetic tree was constructed on JModel Test.

RESULTS AND DISCUSSION

Genomic DNA extraction was analyzed in a 1% agarose gel by electrophoresis and quantified by reading absorbance at 280 nm. Although the analysis on the NanoDrop showed that DNA had a low yield (4.5 µg each sample), it can be observed that it presented no degradation, which is important for DNA polymerase specificity in PCR[15] (**Figure 1**).

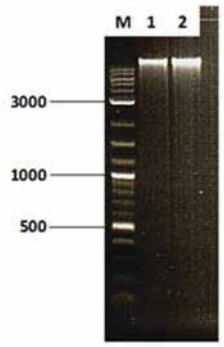


FIGURE 1. Genomic DNA in agarose gel electrophoresis (1%). Lane M: DNA ladder 10 kb. Lane 1: Cf1 DNA sample. Lane 2: Cf2 DNA sample.

PCR amplification showed bands of approximately 1,550 nucleotides, corresponding to the 16S gene as expected[7] (**Figure 2**). After cloning amplicons into pJET1.2 vector, recombinant DNA pJET_16SDNA (4,500 bp) was obtained. Then, competent *E. coli* MC1061 cells were transformed and plasmidic DNA extraction confirmed the presence of pJET_16SDNA transformants.

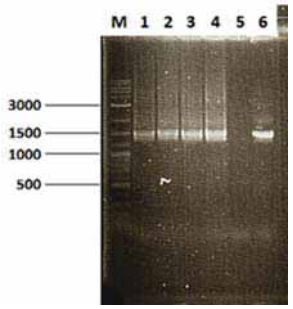


FIGURE 2. Amplification of 16S rDNA. Lane M: DNA ladder 10 kb. Lane 1-4: amplified 16S rDNA from Cf1 and Cf2 samples. Lane 5: negative control. Lane 6: positive control.

Then after, plasmidic DNA was digested by *XbaI* for further analysis (**Figure 3** and **Figure 4**). These results confirmed the presence of transformants by showing the expected size of construction 9 pJET_16SDNA; no transformant clones were discarded from analysis.

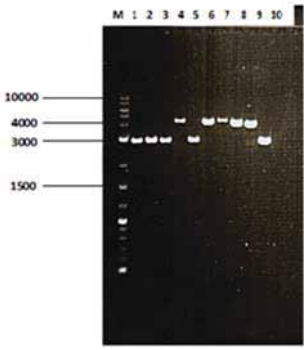


FIGURE 3. Cf1 clones selection with plasmidic DNA linearized by *XbaI*. Lane M: DNA ladder 10 kb. Lane 1-10: pJET _16SDNA clones/*XbaI*.

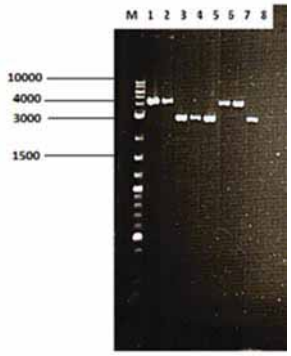


FIGURE 4. Cf2 clones selection with plasmidic DNA linearized by *XbaI*. Lane M: DNA ladder 10 kb. Lane 1-8: pJET _16SDNA clones/*XbaI*.

Sequences analysis reported up to 99% homology for the genus *Geobacter* (**Figure 5A**), *Clostridium* (**Figure 5B**), *Petrimonas* (**Figure 5C**), *Pelobacter* (**Figure 5D**), *Desulfotomaculum* (**Figure 5E**), *Firmicutes* (**Figure 5F**) and *Bacteroidetes* (**Figure 5G**).



FIGURE 5. Sequence alignments

Iron-reducing bacteria (*Geobacter* and *Clostridium*) are known for utilizing Fe(III) as electron acceptor and acetate as electron donor, these bacteria couple the reduction of this metal to its growth[3]. Catabolic metabolism of these is made by the citric acid cycle, also ferric reductase activity is detected in anaerobically grown cells, predominantly in the outer membrane[16]. The c-type cytochromes localized in the outer membrane and in the periplasmic space participate in the electron transfer. *Pelobacter* has similar features to iron-reducing bacteria; it has a fermentative metabolism, accumulating ethanol and producing acetate in the presence of Fe(III)[17].

Firmicutes and *Bacteroidetes* are two phylum of bacteria that belong to the gut microbiota, but can be found in different niches: soil, water and ocean sediments. They can degrade organic matter such as proteins and polysaccharides[18].

Petrimonas and *Desulfotomaculum* are two genus of sulfate-reducing bacteria, which can metabolize organic compounds to carbon dioxide. Their presence indicates and interdependence, due to they can also use Fe(III) and other metals as electron acceptor and couple its reduction in absence of sulfates[19]. Their growth is also owed to the concentration of sulfates in seawater.

CONCLUSION

The identification of iron-reducing bacterial species such as *Geobacter, Clostridium, Petrimonas* and *Desulfotomaculum* was obtained by 16S rRNA. The presence of these genus in water sediments suggests a high iron-reducing activity in the Coatzacoalcos River, which also can be linked to hydrocarbon degradation.

ACKNOWLEDGEMENTS

We thank to the Unit for DNA Sequence and Synthesis of Instituto de Biotecnología of UNAM for the delivered sequences and Ing. Edwin Fariz for collection of samples.

REFERENCES

1. Amils, R. Iron cycle. (2011). In: Gargaud, M., Amils, R., Cernicharo-Quintanilla, J., James, H., Irvine, W. M., editores. Encyclopedia of Astrobiology (pp 849-852). 2nd edition. Departamento de Planetología y Habitabilidad, Centro de Astrobiología (CSIC-INTA), Universidad Autónoma de Madrid Campus Cantoblanco
2. Lovley, D. R. (1991). Dissimilatory Fe(III) and Mn(IV) reduction. *Microbiol. Rev.* 55, 87-259
3. Lovley, D. R. (1997). Microbial Fe(III) reduction in subsurface environments. FEMS Microbiol. Rev. 20: 305-313
4. Shrihari, R. K., Ghandi, K. S. (1990). Modelling of Fe(II) oxidation by *Thiobacillus ferrooxidans*. Appl. Microbiol. Biotechnol. 33(5): 524-528
5. Erbs, M., Spain, J. (2002). Microbial iron metabolism in natural environments.
6. Straub, K. L., Benz, M., Schink, B. (2000). Iron metabolism in anoxic environments at near neutral pH. FEMS Microbiol Ecol. 34: 181-186.
7. Clarridge III, J. E. (2004). Impact of 16S rRNA Gene Sequence Analysis for Identification of Bacteria on Clinical Microbiology and Infectious Deseases. Clin. Microbiol. Rev. 17(4): 840-862

8. Sambrook J, Russell S. W. (2001). *Molecular Cloning: A Laboratory Manual.* 3rd edition. Cold Spring Harbor Laboratory Press; Cold Spring Harbor, NY.
9. Lane D. J. (1991). 16S/23S rRNA sequencing. In: Stackebrandt E, Goodfellow M, editors. Nucleic acid techniques in bacterial systematics. Chichester, United Kingdom: John Wiley and Sons. pp: 115–175.
10. Gutiérrez-Lucas, L. R., Montor-Antonio, J. J., Cortés-López, N. G., Del Moral, S. (2014). Strategies for the Extraction, Purification and Amplification of Metagenomic DNA from Soil Growing Sugarcane. Advances in Biological Chemistry, 4, pp: 281-189.
11. Miller, D. N., Bryant J. E., Madsen E. L., Ghiorse W.C., (1999). Evaluation and optimization of DNA extraction and purification procedure for soil and sediment samples. Appl.Environ.Microbiol. 65: 4715 – 4724
12. Birnboim, H. C., Doly, J. (1979). A rapid alkaline extraction procedure for screening recombinant plasmid DNA. Nucleic. Acids. Res. 7(6): 1513-1523.
13. Sanger, F., Nicklen, S., Coulson, A. R. (1977). DNA sequencing with chain-terminating inhibitors. Proc. Natl. Acad. Sci. 74(12): 5463-5467.
14. Hall, T. A. (1999). BioEdit: a user-friendly biological sequence alignment editor and analysis program for Windows 95/98/NT. Nucl. Acids. Symp. Ser. 41: 95-98.
15. Devereux, R., Wilkinson, S. S. (2004). Amplification of ribosomal RNA sequences. In: Molecular Microbial Ecology Manual, 2nd ed, Netherlands: Kluwer Academic Publishers: 509-522.
16. Schröder, I., Johnson, E., De Vries, S. (2003). Microbial ferric iron reductases. FEMS Microbiol. Rev. 27: 427-447.
17. Lovley, D. R., Phillips, E. J. P., Lonergan, D. J., Widman, P. K. (1995). Fe(III) and S^0 Reduction by *Pelobacter carbinolicus.* Appl. Environ. Microbiol. 61(6): 2132-2138.
18. Eckburg, P. B., Bik, E. M., Bernstein, C. M., Purdom, E., Dethlefsen, L., Sargent, M., Gill, S. R., Nelson, K. E., Relman, D. A. (2005). Diversity of the Human Intestinal Microbial Flora. Science. 308(5728): 1635–1638.
19. Muyzer, G., Stams, A. J. M. (2008). The ecology and biotechnology of sulphate-reducing bacteria. Nature Rev. Microbiol. 6: pp 441-454.

CHAPTER 6.4 EVALUATION OF BIOCIDES IN OILFIELD ENVIRONMENTS USING FLUORESCENT *IN-SITU* HYBRIDIZATION

M. R. Viera *(1,2); C. Terada (3); R. E. Madrid (4); J. C. Felice (4) and M. T. Del Panno (2,3)

(1) CIDEPINT (CICPBA-CONICET) Av.52 s/nº e/ 121 y 122, La Plata, Argentina
(2) Facultad de Ciencias Exactas, Universidad Nacional de La Plata, 47 y 115, La Plata Argentina
(3) CINDEFI (CONICET-UNLP), 50 y 115, La Plata, Argentina
(4) INSIBIO, (CONICET-UNT) and Laboratorio de Medios e Interfases (LAMEIN), Dpto. de Bioingeniería, FACET-UNT. Av. Independencia 1800, S.M. de Tucumán, Argentina

ABSTRACT

Microbiologically influenced corrosion and souring of oilfield reservoirs are process frequently provoked by the sulphate-reducing bacteria. The most common method applied in the industry for preventing or controlling the deleterious effect caused by the presence of microorganisms is the addition of chemical agents (biocides) aimed at killing the microorganisms or inhibiting the microbial growth. Traditionally, biocide selection and testing are based on NACE standard TM0194 which implies the use of culturing for enumerating the bacteria surviving the treatment.

To overcome culturing limitations, we used Fluorescent in-situ Hybridization to assist in the evaluation of biocides applied in water production treatment plants. Biocides were based on THPS (40% (B1); 75% (B2)) and 40% of a mixture (1/1, v/v) of THPS and benzalkonium chloride (B3) applied at two concentrations: 50 and 400 mg/L. The relation between the number of cells visualized with the fluorescent probes Eub338 and SRB385 (for eubacteria and SRB populations respectively) and the DAPI-stained cells (PR%) was used as an indication of the biocide efficiency. B1 and B3 gave a high PR% indicating that the chemical induced the metabolic cell activity. Only the highest B2 concentration showed effectiveness on eubacteria and SRB populations. Thus, through the application of FISH we were able to distinguish concentration effects of the THPS, discriminating sublethal from net inhibitory effects.

The possibility of including FISH into the protocols for the control of the biocides in water treatment plants could improve the biocide selection and the adjustment of their concentration in order to maintain the water system with a low density of metabolically active cells. This would avoid the misuse of chemicals with their consequent economic and ecological impacts.

Keywords: biocides, biocorrosion, fluorescent *in-situ,* hybridization, sulphate-reducing bacteria

---

*Author for correspondence: m.viera@cidepint.gov.ar

INTRODUCTION

A wide range of microorganisms, including both aerobic and anaerobic bacteria and fungi could promote the corrosion process, which reduces the lifetime of industrial materials[1]. Microbiologically influenced corrosion (MIC) and souring of oilfield reservoirs are process frequently provoked by the sulphate-reducing bacteria (SRB). The SRB group's metabolism generates substantial amounts of hydrogen sulfide and insoluble ferrous sulfide in the presence of iron. This often leads to deleterious effects manifested in the form of reduced injectivity of formation water, reservoir souring and plugging and pitting of susceptible steel pipes as well as increased sulfur content in the produced hydrocarbon[2].

Secondary oil recovery (SOR) is a procedure whereby freshwater or seawater is injected into petroleum reservoirs to support pressure and push oil toward producing wells. The water treatment process is chosen according to the source of the water supplied[3]. Because the microbial challenges and environmental parameters of these water sources vary, different microbial control strategies and treatments are required for each source. The most common method applied in the Argentinean industry for preventing or controlling the deleterious effect caused by the presence of microorganisms is the addition of chemical agents (biocides) aimed at killing the microorganisms or inhibiting the microbial growth. Tetrakis (hydroxymethyl) phosphonium sulfate (THPS) and benzalkonium salts (BAC) are among the biocides of choice in the oil industry. THPS can damage the cell membrane and inhibit the lactate dehydrogenase enzyme required for SRB metabolism[4], while BAC interacts with guanine nucleotide triphosphate-binding proteins (G proteins), thereby affecting signal transduction in a variety of cell types and processes[5]. Also, they react with membrane phospholipids causing membrane disorganization, leakage of cell contents, and eventually cell lysis.

Traditionally, biocide selection and monitoring are based on NACE standard TM0194[6] which implies the use of culturing for enumerating the bacteria surviving the treatment. Conventional culture-based methods for studying SRBs are time consuming as a result of slow bacterial growth rates and do not necessarily reflect the role of uncultivated bacteria in the oilfield operation[7]. Fluorescent *in-situ* Hybridization (FISH) is a molecular technique applied to environmental samples, which uses fluorescently-labeled oligonucleotide probes that hybridize specifically to its complementary 16S rRNA target sequence within the intact cell. A major advantage of FISH compared to other microbial ecology techniques is that the abundance of the detected microorganisms can be directly determined. Most frequently, the relative abundance of specific community members is estimated by counting (using an epifluorescence microscopy) the cells stained with a general DNA-binding dye and the cells hybridized with a specific probe. FISH has previously been used for direct identification and quantification of bacteria from natural samples without culturing in drinking water and biofilms[8], acid mine drainages[9] and activated sludge[10].

The aim of this work was to evaluate the utility of FISH in the selection of an appropriate biocide to control the microbial population present in the water treatment plant of an oil secondary recovery plant in an Argentinian oilfield

MATERIALS AND METHODS

Test fluid and Inoculum source. Water samples from two water treatment plants of secondary oil recovery placed in Mendoza and Neuquén provinces, Argentina were used as source of the targeted microorganisms and as fluid medium for biocide challenges. Samples from Mendoza treatment plant were taken at two points: near the water entrance to the plant (EW), and before the exit to the field (SF). Neuquén plant was sampled at a point corresponding to the storage water tank located before the pump to the field (STk). Table 1 shows the physicochemical properties of the waters determined following standard methods. Enrichment cultures in of these water samples prepared in Postgate´s B medium[1] (with the addition of 50 g/L NaCl to approximate the salinity of the produced waters) incubated at their corresponding temperature were tested as inoculum in the biocide inhibition assays. Additionally, a SRB consortium (SRB-OT) of our laboratory culture collection was used.

Chemicals. Three available commercial biocides were used. Biocide 1: 40% (w/w) tetrakis (hydroxymethyl) phosphonium sulfate (THPS); Biocide 2: 75% (w/w) THPS and Biocide 3: 40% of a mixture of THPS and benzalkonium chloride (BAC), 1:1 (v/v).

Table 1. Physicochemical propierties of the three water samples originated in oil fields

Properties / [unit]	EW	SF	STk
PH	7.0	6.7	7.20
Conductivity / [mS/cm]	108.1	107.4	163095.21
Carbonate / [mg/L]	< 1	< 1	< 1
Bicarbonate / [mg/L]	366	329	889.28
Chloride / [mg/L]	43249	42540	68577.08
Sulfate / [mg/L]	1258	1261	1857.00
Calcium / [mg/L]	1063	1043	1763.52
Magnesium / [mg/L]	49	146	807.42
$Na^+ + K^+$ / [mg/L]	27476	26843	41882.71
Total Dissolved Solids / [mg/L]	73461	72162	113283.48
Total Suspended Solids/[mg/L]	59.2	2.7	94.63
Temperature / [°C]	62	60	30
Dissolved oxygen / [ppb]	60	< 10	163.33
Total Sulphide / [mg/L]	9.5	27.9	2.07
Dissolved Sulphide / [mg/L]	6.8	26.1	No determined

Experimental design for the biocide inhibition assays. The assays were done in 10-mL bottles filled with filter-sterilized field water. Anaerobic conditions were achieved by adding thyoglycolate-ascorbic acid solution. A 1% inoculum was added to each bottle. A known volume of a distilled water-based biocide stock solution was added in the reaction bottles. Distilled water instead of biocide stock solution was added to control bottles.

Incubation time (4 h) and temperature (30 or 60°C) were chosen to match field conditions. At the end of the incubation time, 1-mL samples were withdrawn from each bottle to determine the cultivable bacterial counts by extinction method, in R2 broth and Postgate´s B (plus 50 g/L NaCl). Tubes were incubated 3 weeks in the dark at the selected temperature before scoring. The remaining volume was filtered and processed for hybridization. Triplicate assays for each biocide at each concentration were done.

Fluorescence in-situ hybridization. A volume of water sample was filtered onto 0.2 µm nitrate cellulose membrane and fixed in 4 % paraformaldehyde for 2-4 h at 4°C. The volume to be filtered was adjusted in order to get an adequate number of cells on the membranes, usually 10 mL of the sample or 10mL of a 1/10 dilution were used. The membranes with the fixed samples were washed three times with 3 mL phosphate buffered saline [PBS; 130 mM sodium chloride, 10 mM sodium phosphate buffer (pH 7.2)] and stored at –20 ºC.

For hybridization, a section of the membrane filter was dehydrated by successive dipping in 50, 80 and 98% ethanol for 3 min and allowed to air dry. The piece of filter was place on a clean microscope slide and cover with 8 µL of hybridization buffer (20 mM Tris-HCl pH 7.4, 0.9 M NaCl, 0.01% sodium dodecyl sulfate (SDS) and 35% formamide) and 1µL of the fluorescent oligonucleotide probe solution (25ng/mL).

The Eub338 probe was used to detect most members of domain Bacteria and Non338, (complementary to Eub338) was used as the negative control for non-specific binding The SRB385 probe was used to detect most species of SRB belonging to δ-proteobacteria[2]. Al the probes were 5P end-labelled with Cy3.

The slide was placed in a hybridization chamber, equilibrated with the hybridization buffer and incubated at 46º C during 2 h. The hybridization mixture was gently removed with several milliliters of the washing buffer (20 mM Tris-HCl pH 7.4, 0.1% SDS and NaCl) prewarmed at 48°C. The stringency of the washing step was adjusted with 18mM NaCl in the washing buffer. The slides were immersed for 20min in the washing buffer at 48°C. Then they were briefly washed with distilled water, air-dried, stored in the dark.

For the determination of the total number of bacteria in the samples, filters on the slides were stained with 5 µL of the general bacterial stain DAPI (4, 6-diamidino-2-phenylindole dihydrochloride) (1 µg/mL). The slides were covered with antifading solution, and fluorescence was detected with a DMLB microscope coupled to a DC100 camera (Leica Microscopy System) and filter sets 01 (for DAPI staining), and 15 (for Cy3 probes). Among 15 to 20 images were analyzed per sample.

RESULTS AND DISCUSSION

According to the NACE Standard TM0194-2004[6], the organisms used to challenge a biocide to be applied in an oil field should be the bacteria normally found in the oil field waters (which would be the test fluid). Alternatively, up to a 1% inoculum of a fully grown culture originating from the oil field may be used. The hybridization of the water samples with the Eub338 probe done immediately after reception in our laboratory (one week after collection) showed a low number of bacteria stained with DAPI (Figure 1, above left) with very low percentage of the cells emitting the probe-conferred fluorescence. (Figure 1, above, right). This behavior could be attributed to the low metabolic activity of

the cells present in the water samples. Taking into account that the objective of our work was to evaluate the biocide efficacy in the bacteria population present in the oil field environment using FISH, such low hybridization efficiency would reduce the degree of certainty of the results. Thus, enrichment cultures were done. Hybridization of these samples yielded a higher intensity of the fluorescence signal and an increase in the hybridization ratio (**Figure 1**, below). The ratio between the number of cells visualized using the fluorescent probes and the DAPI-stained cells defined the Probe Ratio (PR%). This value was near 80% for the Eub338 probe. This detection yield was comparable to those obtained for activated sludge[4] and sea sediment[5]. Thus, it was decided that the enrichment cultures were inoculated (at 1%) in the test fluid for biocide testing.

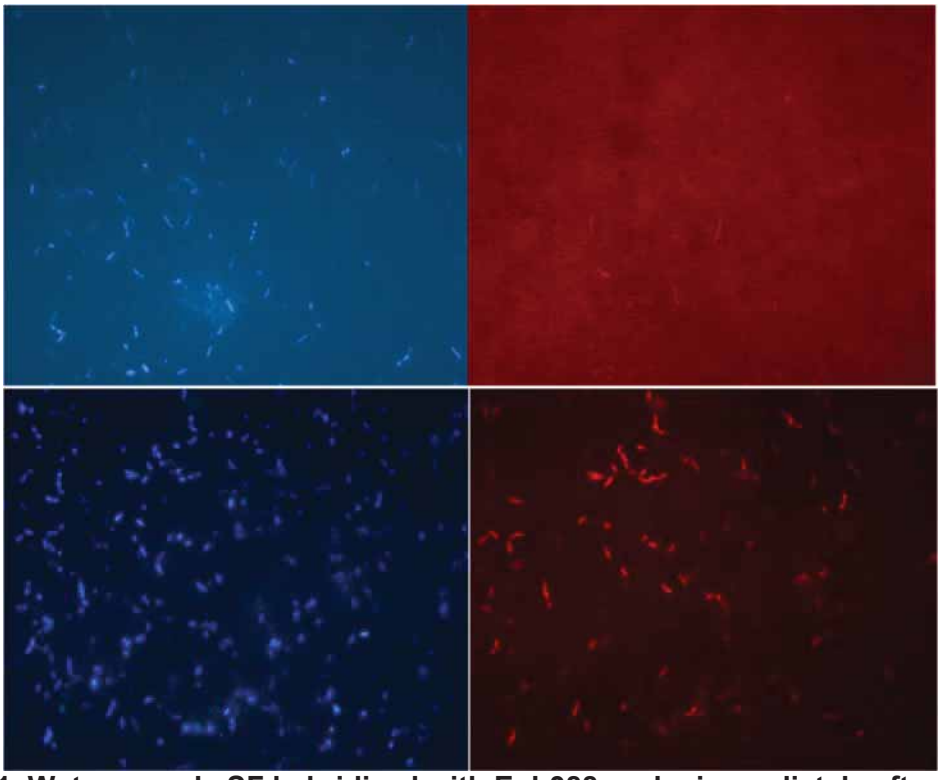


FIGURE 1. Water sample SF hybridized with Eub388 probe immediately after received (above) or after enrichment in Postage´s B medium (below). Left images: DAPI fluorescence; right images: Cy3 fluorescence

Biocide inhibition assays. Two inhibition experiments were done. In the first one, SF was used as test fluid with SRB-OT as inoculum. In this experiment, the viable bacterial population was tested by hybridization using Eub338 probe. In the second experiment, EW was used as test fluid and the enrichment culture originated in this sample was the inoculum. In this case, the bacterial population and the SRBs were detected by hybridization using the Eub338 and SRB385 probes. The efficiency of the biocides was measured through the evaluation of the PR%. A lower PR was expected in the presence of the biocide in relation with the control systems, as an indication of the deleterious effect of the biocide on the bacteria.

Assay 1- Biocide inhibition assay in SF as fluid test and the Eub338 probe. In this case, the inhibitory effects of the three biocides (B1, B2 and B3) at two concentration levels (50 mg/L and 400 mg/L) were evaluated. Both concentrations are usually used in water treatment in the secondary oil recovery process. The results of the viable counts performed in R2 broth and Postage´s B medium for the enumeration of the total bacteria and the SRB showed that the biocides are effective in reducing the number of viable bacteria (**Table 2**), as their number is reduced from 10^3-10^4 cell/mL in the control systems to only 1-10 cells/mL in the presence of 50mg/L of any biocide. At the highest concentration used all the tubes were negatives.

TABLE 2. Viable counts determined by the dilution to extinction method after biocide treatment using SF water sample. The biocides were applied at 50 and 400 mg/L

	Biocide (mg/l)	THPS (mg/l)	BAC (mg/l)	Extinction tubes (R2broth/PGB) 1(1-10)	2(10-10^2)	3 (10^2-10^3)	4 (10^3-10^4)
Control		-	-	+/+	+/+	+/+	+/+
B1	50	20	-	+/+	-/-	-/-	-/-
	400	160	-	-/-	-/-	-/-	-/-
B2	50	37.5	-	+/-	-/-	-/-	-/-
	400	300	-	-/-	-/-	-/-	-/-
B3	50	10	10	+/-	-/-	-/-	-/-
	400	80	80	-/-	-/-	-/-	-/-

Figure 2 shows the PR% values obtained after 4 h of incubation. The first two columns represent the values obtained in the control systems after 15 min and 4h of incubation. A decrease in PR was observed after 4h, attributed to the loss of metabolic activity of the cells during the incubation at 60 °C in the water. Because of this, it was not possible to estimate the percentage of surviving bacteria after the biocide treatments compared to the control. However comparisons amongst biocides were still possible and, interestingly, very different behaviors were detected. As it can be seen, B1 at the lowest concentration gave a high ratio indicating an induction of the metabolic cell activity. At the highest concentration, this biocide reduced the number of metabolically active cells, but not at a level as low as the control. On the other hand, B2 provoked significant inhibitory effects at both concentrations. A different behavior was observed with B3, which did not produce a significant effect at 50 mg/L and induced the metabolic cell activity at 400 mg/L.

The metabolic activation of the bacterial cells observed in the presence of B1 and B3 could be associate to an induced response of the bacteria to an environmental stress (in this case, it could be the presence of a sublethal concentration of biocide). In this situation, bacteria could express numerous stress mechanisms to face with the biocide. Adopting a stress resistant phenotype frequently involves growth arrest and the adoption of a metabolically downregulated state[11]. Maintaining functional growth machinery, such as ribosomes, represents the highest energetic expenditure for stressed cells, which therefore divert their resources towards survival rather than growth when conditions deteriorate[12].

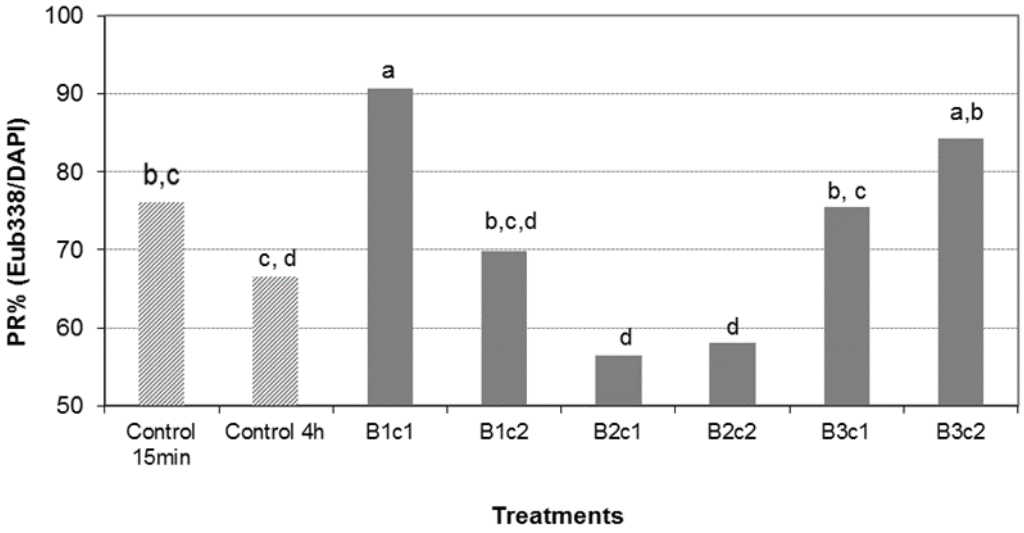


FIGURE 2. PR% values for the Eub338 probe after 4h of incubation with the biocides B1, B2 and B3 at two concentrations: 50 mg/L (c1) and 400 mg/L (c2). (Equal letters indicate no significant difference)

The highest THPS concentration tested (300 mg/L present in 400 mg/L B2) was effective against heterotrophic and SRB population reducing significantly the cultivable cell number to below the detection limit. Although, no significant differences with the control were observed by hybridization, a tendency to provoke cell death could be inferred for 300 mg/L THPS. It has been reported that THPS had little inhibitory effect on E. coli, up to 243.6 mg/L whereas at 487.2 mg/L it lowered CFU/mL by 3 log units after one hour of contact[13]. According to our results, the TPHS effective concentration was lower; however, the FISH results indicated that some cells remained metabolically active in the fluid test.

When THPS was applied along with BAC (B3), a sublethal effect, similar to that obtained when THPS was applied at the lowest concentration (20 mg/L) was observed. The result suggested that there was no synergic effect among both chemicals on the water bacteria community. Mixtures of biocides with a different mode of action are likely to be synergistic. However, in agreement with our results, other authors found that mixtures of THPS with other agents did not exhibit any synergistic effect[14].

Assay 2- Biocide inhibition assay in EW as fluid test with Eub338 and SRB385 probes. In this case, the three biocides were applied at one concentration (200 mg/L) and their inhibitory effects were determined on the total bacterial population and on the SRB populations by counting the cells hybridized with the Eub338 and SRB385 probes. Figure 3 shows the PR% values obtained for 15 min and 4h of incubation. In this experiment, it was not observed a decrease in PR in the control system, after the incubation. The presence of 200 mg/mL of the B1 and B3 produced an increase in PR, associated with a higher metabolic cell activity in the survival cells after the treatment. No significant effect on the total bacterial population was observed with the same concentration of B2.

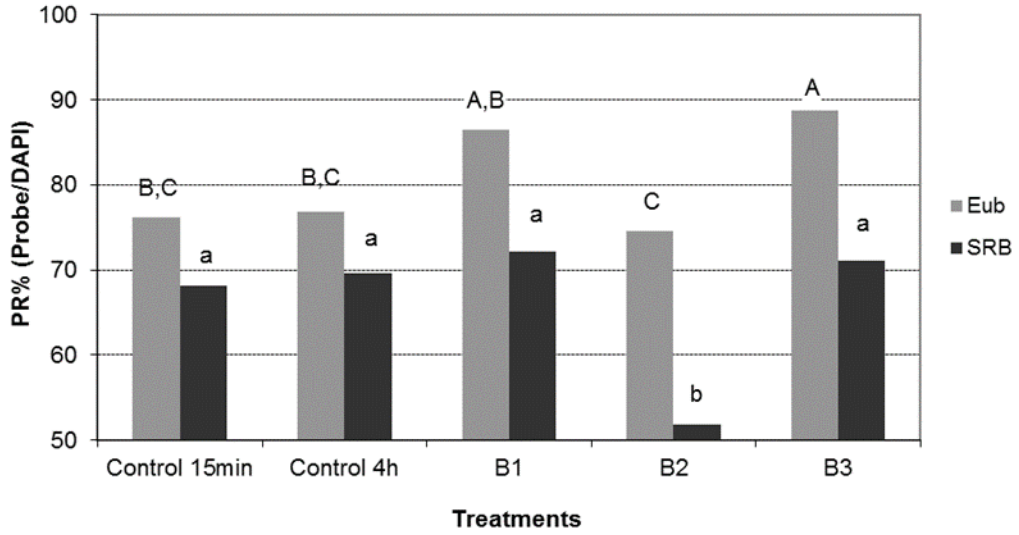


FIGURE 3. PR% values of both probes (Eub338 and SRB385) in EW water after 4h of incubation with the biocides B1, B2 and B3 at 200 mg/L. (Equal letters indicate no significant difference)

The effect of B1 and B3 on the SRB population was not different from that observed in the control system. Instead, a significant inhibitory effect was produced by B2 on this population. In this experiment, the cultivable viable count after 4h of incubation (Table 3) showed that there was no growth in any of the tubes used for enumeration.

TABLE 3. Viable counts determined by the dilution to extinction method after biocide treatment using EW water sample. The biocides were applied at 200 mg/L

	Biocide (mg/l)	THPS (mg/l)	BAC (mg/l)	Extinction tubes (R2broth/PGB) 1(1-10)	2(10-10^2)	3 (10^2-10^3)	4 (10^3-10^4)
Control		-	-	+/+	+/+	+/+	+/+
B1	200	80	-	-/-	-/-	-/-	-/-
B2	200	150	-	-/-	-/-	-/-	-/-
B3	200	40	40	-/-	-/-	-/-	-/-

The THPS effect in this test fluid was similar to that observed in SF, producing metabolic activation of the eubacteria population at the minor concentration (80 mg/L THPS present in 200 mg/L B1) and mixed with BAC (40 mg/L THPS and 40 mg/L BAC present in 200 mg/L B3). Also, no changes in the eubacteria PR% was observed applying 150mg/L THPS (present in 200 mg/L B2) in comparison with the control. However, this concentration of THPS was the only one that significantly reduced the metabolic activity of the SRB population.

The study of the global gene expression resulting from THPS stress on *Desulfovibrio vulgaris* v.H showed that the genes for enzymes related to the energy metabolism were strongly affected[13]. Also, these genes were affected during the treatment with BAC. Although these results were obtained using a pure culture of a typical SRB strain, it

could possible to correlate them with our findings in an enrichment culture of sulphate reducing bacterial community in an actual water production sample. In this sense, we could attribute the increase in the 16SrDNA probe hybridization ratio to an increase in the ribosomal content induced by the application of a sublethal THPS concentration. Likewise, the significant reduction in the hybridization ratio at higher THPS concentration could be attributed to the death of the SRB. In this regard, it is important to point out that even though no culturable cells were detected in the presence of the biocides, at least fifty percent of the cells could be detected by hybridisation with the SRB385 probe. This would mean that survival cells could remain in the water although they were no detected by the conventional cultivable methods.

The use of higher concentrations of biocide might be an alternative to exert its killing action. However, downstream of the treated area there is likely to be a continuum of biocide concentration ranging from the treatment concentration to nil. Thus, sooner or later they can be found in natural environments at low (sub-lethal) concentrations, leading to continuous exposure of water and soil microbial community[15]. As could be shown in our experiment, the usual concentration recommended by the manufacture resulted to be a sublethal dose. This has an unwanted economic and ecological impact. In this sense, the misuse of expensive chemical would condition a habitat where selected tolerant cells may enhance some characteristics potentially useful for colonization of specific environments (biofilm), decreasing the efficacy of biocide treatments and exacerbating the corrosion problems.

Eventually, this scenery could lead to the emergence in the environment of multi-drug resistant strains. Several authors have found a relation between the resistance to biocides and the tolerance to antibiotics[16]. Those results highlight the relevance of the application of sublethal biocide concentrations on the microbial communities from very different habitats.

CONCLUSION

The hybridization assay using ribosomal targeted probes allowed us to detect concentration effects of THPS, discriminating sublethal from net inhibitory effects. Also, it was possible to evidence that the mixture of active compounds such THPS and BAC could not exert a synergistic effect on the heterotrophic and the SRB populations. The possibility of including the FISH technique in the protocols applied in water treatment plants could improve the biocide selection process, contributing to the biocide design targeted to SRB included concentration adjustment in order to maintain the system with an actual low density of metabolically active cells. This would help to avoid the misuse of chemicals with their consequently economic and ecological impacts. This means a cooperative work between the industry and the researchers to improve the protocols for the selection of specific biocides with the ultimate goal of reducing the ecological impact.

ACKNOWLEDGMENTS

This work was funded by YPF SA through a research contract with National University of Tucuman.

REFERENCES

1. Alasvand Zarasvand K., Rai V., Microorganisms: Induction and inhibition of corrosion in metals. Int. Biodeter. Biodegr. 87 (2014) 66-74.
2. Ollivier B., Cayol J., Fauque G., Sulphate-reducing bacteria from oil field environments and deep-sea hydrothermal vents, in: Barton L, Hamilton W., Sulphate-reducing Bacteria: Environmental and Engineered Systems (2007).
3. Mc Inerney M., Sublette K., Oil field microbiology, in: Hurst C., Crawford R., Knudsen G., McInerney M. Stetzenbach L., Manual of Environmental Microbiology (2002).
4. Jones C., Downward B., Hernandez K., Curtis T., Smith, F., Extending performance boundaries with third generation THPS formulations. Corrosion 2010 paper 10257, NACE (2010).
5. Patarca-Montero R., Fletcher M., Effects of Benzalkonium Salts on G-protein-Mediated Processes and Surface Membranes. Relevance to Microbial- and Chemical-Induced Diseases. J. Chronic Fatigue Syndrome 10 (2002) 87-168.
6. NACE Standard TM0194-2004. 2004. Field Monitoring of Bacterial Growth in Oil and Gas System, NACE, Houston, USA, 2004.
7. Larsen J., Zwolle S., Kjellerup B., Frølund B., Nielsen J., Nielsen P., Identification of bacteria causing souring and biocorrosion in the Halfdan Field by application of new molecular techniques, Corrosion 2005 paper 05629, NACE (2005)
8. Manz W., Szewzyk U., Ericsson P., Amann R., Schleifer K., Stenstrom T., In situ identification of bacteria in drinking water and adjoining biofilms by hybridisation with 16S and 23S rRNA-directed fluorescent oligonucleotide probes. Appl. Environ. Microbiol. 59 (1993) 2293-2298.
9. Kock D., Schippers A., Geomicrobiological investigation of two different mine waste tailings generating acid mine drainage. Hydrometallurgy 83 (2006)167-75.
10. Lozada M., Itria R., Figuerola E., Babay P., Gettar R., de Tullio L., Erijman L., Bacterial community shifts in nonylphenol polyethoxylates enriched activated sludge. Water Res. 38 (2004) 2077-2086.
11. Kolter R., Growth in studying the cessation of growth. J. Bacteriol. 181 (1999) 697-699.
12. Geisel N., Vilar J., Rubi J., Optimal Resting-Growth Strategies of Microbial Populations in Fluctuating Environments. PLoS ONE 6 (2011) e18622.
13. Lee M., Caffrey S., Voordouw J., Voordouw G., Effects of biocides on gene expression in the sulfate-reducing bacterium *Desulfovibrio vulgaris* Hildenborough. Appl. Microbiol. Biotechnol. 87 (2010) 1109–1118.
14. Greene E., Brunelle V., Jenneman G., Voordouw G., Synergistic inhibition of microbial sulfide production by combinations of the metabolic inhibitor nitrite and biocides. Appl. Environ. Microbiol. 72 (2006) 7897–7901.
15. SCENIHR (Scientific Committee on Emerging and Newly Identified Health Risks). Assessment of the antibiotic resistance effects of biocides. 2009.
16. Capita R., Riesco-Peláez F., Alonso-Hernando A., Alonso-Calleja C., Exposure of *Escherichia coli* ATCC 12806 to sublethal concentrations of food-grade biocides. Appl. Environ. Microbiol. 80 (2014) 1268–1280.

Section 7.
Wastewater Treatment

Page

Chapter 7.1 Tetra-azo dye direct black 22 decolorization in dual-chamber bioelectrochemical system 432
S.M. Amorim; M. Navarro; C.P. Silva; L. Florencio; M.T. Kato and S. Gavazza

Chapter 7.2 Formation of aerobic granules in sequencing batch reactors applied for diluted domestic wastewater 439
Julliana M. P. Araújo; Poliana M. J. Silva; Oucilane I. M. Alves; Sávia Gavazza; Mário T. Kato and Lourdinha Florêncio

Chapter 7.3 Contaminated water treatment red reactive textile dye by eletroflocculation process 450
José Arruda Biserra Neto; Luiz Gustavo de Sousa Pinto; Armando Morais Correia de Melo Filho and Henrique John Pereira Neves

Chapter 7.4 Evaluation of uasb reactor treating synthetic effluent from industrial denim laundries 456
M. G. P. de Carvalho; S. Amorim; D. Marcelino; L. Florencio; M. T. Kato and S. Gavazza

Chapter 7.5 Reliability analysis of wastewater treatment plants of jeans laundries from Pernambuco-Brazil 466
V. H. Couto; M.T.C. Fonseca; H. K. P. Silva; J. C. Morais and E. A. Pastich

Chapter 7.6 Reliability analysis of eight full-scale stabilization plants in a semiarid region of Brazil 476
V.H. Couto; E. A. Pastich; M. G. Acioly; M. V. Paiva and J. C. Morais

Chapter 7.7 Biopurification system for pesticides mixture degradation in repeated applications 486
M.C Diez; B. Leiva and F. Gallardo

Chapter 7.8 Estudio comparativo de las plantas de tratamiento de aguas residuales en el sur y centro de México 501
Lilian E. Domínguez-Montero and Héctor M. Poggi-Varaldo

Chapter 7.9 Los instrumentos económicos financieros en el tratamiento de aguas residuales municipales en México 515
Lilian E. Domínguez-Montero and Héctor M. Poggi-Varaldo

Chapter 7.10 Diversity and diel variation of phytoplankton community at different depths in a polishing pond 527
J. T. Ferreira; M.L.P.D. Lages; E. A. Pastich; S. Gavazza; M. T. Kato and L. Florencio

Chapter 7.11 Utilización de polietileno poroso en aplicaciones ambientales 538
P. Flores; A. Zalts and J. Monterrat

Chapter 7.12 Comparative evaluation of autochthonous and non-autochthonous sulfate-reducing microbial communities in bench-scale reactor models 546
A. Giordani; E. A. Hayashi; R. P. Rodriguez; L. H. S. Damasceno; H. Azevedo and G. Brucha
Chapter 7.13 Degradación de glifosato a través de biolechos: estudio de diferentes biomezclas 557
M. Lescano; D. Buschiazzo and C. Zalazar
Chapter 7.14 Tratamiento combinado de adsorción y degradación biológica de 4-clorofenol 567
C. Lobo; N. Bertola and N. Zaritzky
Chapter 7.15 Advanced oxidation of commercial herbicide mixtures: experimental design and optimization 577
A. López; A. Coll; M. Lescano and C. Zalazar
Chapter 7.16 Strategy to identify the causes and to solve a granulation problem in anaerobic reactors: application to a plant treating cheese wastewater 588
H. Macarie; M. Esquivel; A. Laguna; O. Baron; R. El Mamouni; S. Guiot and O. Monroy
Chapter 7.17 Treatment of synthetic textile effluent by anaerobic process with micro aerated zone 603
M. S. D. Marcelino; R. Brito; L. Florêncio; M. T. Kato; M. H. R. Z. Damianovic and S. Gavazza
Chapter 7.18 Central composite design applied to post-treatment of stabilized landfill leachate using fenton's reagent 613
Caio Victor Lourenço Rodrigues and Deize Dias Lopes
Chapter 7.19 Greywater treatment in an aerobic sbr: sludge structure and kinetics 625
U. Rojas-Z.; C. Fajardo-O.; I. Moreno-Andrade and O. Monroy
Chapter 7.20 Chemical and microbiological characteristics of effluent from rock filters used for the post-treament of stabilization ponds 636
M.V.A. Santos; T. Köchling; L. R. Martins; S. Gavazza; M. T. Kato and L. Florencio
Chapter 7.21 Methanogenic inhibition of azo and anthraquinone textile dyes 646
C. P. Silva; O. F. Menezes; L. Florencio; M. T. Kato and S. Gavazza
Chapter 7.22 The use of zeolite and lime for sanitization of sewage sludge 654
N. Sasakova; J. Venglovsky; F. Toth; I. Papajova; G. Gregova; R. Hromada and B. Nowakowicz-Debek
Chapter 7.23 Uso de agua residual doméstica tratada y lodo en el cultivo de dos especies de fríjol: productividad y efectos nutricionales en los granos 661
Robson J. Silva; Sávia Gavazza; Lourdinha Florencio; Clístenes W.A. Nascimento; Egídio B. Neto and Mario T. Kato

673

Chapter 7.24 Microbial diversity in sequencing batch reactors used for nutrients removal in domestic sewage
C.N.C. Souto; A.G. Santos Neto; V.V.T. Souza; S. Gavazza; M.T. Kato and L. Florêncio
Chapter 7.25 Use of efluent and sludge from sewage treatment plant in sorghum cultivation 682
E. J. Souza Filho; E. Bezerra Neto; S. Gavazza; L. Florencio and M. T. Kato
Chapter 7.26 Influence of oil concentration and previous oxygenation in las removal in anaerobic reactor
Luiza F.C. Souza*; Tayane Vasconcelos; Lourdinha Florencio; Savia Gavazza and Mario T. Kato 692
Chapter 7.27 Sistema de cultivo hidropónico para el aprovechamiento de efluentes 701
Luiza F. C. Souza, Maria E. Souza, Claudio E. S. Oliveira*
Chapter 7.28 Producción de lípidos empleando una microalga aislada de Tierra Blanca, Veracruz y agua residual de Tilapia
Ana Line Vázquez-Larios; Paula Natalia Robledo-Narváez; Luis Alfredo Ortega-Clemente and Elvira Ríos-Leal 709
Chapter 7.29 Nitrification of industrial nuclear effluent using whole bacterial cell immobilization 716
M. Venturini; D. Camporotondi; P. Silva Paulo; G. Curutchet and R. Pizarro
Chapter 7.30 Combination of photocatalysis and biological oxidation for the degradation of pharmaceuticals in water 727
A. Manassero; K. A. Villón; O. M. Alfano and M. L. Satuf
Chapter 7.31 A hybrid electrooxidation/electrocoagulation system using Ti/ PbO2-Al/Fe electrodes for crystal violet dye removal
Celestino García-Gómez; Eneydi Urias; Pablo Gortáres-Moroyoqui and Ruth Gabriela Ulloa-Mercado 738
Chapter 7.32 Effect of aeration regime on discoloration and breakdown of aromatic amines from azo dye treatment 749
O. F. Menezes; R. Brito; M. G. Carvalho; M. T. Kato; L. Florêncio and S. Gavazza
Chapter 7.33 Biodegradability of paracetamol in anaerobic conditions
C. Nepomuceno; K. K. Barros and L. De Souza 758
Chapter 7.34 Influence of toilet paper in the anaerobic digestion of wastewater
D.P.P. Gomes; M. L. Figueiras; R. B. Pires; S. Gavazza and M. S. Santos 768
Chapter 7.35 Fenton oxidative process evaluation in the treatment of synthetic textile effluent containing dye direct black 22 777
M.A.P. Kelm; D. S. Figueiroa and N.P.S. Lopes

CHAPTER 7.1 TETRA-AZO DYE DIRECT BLACK 22 DECOLORIZATION IN DUAL-CHAMBER BIOELECTROCHEMICAL SYSTEM

S.M. Amorim *(1); M. Navarro (2); **C.P. Silva** (1); L. Florencio (1); M.T. Kato (1) and S. Gavazza (1)

(1) Laboratory Environmental Sanitation, Department of Civil and Environmental Engineering
(2) Laboratory of Organic Electrosynthesis, Department of Fundamental Chemistry
Federal University of Pernambuco, Av. Academico Hélio Ramos s/n, Cidade Universitária, Recife-PE. CEP 50740-530

ABSTRACT

Azo dyes are widely used by the textile industry, and its degradation usually represents the bottleneck of the wastewater treatment system. The bioelectrochemical system is an alternative technology that has, recently, demonstrated improvement in color removal efficiencies and rates in comparison with biological treatment only[1]. In the present study, we investigated the use of a dual-chamber bioelectrochemical system (BES) in lab-scale to treat synthetic textile wastewater. A constant potential of -1.6 V was applied as an external energy source. The anode chamber was fed with glucose (Chemical Oxygen Demand - COD of 1 g O_2 L^{-1}) and nutrients as substrate. The tetra-azo dye Direct Black 22 (DB22) (0.06 mmol.L^{-1}) and nutrients were placed in the cathode chamber. Brewery and textile anaerobic sludge were, respectively, used as biomass in the anode and the cathode chambers. An electrochemical system (ES) essay was conducted in same conditions, without biomass.

The DB22 removal efficiency was 90% and 81% for the BES and ES, respectively. The first-order kinetic constant was 3 times higher for BES (k = 0.03 h^{-1}) than that found for ES (k = 0,01 h^{-1}). Although similar results have been found for the tested systems, the BES exhibited higher pollutants removal rates.

Keywords: azo dyes, bioelectrochemical system, dual-chamber, kinetic.

INTRODUCTION

The dyes present in textile industry effluents usually impair the treatment system efficiency due to their recalcitrance. Environmental and / or operating conditions greatly influence dyes removal and textile effluent treatment behavior [2].

Physical chemical treatment by coagulation/flocculation/filtration is the most applied technology to textile effluents. However, it is expensive and dependent of chemical compounds application. Biological treatment, a more sustainable technology, has demonstrated good performance, even for treating real textile effluents[3]. However, the kinetic of color biodegradation is still low.

Anaerobic treatment can be a viable alternative for the treatment of dye containing wastewaters. In most cases, the azo dyes are easily degraded under anaerobic

---

*Author for correspondence: sandrabio@hotmail.com

conditions. However, the main disadvantage of this reduction is the generation of aromatic amines, which are not well degraded anaerobically[4]. Thus, many researchers have adopted sequential anaerobic-aerobic systems for reaching the complete azo dyes degradation[5].

Recent efforts to develop sustainable wastewater treatment technologies resulted in bioelectrochemical systems (BES) to generate electricity or hydrogen from wastewater in microbial fuel cells (MFC) and microbial electrolysis cell (MEC), respectively, in which an electric potential is applied using an external power supply[6].

The difference between the two types of cells is established at the cathode. In MFCs, the aerobic degradation of organic matter produces a natural difference in the electric potential generating electrical energy. In MECs, the potential is elevated by the electric energy to overcome the thermodynamic constraints of reactions without oxygen (for example, generating hydrogen gas).

This technology is based on electrogenic microorganisms that oxidize the organic matter producing carbon dioxide (CO_2), electrons (e^-) and protons (H^+) with ability of transferring electrons to the anode[7]; then these electrons flow through an external circuit to the cathode, where they are used as electron donors for the oxygen reduction (in MFCs) or for the hydrogen formation (in MECs). Both cathodic reactions can be catalyzed either through direct chemical catalysis (e.g., platinum) or through microbial activity in the biocathode.

In recent years, bioelectrochemical technology has shown great potential for azo dye decolorization due to its innovative features and environmental benefits. Mu et al. used the dual-chamber bioelectrochemical system fed with acetate to decolorization of the azo-dye Acid Orange 7, obtaining decolorization efficiency higher than 78.7%, for 0.19 mM of dye [6].

Then, the concentration gradient of the azo dye was elevated for biofilm acclimatization in the anode chamber, which showed sensitivity to the dye toxicity.

An increase in removal efficiency 10h after adaptation was verified, reaching 73.3%. Results indicate the feasibility of azo dye removal in single-chamber BES. The absence of membrane not only decreased internal resistance, but also increased current density and the azo dye removal.

In the present study, a dual-chamber bioelectrochemical system (BES) was used to investigate the decolorization of the tetra-azo dye Direct Black 22.

MATERIALS AND METHODS

Cyclic voltammetry. Aiming to find the electric potential of the DB22 electrochemical reduction, the behavior of the DB22 reduction process in the cathode was tested using cyclic voltammetry (CV), in a dual-chamber BES. Cyclic voltammetry was performed with an Autolab PGSTAT30 Potentiostat/Galvanostat from -1.8 to 0V vs Ag|AgCl|KCl (sat), using a sweep rate of 100 mV s^{-1}. Solutions were prepared using 0.1 M KCl as the electrolyte, in tests with and without DB22. A three-electrode configuration cell was used with a working glassy carbon electrode (3cm diameter), an auxiliary electrode made of graphite bat, and an Ag|AgCl|KCl(sat) reference electrode. The headspace was displaced using an N_2 stream before each test. For the voltammetry essays, the DB22 dye concentration was 1mM.

Electrochemical cell. The electrochemical cell, H-type, is made of borosilicate glass with a total volume of 200 mL, with 100 mL for each chamber. Each chamber is covered with PVC threaded cap with holes for electrodes accommodation and two side openings (**Figure 1**).

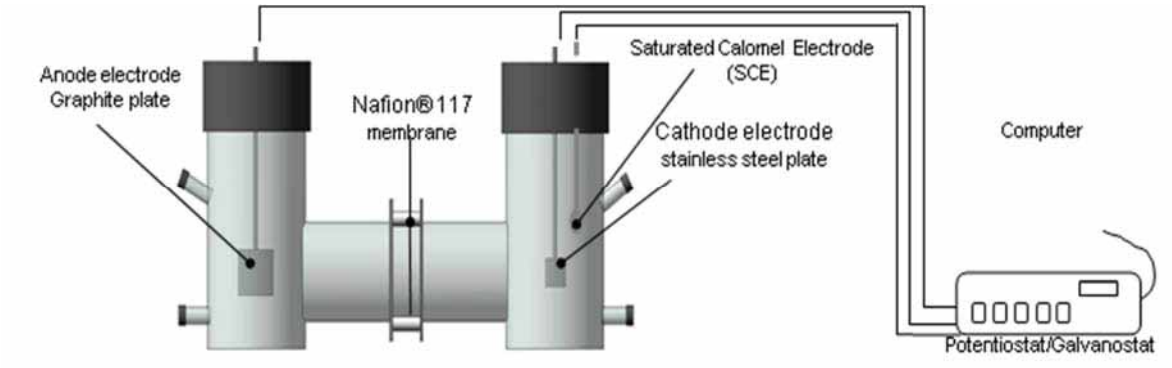


FIGURE 1. Schematic illustration of the electrochemical cell

The anode (5.0 x 3.5 x 0.5 cm, Graphite Store, Buffalo Grove, IL) was made of graphite plate, while the cathode (1.5 x 1.5 x 0.1 cm, LabSolutions) was made of stainless steel plate. The proton exchange membrane Nafion® 117 (DuPont) was placed between anode and cathode chambers. A constant potential of -1.6 V was applied as external energy source (potentiostat/galvanostat Methron Autolab PGSTAT 30). The reference electrode was Saturated Calomel (0.241V *vs* NHE) (CHI150 - CH Instruments, USA).

Brewery anaerobic sludge was used as biomass in the anode, characterizing bioelectrochemical system (BES). A total of 2.37 mL of blended anaerobic granules (3 g of volatile suspended solids [VSS] L^{-1} - concentration in the mixed liquor) from a full-scale UASB reactor, which treats brewery wastewater in Itapissuma (PE - Brazil), was used as inoculum for the anode. An electrochemical system (ES) essay was conducted in same conditions, without biomass.

Both systems were operated batch under constant agitation, temperature (30º±2), in cycles that have been completed when observed stability results. A repeat test was conducted to BES and ES and to check the reproducibility of the process.

The degradation kinetic plotting the left side of the above equations versus time, one can obtain the value of k from the slope of the curve. For BES and ES was used to fit the model of first-order kinetics.

Synthetic wastewater. Synthetic textile wastewater was prepared using the tetra-azo dye Direct Black 22 (DB22, $C_{44}H_{32}N_{13}Na_3O_{11}S_3$; C. I. 35435; CAS 6473-13-8; molecular weight of 1083.97 g mol^{-1}; **Fig.2**), glucose [1000 mg O_2 L^{-1} as chemical oxygen demand (COD)], and macro- and micro-nutrients[8]). The dye was pre-hydrolyzed following the manufacturer's instructions (pH adjustment to 11.0 ± 0.05 with NaOH, 1 h of heating at 80 °C, and pH re-adjustment to 7.0 ± 0.05 using HCl). During the experiment, the dye initial concentration was 0.065 g L^{-1} (0.06 mM). To the prepared substrate was added 1000 mg L^{-1} of NaCl to reach the salinity of real textile effluents[3] of 3.2‰. Additionally, 1000 mg L^{-1} of sodium bicarbonate was also added as buffer.

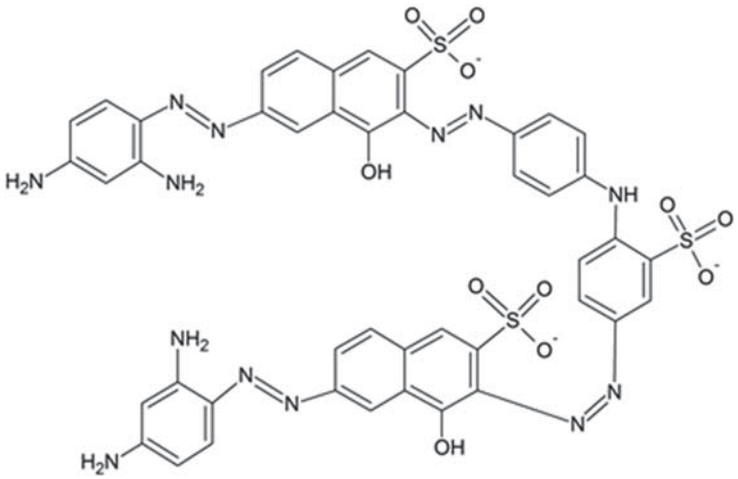


FIGURE 2. Direct black 22 azo dye structure (C. I. 35435)

Analyses. The systems were monitored by measuring dye concentration and pH, daily; COD every two days; and alkalinity at the beginning and at the end of the experiment. Alkalinity, pH, and COD were determined according to Standard Methods for the Examination of Water and Wastewater[9]. The azo dye concentration was measured spectrophotometrically at the wavelength of maximum absorbance for DB22 (476 nm). Samples were centrifuged and diluted (1:1 v/v) in a phosphate buffer (50 mM) to prevent auto-oxidation.

RESULTS AND DISCUSSION

Cyclic voltammetry. The dye DB22 reduction peak was detected in the cathode at −1.6 V in the forward scan (**Figure 3**). Adversely, no catalytic behavior was found in control CV tests using culture medium without DB22, which indicates absence of soluble redox-mediators in the medium. These results indicated that DB22 could be reduced at the cathode using the electric potential of −1.6 V.

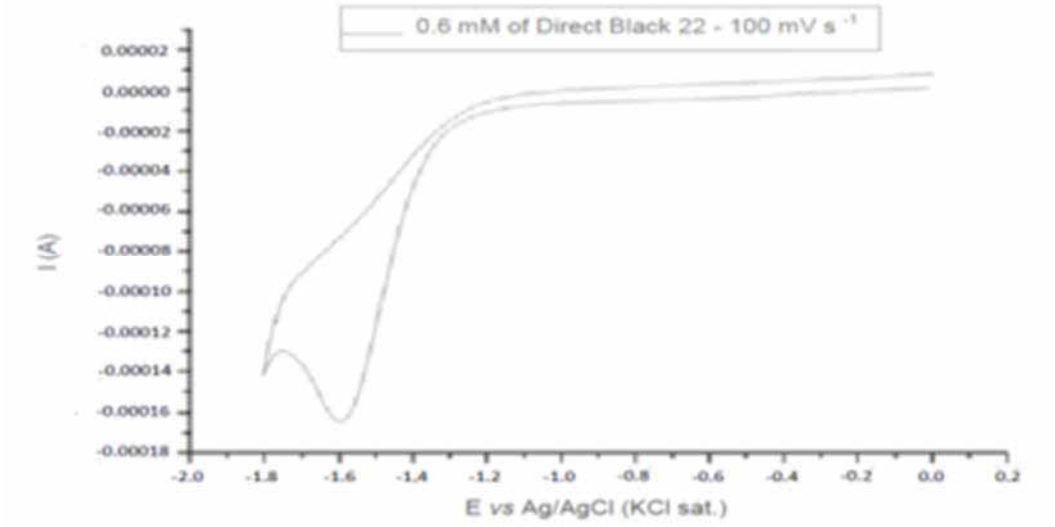


FIGURE 3. Cyclic voltammogram of the azo dye Direct Black 22 (DB22)

pH. At the beginning of the BES experiments the pH was adjusted to 7.0 in both anode and cathode chambers. After 24 hours it had dropped to 3.0 in the anode and 12.0 in the

cathode chambers. Then, it was re-adjusted with NaOH (1N) or NaCl (1N) to pH 7 once more. Few minutes after the 2nd adjustment, the pH decreased to 5.0 at the anode chamber and rose to 12.0 at the cathode chamber, without any new adjustment until the end of the experiment. It is important to highlight the protons exchange through the membrane was probably much slower than the production rate in the anode chamber and also than the consumption rate in the cathode chamber. Cui et al. observed adequate system performance under these pH conditions (5 at anode and 12 at cathode) [10], while Gil et al. recommend buffering the anode chamber for equalize the slow protons transport rate when the authors observed an increase in the pH over 9.5 in the cathode and a decrease to 5.4 in the anode chambers [11]. In our system, after the 2nd pH adjustment the system performance was, apparently, not affected by the pH values.

Dye removal. For BES, 90% of DB22 decolorization efficiency was observed during the experimental period (80% was removed in the first 48 hours). For ES, the corresponding decolorization efficiency was 81% (**Figure 4a and 4b**). This correspond a better behavior of the BES system Appling a much lower potential of 0.5V, Cui et al. obtained 99.2% of decolorization after 48h for the mono-azo dye alizarin yellow R (AYR) in a dual-chamber BES [12]. This high efficiency, even at lower potential, can result from the amount of azo bonds, and / or stability of the molecules.

The values of first-order kinetic constants for BES and ES were 0.03 and 0.01 h^{-1}, respectively. Since the BES degradation rate presents three times greater than that of ES.

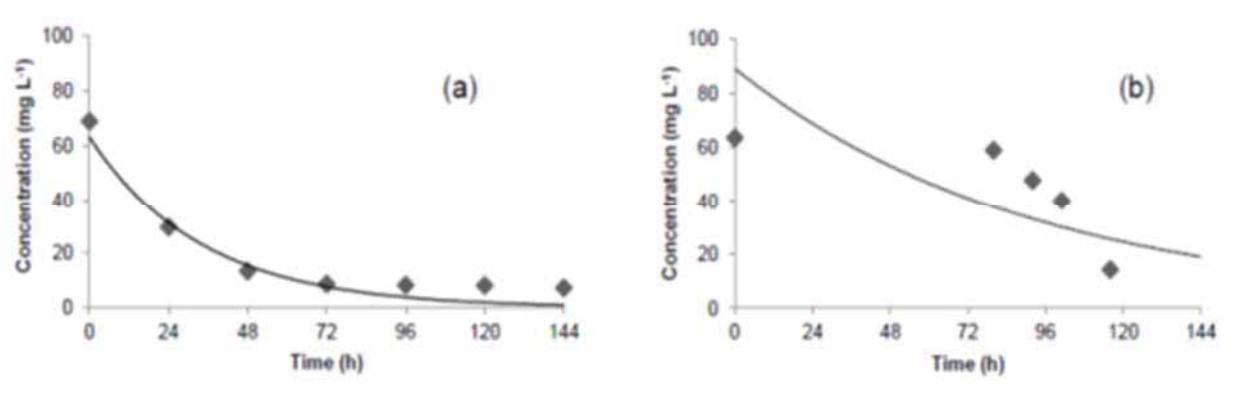


FIGURE 4. (a) degradation kinetics setting for first order model for bio electrochemical system (BES; (b) degradation kinetics setting for first order model for electrochemical system) (ES)

COD removal. The COD removal efficiency was around 56% and 76% for BES and ES, respectively. The low COD removal detected for BES is probably associated with the pH decrease found during the first 24h hours of experiment, with no COD removal during this period (**Figure 5a and 5b**). The pH directly affects biological activity [13]. Under the limited conditions of proton transfer through membrane in our system, the microbial activity and the electron transfer to the electrode in the anode compartment were probably reduced due to the pH change in the anode chamber. **Figure 5a** shows that

when the pH was re-adjusted to 7.0 in the anode, the COD removal started, indicating microbial activity enhancement.

A great advantage of MFCs is that these systems can operate at low COD rates, making possible the biological reduction in COD concentrations ~20 mg COD/L[14]. As COD is added in excess, the BES is a lower removal. Studies show that the effect of variations in operating conditions such as pH of the solution, current density, the number of electrodes, residence times in electrochemical bioreactors and may interfere with the removal of COD. Chatzisymeon et al. varying pH, salinity and current, obtained COD removal efficiencies between 29% and 86% [15].

n the case of ES, in the absence of microorganisms, the glucose (COD source) was oxidized through non-enzymatic reaction (**Figure 4b**).

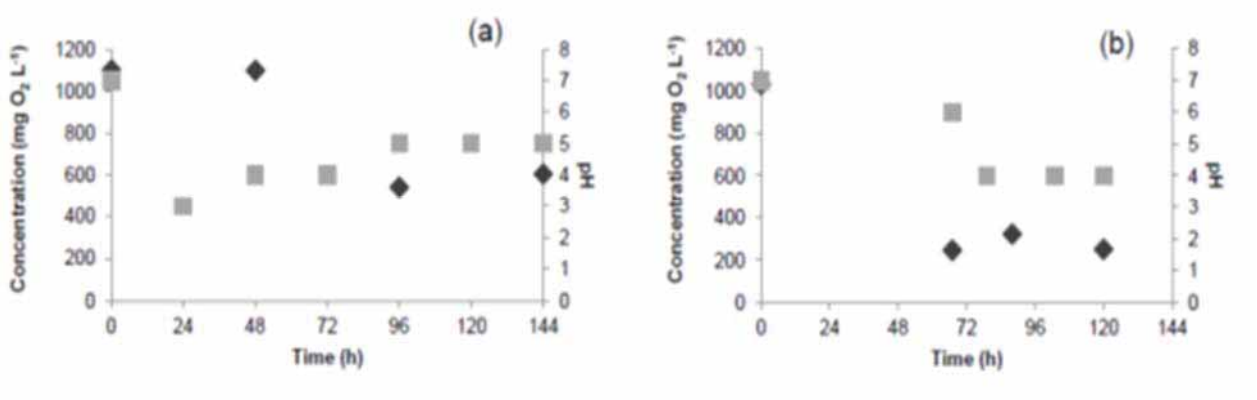


FIGURE 5. (a) COD removal and pH for bio electrochemical system (BES); (b) COD removal and pH for electrochemical system) (ES)

◆ **COD** ■ **pH**

CONCLUSION

The tetra-azo dye Direct Black 22 (DB22) was investigated by bioelectrochemical system dual-chamber.

For this study, BES was more efficient compared to ES, which can be shown by the 90% bleaching efficiency for the BES and 81% for ES and by the constant decolorization speed with 0.03 and 0.01 (h^{-1}) to BES and ES, respectively.

The COD removal efficiency was around 56% and 76% for BES and ES, respectively. The lower efficiency in BES the removal of COD can be in response to various interferences. Studies will be conducted to find an ideal condition.

ACKNOWLEDGMENTS

The authors thank Fundação de Amparo à Ciência e Tecnologia do Estado de Pernambuco (FACEPE - IBPG-0585-3.07/13/ PRONEX - Process: APQ -0603.3-07/14) for the financial assistance and a scholarship provided to the first author and the Brazilian National Counsel of Technological and Scientific Development (CNPq) for financial assistance.

REFERENCES

1. Huang L.P., Cheng S.A. and Chen G.H., Bioelectrochemical systems for efficient recalcitrant wastes treatment. *J Chem Technol Biotechnol.* 2011, 86, 481–491. doi: 10.1002/jctb.2551
2. Pandey A, Singh P, Iyengar L (2007) Bacterial decolorization and degradation of azo dyes. Int Biodeterior Biodegrad 59:73–84. doi:10.1016/j.ibiod.2006.08.006
3. Amaral FM, Kato MT, Florencio L, Gavazza S (2014) Color, organic matter and sulfate removal from textile effluents by anaerobic and aerobic processes. Bioresour Technol 163:364–369. doi:10.1016/j.biortech.2014.04.026
4. van der Zee, F. P., Bouwman, R. H. M., Strik, D. P. B. T. B., Lettinga, G. and Field, J. A. (2001), Application of redox mediators to accelerate the transformation of reactive azo dyes in anaerobic bioreactors. Biotechnol. Bioeng., 75: 691–701. doi:10.1002/bit.10073
5. Albuquerque, M. G. E. et al. Biological sulphate reduction and redox mediator effects on azo dye decolourisation in anaerobic-aerobic sequencing batch reactors. Enzyme and Microbial Technology, v. 36, p. 790–799, 2005. doi: 10.1016/j.enzmictec.2005.01.005
6. Mu, Y. et al. Decolorization of azo dyes in bioelectrochemical systems. Environmental Science and Technology, v. 43, n. 13, p. 5137–5143, 2009. doi: 10.1021/es900057f
7. Wrana, N. et al. Hydrogen gas production in a microbial electrolysis cell by electrohydrogenesis. Journal of Cleaner Production, v. 18, n. SUPPL. 1, p. S105–S111, 2010. doi: 10.1016/j.jclepro.2010.06.018
8. Amorim, S. M. et al. Influence of redox mediators and electron donors on the anaerobic removal of color and chemical oxygen demand from textile effluent. Clean - Soil, Air, Water, v. 41, n. 9, p. 928–933, 2013. doi: 10.1002/clen.201200070
9. American Public Health Association. Standard Methods For The Examination of Water and Wastewater. 22 ed. Washington: APHA, 2012.
10. Liu, L. et al. Microbial fuel cell with an azo-dye-feeding cathode. Applied Microbiology and Biotechnology, v. 85, n. 1, p. 175–183, 2009. doi: 10.1007/s00253-009-2147-9
11. Cui, D., Kong, F. Y., Liang, B., Cheng, H. Y., Liu, D., Sun, Q., & Wang, A. J. (2012). Decolorization of Azo Dyes in Dual-Chamber Bioelectrochemical Systems Seeding with Enriched Inoculum. Journal of Environmental & Analytical Toxicology, 2011. doi: 10.4172/2161-0525.S3-001
12. Kong, F. et al. Improved azo dye decolorization in a modified sleeve-type bioelectrochemical system. Bioresource technology, v. 143, p. 669–73, 2013. doi: 10.1016/j.biortech.2013.06.050
13. Wang, Y. Z. et al. Enhanced azo dye removal through anode biofilm acclimation to toxicity in single-chamber biocatalyzed electrolysis system. Bioresource Technology, v. 142, p. 688–692, 2013. doi: 10.1016/j.biortech.2013.05.007
14. Fernando, E.; Keshavarz, T.; Kyazze, G. Enhanced bio-decolourisation of acid orange 7 by Shewanella oneidensis through co-metabolism in a microbial fuel cell. International Biodeterioration and Biodegradation, v. 72, p. 1–9, 2012. doi: 10.1016/j.ibiod.2012.04.010
15. Madigan, M.T.; Martinko, J.M.; Dunlap, P.V.; Clark, D.P. Microbiologia de Brock. 12. ed., Porto Alegre: Artmed, 2010. 1160 p.

CHAPTER 7.2 FORMATION OF AEROBIC GRANULES IN SEQUENCING BATCH REACTORS APPLIED FOR DILUTED DOMESTIC WASTEWATER

Julliana M. P. Araújo (1); Poliana M. J. Silva (2); Oucilane I. M. Alves (2); Sávia Gavazza (2); Mário T. Kato (2) and Lourdinha Florêncio *(2)

(1) Federal Institute of Education, Science and Technology of the Sertão Pernambucano, Road Tamboril, s/n, Ouricuri, Brazil
(2) Federal University of Pernambuco, Architecture Avenue, s/n, University City, Recife, Brazil

ABSTRACT

Aerobic granulation in sequencing batch reactors (SBR) is an important alternative for wastewater treatment. The granules are formed by increasing the biomass retention in the system, and enabling the simultaneous removal of organic matter and nutrients. However, there are few works that use real wastewater, especially with low organic concentration. Therefore, this study investigated the influence of different volumetric changes in SBR on morphological changes of microbial aggregation during the formation of aerobic sludge pellets treating diluted domestic wastewater. A methodological strategy with two SBRs with different volumetric changes, SBR1 and SBR2 59% to 71% was used. The reactors consisted of transparent acrylic cylindrical column of the same dimensions (total height: 3.0 m; useful height: 2.45 m; inner diameter: 0.245 m; net volume: 115.5 L; total volume: 141.4 L; wall thickness: 0.003 m) and different heights for withdrawing treated effluent (1.0 m to 0.70 m and SRB1 to SRB2). Also the aeration rate of 1.2 to 1.4 $cm.s^{-1}$, ratio of height to diameter 10 and the sedimentation end time between 10 and 15 minutes were used for both reactors. Variations were observed in the behavior of the suspended solids and reduction of cell retention associated with short settling time. The observation of dense and compact granular structures was possible after 71 days of operation for the SBR1 and small granular structures from 91-day operation for volume exchange of 71% (SBR2). It was attributed this difference between the reactors to the constant washing of biomass in SBR2 which was superior to bacterial growth. Phosphorus removal was not observed in both reactors possibly due to no maturation of the granules and the consequent lack of anaerobic microzones. At the end of this work, the viability of granulation process using sewage diluted as a substrate without the presence of inoculum was verified. It was also observed that using lower volumetric exchange this process is qualitatively better with faster granulation, presence of dense granules with improved sludge sedimentation and greater removal of NH4+ and TKN.

Keywords: aerobic granular sludge, sequencing batch reactors, domestic wastewater.

---

*Author for correspondence: flor@ufpe.br

INTRODUCTION

The treatment of domestic wastewater needs obey, among other requirements regulated by legislation, minimum removal efficiency of organic matter and nutrients. The utilization of activated sludge systems is widespread to satisfy these requirements since achieve high efficiency in removal of organic matter. However, due this procedure presenting a low concentration of biomass (volatile suspended solids – VSS) in the aeration tanks it requires specific conditions, such as settling tank intended only to sedimentation; tanks or anaerobic compartments for nutrients removal; and large areas for the system installation. These conditions limit or hinder the use of activated sludge systems, encouraging the search for new treatment technologies to improve their applicability and functionality.

An improvement for retaining biomass in the activated sludge systems is their immobilization by using reactors with biofilms, as biofilters and Moving Bed Biofilm Reactor (MBBR). However these treatments require support material and preventive maintenance for clogging[1]. The aerobic granulation technology is an alternative to immobilization by support material because under specific operating conditions will occur self-immobilization of the biomass[2]. The main advantage of this technology is the existence of microenvironments in the granules, provided by diffusion gradients (**Figure 1**). These gradients allow the growth of bacterias with different metabolic functions and different environmental requirements, enabling coexistence of different species capable of degrading the various compounds present in the wastewater. Among the advantages of its use are: high biomass concentrations[3]; the possibility of processing large volumetric loads[4]; and the opportunity to achieve simultaneous nitrification and denitrification as well as biological phosphorus removal[1].

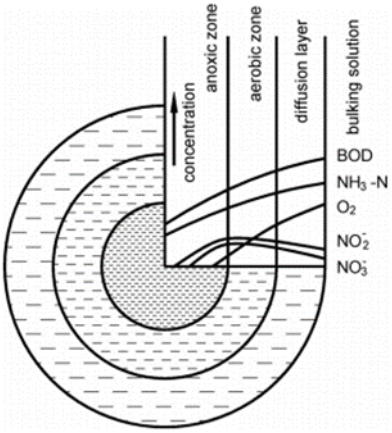


FIGURE 1. Pattern of DO and substrate concentration in sludge[5]

The most researches about the aerobic granulation use laboratory scale and synthetic effluents with high organic load. This fact is due to instability of the granules, which is reported in the literature as one of the major problems affecting its implementation in pilot scale[6]. Thus a better understanding of the formation and characteristics of aerobic granule it possible to identify optimum operating conditions to ensure better stability of the granular biomass and therefore establish this technology as a feasible treatment for domestic wastewater[1]. In this context, this study aimed to

investigate the influence of different volumetric changes in SBRs as operating condition for the development of aerobic granule in the treatment of diluted domestic wastewater.

MATERIALS AND METHODS

Experimental system. The experimental system was installed in the wastewater treatment plant (WWTP) “Mangueira”, located in the city of Recife (Brazil) and automated with the aid of a programmable logic controller (PLC), using ladder language. The system components can be visualized in **Figure 2** and its operation occurred according to the following steps:

1. Initially the influent was pumped after passing the grit chamber WWTP for a storage tank with a capacity of 01 m³;
2. Then, influent was directed by pumping to the two reactors in each filling period of operating cycles;
3. after the period timed by the PLC for reaction (compressor drive for system oxygenation) and sedimentation (settling time, where the compressor was off), the solenoid valve was triggered and the treated effluent was discarded to the grit chamber of the WWTP.

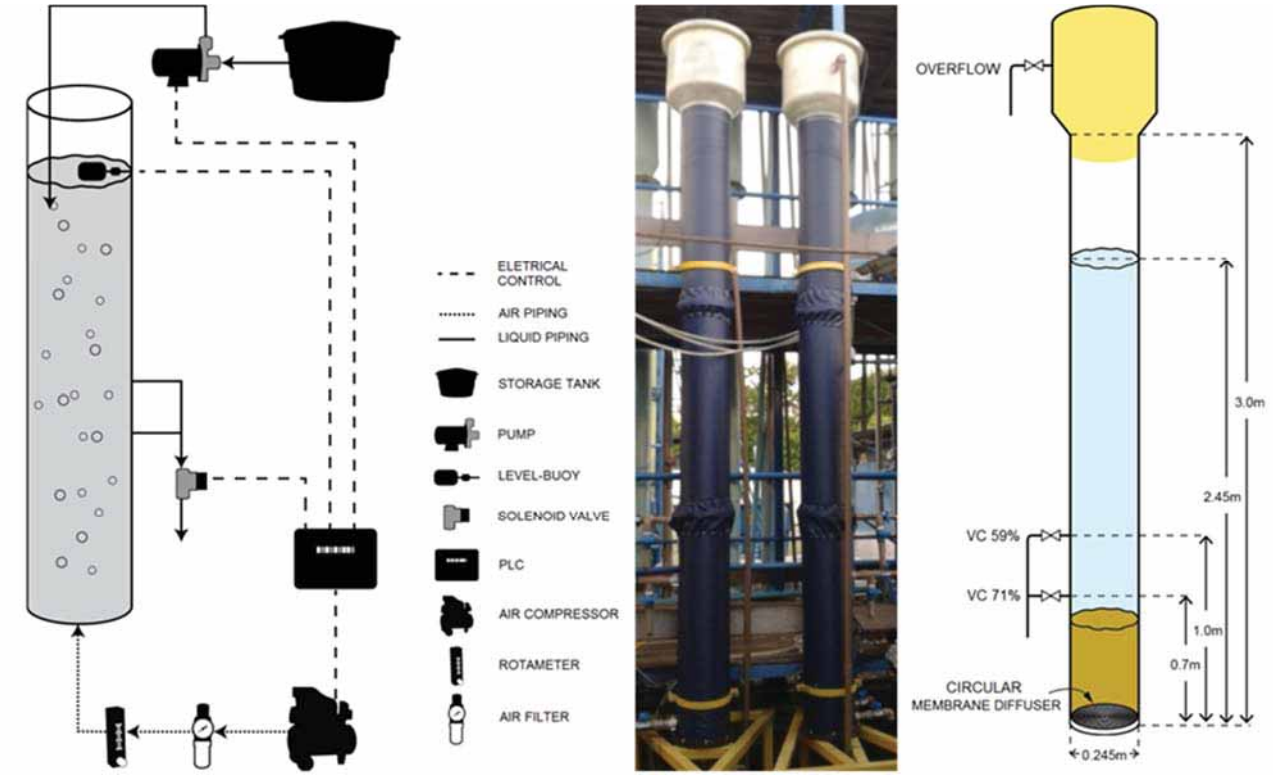


FIGURE 2. Experimental scheme (left); Photography of reactors (center), Graphic diagram (right).

The reactors consisted of two transparent acrylic cylindrical column (**Figure 2**) of the same dimensions (total height: 3.0 m; useful height: 2.45 m; inner diameter: 0.245 m; net volume: 115.5 L; total volume: 141.4 L; wall thickness: 0.003 m) and different

heights for withdrawing treated effluent (1.0 m to 0.70 m and SRB1 to SRB2). They were covered with dark fabric to prevent the algae proliferation.

Operating conditions. Considering the known low organic load of the WWTP influent and the need for high organic load required for the granulation process, the cycle time was set to 3 hours to the both reactors, totaling eight daily cycles. The duration of each phase of the cycle is described in **Table 1** below.

Table 1. Duration of the steps of the operational cycle

Steps of the cycle	Duration of the steps (min) Operation week							
	1th	2th	3th	4th	5th	6th	7th	8th on
Filling	2	2	2	2	2	2	2	2
Reaction	135	140	145	150	155	160	165	160
Sedimentation	40	35	30	25	20	15	10	15
Discard	3	3	3	3	3	3	3	3

It was believed that strategy of reducing the settling period in 5 minutes each week would result in the selection of particle with good and gradual sedimentation, avoiding great initial losses of biomass. Also the aeration rate utilized of 1.2 to 1.4 $cm.s^{-1}$ provides greater shear stress. Finally, the reactors were operated with different volumetric changes (a reactor with 59% SBR1, and the other 71%, SBR2) seeking to compare the influence of the volumetric change in granulation

a) Analysis

Weekly samples were collected from the raw influent (input), from the mixed liquor (mixture of biomass and effluent at the end of the reactors reaction time) and from the treated effluent (outputs of the reactors). The analysis are listed in the Table 2.

TABLE 2. Analysis

Analysis	Methodology	Sample
Volatile Suspended Solids (VSS)	Method 2540-G[7]	Mixed liquor, influent and effluent
Sludge Volume Index (SVI)	Sedimentation[8]	Mixed liquor
Photomicroscopy	Bright field microscopy	Mixed liquor
COD_{total}	Method 5220-C[7]	Influent and effluent
$COD_{soluble}$		
TKN	Method 4500 N_{org} - B[7]	Influent and effluent
$N\text{-}NH_4^+$	Method 4500 NH_3-B e C[7]	Influent and effluent

RESULTS AND DISCUSSION

Figure 3 sets forth the variation of VSS concentration in the mixed liquor (MLVSS) during operation of the reactors.

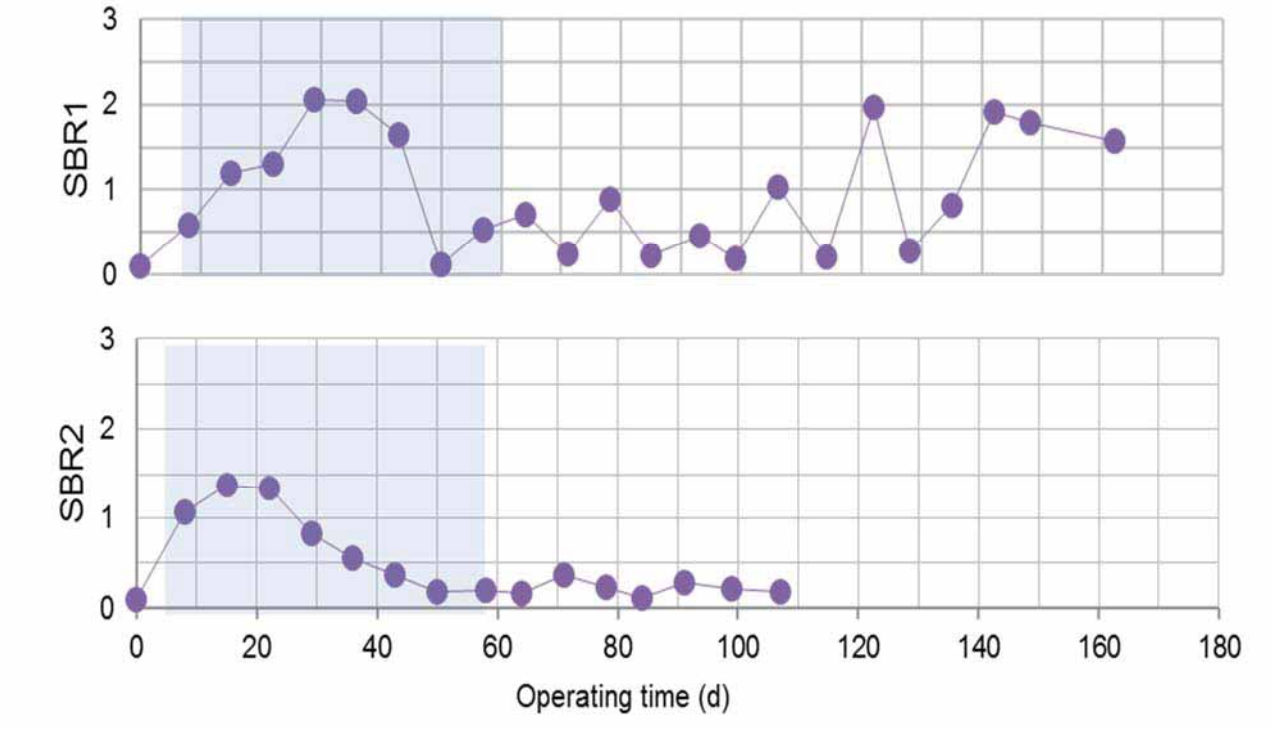


FIGURE 3. MLVSS (g.L^{-1})

As the reactors were not inoculated, the initial concentration of MLVSS is assigned to the raw wastewater. After the operation start, the increase in this concentration was perceived due to the growth of biomass during the first two weeks higher in the reactor with higher volumetric change (SBR2), which was attributed to the different rate of organic load applied. However, with the decrease in settling time on the following weeks was noted a greater biomass loss attributed to a high selection pressure by the volumetric change associated to the short settling time. The highest concentration observed was 2.05 g MLVSS.L^{-1} to 29 days in SBR1 and 1.38 g MLVSS.L^{-1} to 15 days in SBR2.

The gradual decrease in settling time to 10 minutes resulted in a loss of approximately 90% of the MLSSV SBR1, obtaining a concentration of 0.12g MLVSS.L^{-1}. So it was necessary to increase the time decanting for 15 minutes until stabilization of the biomass. Sludge loss during the reduction of the settling time as operating strategy has also been reported in the literature after reduction of the settling time to 10 minutes, which resulted in a loss of about 70% solids (0.7 g MLVSS.L^{-1})[9]. Stabilization can be observed after 140 days of operation in SBR1, with an average concentration of MLSSV 1.76 ± 0.17 g.L^{-1} for the last three collected, corresponding to a coefficient of variation of 9.6%.

Figure 4 sets forth the variation of the SVI in the mixed liquor (MLVSS) during operation of the reactors.

It is known that the reduction in settling time causes a tendency of the SVI achieve lower values due to selection of the particles by gradual increase of pressure seleção[10]. In SBR1 after reduction after increasing the settling time to 15 minutes, the SVI began to

increase gradually, with values near great relationship IVL30 / IVL10 90% for aerobic granular sludge, proposed by Liu and Tay[11].

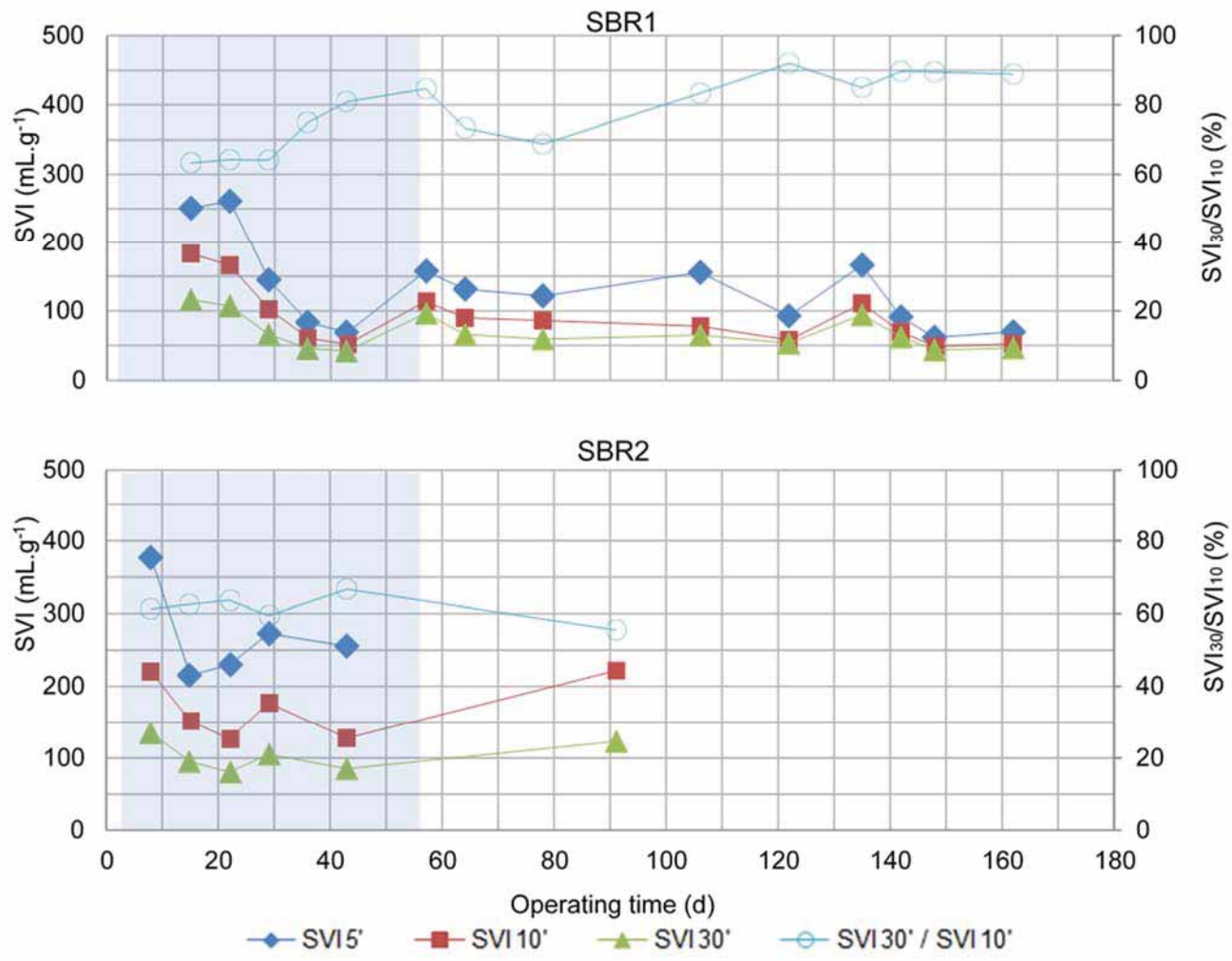


FIGURE 4. SVI 5' (mL.g^{-1}), SVI 10' (mL.g^{-1}), SVI 30' (mL.g^{-1}), SVI30'/SVI10' (%)

However, in SBR2 the low concentration of solids in various samplings precluded SVI analysis, since in these cases the volume measurement decanted resulted in lower values the calibration value in the measuring cylinder. The average values for SVI30, SVI10 and the SVI10 / SVI30 ratio were 170.9 ± 43.0 mL.g^{-1}, 104.0 ± 21.6 mL.g^{-1} and 61.5 ± 3.8% respectively, characterizing the sludge as bad sedimentation. ~~Such a~~ sedimentation associated with short settling time (15 minutes) used in the system contributed to the low concentration of MLVSS.

The data relating to SVI plotted in boxplot in **Figure 8** allow a comparative analysis of the reactors and demonstrate that SBR1 operation resulted in sludge with a better sedimentation compared to SBR2. Although the literature asserting that greater volumetric changes result in lower SVI's, the loss of sludge and constant renewal thereof (lower sludge age) prevented the self-immobilization of biomass.

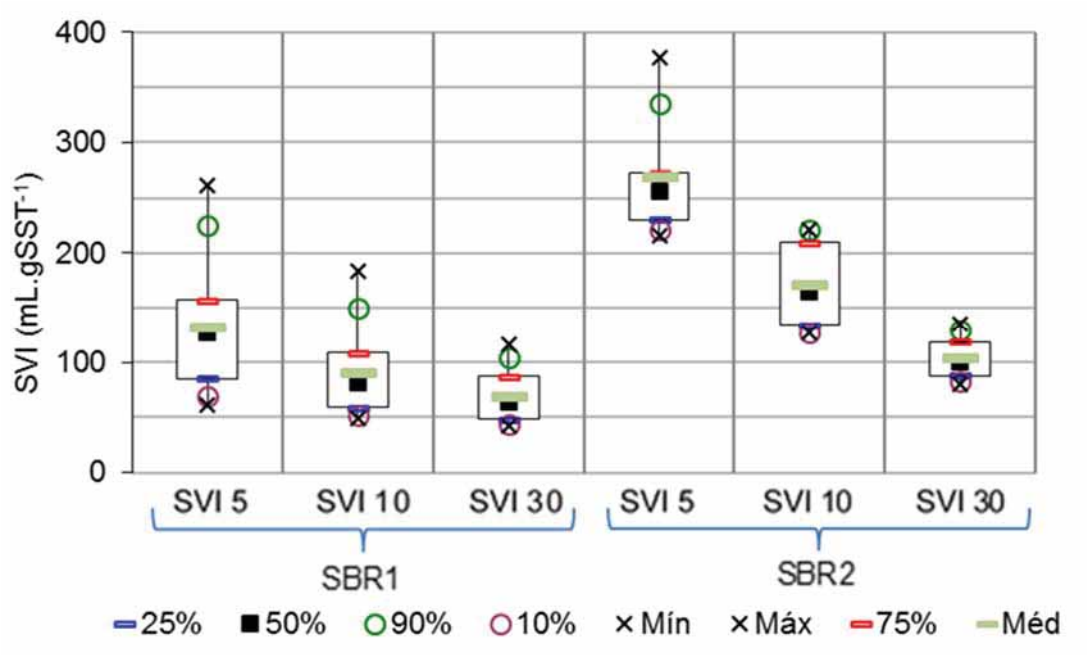


FIGURE 5. Boxplot: SVI_5, SVI_{10} e SVI_{30} for SBR1 and SBR2

The development of granular biomass was monitored by optical microscopy. **Figure 6** shows 100x magnification images for biomass in SBR1, and allows the perception of changes in morphology of microbial aggregation during operation of the reactor. On the 15th day of operation (**Figure 6a**) can be perceived biomass rather dispersed in flakes characteristic of conventional activated sludge system, with very irregular morphological structure. After 36 days (**Figure 6b**) less dispersed flakes and the onset of agglutination of microorganisms for the formation of granule have been observed. Well-formed aerobic granules were observed after 71 days of operation (**Figure 6c** and **6d**), however, aeration issues between the 70th and 85th day of operation caused the partial disintegration of the granules, and these were observed less dense and associated with the presence of flakes in 93 days (**Figure 6e**). In 122-day (**Figure 6f**), there is the reappearance of denser granules, however, still associated with the flocculent sludge.

Figure 7 sets forth the photomicroscopys for the SBR2. Looking at the figure, on day 15 (**Figure 7a**) the biomass found itself rather dispersed into small and irregular flakes. After 36 days (**Figure 7b**), large fluffy and dispersed flakes were observed. After 64 days (**Figure 7c** and **7d**), some flakes were larger and with denser centers. At 78-day (**Figure 7e**), a bit more dense flakes were observed. Only after 91 days of operation (Figure 7f) was observed small granules. However, the interruption of the experiment on 107th day of operation made it impossible to observe a longer period in the presence of granule.

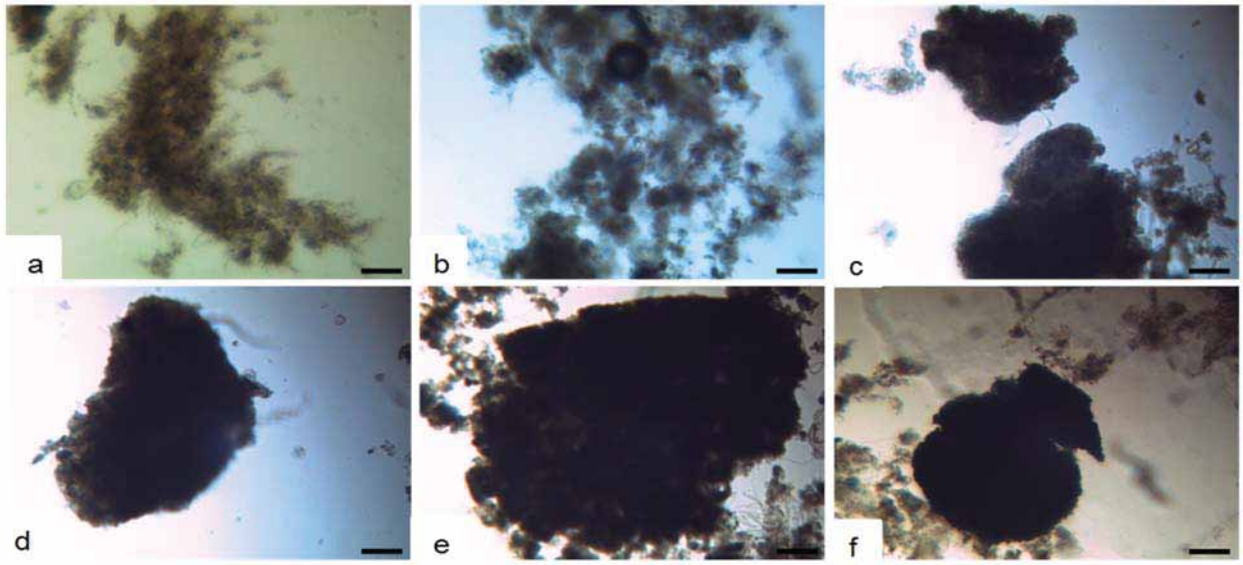


FIGURE 6. Photomicroscopy of the biomass SBR1: Bright field microscopy (100x) operating on different days: (a) 15-day; (b) 36-day; (c) e (d) 71-day; (e) 93-day; (f) 122-day. Bar = 100µm

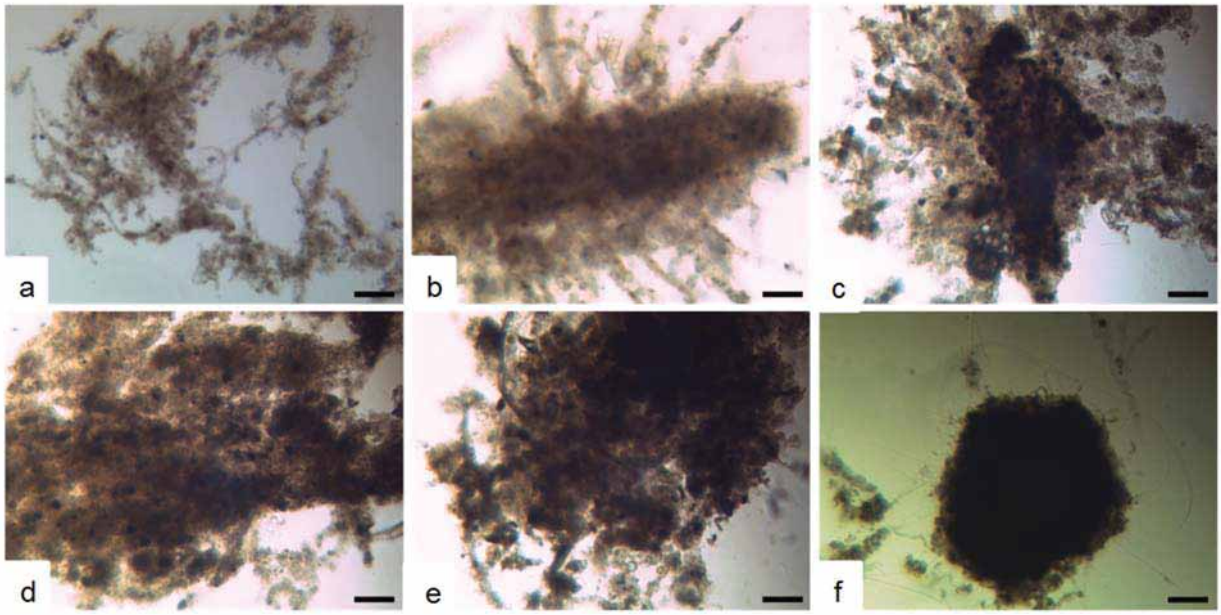


FIGURE 7. Photomicroscopy of the biomass SBR2: Bright field microscopy (100x) operating on different days: (a) 15-day; (b) 36-day; (c) e (d) 64-day; (e) 78-day; (f) 91-day. Bar = 100µm

Equivalently to data found, other authors noted, by monitoring a reactor at 30 ° C using 1.6 kg DQOt.m^{-3}.d^{-1}, low stability of aerobic granules[12]. It was observed complete granulation only after 150 days of operation using an organic load of 2.1 ± 0.5 kg DQOt.m^{-3}.d^{-1} [9] as has also been observed a time of granular development over 400 days using an SBR fed with municipal wastewater with low organic load[13]. Thus, it can

be concluded that the granulation process using domestic wastewater with low organic load demands a long period of observation.

Regarding removal efficiency of reactors, **Figures 8** and **9** show that there was no significant difference between the COD removal efficiency, and the removal efficiency of NH_4^+ and TKN was greater in the SBR1, despite a wide variation (large interquartile range).

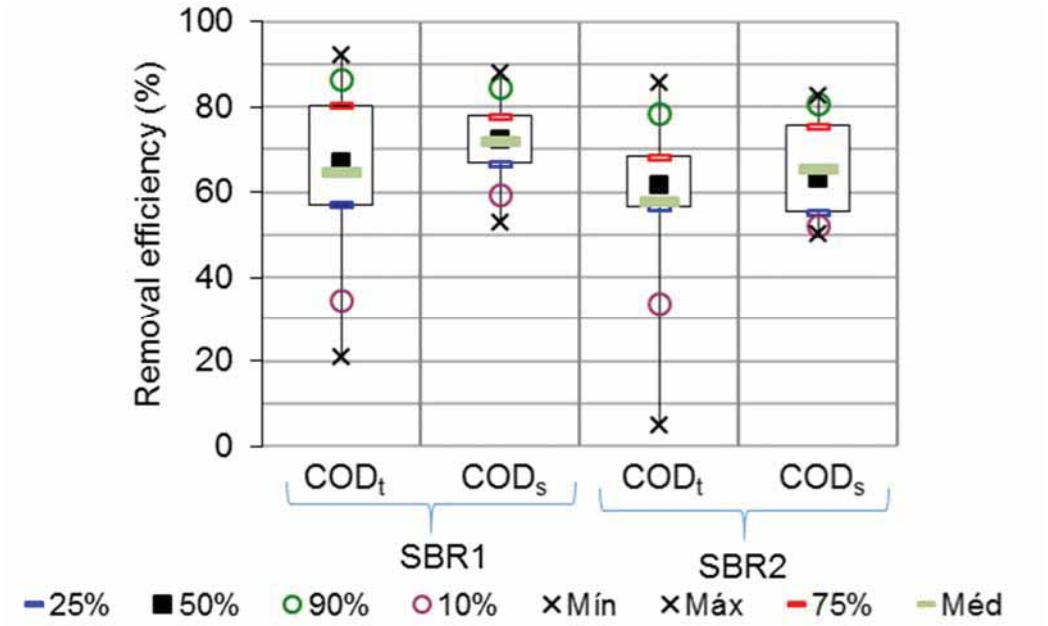


FIGURE 8. Boxplot: Removal efficiency of COD_{total} and $COD_{soluble}$ - SBR1 and SBR2

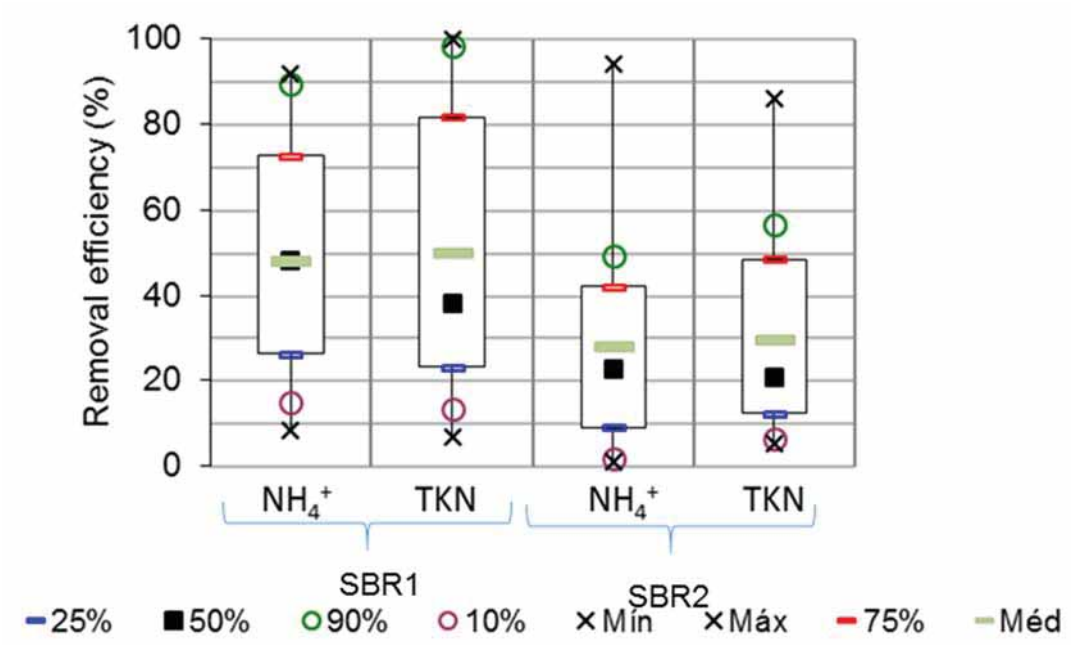


FIGURA 9. Boxplot: Removal efficiency of NH_4^+ and TKN - SBR1 and SBR2

CONCLUSION

Considering the objective of this study, it was possible to verify the viability of the granulation process using diluted domestic wastewater (COD_{total} of 392.1 ± 190.9 and $COD_{solubre}$ of 126.6 ± 28.0) as a substrate without the presence of inoculum. It was also observed that using lower volumetric exchange this process is qualitatively better (faster granulation, sludge presence with improved sedimentation and greater removal of NH_4^+ and TKN).

As for the time necessary for the formation of granules in function of volumetric changes this experiment allowed the observation of dense and compact granular structures from 71 days to the volumetric change of 59% (SBR1) and small granular structures from 91 days of operation for the volumetric change of 71% (SBR2). We attribute this difference to constant washing of biomass in SBR2 which was superior to bacterial growth.

Aeration issues in SBR1 caused partial disintegration system of the granules, increasing the presence of flocculent sludge, it can be inferred that the initial granulation process is very sensitive to variations in air flow applied.

The average removal efficiency COD_{solube} and COD_{total}, there were no significant differences between the two reactors, with the following results: 1) COD_{solube} - 72 ± 10% for the SBR1 and 65 ± 12% for the SBR2; 2) and COD_{total} - 65 ± 21% for the SBR1 and 58 ± 21% for the SBR2. The high coefficient of variation of COD_{total} removal efficiency is associated with the washout of biomass systems, resulting in a higher solids concentration in the treated effluent.

Best results NH_4^+ and TKN removal efficiency was observed for the volumetric change of 59% (SBR1), confirming that a smaller volume exchange is more efficient during the initial granulation process using diluted domestic wastewater diluted.

ACKNOWLEDGMENTS

University Federal of Pernambuco, COMPESA, CAPES, PRONEX, Odebrecht Ambiental, CNPq, FACEPE and Fibra Técnica.

REFERENCES

1. BASSIN, J.P. Tecnologia de granulação aeróbia (Lodo granular aeróbio). In: **Processos biológicos avançados para tratamentos de efluentes e técnicas de biologia molecular para o estudo da diversidade microbiana**. Org: DEZOTTI, M.; SANT'ANNA JR., G. L.; BASSIN, J. P. 1 ed. Interciência: Rio de Janeiro, 2011.
2. ADAV, S. S.; LEE, D. J.; SHOW, K. Y.; TAY, J. H. Aerobic granular sludge: recent advances. **Biotechnology Advances**, v. 26, p. 411-223, 2008.
3. ETTERER, T.; WILDERER, P. A. Generation and properties of aerobic granular sludge. **Water Science and Technology**, v. 43, p. 19-26, 2001.
4. BEUN, J. J. VAN LOOSDRECHT. M. C. M.; HEIJNEN, J. J. Aerobic granulation. **Water Science and Technology**, v. 41, p. 41-48, 2000.
5. HE, S.B.; XUE, G.; WANG, B. Z. Factors affecting simultaneous nitrification and de-nitrification (SND) and its kinetics model in membrane bioreactor. **Journal of Hazardous Materials**, v. 168, p. 704-710, 2009.

6. LEE, D. J.; CHEN, Y. Y.; SHOW, K. Y.; WHITELEY, C. G.; TAY, J. H. Advances in aerobic granule formation and granule stability in the course of storage and reactor operation. **Biotechnology Advances**, v. 28, p. 919-934, 2010.
7. AMERICAN PUBLIC HEALTH ASSOCIATION (APHA). **Standard Methods for the examination of water and wastewater**. 22 ed. United Book Press: Washington, 2011.
8. SCHWARZENBECK, N.; ERLEY, R.; WILDERER, P. Aerobic granular sludge in a SBR-system trating wastewater rich in particulate matter. **Water Science and Technology**, v 49, p 41-46, 2004.
9. AKABOCI, T. R. V. **Tratamento de esgoto sanitário em reator em bateladas sequenciais: desempenho do processo e modelagem matemática**. Dissertation. 169 p. University Federal of Santa Catarina (UFSC): Florianópolis, 2013.
10. QIN, L.; LIU, Y.; TAY, J. H. Effect of settling time on aerobic granulation in sequencing batch reactor. **Biochemical Engineering Journal**, v. 21, p. 47-52, 2004.
11. LIU, Y. Q.; TAY, J. H. Influence of starvation time on formation and stability of aerobic granules in sequencing batch reactors. **Bioresource Technology**, v. 99, p. 980-985, 2008.
12. EBRAHIMI, S.; GABUS, S.; ROHRBACH-BRANDT, E.; HOSSEINI, M.; ROSSI, P.; MAILLARD, J.; HOLLIGER, C. Performance and microbial community composition dynamics of aerobic granular sludge from sequencing batch bubble column reactors operated at 20ºC, 30ºC, and 35º. **Applied Microbiology and Biotechnology**, v. 87, p. 1555-1568, 2010.
13. LIU, Y. Q.; MOY, B.; KONG, Y. H.; TAY, J. H. Formation, physical characteristics and microbial community structure of aerobic granules in a pilot-scale sequencing batch reactor for real wastewater treatment. **Enzyme and Microbial Technology**, v. 46, p. 520-525, 2010.

CHAPTER 7.3 CONTAMINATED WATER TREATMENT RED REACTIVE TEXTILE DYE BY ELETROFLOCCULATION PROCESS

José Arruda Biserra Neto (1); **Luiz Gustavo de Sousa Pinto** (1); Armando Morais Correia de Melo Filho (1) and Henrique John Pereira Neves *(1)

(1) Associação Caruaruense de Ensino Superior e Técnico – ASCES, Av. Portugal, Nº 584, Caruaru - PE, Brasil.

ABSTRACT

In Brazil, the textile sector has a special emphasis on the release of wastewater into rivers and seas, which when not properly treated end up causing serious environmental contamination.
Constating this problem the present study aimed to remove red textile dye reactive of water, by eletroflocculation process, observing as the influence of the concentration of the dye solution, as the time of process and eletrolyte mass variation, in the quality of dye water removing process.
The water treatment was carried out in a reactor operated in batches, a 1-L vessel with two electrodes placed in the reactor via a metal structure in which soldered copper wires were connected to the DC source.
The treated water with eletroflocculation obtained satisfactory results. A comparison of the results of different dye concentrations and NaCl and the time change was made e in the present study was to evaluate an alternative form of water treatment. Eletroflocculation is a simple and effective treatment method.
This work concludes that it is possible to treat the effluent from textile laundries from electricity use low cost and satisfactory results, where the condition is best treatment with lower concentrations of dye and higher mass of NaCl.

Keywords: eletroflocculation, textile effluent, wastewater treatment.

INTRODUCTION

According to Cerqueira[1] the pollution that results from de release of liquid effluents in the rivers and seas, has become a problem of serious proportions, specially with regard to public health and integrity of the environment.

In according to Cerqueira[2] textile industry presents a special emphasis because there is a big volume of effluents generated by the process which if not properly treated, can cause serious environmental contamination.

Peres and Campos[3] state that among the processes in the textile industry, the processing of yarns and fabrics characterized by water intensive use, which ends becoming part of highly polluting liquid effluent, with a high variability and other characteristics that hinder their treatment.

---

*Author for correspondence: henriquejohn@yahoo.com.br

Industrial effluents treatments involve processes required to remove impurities generated in the manufacture of their products. Treatment methods are directly related to the type of effluent generated and to the operational control of industrial activity and the feature of the water used[2].
According to Freitas[4] reducing of effluents volume through recycling and recovery of chemicals and by-products without compromising the final product quality is the greatest challenge faced by the textile industry.

Eletroflocculation is a process that involves the generation of coagulants by dissolving iron and aluminum ions respectively from iron and aluminum electrodes by the action of the electric current applied to this electrodes. The generation of metal ions occurs at the anode , then the hydrogen gas arises at the cathode[2].

The object of this project of study was the removal of reactive red textile dye of water by eletroflocculation process, observing for this the influence of the dye solution concentration, process time and change in mass of electrolyte, in the quality of removed process dye of the water.

MATERIALS AND METHODS

Water treatment was carried out in a reactor operated in batches, in a 1-L container connected to two electrodes placed in the reactors through a metal structure in which copper wires were soldered connected to the DC source.

After it was mounter, a dye solution with a volume of 1L was placed in thereon, initial concentration of 10mg/L. It was made a absorbance(spectrophotometer) at the initial zero time (0), then adding 1g NaCl (electrolyte) in the solution, applying a 12 volt boltage to the electrodes for 10 minutes, making collected every 2 minutes. Then the final product was filtered, from each collect with a paper filter and featured again as the absorbance for the analysis procedure.

This procedure was repeated for the dye solution concentrations of 30 mg/L and 50ml/L to the time of 20 minutes and 30 minutes (each concentration and to each electrolyte mass) and 2g and 3g Na Cl mass (to each concentration and to each time).

RESULTS AND DISCUSSION

Figure 1 presents how the three factors, dye initial concentration, Na Cl mass and time influence the treatment process, as all have a p. 0.05. The three factors influence the process in the case of initial dye concentration, because they have a negative value, it mens this factor influences negatively the process, or, the more concentration increases, dye reduction NaCl mass decreases, because there was a time rising, because there was a positive value. It means that if there is time rising, there will be a greater water dye removal.

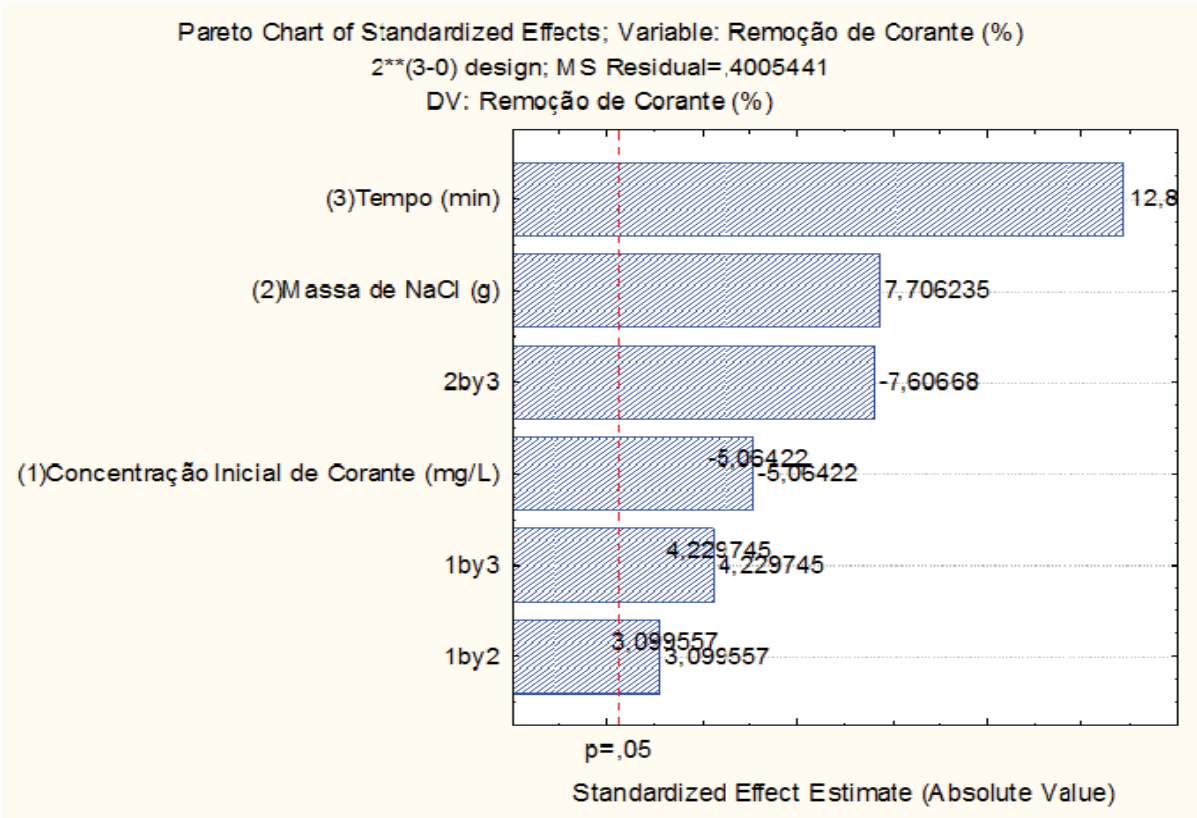


FIGURE 1. Pareto Chart of Standardized Effect

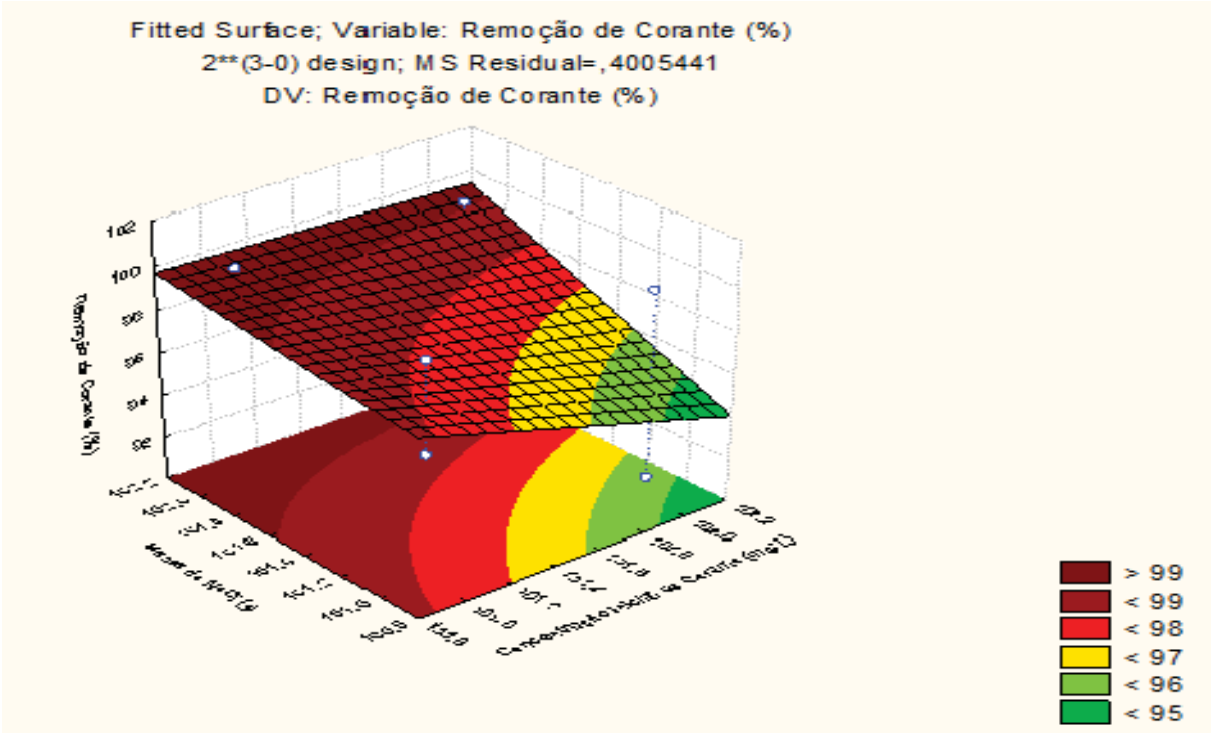


FIGURE 2. Fitted Surface, relation between the factors 'initial dye concentration' and 'NaCl mass'

In the **Figure 2**, which examines the relation between the factors 'initial dye concentration' and 'NaCl mass', one percept that there is a greater removal percentage in the situation which there is a less initial dye concentration (10mg/L) and a greater NaCl mass (3g), a condition representer by the redder, this condition is the best operational condition of the process.

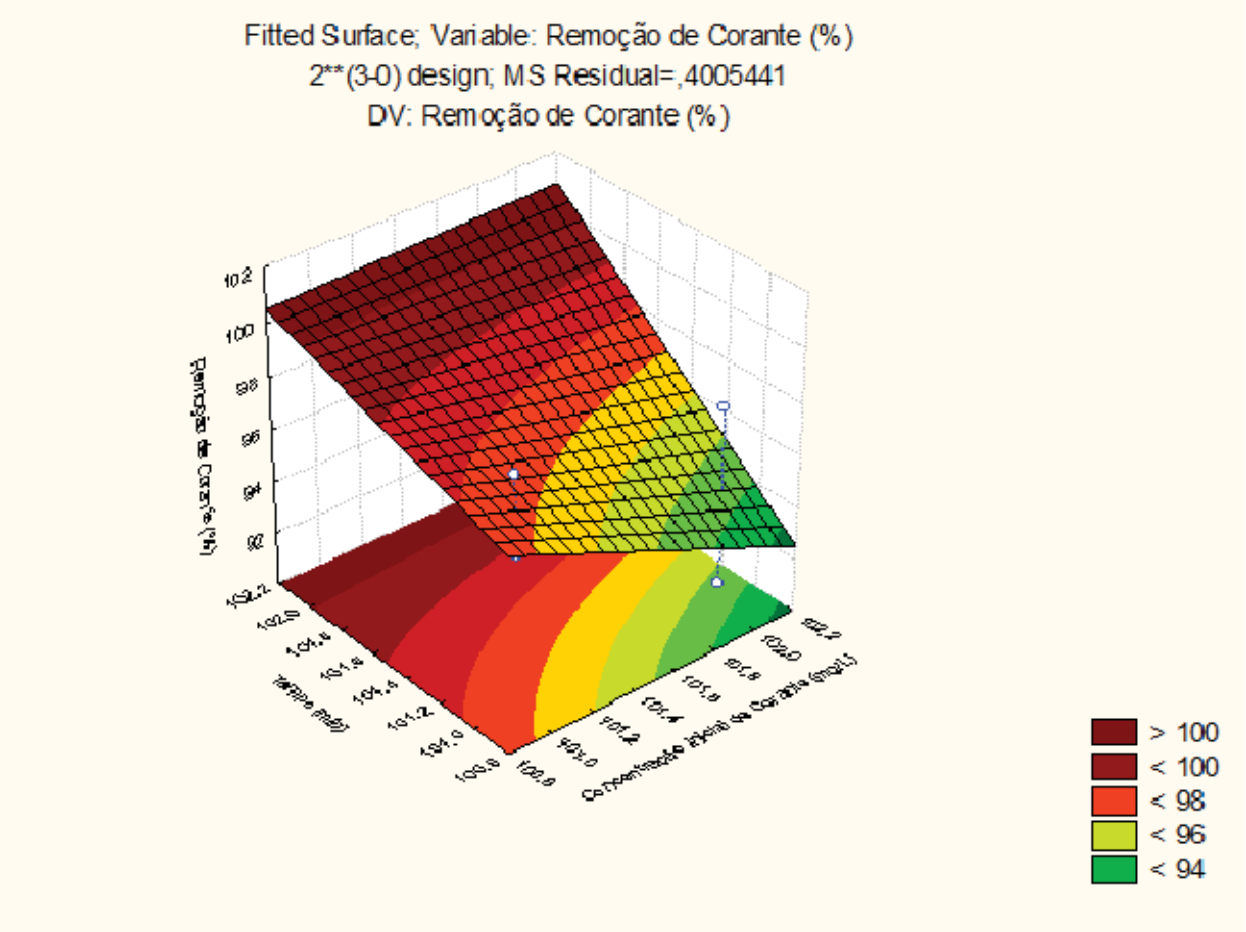


FIGURE 3. Fitted Surface, relation between dye and time initial concentration for greater dye water removal

In this response surface (**Figure 3**), that analyses the relationship between dye and time initial concentration for greater dye water removal, one percept the best condition, represented by redder, should be a less initial dye concentration (10mg/L) and greater time (30m), to have better process operational condition with more dye removal.

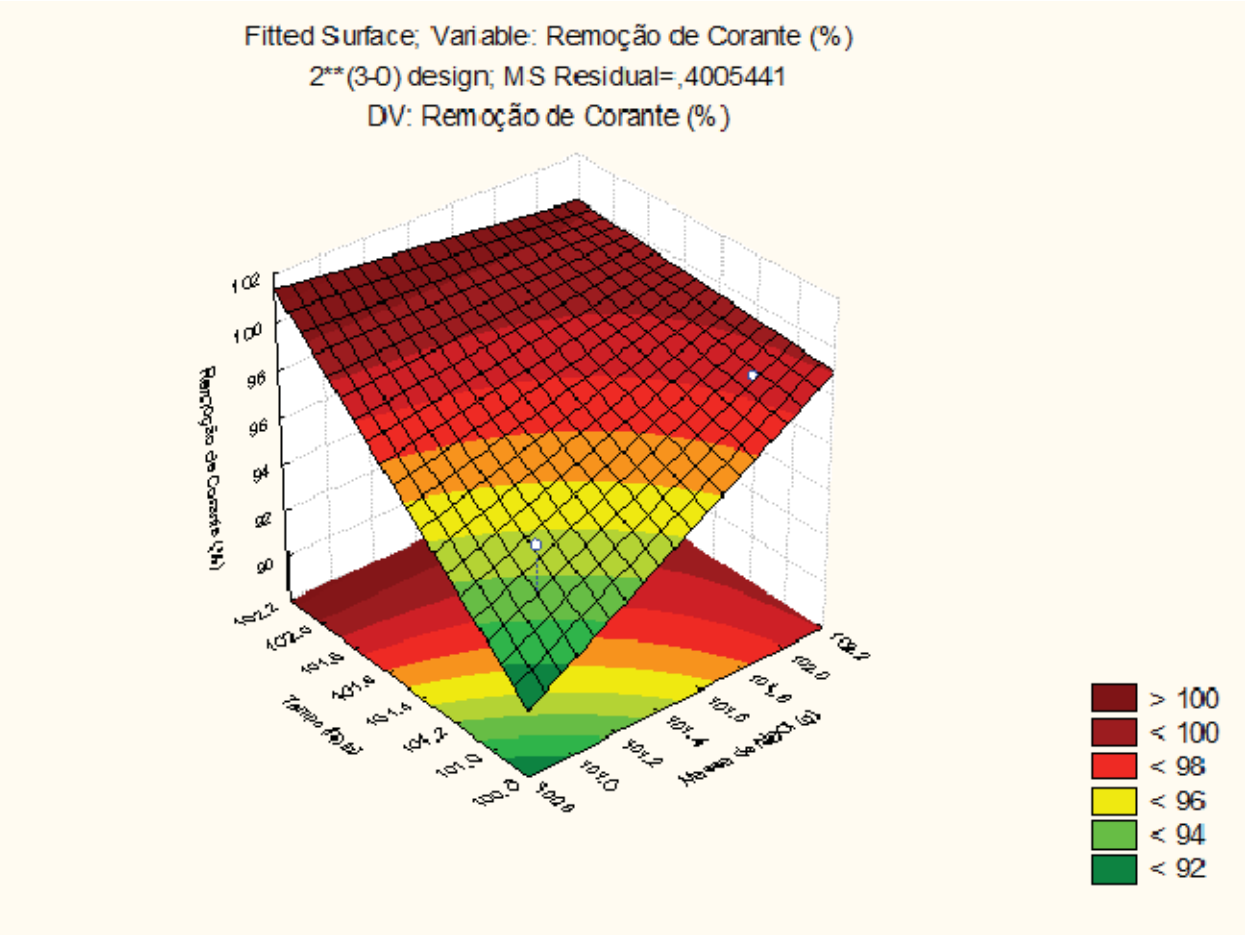


FIGURE 4. Fitted Surface, relation between NaCl mass and time

Figure 4 analyses the relation between NaCl mass and time, one can check the greater dye removal percentage and the better condition of process operation resultant is represented by redder, that means the NaCl mass should be higher (3g) and longer operation time (30m).

CONCLUSION

In the present study it was possible to evaluate an alternative of water treatment. Electrofloculations a simple and effective treatment method. In this work we conclude that is possible to treat the effluent from textile laundries through electricity use without low cost and satisfactory results.

As the textile industry is increasingly expanding in Brazilian Northeast and there is great volume of generation of effluents, electroflocculation was method used with the aim to treat this kind of effluent by the way to let it proper to reuse even in own textile industry with low cost. And we can say from the collected data trat the best treatment condition is with lower concentrations of dye and higher NaCl mass.

REFERENCES

1. CERQUEIRA, A. A., *Utlização de argilas na remoção de íons cromo presentes em efluentes industriais.* 53f. Monografia de especialização em química ambiental – Universidade do Estado do Rio de Janeiro, Rio de Janeiro, 2000.
2. CERQUEIRA, A. A., *Aplicação da técnica de eletrofloculação no tratamento de efluentes têxteis*. Tese com requisito a obtenção do título de Doutor- Universidade do Estado do Rio de Janeiro, Rio de Janeiro, 2006.
3. PERES, A. G.; CAMPOS, M. A., *Tratamento e reciclagem de efluentes finais de lavanderias com uso de carvão ativado de osso bovino*. EPCC, Maringá, 2007.
4. FREITAS, K. R., *Caracterização e reuso de efluentes do processo de beneficiamento da indústria têxtil.* Dissertação de mestrado, Curso de Pós-graduação em Engenharia Química pela Universidade Federal de Santa Catarina, Florianópolis, 2002.

CHAPTER 7.4 EVALUATION OF UASB REACTOR TREATING SYNTHETIC EFFLUENT FROM INDUSTRIAL DENIM LAUNDRIES

M. G. P. de Carvalho (1,2); S. Amorim (2); D. Marcelino (2); L. Florencio (2); M. T. Kato (2) and S. Gavazza (2)

(1) Instituto Federal do Piauí (IFPI), Av, Pedro Freitas, 1020, Teresina-PI, Brasil
(2) Universidade Federal de Pernambuco (UFPE), Av. Prof. Moraes Rêgo, 1235, Recife-PE, Brasil

ABSTRACT

The textile industry is a great driving force behind the development of the Agreste region in the state of Pernambuco, Brazil. Linked to economic benefits there are important environmental problems such as the discharge of effluents with high concentrations of dye, organic matter, salts and sulfate in rivers. Many azo dyes and their degradation products are toxic or mutagenic to aquatic life. Additionally, some dyes and/or their degradation by-products are carcinogenic and persistent in natural environments. Alternatively, to the physical chemical treatment, the ability of microorganisms to conduct decolorization seems to be more advantageous economically, especially due to the lower sludge production. Aiming to evaluate the behavior of a more suitable technology for the treatment of textile wastewater, two bench Upflow Anaerobic Sludge Blanket (UASB) reactors were used to assess the ability of removing the tetra-azo dye Direct Black 22 (DB22 – CAS number 6473-13-8) and chemical oxygen demand (COD), with and without the sulfate influence.

The reactors were fed with synthetic textile wastewater composed by cornstarch (COD of 1,500 mg $O_2.L^{-1}$), 35 mg.L^{-1} of DB22, macro and micronutrients. Each reactor was inoculated with 2 liters of sludge (27 gSTV.L^{-1}). Additionally, Reactor 2 (R2) was fed with 250 mg.L^{-1} of sodium sulfate. Both reactors were operated during 100 days, with hydraulic retention time (HRT), COD and organic loading rates (OLR) that changed along time, thus characterizing three operational phases: P1 (24 h, 570-730 mg $O_2.L^{-1}$, 0.52-0.74 kg COD.$m^{-3}.d^{-1}$); P2 (24 h, 1,080-1,090 mg $O_2.L^{-1}$, 1.08-1.09 kg COD.$m^{-3}.d^{-1}$) and P3 (15 h, 1,300-1,280 mg $O_2.L^{-1}$, 2.08-1.92 kg COD.$m^{-3}.d^{-1}$).

COD removal efficiency was 30% and 38% for Reactor 1 (R1) and R2 in P1, 68% for R1 and R2 in P2, 89% for R1 and R2 in P3. COD results indicate microbial adaptation through the operational time. DB22 removal efficiency was 23% and 15% for R1 and R2 in P1, 58% and 60% for R1 and R2 in P2 and 60% and 51% for R1 and R2 in P3, thus reflecting microbial adaptation, also indicating that sulfate did not negatively influenced the dye removal. The sulfate removal efficiency was 90% in R2 during P2 and P3.

Although good sulfate removal had been achieved in R2, there was no interference on the COD or DB22 removal efficiency, since for most stages efficiencies in R1 were slightly higher than those of R2. Sulfate competes with the dye for the electrons available.

Keywords: Azo dye, Direct Black 22, anaerobic degradation, textile effluent, sulfate.

---

*Author for correspondence: mguerrapc@ifpi.edu.br

INTRODUCTION

In 2015 the Brazilian textile and clothes manufacturing sector exchanged 36.2 billion dollars, with a total investment amounting to US$ 749 million, being the second largest employer in the manufacturing industry[1]. Linked to economic benefits, some environmental problems arises, such as high water consumption, generation of effluents with high concentration of dyes, organic matter, sulfate, toxic substances[10], high concentration of chemicals, reducing agents that are biologically difficult to degrade and inert auxiliaries[20], dye, alkali and sodium chloride[3].

Many dyes are poorly fixed on fabric (50-80%), which results in high amounts of dyes in textile wastewaters[23,24].

The discharge of effluent containing dyes causes aesthetic impacts and affects the photosynthetic processes[6]. Many azo dyes and their degradation products are toxic or mutagenic to life[23,24]. Furthermore, some present a carcinogenic nature[7,8], are toxic to the biological world[9], and are persistent in natural environments[5].

The number of dyes currently used in the textile industry is about 10,000[9,23]. Approximately 75% of the used dyes are azo type[5], whose azo bond cleavage results in aromatic amines as by-products.

Effluents from the textile industry are commonly treated by advanced oxidation processes (AOP)[9]. Azo dyes can be chemically reduced, for example, by Fe (II), other inorganic or organic salts. Although they are effective for the removal of color, physical and chemical processes expend more energy and concentrate pollution in solid or liquid sediments[21], leading to an undesirable increase in salinity or COD of the effluent, or even an increase in the sludge production[15] requiring further treatment or proper disposal.

In opposition to the physical-chemical treatment, the ability of microbes to decolorize dyes has received attention[16] due to its cost effectiveness, reduced production of sludge, and respect for the environment[3, 13; 22, 23].

The anaerobic reduction of azo dyes comprises different mechanisms. The distinction can be made between direct and indirect enzymatic reduction, catalyzed by redox mediators. In addition to these mechanisms, biogenic reducers such as sulfide[23] chemically reduce azo dyes.

Direct reduction consists in the direct electron transference to azo dyes as terminal acceptors through enzymatic activity during bacterial catabolism, linked to the generation of ATP[13]. In this case, organic matter is oxidized and the azo dyes reduction results in the formation of aromatic amines[25].

In the indirect reduction, the rate of azo dye decolorization is usually increased using redox mediators, such as flavins ($FADH_2$, $FMNH_2$) soluble in water, NADH or NADPH. Non-specific enzymes biologically reduce the redox mediator, which act as the electron acceptors from the primary electron donor (usually organic matter). The electrons are then chemically transferred to azo dyes, with the consequent regeneration of the mediator[7,8].

Finally, during the chemical decolorization of azo dyes inorganic compounds such as Fe^{+2} or H_2S donate electrons through chemical reaction[13]. Sulfate, usually detected in textile effluents, can compete with the dyes for the electron donor during the direct enzymatic reduction under anaerobic conditions. Thus, releasing sulfide to the chemical

reduction of azo dyes. Thus, the presence of sulfate in textile effluents can have different effects on the reduction of azo dyes[2].

In this study we evaluated the performance of bench scale UASB reactors treating synthetic textile wastewater, with and without addition of sulfate.

MATERIALS AND METHODS

Two UASB bench reactors (R1 and R2) were operated in parallel. They were made of acrylic, with 114 mm internal diameter and 540 mm useful height (**Figure 1**).
Each reactor was inoculated with 2 liters of anaerobic sludge (27 g STV.L^{-1}) from a soft drink wastewater treatment plant.

Both reactors were fed with synthetic textile wastewater (STW) (peristaltic pump Gilson®, MiniPlus model) at flow rate of 5 L.d^{-1}. The STW was composed of cornstarch (COD of 1,500 mg O_2.L^{-1}), azo dye Direct Black 22 (35 mg.L^{-1} - CAS Number 6473-13-8 – **Figure 2**), NH_4Cl (280 mg.L^{-1}), $K_2PO_4.3H_2O$ (330 mg.L^{-1}), $MgSO_4.7H_2O$ (100 mg.L^{-1}), $CaCl_2.2H_2O$ (10 mg.L^{-1}), $NaHCO_3$ (1,250 mg.L^{-1}), trace element solution (1 mL.L^{-1}). The trace element solution was composed of Fe (562 mg.L^{-1}), B (9 mg.L^{-1}), Zn (24 mg.L^{-1}), Mn (139 mg.L^{-1}), Cu (14 mg.L^{-1}), Mo (4 mg.L^{-1}), Al (10 mg.L^{-1}), Co (495 mg.L^{-1}), Ni (mg.L^{-1}) and Se (49 mg.L^{-1}). To the STW of R2, sulfate (250 mg Na_2SO_4.L^{-1}) was added aiming to evaluate the sulfate influence on the dye removal.

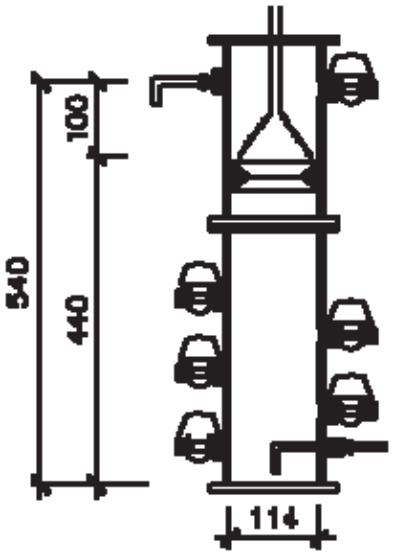


FIGURE 1 - UASB bench reactors

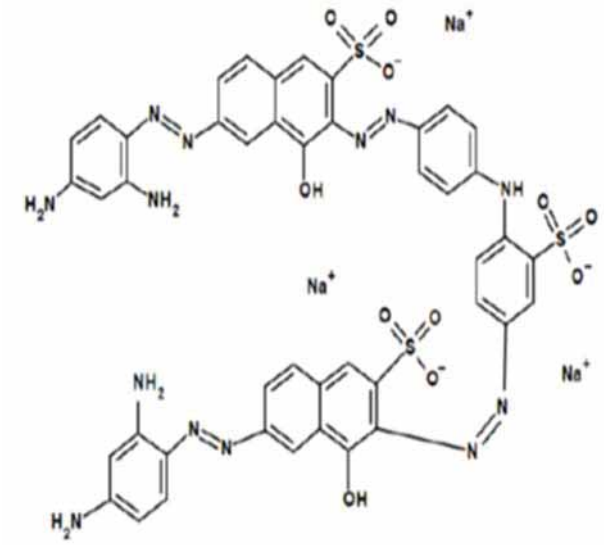


FIGURE 2 - Azo dye Direct Black 22 structure

The operation of R1 and R2 lasted 100 days, with three operational phases distinguished by the application of different organic loading rates (OLR), as shown in **Table 1**. The evaluated parameters and the analytical methods and references are shown in **Table 2**, the analysis were realized twice a week.

Table 1. Average values of COD, HRT and OLR for the reactors per phase

Phase / Parameter	Phase 1 – P1 35 d		Phase 2 – P2 41 d		Phase 3 – P3 23 d	
	R1	R2	R1	R2	R1	R2
COD (mgO_2L^{-1})	570±275	730±274	1,080±219	1,090±291	1,300±114	1,280±281
HRT (h)	24	24	24	24	15	15
OLR (kg COD.$m^{-3}.d^{-1}$)	0.52	0.74	1.08	1.09	2.08	1.92

In P1, in order to promote microbes adaptation was applied recirculation rate 1:1; therefore, the OLRs affluent averages to R1 and R2 were 0.52 and 0.74 $kgCODm^{-3}d^{-1}$, respectively.

TABLE 2. Analysis, analytical methods and reference methods

Parameter	Analytical method	Reference method
Alkalinity	Titrimetric	2320 B (SMWW[a])
pH	Electrometric	4500-H^+ B (SMWW)
ORP	Electrometric	2580 B (SMWW)
DB22	Spectrophotometric	
COD	Spectrophotometric	5220 D (SMWW)
Sulfate	Gravimetric	4500-SO_4^{-2} B (SMWW)
VFA	Titrimetric	5560 C (SMWW)

[a] *Standard Methods for the Examination of Water and Wastewater of American Public Health Association (APHA), the American Water Works Association (AWWA) and the Water Environment Federation (WEF), 22° ed, 2012.*

RESULTS AND DISCUSSION

The averages of COD removal efficiencies were approximately 30±12% for R1 and 38±10% for R2 (**Figure 3**) during P1. The COD results of the first phase suggest microbes adaptation to the new substrate.

During P2, when the OLR increased to 1.08 and 1.09 kg $COD.m^{-3}.d^{-1}$ for R1 and R2, respectively, the average of COD removal efficiency increased to 68±17% for R1 and 68±21% for R2. It was expected, since the organic substrate concentration controls the formation rate of reduction equivalents or intermediate electron donors. Attention to the fact that in P2, once the treatment stability was established, the average of COD removal efficiency were 87±8% and 91±3% for R1 and R2, respectively (**Figure 3**).

For P3, the average COD removal efficiency were 89±8% % for R1 and 89±11% for R2. Thus, considering the results of the P2 treatment stability period and the results of P3, when the ORL was increased to 2.08 and 1.92 $kgCODm^{-3}d^{-1}$ for R1 and R2, respectively, no decrease in COD removal efficiency was observed (**Figure 3**), suggesting microbes ability to degrade organic compounds even after duplicating the OLR.

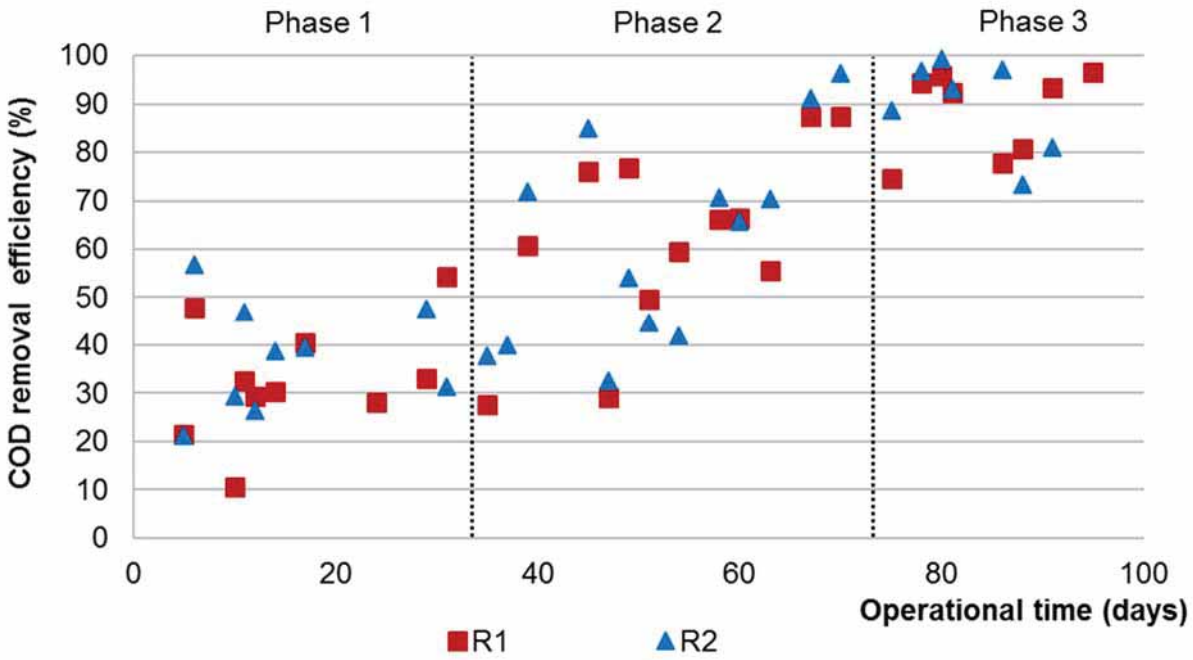


FIGURE 3. COD removal efficiencies of reactors R1 (□) and R2 (▲) during the operation period.

Similarly to the results found in the present work, Naimabadi et al[17] operated a laboratory scale anaerobic baffled reactor (ABR) with five compartments to treat synthetic wastewater containing Reactive Red 2, found increases of COD removal efficiencies ranging from 44 to 61.6% when OLR ranging from 1 to 5 kgCODm^{-3}d^{-1}.

Instead Jonstrup et al[14], in their studies operating anaerobic reactors consisted of glass with a 0.6 L of total volume, to treat synthetic wastewater containing Remazol Red RR, reported that COD removal was higher than 95% for OLRs of 0.38, 0.57 and 0.75 g COD.L^{-1}.d^{-1}. When the authors[14] applied OLRs of 1.13 and 2.26 g COD.L^{-1}.d^{-1} the removal of COD decreased to 82% and 78%, respectively.

Ferraz Jr. et al[10], operating UASB reactors fed with real textile wastewater applying OLR 1.0 to 1.9 kg COD.m^{-3}.d^{-1} found COD removal efficiency ranging from 50 to 59%, after the establishment of steady state conditions. When the OLR was increased from 2.1 to 3.3 kg COD.m^{-3}.d^{-1} the removal dropped to 48%. The authors did not attribute the drop in efficiency to the OLR applied in each stage, but instead to the increase of the real effluent salinity (on a daily basis, values ranging from 28.8 to 73.3 kg/d). The comparison of our results with those found by these authors[10] highlights how different real and synthetic wastewaters are, specially the textiles, where many chemical compounds are used and incorporated to the real wastewater.

Regarding to dye removal, at all stages the average concentration of DB22 affluent was 35±2 mg DB22.L^{-1}, except for P1, which, due to recirculation, was 30±2 mg DB22.L^{-1} for both R1 and R2. The average DB22 removal efficiencies were 23±10% and 15±6% in P1, 58±8% and 60±7% in P2 and 60±9% and 51±2% in P3 for R1 and R2, respectively, as shown in **Figure 4**.

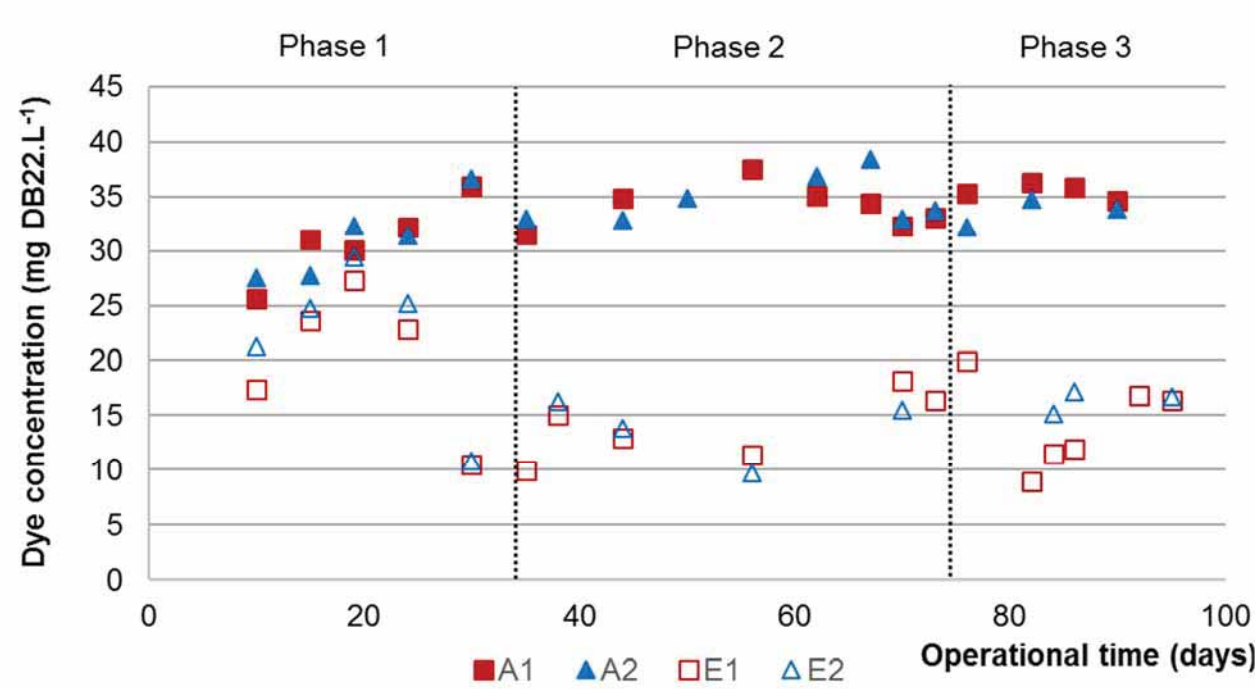


FIGURE 4. DB22 concentrations in affluent of reactors R1 (□) and R2 (▲) and in effluent reactors R1 (□) and R2 (△) during the operation period

Parallel to the low COD removal efficiency detected in P1, there was also low removal of DB22. It can be observed, therefore, that the DB22 removal efficiency was relatively low for OLR lower than 1.00 kg $COD.m^{-3}.d^{-1}$, reinforcing the hypothesis of the direct transfer of reducing equivalents of organic complexes for dyes via anaerobic degradation through enzymes. Furthermore, the dye removal of more expressive in R1 during P1 (23±10%) might be linked to competition between the sulfate and the dye by reduction equivalents available in R2 (15±6%).

For OLRs higher than 1.0 kg $COD.m^{-3}.d^{-1}$ (P2 and P3), there was no difference in the dye removal efficiency between R1 and R2 (DB22 removal efficiency of 58±8% for R1 and 60±7% for R2 during P1 and 60±9% for R1 and 51±2% for R2 during P3). It is possible that the biogenic sulfide, produced from sulfate reduction under anaerobic conditions, may chemically reduced the dye, thus compensating the direct enzymatic electron transfer from organic matter to the dye, expected for anaerobic communities.

It is also important to highlight that the microbes were well adapted when we doubled the OLR from P2 to P3, having similar behavior in these both phases. Similarly, Türgay et al[22] observed that dye removal decreased from only 89.2% to 82.7% after duplication of OLR. The authors concluded that microorganisms were already adapted.

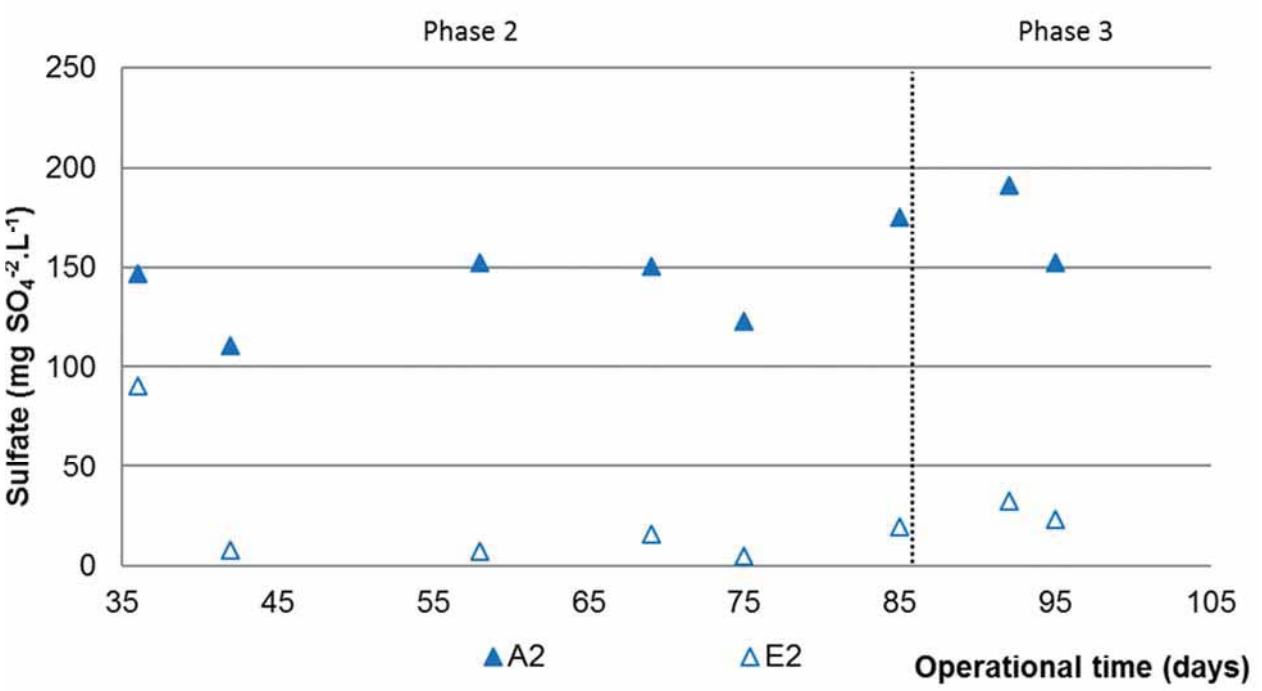


FIGURe 5. SO_4^{-2} concentration in affluent (▲) and effluent reactor R2 (△) during the operation period

Good behavior for sulfate removal was obtained in R2 for P2 (90%) and for P3 (90%) as shown in **Figure 5**, when the sulfate:COD ratios were 0.12 and 0.14, respectively. Apparently there was no interference of sulfate in the DB22 removal efficiency for these both phases. However, during P1 the sulfate may have impaired the dye removal in R2 (15±6%). However, after microbes adaptation (P1), in P2 and P3 biogenic sulfide generated anaerobically might have contributed for the chemical reduction of the dye. Thus, if there is availability, the sulfate acts as an intermediate electron acceptor of the electrons from organic matter, being reduced to sulfide that chemically transfer the electrons to the dye, which is the final acceptor of the azo dyes decolorization. Interesting to note that an intermediate electron acceptor (sulfate) in the reductive decolorization process does not alter the DB22 removal efficiency, suggesting the removal through the direct enzymatic pathway may be compensated by chemical reduction using the biogenic sulfide.

Since azo dyes can chemically react with sulfide, biological activity is not a prerequisite for the reduction of the azo dye. As the sulfide is usually present in effluents from anaerobic digestion of textile wastewaters containing sulfate, chemical reduction of the azo dye would contribute to the overall decolorization process under these conditions.

Libra et al[15], operating batch reactors, demonstrated the importance of sulfur reduction bacteria (SRB) in discoloration of the azo dye C.I. Reactive Orange, because in their experiments decolorization was twice long in the presence of SRBs inhibitors. The authors[15] showed that although delayed, decolorization occurred in enzymatic direct mode.

Regarding to VFA behavior, the influent content was 240±110 mg HAc.L^{-1} for both R1 and R2, while in the effluent 130±50 mg HAc.L^{-1} was detected in average for both R1 and R2. Thus, indicating no accumulation of VFA in the both reactors.

The stability of UASB reactors associated with the production of methane can be achieved to ratio VFA/alkalinity inferior to 0.4. For the results of this work, the VFA/alkalinity ratio ranged from 0.13 to 0.15, indicating the operational stability of the UASB reactors.

CONCLUSION

The UASB reactors showed satisfactory COD removal efficiency only for OLR higher than 1.00 kg COD.m^{-3}.d^{-1} (68% for OLR around 1.0; and around 90% for ORL close to 2,0). For the other phases, once the treatment stability was established, the average COD removal efficiency was over 87%. That is because the organic substrate concentration controls the reduction equivalent formation rate or intermediate electron donors accelerating the degradation of organic matter.

Considering the treatment stability period in Phase 2 and Phase 3, there was no variation of the average efficiency of COD removal when OLR was increased from approximately 1.00 (87 and 91% for Reactor 1 and Reactor 2, respectively) to 2.00 kg COD.m^{-3}.d^{-1} (89% for both reactors), suggesting that the capacity of the biomass present in the reactor to stabilize organic compounds had not been exceeded.

The DB22 dye removal efficiency was related to OLR only for values below 1.00 kg COD.m^{-3}.d^{-1} - reinforcing the hypothesis of direct transfer of electrons of organic matter via reducing equivalents generated by the oxidation of substrates for azo dyes during the bacterial catabolism - being 15% (Reactor 2 with 0.72 kg COD.m^{-3}.d^{-1}) to 23% (Reactor 1 with 0.54 kg COD.m^{-3}.d^{-1}) for Phase 1. However, no difference was observed between the average DB22 dye removal efficiency when the OLR was increased from approximately 1.00 (58 and 60% for Reactor1 and Resctor 2, respectively) to 2.00 kg COD.m^{-3}.d^{-1} (60 and 51 % for Reactor 1 and Reactor 2, respectively), suggesting limits to the capacity of the biomass present in the reactors to promote the reductive decolorization of DB22.

No variation was observed in COD or DB22 removal efficiency due to the addition sulfate to the effluent, reinforcing the hypothesis that sulfate might have different effects on the reduction of azo dyes. This is because although sulfate can compete with the dye as an electron acceptor during oxidation of the organic substrate, biogenic sulfide generated in the reduction of sulfate can chemically reduce the dye.

ACKNOWLEDGMENTS

Thank you IFPI for encouraging the training of their teachers; UFPE for promoting the training of IFPI teachers, especially the Civil Engineering Graduation Program and LEA/CCA/UFPE for providing the necessary support for the development of this work.

REFERENCES

1. ABIT, s.d. ABIT - Associação Brasileira da Indústria Têxtil e de Confecção. [Online] Available http://www.abit.org.br/cont/perfil-do-setor [Acessed July 13, 2016].
2. Amaral, F., Kato, M., Florêncio, L. & Gavazza, S., 2014. Color, organic matter and sulfate removal from textile effluents by anaerobic and aerobic processes. Bioresource Technology, 163, 364-369.
3. Balamurugan, B., Thirumarimurugan, M. & Kannadasan, T., 2011. Anaerobic degradation of textile dye bath effluent using Halomonas sp.. Bioresource Technology, 102, 6365–6369.
4. Behling, E., Diaz, A, Colina, G., Herrera, M., Gutierrez, E., Chacin, E., Fernandez, N. and Foster,. C. F., 1997. Domestic wastewater treatment using a UASB reactor. Bioresource Technology, 61, 239-245.
5. Cervantes, F. J. & Dos Santos, A. B., 2011. Reduction of azo dyes by anaerobic bacteria: microbiological and biochemical aspects. Environ Sci Biotechnol, 10, 125–137.
6. Cervantes, F. J. et al., 2007. Biogenic sulphide plays a major role on the riboflavin-mediated decolourisation of azo dyes under sulphate-reducing conditions. Chemosphere, 68, 1082–1089.
7. dos Santos, A. B., Cervantes, F. J. & van Lier, J. B., 2007. Impact of redox mediators on coulor removal of azo dyes and antthraquinone dyes by anaerobic granular sludge under mesophilic and thermophilic conditions. Eng. sanit. ambient., 12, 102-108.
8. dos Santos, A. B., Firmino, P. I. M., Sousa, M. R. d. & Silva, M. E. R. d., 2012. Sequential Anaerobic/Aerobic Treatment of Dye-Dye-Containing Wastewaters: Colour and COD. Appl Biochem Biotechnol, 166, 1057–1069.
9. Fahmi, C. Z. A. A. & Rahmat, N. R., 2010. Multi-stage Ozonation and Biological Treatment for Removal of Azo Dye Industrial Effluent. International Journal of Environmental Science and Development, 1, nº 2.
10. Ferraz Jr., A. D. N., Kato, M. . T., Florencio, L. & Gavazza, S., 2011. Textile effluent treatment in a UASB reactor followed by submerged aerated biofiltration. Water Science & Technology, 64(8), 1581-1589.
11. Florêncio, L., Jenicek, P., Field, J. A. & Lettinga, G., 1993. Effect of Cobalt on the Anaerobic Degradation of Methanol. Journal os Fermentation and Bioengineering, 75(5), 368-374.
12. Franciscon, E. et al., 2009. Biodegradation of textile azo dyes by a facultative Staphylococcus arlettae strain VN-11 using a sequential microaerophilic/aerobic process. International Biodeterioration & Biodegradation, 63, 280–288.
13. Gurulakshmi, M., Sudarmani, D. & Venba, R., 2008. Biodegradation of Leather Acid dye by Bacillus subtilis. Advanced Biotech, november, 12-18.
14. Jonstrup, M., Kumar, N., Murto, M. & Mattiasson, B., 2011. Sequential anaerobic–aerobic treatment of azo dyes: Decolourisation and amine degradability. Desalination, 280, 339–346.
15. Libra, J., Yoo, E., Borchert, M. & Wiesmann, U., 1997. Series of the CRC 193: Biological Wastewater Treatment. Berlin, s.n.
16. Li, T. & Guthrie, J. . T., 2010. Colour removal from aqueous solutions of metal-complex azo dyes using bacterial cells of Shewanella strain J18 143. Bioresource Technology, 101, 4291–4295.
17. Naimabadi, A., Attar, H. M. & Shahsavani, A., 2009. Decolorization anb biological degradation of azo dye reactive red2 by anaerobic/aerobic sequential process. Iran. J. Environ. Health, 6(2), 67-72.
18. Nigam, P., Banat, I. M., Singh, D. & MarchanV, R., 1996. Microbial Process for the Decolorization of Textile Effluent Containing Azo, Diazo and Reactive Dyes. Process Biochemistry, 31(5), 435-442.
19. Pinheiro, H., Touraud, E. & Thomas, O., 2004. Aromatic amines from azo dye reduction: status review with emphasis on direct UV spectrophotometric detection in textile industry wastewaters. Dyes and Pigments, 61, 121-139.

20. Sarayu, K. & Sandhya, S., 2011. Current Technologies for Biological Treatmentof Textile Wastewater–A Review. Appl Biochem Biotechnol.
21. Shaw, C., Carliell, C. & Wheatley, A., 2002. Anaerobic/aerobic treatment of coloured textile effluents using sequencingbatch reactors. Water Research, 36, 1993–2001.
22. Türgay, O. et al., 2011. The treatment of azo dyes found in textile industry wastewater by anaerobic biological method and chemical oxidation. Separation and Purification Technology, 79, 23-26.
23. van der Zee, F. P., 2002. Anaerobic azo dye reduction. Wageningen: Wageningen University.
24. van der Zee, F. P. et al., 2003. The contribution of biotic and abiotic processes during azo dye reduction in anaerobic sludge. Water Research, 37, 3098–3109.
25. Yoo, E. S., Libra, J. & Adrian, L., 2001. Mechanism of decolorization of azo dyes in anaerobic mixed culture. Journal of environmental engineering, September, 844-849,.

CHAPTER 7.5 RELIABILITY ANALYSIS OF WASTEWATER TREATMENT PLANTS OF JEANS LAUNDRIES FROM PERNAMBUCO-BRAZIL

V. H. Couto *(1); M.T.C. Fonseca (2); H. K. P. Silva (2); J. C. Morais (3) and E. A. Pastich (1)

(1) Federal University of Pernambuco (UFPE-CAA), Caruaru, Brazil.
(2) Institute of Technology of Pernambuco Association (ITEP-OS), Environmental Technology Pos-graduate Programm, Recife, Brazil.
(3) Federal Institut of Pernambuco, Recife, Brazil.

ABSTRACT

The local Productive Arrangement of Pernambuco performs an important role for the Agreste of the State of Pernambuco, a semi-arid region without much economic opportunities, being responsible for a substantial creation of jobs and economic growth. However, the jeans beneficiation process demands large water consumption and the use of chemical products, resulting in an effluent with high organic load, color and toxicity. Many laundries release their effluents the rivers without the proper treatment and the problem is intensified due to long periods of drought and intermittent river regimen that reduce the self-depuration capacity of these rivers. Reliability analysis is an important statistical tool for analyzing wastewater treatment plants (WWTP) because it defines, as a percentage of time, the effluent concentrations compliance for specified standards. The reliability coefficients (RC) of the WWTP performances were calculated in terms of the expected compliance to the legislation of the effluent BOD, pH, TSS and oils and greases. The present study aimed to evaluate the expected compliance with the discharge standards of ten laundries using the reliability analysis. For this study, 334 effluent samples from 10 WWTP were collected during 2012 to 2014 period. All the laundries studied apply physical-chemical treatments (flocculation following sedimentation processes) and the following parameters were evaluated: pH, settleable solids, biochemical oxygen demand (BOD) and oils and greases. Firstly, these samples were used to calculate the reliability coefficient for each laundry. After that, it was possible to evaluate if the WWTP was able to meet the discharge standards at a confidence level of 95%. In terms of pH values, all of the laundries had RC probability of compliance for the standard required in the legislation (pH of 5 to 9). With the exception of one laundry, all of the remaining had >80% probability of compliance for setteable solids (up to 1 $mg.L^{-1}$). The worst scenarios were in relation to oils and greases and BOD concentrations. Only two laundries had a compliance percentage above 80%, within the oils and greases standards (up to 70 $mg.L^{-1}$). In terms of BOD, none of the laundries had a compliance percentage above 80% for an effluent standard of 60 $mg.L^{-1}$.

---

*Author for correspondence: vitorcouto26@outlook.com

Thus, another study should be done to determine whether the problem is the design, operation or maintenance of the WWTP. The discharge of effluent with high pollutants concentrations can result a serious deterioration on the water quality and the ecological equilibrium of the receiving body.

Keywords: environmental impact, statistical analyses, textile effluents

INTRODUCTION

The Agreste of Pernambuco Clothing Pole is the second largest in Brazil, with about 20,000 companies, 100,000 jobs generated and a production of 900 million pieces/year. The Toritama city became a kind of capital in the production of jeans in Brazil, accounting for 16% of national production of jeans[1].

It is situated in semiarid region of Agreste of Pernambucano. The cities of Caruaru, Santa Cruz do Capibaribe and Toritama are the major cities.

In the jeans beneficiation process, there is a high consumption of water and the addiction of chemicals. It is estimated that each piece of jeans demands from 60 to 100 liters of water in the washing process. The city of Toritama, for example, has about 1 million pieces washed per year, which generates 80 million liters of effluents with a high amount of chemicals annually[2].

In the textile industry, one of the major environmental issues comes from the release of liquid waste with a high organic load, sharp color from textile dyes and toxic chemicals.

The release of these effluents into the ecosystem can cause serious environmental impact, both from an aesthetic point of view and from the point of view of pollution and interference in the aquatic ecosystem. Textile effluents are toxic, and have non-biodegradable components resistant to biological treatment. This aspect is due to the high content of dyes, surfactants and additives which are usually organic compounds of complex structures[3].

Thus, despite the fact that the sharp development of the sector has provided significant economic benefit to the region, environmental problems associated with disposal of industrial effluents from laundries have been frequent. From the year 2000, through actions of the State Environment Agency of Pernambuco - CPRH and prosecutors of Pernambuco, several terms of conduct adjustment (TAC) were signed with the laundries of the Clothing Pole, which resulted in the installation of wastewater treatment plants - WWTP's in these establishments, mostly applying physico-chemical processes for the treatment[4].

In this context, the present study investigated the performance of ten (10) WWTP's installed in the Agreste of Pernambuco Clothing Pole of Pernambuco, regarding to the compliance with relevant environmental legislation (CONAMA 430/2011)[5], during the 2012-2014 period, using the reliability analysis as statistical method. For statistical analysis we used the reliability coefficient (RC). The RC lists values of average concentrations observed in relation to a pre-established goal, being an important data analysis tool for the WWTP´s in operation.

MATERIALS AND METHODS

This study was conducted by monitoring the influent and effluent of 10 WWTP´s in the Agreste of Pernambuco Clothing Pole in the city of Caruaru, Pernambuco, Brazil, between the years of 2012 and 2014. The following parameters were evaluated: pH, chemical oxygen demand, biochemical oxygen demand and settleable solids following the methodology recommended by the Standard Methods for the Examination of Water and Wastewater[6].

Data that allows the identification of these laundries have been omitted in this study due to the contractual terms of confidentiality of information of the tests performed, which also resulted in an alternative designation of these companies, so that the 10 laundries studied had their names changed to L-1 to L-10.

Samples were collect in a varied frequency. **Table 1** shows the sample period, the number of samples for each laundry, the drain flow data and the type of coagulant used. All WWTP's studied employ a filtration step with alternating layers of 10 cm of gravel and sand after the step of coagulation / flocculation / sedimentation. The L-5 laundries, L-8 and L-10, make a pH adjustment after filtration with quicklime. The concentrations of reagents applied were not revealed by those responsible for the stations, nor the chemical composition of some flocculants, coagulants and polymers.

Table 1. Monitoring period and total of samples analyzed

Laundries	Studied period	n	Flow rate ($L.h^{-1}$)	Reagents used
L-1	Jan/2012 to Jul/2014	58	554.1	tannin + polymer
L-2	Jan/2012 to Dec/2013	42	165.3	flocculant + polymer
L-3	Jan/2012 to Jul/2014	40	116.7	tannin + polymer
L-4	Jan/2012 to Nov/2013	16	60.0	Coagulant + flocculant
L-5	Feb/2012 to May/2014	24	291.7	aluminum sulfate + polymer
L-6	Jan/2012 to Jul/2014	56	1111.1	flocculant + polymer
L-7	Apr/2012 to Jul/2014	52	155.6	flocculant + polymer
L-8	Feb/2012 to Jul/2013	20	1069.4	flocculant + polymer
L-9	Aug/2012 to Aug/2014	36	3768.5	polymer + aluminum sulfate
L-10	Jan/2012 to Nov/2012	16	777.8	aluminum sulfate + bioflocculant

The statistical analysis was used the descriptive statistics (mean, standard deviation, maximum and minimum value). Additionally, has been used the reliability coefficient (RC) to assess the effluent level of compliance about Brazilian environmental legislation.

The reliability equation allows to estimate the reliability of the treatment plant, that is the fraction of time that the effluent does not exceed the reference standard previously set[7].

The RC values can determine the level of variability of the data, that is, a large RC means that the data have little fluctuations around an average value. From the compliance percentage, it is obtained the probability of compliance of the service to a standard effluent value. For example, a 90 % compliance percentage means that, within a confidence level, 90% of the effluent was released in accordance with the law limit. Release patterns used as standard concentration, Xs, were based on Brazilian law CONAMA Resolution (National Environment Council), Nº. 430 of May 13, 2011.

The RC was calculated according to a specified probability of failure α lying between 0 and 1. Thus, (1- α) is the probability that the variable "x" does not exceed the standard Xs . In this study, the coefficient of variation (CV) was applied to find the appropriate RC.

Low CV values and therefore high RC values do not imply good performance, but only a stable operating condition. Low RC values imply lower values projects effluent concentrations that are required to meet the discharge standards[8].

The coefficient of variation was calculated according to the formulas shown in **Table 2** and then the RC for the following confidence levels of 80 %, 90 %, 95 % and 99 %. In the last step, the average expected concentration was calculated (mx) for each level of confidence.

TABLE 2. Equations used for calculating the reliability coefficient

Parameter	Meaning
average maximum concentration (mx)	mx = (CDC). Xs
Target concentration	X_s
Reliability coefficient (RC)	$\sqrt{CV^2 + 1}$ *exp$\{-Z(1-\alpha) * \sqrt{\ln(CV^2+1)}\}$
Variation coefficient (VC)	δ/μ
Average effluent concentration	μ
Standard deviation	δ
Probability of failure	α
Confidence	$(1-\alpha)\%$
Normal variable	Table Z(1-α)

RESULTS AND DISCUSSION

Hydrogen potential. **Figure 1** shows the pH values measured in the influent and effluent of the WWTP of the 10 laundries studied. Effluents from industrial laundries showed pH values within the standards established by Brazilian law (range 5 - 9), ranging from 5.5 to 9.0. Other values were found, pH range for textile effluent ranging from 8-10, more acid than what was found in this study[9].

In the L-5 and L-10, the physical-chemical treatment resulted in an increase of the pH in the final effluent. In the L-8, the pH level was reduced after the treatment. The other WWTP's evaluated maintained, in general, the same pH range after the treatment

The influent pH range found in the study was between 6 and 7. Other authors[10], using polymeric aluminum sulfate as the coagulant, found the optimal pH range for color removal of textile waste located from 8.2 to 8.5. Even though the tributaries of the studied laundries are outside this range, this may have a direct implication in the removal of color.

In terms of compliance of the pH levels, all the laundries showed more than 80% of compliance to the values established in the legislation (pH between 5 and 9). Furthermore, the mean of the reliability coefficient of the 10 laundries, considering a 95% confidence level, was 0.82 indicating little variability in this parameter.

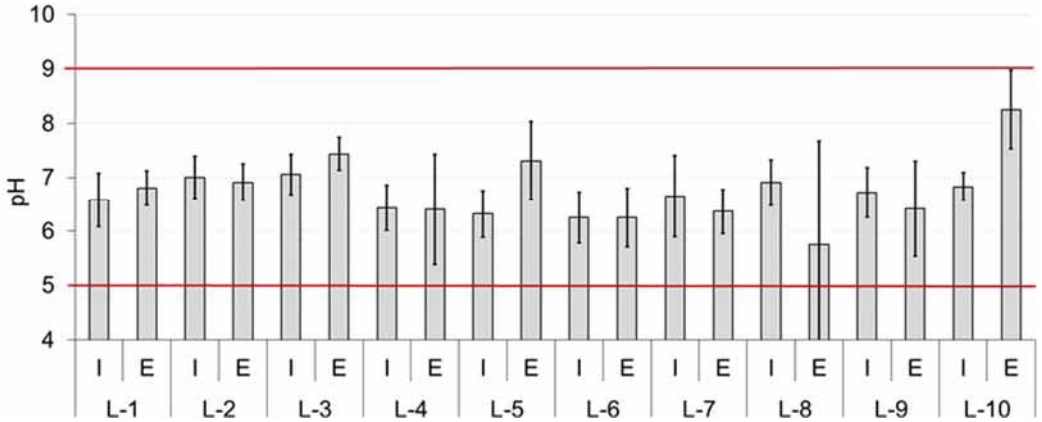


FIGURE 1. pH effluent values from the WWTPs

Settleable Solids. **Figure 2** shows the values of the influent concentration and removal efficiency of total settleable solids by the WWTPs. By analyzing the above figure, it can be seen that the physical-chemical treatment systems used in these textile effluents are satisfactory in removing settleable suspended solids (average efficiencies above 90%). The concentration of SSS influent ranged 13-900 $mg.L^{-1}$, even with this wide variation, the concentration of sedimented solids in the effluent was within the maximum of 1 $mg.L^{-1}$ allowed by CONAMA Resolution 430/2011.

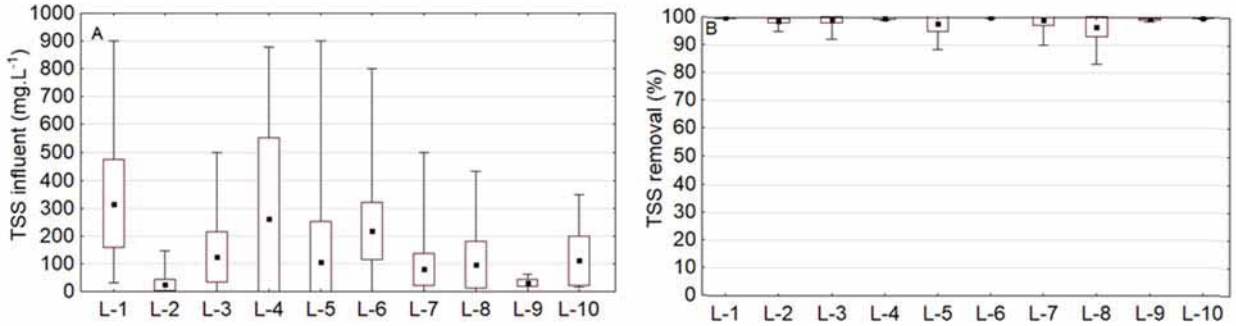


FIGURE 2. A) Influent total sedimentable solids concentration; B) Settleable solids removal.



Table 3 shows the values of reliability coefficients for the settleable solids parameter at the different confidence levels (80, 90, 95 and 99%). For a 1 $mg.L^{-1}$ threshold value (according to the CONAMA Nº 430 legislation), L-2, L-6, L-9 and L-10 had a 100 % compliance percentage. With the exception of L-5 that had a compliance percentage of 69.38%, the remaining WWTPs had a percentage of compliance>80%, what means that the treatment applied by the laundries is suitable for settleable solids.

TABLE 3. Reliability coefficients for settleable solids

R.L (%)	Reliability Coefficients									
	L-1	L-2	L-3	L-4	L-5	L-6	L-7	L-8	L-9	L-10
80	0.76	0.86	0.71	0.71	0.77	0.87	1.00	0.73	0.85	0.81
90	0.44	0.78	0.45	0.46	0.44	0.81	0.48	0.44	0.77	0.71
95	0.28	0.72	0.31	0.32	0.28	0.76	0.26	0.29	0.71	0.63
99	0.12	0.63	0.15	0.16	0.12	0.67	0.08	0.14	0.61	0.51

Organic matter. For the treatment of textile effluents, different techniques are commonly employed. In general, the chemical coagulation technique has shown good results in the removal of organic matter, generating, however, a great amount of sludge, as a byproduct. The conventional biological treatment processes commonly used require a longer hydraulic detention, what results in a higher volume of processing units.

In addition, as biological processes are applied, such systems become more susceptible to toxic compounds present or formed during the process. On the other hand, the biological treatment produces much less sludge that is also more stabilized and that does not require the addition of chemical compounds.

A raw effluent with a ratio COD/BOD less than 2 can be treated by a biological process, as compared to an effluent COD/BOD above 3.33 that impairs or prevents biological treatment[11].

According to **Figure 3**, it was possible to observe an unfavorable condition for the biological treatment (COD/BOD>2). The ratio COD/BOD effluent also points to an unfavorable condition for biological post- treatment. With the exception of L-4 (effluent ratio COD/BOD<2), the other laundries presented a final effluent with high ratio COD / BOD. Other authors[12] observed low specific methanogenic activity in textile sludge and low methane production, which suggests a difficulty in treating this type of waste water biologically in anaerobic biological treatments.

On the other hand, several studies with textile effluents applying biological treatment in laundries in the Agreste Clothing Pole, same region of this present study, showed significant removal of organic matter. In an experimental trial using an UASB - Upflow Anaerobic Sludge Blanket and BAS - Submerged aerated biofilter at different times of the retention time, 12 and 8 hours, 8 and 6 hours, respectively, observed average efficiencies of COD removal equal to 66.7 and 64 %[13].

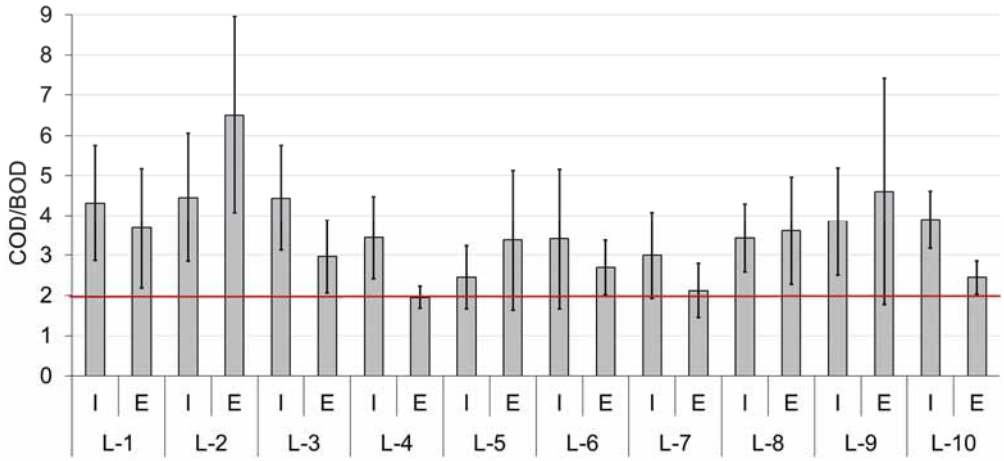


FIGURE 3. COD/BOD relationship

Other authors[14] using the same UASB reactors and BAS reported a BOD removal efficiency at different hydraulic retention times, which ranged from 72.4 % to 96.5 %. The authors state that the OD analysis for textile effluents may not represent the actual concentration of biodegradable organic matter, since toxic compounds can inhibit the biological activity.

Other studies have evaluated the performance of a membrane bioreactor for the treatment of textile effluents and reported a reduction in the COD that have ranged from 60 to 95% and suggested carrying out a post-treatment with nanofiltration to improve the performance of the treatment[15].

The combination of physical- chemicals methods with the biological one may be an attractive option for the treatment of textile effluents, due to the presence of dyes that are normally resistant to degradation in conventional systems[16].

Figure 4 shows the BOD removal efficiency in laundries and the final concentration. Through graphical analysis, it was possible to observe that there is a great instability in the treatment systems that sometimes achieve high removal efficiencies and sometimes demonstrate no removal efficiency.

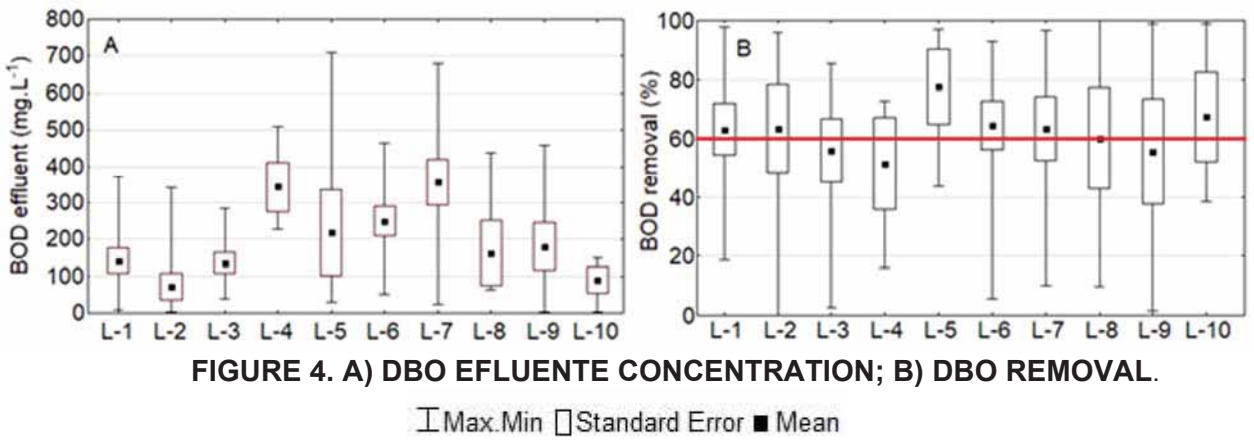


FIGURE 4. A) DBO EFLUENTE CONCENTRATION; B) DBO REMOVAL.

The brazilian legislation CONAMA Nº 430/2011 establishes that an WWTP should perform a minimal BOD reduction of 60% and it is clear that the laundries studied have difficulties to fit within this threshold.

As a result, the effluent BOD concentrations are variable. This is a troublesome finding, since high BOD concentrations cause oxygen consumption dissolved in the receiving body and can lead to death of aerobic organisms such as fish. This factor is further compounded by the fact that most of the rivers in the region are intermittent, which reduces the flow of the river at certain times of the year and, with it, its self-purification capacity.

In **Table 4**, are shown the values of the RC for different confidence levels for the laundries analyzed.

TABLE 4. Reliability coefficients for the BOD removal

R.L	Reliability coefficients									
(%)	L-1	L-2	L-3	L-4	L-5	L-6	L-7	L-8	L-9	L-10
80	0.76	0.86	0.71	0.71	0.77	0.87	1.00	0.73	0.85	0.81
90	0.44	0.78	0.45	0.46	0.44	0.81	0.48	0.44	0.77	0.71
95	0.28	0.72	0.31	0.32	0.28	0.76	0.26	0.29	0.71	0.63
99	0.12	0.63	0.15	0.16	0.12	0.67	0.08	0.14	0.61	0.51

Figure 5 shows the COD data. The effluent COD concentration (**Figure 5A**) is quite variable, as well as the removal efficiencies (**Figure 5B**), with values ranging from zero efficiency and good levels of efficiency (above 90%). Affluent concentrations in WWTP's vary widely (300-2,000 $mg.L^{-1}$), which poses a major challenge in the operation of WWTP's.

The performance of an industrial laundry jeans WWTP in the state of Paraná, Brazil, whose treatment process consisted of primary treatment railing, grease trap, equalization tank, followed by a physical-chemical treatment consisting in coagulation, flocculation and sedimentation was monitored and observed gross mean removal of 71.8% COD and filtered of 63.8%[17].

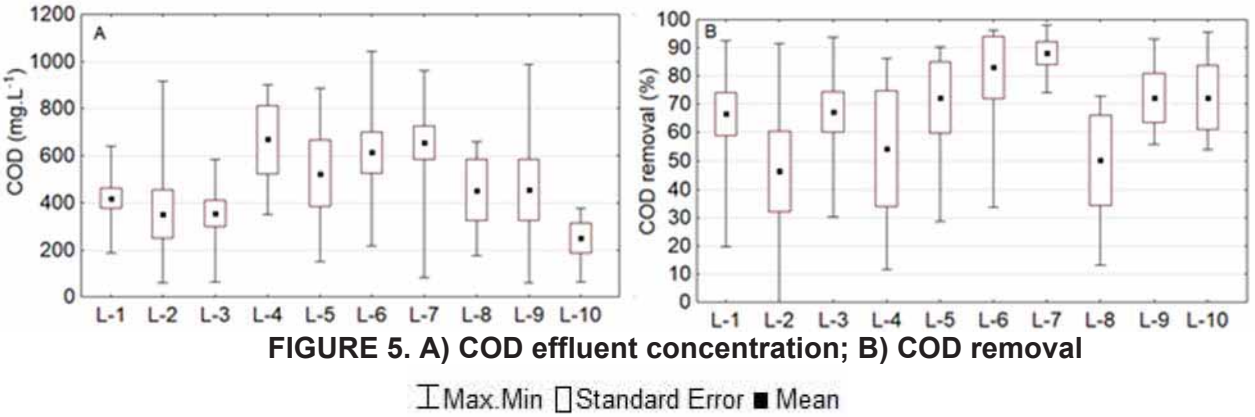


FIGURE 5. A) COD effluent concentration; B) COD removal

The high coefficient of variation in BOD and COD removal efficiencies of the studied laundries (**Figure 4A** and **Figure 5B**) shows that, in general, the operation of WWTPs is

poor, not allowing stability in operation and not the compliance to environmental standards imposed by Brazilian law. Probably, the dosages of reagents, reaction times and size of the treatment plant must be adapted to changes in the affluent charges. The adoption of a roadmap for laboratory tests Jar-test type can be adopted for adjustments in the operation of the WWTPs.

Thus, the combination of physical-chemical and biological treatment can be considered as a strategy not also for assuring environmental compliance but also meeting the economic requirements. Since the region has a predominance of micro and small enterprises, with a high incidence of informality and majority production of popular consumer goods, sophisticated types of treatment are not economic viable [18].

CONCLUSION

The WWTP studied could reach the standard set by Brazilian legislation in relation to the parameters pH and total sedimented solids. However, the organic matter removal efficiency, in terms of BOD or COD showed to be very variable.

The WWTPs studied fail to achieve the desired removal rate necessary to generate an effluent within the standards required for over 80% of monitoring time. This is a serious environmental issue, as the rivers of the region are not perennial and during much of the year have their flow capacity and reduced self-purification.

The study of the COD/BOD indicates a low possibility of a biological treatment for removing the remaining DBO. The high variation of the influent concentration of BOD and COD sets an enormous challenge in optimizing treatment processes.

A greater operating control, reagents dosage optimization and hydraulic detention time optimization are options to ensure the desired efficiency for most of the operating time.

Most of the laundries are small with a high degree of informality which prevents under an economic point of view, the application of more sophisticated and more expensive treatments.

REFERENCES

1. Lacerda A. Agreste tem 2º maior polo têxtil do País*. O Estado de São Paulo, Economia*. 06 de janeiro de 2013. Available at: <http://economia.estadao.com.br/noticias/geral,agreste-tem-2-maior-polo-textil-do-pais-imp>. Access on: 05 setembro14.
2. Jerônimo T. B., Galvão M. B., Falcão J. M. S. L. Proposta de utilização do environment value to businesses em projetos de recursos hídricos de despejo de produtos químicos: estudo de caso das lavanderias no município de Toritama. Revista Eletrônica Sistemas & Gestão. V. 7, n. 3, 2012, pp. 366-378.
3. Perkowski J., Kos L. Decolouration of model dyehouse wastewater with advanced oxidation processes. Fibres & Textiles in Eastern Europe, v. 11, p. 67-71, 2003.
4. CPRH. Diagnóstico Ambiental das Lavanderias de Toritama – PE. Recife: CPRH. Dezembro/2005. 48 p. Available at: <http://www.cprh.pe.gov.br/downloads/toritama.pdf>. Access on: 18 agosto 2014.
5. BRASIL. Resolução CONAMA nº. 430, de 13 DE maio de 2011. Dispõe sobre as condições e padrões de lançamento de efluentes, complementa e altera a Resolução no 357, de 17 de março de 2005, do Conselho Nacional do Meio Ambiente-CONAMA. Diário Oficial da República Federativa do Brasil. Brasília, 2005.

6. APHA/AWWA/WEF. Standard methods for the examination of water and wastewater. 22 ed. Washington, 2012.
7. 7-Niku S., Schroeder E.D., Samaniego F.J. Performance of activated sludge process and reliability-based design. Journal Water Pollution Control Association, v. 51, n. 12, p. 2841 - 2857, Dec., 1979.
8. Silveira A. G. M. Análise de eficiência e confiabilidade em sistemas de baixo custo de tratamento de esgotos do tipo lagoas de estabilização. 2011. 109 f. Dissertação (Mestrado em Engenharia Civil: Saneamento Ambiental) - Centro de Tecnologia, Universidade Federal do Ceará, Fortaleza, 2011.
9. Khandegar V., Saroha A. K. Journal of Environmental Management Volume 128, 15 October 2013, Pages 949–963. Review. Electrocoagulation for the treatment of textile industry effluent – A review
10. Imen Khounia I., Marrot B., Moulinb P., Amar R. B. Decolourization of the reconstituted textile effluent by different process treatments: Enzymatic catalysis, coagulation/flocculation and nanofiltration processes. Volume 268, Issues 1–3, 1 March 2011, Pages 27–37. Desalination.
11. Metcalf, Eddy. Wastewater Engineering – Treatment, Disposal, Reuse. 4º Ed. McGraw-Hill. New York, 2003.
12. Schneiders D., Silva J.D., Till A., Lapa K.R., Pinheiro A.. Atividade metanogênica específica (AME) de lodos industriais provenientes do tratamento biológico aeróbio e anaeróbio. Revista Ambiente & Água: v. 8, n.2, 2013.
13. Amaral F. M., Kato M. T., Florencio L., Gavazza S.. Color, organic matter and sulfate removal from textile effluents by anaerobic and aerobic processes. Bioresource Technology, v. 163, p. 364-369, 2014.
14. Ferraz júnior A. D. N., Kato M.T., Florencio L., Gavazza S. Textile effluent treatment in a UASB reactor followed by submerged aerated biofiltration. Water Science and Technology, v. 64, p. 1581, 2011.
15. Brik M., SchoeberL P., Chamam B., Braun R., Fuchs W. Advanced treatment of textile wastewater towards reuse using a membrane bioreactor. Process Biochemistry (2006), v. 41, n. 8, p. 1751-1757
16. Kunz A., Zamora P., Moraes S., Durán N.. Novas tendências no tratamento de efluentes têxteis. Química Nova, São Paulo, v. 25, n. 1, p. 78 - 82, 2002.
17. Rezende D., Carvalho K., Kreutz C., Arantes E.J., Passig F.H. Avaliação do processo de tratamento de efluentes de uma lavanderia industrial de jeans. Olam –Ciência e Tecnologia. n.2, n.especial, set. 2009, pp .253-270. Rio Claro-SP.
18. SEBRAE. Estudo Econômico do Arranjo Produtivo Local de Confecções do Agreste Pernambucano. Relatório Final. Recife, Maio de 2013. Available at: <http://www.sebrae.com.br/sites/PortalSebrae/ufs/pe/barra_funcionalidade> Access on: 02/09/2014.

CHAPTER 7.6 RELIABILITY ANALYSIS OF EIGHT FULL-SCALE STABILIZATION PLANTS IN A SEMIARID REGION OF BRAZIL

V.H. Couto *(1); E. A. Pastich (1); M. G. Acioly (2); M. V. Paiva (1) and J. C. Morais (3)

(1) Federal University of Pernambuco (UFPE-CAA), Br-104, n/a, Caruaru, Brazil.
(2) Institute of Technology of Pernambuco Association, Prof Luiz Freire St, nº 700, Recife, Brazil
(3) Federal Institute of Pernambuco, Prof. Luiz Freire St, nº 500, Recife, Brazil.

ABSTRACT

San Francisco River it is a resource extremely important for the cities on the shore, because it is responsible for local development, biodiversity conservation and irrigation practices. In this context, the wastewater plants are an indispensable tool to ensure the river's quality. This article presents a reliability analysis of eight full-scale stabilization ponds plants operating in Petrolina city, localized in semi-arid region of Brazil. The climate that the ponds are located is classified as warm and semi-arid (the BSh type in climatic classification of Köppen), with the scarcity and irregularity of rainfall, as well as the strong evaporation due to high temperatures (averages of 26 to 39ºC). All these climate conditions are proper to stabilization ponds treatment, because favor the biology metabolisms present in the ponds: aerobic respiration (bacteria) and photosynthesis (algae).
The methodology used to analyze the plants performance was developed in 1979. It is used to determinate the coefficients of reliability (COR), in terms of the compliance of effluent parameters to discharge standards. For this study, effluent samples of Total Nitrogen (TN), BOD, Total Phosphorus (TP) and thermos tolerant coliforms were collected from 8 WWTP throughout the years of 2006 to 2014.
In general, the WWTP's performances were within expected. It was explained as a consequence of high solar radiation and high temperatures that stimulated the microbiologic metabolism. In terms of thermotolerant coliform, efficiencies were observed ranging from 70 to 99.98%, with average of 99%. Dissolved oxygen concentrations increased, as photosynthesis consequences (influent average was 0.2 $mg.L^{-1}$ and effluent average was 5 $mg.L^{-1}$). Each wastewater plant showed a good performance in BOD removal, with above 80% of compliance percentage.
The compliance regarding total nitrogen removal was 99% of samples during the monitoring period. However, the other parameters like TP and coliforms have not had an expected compliance percentage (below 80%). The results showed that plants, under the observed operating conditions, would be able to present reliable performances in terms of compliance with the discharge standards. On the other hand, the effluent quality for some constituents, as a phosphorus concentration, was not very good and can to induce the eutrophication.

Keywords: performance, statistical analysis, wastewater

---

*Author for correspondence: vitorcouto26@outlook.com

INTRODUCTION

The city of Petrolina-PE is extremely important for the economic growth of Pernambuco's semiarid region. The city is strategically located close to San Francisco's river and possesses a lot of irrigated agriculture. Different types of fruits are cultivated in this city, such as, grape, mango, guava and banana [1].

Because of the importance of water to this city, it is necessary to see Petrolina's WWTP as a major key to guarantee the water's quality of San Francisco River. San Franciso river is the receiving body for effluents generated in the WWTP of the region and is also the water source for the irrigated agriculture.

The applications of sewage simplified treatments, especially in terms of costs involved, and take local weather as an advantage are always a priority. In developing countries stabilization ponds are commonly used as alternative systems. The advantages of stabilization ponds include their low cost of construction and maintenance, satisfactory pollutant removal efficiency and self-sustainability [2]. Despite the operational simplicity, as well as any system of treatment, stabilization ponds should be monitored and operated in a systematic and proper manner [3]. Stabilization pond is a type of biological treatment of sewage that is designed to increase the efficiency of self-depuration capacity [4].

The matter organic aerobic stabilization mechanism is based in the metabolic activity of oxidative bacteria. The oxidative processes decompose organic matter into more stable molecules and lower energy value. As consequence about this process, some substances were formed, such as carbon dioxide and minerals. These substances will be important to algae development who releasing oxygen to maintain aerobic conditions in the environment [5]. Stabilization ponds are perfectly suited for subtropical and tropical countries, since availability of light and temperature are the main factors influencing the sewage treatment efficiency [6].

Additionally, the environmental conditions to which the sewage is subjected within these ponds allow death of pathogenic microorganisms. The removing protozoan cysts and helminth eggs are due to sedimentation process, since the long hydraulic retention time is sufficient to allow this process.

Already the coliforms removal occurs primarily as a result of light intensity [7]. Other environmental factors are also related as high values of dissolved oxygen, temperature and pH. Thus, to improve the effluent disinfection, about coliforms, is important to increase the exposure to light, with longer hydraulic retention and increased surface area.

Brazil's semiarid region displays high levels of air temperatures (above 25ºC) and solar radiation, which are perfect for sewage treatment using stabilization ponds. Thus, this study had the purpose to assess the behavior and performance of eight WWTP that uses stabilization ponds to treat sewage. For the statistical evaluation of the data, the coefficient of reliability (COR) was used. The COR correlate the observed effluent average with discharge standards. It is an essential tool to analyze data from WWTP in full operation.

MATERIALS AND METHODS

This study was made through monitoring of eight WWTP in Petrolina-PE. The treatment plants were arranged as SP-1 to SP-8, where SP is a short term of stabilization pond, and the receiving body of all of them is the San Francisco river.

The local climate is classified as warm and semi-arid (the BSh type in climatic classification of Köppen), with the scarcity and irregularity of rainfall, as well as the strong evaporation due to high temperatures (averages of 26 to 39ºC). All these climate conditions are proper to stabilization ponds treatment, because favor the biology metabolisms present in the ponds: aerobic respiration (bacteria) and photosynthesis (algae).

All of the WWTP analyzed had stabilization pond as the mechanism to treat sewage. The **Table 1** displays the operational data. Effluent samples of BOD, QOD, TSS, FC, TP and TN.

TABLE 1. Operational data from the WWTP analyzed

WWTP	Flow-rate ($L.s^{-1}$)	Sewage treatment
SP1	56	Series of three stabilization ponds, the first of which is a facultative pond followed by two maturation ponds
SP2	18	Series of three stabilization ponds, the first of which is a facultative pond followed by two maturation ponds
SP3	22	Series of three stabilization ponds, the first of which is a facultative pond followed by two maturation ponds
SP4	91	One facultative pond
SP5	27	Series of three stabilization ponds, the first of which is a facultative pond followed by two maturation ponds
SP6	33	Series of three stabilization ponds, the first of which is a facultative pond followed by two maturation ponds
SP7	66	One facultative pond
SP8	20	Series of three stabilization ponds, the first of which is a facultative pond followed by two maturation ponds

For the statistical analysis, in addition to average, standard error, maximum and minimum value the COR were calculated in order to obtain the compliance percentage to Brazil's discharge standards. The Percentage of effluent concentration that did not meet the discharge standard during the time analyzed can be obtained using COR [8].

Using the values of COR calculated it is possible to obtain the variability of the data, in other words, a COR close to 1 means that the data analyzed had little variability. The compliance percentage, according to a reliability level, is the percentage that an effluent met the discharge standard. As an example, a compliance percentage of 90% means that 90% of the effluent discharge met the standard.

In this study, the discharge standards used as the fixed standard (X_s) were based in the Brazilian legislation [9]. The COR were calculated for a reliability level of 80%, 90%, 95% and 99%. Equations used in this study are shown in **Table 2**.

TABLE 2. Equations used to calculate COR

Parameter	Definition
Mean constituent value (mx)	mx = (COR). Xs
Fixed standard	X_s
Coefficient of reliability (COR)	$\sqrt{CV^2 + 1}$ *$\exp\{-Z(1-\alpha) * \sqrt{\ln(CV^2+1)}\}$
Coefficient of Variation (CV)	δ/μ
Effluent average concentration	μ
Standard deviation	δ
Failure percentage	α
Reliability level	$(1-\alpha)\%$
Percentiles	$Z(1-\alpha)$

RESULTS AND DISCUSSION

The pH values Influent and effluent from all of the eight WWTP are shown on **Figure 1**. The pH levels increased in the effluent, however, most of the effluent samples were between 5 and 9, inside Brazilian legislation standard value [9].

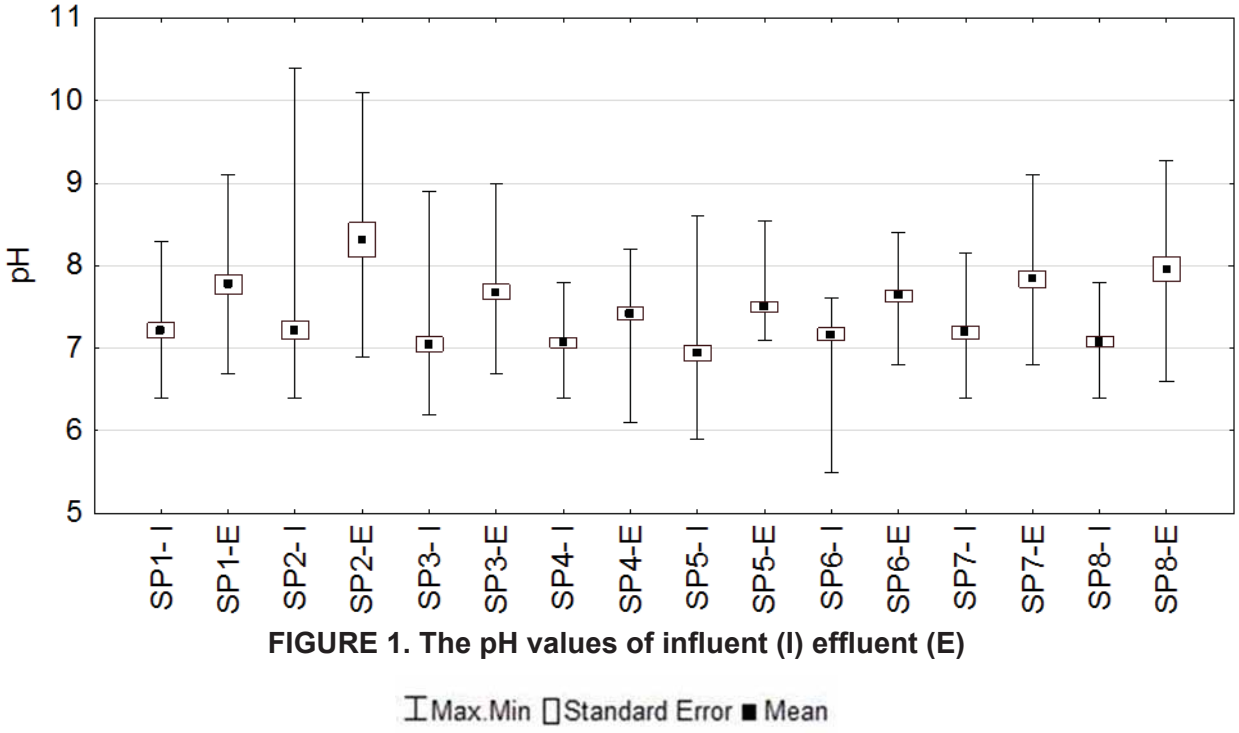


FIGURE 1. The pH values of influent (I) effluent (E)

In generally, the pH changes in stabilization ponds are consequences of CO_2 algae uptake in the light period daily. Already during the night, there is an increase of CO_2 and consequently a decrease in pH because of the breath of both algae as bacteria [10]. As the samples were taken during the day, it was observed high values of pH.

The phytoplankton metabolism is influenced by pH of the water, mainly due to CO_2 bioavailability for photosynthesis and absorption of nutrients in ionic form [11].

The CO_2 availability for photosynthesis depends directly on aerobic oxidation of the matter organic from sewage by heterotrophic bacteria [12]. The pH optimum for most algae is around 8, pH values far above or below could decrease the productivity [13]. The heterotrophic aerobic bacteria responsible for the removal of organic matter in stabilization ponds, have their pH optimum around 8.3; higher values may inhibit bacterial activity [14].

Dissolved oxygen concentrations are shown in **Figure 2**. The sewage treatment of domestic effluent using facultative and maturation ponds provides an advantage for dissolved oxygen. In these types of treatment the dissolved oxygen increases naturally, in other words, there is no need of diffusers.

The photosynthetic algae activity provides daily variations in the dissolved oxygen (DO) concentration, which can reach values of 20 $mg.L^{-1}$ in a supersaturation condition. The pH values can reach values greater than 9.4 [6]. The final effluent from ETE's studied had average concentrations of dissolved oxygen within the established laws (minimum 5 $mg.L^{-1}$) [9].

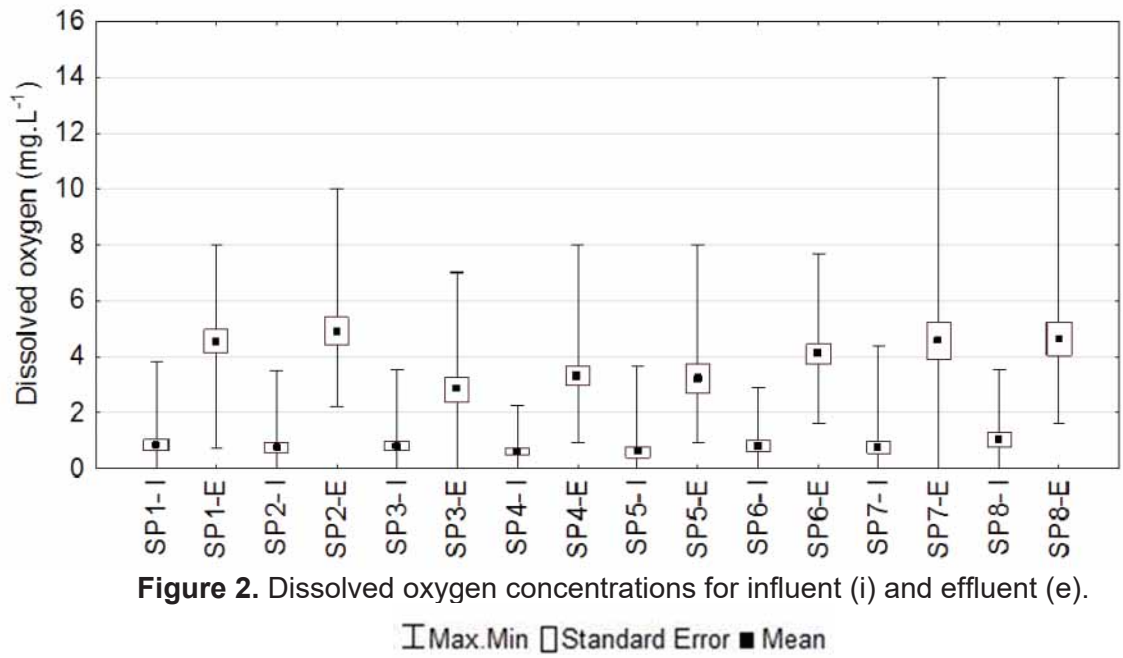


Figure 2. Dissolved oxygen concentrations for influent (i) and effluent (e).

The **Table 3** displays the reliability analysis for BOD from each WWTP, according to a discharge standard of 120 $mg.L^{-1}$. The results showed that the WWTP did not have any trouble to meet the discharge standard, for a reliability level of 90%. Its means that the WWTP's, during 90% of the time, met the Brazilian legislation for BOD discharge concentration. In addition to that, SP-2 and SP-7 had a 95% of compliance percentage, which was better than the rest.

TABLE 3. Reliability analysis for BOD

RL (%)	Coefficient of reliability

	SP-1	SP-2	SP-3	SP-4	SP-5	SP-6	SP-7	SP-8
80	0.73	0.71	0.70	0.70	0.73	0.72	0.70	0.72
90	0.56	0.51	0.50	0.47	0.57	0.54	0.50	0.54
95	0.45	0.39	0.38	0.34	0.47	0.43	0.38	0.43
99	0.31	0.24	0.22	0.18	0.32	0.28	0.22	0.28
RL (%)	**Design mean concentration (mg/L)**							
	SP-1	**SP-2**	**SP-3**	**SP-4**	**SP-5**	**SP-6**	**SP-7**	**SP-8**
80	87.08	84.63	84.36	84.41	87.79	86.05	84.41	86.04
90	67.40	61.11	59.93	56.42	68.85	65.14	60.19	65.12
95	54.56	46.72	45.20	40.47	56.34	51.77	45.54	51.75
99	36.71	28.23	26.63	21.70	38.68	33.65	26.98	33.63
AV	55.03	55.24	58.47	57.23	63.66	62.07	44.68	62.64

Note: RL= reliability level; SP=stabilization pond; AV= average

In Brazil, a study was conducted in 166 WWTP's in operation [15]. The authors observed in facultative pond effluent BOD concentrations from 86 to176 $mg.L^{-1}$. These concentrations are larger than the range shown in the general literature on facultative pond (50 and 80 $mg.L^{-1}$).

In the present study the effluent ranged 26.6 to 38.3 $mg.L^{-1}$ this confirming the good performance of stabilization ponds for BOD removal.

The **Figure 3** shows BOD concentrations for interfluent and effluent from the eight WWTP. According to the **Figure 3** it is possible to notice that stabilization ponds can show an excellent performance of organic matter removal, even though most of the systems are simplified. The removal efficiency considering interfluent BOD and effluent varies between 77.6% and 84.7%.

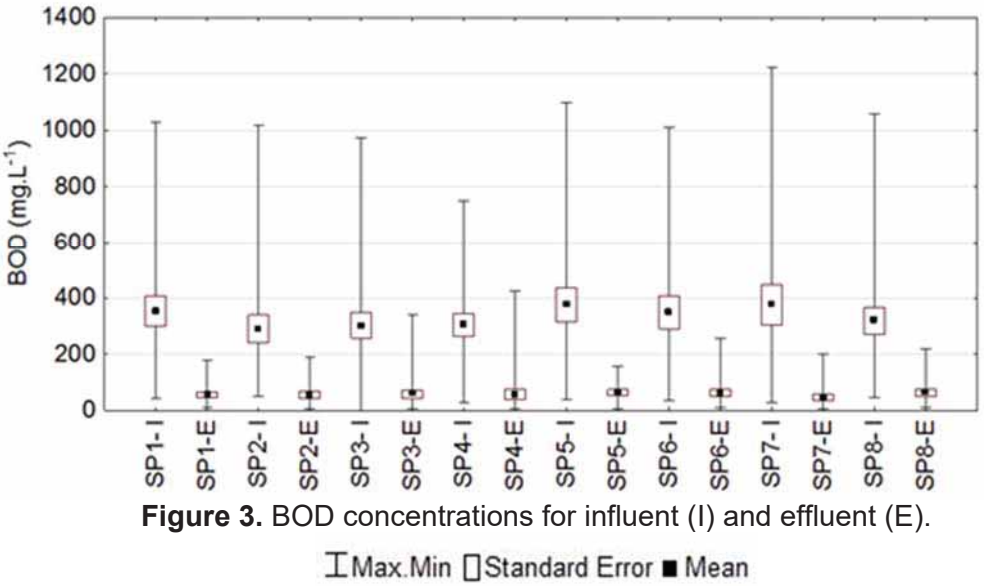


Figure 3. BOD concentrations for influent (I) and effluent (E).

The **Table 4** presents the reliability analysis for thermotolerant coliforms for a discharge standard of 10^5 $NMP.100.mL^{-1}$ [19].

TABLE 4. Reliability analysis for thermotolerant coliforms

RL	Coefficient of reliability							
(%)	SP-1	SP-2	SP-3	SP-4	SP-5	SP-6	SP-7	SP-8
80	0.76	0.99	0.74	0.75	0.82	0.81	0.99	1.15
90	0.44	0.47	0.44	0.44	0.44	0.44	0.47	0.51
95	0.28	0.26	0.29	0.28	0.27	0.27	0.26	0.26
99	0.12	0.08	0.13	0.12	0.10	0.11	0.08	0.08
RL	**Design mean concentration (E.coli/100mL)**							
(%)	**SP-1**	**SP-2**	**SP-3**	**SP-4**	**SP-5**	**SP-6**	**SP-7**	**SP-8**
80	$7.61x10^4$	$9.91x10^4$	$7.40x10^4$	$7.55x10^4$	$8.15x10^4$	$8.05x10^4$	$9.86x10^4$	$1.15x10^5$
90	$4.40x10^4$	$4.75x10^4$	$4.43x10^4$	$4.40x10^4$	$4.42x10^4$	$4.41x10^4$	$4.73x10^4$	$5.12x10^4$
95	$2.80x10^4$	$2.59x10^4$	$2.90x10^4$	$2.82x10^4$	$2.67x10^4$	$2.69x10^4$	$2.59x10^4$	$2.63x10^4$
99	$1.20x10^4$	$8.27x10^3$	$1.31x10^4$	$1.23x10^4$	$1.04x10^4$	$1.06x10^4$	$8.31x10^3$	$8.31x10^3$
AV	$3.71x10^4$	$3.12x10^4$	$6.39x10^4$	$3.64x10^4$	$4.73x10^5$	$1.06x10^5$	$1.45x10^5$	$6.38x10^5$

Note: RL= reliability level; SP=stabilization pond; AV= average

In stabilization ponds, the mechanism predominant to fecal coliforms removal is sunlight exposure [7]. Due to the semi-arid climate that the ponds studied was situated was expected high coliform removal efficiencies. However, according to the statistical analysis (**Table 4**), only three WWTP (SP-1, SP-2 and SP-4) should that. The SP-3 had compliance percentage of 80%, and the others stabilizations ponds had a performance below 80%, which is not enough.

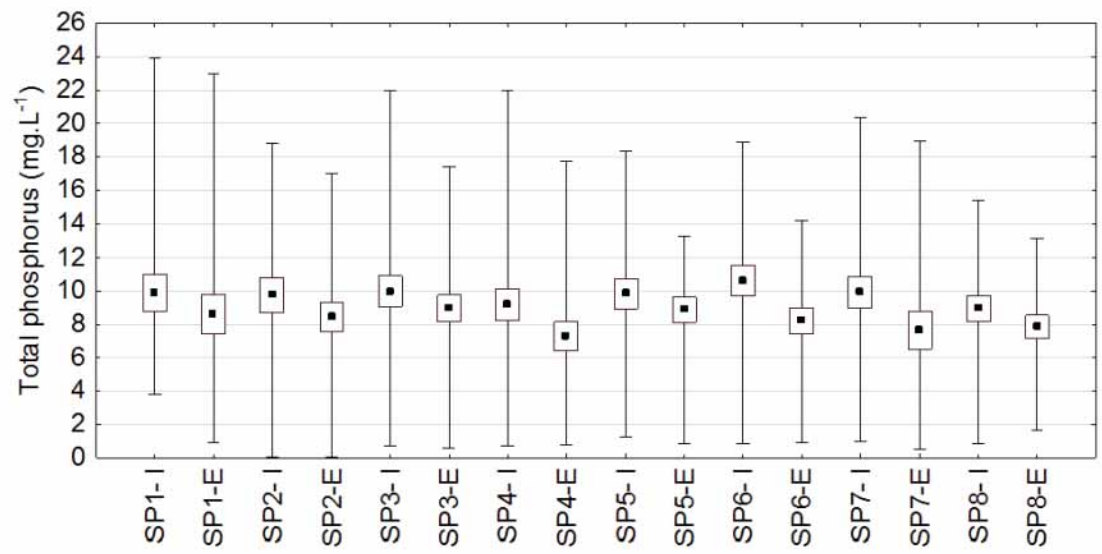


FIGURE 4. Phosphorus concentrations for influent (I) and effluent (E)

This level of performance did not have any relation with the stabilization ponds capacity, other operational reason that was not monitored in this study like superficial application rate, hydraulic detention time and depth could explain this problem.However, this microbiology quality is enough some activities like crop restrict irrigation or Aquaculture reuse [6].

The Brazilian legislation did not establish standard for phosphorous and nitrogen discharges, which incapacitate a reliability analysis to these parameters. The **Figure 4 and 5** summarizes the interfluent and effluent concentration for total phosphorus and Total Nitrogen kjeldahl.

The insoluble phosphate salts precipitation together the assimilation by the biomass are the major phosphorus removal mechanisms in stabilization ponds [16]. In general, the phosphorus removal is relatively low and may reach values of around 50%, but these values depend on the number of maturation ponds in the system [6].

On present research the phosphorus efficiency removal was below 20%. Stabilization ponds, in general, cannot remove phosphorus, once requires high levels of pH in order to form and decant of phosphorus salts. The pH varied from 7 to 8.3.

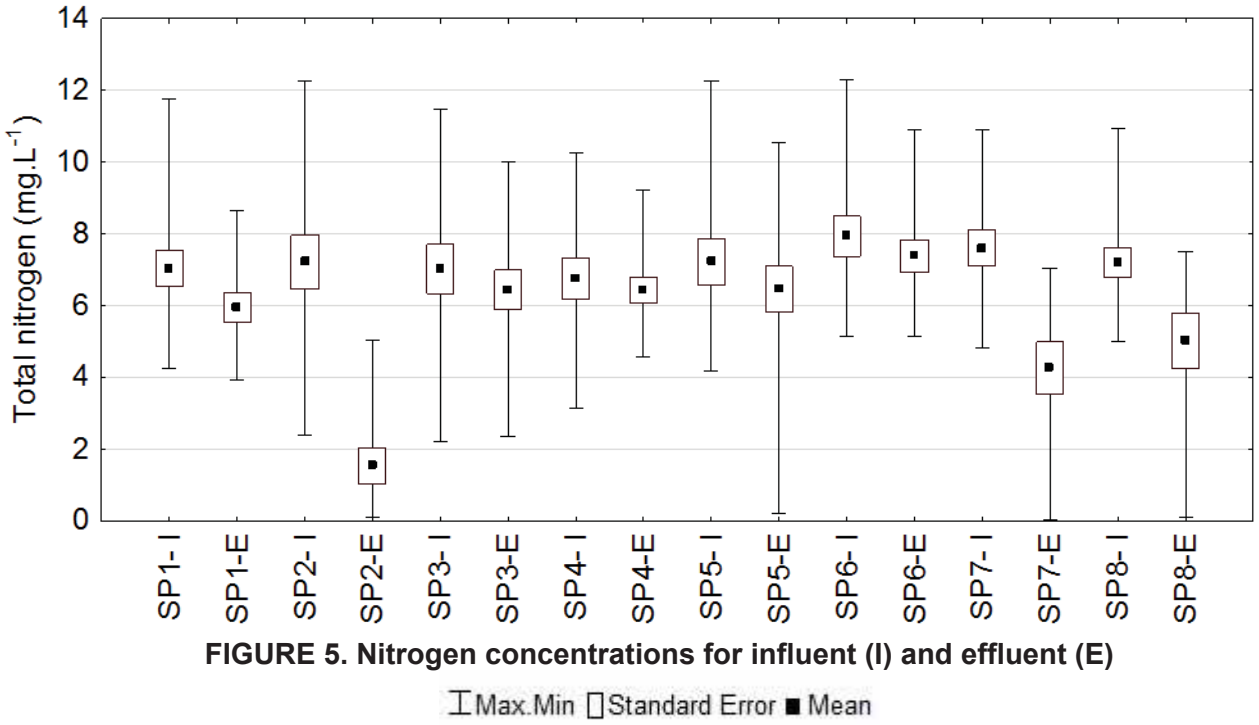


FIGURE 5. Nitrogen concentrations for influent (I) and effluent (E)

For the total nitrogen (NTK), the best removal efficiencies were 77%, 42% and 35% for the SP-2, SP-7 and SP-8, respectively. The others WWTP had removal efficiency below 20%. The average efficiency for stabilization ponds in Brazil is 44%.

Thus, for NKT parameter was a significant variation in average effluent and hence the efficiency. This variation is within the average observed in facultative ponds systems in Brazil (44 %) [17].

The ammonia volatilization and ammonia uptake biomass are the major nitrogen removal mechanisms in stabilization ponds. Both processes are associated with high pH values (around 9). In ponds evaluated in this study the pH range was about 7 to 8.3, not favoring in this way the ammonia volatilization [18].

CONCLUSION

The stabilization ponds analyzed had a great efficiency for BOD removal. However, the efficiencies for thermotolerant coliforms were not so good, which indicates a contamination in the effluent generated. However, this microbiology quality can be enough to some activities like crop restrict irrigation or Aquacultural reuse.
The WWTP, in general, did not have a great performance for nutrients removal (phosphorus and nitrogen), which can increase the eutrophication in the receiving body. On the other hand, the effluent can be used in others uses. For example, effluent with nutrients can be positive for agriculture.
The reliability analysis showed as an important tool to evaluate and controls the effluent concentration, which can be used for environmental agencies to guarantee the compliance of the discharge standards. Using this data, the WWTP can be arranged to remove the parameter that did not meet the discharge standard.

REFERENCES

1. IBGE. *Instituto Brasileiro de Geografia Estatística*. Disponível em: <http://cidades.ibge.gov.br> 2014.
2. Von Sperling M., Mascarenhas L.C.A.M. *Performance of very shallow ponds treating effluents from UASB reactors*. Water Science and Technology, vol. 51, nº 12, pp. 83-90, 2005.
3. Dias D.F.C.; Nascimento T.E.P F., Rodrigues V.J.P., Von Sperling, M.. *Overall performance evaluation of shallow maturation ponds in series treating UASB reactor effluent: ten years of intensive monitoring of a system in Brazil*. Ecological Engineering , v. 71, p. 206-214, 2014
4. Pastich EA, Gavazza S, Casé MCC, Florencio L, Kato MT. *Structure and dynamics of the phytoplankton community within a maturation pond in a semiarid region*. Brazilian Journal of Biology 76, (1): 144-15, 2016
5. Masseret E., Amblard C., Bourdier G., Sargos D.. *Effects of a waste stabilization lagoon discharge on bacterial and phytoplanktonic communities of a stream*. Water Environmental Research, 72 (3) 285-294, 2000.
6. Varón M.P., Mara D..*Waste stabilization ponds*. IRC: International Water and Sanitation Centre, 2004.
7. Davies-Colley R.J., Donnison A.M., Speed D.J., Ross C.M., Nagels J.W. *Inactivation of faecal indicador microorganisms in waste stabilization ponds: interactions of environmental factors with sunlight***.** Water Research, 33, (5), 1220-1230, 1999.
8. Niku S., Schroeder E.D., Samaniego F.J.*. Performance of activated sludge process and reliability-based design*. Journal Water Pollution Control Association, v. 51, n. 12, p. 2841 - 2857, 1979.
9. BRASIL. Ministério do Meio Ambiente Conselho Nacional do Meio Ambiente (CONAMA) Resolução Nº430, de 13 de maio de 2011.
10. Kayombo S., Mbwette T.S.A, Mayo A.W., Katima J.H.Y., Jorgensen S.E.. *Diurnal cycles of variation of physical-chemical parameters in waste stabilization ponds*. Ecological Engineering, 18, 287-291, 2002.
11. Park J.B.K., Craggs R.J. and Shilton A.N.. Wastewater treatment high rate algal ponds for a biofuel production. Bioresource Technology, 102, 35-42, 2011.
12. Craggs, R.J.. *Advanced integrated wastewater ponds*. In: Shilton, A. (Ed.), Pond Treatment Technology, IWA Scientific and Technical Report Series, IWA, London, UK, 282-310, 2005
13. Kong QX., Li L., Martinez B., Chen P., Ruan R.. *Culture of Microalgae Chlamydomonas reinhardtii in Wastewater for Biomass Feedstock Production*. Applied Biochemistry and Biotechnology, 160 (1) 9-18, 2010.

14. Craggs R. J., Heubeck S., Lundquist T. J., Benemann J.R.. Algal biofuels from wastewater treatment high rate algal ponds, Water Science & Technology, 63 (4) 660–665, 2011.
15. Oliveira S.M.A.C., Von Sperling M.. *Avaliação de 166 ETE em operação no país, compreendendo diversas tecnologias. parte 1 - análise de desempenho*. Revista Engenharia Sanitária e Ambiental , v. 10, Nº 4, 2005.
16. Cavalcanti P.F.F., van Haandel A., Kato M.T., von Sperling M., Luduvice M.L., Monteggia, L.O. *Pós-tratamento de efluentes de reatores anaeróbios por lagoa de polimento*. In: Chernicharo, C.A.L (coordenador) Pós-tratamento de reatores anaeróbios. Belo Horizonte: PROSAB, cap 3, 2001.
17. Oliveira S. C., von Sperling M. *Performance evaluation of different wastewater treatment technologies operating in a developing country*. Journal of Water, Sanitation and Hygiene for Development, 1, 37-56, 2011.
18. Camargo Valero M. A., Mara D.D., Newton R.J..*Nitrogen removal in maturation ponds via biological uptake and sedimentation of dead biomass*. Water Science and Technology, 61 (4), 1027-1034, 2010.
19. PERNAMBUCO. Norma Técnica 2007. CPRH Agencia Estadual do Meio Ambiente. Coliformes Fecais – Padrão de Lançamento para Efluentes Domésticos E/Ou Industriais.

CHAPTER 7.7 BIOPURIFICATION SYSTEM FOR PESTICIDES MIXTURE DEGRADATION IN REPEATED APPLICATIONS

M.C Diez *(1,3); B. Leiva (3) and F. Gallardo (2,3)

(1) Chemical Engineering Department, La Frontera University, PO Box 54D, Temuco, Chile.
(2) Chemical Sciences and Natural Resource Department, La Frontera University, Temuco, Chile
(3) Biotechnological Research Center Applied to the Environment- Scientific and Technological Bioresource Nucleus (CIBAMA-BIOREN)

ABSTRACT

A biopurification system based on the adsorption and degradation capacity of a biomixture was evaluated to degrade a mixture of pesticides (35 mg of each a.i. kg^{-1}) in repeated applications (0, 30 and 60 days). The biomixture contained soil, peat, and wheat straw (1:1:2 v v^{-1}). Tanks of 1 m^3 packed with 125 kg of biomixture (ρ 0.29 g mL^{-1}), with and without vegetal cover were used. Pesticides concentration, biological activities (urease, phenoloxidase and dehydrogenase) and microbial community changes (DGGE and qPCR) were evaluated periodically. Pesticides degradation was higher in tanks with vegetal cover (>95%) and no variation was observed after the three applications; besides, no metabolites of these compounds were detected in biomixture. Contrarily, pesticides dissipation decreased in tank without vegetal cover after each application. Besides, the vegetal cover collaborated with retention of pesticides being only hydroxiatrazine (HA) detected in lixiviates. Biological activities were not affected by the application of pesticides, showing some differences between tanks with and without vegetal cover. High similarity between microbial groups (actinobacterias, bacteria and fungi) was observed, being not affected by reapplications of pesticides. The numbers of copies of bacteria and actinobacterias remain almost constant during the assay. However, the number of copies of fungi was significantly higher in non contaminated tank without vegetal cover

Keywords: Biopurification system; pesticide dissipation, biological activities, DGGE.

INTRODUCTION

The use of pesticide has increased in the last years, generating an important environmental concern. Once in the environment, these compounds and their metabolites can produce significant effects in human and animal health. Pesticide residues can be found in soil, water and air, producing alterations in food chains and microorganisms[1]. Accidental spillages during tank filling or cleaning the spraying equipment can occur due unsatisfactory management in farms generating point's source of contamination[2]. Therefore, it is necessary to develop green technologies to protect the environment and human health.

---

*Author for correspondence: cristina.diez@ufrontera.cl

Different biological technologies can be used to decrease the contamination by pesticides. The biopurification system named biobed has been proposed as an ecological and cost effective technology to decrease pesticide contamination of soil and water[3]. This biopurification system is based on the adsorption and degradation of pesticides by an organic biomixture composed by active soil, peat and straw. The organic biomixture has active microbial activity, which degrade pesticides and its metabolites at high concentrations[4-5], and could be modified to improve its capacity to dissipate pesticides[6-8].

The use of vegetation over the biomixture of biobed can keeps a good moisture balance by evaporating excess water, and prevents the top layer from drying out[4]. Research showed that grasses (Carex spp.) are more resistant to herbicides, but bushes and trees (Salix spp.) have higher evaporation capacities. Carex spp. increased the evaporation of the system by more than 500 liters per planted m² per year while Salix spp. increased the evaporation by about 1000 or more liters per year. When using enough plant units to evaporate excess water, open biofilter systems can become zero leachate systems. Also, the root system can improve soil conditions for microorganisms, which are responsible for the degradation of organic pollutants, between them pesticides. However, some phytoxicity of the grass cover can occur when high concentration of pesticides (especially herbicides) is directly charged onto a biobed. Studies on plant root growth have shown that it can only survive contamination up to a certain critical toxic concentration in soil that varies according to plants species[10]. Wang and Oyaizu (2009)[11] evaluated the phytoremediation potential of four plants species for dibenzofuran-contaminated soil. The authors found that white clover had not only the highest root biomass, but also the highest dibenzofuran-degrading bacterial numbers compared to those of the other three grasses.

The pesticide dissipation increases quickly from planted biomixture than non-planted[12]. The rhizosphere effect in the dissipation of pesticides has not been extensile studied in the biobed system in spite of its positive effect. In several studies, rhizodegradation is a specific type of phytoremediation that involves both plants and their associated rhizosphere microbes; this interaction was effective for removal and degradation of pesticides compared with unplanted soil[13]. Plant-microbial interaction increases microbial activity at the root-soil interface where physical, chemical, and/or biological parameters are being modified by the presence of the roots by their exudates[14]. Few studies on the importance of plants in biopurification systems involved in pesticide dissipation at laboratory scale are available[15,12]. The rhizosphere of plants appears to provide an environment conductive to co-metabolism due the proliferation of microorganisms in surface soil by exuding carbohydrates, enzymes and root exuded as citrate, oxalate, malate, citric, fumarate and acetate[16]. However, native microorganisms in rhizosphere are usually modified in abundance and composition after the application of pesticides in soil.

The microbial communities in soil can be studied qualitatively by fingerprint molecular methods such as PCR amplification of polymorphic DNA and PCR-DGGE[17]. Different reports have been proposed, these studies have been analyzed by DGGE technique, demonstrating shifts in time on microbial communities of bacteria, fungi and actinobacteria[18-19]. Coppola et al. (2011)[20] studied shifts in fungal and bacterial diversity after the addition of pesticides and which demonstrated that yeasts and ascomycete

filamentous fungi seemed to be involved in the pesticides degradation in biopurification system. Tortella et al. (2013a)[21] monitored fungi and bacterial communities' structure during atrazine degradation in a biopurification system and observed little impact in time.

For this reason, the influence of rhizosphere microbial communities and their exudates may increase the dissipation of pesticide and decrease the impact over rhizospheric microorganisms. Therefore, the main aim of this study was to evaluate the pesticide dissipation and its impact on the microbial communities in a field biopurification system after repeated applications of a pesticide mixture.

MATERIALS AND METHODS

Chemicals. Analytical standard atrazine (ATZ), chlorpyrifos (CHL) and iprodione (IPR), all of them 99% purity, were purchased from Sigma Aldrich, Chile. MBTH (3-methyl-2-benzothiazolinone hydrazone) and DMAB (3-dimethyl-amino benzoic acid) were purchased from Sigma Aldrich, Chile. All other chemicals and solvent were of analytical reagent grade and were purchased from Equilab Ltda. and Merck S.A (Chile).

Biomixture formulation. The biomixture was prepared mixing an Andisol topsoil (37% sand, 34% silt, 28% clay, 7% organic carbon, pH 5.4), commercial peat (36% organic carbon), and wheat straw (34% organic carbon), in a proportion of 1:1:2 by volume respectively. The soil, which belonged to the Freire series (38º50'S, 72º41'W) at Maquehue Experimental Station of Universidad de La Frontera in southern Chile, was collected at a depth of 0 to 20 cm, air-dried at room temperature and sieved through a 2 mm mesh. The straw was collected from crop residues in a local farm and was chopped to obtain fractions of 5 to 10 cm length. The constituents were mixed vigorously to obtain a homogeneous biomixture; this biomixture, with 60 % of water holding capacity (WHC), was deposited on a surface, covered with plastic to avoid the effects of rain, and left to compost for 60 days until use. The resulting biomixture had pH 5.5, 33% organic carbon and 0.6% total nitrogen.

Experimental design and assay setup. We used a field biopurification system installed at Maquehue Experimental Station of Universidad de La Frontera, described previously by Diez et al. (2015). Briefly the installation consisted in plastic tanks of 1 m^3 packed with 125 kg of biomixture (bulk density (ρ) 0.29 g mL^{-1}), to a height of 60 cm. The biopurification system had previously been used to treat a mixture of pesticides of ATZ, CHL and IPR (35 mg kg^{-1} of each active ingredient (a.i.)) and humidity was maintained by addition of tap water to maintain 65-70% of water holding capacity (WHC). The assay included two tanks with vegetal cover plus pesticide mixture (L1), two tanks with vegetal cover without pesticide mixture (L2), two tanks without vegetal cover with pesticide mixture (L3) and two tanks without plants and without pesticide mixture (L4). The vegetal cover was maintained at a height of 5 cm. The tanks L1 and L2 were artificially contaminated spraying a water solution containing a mix of formulated ATZ, CHL and IPR (35 mg a.i. kg^{-1}) at three times (0, 30 and 60 days). The tanks L3 and L4 were maintained only with water for control purposes. Tap water was added at a rate of 1.2 L d^{-1} to each tank during the assay (90 days). The assay was kept under field conditions and, the tanks were installed beneath a rain protection roof. Biomixture samples were

taken from each tank (first 15 cm below the vegetal cover) and analyzed for pesticides and their metabolites, biological activities (phenoloxidase, dehydrogenase and urease) and microbial communities (fungi, bacteria and actinomycetes) at regular time intervals. All experiments were conducted using three independent replicates and statistical analysis was assessed. Data were subjected to a one-way analysis of variance and the averages were compared by Tukey's range tests. Pesticide kinetics was analyzed by stargraphic program.

Pesticide extraction and analytical procedures. Samples for pesticides analyses from L1 and L2 tanks (5 gr dry weight) were extracted by shaking (1 h at 250 rpm) with 20 mL of acetone and by ultrasonication (30 min). After centrifuging (10,000 rpm) 5 mL of the supernatant was collected, filtered through a PTFE membrane (0.2 μm pore size) and evaporated to dryness under an N_2 flow, after which the residue was dissolved with 1 mL of acetonitrile. Recovery of ATZ, CHL and IPR was >85%. The pesticide concentrations were determined by HPLC using a Merck Hitachi L-2130 pump that was equipped with a Rheodyne 7725 injector and a Merck Hitachi L-2455 diode array detector. Separation was achieved using a C18 column (Chromolit RP-8e, μm 4.6 x 100 mm). Eluent A was 1mM ammonium acetate and eluent B was acetonitrile. The gradient conditions used for pesticide separation was as follow: 0-2 min of 95% A, 2-4 min of 95-70% A, 4-7 min of 70% A, 7-12 min of 70-30% A, 12-16 min of 30% A, 16-17 min of 30-95% A and 17-20 min of 95% A. The flow rate was set as follows: 0-12 min at 1 mL $min^{-1,}$12-16 min at 1-2 mL $min^{-1,}$ increase 16-20 min at 2 mL min^{-1}. The column T° was maintained at 30±1 °C. The detector was set at 3 wavelengths for data acquisition 220, 245 and 290 nm. Instrument calibrations and quantifications were performed against pure reference standards (0.1-10 mL min^{-1}) for each compound.

Enzymatic activities. Phenoloxidase activity was assessed using MBTH/DMAB method (adapted from Castillo et al., 1994)[35]. Briefly, samples (10 g dw) of the biomixtures were shaken (150 rpm, 2 h) with 25 mL of a 100 mM succinate–lactate buffer (pH 4.5). The samples were centrifuged (4000 rpm, 20min). The supernatant of each sample was collected, filtered through 0.45 lm membrane and measured immediately. The reaction mixture contained 300 μL of 6.6 mM DMAB, 100 μL of 1.4 mM MBTH, 30 μL of 20 mM $MnSO_4$ and 1560 μL of the filtered sample; the reaction was initiated with the addition of 10 μL of 10 mM H_2O_2. The reaction was observed in a Spectronic Genesis 2PC spectrophotometer at 590 nm (e =0.053 μM^{-1} cm^{-1}). For the possible presence of lignin peroxidase (LiP) and Laccase (Lac) activity, no correction was made, thus measurement may represent the sum of manganese peroxidase, LiP and Lac and is expressed as phenoloxidase activity[4]. Penoloxidase activity is expressed as U kg^{-1}.

Urease activity was measured by the method of Alef and Nannipieri (1985)[30]. Briefly, 12 mL of 0.1 M phosphate buffer (pH 6), 3 mL of distilled water and 1 mL of 1.067 M urea were added to 3 g rhizosphere soil samples. The samples were incubated at 37 °C for 2 h. Thereafter, 15 mL of 2M KCl shaking for 60 min. Subsequent filtration was done through Whatman Nº 40 filter papers. The $N\text{-}NH_4^+$ was determined by ion selective electrode. Three replicates of each sample were tested and a control sample without urea was prepared. All the results were expressed as μmol of $N\text{-}NH_4^+$ g^{-1} h^{-1}.

Dehydrogenase activity was determined using the methodology proposed by Casida (1977)[34]. Moist biomixture (equivalent to 2 g of dry matter) was incubated for 24 h at 37ºC with 4 mL of buffer Tris (pH 6) and 2 mL of 1% 2,3,5 triphenyl tetrasolium chloride (TTC) as a substrate. After incubation, 10 mL of methanol was added and tubes were vigorously agitated to extract the reaction product triphenyl formasan (TPF). The pink liquid was centrifuged at 4,500 rpm for 10 min at 4ºC. TPF concentration was measured at 485 nm and dehydrogenase activity was expressed as μg TPF g^{-1} h^{-1}.

Microbial community analyses. DNA was isolated from the different biomixtures of the tanks at 10, 30, 60 and 90 days, using the FastDNA® Spin Kit for soil. Isolation was performed on 0.5 g of biomixture following the manufacturer´s instructions, 1% agarose gel electrophoresis in 0.5x TBE was used to analyze the quality and quantity of extracted DNA. The soil extraction was.

PCR conditions for bacteria. Bacterial DNA was amplified with primers F341-GC (2) (GC) CCTACGGGAGGCAGCAG region 16S rDNA S and R534 ATTACCGCGGCTGCTGG region 16S rDNA[38], Combination of both primers generates a PCR fragment of about 200 bp suitable for a subsequent PCR-DGGE analysis. For PCR 10 μL buffer “Green GoTaq® Flexi” 5X, 2,5 μL de MgCl2 (25 mM), 1 μL de DNTP’S (10 mM), 1 μL forward primer (10 mM), 1 μL reverse primer (10 mM), 0,25 μL Taq (5U μL, Go Taq® Flexi DNA polimerase, Promega Corp), 3 μL ADN (50 ng μL) y 31,25 μL water. For PCR program the initial denaturation was 8 min at 94°C, 32 denaturation cycles in 30 s at 94°C, hybridization at 30 s to 58°C. Primer extension was carried out at 72 °C for 1 min. Finally, the samples were incubated for 5 min at 72 °C (final extension). The presence of PCR products was ascertained by agarose (1.5% w/v) gel electrophoresis, at 90 V for 40 minutes.

PCR conditions for actinomycetes. Bacterial DNA was amplified with primers F243 GGATGAGCCCGCGGCCTA region 16S rDNA S and R1378 CGGTGTGTACAAGGCCCGGGAAC region 16S rDNA[37], combination of both primers generates a PCR fragment of about 200 bp suitable for a subsequent PCR-DGGE analysis. For PCR 10 μL buffer “Green GoTaq® Flexi” 5X, 2,5 μL de MgCl2 (25 mM), 1 μL de DNTP’S (10 mM), 1 μL forward primer (10 mM), 1 μL reverse primer (10 mM), 0,25 μL Taq (5U μL, Go Taq® Flexi DNA polimerase, Promega Corp), 3 μL ADN (50 ng μL) y 31,25 μL water. For PCR program the initial denaturation was 5 min at 95°C, 35 denaturation cycles in 30 s at 95°C, hybridization at 30 s to 60°C. Primer extension was carried out at 72 °C for 1 min. Finally, the samples were incubated for 10 min at 72 °C (final extension). The presence of PCR products was ascertained by agarose (1.5% w/v) gel electrophoresis, at 90 V for 40 minutes. PCR conditions for fungi. DNA was amplified with primers ITS 3-GC (1) (GC) ATCGATGAAGAACGCAGC region 5, 8 S rDNA S and ITS 4 TCCTCCGCTTATTGATATGC 5, 8 S rDNA[40], Combination of both primers generates a PCR fragment of about 200 bp suitable for a subsequent PCR-DGGE analysis. For PCR 10 μL buffer “Green GoTaq® Flexi” 5X, 2,5 μL de MgCl2 (25 mM), 1 μL de DNTP’S (10 mM), 1 μL forward primer (10 mM), 1 μL reverse primer (10 mM), 0,25 μL Taq (5U μL, Go Taq® Flexi DNA polimerase, Promega Corp), 3 μL ADN (50 ng μL) y 31,25 μL water. For PCR program the initial denaturation was 8 min at 94°C, 35 denaturation cycles in 30 s at 94°C, hybridization at 30 s to 58°C. Primer extension was carried out at 72 °C for 1 min. Finally, the samples were incubated for 5 min at 72 °C

(final extension). The presence of PCR products was ascertained by agarose (1.5% w/v) gel electrophoresis, at 90 V for 40 minutes.

PCR-DGGE analysis. For the analysis of microbial communities of bacteria, actinomycetes and fungi PCR products were analyzed by PCR-DGGE by using a Bio-Rad Dcode. Electrophoresis experiments were performed at 60 °C by using gels containing urea-formamide denaturing gradient (40-70% bacteria; 20-50% actinomycetes; 30-60% fungi). The gels were analyzed by gel electrophoresis for 17 h at 60°C and 80 V, stained with silver nitrate described by Sanguinetti et al. (1994)[39]. The PCR-DGGE dendrogram profile was constructed using Phoretix 1D analysis software.

Q-PCR analysis. The reactions used to determine the relative abundance of fungal and bacterial ribosomal gene copy numbers were performed with a StepOnePlus Real-Time PCRT System (Applied Biosystems) and HOT FIRE Pol® EvaGreen® qPCR Mix Plus. Bacterial 16S rRNA copy numbers were estimated using set Eub338 (5´ACTCCTACGGGAGGCAGCAG) and Eub518 (5´ ATTACCGCGGCTGCTGG)[38]. Fungal 16S rRNA copy numbers were estimated using set FR1 (5´ AICCATTCATCGGTAIT) and FF390 (5´ CGATAACGAACGAGACCT) (Vainio and Hantula, 1999). PCR amplifications used the following program: 95 ºC for 2 min; 40 denaturation cycles at 95 ºC for 15 s, annealing at 63 ºC (bacteria) and 58 ºC (fungi) for 20 s, and extension at 72 ºC for 20 s. Each 20 µL reaction contained 4 µL of EvaGreen®, 0.6 µL of each primer (10 µM), 9.8 µL sterilized milli-Q water, and 2 µL template DNA (0.5 ng µL-1). Standard curves (r2 > 0.995) were generated using triplicate 10-fold serial dilution of a plasmid containing a full-length copy of either the Escherichia coli 16S rRNA gene or theA.discolor 16S rRNA gene.

RESULTS AND DISCUSSION

Pesticide dissipation. **Figure 1** shows the pattern of ATZ, CHL and IPR dissipation from the biomixture after repeated applications. A rapid and high dissipation of the three pesticides evaluated was observed (> 95%) in biomixtures with vegetal cover (L1 tank) after three application of pesticides, demonstrating the great influence of the rhizosphere of the biobed over pesticides dissipation. These finding are associated with the positive effect of the rhizosphere of the biopurification system on the pesticides degradation. Diez et al. (2015)[15] concluded that the vegetal cover diminished the lixiviation of ATZ, CHL and IPR and their metabolites at the same time that increased the degradation of the pesticides in planted biomixture after one application of these compounds at the same concentration. Besides, might be due to the adaptation of the degrading microorganisms in the biomixture after repeated pesticide applications. Yu et al. (2009)[22] reported that the dissipation of carbendazim in soil could be accelerated by repeated pesticide applications.

On the other hand, the dissipation of the pesticides decreased in unplanted tank (L3) after the three successive applications. ATZ dissipation decreased from 83.6% to 79% and 64.8% after the first, second and third application, respectively (**Figure 1a**) and, the same behaviour was observed with CHL dissipation, decreasing from 82.5% to 73,7% and 64% (**Figure 1b**) and IPR decreasing from 91.2 % to 83.8% and 75%, after the first, second and third application, respectively (**Figure 1c**). Accelerated dissipation of ATZ

has been reported in the biomixture of a laboratory biobed system without vegetal cover[21]. The authors reported that after the second application of ATZ, the dissipation efficiency slightly decreased (from 96% to 78%), but the system was able to recover and show a positive performance after the 3rd ATZ application with 95% of dissipation. Vischetti et al. (2008)[23] used a modified biomixture of biobed composed of vine/branches and urban waste/garden compost. They found that the fungicide metalaxyl was rapidly degraded after 3 successive applications and that the half-life (t ½) was reduced from 37 d after the first metalaxyl application to just 4 d after the third application. An opposite situation was found for CHL and a decreasing in pesticide dissipation was observed and, the authors explained that the accumulation of TCP in the biomixture may affect the microbial activity, due to antimicrobial properties of this compound.

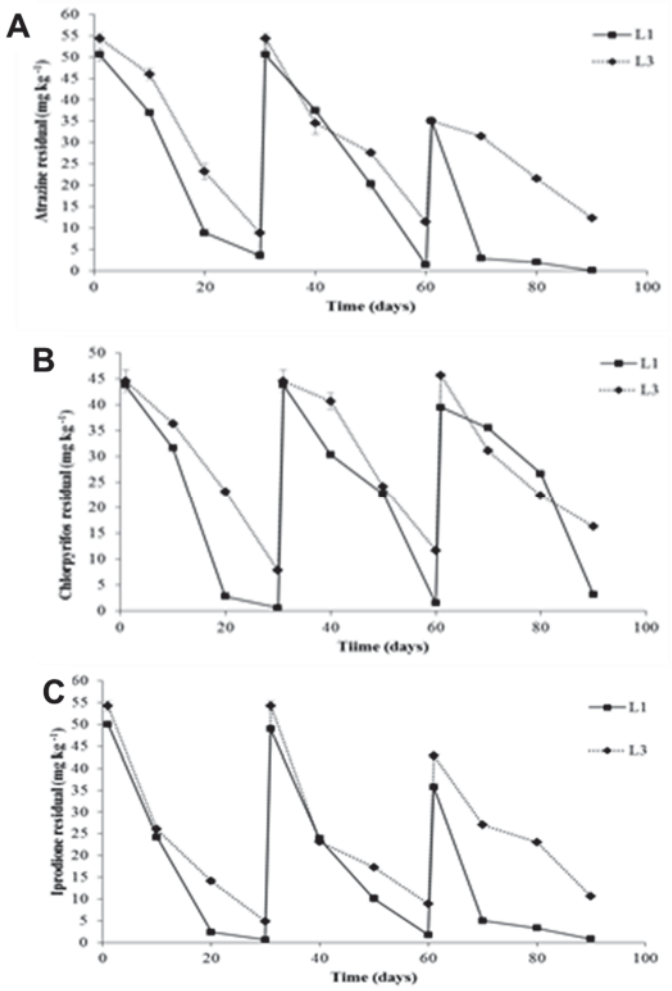


FIGURE 1. Concentration of pesticides ATZ (A), CHL (B) and IPR (C) in the biomixture of biobeds after repeated applications of the mixture of pesticides at 50 mg kg^{-1}, during 90 days. Treatment L1, with pesticide and vegetal cover; L3, with pesticide and without vegetal cover.

Biological Activities. Phenoloxidase activity has been monitored due its positive correlation with pesticide dissipation in biopurification systems[12,24]. Plant and microbial

phenoloxidase can play an important role in the dissipation of pesticides. Some pesticide, in particular those containing amino or hydroxyl functional groups, may increase the dissipation by root-associated or free extracellular enzymes[25]. Contrarily to those results of dehydrogenase and urease activities, phenoloxidase activity showed a tendency towards no stabilization after 90 days of evaluation in all treatments and, the highest values were obtained at this time (0.28 to 0.45 U kg^{-1}) (**Table 1**). An oscillatory behavior was observed in tanks L1 and L2, due to the presence of plants and microorganism in the biomixture that promote the hydrolysis of nitrogen compounds. The lowest values of urease activity in tanks L1 and L3 were observed after each reapplication (30 and 60 days) demonstrating some inhibitory effect by the presence of the pesticides. The result obtained in this study are concordant with Tortella et al. (2013c)[26] who found an inhibitory effect on the phenoloxidase activity in a biomixture without vegetal cover, obtaining values 0.2-0.6 U kg^{-1} during ATZ dissipation. In addition, Urrutia et al. (2013)[7] monitored the phenoloxidase activity in the range of 0.5-3.0 U kg^{-1} during the dissipation of ATZ, CHL and isoproturon in a biomixture without plants. However, some studies have proposed contrasting values of phenoloxidase during pesticide dissipation. Tortella et al. (2012)[27] found greater values of phenoloxidase activity (2-14 U $kg^{-1)}$ at high CHL dissipation in a biomixture. Moreover, Fernández et al. (2012)[36] found values in the range of 1.6-2.8 U kg^{-1} during CHL dissipation (160 mg a.i. kg^{-1}) after 40 days.

Dehydrogenase is the enzyme used as an indicator of overall microbial activity in soils. In our study, dehydrogenase activity showed a tendency towards stabilization after 90 days of evaluation in all treatments (43.00 to 60.86 µg TPF g^{-1} h^{-1}). Dehydrogenase activity remained almost constant in L1 tank, with values of 59.8 and 49.99 µg TPF g^{-1} h^{-1} at the initial and final time of evaluation, respectively, and no effect was observed after each reapplication of pesticides. On the other hand, in L2 tank an oscillatory behavior was observed, with the maximum value after 30 days of evaluation (71.30 µg TPF g^{-1} h^{-1}). The major values were obtained in L3 tank at time 0 and after 10, 30 and 50 days of evaluation. In L4 tank dehydrogenase activity decreased from 64.87 to 42 µg TPF g^{-1} h^{-1} at day 20 and then the activity remained constant until the last evaluation (Table 2). Comparing dehydrogenase activity in tanks contaminated with pesticides (L1 and L3), we can observe that plants in L1 had a regulatory effect over this enzyme and no major fluctuations were observed. L4 tank showed lower values than those observed in the other tanks, which could be explained by the lack contribution of the vegetal cover in keeping the moisture in the system and the lack of the beneficial effect of the interaction between plants and microorganisms due to the exudation of organic acids (Wang et al., 2014). Plants increase or improve root exudation under chemical stress, which increases microbial activity and community numbers thus enhancing the degradation of pollutants (Chaudhry et al., 2005); this could explain the lower concentrations of ATR CHL and IPR found in tank with vegetal cover (L1).

Urease is an enzyme studied for its relationship with soil fertility and is largely related to microbial biomass. It is characterized to be very sensible to changes in a particular medium, so urease activity has been used as an indicator of environmental contamination by heavy metals or pesticides. Similarly to dehydrogenase activity, urease showed a tendency towards stabilization after 90 days of evaluation in all treatments (11.36 to 16.58 µmol g^{-1} h^{-1}) (**Table 2**). However, an oscillatory behavior was

observed in all tanks with picks of urease activity at times 20 and 60 days, not necessarily associated with the reapplications of the pesticides. The highest values were obtained in contaminated tank without plants (L3) probably due to the reaction of native microorganisms in the presence of the contaminant, and the lowest values were obtained in uncontaminated tank without plants (L4).

TABLE 2. Enzymatic activities in the biomixture of biobeds after repeated applications of the mixture of pesticides at 50 mg kg^{-1}

Enzymatic Activities	Tanks	Days									
		0	10	20	30	40	50	60	70	80	90
Phenoloxidase (U kg^{-1})	L1	0.28	0.43	0.27	0.15	0.22	0.31	0.15	0.23	0.33	0.37
	L2	0.37	0.38	0.30	0.23	0.32	0.39	0.25	0.34	0.42	0.45
	L3	0.19	0.22	0.18	0.12	0.15	0.18	0.14	0.14	0.21	0.28
	L4	0.32	0.39	0.36	0.32	0.29	0.31	0.37	0.28	0.34	0.38
Dehydrogenase µg TPF g^{-1} h^{-1}	L1	59.80	55.02	64.17	54.81	52.72	56.09	47.55	62.61	50.14	49.99
	L2	64.48	39.48	37.00	71.30	47.54	35.85	49.06	49.07	36.28	51.97
	L3	87.46	91.47	44.67	79.36	59.89	75.52	65.15	46.21	54.25	60.86
	L4	64.87	57.64	42.00	42.31	35.16	42.91	35.84	36.70	40.00	43.00
Urease µmoles N-NH4^{+}g^{-1} h^{-1}	L1	6.39	12.9	31.4	26.9	17.8	14.1	36.9	26.6	20.8	13.9
	L2	8.29	13.3	26.9	14.3	16.3	29.6	35.1	24.2	12.0	16.58
	L3	6.80	19.7	44.4	34.4	23.1	36.4	48.0	35.7	23.3	15.2
	L4	7.04	10.7	38.2	14.7	8.2	16.8	29.2	32.5	11.7	11.36

Samples were obtained at 0-10 cm depth during 90 days. L1, with pesticide and vegetal cover; L2, without pesticide and with vegetal cover; L3, with pesticide and without vegetal cover and L4, without pesticide or vegetal cover.

PCR-DGGE analysis. Ours results revealed a similar intense of DGGE bands in all the analyzed samples, indicating the presence of a large number of equally abundant ribotypes in both treated and untreated biomixtures (**Figure 2**). The patterns of fungal communities (**Figure 2C**) in the biopurification system contaminated showed high similarity (>80%) (**Figure 2C**). The cluster analyzes revealed the existence of several groups with higher similarity. The control non-contaminated and contaminated, shown small difference between treatments. These finding suggest that after the pesticide application the fungal communities were not affected for the ATZ, CHL or IPR repeated applications. Similar situation was found for bacteria ribotypes (**Figure 2A**) that showed higher similarity indices (80%). The cluster analyzes revealed the existence of several groups with a similarity more than 90% between treatments. Therefore, pesticide application at the concentration evaluated in this study revealed shortly shifts compared to control. These results are in accordance with the results reported by Tortella et al (2013a)[21], where after repeated application of pesticide in the biomixture a small shift

was detected in fungal or bacterial communities that were principally attributed to variations to carbon sources easily available.

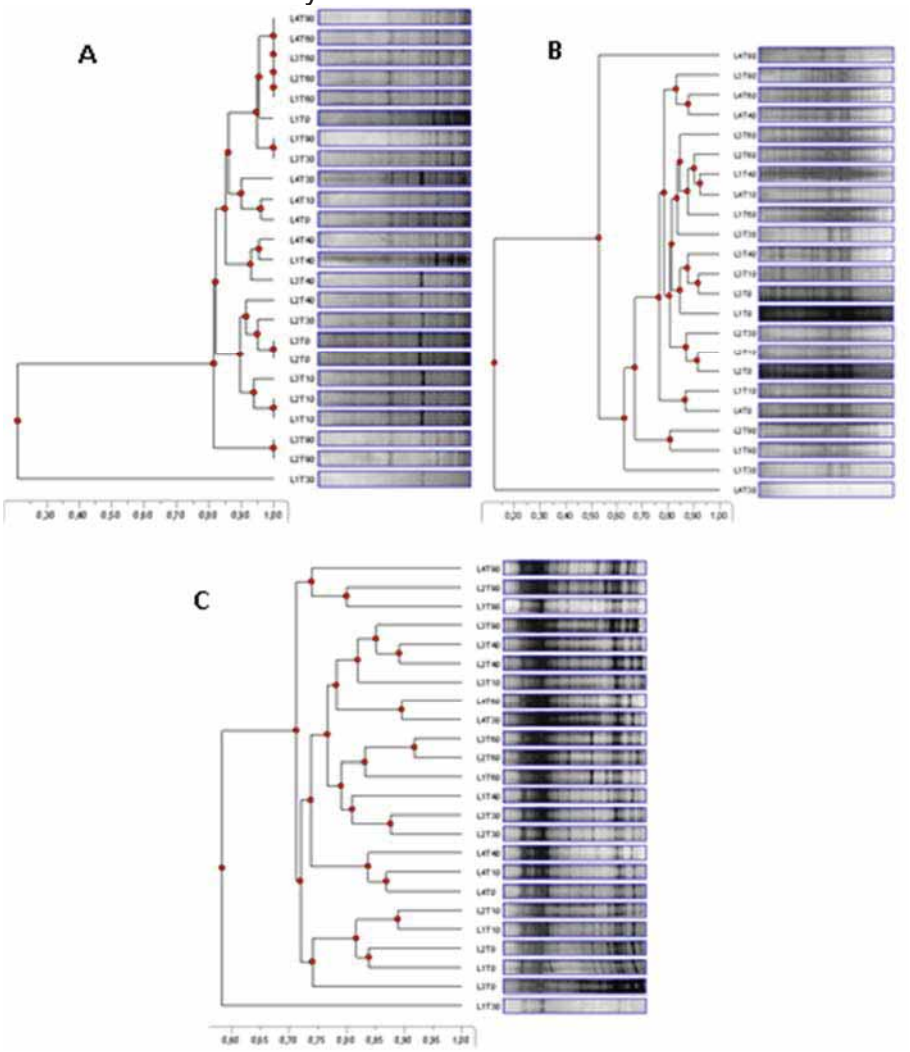


FIGURE 2. Cluster analysis of DGGE profiles of 16S rDNA of bacterial (A) and actinobacteria (B) and fungal (C) 18S rDNA amplicons in the biomixture after repeated applications of a pesticide mixture

On the other hand, DGGE patterns for actinobacterias communities showed a similarity index (>75%). The cluster analyzes revealed the existence of five groups with a similarity more than 70% between treatments. The method showed that fingerprint of actinobacterias communities did not differ from each other.

The results monitored shown intense bands in all samples analyzed, demonstrating a high number of ribotypes in the control and the system contaminated. The results obtained in this present work are corroborated by previous studies by Tortella et al., (2013a), who described the effect of ATZ in microbial activities in a biomixture of biobed without vegetal cover. They found the microbial diversity of bacteria, fungi and actinomycete after 60 days was similar for all the treatment evaluated. In addition, Urrutia et al. (2015) found high abundance of bacteria and fungi during pesticide dissipation by real-time PCR in a biopurification system. Coppola et al. (2011)[20]

monitored the fungicide effect in microbial communities, describing a small change in fungal and bacterial communities but recovered at the end of the experiment. Tortella et al. (2013b)[19] evaluated the microbial communities during ATZ dissipation in a biopurification system. They found transitory effect during the ATZ application. Besides, Tortella et al. (2013b)[19] found that microbial communities monitored by DGGE in a biopurification system. They showed a significantly effect after pesticide application but recovered at the end of the experiment. Tortella et al. (2014)[28] monitored the microbial communities during diazinon dissipation in a biopurification system. They found a decrease size in fungal and bacterial communities after diazinon application.

The structure of microbial communities represents the abundance and proportion of phylogenetic and functional groups. The disappearance of different microbial communities as a result of pesticide exposure may eliminate key ecosystem functions and/or impair the ability of communities to respond to other environmental perturbations[29].

***q-PCR analysis*.** The fungal, bacterial and actinobacteral populations were estimated by real-time PCR (**Figure 3**). The highest value of actinobacteria population was observed in L3 tank (16 x 10^5 g^{-1}) at 30 days, decreasing to 4 x 10^5 g^{-1} at 90 days of evaluation. Numbers of copies of actinobacteria were similar in tank L1 during 40 days, decreasing then to 3.5 x 10^5 g^{-1}. In L2 tank numbers of copies were similar during 60 days varying between 7.5 to 11 x 10^5 g^{-1}, decreasing near 3.5 x 10^5 g^{-1} at 90 days of evaluation. On the other hand, actinobacteria population in L4 tank remained almost constant during all the evaluation period (aprox 7.5 x 10^5 g^{-1}) (Figure 3a). The increasing values of actinobacteria copies in L3 tank could be a reaction due to pesticides reapplication at day 30, by the natural actinobacteria present in the biomixture; however, not the same behavior was observed after the third reapplication (60 days). In contaminated biomixture with vegetal cover (L1), the degradation of pesticides was associated both by rhizospheric bacteria and by natural actinobacteria present in the biomixture. The soil used to formulate the biomixture used in this study has a natural quantity of pesticides-degrading actinobacteria[31,32]. Briceño et al. (2012)[33] isolated actinobacteria from a soil that had received continuous application of CHL and found high degradation of CHL (90%) and, also observed 3,5,6-trichloro-2-pyridinol (TCP) formation and later degradation by the CHL degrading actinobacteria.

Bacteria population varied from 3 to 9 x 10^7 g^{-1} in all biomixtures analyzed (**Figure 3b**). Biomixture of contaminated L1 tank with vegetal cover presented lower values of bacteria copies compared with biomixture of contaminated L3 tank without vegetal cover. This result suggests that natural bacteria of the biomixture in L3 tank are not affected by the contamination with the mixture of pesticides. Therefore, the lesser quantity of bacteria population in tank L1 did not effected the degradation of the pesticides as we can observe in Figure 1. At the same time, no negative effect was observed after pesticides reapplications at days 30 and 60 in L1 and L3 tanks. On the other hand, no difference was observed between biomixtures in L2 with vegetal cover and L4 without vegetal cover tanks after 40 days of evaluation.

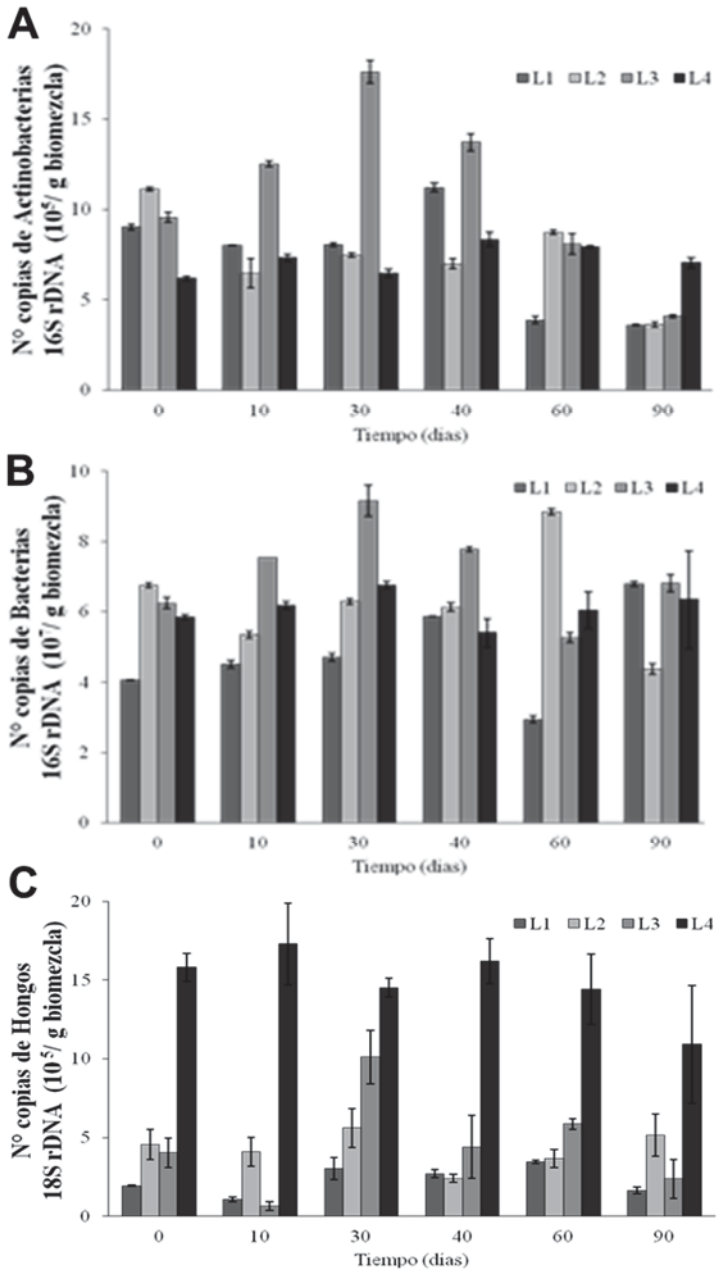


FIGURE 3. 16S rDNA copy numbers for bacteria (A) and Actinobacterias (B) and 18S rDNA copy number for Fungi (C) from qPCR analysis after repeated applications of pesticide mixture at 50 mg kg-1 after 90 days of incubations. L1, with pesticide and vegetal cover; L2, without pesticide and with vegetal cover; L3, with pesticide and without vegetal cover and L4, without pesticide or vegetal cover.

Fungal population was lowest in biomixture of contaminated L1 tank with vegetal cover during all evaluated period. On the other hand, fungal population was highest in uncontaminated biomixture of L4 tank without plants. The biomixture contains 50% of wheat straw, therefore promote fungal growth that has extracellular ligninolytic enzymes capable to degrade lignin from wheat straw of the biomixture. Lignin degradation by fungal attack was observed by Diez et al. (2015)[15] by confocal laser scanning

microscopy (CLSM). Wheat straw samples taken from the same biomixtures used in our study (L1 to L4) showed an increment in lignin colonisation and degradation by fungi in all treatments evaluated. Besides, wheat straw degradation and colonization by natural fungi from the biomixture have been observed by SEM microscopy[5].

CONCLUSION

Vegetal cover of the biopurification system increased pesticides dissipation compared with the system without vegetal cover. Pesticides degradation was higher in tanks with vegetal cover (>95%) and no variation was observed after the three applications. Contrarily, pesticides dissipation decreased in tank without vegetal cover after each repeated application. Biological activities were not affected by repeated application,showing some differences between tanks with and without vegetal cover. High similarity between microbial groups was observed, being not affected by reapplications of pesticides. The numbers of copies of bacteria and actinobacterias remain almost constant; however, the number of copies of fungi was significantly higher in non contaminated tank without vegetal cover.

ACKNOWLEDGMENTS

This research was supported by FONDECYT 1120963 and, partially by 1161481 and CONICYT/FONDAP/15130015 projects.

REFERENCES

1. Carter, A. (2000). How pesticides get into water-and proposed reduction measures. Pesticide outlook, 11(4), 149-156.
2. Torstensson, L., & Castillo, M. (1997). Use of biobeds in Sweden to minimize environmental spillages from agricultural spraying equipment. Pesticide Outlook (United Kingdom).
3. Castillo, M. D. P., & Torstensson, L. (2007). Effect of biobed composition, moisture, and temperature on the degradation of pesticides. Journal of agricultural and food chemistry, 55(14), 5725-5733.
4. Castillo, M. D. P., Torstensson, L., & Stenström, J. (2008). Biobeds for environmental protection from pesticide use--a review. Journal of Agricultural and Food Chemistry, 56(15), 6206–19.
5. Diez, M.C., Tortella, G.R., Briceño, G., Castillo, M.P., Díaz, J., Palma, G., Altamirano, C., Calderón, C. & Rubilar, O. (2013a). The influence of novel lignocellulosic residues in a biobed biopurification system on the degradation of pesticides applied in repeated high doses. Electronic Journal of Biotechnology DOI: 10.2225/vol16-issue6-fulltext-17.
6. Karanasios, E., Tsiropoulos, N. G., Karpouzas, D. G., & Ehaliotis, C. (2010). Degradation and adsorption of pesticides in compost-based biomixtures as potential substrates for biobeds in Southern Europe. Journal of agricultural and food chemistry, 58(16), 9147-9156.
7. Urrutia, C., Rubilar, O., Tortella, G. R., & Diez, M. C. (2013). Degradation of pesticide mixture on modified matrix of a biopurification system with alternatives lignocellulosic wastes. Chemosphere, 92(10), 1361-1366.
8. Diez, M. C., Levio, M., Briceño, G., Rubilar, O., Tortella, G., & Gallardo, F. (2013b). Biochar as a partial replacement of peat in pesticide-degrading biomixtures formulated with different soil types. Journal of Biobased Materials and Bioenergy, 7(6), 741–747
9. Debaer, C. & Jaeken, P. (2006). Modified biofilters to clean up leftovers from spray loading and cleaning; experience from pilot installations. Aspects Appl. Biol. 2006, 77, 247–252.

10. Chaudhry, Q., Blom-Zandstra, M., Gupta, S., Joner, E. (2005). Utilising the synergy between plants and rhizosphere microorganisms to enhance breakdown of organic pollutants in the environment. Environ. Sci. Pollut. Res. 12(1), 34-48.
11. Wang, Y. & Oyaizu, H. (2009). Evaluation of the phytoremediation potential of four plant species for dibenzofuran-contaminated soil Journal of Hazardous Materials 168, 760–764.
12. Urrutia, C., Rubilar, O., Tortella, G., Castillo, J. M., Romero, E., Azcón, R., & Diez, M. C. (2015). Influence of the rhizosphere in a biopurification system on the dissipation of a pesticide mixture. Journal of soil science and plant nutrition,15(4), 914-927.
13. Merini, LJ., Bobillo, C., Cuadrado, V., Corach, D. and Giulietti, AM. 2009. Phytoremediation potential of the novel atrazine tolerant Lolium multiflorum and studies on the mechanisms involved. Environmental Pollution. 157, 3059–3063.
14. Barea J.M, Pozo M.J, Azcón R, Azcón-Aguilar C. (2005). Microbial co-operation in the rhizosphere. J Exp Botany 56: 1761-1778.
15. Diez, M. C., Schalchli, H., Elgueta, S., Salgado, E., Millahueque, N., & Rubilar, O. (2015). Rhizosphere effect on pesticide degradation in biobeds under different hydraulic loads. Journal of Soil Science and Plant Nutrition, 15(2), 410–21.
16. Ryan, P. R., Delhaize, E., & Jones, D. L. (2001). Function and mechanism of organic anion exudation from plant roots. Annual review of plant biology, 52(1), 527-560
17. Kirk, J. L., Beaudette, L. A., Hart, M., Moutoglis, P., Klironomos, J. N., Lee, H., & Trevors, J. T. (2004). Methods of studying soil microbial diversity. Journal of microbiological methods, 58(2), 169-188
18. Marinozzi, M., Coppola, L., Monaci, E., Karpouzas, D. G., Papadopoulou, E., Menkissoglu-Spiroudi, U., & Vischetti, C. (2013). The dissipation of three fungicides in a biobed organic substrate and their impact on the structure and activity of the microbial community. Environmental Science and Pollution Research International, 20(4), 2546–55.
19. Tortella, G. R., Mella-Herrera, R. A., Sousa, D. Z., Rubilar, O., Briceño, G., Parra, L., & Diez, M. C. (2013b). Carbendazim dissipation in the biomixture of on-farm biopurification systems and its effect on microbial communities. Chemosphere, 93(6), 1084–1093.
20. Coppola, L., Comitini, F., Casucci, C., Milanovic, V., Monaci, E., Marinozzi, M., Taccari, M., Ciani, M. & Vischetti, C. (2011). Fungicides degradation in an organic biomixture: Impacto on microbial diversity. New Biotechnology, Doi 10.1016/j.nbt.2011.03.005.
21. Tortella, G. R., Mella-Herrera, R. A., Sousa, D. Z., Rubilar, O., Acuña, J. J., Briceño, G., & Diez, M. C. (2013a). Atrazine dissipation and its impact on the microbial communities and community level physiological profiles in a microcosm simulating the biomixture of on-farm biopurification system. Journal of Hazardous Materials, 260, 459–467.
22. Yu, Y., Chu, X., Pang, G., Xiang, Y., Fang, H. 2009. Effects of repeated applications of fungicide carbendazim on its persistence and microbial community in soil. Journal of Environmental Science. 21, 179-185.
23. Vischetti, C., Monaci, E., Cardinali, A., Casucci, C. & Perucci, P. (2008). The effect of initial concentration, co-application and repeated applications on pesticide degradation in a biobed mixture. Chemosphere 72(11), 1739-1743.
24. Castillo, M. P., Ander, P., & Stenström, J. (1997). Lignin and manganese peroxidase activity in extracts from straw solid substrate fermentations, Biotechnology Techniques 11(9), 701–706.
25. Shaw, L. J., & Burns, R. G. (2003). Biodegradation of organic pollutants in the rhizosphere. Advances in applied microbiology, 53, 1-60.
26. Tortella, G. R., Rubilar, O., Stenström, J., Cea, M., Briceño, G., Quiroz, A.Diez, M.C., & Parra, L. (2013c). Using volatile organic compounds to enhance atrazine biodegradation in a biobed system. Biodegradation, 24(5), 711-720.
27. Tortella, G. R., Rubilar, O., Castillo, M., Cea, M., Mella-Herrera, R., & Diez, M. C. (2012). Chlorpyrifos degradation in a biomixture of biobed at different maturity stages. Chemosphere, 88(2), 224-228.
28. Tortella, G. R., Salgado, E., Cuozzo, S. A., Mella-Herrera, R. A., Parra, L., Diez, M. C., & Rubilar, O. (2014). Combined microbiological test to assess changes in an organic matrix used to avoid agricultural soil contamination, exposed to an insecticide. Journal of soil science and plant nutrition, 14(4), 869-880.

29. Zabaloy, M. C., Zanini, G. P., Garland, J. L., Gomez, M. A., & Bianchinotti, V. (2011). Herbicides in the soil environment: linkage between bioavailability and microbial ecology. INTECH Open Access Publisher.
30. Alef, K., and Nannipieri, P. (1985). Methods in Applied Soil Microbiology and Biochemistry. (K. Alef and P. Nannipieri, Eds.) The Journal of Applied Ecology. Academic Press.
31. Briceño, G., Fuentes, M.S., Rubilar, O., Jorquera, M., Tortella, G.R., Palma, G., Amoroso, M.J. & Diez, M.C. (2015). Removal of the insecticide diazinon from liquid media by free and immobilized Streptomyces sp. Isolated from agricultural soil. Journal of Basic Microbiology, Special Issue:Microbes in bioremediation, Vol 55, Issue 3, pages 293-302.
32. Campos, M., Perruchon, C., Vasilieiadis, S., Menkissoglu-Spiroudi, U., Karpouzas, D. & Diez, M.C. (2015). Isolation and characterization of bacteria from acidic pristine soil environment able to transform iprodione and 3,5-dichloraniline. International Biodeterioration and Biodegradation 104, 201-211
33. Briceño, G., Fuentes, M.S., Palma, G., Amoroso, M.J., Diez, M.C. (2012). Chlorpyrifos degradation by consortium of actinobacteria isolated from contaminated environment. *New Biotechnology* vol. 29 September 23-26 p. S179. DOI: 10.1016/j.nbt.2012.08.501. ISSN: 1871-6784.
34. Casida Jr. L.E (1977). Microbial metabolic activity in soil as measured by dehydrogenase determinations, Appl. Environ. Microbiol. 34 (1977) 630–636.
35. Castillo, M. D.P, Stenstrom, J., & Ander, P. (1994). Determination of manganese peroxidase activity with 3-methyl-2-benzothiazolinone hydrazone and 3-(dimethylamino) benzoic acid. Analytical biochemistry, 218(2), 399-404.
36. Fernández-Alberti, S., Rubilar, O., Tortella, G. R., & Diez, M. C. (2012). Chlorpyrifos degradation in a Biomix: Effect of pre-incubation and water holding capacity. Journal of soil science and plant nutrition, 12(4), 785-799.
37. Heuer, H., Krsek, M., Baker, P., Smalla, K., & Wellington, E. M. (1997). Analysis of actinomycete communities by specific amplification of genes encoding 16S rRNA and gel-electrophoretic separation in denaturing gradients. Applied and environmental microbiology, 63(8), 3233-3241.
38. Muyzer, G., De Waal, E. C., & Uitterlinden, A. G. (1993). Profiling of complex microbial population by DGGE analysis of polymerase chain reaction amplified genes encoding for 16S rRNA. Appl Environ Microbiol, 62, 2676-2680.
39. Sanguinetti, C. J., Dias, N. E., & Simpson, A. J. (1994). Rapid silver staining and recovery of PCR products separated on polyacrylamide gels.Biotechniques, 17(5), 914-921.
40. White, T. (1990). Analysis of phylogenetic relationships by amplification and direct seaquencing of ribosomal RNA genes. PCR protocols: a guide to methods and applications.

CHAPTER 7.8 ESTUDIO COMPARATIVO DE LAS PLANTAS DE TRATAMIENTO DE AGUAS RESIDUALES EN EL SUR Y CENTRO DE MÉXICO

Lilian E. Domínguez-Montero (1) and Héctor M. Poggi-Varaldo *(1,2)

(1) Grupo de Biotecnología Ambiental y Energías Renovables, Programa Transdisciplinario en Desarrollo Científico y Tecnológico para la Sociedad, Centro de Investigación y Estudios Avanzados del IPN, Av. Instituto Politécnico Nacional 2508, Ciudad de México, México.
(2) Grupo de Biotecnología Ambiental y Energías Renovables, Departamento de Biotecnología y Bioingeniería, Centro de Investigación y Estudios Avanzados del IPN, Address ibidem.

RESUMEN

De acuerdo con la Comisión Nacional del Agua, México cuenta con 2387 Plantas de Tratamiento de Aguas Residuales Municipales (PTARM) distribuidas en toda la República. El objetivo de este trabajo fue comparar PTARM representativas (selectas) en la Ciudad de México (CDMX), y de un estado del sur de México (Oaxaca, OAX) ubicando varios aspectos clave para su funcionamiento (caudal tratado, infraestructura, proceso, presupuesto, calidad del agua, entre otros) así como discutir cuáles son las barreras y retos que se deben superar para lograr que el tratamiento de agua (TAR) alcance el 100% de su capacidad instalada y una calidad que cumpla con la normatividad vigente. Se tomó una muestra aleatoria de 12 PTARM para cada estado, además se realizó visitas personales y entrevistas al personal a cargo de las PTARM.
De las PTARM estudiadas en OAX, sólo 7 se encuentran operando, 4 se encuentran sin funcionar desde hace más de 5 años y 1 se encuentra en rehabilitación. Los principales problemas que presentan son infraestructura mal diseñada, nulo o bajo presupuesto para su funcionamiento, mala calidad de agua, y monitoreo deficitario. En comparación, las 12 PTARM de CDMX se encuentran en funcionamiento, aunque sus principales dificultades fueron la existencia de equipo y estructura civil deteriorada, bajo presupuesto otorgado para el funcionamiento y mantenimiento; un tardío seguimiento de los análisis del agua tratada y escaso tratamiento de los lodos generados los cuales en su mayoría se van al drenaje. El índice caudal real tratado sobre el caudal tratado del inventario declarado oficialmente es 74.8 y 80.9% para OAX y CDMX, respectivamente. La cobertura de tratamiento real (caudal real tratado sobre caudal colectado) es de 39 y 56% para las PTARM de OAX y las de CDMX, respectivamente lo que todavía no alcanza el 60% que es la meta del Programa Nacional Hídrico 2014-2018.
En conclusión, podemos decir que el Gobierno Mexicano ha hecho esfuerzos para lograr el saneamiento de aguas residuales a través de la construcción de PTARM en México; éstas parecen haber favorecido a las comunidades urbanas como es el caso de la CDMX mientras que, por otro lado, hay insuficiencias marcadas en zonas con comunidades rurales, OAX. Con las insuficiencias detectadas en las PTARM de los

---

*Author for correspondence: r4cepe@yahoo.com

estados analizados, y si las PTARM del resto del país siguen esta tendencia, en los siguientes años se complicará llegar a la meta establecida en el PNH 2014-2018, el cual establece el tratamiento del 60% de agua residual colectada.

Palabras clave: Ciudad de México, plantas de tratamiento de aguas residuales, Oaxaca.

INTRODUCCIÓN

Las plantas de tratamiento de aguas residuales municipales (PTARM) son utilizadas para la remoción de contaminantes presentes en el agua residual cruda; el agua tratada generada en la PTARM para su reúso, así como los lodos resultantes durante el tratamiento del agua residual (TAR), deben reunir una determinada calidad de acuerdo a la normatividad impuesta por el Gobierno. En el caso de México debe apegarse a lo establecido en la NOM-001-SEMARNAT-1996, NOM-002-SEMARNAT-1996, NOM-003-SEMARNAT -1997 y NOM-004- SEMARNAT-2002.

Para que una PTARM funcione adecuadamente deben considerarse varios aspectos para su construcción y operación como son: la ubicación de la planta; el tipo de influente que se recibe; el proceso y la tecnología apropiada para el ambiente local; el cumplimiento normativo para lograr una buena calidad del agua residual tratada; la evaluación de la viabilidad económica; la evaluación de factores tecnológicos de operación y mantenimiento; el presupuesto asignado para su funcionamiento y operación futura; entre otros. [1-4]

Actualmente, el Gobierno Mexicano ha identificado que los principales problemas de las PTARM son la falta de recursos financieros para la construcción, rehabilitación y mantenimiento de la infraestructura; así como los altos costos de energía eléctrica y reactivos químicos para la operación[5]. Por ello, en el Programa Nacional Hídrico (PNH) 2014-2018, se tiene como uno de los objetivos:

"Fortalecer el abastecimiento de agua y el acceso a los servicios de agua potable, alcantarillado y saneamiento" [5]

Por ello para el 2018 se ha dejado la misma meta establecida en el PNH 2007-2012, la cual es lograr en México una cobertura del 60% de las aguas residuales colectadas[5].

En el 2013, en México se generaron 230162 l/s de aguas residuales, de los cuales se trataron el 50.2% de ellas[6]. En ese mismo año, de acuerdo con la Comisión Nacional del Agua (Conagua), México contaba con 2387 PTARM distribuidas en todo el país.

Oaxaca (OAX) es uno de los tres estados pertenecientes de la región sur del territorio mexicano; cuenta con una superficie de 93793 km², equivalentes al 4.8 por ciento del país, ocupando el quinto lugar en extensión[7]. De acuerdo con el Censo de Población y Vivienda 2010[8], OAX tiene una población de 3901962 habitantes; además OAX ocupa el tercer lugar en el índice de marginación, el cual abarca educación, vivienda, distribución de población e ingresos por trabajo[9].

El sistema hidrológico de OAX se usa principalmente en la agricultura, seguido del abastecimiento público y la industria autoabastecida[10]. Respecto a la infraestructura hidráulica de OAX, de acuerdo al Inventario Nacional de Plantas Municipales Tratamiento de Aguas Residuales (INPTARM)[6] se tienen registradas 69 PTARM funcionando en OAX con una capacidad de 1520.5 l/s.

El volumen de agua residual cruda generada en OAX, en 2013, fue de 2985 l/s, mientras que el volumen de agua residual colectada fue de 2132 l/s. De acuerdo a Conagua del agua colectada se trataron 986.1 l/s, lo que significa que solo un 33% de las aguas generadas son tratadas.

Por otra parte, la Ciudad de México (CDMX), antes Distrito Federal, se localiza en el Valle de México y pertenece a uno de los 8 estados de la región centro de México; cuenta con una superficie 1485 km², que representa el 0.08% del territorio[7]. La población dada en el Censo del INEGI 2010[8] fue de 8851080 habitantes, y se ubica en el puesto número 32 con índice de marginación[9]. Los principales usos del agua en la CDMX son para abastecimiento público con un 97% y para la industria autoabastecida con el resto[10].

Las 16 delegaciones pertenecientes a la CDMX en el año 2013 generaron un volumen de agua residual de 22956 l/s, y se colectó el 71.42% de dichas aguas. Del volumen de agua total colectada se trataron solamente 3113 l/s en las 29 PTARM[6] que se encuentran disponibles de acuerdo al INPTARM de Conagua.

Por ello, el objetivo de este trabajo fue comparar PTARM representativas (selectas) en la Ciudad de México, y de un estado del sur de México (OAX) ubicando varios aspectos clave para su funcionamiento (caudal tratado, infraestructura, proceso, presupuesto, calidad del agua, entre otros) así como discutir cuáles son las barreras y retos que se deben superar para lograr que el tratamiento de agua (TAR) alcance el 100% de su capacidad instalada y una calidad que cumpla con la normatividad vigente.

MATERIALES Y MÉTODOS

Se seleccionaron dos estados de México, de la región sur y centro del país para llevar a cabo una serie de visitas y entrevistas al personal en las PTARM.

De los tres estados pertenecientes a la región sur (Chiapas, Guerrero y Oaxaca), se seleccionó el estado de Oaxaca por los aspectos referentes a: condiciones hidrológicas, superficie territorial, número de habitantes, índice de marginación y número de PTARM.

La región centro de México cuenta con ocho estados: Ciudad de México, Guanajuato, Hidalgo, México, Morelos, Puebla, Querétaro y Tlaxcala; de dichos estados se seleccionó la Ciudad de México por los siguientes aspectos: ser la capital del país, el número de habitantes, el índice de marginación bajo, el volumen de agua residual generada y el número de PTARM en operación.

Usando como base de datos el INPTARM elaborado por la Conagua (Conagua, 2014), y utilizando el programa R Studio, se obtuvo una muestra aleatoria de 12 PTARM para cada estado; en cada muestra se buscó que hubiera distribución geográfica a lo largo de cada estado; que el caudal de tratamiento fuera bajo, medio y alto; y que las PTARM contaran con diversos procesos de tratamiento.

Al mismo tiempo, se elaboró una encuesta donde se incluyeron los siguientes puntos:

- Status de la PTARM: caudal tratado, proceso, tratamiento de lodos, entre otros.
- Volúmenes de aguas residuales en la PTARM: capacidad instalada, caudal real tratado.

- Calidad del agua residual tratada: análisis realizados, parámetros dentro de la normatividad, entre otros.
- Aspectos económicos de las PTARM: presupuesto anual, origen del ingreso, apoyo de programa para TAR, entre otros.
- Necesidades actuales y futuras para mejorar las PTARM: barreras y retos que se deben superar para lograr que el TAR alcance el 100% de su capacidad instalada y una calidad que cumpla con la normatividad vigente.

Se realizaron visitas guiadas por las instalaciones de las PTARM en ambos estados; así como entrevistas en donde los encargados de las PTARM contestaron la encuesta elaborada. Posteriormente se realizó el análisis de la información recolectada.

RESULTADOS Y DISCUSIÓN

Status de las Plantas de Tratamiento de Aguas Residuales Municipales. De las PTARM estudiadas en OAX, sólo 7 se encuentran operando, 2 se encuentran sin funcionar desde hace 6 años, 2 más tienen sin funcionar más de 10 años y 1 se encuentra en rehabilitación. Cabe señalar que en dos PTARM no nos pudieron proporcionar datos, ya que en ambos casos los municipios encargados de las plantas desconocían sus existencias. En comparación, las 12 PTARM de CDMX se encuentran en operación.

Como se observa en la **Figura 1a**, las PTARM de la CDMX entraron en función desde hace más de 60 años, y sola una es de reciente creación; mientras que las PTARM de OAX, son más recientes, a pesar de ello, cuatro no están en funcionamiento y en dos no pudieron dar información sobre el año en que iniciaron operaciones.

El tipo de proceso que tienen las PTARM (**Figura 1b**) se encuentra especificado en el INPTARM; sin embargo, en los casos de OAX se especificaba solo como tratamiento anaerobio cuando en algunas ocasiones eran humedales, y la PTARM que no estaba especificada en el INPTARM resultó ser un proceso de tratamiento químico. Por otra parte, las PTARM de la CDMX tienen el proceso señalado en el INPTARM, el cual en el 92% de los casos es lodos activados.

El 83.33% del efluente que llega a las PTARM de la CDMX es agua residual municipal **(Figura 1c)**, mientras que el resto proviene de zonas donde hay una gran amplitud de pequeños comercios dedicados a la fabricación de alimentos.

En la **Figura 1d**, se observa que 6 PTARM en OAX cuentan con tratamiento de lodos funcionando el cual es lecho de secados (**Figura 1e**); además existe la infraestructura de lecho de secado en las 4 PTARM sin funcionar. En los 2 casos donde no existe tratamiento de lodos este pasa directamente al drenaje.

El tratamiento de lodos en la CDMX es muy diferente de OAX, ya que en las 12 PTARM los lodos resultantes del TAR se descargan directamente al drenaje, y no se hace un monitoreo para cumplir con la NOM-004-semarnat-2002, la cual indica las especificaciones y límites máximos permisibles (LMP) de contaminantes para el aprovechamiento y disposición final de los lodos y biosólidos provenientes de las plantas de tratamiento de aguas residuales[11].

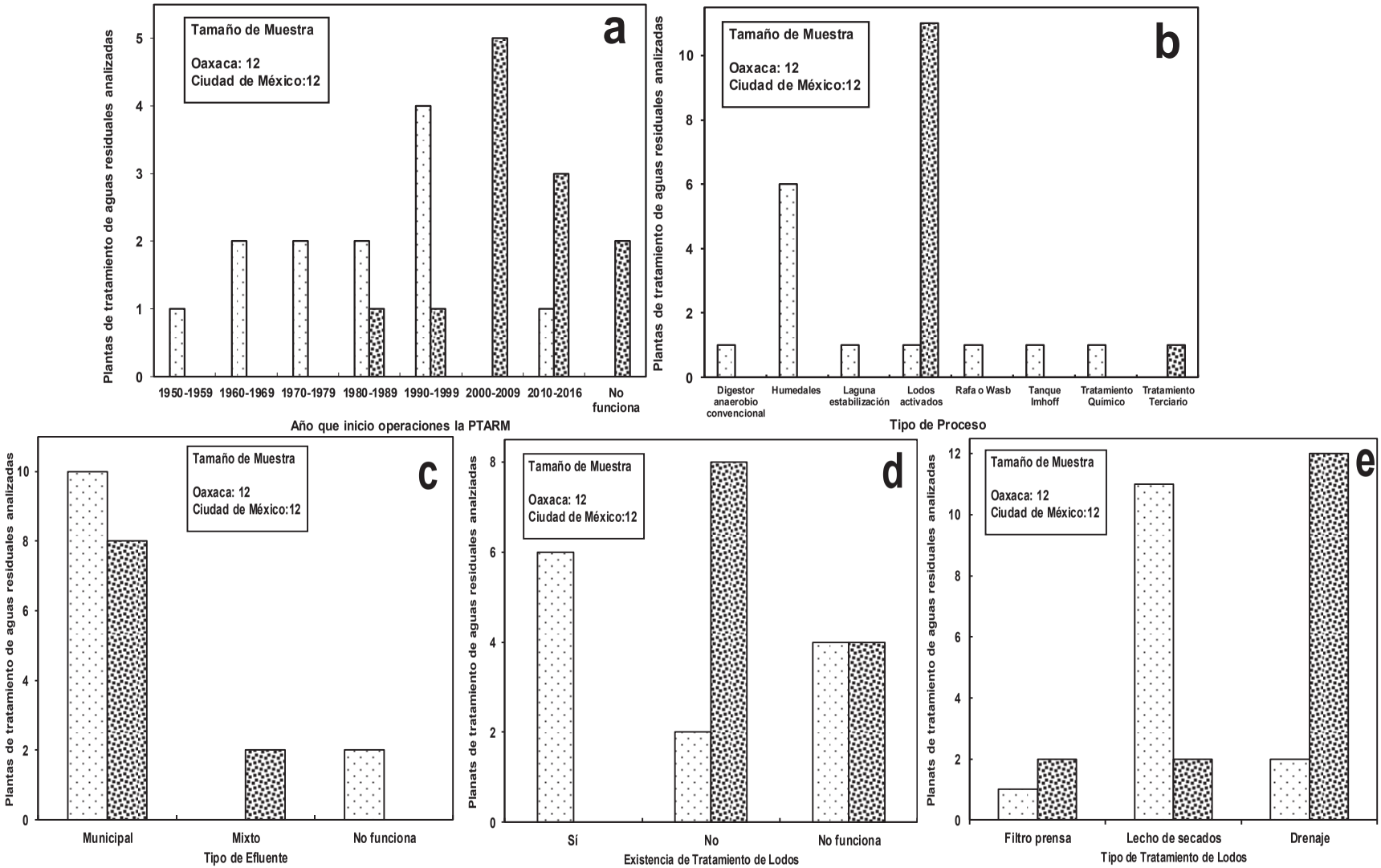


FIGURA 1. Status de las plantas de tratamiento de aguas residuales municipales analizadas en Oaxaca y la Ciudad de México: (a) Año de inicio de operaciones, (b) Tipo de proceso, (c) Tipo de efluente recibido, (d) Existencia de tratamiento de lodos, (e) Tipo de tratamiento de lodos y disposición final ☐ Oaxaca ▨ Ciudad de México

Volúmenes de aguas residuales en las Plantas de Tratamiento de Aguas Residuales Municipales. En las PTARM seleccionadas para la CDMX se observa en la **Tabla 1** que los volúmenes reportados de capacidad instalada son los mismos tanto de Conagua como los recolectados en las encuestas, esto posiblemente se debe a que estas PTARM fueron de las primeras en construirse en el país por lo que los datos no han cambiado desde aproximadamente 60 años[12].

Por el contrario, en OAX los valores de los volúmenes de la capacidad instalada (**Tabla 1**) están por encima de los volúmenes reportados a Conagua; esto se debe a que hace 5 años aproximadamente, los habitantes y a los municipios de dos comunidades tomaron la iniciativa de construir nuevos tanques al ver que tenían mayor volumen de agua residual con lo que se amplió la capacidad instalada.

Los datos arrojados en el volumen de caudal tratado son muy diferentes al caso anterior. Podemos observar que los datos reportados por Conagua tanto para OAX como la CDMX son mayores a lo que realmente se está tratando en las PTARM.

En el caso de la CDMX, el caudal tratado de las 12 PTARM seleccionadas es 19.1% menor del establecido en los reportes (**Tabla 1**); si aunado a esto vemos que la cobertura de tratamiento total de la ciudad es del 13.63%, la mayor parte del agua residual generada en la CDMX es eliminada sin recibir tratamiento alguno. De acuerdo a Breña Puyol y Breña Naranjo, el agua sin tratamiento pasa primero al río Moctezuma, después al río Pánuco y finalmente desemboca en el Golfo de México[13], lo que genera un grave problema de contaminación del agua durante su trayecto; además, durante este recorrido se encuentras zonas agrícolas las cuales reúsan dichas aguas para el riego[14].

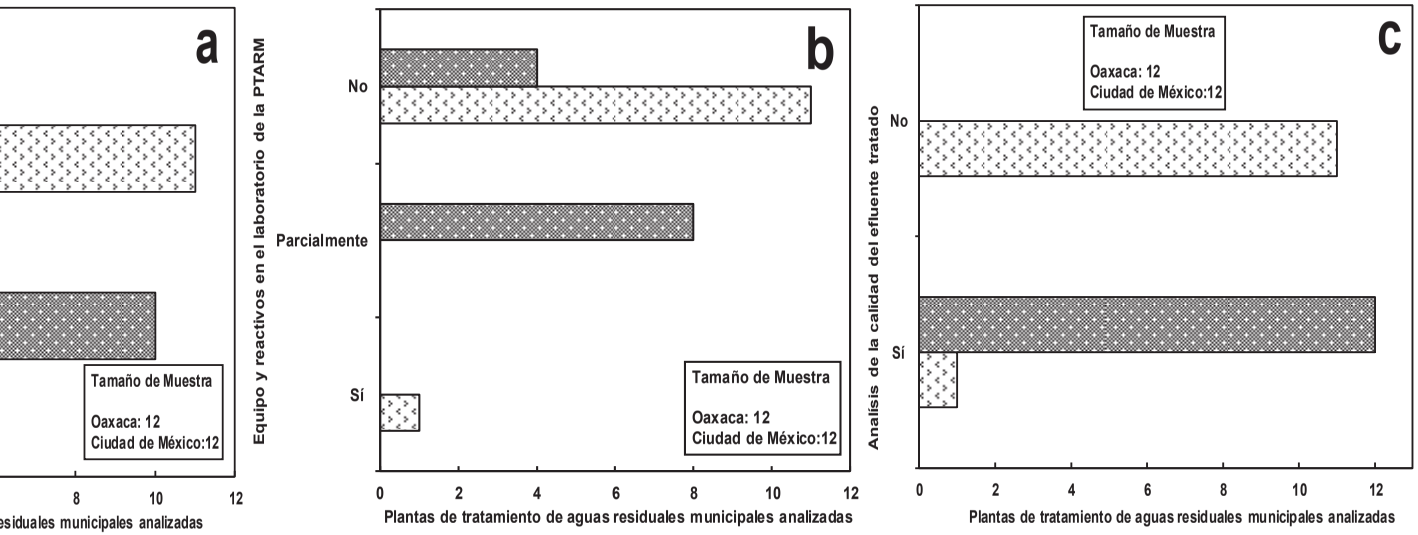
En OAX la situación no es mejor, a pesar de que el agua residual generada es menor por ser un estado que en su mayoría se compone de comunidades rurales[7], el caudal tratado es 25.2% menor del reportado por Conagua. Esta disminución en parte se debe a las PTARM que se encuentran fuera de servicio y en rehabilitación; si consideráramos los l/s que estas PTAR trataran se tendría un aumento de 43 l/s. Sin embargo, la única PTARM que podría considerarse para mejorar el volumen de agua residual tratada es la que se encuentra en rehabilitación y que entrara en operación en 2017 con un caudal de 20 l/s.

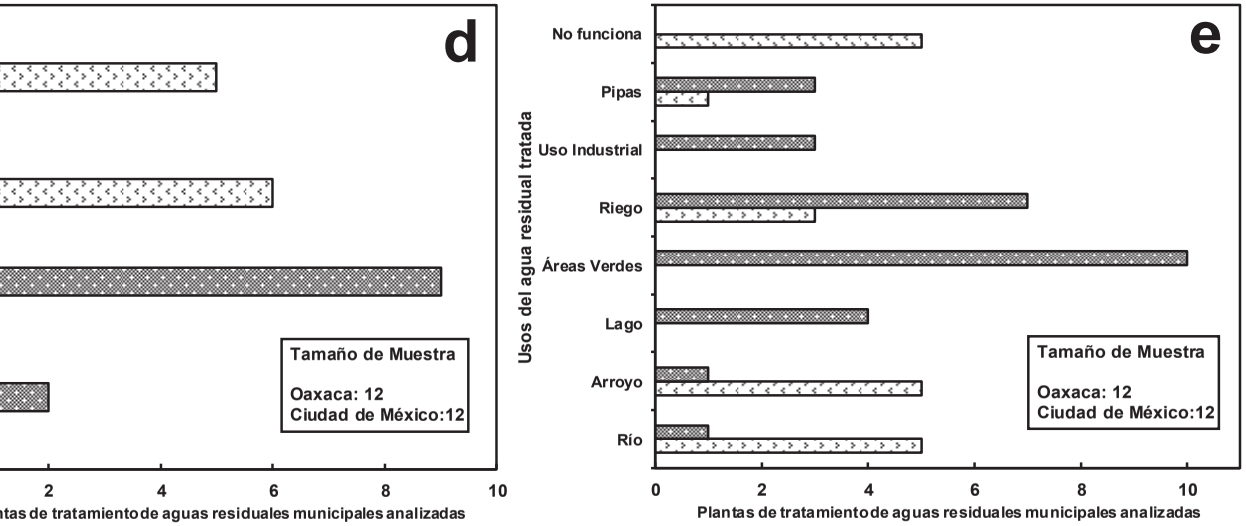
TABLA 1. Capacidad instalada y caudal tratado de aguas residuales reportadas por la Comisión Nacional del Agua y las reportadas en las encuestas

	Ciudad de México		Oaxaca	
	Conagua	**Encuestas**	**Conagua**	**Encuestas**
Capacidad instalada (l/s)	4,233.00	4,233.00	679.20	711.50
Caudal tratado (l/s)	2,820.00	2,282.00	352.90	264.00

Fuente: Conagua, 2015

La cobertura de tratamiento real (caudal real tratado sobre caudal colectado) es de 39 y 56% para las PTARM de OAX y las de CDMX, respectivamente lo que todavía no alcanza el 60% que es la meta del PNH 2014-2018[5].





del agua residual tratada en las plantas de tratamiento de aguas residuales municipales analizadas en l de México: (a) Laboratorio para analizar aguas residuales, (b) Equipo y reactivos necesarios para los sis de la calidad del efluente tratado, (d) Parámetros del efluente tratado dentro de la normatividad (e) Disposición final y usos del efluente tratado. ▨ Ciudad de México ▨ Oaxaca

Calidad del agua residual tratada. Para lograr una buena calidad del efluente tratado y cumplir con la normatividad mexicana la cual estipula los LMP de contaminantes que se pueden descargar en las aguas residuales en aguas y bienes nacionales (NOM-001-SEMARNAT-1996[15]), en sistemas de alcantarillado urbano o municipal (NOM-002-SEMARNAT-1996[16]) y para el reúso de agua tratada en servicios al público (NOM-003-SEMARNAT-1997[17]), es necesario realizar un monitoreo a través de un laboratorio, el cual puede encontrarse dentro de las instalaciones o ser uno externo que este certificado para análisis de aguas residuales.

Sin embargo, al monitorear los laboratorios de las PTARM de OAX y la CDMX, se observó que las PTARM de la CDMX son las que cuentan con un mayor número de laboratorios dentro sus instalaciones (**Figura 2a**), mientras que OAX solamente tiene un laboratorio en todas la PTARM visitadas.

A pesar de que las PTARM de la CDMX cuentan con un mayor número de laboratorios, sus condiciones no son óptimas para realizar todas las mediciones requeridas, ya que algunos equipos de medición son obsoletos, y hay escasez o son insuficientes los reactivos químicos (**Figura 2b**). Sin embargo, existe un laboratorio central que toma muestras del influente y efluente, de dos o cuatro veces al mes, en las 29 PTARM de la CDMX, donde obtienen todos los parámetros necesarios para conocer las condiciones del agua, y los resultados son entregados a la semana siguiente de la toma de la muestra (**Figura 2c**).

En un 75% de las PTARM de la CDMX, como se observa en la **Figura 2d,** los resultados del efluente tratado no cumplen con los parámetros establecidos por las Normas Oficiales Mexicanas (NOM´s). Los parámetros que están por encima de los LMP son los de coliformes fecales establecido en la NOM-001-SEMARNAT.1996[15]; mientras que hay parámetros establecidos en las NOM´s que no son determinados como son los casos del cianuro y níquel cuyos LMP son solicitados en la NOM-002-SEMARNAT-1996[16], y el de huevos de hemilto que solicita la NOM-003-SEMARNAT-1997[17].

En Oaxaca la situación es muy diferente, como ya se comentó solo cuenta con un laboratorio para análisis que se ubica en una de las PTARM más grande del estado; el resto de las plantas no cuentan con laboratorio, y no se han mandado a realizar análisis desde que entraron en funcionamiento (**Figura 2a, 2b, 2c**). Por otra parte, sin los análisis del efluente tratado se desconoce si las PTARM cumplen o no con las NOM´s, por lo que la calidad del agua tratada es dudosa (**Figura 2d**).

El uso del efluente tratado en OAX es principalmente para riego, ríos y arroyos; mientras que en la CDMX tiene una mayor cantidad de usos como se observa en la **Figura 2e**.

Aspectos económicos de las Plantas de Tratamiento de Aguas Residuales Municipales. La inversión anual que requieren diariamente las PTARM fue una de los aspectos más difícil de conseguir a la hora de las entrevistas tanto para OAX y CDMX.

En el caso de OAX, la parte económica en la mayoría de los casos está a cargo de los municipios (**Figura 3a**). El personal que maneja las PTARM es de obras pública, y si el municipio es muy pequeño el presidente municipal y su personal de confianza lo hacen. El personal del municipio dura a cargo de las funciones un año o más tardar 2

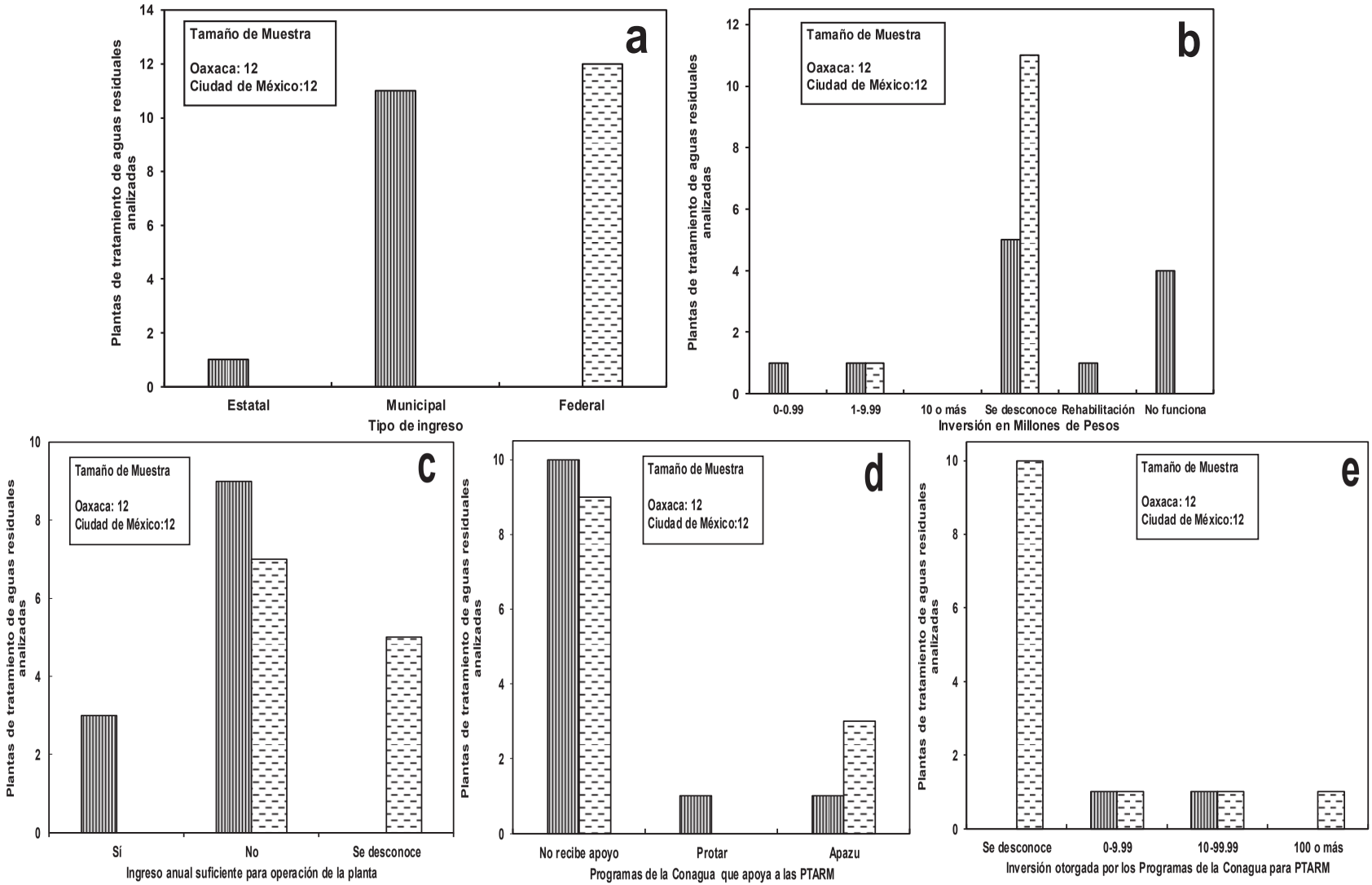


FIGURA 3. Aspectos económicos de las plantas de tratamiento de aguas residuales municipales analizadas en Oaxaca y la Ciudad de México: (a)Tipo de ingreso, (b) Inversión anual en millones de pesos, (c) Ingreso anual suficiente para operación, (d) Programas de Conagua que otorgan apoyo para tratamiento de aguas residuales (e) Inversión otorgada por los programas de Conagua. ▫ Ciudad de México ▥ Oaxaca

años, por lo que los montos para las PTARM ya es un presupuesto asignado y constante, y por ende se desconoce lo que se invierte anualmente (**Figura 3b**).

Sin embargo, a pesar de que en OAX tienen un ingreso fijo asignado a las PTARM, los encargados de éstas saben que requieren una mayor inversión para funcionar correctamente, pero o desconocen cómo obtener apoyos económicos, o no pueden invertir presupuesto para otras funciones básicas en la comunidad (**Figura 3c**).

Solo dos PTARM de OAX han obtenido apoyo de los programas que el Gobierno Federal otorga a través de Comisión Nacional del Agua (Conagua) para TAR[18]; uno de esos apoyos es a la PTARM en rehabilitación, y otro fue otorgado hace 3 años (**Figura 3d, 3e**).

En el caso de la CDMX, la mayoría de las PTARM están a cargo del Sistema de Aguas de la Ciudad de México (SACMEX) por ello el ingreso asignado a las PTARM es federal (**Figura 3a**). El Director a cargo de TAR manera la situación financiera de éstas, por lo que la información es confidencial, por ello el personal a cargo desconoce los montos asignados a cada PTARM (**Figura 3b**).

Como se observa en la **Figura 3c,** el personal a cargo considera que el monto asignado anualmente para operación de las PTARM es insuficiente debido a que no logran cubrirse varios rubros que requieren atención inmediata para el correcto funcionamiento de la planta como son equipo e infraestructura, tema que se tratará más adelante (**Figura 4b**).

En la CDMX, existen 3 PTARS de las 12 analizadas hay recibido o están recibiendo apoyo; dos se encuentran en rehabilitación parcial, y la más reciente fue para su construcción total en el 2014 (**Figura 3d, 3e**).

Necesidades actuales y futuras para mejorar las Plantas de Tratamiento de Aguas Residuales Municipales. En la **Figura 4a**, se observa que ninguna PTARM de la CDMX y OAX requieren una ampliación de instalaciones en un futuro, esto debido a que las plantas en muchos casos no les llega suficiente volumen de aguas residual cruda para tratar por lo que una parte de la infraestructura de las PTARM se queda sin funcionar.

Tanto para las PTARM de CDMX como de OAX los encargados de las plantas, mencionaron más de una opción acerca de que rubros requieren en una mayor inversión (**Figura 4b**). En el caso de CDMX los rubros que requieren mayor inversión son: equipo, infraestructura y laboratorio, mientras que en OAX los rubros son equipo, infraestructura y rehabilitación total de la PTAR; este último rubro se dio con las 4 PTARM que no están en funcionamiento.

Para el caso de mejoras que requiere la PTARM para alcanzar el 100% de la capacidad instalada (**Figura 4c**), nuevamente los rubros de equipo, infraestructura y mantenimiento de equipo fueron los que sobresalen. En 4 PTARM de la CDMX también predomino que es necesario que se les envíe un mayor volumen de agua residual para su tratamiento. Como se ha venido mencionando, en OAX, 4 PTARM que están fuera de operación dicen que requieren una rehabilitación; en 2 casos a pesar de tener el terreno y parte de la infraestructura sería necesario una construcción nueva de la PTARM.

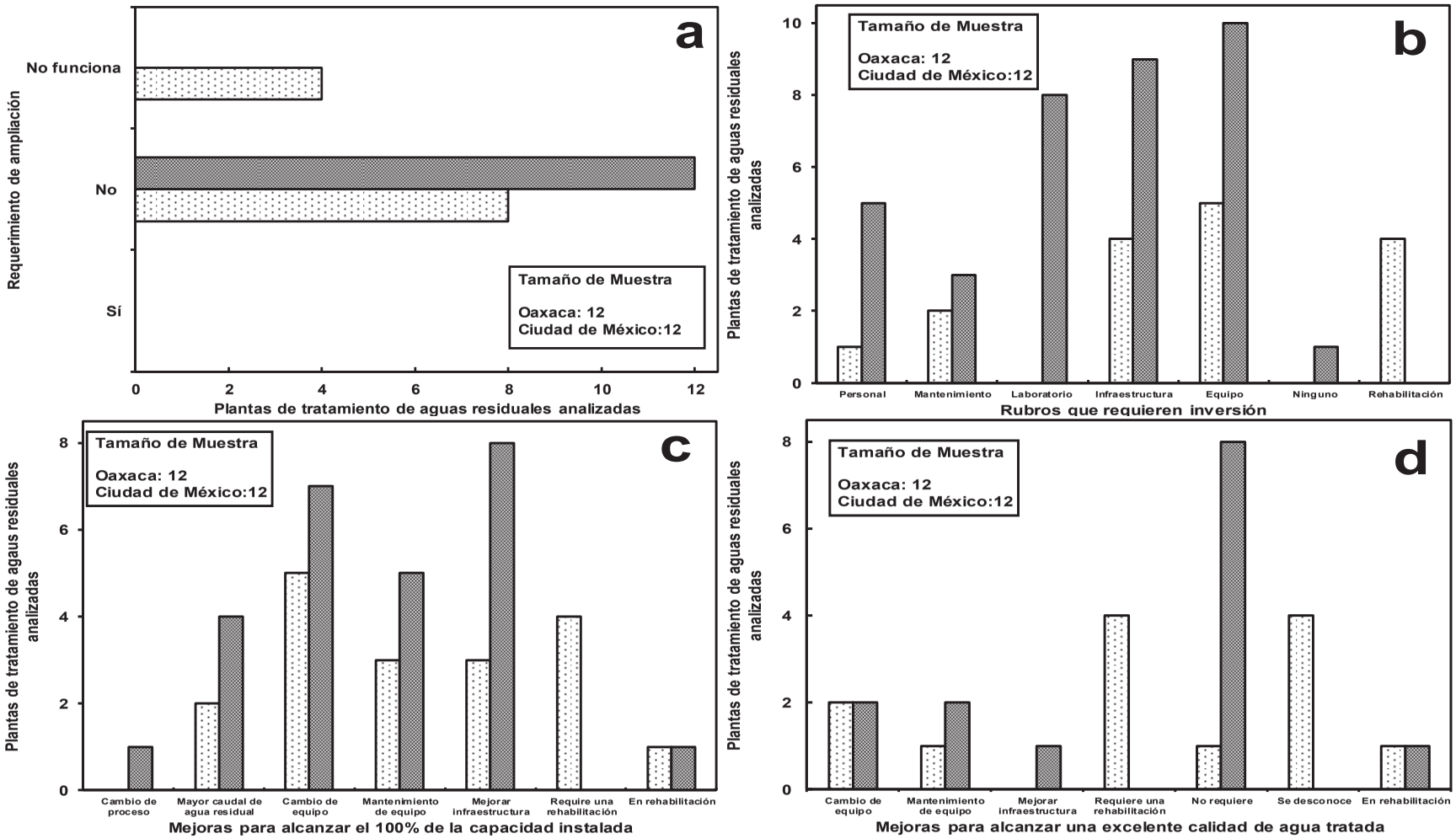


FIGURA 4. Necesidades actuales y futuras para mejorar las Plantas de Tratamiento de Aguas Residuales Municipales: (a)Requerimiento de ampliación, (b) Rubros que requieren inversión, (c) Mejoras para alcanzar el 100% de la capacidad instalada, (d) Mejoras para alcanzar una excelente calidad del agua tratada. ⊡ Oaxaca ▨ Ciudad de México

Finalmente, al solicitar que mejoras se necesitan para alcanzar una excelente calidad del agua tratada (**Figura 4d**), las respuestas fueron distintas en ambos estados. En el estado de OAX, predomino que 4 PTARM dijeron desconocer que hacer para mejorar la calidad y 2 PTARM dijeron necesitar cambio de equipo.

En la CDMX la situación es diferente, en 8 de 12 PTARM analizadas, dijeron no requerir mejora alguna para lograr una buena calidad del agua; sin embargo, esto se contradice con los resultados observados en la **Figura 2d** donde se observa que 9 PTARM no cumplen con los LMP señalados por las NOM´s por lo que el agua obtenida no es de buena calidad.

CONCLUSIÓN

El Gobierno Mexicano ha hecho esfuerzos para lograr el saneamiento de aguas residuales a través de la construcción de plantas de tratamiento de aguas residuales municipales en México; éstas parecen haber favorecido a las comunidades urbanas como es el caso de la mientras que, por otro lado, hay insuficiencias marcadas en zonas con comunidades rurales como sucede en Oaxaca.

Las plantas de tratamiento de aguas residuales municipales que se encuentran en operación tanto en la Ciudad de México como en Oaxaca, actualmente requieren mejoras en cuanto a equipo, rehabilitación de estructura civil, mayor presupuesto económico para mantenimiento y operación, personal con conocimientos de tratamiento de aguas residuales, realizar el tratamiento adecuado de los lodos generados durante el proceso y un monitoreo constante para lograr la calidad del agua residual tratada que solicita la normatividad mexicana.

Es necesario que las instancias encargadas de dar seguimiento a las plantas de tratamiento de aguas residuales municipales, actualicen la información del inventario declarado oficialmente que tienen disponible, ya que existen plantas de tratamiento que se encuentran fuera de operación desde hace más de 5 años; además, los volúmenes de cobertura de tratamiento real tratada que se tienen registrados son menores a los señalados debido a las problemáticas que viven día a día las plantas.

Con las insuficiencias detectadas en las plantas de tratamiento de aguas residuales municipales de los estados analizados, y si las plantas del resto del país siguen esta tendencia, en los siguientes años se complicará llegar a la meta establecida en el PNH 2014-2018, el cual establece el tratamiento del 60% de agua residual colectada.

AGRADECIMIENTOS

Los autores agradecemos al CINVESTAV del IPN por el respaldo parcial a esta investigación. Uno de los autores (Lilian Edith Domínguez Montero) agradece al Consejo Nacional de la Ciencia y la Tecnología por la beca de posgrado para la realización de esta investigación.

Se agradece también a la Comisión Estatal del Agua de Oaxaca y al Sistema de Aguas de la Ciudad de México por las facilidades otorgadas para las visitas de las Plantas de Tratamiento de Aguas Residuales Municipales.

REFERENCIAS

1. Romero A. H., García O. J. y Janetti, D. J. (1996). Las vicisitudes de las plantas de tratamiento de aguas residuales en México. Ingeniería Civil. 330, 12-18.
2. Escalante, V., Cardoso, L., Ramírez, E., Moeller, G., Mantilla, G., Montecillos, J. y Villavicencio, F. (2003). El reúso del agua residual tratada en México. Memorias. Seminario Internacional sobre Métodos Naturales para el Tratamiento de Aguas Residuales. Cali, Colombia. 230-236.
3. Rodríguez Miranda, J. P., García Ubaque, C. A. y Pardo Pinzón, J. (2015). Selección de tecnologías para el tratamiento de aguas residuales municipales. Tecnura. 19, 149-164.
4. Ramón L.V. (2010). Infraestructura sustentable: Las plantas de tratamiento de aguas residuales. Quivera. 12 , 58-69.
5. SEMARNAT (2013). Programa Nacional Hídrico 2014-2018. Secretaría de Medio Ambiente, Recursos Naturales y Pesca. Diario Oficial de la Federación. 8 de abril de 2014.
6. CONAGUA (2014). Inventario Nacional de Plantas Municipales de Potabilización y de Tratamiento de aguas residuales en Operación. Diciembre de 2014. Comisión Nacional del Agua, Subdirección General de Agua Potable, Drenaje y Saneamiento. Informe. México, D.F.
7. INEGI (2016). México en cifras, Información Nacional por Entidad Federativa y Municipios [en línea]. Instituto Nacional de Estadística y Geografía. http://www3.inegi.org.mx/sistemas/mexicocifras 12/07/2016
8. INEGI (2016a). Censo de Población y Vivienda 2010: Tabulados del Cuestionario Básico [en línea] Instituto Nacional de Estadística y Geografía. http://www3.inegi.org.mx/sistemas/TabuladosBasicos/Default.aspx?c=27302&s=est 12/07/2016
9. CONAGUA (2013). Atlas del agua en México 2012. Comisión Nacional del Agua. México, D. F..
10. CONAGUA (2015). Situación del Subsector de Agua Potable, Alcantarillado y Saneamiento. Comisión Nacional del Agua, Subdirección General de Infraestructura Hidráulica Urbana. Informe. Edición 2004. México, D. F.
11. SEMARNAT (2002). Norma Oficial Mexicana NOM-004-SEMARNAT-2002. Lodos y biosólidos. Secretaría de Medio Ambiente, Recursos Naturales y Pesca. Diario Oficial de la Federación. 15 de agosto de 2003.
12. Ochoa Elizondo, R. E. (1956). Estudio sobre el tratamiento de aguas negras de la Ciudad de México-Planta Piloto. Boletín de la oficina sanitaria Panamericana.166-170.
13. Breña Puyol, A. F. y Breña Naranjo, J. A. (2009). Problemática del recurso agua en grandes ciudades: zona metropolitana del valle de México. ContactoS. 74, 10-28.
14. Jiménez Cisneros, B. E. (2007). Información y calidad del agua en México. Trayectorias: revista de ciencias sociales de la Universidad Nacional de Nuevo León.24, 45-56.
15. SEMARNAT (1997). Norma Oficial Mexicana NOM-001-SEMARNAT-1996. Que establece los límites máximos permisibles de contaminantes en las descargas de aguas residuales en aguas y bienes nacionales. Secretaría de Medio Ambiente, Recursos Naturales y Pesca. Diario Oficial de la Federación. 6 de enero de 1997.
16. SEMARNAT (1998). Norma Oficial Mexicana NOM-002-SEMARNAT-1996.Que establece los límites máximos permisibles de contaminantes en las descargas de aguas residuales a los sistemas de alcantarillado urbano o municipal. Secretaría de Medio Ambiente, Recursos Naturales y Pesca. Diario Oficial de la Federación. 3 de junio de 1998.
17. SEMARNAT (1998). Norma Oficial Mexicana NOM-003-SEMARNAT-1997. Que establece los límites máximos permisibles de contaminantes para las aguas residuales tratadas que se reúsen en servicios al público. Secretaría de Medio Ambiente, Recursos Naturales y Pesca. Diario Oficial de la Federación. 21 de septiembre de 1998.

18. Domínguez-Montero, L. E. y Poggi-Varaldo, H. M. (2016). Los instrumentos económicos financieros en el tratamiento de aguas residuales municipales en México. In: Candal, R.; Curutchet, G.; Domínguez-Montero, L.; Macarie, H.; Poggi-Varaldo, H.; Vazquez, S.; Sastre, I. (Editors): Book of Abstracts Environmental Biotechnology and Engineering – 2016. Ed. Cinvestav, México D.F., México.

CHAPTER 7.9 LOS INSTRUMENTOS ECONÓMICOS FINANCIEROS EN EL TRATAMIENTO DE AGUAS RESIDUALES MUNICIPALES EN MÉXICO

Lilian E. Domínguez-Montero (1) and Héctor M. Poggi-Varaldo *(1,2)

(1) Grupo de Biotecnología Ambiental y Energías Renovables, Programa Transdisciplinario en Desarrollo Científico y Tecnológico para la Sociedad, Centro de Investigación y Estudios Avanzados del IPN, Av. Instituto Politécnico Nacional 2508, Ciudad de México, México.
(2) Grupo de Biotecnología Ambiental y Energías Renovables, Departamento de Biotecnología y Bioingeniería, Centro de Investigación y Estudios Avanzados del IPN, Dirección ibídem.

RESUMEN

En México es necesario contar con sistemas apropiados para el tratamiento de aguas residuales (TAR) con el fin de mitigar los problemas de contaminación ambiental y del agua, así como disminuir el consumo de agua potable. El objetivo de este trabajo fue analizar la inversión y financiamiento que ha otorgado el gobierno de México por medio de la Comisión Nacional del Agua en los últimos 7 años al TAR, así como comparar la situación con la de otros países del mundo con un nivel de desarrollo similar, Brasil; y con países desarrollados de la Organización para la Cooperación y el Desarrollo Económico (OCDE), Estados Unidos y Francia.
En comparación, durante el periodo 2007-2013 el país con mayor porcentaje de cobertura (γ) de m^3 agua residual tratada por m^3 agua residual colectada es Francia con una γ= 84.39%, seguido de Estados Unidos con γ=80.00%, mientras que Brasil tiene una γ= 68.05%, y México con la menor cobertura γ= 44.24%. Además, al realizar el cálculo de la inversión en millones de dólares constantes al año 2007 ($MUSD_{2007}$) por m^3/s de agua tratada (ω) se obtiene que México es el país con menor ω con un valor de 3.81 $MUSD_{2007}$/(m3/s), mientras que Brasil que es un país con un nivel desarrollo similar a México tiene una ω= 15.92 $MUSD_{2007}$/ (m3/s), lo que es 4 veces más que en México. A la vez se obtuvo la inversión per cápita (η) en $MUSD_{2007}$ por cada 100 mil habitantes y se observa que México está muy por debajo de los demás países con una η= 2.09, mientras que Francia que es el país con mayor inversión y un mayor porcentaje de cobertura en TAR tiene una η= 90.32. En cuanto a la evolución dinámica de la inversión en México, los resultados muestran que a pesar de que los recursos económicos asignados al TAR parecen ir en aumento (15.17% en el período 2007-2013, recursos expresados en dólares constantes 2007), tanto el retraso en el punto de partida como la situación económica mundial y la crisis financiera que ha sufrido en los últimos años se ha traducido en que el aumento de la inversión en dólares constantes en este subsector no ha sido suficiente. Este es posiblemente un factor que ha influido en que la meta establecida en México por el Programa Nacional Hídrico (PNH) 2007-2012 de tratar el 60% de las aguas residuales colectadas no se cumpla todavía, ya que para lograr dicha meta se necesitaría invertir 5,824.47 $MUSD_{2007}$, lo que significaría un aumento del presupuesto del 126% en un muy corto plazo.

---

*Author for correspondence: r4cepe@yahoo.com

Palabras claves: Brasil, Francia, instrumentos económicos financieros, México, tratamiento de aguas residuales

INTRODUCCIÓN

Los centros urbanos, comercios, industrias, y áreas agrícolas se han convertido en los focos de contaminación del agua[1] debido a la descarga de aguas residuales con materia orgánica, microorganismos, metales y sustancias químicas[2]. El Tratamiento de Aguas Residuales (TAR) permite el saneamiento de las aguas residuales además de mitigar los problemas de contaminación del agua y disminuir el consumo de agua limpia, para ello se requiere de inversión económica para la construcción de nuevas plantas de tratamiento de aguas residuales (PTAR), así como el correcto funcionamiento de las ya existentes.

Los instrumentos económicos en el medio ambiente son herramientas que buscan principalmente la reducción de la contaminación ambiental por medio de beneficios y apoyos económicos como son impuestos por contaminación, incentivos por cumplimiento y subsidios[3-7]. De acuerdo a la Ley General del Equilibrio Ecológico y Protección Ambiental (LGEEPA)[8] de México, los instrumentos económicos están definidos como:

"Los mecanismos normativos y administrativos de carácter fiscal, financiero o de mercado, mediante los cuales las personas asumen los beneficios y costos ambientales que generen sus actividades económicas, incentivándolas a realizar acciones que favorezcan el ambiente."

A su vez, como instrumentos económicos financieros (IEF) se reconocen como:

"los créditos, finanzas, seguros de responsabilidad civil, los fondos y los fideicomisos, siempre que sus objetivos estén dirigidos a la preservación, protección, restauración o aprovechamiento sustentable de los recursos naturales y el ambiente, así como al financiamiento de programas, proyectos, estudios e investigación científica y tecnológica para la preservación del equilibrio ecológico y protección del ambiente"[8].

Para el sector del agua en México, los IEF son apoyos financieros otorgados a través del Gobierno Federal y se ubican principalmente en la Comisión Nacional del Agua (Conagua), a través de la aplicación de programas y acciones que impulsen el incremento en sus eficiencias y la prestación de mejores servicios para agua potable, drenaje y saneamiento[9]; en el concepto de saneamiento se considera el acopio, transporte y tratamiento del agua residual[10]. Los programas encargados del TAR son seis[11-17] , el Programa de Agua Potable y Alcantarillado en Zonas Urbanas (APAZU), Programa de Devolución de Derechos (Prodder), Programa de Modernización de Organismos Operadores de Agua (Promagua), Programa para la Sostenibilidad de los Servicios de Agua Potable y Saneamiento (Prossapys), Programa de Tratamiento de Aguas Residuales (Protar) y el Programa de Sustentabilidad Hídrica de la Cuenca del Valle de México (PSHCVM); los cuales aportan apoyo económico y técnico a los gobiernos estatales y municipales para la construcción de las PTARM, posteriormente la operación queda a cargo de los gobiernos municipales y estatales[18].

En Brasil, la situación del TAR es similar a México. El apoyo financiero es proporcionado con fondos públicos a la Secretaria de Recursos Hídricos del Ministerio

de Medio Ambiente quien es responsable de otorgar los recursos económicos a la Secretaría Nacional de Saneamento Ambiental (SNSA) quien gestiona los programas de Saneamiento Básico, Saneamiento para Todos, Saneamiento Rural y de Servicios Urbanos de Agua y Alcantarillado Sanitario[19,20], quien le brinda apoyo económico a los municipios y estado del país[21].

Por otra parte, en Francia los servicios de agua potable y saneamiento son servicios públicos descentralizados, y las municipalidades están encargadas de la organización del servicio y son propietarios de las infraestructuras[22]. El gobierno francés a través de las seis Agencias del Agua son los encargados de gestionar las inversiones para el TAR quienes a su vez otorgan los IEF a las autoridades locales[23]. Cabe señalar que en dicho país los hogares son quienes financian el 43% de los servicios públicos de agua potable y saneamiento[22].

Estados Unidos a pesar de ser una de las naciones con mayor desarrollo económico mundial se enfrenta a los mismos problemas hídricos que el resto de los países de América Latina con excepción que la mayor parte de la población americana cuenta con acceso a fuentes de agua potable y servicios sanitarios adecuados. Para la gestión del TAR, el gobierno federal otorga el financiamiento a la U.S. Environmental Protection Agency (EPA) quien a su vez otorga los recursos a la Office of Wastewater Management (OWM) responsable del tratamiento, disposición y gestión de las aguas residuales[24].

El objetivo de este trabajo fue analizar la inversión y financiamiento en dólares constantes que ha otorgado el Gobierno de México por medio de la Conagua en los últimos 7 años a los programas encargados del saneamiento del agua a través del tratamiento de las aguas residuales, así como comparar la situación con la de otros países del mundo con un nivel de desarrollo similar, Brasil; y con países desarrollados de la Organización para la Cooperación y el Desarrollo Económico (OCDE), Estados Unidos y Francia.

MATERIALES Y MÉTODOS

Método para estimar el presupuesto para el tratamiento de aguas residuales en dólares constantes para México y países selectos. El método utilizado para la búsqueda de los presupuestos otorgados para TAR en el periodo 2007-2013 para México, Brasil, Estados Unidos y Francia, se centró en los informes proporcionados por los gobiernos de cada país respectivamente. Para el caso de México se obtuvo de los informes anuales que proporciona Conagua titulados “Situación del subsector agua potable, drenaje y saneamiento”; el Sistema Nacional de Informes sobre Saneamiento (SNIS) en Brasil realiza anualmente un reporte titulado “Diagnóstico dos Serviços de Água e Esgotos”[25-31] donde se da la información sobre el agua residual colectada y tratada, así como la inversión anual para TAR; en Francia, la instancia encargada de realizar el informe sobre la inversión anual que se otorga para el TAR es el Servicio de Estadística del Ministerio de Desarrollo Sostenible (SoeS); y en Estados Unidos la OWM[32-38] entrega anualmente.

La inversión y financiamiento otorgado a TAR en cada país está influenciado por la inflación de cada año, por ello para medir el crecimiento real se realiza la conversión a moneda constante, en este caso dólares. Primero se adquieren los Índices de Precios

de Consumo (IPC) para cada país (**Tabla 1**); posteriormente se calculan los factores IPC como se muestra
en la Ecuación 1 a 4 tomando como base el año 2007; luego se multiplica el correspondiente valor del precio actual en moneda local por el resultado del factor IPC de cada año para obtener el monto en moneda local constante.

TABLA 1. Índices de Precios de Consumo, 2007-2013

País	2007	2008	2009	2010	2011	2012	2013
Brasil	0.045	0.059	0.041	0.059	0.065	0.058	0.059
EEUU	0.041	0.001	0.027	0.015	0.030	0.017	0.015
Francia	0.026	0.010	0.009	0.018	0.025	0.013	0.007
México	0.038	0.065	0.036	0.044	0.038	0.036	0.040

Fuente: Banco Mundial, 2016

$$IPC_n = \prod_{j=2007}^{n} \frac{1}{(1+IPC_j)} \quad (1)$$

donde

IPC_n es el factor de índices de precios de consumo
$2007 \leq n \leq 2016$
IPC 2007=1
π representa la "productiva"

Debido a que los datos están dados en moneda local después se convierten a dólares, usando los tipos cambiarios oficiales de cada año. Finalmente se divide cada monto correspondiente actual en dólares sobre el resultado del factor IPC de Estados Unidos con referencia a 2007.

Determinación de indicadores relacionados con la inversión y el tratamiento de aguas residuales en México y países selectos. Con los datos obtenidos de las fuentes de información de México, Brasil, Francia y España (**Tabla 2**) se determinaron 5 indicadores descritos por las Ecs. 2 a 6 que permitan analizar la relación entre países. Estos indicadores miden la inversión en dólares constantes respecto al agua residual tratada, colectada y sin tratamiento en m^3/s, así como por el número de habitantes de cada país. Todos los indicadores se obtuvieron en el mismo periodo de tiempo (2007-2013).

TABLA 2. Información promedio sobre el Tratamiento de Aguas Residuales en Brasil, Estados Unidos, Francia y México, 2007-2013

País	Inversión ($MUSD_{2007}$)	Agua Residual Colectada (m^3/s)	Agua Residual Tratada (m^3/s)	Agua Residual No Tratada (m^3/s)	Población Total [e] (100 mil Habitantes)
Brasil [a]	10,903.76	1,006.75	685.08	321.66	1,986
Estados Unidos [b]	42,310.22	13,034.26	10,427.41	2,606.85	3,091
Francia [c]	58,709.63	2,356.50	1,988.61	367.89	650
México [d]	2,471.98	1,464.67	647.99	816.68	1,185

[a] Sistema Nacional de Informações sobre Saneamento (SNIS); [b] Office of Wastewater Management (OWM);
[c] Service de l'Observation et des Statistiques (SOeS); [d] Comisión Nacional del Agua (Conagua); [e] Banco Mundial, 2016; población promedio de los años 2007 al 2013.

$$\omega = \frac{IMDC_{TAR}}{Q_{ART}} \tag{2}$$

donde

ω es la inversión para tratamiento de aguas residuales por m^3/s de agua residual tratada en MUSD/ (m^3/s);
IMDC $_{TAR}$ representa la inversión en millones de dólares constantes para tratamiento de aguas residuales; y
Q $_{ART}$ es el gasto de agua residual tratada en m^3/s.

$$\eta = \frac{IMDC_{TAR}}{100 \quad mil \quad habitantes} \tag{3}$$

donde

η es la inversión per cápita (MUSD/100 mil habitantes)
IMDC $_{TAR}$ representa la inversión en millones de dólares constantes para tratamiento de aguas residuales

$$\gamma = \frac{Q_{ART}}{Q_{ARC}} \times 100 \tag{4}$$

donde

γ es la cobertura de tratamiento de aguas residuales en %

Q_{ART} representa el gasto de agua residual tratada en m^3/s
Q_{ARC} es el gasto de agua residual colectada en m^3/s

$$\sigma = \frac{IMDC_{TAR} \times Q_{ARNT}}{Q_{ART}} \quad (5)$$

donde

σ es la inversión requerida en millones de dólares constantes para aguas residuales no tratadas (MUSD)
$IMDC_{TAR}$ representa la inversión en millones de dólares constantes para tratamiento de aguas residuales
Q_{ART} es el gasto de agua residual tratada en m^3/s
Q_{ARNT} representa el gasto de agua residual no tratadas en m^3/s

$$\theta = \frac{\sigma}{IMDC_{TAR}} \times 100 \quad (6)$$

donde

θ es el incremento de la inversión requerido para alcanzar cobertura total de tratamiento de aguas residuales en %

σ representa la inversión aproximada para aguas residuales no tratadas en USD constantes
$IMDC_{TAR}$ es la inversión en millones de dólares constantes para tratamiento de aguas residuales

RESULTADOS Y DISCUSIÓN

Presupuesto otorgado al tratamiento de aguas residuales en México y países selectos. Como se observa en la **Figura 1**, los países que tuvieron una mayor inversión para TAR durante el periodo 2007-2013 son Francia y Estados Unidos. La inversión de Francia es de 58,709.63 millones de dólares con año base 2007 ($MUSD_{2007}$), con lo cual le permite lograr el 84.39% de cobertura. Estados Unidos ocupa el segundo puesto en inversión con un total de 42,310.22 $MUSD_{2007}$, siendo el 2009 el año con mayor inversión, esto debido a la Ley de Recuperación y Reinversión (ARRA por sus siglas en inglés) firmada por el presidente Barack Obama, el cual otorgó al programa Clean Water State Revolving Fund (CWSRF) un apoyo de 4000 MUSD para mejorar los sistemas de aguas residuales y la calidad del agua[34y39]; dicha aportación ha sido gastada a lo largo del periodo 2009-2012.

Brasil ocupa el tercer lugar de los países analizados, con una inversión en TAR de 10,903.76 $MUSD_{2007}$ de acuerdo a los reportes del Sistema Nacional de Informações sobre Saneamento (SNIS), mientras que México es el país con menor inversión en dicha área con 2,471 $MUSD_{2007}$. Aunque actualmente México y Brasil son las dos principales economías en América Latina, la inversión lograda para TAR por este último país es 4.41 veces mayor que en México; debido a que Brasil ha logrado en los últimos

años un progreso institucional en la organización de los recursos hídricos viéndose reflejado en los montos invertidos[40].

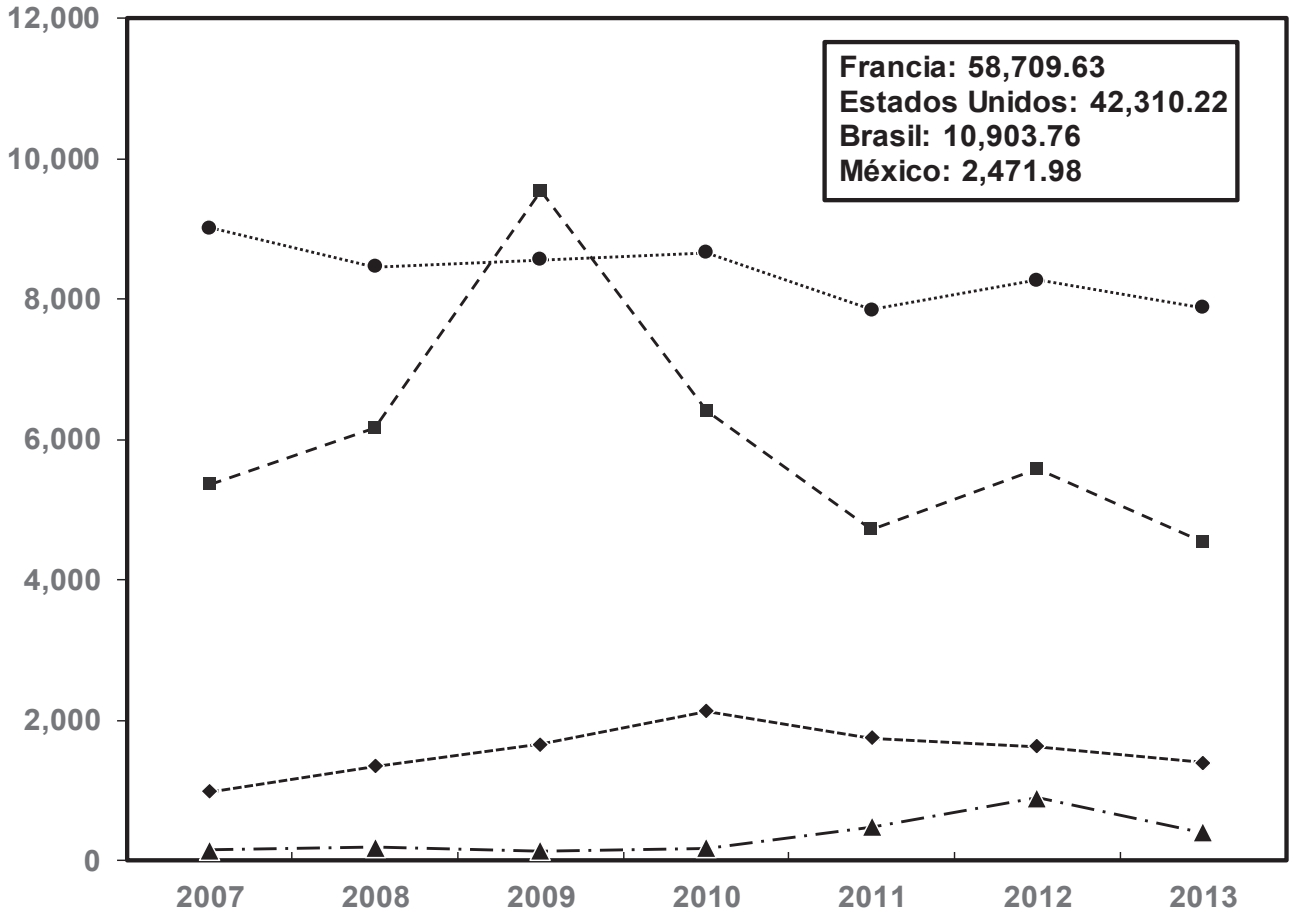


FIGURA 1. Presupuesto otorgado al tratamiento de aguas residuales municipales en México, Brasil, Francia y Estados Unidos, 2007-2013

Fuente: Conagua; EPA-OWM; SNIS y SoeS

Al realizar el cálculo de la inversión en $MUSD_{2007}$ por m^3/s de agua tratada (ω), **Tabla 3,** se ve que México es el país con menor ω con un valor de 3.81 MUSD/(m3/s); mientras que Brasil que es un país con un nivel de desarrollo similar a México económicamente tiene una ω= 15.92 MUSD/ (m3/s), lo que es más de 4 veces superior. Por el contrario, Francia es el país con mayor ω con un valor de 29.52 MUSD/ (m^3/s).

A la vez se obtuvo la inversión per cápita (η) en $MUSD_{2007}$ por cada 100 mil habitantes, y se observa que México está muy por debajo de los demás países con una η= 2.09 MUSD/100 mil habitantes, mientras que Francia nuevamente es el país con mayor porcentaje de cobertura en TAR teniendo una η= 90.32 MUSD/100 mil habitantes.

En comparación, durante el periodo 2007-2013 el país con mayor porcentaje de cobertura (γ) de m^3 ART por m^3 ARC es Francia con una γ= 84.34%, seguido de

Estados Unidos con γ=79.37%, mientras que Brasil tiene una γ= 67.95%, y México con el menor porcentaje de cobertura γ= 43.55%.

TABLA 3. Indicadores para el Tratamiento de Aguas Residuales en Brasil, Estados Unidos, Francia y México, 2007-2013

País	ω (MUSD/ m^3/s)	η (MUSD/100 mil habitantes)	γ (%)	θ (%)
Brasil	15.92	5.49	68.05	46.95
Estados Unidos	4.06	13.69	80.00	25.00
Francia	29.52	90.32	84.39	18.50
México	3.81	2.09	44.24	126.03

Respecto a la inversión promedio requerida para alcanzar la cobertura total de TAR (θ), se observa que México es el único país que requeriría invertir más del 100% para lograr dicho objetivo. Por otra parte, a pesar de que Brasil es el país de América Latina con mayores similitudes a México, la inversión que realiza en TAR es superior, por lo que solo requeriría invertir 46.95% más de lo ya realizado durante este periodo. Por el contrario, Francia y Estados Unidos son los países que requerirían realizar una inversión menor.

Situación del presupuesto otorgado al tratamiento de aguas residuales en México, 2007-2013. Como se observó anteriormente, la inversión para TAR en México ocupa el último lugar dentro de los países analizados; a pesar de ello la inversión para TAR, asignado por el gobierno federal en $MUSD_{2007}$ parece ir en aumento (**Figura 2)**, siendo el presupuesto asignado en 2013 un 15.17 % mayor que el de 2007, en dólares constantes 2007.

Dicho aumento se debe a la construcción de la PTAR de Atotonilco cuya construcción se inició en 2009 y se aceleró en 2011-2012, y se planea sea la PTAR más grande del país con una capacidad promedio para tratar 23 m^3/s [16]. La inversión para la construcción de la PTAR Atotonilco entra dentro del Programa de Sustentabilidad Hídrica de la Cuenca del Valle de México (PSHCVM), que en el año 2012 representó el 40.94% del presupuesto asignado a saneamiento en México ese año, siendo el resto del presupuesto para mantenimiento de las 2342 PTARM ya existentes y la construcción de otras PTAR en el resto del país.

En la **Figura 2** también se observa que la cobertura de TAR ha ido en aumento siendo en el año 2007 del 38.28% mientras que el 2013 alcanzó el 50.19%. Tanto el aumento presupuestal para TAR y el aumento en la cobertura de tratamiento podrían estar relacionados con el Programa Nacional Hídrico (PNH) 2007-2012 y 2013-2018, en los cuales la meta establecida es tratar el 60% de las ARC en 2018[41,42]. Para lograr dicho propósito se requieren invertir 5,824.47 $MUSD_{2007}$ lo que representa un 135.62% más de la inversión que actualmente se ha hecho en este rubro; y si México quisiera igualar el porcentaje tratado por Francia (84.39%), país con mejores indicadores para

TAR (**Tabla 3**), México necesaria invertir la cantidad 7,187.26 $MUSD_{2007}$, 1.90 veces más del presupuesto actual. En el mismo sentido, si México se propusiera lograr el tratamiento total del agua residual colectada, la inversión promedio que se requeriría sería de 8059.46 $MUSD_{2007}$, 126% más de lo invertido actualmente.

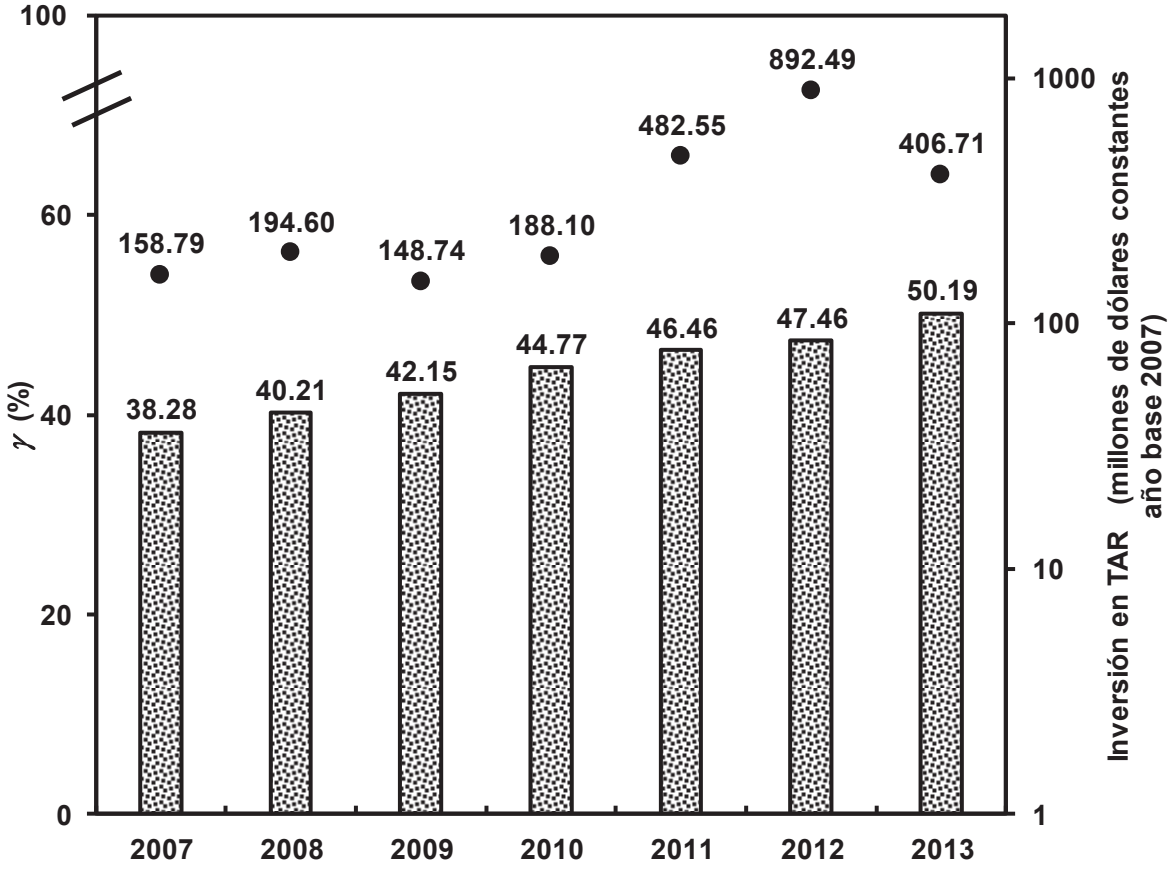


FIGURA 2. Inversión y cobertura en el tratamiento de aguas residuales municipales en México, 2007-2013. Notar que la escala derecha es logarítmica, por lo que cualquier incremento de la variable se aprecia como relativamente más bajo que el incremento real. Fuente: Conagua 2007-2013.

Es importante notar que, si se implementara desarrollo tecnológico de origen mexicano en las PTAR, se reducirían los costos de construcción y operación de las PTAR[43], lo que permitiría que la inversión que el gobierno federal aporte sea suficiente para tener PTAR que logren la cobertura de tratamiento planeada (60%) y que esta sea eficientemente.

Finalmente, estos resultados pueden servir de apoyo para futuros proyectos para el aumento de instrumentos económicos financieros, así como implementar políticas públicas para el subsector de tratamiento de aguas residuales.

CONCLUSIÓN

México es el país con menor inversión per cápita, menor inversión en dólares constantes, con una cobertura de tratamiento de aguas residuales muy por debajo del resto de los países analizados, y sería el único país que requeriría invertir más del 100% de la inversión actual para lograr el tratamiento total de las aguas residuales colectadas.

En el caso contrario, Francia es un país con un tratamiento de aguas residuales superior a todos los países analizados al lograr una cobertura del 84.5%, esto se debe a que la inversión que el Gobierno otorga a este subsector es de las más altas en el análisis.

La evolución dinámica de la inversión que el Gobierno de México ha otorgado al tratamiento de aguas residuales ha ido en aumento; sin embargo, dicho aumento en dólares constantes en este subsector no ha sido suficiente ya que en comparación con otros países el volumen de agua residual tratada es menor. Este es posiblemente un factor que ha influido en que la meta establecida en México por el PNH 2007-2012 de tratar el 60% de las aguas residuales colectadas no se cumpla todavía, y que para lograr una cobertura de TAR en un corto plazo se requiera de una fuerte inversión en el subsector.

Por ello estos resultados pueden servir de apoyo para futuros proyectos para el aumento de instrumentos económicos financieros, así como para implementar políticas públicas para el subsector de tratamiento de aguas residuales.

AGRADECIMIENTOS

Los autores agradecemos al CINVESTAV del IPN por el respaldo parcial a esta investigación. Uno de los autores (Lilian Edith Domínguez Montero) agradece al Consejo Nacional de la Ciencia y la Tecnología por la beca de posgrado para la realización de esta investigación, así como al Consejo Mexiquense de Ciencia y Tecnología (Comecyt) por las facilidades otorgadas para la participación en el 5th International Symposium on Environmental Biotechnology and Engineering.

REFERENCIAS

1. Aboites Aguilar L., Birrichaga Gardida D. y Garay Trejo, J.A. (2010). El manejo de las aguas mexicanas en el siglo XX. En: *El agua en México: cauces y encauces*. (B. Jiménez, M. Torregrosa, L. Aboites, Eds.) Academia Mexicana de Ciencias, D.F., México. pp. 19-50.
2. FEA y CEMDA (2006). El agua en México: lo que todas y todos debemos saber. Fondo para la Comunicación y la Educación Ambiental, A.C. y Centro Mexicano de Derecho Ambiental, A.C.
3. Rodríguez Tapia L. y Morales Novelo J. A. (2000). La aplicación de instrumentos económicos para disminuir la contaminación del agua: experiencias en el uso de cuotas por descargas de aguas residuales. Análisis Económico. 15, 11-135.
4. Silva Arroyave S. M. y Correa Restrepo F. (2010). Los instrumentos económicos como incentivos a la internalización de costos ambientales en empresas floricultoras. Pensamiento & Gestión. 29, 25-55.

5. Pérez Calderón J. P. (2010). La política ambiental en México: Gestión e instrumentos económicos. El Cotidiano. 162, 91-97.
6. Rodríguez J.K. y Ávila Foucat S. (2013). Instrumentos económicos voluntarios para la conservación: una mirada a su surgimiento y evolución en México. Sociedad y Economía. 25, 75-105.
7. Vasile A. J. (2013). Economic instruments for environmental policy in Serbia. Memorias. InInternational Scientific Conference. Sustainable Agriculture and Rural Development in Terms of the Republic of Serbia Strategic Goals Realization Within the Danube Region, Achieving regional competitiveness. Topola, Serbia. 5 de diciemcbre 2013. 331-346 pp.
8. LGEEPA (2012). Ley General del Equilibrio Ecológico y la Protección al Ambiente. Diario Oficial de la Federación. 4 de Junio de 2012.
9. Canizales Pérez R., González Gutiérrez G. y Florez Romero E. (2011). Instrumentos económicos en la gestión del agua en México: caracterización de los incentivos fiscales, financieros y de mercado en el sector. Gaceta de Administración del Agua. 1, 14-25.
10. De la Peña M.E., Ducci J. y Zamora Plascencia V. (2013). Tratamiento de aguas residuales en México. Banco Interamericano de Desarrollo,19 pp
11. Conagua (2008), Situación del Subsector de Agua Potable, Alcantarillado y Saneamiento, Edición 2008. Comisión Nacional del Agua. Informe. México, D.F.
12. Conagua (2009), Situación del Subsector de Agua Potable, Alcantarillado y Saneamiento, Edición 2009. Comisión Nacional del Agua Informe. México, D.F.
13. Conagua (2010), Situación del Subsector de Agua Potable, Alcantarillado y Saneamiento, Edición 2010. Comisión Nacional del Agua Informe. México, D.F.
14. Conagua (2011), Situación del Subsector de Agua Potable, Alcantarillado y Saneamiento, Edición 2011. Comisión Nacional del Agua Informe. México, D.F.
15. Conagua (2012), Situación del Subsector de Agua Potable, Alcantarillado y Saneamiento, Edición 2012. Comisión Nacional del Agua. Informe. México, D.F.
16. Conagua (2013), Situación del Subsector de Agua Potable, Alcantarillado y Saneamiento, Edición 2013. Comisión Nacional del Agua. Informe. México, D.F.
17. Conagua (2014), Situación del Subsector de Agua Potable, Alcantarillado y Saneamiento, Edición 2014. Comisión Nacional del Agua. Informe. México, D.F.
18. De la Peña M.E., Ducci J. y Zamora Plascencia V. (2013). Tratamiento de aguas residuales en México. Banco Interamericano de Desarrollo,15 pp
19. Banco Mundial, UNICEF y BID. (2007). Saneamiento para el desarrollo:¿ cómo estamos en 21 países de América Latina y el Caribe?. Banco Mundial, United Nations International Children's Emergency Fund y Banco Interamericano de Desarrollo. Informe. Perú, Lima.
20. SNIS (2013). Diagnóstico dos serviços de água e esgotos- 2011. Sistema Nacional de Informações sobre Saneamento.
21. Tucci, C., Hespanhol, I. y Cordeiro, O. (2000). Relatório nacional sobre o gerenciamento da água no Brasil. En: Agua para el Siglo XXI: De la Visión a la Acción.América del Sur. (GWP y SAMTAC, Eds.) Global Water Partnership y Comité Técnico Asesor para Sud América.
22. OIA (2009). Organización de la gestión del agua en Francia. Oficina internacional del Agua. Informe. Francia, París.
23. SOeS (2014). L'économie de l'environnement en 2012: Rapport de la Commission des comptes et de l'économie de l'environnement. Edición 2014. Service de l'Observation et des Statistiques. Francia, París.
24. Henry Vaux, Jr. (2012). Los recursos hídricos de los Estados Unidos. En: Diagnóstico del agua en las Américas. (Cisneros, B. J. y Tundisi, J. G. , Eds.)Red Interamericana de Academias de Ciencias. México: Foro Consultivo Científico y Tecnológico. 267-279.

25. SNIS (2009).Diagnóstico dos serviços de água e esgotos- 2007: Parte 1 – Texto Visão Geral da Prestação de Serviços. Sistema Nacional de Informações sobre Saneamento
26. SNIS (2010). Diagnóstico dos serviços de água e esgotos- 2008: Tabelas de Informações e Indicadores. Sistema Nacional de Informações sobre Saneamento
27. SNIS (2011). Diagnóstico dos serviços de água e esgotos- 2009. Sistema Nacional de Informações sobre Saneamento
28. SNIS (2012). Diagnóstico dos serviços de água e esgotos- 2010. Sistema Nacional de Informações sobre Saneamento
29. SNIS (2013). Diagnóstico dos serviços de água e esgotos- 2011. Sistema Nacional de Informações sobre Saneamento
30. SNIS (2014). Diagnóstico dos serviços de água e esgotos- 2012. Sistema Nacional de Informações sobre Saneamento
31. SNIS (2014b). Diagnóstico dos serviços de água e esgotos- 2013. Sistema Nacional de Informações sobre Saneamento
32. EPA and OWM (2008). OWM Accomplishments Report 2007. United States Environmental Protection Agency and Office of Wastewater Management. Informe. Whashington, D.C.
33. EPA and OWM (2009). 2008 OWM Accomplishments Report: Clean and sustainable water now and in the future. United States Environmental Protection Agency and Office of Wastewater Management. Informe. Whashington, D.C.
34. EPA and OWM (2010). 2009 OWM Annual Accomplishments Report. United States Environmental Protection Agency and Office of Wastewater Management. Informe. Whashington, D.C.
35. EPA and OWM (2011). Office of Wastewater Management: 2010 Annual accomplishments report. United States Environmental Protection Agency and Office of Wastewater Management. Informe. Whashington, D.C.
36. EPA and OWM (2012). Office of Wastewater Management: 2011 Annual report. United States Environmental Protection Agency and Office of Wastewater Management. Informe. Whashington, D.C.
37. EPA and OWM (2013). Office of Wastewater Management: 2012 Annual report. United States Environmental Protection Agency and Office of Wastewater Management. Informe. Whashington, D.C.
38. EPA and OWM (2014). Office of Wastewater Management: 2013 Annual report. United States Environmental Protection Agency and Office of Wastewater Management. Informe. Whashington, D.C.
39. Harrington, W., & Malinovskaya, A. (2015). Expected versus Actual Outcomes of Environmental Policies: The Clean Water State Revolving Fund. Resources for the Future Discussion Paper, 15-46.
40. Galizia Tundisi, J. y Barnsley Scheuenstuhl, M. C. (2012). Los recursos hídricos de Brasil. En: Diagnóstico del agua en las Américas. (Cisneros, B. J. y Tundisi, J. G. , Eds.)Red Interamericana de Academias de Ciencias. México: Foro Consultivo Científico y Tecnológico. 97-111.
41. PNH (2008). Programa Nacional Hídrico 2007-2013. Diario Oficial de la Federación. 30 de Diciembre de 2008.
42. PNH (2014). Programa Nacional Hídrico 2014-2018. Diario Oficial de la Federación. 8 de Abril de 2014.
43. Dominguez-Montero, L. E., Poggi-Varaldo, H.M., Pérez Angón, M.A., Jimenez Cisneros, B.E., Cañizares Villanueva, R.O, Caffarel Méndez,S., Frixione Garduño,E. (2016). Instrumentos tecnologicos patentados en Mexico para tratar aguas residuales. Número Especial de Biotecnología e Ingeniería Ambientales. Revista Internacional de Contaminación Ambiental. En prensa

CHAPTER 7.10 DIVERSITY AND DIEL VARIATION OF PHYTOPLANKTON COMMUNITY AT DIFFERENT DEPTHS IN A POLISHING POND

J. T. Ferreira *(1); M.L.P.D. Lages (1); E. A. Pastich (2); S. Gavazza (1); M. T. Kato (1) and **L. Florencio (1)**

(1) Laboratory of Environmental Sanitation, Department of Civil Engineering, Federal University of Pernambuco, Av. Acadêmico Hélio Ramos s/n, Cidade Universitária, Recife-Brazil.
(2) Laboratory of Environmental Engineering, Academic Center of Agreste, Federal University of Pernambuco, BR-104, Km 62, Caruaru-Brazil

ABSTRACT

The phytoplankton community in stabilization ponds is directly influenced by the availability of nutrients and solar radiation that reaches the different depths of the water column. The density and dominance of some phytoplankton species can vary with depth due to the demand for better light conditions. The quality of the final effluent may be favored by lower density of algae, whereas the phytoplankton is essential for the dissolved oxygen production by photosynthesis, and contributes to the high concentration of suspended solids in the final effluent of stabilization ponds.
Phytoplankton dynamics knowledge in stabilization ponds can contribute to the design of the effluent output devices ponds aiming improving the final effluent quality, since the algae density floats in the water column. Thus, the goal of this study was to characterize the phytoplankton dynamics at nictimeral and time scale, and also their correlation with abiotic parameters.
Monthly campaigns were conducted between August 2015 and January 2016, in a polishing pond located at Rio Formoso county of Pernambuco State, which is applied as post-treatment of a UASB reactor. In each campaign were evaluated three points: affluent, a point inside the pond with collections at different depths, and effluent. The times defined for collections were 9h, 11h, 13h, 15h, and 17h. For phytoplankton quantification was used Utermöhl method. Ecological indexes as relative abundance and frequency of occurrence were used for the interpretation of phytoplankton dynamic.
The phytoplankton community was represented by 12 taxa, distributed in Cianophyta divisions (54%), Chlorophyta (45%), and Bacillariophyta (1%). The following taxa were identified: *Planktothrix agardhii*, *Phormidium sp*, *Merismopedia tenuissima*, *Pseudonabaena catenata*, *Microsystis sp*, *Closteriopsis acicularis*, *Desmodesmus sp.1*, *Desmodesmus sp.2*, *Monoraphidium arcuatum*, *Monoraphidium circinale*, *Monoraphidium contortum,* and *Nitzschia sp*. All found taxa have been observed in other studies about stabilization ponds.
Compared the versatile metabolism of Cyanobacteria was not observed any behavior pattern along the water column; it is not possible to point to a specific depth for installation of output devices of the effluent in order to avoid the group. However, in relation to dissolved oxygen parameter, most superficial layers showed higher

---

*Author for correspondence: ferreira.juceliat@gmail.com

concentrations. The months of November, December, and January provided the highest densities of Cyanobacteria. In these months should be intensified monitoring of potentially toxic species and should be included in the monitoring analysis of the concentration of toxins.

Keywords: cyanobacteria, domestic sewage, phytoplankton, polishing pond.

INTRODUCTION

The phytoplankton community in stabilization ponds is directly influenced by the availability of nutrients and solar radiation that reaches the different depths of the water column. The dominance of some species can vary with depth due to the search for better environmental conditions the light availability. The main phytoplankton groups registered in stabilization ponds are the cyanobacteria, Chlorophyceae, Bacillariophyceae and Euglenophyceae[1,2,3].

Phytoplankton is essential for the sewage treatment, because, for carrying out photosynthesis, they release oxygen in into the environment. This oxygen is used by aerobic bacteria to oxidize the organic matter. However, higher densities of phytoplankton in the final effluent of stabilization ponds generate an effluent with high turbidity and suspended solids[4].

In addition, phytoplankton can be dominated by cyanobacteria that are potential producing toxins. In the shallow and eutrophic water with temperatures above 20°C and high sunlight, cyanobacteria can become dominant[5].

This can create imbalances in the aquatic ecosystem of the receiving water body, as well as public health problems if it is used for the supply or fishing activities. Several studies report the presence of cyanobacteria in stabilization ponds[6,7].

In Brazil, the stabilization ponds are widely used for the treatment of domestic sewage, over the tropical climate that is quite favorable. However, there are only few studies on the dynamics of the phytoplankton community in these ecosystems.

Knowledge of the dynamics of phytoplankton community in stabilization ponds and the parameters that influence this dynamic can help in the ponds management and choosing the best depth for installation of effluent output devices. Thus, it may be possible to avoid depths with greater density of phytoplankton or cyanobacteria.

This study aimed to characterize the dynamics of phytoplankton at different depths in the water column of a polishing pond in nictimeral and timescale, and its correlation with abiotic parameters.

MATERIALS AND METHODS

The WWTP of Rio Formoso county, located in northeastern Brazil (08°39'31"S, 08°39'31"W), was studied in this work. It is distant 92 km from Recife, capital of Pernambuco. The WWTP includes an Upflow Anaerobic Sludge Blanket (UASB) reactor followed by a maturation pond, and a set of four stone percolators filters as a pond post-treatment.

Sampling was conducted during six months (August, September, October, November, December of 2015 and January of 2016). In each sampling campaign were assessed three points: influent pond (P1), column sample at different depths (P2, P3, P4 and P5 to 10, 20, 30, 60 and 90 cm from the surface, respectively) and effluent pond (P6).

The samples used to assess the phytoplankton composition were collected in four sampling points on water column (P2, P3, P4 and P5) and 1 point at the effluent (P6). The samples were collected at five different times (9 a.m., 11 a.m., 1 p.m., 3 p.m., and 5 p.m.), totaling 150 samples (6 months x 5 sampling points x 5 hours).

The samples used to analyze physicochemical characteristics were collected in three points: affluent pond (P1) collected only at 9 a.m., composite sample of the water column (PC) collected in five times and effluent point (P6) also collected in 5 times, totaling 66 samples.

The phytoplankton quantification was conducted in an inverted microscope. The dynamic phytoplankton analysis was performed using the Specific density.

The Specific density[8] was calculated according to the following equations:

$$D = N/V_c \quad (1)$$

$$Vc = A_c \times V/Ta \quad (2)$$

Where:

D = Specific Gravity (cell.mL^{-1})
N = Number of cells counted
Vc = Volume counted (mL)
Ac = Area counted
V = Volume sedimented in Utermöhl chamber (mL)
Ta = Total area of the counting chamber

The depths samples were collected with a Van Dorn collecting bottle. All samples for the phytoplankton identification and quantification were preserved with 4% acetic lugol.

The following physicochemical parameters were analyzed: the total Kjeldahl nitrogen (N-NTK), ammonia (ammonia-N), orthophosphate, total phosphorus, alkalinity, turbidity and BOD. The methods used were carried out according to the methodology described in Standard methods[9].

RESULTS AND DISCUSSION

Table 1 presents the average concentrations observed in the following points: P1 (pond influent, collected only at 9:00), PC (sample of the water column collected in time 9 a.m., 11 a.m., 1 p.m., 3 p.m., and 5 p.m.) and P6 (pond effluent).

The total alkalinity did not present any variations throughout the day. On the P1 point was observed an average of 235 mg.L^{-1}. For the PC point was observed an average of 150.3 mg.L^{-1}. However, for P6 point was observed average ranged from 165.8 mg.L^{-1} at 9 a.m. to 158.4 mg.L^{-1} at 5 p.m.

TABLE 1. Average values and standard deviation for physicochemical parameters

SP	N-TKN ($mg.L^{-1}$)	$N\text{-}NH_4^+$ ($mg.L^{-1}$)	$P\text{-}PO_4^{-3}$ ($mg.L^{-1}$)	PT ($mg.L^{-1}$)	Alkalinity ($mg.L^{-1}$)	Turbidity (NTU)
P1 - 9h	35±4.8	32±1.9	2.7±1	2.7±1.6	235.7±517.3	57.9±16.7
PC - 9h	20±4.5	13±2.2	1.2±0.6	2.5±1.5	152.4±9.2	99.8±53.0
PC - 1h	19±5.4	13±2.2	1.3±0.8	2.4±1.3	150.9±8.2	90.4±44.9
PC - 13h	20±3.9	13±2.6	1.2±0.9	2.3±1.4	150.5±5.4	93.0±39.1
PC - 15h	21±3.8	13±1.8	1.2±0.9	2.4±1.3	151.3±7.0	91.7±41.1
PC - 17h	17±5.6	13±2.4	1.3±0.9	2.2±1.2	157.1±5.2	89.0±45.1
P6 - 9h	20±4.8	14±3.2	1.1±0.6	2.4±1.3	165.8±15.9	99.5±45.1
P6 - 11h	19±4.9	15±3.3	1.2±0.8	2.4±1.4	156.2±7.1	97.5±38.4
P6 - 13h	19±4.5	12±3.5	1±0.9	2.4±1.4	156.5±10.2	92.2±37.7
P6 - 15h	17±6.1	13±3.1	1.2±0.9	2.3±1.3	160.6±13.7	95.0±41.4
P6 - 17h	18±5.5	13±2.6	1±0.8	2.4±1.3	158.4±8.0	95.9±38.2

Note: SP = sample point at different times of collection; P1 = pond influent, PC = sample of the water column and P6 = effluent pond.

The total nitrogen values (N-TKN) in the influent point (P1) presented a short variation throughout the monitoring period. The average was 35.2 $mg.L^{-1}$. On the other hand, in the water column (PC), the lowest values were observed at 5pm (average 16.6 mgL-1). On pond effluent (P6), the lowest value was observed at 3 p.m. (17.1 $mg.L^{-1}$).

In the period of the day that solar radiation increases, the photosynthesis and carbon dioxide consumption by the algae can raise the pH and, as a consequence, promote the volatilization of ammonia.

Changes in the pH value in stabilization ponds are generally a consequence of the CO_2 consumption by algae during the photosynthesis. Already during the night, there is an increase in CO_2 concentration in pond, so, there is a pH decreasing because both algae and bacteria oxidative process[10].

High pH may lead to volatilization of ammonia[11], which may explain the observed lower concentration of TKN to 3 pm.

Overall, the results for nitrogen corroborate to Viçosa-MG study[12], who observed average values between 10 $mg.L^{-1}$ and 45 $mg.L^{-1}$, in a UASB system followed by polishing ponds.

The total phosphorus removal did not occur in this study. The concentrations were between 2.8 $mg.L^{-1}$ in P1 (influent) and 2.5 $mg.L^{-1}$ in P6 (effluent). The phosphorus removal in stabilization ponds occurs on a small scale, since the pH does not reach these units in general, the high values required for significant removal[13]. The pH observed during the study (being the highest value at 8.2 $mg.L^{-1}$) did not favor the phosphorus precipitation.

Total phosphorus almost had no removal and the values were between 2.8 $mg.L^{-1}$ in P1 and 2.5 $mg.L^{-1}$ in P6. As to the orthophosphate were obtained ranges of 2.7 $mg.L^{-1}$ at P1 and 1.1 $mg.L^{-1}$ at P6 (5 p.m.). Higher concentrations were found in the Viçosa-MG study using an UASB system followed by polishing ponds[12].

The ranges for BOD were 30.6 $mg.L^{-1}$ (P1) and 6.6 $mg.L^{-1}$ (P6). The algae density increase inside ponds can influence the BOD increasing in effluent[14].

Over a period of stratification that occurs inside the pond there is an intense growth of algal biomass and zooplankton that is not able to consume phytoplankton and promote the clarification the water. The consequence is an accumulation of algal biomass and disruption of the food chain in the pond stabilization, which reduces the treatment efficiency[15]. Among the stratification consequences, the main one is the useful volume reduction of the pond. This happen because the pond is divided into a more active surface layer and less dense and another layer deeper, denser and less active[16].

For turbidity were observed 57.9 NTU at P1, 100 NTU (9h) and 89 NTU (17h) at PC, and 99.5 NTU (9h) and 96 NTU (17h) for P6. The turbidity results were generally equivalent to other studies in stabilization ponds[17,18].

The **Figure 1** shows the temperature profile along the water column. The temperature ranged between 30.9°C (9:00) to 25.2°C (17:00). For all the months studied, the highest values were observed in the highest solar radiation range (from 1 p.m. to 3 p.m.). The average water temperatures were increasing from August to December (**Figure 1 A, B, C, D and E**). After that, the temperature reduced again in January (**Figure 1**).

The temperature gradient of 0.6°C.m^{-1} is enough to denote thermal stratification in the water column of stabilization ponds[15]. In the present study thermal stratification occurred in August and September at the times 15h and 17h. In the months October and November, the pond was stratified during the largest time. In January, the thermal stratification was not be observed.

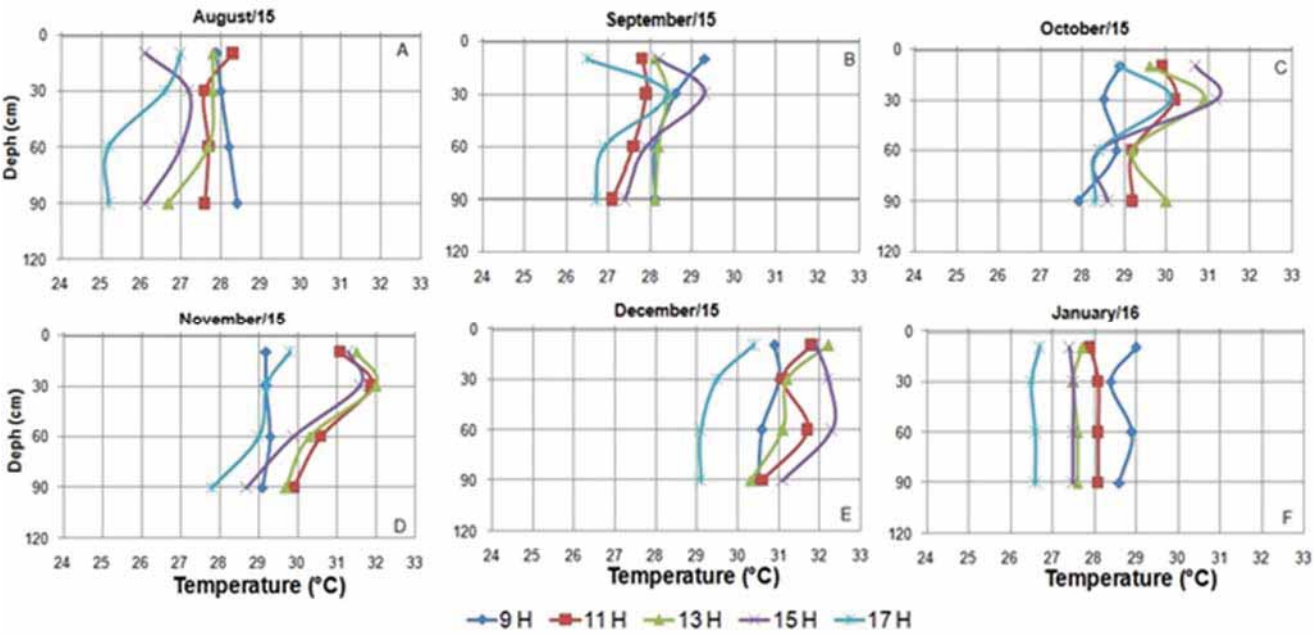


FIGURE 1. Temperature (°C) obtained during the sampling months (A, B, C, D, E and F), at points P2 (10 cm), P3 (30 cm), P4 (60 cm) and P5 (90 cm), in time 9:00, 11:00, 1pm, 3pm and 5pm of ETE polishing pond - Rio Formoso

Other studies reported the stratification dynamics of three stabilization ponds during 596 days[19]. The authors highlighted three types of behavior on same pond: complete mixing model without stratification, stratification during the day and complete mixing at

night, and continuous stratification throughout the day. In this study, the pond was stratified during the day and at night remaining mixed, except on January when the pond was not stratified.

In stabilization pond systems in series, the first units receiving greater organic loads, the daily variation in the parameters pH, temperature and dissolved oxygen are smaller and,

with this, the mixture is greater[10,20]. The study pond is not a post-treatment of a UASB reactor, thus, much of the organic matter has been removed from the reactor.

The organic load in the pond is low (average 95.8 Kg $BOD.ha^{-1}.day^{-1}$), which promotes the stratification. The increased thermal stratification favors the development of potentially producing cyanobacteria toxinas[21].

The **Figure 2** presents the pH changes along the water column. The average pH values were increased from August to December (**Figure 2A, 2B, 2C, 2D** and **2E**) as well as temperature data, returning to reduce in January/2016.

The pH in a stabilization pond is strongly influenced by carbon dioxide uptake by algal biomass, reducing acidity of the environment and increasing pH. The temperature increased accelerates the microbial metabolism[10].

Thus, as expected, the pH varies proportionally to the temperature, but less intensely. This same behavior was observed in another study[7], which studied the diurnal variation in two stabilization pond systems. The higher pH values were generally at 1pm to 3pm. In January (**Figure 2F**), there was not stratification in pH, as well as temperature.

Regarding concentration of dissolved oxygen in the water column (**Figure 3**), the months with highest chemical stratification were October, November and December, following the same trend in temperature.

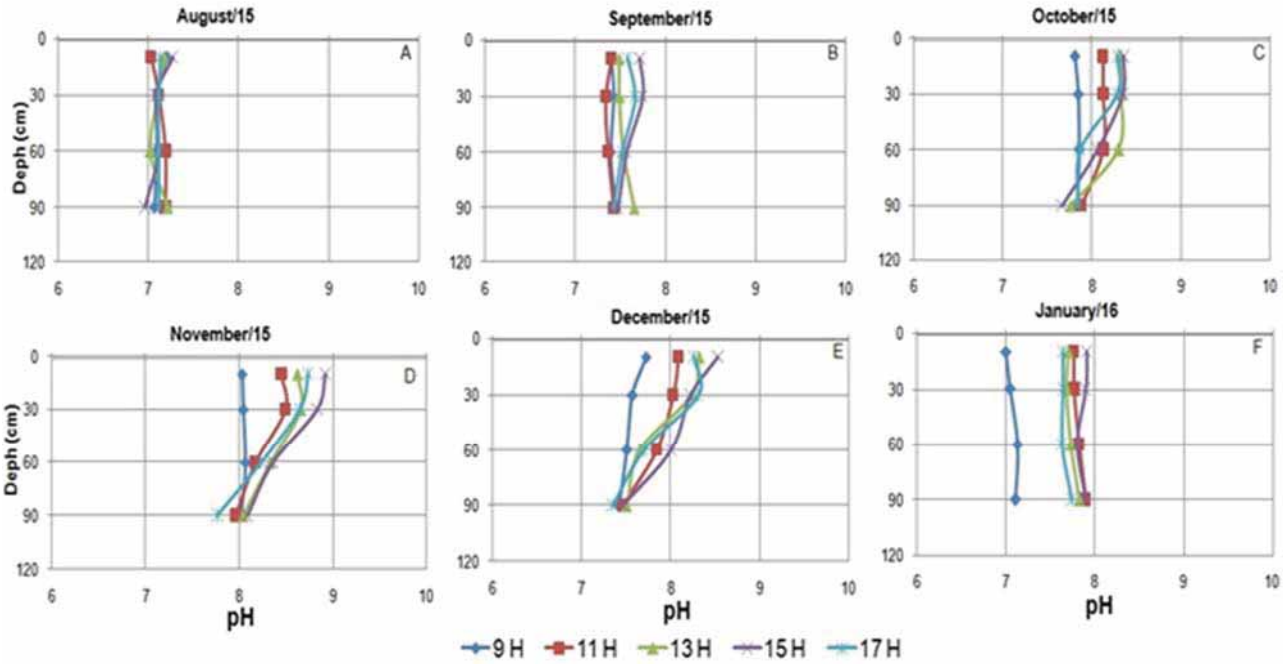


FIGURE 2. The pH values obtained during the sampling months (A, B, C, D, E, F), at P2 (10 cm), P3 (30 cm), P4 (60 cm) and P5 (90 cm) points, in time 9:00, 11:00, 1pm, 3pm and 5pm of ETE polishing pond - Rio Formoso.

Increasing the temperature influencing the algal metabolism may also be added to the understanding of dissolved oxygen parameter. The fast metabolism causes the algal biomass performs of photosynthesis at a high rate providing dissolved oxygen as by product.

During the first hour of the day, the water surface temperatures are higher than bottom, which results in the pond become chemically stratified[7]. During the night, the decrease of air temperature cools the surface layer and eliminates stratification. Without the photosynthetic activity of Phytoplankton, all the oxygen produced during the day is consumed by heterotrophic organisms at night, and so, the ponds become anoxic.

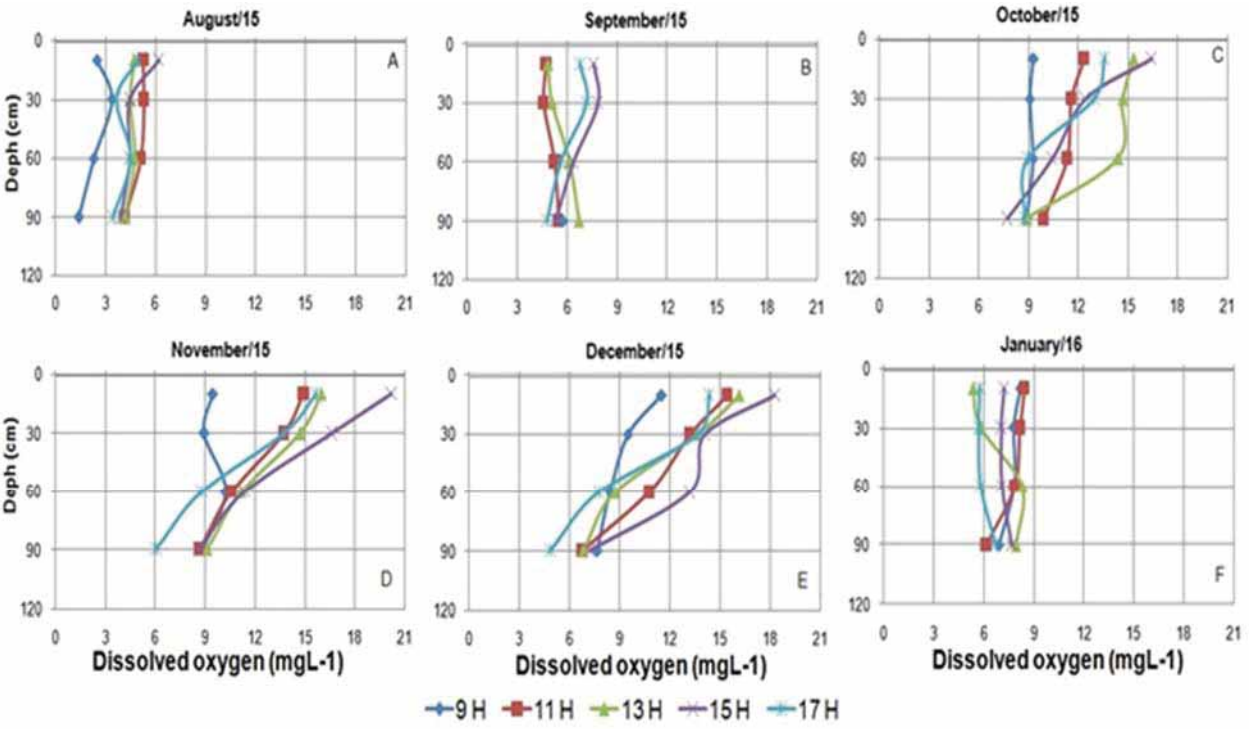


FIGURE 3. The Dissolved Oxygen (mg.L^{-1}) obtained during the months (A, B, C, D, E, F), at P2 (10 cm), P3 (30 cm), P4 (60 cm) and P5 (90 cm) points, in time 9 a.m., 11 a.m., 1 p.m., 3 p.m. and 5 p.m. of ETE polishing pond - Rio Formoso.

The phytoplankton community was represented by 12 taxa, distributed in following divisions: Cyanophyta (54%), Chlorophyta (45%) and Bacillariophyta (1%). The following taxa were identified: *Planktothrix agardhii*, *Phormidium* sp, *Merismopedia tenuissima*, *Pseudonabaena catenata*, *Microsystis* sp., *Closteriopsis acicularis*, *Desmodesmus* sp.1, *Desmodesmus* sp.2, *Monoraphidium arcuatum*, *Monoraphidium circinale*, *Monoraphidium contortum* and *Nitzschia* sp.. All taxa founded have been observed in other studies of stabilization ponds[1,3,22,23,].

Cyanophyta was dominant division in this study. On Barbalha, south of Ceará-Brazil, the same behavior was observed: the most representative groups were Cyanophyta, Chlorophyta followed by Bacillariophyta[1].

Figure 4 shows Cyanophyta density at different depths by the water column. The months showed the highest density were November/15, December/15 and January/16.

Even in the months, when there were thermal and chemical stratification, Cyanobacteria dominated the water column at all depths. So, was not possible to establish a more appropriate depth for installation of output devices in order to avoid the higher densities. As Cyanobacteria have a very versatile metabolism they can occupy different ecological niches[7].

However, the months when the Cyanophyta presented higher densities, is the greatest risk for the production of toxins.

The dominance of cyanobacteria found during the study corroborates with other studies[3,22], which found cyanobacteria in stabilization ponds treating domestic sewage. The dominance of this group in stabilization ponds can cause public health problems in the receiving water body because the toxins production[3]. In the present study was found gender *Microsystis sp*., which is seen as potentially toxic[24].

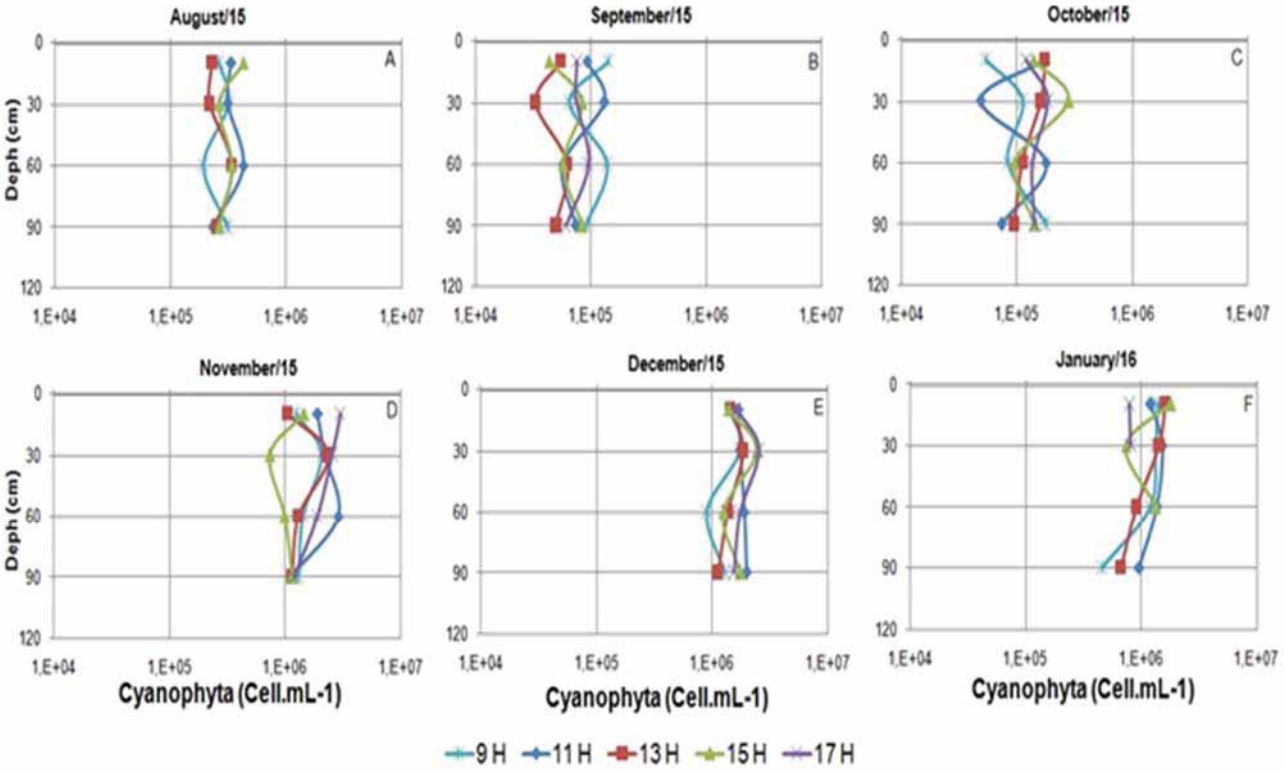


FIGURE 4. Cyanophyta density (cell.mL^{-1}) obtained during the months (A, B, C, D, E and F), at P2 (10 cm), P3 (30 cm), P4 (60 cm) and P5 (90 cm) points, in time 9 a.m., 11 a.m., 1 p.m., 3 p.m. and 5 p.m. of ETE polishing pond - Rio Formoso.

The **Figure 5** shows the densities of the Chlorophyta group. The months of October, November and January had the highest group density, but throughout the period studied the density was lower than that observed in Cyanophyta. The same pattern of dominance was observed in other ponds polimento[1].

The highest densities were observed in November (2,160 cell.mL^{-1}) (P5- August/15) and 2,360 cell.mL^{-1} (P5-September/15) at 15h, respectively. In October, November and December the highest densities were 3,820 cell.mL^{-1} (P5-9h), 3,200 cell.mL^{-1} (P5-15h) and 1,760 cell.mL^{-1} (P5-9h), respectively.

Chlorophyta was the second group most representative during the study period, in accordance with other works in polishing ponds[1]. Bacillariophyta showed no significant values of density.

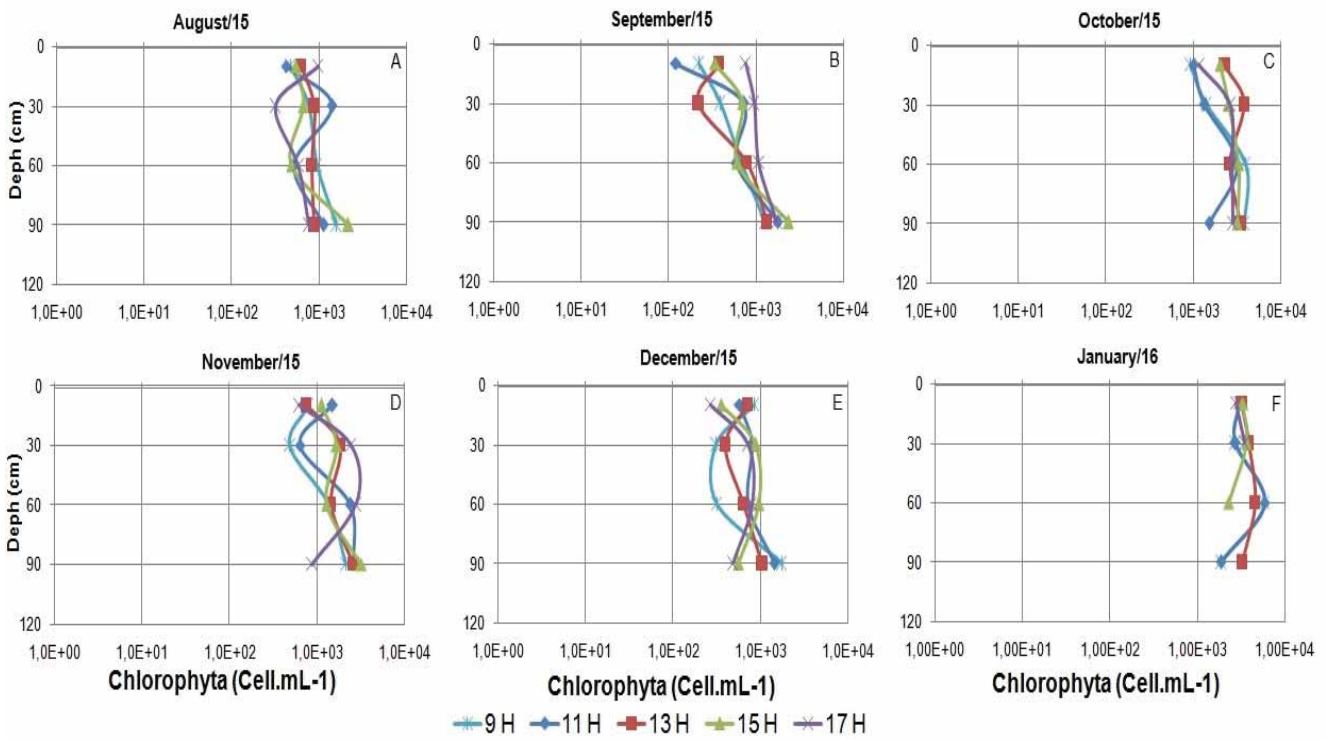


FIGURE 5. Chlorophyta density (Cell.mL) obtained during the months (A, B, C, D, E and F), at P2 in (10 cm), P3 (30 cm), P4 (60 cm) and P5 (90 cm) points, in time 9 a.m., 11 a.m., 1 p.m., 3 p.m. and 5 p.m. of ETE polishing pond - Rio Formoso.

CONCLUSION

The variations of concentrations were not observed at throughout the day of the following parameters: total nitrogen (N-TKN), total phosphorus and orthophosphate.
The turbidity increase in in the pond was observed due to the growth of algal biomass.
The months of October and November were the pond was more stratified time. On January did not occur thermal stratification. The variation in pH values were similar to that observed in relation to temperature. For dissolved oxygen the months with higher chemical stratification were October, November and December.
The phytoplankton community was dominated by Cyanobacteria throughout the monitoring period and all depths studied in the water column. The dominance of Cyanobacteria was the same regardless of stratification. It was not possible to observe variations along the water column for algae density.
However, with respect to dissolved oxygen, the superficial layers had the highest stall concentrations.

ACKNOWLEDGES

We appreciate the Higher Education Personnel Improvement Coordination (CAPES) granting post-graduate scholarship and Environmental Sanitation Laboratory of UFPE for providing necessary infrastructure for development of this study.

REFERENCES

1. Aquino, E. P., Oliveira, E. C. C. Fernandes, U. L. & Lacerda, S. R. Fitoplâncton de uma lagoa de estabilização no nordeste do Brasil. Braz. J. Aquat. Sci. Technol.15 (2011) (1):71-77.
2. Soldatelli, F. V.; Schwarzbold, A. Comunidade fitoplanctônica em lagoas de maturação, Caxias do Sul, Rio Grande do Sul, Brasil. IHERINGIA, Sér. Bot., Porto Alegre, 65 (2010), 1, 75-86, junho.
3. Vasconcelos V. M, Pereira E. Cyanobacteria diversity and toxicity in a wastewater treatment plant (Portugal). Water Research 35 (2001), (5): 1354-1357.
4. Esteves, F. A. *Fundamentos de limnologia*, 2ª. ed. Rio de Janeiro: Interciência, 602(1998).
5. Calijuri, M. C.; Alves, M. S. A.; Dos Santos, A. C. A. Cianobactérias e Cianotoxinas em Águas Continentais. 1. ed. São Carlos: Rima, 1 (2006), 109.
6. Aquino, E. P.; Lacerda, Sírleis Rodrigues; Freitas, Antônia Ionara Gonçalves de. Cianobactérias das Lagoas de Tratamento de Esgoto no Semi-árido Nordestino (Ceará, Brasil) *Revista de Botânica – Journal of Botany Florianópolis*, 39 (2010), 34-46.
7. Pastich, E.A., Silvia M. Barbosa, Lourdinha Florencio, Savia Gavazza and Mario T. Kato. The influence of environmental factors on the diel variation of phytoplankton in stabilization ponds. Interciencia, vol. 41, núm. 5, mayo, (2016), pp. 330-333. (A)
8. Villafañe, V. Reid, F. (1995). Metodos de Microscopia para la Quantificacion Del Fitoplancton. In: Alveal K, Ferrario M, Oliveira E, Sar E (eds) Manual de Métodos Ficológicos. Universidad de Concepcion. Concepcion, Chile, p. 169-185.
9. APHA, AWWA, WEF. *Standard methods for the examination of water and wastewater*. American Public Health Association, American Water Works Association, Water Environmental Federation, 22st ed. Washington (2012).
10. Kayombo S., Mbwette T.S.A, Mayo A.W., Katima J.H.Y and Jorgensen S.E. Diurnal cycles of variation of physical-chemical parameters in waste stabilization ponds. Ecological Engineering, 18 (2002), 287-291.
11. Zimmo O.R., van der Steen N.P. and Gijzen H.J. Comparision of ammonia volatilisation rates in algae and duckweed waste stabilization ponds treating domestic waste water. Water Research, 37(2003), 4587-4594.
12. Bastos, R.K.X., Dornelas, F.L., Rios, E.N., D.B.Ruas, W.Y. Okano. Dinâmica da qualidade da água e da comunidade planctônica em lagoas de polimento. Estudo de caso no Sudeste Brasileiro. Revista AIDIS de Ingeniería y Ciencias Ambientales: Investigación, desarrollo y práctica. Vol. 3, 2010, No. 1, 97-107.
13. Von Sperling, M. et al. Lagoas de estabilização. In: GONÇALVES, R.F. (ed). Desinfecção de efluentes sanitários. Rio de Janeiro: ABES/ Projeto: PROSAB 3, (2003), 277-336.
14. H. E. Maynard, M, S. K. Ouki. M and S. C. Williams. tertiary lagoons: a review of removal mechanisms and performance. Wat. Res. Vol. 33 (1999), No. 1, pp. 1±13.
15. Arauzo M. Harmful effects of un-ionised ammonia on the zooplankton community in a deep waste treatment pond. Water Research, 37(2003) 1048-1054.
16. Kellner, E. and Pires, E.C., The influence of thermal stratification on the hydraulic behavior of waste stabilization ponds. Water Science and Technology, vol. 45 (2002), no. 1, pp. 41-48.

17. Caterina Amengual-Morro, Gabriel Moyà Niell, Antoni Martínez-Taberner. Phytoplankton as bioindicator for waste stabilization ponds. Journal of Environmental Management 95 (2012)., S71e S76.
18. Pastich EA, Gavazza S, Casé MCC, Florencio L, Kato MT. Structure and dynamics of the phytoplankton community within a maturation pond in a semiarid region. Brazilian Journal of Biology 76 (2016), (1): 144-15. (B)
19. Ruochuan G. and Stefan H.G. Stratification dynamics in wastewater stabilization ponds. Water Research, 29 (1995), (8), 1909-1923.
20. Tadesse I., Green F.B. and Puhakka J.A. Seasonal and diurnal variations of temperature, pH and dissoved oxygen in advanced integrated wastewater pond system treating tannery effluent. Water Research, 38 (2004), 645-654.
21. Paerl, H.W. and Paul, V.J. Climate change: links to global expansion of harmful cyanobacteria. Water Research, vol. 46 (2012), no. 5, pp. 1349-1363.
22. Furtado ALFF, Calijuri MC, Lorenzi AS, Honda RY, Genuário DB, Fiore MF Morphological and molecular characterization of cyanobacteria from a Brazilian facultative wastewater stabilization pond and evaluation of microcystin production. Hydrobiologia: 627(2009), (1): 195-209.
23. Kotut K, Ballot A, Wiegand C, Krienitz L Toxic cyanobacteria at Nakuru sewage oxidation ponds – A potential threat to wildlife. Limnologica 40 (2010), 47-53.
24. Catarina Paula da Silva Ramos,Talita Gomes Calaça Menezes, Almerinda Agrelli, Iasmine Andreza Basilio dos Santos Alves, Jaylla Cavalcanti da Luz, Cícero Tiago Gomes da Silva, Irapuan Oliveira Pinheiro, Agenor Tavares Jácome Júnio. Cianobactérias e microcistina em águas de rio destinadas ao abastecimento de centro industrial de Caruaru, PE, Brasil. Vigil. sanit. debate (2016);4(1):27-35

CHAPTER 7.11 UTILIZACIÓN DE POLIETILENO POROSO EN APLICACIONES AMBIENTALES

P. Flores (1,2); A. Zalts (1) and J. Monterrat *(1,2)

(1) Área de Química, Instituto de Ciencias, Universidad Nacional de General Sarmiento, J.M. Gutiérrez 1150, Los Polvorines, Prov. Buenos Aires, Argentina
(2) CONICET

RESUMEN

La actividad agrícola utiliza una gran cantidad de cubiertas de polietileno (PE) para la fabricación de silobolsas, invernaderos, túneles y recubrimientos de lomo (mulching). En el caso particular de las producciones hortícolas periurbanas, estas películas plásticas quedan en el propio predio productivo incorporándose al suelo.[1] En nuestro grupo de trabajo se desarrolló un proceso de reciclado de estas cubiertas plásticas para transformarlas en un material poroso (pPE), con porosidades globales en el rango 60-80%. Este material resultó mecánicamente estable y pudo hilarse (patente en proceso de presentación).

En este trabajo se explora la aplicación del pPE para la adsorción de sustancias hidrofóbicas, tales como los hidrocarburos y los ácidos grasos que pudieran encontrarse en matrices acuosas. También se exploró la posibilidad de "decorar" el pPE con Fe^0 microparticulado para utilizarlo como un soporte catalítico para degradar paracetamol en solución ácida mediante una reacción de tipo Fenton.

Palabras claves: ácidos grasos, biodiesel, cubiertas agrícolas, polietileno.

INTRODUCCIÓN

Un problema significativo en las zonas cultivables de la Argentina (y de gran parte del mundo) es el uso intensivo de cubiertas de PE para la fabricación de silobolsas, túneles y recubrimientos de lomo (mulching). Se estima, en términos generales, que el consumo de plástico en Argentina es de 1,7 millones de toneladas, de los cuáles el 50% corresponde a envases, embalajes y plásticos agrícolas con alto contenido de PE, siendo en su mayoría enviados a enterramiento.[2]

Pasada su vida útil, estas cubiertas son normalmente abandonadas e incluso quemadas dentro del mismo predio productivo. Usualmente, estos plásticos pueden retener ciertos contaminantes propios de la actividad agrícola (por ejemplo, plaguicidas), por lo que resulta importante la búsqueda de métodos adecuados de reciclado y reutilización de los mismos. La producción de pPE podría ser una alternativa interesante.

---

*Author for correspondence: jmontser@ungs.edu.ar

En este trabajo se explora la aplicación del pPE para la adsorción y remoción de sustancias hidrofóbicas, tales como los hidrocarburos y los ácidos grasos que pudieran encontrarse en matrices acuosas. Los ácidos grasos, por ejemplo, son componentes importantes de los efluentes cloacales y tienen un valor químico importante ya que podrían ser utilizados como materia prima en procesos de obtención de biodiesel de segunda generación.

También se exploró la posibilidad de "decorar" el pPE con Fe^0 microparticulado para utilizarlo como un soporte catalítico para degradar paracetamol (molécula modelo de contaminante emergente) en solución ácida mediante una reacción de tipo Fenton. Esta reacción provoca la oxidación de materia orgánica por vía radicalaria. La generación de estos radicales requiere de Fe(II) y agua oxigenada, según las siguientes etapas[3]:

$$Fe^{2+}_{(ac)} + H_2O_{2(ac)} \rightarrow Fe^{3+}_{(ac)} + HO\bullet_{(ac)} + OH^-_{(ac)} \quad (1)$$

$$Fe^{3+}_{(ac)} + H_2O_{2(ac)} \rightarrow Fe^{2+}_{(ac)} + HOO\bullet_{(ac)} + H^+_{(ac)} \quad (2)$$

De esta manera, se busca emplear el pPE hilado con Fe como fuente de Fe(II) para así catalizar la completa degradación del paracetamol.

MATERIALES Y MÉTODOS

Materiales. Se emplearon películas de PE (Termoagro® Premium Plus) con un porcentaje no determinado de etilenvinil acetado (EVA) y 100 micrones de espesor como materia prima para la obtención del pPE. El ácido mirístico empleado fue recristalizado a partir de ácido mirístico de grado técnico. Asimismo, se emplearon los siguientes compuestos, sin purificaciones adicionales: hexano (Dorwil, p.a.), acetato de etilo (Dorwil, p.a.), ciclohexano (Anedra, p.a.), ácido oleico (Wisconsin, grado técnico), biodiesel proveniente de la planta municipal del partido de Malvinas Argentinas, Fe^0 en polvo (Aldrich, 97%, ~325 mesh), H_2O_2 30% (Anedra), KSCN (Merck, p.a.), $FeCl_3 \cdot 6H_2O$ (Anedra, r.a.), paracetamol (Sigma-Aldrich), acetonitrilo (Merck, para HPLC), ácido orto-fosfórico 85% (Riedel-de Haën) y HNO_3 concentrado (Anedra, p.a.).

Preparación de hilos de pPE(-). A 20 g de PE previamente cortado en secciones de hasta 0,5 cm x 0,5 cm, se agregaron 80 g de mezcla de solvente hidrofóbico (patente en proceso de presentación). La mezcla obtenida fue calentada gradualmente bajo agitación mecánica constante, hasta homogeneización del fundido. La mezcla fundida fue vertida en un tubo extrusor a la misma temperatura, obteniéndose hilos de no más de 1 mm de diámetro. Éstos fueron recogidos en agua fría bajo agitación constante y se los dejó secar unas horas, tras lo cual se les extrajo la mezcla de solventes hidrofóbicos con hexano en un dispositivo tipo Soxhlet. Se dejó secar a temperatura ambiente para eliminar el hexano residual en el PE. A este sistema se lo denominó pPE(-).

Preparación de hilos de pPE(-)+Fe. A 20 g de PE previamente cortado en secciones de hasta 0,5 cm x 0,5 cm, se agregaron 80 g de mezcla de solvente hidrofóbico (patente en proceso de presentación) con una proporción adecuada de Fe° finamente dividido. La **Tabla 1** muestra las masas medidas para la preparación del fundido.

TABLA 1. Masas medidas (g) para la preparación del fundido

PE	Fe°	Solvente Hidrofóbico	Sistema Total	% Fe
20,0	1,0	79,0	100,0	1,0
20,0	5,0	75,0	100,0	5,0
20,0	10,0	70,0	100,0	10,0
20,0	15,0	65,0	100,0	15,0

La mezcla obtenida fue calentada gradualmente bajo agitación mecánica constante, hasta homogeneización del fundido. La mezcla fundida fue vertida en un tubo extrusor a la misma temperatura, obteniéndose hilos de no más de 1 mm de diámetro. Éstos fueron recogidos en agua fría bajo agitación constante y se los dejó secar unas horas, tras lo cual se les extrajo la mezcla de solventes hidrofóbicos con hexano en un dispositivo tipo Soxhlet. Se dejó secar a temperatura ambiente para eliminar el hexano residual. A este sistema se lo denominó pPE(-)+Fe.

Cinética de sorción de emulsión de ácidos grasos. En un frasco de 50 mL se vertieron 30 mL de agua destilada y 0,16 g de un ácido graso en particular. Los ácidos grasos estudiados fueron: ácido mirístico, ácido oleico. También se utilizó como sorbato biodiesel (ésteres metilados de ácidos grasos). La **Tabla 2** muestra las condiciones de trabajo para cada cinética estudiada.

Tras asegurar la formación de una emulsión según el método descrito en la **Tabla 2**, se agregaron 0,2 g de hilos de pPE(-). El sistema se mantuvo en agitación durante un tiempo deseado (ver **Tabla 2**). Para el ácido mirístico y el ácido oleico, el pH se fijó con el agregado de HCl 1 M o NaOH 1 M, según fuese necesario. Se trabajó por triplicado.

Una vez alcanzado el tiempo de exposición, se retiraron los hilos de pPE(-), la mezcla resultante se acidificó a pH 1 con HCl 1 M y se extrajo el sobrenadante según lo indicado en la **Tabla 2**. La fase orgánica fue secada con Na_2SO_4 anhidro, filtrada y rotaevaporada hasta sequedad.

TABLA 2. Condiciones de trabajo para las cinéticas de sorción de ácidos grasos y biodiesel

Compuesto	Formación de la Emulsión	pH de la Emulsión	Tiempos Medidos	Extracción
Ácido Mirístico	Calentamiento a 62ºC	3, 5 y 7	0, 10, 20, 30, 60 y 90 minutos	Acetato de Etilo (3 x 20 mL)
Ácido Oleico	Sonicación por 30 minutos	3 y 5	0, 10, 20, 30, 60 y 90 minutos	Ciclohexano (3 x 20 mL)
Biodiesel	Sonicación por 30 minutos	5	0, 15, 30, 60, 90 y 120 minutos	Hexano (3 x 20 mL)

Capacidad máxima de sorción y reutilizabilidad. Para determinar la capacidad de sorción de los hilos de pPE(-), en un frasco de 50 mL se vertieron 50 mL de biodiesel y se le agregó 0,2 g de hilos de pPE(-). El sistema se dejó en agitación durante 20 hs, tras lo cual se retiró el pPE(-) y se lo pesó. La capacidad de sorción se calculó según:

$$q_m = \frac{m_f - m_0}{m_0} \qquad (1)$$

donde q_m es la capacidad máxima de sorción (en g sorbidos sobre g de sorbente), m_f es la masa del sorbente tras 20 hs de agitación y m_0 es la masa inicial del sorbente. Se trabajó por triplicado.

Una vez determinado q_m, se extrajo el biodiesel sorbido con hexano en un dispositivo de tipo Soxhlet. A continuación, se pesó nuevamente el hilo de pPE(-) para detectar posibles pérdidas de masa debida a la extracción con hexano, y se reintrodujo nuevamente en 30 mL de biodiesel, repitiendo así la determinación de q_m. Esto se realizó un total de 11 veces.

Ángulo de contacto. Se determinó la tensión superficial del pPE(-) a partir del método de Zismann y se le comparó con el del polietileno de baja densidad (PEBD). Para ello, se midió el ángulo de contacto de varias soluciones de etanol/agua y ácido acético/agua de tensión superficial conocidas. Se empleó un dispositivo de construcción propia con un microscopio digital USB. Las fotos obtenidas fueron analizadas con el software ImageJ. Como sustrato se emplearon recortes cuadrados no mayores a 5x5 cm de pPE(-) y de PEBD.

Degradación de paracetamol por reacción Fenton. A fin de eliminar el óxido férrico de la superficie metálica, 0,2 g de hilos de pPE(-)+Fe fueron lavados con 30 mL de una mezcla de HCl 10^{-2} M y H_2O_2 10^{-3} M. Esta mezcla fue sometida a agitación por 30 minutos, tras lo cual se guardaron las aguas de lavados para la determinación de Fe libre. Se trabajó por triplicado por cada proporción de Fe en los hilos de pPE(-)+Fe.

A continuación, en un frasco de 50 mL se vertieron 30 mL de solución de paracetamol 10^{-3} M en HCl 10^{-2} M (pH 2) y se le agregó el hilo de pPE(-)+Fe lavado. Esto se realizó por triplicado para cada proporción de Fe (1%, 5%, 10% y 15%). El sistema fue sometido a agitación por 30 minutos y se tomaron muestras de 1,5 mL para analizar posibles cambios en la concentración de paracetamol por sorción en el sorbente. Seguidamente, se agregaron 10 µL de H_2O_2 30% y se dejó agitando durante 3 hs, tomando alícuotas de 1,5 mL a los 30 y 180 minutos.

Las muestras tomadas fueron centrifugadas y las fracciones superiores fueron trasvasadas a sendos viales. Se determinó el paracetamol remanente por cromatografía líquida de alta resolución (HPLC), empleando una columna de fase reversa C-18 (Inertsil ODS-3 de Interscience) y una fase móvil de acetonitrilo y H_3PO_4 a pH 3 (5/95 por 2 minutos, seguido de 1 minuto a 20/80 y 4 minutos finales a 5/95) a 1 mL/min. Todas las mediciones se realizaron a 230 nm.

Determinación de hierro remanente. Se determinó el Fe total remanente en las soluciones de lavado (tres soluciones por cada proporción de Fe: 1%, 5%, 10% y 15%). Se recurrió a la determinación espectrofotométrica mediante la formación del complejo $Fe(SCN)^{2+}$. Para ello, se tomaron 5 mL de cada solución, se las diluyó con KSCN 0,1 M (a la mitad para las soluciones con hilos de pPE(-)+Fe 1%, a la vigésima parte para las soluciones con restantes) y se midió la absorbancia a 460 nm. Se empleó un espectrofotómetro Jenway 7305.

Tras la degradación del paracetamol por reacción Fenton, el Fe remanente en las soluciones también fue determinado por espectrofotometría. Como la solución adquirió un color ámbar tras la degradación (posiblemente debido a los productos de degradación del paracetamol), se tomaron alícuotas de 3-4 g y se las irradió mediante una lámpara de Hg durante 2,5 hs en presencia de 0,5 mL de HNO_3 concentrado, a fin de eliminar toda traza de compuestos orgánicos que pudiesen interferir con la determinación del Fe(III) libre. A continuación, se trasvasaron cuantitativamente las soluciones a sendos tubos Hatch®, donde fueron tratadas con KSCN 0,1 M y se midió la absorbancia a 460 nm.

RESULTADOS Y DISCUSIÓN

Cinética de sorción de emulsión de ácidos grasos. La **Tabla 3** muestra los resultados de las cinéticas de sorción para cada ácido graso.

La temperatura de trabajo es distinta para el ácido mirístico (62ºC) porque era necesaria para obtener una emulsión de ácido en agua. Para el oleico y el biodiesel, en cambio, bastó con sonicar para alcanzar la formación de la emulsión. Esto puede deberse a que el ácido mirístico es un sólido, mientras que el oleico es un líquido.

TABLA 3. Resultados de Cinéticas de Sorción

Compuesto	pH	T / ºC	$t_{50\%}$ / min	$t_{80\%}$ / min
Ácido Mirístico	3	62	5	10
	5	62	5	20
	7	62	NM	NM
Ácido Oleico	3	20	5	7
	5	20	7	17
Biodiesel	5	20	10	60

Capacidad máxima de sorción y reutilizabilidad. La **Figura 1** muestra cómo varía tanto la capacidad máxima de sorción de biodiesel como la masa del pPE(-).

Aunque la capacidad máxima de sorción (q_m) varía notablemente, siempre se mantiene entre 5 y 8 veces su propio peso en biodiesel. Asimismo, se observa que tras once ciclos de uso y extracción con hexano, la masa de pPE(-) decae solamente un 5% y se mantiene estable en torno a los 0,19 g. Esto implicaría que, para once usos, el material se mantiene estable y es capaz de sorber por lo menos 6 veces su propio peso en biodiesel en cada uso.

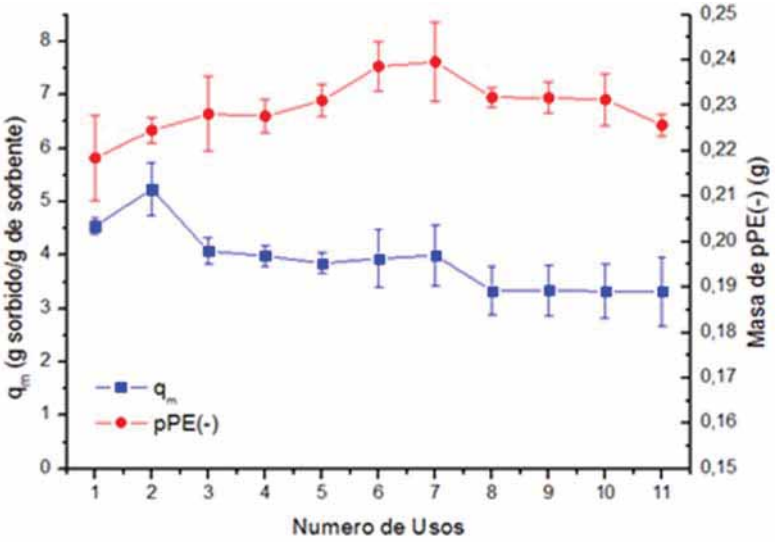


FIGURA 1. Reutilizabilidad del pPE(-)

***Ángulo de contacto*.** La **Figura 2** muestra las curvas de calibración obtenidas para el pPE(-) y para el PEBD.

Por extrapolación a cos (θ) = 1, se puede calcular la tensión superficial crítica para ambos sustratos: 25 mN/m ± 1 mN/m para el pPE(-) y 20 mN/m ± 3 mN/m para el PEBD. Si bien los intervalos de confianza no se superponen, puede observarse la poca discrepancia entre ambos valores. Esto indicaría que las propiedades superficiales de ambos sustratos no cambiarían demasiado a pesar de la transformación realizada sobre el PE.

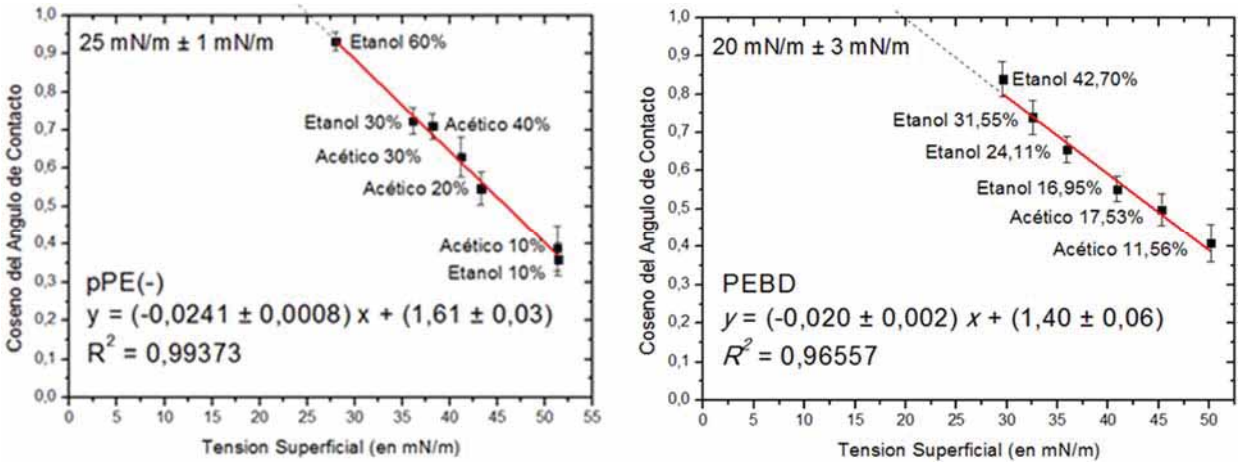


FIGURA 2. Curvas de calibración para pPE(-) y PEBD

Degradación de paracetamol por reacción Fenton. La **Tabla 4** muestra cómo varía el porcentaje de paracetamol remanente en solución para los cuatro porcentajes de Fe° en el pPE(-). No se observaron cambios en la concentración, únicamente por sorción, mayores al 1% de la concentración inicial de paracetamol

TABLA 4. Porcentaje de Paracetamol Remanente

$t_{reacc.}$/min	Contenido de Feº en pPE(-) (%)			
	1	5	10	15
30	42% ± 2%	37% ± 1%	35% ± 3%	31% ± 2%
180	2,7% ± 0,2%	2,44% ± 0,06%	2,4% ± 0,2%	4,5% ± 0,3%

Puede observarse que tras 30 minutos de reacción se mantiene entre un 31-42% de la concentración inicial de paracetamol. Si bien estos valores son similares, puede verse que el porcentaje de degradación crece con la proporción de Fe en la mezcla de preparación del pPE(-)+Fe. Finalmente, tras 180 minutos de reacción, las concentraciones son aproximadamente las mismas. De esta forma, a las 3 hs de reacción, no habría diferencia cualitativa entre cualquiera de las cuatro proporciones de Fe.

Determinación de hierro remanente. La **Tabla 5** muestra las concentraciones de Fe(III) remanente en las soluciones tras los lavado con HCl y H_2O_2, y tras la degradación del paracetamol.

La dispersión de los datos es debida a la heterogeneidad del material. Aún así, es claro que a mayor contenido de Feº en el pPE(-) mayor será la cantidad de Fe liberado al medio. Cabe destacar, además, que la concentración de Fe(III) liberado para el pPE(-)+Fe 1% es la misma tras el lavado y tras la degradación: 2 ppm, un valor menor al recomendado de 10 ppm para vertido de aguas residuales.[4]

TABLA 5. Concentraciones de Fe(III) remanente en solución (en ppm)

Etapa	Contenido de Feº en pPE(-) (%)			
	1	5	10	15
Lavado	2 ± 1	55 ± 8	75 ± 18	91 ± 26
Degradación	2 ± 2	17 ± 11	25 ± 5	145 ± 75

CONCLUSIÓN

Los resultados obtenidos muestran que el material poroso obtenido puede sorber eficientemente contaminantes hidrofóbicos presentes en medios acuosos. Resultó especialmente efectivo al momento de sorber ácidos grasos en tiempos menores a los 20 minutos al trabajar en medios ácidos. Asimismo, pudo verificarse que las propiedades superficiales del material no distan mucho a los del PEBD, al menos en cuanto a tensión superficial se refiere.

Por otra parte, el agregado de partículas de Fe° pudo realizarse mediante un método sencillo y de bajo costo. La degradación de soluciones de paracetamol también fue realizable, obteniendo degradaciones casi totales para los cuatro contenidos de Fe° elegidos. En particular, al trabajar con 1% de Fe° en el contenido inicial, se asegura la completa degradación a las 3 hs, seguida de una liberación de hasta 2 ppm de Fe(III) al medio acuoso. Cabe destacar que la reacción requirió de un medio de acidez elevada (pH 2), típico de la reacción Fenton.

AGRADECIMIENTOS

Se agradece a la Universidad Nacional de General Sarmiento y a CONICET por la financiación.

REFERENCIAS

1. L. Ramos, G. Berenstein, E. Hughes, A. Zalts, J. M. Montserrat. Polyethylene film incorporation into the horticultural soil of small periurban production units in Argentina. *Sci. Tot. Environment 523*, 74-81, **2015**.
2. Informe sectorial. Sector del Plástico. Dirección de Oferta Exportable. Dirección General de Estrategias de Comercio Exterior. Subsecretaría de Comercio Internacional. **2011**.
3. D.F. Laine, I. F. Cheng. The destruction of organic pollutants under mild reaction conditions: A review. *Microchemical Journal 85*, 183-193, **2007**.
4. Ministerio de Obras y Servicios Públicos, Administración General de Obras Sanitarias, Provincia de Buenos Aires, Resolución Nº 389/1998. **1998**.

CHAPTER 7.12 COMPARATIVE EVALUATION OF AUTOCHTHONOUS AND NON-AUTOCHTHONOUS SULFATE-REDUCING MICROBIAL COMMUNITIES IN BENCH-SCALE REACTOR MODELS

A. Giordani *(1); E. A. Hayashi (1); R. P. Rodriguez (1); L. H. S. Damasceno (1); H. Azevedo (2) and G. Brucha (1)

(1) Universidade Federal de Alfenas, Rodovia José Aurélio Vilela, 11999, Poços de Caldas, Brazil.
(2) Comissão Nacional de Energia Nuclear, Rodovia Poços de Caldas-Andradas, km 13, Poços de Caldas, Brazil.

ABSTRACT

Acid Mine Drainage (AMD) is a serious environmental problem in mining industries because of the low pH, high levels of sulfate and dissolved metals present in this wastewater. This study focus on evaluating the performance and microbial diversity on anaerobic batch reactors models, of autochthonous (INB) and non-autochthonous (LAC) biomass derived from enrichment culture of AMD sediments and pre-acclimated sludge from industrial wastewater treatment plant, respectively. Results showed a maximum sulfate removal of 57% for INB and 62% for LAC, with maximum COD removal of 29% for INB and 89% for LAC, and the maximum hydrogen sulfide production of 608 mg/L for INB and 650 mg/L for LAC reactor. Phylogenetic study of the sulfate-reducing group revealed the presence of *Desulfotomaculum*-related bacteria in INB community, while *Desulfovibrio* was the predominant genus found in LAC-derived community. The equivalent sulfate reducing activity indicated that INB culture could be used for local AMD decontamination instead of pre-acclimated sludges from wastewater treatment plants.

Keywords: acid mine drainage, anaerobic batch reactor, autochthonous, sulfate-reducing bacteria

INTRODUCTION

Mining and metallurgy exploitation of sulfide minerals can lead to the formation of Acid Mine Drainage, also called AMD[1]. The AMD generation can occur by sulfide metals exposure to air and water, what can lead to the accumulation of low pH waters, with high concentrations of sulfate and metals and, generally, low organic carbon content. AMD is a serious problem of environmental contamination and it can cause severe impacts on biodiversity and watercourses if not controlled.

Traditional chemical processes for treatment of AMD include many disadvantages as high cost of the chemical reagents, inefficient sulfate removal and large sludge generation[1]. Due to high efficiency, cost-effective and environmental safety, anaerobic techniques using biological treatment have been considered an important substitute for conventional AMD treatment.

---

*Author for correspondence: giordani.alessandra1211@gmail.com

A viable alternative is the bioremediation of AMD using Sulfate-reducing Bacteria (SRB). During metabolic transformation of organic matter, SRB have the capacity of using sulfate (SO_4^{-2}) as electron acceptor, reducing it to hydrogen sulfide (H_2S) and producing bicarbonate (HCO_3-), as shown in Reaction 1[2]:

$$SO_4^{2-} + CH_2O \rightarrow H_2S + HCO_3\text{-} \quad (1)$$

The generated bicarbonate can increase the acidic pH to neutral or alkaline values[3] and the produced sulfide makes possible to remove metals by forming stable precipitates[4] (Reaction 2):

$$H_2S + M^{2+} \rightarrow \downarrow MS + 2\ H^+ \quad (2)$$

SRB can be classified into two main groups: incomplete oxidizing SRB, which degrade organic matter incompletely to acetate and the complete oxidizing SRB, which degrade organic compound completely to carbon dioxide[5].

SRB can use a large number of organic matter as electron donors such as lactate, acetate, propionate, pyruvate, malate, ethanol[6]. The group can also exist in many locations as soil, sediments, domestic, industrial and mining wastewaters, marine and fresh waters, which can amplify the economic, environmental and biotechnological interest on this microbial communities[7]. Their ubiquitous capacity can make possible the use of autochthonous SRB on AMD treatment. In general, the use of autochthonous microorganisms is more recommended due to environmental safety and microbial adaptability issues.

The purpose of this study is to compare performance and microbial diversity of autochthonous and non-autochthonous sulfate-reducing bacteria communities in batch anaerobic reactors using Postgate C as enrichment medium. The production of sulfide and removal of sulfate were analyzed to explore the autochthonous microbial community's potential for bioremediation of AMD.

MATERIALS AND METHODS

SRB Enrichment. Enrichment of SRB was made using Postgate C medium[8] containing sodium lactate as carbon source and electron donor. Two different samples of biomass were used as inoculum. One sample derived from a stable sulfidogenic reactor using a pre-acclimated sludge from an up-flow anaerobic sludge bed reactor (UASB) treating slaughterhouse waste from an industry in Tietê, São Paulo, Brazil (here named LAC culture) and other from the sediment from an uranium mine site containing AMD located in Poços de Caldas, Minas Gerais, Brazil (INB culture). LAC culture was prepared by dissolving 10 mL of the inoculum from the sulfidogenic reactor, previously cited, on 25 mL of distillated water. INB culture consisted in uranium acid mine samples enriched in Postgate C medium. 10 mL of LAC culture (4% of inoculum) and 25 mL of INB culture (10% of inoculum) were inoculated in 500 mL anaerobic batch reactors containing 250 mL of Postgate C medium, previously sterilized and kept aseptic and under constant flow of nitrogen. The system was incubated at 30ºC, under agitation at 100 rpm for 41 days.

Physical chemical analysis. Samples were previously centrifuged using MCD-2000 HEMATOCRIT micro type centrifuge at 8000 rpm during 10 min for COD and sulfate measurements. COD, pH and concentrations of sulfate and dissolved sulfide were monitored according to APHA[9]. COD, sulfate and sulfide were determined weekly, while pH was measured only at the beginning and the end of enrichment.

Molecular Analyses. Samples of INB and LAC reactors were taken every week along one month, for Bacteria domain and SRB diversity study through PCR-DGGE analysis. It was named INB 1 and LAC 1 the collected samples on January 22th, INB 2 and LAC 2 on January 29th, INB 3 and LAC 3 on February 3rd, INB 4 and LAC 4 on February 12th , INB 5 and LAC 5 on February 19th.

DNA extraction. Total DNA was extracted using Wizard® Genomic DNA Purification Kit (Promega®), according to manufacturer's instructions. The DNA extraction was confirmed by electrophoresis (DIGEL®) on 1.5% agarose gels at 120 V for 30 min.

PCR-DGGE Analyses. For PCR analyses, 50 µl of mixtures consisting of 10 mM Tris-HCl buffer, 1.5 mM $MgCl_2$, 0.2 mM of each dNTP, 0.5 U of Taq DNA polymerase (Promega), 0.2 µmol of each primer, and 50-100 ng of DNA were used. Dissimilatory sulfite redutase subunity B gene (dsrB) was amplified by PCR using the primers DSRp2060F (5'-CAACATCGTYCAYACCCAGGG-3') and DSR4R (5'-GTGTAGCAGTTACCGCA-3')[10]. Bacterial 16S rRNA gene was amplified using the primers 968F (5'-AAC GCG AAG AAC CTT AC) and 1401R (5' CGG TGT GTA CAA GGC CCG GGA ACG). The 5' end of forward primers were GC-clamped (5' CGC CCG CCG CGC GCGGCG GGC GGG GCG GGG GCA CGG GGG G)[11]. Amplification was performed in a MaxyGene Gradient Thermal Cycler (Axygen) according to the following protocol: initial denaturation step at 94ºC for 4 min; 35 cycles of denaturation at 94ºC for 1 min, primer annealing at 55ºC for 1 min, and extension at 72ºC for 1 min; final extension step at 72ºC for 10 min. PCR amplification were confirmed by electrophoresis (DIGEL®) on 1.5% agarose gels at 120 V for 30 min.

For DGGE analyses, a Loccus Biotecnologia system was used. The conditions were 80 V at 60°C for 17 h in a 7.5% polyacrilamide gel with a 30-70% urea-formamide denaturing gradient. Bionumerics software (Applied Maths) using Dice coefficient and UPGMA method were used for study of DGGE profiles. Bands from dsrB DGGE were excised and reamplified without GC-clamp, but using the same primers as for DGGE. Wizard ® SV Gel and PCR Clean-Up System (Promega) were used for purification of reamplificated products. ABI 3730 DNA Analyzer (Perkin- Elmer) was used for sequencing reamplicated bands. Sequences alignment was done by BLASTN program, found on Geobank database.

RESULTS AND DISCUSSION

Performance of INB and LAC Reactors. Sulfate reduction was very similar for INB and LAC reactors, as shown in **Table 1**, that summarizes the performance of INB and LAC reactors. A maximum sulfate removal of 57% was obtained for INB reactor and 62% for LAC reactor. COD removal was lower in INB reactor, with only 29%, compared to the

89% removal for LAC reactor. The increase of pH was observed for the two reactors. Singh et al. (2011)[7] enriched an anaerobic digester sludge collected from sewage treatment plant using Postgate C medium in batch reactors and obtained a final pH of 8.13, a sulfate removal of 20.5% and a COD removal of 12% during 3 days of incubation. Rampinelli et al. (2008)[12] studied the growth of an isolated SRB collected from an AMD site using batch experiments containing Postgate C. The initial pH was 5.5 and 7.0, showing that the strain could growth at acid conditions, increasing pH. The removal of sulfate was 50% after 144 h.

Hydrogen sulfide production was slightly superior for LAC reactor. During 11 days of cultivation, 650 mg/L of sulfide was produced in LAC and 608 mg/L in INB reactor. Thus, the sulfidogenic activity was equivalent for INB and LAC reactors. Vainshtein et al. (2003)[13] obtained a maximum sulfide production around 100 mg/L after 38 days of cultivation. They also observed the presence of two stages of sulfate reduction of a bacterial consortium isolated from a soil sample of aerobic/anaerobic gradient ecosystem: a slow one, with no accumulation of hydrogen sulfide, and a rapid one, with sulfide accumulation. The first stage remained during 20 days, and the tiny sulfate concentration decrease was accompanied by an accumulation of unknown sulfur intermediates.

TABLE 1. Parameters obtained by physical chemical analyzes during cultivation time

Parameters	Reactor INB	Reactor LAC
Initial pH	6.65±0.10	6.20±0.10
Final pH	7.86±0.10	7.91±0.10
COD/SO_4^{2-}	1.26±0.16	1.30±0.18
Initial COD concentration (mg/L)	$(4.03\pm0.13)10^3$	$(4.76\pm0.13)10^3$
Final COD concentration (mg/L)	$(4.03\pm0.11)10^3$	$(9.04\pm0.54)10^2$
Maximum COD Removal (%)	29.1±3.4	88.8±3.7
Initial Sulfate concentration (mg/L)	$(3.95\pm0.51)10^3$	$(3.67\pm0.50)10^3$
Final Sulfate concentration (mg/L)	$(1.89\pm0.18)10^3$	$(1.52\pm0.17)10^3$
Maximum Sulfate Removal (%)	57±15	62±17
Initial Sulfide concentration (mg/L)	0.2±2.3	11.8±4.7
Final Sulfide concentration (mg/L)	308±17	449±18
Maximum Sulfide Production (mg/L)	608±27	648±27

Figure 1 shows an adaptation time of around 10 days necessary for INB culture. During this period, the SRB activity was slower in INB reactor than LAC reactor, which

can be noted by high sulfate removal and sulfide production on LAC reactor compared to INB one. For INB reactor, sulfide and sulfate concentrations remained almost the same at lag phase, with a small removal of sulfate and production of sulfide. This lag phase was not observed for LAC culture, probably because LAC biomass was pre-acclimated at lower pH values in a stable sulfidogenic reactor. Martins et al. (2009)[14] observed the presence of a lag phase when studying metal resistant sulfate-reducing bacteria to be used in acid mine drainage treatment in batch reactor under anaerobic conditions. In that study, a variety of environmental samples, as soil, sediments and sludge from wastewater treatment plants, were used as biomass source. Meier et al. (2012)[15] studied batch models containing enriched cultures from acidic sediments of a pit lake under different initials pH with high concentrations of Fe^{2+} and Al^{3+}. An extended lag phase was noted for initial pH values of 3 and 4, indicating the necessity of SRB adaptation to acidic conditions.

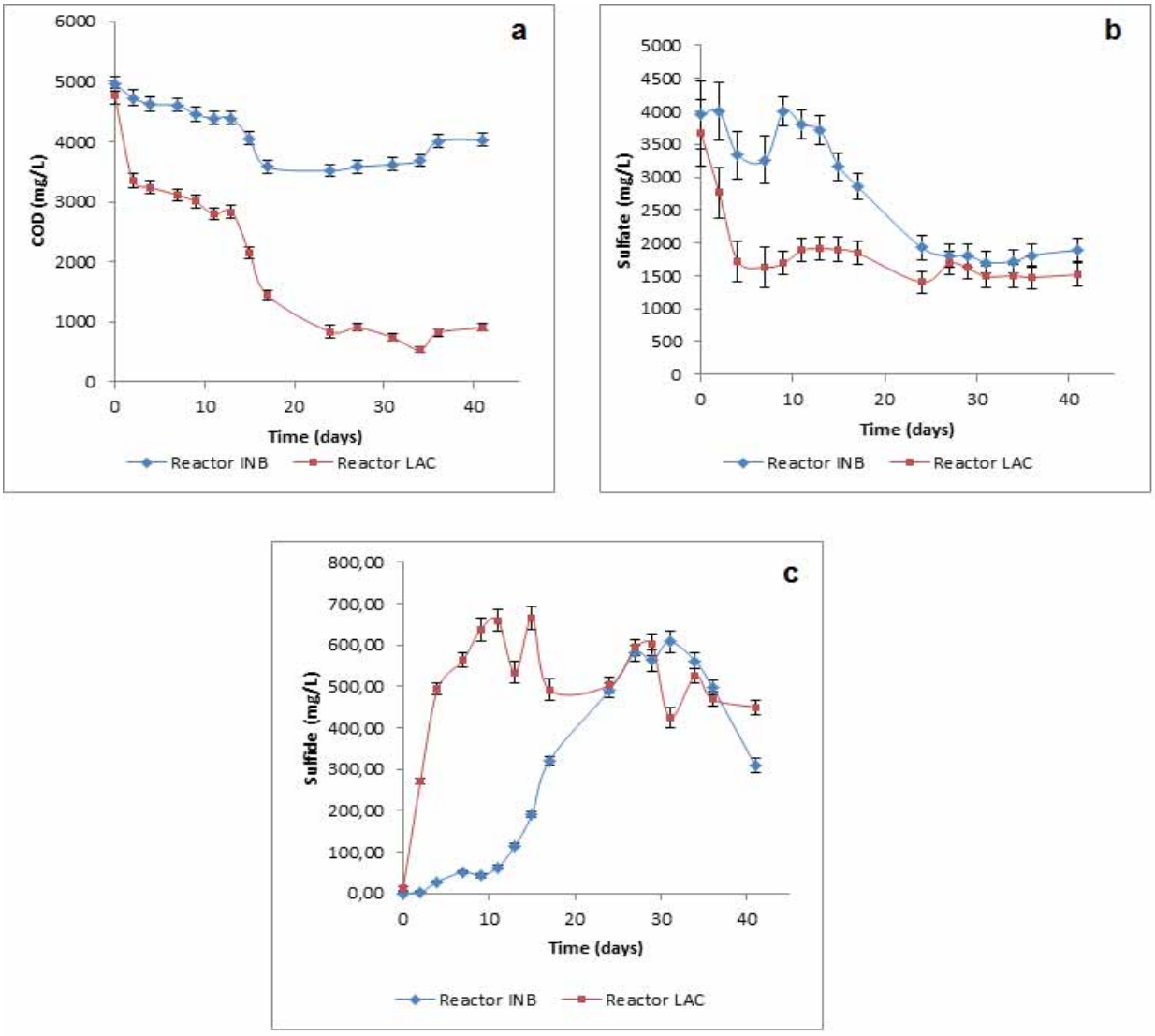


FIGURE 1. Overall performance of INB and LAC reactors during the experiment: (a) COD; (b) sulfate; (c) sulfide

After the acclimation period, necessary for INB, both cultures had equivalent SRB activity, resulting in similar values of sulfate removal and sulfide production (**Table1**). Luptakova and Kusnierova (2005)[16] studied the removal of metals from acid mine drainage using isolated SRB from natural and industrial sources, cultivated at Postgate C medium, and copper precipitation by produced hydrogen sulfide was observed. Results showed similar high sulfate-reducing activity for both cultures.

Comparative Evaluation of Microbial Community. **Figure 2** contains the DGGE profile for Bacteria domain and SRB group. It revealed that LAC and INB reactors have distinct community structures and demonstrated that Bacteria and SRB diversity remained stable during all the enrichment. Both reactors had high microbial diversity for Bacteria domain during the cultivation period (**Figure 2a**). For SRB group, INB showed a low diversity compared to the LAC reactor (**Figure 2b**). According to Martin et. al (2011)[17], the diversity in bacterial community and the functional role of the corresponding partners could be the reason to the effectiveness of AMD bioremediation.

It was not possible to amplify SRB dsrB gene during the 2 first weeks of enrichment for INB reactor (INB 1 and INB 2), as shown in **Figure 2b**. This period corresponded to the adaptation time and a low sulfide production (**Figure 1c**), and the scarce SRB numbers during this cultivation time probably was not sufficient to allow the PCR amplification and DGGE analyses of that group. This did not occur for Bacterial 16S rRNA gene PCR-DGGE analyses (**Figure 2**).

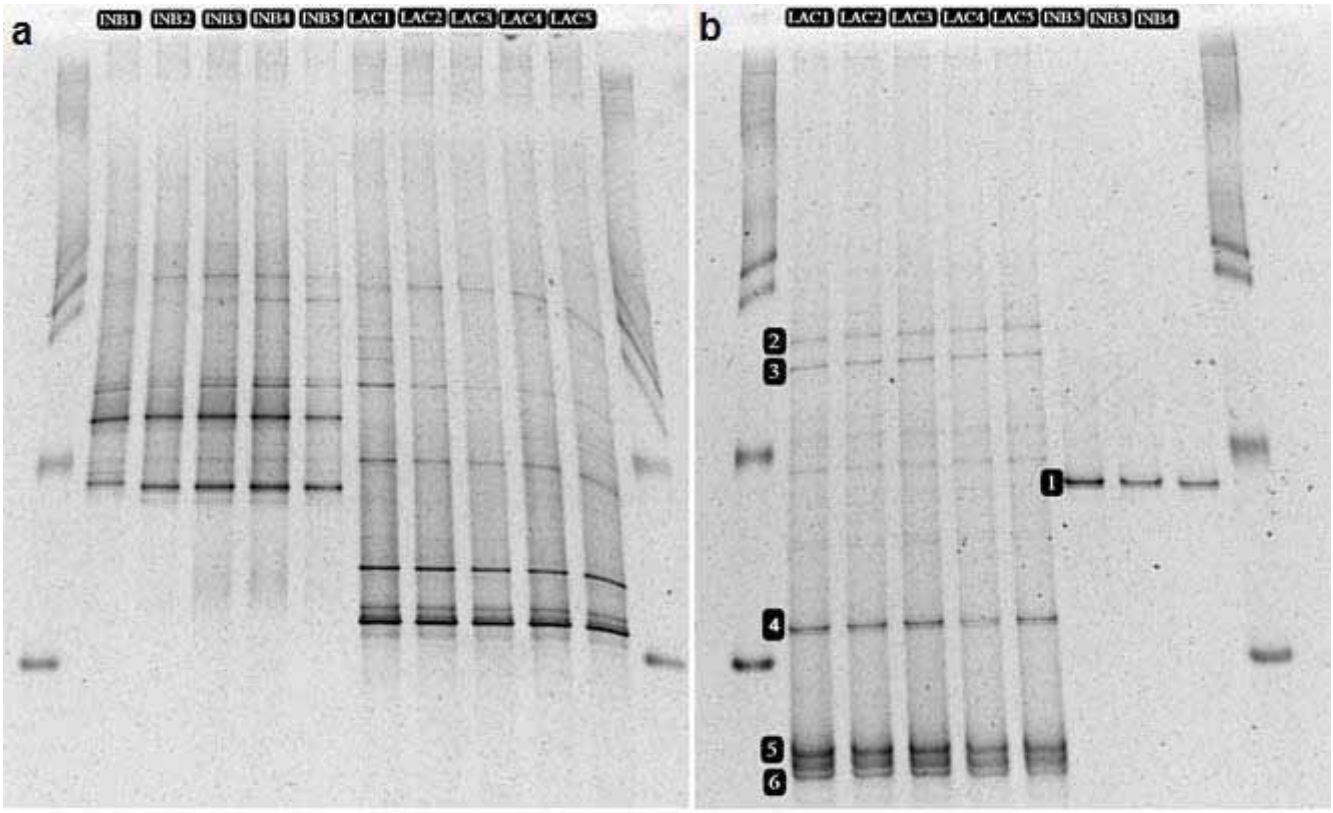


FIGURE 2. DGGE profile for Bacterial 16S rRNA gene(a) and dsrB gene (b). Numbers presented on gel image (b) represent sequenced bands

Table 2 resumes the results of chosen sequenced dsrB-DGGE bands. Band 1 (INB reactor) belonged to Clostridia group, and showed more similarity to *Desulfotomaculum* genus, while all other isolated bands (LAC reactor) belonged to Delta Proteobacteria, and had more similarity to *Desulfovibrio* genus. Band 1, was 91% similar to *Desulfotomaculum gibsoniae* DSM 7213 strain, a mesophilic SRB isolated from a freshwater ditch in Bremen, Northern Germany[18]. This SRB have the capacity of growing on a large variety of substrates including organic compounds, long-chain fatty acids and several aromatic compounds. The oxidation of substrates is usually complete to CO_2, but when high substrate concentrations are observed, acetate and other fatty acids can accumulate[19]. All LAC reactor bands were more similar to an isolated SRB strain sequence from an AMD site with sulfate reducing capacity to growth in moderately acidic conditions[12]. Band 2 closest cultured strain was *Desulfovibrio fructosivorans* JJ DSM 3600 (97%). Band 3 closest relative strain was *Desulfovibrio magneticus* RS-1, with a similarity of 95%. Band 5 was 94% related to *Desulfovibrio carbinolicus* DSM 3852 strain. Band 6 showed more similarity to *Desulfovibrio magneticus RS-1* strain (98%). *Desulfovibrio* species are the fastest growing SRB using low molecular mass organic acids as substrates, such as lactic acid, acetic acid and ethanol[20].

TABLE 2. Phylogenetic affiliations of sequenced bands from dsrB gene DGGE profiling

Band (Genbank Acession Number)	Closest Sequence (Genbank Acession Number)	Similarity (Query Cover)	Closest cultured strain (Genbank Acession Number)	Similarity (Query Cover)*	Phylogenetic group
1 (KX351203)	*Desulfotomaculum gibsoniae* DSM 7213 (CP003273)	91% (100%)	*Desulfotomaculum gibsoniae* DSM 7213 (CP003273)	91% (100%)	Clostridia[12]
2 (KX351204)	Bacterium AMD.C1 (EU086051)	97% (100%)	*Desulfovibrio fructosivorans* JJ DSM 3600 (AF418187)	97% (95%)	Delta Proteobacteria
3 (KX351205)	Bacterium AMD.C1 (EU086051)	97% (100%)	*Desulfovibrio magneticus* RS-1 (AP010904)	94% (100%)	Delta Proteobacteria
5 (KX351206)	Bacterium AMD.C1 (EU086051)	98% (100%)	*Desulfovibrio carbinolicus* strain DSM 3852	94% (100%)	Delta Proteobacteria
6 (KX351207)	Bacterium AMD.C1 (EU086051)	99% (100%)	*Desulfovibrio magneticus* RS-1 DNA (AP010904)	94% (99%)	Delta Proteobacteria

* Defined using BLASTN search tool.

When lactate is used as an electron donor for sulfate reduction, these SRB incompletely oxidize it to acetate[21]. *Desulfovibrio fructosivorans* species has a unique ability among all SRB, that is the capacity to oxidize fructose[22]. One of the co-existing species was affiliated to *Desulfovibrio magneticus*, reported by Altun et al. 2014[23] in a sulfidogenic fixed-bed column bioreactor for arsenic removal. These interesting magnetotactic bacteria are capable of producing extracellular magnetic iron sulfide.

Zhang and Wang (2016)[21] treated AMD containing high concentrations of heavy metals using sludge from a wastewater treatment plant. In the present study, band 4 (**Figure 2**), despite not registered in GenBank due to its relatively short sequence, was closely related to *Desulfovirio desulfuricans* (92%). Among the SRB in the up-flow anaerobic packed-bed bioreactor used, *Desulfovibrio desulfiricans*-related organisms and anaerobic fermentative bacteria with ability to use lactate as electron donor were detected. The study indicated that many of the electrons produced from incomplete COD oxidation could be utilized by co-existing anaerobic fermentative organisms. Thus, it could help explaining the high COD removal by LAC reactor, more than expected based on sulfate reduction (**Figure 1a**).

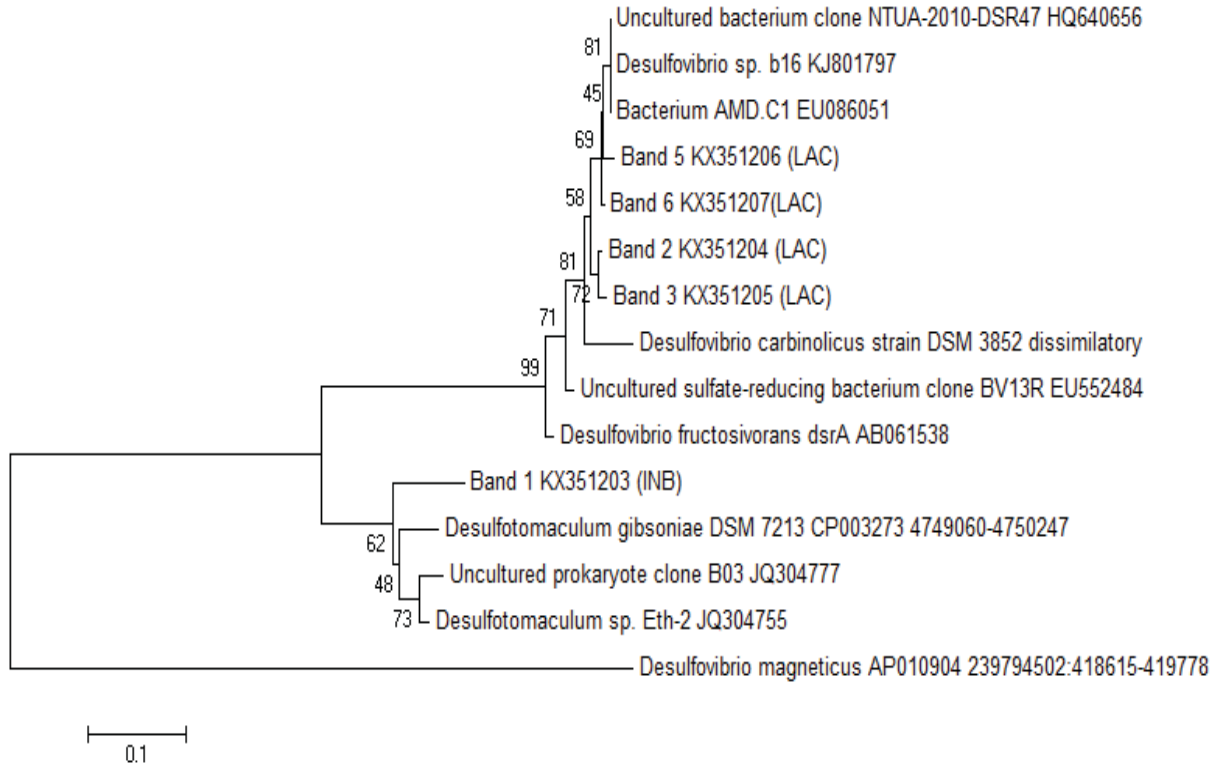


FIGURE 3. Phylogenetic tree constructed by comparing sequenced bands from dsrB gene DGGE profiling with some of the closest relatives retrieved from GenBank database. The tree was created with neighbor-joining method using MEGA 5.0 software. Bootstrap values are indicated at the nodes. The scale bar represents two nucleotide substitutions per 100 nucleotides.

A study of an AMD bioremediation system based on sulfate reduction during a high acid treatment with an initial pH of 2.0 by Lu et al. (2011)[24] showed that *Desulfotomaculum* species can tolerate high acid conditions and heavy metals presence maintaining an efficient sulfate removal. This species, which ones INB reactor showed more similarity, despite having low SRB diversity compared to *Desulfovibrio* ones, demonstrated the same performance as LAC reactor on sulfate removal, as shown in **Figure 1**. This performance results and the possibility of acid tolerance by

Desulfotomaculum organisms can bring significant environmental advances for AMD bioremediation.

CONCLUSION

The study showed that sulfate reducing activity of the selected autochthonous population was similar to a non-autochthonous one after de acclimation period, showing that INB culture could be used for local AMD treatment and probably be more indicated for bioremediation than generally tested sludges from wastewater treatment plants.
The low COD removal for INB reactor revealed that the high substrate concentrations present in Postgate C medium, probably lead to accumulation of acetate and other fatty acids. As Postgate C is a favorable medium for incomplete oxidizing SRB[25], high COD removal at LAC reactor could be explained by the syntrophic relationship of SRB with other microorganisms, such as methanogenic archaeas and acetogenic bacteria[5].
DGGE analyses demonstrated that for both reactors, Bacteria and SRB diversity stayed stable during all the cultivation period. LAC and INB had a distinct community structures both in Bacteria and SRB. Low diversity in SRB group was found in INB compared to the LAC reactor, however, it did not affect the sulfidogenic potential of INB reactor.
Phylogenetic affiliation study indicated that the main SRB representative in INB culture belonged to Desulfotomaculum genus, instead of LAC reactor, which showed more similarity to Desulfovibrio-related organisms.

ACKNOWLEDGMENTS

The authors are sincerely grateful to Fundação de Amparo à Pesquisa de Minas Gerais (FAPEMIG) for providing research funding and Universidade Federal de Alfenas (UNIFAL) for providing scholarship.

REFERENCES

1. Kaksonen A.H., Plumb J.J., Robertson W.J., Riekkola-vanhanen M., Franzmann P.D., Puhakka J.A. The performance, kinetics and microbiology of sulfidogenic fluidized-bed treatment of acidic metal- and sulfate-containing wastewater. Hydrometallurgy 83 (2006) 204–213.
2. Vitor G., Palma T.C., Vieira B., Lourenço J.P., Barros R.J., Costa M.C. Start-up, adjustment and long-term performance of a two-stage bioremediation process, treating real acid mine drainage, coupled with biosynthesis of ZnS nanoparticles and ZnS/TiO2 nanocomposites. Minerals Engineering 75 (2015) 85–93.
3. Sahinkaya E., Gunes F. M., Ucar D., Kaksonen A. H. Sulfidogenic fluidized bed treatment of real acid mine drainage water. Bioresource Technology 102 (2011) 683–689.
4. Bekmezcia O. K., Ucara D, Kaksonen A. H., Sahinkayaa E. Sulfidogenic biotreatment of synthetic acid mine drainage and sulfide oxidation in anaerobic baffled reactor. Journal of Hazardous Materials 189 (2011) 670–676.
5. Muyzer G.,Stams A. J. M. The ecology and biotechnology of sulphate-reducing bacteria. Nature Publishing Group 6 (2008) 441-454.
6. Purushothaman J. G. C.S., Shouche S. Y. Isolation and characterization of sulphate-reducing bacteria Desulfovibrio vulgaris from Vajreshwari thermal springs in Maharashtra, India. World J Microbiol Biotechnol (2008) 24:681–685.

7. Singh R., Kumar A., Kirrolia A., Kumar R., Yadav N., Bishnoi Narsi R. Lohchab Rajesh K. Removal of sulphate, COD and Cr(VI) in simulated and real wastewater by sulphate reducing bacteria enrichment in small bioreactor and FTIR study. Bioresource Technology 102 (2011) 677–682.
8. Ilham-Sungur, E.; Cansever,N.; Cotuk,A. Microbial corrosion of galvanizedsteel by a freshwater strain of sulphate reducing bactéria (dessulvovibrio sp.) Corrosion Science (2007) 1097-1109.
9. APHA - AMERICAN PUBLIC HEALTH ASSOCIATION. Standard Methods for the examination for water and wastewater. 22th ed. New York. 2012.
10. Lopez,M.V.; Dias, A. C. F.; Fasanella, C. C.; Durrer, A.; Melo, I.S.; Kuramae, E.E.; Andreote, F.D. Sulphur-oxidizing and sulphate-reducing communities in Brazilian mangrove sediments. Environmental Microbiology 16 (2014) 845-855.
11. Heuer H., Krsek M., Baker P.,Smalla K., Wellington E. M. H. Analysis of actinomycete communities by specific amplification of genes encoding 16S rRNA and gel-electrophoretic separation in denaturing gradients. Applied and Environmental Microbiology 63 (1997) 3233–3241.
12. Rampinelli L. R., Azevedo R. D., Teixeira M. C., Guerra-Sa R., Leão V. A. A sulfate-reducing bacterium with unusual growing capacity in moderately acidic conditions. Biodegradation 19 (2008) 613–619.
13. Vainshteina M., Kuschkb P.,Mattuschb J.,Vatsourinaa A., Wiessnerb A. Model experiments on the microbial removal of chromium from contaminated groundwater. Water Research 37 (2003) 1401–1405.
14. Martins M., Faleiro M. L., Barros J. R., Veríssimo A. R., Barreiros M. A., Costa M. C. Characterization and activity studies of highly heavy metal resistant sulphate-reducing bacteria to be used in acid mine drainage decontamination. Journal of Hazardous Materials 166 (2009) 706–713.
15. Meier J., Piva A., Fortin D.. Enrichment of sulfate-reducing bacteria and resulting mineral formation in media mimicking pore water metal ion concentrations and pH conditions of acidic pit lakes. FEMS Microbiol Ecol 79 (2012) 69–84.
16. Luptakova A., Kusnierova M. Bioremediation of acid mine drainage contaminated by SRB. Hydrometallurgy 77 (2005) 97–102.
17. Martins M., Santos E. S., Faleiro, M. L., Chaves, S., Tenreiro R., Barros R. J., Barreiros A., Costa M. C. Performance and bacterial community shifts during bioremediation of acid mine drainage from two Portuguese mines. International Biodeterioration & Biodegradation 65 (2011) 972-981.
18. Kuever J.,Visser M., Loeffler C., Boll M., Worm P, Sousa Z. D., Plugge M. C., Schaap J. P., Muyzer G., Pereira A.C. I., Parshina N. S., Goodwin A. L., Kyrpides C. N., Detter J., Woyke T., Chain P., Davenport W. K., Rohde M., Spring S., Klenk H., Stams J. M. A. Genome analysis of Desulfotomaculum gibsoniae strain GrollT a highly versatile Gram-positive sulfate-reducing bacterium. Standards in Genomic Sciences 9 (2014) 821-839.
19. Kuever J., Rainey A., Hippe H.. Description of Desulfotomaculum spa Groll as Desulfotomaculum gibsoniae spa nova.International Journal of Systematic Bacteriology 49 (1999) 1801 -1808.
20. Cabrera G., Perez R., Gomez J.M., Abalos A., Cantero D. Toxic effects of dissolved heavy metals on Desulfovibrio vulgaris and Desulfovibrio sp. strains. J Hazard Mater: 135(2005) 40-46.
21. Zang W., Wang H. Preparation of immobilized sulfate reducing bacteria (SRB) granules for effective bioremediation of acid mine drainage and bacterial community analysis. Minerals Engineering 92 (2016) 63–71.
22. Moreau J. W.,. Zierenberg R. A., Banfield J. F. Diversity of Dissimilatory Sulfite Reductase Genes (dsrAB) in a Salt Marsh Impacted by Long-Term Acid Mine Drainage. Applied and environmental microbiology 76 (2010) 4819–4828
23. Altun M., Sahinkaya E., Durukan I., Bektas S., Komnitsas K.. Arsenic removal in a sulfidogenic fixed-bed column bioreactor. Journal of Hazardous Materials 269 (2014) 31–37.

24. Lu J., Chen T., Wua J., Wilson C. P., Hao X., Qian J. Acid tolerance of an acid mine drainage bioremediation system based on biological sulfate reduction. Bioresource Technology 102 (2011) 10401–10406.
25. Bertolino S. M., Rodrigues I. C. B., Guerra-Sá R., Aquino S. F., Leão V. A.Implications of volatile fatty acid profile on the metabolic pathway during continuous sulfate reduction. Journal of Environmental Management 103 (2012) 15-23.

CHAPTER 7.13 DEGRADACIÓN DE GLIFOSATO A TRAVÉS DE BIOLECHOS: ESTUDIO DE DIFERENTES BIOMEZCLAS

M. Lescano *(1); D. Buschiazzo (1) and C. Zalazar (1,2)

(1) INTEC (UNL-CONICET), Colectora RN 168 km 472.5, Santa Fe, Argentina
(2) FICH-UNL-Depto Medio Ambiente, Ciudad Universitaria, Santa Fe, Argentina

RESUMEN

Los biolechos son empleados para colectar y decontaminar efluentes que contienen alta concentración de pesticidas. Consisten en una biomezcla de tres componentes: suelo, materiales lignocelulósicos y humidificantes mezclados en diferentes relaciones de volúmenes. Los materiales paja y turba fueron utilizados en los primeros biolechos construidos en Suecia. La biomezcla tiene la capacidad de retener y degradar pesticidas: el suelo provee la capacidad de retención y una comunidad activa de microorganismos para la degradación de los pesticidas; la turba incrementa la capacidad de retención y contribuye con el control de la humedad del lecho y la paja estimula la actividad de hongos lignolíticos y la formación de enzimas que degradan la lignina y una amplia variedad de pesticidas. Para aplicar este tipo de sistemas en Argentina, es necesario proponer diseños que tengan en cuenta materiales locales disponibles de bajo costo que puedan degradar la más amplia variedad de pesticidas aplicados en campo. En esta línea, el glifosato se ha convertido en el herbicida más empleado en los últimos años produciendo una alta concentración de residuos que deben ser debidamente tratados. Por lo tanto, en este estudio, se proponen nuevos diseños de biolechos para tratar efluentes contaminados con glifosato. Dado que la turba es un recurso escaso y de alto costo en Argentina, se propone sustituirlo por otro material abundante en la región y de bajo costo llamado “resaca” el cual puede ser fácilmente obtenido del río. Además, dos tipos de suelos [un suelo que ha sido cultivado con soja durante 30 años (A) y un suelo que no ha sido cultivado (B)] y dos materiales lignocelulósicos (paja de alfalfa y rastrojo de trigo) fueron ensayados. Se construyeron ocho biolechos a escala laboratorio empleando cajas de vidrio conteniendo diferentes biomezclas (B1: suelo B+ paja + resaca; B2: suelo B + rastrojo; B3: suelo B + rastrojo + resaca; B4: suelo B + paja; A1: suelo A + rastrojo + resaca; A2: suelo A + paja; A3: suelo A + paja + resaca; A4: suelo A + rastrojo). Las biomezclas fueron maduradas durante 50 días registrando la temperatura y humedad diariamente. Luego, se pulverizaron todas las cajas con una solución preparada a partir de un formulado comercial de glifosato para obtener una concentración final de 1000 mg de glifosato/kg de biomezcla seca. Los ensayos de degradación se llevaron a cabo durante 63 días tomando muestra al día 0 (inicial) y luego a los 4, 25, 45 y 63 días. Se realizó la extracción y luego la cuantificación del glifosato y su primicial metabolito, el ácido aminometilfosfónico (AMPA) mediante técnicas cromatográficas.
Los resultados mostraron que en todas las biomezclas ensayadas se logró una alta degradación de glifosato (porcentajes mayores al 90%) luego de transcurridos los 63

---

*Author for correspondence: mlescano@intec.unl.edu.ar

días de ensayo, siendo la caja A4 (suelo A + rastrojo) aquella que presentó mayor velocidad de degradación (70% de degradación de glifosato en 25 días). Además, se observó una buena capacidad de las biomezclas para degradar el AMPA. En este estudio se ha comprobado que el empleo de materiales locales de bajo costo es adecuado para construir biolechos económicos eficientes para tratar efluentes con alta concentración de glifosato.

Palabras clave: biolechos, biopurificación, glifosato

INTRODUCCIÓN

La contaminación del ambiente por pesticidas puede ser originada mediante fuentes puntuales o difusas, las cuales muchas veces no están claramente diferenciadas. La contaminación difusa ocurre durante la aplicación de pesticidas en campo, principalmente por pérdidas por escorrentía y deriva. Mientras que la contaminación puntual se origina en el lugar de preparación de los pesticidas, previo a su aplicación o cuando se produce el manejo inadecuado de los agroquímicos y sus envases.

Dentro de los agroquímicos más usados se encuentran los herbicidas seguidos de los insecticidas. En Argentina, en el año 2009, los herbicidas representaron un 63 % del mercado total mientras que los insecticidas representan un 20 %[1]. Dentro del grupo de los herbicidas, el glifosato es uno de los más utilizados en el mundo, debido a su amplio espectro, bajo costo y no selectividad y, por sobre todo, a la adopción de cultivos resistentes al glifosato. En Argentina, por ejemplo, el uso de este plaguicida se incrementó de 1 millón de litros en 1991 a 180 millones de litros en 2007[2] . Las consecuencias ambientales que provoca la contaminación con glifosato sobre la salud humana expuesta directa e indirectamente son poco conocidas y estudiadas a pesar de ser el herbicida más utilizado. Recientemente la Agencia Internacional para la Investigación sobre el Cáncer (Iarc), dependiente de la OMS, declaró al glifosato como “probable “carcinógeno para humanos. El incremento en su uso y su empleo rutinario generan sin duda una importante cantidad de residuos y, más allá de la controversia que existe actualmente sobre su toxicidad, el glifosato es un químico y como tal debe ser usado correctamente y sus residuos, tratados debidamente.

Los sistemas de biopurificación (BPS), también conocidos como biolechos, están diseñados para colectar y descontaminar líquidos residuales con alta concentración de pesticidas. Los biolechos están constituidos básicamente por excavaciones impermeabilizadas rellenas con una matriz activa biológicamente (denominada biomezcla) que consiste en suelo, material lignocelulósico y un sustrato orgánico humidificante, mezclados en relaciones de volúmenes variables y cubiertas por una capa vegetal[3]. La biomezcla es el componente más importante de los lechos biológicos ya que permite la retención y posterior degradación de los pesticidas por acción de los microorganismos que se desarrollan en la misma. La típica biomezcla (en su diseño original) está compuesta por paja, suelo y turba. La paja estimula la actividad de hongos ligninolíticos y la formación de enzimas que degradan la lignina y que también degradan una amplia variedad de pesticidas. El suelo provee capacidad de retención y es fuente de otros microorganismos degradadores de pesticidas. La turba contribuye también con capacidad de retención y a su vez ayuda a mantener la humedad de la mezcla. La capa

de césped en la superficie es importante para mantener la humedad y sirve asimismo como indicador de derrame de pesticidas[4,5]. Los biolechos han adquirido importancia en países europeos por su sencillez y eficacia en degradar y retener altas cargas de pesticidas que son descargados durante los períodos de fumigación[6,7,8]. En estos países se están realizando estudios de adaptación de los biolechos a las condiciones de cada región y en la actualidad se llevan a cabo estudios similares en otras partes del mundo tales como Perú, Guatemala, Costa Rica, México, Ecuador, Vietnam e India. Sin embargo, en Argentina, este tipo de sistemas de purificación todavía no se han implementado. Para ello es importante proponer diseños que tengan en cuentas materiales de bajo costo y disponibles en la región para preparar biomezclas que puedan emplearse para degradar glifosato. Un importante desafío es, sin duda, ensayar materiales que reemplacen la turba (componente humidificante de los primeros biolechos desarrollados en Suecia) ya que se trata de un recurso escaso y de alto valor económico[9].

En este contexto, en el presente trabajo, se prepararon diferentes biomezclas en donde se favoreció el desarrollo de hongos y/o de bacterias a fin de evaluar la eficiencia de los lechos biológicos para la degradación de un efluente con altas concentraciones de glifosato empleando materiales locales de bajo costo. La evaluación de la eficiencia de los biolechos se llevó a cabo a través de la medición de la concentración de glifosato y su principal metabolito (ácido aminometilfosfónico, AMPA) a diferentes tiempos a lo largo del ensayo.

TABLA 1. **Caracterización fisicoquímica de los suelos empleados en las biomezclas**

Determinación	Suelo A	Suelo B
Granulometría	Arena (6,4%) Limo (66,6%) Arcilla (27,0%)	Arena (52,3%) Limo (33,9 %) Arcilla (13,8%)
Carbono base seca %	1,97	2,40
Materia orgánica %	3,40	4,12
Fósforo base seca (ppm)	0,023	0,029
Densidad real base seca (g/cm^3)	2,674	2,392
Porosidad %	70,7	58,9
pH (1:2,5)	5,96	6,88
Cenizas (%) - estufa (105 -110º	94,83	92,15
Potasio (mg /kg suelo)	462,71	472,99
Calcio (mg /kg suelo)	184,88	532,96
Magnesio (mg /kg suelo)	84,36	51,89
Sodio (mg /kg suelo)	10,39	27,74
Nitrógeno (%)	0,153	0,270
Relación C/N	12,9	8,9

MATERIALES Y MÉTODOS

Se prepararon 8 biomezclas empleando dos tipos de suelo (suelo que ha sido cultivado con soja [A] y otro sin historial de cultivo de soja [B]), dos residuos lignocelulósicos (paja de alfalfa y rastrojo de trigo) y resaca de río como material humidificante. Tanto las muestras de suelo A como los residuos lignocelulósicos fueron recolectados en un campo de la localidad de Margarita (norte de la provincia de Santa Fe, Argentina). Las muestras de suelo B fueron recolectadas del jardín de un domicilio particular de la localidad de Santa Fe (Santa Fe). La resaca de río se adquirió en un vivero de la zona de Santa Fe. Las características fisicoquímicas de los materiales se muestran en las **Tablas 1** y **2**.

TABLA 2. Caracterización fisicoquímica de los materiales lignocelulósicos empleados en las biomezclas

Determinación	Paja de alfalfa	Rastrojo de trigo
Materia orgánica (%)	79,5	82,2
Materia seca (%)	89,6	91,3
Cenizas (%)	10,1	9,1
Fibra bruta (%)	23,6	38,4
Fósforo (%)	0,4	No se detecta
Nitrógeno (%)	2,3	0,46

El rastrojo y la paja se cortaron hasta obtener trozos de aproximadamente 2-3 mm. El suelo fue tamizado (3mm) para separar otros materiales presentes como piedras, palos, etc. Las biomezclas se prepararon mezclando los componentes en diversos porcentajes en volumen según se muestra en la **Tabla 3**. Las biomezclas se dispusieron en cajas de vidrio de 30 litros (20×30×50 cm).

TABLA 3. Biomezclas preparadas

Biomezcla	Suelo		Material lignocelulósico		Material Humidificante
	A %	B %	Rastrojo %	Paja %	Resaca %
B1	-	25	-	50	25
B2	-	50	50	-	-
B3	-	25	50	-	25
B4	-	50	-	50	-
A1	25	-	50	-	25
A2	50	-	-	50	-
A3	25	-	-	50	25
A4	50	-	50	-	-

La maduración fue realizada en las mismas cajas durante 50 días entre los meses de febrero – abril. Se realizaron controles de humedad y pH de las biomezclas a lo largo de toda la etapa de maduración. El pH se mantuvo en todos los casos entre 7,5 – 8 y la humedad se controló pulverizando agua destilada sobre las biomezclas cada vez que fue necesario de manera de mantenerla entre 70 – 80 %. El registro de pH y humedad se realizó con un medidor de jardín (TFA).

Finalizada la etapa de maduración, cada biolecho fue pulverizado con una solución de glifosato preparada con el formulado comercial Eskoba (Red Surcos, Argentina, 35,6% principio activo) de tal manera de obtener una concentración inicial de ingrediente activo de 1000 mg i.a./kg de biomezcla seca. Se tomaron muestras en los siguientes días de ensayo: 0 (inicial), 10, 16, 25, 43 y 63 para determinar la concentración de glifosato y AMPA. Cuando fue necesario restablecer los valores de humedad se pulverizó con agua destilada. En la **Figura 1** puede observarse una fotografía de las cajas con las biomezclas (biolechos a escala laboratorio) utilizadas para evaluar la degradación de glifosato.



FIGURA 1. Biolechos a escala laboratorio

Técnica de extracción de glifosato y AMPA. La extracción de glifosato y AMPA se llevó a cabo adaptando diferentes técnicas presentes en bibliografía[10,11,12].

Para la puesta a punto de la misma se llevaron a cabo ensayos de recuperación (variando masa de muestra, concentración y tipo de extrayente, tiempo de agitación y tratamiento de muestra), empleando la misma matriz de trabajo y aplicando concentraciones conocidas del formulado en el rango de trabajo. Se obtuvieron recuperaciones entre el 70 y 80 % para las condiciones óptimas encontradas. Se empleó una solución de KH_2PO_4 0,1 M como extrayente, filtrando el sobrenadante mediante filtros de jeringa de Nylon de 0,45 µm luego del proceso extractivo.

Técnica de cuantificación de glifosato y AMPA. La técnica de cuantifiación de glifosato y AMPA se puso a punto mediante HPLC/UV derivatizando previamente la muestra con cloruro de p-toluensulfonilo (Sigma Aldrich) adaptando la técnica de Kawai et al.[13]. La fase móvil empleada fue NaH_2PO_4 (ajustada con ácido fosfórico a pH 2,3) – Acetonitrilo (85:15). Para la derivatización, se tomó 1 mL de muestra y se le agregaron 500 µL de buffer fosfato (pH 11) y 200 µL del derivatizante calentando luego a 50 ^{0}C por 5 min. Luego se realizó la inyección, trabajando a una longitud de onda de 240 nm.

Se realizó una curva de calibrado, siendo el rango lineal 10-80 ppm y el límite de detección, LD = 10 ppm.

RESULTADOS Y DISCUSIÓN

Extracción y cuantificación. En los primeros 16 días del ensayo se registraron porcentajes de degradación de glifosato cercanos al 15% en B2, 50 % en las biomezclas B1, B3, A3 y del 30% en las biomezclas B4, A1 y A2; mientras que la A4 alcanzó el 70 %. Al tiempo de 46 días de ensayo, todas las biomezclas evaluadas superaban el 60% de degradación. En el tiempo de finalización del ensayo (63 días), las mismas alcanzaron porcentajes de degradación de glifosato mayores al 90%, siendo A4, la que presentó mayor velocidad de degradación. Las biomezclas B3, A1 y A3 también mostraron una alta velocidad de degradación (**Figura 2**). Es importante resaltar que las cuatro biomezclas que exhibieron mayor poder de degradación de glifosato (excepto B3), están constituidas mayoritariamente por suelo que ha sido cultivado por muchos años con soja (por lo tanto, estuvo expuesto a glifosato) y con rastrojo extraído del mismo campo de donde fue obtenido el suelo (a excepción de A3). Posiblemente ambos componentes contribuyan con flora microbiana ya adaptada a la presencia de glifosato y, por lo tanto, con mayor capacidad para su degradación.

Por otro lado, en la **Figura 3**, se observa claramente la formación de AMPA (intermediario) en todas las biomezclas ensayadas. En general se observa la producción de un máximo y luego una tendencia a la degradación con la evolución de los días de ensayo. Seguramente si el ensayo se hubiera prolongado (más de 63 días), se hubiera logrado reducir aún más la concentración de este intermediario.

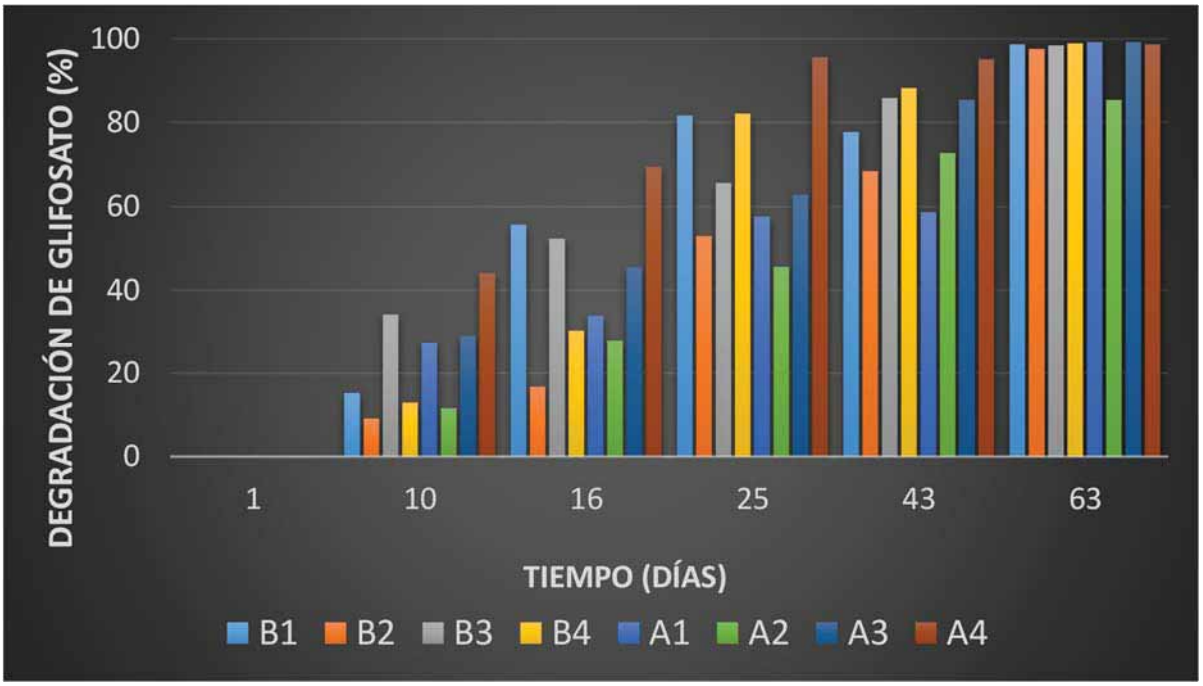


FIGURA 2. Porcentajes de degradación de glifosato en las biomezclas en función del tiempo

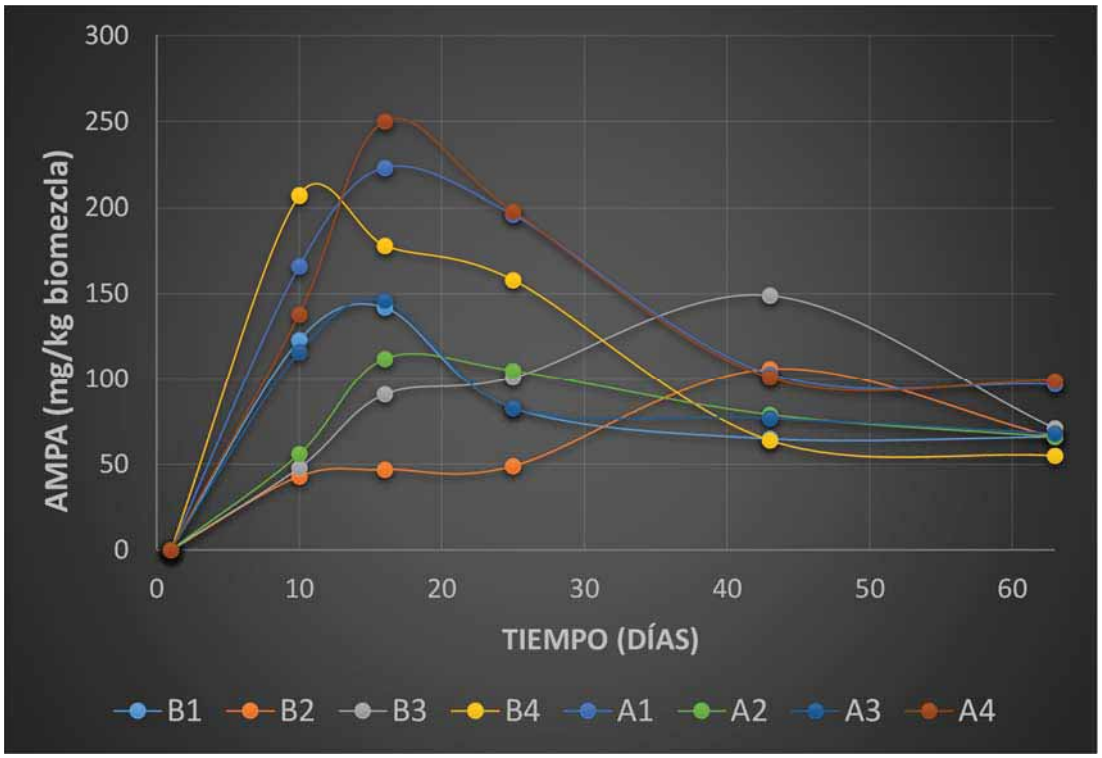


FIGURA 3. Concentración de AMPA en las biomezclas en función del tiempo de ensayo

La **Figura 4** muestra el comportamiento del glifosato y el AMPA de manera comparativa para las biomezclas más eficientes en la degradación de glifosato (B3, A1, A3 y A4), siendo la A4 aquella biomezcla en donde se obtuvo la mayor velocidad de degradación. Es importante destacar que la biomezcla A1 (con resaca de río), mostró en general una mayor capacidad para conservar la humedad lo que sugiere que este material residual puede ser conveniente para reemplazar la turba, un recurso escaso y costoso.

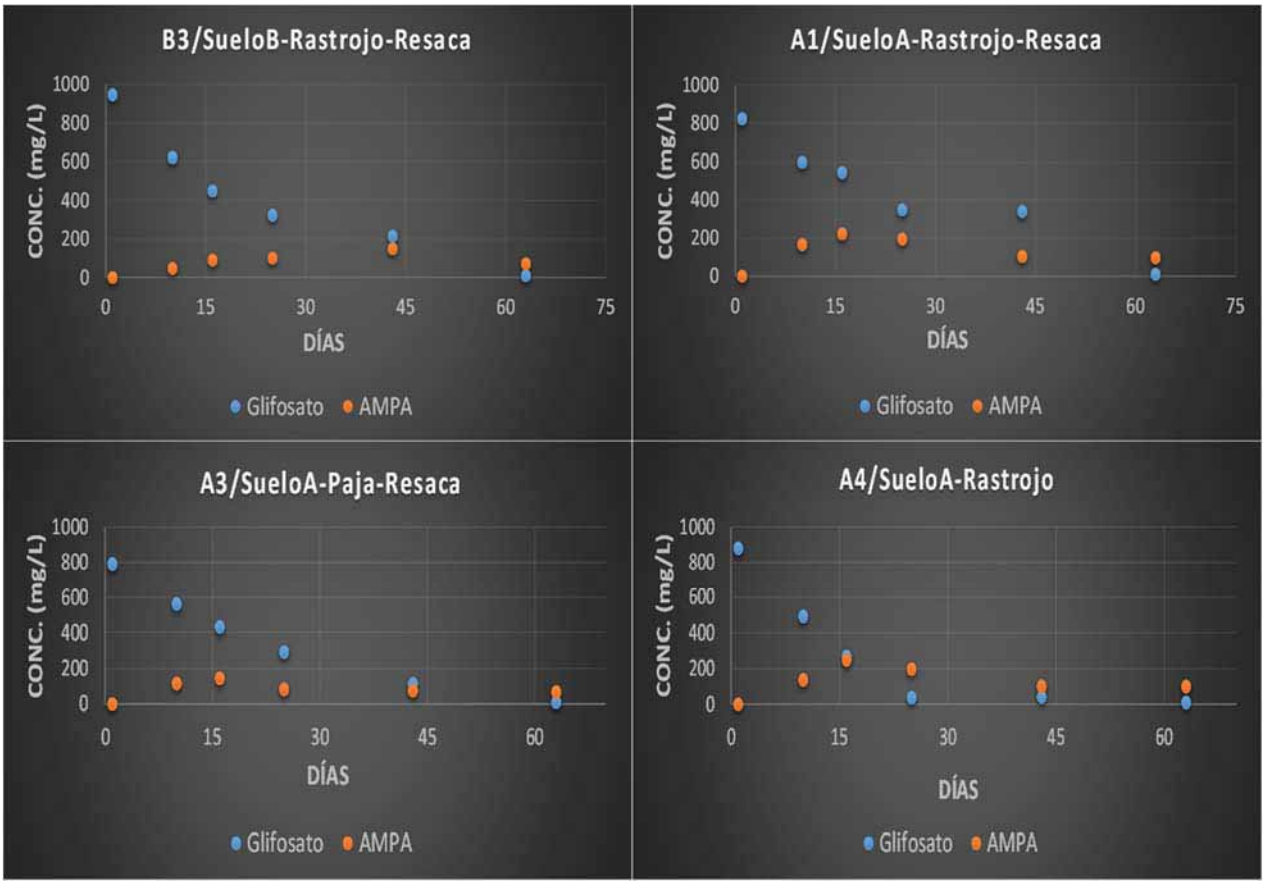


FIGURA 4. Evolución de glifosato y AMPA durante el ensayo en la biomezclas B3, A1, A3, A4

CONCLUSIÓN

En todas las biomezclas ensayadas se lograron altos porcentajes de degradación de glifosato, siendo las mezclas compuestas por suelo A (que ha sido cultivado durante muchos años con soja) y rastrojo de trigo mayoritariamente, las que presentaron mayor velocidad de degradación. También se evidenció en estas biomezclas buena capacidad para degradar el AMPA. En todos los casos se pulverizó con una solución comercial de glifosato y se emplearon materiales disponibles en la región. En el caso particular del rastrojo de trigo, es un material residual abundante y, por lo tanto, ampliamente disponible en nuestros campos. La biomezcla constituida por suelo A, rastrojo y resaca de río además presentó buena capacidad para conservar la humedad lo que hace que

sea una biomezcla ideal para construir biolechos a escala campo donde el control de variables es más difícil.
Los resultados hallados permiten establecer las biomezclas B3, A1, A3, A4 como las más eficientes para la degradación de glifosato. Sin embargo, es necesario realizar nuevos ensayos prolongando su duración para verificar que también puede lograrse una alta degradación de AMPA.
Si bien se lograron resultados preliminares promisorios, se deben realizar nuevos ensayos con las biomezclas más eficientes de manera de lograr optimizar las variables del proceso. Además, sería de gran utilidad poder evaluar en próximos ensayos la inocuidad de las biomezclas empleadas mediante la aplicación de bioensayos.

AGRADECIMIENTOS

Los autores agradecen a la Universidad Nacional del Litoral (UNL), a la Secretaría de Ciencia, Tecnología e Innovación de Santa Fe, a la ANPCyT y al Consejo Nacional de Investigaciones Científicas y Técnicas (CONICET) por el apoyo económico a través de diferentes proyectos.

REFERENCIAS

1. CASAFE (Argentine board of agricultural health and fertilisers), *Guía de Productos Fitosanitarios para la República Argentina*, Buenos Aires, Argentina, 2011.
2. Binimelis R,Pengue W,Monterroso I(2009) Transgenic treadmill: Responses to the emergence and spread of glyphosate- resistant johnsongrass in Argentina, Geoforum, 40, 623–633.
3. Castillo M. P., Torstensson L., Stenström J. Biobeds for environmental protection form pesticide use. A review. Journal of agricultural and food chemistry 56 (2008) 6206-6219.
4. Fogg P., Boxall A. B. A. Degradation of pesticides in biobeds. Journal of Agricultural and Food Chemistry 52 (2004) 5643-5652.
5. Coppola L., Castillo M., Monaci E., Vischetti C. Adaptation of the biobed composition for chlorpyrifos degradation to Southern Europe conditions. Journal of Agricultural and Food Chemistry 55 (2007) 396-401.
6. Antonious G. F. On-farm bioremediation of dimethazone and trifluralin residues in runoff water from an agricultural field. Journal of Environmental Science and Health B 47 (2012) 608-621.
7. Karanasios E., Tsiropoulos N., Karpouzas D. On-farm biopurification systems for the depuration of pesticide wastewaters: recent biotechnological advances and future perspectives. Biodegradation 23 (2012) 787-802.
8. Tortella G., Rubilar O., Castillo M., Cea M., Mella-Herrera R., Diez M. Chlorpyrifos degradation in a biomixture of biobed at different maturity stages, Chemosphere 88 (2012) 224-228.
9. Gao W., Liang J., Pizzul L., Zhang K., Castillo M. P. Evaluation of spent mushroom substrate as substitute of peat in Chinese biobeds.International Biodeterioration& Biodegradation 98 (2015) 107–112.
10. Aparicio V., De Gerónimo E., Marino D., Primost J., Carriquiriborde P., Costa J. Environmental fate of glyphosate and aminomethylphosphonic acid in surface waters and soil of agricultural basins. Chemosphere 93 (2013) 1866-1873.
11. Araujo A., Monteiro R., Abarkeli R. Effect of glyphosate on the microbial activity of two Brazilian soils. Chemosphere 52 (2003) 799-804.

12. Peruzzo P., Porta A., Ronco A. Levels of glyphosate in surface waters, sediments and soils associated with direct sowing soybean cultivation in north pampasic region of Argentina. Environmental Pollution 156 (2008) 61-66.
13. Kawai S.,Uno B. Determination of glyphosate and its major metabolite aminomethylphosphonic acid by high-performance liquid chromatography after derivatization with p-toluensulphonyl chloride. Journal of Chromatography 540 (1991) 411-415.

CHAPTER 7.14 TRATAMIENTO COMBINADO DE ADSORCIÓN Y DEGRADACIÓN BIOLÓGICA DE 4-CLOROFENOL

C. Lobo (1); N. Bertola (1) and N. Zaritzky *(1,2)

(1) Centro de Investigación y Desarrollo en Criotecnología de Alimentos CONICET La Plata, Argentina.
(2) Facultad de Ingeniería, Universidad Nacional de La Plata. Argentina.

RESUMEN

Los compuestos fenólicos están presentes en una amplia variedad de efluentes industriales, tales como los generados por petroquímicas, farmacéuticas y herbicidas. Entre los compuestos fenólicos se destacan por su toxicidad los clorofenoles. Si bien, el tratamiento biológico es adecuado para fenoles, su aplicación para elevadas concentraciones de clorofenoles tiene severas limitaciones debido al alto grado de toxicidad para los microorganismos. Por esa razón resulta recomendable la combinación de un pre-tratamiento fisicoquímico seguido de un tratamiento biológico. Si bien se han realizado numerosos estudios sobre la adsorción de compuestos fenólicos en carbón activado, los altos costos del carbón activado y la eliminación del carbón utilizado condujeron a la investigación de materiales alternativos más económicos tales como almidón catiónico insoluble quitina y quitosano. En el presente trabajo se analizó la remoción de 4-clorofenol (4CF) por medio de adsorción en quitosano comercial como un posible tratamiento previo al sistema biológico. Posteriormente, se analizó el empleo de un reactor biológico de barros activados (BA) que fueron previamente aclimatados a 300 mg/L de fenol para la biodegradación de 4CF. En los ensayos de adsorción se estudió la remoción de 7.7 mM de 4CF en suspensiones 4g/L y 1g/L de quitosano a pH=4.5, 25ºC. En los ensayos biológicos se caracterizó la biodegradación de 0.78mM de 4CF y se estudió el efecto de pulsos sucesivos sobre los BA mediante la técnica de respirometría abierta (método ISO 8192, OECD 301F). En cada ensayo la concentración de 4CF se determinó por el método colorimétrico de 4-aminoantipirina y como demanda química de oxígeno (DQO).
En los ensayos de adsorción, la remoción de 7.7mM de 4CF fue de 15.4% para 4g/L quitosano, alcanzándose el equilibrio en un tiempo de 213 h. Se analizó la cinética de adsorción de 4CF en quitosano y se realizó el ajuste a la ecuación de Langmuir obteniéndose una constante de adsorción máxima (q_{max}) de 56.3 mg4CF/g quitosano y una constante de Langmuir (K_L) de 0.004 L/mg4CF. Por otra parte, en los ensayos de respirometría se determinó que los BA previamente aclimatados a fenol fueron capaces de biooxidar 0.78 mM de 4CF, con una remoción de 99.3% para anillos arómaticos y de 82.3% para DQO. Cuando se adicionaron pulsos sucesivos de 4CF, se observó una disminución en la biodegradación. La concentración acumulada de sustrato que redujo un 50% la velocidad específica de consumo de oxígeno (EC50) fue 2.25mM para 4CF, mientras que el coeficiente de oxidación (yO/S) se mantuvo constante con un valor de 2.15mmol4CF/mmolO_2.

---

*Author for correspondence: zaritzkynoemi@gmail.com

En conclusión, la optimización de la adsorción de 4CF en biopolímeros como el quitosano podría ser una alternativa para disminuir la concentración del contaminante al inicio del tratamiento biológico, evitando así la inhibición de los barros activados.

Palabras clave: 4-clorofenol, adsorción, biodegradación, barros activados

INTRODUCCIÓN

Los compuestos fenólicos están presentes en una amplia variedad de efluentes industriales, tales como los generados por petroquímicas, farmacéuticas y herbicidas[1]. Entre los compuestos fenólicos se destacan por su toxicidad los clorofenoles, debido a ello han sido clasificados como contaminantes prioritarios por *United States Environmental Protection Agency (US EPA)*[2].

Está ampliamente demostrado que los compuestos fenólicos, en particular los clorados, son sumamente persistentes en el medio ambiente. Si bien han sido aislados numerosos microorganismos capaces de biodegradarlos en general, esta velocidad de biodegradación suele ser muy lenta. Además, estos compuestos químicos son tóxicos, recalcitrantes y potencialmente carcinogénicos y/o mutagénicos. Es decir, son considerados residuos peligrosos y regulados como tales – por ejemplo, por la Ley Nacional N°24051/92 (Argentina), con un límite de descarga en agua superficial de 30 μg L^{-1}(Decreto 831/93).

Se han estudiado diferentes métodos de remoción de clorofenoles tales como: adsorción[3], degradación fotoquímica[4] y biodegradación[5]. Varios estudios se han focalizado en la obtención de barros activados aclimatados a clorofenoles[6]. Sin embargo, este proceso requiere de largos períodos de adaptación de los microorganismos, principalmente durante la fase lag. Una estrategia promisoria para la biodegradación de clorofenoles es el empleo de biomasa con potencial afinidad para biodegradarlos.

Si bien, el tratamiento biológico es adecuado para compuestos fenólicos, su aplicación para elevadas concentraciones de clorofenoles tiene severas limitaciones debido al alto grado de toxicidad para los microorganismos. Por esa razón resulta recomendable la combinación de un pretratamiento fisicoquímico seguido de un tratamiento biológico. Si bien se han realizado numerosos estudios sobre la adsorción de compuestos fenólicos en carbón activado[7], los altos costos del carbón activado y la eliminación del carbón utilizado condujeron a la investigación de materiales alternativos más económicos tales como almidón catiónico insoluble, quitina y quitosano.

La quitina (poli-β-(1,4)-N-acetil-D-glucosamina), segundo polisacárido natural más abundante después de la celulosa, es uno de los componentes principales de las paredes celulares de los hongos, y del exoesqueleto de crustáceos e insectos; es altamente insoluble en agua y solventes orgánicos. Por desacetilación se transforma en quitosano (poli-β-(1,4)-D-glucosamina-N-acetil-D-glucosamina), un polielectrolito catiónico que exhibe características fisicoquímicas de notable interés (elevada proporción de grupos amino libres, mayor solubilidad comparada con la quitina, biocompatibilidad y biodegradabilidad), lo cual hace que presente múltiples aplicaciones en medicina, industria cosmética, agricultura, biotecnología, industria alimentaria, industria papelera, y en el tratamiento de aguas y efluentes residuales e industriales.

El objetivo del presente trabajo fue analizar la factibilidad de lograr remoción de 4-clorofenol (4CF) de aguas residuales por medio de una etapa primera de adsorción en quitosano comercial previo al tratamiento biológico para reducir los niveles de 4CF y la toxicidad del sistema. Posteriormente a esta etapa se analizó el empleo de barros activados (BA) que fueron previamente aclimatados a 300 mg/L de fenol para la biodegradación de 4CF y de pulsos sucesivos del contaminante. Los resultados obtenidos de adsorción se modelaron matemáticamente con la isoterma de adsorción de Langmuir; por otro lado, los resultados obtenidos mediante tratamiento biológico permitieron obtener constantes cinéticas y estequiométricas.

MATERIALES Y MÉTODOS

Reactivos. Las sales inorgánicas fueron de grado reactivo Anedra (San Fernando, Argentina). Quitosano de peso molecular medio, fenol (PM 94.11 Da) y 4-Clorofenol (4CF; PM 128.6 Da) de grado analítico fueron adquiridos de Sigma (St. Louis, MO, USA).

Ensayo de adsorción. Se estudió la remoción de 7.7 mM (990 mg L^{-1})de 4CF en 4g/L de quitosano pH 4.5, luego se analizó la cinética de adsorción en 1g/L de quitosano pH 4.5, 25ºC para diferentes concentraciones iniciales de 4CF 0-6.22 mM (0-800 mg L^{-1}). Luego de alcanzar el equilibrio, se determinó la concentración de 4CF. La capacidad de adsorción se calculó como:

$$q_e = \frac{(C_e - C_0) * V}{m} \quad (1)$$

donde q_e es la capacidad de adsorción en el equilibrio (mg/g), C_0 y C_e corresponden a la concentración inicial y de equilibrio de 4CF, respectivamente, V es el volumen y m la masa del adsorbente (g)[8].

Barros Activados y condiciones de cultivo. Los barros activados fueron cultivados en un reactor semicontinuo de escala laboratorio (2.5 L); el tiempo de residencia hidráulico fue de 3.3 días y el tiempo de residencia celular de 20 días. La concentración de oxígeno disuelto fue mayor a 4 mgO_2 L^{-1}, la concentración de biomasa fue de 4 g L^{-1} y el pH final fue ajustado en 8. La biomasa fue aclimatada con un medio de cultivo con 300 mg L^{-1} de fenol como única fuente de carbono y energía[9]. Cuando se alcanzó el estado estacionario, los barros activados fueron utilizados como fuente de biomasa para todos los ensayos de respirometría.

Procedimientos Analíticos. La concentración de biomasa fue determinada como sólidos suspendidos totales (SST, g L^{-1}) y la concentración de 4CF fue medida por el método 4-amino antipirina y como Demanda Química de Oxígeno (DQO, mgL^{-1})[10].

Respirometría. Los ensayos respirométricos fueron realizados en un respirómetro de 500 mL de volumen. La muestra de barros fue agitada y aireada de modo que la concentración de oxígeno disuelto (OD) en todo momento del ensayo fuera mayor a 4 mgO_2 L^{-1}. La concentración de OD se determinó con un electrodo de oxígeno (YSI modelo 5739) conectado a una computadora la cual almacenaba 1 dato/seg. Antes de cada pulso del compuesto a estudiar se determinó el coeficiente de transferencia de oxígeno (k_La) y la velocidad de respiración endógena (OUR_{en}) mediante un método dinámico[11]. Posteriormente, se determinó la velocidad de respiración exógena (OUR_{Ex}) que se produce en respuesta al agregado del compuesto ensayado. A partir del balance de masa de OD en el reactor se obtiene:

$$OUR_{Ex} = k_L a(C_e - C) - \frac{dC}{dt} \quad (2)$$

donde C_e es la concentración de OD en ausencia de sustrato y C es la concentración de OD instantánea. A partir de los datos de C en función del tiempo, se puede calcular el término dC/dt mediante una derivación numérica; asumiendo que OUR_{en} es constante durante todo el experimento; la ecuación (2) permite calcular la velocidad de respiración asociada al consumo del sustrato agregado (OUR_{Ex}). La velocidad específica de respiración (q_{Ex}, mgO_2 $gSST^{-1}$ h^{-1}) se calculó como el cociente entre OUR_{Ex} y la concentración de barros en el respirómetro (X).

El coeficiente de oxidación (yO/S) correspondiente al compuesto estudiado, representa la cantidad de oxígeno consumido por unidad de sustrato oxidado y se calculó mediante la siguiente expresión:

$$yO/S = \frac{OC}{S_0} = \frac{\int_0^t OUR_{Ex}\, dt}{S_0} \quad (3)$$

donde OC es el oxígeno consumido durante la oxidación del sustrato y S_0 es la concentración inicial del compuesto estudiado[12].

Para realizar los ensayos respirométricos se tomó una muestra de barros del reactor en estado estacionario, los barros activados aclimatados a 300 mg L^{-1} de fenol fueron centrifugados a 2000 rpm y resuspendidos en 500 mL de buffer fosfato (K_2HPO_4 1000 mg L^{-1}, KH_2PO_4 500 mg L^{-1}). El pH fue ajustado en 7,5 por medio de adición de gotas de una solución concentrada de NaOH o H_2SO_4. Los barros activados lavados fueron colocados en el respirómetro y se comenzó la aireación de los mismos hasta obtener una lectura de OD constante, la cual indicaba una velocidad de respiración endógena constante. La aireación fue mantenida estable en 1 L min^{-1} utilizando un caudalímetro de alta precisión (Bruno Schilling). Cuando se alcanzó una concentración estable de OD se adicionó un pulso de 0.78 mM (100 mg L^{-1}) de 4CF. Por otro lado, se adicionaron 5 pulsos sucesivos de 0.64 mM de 4CF.

RESULTADOS

Adsorción de 4CF en quitosano. En los ensayos de adsorción, se estudió la remoción de concentraciones elevadas de 4CF 7.7mM (990 mg L^{-1}) en 4g L^{-1} quitosano. El tiempo empleado en alcanzar el equilibrio fue de 213 h, con un porcentaje de remoción de 15.4 %.

En la **Figura 1** se muestra la isoterma de adsorción que relaciona la capacidad de adsorción y la concentración de 4CF en el equilibrio. La ecuación de Langmuir ha sido aplicada ampliamente para procesos de adsorción de compuestos orgánicos:

$$q_e = \frac{K_L q_{max} C_e}{1 + K_L C_e} \qquad (4)$$

donde q_e es la capacidad de adsorción en condiciones de equilibrio (mg g^{-1}), C_e es la concentración de 4CF en el equilibrio, q_{max} y K_L corresponden a la máxima capacidad de adsorción (mg g^{-1}) y la constante de Langmuir, respectivamente. A partir del ajuste no lineal de q_e en función de C_e[13], se obtuvo un q_{max} 56.3 mg4CF(g quitosano)$^{-1}$ y una constante de Langmuir ($K_{L=}$ 0.004 L (mg4CF)$^{-1}$ (r^2=0.98). Estos valores fueron mayores a los obtenidos por Li y col[8]; quienes obtuvieron un q_{max} =2.58 mg g^{-1}y K_L= 0.001 mg g^{-1}para quitosano a pH 7, 30°C. Zhou y col, 2014[13], estudiaron la adsorción de compuestos fenólicos en quitosano modificado químicamente.

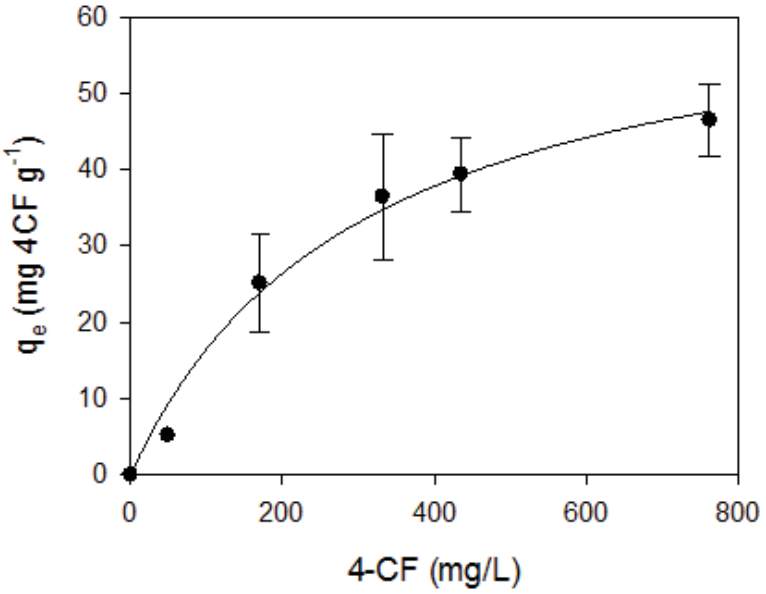


FIGURA 1. Isoterma de adsorción de 4-clorofenol en quitosano pH 4.5, 25ºC. La línea continua corresponde al ajuste a la ecuación de Langmuir

Los valores de q_{max} obtenidos para quitosano modificado con β-ciclodextrina y quitosano con salicilaldheído fueron del orden obtenido en el presente trabajo: 37.04 y 31.27 mg4CF g^{-1}., respectivamente.

Por lo tanto, la adsorción de 4CF en quitosano podría emplearse para disminuir la concentración de 4CF a un valor que sea factible para el tratamiento biológico.

Biodegradación de 4CF por barros activados aclimatados a fenol. En la **Figura 2** se encuentra la variación de la velocidad específica de respiración exógena (q_{Ex}) y la concentración de 4CF en función del tiempo para la biodegradación de 0.78mM (100 mg L^{-1}) de 4CF. Como puede observarse, cuando se adicionó el sustrato (4CF) a t=0, los valores de q_{Ex} se incrementaron rápidamente hasta un máximo valor de aproximadamente 2.3 mmolO_2 (gSST h)$^{-1}$. Finalmente, en el instante que se agotó el sustrato, q_{Ex} retorno a su valor inicial (Fig.2 línea punteada).

La remoción de 4CF obtenida en el tratamiento biológico fue de 99.3%, mientras que la remoción en DQO fue de 82.3%. Esta diferencia puede atribuirse a la acumulación de un intermediario de la biodegradación de 4CF en el sobrenadante. Los porcentajes de remoción de 4CF obtenidos fueron mayores a los informados por Sahinkaya y Dilek[14], quienes determinaron porcentajes de remoción en DQO de 46% para 0.87 mM de 4CF en barros activados. Por otra parte, Uysal y Turkman[15], calcularon porcentajes de remoción de 4CF y DQO de 98.9 y 95.3%, respectivamente. Estos valores fueron similares a los obtenidos en el presente trabajo, sin embargo estos autores emplearon barros activados alimentados con 4CF y glucosa como co-sustrato con adición de un biosurfactante. En cambio, en el presente trabajo se empleo 4CF como único sustrato.

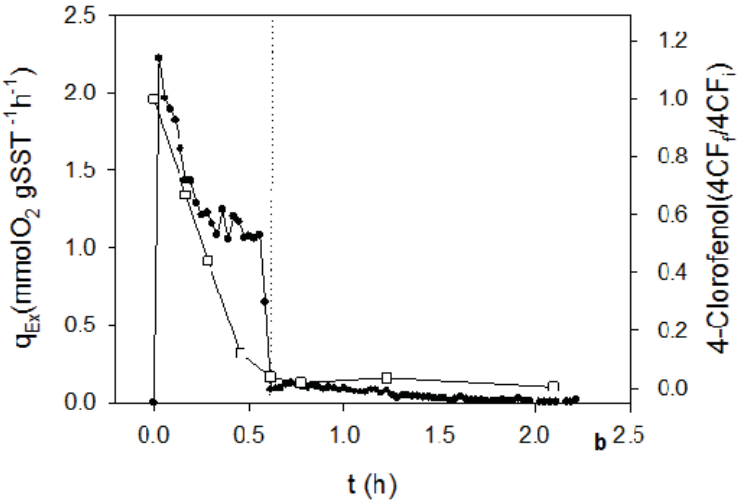


FIGURA 2. Variación de la velocidad especifica de respiración exógena (q_{Ex}; ●) y concentración de 4-clorofenol (□) en función del tiempo, durante la adición de 0.78 mM de 4-clorofenol. La línea punteada indica el tiempo en el que se agota el sustrato.

Por otro lado, se estudió el efecto de la adición de pulsos sucesivos de 4CF sobre la q_{Ex} en función del tiempo para barros activados aclimatados a fenol. Como puede observarse en la **Figura 3** los barros activados fueron capaces de bio-oxidar pulsos sucesivos de 0.64 mM (82.3 mg L^{-1}) de 4CF; sin embargo, q_{Ex} disminuyó en función de la adición de 4CF. El valor de q_{Ex} correspondiente al pulso #5 fue un 40% respecto del valor máximo inicial.

En la **Figura 3** se puede observar que los perfiles respirométricos obtenidos variaron en función de la adición de sustrato. Por ello, para evaluar el efecto tóxico de 4CF sobre la biodegradación se determinó la velocidad específica de respiración exógena media ($q_{Exmedia}$). Cuando se adiciona un pulso de sustrato oxidable en el respirómetro se obtiene un incremento de $q_{Ex,}$ una vez que el sustrato se agota el valor de q_{Ex} retorna al valor inicial. De esta forma se puede definir el tiempo de degradación total (t_d) como el intervalo en que se observa un incremento y decrecimiento del valor de q_{Ex}. Esta estrategia fue utilizada por Buitrón y col[16] como herramienta de control para optimizar el tiempo de reacción en un SBR a partir de perfiles de OD. Por lo tanto, $q_{Exmedia}$ se determinó como:

$$q_{Exmedia} = \frac{OC}{t_d\, X} \qquad (5)$$

donde OC corresponde al oxígeno consumido, t_d es el tiempo total de degradación y X es la concentración de biomasa en el respirómetro. Los valores de $q_{Exmedia}$ variaron entre 1.62 $mmolO_2\, gSST^{-1}\, h^{-1}$ ($q_{Exmedia\ 1}$ en el pulso #1) a 0.29 $mmolO_2\, gSST^{-1}\, h^{-1}$ (pulso #5). Estos valores fueron similares a los informados por Moreno-Andrade y Buitrón[5] para barros activados durante la aclimatación a 0.77 mM de 4CF en un reactor en batch secuencial.

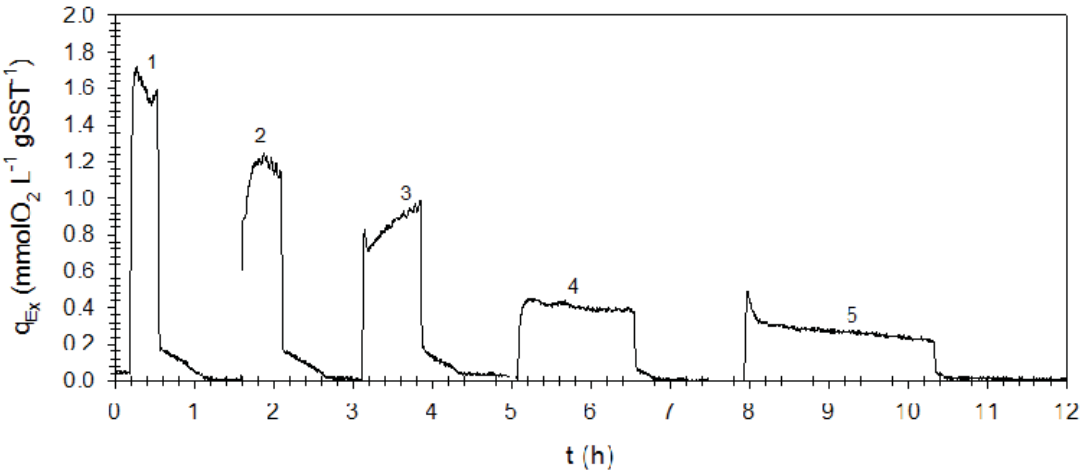


FIGURA 3. Velocidad específica de respiración exógena (q_{Ex}) en función del tiempo para barros activados aclimatados a fenol durante la adición de cinco pulsos sucesivos de 4-clorofenol

En la **Figura 4a** se puede observar la variación de $q_{Exmedia}$ para la adición de pulsos sucesivos de 4CF. Los resultados fueron expresados como porcentaje respecto del valor del primer pulso adicionado ($q_{Exmedia1}$). Para 4CF la concentración acumulada de sustrato correspondiente a $q_{Exmedia}/\ q_{Exmedia\ 1}$= 0.5 (EC50) fue de 2.25 mM (289 mg L^{-1}). Lim y col[17], calcularon un EC50= 0.77mM basado en la velocidad especifica de crecimiento de la biomasa para barros activados aclimatados a fenol. Por el contrario, Kargi y Konya[18], obtuvieron un valor de EC50 3.88 mM para la biodegradación de 4CF en barros activados previamente adaptados a degradar 4CF.

Estas diferencias en el valor de EC50 pueden deberse a el empleo de diferentes inóculos de barros activados. En el presente trabajo los barros activados fueron aclimatados a fenol como única fuente de carbono y energía, mientras que Kargi y Konya[18] emplearon 4CF como fuente de carbono durante la aclimatación de los barros activados.

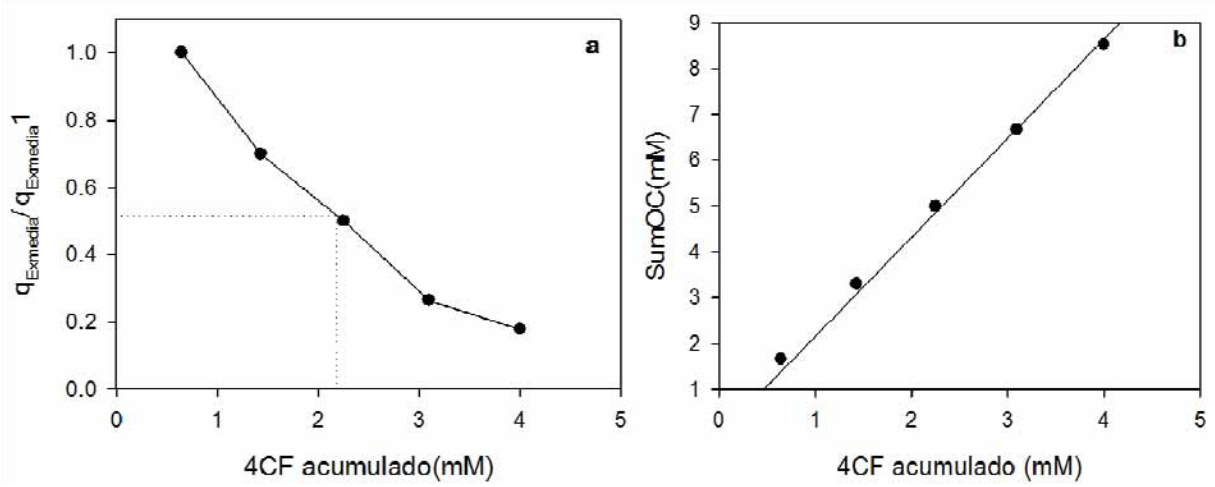


FIGURA 4. a. Variación de velocidad específica de respiración exógena media referido al valor del primer pulso ($q_{Exmedia}/ q_{Exmedia1}$) en función de la concentración acumulada de 4-clorofenol. La línea punteada señala el valor de EC50. b. Oxígeno consumido acumulado en función de la concentración acumulada de 4-clorofenol.

A partir de los respirogramas obtenidos en la Fig. 3 se calculó el coeficiente de oxidación (yO/S) para 4CF como la pendiente de la regresión lineal de la suma de oxígeno consumido (Sum(OC)) en función de la concentración acumulada de 4CF (**Figura4b**). El valor de yO/S calculado fue de 2.15 $mmolO_2$ $mmol4CF^{-1}$(r^2 = 0.99). Lamentablemente, no se encontraron en literatura valores de yO/S para la biodegradación de 4CF; sin embargo, el valor obtenido de yO/S fue similar al calculado para la adición de pulsos sucesivos de otros compuestos fenólicos en barros activados aclimatados a fenol[12], tales como resorcinol (yO/S = 2.00 $molO_2$ mol resorcinol^{-1}) y p-hidroquinona (yO/S = 2.06 $molO_2$ mol p-hidroquinona^{-1}).

CONCLUSIÓN

En el presente trabajo se estudió en una primera etapa la remoción de 4CF por medio de adsorción en quitosano a los efectos de alcanzar una concentración de 4CF adecuada para poder someterse a un proceso posterior de biodegradación en barros activados aclimatados a fenol. Cuando se adicionaron pulsos sucesivos de 4CF a los barros activados aclimatados a fenol se observó una disminución en la velocidad específica de respiración exógena debido a la inhibición de los microorganismos, sin embargo el coeficiente de oxidación yO/S se mantuvo constante.
Los resultados obtenidos demostraron que una etapa preliminar de adsorción de 4CF en biopolímeros como el quitosano podría ser una alternativa para disminuir la concentración del contaminante al inicio del tratamiento biológico, evitando así la inhibición de los barros activados.

AGRADECIMIENTOS

Los autores agradecen el financiamiento otorgado por la Agencia Nacional de Promoción Científica y Tecnológica (ANPCYT), el Consejo Nacional de Investigaciones Científicas y Técnicas (CONICET) y a la Universidad Nacional de La Plata, Argentina.

REFERENCIAS

1. Kim, J.-H., et al., Biodegradation of phenol and chlorophenols with defined mixed culture in shake-flasks and a packed bed reactor. Process Biochemistry, 2002. 37(12): p. 1367-1373.
2. EPA, U.S., TOXICOLOGICAL PROFILE FOR CHLOROPHENOLS DEPARTMENT OF HEALTH AND HUMAN SERVICES Public Health Service Agency for Toxic Substances and Disease Registry, 1999.
3. Nadavala, S.K., et al., Biosorption of phenol and o-chlorophenol from aqueous solutions on to chitosan–calcium alginate blended beads. Journal of Hazardous Materials, 2009. 162(1): p. 482-489.
4. Pino, E. and M.V. Encinas, Photocatalytic degradation of chlorophenols on TiO2-325mesh and TiO2-P25. An extended kinetic study of photodegradation under competitive conditions. Journal of Photochemistry and Photobiology A: Chemistry, 2012. 242: p. 20-27.
5. Moreno-Andrade, I. and G. Buitrón, Variation of the microbial activity during the acclimation phase of SBR system degrading 4-chlorophenol, 2004. p. 251-258.
6. Monsalvo, V.M., et al., Cometabolic biodegradation of 4-chlorophenol by sequencing batch reactors at different temperatures. Bioresource Technology, 2009. 100(20): p. 4572-4578.
7. Aktaş, Ö. and F. Çeçen, Adsorption, desorption and bioregeneration in the treatment of 2-chlorophenol with activated carbon. Journal of Hazardous Materials, 2007. 141(3): p. 769-777.
8. Li, J.-M., et al., Adsorption of phenol, p-chlorophenol and p-nitrophenol onto functional chitosan. Bioresource Technology, 2009. 100(3): p. 1168-1173.
9. Nuhoglu, A. and B. Yalcin, Modelling of phenol removal in a batch reactor. Process Biochemistry, 2005. 40(3-4): p. 1233-1239.
10. Ferro Orozco, A.M., E.M. Contreras, and N.E. Zaritzky, Simultaneous biodegradation of bisphenol A and a biogenic substrate in semi-continuous activated sludge reactors. Biodegradation, 2015: p. 1-13.
11. 11- Lobo, C., N. Bertola, and E. Contreras, Error propagation in open respirometric assays Brazilian Journal of Chemical Engineering, 2014. En proceso de edición.
12. Lobo, C.C., N.C. Bertola, and E.M. Contreras, Stoichiometry and kinetic of the aerobic oxidation of phenolic compounds by activated sludge. Bioresource Technology, 2013. 136(0): p. 58-65.
13. Zhou, L.-C., et al., Highly efficient adsorption of chlorophenols onto chemically modified chitosan. Applied Surface Science, 2014. 292: p. 735-741.
14. Sahinkaya, E. and F.B. Dilek, Biodegradation of 4-chlorophenol by acclimated and unacclimated activated sludge—Evaluation of biokinetic coefficients. Environmental Research, 2005. 99(2): p. 243-252.
15. Uysal, A. and A. Turkman, Biodegradation of 4-CP in an activated sludge reactor: Effects of biosurfactant and the sludge age. Journal of Hazardous Materials, 2007. 148(1–2): p. 151-157.
16. Buitrón, G., et al., Evaluation of two control strategies for a sequencing batch reactor degrading high concentration peaks of 4-chlorophenol. Water Research, 2005. 39(6): p. 1015-1024.
17. Lim, J.-W., J.-Z. Tan, and C.-E. Seng, Performance of phenol-acclimated activated sludge in the presence of various phenolic compounds. Applied Water Science, 2013. 3(2): p. 515-525.

18. Kargi, F. and I. Konya, COD, para-chlorophenol and toxicity removal from para-chlorophenol containing synthetic wastewater in an activated sludge unit. Journal of Hazardous Materials, 2006. 132(2–3): p. 226-231.

CHAPTER 7.15 ADVANCED OXIDATION OF COMMERCIAL HERBICIDE MIXTURES: EXPERIMENTAL DESIGN AND OPTIMIZATION

A. López (1); A. Coll (1); **M. Lescano ***(1) and C. Zalazar (1,2)

(1) INTEC-UNL-CONICET, Colectora RN 168 km 472.5, Santa Fe, Argentina.
(2) FICH-UNL-Depto. Medio Ambiente, Ciudad Universitaria, Santa Fe, Argentina.

ABSTRACT

Advanced oxidation processes (AOPs), a special kind of wastewater treatment technologies, have been successfully applied for recalcitrant pollutants degradation as herbicides. The studies are generally performed employing single compounds at higher concentrations than the values that can be found in the environment. Few researches report mixtures degradation. The application of aqueous commercial herbicide mixtures is nowadays a common practice in agriculture-intensive South American countries. Glyphosate is combined, for example, with other herbicides such as 2,4-dichlorophenoxyacetic acid (2,4-D) and atrazine. The disposal of aqueous herbicide wastewaters is still an unresolved environmental issue in many of these countries. An advanced oxidation technology as the UV/H_2O_2 process is an effective and attractive alternative to treat this kind of contamination. The UV/H_2O_2 process has certain advantages in comparison with the most renowned AOPs: relatively low capital and operating costs as well as simplicity in its operation.
In this study, the suitability of the UV/H_2O_2 process for commercial herbicide mixtures degradation (glyphosate, 2,4-D and atrazine) is studied. Optimization of specific operating conditions as H_2O_2 to Total Organic Carbon molar ratio (R) and pH is also evaluated. Experimental runs were carried out in a batch photo-reactor, samples were taken each one hour, reaction temperature was set at 25 ºC and radiation was supplied by two low-pressure mercury vapor lamps (λ = 253.7 nm). Optimization of the selected operating conditions was assessed by the response surface methodology (RSM) technique. Employing this kind of method, a minimum set of assays adequately distributed in the experimental region was tested ($1.4 \leq R \leq 17.1$, $3 \leq pH \leq 10$). A 3-level full factorial design with two factors (R, pH) was selected. The Total Organic Carbon (TOC) conversion (%) at 8 hours was defined as the response.
Results have shown that second-order polynomial regression model could well describe and predict the system behavior within the tested experimental region. The model satisfies the assumptions of the analysis of variance (ANOVA). According to the probability value for calculated Fisher F-test ($p < 0.05$) as well as the coefficient of determination value ($R^2 > 0.9$), it can be observed that the model is statistically significant. Experimental values agreed with the modeled ones confirming the significance of the model and highlighting the success of RSM for UV/H_2O_2 process modeling.

---

*Author for correspondence: mlescano@intec.unl.edu.ar

The UV/H_2O_2 process could be suitable for aqueous commercial herbicide mixtures degradation. The optimum operating conditions found could be useful for real field applications.

Keywords: herbicides, response surface methodology, UV/H_2O_2 process

INTRODUCTION

Glyphosate (N-phosphonomethyl glycine) is the most widely herbicide used in the world. In Argentina, glyphosate use increased from 1 million to more than 200 million liters[1]. The widespread use of this herbicide causes two important problems: water pollution, due to its high solubility, and the emergence of resisting weeds. In order to prevent the growth of glyphosate resistant weeds, a typical recommended management strategy is to use herbicide mixtures[2]. Application of aqueous commercial herbicide mixtures is nowadays a common practice in agriculture-intensive South American countries. Glyphosate is combined with other herbicides that have different modes of action and soil residual activity, for example 2,4-D (2,4-dichlorophenoxyacetic acid) and atrazine (2-chloro-4-ethylamino-6-isopropylamino-1,3,5-triazine)[3, 4].

The disposal of aqueous herbicide wastewaters is still an unresolved environmental issue in many of these countries. Wastewaters are frequently produced through rinsing operations of empty herbicide containers or spray equipment. The resulting complex mixture[5] may represent a potential long-term impact in human health[6].

Advanced oxidation processes (AOPs) are defined as processes based on the in situ generation of powerful oxidizing agent, such as hydroxyl radical (HO•), to effectively decontaminate waters[7]. Indeed, they constitute promising, efficient and cost-effective methods for recalcitrant pollutants removal or degradation, like herbicides[8]. An advanced oxidation technology like the UV/H_2O_2 process is a potentially effective and efficient alternative to treat herbicide wastewaters[9, 10]. Even when it is an extensive electricity consumer, the UV/H_2O_2 process can be carried out under natural conditions and has certain advantages in comparison with the most renowned AOPs: relatively low capital and operating costs and simplicity in its operation[11]. The process can reach appreciable rates of contaminants oxidation and offers a wide range of applications[12].

As Ikehata and Gamal El-Din explained[13], commercial herbicide formulations contain additives apart from active ingredients such as solvents, surfactants, carriers and intensifiers. Even so, degradation studies are generally performed employing single compounds at higher concentrations than the values that can be found in the environment[14, 15]. Few researches report mixtures degradation[16, 17]. Murcia et al.[14] proposed a possible reaction pathway focusing on the formation of chlorophenols for 2,4-D oxidation by the UV/H_2O_2 process. The authors then derived a model based on pseudo-first order kinetics. In the same direction, the work by Sarmento and Miranda[15] dealt with the formulation of a mechanistic kinetic model for atrazine degradation employing the UV/H_2O_2 process. In addition, Nienow et al.[9] and Gao et al.[10] explored the UV/H_2O_2 process optimization. These works are focused on single contaminant degradation.

Response surface methodology (RSM) is a set of mathematical and statistical methods to design experiments, build models and evaluate the effects of independent

variables (factors) on a dependent variable (response)[18, 19]. Estimation of linear, interaction and quadratic effects of input factors and the establishment of a mathematical model for prediction of the response are also accounted by this technique[19]. Response surface models have been derived for modeling and optimization of different kinds of advanced oxidation processes. Examples can be found ranging from the oxidation of synthetic organic dyes solutions by UV/H_2O_2 process[20, 21] to complex industrial wastewaters degradation by Fenton-type processes[22, 23]. Nevertheless, the UV/H_2O_2 process modeling by RSM for commercial herbicide mixtures degradation has not been reported yet.

In this study, the suitability of the UV/H_2O_2 process for commercial herbicide mixtures degradation (glyphosate, 2,4-D and atrazine) was studied. Modeling of the process response related to specific operating conditions like initial pH and H_2O_2 to Total Organic Carbon molar ratio (R) was assessed by RSM.

MATERIALS AND METHODS

Reagents. The following reagents were used: (a) commercial glyphosate formulation, 67.9% w/v as acid (Round Up Ultra Max, N-phosphonomethyl glycine salt), (b) commercial 2,4-D formulation, 50 g/100 ml as acid (Chemotécnica, dimethylamine salt) and (c) commercial atrazine formulation, 50 g/100 ml. Hydrogen peroxide solution (Ciccarelli, 30% w/w) was used as the source of H_2O_2. Catalase enzyme from bovine liver (Fluka, > 2000 units/milligram) was employed for H_2O_2 decomposition (1 unit decomposes 1 μmol H_2O_2 per minute at pH 7.00 and 25 °C). Ultrapure water (0.055 μS/cm) was used in all experimental runs.

Equipment, operating conditions and procedure. The reaction was carried out in a 110 cm^3 batch cylindrical photoreactor made of Teflon® closed with two flat, circular quartz windows. Each window permitted the interposing of one shutter to block the passage of light when necessary. Radiation was supplied by two low-pressure mercury vapor lamps with one emission wavelength at λ = 253.7 nm.

The reactor was part of a closed recycling system including: a 2000 cm^3 glass storage tank with mechanical stirring and provisions for sampling, pH and temperature measurements, and a high flow rate recirculation pump (2 L s^{-1}). A heat exchange system is also included to keep a constant reaction temperature (25 ºC). A detailed description of the experimental set up has been presented previously[24].

Experimental runs were performed by varying two of the most significant factors related to the efficiency of the UV/H_2O_2 process: initial pH (between 3 and 10) and H_2O_2 concentration (between 120 and 1450 mg L^{-1}) at constant Total Organic Carbon (TOC) initial concentration (30 mg L^{-1}) and spectral fluence rate (22.4 x 10^{-9} Einstein cm^{-2} s^{-1}). The total reaction time was 8 hours.

For each run, the following procedure was followed: with shutters on, the lamps were turned on and they were allowed for at least 30 minutes to reach electrical stability. A working mixture (1000 cm^3) of glyphosate, 2,4-D and atrazine was prepared employing ultrapure water. The pH was adjusted with H_2SO_4 (1 N) or NaOH (1 N). The mixture was added to the reactor and the recirculation was established. Once reaction temperature was constant, the shutters were removed indicating the time t = 0 of the reaction.

Samples (35 ml) were taken each one hour. After a typical run, the equipment was carefully washed.

Analyses. The following analyses were performed: H_2O_2 concentration was analyzed by a spectrophotometric method at 350 nm[25] employing a Perkin Elmer® spectrophotometer. Immediately after sampling and prior to the analysis, catalase enzyme solution was added to each sample in order to decompose the remaining H_2O_2 and to avoid further (direct) oxidation. The pH was measured with a HQ 40 d Hach® pH meter (accuracy: ±0.1) and TOC was analyzed with a Total Elementar® organic carbon analyzer.

Experimental design. Modeling of the process response related to specific operating conditions as initial pH and R ratio was assessed by RSM. A minimum set of assays adequately distributed in the experimental region was tested ($1.4 \leq R \leq 17.1$, $3 \leq pH \leq 10$). Design-Expert Software® (V10) was used for regression analysis and coefficients estimation. Initial pH and H_2O_2 concentration ranges were selected according to previous works where the UV/H_2O_2 process was applied for commercial herbicide degradation under similar experimental conditions[26, 27]. Total Organic Carbon (TOC) conversion (%) at 8 hours was defined as the response.

A 3-level full factorial design with two factors (R, pH) was selected[28]. Being k the number of factors, it is common to specify the design as a 3^k design and the level of each factor as low, center and high (coded as -1, 0 y +1, respectively). For two factors and three levels 12 experimental runs were performed. RSM is mainly based on second-order equations[28]. Therefore, a second-order polynomial model was derived for the correlation of the response:

$$Y = b_0 + b_1 X_1 + b_2 X_2 + b_{12} X_1 X_2 + b_{11} X_1^2 + b_{22} X_2^2 + e$$

Y states for the response, X_1 and X_2 are the factors in its coded form (initial pH and R ratio, respectively), b_i are the regression coefficients for linear (main) effects, b_{ii} reflect the quadratic (squared) effects and the b_{ij} account for the interaction (cross-factor) effects. The term 'e' denotes the random error component that represents different sources of variability, including effects such as measurement error on the response, non-studied factors and other sources of variability of the system itself[29].

In order to evaluate the statistical significance, adequacy and quality of fit of the second-order regression model, analysis of variance (ANOVA) statistics (Fisher F-test, adequate precision ratio, determination coefficient) and diagnostic plots (residuals) were examined. Actual (i.e., experimental) and predicted responses were then compared to validate the model.

RESULTS AND DISCUSSION

Full factorial design model. The experimental grid is presented in **Table 1**. Once the model was derived, the significance of each term was evaluated by ANOVA. Not significant terms were removed through backward elimination as the chosen strategy, with a 95% confidence level. The outliers (i.e., abnormal data points) were also discarded according to specific diagnostic plots[29]. The fitted second-order model

(without interaction) to describe and predict the system behavior is, in its non-coded form:

$$X\ TOC\ (\%) = 29.13389\ pH + 5.05947\ R - 2.06576\ pH^2 - 0.26108\ R^2 - 62.21186$$

As it can be appreciated, factors are not involved in any significant interaction (i.e., the initial pH-effect is not dependent on the R-level). On the other hand, the pH-coefficient is almost six times the R-coefficient and pH-term seems to be the most significant one (see model evaluation subsection).

As it can be expected, an optimum R-level exists whatever the level of the pH-factor. In AOPs, it has been extensively demonstrated that organic matter degradation usually increases with an increase in H_2O_2 concentration[7]. However, degradation reactions progress up to a certain limit, at which H_2O_2 starts to inhibit the photolytic degradation process[8]. Once this limit is exceeded, H_2O_2 begins to act as a HO• scavenger.

TABLE 1. 3-level full factorial design grid. Actual and predicted responses

Run	pH	R	Exp.†	Pred.
1	3 (-1)	1.5 (-1)	10.5	13.6
2	10 (+1)	1.6 (-1)	26.9	29.98
3	5 (0)	17.1 (+1)	41.4	41.99
4	10 (+1)	14.65 (+1)	41.45	40.64
5	3 (-1)	17.6 (+1)	36.5	-
6	10 (+1)	6.9 (0)	47.3	45.03
7	5 (0)	1.4 (-1)	44.5	38.39
8	5 (0)	8.3 (0)	61.2	-
9	5 (0)	7.85 (0)	53.6	55.44
10	5 (0)	7.9 (0)	56.5	55.49
11	5 (0)	7.8 (0)	50.7	55.39
12	3 (-1)	8.6 (0)	33.9	30.8

† Outliers: runs 5 and 8.

The scavenging effect and the existence of an optimum R-level are shown through the corresponding quadratic term of the model, preceded by a minus sign. The existence of an optimum initial operating pH can also be anticipated, for each H_2O_2 concentration (i.e., for each R-level). In this sense, for a given H_2O_2 concentration TOC conversion increases for higher pH-levels up to a certain value where it begins to decrease.

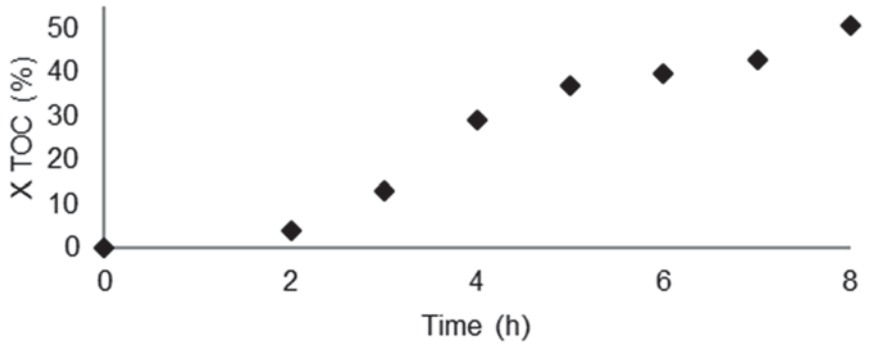


FIGURE 1. TOC conversion (%) for pH (initial) = 5 and R = 7.8

Conditions for highest TOC conversion were obtained for center level of both factors (see **Table 1** and **Figure 1**). The H_2O_2 conversion for such conditions is also shown in **Figure 2**. The optimum operating conditions to maximize the TOC conversion were evaluated employing a numerical technique based on the fitted model and the factors in their critical range as the constraints. The conditions found were: pH (initial) = 7.05 and R = 9.69 for 65.02% TOC conversion.

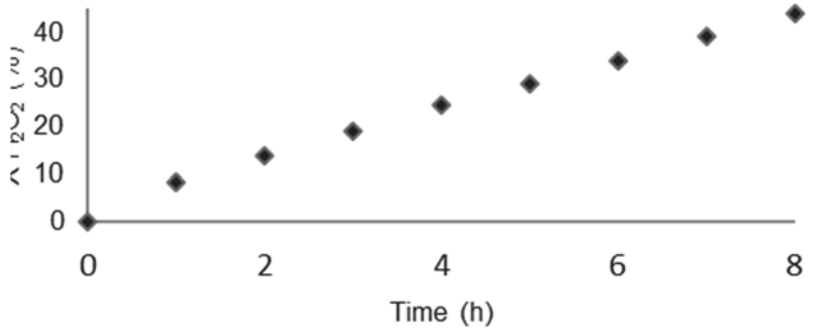


FIGURE 2. H_2O_2 conversion (%) for pH (initial) = 5 and R = 7.8

In order to show the effect of each factor in TOC conversion, a 3-D plot based on the fitted model is presented in **Figure 3**.

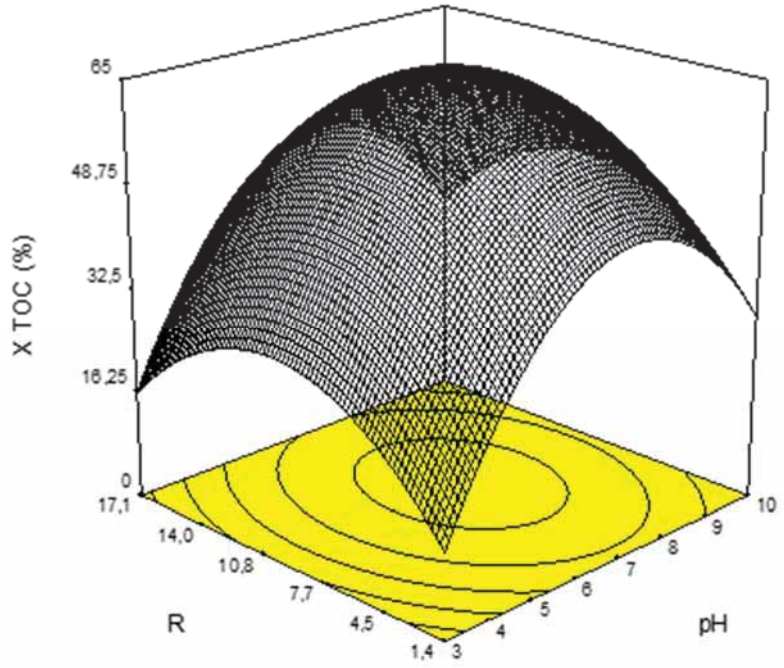


FIGURE 3. Response surface plot for TOC conversion (%) as a function of initial pH and R ratio

***Model evaluation: variance analysis*.** The statistical significance of the regression model to describe and predict the system behavior was evaluated by typical ANOVA statistics (Fisher F-test, adequate precision ratio). **Table 2** shows ANOVA results of the fitted model for TOC conversion.

TABLE 2. ANOVA results for predicted TOC conversion (%)

Source	Sum of squares	Degrees of freedom	Mean Square	F	p
Model	1625.14	4	406.28	20.59	0.0026
pH (X_1)	294.08	1	294.08	14.9	0.0119
R (X_2)	45.36	1	45.36	2.3	0.1899
pH^2	834.79	1	834.79	42.3	0.0013
R^2	487.22	1	487.22	24.69	0.0042
Residual error	98.68	5	19.74	-	-

R^2 = 0.9428; Adeq. precision = 13.335; RMSE = 0.9868 mg L^{-1}

Fisher F-test relies in the calculation of the F-value which is computed through the ratio between the mean square of the model (df = 4) and the mean square of the residual error (df = 5). The value (20.59) is greater than the tabulated critical one ($F_{4,5;0.05}$ = 5.19) for a 95% confidence level. Therefore, according to the computed F-value and the low probability value for calculated Fisher F-test ($p < 0.05$) it can be observed that the model is statistically significant. The model terms can be considered statistically significant because their respective values are not greater than 0.1[20]. R-term represents an exception, in this sense; however, after the backward elimination regression (at the selected confidence level), it was keep to maintain the hierarchy of the model[29]. According to ANOVA results, it is expected that this model would produce a signal comparatively larger than the total of the variability[22]. The adequate precision ratio (i.e., a signal-to-variability ratio) statistic reinforces these findings. In this sense, it could be said that the model is an appropriate tool to describe the system behavior when an operator navigates within the completely experimental region (adeq. precision > 4).

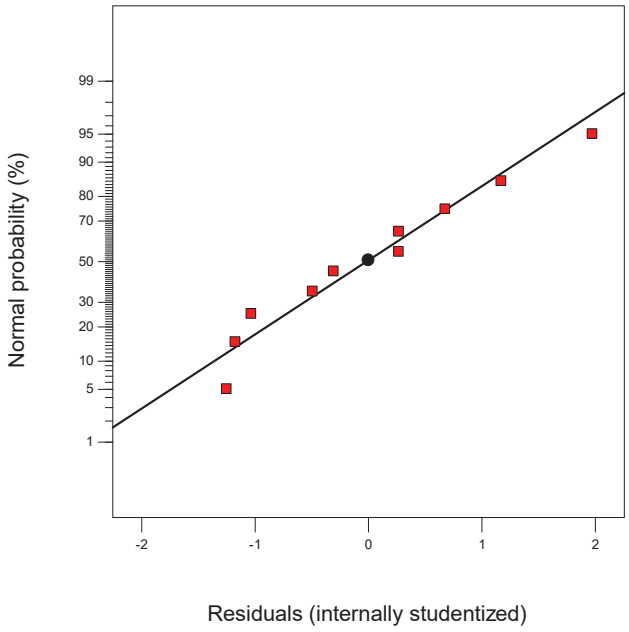


FIGURE 4. Normal probability plot as a function of residuals

Model adequacy check: diagnostic analysis. Even though it was demonstrated that the model is statistically significant it becomes essential to check diagnostic plots and determination coefficient (R^2) value in order to determine if the model explains correctly the variability through the experimental data[29]. The adequacy of the regression model was first assessed by checking residuals diagnostic plots.

As it was mentioned, residuals (i.e., the random error component) represent other sources of variability not accounted for the fitted model and it is expected that they follow a normal distribution. The normal probability plot is the appropriate graphical proof to decide whether the residuals occur according to a normal distribution, which is indeed one of the basic assumptions for ANOVA validation[29]. The normal probability plot is shown in **Figure 4**. As can be seen, residuals are distributed around a straight line; at the same time, residuals do not describe a defined shaped pattern (figure not shown). Therefore, the existence of a homogeneous variance (other basic assumption for ANOVA validation) is positively evaluated[29].

The model quality of fit was evaluated, quantitatively, by computing R^2 statistic (see **Table 2**). Good correlation between the experimental data and the predicted responses was obtained indicating that the fitted model explains 94.28% of the total variability that affects the response.

Another supplementary statistic, the root mean square error (RMSE), reinforces this result (see **Table 2**). The RMSE (i.e., the positive square root of the sum of squares of the residual error divided by the effective total number of experimental runs) is a measure of the total variability that is not explained by the model[30].

TOC conversion was finally validated by comparing experimental and predicted responses. As it is shown in **Figure 5**, the majority of the experimental data were in good agreement with the predicted responses under the operating conditions studied, with a correlation coefficient r = 0.97.

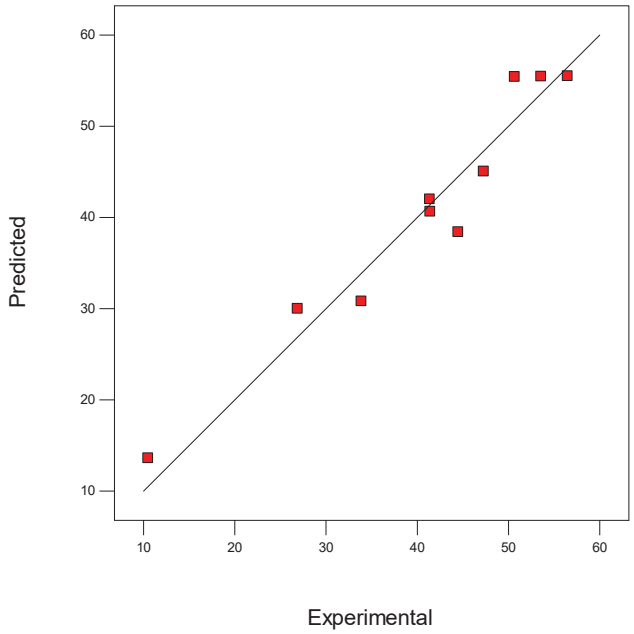


FIGURE 5. Predicted TOC conversion (%) vs. experimental

CONCLUSION

In this study, the suitability of the UV/H_2O_2 process for commercial herbicide mixtures degradation was studied. Modeling of the process response related to specific operating conditions was successfully assessed by RSM.
A second-order polynomial model was derived for the correlation of the response. This model could describe the effects of the selected factors (initial pH, R ratio) on the UV/H_2O_2 process efficiency. Its structure has shown that the factors were not involved in any significant interaction under the operating conditions studied. TOC conversion was highly influenced by the initial pH while the influence of the R ratio was smaller.
The statistical significance, adequacy and quality of fit of the model were evaluated. The model satisfied the assumptions of ANOVA. According to the probability value for calculated Fisher F-test ($p < 0.05$) as well as the determination coefficient value ($R^2 > 0.9$) it can be observed that the model is statistically significant. The model could well describe and predict the system behavior within the tested experimental region. It also correctly explained the variability in the experimental data.
TOC conversion was validated by comparing experimental and predicted responses. Experimental values were in good agreement with the modeled ones confirming the significance of the model and highlighting the success of RSM for UV/H_2O_2 process modeling.
The UV/H_2O_2 process could be suitable for aqueous commercial herbicide mixtures degradation. The optimum operating conditions found could be useful for real field applications.

ACKNOWLEDGMENTS

The authors would like to thank the Universidad Tecnológica Nacional (UTN), Universidad Nacional del Litoral (UNL) and Consejo Nacional de Investigaciones Científicas y Técnicas (CONICET) for their financial support.

REFERENCES

1. Binimelis R., Pengue W., Monterroso I. Transgenic treadmill: responses to the emergent and spread of glyphosate-resistant johnongrass in Argentina. Geoforum 40 (2009) 623-633.
2. Diggle A., Neve P., Smith F. Herbicides used in combination can reduce the probability of herbicide resistance in finite weed populations. Weed Res. 43 (2003) 371-382.
3. Viglizzo E., Ricard M., Jobbágy E., Frank F., Carreño L. Assessing the cross-scale impact of 50 years of agricultural transformation in Argentina. Field Crops Res. 124 (2011) 186-194.
4. Baldé A., Scopel E., Affholder F., Corbeels M., Da Silva F., Xavier J., Wery J. Agronomic performance of no-tillage relay intercropping with maize under smallholder conditions in Central Brazil. Field Crops Res. 124 (2011) 240-251.
5. Groten J., Feron V., Sühnel J. Toxicology of simple and complex mixtures. Trends Pharmacol. Sci. 22 (2001) 316-322.
6. Hernández A., Parrón T., Tsatsakis A., Requena M., Alarcón R., López-Guarnido O. Toxic effects of pesticide mixtures at a molecular level: their relevance to human health. Toxicology 307 (2013) 136-145.

7. Gogate P., Pandit A. A review of imperative technologies for wastewater treatment I: oxidation technologies at ambient conditions. Adv. Environ. Res. 8 (2004) 501-551.
8. Wang J., Xu L. Advanced oxidation processes for wastewater treatment: formation of hydroxyl radical and application. Crit. Rev. Env. Sci. Tec. 42 (2012) 251-325.
9. Nienow A., Bezares-Cruz J., Poyer I., Hua I., Jafvert C. Hydrogen peroxide-assisted UV photodegradation of lindane. Chemosphere 72 (2008) 1700-1705.
10. Gao N., Deng Y., Zhao D. Ametryn degradation in the ultraviolet (UV) irradiation/hydrogen peroxide (H_2O_2) treatment. J. Hazard. Mater. 164 (2009) 640-645.
11. Aleboyeh A., Olya M., Aleboyeh H. Electrical energy determination for an azo dye decolorization and mineralization by UV/H_2O_2 advanced oxidation process. Chem. Eng. J. 137 (2008) 518-524.
12. Stefan M., Hoy A., Bolton J. Kinetics and mechanism of the degradation and mineralization of acetone in dilute aqueous solution sensitized by the UV photolysis of hydrogen peroxide. Environ. Sci. Technol. 30 (1996) 2382-2390.
13. Ikehata K., Gamal El-Din M. Aqueous pesticide degradation by hydrogen peroxide/ultraviolet irradiation and Fenton-type advanced oxidation processes: a review. J. Environ. Eng. Sci. 5 (2006) 81-135.
14. Murcia M., Vershinin N., Briantceva N., Gomez M., Gomez E., Cascales E., Hidalgo A. Development of a kinetic model for the UV/H_2O_2 photodegradation of 2,4-dichlorophenoxiacetic acid. Chem. Eng. J. 266 (2015) 356-367.
15. Sarmento S., Miranda J. Kinetics of the atrazine degradation process using H_2O_2-UVC. Water Sci. Technol. 69 (2014) 2279-2286.
16. Huston P., Pignatello J. Degradation of selected pesticides active ingredients and commercial formulations in water by the photo-assisted Fenton reactions. Water Res. 33 (1999) 1238-1246.
17. Jiménez M., Oller I., Maldonado M., Malato S., Ramírez A., Zapata A., Peralta-Hernández J. Solar photo-Fenton degradation of herbicides partially disolved in water. Catal. Today 161 (2011) 214-220.
18. Rauf M., Marzouki N., Körbahti B. Photolytic decolorization of Rose Bengal by UV/H_2O_2 and data optimization using response surface method. J. Hazard. Mater. 159 (2008) 602-609.
19. Kasiri M., Khataee A. Photooxidative decolorization of two organic dyes with different chemical structures by UV/H_2O_2 process: experimental design. Desalination 270 (2011) 151-159.
20. Körbahti B., Rauf M. Application of response surface analysis to the photolytic degradation of Basic Red 2 dye. Chem. Eng. J. 138 (2008) 166-171.
21. Zuorro A., Fidaleo M., Lavecchia R. Response surface methodology (RSM) analysis of photodegradation of sulfonated diazo dye Reactive Green 19 by UV/H_2O_2 process. J. Environ. Manage. 127 (2013) 28-35.
22. Sekaran G., Karthikeyan S., Boopathy R., Maharaja P., Gupta V., Anandan C. Response surface modeling for optimization heterocatalytic Fenton oxidation of persistence organic pollution in high total dissolved solid containing wastewater. Environ. Sci. Pollut. Res. 21 (2014) 1489-1502.
23. Bianco B., Michelis I., Vegliò F. Fenton treatment of complex industrial wastewater: optimization of process conditions by surface response method. J. Hazard. Mater. 186 (2011) 1733-1738.
24. Zalazar C., Labas M., Brandi R., Cassano A. Dichloroacetic acid degradation employing hydrogen peroxide and UV radiation. Chemosphere 66 (2007) 808-815.
25. Allen A., Hochanadel C., Ghormley J. Descomposition of water and aqueous solutions under mixed fast neutron and gamma radiation. J. Phys. Chem. 56 (1952) 575-586.
26. Vidal E., Negro A., Cassano A., Zalazar C. Simplified reaction kinetics, models and experiments for glyphosate degradation in water by the UV/H_2O_2 process. Photochem. Photobiol. Sci. 14 (2015) 366-377.

27. Mariani M., Romero R., Zalazar C. Modeling of degradation kinetic and toxicity evaluation of herbicides mixtures in water using the UV/H_2O_2 process. Photochem. Photobiol. Sci. 14 (2015) 608-617.
28. Sakkas V., Islam M., Stalikas C., Albanis T. Photocatalytic degradation using design of experiments: a review and example of the Congo red degradation. J. Hazard. Mater. 175 (2010) 33-44.
29. Vera Candioti L., De Zan M., Cámara M., Goicoechea H. Experimental design and multiple response optimization. Talanta 124 (2014) 123-138.
30. Mendes C., Magalhes R., Esquerre K., Queiroz L. Artificial neural network modeling for predicting organic matter in a full-scale up-flow anaerobic sludge blanket (UASB) reactor. Environ. Model Assess. 20 (2015) 625-635.

CHAPTER 7.16 STRATEGY TO IDENTIFY THE CAUSES AND TO SOLVE A GRANULATION PROBLEM IN ANAEROBIC REACTORS: APPLICATION TO A PLANT TREATING CHEESE WASTEWATER

H. Macarie *(1); M. Esquivel (2); A. Laguna (2); O. Baron (2,3); R. El Mamouni (4); S. Guiot (4) and O. Monroy (2)

(1) Aix Marseille Univ, Avignon Univ, CNRS, IRD, IMBE, Marseille, France
(2) Universidad Autónoma Metropolita-Iztapalapa, Depto Biotecnología, México D.F., Mexico
(3) FERMEX, Edo Veracruz, Mexico
(4) NRCC, Royalmount Avenue, 6100, Montréal H4P 2R2, Canada

ABSTRACT

Granulation of biomass is at the basis of the operation of the most successful anaerobic systems (UASB, EGSB & IC reactors) applied worldwide for wastewater treatment. Despite of decades of studies of the biomass granulation process, it is still not fully understood and controlled. “Degranulation/lack of granulation” is a problem that occurs sometimes in anaerobic systems resulting usually in heavy loss of biomass and poor treatment efficiencies or even complete reactor failure. Such a problem occurred in Mexico in two full-scale UASB reactors treating cheese wastewater. A close follow up of the plant was performed to identify the factors responsible for the phenomenon. Basically the list of possible causes to a granulation problem that were investigated can be classified among nutritional, i.e related to wastewater composition (e.g. deficiency or excess of macro- or micronutrients, too high COD proportion due to proteins or volatile fatty acids, high ammonium, sulphate or fat concentrations, presence of toxicants), operational (excessive loading rate, sub or over-optimal water upflow velocity) and structural (poor hydraulic design of the plant). Based on literature results, an attempt to artificially granulate the reactor biomass through the addition of a cationic polymer was also tested. While the causes of the granulation problems could not be identified, the present case remains an example of the strategy that must be followed to identify these causes and could be used as a guide for plant operators or consultants who are confronted with a similar situation independently of the type of wastewater.

Keywords: Anaerobic digestion, cationic polymers, granulation, UASB

INTRODUCTION

Granulation of biomass is at the basis of the operation of the most successful anaerobic systems (UASB, EGSB & IC reactors) applied worldwide for wastewater treatment[1]. Despite of decades of studies of the biomass granulation process, it is still not fully understood and controlled[2]. “Degranulation/lack of granulation” is a problem that occurs sometimes in anaerobic systems resulting usually in heavy loss of biomass and poor treatment efficiencies or even complete reactor failure[3,4,5,6].

---

*Author for correspondence: herve.macarie@ird.fr

The causes of granulation problems observed remain uncertain in most cases. Nevertheless, the information available in the literature suggests that they can be related to nutritional or non-nutritional factors such as:

1. a deficiency or excess of some macro (N, P, S) or micronutrients (Fe, Ni, Co, Mo, Ca, Al, Na, K) that affect sludge growth, granule stability, or may cause their mineralization[7,8,9,10,11,12].
2. a high concentration of proteins, ammonium, phosphate or sulfate[13,14].
3. a conversion of substrates to volatile fatty acids (VFA) higher than 40% of COD in the buffer tank[14].
4. a high concentration of fats (long chain fatty acids or triglycerides) that adsorb to the biomass inducing its flotation and possibly granule disintegration[15,16].
5. the presence of toxic compounds such as those brought by the disinfectants used by the industries which may induce cell lysis and deteriorate granule strength[17].
6. a wastewater liquid surface tension where granule formation is thermodynamically difficult if not impossible, or selects for granules with a hydrophobic external layer allowing biogas bubbles adherence and leading to sludge washout[18].
7. a low selection pressure due to, for example, low water and gas superficial velocities[19,20,21].

Degranulation was identified at the anaerobic wastewater treatment plant of a cheese factory near the city of Queretaro in Mexico. During the 33rd and 34th months of the reactor operation, a close inspection of the plant was performed in order to determine if some of the above factors were involved. In parallel to this investigation, an artificial granulation of the biomass was attempted by dosing the reactors with a high molecular weight cationic polymer. This endeavour was based on the excellent results of enhanced granulation obtained at lab scale by Cail and Barford as early as 1985[22] and reproduced since then with success regularly in the literature with different lab scale anaerobic systems, wastewaters and polymers[e.g 23]. The results of these surveys are the object of the present paper.

MATERIALS AND METHODS

Description of the anaerobic treatment plant. The cheese factory where the treatment plant is operating generates 130 to 172 m^3/d of wastewater resulting mainly from washing operations involving detergents (caustic soda or phosphoric acid based) and disinfectants (sodium hypochlorite, peracetic acid, hydrogen peroxide, iodine) and for a smaller part (~12 m^3/d) from the staff toilets and showers. Whey is normally commercialized. Occasionally however, when it acidifies and cannot be sold, it is also discharged into the sewers. The treatment plant was composed of a buffer tank with 12 hours hydraulic retention time (HRT), a pre-treatment based on dissolved air flotation (DAF) to remove fat, phosphate and suspended solids and two 60 m^3 upflow anaerobic reactors (D1 and D2) without gas-liquid-solid separator (GLS) designed to operate in parallel at the same organic loading rate and HRT. In this scheme, the sanitary wastewaters were treated separately in septic tanks before being mixed in a pumping

well (PW) with the rest of the wastewater flow coming from the DAF and being fed to the anaerobic reactors.

Analytical procedures. All measurements were performed on 24 h composite water samples. COD, total and volatile suspended solids (TSS & VSS), pH, redox potential, temperature, fats, oil and grease, SO_4^{2-} and Sludge Volume Index (SVI) were determined according to Standard Methods[24]. The concentrations of total nitrogen (including nitrate & nitrite), total phosphorus and ortho-phosphate were obtained respectively with the Hach test N tube methods #10022, #10013 and #8048. Trace metals and cations were analysed with a Perkin Elmer 500 IC plasma according to the instructions of the manufacturer. Biogas CH_4 and VFA in wastewater were measured according to Celis-García *et al*.[25] and the sludge particle size distribution as described by Laguna *et al*.[26].

Sludge methanogenic activity. The methanogenic activity of the sludge was determined with serum bottles of 100 mL filled under N_2 with a mixture of PW wastewater and sludge to have a COD/VSS ratio of 1 and a VSS concentration between 3-5 g/L. The bottles were incubated at 35°C with shaking and their gas phase was regularly sampled in order to follow the CH_4 concentration. The specific activity was determined from the slope of the linear phase of methane production divided by the amount of VSS in the bottle. Methane was later converted to COD considering that 15.625 mmole of CH_4 are produced per g of COD degraded.

Polymer addition. The cationic polymer Percol 763 (Allied Colloids Inc., USA) used for the artificial granulation attempt as well as its discontinuous dosage to the reactors while they are in operation were selected based on the work of El-Mamouni *et al.*[27]. The dosage, necessary to obtain an optimal sludge flocculation, was predetermined through Jar tests and was found at 1 mg/g TSS. The polymer was added 7 times to the cheese factory reactor D2 in the form of a 0.25 or 0.5% (w/v) solution in tap water. The solution was dosed at different points of the plant and the dosage was adjusted from 0.12 to 1 mg polymer/g TSS. Reactor D1 was initially used as control but received the final two doses of Percol 763. Originally, the dosage frequency was to be determined on the amount of TSS at the exit of the reactor. In reality, each polymer dosage was separated by 3 to 8 days.

Test of the effect of water upflow velocity (Vup) on granulation at lab-scale. This test was done with 2 lab-scale UASB reactors of 2 litres inoculated with the sludge of the cheese factory D2 reactor. Before start-up, the ratio "sludge volume/reactor working volume" was of 50% as in the full-scale reactor. The HRT (2 days) and the sludge organic loading rate (0.05-0.15 kg COD/kg VSS.day) applied to both reactors throughout the experiment were identical to those of the real plant but one was operated at a Vup of 0.5 m/h and the other at the Vup of the full-scale reactors (0.06 m/h). Such Vup were achieved by water recycling. The wastewater feed was sampled monthly at the level of the pumping well and was stored under refrigeration.

RESULTS AND DISCUSSION

Reactor start-up, detection of the granulation problem, consequences and first tentative corrective actions. The two full-scale digesters were inoculated with the granular sludge of an anaerobic lagoon treating the wastewater of another cheese factory[28]. When wastewater was introduced, the size of the granules started to decrease. The smaller particles were washed out of the reactors resulting in a heavy loss of biomass (effluent TSS > 200 mg/l). As a result, 19 months after the start up, almost half of the initial sludge mass had been lost and 54 to 63% of the VSS (Volatile Suspended Solids) still present in the digesters corresponded to particles smaller than 0.59 mm (**Figure 1** see values for day 597). The sludge organic loading rate had also reached values as high as 2 – 3 kg COD/kg VSS.day while the sludge methanogenic specific activity was only 0.07 – 0.11 kg COD/kg VSS.day. The solid retention time (SRT) was less than 12-22 days. As a consequence, the reactors never reached the design performances (75% COD removal) and presented total COD removals of only 14-20% (22-24% for soluble COD). A reduction of the wastewater flow to reactor D2 during the same period in order to adjust its specific loading rate to 1 kg COD/kg VSS.day had no beneficial effect on COD removal. Despite the overload imposed to the digesters, their mixed liquors always presented an adequate pH (6.6-6.7) and redox potential ($E_{AgCl/Ag}$ = -389 / -398 mV).

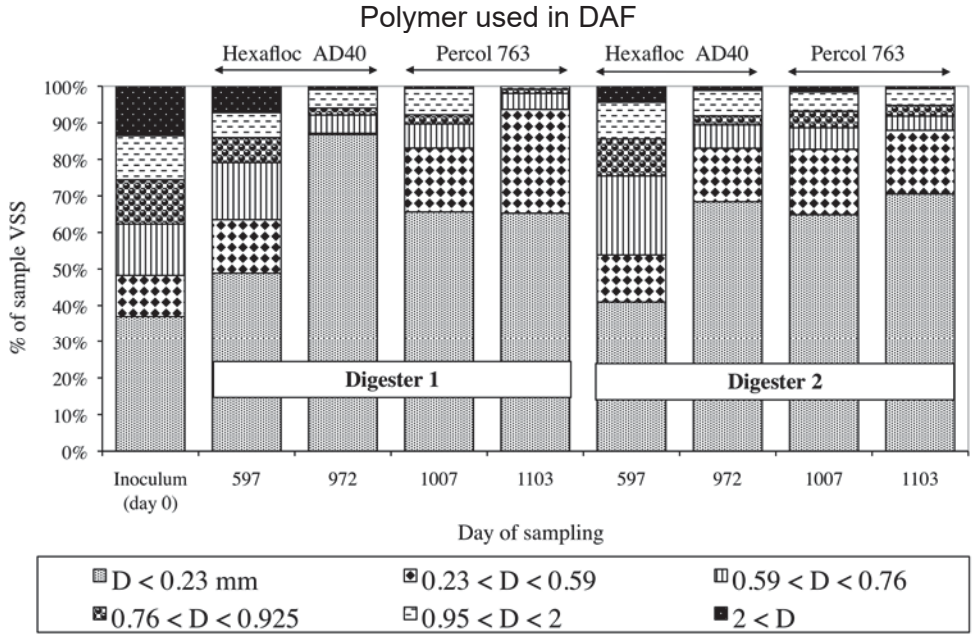


FIGURE 1. Evolution of the granulometry of reactor D1 and D2 sludge over time

In an attempt to increase the treatment plant performance, 1 year and 8 months after the start up, the anaerobic reactors were transformed into UASB systems. The reactor modification included the installation of a GLS device to improve biomass retention (new reactor working volume 88.4 m^3) and the addition of new feeding points (one each 5.6 m^2 of reactor bottom) to ensure better distribution of wastewater within the sludge bed.

Once the transformations were completed 3 months later, the reactor biomass content was also increased to 30 m^3 through the addition of fresh sludge from the same source as the original inoculum. The re-start up strategy consisted in adjusting the digesters' feeding rate to their biomass real treatment capacity. With these modifications, the reactor performances improved drastically. On day 972 (2 years and 9 months after the 1st start-up), they removed more than 74% and 87% of the total and soluble COD respectively. However, until this date the flow rate that they accepted was limited to 14% of the flow rate reaching the plant (2 L/s) and any increase of this value was immediately translated into an important biomass washout. Additionally, the sludge granulometry remained poor with 83 to 87% of the sludge VSS corresponding to sludge particles smaller than 0.59 mm of which at least 68% were smaller than 0.23 mm (Fig. 1, see day 972). It is when possible causes for the degranulation/lack of granulation started to be investigated.

Search of Nutritional factors: characterization of wastewater composition.

COD/N/P/S ratio. The characterisation of the wastewater at different points of the plant (**Table 1**) showed that the DAF removed 71.9±19.8% of the fats, 76.7±10.4% of the TSS, 28.2±16.7% of total nitrogen, 69±9.5% of total phosphorus and 80% of the particulate COD while soluble COD removal was almost negligible (less than 10%). The concentrations remaining in the wastewater after mixing with the sanitary flow in PW resulted in a COD/N/P/S ratio of 100/2.3/0.95/6.58 which indicated that nitrogen, phosphorus and sulphur were respectively 1.6, 3 and 87 times in excess compared to the minimum ratio (100/1.43/0.28/0.075) usually recommended for biomass growth and so granule formation in anaerobic digestion.

Different forms of N, P and S in the wastewater and their impact on granulation. The forms under which nitrogen and sulphur were present in the wastewater were not investigated. Nitrogen was probably present incorporated in proteins or as free ammonium or both since, unlike most other cheese plants, nitric acid cleaning agents were not used here[29]. The presence of sulphur was only determined as SO_4^{2-}. The majority (72.8%) was introduced in the wastewater through the dosage of 640 mg $Al_2(SO_4)_3$/L to the DAF. The resulting COD/SO_4^{2-} ratio of 5 in PW indicated that sulphate reduction should be important in the reactors. This was confirmed by a substantial decrease (80 to 100%) of sulphate concentration in their effluents (**Table 1**) and visually by the black colour of their biomass. In addition, sulphate reducers growing on lactate and some amino acids could be isolated from their sludge. Irrespective of the point of sampling, 70 to 86% of the total phosphorus (72% in PW) corresponded to ortho-phosphate (**Table 1**). This was logical since 73% of the phosphorus detected in the raw wastewater could be attributed to the phosphoric acid based detergents used to clean the pasteurisation and ultrafiltration equipments of the factory.

TABLE 1. WW composition at different points of the WW treatment plant (day 973 to 1033) *

Samp Point	T	pH	FOG	TSS	COD		N	Phosphorus		SO_4^{2-}	VFA
					Total	Soluble	Total	Total	Reactive		
(exit)	°C		mg/L	mg/L	mg O_2/L	mg O_2/L	mg N/L	mg P/L	mg P/L	mg/L	mg O_2/L
HT	27.8 ±2.1	5.4 ±0.4	652.2 ±431	837.1 ±526	3275.5 ±827.2	1766.3 ±655.8	67.6 ±17.3	55.8 ±9.9	49.7 ±8.5	36.0 ±53.3	-
DAF	27.5 ±2.1	6.5 ±0.6	-	154.2 ±71.2	1752.2 ±498.2	1605.7 ±584.1	47.8 ±13.3	17.5 ±6.3	12.3 ±4.3	269.4 ±98.8	-
PW	**27.4 ±1.9**	**6.6 ±0.5**	**156.1 ±150**	**183.8 ±58.6**	**1874.3 ±356.7**	**1575.7 ±449.0**	**42.7 ±19.3**	**17.7 ±6.2**	**12.8 ±4.6**	**369.8 ±99.7**	**272.4 ±166.0**
D1	23.1 ±1.4	7.2 ±0.2	-	186.9 ±59.1	393.8 101.2	137.3 ±113.6	60.4 ±27.2	16.9 ±7.7	14.7 ±2.2	67.3 ±101	235.4 ±101.9
D2	23.2 ±1.4	7.3 ±0.1	-	230.4 ±98.1	451.8 ±111.2	183.3 ±128.3	55.0 ±11.5	19.4 ±5.4	14.7 ±2.9	20.4 ±31.0	223.9 ±151.1

(*) HT: Homogenisation tank; DAF: Dissolved Air Flotation; PW: Pumping Well; D1: Digester 1; D2: Digester 2; T: Temperature; FOG: Fats, Oils and Grease; TSS: Total Suspended Solids; N: Nitrogen; Total Phosphorus = organic + mineral phosphorus; reactive phosphorus = H_3PO_4 + $H_2PO_4^-$ + HPO_4^{2-} + PO_4^{3-}; VFA: Volatile Fatty Acids expressed in COD Equivalent; values after ± correspond to standard deviation.

Ammonium and proteins. Both ammonium and proteins are known to negatively affect the formation and growth of granular sludge pellets[13]. This occurs at ammonium concentrations over 1167 mg N-NH_4/L (pH > 7.4) or when the proteins are at a concentration which cause a COD/N ratio higher than 100/3[13], two conditions never reached at the level of PW (**Table 1**).

Indirect impact of reactive phosphorus and sulphate. An excess of reactive phosphorus and SO_4^{2-} may also be detrimental for sludge granulation. This is related to the capacity of PO_4^{3-}, HPO_4^{2-} and S^{2-} (product of sulphate reduction) to form poorly soluble complexes (solubility products between 10^{-7} to 10^{-35}) with several micronutrients indispensable for the growth of methanogens (Al, Co, Fe, Ni) or the stability of sludge aggregates (Ca^{2+}) and which will not be or will be less accessible to the microorganisms under a precipitated form. Theoretical calculations using expected concentrations of PO_4^{3-}, HPO_4^{2-} and S^{2-} in the anaerobic reactors and the solubility products (Ksp) of the different predicted complexes, suggested that the concentrations of Ca^{2+}, Co^{2+}, Fe^{2+} and Ni^{2+} in the mixed liquors of the reactors could be below the recommended levels (**Table 2**). The direct analysis of these elements showed that in fact they were all present in adequate amounts in the reactors' mixed liquors (see concentration at the reactor exit) except Co and Mo which could not be detected (**Table 2**). Co and Mo were also not detected in the sludge of reactor D1 while Mo was found in the sludge of reactor D2 but in very low amounts (**Table 2**).

TABLE 2. Concentration of some trace metals and cations at different points of the plant (in mg/L) and in the sludge of the reactors (in mg/g TSS) and comparison to the expected solubility in the reactors' mixed liquor calculated from solubility products (Ksp) but also to the optimum concentrations reported for growth of methanogenic *Archaea* or granule formation (both in mg/L)

Metal	Water sampling points					Reactor sludge		Maximum solubility for complexes with		Optimum concentration for growth or granulation
	HT	DAF	PW	D1	D2	D1	D2	$PO4^{3-}/HPO_4^{2-}$	S^{2-}	
Al	1.0	1.2	1.0	1.1	1	11.29	6.7	$8.23\ 10^{-6}$	$> 10^{13}$	NA
Ca	125	125	109	125	94	46.88	39.12	8.5-145	NA	80 - 200
Co	< 0.006					< 0.00096		0.1	$2\ 10^{-12}$-$6\ 10^{-8}$	0.00059 - 0.059
Fe	0.0	0	0.2	0.1	0.3	11.82	8.35	NA	$9\ 10^{-6}$-$8\ 10^{-5}$	0.28 - 50.4
K	156	188	188	266	484	15.62	31.25	NA	NA	< 3510
Mo	< 0.0079					$< 10^{-3}$	$1.2\ 10^{-3}$	NA	NA	0.00096 - 0.048
Na	813	1125	1219	1141	1000	39.12	70.37	NA	NA	< 4600
Ni	6.8	10	4.5	4	5.6	0.5	0.7	2.87	$2\ 10^{-13}$-$4\ 10^{-6}$	0.0059 - 5

An experiment was then set up to test further this apparent deficiency. It consisted to determine the methanogenic activity of reactor D2 sludge in presence of Co and Mo added separately or together at a concentration of 0.25 or 0.5 mg/L. No difference in the rate of methane production was observed compared to the activity determined in absence of added metals (**Figure 2**). A similar result was obtained when acetate was used as carbon source instead of wastewater (data not shown). This suggested that, although undetectable with the analytical equipment used, the levels of Co and Mo in the wastewater were sufficient for not interfering with the methanogenic capabilities of the sludge.

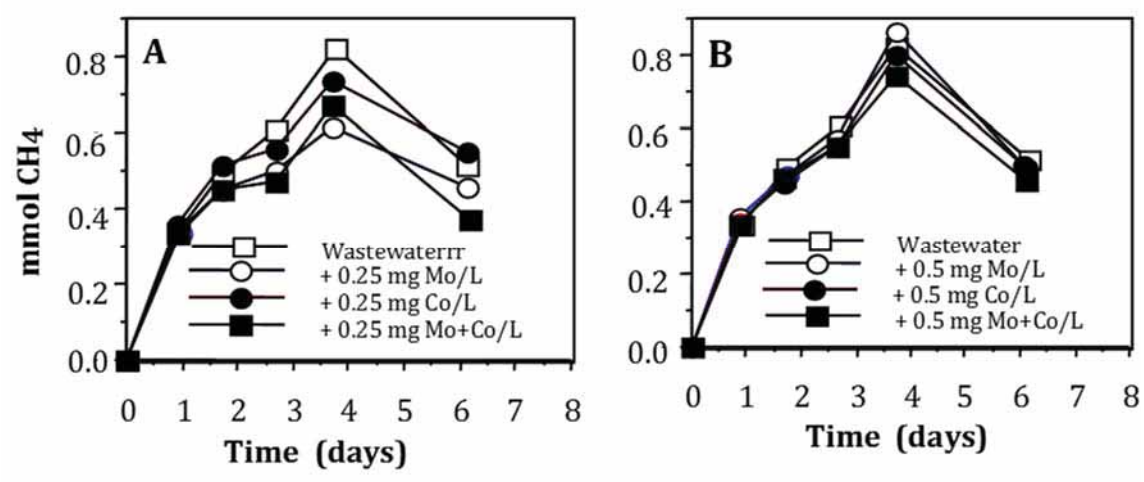


Figure 2. Evolution of the methane production of reactor D2 sludge on PW wastewater at a COD/VSS ratio of 1 in presence and absence of 0.25 (A) or 0.5 mg/L (B) of Co and Mo or both of them

Direct impact of sulphate and its reduction products. Beside the capacity of S^{2-} to form insoluble complexes with trace metals, other product of sulphate reduction, soluble free H_2S, may equally affect the granulation process since it is known to inhibit the activity of the methanogenic *Archaea* and acetogenic *Bacteria*[30]. The concentrations of soluble free H_2S in the digesters which could be calculated accounting for (1) a complete reduction of the SO_4^{2-} present in PW, (2) the stripping due to biogas production estimated from COD removal and (3) the pH of their mixed liquors, were of 42 and 36.9 mg H_2S-S/L for D1 and D2 respectively. Such H_2S levels may reduce the methanogenic acetoclastic activity by 20-30%[30]. Nevertheless, no negative effects on granulation build-up have been observed with sulphide concentrations up to 600 mg/L[14]. Even if the products of sulphate reduction (S^{2-}, H_2S) have no impact on sludge granulation, the fact that sulphate reducing bacteria may represent a big part of the microflora could affect granular stability since the ability of these bacteria to flocculate seems very poor[31]. Fortunately, for a COD/SO_4^{2-} ratio between 5 and 10, the impact on sludge granulation appears to be limited to a 10-20% reduction of the granule growth yield compared to granules grown in the same conditions but in absence of sulphate[14] and so should not apply in the present case.

Na and K content in wastewater. Due to the use of brines for cheese processing, the NaCl and the other salts added could negatively affect sludge growth as members of the microbiota show specific halotolerance levels, outside of which the salts become toxic or growth arresting. Levels of sodium and potassium were followed in parallel with trace metals and calcium. Their concentrations in PW (Table 2) were at levels much lower than those known to cause 10% inhibition of the acetoclastic methanogenic activity[32,33]. Potassium was at a concentration close to the value (0.01 M or 390 mg/L) for which it gives an optimum antagonistic effect to the toxicity of sodium[32]. An increase of the ionic strength, related to the presence of these cations, could also negatively impact the physical integrity of the granules. However, it has been reported that NaCl concentrations of 125 mM (2.36-fold higher than at the digester entrance) do not affect the resistance of methanogenic granules to abrasion[34].

VFA content in wastewater. It was found that VFA represented 15.3±11.15% of total COD and 19.7±16.9% of the soluble one at the level of PW (**Table 1**). With the analytical conditions used, only acetic, propionic and butyric acid could be detected. They represented respectively 47.6±6, 43.4±7.6 and 9.1±4.2% of the VFA COD. According to previous works on acidogenesis of dairy effluents[35], it is probable however that other compounds such as lactic acid and alcohols' (methanol, ethanol, others) were also produced in the buffer tank taking into account its pH (**Table 1**) and residence time (12 hours). Further evolution of the wastewater in the DAF and PW was not expected due to the very short hydraulic retention time there (30 min and 12 min respectively). Lactic acid and alcohols are high-energy substrates (the Gibbs free energy of their conversion to CH_4 and CO_2 is higher than –0.9 kJ/g COD for the alcohols and -1.145 kJ/g COD for lactate), and as so are good carbon sources for granulation[14]. This means that the COD of the detected VFA, which on the contrary are poor inducers of granulation, is sufficient to conclude that the level of acidification in the buffer tank was within the recommended range to avoid granulation problems[36].

Fats, oil and grease content in Wastewater. Some 156.06±149.82 mg/L of fats, oils and grease (FOG) were found at the entrance of the digesters (**Table 1**). Most of these corresponded to milk fat not removed by the DAF and were probably in the form of triglycerides and long chain fatty acids (LCFA) resulting from the expected rapid hydrolysis of the triglycerides in the buffer tank[37]. The composition of the LCFA in PW was not determined, but could be approximated with that of milk which contains in % (w/w) of total LCFA[37] 7% lauric (2.72), 6% myristic (2.807), 21% palmitic (2.875), 6% stearic (3.104), 2% palmitoleic (2.834), 39% oleic (2.894) and 13% linoleic acids (2.82) (values in parenthesis correspond to the theoretical COD of each LCFA in g O_2/g). Since the theoretical COD of the LCFA and of their corresponding triglycerides is very similar, it is possible to estimate that 1 g of milk LCFA or triglycerides or mixture of them generates a theoretical COD of 2.7 g O_2 (= $\sum$ [($LCFA_i$ $COD_{theoretical}$) x (% of $LCFA_i$ in LCFA milk)]). This means that 156.06±149.82 mg/L of FOG should represent some 421.4±404.5 mg COD/L. It results from this value that the FOG loading rates supported by the digesters (0.017-0.048 mg $COD_{equivalent}$/kgVSS.d) were well below the rate (0.09 g LCFA-COD/g VSS.d) over which sludge flotation has been reported to start[38]. Moreover, this should remain true even if the digesters received all the wastewater flow from the cheese factory (1 L/s or 86.4 m^3/day each). As a consequence, the levels of FOG are presumably unrelated to the observed granulation problems. Nevertheless, this cannot be definitively excluded as an almost complete washout of granular biomass has been reported in the literature[3] for a full scale UASB reactor treating at a similar FOG loading rate, (0.028 g FOG/g TSS.d, estimated from given biomass inventory), the wastewater of a baking company containing also after pre-treatment by DAF a similar FOG concentration (136 mg/l). In this case, biomass loss could be clearly associated to FOG and solved by an improvement of FOG removal below 50 mg/l at the level of the DAF. It must be noted however that the reactor described in this study was operated at much higher loading rate (6.8 kg COD/m^3.d) and lower HRT (7 hours) than the present cheese factory reactors resulting in much higher water (0.65 m/h) and biogas (0.23 m/h) superficial velocities which would drastically increase the potential for sludge flotation and washout.

Polymer addition. The first two additions of Percol 763 resulted in the formation of a 60 cm layer of floating biomass at the surface of reactor D2 giving a temporary important loss of solids. This occurred despite the use of a Percol dosage (0.23 mg/g sludge TSS) below the optimum value. The problem was probably related to the trapping of biogas in the flocs. After several trials acting on the percol amount dosed to the reactor, as well as the place and duration of addition, sludge flotation could be controlled and reduced to a minimum by dosing it to PW along 1 to 7 hours to achieve a dose of 0.1 to 0.37 mg percol/g sludge VSS. The day before the 7^{th} and last addition of Percol (day 1007), the measurement of the particle size distribution of the sludge of both reactors showed that no granulation had been obtained (**Figure 1**). Over 60 % of D2 sludge VSS still corresponded to particles smaller than 0.23 mm as at the beginning of the plant follow up 35 days before (day 972). The apparent improvement of D1 sludge granulometry on the same day was probably a sampling artefact. In a similar manner, over the same period, no improvement of the SVI of D2 sludge compared to D1 sludge was observed.

Following visual inspection, it appeared that the flocs obtained with Percol 763 disaggregated 2 or 3 days after being formed. This is common and usually due to the loss of stability of the polymers over time. Nevertheless, in the present case, this phenomenon was apparently the result of an antagonistic effect due to a fraction of the high molecular weight anionic polymer (Hexafloc AD40 from Technics International) used in the DAF which did not react locally and was lost to the wastewater. Qualitative experiments clearly demonstrated that D2 sludge flocculated with Percol 763 (0.5 mg/g TSS) could not maintain its structure after addition of Hexafloc AD40 (0.5 mg/g TSS).

As Percol 763 is also recommended for phosphorus removal in combination with alum, on day 998, it was decided to use it instead of Hexafloc AD40 in the DAF operation. Immediately after this change, it was possible to increase the flow rate of wastewater to the reactors without observing any biomass washout or deterioration of their COD removal efficiencies (data not shown). The DAF COD, FOG, TSS, phosphorus and nitrogen removal efficiencies remained unaffected by the change of polymer (data not shown). Two more additions of Percol 763 to PW were still done after day 998. One week after the second addition, D2 sludge became suddenly bulker. No clear explanation to this phenomenon was identified but the decision was taken to stop the direct dosage of Percol to the digesters.

At the end of the period of study (day 1033), both reactors were treating 79.1±12.4 % of the total wastewater flow produced by the factory. The activities of D1 and D2 sludge measured on day 1007 (0.601±0.03 and 0.417 ± 0.032 g COD/g VSS.d for reactors D1 and D2 respectively), showed nevertheless that the reactors had the capacity to treat the daily COD load remaining after the physicochemical pre-treatment. In agreement with this, according to the cheese factory staff, the reactors were finally able to treat the nominal flow rate. The last granulometry determination performed on day 1103, indicated however that 3 months after the switch of polymers in the DAF, the reactors' biomass was still flocculent (**Figure 1**). This was unchanged after one year of operation using these new conditions (see values for the inoculum on **Figure 3**).

Upflow velocity. The two lab scale reactors, operated respectively at Vup of 0.06 and 0.5 m/h, to see if an action on this parameter could induce biomass granulation presented very similar performances (data not shown). The main difference between the two reactors was that, logically, the one operated at the higher Vup showed a slightly higher loss of suspended solids to the effluent (53±94 against 37±41 mg TSS/L). In both cases, the loss of TSS was however 5 to 6 times lower than that observed at full scale while the COD removal was improved by 10 to 20%. The differences between the lab and full scale reactors were probably the result of the higher temperature at which the lab scale experiment was performed (33.5 against 23°C) but were considered not so important as to affect the analysis of the increase of the upflow velocity on the granulation process and its transposition to full scale.

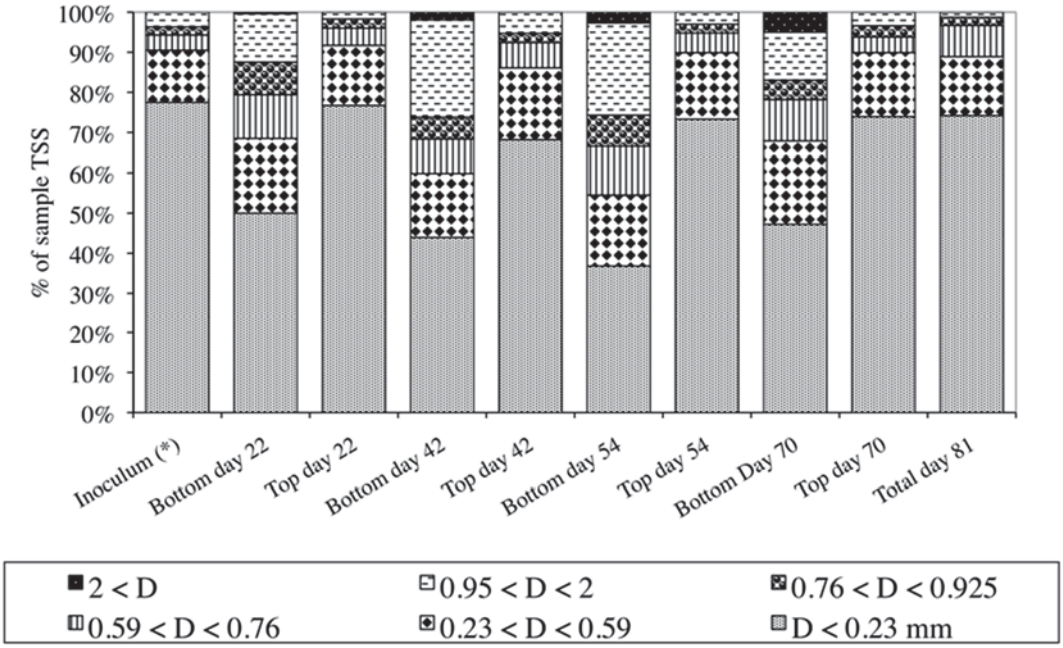


FIGURE 3. Evolution of the sludge granulometry of the lab scale reactor operated at 0.5 m/h (*sludge sampled on reactor D2 on day 1344)

The biomass of the reactor operated at 0.06 m/h did not show a positive evolution of its particle size distribution. Only a slight segregation of the particles within the sludge bed could be immediately noticed, the biggest granules being logically in higher amounts at the bottom of the reactor (data not shown). The reactor operated at 0.5 m/h presented also a segregation by size of the granules within its sludge bed, but much more noticeable than previously (**Figure 3**). A positive evolution of the sludge particle size distribution was observed initially. For instance, on day 54 of operation, less than 40% of the sludge TSS corresponded to particles smaller than 0.23 mm at the bottom of the reactor, while they represented almost 80% of the TSS in the inoculum. Nevertheless, for the next sampling performed on day 70, the sludge particle size distribution had returned to the values found on day 22 (**Figure 3**). On the same way, the granulometry of the sludge at the top of the reactor, which had improved during the 42 first days of operation started to deteriorate in the subsequent samplings. This deterioration occurred after a change in the quality of the wastewater used to feed the reactors which presented a higher content of organic matter (3000-4000 mg COD/L against 800 mg/L) as well as a thin layer of floating material with an oily appearance.

After 81 days, both reactors were emptied and their sludge beds were homogenised for a last granulometry determination. Surprisingly, no differences were identified. In addition, their particle size distributions remained almost identical to the initial one as well as their SVI (28.9 and 27.4 mL/g TSS for the reactors operated at 0.5 and 0.06 m/h against 26.5 mL/g for the inoculum). The length of the experimentation (almost 12 weeks) could possibly be too short to see any positive effect of an increase of the upflow velocity. Ten weeks had been however sufficient for a similar study performed with crushed granular sludge and sucrose, an easily biodegradable compound, as substrate[19]. At least the present experiment showed that an increase of the upflow

velocity had no detrimental effect on the performances of the reactors and the granulometry of their sludge.

CONCLUSION

The factors responsible of the disintegration/lack of granulation in the present case study could not be identified although the role of milk fat not removed in the DAF pre-treatment could not be completely discarded. It was shown that the granulation problem was not related to (1) a deficiency or excess of some macro- or micronutrients, (2) a high proportion of COD due to proteins or volatile fatty acids, (3) a high concentration of ammonium, (4) a high development of sulphato-reduction and (5) a sub-optimum selection pressure due to a low water upflow velocity.
The initiative to artificially granulate the sludge through the addition of a cationic polymer failed and instead caused a heavy sludge flotation. This shows that despite the excellent results reported in the literature at lab scale, it is premature to advise the dosage of such polymers to promote sludge granulation in running (biogas producing) full-scale UASB-like reactors. Their use should be accepted only if successful reports on their application at full scale and detailed procedures for their dosage become available. A more promising way to induce granulation with polymers may correspond to a process similar to the one patented by Biothane[39]. In this process, the sludge is pre-granulated outside the reactor through the addition of an organic cationic polymer followed by the addition of an inorganic anionic polymer plus some additives (activated carbon, calcium, etc). Published results suggest that the granules obtained in such a way have excellent settling properties and keep their integrity (no degranulation) in the long-term operation of UASB reactors[40].
Despite of being limited to a specific case, the present work has a broader perspective since it gives an example of most of the points that must be investigated when a granulation problem occurs, an example that is true for any type of wastewaters.
In the case under study, at the end of the survey, the lack of granulation was not a problem anymore since the SRT of the remodelled reactors was higher than 100 days. This means that contrarily to the beginning they had acquired an excellent capacity to retain the flocculent biomass, a capacity associated to stable and high COD removal.

ACKNOWLEDGMENTS

For this study, Maricela Esquivel was financially supported by the cheese factory and Acela Laguna and Olivier Baron by IRD. The authors thank the cheese factory and particularly its employees Paulino Rivas, Gerardo Gonzalez, Omar Reyes, and Abelardo Villareal for their interest and kind assistance during the realisation of this project. They also thank Sébastien Prunier and Graciela Famá for technical help at the early stage of the work, German Buitrón and Ilangovan Kuppusamy for the loan of a Hach spectrophotometer and a jar test equipment respectively and Mark Spanevello for help with English language.

REFERENCES

1. Van Lier J.B., Van der Zee F.P., Frijters C.T.M.J., Ersahin M.E. Celebrating 40 years anaerobic sludge bed reactors for industrial wastewater treatment. Rev. Environ. Sci. Bio/Technol. 14 (2015) 681-702.
2. McHugh S., O'Reilly C., Mahony T., Colleran E., O'Flaherty V. Anaerobic granular sludge bioreactor technology. Rev. Environ. Sci. Bio/Technol. 2 (2003) 225-245.
3. Maat D.Z., Gorur S.S. Start-up and performance testing of a full scale UASB anaerobic wastewater treatment facility, in: Proceedings 44th Industrial Waste Conference, Purdue University, Lewis Publishers Inc, Chelsea, MI, USA, pp. 209-214 (1990).
4. Borzacconi L., López I., Passeggi M., Etchebehere C., Barcia R. Sludge deterioration in a full scale UASB reactor after a pH drop working under low loading conditions. Water Sci. Technol. 57 (2008) 797-802.
5. Li J., Hu B., Zheng P., Qaisar M., Mei L. Filamentous granular sludge bulking in a laboratory scale UASB reactor. Bioresource Technol. 99 (2008) 3431-3438.
6. Sekiguchi Y., Ohashi A., Parks D.H., Yamauchi T., Tyson G.W., Hugenholtz P. First genomic insights into members of a candidate bacterial phylum responsible for wastewater bulking. PeerJ, 3 (2015) e740.
7. Alphenaar P.A., Sleyster R., De Reuver P., Ligthart G. J., Lettinga G. Phosphorus requirement in high rate anaerobic wastewater treatment. Water Res. 27 (1993) 749-756.
8. Grotenhuis J.T.C., van Lier J.B., Plugge C.M., Stams A.J.M., Zehnder A.J.B. Effect of ethylene glycol-bis(b-aminoethyl ether)-N,N-tetraacetic acid (EGTA) on stability and activity of methanogenic granular sludge. Appl. Microbiol. Biotechnol. 36 (1991) 109-114.
9. Guiot S.R., Gorur S.S. Kennedy K.J. Nutritional and environmental factors contributing to microbial aggregation during upflow anaerobic sludge bed-filter (UBF) reactor start-up, in: Hall E.R. and Hobson P.N. (Eds.), Anaerobic Digestion 1988, Proceedings 5th International Symposium, Pergamon Press, London, UK, pp. 47-53 (1988).
10. Kim Y.H., Yeom S.H., Ryu J.Y., Song B.K. Development of a novel UASB/CO_2-stripper system for the removal of calcium ion in paper wastewater. Process Biochem. 39 (2004) 1393-1399.
11. Speece R.E. Anaerobic Biotechnology and Odor/Corrosion Control for Municipalities and Industries. Chapter 16, Trace Metals. Archae Press, Nashville, Tennessee, USA, pp. 405-430 (2008).
12. Zandvoort M.H., van Hullenbusch E.D., Gieteling J., Lens P.N.L. Granular sludge in full-scale anaerobic bioreactors: trace element content and deficiencies. Enzyme Microb. Technol. 39 (2006) 337-346.
13. Thaveersi J., Gernaey K., Kaonga B., Boucneau G., Verstraete W. Organic and ammonium nitrogen and oxygen in relation to granular sludge growth in lab-scale UASB reactors. Water Sci. Technol. 30 (12) (1994) 45-53.
14. Vanderhaegen B., Ysebaert E., Favere K., van Wambeke M., Peeters T., Pánic V., Vandenlangerbergh V., Verstraete W. Acidogenesis in relation to in-reactor granule yield. Water Sci. Technol. 25 (7) (1992) 21-30.
15. Amaral A.L., Pereira M.A., da Motta M., Pons M.N., Mota M., Ferreira E.C., Alves M.M. Development of image analysis techniques as a tool to detect and quantify morphological changes in anaerobic sludge: II. Application to a granule deterioration process triggered by contact with oleic acid. Biotechnol. Bioeng. 87 (2004) 194-199.
16. Chipasa K.B., Medrzycka K. Behaviour of lipids in biological wastewater treatment processes. J. Ind. Microbiol. Biotechnol. 33 (2006) 635-645.
17. 17-Zitomer D.H., Burns R.T., Duran M. Vogel D.S. Effect of sanitizers, rumensin and temperature on anaerobic digester biomass. Transactions of the ASABE 50 (2007) 1807-1813.

18. Thaveersi J., Daffonchio D., Liessens B., Vandermeren P., Verstraete W. Granulation and sludge stability in upflow anaerobic sludge bed reactors in relation to surface thermodynamics. Appl. Environ. Microbiol. 61 (1995) 3681-3686.
19. Arcand Y., Guiot S.R., Desrochers M., Chavarie C. Impact of the reactor hydrodynamics and organic loading on the size and activity of anaerobic granules. Chem. Eng. J. 56 (1994) B23-B25.
20. O'Flaherty V., Lens P.N.L., de Beer D., Colleran E. Effect of feed composition and upflow velocity on aggregate characteristics in anaerobic upflow reactors. Appl. Microbiol. Biotechnol. 47 (1997) 102-107.
21. Bhunia P., Ghangrekar M.M. Influence of biogas-induced mixing on granulation in UASB reactors. Biochem. Eng. J. 41 (2008) 136-141.
22. Cail R.G., Barford J.P. The development of granulation in an upflow floc digester and an upflow anaerobic sludge blanket digester treating cane juice stillage. Biotechnol. Lett. 7 (1985) 493-498.
23. Wang J.S., Hu Y.Y., Wu C.D. Comparing the effect of bioflocculant with synthetic polymers on enhancing granulation in UASB reactors for low-strength wastewater treatment. Water SA 31 (2005) 177-182.
24. Standard Methods for the Examination of Water and Wastewater, 19th edn. American Public Health Association/American Water Works Association/Water Environment Federation, Washington DC, USA (1995).
25. Celis-Garcia L.B., Razo-Flores E., Monroy O. Performance of a down-flow fluidized-bed reactor under sulfate reduction conditions using volatile fatty acids as electron donors. Biotechnol. Bioeng. 97 (2007) 771-779.
26. Laguna A., Ouattara A., Gonzalez R.O., Baron O., Famá G., El Mamouni R., Guiot S., Monroy O., Macarie H. A simple and low cost technique for determining the granulometry of upflow anaerobic sludge blanket reactor sludge. Water Sci. Technol. 40 (8) (1999) 1-8.
27. El Mamouni R., Leduc R., Guiot S.R. Influence of synthetic and natural polymers on the anaerobic granulation process. Water Sci.Technol. 38 (8-9) (1998) 341-347.
28. Monroy O., Vázquez F., Derramadero J.C. Guyot J.P. Anaerobic-aerobic treatment of cheese wastewater with national technology in Mexico: the case of « El Sauz ». Water Sci. Technol. 32 (12) (1995) 149-156.
29. Danalewich J.R., Papagiannis T.G., Belyea R.L., Tumbleson M.E., Raskin L. Characterization of dairy waste streams, current treatment practices, and potential for biological nutrient removal. Water Res. 32 (1998) 3555-3568.
30. Rinzema A., Lettinga G. Anaerobic treatment of sulfate containing wastewater, in: Wise D.L. (Ed.), Biotreatment Systems, Vol. III, CRC Press, Boca Raton, Florida, USA, pp. 65-109 (1988).
31. Visser A., Alphenaar P.A., Gao Y., van Rossum G., Lettinga G. Granulation and immobilisation of methanogenic and sulfate-reducing bacteria in high-rate anaerobic reactors. Appl. Microbiol. Biotechnol. 40 (1993) 575-581.
32. Kugelman I.J., Chin K.K. Toxicity, synergism and antagonism in anaerobic waste treatment processes. Adv. Chem. Ser. 105 (1971) 55-90.
33. Rinzema A., van Lier J., Lettinga G. Sodium inhibition of acetoclastic methanogens in granular sludge from a UASB reactor. Enzyme Microb. Technol. 10 (1988) 24-32.
34. Pereboom J.H.F. Strength characterisation of microbial granules. Water Sci. Technol. 36 (6-7) (1997) 141-148.
35. Yu H.Q., Fang H.H.P. Acidification of mid- and high-strength dairy wastewaters. Water Res. 35 (2001) 3697-3705.
36. Lettinga G., Hulshoff Pol L.W. UASB-process design for various types of wastewaters. Water Sci. Technol. 24 (8) (1991) 87-107.

37. Hwu C.S. Enhancing anaerobic treatment of wastewaters containing oleic acid. PhD thesis, University of Wageningen, The Netherlands, ISBN 90-5485-733-1 (1997).
38. Hwu C.S., Tseng S.K., Yuan C.Y., Kulik Z., Lettinga G. Biosorption of long-chain fatty acids in UASB treatment process. Water Res. 32 (1998) 1571-1579.
39. Frankin R.J. de Pijper M.A.M. Process for producing granular biomass. WO Patent 2007/089144 A1, 10 pages (2007).
40. Jeong H.S., Kim Y.H., Yeom S.H., Song B.K., Lee D.I. Facilitated UASB granule formation using organic-inorganic hybrid polymers. Process Biochem. 40 (2005) 89-94.

CHAPTER 7.17 TREATMENT OF SYNTHETIC TEXTILE EFFLUENT BY ANAEROBIC PROCESS WITH MICRO AERATED ZONE

M. S. D. Marcelino (1); R. Brito (1); **L. Florêncio ***(1); M. T. Kato (1); M. H. R. Z. Damianovic (2) and S. Gavazza (1)

(1) Laboratory of Environmental Sanitation, Department of Civil Engineering, Federal University of Pernambuco, Av. Acadêmico Hélio Ramos S/N, Cidade Universitária, 50740-530, Recife PE, Brazil
(2) Laboratory of Biological Process, Department of Hydraulic and Sanitation, University of São Paulo, 13566-590, São Carlos SP, Brazil.

ABSTRACT

Azo dyes are synthetic compounds containing one or more azo group (–N=N–) bonded to aromatic structures. Among the dyes applied to the textile processing, around 70% belongs to the azo-type[1]. These elements, when released into water bodies, can negatively affect the environment and human health, causing changes in water color, resulting in aesthetic problems and photosynthetic activity reduction, as well as increasing the toxicological risk to river living beings and humans.
For the complete biological degradation of azo dyes, it is typically required two stages: An anaerobic first stage, where the azo bonds are broken, releasing aromatic amines as degradation by-products, and a second aerobic stage, required for biodegradation of such toxic by-products. This process is usually conducted into of two separates treatment units. Aiming to reduce the process to one treatment unit, and obviously, the costs, in the present study we micro-aerated the middle zone of a lab-scale UASB reactor (R2) for the treatment of synthetic textile wastewater. A control conventional anaerobic UASB reactor (R1) was also essayed.
The cylindrical reactors volume was 5L (60 cm x 11 cm), and in the R2 an air diffusor was placed just after the sludge blanket (25 cm from the bottom). In this point the dissolved oxygen (DO) was kept between 0.2 and 0.3 mg O_2 L^{-1}. Both reactors were fed with synthetic textile wastewater, composed by starch (COD of 1500 mg O_2 L^{-1}), 60 mg/L of the tetra-azo dye Direct Black 22 (DB22-CAS n° 6473-13-8), 500 mg L^{-1} of sulfate, macro and micronutrients. The operational time was 120 days at room temperature of 28 ± 2°C, and 24 hours of hydraulic retention time (HRT). Thus, the COD mass ratio to the oxygen mass fed in the partially-aerated reactor, varied between 5000 to 7500 g COD-starch/g O_2.
The COD removal efficiency in R1 (71.34%) was slightly higher than in R2 (66.51%), while R1 effluent was 441.42 ± 171.81 mg O_2 L^{-1}, R2 effluent was 513.76 ± 216.70 mg O_2 L^{-1}, suggesting that micro-aeration did not have a strong positive influence on the overall organic matter removal. The color removal efficiencies were also similar in both reactors (61.6% for R1 and 65.1% for R2), indicating R1 small disadvantage in dye reduction, and a slightly competition with sulfate reducing bacteria by available electrons. The sulfate effluent concentrations were 156.18 ± 76.49 and 276.56 ± 64.78 mg SO_4^{2-} L^{-1} in R1 and R2, respectively, resulting in 68.64 and 44.63% of removal

---

*Author for correspondence: denise_msm@yahoo.com.br

efficiency to R1 and R2, respectively. Moreover, the aromatic amines were removed in R2. In contrast, aromatic amines accumulated in R1 effluent, confirming the ability of micro-aeration stage in the UASB reactor in promoting the complete azo-dye degradation with the advantage of using one single-unit treatment.

Keywords: aromatic amines, azo dye, micro-aeration, textile effluent.

INTRODUCTION

Due to the great diversity and quantity of dyes used in the textile industry, they are responsible for giving color to textile effluents. The most significant environmental impact is due to the discharge of dyes into water bodies, since many of these dyes are difficult to degrade in the natural environment. Some dyes have a low degree of fixation (50-80%) in fabric, which results in heavy load in wastewater[1].

The azo dyes are characterized by one or more chromophore groups of the type –N=N– liked to substituted aromatic structures. They are the largest class (70%) of dyes applied to textile processes[1]. The use of this type of dye associated with the low level of fixation (considering that many dyes are visible in water at concentrations as low as 1 mg L^{-1}) is generated highly colored effluents[2].

In general, the azo dyes biodegradation process by microorganisms occurs in two stages. The first stage involves the reductive cleavage of azo bonds (–N=N–), under anaerobic conditions, which results in the formation of aromatic amines; these compounds are, in general, free color, but still toxic[3,4]. In the second stage, aerobic microbes respire these amines in organic acids or CO_2 and H_2O[5].

High sulfate content is also common in textile effluents and it is due to sodium metabisulfite, sulfide and dithionite compounds, which are widely used during industrial process. Sulfate reducing process can interfere the azo dyes biological degradation[2]. The sulfate can play different functions in the reducing dyes process; negatively, when competing with dyes for the available electrons; and positively, being the precursor of sulfide, which acts as electron donor for chemical decoloration. Another interfering compound in textile wastewater is sodium chloride, usually applied for dye fixation in industrial process, conferring high salinity to the wastewater, increasing the toxicity due to the high osmotic pressure[6].

Studies for the treatment of textile effluents using sequential anaerobic-aerobic system f indicate that aeration provides improvement of COD removal and acts as an important complement to the anaerobic removal of color[7,8]. However, recent studies have confirmed that the aromatic amines degradation is also well performed at low oxygen concentration. Furthermore, the limited oxygen introduction into the anaerobic digesters creates favorable microaerophilic conditions for the removal of hydrogen sulfide formed from the sulfate reduction[9]. The oxidation of sulfide in the oxygen presence, occurs both chemically and biologically[10].

The use of a single unit in the biological treatment of textile effluents would be promising, due to the low operating costs, the ability to reduce dyes and its intermediate metabolites, organic matter and sulfide, minimizing environmental impacts. Thus, in this study we evaluated the effect of adding a micro-aerated zone in an UASB reactor for the treatment of synthetic textile wastewater, containing azo dye, sulfate and salinity.

MATERIALS AND METHODS

Biomass. Flocculent sludge from a 5 L bench type UASB feed by a synthetic textile effluent was used. Previously to the inoculation into the experimental set reactors, the humid biomass was stored at 4ºC. To perform the experiment startup, it was necessary submit the biomass to a 30ºC acclimatization during 48 hours, in order to increase the microorganisms metabolic activity.

The sulfate-reducing microorganisms were already identified in the biomass, due to sulfate addition into the synthetic effluent in a previous work, then, the sludge was already adapted to textile dyes. The sludge volume used was 0.66 L, resulting in 0.044 and 0.050 g VSS/TSS in R1 reactor (UASB) and R2 reactor (UASB micro-aerated zone) respectively.

Synthetic textile effluent. The tetra azo dye Direct Black 22 (CI 35435, CAS 6473-13-8) was used in this experiment set (**Figure 1**). It was acquired from the Brazilian company Exatacor Araquímica Indústria e Comércio de Corantes. This dye is the most commonly used in the textile industries located in the state of Pernambuco, Brazil[11].

Before being used in the experiment, the dye was submitted to hydrolysis. This stage consists in adjusting the pH of the dye stoke solution prepared in deionized water to 11.0 ± 0.05 using 20% NaOH, followed by 1 hour of heating at 80°C; after cooling the solution, it is neutralized to pH 0.05 ± 7.0 using HCl[12]. Similar hydrolyzing procedures are applied in textile industries [13,14]. The dye concentration in the synthetic textile wastewater was 0.06 mM.

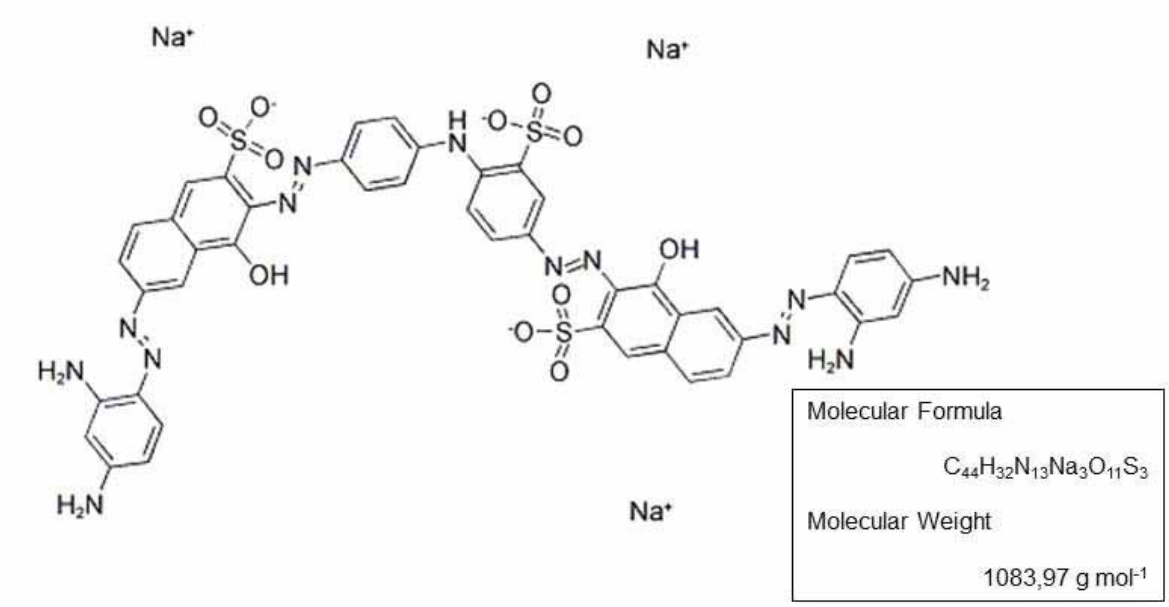


FIGURE 1. Molecular structure of the azo dye *Direct Black 22* (CAS 6473-13-8)

Starch was used as electron donor because this compound contributes to the COD concentration of textile effluents, given that it is used in the degumming process stage. Besides the dye *Direct Black 22* and electrons donor, the synthetic textile effluent, is

also composed for a macro and micronutrients solution (described in **Tables 1** and **2**). Sodium sulfate (Na_2SO_4) and sodium chloride (NaCl) was also added.

The starch solution was heated (90°C for 30 min) before the introduction to the set reactors to in order to improve the solubilization compound capacity in the aqueous phase.

TABLE 1. **Composition of the synthetic effluent in study**

Composition	Concentration of reactors
Electron donor (starch)	COD of 1200 mg $O_2.L^{-1}$
Dye *Direct Black 22*	65 mg L^{-1} (0.06 mM)
Ammonium chloride (NH_4Cl)	280 mg L^{-1}
Potassium phosphate dibasic (K_2HPO_4)	252 mg L^{-1}
Magnesium sulfate hydrate ($MgSO_4.7H_2O$)	100 mg L^{-1}
Calcium chloride ($CaCl_2$)	7 mg L^{-1}
Sodium bicarbonate ($NaHCO_3$)	1200 mg L^{-1}
Sodium sulfate (Na_2SO_4)	700 mg L^{-1}
Sodium chloride (NaCl)	1000 mg L^{-1}
Micronutrient solution	1 mL L^{-1}

For composing 30L of the synthetic wastewater 30 and 1 mL of macronutrients and micronutrients stock solution were added, respectively. The micronutrients solution composition is shown in **Table 2**.

TABLE 2. **Composition of the micronutrients solution of the synthetic effluent in study**

Composition	Concentration stock solution
$FeCl_2$	1275.6 mg L^{-1}
$ZnCl_2$	50 mg L^{-1}
$NiCl_2.6H_2O$	142 mg L^{-1}
$Mn.Cl_2.4H_2O$	500 mg L^{-1}
$Na_2SeO_3.5H_2O$	164 mg L^{-1}
H_3BO_3	50 mg L^{-1}
$CuCl_2.2H_2O$	38 mg L^{-1}
$CoCl_2.6H_2O$	2000 mg L^{-1}
$AlCl_3.6H_2O$	90 mg L^{-1}
$(NH_4)_6Mo_7O_{24}.4H_2O$	50 mg L^{-1}
EDTA	1000 mg L^{-1}
HCl	1 mL L^{-1}

Reactors and operating procedure. It was used two acrylic made cylindrical reactors with 5 L of volume (60 cm of high and 11 cm of internal diameter). Sampling valves were placed at 4 and 14 cm from the bottom (**Figure 2**). Both reactors were operated with Hydraulic Retention Time (HRT) of 24 hours and an Organic Loading Rate (OLR) of 1.5 Kg COD $m^3.d^{-1}$. The difference between the configurations of the two reactors is that R1 reactor is used as control (conventional configuration of UASB reactors), and in the R2 reactor an air diffuser (porous stone) was located after the sludge blanket bed (25 cm

from the bottom). Dissolved oxygen (DO) was kept between 0.2 and 0.3 mg O_2 L^{-1} (aquarium pump and control valve).

The synthetic effluent was stored in a refrigerator (9 ± 1ºC) and pumped for continuously feeding the two reactors using a peristaltic pump. The reactors were operated in a 28°C (± 2°C) acclimatized room.

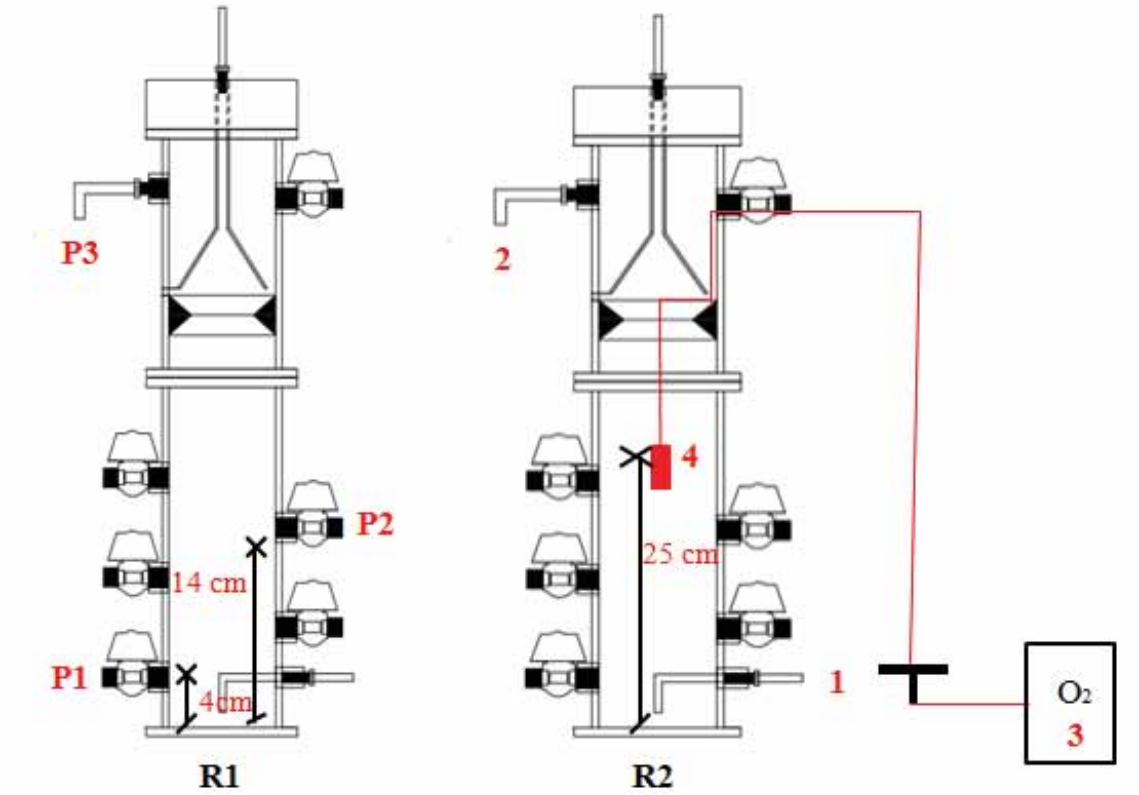


FIGURE 2. Schematic illustration of the operated reactors in bench scale, indicating the sampling points (P1, P2 and P3). 1 - Influent; 2 - Effluent; 3 - Aaquarium pump; 4 - Aerator

Evaluation of aromatic amines.Spectrofotometric scanning in the light absorption range of 200 to 500 nm was performed with influent and effluents samples of R1 reactor (UASB) and R2 (UASB with micro-aerated zone), in order to qualitatively assess the formation of aromatic amines as by-products of the anaerobic degradation of the azo dye DB22. Aromatic amines show strong light absorption in the range 260-300 nm[15]. In this range it is not observed interference from contaminants usually present in textile wastewaters and by-products of anaerobic degradation.

Monitoring parameters. The reactors were monitored by analysis of parameters and frequencies shown in **Table 3**. The physicochemical parameters were analyzed according to the *Standard Methods for The Examination of Water and Wastewater*[16].

TABLE 3. Parameters and frequencies monitoring of reactors

Parameters	Frequency
pH Temperature (ºC) ORP (mV) Dissolved oxygen (mg $OD.L^{-1}$) Salinity Total alkalinity (mg $CaCO_3.L^{-1}$) COD (mg $O_2.L^{-1}$) Color (mg $DB22.L^{-1}$)	3 times per week
Sulfate (mg $SO_4^{2-}.L^{-1}$) Aromatic amines	2 times per week

RESULTS AND DISCUSSION

Reactors Monitoring. The reactors were monitored during 120 days. **Table 4** shows the results of monitoring parameters of R1 and R2 during the operational period.

It is worth highlight that the influent, although stored in the refrigerator, already had oxidation-reduction potential (ORP) variation between -321.8 to -510.1 mV, indicating that the degradation may have started during the 7 days of storing in the refrigerator. Similar variation was detected in the effluent of R1 and R2, with variation from -422.3 to -311.7, and from -336 to -267.1 mV, respectively. Despite to the significant sulfate reduction in R1 reactor (68.64%), the ORP was sometimes more representative of methanogenic (-350 to -600 mV)[17] than the sulfate reduction (-220 mV)[18] conditions. The ORP in the effluent of R2 was less negative than in the effluent of R1, reflecting a slight interference of the micro-aeration in R2.

TABLE 4. Influent and effluent characteristics of R1 and R2 along the operational period

Parameters	Influent	R1 effluent	R2 effluent
pH	7 – 8.3	7 – 8.3	7 – 8.1
Temperature (ºC)	9 ± 1.32	26 ± 0.04	26 ± 0.03
ORP (mV)	-416.3 ± 48.08	-368.40 ± 26.24	-299 ± 19.40
Dissolved oxygen (mg $OD.L^{-1}$)	nd	nd	0.25 ± 0.03
Salinity	2.85 ± 0.17	2.71 ± 0.13	2.62 ± 0.11
Total alkalinity (mg $CaCO_3.L^{-1}$)	639 ± 124.37	930 ± 91.85	818 ± 88.83

nd – not detected

The total alkalinity (Table 4) increased from the influent to the effluent of both R1 and R2, indicating self-sufficiency of treatment systems in the production of alkalinity, ensuring stable operating conditions, remaining above the ideal value for anaerobic degradation (> 300 mg $CaCO_3$ L^{-1})[19].

COD removal. The temporal behavior of COD for R1 and R2 during the operational period is presented in **Figure 3**. The results of COD removal efficiency suggest that the micro-aerated zone did not favor the organic matter removal in R2 reactor, reaching an average removal efficiency of 66.51%, even lower than the detected in R1 (71.34%). According to the analysis of the t-test there was no significant difference ($p>0.05$) between the two reactors ($p = 0.10$). Probably the microbial community activity was reduced due to the salinity imposed on the treatment (2.85). Amaral[20] when operating the same reactor configuration with salinity of 1.9 reached COD removal efficiencies of 72 and 78%, respectively, for R1 and R2. When the author[20] increased the salinity to 3.2, decreased efficiencies were obtained, particularly in R2 reactor, of 67 and 59%, respectively for R1 and R2. Thus, indicating microbial community sensitivity to the imposed salinity.

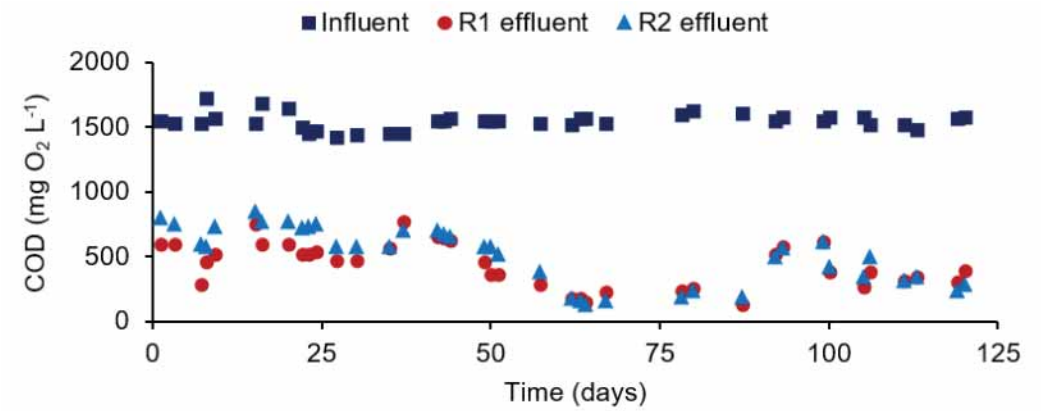


FIGURE 3. COD values in the influent and effluents along the operating period

Much higher COD removal efficiency of 97% (OLR of 7.2 kg COD $m^3.d^{-1}$) and 79% (kg COD $m^3.d^{-1}$) was obtained by Balapure, Bhatt and Madamwar[21] during the operation of a microaerophilic reactor (0.06 to 0.08 OD mg L^{-1}) to the treatment of textile effluent (azo dyes, salt, starch and glucose). In this study we used a mixture of azo dyes (Reactive Red 2, Reactive Red 198, Reactive Red 120, Reactive Blue 160, Reactive Blue 13 and Reactive Blue 172), with total concentration of 300 mg L^{-1} and salinity 1000 mg L^{-1}.

Color removal. Regarding to the average of color removal efficiency (**Figure 4**), the behavior were similar in R1 and R2, with R2 behavior (65.15%) slightly higher than the found for R1 (61.60%). This small disadvantage of reducing the dye in R1 may be explained by the competition with sulfate reducers bacteria, once the sulfate reduction was higher in R1. The influent color averaged 60.81 ± 3.45 mg DB22 L^{-1} and the effluent from reactors R1 and R2 23.45 and 21.20 mg DB22 L^{-1}, respectively (**Figure 4**). According to the analysis of the t-test there was also no significant difference ($p> 0.05$) between the two reactors ($p = 0.09$).

The efficiency values obtained were similar to Amaral[20], with the similar operational conditions (DB22, starch, sulfate and salt), reaching 65 and 69%, removal efficiencies respectively, in R1 and R2. Balapure *et al*. (2016)[22], using microaerophilic sequential

anaerobic-treatment system for textile effluent treatment containing azo dyes, achieved maximum removal efficiency in 60 hour HRT, of 99% efficiency. In this case, 80% efficiency was achieved only in anaerobic, as a complement in color removal and its intermediates.

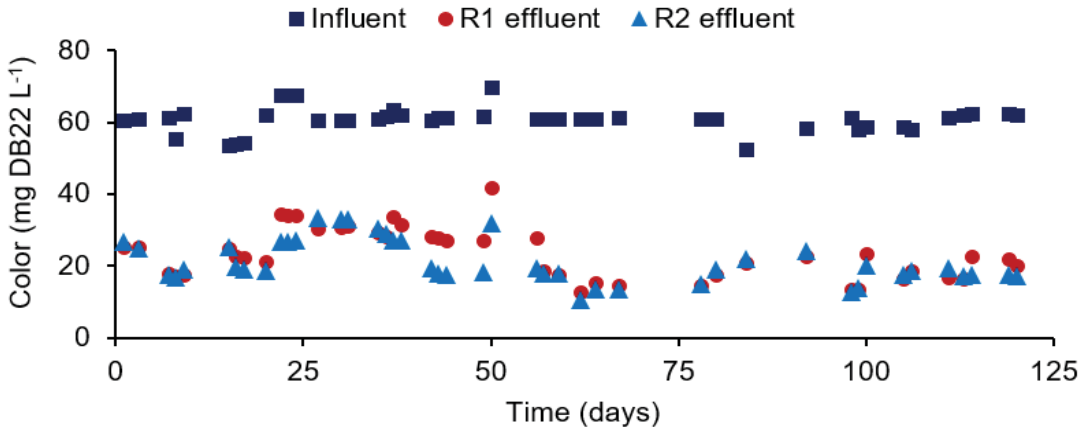


FIGURE 4. Color values in the influent and effluents along the operating period

***Aromatic amines*. Figure 5** shows the 200 to 500 nm scanning of influent and R1 and R2 effluents, conducted to qualitatively evaluate the formation of aromatic amines. It is observed that from 400 nm wavelengths, the absorbance of the influent starts to increase and effluents of R1 and R2 started to decrease, reflecting the degradation process of the dye DB22, which maximum absorption wavelength is 476nm. The scanning of R1 (anaerobic) effluent reveled higher absorbance values in the range of aromatic amines formation (260-300 nm)[15] than in R2 for the same wavelength range. This fact indicates subsequent removal of aromatic amines under microaerophilic conditions (0.25 ± 0.03 mg OD L^{-1}) in R2.

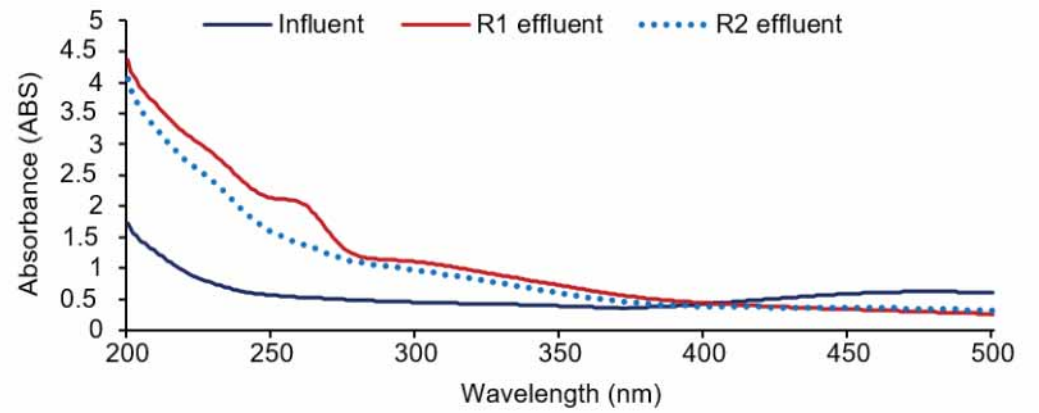


FIGURE 5. UV/VIS absorption spectrum for samples for influent and effluents

Sulfate reduction. The results of sulfate removal efficiency (**Figure 6**) with influent average of 513.46 ± 111.39 mg SO_4^{2-} L^{-1}, and R1 and R2 effluent of 156.18 ± 76.49 and 272.56 ± 64.78 mg SO_4^{2-} L^{-1}, respectively, indicate better removal in R1 (68%) than in

R2 (44%). Possibly the micro-aeration favored the conversion of sulfide, formed under anaerobic condition, back to sulfate in the presence of oxygen. Analysis of the t-test showed a significant difference ($p < 0.05$) between the two reactors ($p = 0.002$), and confirmed the best sulfate removal performance in the anaerobic reactor (R1).

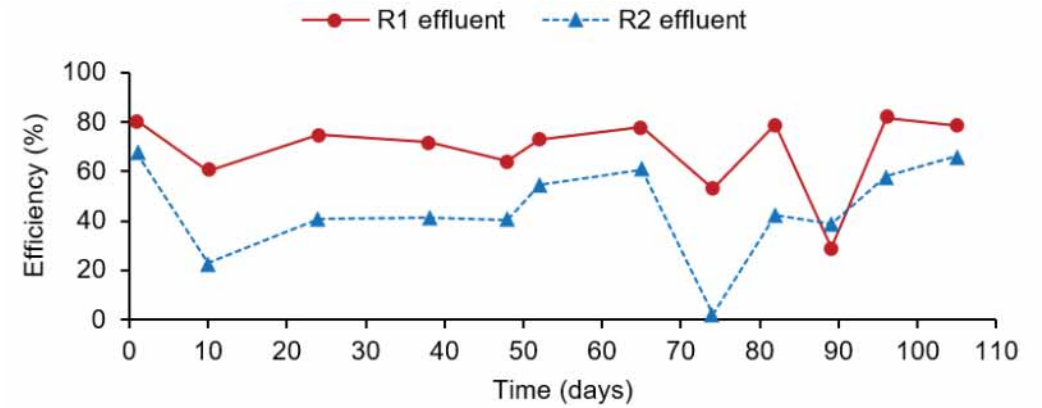


FIGURE 6. Sulfate removal efficiency for R1 and R2 along the operating period

CONCLUSION

The micro-aerated zone in the UASB reactor (R2) did not favor the removal of COD and color, with lower COD removal efficiency than the found in the UASB control reactor (R1). Probably the high salinity (2.85 ‰) caused sensitivity to microbial community. In R2 reactor, the color removal efficiency was slightly higher than the R1 reactor. Removal of the azo dye occurred in the R1 reactor by formation of aromatic amines, and R2 reactor occurred formation and subsequent removal of aromatic amines under microaerophilic conditions. Regarding the removal of sulfate the R1 reactor behaved as expected with an average removal efficiency of 68.64%, higher than the R2 reactor (44.63%). For the R2 reactor, micro-aeration reconverted part of sulfide formed sulfate in the presence of oxygen.

ACKNOWLEDGMENTS

The development agencies FACEPE and CNPq for the PhD scholarship and financial support, and Laboratory of Environmental Sanitation for the technical and scientific support.

REFERENCES

1. Van der Zee, F. Anaerobic azo dye reduction. Environmental Technology. Wageningen University, Wageningen, The Netherlands, 2002.
2. Trindade, B., Kato, M. T., Florêncio, L., Gavazza, S. Effect of starch and ethanol as electron donors, and sulfate on the reductive decolourisation of azo dye Direct Black 22. *13th World Congress on Anaerobic Digestion*, IWA, Santiago de Compostela, Spain, 2013.
3. Mendez-Paz, D., Omil, F., Lema, J.M. Anaerobic treatment of azo dye Acid Orange 7 under fed-batch and continuous conditions. *Water Resources*. 39, 771–778, 2005.

4. Razo-Flores, E.; Donlon, B.A.; Field, J.A.; Lettinga, G. Biodegradability of n-substituted aromatics and alkylphenols under methanogenic conditions using granular sludge. *Water Science and Technology*. 33 (3), 47–57, 1996.
5. Tan, N. C. G., Borger, A., Slender, P., Svitelskaya, A.V., Lettinga, G., Field, J.A. Degradation of azo dye Mordant Yellow 10 in a sequential anaerobic and aerobic reactor. *Water Science and Technology*. 42, 337–344, 2000.
6. Yerkes, D. W., Boonyakitombut, S., Speece, R. E. Antagonism of sodium toxicity by the compatible solute betaine in anaerobic methanogenic systems. *Water Science and Technology*. (37): 15–24, 1997.
7. Ferraz, A.D.N., Kato, M.T., Florencio, L., Gavazza, S. Textile effluent treatment in a UASB reactor followed by submerged aerated biofiltration. *Water Sci. Technol*. 64, 1581–1589, 2011.
8. Amaral, F. M., Kato, M. T., Florêncio, L., Gavazza, S. Color, organic matter and sulfate removal from textile effluents by anaerobic and aerobic processes. *Bioresource Technology*, 163: 364–369, 2014.
9. Jenicek, P., Koubova, J., Bindzar, J., Zabranska, J. Advantages of anaerobic digestion of sludge in microaerobic conditions. *Water Sci. Technol*., 62, 427–434, 2010.
10. Van der Zee, F. P.; Villaverde, S.; Garcia, P. A. Sulfide removal by moderate oxygenation of anaerobic sludge environments. *Bioresource Technology*, v. 98, n.3, p. 518–524, 2007.
11. Amorim, S. M., Kato, M. T., Florêncio, L., Gavazza, S. Influence of redox mediators and electron donors on the anaerobic removal of color and chemical oxygen demand from textile effluent. *Clean – Soil, Air, Water*, 41(9): 928–933, 2013.
12. Dos Santos, A. B. Reductive decolourisation of dyes by thermophilic anaerobic granular sludge. 176p. Thesis (Postgrad) – Wageningen University, Wageningen, The Netherlands, 2005.
13. Albuquerque, M. G. E., Lopes, A. T., Serralheiro, M.L. Biological Sulphate Reduction and Redox Mediator Effects on Azo Dye Decolourisation in Anaerobic-Aerobic Sequencing Batch Reactors. *Enzyme and Microbial Technology,* v 36, p. 790–799, 2005.
14. Gavazza, S., Gusman, Juan J. L., Angenent, Largus, T. Electrolysis within anaerobic bioreactors stimulates breakdown of toxic products from azo dye treatment. Biodegradation. 26(2):151-60, 2015.
15. Pinheiro H. M., Touraud E., Thomas O. Aromatic amines from azo dye reduction: status review with emphasis on direct UV spectrophotometric detection in textile industry wastewaters. *Dyes and Pigments*. 61: 121–139, 2004.
16. American Public Health Association (APHA). Standard Methods for the Examination of Water and Wastewater. 21sted. Washington DC, USA: American Water Works Association/ Water Environment Federation, 2005.
17. Rau, J., Stolz, A. Oxygen-insensitive Ntroreductases NfsA and NfsB of Escherichia coli Function under Anaerobic Conditions as Lawsone-dependent Azo Reductases. *Applied Environmental Microbiology*, v. 69, p. 3448-3455, 2003.
18. Yoo, E. S., Libra, J., Adrian, L. Mechanism of Descolorization of azo Dyes in a Anaerobic Mixed Culture. *Journal of Enviironment Engineering*, v. 127, p. 844-849, 2001.
19. Metcalf e Eddy – Wastewater Engineering – Treatment, Disposal, Reuse. 4° ed. Nova York, 2003.
20. Amaral, F. M. Tratamento de efluente têxtil por processo anaeróbio e aeróbio. 104p. Thesis (Postgrad) – Universidade Federal de Pernambuco, 2015.
21. Balapure, K., Bhatt, N., Madamwar, D. Mineralization of Reactive Azo Dyes Present in Simulated Textile Wastewater using Down Flow Microaerophilic Fixed Film Bioreactor. *Bioresource Technology*, v. 175, p. 1-7, 2015.
22. Kshama Balapure, K., Jain, K., Bhatt, N., Madamwar, D. Exploring bioremediation strategies to enhance the mineralization of textile industrial wastewater through sequential anaerobic-microaerophilic process. *International Biodeterioration & Biodegradation*. 106: 97-105, 2016.

CHAPTER 7.18 CENTRAL COMPOSITE DESIGN APPLIED TO POST-TREATMENT OF STABILIZED LANDFILL LEACHATE USING FENTON'S REAGENT

Caio Victor Lourenço Rodrigues *(1) and **Deize Dias Lopes** (2)

(1) Universidade Estadual de Londrina, Rod. C. Garcia Cid, Pr 445 Km 380, CEP 86.057-970, Londrina - PR, Brazil
(2) Universidade Estadual de Londrina, Rod. C. Garcia Cid, Pr 445 Km 380, CEP 86.057-970, Londrina - PR, Brazil

ABSTRACT

This study aimed to evaluate the application of Fenton's reagent for removing recalcitrant organic matter and color from mature landfill leachate, after biological pretreatment. Most of the organic matter in mature leachate is formed by complex molecules. Humic substances are the main group of these molecules, which are responsible for the dark color of the leachate. These molecules are recalcitrant, so that the physicochemical treatments are more appropriate for their removal. The AOPs can oxidize partially or fully organic molecule through $OH^{\bullet}$ radical, generated by the activation of any oxidizing substance. Fenton's reagent based on the activation of H_2O_2 by iron salts, which are able to remove recalcitrant organic and color from mature leachate. The Fenton's reagent involves a number of variables, as dosage of each reagent, molar ratio between them, pH of the reaction and addition modes of the reagents. For correct dosing of reagents and optimization of the treatment is adequate to evaluate the interaction effect between these variables.
In this study was evaluated the application Fenton's reagent to biologically treated leachate and the interaction among the involved variables. For the study of the physical-chemical treatment was developed an experimental design, divided into three steps. The results were evaluated by means of the response variables COD (Y_1) and color (Y_2). In Step I was determined from the literature which variables would be studied and after the effect of the variables were analyzed separately to get their value range. In Step II was used a fractional factorial design to evaluate which of these variables and interactions were significant. In Step III was used a CCD. It was established the conditions that resulted in the highest COD and color removal efficiency moreover was estimated the model that best represents the application of the Fenton's reagent conditions. Four independent variables were evaluated: $[H_2O_2]$, $[H_2O_2]/[Fe^{2+}]$, pH and addition mode of reagents.
Based on the variables studied the efficiency of COD removal was 89% and the color was 99% to the following parameters: $[H_2O_2]$=480 mM; $[H_2O_2]/[Fe^{2+}]$=6; pH=3.5 and fractioning the dose in four stages. The model that best represents the application of Fenton's reagent counted only the variable $[H_2O_2]$, linear and quadratic. However, tests have indicated that the other variables, while were not significant in relation to the

---

*Author for correspondence: caiovlrodrigues@gmail.com

response variables have any influence on the system operation, for example, the generation of sludge and therefore must not be disregarded.

Keywords: COD, Fenton, landfill, leachate

INTRODUCTION

In mature landfill leachate dissolved organic matter is formed by organic molecules which are resistant to biodegradation. Humic substances (HS) are the largest constituent of leachate organic matter (70-85%), whose molecules have molecular weight between 1800 to 2600 Da. These species are main responsible for the color leachate.[1-6] Recalcitrant organic does not cause immediate oxygen consumption in water bodies but its presence can cause problems in the drinking water.[7,8]

The biological treatment may not be effective in the removal of recalcitrant organic matter, therefore, the combination with physicochemical processes is recommended. The Advanced Oxidation Processes (AOPs) are an alternative to the removal of recalcitrant organic matter and color of stabilized leachate. AOPs are based on the high oxidation power and low selectivity of the hydroxyl radical (OH●) released during the redox reactions of some oxidizing compounds such as hydrogen peroxide (H_2O_2), ozone (O_3), oxide zinc (ZnO) and titanium dioxide (TiO_2). The OH● radical has a higher oxidation potential compared to conventional oxidants.[9,10] The formation of the OH● radicals from the reaction between iron salts and H_2O_2 is known as Fenton's reagent. In this reaction, ferrous salts activate the H_2O_2, which releases the OH● radical. This reaction redox involves a chain of reactions, the main are represented in Equations 1 and 2. [10-14]

$$Fe^{2+} + H_2O_2 \rightarrow Fe^{3+} + OH^{\bullet} + OH^{-} \quad (1)$$

$$2Fe^{2+} + H_2O_2 + 2H^{+} \rightarrow Fe^{3+} + 2H_2O \quad (2)$$

The Fenton's reagent is a technique that employs low-cost reagents. Other advantages are the lower generation of toxic byproducts and there is no limit for the mass transfer.[10,15-17] The main disadvantage is the high dosage of reagents because overdosing generates large volumes of sludge rich in iron. Another disadvantage reported by researchers is the need to reduce the pH. [4,11,16,18-20] The OH● radical promotes the oxidation of organic matter through its complete mineralization or reduction in size of organic molecules which can enhance the biodegradability of these substances. The combination of the application of the Fenton's reagent with other processes becomes appropriate.[11,21] The average efficiency achieved in research applying Fenton's reagent to mature leachate was 70%. [4,5,12,15,17,22-27]

The treatment with Fenton reagent consists essentially of the following steps: pH adjustment, addition of reagents, hydroxyl radical liberation, time for oxidation and neutralization and after coagulation/flocculation and sedimentation.[11,18,19] In spite of its simplicity, the treatment with Fenton's reagent involves a number of independent variables such as: dosage of each reagent, molar ratio between them, alkalinity,

characteristics of the organics in the influent, reaction time, addition mode of reagents, pH, temperature and dissolved oxygen in medium.[11,15]

The presence of H^+ ions indicate that the reaction between Fe^{2+} and H_2O_2 (Eq. 02) must occurs in acid medium.[10] Prior to the addition of the reagents, the pH of the medium should be adjusted to acidic values (2.0-4.5).[11] After medium acidification, Fe^{2+} and H_2O_2 is added and *i*mmediately starts the time required for the generation of OH● radicals and oxidation of the present compounds. In general, increasing the dosage of these reagents promotes greater removal of organics, however, it must be checked the saturation point of each reagent. The excess H_2O_2 can react with the OH● radical itself to forming hidroperoxila radical (HO_2) that is less oxidant.[5,15,28] In addition to the activating effect of H_2O_2, iron also has coagulant power, thus increasing its dosage promotes coagulation, on the other hand there is higher sludge production and of dissolved solids on effluent. After the oxidation time, the medium should be neutralized to interrupt oxidation reactions.[2,10-12] Regarding application of reagents, there is a preference for single dosage. However, this option can create an excess of reagent at the time of application, causing side effects of overdosing. Adding the reagents in steps, the reaction carried out gradually over time.[15,11]

The aforementioned variables are those reported in the literature as the most important in the application of the Fenton´s reagent. However, most of the results are obtained by analysis of variables separately, which do not take into account the interaction between them. The objective of this study is to evaluate and define what are the variables and meaningful interactions, as well as ideal conditions for the application of Fenton's reagent

MATERIALS AND METHODS

Leachate. Leachate used in the experiment collected from the municipal solid waste landfill in Londrina (PR, Brazil). It was operated between the years 1974 and 2010. The collected leachate was stored in the laboratory for supplying the experimental system. Physicochemical composition of the leachate was: pH: 8.2-8.5; Alkalinity: 4831-7205 $mgCaCO_3.L^{-1}$; BOD: 145-211 $mgO_2.L^{-1}$; $COD_{Filtered}$:1985-3096 $mgO_2.L^{-1}$; COD_{Total}: 2015-3576 $mgO_2.L^{-1}$; Ammonia: 819-1370$mgN\text{-}NH_3.L^{-1}$. The range of variation in some parameters reflects rainfall variation throughout the year in Londrina - humid subtropical climate region, with average rainfall of 1626 mm/year and average temperature of 21.1ºC.[29]

Before physicalchemical treatment the leachate was undergone to a biological treatment to remove nitrogen. The biological treatment consisted of an aerobic reactor (90L) followed by anoxic (27L) and clarifier. In **Table 1** the leachate characteristics were shown after the biological treatment. This effluent was used in the treatment with Fenton's reagent.

TABLE 1. Characteristics Leachate after biological treatment

Parameters	Steps	
	I e II	III
pH	8.0±0.1	7.8±0.12
Alkalinity ($mgCaCO_3.L^{-1}$)	1095±41.5	527±58.0
Color (uC)	7416±176.4	10432±119.6
COD $_{Filtered}$ ($mgO_2.L^{-1}$)	2248±49.4	2713±93.4
Ammonia-($mgN\text{-}NH_3.L^{-1}$)	208±88.9	126±41.6
Nitrite ($mgN\text{-}NO_2.L^{-1}$)	4.0±1.67	394.4±162,29
Nitrate ($mgN\text{-}NO_3.L^{-1}$)	199.1±99.6	7.1±2.61

Treatment with Fenton's reagent. Assays with Fenton's reagent were performed using a jar-test unit. The first step consisted in adjust the pH, that was tested for the interval from 2.0 to 5.0. The H_2O_2 solution was used in 30% (v/v), analytical grade (MW=34.01g and ρ=1.11g.cm^{-3}). The Fe^{2+} ions were obtained using granular ferrous sulfate heptahydrate ($Fe(SO_4).7H_2O$) (MW=278.01 g). The pH was adjusted with NaOH (6N) or H_2SO_4 (6N). For operational reasons, the volume used in each reactor was 1.0L. Firsty, H_2O_2 was addicted and after a short interval ferrous sulfate. After, the temperature and pH were checked. Stirring speed was maintained around 175s^{-1} for 2.5h. The final pH was adjusted to the values near neutral to stop the oxidation reaction. The settling time was determined from the beginning of the neutralization. Samples were collected for analysis (COD and color). The summary of the experimental procedure to three steps is shown in **Table 2**.

TABLE 2. Summary of the experimental procedure to Steps I, II and III

Experimental Procedure	Steps		
	I	II	III
Volume of leachate (L)	1.5-2.0	1.0	1.0
Initial pH Adjustment	yes/no	Yes	Yes
Temperature Control	yes/no	Yes	Yes
Reaction time (h)	2.0	2.5	2.0
Velocity Gradient (s^{-1})	175	175	175
Final pH Adjustment	No	Yes	Yes
Settling time (h)	1.0	1.0	1.0
COD	total	filtered	filtered
Color determination	No	Yes	Yes

Physicochemical analysis. The physicochemical analyses were carried out according to APHA[30], except for the nitrate, which followed the method of salicylic acid.[31] Samples for determination of color and COD were filtered through glass fiber membrane # 1.20µm. The presence of H_2O_2 may interfere with the results of the COD values overestimating them. However, there are not standardized methods yet for determining the residual H_2O_2, so in this study, it was disregarded, since the efficiency achieved in the tests will be underestimated.[32,33]

Experimental planning. In the experimental design two variables responses were used: Y1 for removing the organic matter, measured as COD, and Y2 for the removal of color. The experimental design was divided into three steps (Tab. 3). The statistical analysis was performed using the *R Statistical Software*, to a significance level of 5%.

The objective of the Step I was to determine the ranges of values to be used for each independent variable along the Step II. The variables were chosen based on two criteria. The first one considered the influence of these in the release mechanism OH● radical and oxidation. The second was based on the evaluation of the relevance of these variables, according to the literature. Most of the results presented in the literature were obtained by the analysis of the variables separately but do not consider the interaction between them. It was used as independent variables the concentration of H_2O_2 (x1), the molar ratio H_2O_2/ Fe^{2+} (x2), the pH of reaction (x3) and the number of reagent dosages (x4). In this step the variables were evaluated separately and only for the response variable Y1 (COD). The results were used to study each variable and the interactions between them in the Step II.

TABLE 3. **Steps of statistical analysis**

Steps	Objectives
I – Initial Tests	Identifying a range of values for the independent variables
II – Fractional Factorial Design 2^{4-1}	select the significant independent variables
III – Central Composite Desing (CCD)	Obtain the final model and the response surface

The interaction of independent variables was studied for the response variables by application of fractional factorial design (2^{4-1}) to levels (-1, 0, 1) in II. The level "0" (zero) refers to center points, which together with the replicas are used for the calculation of the error analyzes. Four center points were used for each variable. After the determination of significant variables and their interactions (Step II), the Central Composite Desing (CCD) was applied to obtain the final model for the response variables (Step III). A generic model can be seen from Equation 3.

$$Y= \beta_0 + x1\beta_1 + x2\beta_2 + x3\beta_3 + x4\beta_4 \quad (3)$$

The model was obtained from the CCD, formed by the full factorial design levels (-1, 0, +1), plus the axial points ($-\alpha$, 0, $+\alpha$). The levels of axial points were obtained from Equation 4, resulting α=2. The center points were the same for the fractional and to CCD factorial. The values of the independent variables are shown in **Table 4**.

$$\alpha = \left(2^k\right)^{1/4} \quad (4)$$

TABLE 4. Full Factorial design (2^4) and CCD

Independent Variables	Coded Values				
	-2	**-1**	**0**	**1**	**2**
x1 - [H_2O_2] (mM)	30	143	255	368	480
x2 - [H_2O_2]/Fe	2	4	6	8	10
x3 – pH	2.0	2.8	3.5	4.3	5.0
x4 – Dosage Steps	1	2	3	4	5

RESULTS AND DISCUSSION

The proposed experimental design was carried out to analyze the independent variables (x1, x2, x3, x4) for the responses variables Y1 (COD) and Y2 (color). After defining the range of values in Step I, fractional factorial design (2^{4-1}) was used in Step II to evaluate the interactions between variables and to determine the most significant independent variables. In Step III through CCD based on factorial design planning plus axial points, it was possible to assess all interactions between independent variables and define the optimal conditions for the application of Fenton's reagent, and the significant variables for the treatment.

Step I - Definition of the range of values for the independent variables. In Step I tests were conducted to select the range of values for the independent variables and only response variable Y1 (COD) was used. Value ranges were the following: x1 ([H_2O_2]) from 30 to 480mM; x2 ([H_2O_2]/[Fe^{2+}]) was between 2 to 10. The pH (x3) was assessed between 2 and 5 and in relation to the dosage, it was worked with a single dose fractionation to 5 doses throughout the reaction time. Keeping the same molar ratio [H_2O_2]/[Fe^{2+}], it was expected that the larger H_2O_2 concentration the greater the production of OH● radicals and therefore the removal of organic matter should be greater until a saturation concentration. In this step, this tendency was not observed, for that it was necessary to expand the range of values to study. Regarding the pH of the medium, tests were performed for three different conditions: adjusting the pH just prior to application of reagents, only the neutralization of the medium at the end of the reaction time and no pH adjustment. Organic matter was removed (86% removal of COD) when there was no initial adjustment of pH different from what was reported in the literature. These results attracted the attention to the possibility of participation of other factors, including the presence of some ions in the effluent and the characteristics of HS.

Step II - Analysis of variance to define the significant variables. In the analysis of variance, the significance of the independent variables and the interaction between them can be verified by the F-test and the p-value. The results of the analysis of variance (ANOVA) are presented in **Table 5** to responses variables (Y1 and Y2) with $F_{statistic}$ values and p-values.

In **Table 5** the significant variables are x1, x2, and the interaction between them (x1x2). The $F_{statistic}$ for these variables was higher than F_{critic} (4.35) and p-value less than 0.05. This result confirms the importance of [H_2O_2] (x1) and its relation to the [Fe^{2+}] (x2) in the production of OH● radicals. The applied dosage was in the range of 0.45 to 7.26

mgH_2O_2/gDQO and 0.37 to 1.19 mgFe^{2+}/gDQO. By comparing the p-value of the variables x1 and x2 it can be said that the [H_2O_2] has an importance which is greater than its activator. This suggests the possibility of using other activators. Rivas[20] have used another form iron ion, Fe^{3+}, obtaining organic matter removal efficiency very close to traditional systems, about 80% to [Fe^{3+}] equal to 0.01 M and [H_2O_2] equal to 1.0M.

Table 5. **Step II Analysis of variance for the response variable Y1 (COD) and Y2 (color)**

Variab.	DF	Sum of squares		Mean Squares		$F_{statistic}$		p-value	
		Y1	Y2	Y1	Y2	Y1	Y2	Y1	Y2
x1	1	3528.4	2882.0	3528.4	2882.0	86.01	35.42	1.11e-08**	8.052e-06**
x2	1	273.4	477.0	273.4	477.0	6.66	5.86	0.0178*	0.0251*
x3	1	35.0	12.0	35.0	12.0	0.85	0.15	0.3664	0.7045
x1:x2	1	672.0	4293.4	672.0	4293.4	16.38	52.77	6.295e-04**	5.003e-07**
x1:x3	1	57.0	126.0	57.0	126.0	1.39	1.55	0.2522	0.2276
x2:x3	1	35.0	45.4	35.0	45.4	0.85	0.56	0.3664	0.4639
x1:x2:x3	1	108.4	77.0	108.4	77.0	2.64	0.95	0.1197	0.3421
Regr.	7	4709.2	7912.8	672.74	1130.4				
Resid.	20	820.4	1627.1	41.0	81.4				
Total	27	5529.6	9539.9	204.8	353.3				

R^2 = 0.80; $F_{critic(0.05;\ 1;\ 20)}$ = 4.35; *significant; ** more significant

It was also observed that significant independent variables were the same for COD removal (Y1) and true color (Y2), which indicates a strong relationship between the removal of organic matter and color leachate. Christensen[1] and Kang[32] who found similar condition concluded that the HS in addition to being a major portion of the organic matter in mature leachate also is responsible for the color of leachate.

The concentration of iron ions increases the color of the treated effluent due to the presence of iron in excess besides the increase in sludge production. Other authors also observed this situation, according to Wu[5], Fe^{2+} ions dosages greater than 160 mM may increase the salinity and conductivity of the treated effluent.[4,12,19,24,28]

The analysis of variance with variable pH (x3) was not significant, although the graphs of interactions for the two levels of the variables x1 and x3, for both responses variables (Y1 and Y2), had indicate that x1x3 interaction there may be statistically significant.

Unlike than what was reported in the literature, the variables x3 and x4 were not significant, except for interaction between them. Thus, Step III should be carried out only with variables x1, x2 and x1x2 interaction. However, we chose not to discard any variable.

Step III - Definition of the significant variables and definition of the final model. After keeping the four independent variables (x1. x2. x3 and x4), we proceeded to the experimental design of Step III. In order to evaluate the behavior of the variables and their interactions, a model was initially tested with all variables and possible interactions (1st. 2nd. 3rd and 4th order). It was found that some variables and interactions were not

significant then other designs with fewer variables and interactions were tested until the decision for the final model. Models tested by the CCD for both variables Y1 (COD) and Y2 (color) are shown in **Table 6**.

From the adjusted coefficient of determination (R^2), the models were selected (i.e. IV, V, VI, IX and X) whose adjusted R^2 values were greater than 0.79 and 0.72 for COD and color. So these selected models explain at least 79 and 72% of the total variation of responses. It appears that these models simultaneously satisfy the response variables, indicating that there is a dependency between them. Christensen[1] and Kang[32] also observed this condition. For the authors, the HS in addition to being a major portion of the organic matter present in mature leachates, also contribute to the color of it. In all models previously selected at least one of the terms was quadratic indicating a 2nd degree function which best represents the relationship between the independent and dependent variables. It is observed that for the models selected at least one of the variables x1, x2 or x1x2 are present. This observation confirms the statistical analysis in Step II, which pointed these variables as significant. Then, one should adopted model to represent the dependent variable and the efficiency curve, according to the independent variables related to treatment. In **Figure 1** results of the responses variables Y1 and Y2 are represented in function of the independent variable $[H_2O_2]$ and $[H_2O_2]/[Fe^{2+}]$, for the model VII.

TABLE 6. **Models tested in CCD (Central Composite Desing)**

Models	Variables Analyzed	Adjusted R^2	
		Y1	Y2
I	x1. x2. x3. x4. x12. x13. x14. x23 x24. x34. x123. x124. x134. x234. x1234	0.59	0.19
II	x1. x2. x3. x4. x12. x13. x14. x23 x24. x34. x123. x124. x134. x234	0.60	0.21
III	x1. x2. x3. x4. x12. x13. x14. x23 x24. x34	0.63	0.29
IV	x1. x2. x1(Q). x12	0.82*	0.72*
V	x1. x2. x1(Q). x2(Q)	0.82*	0.72*
VI	x1. x2. x1(Q). x2(Q). x12	0.81*	0.72*
VII	x1. x2. x12	0.66	0.38
VIII	x1. x2	0.66	0.39
IX	x1. x2. x1(Q)	0.82*	0.73*
X	x1. x1(Q)	0.79*	0.73*

*selected models; (Q) – quadratic

The adjusted correlation coefficients of the selected models are very close. We used the partial F-test in order to determine the best set of regressors to the model. In the case of partial F if $F_{statistic}<F_{critic}(4.05)$, it accepts the null hypothesis. It is concluded that the variables x1x2, x2 and x2 (Q) does not significantly contribute to the model. The model that best represented the application of the Fenton's reagent was X (x1, x1(Q)), (Eq. 5 and 6).

$$Y1 = 53.0826 + 0.1714x1 - (0.0002x1^2) \quad (5)$$

$$Y2 = 62.3748 + 0.2371x1 - (0.0004x1^2) \quad (6)$$

From the response surfaces shown in **Figure 1** it is observed that the saturation point for the dosage of H_2O_2 is equal to approximately 300 mM, or from this point increasing the dosage does not result on gain efficiency. For Y2 variable it is possible to verify that after this point there is a drop in efficiency which may be caused by reaction between the excess H_2O_2 and OH● radicals, that besides the consumption of OH● radical own generates radicals $•HO_2$ with lower oxidation potential.[5.15.28] The point of saturation obtained in this work is close to the values obtained by Deng[15] and Wu[5], but higher than those found by Lau[12] and Lopez[17]. This difference to the saturation point of the dosage of H_2O_2 can be explained by variability in the leachate.

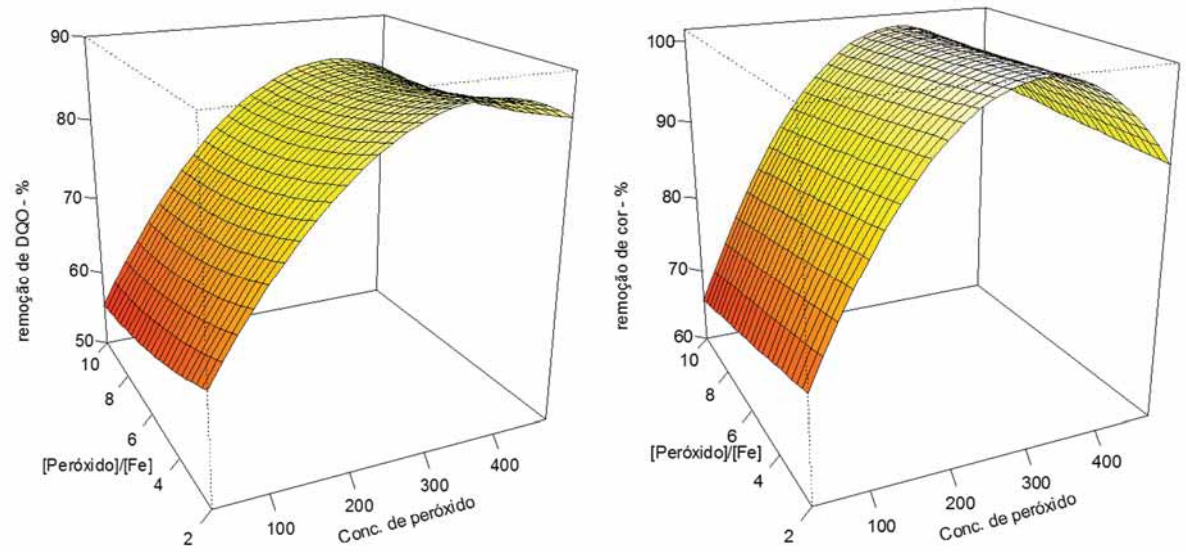


FIGURE 1. Response surface to removal efficiency dependent variables Y1 (a) and Y2 (b) to the independents variable $[H_2O_2]$ and $[H_2O_2]/[Fe^{2+}]$

Regarding iron ions, the present study evaluated the relationship between $[H_2O_2]/[Fe^{2+}]$ and not the isolated action of iron ions. The non-significance of the variable x2 does not indicate that the presence of iron ions is unnecessary, but the concentration of these in the studied ranges did not influence the efficiency of treatment for leachate in question and the conditions studied. The presence of iron ions in the medium is essential for oxidation to occur, since these are activators of H_2O_2 to form the radical hydroxyl.[5,24,28,32] From the results obtained, it is suspected there is a minimum dosage of iron for this reaction to occur. It can search in future work only the necessary dosage H_2O_2 activation, lower than that one used in this study ($[Fe^{2+}]$<80 mM). There will be reduction in reagent consumption and increased participation of oxidation and less sludge production, probably for the same removal efficiency.

Analysis used in this study allowed for the variables x1, x2, x3 and x4 were studied concurrently, or all possible interactions were evaluated. Although some of these variables are not significant, it was possible to find the values of these combinations that resulted in improved organic matter removal efficiencies (Y1) 89% and color (Y2) 99%. The parameters that provide the best results were $[H_2O_2]$=480 mM $[H_2O_2]/[Fe^{2+}]$=6, initial

pH of 3.5 and dosage divided into 03 fractions dosage. The COD removal efficiency obtained in this study, mean values of 89%, was high when compared to other treatment processes reported in the literature for leachate with similar characteristics.

The variable x4, relating to fractionation of the dosage of the reagents was no significant for the studied ranges of values. However, it was found that an operational way contribute to the process, with a lower foaming. The statistical analyzes performed in Step II and III possible to concludes that the variable x3 (pH) was not significant in the application of the Fenton's reagent. This observation differs from much of recommendation consulted researches, who point to the need to reduce the pH reaction at the beginning of the test, aiming to meet the balance of reactions triggered by Fenton's reagent.

According to Equation 2, the equilibrium of the reaction occurs in the presence of H^+ ions, acid medium. According Kang[32], the appropriate pH range for the reaction is between 3.0 and 5.0. However, this value range can be obtained during their own Fenton's reagent reactions, with no need for prior adjustment of the pH. This may justify variable x3 not be significant in the analysis of variance. In the literature, there is not a separation in the analysis of the reaction medium for the formation of hydroxyl radicals and the oxidation of organic matter. Equation 2 indicates that the formation of radicals should take place in an acid medium. This condition is also treated and discussed as ideal for the oxidation of organic matter. Others researches have applied Fenton's reagent without performing the reduction prior to the pH of the medium and yet achieved satisfactory results in the removal of organic matter with relative values between 60 and 85%.[22,25]

Therefore, to some authors the acidification of the medium prior to the application of the Fenton's reagent does not have the effect of reducing the pH of the medium, but it reduces the alkalinity of effluent to be treated. The carbonates and bicarbonates ions may react with the OH● radical, the radicals available for reducing degradation of desired compounds.[34,35] In the mature landfill leachate, in addition to carbonates and bicarbonates ions, attention should be paid to the presence of chlorides and sulfates.[36]

Finally, the model adopted in this study indicates that the variable pH is not significant, since the medium can become acid by addition of reagents which is inherent to the treatment, but based on the results obtained there is no basis for this statement. A study further deepening of the relationship between the initial alkalinity, reducing the pH by the addition of reactants and efficiency should be achieved conducted to evaluate more specifically to such arrangements.

CONCLUSION

Through statistical design developed, it was observed that for each conditions used in this study and for the tested values ranges for each independent variable, only the variables $[H_2O_2]$ and $[H_2O_2]/[Fe^{2+}]$ were significant, opposite to what is indicated by the literature;

The variable pH has not been identified in this study as a significant variable. It noted that the alkalinity and the characteristics of the leachate used may interfere in the application efficiency of the Fenton's reagent, deserving further research. Fractionation of the reagents was no significant treatment by Fenton's reagent. It is recommended to

fractional dosage for optimal system operation, avoiding foam formation in the reactor;
In this study was achieved organic matter, measured as COD, and color removal efficiencies of 85% and 98% from mature leachate using a dosage of 7.26 mgH_2O_2/gCOD removed and 1.19mgFe^{2+}/gCOD removed. The reagents were applied in a single dose, with the correction of the initial pH to 2.0.

REFERENCES

1. Christensen. J.B.; Jensen. D.L.; Gron. C.; Filip Z.Z.; Christensen. T.H.. *Characterization of dissolved organic carbon in landfill leachate-polluted groundwater*. Water Res.. v. 32. p. 125-135. 1998.
2. Kang. K.; Shin. H.S.; Park. H.. *Characterization of humic substances present in landfill leachates with different landfill ages and its implications*. Water Res.. v. 36. p. 4023-4032. 2002.
3. Kurniawan. T.A.; Lo. W.; Chan. G.Y.. *Physico-chemical treatments for removal of recalcitrant contaminants from landfill leachate.* Journal of Hazardous Materials. v.129. p.80-100. 2006.
4. Moravia. W.G.; Amaral. MC.S.; Lange. L.C.. *Evaluation of landfill leachate treatment by advanced oxidative process by Fenton's reagent combined with membrane separation system*. Waste Manage. v.33. p.89-101. 2013.
5. Wu. Y.; Zhou. S.; Qin. F.; Peng. H.; Lai. Y.; Lin. Y.. *Removal of humic substances from landfill leachate by Fenton oxidation and coagulation*. Process safety and Environ. Protection. v. 88. p. 276-284. 2010.
6. Zhao. R.; Gupta. A.; Novak. J.T.; Goldsmith. C. D.; Driskill. N.. *Characterization and treatment of organic constituents in landfill leachates that influence the UV disinfection in the publicly owned treatment works (POTWs)*. J. of Hazardous Materials. v. 258-259. p.1-9. 2013.
7. Fabris. R.; Chow. C.W.K.; Drikas. M.. *Practical application of a combined treatment process for removal of recalcitrant NOM–alum and PAC.* Wat. Sci. and Technol.: Wat. Supp.. v. 04. p.89-84. 2004.
8. Marttinen. S.K; Kettunen. R.H; Sormunen. K.M; Soimasuo. R.M; Rintala. J.A.. *Screening of physical–chemical methods for removal of organic material. nitrogen and toxicity from low strength landfill leachates.* Chemosphere. v. 46. p. 851-808. 2002.
9. EPA – United States Environmental Protection Agency.. *Handbook on Advanced Photochemical Oxidation Processes.* U.S. Enviroment Protection Agency – Technology Trasnfer. 1998.
10. Huang. C. P; Dong. C.; Tang. Z.. *Advanced chemical oxidation: Its present role and potential future in hazardous waste treatment*. Waste Manage.. v. 13. p.61-377. 1993.
11. Deng. Y.; Englehardt. J.. *Treatment of landfill leachate by the Fenton process*. Water Res.. v.40. p.3683-3694. 2006.
12. Lau. I.W.C.; Wang. P.; Fang. H.H.P.. *Organic removal of anaerobically treated leachate by Fenton coagulation*. J. of environ. Engineering. v. 127. p.666-669. 2001.
13. Neyens. E; Baeyens. J.. *A review of classic Fenton's peroxidation as an advanced oxidation technique.* J. of Hazardous Materials. v. 98. p.33-50. 2003.
14. Walling. C.; Goosen. A.. *Mechanism of the ferric ion catalyzed decompostion of hydrogen peroxide*. J. of the American Chemical Society. v. 95. p.2987-2991. 1973.
15. Deng. Y.. *Physical and oxidative removal of organics during Fenton treatment of mature municipal landfill leachate*. J.l of Hazardous Materials. v. 146. p. 334-340. 2007.
16. Li. W.; Zhou. Q.; Hua. T.. *Removal of organic matter form landfill leachate by advanced oxidation process: A review*. Hindawi Publishing Corporation. v. 2010. DOI 10.1155/2010/270532. 2010

17. Lopez. A; Pagano. M.; Volpe. A.; Di pinto. A. C.. *Fenton's pre-treatment of mature landfill leachate*. Chemosphere. v. 54. p.1005-1010. 2004.
18. Georgi. A; Schierz. A.; Trommler. U.; Horwitz. C.P.; Collins. T.J.; Kopinke. F. D.. *Humic acid modified Fenton reagent for enhancement of the working pH range*. App. Catalysis B: Environ. v.72. p. 26-36. 2007.
19. Gotvajn. A.Z.; Zagorc-koncan. J.; Cotman. M.. *Fenton's oxidative treatment of municipal landfill leachate as an alternative to biological process.* Desalination. v. 275. p.269-275. 2011.
20. Rivas. F.J.; Beltran. F.; Carvalho. F.; Acedo. B.; Gimeno. O.. *Stabilized leachates: sequential coagulation–flocculation+chemical oxidation process*. J. of Hazardous Mat. B. v. 116. p. 95-102. 2004.
21. Chamarro. E.; Marco A.; Esplugas. S.. *Use of Fenton reagent to improve organic chemical biodegradability.* Water Research. v.35. p.1047-1051. 2001.
22. Chen. Y.; Liu. C.; Nie. J.. *Removal of COD and decolorizing from landfill leachate by Fenton´s reagent advanced oxidation.* Clean Techn Environ Policy. v. 16. p. 189-193. 2014.
23. Hermosilla. D.; Cortijo. M.; Huang. C.P.. *Optimizing the treatment of landfill leachate by conventional Fenton and photo-Fenton processes*. Sci. of the Total Environ..v.407. p.3473-3481. 2009.
24. Kim. Y.; Huh. I.. *Enhancing Biological Treatability of Landfill Leachate by Chemical Oxidation*. Environmental Engineering Science. v. 14. p. 73-79. 1997.
25. Koc-jurczyk. J.; Jurczyk. L.. *The efficiency of landfill leachate treatment using the Fenton´s reagent*. Journal of Ecological Engineering. v.16. p.70-76. 2015.
26. Pala. A.; Erden. G.. *Chemical Pretreatment of Landfill Leachate Discharged into Municipal Biological Treatment Systems*. Environmental Engineering Science. v. 21. p. 549-557. 2004.
27. Sun. J.; Li. X.; Feng. J.; Tian. X.. *Oxone/CO_2^+ oxidation as an advanced oxidation process: Comparison with traditional Fenton oxidation for treatment of landfill leachate*. Water Research. v.43. p. 4363-4369. 2009.
28. Gogate. P.R.; Pandit. A.B.. *A review of imperative technologies for wastewater treatment I: oxidation technologies at ambient conditions*. Advances in Environmental Research. v. 8. p.501-551. 2004.
29. Instituto Agronômico do Paraná. Agrometeorologia. *Dados diários de Londrina 2016*. Londrina. 2016.
30. Apha. *Standard methods for the examination of water and wastewater*. 20th. Edition. Washington. 2005.
31. Cataldo. D.A.; Haroon. M.; Schrader. L.E.; Youngs. V.L.. *Rapid colorimetric determination of nitrate in plant tissue by nitration of salicylic acid*. Comm. in Soil Sci. and Plant Analysis. v.6. p.71-80. 1975.
32. Kang.Y. W.; Hwang. K.. *Effects of reaction conditions on the oxidation efficiency in the Fenton process*. Water Res.. v. 34. p. 2786-2790. 2000.
33. Peixoto. A.L.C.; Brito. R.A.; Salazar. R.F.S.; Guimarães. O.L.C.; Filho. H.J.I.. *Predição da Demanda Química de Oxigênio em chorume maduro contendo reagente de Fenton. por meio de modelo matemático empírico gerado com planejamento fatorial completo*. Quím. Nova. v. 31. p. 1649-1647. 2008.
34. Cho. S. P.; Hong. S. C.; Hong. S.. *Photocatalytic degradation of the landfill leachate containing refractory matters and nitrogen compounds*. Appl. Catalysis B: Environ.. v. 39. p.125-133. 2002.
35. Lin. S.; Gurol. M.. D.. *Catalytic decomposition of hydrogen peroxide on iron oxide: Kinetics. mechanism. and implications*. Environ. Sci. Technol.. v. 32. p.1417-1423. 1998.
36. Deng. Y.; Rosario-muniz. E.; Ma. X.. *Effects of inorganic anions on Fenton oxidation of organic species in landfill leachate*. Waste Manage. & Res.. v.30. p.12-19. 2012.

CHAPTER 7.19 GREYWATER TREATMENT IN AN AEROBIC SBR: SLUDGE STRUCTURE AND KINETICS

U. Rojas-Z. (1); C. Fajardo-O. (1); I. Moreno-Andrade (2) and O. Monroy *(1)

(1) Department of Biotechnology, Universidad Autónoma Metropolitana-Iztapalapa, Av San Rafael Atlixco, No 186, Mexico City, Mexico.
(2) Laboratory for Research on Advanced Process for Water Treatment, Unidad Académica Juriquilla, Instituto de Ingeniería, Universidad Nacional Autónoma de México, Blvd. Juriquilla, No 3001, Querétaro, México.

ABSTRACT

The effect of the composition of the influent on the granulation process was evaluated using a synthetic media (SM) and greywater (GW) as feedstock in the operation of two SBR. The feeding with a balanced SM led to the growth of the first granules after 3 weeks from the start up, and on day 139 the biomass was dominated by mature and compact granules, with a sludge volume index (SVI) of 22.4 mL g^{-1}, a zone settling velocity (ZSV) of 13.1 m h^{-1} and a density of 56.7 g L^{-1}. In contrast, the physical properties of the granules in the SBR fed with GW were dependent on the existence of famine periods which in turn depended of the specific organic loading rate (Bx) applied. When this system was operated at a high mean Bx of 4.4 kg COD $kgVSS^{-1}$ d^{-1} the biomass was dominated by filamentous aggregates with poor physical properties. However when the Bx was reduced from to 2.9 kg COD $kgVSS^{-1}$ d^{-1}, the existence of famine periods was allowed, and a considerable improvement in the settling properties and compactness of the granules was observed. It was found that the cell growth kinetics of microorganisms in aerobic granules is also dependent of the influent composition. In this study, granules cultivated with SM were formed by fast growing microorganism with high substrate utilization rates, whereas granules cultivated in greywater presented a much lower cell growth and substrate utilization rates.

Keywords: Aerobic granules, greywater treatment, kinetic parameters, sequencing batch reactors

INTRODUCTION

Greywater is the fraction of domestic wastewater composed by bathroom (shower & hand basin), laundry and kitchen discharges[1]. Since this effluent does not contain faeces, urine and toilet paper, it is considered as less polluted than municipal wastewater, and its reclamation for non-potable uses has been considered as an attractive option to reduce the domestic water demand[2,]. However, greywater composition is highly dependent on household activities, source and water availability, and in many cases may present high pollutants concentrations of dissolved and suspended organic matter, salts, organic chemicals oils, detergents and pathogens[3].

---

*Author for correspondence: ulises.rojaz@gmail.com

Therefore, the most suitable alternative of reuse is after and efficient, robust and decentralized treatment that allows the removal of its pollutants.

To date, different biological technologies have been applied for greywater treatment. These include constructed wetlands[4], membrane bioreactors[5], upflow anaerobic sludge blanket (UASB) reactors and sequencing batch reactors (SBR)[6]. Among these, SBR systems are advantageous due to the possibility to carry out the simultaneous removal of organic matter and nutrients at relative low hydraulic retention times[7,8], demanding a small footprint due to the absence of secondary clarifiers.

In addition to the mentioned qualities, in the last 20 years the study of the operation of the SBR has been focused in the study of cultivation and application of granular activated sludge, which presents a high settling velocity, a regular and dense structure, and the ability to resist toxics and the operation at high organic loading rates[9]. So far, aerobic granulation has been widely studied using synthetic media with readily biodegradable carbon sources, like glucose, acetate, phenol and ethanol[10], and in some cases with industrial wastewaters[8]. However, the analysis of the granulation process using greywater as feedstock has not been addressed to date. This is an important question that must be studied to define the effect of the particular composition of this effluent on the granulation process and the viability of the granular technology as an efficient alternative the stabilization of greywater.

This study aims to analyze the granulation process in a SBR using greywater as feedstock and the effect of the specific organic loading rate in the stability and properties of the biomass. The results were compared with an identical system fed with a well-balanced synthetic media (SM) in order to analyze the effect of the influent composition over the biomass development and structure.

MATERIALS AND METHODS

SBR. Two SBR of 3.3 L of working volume and a L/D ratio of 10.2 were used during experimentation for the cultivation of aerobic activated sludge. Oxygen was provided by a 70 W air blower connected to fine bubble diffusers fixed at the bottom of the reactors. The influent was fed through a port positioned near the bottom of the reactor, and the effluent was discharged through a port located at the middle of the working height. The control of pumps and blower was carried out using time programmable devices.

***Operation*.** The SBR were fed with a Synthetic media (SM) and greywater (GW). SM was prepared according to Beun et al. (1999)[11], except for the concentrations of sodium acetate and mono and dibasic potassium phosphate, which were adjusted to higher concentrations. GW samples were obtained from a household in Mexico City by mixing subsamples from kitchen sink, bathroom and washing machine. Samples were stored in 20 L containers at 8.0±1.0°C, and its composition is shown in **Table 1**. Both systems were inoculated with activated sludge (3.2 g L^{-1} VSS) from a municipal wastewater treatment plant, which had an irregular floc structure.

The SBR were operated in successive cycles of 4 h, with 10 min for feeding, variable reaction and settling times, and 3 min for discharge. The settling time was gradually reduced from 8 to 1 min in the reactor fed with synthetic wastewater (SMr) and from 8 to 3 min in the reactor fed with greywater (GWr). The effluent exchange ratio was fixed at

50%, and the aeration flow was maintained at 4.5 L min^{-1}, equivalent to a superficial airflow velocity of 1.43 cm s^{-1}. The temperature was controlled at 30 ± 2.0°C.

TABLE 1. Composition of SM and GW

	SM	GW
tCOD (mg L^{-1})	1,110-1,908	610-2,610
sCOD (mg L^{-1})	--	273-1,190
NH_4^+(mg NH_4^+ - N L^{-1})	149	0.36-10.5
PO_4^{3-} (mg PO_4^{3-}-P L^{-1})	149-172	3.6-45.1
Anionic surfactants (mg L^{-1})	--	5.3-90.3
TSS (mg L^{-1})	--	0.19-1.25

***Analytical methods*.** The determination of total and soluble chemical oxygen demand (tCOD, sCOD), total and volatile suspended solids (TSS, VSS), sludge volume index (SVI) and zone settling velocity (ZSV) were carried out following standard methods[12]. Ammonia was determined in samples previously centrifuged at 2500 rpm for 15 min, using a Hanna electrode, model HI 83141. Anionic surfactants were analyzed according to the method of Jurado et al. (2006)[13]. Biomass density was analyzed by the blue dextran method, proposed by Beun et al. (2002)[14]. The integrity coefficient of granular biomass was determined as the ratio of solids in the supernatant to the total weight of the granular sludge, by measuring the amount of detached material after a sample was stirred at 200 rpm for 5 min, following the procedure suggested by Ghangrekar et al. (2005)[15]. For the analysis of the biomass morphology a Nikon optical microscope, model BX50, and a digital cell camera were used.

***Aerobic granular sludge kinetics*.** The substrate uptake rate and cell growth rate of the aerobic granular biomass cultivated using SM and GW was evaluated. The experimental results were fitted with the linearized form of the Monod model, using the Lineweaver-Burk plot method (Eq. 1):

$$\frac{1}{\mu} = \frac{K_S}{\mu_{max}} \frac{1}{S} + \frac{1}{\mu_{max}} \quad (1)$$

Where μ is specific growth rate (h^{-1}), μ_{max} is the maximum specific growth rate (h^{-1}), S is limiting substrate concentration (g L^{-1}) and K_s is the affinity constant (g L^{-1}).The values of μ_{max} and Ks were obtained by the intercept and the slope of a plot of 1/μ versus 1/S.

For the experiment it was taken a sample of granules from each SBR, which were disaggregated using a mortar. The culture from SMr was fed with a synthetic media with a tCOD of 16.9 g L^{-1}, and the culture from GWr was fed with greywater with a COD of 5.6 g L^{-1}. The experiments were carried out in the same SBR used for granular biomass

cultivation, applying the same hydraulic conditions and following the COD consumption and the cell growth in time.

Parameters calculation. Although the operation of the SBR is carried out in a batch mode, the constant repetition of the cycles under the same conditions allows its analysis as continuous systems. To obtain the cell mass yield coefficient (Y_x) there were considered the suspended solids washed out with the effluents as follows:

$$Y_x = \frac{\left[(X - X_0) + \frac{V_e}{V}\sum_{i=0}^{n} X_e\right]}{\sum_{i=1}^{n}(S_0 - S)} = \frac{[(X - X_0) + r_e \sum_{i=0}^{n} X_e]}{\sum_{i=1}^{n}(S_o - S)} \quad (2)$$

Where X_0 and X (gVSS L^{-1}) corresponds to the biomass concentration in the reactor at the beginning and after "n" cycles respectively, S_0 and S (g L^{-1}) are de tCOD in the influent and effluent in "n" cycles respectively, and Xe is the effluent solids content in "n" cycles.

The equation 2 estimates Y_x from the biomass growth, substrate utilization and the effluent solids content in several operational cycles of the granular SBR, which is convenient for a more accurate estimation.

The control of the specific organic loading rate Bx (g COD g VSS-1 d-1) (Eq. 3) is important in the development of the granulation process and the performance of the system. If this parameter is not controlled the formation, size and stability of granules could be affected.

$$B_x = \frac{S_{inf} \,.\, C}{X} \cdot \frac{V_e}{V} = \; B_x = \frac{S_{inf} \,.\, C}{X} \cdot r_e \quad (3)$$

RESULTS AND DISCUSSION

The behavior of both systems was quite different in terms of physical properties and kinetics of the biomass, pollutants removal efficiency and effluent quality considering its solids content.

Granulation process. The application of a high aeration rate along with the gradual reduction in the settling time, led to the washout of the biomass with the poorer settling properties and to the formation of small and dense aggregates, of about 0.2 mm, in both systems during the first 10 days. In GWr the biomass started to show filamentous outgrowths from the second week, fostering the predominance of aggregates with a fluffy and filamentous structure until day 145. Thereafter, with the reduction in the Bx from 4.1 to 2.9 kg COD kg VSS^{-1} d^{-1}, a considerable reduction in the filamentous outgrowths of the granules from GWr was observed (**Figure 1**). In this system the SVI increased during start up to values closer to 250 mL g^{-1} and remained stable during the first 145 d. Subsequently, with the reduction in Bx, it was observed an improvement in

the settling properties of the granules, reaching to the maximum compactness and velocity just during the last 70 days of operation, when the SVI was closer to 100 mL g^{-1} (**Table 2**). In contrast, the feeding with a readily biodegradable substrate in SMr led to the formation of the first granules just after three weeks from the start up, and after 60 days, the flocs disappeared from the system and the biomass was dominated by mature and compact granules (**Figure 1**, SMr day 224), which were much smaller than granules in the GWr (**Table 2**). The faster granulation attained using synthetic media led to the increase in the settling properties since the first 4 weeks, which was reflected in a continuous drop in SVI from day 20 until day 50 up to values lower than 50 mL g^{-1}.

Table 2 shows the physical properties of the granular biomass from SMr and GWr in two operational days. In day 139, granules from GWr presented a high fraction of filamentous, while in day 253 granules presented a more regular morphology, with a considerably lower fraction of filaments (Figure 1, GWr day 264). On the other hand, granules from SMr did not show a difference in the morphology from day 139 to day 217 to day 2.

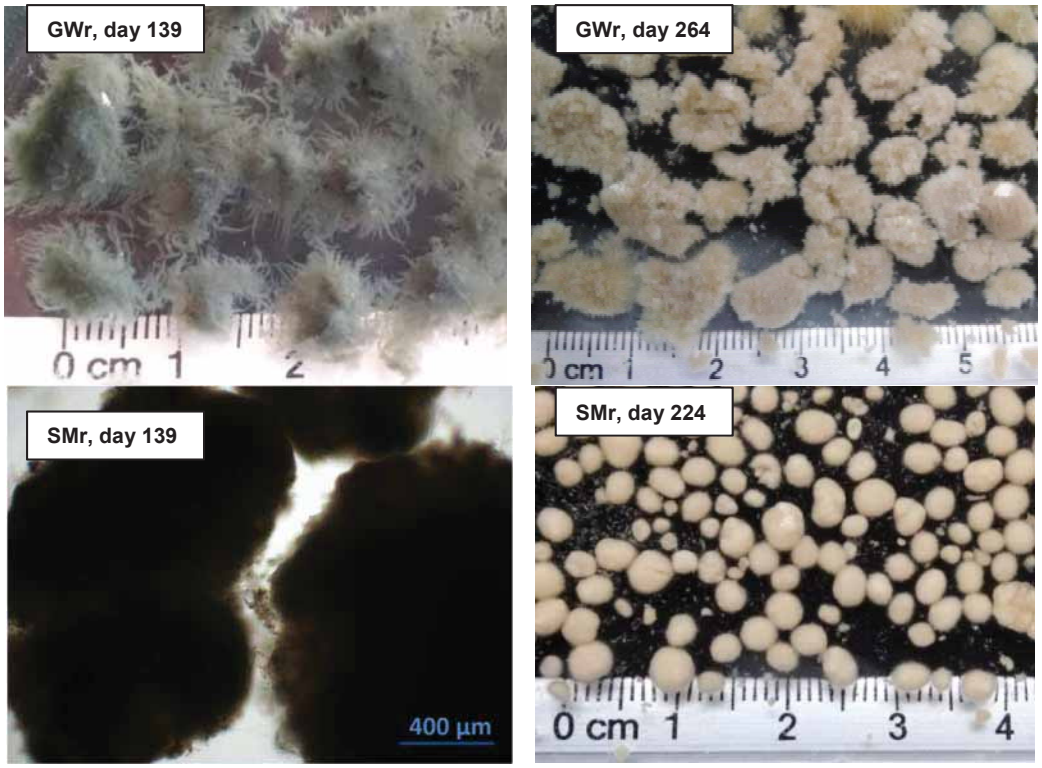


FIGURE 1. **Morphology of granules from GWr and SMr in different operational days**

The data showed in **Table 2** indicated that aerobic granules cultivated using synthetic media presented better physical properties than granules formed using greywater. The difference in the properties was considerably high on day 139, when GWr was operated at a Bx 4.4 kg COD kg SSV^{-1} d^{-1}. However when the Bx was reduced to 2.9 kg COD kg SSV^{-1} d^{-1} it was observed a remarkable improvement in the physical properties of the biomass in GWr, and as result the SVI decreased from 164.8 to 98.0 mL g^{-1} and the ZSV and density increased from 9.8 to 13.3 m h^{-1} and from 13.1 to 21.7 g L^{-1}

respectively. The lower integrity coefficient and size of granules from SMr also indicated a higher strength and compactness, although with the reduction in Bx in the operation of GWr it was observed an improvement in the strength of its granular biomass, and therefore the integrity coefficient decreased from 4.2 to 2.0.

TABLE 2. Physical properties of the biomass from SMr and GWr on two different operational days

Biomass	ZSV ($m\ h^{-1}$)	SVI ($mL\ g^{-1}$)	Density ($g\ L^{-1}$)	Integrity coefficient (%)	Predominant size (mm)
SMr (d 139)	13.1	22.4	56.7	0.4	0.9 < D < 1.7
(d 217)	17.6	43.1	31.4	0.6	1.7 < D < 2.8
GWr (d 139)	9.8	164.8	13.1	4.2	D > 4.8
(d 253)	13.3	98.0	21.7	2.0	2.8 < D < 4.8

Despite of the improvement in the properties of granules from GWr, the compactness and settling velocity never were superior to that of granules cultivated using synthetic media. This indicates that the composition of the influent is also a factor in the conformation of the granular biomass. The feeding with a non-complex influent in SMr allowed the formation of aerobic granules with a regular, dense and strong microbial structure, which are characteristics of heterotrophic granular sludge[14]. On the other hand, the poorer physical properties of granules cultivated in GWr were due to the presence of protozoa and other organisms **(Figure 1**, GWr day 139). When the reactor is fed with a complex media like greywater, the slowly biodegradable matter must be extracellularly hydrolyzed to soluble components before bacterial absorption[16]. This slow process, which results in the limitation of the growth of heterotrophic bacteria, is commonly related with the presence of protozoa, which coexist with filamentous microorganisms and finger type structures at the surface of granules[17]. It has been reported that protozoa presents a high affinity to slowly biodegradable matter and solids[17, 18]. So, the formation of filamentous outgrowths in aerobic granules can be analyzed as an adaptation of the biomass to the presence of slowly biodegradable compounds. This behavior is similar to the one reported by Schwarzenbeck et al. (2005)[18], who obtained filamentous aggregates using dairy wastewater, with lower settling properties than granules cultivated with synthetic media.

Relationship between Bx and famine time and its effect in biomass structure. The sCOD degradation profiles of two cycles from different operational days are shown in **Figure 2**. In SMr the degradation of practically all the organic matter occurred within the first half hour of the cycle, giving a first order constant (k) of 5.5 h^{-1}. In contrast, for GWr the sCOD consumption rate was significantly lower (k = 1.61 h^{-1}), allowing the substrate availability during a long fraction of the cycle. This phenomenon was mainly observed during the first 145 operational days, when GWr was operated at a mean Bx of 4.1 kg COD kg VS^{-1} d^{-1}, however, when the Bx was reduced to 2.9 kg COD kg VS^{-1} d^{-1}, the sCOD consumption occurred during the first 1.7 h of the cycle (second profile of GWr on **Figure 2**), allowing the existence of famine periods. Therefore, the evolution in the

morphology of the biomass observed with the reduction in Bx, from non-dense filamentous aggregates to more dense granules with a regular structure, was probably encouraged by the existence of famine periods in the operation cycles.

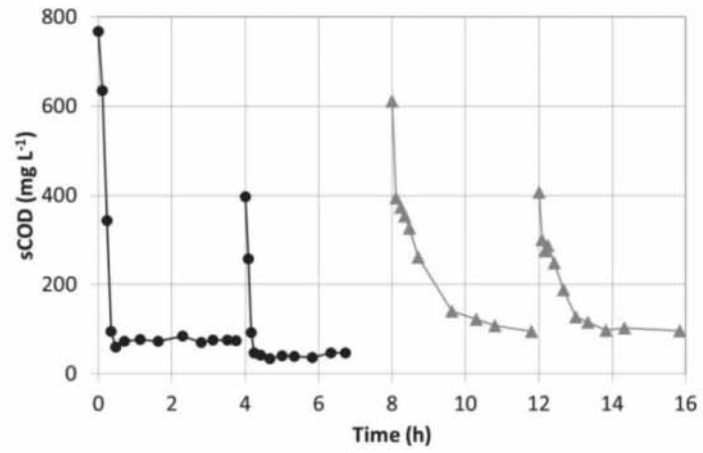


FIGURE 2. sCOD degradation profiles of SM (●) and GW (▲) in cycles of two operational days

It is reported that filamentous microorganism, which have a very low values of Monod affinity constant (Ks) and maximum specific growth rate (μ_{max}), are able to compete with flocs forming bacteria at continually low substrate concentrations or when there are not feast-famine conditions[19]. The treatment of real high complexity wastewater at high tCOD loading rates may led to the growth of filamentous aggregates, since the removal of the slowly biodegradable compounds is carried out at low substrate uptake rates, which promotes a continuous substrate availability during practically all the cycle time, reducing the famine conditions to the minimum. This situation does not occur with synthetic media, where usually the carbon source is a readily biodegradable compound (eg. ethanol, acetate or glucose) which is consumed rapidly, allowing a long famine phase. According with this, the presence of filamentous granules has been specially observed in the treatment of sewage, like effluents from pig farm[10], dairy industry[18], and domestic sewage[20], in which the pollutants removal is carried out at low substrate uptake rates and therefore it is required to apply a low ratio of substrate to microorganisms (Bx) to attain famine conditions in the cycles and the formation of compact granular biomass.

Kinetics of granular biomass. The evaluation of the cell growth kinetics and the substrate utilization rate is a key aspect in the design, operation, and prediction of the performance of biological systems. In this study the kinetic constants Ks, μ_{max} and Y_x of granules cultivated with synthetic media and greywater were evaluated. The results of the analysis are presented and compared with those from another works in **Table 3**.

The values of μ_{max} and Ks showed in **Table 3** indicated that granules from GWr are composed by slow growing microorganism with a high affinity to the substrate, while granules from SMr are composed by fast growing microorganism, maybe dominated by zoogleal bacteria, with a lower affinity for substrate. The low value of μ_{max} for the

granules from GWr is probably related to the fact that this biomass comes from filamentous aggregates, which according to Liu and Liu (2006)[19], presents a higher substrate affinity and lower maximum growth rate than non-filamentous organisms.

TABLE 3. Kinetics parameters of granular and fungi biomass fed with different substrates

System (influent)	X ($g\ L^{-1}$)	K_s ($g\ L^{-1}$)	μ_{max} (h^{-1})	Y_x ($gVSS\ gCOD^{-1}$)	r_x ($g\ L^{-1}\ h^{-1}$)	Reference
Granular SBR (SM)	4.5	0.23	0.22	0.65	0.72	This work
Granular SBR (GW)	1.8	0.14	0.11	0.10	0.20	This work
Granular SBR (SM)	4.7			0.23	---	Chen et al. (2008)[21]
Granular SBR (SM)	8.0	0.27		0.18-0.25	---	Liu et al. (2005)[22]

The Ks values of the granules cultivated in SMr, using sodium acetate as carbon source, are similar to that reported by Liu et al. (2005) for granules cultivated using glucose. However, the Y_x value of granules cultivated with sodium acetate is considerable higher. The difference may be due to the different operational conditions among both experiments, since according with Sponza (2001)[23], the rate of substrate utilization is directly related with the microorganism content inside the granules and with the concentration of substrate surrounding the granule. On the other hand, it is important to notice that there were not found values of μ_{max} for microorganism in aerobic granules cultivated with greywater or even real wastewaters, so the values obtained in this experiment cannot be compared with others.

System Performance. **Figure 3** shows the tCOD in the influent and effluent and the COD in the reactor at the beginning of the reaction stage. The overall tCOD removal efficiency of SMr and GWr were 74.2 % and 83.0 %, respectly, with a HRT = 8.0 h. In both systems the COD removal efficiency was directly affected by the presence of suspended solids (SS) in the effluents, coming from biomass washouts. It was found that the factors that determined the amount of washed out solids were the biomass concentration inside the reactor and its cell growth kinetics. The higher the cell growth kinetics, the higher the impact by suspended solids in the effluent. This was confirmed by the results of the operation of SMr and GWr; where the high value of Y_x of granules cultivated in SMr led the operation of this system with a high X (4.5 g VSS L^{-1}), and to the washout of the recently formed biomass, resulting in a mean effluents solids concentration of 0.31 g TSS L^{-1}. In contrast, the lower cell mass yield coefficient of the granules formed with greywater (**Table 3**), led to the operation of GWr with a X of 1.8 g VSS L^{-1} and to a lower solids concentration in effluents (0.073 g TSS L^{-1}).
The effect of solids in the effluent quality can be determined by the difference between tCOD and sCOD. As it can be seen in **Figure 3**, the high content of solids in effluents

from SMr led to a difference between tCOD and sCOD higher than 100%, while in GWr that difference was of 49%. It must be noted that the solids in effluents from SMr were only due to biomass washouts, whereas the solids in effluents from GWr were from biomass washouts, and from the solids coming in the influent which were not retained or removed by the system. The negative effect of the solids in the effluents quality due to the application of very short settling times in aerobic granules systems, has already been commented in other studies[8,18], in which is recommended a post-treatment of the effluents from these systems to improve its quality.

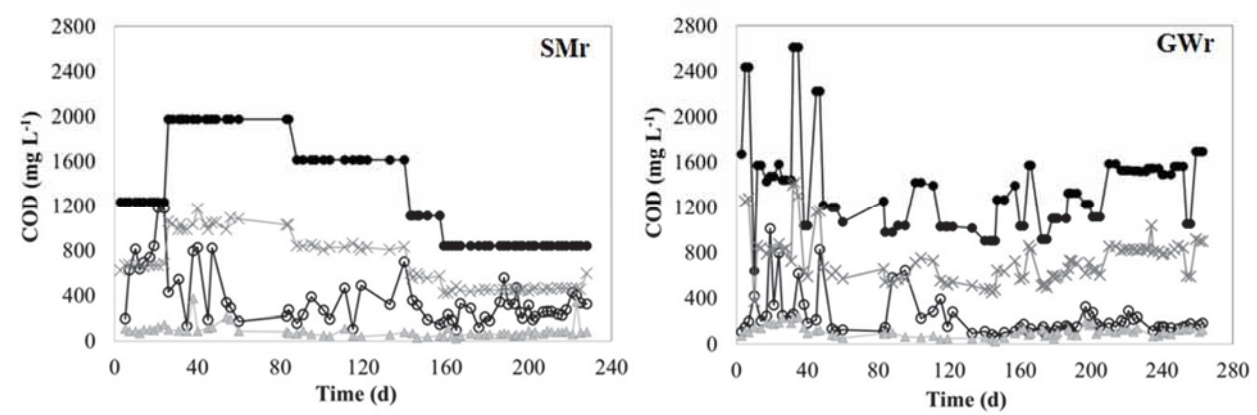


FIGURE 3. tCOD in influents (●), effluents (○) and in the reactor after fill up (x), and sCOD in effluents from SMr and GWr.

CONCLUSION

The operation of a SBR using a balanced synthetic medium as feedstock led to the formation of aerobic granules with a regular structure, high compactness and settling properties, whereas the operation of a SBR fed with greywater conducted to the formation of granules with a fluffy structure, lower compactness and settling properties.

The factor that directly affected the physical properties and the growth of the granular biomass seems to be the predominance of feast famine conditions, which in turn are directly dependent of the specific organic loading rate (Bx). When the value of Bx was about 4.4 kg COD kg SSV^{-1} d^{-1} there were not observed famine periods in the cycles and the granules presented a considerably light structure with filamentous outgrowths, however, when Bx was reduced to 2.9 kg COD kg SSV^{-1} d^{-1}, the existence of famine periods was allowed and it was observed a significant improvement in the physical properties of the granules.

The Ks values indicated that granules cultivated using greywater are composed by slow growing microorganism with high affinity for the substrate, while granules from SMr are composed by fast growing microorganism, with a higher cell mass yield coefficient. It is important to notice that granules in GWr were formed from filamentous aggregates, which presents a high substrate affinity and a low value of μ_{max}, and therefore it is possible that those granules were still contained a fraction of filamentous microorganisms.

ACKNOWLEDGMENTS

To the Universidad Autónoma Metropolitana and the Consejo Nacional de Ciencia y Tecnología from Mexico by granting the necessary resources for the development of the project and assistance to the symposium.

REFERENCES

1. Jabornig S., Podmirseg S.M. A Novel Fixed Fibre Biofilm Membrane Process for On-Site Greywater Reclamation Requiring No Fouling Control. Biotechnology and Bioengineering. 112 (2015) 484-493.
2. Friedler, E. Quality of individual domestic greywater streams and its implication for on-site treatment and resuse possibilities. Environmental Technology. 25 (2004) 997-1008.
3. Travis, M.J., Wiel-Shafran, A., Weisbrod, N., Adar, E., Gross, A. Greywater reuse for irrigation: Effect on soil properties. Science of the Total Environment. 408 (2010) 2501–2508.
4. Hyun, K., Choi, J., Ki, D., Park, J., Ahn, S., Oh, H., Choung, Y.K. Bathroom wastewater treatment in constructed wetlands with planting, non-planting and aeration, non-aeration conditions. Desalination and water treatment. 57 (2015) 1-9.
5. Lamine, M., Samaali, D., and Ghrabi, A. Greywater treatment in a submerged membrane bioreactor with gravitational filtration. Desalination and Water Treatment 46 (2012) 182-187.
6. Hernández Leal, L., Temmink, H., Zeeman, G., Buisman, C.J.N. Comparison of three systems for biological greywater treatment. Water. 2 (2010) 155-169.
7. Obaja, D.S., Mace, J., Costa, C., Sans, J., Mata-Alvarez, J. Nitrification, denitrification and biological phosphorus removal in piggery wastewater using a sequencing batch reactor. Bioresource Technology. 87 (2003) 103–111.
8. Arrojo, B., Mosquera-Corral, A., Garrido, J.M., Méndez, R. Aerobic granulation with industrial wastewater in sequencing batch reactors. Water Research. 38 (2004) 3389-3399.
9. Adav, S.S, Lee, D.-J., Show, K.-Y., Tay, J.-H. Aerobic granular sludge: Recent advances. Biotechnology Advances. 26 (2008) 411–423.
10. 10-Val del Río, A., Figueroa, M., Arrojo, B., Mosquera-Corral, A., Campos, J.L., García-Toriello, G. Aerobic granular SBR systems applied to the treatment of industrial effluents. Journal of Environmental Management. 95 (2012) 88-92.
11. Beun, J.J., Hendriks, A., van Loosdrecht, M.C.M., Morgenroth, E., Wilderer, P.A., Heijnen, J.J. Aerobic granulation in a sequencing batch reactor. Water Research. 33 (1999) 2283-2290.
12. APHA. Standard methods for the examination of water and wastewater, 19t^{h} edition, (1995).
13. Jurado, E., Fernández-Serrano, M., Núñez-Olea J., Luzón, G., Lechuga, M. Simplified spectrophotometric method using methylene blue for determining anionic surfactants: Applications to the study of primary biodegradation in aerobic screening tests. Chemosphere. 65 (2006) 278-285.
14. Beun, J.J., van Loosdrecht, M.C.M., Heijnen, J.J. Aerobic granulation in a sequencing batch airlift reactor. Water Research. 36 (2002) 702–712.
15. Ghangrekar, M.M., Asolekar, S.R., Joshi, S.G. Characteristics of sludge developed under different loading conditions during UASB reactor start-up and granulation. Water Research. 39 (2005) 1123–1133.
16. Henze, M., Grady Jr., C.P.L., Gujer, W., Marais, C.V.R., Matsuo, T. A general model for single-sludge wastewater treatment systems: an abbreviated report. Water Research. 21 (1987) 505–515.

17. De Kreuk, M.K., Kishida, N., Tsuneda, S., Van Loosdrecht, M.C.M. Behavior of polymeric substrates in an aerobic granular sludge system. Water Research. 4 (2010) 5929 -5938.
18. Schwarzenbeck, N., Borges, J.M., Wilderer, P.A. Treatment of dairy effluents in an aerobic granular sludge sequencing batch reactor. Applied Microbiology and Biotechnology. 66 (2005) 711718.
19. Liu, Y., Liu Q.S. Causes and control of filamentous growth in aerobic granular sludge sequencing batch reactors. Biotechnology Advances. 24 (2006) 115–127.
20. De Kreuk, M.K., Van Loosdrecht, M.C.M. Formation of Aerobic Granules with Domestic Sewage. Journal of environmental Engineering. 132 (2006) 694-697.
21. Chen, Y., Wenju, J., Tee – Liang, D., Hwa-Tay, J. Biodegradation and kinetics of aerobic granules under high organic loading rates in sequencing batch reactor. Applied Microbiology and Biotechnology. 79 (2008) 301–308.
22. Liu, L., Wang, Z., Yao, J., Sun, X., Cai, W. Investigation on the formation and kinetics of glucose-fed aerobic granular sludge. Enzyme and Microbial Technology. 36 (2005) 487–491.
23. Sponza, D.T. Anaerobic granule formation and tetrachloroethylene (TCE) removal in an upflow anaerobic sludge blanket (UASB) reactor. Enzyme and Microbial Technology. 29 (2001) 417–427.

CHAPTER 7.20 CHEMICAL AND MICROBIOLOGICAL CHARACTERISTICS OF EFFLUENT FROM ROCK FILTERS USED FOR THE POST-TREAMENT OF STABILIZATION PONDS

M.V.A. Santos *(1); T. Köchling (1); L. R. Martins (1); S. Gavazza (1); M. T. Kato (1) and L. Florencio (1)

(1) Federal University of Pernambuco, Department of Civil Engineering, Laboratory of Environmental Sanitation. Av. Acadêmico Hélio Ramos, s/n. Cidade Universitária. CEP: 50740-530 Recife PE, Brazil.

ABSTRACT

Effluent of wastewater stabilization ponds can present high turbidity, some nutrients, suspended solids and high density of phytoplankton that may contain cyanobacteria. An alternative to remove phytoplankton is to use rock filter after the stabilization ponds. However, in the case of cyanobacteria, there is lack of knowledge about their production and potential toxicity in stabilization ponds, and the removal efficiency in rock filters. This study aimed to determine the effectiveness of two parallel horizontal flow rock filters by studying the chemical and microbiological aspects. Monitoring consisted of sample analyses of physicochemical parameters and using PCR-DGGE technique by amplifying 16S rRNA gene. The presence of microcystin was verified by specific PCR with *mcyE* gene. The samples were collected every 15 days, during a period of 230 days.

The results showed that the rock filters were effective in the total COD removal with efficiency of about 79%, corresponding to effluent concentration of 27 $mg.L^{-1}$. Very good removal of about 96%, corresponding to effluent turbidity of 5±3 NTU, was obtained; and the TSS removal efficiency was 65% which corresponded to effluent mean values of 33 $mg.L^{-1}$. The total removal of phytoplankton cells was 98% for both rock filters, with a mean density in the effluent of 2,464 $cel.mL^{-1}$. The result of the t-test for all the 14 samples collected in the effluent from each rock filters was 0.744, which was lower than the value of 2.16 from the 5%-t_{tab} showing that the two rock filters had similar performance behavior.

Regarding the *Bacteria* domain, the relevant genres during the study period were: *Planktothrix*, which prefers shallow water body, rich in nutrients and mixed by the wind; *Campylobacter*, microaerophilic bacteria; *Halothiobacillus,* mandatory chemolithoautotrophic bacteria that oxidize H_2S to SO_4^{-2}; and *Thiovirga* that obtain energy from reduced sulfur compounds. The genres carriers of the *mcyE* gene showed no favorable release of microcystin.

Therefore, rock filters are effective to remove turbidity, suspended solids and cyanobacteria, and under the studied conditions, the genus *Microcystis* did not favor the production of microcystin, as confirmed by specific PCR.

Keywords: bacteria domain, cyanobacteria, PCR-DGGE technique, turbidity

---

*Author for correspondence: mvinicius86@gmail.com

INTRODUCTION

In northeastern Brazil, the stabilization ponds have been widely used for wastewater treatment due to environmental conditions (temperature, incidence of solar radiation) and availability of land favorable to the application of this technology. In addition, they have low construction costs, operation and maintenance, and high removal efficiencies of organic matter and pathogens[1]. However, its effluent still has a high content of suspended solids and phytoplankton containing cyanobacteria[2].
Many cyanobacterial genres can produce varieties of cyanotoxins[3]. In stabilization ponds is common the presence of *Microcystis* and *Planktothrix* (*Oscillatoria*), potential producers of microcystin[4,5].

The application of rock filter into the post-treatment stabilization pond could be an attractive alternative for the removal of suspended solids and therefore cyanobacteria of these effluents. However, little is known about the removal of cyanobacteria rock filters and neither the capability of producing of the same toxicity cultivated in this environment.

Thus, this study aimed to evaluate the rock filter efficiency as post-treatment stabilization ponds for removal of cyanobacteria. For that they were determined physico-chemical and microbiological parameters, by PCR-DGGE technique. Moreover, the presence of microcystin was assessed by amplification of *mcyE* gene.

MATERIALS AND METHODS

Description of Rio Formoso wastewater treatment plant. Rio Formoso wastewater treatment plant (WWTP) consists of a primary treatment (railing and sandbox), UASB reactor with three cells operating in parallel (324 m^3), a stabilization pond (28,050 m^3). The Two rock filters present main feature: the length of 120 m, width of 30 m, bed height of 0.55 m, volume of 1980 m^3, average flow of 504 m^3 d^{-1}, hydraulic loading rate of 30 m^3/m^2 d^{-1} and hydraulic retention time of 3 days. In this study, it was analyzed the efficiency of each filter individually and collection points can be seen in **Figure 1**.

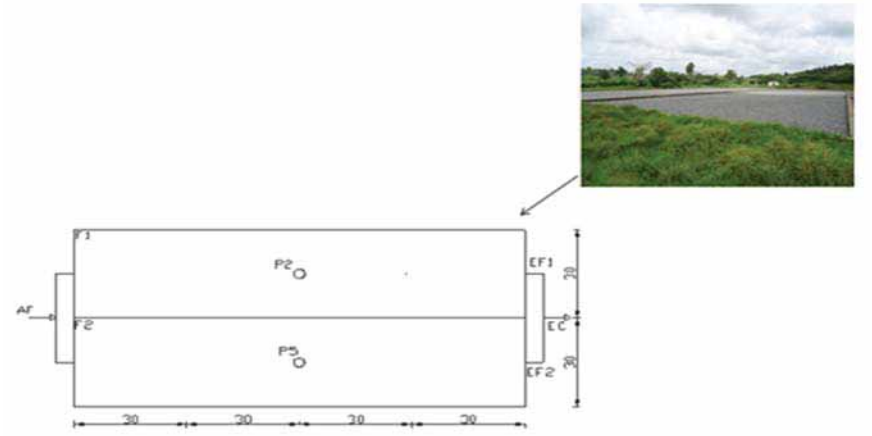


FIGURE 1. Location of collection points in rock filters. Influent – AF; Filter Effluent 1–EF1; Filter Effluent 2 – EF2; Effluent from the box – EC; P2 – median point of horizontal flow of rock filter 1 (F1); P5 - median point of horizontal flow of rock filter 2 (F2). Scale in meters (m)

The system was monitored every 15 days, from October 2013 until June 2014 (total of 230 days). The Collection points in the present study were the following: Influent (**AF**), point on the distribution box from the effluent to the stabilization pond; points two ($\mathbf{P_2}$) and five ($\mathbf{P_5}$), median points of horizontal flow of rock filter, located 60m from AF; rock filter effluent 1 ($\mathbf{EF_1}$) and rock filter effluent 2 ($\mathbf{EF_2}$). Regarding the study molecular biology were used: Influent (**AF**), two point (P2) and effluent unit box (EC), where the two rock filters receive the effluent together.

Physicochemical analysis. The field parameters were measured *in situ* aided by multiparameter (HACH, 40D) and turbidimeter (HACH, 2100 P). These parameters were: pH, temperature (°C), dissolved oxygen ($mgO_2\ L^{-1}$), electric conductivity (µs/cm), turbidity (NTU). Analyzes performed in the laboratory were: total chemical oxygen demand ($mgO_2\ L^{-1}$), total biochemical oxygen demand ($mgO_2\ L^{-1}$), total phosphorus ($mgP_{Total}\ L^{-1}$), orthophosphate ($mgP\text{-}PO_4^{-3}\ L^{-1}$) nitrite ($mgNO_2^-\ L^{-1}$), nitrate ($mgNO_3^-\ L^{-1}$), ammonium ion ($mgN\text{-}NH_4^+\ L^{-1}$) and total suspended solids ($mgSST\ L^{-1}$).

All samples were immediately transported to the laboratory and the collection methods of analysis and preservation[6].

Molecular analysis. DNA extraction was performed by Power Soil™ DNA Isolation Kit MO BIO laboratory Inc. 100 mL of samples was filtered, through a membrane of 0.22 µm (esters of mixture membrane filter), in order to retain the microorganisms. Subsequently,100 µL of genomic DNA was stored at -20°C until further process.

Genomic DNA extracts were submitted to amplification by polymerase chain reaction (PCR). Amplification of the 16S rRNA gene fragments to denaturing gradient gel electrophoresis (DGGE) was performed by the specific primer for the *Bacteria* domain 968F-GC e 1392 R[7].

Amplification was carried out by My cycle thermocycle (Bio Rad) using the following sequence: initial denaturation at 94°C for 5 min, 30 cycles of denaturation (at 94°C for 30 seg), annealing (at 48°C for 30 seg), extension (at 68°C for 1 min) and final extension 68°C for 10 min.

For the amplification of microcystin it was used the primer set mcyE-2F and Mic mcyE-8R[8] following the sequence: initial denaturation at 95°C for 3 min, 30 cycles of denaturation (at 94°C for 30 seg), annealing (at 58°C for 30 seg), initial extension (at 68°C for 1 min) and final extension 68°C for 10 min.

PCR products of Bacteria domain were subjected to DGGE[9] and run in Dcode systems (Bio Rad). The Gradient conditions were 40% to 60% of urea and formamide (UF), 8% acrylamide gel.

After electrophoresis at 250 V for 5 hours 60°C in TAE buffer (80 mM Tris base, 2.0 mM EDTA), the gel was colored with ethidium bromide (0.5 ug / ml) and visualized with an ultraviolet transilluminator (UVP, TMW-20).

Purification of the PCR products from the bands of DGGE and sequencing reactions were performed by Macrogen (South Korea). It was used the Big Dye Terminator version 3.1 sequencing kit in automatic ABI 3730XL Analyzer-96 capillary type. Sequences were submitted for a BLAST search[10] to obtain an indication of the phylogenetic affiliation.

For the DGGE patterns bands it was done a dendrogram analysis by clustering to the *Bacteria* domain by distance measure: Jaccard index; algorithm: UPGMA. Cophenetic correlation coefficient: 1.0.

Statistic. Box plot and Whiskers graphs were used through the Statistic software (StatSoft-Six Sigma). Concerning the correlation, r and p values were calculated with the purpose to confection correlation map (heatmap) to the temperature, turbidity, pH, electric conductivity, dissolved oxygen, total chemical oxygen demand, filtered chemical oxygen demand, ammonia ion, nitrite, total phosphorus and orthophosphate parameters applied with 95% confidence level.

T-test with two paired samples for means was accomplished for the purpose of ascertains the similarity between the horizontal flow rock filter effluents. The parameters analyzed were total suspended solids, and total quantity of phytoplankton cells. T table for 13 degrees of freedom (df), considering 5% was 2.16

RESULTS AND DISCUSSION

***Total chemical oxygen demand*.** The average concentration of total chemical oxygen demand (COD) present in influent was 127±31 mgO_2L^{-1}. Concerning the rock filter 1 effluent, the average concentration was 27±19 $mgO_2\ L^{-1}$ while rock filter 2 effluent was of the 28±19 $mgO_2\ L^{-1}$ (**Figure 2A** and **Table 1**).

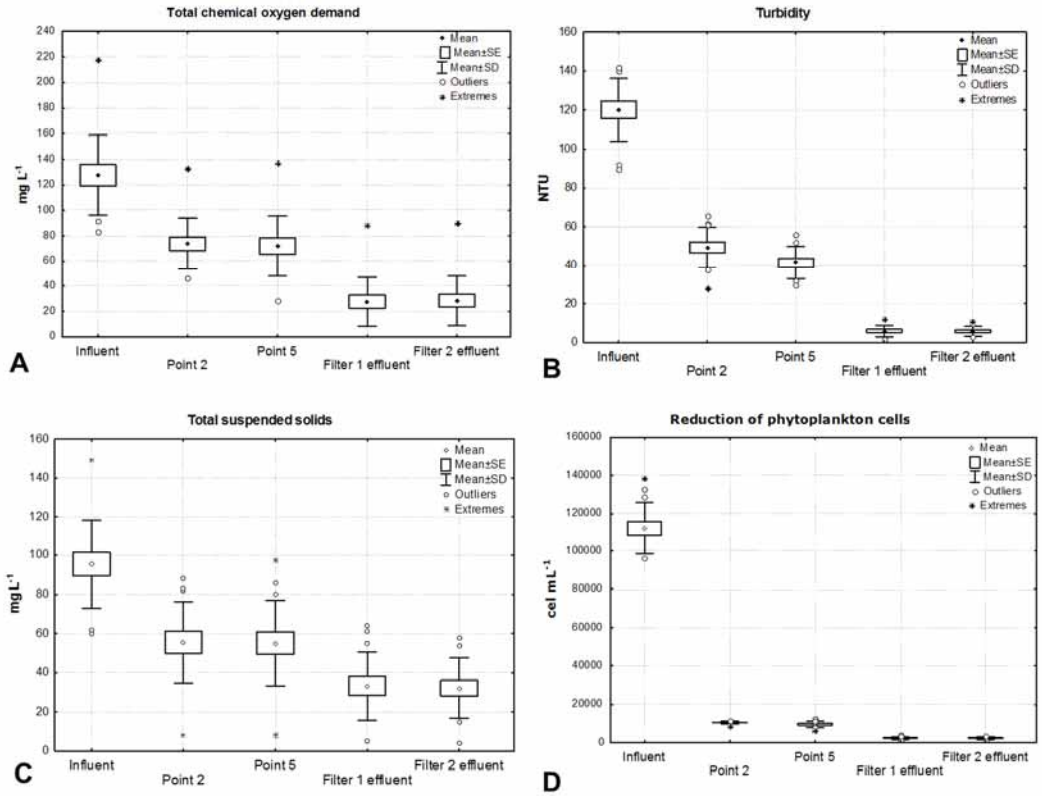


FIGURE 2. Variation of parameters: A) Total COD, B) Turbidity, C) SST, D) cell reduction of phytoplankton, in influent, midpoint of the rock filters and effluent rock

TABLE 1. Means of physicochemical parameters found during the study period

Parameters	Average		
	Influent	Filter 1 effluent	Filter 2 effluent
Turbidity (NTU)	120±16	5±3	5±2
pH	7.9±0.3	7.5±0.1	7.5±0.1
Temperature (°C)	30±1.0	29±0.8	29±0.8
Conductivity (µs/cm)	1,242±155	1,130±139	1,137±138
Dissolved oxygen (mg L^{-1})	4±0.9	5±0.5	5±0.5
Total BOD (mg L^{-1})	41±13	11±0	12±0
Filtered BOD (mg L^{-1})	12±4.3	5±1.4	4±1.4
Total COD (mg L^{-1})	127±31	27±19	28±19
Filtered COD (mg L^{-1})	39±13	15±6	15±6
Orto-P (mg L^{-1})	1.7±0.6	1.8±0.5	1.9±0.4
P total (mg L^{-1})	3.3±0.3	2.5±0.4	2.5±0.4
NH_4^+ (mg L^{-1})	15±2,7	12±2.8	12±3.4
NO_2^- (mg L^{-1})	0.1±0.2	0.3±0.1	0.2±0.1
NO_3^- (mg L^{-1})	1.2±0.1	1.9±0.1	1.8±0.1
SST (mg L^{-1})	95±22	33±17	32±15
Phytoplankton (cel mL^{-1})	112,195±13,441	2,464±766	2,248±728

The result demonstrates satisfactory removal of organic matter (COD Total), with 79% reduction for the filter 1 and 78% for the filter 2. Previous work showed efficiencies in the range of 50% to 75%[11,12].

The removal organic matter showed a positive strong correlation with the turbidity parameter (r = 0.91 e p = 0.01), with no significant difference (**Figure 3**).

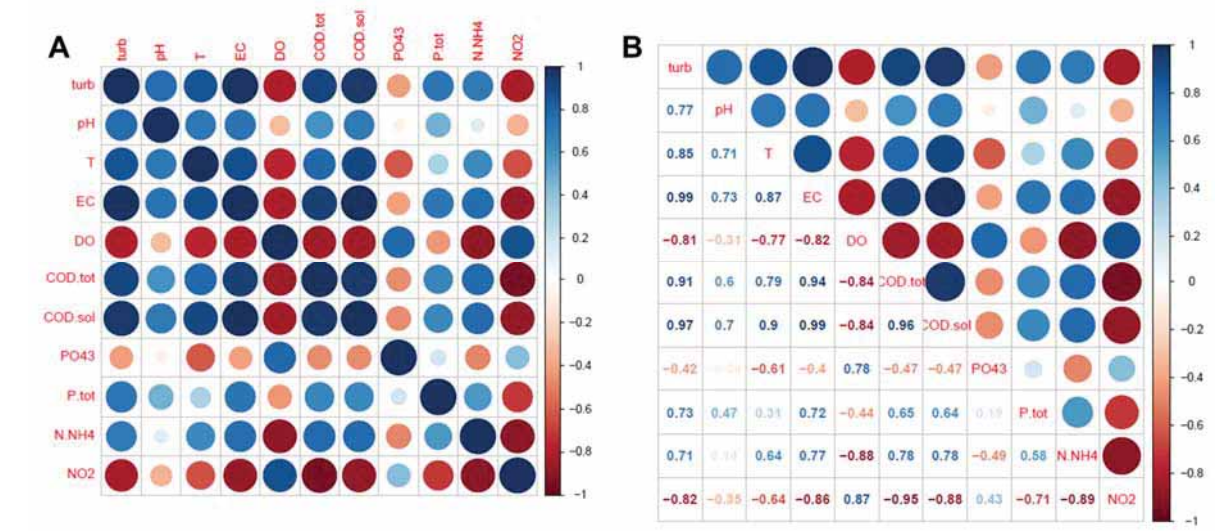


FIGURE 3. Correlation of physicochemical parameters in the heatmap graphic, found the rock filters during the study (Correlation the stronger positive shows blue color, while the strongest negative correlation shows red color); B) Values of the correlations of the physicochemical parameters, the heatmap graphic, found the rock filters during the study.

Algal biomass present in the influent was adhered at the interfaces support material to pass through the treatment. Bacteria oxidize biodegradable organic compounds to obtain cellular energy, finally suiting the wastewater system to the receiver body.

Turbidity. Regarding the turbidity, the average concentration of the influent was 120 NTU, while in the effluent of both rock filters it was 5 NTU (**Figure 2B** and **Table 1**). The Mean removal efficiency presented by rock filters was about 96%.

High turbidity values directly affect the entry of light, therefore the growth of cyanobacteria. In the study, high turbidity values were related to the reduction of influent residence time, due to the rain that occurred during the study period.

The reduction of turbidity in the rock filters varies from 70% to 90%[13,14]. The main mechanism for reducing turbidity was concerning the decomposition of cyanobacteria and algae on the support material.

As well, the gas vesicle collapses by increased turgor pressure. The amount of gas vesicle collapses under pressure causes a decrease in turbidity[15,16,17].

Total suspended solids. Average concentration in influent was of 95±22 mgSST L^{-1}, concerning rock filter 1 effluent was 33±17 mgSST L^{-1}, while rock filter 2 effluent was of the 32±15 mgSST.L^{-1} (**Figure 2C** and **Table 1**). TSS removal efficiency of the effluent for rock filters 1 and 2 was 65% and 66%, respectively.

The reduction of suspended solids in rock filters varies from 60% to 80%[11,12]. Rock filter used in the post treatment stabilization ponds allows an attractive set in the reduction of suspended solids, when low or moderate concentrations are required.

Results for T-test between 14 observations rock filter effluent was equal to 0.744. This result was lower than the tab t the 5% (t=2.16), this means that the average values showed no significant differences.

Phytoplankton of removal. The total removal of phytoplankton cells was 98% for both rock filters, with a mean density in the rock filter 1 effluent of 2,464 cel mL^{-1} and rock filter 2 effluent exhibited a mean value of 2,248±728 cel mL^{-1}.

The result for the t test between the 14 observations of the effluent from rock filter was 0.195. This result was less than 5% tab t (t = 2.16), this means that the average values showed no significant differences.

Molecular biology. PCR products of the samples to the *Bacteria* domain were subjected to denaturing gradient gel electrophoresis (**Figure 4A**).

Population dynamics in horizontal flow rock filters was associated the influence of low light condition caused by support material, mesophilic temperature, competition for nutrients between bacteria and cyanobacteria under aerobic conditions.

Candidatus (Figure 4B e Table 3) showed the lower level of similarity between all microorganisms. Phosphorus concentrations above 3.0 mg L^{-1} in the samples A (Table 2) favored a competitive advantage in stock up phosphorus in the aerobic condition on the microbial community studied.

In the aerobic phase, *Candidatus accumilibacter* containing reserves of polyhydroxyalkanoate (PHA) can assimilate phosphorus and store it in the form of intracellular polyphosphate[18].

The bands 5 and 6 correspond to the *Campylobacter* genre (**Figure 4B** and **Table 3**). They show a similarity with the bands 3 and 8 highlight by *Planktothrix*.

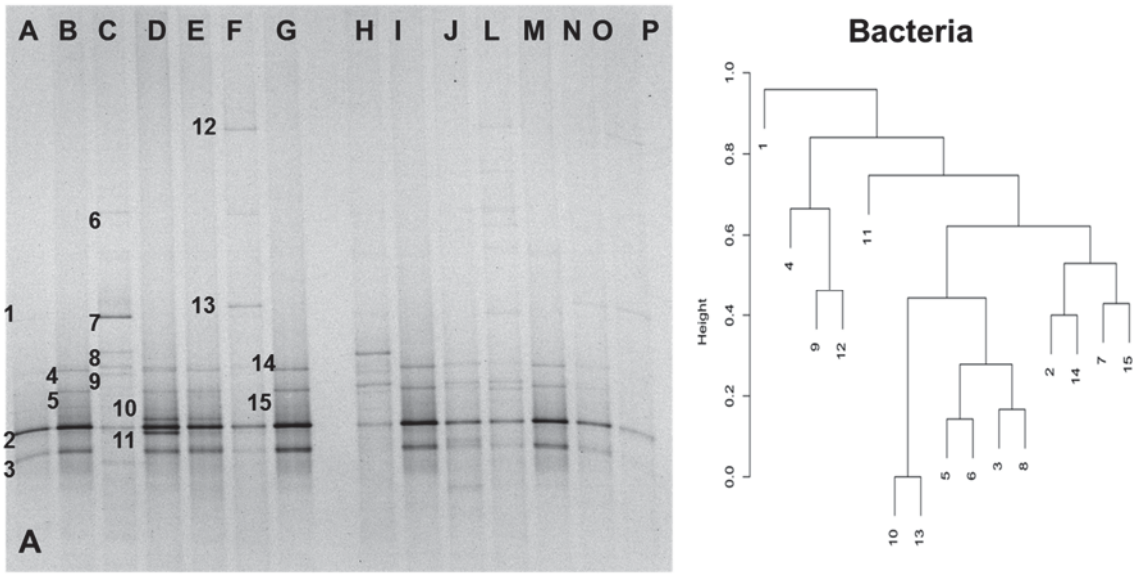


FIGURE 4. A) DGGE bands profile *Bacteria* domain B) Standards of DGGE bands and dendrogram of the analysis by "clustering" for the *Bacteria* domain. Distance measure: Jaccard index; algorithm: UPGMA. Cophenetic correlation coefficient: 1.0.

Campylobacter was present in the samples B and C (**Table 2**) belonging to the ε-Proteobacteria phylum, gram negative, chemoorganotrophic and optimal growth requires anaerobic or microaerophilic growth in the presence fumarate[19].

Campylobacter was removed by sensitivity presenting the average concentration of 4 to 5 mgO_2L^{-1} for anaerobic and microaerophilic genres.

Halothiobacillus (**Figure 4B** and **Table 3**) had a great similarity with the *Planktothrix* (12 band). *Halothiobacillus* responsible for oxidizing elemental sulfur (S^0) to sulfate (SO_4^{-2})[19] was present in the sample D (**Table 2**). It belongs to the γ-Proteobacteria phylum, gram negative, chemolithoautotrophic, grow in neutral pH conditions, mesophilic, dwelleth biofilm wastewater[20].

Thiovirga (**Figure 4B** and **Table 3**) was present in the Sample D (**Table 2**), it belongs to γ-Proteobacteria phylum, mandatorily chemolithoautotrophic, gram negative. This genre gets energy from reduced inorganic sulfur compounds[21]. *Thiovirga* showed similarity to *Campylobacter* (4 band) and *Candidatus* (1 band).

The most represented taxonomic group in all samples belonged to the *Cyanobacteria* phylum. *Planktothrix* was the dominant microorganism of the microbial communities during the study period (**Figure 4B** and **Table 3**). *P. agardhii* prefers shallow body of water, mixed by wind and rich in nutrients[22], while the species *P. rubescens* adapts in lakes metalimnion oligo-mesotrophic[23].

TABLE 2. Samples used in the particular study period and points characterized in the formation the DGGE gel *Bacteria* domain

Dates	Points	Period
Dec. 02, 2013	A → Influent B → Midpoint C → Effluent	Dry season
Dec. 18, 2013	D → Influent E → Midpoint F → Effluent	
Jan. 16, 2014	G → Influent H → Midpoint I → Effluent	
May 21, 2014	J → Influent L → Midpoint M → Effluent	Rainy season
Jun. 10, 2014	N → Influent O → Midpoint P → Effluent	

Rock filters present depth of 0.55 m, turbulence, nutrients (phosphorus and nitrogen) and reduced sunlight caused by the material support. Thus, the *Planktothrix* genre has a competitive advantage about *Microcystis*, *Merimospedia*, *Pseudoanabaena* present in rock filters.

In this study it was used the primers set mcyE-F2 and MicmcyE-R8 to check the possible potential microcystin present in this environment. However, amplifications of all samples proved to be negative (Data not show). Therefore, positive control was added (*Microcystis*) and the set primer amplified its sample.

Microcystis is known worldwide for producing secondary metabolites, being released into the environment during flowering or occurrence of cell lysis.

TABLE 3. Phylogenetic affiliation of the corresponding microorganisms during the study period (DGGE-*Bacteria*)

Band	Phylum	Class	Genre
1	*Chlamydiae*	*Chlamydiia*	*Candidatus*
2-4	*Cyanobacteria*	*Oscillatoriophycideae*	*Planktothrix*
5-6	*Proteobacteria*	*Epsilonproteobacteria*	*Campylobacter*
7-8	*Cyanobacteria*	*Oscillatoriophycideae*	*Planktothrix*
9	*Proteobacteria*	*Gammaproteobacteria*	*Halothiobacillus*
10	*Cyanobacteria*	*Oscillatoriophycideae*	*Planktothrix*
11	*Proteobacteria*	*Gammaproteobacterae*	*Thiovirga*
12-15	*Cyanobacteria*	*Oscillatoriophycideae*	*Planktothrix*

CONCLUSION

Regarding the similarity between the rock filter for the t-test, these did not show significant differences between the 14 observations.
Rock filters presented satisfactory removal of total COD, turbidity and total suspended solids.
Rock filters have promoted removal of phytoplankton cell number, being far below the limits of CONAMA 357/05 legislation which is 50,000 cel mL^{-1}.
Regarding the *Bacteria* domain, the relevant genres during the study period were: *Planktothrix*, which prefers shallow water body, rich in nutrients and mixed by the wind; *Campylobacter*, microaerophilic bacteria; *Halothiobacillus,* mandatory chemolithoautotrophic bacteria that oxidize H_2S to SO_4^{-2}; *Thiovirga* that obtain energy from reduced sulfur compounds and *Candidatus* stores it phosphorus under aerobic conditions.
Microcystis species capable of producing microcystin toxins were not detected by specific PCR during the study period.

ACKNOWLEDGMENTS

This work was financially supported by the Brazilian agencies CAPES (Higher Education Personnel Training Coordination) and CNPq (National Council for Scientific and Technological Development) through the Program PRONEX, the Environmental Sanitation Laboratory (LSA - UFPE). We also thank the Pernambuco Sanitation Company (COMPESA) for the assistance in the Rio Formoso Plant.

REFERENCES

1. Von Sperling M., Bastos R. K. X., KATO M.T. Removal of E. coli and helminth eggs in UASB - polishing pond systems in Brazil. Wat. Sci. Techn. 51(12), (2005) 91-97.
2. Pastich E. A., Gavazza S., Casé M. C. C., Florencio L., Kato M. T. Structure and dynamics of the phytoplankton community within a maturation pond in a semiarid region. Braz. Journ. Biol. 76 (2016) 144-153.
3. Carmichael W. W. The toxins of cyanobacteria. Scient Americ. 270 (1994) 78-86.
4. Hautala H., Lamminmäki U., Spoof L., Nybom S., Meriluoto J., Vehniäinen M. Quantitative PCR detection and improved sample preparation of microcystin-producing *Anabaena*, *Mycrocystis* and *Planktothrix* Ecotoxic.Environ.Safe*.* 87 (2013) 49-56.
5. Borges H. L F., Branco L. H. Z., Martins M. D., Lima C. S., Barbosa P. T., Lira G. A. S. T., Bittencourt-Oliveira M. C., Molica R.J.R. Cyanotoxin production and phylogen of benthic cyanobacterial strains isolated from the northeast of Brazil. Harm.Alg. 43 (2015) 46-57.
6. APHA, AWWA, WPCF. *Standards Methods for the Examination of Water and Wastewater*. 22th ed. Washington DC, USA, 2012.
7. Nielsen A T., Liu W., Filipe C., Grady L., Molin S., Stahl D. A. Identification of a novel group of bacteria in sludge from a deteriorated biological phosphorus removal reactor. *Appl.Environ.Microbiol.* 65(3) (1999) 1251 – 1258.
8. Vaitomaa J., Rantala A., Halinen K., Rouhianen L., Tallberg P., Mokelke L., Sinvonen K. Quantitative real-time PCR for determination of microcystin-synthetase E copy numbers of *Microcystis* and *Anabaena* in lakes. Appl.Environ.Microb.69 (12) (2003) 7289–7297.

9. Muyzer G., Smalla K. Application of denaturing gradient gel electrophoresis (DGGE) and temperature gradient gel electrophoresis analysis of polymerase chain reaction amplified genes coding for 16S rRNA. Kluw.Acad. Pub. 73 (1998) 127-141.
10. Altschul S. F., Madden T. L., Schaäffer, A. A., Zhang J., Zhang Z., Miller W., Lipman D. J. 1997 Gapped BLAST and PSI-BLAST: a new generation of protein datebase search programs. *Nuc. Aci. Research* 25 (17) (1997) 3389-3402.
11. Von Sperling M., Andrada J. G. B., Melo W. R. Coarse filters for pond effluent polishing: comparison of loading rates and grain sizes. Wat.Scien.Techn. 11 (2007) 121-126.
12. Dias D. F.C., Possmoser-Nascimento T. E., Rodrigues V. A. J., von Sperling M. Overerall performance evaluation of shallow matuation ponds in series treating UASB reactor efluente: Tem years of intensive monitoring of a system. Ecolog.Egineer. 71 (2014) 206-214.
13. Ahsan T., Alaerts G., Buiteman P. Direct horizonatal flow roughing filtration. Part II: performance and operational guideline. Aqua, (1996) 45 191-281.
14. Nkwonta O., Ochieng G. Roughing filter for water pre-treatment technology in developing countries: A review. Internat. Journ. Phys.Scien. 4(9) (2009) 455-463
15. Walsby A. E. Gas vesicles. Microbiol. Rev., 58 (1994) 94-144.
16. Porat R., Teltsch B., Mosse A., Dubinsky Z., Walsby E. Turbidity changes caused by collapse of cyanobacterial gas vesicles in water pumped from Lake Kinneret Into the Israeli national water carrier. Wat.Res. Vol. 33, No. 7, pp. (1999) 1634-1644.
17. Belenky M., Meyers R., Herzfeld J. Subunit structure of gas vesicles: A MALLDI-TOF mass spectrometry study Biophys. Journ. 86 (2004) 499-505.
18. Ahn J., Schroeder S., Beer M., Mcllroy S., Bayly R. C., May J. W., Vasiliadis G., Seviour R. J. Ecology of the microbial community removing phosphate from wastewater under continuously aerobic conditions in a sequencing batch reactor. Appl. Environ.Microb. 73 (7) (2007) 2257 – 2270.
19. Ito T., Sugita K., Okabe S. Isolation, characterization, and in situ detection of a novel chemiolithoautotrophic sulfur-oxidizing bacterium in wastewater biofilms growing under microaerophilic conditions. Appl. Environ. Microb. 70(5) (2004) 3122-3129.
20. Brenner D. J., Krieg N. R., Staley J. T. *Bergey's Manual of Systematic Bacteriology*, volumen 2. Springer. 2005.
21. Ito T., Sugita K., Yumoto I., Nodasaka Y., Okabe S. *Thiovirga sulfuroxydans* gen. nov., sp., a chemiolitothoautotrophic sulfur-oxidizing bacterium isolated from a microaerobic wastw-water biofilm. Internat. Journ. System. Evolut. *Microbiol.*55 (2005) 1059-1064.
22. Akcaalan R., Young F., Metcalf J. E., Morrison L. F., Albay M., Codd G. A. Microcystin analysis in single filamentous of *Planktothrix* spp. in laboratory cultures and environmental blooms. *Wat. Res.* 40 (2006) 1583-1590.
23. Barco M., Flores C., Josep R., Caixach, J. Determination of microcystin variants and related peptides present in a water bloom of *Planktothrix* (*Oscillatoria*) *rubescens* in a Spanish driking water reservoir by LC/ESI-MS. *Toxic.* 44 (2004) 881-886.

CHAPTER 7.21 METHANOGENIC INHIBITION OF AZO AND ANTHRAQUINONE TEXTILE DYES

C. P. Silva (1); O. F. Menezes (1); L. Florencio (1); M. T. Kato (1) and S. Gavazza *(1)

(1) Laboratory Environmental Sanitation, Department of Civil and Environmental Engineering Federal University of Pernambuco, Av. Academico Hélio Ramos s/n, Cidade Universitária, Recife-PE, CEP 50740-530

ABSTRACT

Research on decolorization and detoxification of textile effluents are important and have been reasons for frequent studies. Considering both the volume discharged and the effluent composition, the wastewater generated by the textile industry is rated as the most polluting among all industrial sectors. Some dyes are known by the toxicity to humans and environment. As the use of anaerobic technology has increased for the treatment of textile effluents, it is important to evaluate the toxicity response of dyes to the methanogenic microbes, which are the most sensitive of the anaerobes. Then, this study aimed to evaluate the individual influence of a di-azo dye, the Direct Orange 4 (DO4), a tetra-azo dye, the Direct Black 22, and an anthraquinone dye, the Reactive Blue 19 (RB19) on the Specific Methanogenic Activity of anaerobic microbes. Systems were assembled in 1 L glass flasks, using anaerobic sludge (3 g VSS·L^{-1}), substrate (VFA mixture for 2 g COD·L^{-1}), individual azo dyes, buffer, and nutrients. Dye solutions were used after the hydrolysis process and in five predetermined concentrations (0.30, 0.60, 0.90, 0.12, and 0.24 mM to DB22; and 0.50, 1.00, 2.00, 3.00, and 4.00 mM to both DO4 and RB19). A control test was essayed without dyes. The azo dyes DB22 and DO4 did not inhibit the methanogenic activity. However, the anthraquinone dye RB19 demonstrated the inhibitory effect on the methanogenic activity for the concentrations higher than 1 mM.

Keywords: anthraquinone dye, azo dye, inhibition, specific methanogenic activity.

INTRODUCTION

Dyes used by the textile industries are, in majority, synthetic. Molecules of these dyes include aromatic groups able to absorb visible light (chromophore), a group responsible for fixing the dye on the fiber, and an electron acceptor and/or donor groups, which enhance the color of the chromophore (auxochromes). The most common chromophores are azo (-N=N-), carbonyl (-CO-), methine (-CH=), nitro (-NO_2), or quinoid groups[1].

Chromophore of the azo type is the most commonly comprising up to 60-70%[2] of all textile dyes produced, followed by anthraquinones (characterized by an anthracene core linked to a quinone group)[3-5]. Amine (-NH_2), carboxyl (-COOH), sulfonic acid (-SO_3H)

---

*Author for correspondence: savia@ufpe.br

and hydroxyl (-OH) are among the most important auxochromes. Sulfonate groups confer high solubility of dyes in water. Dye auxochromes usually belong to classes acid, azoic, basic, direct, disperse, mordant, reactive, solvent, sulfur, and vat[1,4].

Regarding to azo dyes, anaerobic environment is the most adequate for the degradation of azo compounds. The first step in the microbial degradation under anaerobic conditions is the reduction of the azo bond (-N=N-). This reduction may involve different mechanisms such as enzymatic, chemical reduction through low molecular weight redox mediators, chemical reduction by biogenic reducers as sulfide, or a combination of these mechanisms[6]. After decolorization (obtained by breaking the bond -N=N-), very stable aromatic amines are produced, which are more easily mineralized aerobically. The original dyes, or these aromatic amines are potentially toxic and may cause inhibition of the most sensitive of anaerobes, the methanogenic microbes.

The aim of this study was to investigate the inhibitory effects of azo and anthraquinones dyes on the specific methanogenic activity (SMA) during the anaerobic treatment of textile wastewaters.

MATERIALS AND METHODS

Dyes and chemicals. The dyes used were the di-azo dye Direct Orange 4 (DO4), the tetra-azo dye Direct Black 22 (DB22) and the anthraquinone dye Reactive Blue 19 (RB19), illustrated in **Figure 1**. These dyes were hydrolyzed at pH 11 with NaOH for 60 minutes at 80 °C and after the hydrolysis the pH was adjusted to 7.0 with 2 mol·L^{-1} HCl. The hydrolysis was conducted because dyes are commonly hydrolyzed during the textile application process and it is how they are released in real textile wastewater[7,8]. For each dye the experiment was performed in five predetermined concentrations (0.30, 0.60, 0.90, 0.12, and 0.24 mM to DB22; and 0.50, 1.00, 2.00, 3.00, and 4.00 mM to both DO4 and RB19). The experiments were performed in triplicate for each dye concentration.

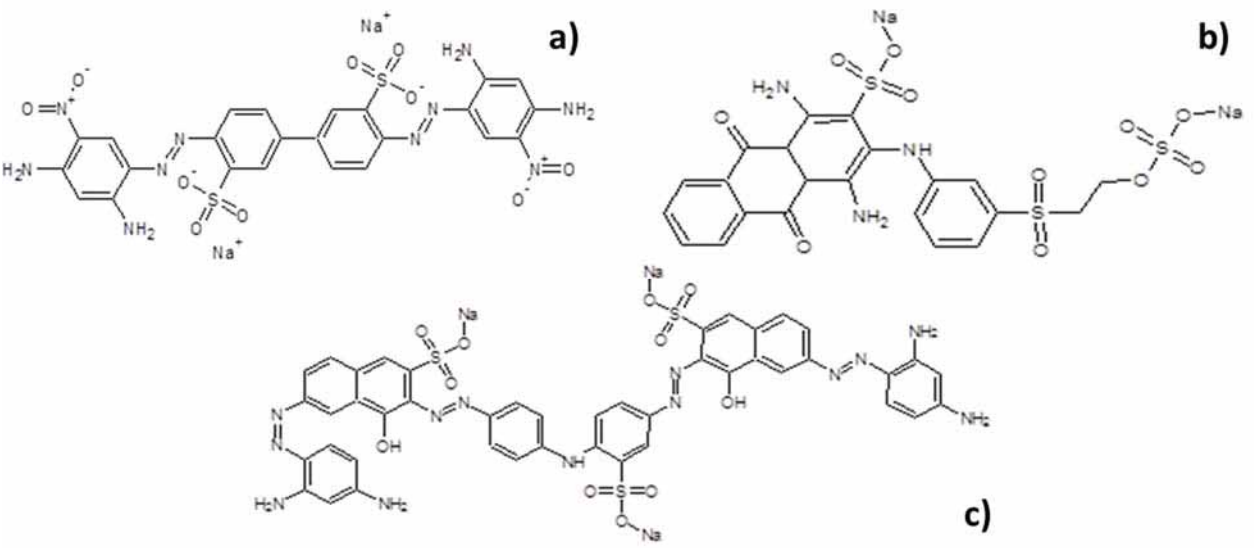


FIGURE 1. Chemical structure of the dyes (a) Direct Orange 4 - DO4, (b) Reactive Blue 19 - RB19, and (c) Direct Black 22 - DB22

These dyes belong to two different groups in relation to their functions and have different physical and chemical properties and they have been widely used in the textile industry[9].

Basal Medium. Composition of essay medium consisted inorganic nutrients and trace elements, bicarbonate buffer, and volatile fatty acids. The basal medium was composed of inorganic nutrients ($g \cdot L^{-1}$): NH_4Cl (0.280), K_2HPO_4 (0.252), $MgSO_4.7H_2O$ (0.100), $CaCl_2$ (0.007), $NaHCO_3$ (0.400), yeast extract (0.100); 1 mL of trace elements solution ($g \cdot L^{-1}$): $FeCl_2.4H_2O$ (2.000), $ZnCl_2$ (0.050), $MnCl_2.4H_2O$ (0.500), $NiCl_2.6H_2O$ (0.142), $NaSeO_3.5H_2O$ (0.164), H_3BO_3 (0.050), $CuCl_2.2H_2O$ (0.038), $CoCl_2.6H_2O$ (2.000), $AlCl_3.6H_2O$ (0.090), $(NH_4)_6.Mo_7O_{24}.4H_2O$ (0.050), EDTA (1.000), resazurin (0.200), and HCl (1 $mL \cdot L^{-1}$)[10-12].

To determine the full methanogenic activity taking into consideration the production of methane by acetoclastic and hydrogenotrophic anaerobes, as well as syntrophic capacity of the system (**Figure 2**), the tests were carried out with a mixture of volatile fatty acids (VFAs): a mixture acetate, propionate and butyrate (1:1:1, based on COD-values / 2 $gCOD \cdot L^{-1}$ in systems)[13] formed the substrate. As buffer 1 g $NaHCO_3$ per g COD was added to this substrate.

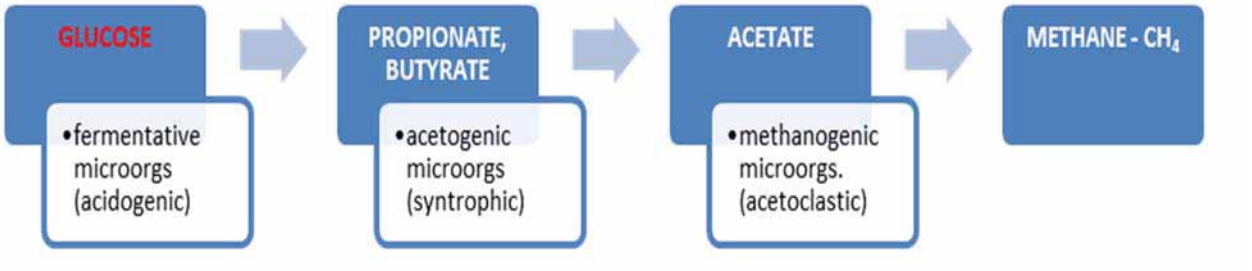


FIGURE 2. Sequence of transformations and types of microorganisms involved in methanogenic activity

Inoculum. The inoculum sludge was obtained from a brewery wastewater treatment plant (non-adapted to dye removal). The flaks reactors were inoculated with a sludge concentration of 3 $g\ VSS \cdot L^{-1}$.

Essays. The specific methanogenic activity (SMA) tests were performed according the methods described by Owen *et al* [14]. Anaerobic serum bottles (100 mL total and 80 mL working volume) were fed with basal medium (16 mL), inoculum (3 $g\ VSS \cdot L^{-1}$), dye and substrate, and kept at room temperature for monitoring of gas production at regular time intervals. Daily weight measurements of the displaced hydroxide were used to plot the cumulative production of CH_4 over the experimental time, and calculate the SMA. The SMA was calculated according to Equation 1.

$$SMA = \left(\frac{V_{CH_4 max}}{m_{VSS} \cdot t}\right) \cdot \left(\frac{64}{0{,}082} \cdot \frac{P}{T}\right) \quad (1)$$

Where calculation of SMA given temperature and pressure conditions under which the test was performed (*V* is volume in Liters, *m* is the mass in grams, *P* is pressure in atmospheres, and *T* is temperature in Kelvin).

Analytical Techniques. Concentration of the dyes DB22, DO4, and RB19 was determined by measuring the spectrophotometric absorbance at the wavelengths of 480, 490, and 592 nm, respectively. Total and volatile suspended solids (TSS and VSS), and COD determinations were performed according to Standard Methods[15]. VFA concentration and the carbonate alkalinity were determined by titration, according to the method adapted to Standard Methods[15].

RESULTS AND DISCUSSION

Determining the SMA. The methane accumulated production, obtained for each dye concentration, are shown in **Figure 3**. In the graph of **Figure 3a** and **3b**, there is not a clear relationship showing a tendency of variation of the volume of methane produced with the dye concentration. As in the previous case (DB22), the concentrations should be increased to find the inhibitory concentration.

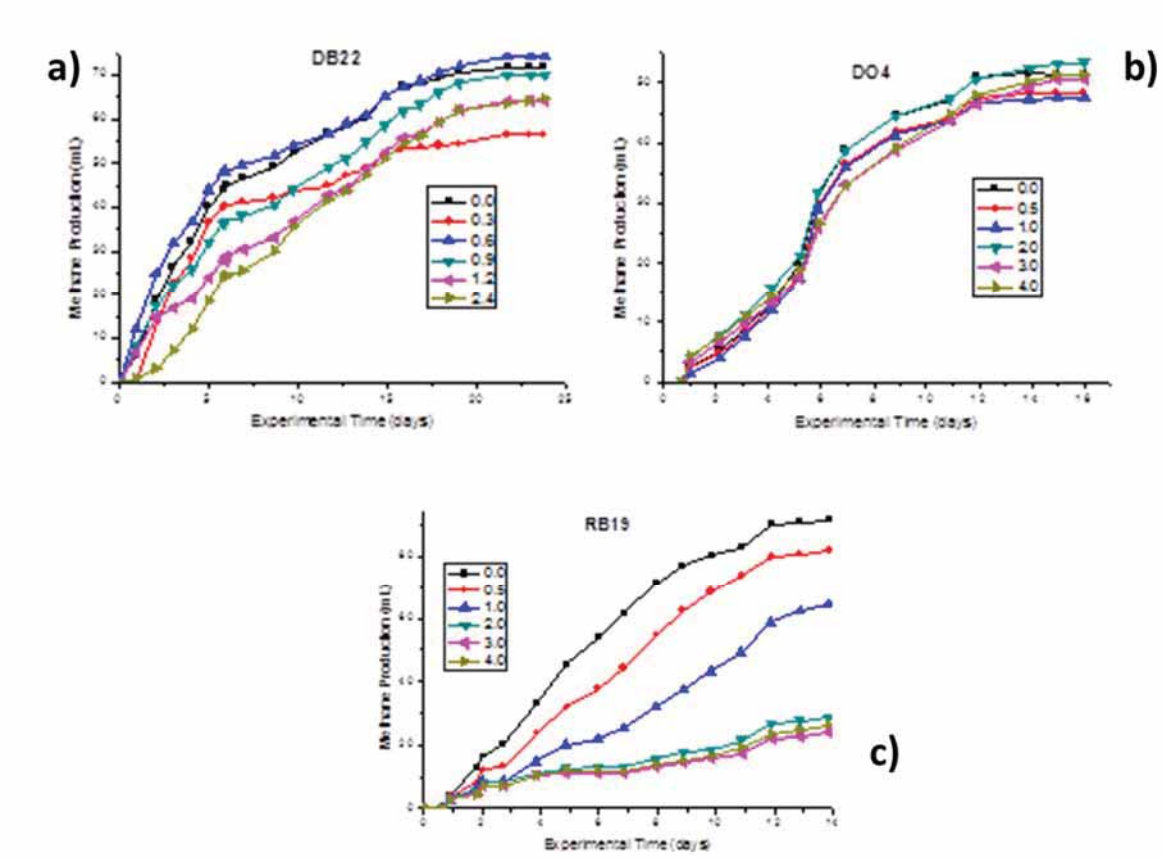


FIGURE 3. Cumulative production of methane in SMA tests for (a) the tetra-azo dye Direct Black 22, (b) the di-azo dye Direct Orange 4, and (c) the anthraquinone dye Reactive Blue 19

For the anthraquinone dye RB19, these concentrations have clearly shown that inhibitory concentration methanogenic activity, in this case, lies between 1.0 mmol·L^{-1} and 2.0 mmol·L^{-1}. The values of concentration 2, 3 and 4 mmol·L^{-1} show a similar production of methane so that we can infer that these concentrations must be greater than the concentration that will generate the maximum inhibition for SMA with this dye.

Daily production of methane. To check the days of higher methane production, daily methane production was plotted over the time (**Figure 4**).

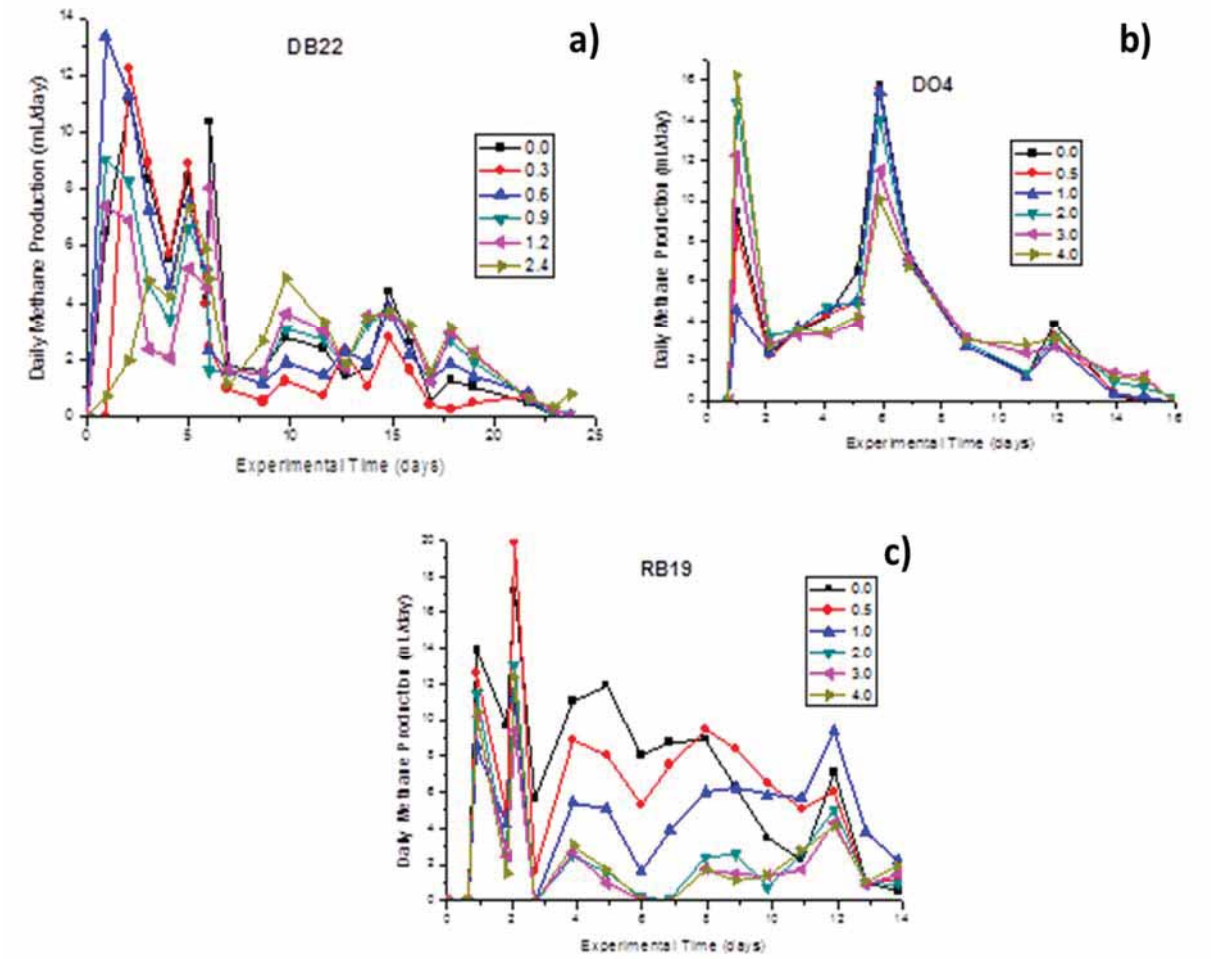


FIGURE 4. Daily methane production in SMA tests for (a) the tetra-azo dye Direct Black 22, (b) the di-azo dye Direct Orange 4, and (c) the anthraquinonic dye Reactive Blue 19

The SMA obtained values and percentage of methanogenic activity inhibition are presented in **Table 1** and **2**.

For the dye DB22 there is not a clear relationship between the DB22 concentrations and the percentage of inhibition. Instead, for the lowest DB22 concentration applied (0.3 and 0.6 mM) a kind of stimulation was detected, with higher SMA than the control reactor.

Table 1. SMA values obtained in the tests with the dye DB22, using the maximum values daily methane production

DB22 Molarity ($mmol \cdot L^{-1}$)	$V_{max}CH_4 \cdot day^{-1}$ (mL)	SMA ($gCOD \cdot gVSS^{-1} \cdot day^{-1}$)	Inhibition %
0.00	11.12	0.010	0.00
0.30	12.22	0.011	-9.89
0.60	13.34	0.012	-19.96
0.90	9.03	0.008	18.79
1.20	8.04	0.007	27.70
2.40	7.36	0.006	33.81

TABLE 2. SMA ($gCOD \cdot gVSS^{-1} \cdot day^{-1}$) values obtained in the test with the dye DO4 and RB19, using the maximum values daily methane production

	DO4			RB19		
Molarity ($mmol \cdot L^{-1}$)	$V_{max}CH_4$ ($mL \cdot day^{-1}$)	SMA	Inhibition %	$V_{max}CH_4$ ($mL \cdot day^{-1}$)	SMA	Inhibition %
0.00	15.71	0.169	0.00	17.20	0.185	0.00
0.50	15.56	0.167	0.95	19.84	0.213	-15.35
1.00	15.46	0.166	1.59	11.19	0.120	34.94
2.00	14.07	0.151	10.44	13.01	0.140	24.36
3.00	11.53	0.124	26.61	10.25	0.110	40.41
4.00	10.06	0.108	35.96	12.33	0.132	28.31

For the essays conducted with the dye DO4, there is a clear correlation between the dye concentration and the inhibition percentage (**Table 2** and **Figure 5**). By extrapolation of the results plotted in **Figure 5**, the DO4 concentration that could generate 100% of SMA inhibition is 0.96 $mol \cdot L^{-1}$.

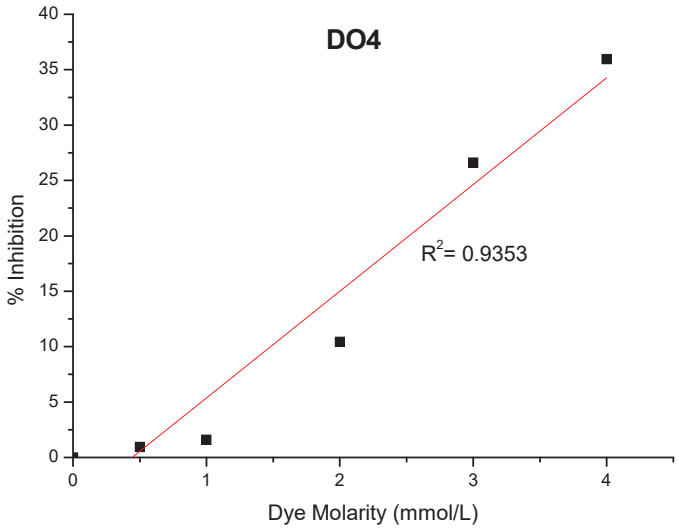


FIGURE 5. Correlation between molarity and percent inhibition observed for the dye DO4

CONCLUSION

The dyes belonging to the azo category (tetra-azo DB22 and di-azo DO4) did not inhibit the methanogenic activity for the tested concentration. Instead, the lowest concentration applied of the DB22 (0.3 and 0.6 mM) was stimulatory for the maximum specific methanogenic activity. However, the dye RB19, which belongs to the anthraquinone category, inhibited the methanogenic activity from 1 mM. RB19 dye in concentration between 2 and 3 mM empire the methane production, before the consumption of one-half of the organic matter supplied. Thus, indicating that the anthraquinone tested dye was more toxic to methanogens that the azo dyes used, for the tested concentration.

REFERENCES

1. Sarayu K.; Sandhya S. Current Technologies for Biological Treatment of Textile Wastewater–A Review. *Applied Biochemistry and Biotechnology***,** v. 167, n. 3, p. 645-661, 2012. ISSN 0273-2289
2. Dos Santos A. B. et al. Effect of different redox mediators during thermophilic azo dye reduction by anaerobic granular sludge and comparative study between mesophilic (30 °C) and thermophilic (55 °C) treatments for decolourisation of textile wastewaters. Chemosphere, v. 55, n. 9, p. 1149-1157, 2004. ISSN 0045-6535.
3. Kunz A. et al. Novas tendências no tratamento de efluentes têxteis. Química Nova, v. 25, p. 78-82, 2002. ISSN 0100-4042.
4. Vandevivere P. C.; Bianchi R.; Verstraete W. Review: Treatment and reuse of wastewater from the textile wet-processing industry: Review of emerging technologies. Journal of Chemical Technology & Biotechnology, v. 72, n. 4, p. 289-302, 1998. ISSN 1097-4660.
5. Cervantes F. J. et al. Biogenic sulphide plays a major role on the riboflavin-mediated decolourisation of azo dyes under sulphate-reducing conditions. Chemosphere, v. 68, n. 6, p. 1082-1089, 2007. ISSN 0045-6535.
6. Pandey A.; Singh P.; Iyengar L. Bacterial decolorization and degradation of azo dyes. International Biodeterioration & Biodegradation, v. 59, n. 2, p. 73-84, 2007. ISSN 0964-8305.
7. Dos Santos A. B. et al. Enhancing the electron transfer capacity and subsequent color removal in bioreactors by applying thermophilic anaerobic treatment and redox mediators. Biotechnology and Bioengineering, v. 89, n. 1, p. 42-52, 2005. ISSN 1097-0290.
8. Yoo E. S.; Libra J.; Wiesmann U. Reduction of azo dyes by desulfovibrio desulfuricans. London, ROYAUME-UNI: International Water Association, 2000. VIII, 272 p.
9. Michniewicz A. et al. Kinetics of the enzymatic decolorization of textile dyes by laccase from Cerrena unicolor. Dyes and Pigments, v. 77, n. 2, p. 295-302, 2008. ISSN 0143-7208.
10. Field J. A.; Lettinga G.; Geurts M. The methanogenic toxicity and anaerobic degradability of potato starch wastewater phenolic amino acids. Biological Wastes, v. 21, n. 1, p. 37-54, 1987. ISSN 0269-7483.
11. Florencio L. The Fate of Methanol in Anaerobic Bioreactors. Landbouwuniversitet te Wageningen, 1994. ISBN 9789054852728.
12. Florencio L. et al. Effect of cobalt on the anaerobic degradation of methanol. Journal of Fermentation and Bioengineering, v. 75, n. 5, p. 368-374, 1993. ISSN 0922-338X.
13. Aquino S. F. et al. Metodologias para determinação da atividade metanogênica específica (AME) em lodos anaeróbios. Engenharia Sanitaria e Ambiental, v. 12, p. 192-201, 2007. ISSN 1413-4152
14. Owen W. F. et al. Bioassay for monitoring biochemical methane potential and anaerobic toxicity. Water Research, v. 13, n. 6, p. 485-492, 1979/01/01 1979. ISSN 0043-1354.

15.A P H A. Standard methods for the examination of water and wastewater / prepared and published jointly by the American Public Health Association, American Water Works Association, Water Pollution Control Federation ; joint editorial board, Michael J. Taras, Arnold E. Greenberg, R.D. Hoak. Washington, D.C. : : American Public Health Association, 1971. ISBN 0875530605

CHAPTER 7.22 THE USE OF ZEOLITE AND LIME FOR SANITIZATION OF SEWAGE SLUDGE

N. Sasakova *(1); J. Venglovsky (1); F. Toth (2); I. Papajova (2); G. Gregova (1); R. Hromada (1) and B. Nowakowicz-Debek (3)

(1) University of Veterinary Medicine and Pharmacy in Kosice, Komenského 73, 041 81 Košice, The Slovak Republic;
(2) Parasitological Institute of the Slovak Academy of Sciences, Hlinkova 3, 040 01 Košice, The Slovak Republic;
(3) University of Life Sciences in Lublin, Akademicka 13, 20-950 Lublin, Polska

ABSTRACT

The study focused on monitoring and evaluation of relevant parameters in samples of sewage sludge obtained from municipal wastewater treatment plant (WWTP). In the WWTP, the produced sewage sludge was sanitized by addition of lime and zeolite with the aim to achieve high level of devitalisation of potential pathogens. Microbiological examination included the groups of micro-organisms which indicate hygiene risk, particularly total coliforms, thermotolerant coliforms and faecal streptococci. Complete sanitization of raw municipal sludge was achieved by treatment at the following ratios in per cent: raw sludge : CaO : zeolite ─ 90 : 5 : 5. After treatment with lime and zeolite no representatives of any of the above groups of micro-organisms could be recovered from the treated sludge. Thus the microbiological values limiting the application of sludge to soil were not exceeded. Chemical examination of sewage sludge included determination of pH, chemical oxygen demand (COD), dry matter content (DM), organic matter (OM), water soluble ammonium nitrogen ($N\text{-}NH_4^+$), total nitrogen (N_t) and total phosphorus (P_t), important for utilization of this substrate by application to soil. The quantity of sludge applied per hectare of agricultural soil is limited by legislative requirements taking into consideration DM content, microbiological counts and the content of selected heavy metals.

Keywords: lime, sanitization, sewage sludge, wastewater treatment, zeolite

INTRODUCTION

Wastewater treatment is an important part of environmental protection. The products of treatment of municipal wastewater are treated water and waste sludge. Optimum technological processes can ensure high level of wastewater treatment so the effluent can be discharged to surface water. However, disposal of waste sludge poses some problems. The annual world-wide production of sludges from WWTP has been estimated to approx. 20 x 10^9 tonnes. The proportion of organic substances in sludge reaches 40−90 % and thus this substrate could be used for manuring.

---

*Author for correspondence: nada.sasakova@uvlf.sk

The progressive implementation of the Urban Waste Water Treatment Directive 91//271/EEC in all EU Member States is increasing the quantities of sewage sludge requiring disposal. The principal controversies surrounding their land application involve heavy metals and pathogens[1].

However, sludges contain far more heavy metals and other elements than artificial fertilisers. They may accumulate in the soil from which they can be mobilised for example by acidification and taken up by soil organisms and plant roots, or leached into groundwater. For this reason, relevant legislative requirement set the limits on the content of selected heavy metals and the quantity of sludge that can be applied to soil. Adequate treatment of sewage sludge including its sanitization, and observation of relevant legislative requirements help to avoid potential hygiene risks related to utilisation of this valuable substrate [2].

In general, stabilised sludge is the term used for sludge which has no negative effect on the environment causes no hygienic problems to humans and animals which manipulate or come into contact with this substrate. According to Juriš et al.[2], the counts of micro-organisms in sewage sludge generally reach 10^6 colony forming units (CFU) in 1 g, of that about 10 % are pathogenic to man and animals. It has been stated than 1% of healthy humans or animals eliminate pathogenic germs which then pass via wastewaters to wastewater treatment plants (WWTP). Thus sewage sludge can contain a range of bacterial and viral pathogens including *Salmonella* spp., *Shigella* spp., *Yersinia* spp., as well as eggs of parasites, e.g. *Ascaris lumbricoides* and oocysts of *Cryptosporidium* spp. and *Giardia* spp. Competition for nutrients and their elimination in the process of decomposition of organic substances, increased temperatures and other factors during processing of sludge inactivate and eliminate these pathogens[3].

Various methods can be used for sanitization of sewage sludge. Advantageous is the use of natural materials such as calcium oxide or calcium hydroxide. These substances are effective in devitalization of potential pathogens present in sludge, particularly by increasing pH, and have positive effects also after application of sludge to soil. After addition of calcium oxide to sludge, calcium hydroxide is produced at the release of heat. Zeolite also plays a positive role after application of amended sludge to soil.

Besides showing a devitalisation effect on bacteria and viruses, lime is effective also against eggs of parasites which accumulate in the sludge in the process of treatment of municipal wastewaters.

Papajová and Juriš[4] reported that liming decreases viability of pathogens but does not always destroys them completely and thus additional methods of treatment of contaminated substrates should be used, such as pasteurisation, chemical disinfection, composting or at least long-term storage on sludge fields.

In Slovakia, the Act No. 188/2003 Coll.[5] about application of sewage sludge and bottom sediments limits the use of sludge in such a way that only treated sludge with minimum content 18 % of dry matter and concentration of risk substances not exceeding the specified limits can be applied to forest or agricultural soil.

The aim of the study was to carry out over the period of 5 months microbiological examination of sludges from different stages of WWTP and to asses effectiveness of its treatment with calcium oxide and zeolite.

MATERIALS AND METHODS

Sewage sludge was obtained from four different stages of municipal aerobic mechanical-biological WWTP. In the WWTP the dewatered sludge was treated by addition of the following natural materials:

1. White dolomite lime – calcium oxide CaO, non-slaked.
2. Nitrosorb – natural zeolite clinoptilolite hydrated aluminosilicate of alkaline metals and metals of alkaline earths), commercial name Zeo Cem Eco Dust. Physico-chemical properties and composition: ground zeolite – crystalline porous adsorbent. Crystalline aluminosilicate of alkaline metals with ion exchange properties.

The aim of manipulation with sludge in WWTP is to reduce the volume of raw sludge (mixture of primary and secondary sludge) by thickening and dewatering. The dewatered sludge is subsequently treated by calcium oxide and zeolite and stored before transportation to purchasers. The treatment should eliminate hygiene risks by devitalization of potential pathogens which is ensured by addition of lime. Because the purchasers use the sludge for production of industrial composts, zeolite is also added during the processing in WWTP to decrease the losses of ammonia after addition of lime and retain this valuable nutrient in the sludge.

The amount and ratio of both components as well as the length of mixing can be adjusted. The aim is to produce alkaline environment with minimal pH = 12.

We determined counts of relevant micro-organisms in four stages of WWTP where sludge was produced and eventually treated:

1. Primary sludge containing considerable proportion of water,
2. Secondary sludge from the second stage of treatment, after dewatering,
3. Dewatered non-sanitized sludge treated with addition of organic flocculation agent,
4. Sanitized sludge – after treatment with lime and zeolite.

Raw municipal sludge was sanitized using the following ratios in per cent: raw sludge : CaO : zeolite ─ 90 : 5 : 5.

Microbiological examination carried out during our study included determination of the groups of micro-organisms which indicate hygiene risk, particularly total coliforms, thermotolerant coliforms and faecal streptococci. Plate counts of micro-organisms (colony forming units − CFU) were determined by cultivation as follows: mesophilic micro-organisms on meat peptone agar at 37°C; total coliforms and thermotolerant coliforms on Endo agar at 37°C and 42°C, resp.; faecal streptococci on Slanetz-Bartley agar at 37°C.

The following changes in physical and chemical properties of the sludges were monitored: pH and ammonium nitrogen in water extracts (1:10) of respective substrates, dry matter content (DM), chemical oxygen demand (COD), organic matter (OM), water soluble ammonia nitrogen ($N\text{-}NH_4^+$), total nitrogen (N_t) and total phosphorus (P_t). The samples were examined for the pH using a pH electrode (HACH Company, Loveland, Colorado, USA). Dry matter was determined by drying at 105 °C to a constant weight, organic matter by the method of Navarro[6], water soluble ammonium nitrogen by titration (Mulvaney[7]), COD by consumption of potassium bichromate for oxidation of sample in sulfuric acid medium during 2-hour boiling in a COD reactor (HACH Company, Loveland,

Colorado, USA). Total nitrogen and total phosphorus were determined by mineralisation of samples using equipment DIGESDAHL (HACH Company, Loveland, Colorado, USA).

RESULTS AND DISCUSSION

Microbiological examination of samples of sewage sludge focused on selected groups of micro-organisms which indicate hygiene risk and on total coliform counts. The detected plate counts − CFU.g^{-1} dry matter (DM) are presented in **Table 1**.
Our results showed that the plate counts of mesophilic micro-organisms in sludge decreased during the treatment in WWTP by one to three orders. Total coliforms counts were also reduced mostly by 2 to 3 orders in the first 3 stages and after sanitization of sludge with lime and zeolite were no more recovered.

Except for the last sampling, thermotolerant coliforms were not detected in dewatered and sanitized sludge. Similar situation was observed for faecal streptococci with complete absence of these micro-organisms in the sanitized sludge.

The Act of the National Council of SR No. 188/2003 Coll.[5] on application of sewage sludge and bottom sediments to soil stipulates that only treated sludge can be applied to soil and sets the limit for thermotolerant coliform bacteria and faecal streptococci to $2x10^6$ CFU.g^{-1}, thus the treatment used in the examined WWTP ensured adequate sanitization of sludge.

TABLE 1. Results of microbiological examination of sewage sludge

CFU. g^{-1} DM	July 9 2013	Sept. 27 2013	October 28 2013	November 5 2013	December 10 2013
Mesophilic micro-organisms (MM)					
1	$1.5x10^7$	$6.0.x10^6$	$4.2x10^6$	$1.8x10^7$	$1.7x10^7$
2	$6.5x10^6$	$8.0x10^5$	$2.2x10^6$	$3.5x0^5$	$2.4x10^5$
3	$2.0x10^6$	$3.2x10^5$	$3.1x10^5$	$2.1x10^5$	$3.0x10^4$
4	$1.9x10^5$	$4.5x10^5$	$4.0x10^5$	$4.0x10^4$	$3.5x10^4$
Total coliformns (TC)					
1.	$6.8.10^6$	$2.2x10^6$	$1.2x10^6$	$2.2x10^6$	$1.1x10^6$
2	$1.4x10^6$	$5.5x10^5$	$7.7x10^5$	$5.8x10^4$	$1.0.x10^4$
3	0	$1.3x10^4$	$8.0x10^3$	0	$1.0x10^3$
4	0	0	0	0	0
Thermotolerant coliforms (TC)					
1	$4.1x10^5$	$2.2x10^5$	$2.5x10^5$	$3.0x10^5$	$3.0x10^5$
2	$1.1x10^4$	$1.8.x10^4$	$3.6x10^4$	$7.2x10^3$	$1.1x10^3$
3	0	0	0	0	$2.5x10^2$
4	0	0	0	0	0
Faecal streptococci (FS)					
1	$1.0x10^4$	$1.0x10^4$	$7.0x10^3$	$1.2x10^4$	$4.0x10^3$
2	$5.0x10^3$	0	$2.0x10^3$	$2.0x10^3$	$3.9x10^3$
3	0	0	0	$3.0x10^2$	$2.1x10^2$
4	0	0	0	0	0

Good bactericidal effects of lime and slaked lime were observed also after addition of these chemicals to animal slurry and the treated slurry had no negative effect when applied to soil as it did not contain harmful residues nor had any phytotoxic effects.

TABLE 2. Results of physical and chemical examination of sewage sludge

Samples	July 9 2013	September 27 2013	October 28 2013	November 5 2013	December 10 2013
			pH		
1	7.7	8,25	8,77	7,78	8,06
2	7.71	9,98	8,34	7,94	7,87
3	9.38	9.12	8,99	8,75	8,71
4	11.79	10.86	11,47	11,52	12,25
			COD (mg.kg-DM)		
1	9900	9670	8990	7670	8400
2	3940	2890	4550	1550	5520
3	1570	1415	1113	1017	1119
4	3000	3716	3477	2987	2228
			Dry Matter (%)		
1	1,34	1,22	1,67	1,31	2,05
2	2,87	1,535	2,02	0,88	0,88
3	26,6	20,09	25,55	22,94	25,5
4	32,8	22,0	25,6	26,33	39,36
			Organic Matter (%)		
1	99,7	99,1	98,3	99,5	98,8
2	98,7	99,79	95,5	99,8	99,7
3	86,8	89,4	89,3	87,6	89
4	80,6	85,9	89,1	91,96	71,8
			$N\text{-}NH_4$ ($mg.kg^{-DM}$)		
1	42,0	235	89,6	20	12
2	14,0	44,8	89,6	90	112
3	364,0	501	159	476,2	796
4	280	504	358,6	280,14	224,1
			N_t ($mg.kg^{-DM}$)		
1	1058,6	1259	2332	1021	687
2	876,3	1039	1418	853	526.6
3	793,5	920	1005	739	455
4	702,7	863	755	701,5	394
			P_t ($mg.kg^{-DM}$)		
1	116,3	124.7	154	37.1	143
2	90,3	29.2	53.3	33.5	37
3	778	90.9	899.8	816.9	612
4	854	948	929.9	943.9	501

After addition of lime, ammonia is released which also exerts some sanitizing effect and helps to devitalise bacterial pathogens and even support inactivation of parasitic protozoan stages, such as Cryptosporidium oocysts inactivation[8,9]. Moreover, CaO reacts with water present in slurry or sludge by exothermic reaction which may result in

increased temperature of the substrate and thus increase devitalisation of pathogens as reported Wong and Fang[10] and Sasáková[11].

The changes in physical and chemical properties of the sludges determined during the study are presented in **Table 2**.

The concentration of risk substances, namely selected heavy metals (As, Ca, Pb, Hg, Zn, Ni, Cr, Cu), must not exceed the relevant limits specified as $mg.kg^{-1}$ DM. Results of determination of these substances will be reported elsewhere.

From the chemical parameters important are changes in pH, as for effective sanitization pH above 12 is recommended. The pH determined in our study in the treated sludge showed that the pH level varied from 11.47 to 12.25 and only at one sampling was below 11 (10.86), and thus quite high to ensure sufficient sanitization of sludge. Raising the pH is one option for sludge treatment, but the effectiveness of this option varies greatly. Factors that may contribute to this variability and thus affect survival of pathogens include temperature, the type and dose of alkalizing agent, the maximum pH attained, and the pH profile during storage [12,13].

The content of dry matter in the dewatered and treated sludge was higher (22.0 – 39.36 %) than 18 % required by the Act[3].

High content of organic matter (71.8−91.96 %) total nitrogen (394−863 $mg.kg^{-1}$) and total phosphorus (501−929.9 $mg.kg^{-1}$) indicate that the treated sludge can be a valuable substrate and a source of nutrients for plants and thus, when it complies with the hygiene requirements, could be utilised for application to soil. However, constant monitoring of its quality should be ensured as considerable variations in its quality may occur as indicated also by our study.

CONCLUSION

Results obtained in this study indicate good effectiveness of technological processes of wastewater and sewage sludge treatment, particularly the final treatment with lime and zeolite which ensured adequate sanitization of this waste material.

The treated waste sludge corresponded to the legislative requirements on its microbiological quality and due to its high content of organic matter, nitrogen and phosphorus can serve as a valuable additive to composts or for other application to agricultural soil. However, the relevant legislative requirements including microbiological quality and chemical composition of the treated sludge, particularly the content of heavy metals, must be fulfilled and frequent monitoring of quality is highly recommended[14].

ACKNOWLEDGEMENTS

The study was supported by Ministry of culture and education grant agency N. 003UVLF-4/2016.

REFERENCES

1. Epstein, E. Land application od sewage sludge and biosolids. 2002, CRC Press.

2. Venglovský, J., Martinez, J., Plachá, I. Hygienic and ecological risks connected with utilization of animal manures and biosolids in agriculture. Livestock Science. ISSN 1871-1413, 2006, Vol. 102, No. 3, 197–203.
3. Dubinský, P., Juris, P., Moncol, D. J. et al. Environmental protection against the spread of pathogenic agents of diseases through the wastes of animal production in the Slovak republic. Harlequin, Ltd., 2000, Kosice.
4. Papajová, I. and Juriš, P. The effect of composting on the survival of parasitic germs. In: Pereira, J. C., Bolin, J. L. (Eds.) *Composting: Processing, Materials and Approaches*. New York: Nova Science Publishers, 2009, 113−154. ISBN 978-1-60741-438-4.
5. Act of the National Council of SR No. 188/2003 Coll. On application of sewage sludge and bottom sediments to soil.
6. Navarro, A. F., Cegarra, J., Roig, A., Garcia, D.. Relationships betwen organic matter and carbon contents of organic wastes. Bioresource Technology, 44, 1993, 203-207.
7. Mulvaney, R. L. Nitrogen – inorganic forms. In SPARKS, D. L. (Ed) Methods of Soil Analysis. Madison, WI: SSSA Inc., 1996, 1123 – 1184.
8. Jenkins, M.B., Bowman, D.D., Ghiorse, W.C. Inactivation of Cryptosporidium parvum oocysts by ammonia. Appl. Environ. Microbiol. 64, 1998, 784–788.
9. Jenkins, M.B., Walker, M.J., Bowman, D.D., Anthony, L.C., Ghiorse, W.C., 1999. Use of a sentinel system for field measurements of Cryptosporidium parvum oocysts inactivation in soil and animal waste. Appl. Environ. Microbiol. 65, 1998–2005.
10. Wong, J.W.C. – Fang, M. Effects of lime addition on sewage sludge composting process. In *Water Research*. ISSN 0043-1354, 2000, Vol. 34, No. 11, 3691−3698.
11. Sasáková, N., Vargová, M., Ondrašovičová, O. Environmental pollution and health risk related to metals in the solid fraction and effluent from waste water treatment. Bull. Environ. Contam. Toxicol. 76, 2006, 671−676.
12. Pescon, B. M., Nelson, K .L. Inactivation of Ascaris suum eggs by ammonia. Environ. Sci. Technol. 39, 2005, 7909–7914.
13. Varadyova, Z., Zelenak, I., Siroka, P., Dubinsky, P., 2001. In vitro fermentation of cellulosis amorphous and meadow hay in experimentally Ascaris suum infected lambs. Small Rumin. Res. 40, 155–164.
14. Juriš, P., Rataj, D., Ondrašovič, M., Sokol, J., Novák, P. Hygiene and ecological requirements on recycling organic wastes in agriculture. Publ. M. Vaška, Prešov, 2000, ISBN 80-7165-257-1.

CHAPTER 7.23 USO DE AGUA RESIDUAL DOMÉSTICA TRATADA Y LODO EN EL CULTIVO DE DOS ESPECIES DE FRÍJOL: PRODUCTIVIDAD Y EFECTOS NUTRICIONALES EN LOS GRANOS

Robson J. Silva (1); Sávia Gavazza (2); Lourdinha Florencio (2); Clístenes W.A. Nascimento (3); Egídio B. Neto (3) and **Mario T. Kato ***(2)

(1) Universidad Federal Rural de Pernambuco, Departamento de Ingeniería Civil, Calle Antigua Carretera, 4360, CEP: 54503-900, Cabo de Santo Agostinho, PE, Brasil
(2) Universidad Federal de Pernambuco, Departamento de Ingeniería Civil, Avenida Acadêmico Hélio Ramos, s/n, CEP: 50740-530, Recife, PE, Brasil
(3) Universidad Federal Rural de Pernambuco, Departamento de Agronomía, Calle D. Manoel de Medeiros, s/n, CEP: 52171-900, Recife, PE, Brasil

RESUMEN

Se ha evaluado el cultivo de especies de frijol - *Phaseolus vulgaris* L. y *Vigna unguiculata* - con efluente y lodo de una Planta de Tratamiento de Aguas Residuales (PTAR). Esta planta está formada por reactor UASB seguido de laguna de estabilización y filtros de piedra. El experimento se realizó en bloques al azar en el sistema factorial 10 x 2, con tres repeticiones. Los tratamientos consistieron en: T0 (agua de abastecimiento), T1 (agua de abastecimiento + fertilizante NPK), T2 (agua de abastecimiento + inoculación por bacteria *Rhizobium*), T3 (agua de abastecimiento + inoculación por *Rhizobium* + fertilizante PK), T4 (efluente), T5 (efluente + inoculación por *Rhizobium*), T6 (efluente + inoculación por *Rhizobium* + fertilizante PK), T7 (lodo), T8 (lodo + inoculación por *Rhizobium*) y T9 (lodo + inoculación por *Rhizobium* + fertilizante PK). Para el cultivo de las dos especies de frijol, fueron utilizadas macetas, con capacidad para 10 kg de tierra, riego diario controlado por el peso y índice WPC del suelo. Para el peso de 1.000 semillas, el T9, con 268,63g, se destacó como el mejor tratamiento para la especie *Phaseolus vulgaris* L. Por otra parte, los tratamientos T9, T6 y T7 fueron los mejores para la especie *Viguina unguiculata*, con los respectivos pesos de 279,60g, 260,25 g y 255,31g. En lo que se refiere al contenido de hierro detectado en los granos de la primera especie, los tratamientos con efluente (T4), lodo (T7) y las variaciones (T5, T6, T8 y T9) ostentaron las concentraciones más altas: 145,48g kg^{-1}, 148,63g kg^{-1}, 151,72g kg^{-1},150,33g kg^{-1}, 156,88g kg^{-1} e 187,24g kg^{-1}, respectivamente. Para la segunda especie, el mejor rendimiento fue para el tratamiento T9, por el acrécimo de la concentración para 161,22g kg^{-1} de este nutriente. En cuanto a la concentración de zinc en ambas especies, se verificó que los resultados fueron satisfactorios también para los procedimientos T4, T5, T6, T7, T8 y T9. Los tratamientos con efluente, lodo y sus variaciones cobraron importancia tanto en la producción de granos, como en su calidad nutricional, lo que evidencia la viabilidad del uso de lodo y aguas residuales tratadas en el cultivo de las especies de frijol *Phaseolus vulgaris* L. y *Vigna unguiculata*.

---

*Author for correspondence: rob.engenhariacivil@gmail.com

Palabras clave: laguna de estabilización, *Phaseolus vulgaris* L., reactor UASB, *Vigna unguiculata*

INTRODUCCIÓN

La calidad del agua y su cantidad en niveles satisfactorios son unos de los mayores retos que enfrenta la mayoría de los países, en los días actuales. Según la Organización de las Naciones Unidas (ONU), cerca del 70% de toda agua potable disponible en el mundo se utiliza para el riego, el 20% para las actividades industriales y el 10% para el uso hogareño. En el proceso de economía de agua potable, sobre todo en el área de riego, el efluente de las Plantas de Tratamiento de Aguas Residuales (PTAR) puede asumir un papel cada vez más importante, ya que presenta concentraciones significativas de macronutrientes tales como nitrógeno (N), fósforo (P) y potasio (K), esenciales al adecuado desarrollo del cultivo de vegetales. Por otra parte, y en concentraciones más bajas, también se pueden encontrar en el efluente algunos metales como hierro (Fe) y zinc (Zn), también requeridos por las plantas, pero en pequeñas cantidades.

El fríjol es un alimento de excelente valor nutritivo, cultivado principalmente en la producción de granos para el consumo humano. Brasil es el mayor productor mundial de frijoles con producción anual promedia de 3,5 millones de toneladas y crecimiento anual del 1,22%. A medida que el consumo de frijoles se generaliza en todo el mundo, el trabajo con vistas a su mejoría nutricional se ha convertido en objeto de varios estudios.

El presente estudio tuvo como meta principal demostrar la productividad y mejoría nutricional en granos de frijoles, desde la utilización de efluente y lodo, en diferentes configuraciones de fertirrigación. En su cultivo las bacterias de la clase *Rhizobium* también se han insertado en el proceso, ya que son capaces de captar el nitrógeno del aire y liberarlo en el suelo bajo la forma de nitrato, que puede ser absorbido por la planta de frijol y aportar beneficios en su productividad.

MATERIALES Y MÉTODOS

La PTAR de este estudio comprende un sistema que comporta reactor UASB, seguido de laguna de estabilización y filtros de piedra. El tiempo de retención hidráulica del sistema es de 10,4 días, con flujo de 30 L s^{-1}, como se muestra en la **Tabla 1**.

Tabla 1. Datos de la Planta de Tratamiento de Aguas Residuales

Datos	Conjunto reactor UASB	Laguna de estabilización	Filtros de piedra
Longitud (m)	12	170	120
Anchura (m)	6	90	120
Profundidad (m)	4,5	1,5	0,5
Superficie (m^2)	72	15300	14400
Volumen (m^3)	324	28050	7920
TDH (d)	0,3	8,1	2

Se han utilizado el efluente de la PTAR y el lodo del reactor UASB para el cultivo de dos especies de frijol: *Phaseolus vulgaris* L. y *Vigna unguiculata*, y a partir de eso, los efectos sobre la productividad y mejoría nutricional de los granos.
El experimento se llevó a cabo por medio de bloques al azar, en el sistema factorial de 10 x 2, con tres repeticiones cada uno. Los tratamientos se describen en la **Tabla 2**.

TABLA 2. Tratamientos utilizados para las dos especies de frijoles

Tratamiento	Descripción
T0 (A)	Agua de abastecimiento
T1 (A + NPK)	Agua de abastecimiento + fertilizante NPK
T2 (A + I)	Agua de abastecimiento + inoculación por bacteria *Rhizobium*
T3 (A + I + PK)	Agua de abastecimiento + inoculación por *Rhizobium* + fertilizante PK
T4 (E)	Efluente
T5 (E + I)	Efluente + inoculación por *Rhizobium*
T6 (E + I + PK)	Efluente + inoculación por *Rhizobium* + fertilizante PK
T7 (L)	Lodo
T8 (L+ I)	Lodo + inoculación por *Rhizobium*
T9 (L + I + PK)	Lodo + inoculación por *Rhizobium* + fertilizante PK

Las especies de frijol *Phaseolus vulgaris L.* y *Vigna unguiculata*, así como los inoculantes de *Rhizobium*, fueron proporcionados por el Instituto Agronómico de Pernambuco, para el experimento.

El experimento se realizó en un invernadero ubicado en el Departamento de Energía Nuclear de la Universidad Federal de Pernambuco (**Figura 1**). Las plantas se cultivaron en macetas que contenían 10 kg de suelo. Inicialmente, se plantaron 5 semillas en cada maceta. A los 12 días después de la germinación, se llevó a cabo el adelgazamiento, dejando sólo dos plantas por maceta.



FIGURA 1. Invernadero ubicado en el Departamento de Energía Nuclear de la Universidad Federal de Pernambuco

TABLA 3. Análisis químico y de textura del suelo utilizado

N	P	Cu	Zn	Mn	Fe	pH	K	Na	Al	Ca	Mg	Arcilla	Limo	Arena
(dag kg^{-1})			(mg dm^{-3})			(-)			(cmol dm^{-3})				(%)	
0,20	1,00	0,20	5,60	4,70	5,40	4,60	0,06	0,10	1,50	0,30	0,30	25	52	23

El control del riego se dio por pesada. El suelo se regó todos los días hasta alcanzar la lámina correspondiente a 80% del índice WPC. Tal coeficiente fue adoptado por expresar el contenido de agua retenida por el suelo, después de la saturación, y el consiguiente procesamiento de drenaje por gravedad [1, 2].

TABLA 4. Análisis químico de los efluentes de los filtros de piedra

Parámetros	Unidad	Número de muestras	Concentración
pH	-		7,3
Temperatura	°C		27
Conductividad electrica	µS cm^{-1}		974
Sólidos totals	mg L^{-1}		1286
Sólidos totales fijos	mg L^{-1}		1040
Sólidos totales volátiles	mg L^{-1}	13	246
Sólidos suspendidos totals	mg L^{-1}		43
Sólidos suspendidos fijos	mg L^{-1}		15
Sólidos suspendidos volátiles	mg L^{-1}		18
Sólidos disueltos totals	mg L^{-1}		1243
Sólidos disueltos fijos	mg L^{-1}		1025
Sólidos disueltos volátiles	mg L^{-1}		218
DQO	mg L^{-1}		72,60
NTK	mg L^{-1} N-NTK		13,10
Amonio	mg L^{-1} $N\text{-}NH_3$		10,60
Nitrito	mg L^{-1} $N\text{-}NO_2$		1,09
Nitrato	mg L^{-1} $N\text{-}NO_3$	10	2,17
Fósforo	mg L^{-1}		2,39
Potasio	mg L^{-1}		11,20
Hierro	mg L^{-1}		0,81
Zinc	mg L^{-1}		0,13
Coliformes totales	NMP/100mL		4,0E3
Coliformes termotolerantes	NMP/100mL	8	1,8E3
Huevos de helmintos	Huevo L^{-1}		0,0

El peso de 1.000 semillas fue el parámetro establecido para evaluar el rendimiento de la productividad, mientras que el contenido de hierro y zinc se consideró para evaluar el estado nutricional de los granos. Dado el diseño de bloques al azar, los resultados se evaluaron estadísticamente mediante análisis de varianza y la prueba F,

en los niveles 1 y 5%. Por último, las hipótesis fueron probadas para encontrar posibles diferencias significativas entre los tratamientos de la prueba de Tukey ($p > 0,05$).

Se obtuvo el suelo para el experimento en el municipio de Jaboatão, en la región de la Zona da Mata de Pernambuco. Este suelo se clasifica como rojo-amarillo, con base en el Sistema Brasileño de Clasificación de Suelos [3], presentando una textura de mediana a mucho arcillosa.

TABLA 5. Análisis químico del lodo proveniente del lodo de UASB

Parámetros	Unidad	Concentración
pH	-	6,4
Umidade, a 60 – 65 °C	% (m/m)	24,4
Sólidos totales	% (m/m)	67,8
Sólidos suspendidos volátiles	% (m/m)	31,7
Carbono Orgánico	g de C kg^{-1}	151,0
NTK	g de N kg^{-1}	20,3
Amonio	mg de N kg^{-1}	1677,0
Nitrato-nitrito	mg de N kg^{-1}	59,2
Arsenio	mg de As kg^{-1}	5,0
Selenio	mg de Se kg^{-1}	ND
Mercurio	mg de Hg kg^{-1}	ND
Potasio	mg de K kg^{-1}	949,0
Sodio	mg de Na kg^{-1}	611,0
Boro	mg de B kg^{-1}	no se detectó
Cadmio	mg de Cd kg^{-1}	2,0
Calcio	mg de Ca kg^{-1}	12,5
Chumbo	mg de Pb kg^{-1}	20,7
Cobre	mg de Cu kg^{-1}	120,0
Cromo	mg de Cr kg^{-1}	22,8
Hierro	mg de Fe kg^{-1}	20668,0
Fósforo	g de P kg^{-1}	5,2
Magnesio	g de Mg kg^{-1}	2,3
Manganeso	mg de Mn kg^{-1}	191,0
Molibdeno	g de P kg^{-1}	17,5
Níquel	mg de Ni kg^{-1}	18,3
Zinc	mg de Zn kg^{-1}	579,0
Coliformes termotolerantes	NMP g^{-1}	5,7E3
Huevos de helmintos	Huevos g^{-1}ST	0,11

Cabe subrayar que el suelo fue elegido estratégicamente, por presentarse como pobre en nutrientes, ya que el objetivo era obtener respuestas directamente relacionadas con la asimilación de los nutrientes contenidos en las aguas residuales y lodo.

Los análisis del suelo se llevaron a cabo según los métodos propuestos por EMBRAPA [4], en el Laboratorio de Suelos de la Estación Experimental de Caña de Azúcar de la Universidad Federal Rural de Pernambuco. Para la corrección de la acidez, se introdujo el carbonato de calcio, a una dosis de 0,6 g kg^{-1} de suelo seco, aplicado a todas las macetas del experimento.

Para los tratamientos basados en la adición de NPK (T1) y PK (T3, T6 y T9), las dosis de nutrientes N, P y K se aplicaron de acuerdo con las recomendaciones del IPA [5], para la fertilización de las respectivas especies de frijoles. Los fertilizantes minerales utilizados para satisfacer a las necesidades de estos nutrientes fueron sulfato de amonio, superfosfato y cloreto de potasio, respectivamente.

El efluente de la PTAR oriundo de los filtros de piedra se utilizó en los riegos de los tratamientos T4, T5 y T6 y su caracterización [6] se evidencia en la **Tabla 4**.

El lodo utilizado en los tratamientos T7, T8 y T9 fue sometido a proceso de compostaje natural por un período de 60 días. Los análisis de caracterización se llevaron a cabo en el Instituto Agronómico de Campinas São Paulo y los resultados se muestran en la **Tabla 5**.

Las dosis de lodo para el cultivo de las dos especies de granos de frijol se calcularon de acuerdo con la cantidad de nitrógeno recomendada para cultivos en relación con lo disponible en el lodo [7].

Es importante destacar que las concentraciones de coliformes, huevos de helmintos y metales pesados estuvieron por debajo de los niveles mínimos recomendados para el cultivo de frijol [8].

El suministro de agua potable utilizados en los tratamientos T0, T1, T2 y T3 tiene su caracterización [6] demostrada en la **Tabla 6**.

TABLA 6. Análisis químico del agua de abastecimiento

Parámetros	Unidad	Número de muestras	Concentración
pH	-	13	6,4
Temperatura	°C		29,7
Conductividad electrica	µS cm^{-1}		423
OD	mg L^{-1}	10	2,56
NTK	mg L^{-1} N-NTK		0,0
Amonio	mg L^{-1} $N\text{-}NO_3$		0,0
Hierro	mg L^{-1}		no se detectó
Fósforo	mg L^{-1}		0,01
Zinc	mg L^{-1}		no se detectó
Potasio	mg L^{-1}		0,0
Coliformes totales	NMP/100mL	8	no se detectó
Coliformes termotolerantes	NMP/100mL		no se detectó
Huevos de helmintos	Huevos L^{-1}		0,0

RESULTADOS Y DISCUSIÓN

Peso de 1.000 semillas. El resultado del método estadístico de Tukey, con probabilidad de 5%, se encuentra en la **Tabla 7**. Los tratamientos con la presencia de efluente y lodo en su composición mostraron desempeños satisfactorios en ambas especies de frijoles.

Para la especie *Phaseolus vulgaris L*., las estadísticas apuntan con destaque la eficiencia del método del tratamiento T9. La combinación respectiva del lodo + inoculación + PK fue capaz de lograr el índice de 268,63g para el peso de 1.000 semillas. Ningún otro tratamiento fue emparejado con el desempeño estadístico del T9.

A continuación, y para la misma especie, se pueden destacar los tratamientos T1 (agua + NPK), T6 (efluente + inoculación + PK) y T7 (lodo), con pesos respectivos de 195,72g, 192,83g y 169,73g.

TABLA 7. Resultado de la prueba de Tukey (p>0,05), para el parámetro peso de 1.000 semillas

Tratamientos	Peso de 1.000 semillas (g)	
	Phaseolus vulgaris L.	***Vigna Unguiculata***
T0 (A)	99,26 e	89,23 f
T1 (A + NPK)	195,72 b	203,12 b
T2 (A + I)	99,95 e	90,28 ef
T3 (A + I + PK)	125,69 de	157,07 cd
T4 (E)	124,16 de	131,76 de
T5 (E + I)	120,04 de	123,02 def
T6 (E + I + PK)	192,83 b	260,25 a
T7 (L)	169,73 bc	255,31 a
T8 (L+ I)	149,06 cd	184,43 bc
T9 (L + I + PK)	268,63 a	279,60 a

Por la prueba de Tukey (p>0,05), valores con la misma letra no difieren significativamente entre sí. Los mejores tratamientos presentan la letra a.

Para la especie *Vigna unguiculata*, los tratamientos T9, T6 y T7 se destacaron por presentar, respectivamente, los coeficientes de 279,60g, 260,25g y 255,31g para el peso de 1.000 semillas. Estadísticamente, no hubo diferencias significativas entre los tres, lo que muestra que para esta especie, las respectivas combinaciones de lodo + inoculación + PK (T9); efluente + inoculación + PK (T6); y lodo (T7) ofrecen las mejores condiciones para la producción de estos granos. Vale la pena señalar que, en este caso, sólo el lodo (T7) fue capaz de lograr los resultados obtenidos por los tratamientos T9 (lodo + inoculación + PK) y T6 (efluente + inoculación + PK).

Por lo general, el buen desempeño de una cultura puede estar asociado principalmente con el contenido de macronutrientes disponible y absorbido por la planta:

nitrógeno, fósforo y potasio. La absorción del nitrógeno está asociada con la asimilación de carbono a través de la fotosíntesis y con el crecimiento de la acumulación de biomasa vegetal [9]. El fósforo interviene en diversas funciones clave de las plantas, incluyendo la transferencia de energía; la fotosíntesis; la transformación de los azúcares y almidones; el movimiento de nutrientes dentro de la planta; y la transferencia de las características genéticas de una generación a la siguiente de frijol [10]. El potasio también participa en la activación de varios sistemas de enzima, fotosíntesis y la respiración [11].

Varios estudios [1,12] señalan el fuerte crecimiento de las plantas que se riegan con efluente: eucalipto, maíz, algodón, papaya, etc. El lodo es también una excelente alternativa de macronutrientes, con excelentes trabajos [13] y unos resultados muy satisfactorios en lo que se atiene al cultivo de frijol [14], especialmente para la especie *Phaseolus vulgaris L*. La viabilidad y el potencial de este tipo de riego se quedó demostrada también con el *Vigna unguiculata*.

Comparándose los tratamientos por equivalencia de fertiirrigación, se observó que el efluente y el lodo, así como sus derivaciones, también ostentaron un rendimiento satisfactorio en relación a los tratamientos basados en suministro de agua potable.

Para la especie *Phaseolus vulgaris* L., es posible comparar los tratamientos T0 (agua), T4 (efluente) y T7 (lodo) para el peso de 1.000 semillas (**Figura 2a**). Así como en la estadística, se hizo evidente el mejor desempeño de los tratamientos con lodo y efluente en lo se refiere al tratamiento de control, que utiliza sólo agua potable sin acrécimo de fertilizante. Eso resulta en una alternativa viable a los agricultores de bajos ingresos que no tienen las condiciones financieras para una plantación fertilizada. El contenido de N, P y K en el lodo (**Tabla 5**) y en el efluente (**Tabla 4**) justifican tal resultado. Lo mismo ocurre cuando se comparan los tratamientos T2 (agua + inoculación), T5 (efluente + inoculación) y T8 (lodo + inoculación), de acuerdo a la **Figura 2a**.

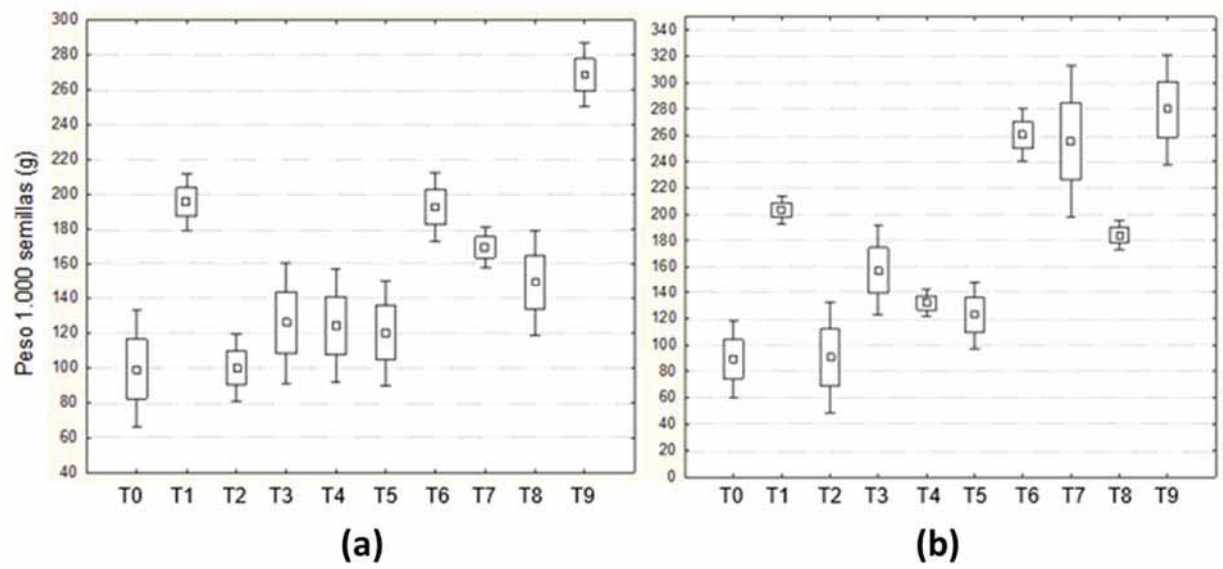


FIGURA 2. Equivalencia de los tratamientos: peso de 1.000 semillas para la especie *Phaseolus vulgares* L. (a) y *Vigna unguiculata* (b).

Para los tratamientos con el uso de fertilizantes T1 (agua + NPK), T3 (agua + inoculación + PK), T6 (efluente + inoculación + PK) y T9 (lodos + inoculación + PK), el desempeño del efluente y del lodo fueron todavía mayores, como lo demuestra la **Figura 2a**.

Para la especie *Vigna unguiculata*, también se destacaron los tratamientos con efluente y lodo en su composición. En la **Figura 2b**, los tratamientos T7 (lodo) y T4 (efluente) presentan mayor peso con base en las 1.000 semillas en relación al tratamiento de control T0 (agua). Los tratamientos T8 (lodo + inoculación) y T5 (efluente + inoculación) prevalecen sobre el tratamiento T2 (agua + inoculación). Y, comparándose los tratamientos T1 (agua + NPK), T3 (agua + inoculación + PK), T6 (efluente + inoculación + PK) y T9 (lodo + inoculación + PK), la **Figura 2b** confirma las estadísticas donde T6 y T9 se destacan como los mejores resultados.

Hierro y zinc. Para evaluar la nutrición de los granos, se han considerado las concentraciones de hierro y zinc, en vista de la importancia de estos metales en la composición del frijol. Muchos expertos en salud recomiendan estos granos como fuente nutricional en la dieta de los niños, mujeres embarazadas, etc. En la planta, el hierro es esencial para la síntesis de proteínas y ayuda en la formación del sistema respiratorio enzimático, teniendo también participación en la fotosíntesis y la transferencia de energía. Por su parte, el zinc es esencial en la actividad, regulación y estabilización de la estructura proteica de la planta. En los seres humanos, el hierro actúa en la síntesis de las células rojas de la sangre y en el transporte del oxígeno a todas las células del cuerpo. Según la WHO [15], su deficiencia se asocia con anemia y hábitos alimenticios. Dado que el zinc ayuda al sistema inmunológico, para atender la defensa del cuerpo, ayuda en la cicatrización, además de ser también un antioxidante [16].

En lo que se refiere a la evaluación del contenido de hierro en los granos de la especie *Phaseolus vulgaris* L., la prueba de Tukey (**Tabla 8**) mostró que los mejores tratamientos de cultivo fueron T4 (efluente), T5 (efluente + inoculación), T6 (efluente + inoculación + PK), T7 (lodo), T8 (lodo + inoculación) y T9 (lodo + inoculación + PK). Los 6 tratamientos no mostraron diferencias significativas entre sí, como bien lo demuestra los respectivos índices de 145,48g kg^{-1},148,63g kg^{-1}, 151,72g kg^{-1}, 150,33g kg^{-1},156,88g Kg^{-1} y 187,24g kg^{-1}. Esos resultados reflejan que el efluente y el lodo proporcionan niveles satisfactorios de hierro a la planta y esto se verifica en la calidad de los granos.

En cuanto a la especie *Vigna unguiculata*, el mayor destaque se concentró en el tratamiento T7 (lodo), cuya producción de granos alcanzó una concentración de hierro de 168,20g kg^{-1}.

Sobre los niveles de zinc para la especie *Phaseolus vulgaris* L., la prueba de Tukey (**Tabla 8**) mostró que las mejores actuaciones fueron obtenidas por los tratamientos T0 (agua), T2 (agua + inoculación), T4 (efluente), T5 (efluente + inoculación), T6 (efluente + inoculación + PK), T7 (lodo), T8 (lodo + inoculación) y T9 (lodo+ inoculación + PK), con los respectivos índices de 61,58g kg^{-1}; 61,83g kg^{-1}; 63,58g kg^{-1}; 66,08g kg^{-1}; 56,25g kg^{-1}; 71,00g kg^{-1}; 62,92g kg^{-1}; y 70,42g kg^{-1}. En este caso, los tratamientos con agua (sin fertilizante añadido) fueron capaces de proporcionar zinc a la planta de la misma manera que los tratamientos con efluente y lodo. Como en el suministro de agua potable no se detectó ninguna concentración de zinc (**Tabla 8**), es posible atribuirse el

buen desempeño de T0 (agua) y T2 (agua + inoculación) al contenido de zinc encontrado en el suelo (**Tabla 3**). Los peores desempeños fueron para los tratamientos con fertilizantes: T1 (agua + NPK) y T3 (agua + inoculación + NPK), que presentaron las concentraciones más bajas de zinc: 41,43g kg^{-1} y 51,83g kg^{-1}, respectivamente. Esto apoya la línea de estudio que evalúa la pérdida de la fijación de zinc inducida por los fertilizantes de fosfato [17]. Este comportamiento también se repitió en la especie *Vigna unguiculata*. Los mejores tratamientos fueron los mismos de la especie anterior y las peores concentraciones fueron 41,43g Kg^{-1} y 51,85g kg^{-1} para los tratamientos T1 (agua + NPK) y T3 (agua + inoculación + PK), ambos con agua y adición de fertilizante mineral.

TABLA 8. Resultados de la prueba de Tukey (p>0,05), para el hierro y el zinc

Tratamientos	Hierro (g kg^{-1})		Zinc (g kg^{-1})	
	Phaseolus vulgaris L.	***Vigna Unguiculata***	***Phaseolus vulgaris L.***	***Vigna Unguiculata***
T0 (A)	110,27 b	74,17 b	61,58 a	60,75 ab
T1 (A + NPK)	133,05 b	69,43 b	41,62 b	41,43 c
T2 (A + I)	118,38 b	83,05 b	61,83 a	58,17 abc
T3 (A + I + PK)	126,60 b	86,93 b	40,00 b	51,83 bc
T4 (E)	145,48 ab	95,55 b	63,58 a	58,33 abc
T5 (E + I)	148,63 ab	90,80 b	66,08 a	56,83 abc
T6 (E + I + PK)	151,72 ab	88,42 b	56,25 ab	56,67 abc
T7 (L)	150,33 ab	161,22 a	71,00 a	73,58 a
T8 (L+ I)	156,88 ab	97,97 b	62,92 a	57,92 abc
T9 (L + I + PK)	187,24 a	93,25 b	70,42 a	64,50 a

Por la prueba de Tukey (p>0,05), valores con la misma letra no difieren significativamente entre sí. Los mejores tratamientos presentan la letra a.

CONCLUSIÓN

Los tratamientos con efluente, lodo y sus variantes ostentaron desempeños satisfactorios en cuanto a la producción, evaluados con base en el peso de 1.000 semillas, y la mejoría nutricional. Para la especie *Phaseolus vulgaris* L., los tratamientos con efluente (T4) y lodo (T7) obtuvieron, respectivamente, una producción del 24% y 70% superior al tratamiento con agua (T0). Para la especie *Vigna unguiculata*, los tratamientos T4 y T7 superaron el 47% y 186%, respectivamente. Eso representa un resultado excelente. Sin embargo, los mejores resultados de la producción de la primera especie se concentraron en el tratamiento T9 (lodo + inoculación + PK), mientras que para la segunda se concentró en T9 (lodo + inoculación + PK), T6 (efluente + inoculación + PK) y T7 (lodo).

En cuanto a la nutrición de los granos, el destaque fue todavía mayor en virtud de las concentraciones de Fe y Zn del efluente, del lodo y de sus variaciones. Para la especie

Phaseolus vulgaris L. los tratamientos T4, T5, T6, T7, T8 y T9 superaron el T0 en al menos 31%. En cuanto a las especies *Vigna unguiculata* el mejor desempeño fue para el T7.

Los tratamientos con efluente, lodo y sus variaciones adquirieron importancia tanto en la producción como en la nutrición de los granos, lo que muestra la viabilidad del uso de aguas residuales tratadas y lodo en el cultivo de las especies de frijol *Phaseolus vulgaris* L. y *Vigna unguiculata*.

AGRADECIMIENTOS

Las instituciones que financiaron la realizacion del trabajo: CAPES, CNPq, UFPE y UFRPE.

REFERENCIAS

1. Silva R., Gavazza S., Florencio L., Nascimento C., Kato M. El cultivo de plantas de eucaliptos con aguas residuales domésticas tratadas. Rev. Eng. Sanit. Ambent. 20 (2), (2015) 323-330.
2. Souza C., Oliveira F., Silva I., Amorim Neto M. Evaluación de métodos para la determinación de agua y la gestión del riego algodón herbáceo disponible en el suelo rojo. Rev. Bras. Eng. Agríc. Ambient. 4 (3), (2000) 338-342.
3. Lima J., Schulze S., Ribeiro M., Barreto S. Mineralogía de un argissuelo rojo-amarillo de la zuena úmida costeira del Estado de Pernambuco. Rev. Bras. Ciênc. Solo. 32 (2008) 88-892.
4. EMBRAPA El análisis manual de química para el suelo, y las plantas de fertilizantes, en: Silva, F.C. (Ed.), Empresa Brasileira de Pesquisas Agropecuárias, Brasil, (1999) 75-223.
5. IPA Recomendaciones para fertilización en el Estado del Pernambuco, 2nd edición. Instituto Agronômico de Pernambuco, Comissão Estadual de Fertilidade do Solo, Recife, Brasil, 2008.
6. APHA, AWWA, WEF Standard methods for the examination of water and wastewater. American Public Health Association, American Water Works Association, Water Environmental Federation, 22nd edition, Washington, USA, 2012.
7. Andreoli C., Von Sperlin M., Fernandes F., Lodo de esgotos: tratamiento y disposición finale, 6 volume (2001).
8. Santos H., Tsutiya M., Miki M., Ebert R., Delatorre M. Critérios para el uso agricola de biossolido de PTAR de la SABESP. En: AESABESP, SANEAS, 10 (1997).
9. Gastal, F., Lemaire, G. N uptake and distribution in crops: an agronomical and ecophysiological perspective. J. Exp. Bot., 53 (2002) 789-799.
10. Zucareli C., Prando A., Ramos Jr E.U. El fósforo en la productividad y calidad de las semillas de frijol carioca cultivada durante la temporada de lluvias. Rev. Ciênc. Agron. 4 (1), (2011) 32-38.
11. Ernani, P., Almeida, J., Santos, F. Potasio. En: Novais, R.; Alvarez, V., Barros, N., Fontes, R., Cantarutti, R., Neves, J. Fertilidade do solo. Viçosa: UFV. 1017 p, 2007.
12. Barros, K., Nascimento, C., Florencio, L. Nematode suppression and growth stimulation in corn plants (Zea mays L.) irrigated with domestic effluent. Water Sci. Technol. 66 (2012) 681-688.
13. Barbosa G., Tavares Filho J. El uso agrícola de lodos: influencia sobre las propiedades químicas y físicas del suelo, la productividad y la recuperación de áreas degradadas. Ciênc. Agrar., 27 (4), (2006) 565-580.
14. Nascimento C., Barros D., Melo E., Oliveira A. Cambios químicos en las plantas del suelo y el crecimiento de maíz y frijol con uso de lodos. R. Bras. Ciênc. Solo 28 (2004) 385-392.

15. WHO Health guidelines for the use of waste water in agriculture and aquaculture, World Health Organization, Technical Report, Series nr. 778, Geneva, Switzerland, 1998.
16. Mafra D., Cozzolino S. The importance of zinc in human nutrition. Rev. Nutr. Campina 17(1), (2004) 79-87.
17. Warnock E. Micronutrient uptake and mobility within corn plants (Zea mays L.) in relation to phosphorus-induced zinc deficiency. Soil Sci. Soc. Amer. Proc. 34 (1970) 765-769.

CHAPTER 7.24 MICROBIAL DIVERSITY IN SEQUENCING BATCH REACTORS USED FOR NUTRIENTS REMOVAL IN DOMESTIC SEWAGE

C.N.C. Souto (1); A.G. Santos Neto (1); V.V.T. Souza (1); S. Gavazza (1); M.T. Kato (1) and L. Florêncio *(1)

(1) Federal University of Pernambuco, Department of Civil Engineering, Laboratory of Environmental Sanitation, Av. Acadêmico Helio Ramos, s/n, Cidade Universitária, Recife, Brazil.

ABSTRACT

Sequencing batch reactors (SBRs) can promote nutrients removal in wastewater through biological process. Exposing a microbial population to cyclical anaerobic, aerobic and/or anoxic conditions provides phosphorus removal by storage inside the cells and simultaneously the nitrogen removal by nitrification-denitrification reactions.
In this work, two SBRs (140 L) were operated with low organic load (0,485 kg COD.m^{-3}.d^{-1}) and cycles of 8 hours, being operated with 2 h, 4 h, 1,25 h and 0,75 h period under anaerobic, aerobic, anoxic, sedimentation and emptying, respectively. One SBR was continuously aerated and the other intermittently. Along the 223 d operational period, nitrogen and phosphorus removal were monitored and batching time profiles were carried out in order to observe metabolic pathways.
Abundance of *Nitrospira*, denitrifiers, anammox, ammonia-oxidising bacteria (AOB) and polyphosphate accumulating organisms (PAOs) were evidenced by Polimerase Chain Reaction (PCR). Both reactors provided satisfactory phosphorus removal reaching total concentration below 1 mg.L^{-1}. Although the reactor with intermittent aeration has showed a faster biomass growth than the continuously aerated reactor, it was not more efficient to the nutrients removal.

Keywords: enhanced biological phosphorus removal, nitrification and denitrification, polyhydroxyalkanoates, polyphosphate accumulating organisms.

INTRODUCTION

Biological nutrients (N and P) removal in sewage involves four major groups of microorganisms: autotrophic nitrifying that oxidize ammonium to nitrite and nitrate aerobically; heterotrophic denitrifying, responsible for the reduction of nitrate to nitrogen gas under anoxic conditions; polyphosphate accumulating organisms (PAOs), which accumulate phosphorus taking up oxygen as electron acceptor; and denitrifying polyphosphate accumulating organisms, which store phosphorus using nitrate or nitrite as electron acceptor.

---

*Author for correspondence: flor@ufpe.br

A serie of reactors operating under environmental conditions to stimulate the development of specific microbial populations improves efficiency of nutrients removal. The use of a single reactor, creating different conditions in distinct zones or different operation times, reduces space requirement and operational costs. A sequencing batch reactor (SBR) operating with alternating conditions (anaerobic/aerobic and/or anoxic) can be useful for this aim[1].

Enhanced Biological Phosphorus Removal (EBPR) is a process that provides high phosphorus removal efficiency avoiding eutrophication of waterways. EBPR occurs due to metabolic activity of polyphosphate accumulating organisms (PAOs) which take up phosphorus and store into their cells as poly-P[2].

EBPR process is mainly expose activated sludge biomass to anaerobic and aerobic conditions providing organic matter during anaerobic period, where microorganisms rather utilize acetate and propionate as carbon source to produce polyhydroxyalkanoates (PHAs) and store inside the cells. The energy required is obtained from the hydrolysis of polyphosphates and glycogen oxidation, also storage compounds inside the cells[3].

Therefore, phosphate releasing takes place in the anaerobic stage, whereas organisms metabolize PHA in the aerobic stage, providing energy to cell growth while they accumulate glycogen and polyphosphate. In this stage, phosphate previously released is taken up and the influent phosphate is consumed. Thus, total phosphorus is removed with the excess sludge produced during the process[4,5].

Batching reactors are commonly used to the EBPR study in laboratory-scale, where required conditions are feasible provided to the microbial community and also allows a higher monitoring.

Biological nutrient removal (BNR) combines phosphorus and nitrogen removal. Most BNR Wastewater Treatment Plants (WWTPs) operates the denitrifying stage (anoxic) at upstream from the anaerobic zone. Since ammonia must be aerobically oxidized to the denitrification happen, this configuration needs high mixed liquor recycle rates to provide nitrate in the anoxic phase. Instead, locating the anoxic stage at downstream of the nitrification zone (aerobic) allows achieve higher total nitrogen removal, excluding mixed liquor recycle requirements[6].

In this work, two SBR (140 L) fed with real sewage were exposed to alternating conditions (anaerobic/aerobic/anoxic) with the same operational conditions, except for the aeration (continuously/intermittently) in order to improve activity of the microorganisms involved in the nutrients (N e P) removal.

MATERIALS AND METHODS

Experimental setup. Two sequencing batch reactors in pilot scale were operated and fed with real sewage from the pre-treatment of the WWTP Mangueira, Recife-PE, Brazil. Both SBRs with 140 L of working volume and operated for over 223 days. The systems were operated with 8 h cycles consisted of 2 h anaerobic (including 5 min for charging), 4 h aerobic, 1.25 h anoxic and 0.75 h for settling and emptying. The system was automated with two control valves for charging and emptying of reactors, connected to a programmable logic controller (PLC) and air compressors were active in aerobic stage. Mechanical mixers promoted complete mix into reactors. Regarding aeration, one

reactor was continuously aerated (SBR2) and the other intermittently (SBR1) for the purpose of compare influence in the treatment.

Phosphorus, nitrogen and others control parameters were analyzed in order to evaluate nutrients removal along the operational period. Batching time profiles were carried out to evaluate all the treatment process and metabolic pathways.

Chemical analysis. Influent and effluent samples were analyzed weekly along the operational time and the SBRs also were monitored along the anaerobic/aerobic/anoxic phases (batching time profiles). Total phosphate, orthophosphate (PO_4-P) and the nitrogen serie (NH_3-N, NO^-_3-N, NO^-_2-N) were determined using standard methods, SM 4500 E, SM 4500 C, SM 4500 B, respectively. [7]

Intracellular PHA was quantified by the adapted method of Oehmen et al.[8] using a gas chromatography equipped with a flame ionization detector (GC-FID). Mixed liquor samples of 100 mL were collected during the cycles and then centrifuged at 2000 rpm for 10 min and the supernatant was removed. Then, samples were lyophilized until complete drying. Approximately 20 mg of lyophilized sludge samples, 2 mL of chloroform and 2mL of an acidified methanol solution (10% H_2SO_4) containing benzoic acid as internal standard were added to glass tubes of 10 mL, and the samples were digested in tightly at 100 °C for 3.5 h to PHAs esterification. After digestion, samples were cooled to room temperature and about 1 mL of ultra pure water (Milli-Q®) was mixed with samples to remove particulate debris and then, were shaken in a vortex for 5 min and centrifuged for 3 min to promote phases separation. The chloroform phase (at the bottom) was extracted and injected into the Agilent GC-FID operated with a DB-WAX column (30 m x 0.25 mm x 0.25 µm), a split injection ratio of 1:15 and hydrogen as carrier gas (1 $mL.min^{-1}$). The FID unit was operated at 300 ºC with an injection temperature of 210 ºC. The oven was set to 100 ºC for 1 min increasing 8 $°C.min^{-1}$ until 160 ºC, and then to 270 ºC at 45 $°C.min^{-1}$ holding for 3 min. The injection volume was 1 µL.

***Microbial monitoring*.** Microscopic visualization analyses were performed in order to evaluate microbial population involved in the treatment process herein studied. Fresh samples of mixed liquor were collected from the both reactors. A portion of each sample was placed on a slide and covered with a cover slip, and then visualized by an optical microscope (Leica®), analyzing structure and dominant microorganisms in the sludge.

Furthermore, genomic DNA was extracted from each reactor in order to apply the molecular biology technics of polymeric chain reaction (PCR). Specific primers, the mix and a Platinum Taq DNA polymerase (Invitrogen) were used in the PCR reaction to assess abundance of major groups involved in nitrogen and phosphorus removal: ammonia-oxidising bacteria[9] – AOB- (primer 190F/1225R); the nitrite-oxidising bacteria *Nitrospira*[10] (primer NTS232F/NTS1225R); denitrifying bacteria[11] (primer NirS 2F - GC/NirS 3R); Anammox[12] (primer AMX368F/AMX820R) and PAOs[13] (primer 651F/846R). Extraction was performed by a Power Soil™ DNA Isolation Kit MOBIO laboratory. Amplification was carried out in the termocycle “My cicle” (Bio Rad).

RESULTS AND DISCUSSION

Chemical analysis. Removal efficiency of phosphorus only was reached after 160 days of operation for both reactors (**Figure 1**), required period for biomass development and stabilization. Phosphorus removal reached 80 - 98% (SBR2) and 80 - 95% (SBR1). Optimal efficiency to SBR1 was reached in 174 days with volatile suspended solids on mixed liquor (MLVSS) of 434 $mg.L^{-1}$ and SBR2 reached optimal efficiency at 165 days and MLVSS of 793 $mg.L^{-1}$.

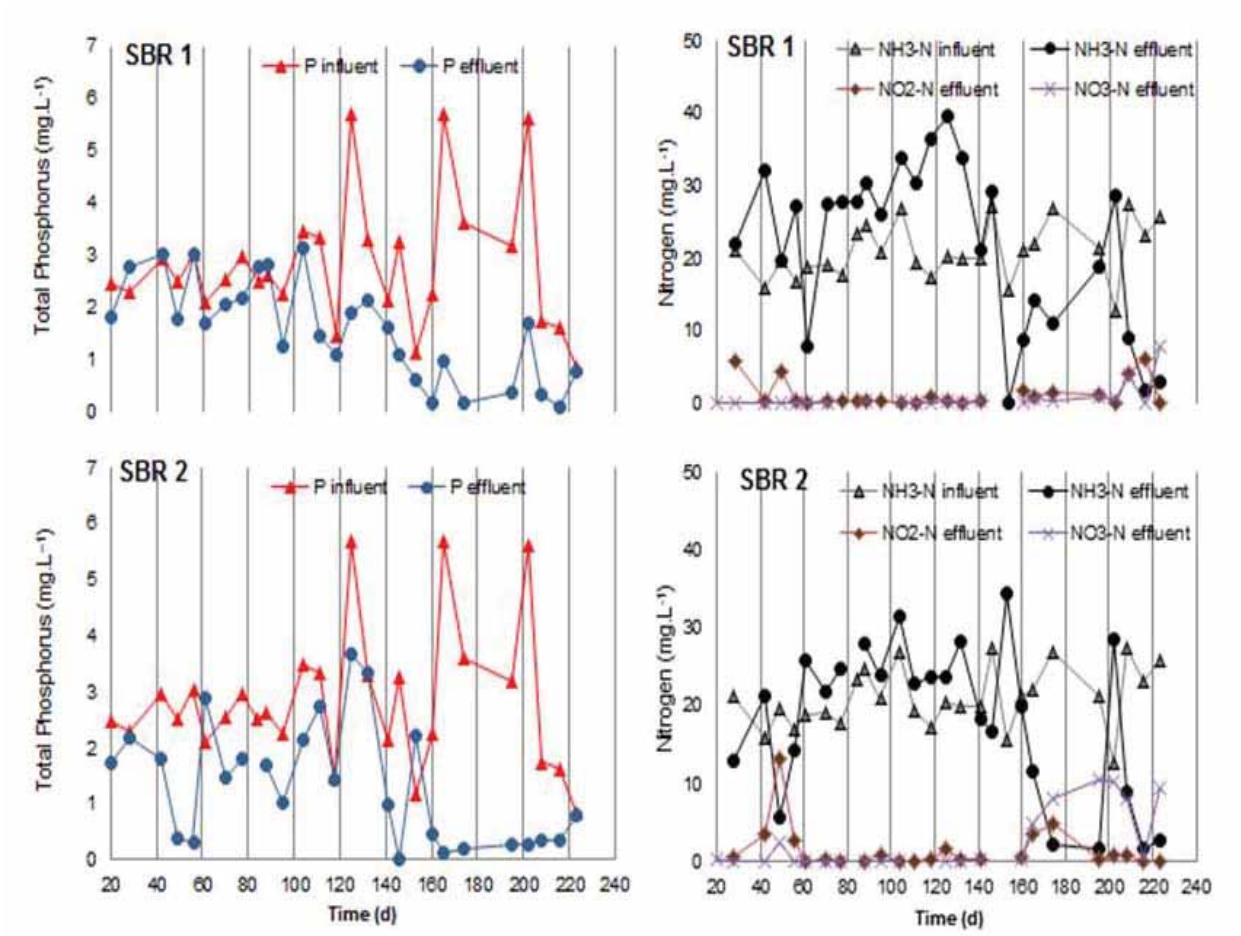


FIGURE 8. Total phosphorus and nitrogen influent and effluent along operational period

Regarding nitrogen removal, SBR2 achieved higher efficiency than SBR1. However, nitrification/denitrification in both reactors only occurs after 160 operation days (Figure 1). In the steady state of SBR1 and SBR2 (**Figure 2**) there is not high variation to the phosphorus removal of both reactors (most of 80 – 90%) while total nitrogen exhibited variation but the majority reached removal of 50 - 67% (SBR2) e 50 – 60% (SBR1).

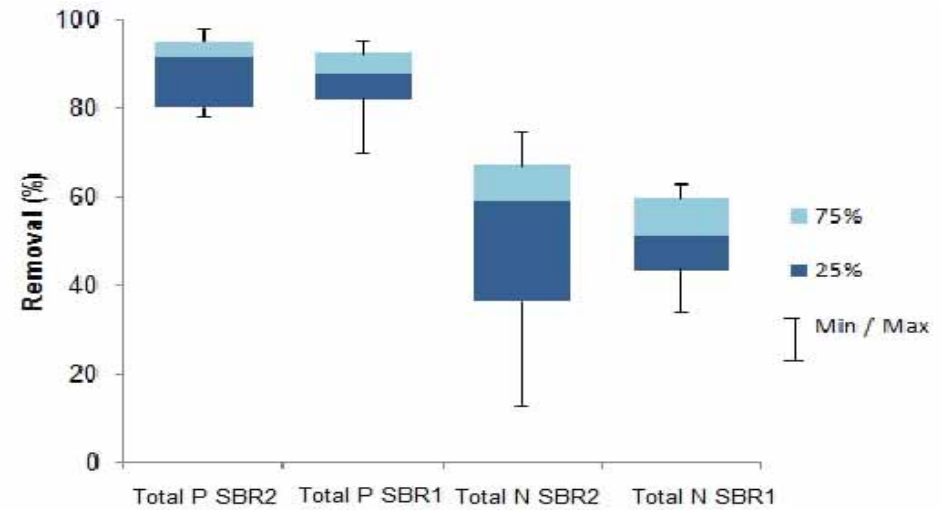


FIGURE 9. Removal of P and N after steady state of reactors

Results obtained through the batching time profiles (**Figure 3**) exhibited the immediately releasing of phosphate at the beginning of anaerobic stage to both reactors. At the first hour of the cycle phosphorus reaches maximum concentration and is consumed from the second hour to the end of aerobic stage. PHAs production and consumption are related with the phosphorus profile such that the PAOs break the polyphosphate stored to provide energy source at same time that release PO_4^{3-} and store volatile fatty acids (VFAs) as polyhydroxyalkanoates (PHAs) under anaerobic conditions. In the aerobic stage, PHAs are degraded, providing carbon and energy and accumulating PO_4^{3-} inside the cells that is removed with the excess sludge.

SBR2 achieved higher nitrogen removal than SBR1. Along the operational period SBR1 exhibited unsteady to the N removal. Increasing amounts of nitrite and nitrate were observed in the effluent that suggests incomplete denitrification. The reduction in the aerobic phase and increase the anoxic time would favor the nitrogen removal in both reactors without damaged phosphorus removal, since it was achieved with only 3 hours of aeration.

***Microbial monitoring*.** The biomass development presented typical characteristics of activated sludge. Initially, it was observed proliferating of filamentous microorganisms (**Figure 4a**) contributing to the flakes agglomerating. However, excess of filamentous denote nutrients dissolved oxygen deficiencies and is responsible for low sludge settleability. Protozoa and fixed ciliates (**Figure 4b**) occurred more frequently in SBR2. The ciliates *Aspidisca costata* (**Figure 4c**) in SBR2 denotes satisfactory removal of settleable solids and low nitrification. SBR1 exhibited low microbial diversity.

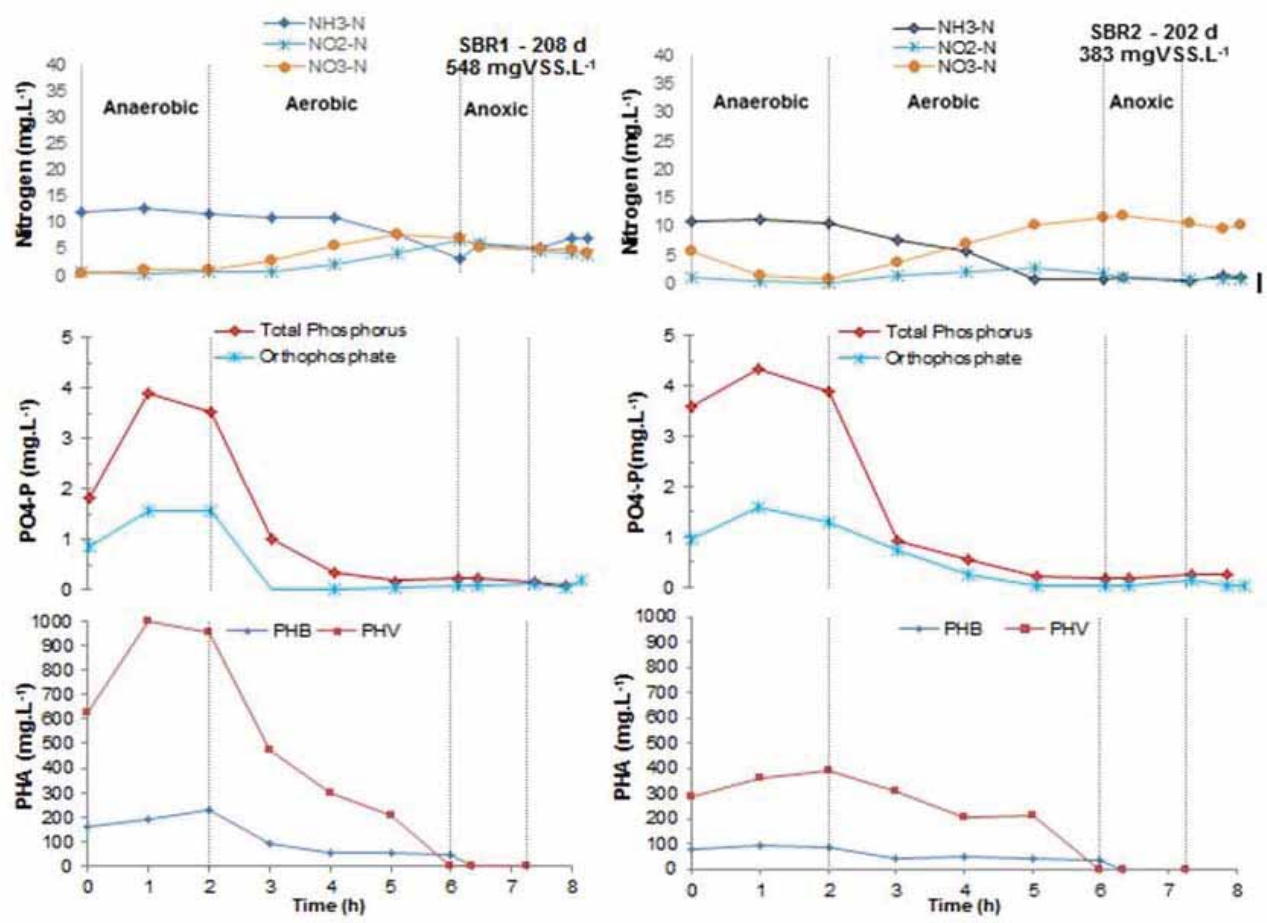


FIGURE 10. Batching time profiles of SBR1 and SBR2 after steady state

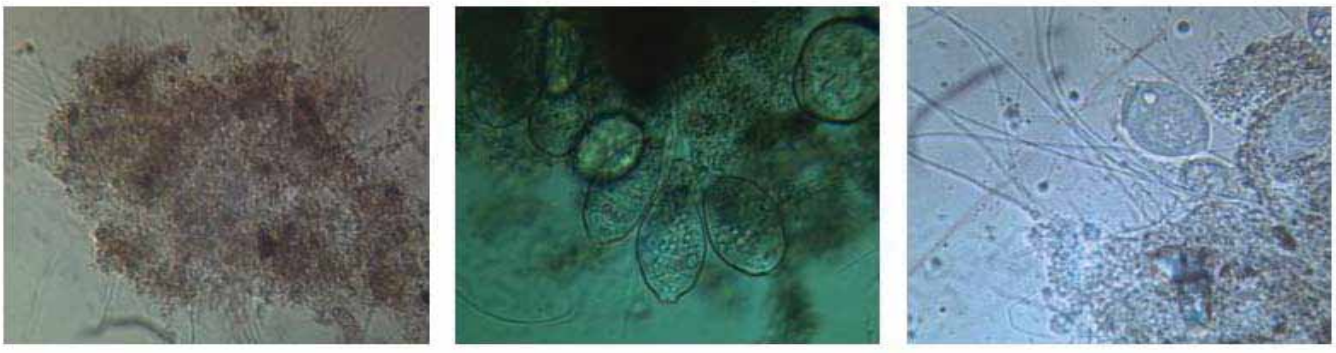


FIGURE 4. Microbial diversity observed by optical microscope: (a) Filamentous; (b) *Opercularias* SP (fixed ciliates); (c) *Aspidisca costata* (free ciliates).

PCR analyses (**Figure 5**) confirmed presence of the main groups: ammonia-oxidising bacteria, denitrifiers bacteria, anammox, *Nitrospira* (in a sample of SBR2) and polyphosphate accumulating organisms in both reactors.

Batching time profiles of the two reactors concerning phosphorus removal and the presence of PAOs confirmed by PCR, characterize EBPR process occurring in both SBRs.

Regarding nitrogen removal, the appearing of *Nitrospira* in one sample is not representative to denote conventional nitrification occurring. The positive result for anammox suggests a N-NH_3 removal by ammonia oxidising with NO_2^- as electron acceptor in anaerobic conditions, that probably happens in SBR1 (anoxic stage), where occurs an elevation of NH_3 (due the addition of sewage as carbon source to the denitrification) and consumption of NO_2^-. Positive result for the ammonia-oxidising bacteria suggests nitrification occurrence in both SBRs. Despite the confirmed presence of denitrifiers, denitrification was incomplete in both, mainly in SBR2.

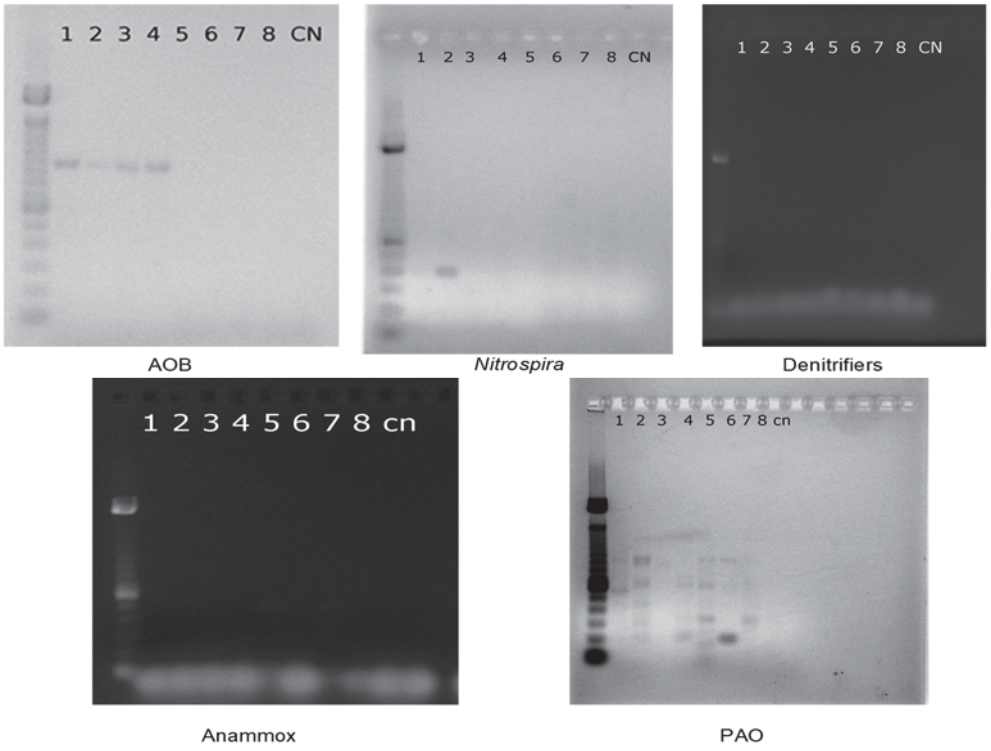


FIGURE 5. PCR analyses of samples collected along operational time

CONCLUSION

This study presented main aspects involved on the biological phosphorus and nitrogen removal focused in operational conditions provided to the development of microbial population responsible for these processes.

It was finding that a period of 160 days was required to development and stabilization of biomass in both reactors. Satisfactory phosphorus removal was obtained in both

reactors after this adaptation period, reaching efficiencies higher than 80%. Regarding the nitrogen removal, both SBRs exhibited unstable along operational period and increasing amounts of nitrite and nitrate on the final effluent denoted incomplete denitrification.
In order to promote complete denitrification in both systems (SBR1 and SBR2), a reduction in the anaerobic stage time and an increase in anoxic stage would provide complete nitrogen removal.
The PCR analysis confirmed presence of the expected microbial population: AOB, denitrifiers, anammox, *Nitrospira* and PAOs.
Phosphorus results were more consistent and EBPR process occurred as expected. PHAs metabolism was related with phosphorus removal such that followed the phosphorus behavior in each reaction stage during the cycles.
Although the both reactors exhibited satisfactory phosphorus removal reaching concentration below 1 $mg.L^{-1}$ SBR1 was not more efficient to the nutrients removal, since the SBR2 reached higher rates of removal also to nitrogen.

ACKNOWLEDGMENTS

We are grateful to the Brazilian Agencies that supported this study: Capes, CNPq, FACEPE, COMPESA and Finep, Federal University of Pernambuco (UFPE), Laboratory of Environmental Sanitation (LSA).

REFERENCES

1. Freitas F., Temudo M., Reis M.A.M. Microbial population response to changes of the operating conditions in a dynamic nutrient-removal sequencing batch reactor. Bioprocess Biosyst. Eng. 2005, 28: 199-209
2. Mesquita D.P., Amaral A.L., Leal C., Carvalheira M., Cunha J.R., Oehmen A., Reis M.A.M., Ferreira E.C. Monitoring intracellular polyphosphate accumulation in enhanced biological phosphorus removal systems by quantitative image analysis. Water Science & Technology 2014, 69.11: 2315-2323
3. Kang D., Noguera D.R. *Candidatus* Accumulibacter phosphatis: Elusive Bacterium Responsible for Enhanced Biological Phosphorus Removal. Journal of Environmental Engineering 2014, 140: 2-10
4. Martín H.G., Ivanova N., Kunin V., Warnecke F., Kerrie W.B., McHardy A.C., Yeates C., He S., Salamov A.A., Szeto E., Dalin E., Putnam N.H., Shapiro H.J., Pangilinan J.L., Rigoutsos I., Kyrpides N.C., Blackall L.L., McMahon K.D., Hugenholtz P. Metagenomic analysis of two enhanced biological phosphorus removal (EBPR) sludge communities. Nature biotechnology 2006, 24: 1263-1269
5. Zeng R.J., Yuan Z., Keller J. Improved understanding of the interactions and complexities of biological nitrogen and phosphorus removal processes. Environmental Science & Bio/Technology 2004, 3: 265-272
6. Winkler M., Coats E.R., Brinkman C.K. Advancing post-anoxic denitrification for biological nutrient removal. Water Research 2011, 45: 6119-6130
7. APHA : American Public Health Association. Standard Methods For The Examination of Water and Wastewater, 22 ed. Washington, 2012.
8. Oehmen A., Keller L. B., Zeng R. J., Yuan Z., Keller, J. Optimisation of poly-β-hydroxyalkanoate analysis using gas chromatography for enhanced biological phosphorus removal systems. Journal of Chromatography 2005, 1070: 131-136

9. Hikuma M., Nakajima M., Hirai T., Matsuoka H. Rapid Detection of Ammonia-oxidizing Bacteria in Activated Sludge Based on 16S-rRNA Gene by Using PCR and Fluorometry. Biotechnol. Bioprocess Eng. 2002, 7: 323-326
10. Lim J., Do H., Shin S.G., Hwang S. Primer and Probe Sets for Group-Specific Quantification of the Genera Nitrosomonas and Nitrosospira Using Real-Time PCR. Biotechnology and Bioengineering 2008, 99(6): 1374 -1383
11. Nittami T., Kurisu F., Satoh H., Mino T. Analysis of the populations of denitrifying bacteria in activated sludge by PCR-DGGE analysis of the nirS nitrite reductase genes. J. Japan Society on Water Environ. 2003, 26: 583-588
12. Schmid M., Walsh K., Webb R., Rijpstra W.I.C., van de Pas-Schoonen K., Verbruggen M.J., Hill T., Moffett B., Fuerst J., Schouten S., Damsté J.S.S., Harris J., Shaw P., Jetten M., Strous M. Candidatus “Scalindua brodae”, sp. nov., Candidatus “Scalindua wagneri”, sp. nov., Two New Species of Anaerobic Ammonium Oxidizing Bacteria. Systematic and applied microbiology 2003, 26: 529-538
13. Crocetti G.R., Hugenholtz P., Bond P.L., Schuler A., Keller J., Jenkins D., Blackall L.L. Identification of Polyhosphate-Accumulating Organisms and Design of 16S rRNA-Directed Probes for Their Detection And Quantitation. Applied and Environmental Microbiology 2000, 66: 1175-1182

CHAPTER 7.25 USE OF EFLUENT AND SLUDGE FROM SEWAGE TREATMENT PLANT IN SORGHUM CULTIVATION

E. J. Souza Filho *(1); E. Bezerra Neto (2); S. Gavazza (1); L. Florencio (1) and M. T. Kato (1)

(1) Laboratory of Environmental Sanitation, Department of Civil Engineering, Federal University of Pernambuco, Av. Acadêmico Hélio Ramos S/N, Cidade Universitária, 50740-530, Recife-PE – Brazil
(2) Department of Chemistry, Federal Rural University of Pernambuco, Recife, PE, Brazil.

ABSTRACT

The use of treated wastewater for irrigation is very interesting because it is a water source with presence of nutrients that can meet the needs of the plants. Sorghum (*Sorghum bicolor L*.) is a plant of African origin and adapts well to semi-arid regions; in some African countries, it is used as human food. In Brazil, there are cases where sorghum flour is mixed with wheat flour for bread production; however, sorghum is more widely used for animal feed. The use of treated wastewater for irrigation of crops for animal feed is considered as highly recommended. Therefore, the study of nutritional effects on pasture crops irrigated with wastewater is important. This work provides a study of the use of wastewater and sludge in the sorghum crop, evaluating the productivity and the nutrient input. The experiment was conducted in a greenhouse where the sorghum plants were grown in pots of 10 dm^3, and irrigation was performed daily in order to leave the soil with 70% to 80% of saturation. The soil type was Quartzipsamment. Six treatments (T) and five repetitions each were tested: T1 = irrigation with potable water, T2 = irrigation with potable water + chemical fertilizer (NPK), T3 = irrigation with potable water + fertilization with sludge, T4 = irrigation with wastewater, T5 = irrigation with wastewater + chemical fertilizer (PK), T6 = wastewater irrigation + fertilization with sludge. The treatment plant consisted of anaerobic reactor type UASB (upflow anaerobic sludge blanket) and stabilization pond. The used sludge came from the UASB reactor. The plants were monitored through growth physical parameters (height, stem diameter), production (grain number and weight of 100 grains) and biochemical characteristics (chlorophyll, nitrogen, phosphorus and potassium). The results showed that the use of sludge and effluent under controlled conditions enhance the sorghum production when compared with the use of chemical fertilizers.

Keywords: agronomic behavior, anaerobic reactor, stabilization ponds, water reuse.

INTRODUCTION

The demand for water of good quality is increasing due to several factors, like population growth, pollution of water resources, economic growth and consequently, increased consumption. These factors make uncertain the future availability. Only in China, it is estimated that a total of 280 million people use poor quality water for consumption[1]. The

---

*Author for correspondence: edecio.souza@yahoo.com.br

possible shortage of water, especially in agriculture, is an urgent problem that currently affects approximately one third of the world population[2,3,4], considering that most of the water is consumed in agriculture.

Given this scenario, it is necessary greater protection of the existing water resources. The reuse of water is an alternative to scarcity. In addition to enabling the reduction of discharges of treated effluent into water bodies, this activity provides the use of better quality water for more noble purposes. Considering that agriculture is the activity that more demands thef water resources, water reuse becomes very attractive. The irrigation with treated sewage can cause beneficial effects on plants, especially on increased production[5].

The nutrients present in the effluent of sewage treatment plants are utilized by plants, often reaching good crop development, contributing to reduce the use of artificial fertilizers in irrigation[6,7]. The amount of N present in the wastewater is sufficient for the plants; however, the levels of P and K are not enough to meet the needs of most cultivars[8].

The sludge disposal originating from sewage treatment plants is also characterized as environmental concern; however, this product is rich in organic matter and nutrients, being very indicated its use in agriculture after previous treatment[9].

Sorghum (*Sorghum bicolor L*.) is a plant originated in Africa and belongs to the same family of corn. It has being widely used in animal feed and has showed characteristic of good adaptation to semi-arid regions[10]. Sorghum is a potential source of phytochemicals with an important role in promoting human health, but it is currently underutilized as food. Because it does not have gluten, that cereal can be a viable alternative to replace wheat in the development of products for celiacs[11,12,13].

The objective of this study was to evaluate the environmental and agronomic feasibility of using the effluent and sludge from sewage treatment plant in sorghum cultivation.

MATERIALS AND METHODS

The experiment was conducted at the Department of Nuclear Energy of the Federal University of Pernambuco. The used effluent and sludge came from a treatment plant located in Rio Formoso city and consisted of preliminary treatment, an upflow anaerogic sludge bed (UASB) reactor, a stabilization pond and stone filters and served a population of 15,830 people. The effluent was collected after the stabilization pond and the sludge from the UASB reactor.

Sorghum (cultivar IPA-2502) was cultivated in a greenhouse in pots with capacity of 10 dm^3 with 15 kg of soil. Planting was carried out directly in pots with three seeds each; after seven days of the emergency, thinning was done resulting in one plant per pot. Irrigation was performed daily manually, reaching 80% of the pot capacity. The pot capacity is the water content of the soil after suffering saturation until ceasing drain[14]. Irrigation was controlled by weighing the pots daily.

Fertilization was defined by the results of soil fertility analyses and recommendation of the IPA[15] for sorghum grain production. The sludge was treated and used in the soil according to Tsutiya et al[16]; the dose depended on the available nitrogen.

Physicochemical analyses were performed according to the methods described in Standards Methods for the Examination of Water and Wastewater[17]. The parameters evaluated were: electrical conductivity, chemical oxygen demand (COD), biochemical oxygen demand (BOD), total nitrogen Kjeldahl (TNK), ammonia nitrogen, phosphorus, potassium, sulfate, chloride, sodium, calcium hardness and magnesium hardness.

The harvest of sorghum was carried out 94 days after the planting, according to the characteristics shown by the grain The parameters evaluated in the plants were height, diameter stem, leaf area, phosphorus, chlorophyll, carbohydrates, potassium, sodium, calcium, number of grains and weight of 100 grains. The physical parameters were measured with the aid of a pachymeter and length measuring tape. The chemical and biochemical parameters of the plants were obtained following the recommendations of Bezerra Neto and Barreto[18]. The weighing of grain was carried out with an analytical balance.

The type of soil used was Quartzipsamment[19]. It was collected in the city of Petrolândia, situated in the semi-arid region of Pernambuco, Brazil. The granulometric composition of the natural soil at a depth of 0-20 cm was 51.4% of coarse sand, 42.71% of fine sand, 0.2% of silt and 5.58% of clay. Soil chemical analyses of pH, copper, iron, potassium and phosphorus were performed according to a manual of chemical analyzes of soil, plants and fertilizers[20].

The sludge used from a UASB reactor contained 20.3 g kg^{-1} of total nitrogen, 949 mg kg^{-1} of potassium and 5.2 g kg^{-1} phosphorus[21].

The experimental design was completely randomized with five repetitions, as the environmental conditions of the pots were similar. The variations were only the treatments, with a total of six as shown in **Table 1**, totaling 30 experimental units. Tukey test at 5% probability was carried out for the evaluated parameters.

TABLE 1. Description of the treatments used in the experiment

Treatments	Description
T1	Irrigation water without chemical fertilization
T2	Irrigation with water + chemical fertilizer (NPK)
T3	Water irrigation + fertilization with sludge
T4	Irrigation with wastewater without chemical fertilization
T5	Irrigation with wastewater + chemical fertilizer (NPK)
T6	Irrigation with wastewater + fertilization with sludge

RESULTS AND DISCUSSION

Wastewater. The results of the analyses of the treated effluent are shown in **Table 2**. The values of N, P and K of the treated effluent were used for calculation of chemical fertilizer levels necessary to complement the crop nutrient requirements.

TABLE 2. Physical and chemical characteristics of the effluent

Parameter	Unit	Average value
pH	-	7.36
Conductivity	mS cm^{-1}	1021.0
COD	mg O_2 L^{-1}	127.4
BOD	mg O_2 L^{-1}	40.0
N-TNK	mg L^{-1}	19.1
$N\text{-}NH_4^+$	mg L^{-1}	11.4
$P\text{-}PO_4^{-3}$	mg L^{-1}	2.3
K	mg L^{-1}	12.0
$S\text{-}SO_4^{-2}$	mg L^{-1}	31.7
Na	mg L^{-1}	40.0
Calcium hardness	mg $CaCO_3$ L^{-1}	28.0
Magnesium hardness	mg $CaCO_3$ L^{-1}	37.0

Soil. The results of soil chemical analyses are shown in **Table 3.** The pH average was 6.7, therefore, it was not necessary chemical soil correction. The values of P and K, were 12.7 mg dm^{-3} and 0.19 mg dm^{-3}, respectively, and served for the determination of chemical fertilization required for some treatments in accordance with IPA[15].

TABLE 3. Results of chemical analyzes of soil

Parameter	Unit	Average value	Parameter	Unit	Average value
Fe	mg dm^{-3}	18.2	Ca	cmolc dm^{-3}	1.74
Cu	mg dm^{-3}	0.57	Mg	cmolc dm^{-3}	0.53
Zn	mg dm^{-3}	4.10	Al	cmolc dm^{-3}	0.02
O.M*	%	0.52	SB	cmolc dm^{-3}	2.65
P	mg dm^{-3}	12.7	CEC***	cmolc dm^{-3}	3.63
pH	-	6.71	Na	cmolc dm^{-3}	0.19
K	cmolc dm^{-3}	0.19	SAR**	mmolc dm^{-3}	0.18

*O.M: Organic matter; **SAR: Sodium adsorption ratio; ***CEC: Cation exchange capacity.

Plants and grains

Plant height. Larger plants were obtained in the treatments T2, T3 T4 and T5 with average values of 156 cm, 154 cm, 149 cm and 153 cm respectively, but showing no significant differences by Tukey test at 5% probability. The plants obtained from the T1 and T6 treatments had the lowest heights, 137 cm and 132, respectively (**Figure 1**). The lower height observed in T1 can be explained by nutrient deficiency, because this treatment cultivation was carried out without supplementation. Regarding the T6

treatment, the smaller heights may be justified due to excess nutrients because in the treatment fertilization was used with the sludge and irrigation with treated effluent. Thus, excess of some nutrients may inhibit availability of other compounds.

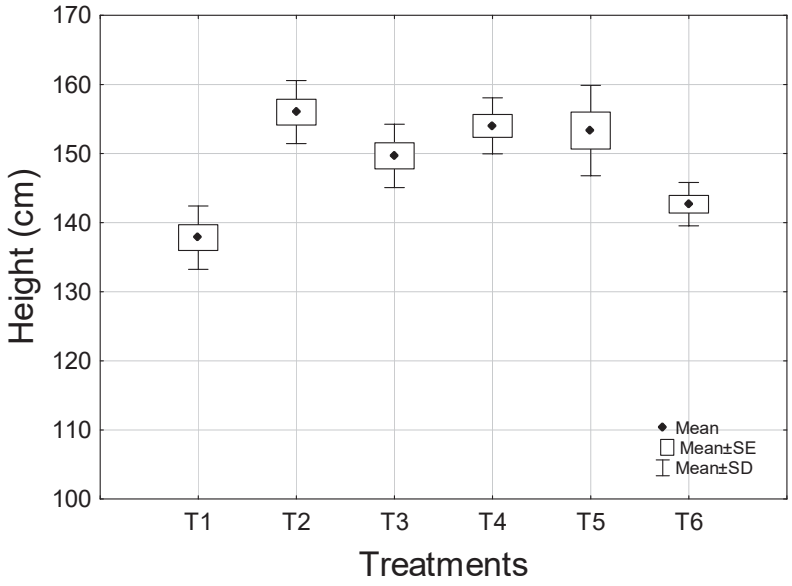


FIGURE 1. Height of sorghum plants after 94 days of growth. Treatment T1: irrigation water without fertilization; T2: irrigation water and chemical fertilizers (NPK); T3: water irrigation and fertilization with WWTP sludge; T4: irrigation with sewage without fertilization; T5: irrigation with sewage and chemical fertilization (PK); T6: irrigation with sewage and fertilizer with WWTP sludge.

Stem diameter. **Figure 2** shows average values of the diameter of the stem of plants. Highest values were observed in the treatments T2, T4 and T5, of 1.80 cm, 1.74 cm and 1.74cm, respectively, with differences in relation to T1, T3 and T6 with values of 1.18 cm, 1:49 cm and 1:42 cm, respectively.

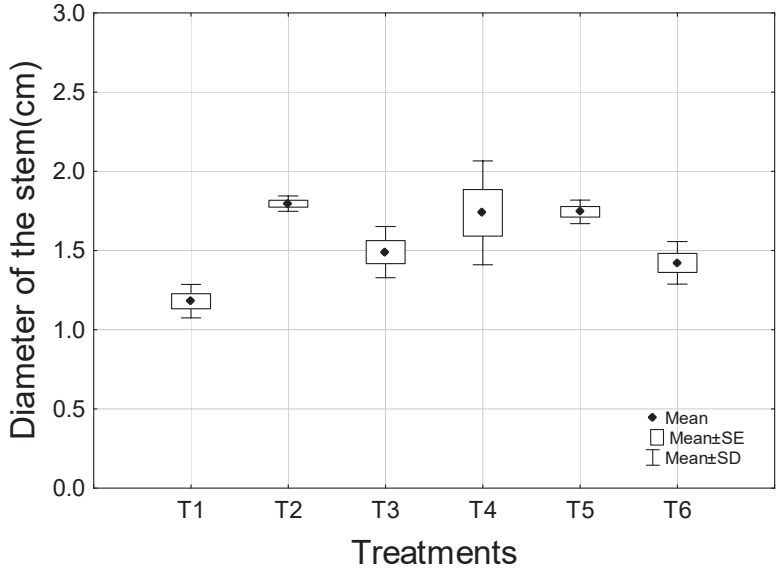


FIGURE 2. Stem diameter, measured at 50 cm from the ground

Chlorophyll A and B in plant. **Figure 3** shows a graph of results of chlorophyll A and B of plant foliage. The average values of chlorophyll A ranged from 1.64 mg g^{-1} to 1.94 mg g^{-1} and chlorophyll B, 0.83 mg g^{-1} to 0.87 mg g^{-1}, with no significant differences by the 5%Tukey test.

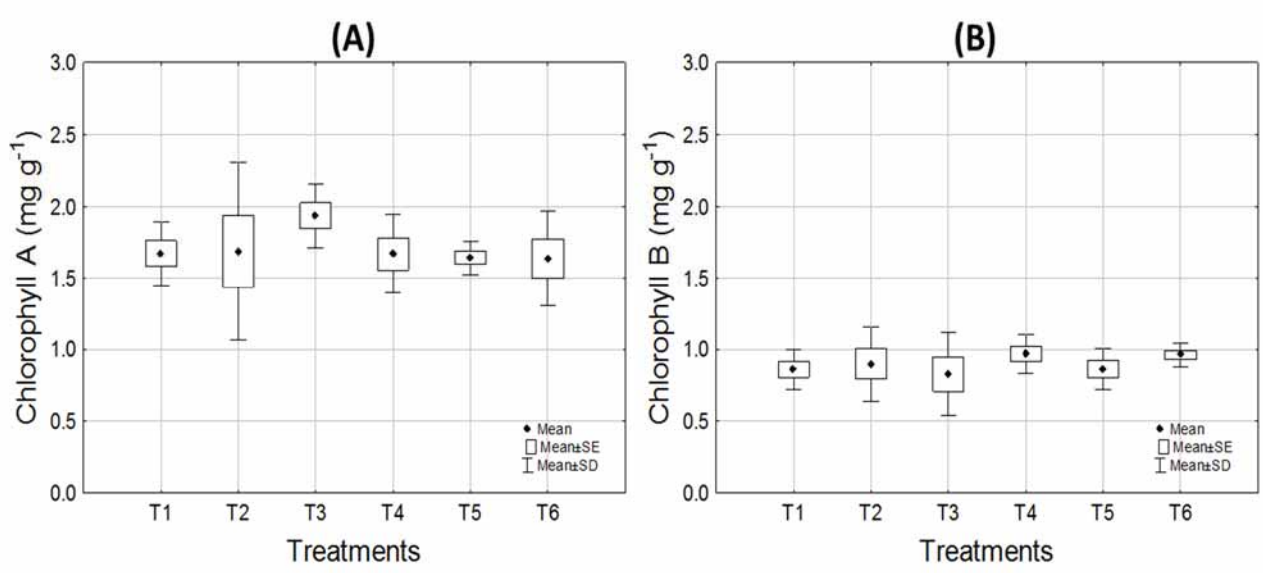


FIGURE 3. (A): The chlorophyll A concentration in the sap of the plant; (B): The chlorophyll B concentration in the plant sap

Phosphorus in plant. **Figure 4** shows the phosphorus concentration results in the plant foliage, higher concentrations were observed in T2 and T5 treatment, with mean values of 3.22 mg kg^{-1} and 2.70 mg kg^{-1}, respectively, and showing significant difference using 5% Tukey test.

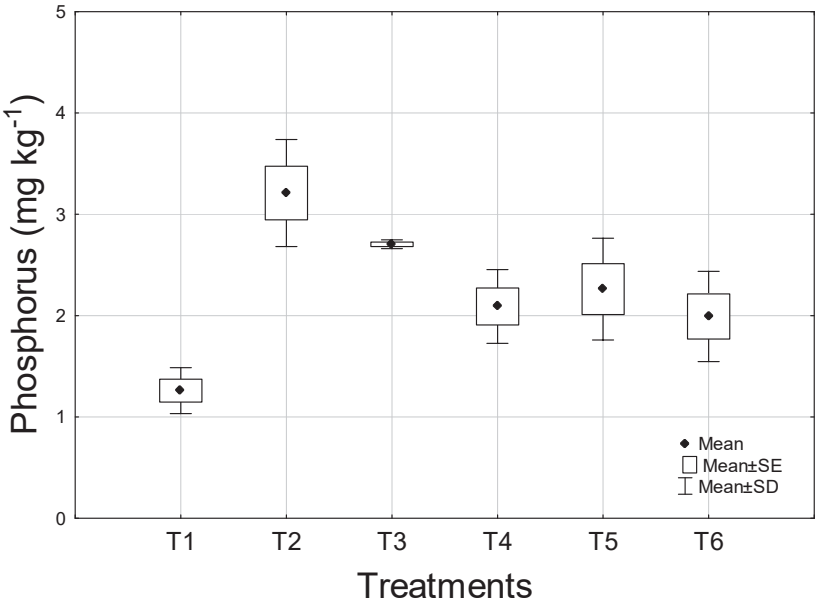


FIGURE 4. Phosphorus concentration in plant leaves

Nitrogen in plant. Nitrogen values ranged from 8.12 mg g^{-1} and 14.85 mg g^{-1}, with no significant difference between the treatments. The results are depicted in **Figure 5**.

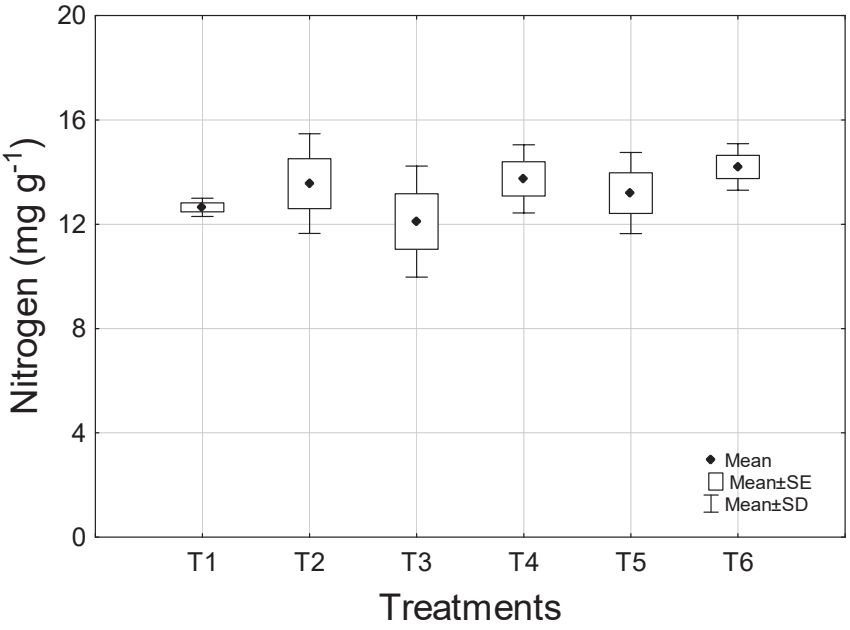


FIGURE 5. Concentration of total nitrogen in plant leaves

Potassium in plant. The concentrations of potassium in plants are shown in the **Figure 6**; the treatment which showed the highest value was T5 showing average value of 52.3 mg kg^{-1}. The treatments T2, T3, T4 and T6 showed values of 18.7 mg kg^{-1}, 30,0 mg kg^{-1}, 21.82 mg kg^{-1} and 27.8 mg kg^{-1}, respectively.

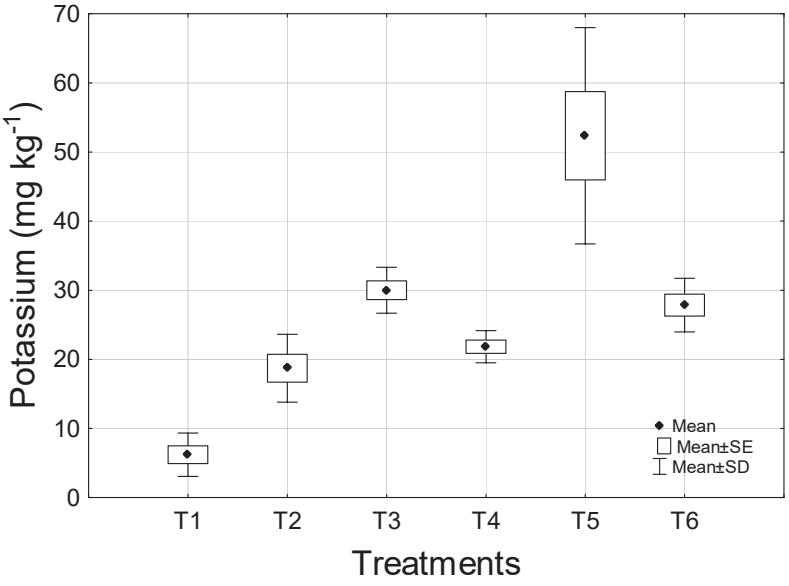


FIGURE 6. Potassium concentration in leaves

Amount of grains and weight of 100 grains. The amount of beans and weighing of 100 grains are shown in **Table 4**. The lowest average value was obtained in T1 (1276.6 units). The treatments T2, T3, T4, T5 and T6 showed no differences by 5% Tukey test. No significant differences were found in the 100-grain weight values.

Table 4. **Mean values of the amount of grain and weight of 100 grains**

Parameter	Treatments					
	T1	**T2**	**T3**	**T4**	**T5**	**T6**
Quantity of grains	1274.6b	1668.4a	1453.0a	1636.4[a]	1605.0a	1531.6a
Weight of 100 grains (g)	3.02b	3.53a	3.49a	3.40[a]	3.45a	3.31a

Means followed by the same letter, in the same lines do not differ 5% probability by Tukey test.

CONCLUSION

The treatments T2, T4 and T5 showed better results regarding the physical characteristics of the plant (height and stem diameter), being T4 treatment more attractive due to non use of mineral fertilizers. The lower values of T1 treatment is explained by the fact of not using nutritional supplementation in sorghum cultivation. T6 treatment may be explained by the use excess of nutrients, since the abundance of an element can inhibit the availability of other, which is also important for plant growth.
Higher accumulation of nutrients in plant leaves was observed in T5 treatment, which had higher values of phosphorus in the plant, as well as the treatment T2. This last also showed higher potassium values reaching an average of 52.3 mg kg^{-1}, which is higher than all other treatments. The use of irrigation with treated sewage combined with chemical fertilization favors the transport of nutrients to the plant leaf.
The nutritional supplementation is very important to get larger and heavier grains, given that only the treatment T1 (without nutritional replacement) showed significantly lower values compared to the other treatments.

ACKNOWLEDGMENTS

To CNPq for the financial support and fellowship to the first author to conduct this research; the Department of Nuclear Engineering of the UFPE for providing the area for experimentation; UFRPE to the soil analyses and availability of the structure of the Experimental Station Carpina PE; Laboratory of Chemistry of Vegetables of UFRPE for their support in the plant chemical analyses.

REFERENCES

1. 1-Xinhua News (2014). Drinking water for 280 million residents unsafe: Areport released by the Ministry of Environmental Protection of China. http://news.xinhuanet.com/english/china/201403/14/c_133187044.htm (accessed May 16,).
2. 2-Kummu, M.; Gerten, D.; Heinke, J.; Konzmann, M.; Varis, O. Climate-driven interannual variability of water scarcity in food production potential: a global analysis. Hydrology and Earth System Sciences. n. 18, p. 447–461, 2014.
3. 3-Hoekstra, A. Y.; Mekonnen, M. M.; Chapagain, A. K.; Mathews, R. E.;, Richter, B.D. Global Monthl Water Scarcity: Blue Water Footprints versus Blue Water Availability. PLOS ONE. n. 7, 2012.
4. 4.Porkka, M.; Gerten, D.; Schaphoff, S.; Siebert, S.; Kummu, M. Causes and trends of water scarcity in food production. Environmental Research Letters. v. 11, n. 1, p. 1-12, 2016.
5. 5.Araviadis, R. V. The Effects of Irrigation with Treated wastewater on Crops and Human Populations – A Review. European Journal of Engineering and Natural Sciences. v. 1, p. 15-22, 2016.
6. 6.Bastos, R. K. X (Coord.). *Utilização de esgotos tratados em fertirrigação, hidroponia e piscicultura*. Programa de Pesquisa em Saneamento Básico - PROSAB. Rio de Janeiro: ABES, 2003. 267 p.
7. 7.Florencio, L. Bastos, R. K. X.; Aisse, M. M. Uso do Esgotos Tratados para Produção Animal. In: Florencio, L. M. (Coord.). Tratamento e utilização de esgotos sanitários. Projeto PROSAB. Rio de Janeiro: ABES, 2006. p. 301-330.
8. 8.Wolterdorf, L.; Scheidegger, R.; Liehr, S.; Doll, P. Municipal water reuse for urban agriculture in Namibia: Modeling nutrient and salt flows as impacted by sanitation user behavior. Journal of Environnmental Management. v. 169, p. 272-284, 2016.
9. 9.Lemainski, J.; Silva, J. E. Utilização de Biossólido da CAESB na produção de milho no Distrito Federal. Revista Brasileira de Ciência do Solo. v. 30, p. 741-750, 2006.
10. 10.Dicko, M. H.; Gruppen, H.; Traoré, A. S.; Voragen, A. G. J.; Berkel, W. J. H. V. *Sorghum grain as human food in Africa : relevance of content of starch and amylase activities*. African Journal of Biotechnology. v. 5 p. 384–395, 2006.
11. 11.Queiroz, V. A. V.; moraes, E. A.; martino, H. S. D.; paiva, C. L.; menezes, C. B. Potencial do sorgo para uso na alimentação humana. Informe agropecuário. v. 35, n. 278, p. 7-12, 2014.
12. Magalhães, P. C.; Durães, F. O M.; Rodrigues, J. A. S. Cultivo do Sorgo: Aspectos gerais dos efeitos ambientais dobre o crescimento do sorgo. Embrapa Milho e Sorgo. 2007. http://www.cnpms.embrapa.br/publicacoes/sorgo_1_ed/ambientais.htm. (accessed Jan 16).
13. 13.Santos, O. O.; Falcão, H.; Antonino, A. C. D.; LIMA, J. R. S.; Lustosa, B. M.; Santos, M. G. Desempenho ecofisiológico de milho, sorgo e braquiária sob déficit hídrico e reidratação. Bragantia. v. 73, p. 203-212, 2014.
14. Souza, C. C.; Oliveira, F. A.; Silva, I. F.; Amorim Neto, M. S. Avaliação de métodos de determinação de água disponível e manejo da irrigação em terra roxa sob cultivo de algodoeiro herbáceo. Revista Brasileira de Engenharia Agrícola e Ambiental. v.4, p.338-342, 2000.
15. IPA – INSTITUTO DE PESQUISAS AGROPECUÁRIAS Recomendações de adubação para o Estado de Pernambuco. Cavalcanti, F. J. A. (coord.). 2ª aproximação. Recife PE, 2008.
16. Tsutiya, M. T.; Comparini, J. B.; Alem Sobrinho, P.; Hespanhol, I.; Carvalho, P. C. T.; Melfi, A. J.; Melo, W. J.; Marques, M. O. Biossólidos na agricultura. São Paulo: ABES. 2002, 468p.
17. 17.APHA, AWWA, WEF. *Standard methods for examination of water and wastewater*. 22nd edn. American Public Health Association, American Water Works Association, Water Environmental Federation. Washington DC, 2012.

18.18.Bezerra Neto, E.; Barreto L. P. *Análises químicas e bioquímicas em plantas*. 1*nd edition*. (2011).
19.19.Silva, A. B.; Silva, A. C. S.; Menezes, A. A. A.; Mello, C. M. L.; Zenaide, E. S.; Silva, F. H. B. B.; Araújo Filho, J. C.; Santos, J. C. P.; Oliveira Neto, M. B.; Silva, R. R. Coordenação: Barros, A. H. C. Mapa Exploratório - Reconhecimento de solos do município de Petrolândia - PE. Zoneamento Agroecológico de Pernambuco - ZAPE. Direitos reservados: Embrapa Solos, UEP Recife. 2001.
20.20.EMBRAPA *Manual de análises químicas de solos, plantas e fertilizan*tes. Brazil, Recife 1999.
21.21.Silva, R. J.; Gavazza, S. ; Florencio, L.; Nascimento, C. W.A; Bezerra Neto, E.; Kato, M. T. . Uso de agua residual doméstica tratada y lodo en el cultivo de dos especies de fríjol: productividad y efectos nutricionales en los granos. In: The Fifith International Symposium on Environmental Biotechnology and Engineering, 2016, San Martin-Argentina. Wastewater Treatment, 2016.

CHAPTER 7.26 INFLUENCE OF OIL CONCENTRATION AND PREVIOUS OXYGENATION IN LAS REMOVAL IN ANAEROBIC REACTOR

Luiza F.C. Souza*; Tayane Vasconcelos; Lourdinha Florencio; Savia Gavazza and Mario T. Kato

Federal University of Pernambuco, Department of Civil Engineering, Laboratory of Environmental Sanitation. Av. Acadêmico Helio Ramos, s/n, Cidade Universitária, Recife, Brazil

ABSTRACT

The linear alkylbenzene sulfonate (LAS) is an anionic tensoative widely used in cleaning products. It is known as highly biodegradable under aerobic conditions, but some questions arise when anaerobic reactors are used. In Brazil and many countries, anaerobic reactors have been frequently used in sewage treatment plants. However, when treating domestic sewage in that reactor, LAS removal can be influenced by many factors involving the influent characteristics and reactor operation conditions.

Two of the factors were studied in a 32.7L UASB reactor under controlled conditions (pH 8 and HRT 12 h). The effect of oil concentration (0 and 0.25 $mg.L^{-1}$) and previous oxygenation (with and without) of the influent domestic sewage was evaluated. A 2^k factorial design was used to analyze the effect and interactions of both factors, resulting in 4 phases with a 40day period each. The COD and LAS concentrations in the influent sewage varied from 218 to 518 $mgO_2.L^{-1}$ and 3 to 7 $mg.L^{-1}$, respectively.

The results showed that increasing the oil concentration alone, the adsorption increased by 19%; and with previous oxygenation alone, the increase was 19%. Under the same experimental conditions, the biodegradation decreased by 7 % and 9%, respectively. The effects on adsorption and biodegradation were different when there was interaction between both factors. Without LAS oxygenation but increasing oil concentration from 0 to 0.25 $mg.L^{-1}$, there was no change in adsorption and biodegradation removal. However, with previous oxygenation and increasing the oil concentration, there was a 38% increase in the adsorption and a 13% decrease in biodegradation.

The highest biodegradation of 15% was achieved when there was no LAS adsorption and when some desorption was observed. This occurred in two experimental conditions, the first when there was no previous oxygenation and no oil was added; the second, also when there was no oxygenation but by adding 0.25 mg $oil.L^{-1}$. In this study, the LAS highest biodegradation was lower than that obtained in other works and this can also be attributed to its much lower concentration in the influent.

The adsorption enhanced when the biodegradation was inhibited. The highest adsorption of 37% was achieved when there was no biodegradation. Therefore, LAS adsorption inhibited biodegradation under anaerobic conditions, and the oil influence occurred only when there was previous influent oxygenation.

Keywords: adsorption, biodegradation, influent oil concentration, previous oxygenation

---

*Author for correspondence: luizas@gmail.com

INTRODUCTION

The purpose of developing the linear alkylbenzene sulfonate (LAS) was to reduce the environmental impact caused by alkylbenzene sulfonate (ABS) and create a biodegradable compound[1]. Efficiency of LAS removal by aerobic and anaerobic wastewater treatment (WTP) is around 95±5% e 50±20%, respectively[2,3]. In aerobic environment, oxygen dissolved in water enhances the oxygenation reaction of the LAS molecule (ϖ-oxidation), turning it in sulfophenylcarboxylated (SPC), which are easily assimilated by microorganisms. Therefore, complete mineralization of LAS in aerobic environment depends on the ϖ-oxidation. After that, SPC is β-oxidized many times decreasing the alkyl chain size. Desulfonation and the cracking aromatic ring are the next steps to form carbonic gas and water. These four steps are performed by distinct microorganisms[4,5].

In anaerobic environment, SPCs formation is unknown, mainly by the absence of dissolved oxygen, but some authors suggest SPCs formation as a first step of anaerobic degradation of LAS. Lara-Martin et al.[6] suggested ϖ-oxidation of the LAS and β-oxidation of the SPC in anaerobic environment by fumarate, instead of dissolved oxygen, however it was not proven. Desulfonation and cracking aromatic ring can occur in both environments[7,8,9], soon these steps would not limiting.

Nevertheless, LAS removal in anaerobic wastewater treatment is observed and explained both by biodegradation and by adsorption on biomass[10]. LAS molecule have two different ends, one hydrophobic and one hydrophilic, and can adhere on polar and nonpolar surfaces or remain soluble in organic solvents and aqueous solution. Thus, LAS solubility or adsorption depend on the solid and liquid composition[11,12]. Souza et al.[13] reported reduction of the LAS degradation when the environment was favorable to LAS adsorption.

Influence of the operational factors of wastewater treatment plants and influent composition in LAS biodegradation were studied by Khleifat[14]. Mixed and pure facultative culture were used to evaluate pH, temperature, carbon and nitrogen source, aeration and LAS concentration influence in LAS degradation. In this work, mixed culture, pH 8.5, 32ºC, carbon and nitrogen source addition, higher aeration (250 rpm) and 200 mg $LAS.L^{-1}$ were the best conditions to LAS degradation. Similar studies of the Khleifat's[14] have been held but the results were distincts. In Eniola's work[15], LAS degradation was also better by mixed culture of microorganisms than by pure culture, but addition of carbon and nitrogen source decreased LAS degradation in aerobic environment. Similar results were observed in Okada et al's work[16], high LAS degradation (76%) occurred without carbon addition in anaerobic reactors.

In all studies showed above, the experiments was held in bench scale, factors influence were individually evaluated, varying one factor at a time; and distinct responses were observed during the study of the same factor. Operating conditions of the WTP and influent composition can be the reason for those results. Because of these, the aim of this study were to evaluate the influence of influent oxygenation previous to anaerobic reactor in LAS degradation, the influence of the oil concentration in the adsorption/desorption dynamics of LAS in biomass and the interaction between these

factors to reduction the adsorption and increase the LAS degradation in anaerobic reactor in lab scale and fed with real wastewater.

MATERIALS AND METHODS

Anaerobic Reactor. Acrylic UASB reactor (upflow anaerobic sludge blanket), 32 L useful volume, height: 203.6 cm and diameter:14.3 cm (**Figure 1**). Flocculant anaeróbic sludge was utilized to inoculate the reactor. Volatile solids concentration of the sludge was 21 ± 2,0 $g.L^{-1}$ in reactor, corresponding to 11 L of the sludge from a WTP fed with domestic wastewater and real scale. Operation conditions were 12 hour of hydraulic detention time (HDT), average flow 2.66 $L.h^{-1}$, continuous feed with real wastewater, without LAS and co-substrate addition. However, chemical oxygen demand (COD) and LAS concentration were between 218 to 518 mg $O_2.L^{-1}$ and 3 to 7 $mg.L^{-1}$, respectively.

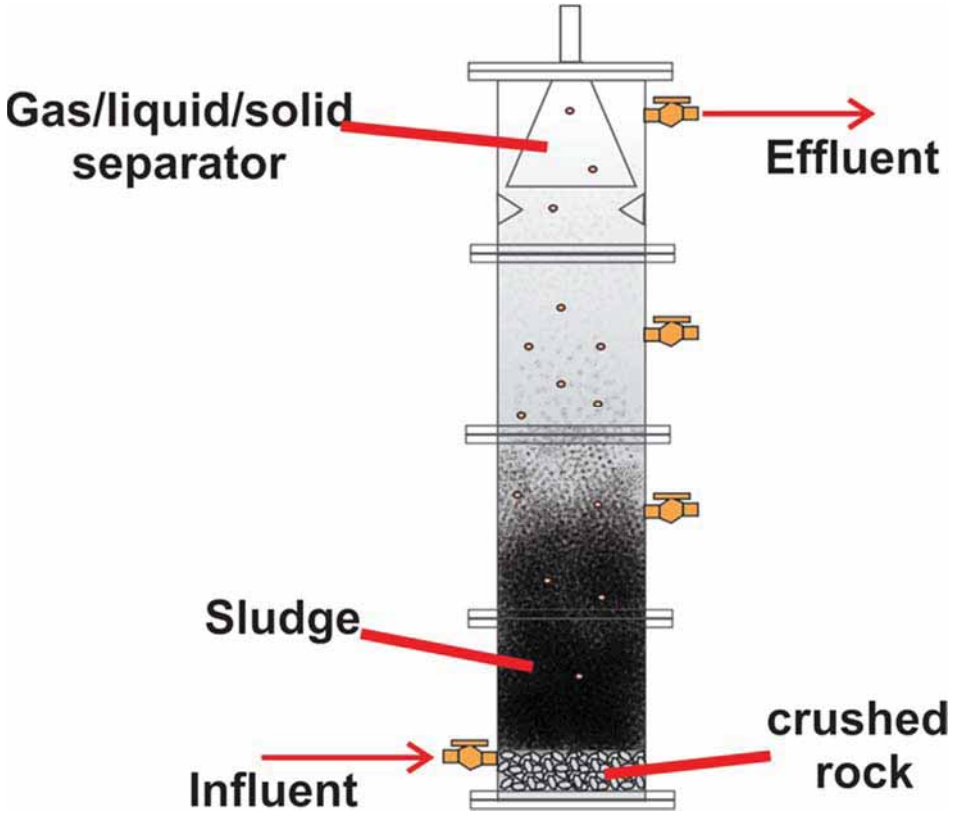


FIGURE 1. UASB reactor

2^K Factorial Design. The reactor was operated simultaneous variation of the oil concentration and influent oxygenation. 2^2 factorial design was utilized to evaluate the influence and interaction effects of these factors, resulting in four operational phases with 40 days duration each one (**Table 1**)

TABLE 1. Influent characterization in each operational phases

Phase	Oil concentration ($g.L^{-1}$)	Oxygenation
1	0	without
2	0	with
3	0.25	without
4	0.25	with

Sodium hydroxide was utilized to adjust the pH to 8, following Khleifat[14] recommendations, because of the high LAS degradation in this pH value. Commercial soybean oil was added in influent to be the oil source and to obtain the experimental concentration. Aquarium aerator was used to promote previous oxygenation in influent. The influent was aerated for four minutes and after one hour resting it was pumped to the anaerobic reactor. This was a simulation of the aeration procedure in previous units of the reactors, in real WTP, promoting contact between LAS molecule and atmospheric oxygen. After that, oxygenation of the molecule can occur, LAS becomes SPC, more easily degradaded by microorganisms.

Monitoring. Influent and effluent samples were collected twice a week and COD and LAS homologues (C10. C11, C12 and C13) were determined. Sludge samples were collected at the beginning of the operation and after each phase. Concentration of the LAS homologues adsorbed in sludge was determined.

Analyses. COD was determined by colorimetric methods established by Standard Methods[17]. LAS concentration in liquid and solid phase was determined by high performance liquid chromatography (HPLC). Liquid samples were injected directly in chromatograph after filtration with 0.22 μm nylon membrane. Solids samples were extracted by soxhlet extraction technique using methanol followed injection in chromatograph. Nylon membrane (0.22 μm), Chromosep column (Merck), 100 μL injection volume, 1.00 mL.min-1 flow, 230 nm wave-lenth, and two eluents A trimethylamine acetic acid 4.5 mM) and B (acetonitrile) were utilized following the lab protocol.

RESULTS AND DISCUSSION

Adsorption. Adsorption process is one way to removal soluble LAS molecule of the liquid phase (influent), however only mass transference occur, LAS molecule remains intact. Favoring adsorption, WTP efficiency increase and treat effluent quality enhances too. Nevertheless, sludge need to be treated before disposal into the environment. The **Table 2** shows the influent oxygenation and oil concentration effect in LAS adsorption on sludge.

TABLE 2. Individual and interaction effects of the influent oxygenation and oil concentration in adsorption of total and LAS homologues in the sludge

Factor	Individual Effect				
	C10 (%)	C11 (%)	C12 (%)	C13 (%)	LAS (%)
Oil	13	56	44	11	19
Aeration	13	-19	-7	28	19
Interaction Effect					
Oil x Aeration	13	-28	-7	11	19

Adsorption of the all LAS homologues was enhanced by increasing oil concentration, mainly C11 and C12, 56% e 44% increase, respectively. Increasing oil concentration in liquid phase, decrease the solution polarity, benefiting homologues adsorption in the sludge.

Interaction effect between studies factors was significant. In **Figure 2**, graphics show the interaction effect of the factors in each homologue adsorption.

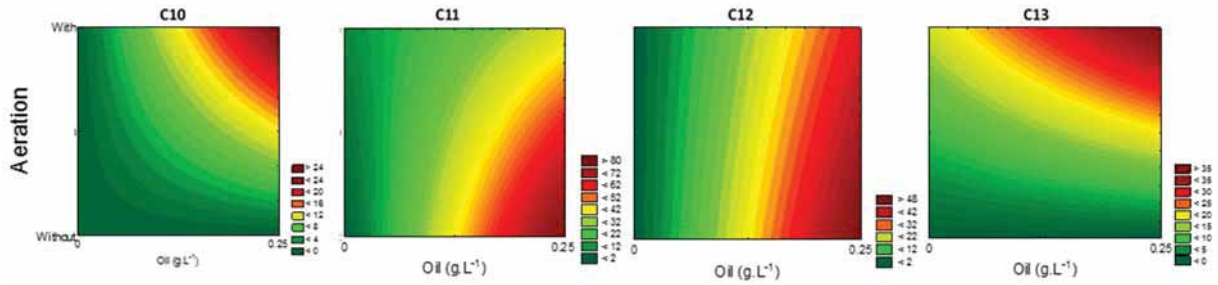


FIGURE 2. Adsorption efficiency of LAS homologues in anaerobic sludge with different conditions of oil concentration and influent oxygenation

In **Figure 2**, for each homologues, the higher adsorption efficiency can be observed in red graph region. Similar characteristics in C10 and C13 homologues graphs were observed. The higher adsorption for these homologues, 25% and 39%, respectively, occurred when the oil concentration was 0.25 $g.L^{-1}$ and with oxygenation. Without oxygenation and increasing oil concentration no significant change of the adsorption was observed. C11 and C12 adsorption were also enhanced increasing oil concentration; however, C11 adsorption is higher without oxygenation than with oxygenation, 83% and 37%, respectively. C12 adsorption efficiency was lower than C11, 50% and 37%, without and with oxygenation, respectively.

Oxygenation process favored the LAS adsorption in sludge, 19% increasing. However, although increasing C10 and C13 adsorption, 13% and 28% increase, respectively, C10 and C12 adsorption decreased, 19% and 7%, respectively. Among the LAS homologues, C10 is the most hydrophilic and C13 is the most hydrophobic. Oxygenation process makes the environment more hydrophilic, favoring C10 and C13 adsorption on hydrophilic and hydrophobic sites in sludge, respectively[18]. C11 and C12 are intermediate homologues, and their interaction with the sites is weaker than C10 and C13 interaction, causing dessorption.

Biodegradation. In **Table 3**, the individual and interaction effects of the studies factors in LAS homologues biodegradation in anaerobic reactors is showed.

TABLE 3. Individual and interaction effects of influent oxygenation and oil concentration in Biodegradation of total and LAS homologues by the anaerobic sludge

Factor	Individual Effect				
	C10 (%)	C11 (%)	C12 (%)	C13 (%)	LAS (%)
Oil	-4	-55	-40	18	-7
Aeration	-16	-33	23	-18	-9
Interaction Effect					
Oil x Aeration	-10	-33	-23	-18	-7

Oxygenation process and oil concentration decreased total LAS biodegradation in 7% and 9%, respectively. Oxygenation process caused 23% increase C12 biodegradation and 16%, 33% and 18% decrease C10%, C11% and C13% biodegradation, respectively. Increasing oil concentration caused 4%, 55% and 40% decrease C10, C11 and C12 biodegradation, respectively. Inverse effect of the oil concentration in C13 biodegradation was observed, increasing around 18%. The influence of the factors in biodegradation was opposed to influences in adsorption. Soon, when adsorption was favored, the biodegradation was inhibited.

Interaction effect of the factors in anaerobic biodegradation of each LAS homologues can be observed in **Figure 3**.

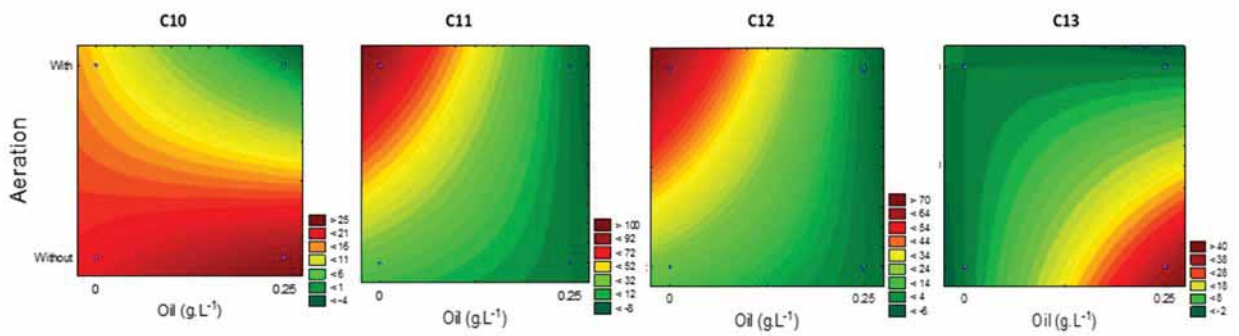


Figure 3. Biodegradation efficiency of LAS homologues in anaerobic sludge with different conditions of oil concentration and influent oxygenation

C10 biodegradation was not altered by oil concentration and without oxygenation process, only 5% decrease when increasing oil. With oxygenation, C10 biodegradation was 14% higher when increased oil concentration. The higher C11 and C12 biodegradation efficiency were 88% and 63%, respectively, when oil concentration was 0 $g.L^{-1}$ and with oxygenation. Higher C13 biodegradation efficiency was 35% without oxygenation and 0.25 g $oil.L^{-1}$.

LAS standard was composed by four homologues, C10, C11, C12 and C13, but the amount of each one in the standard is different. Different LAS standards were used in different household products. Soon, LAS standard has different composition and concentration of homologues and total LAS removal depends on the homologues

concentration. In **Figure 4**, the interaction effect of oxygenation and oil concentration in total LAS biodegradation can be observed.

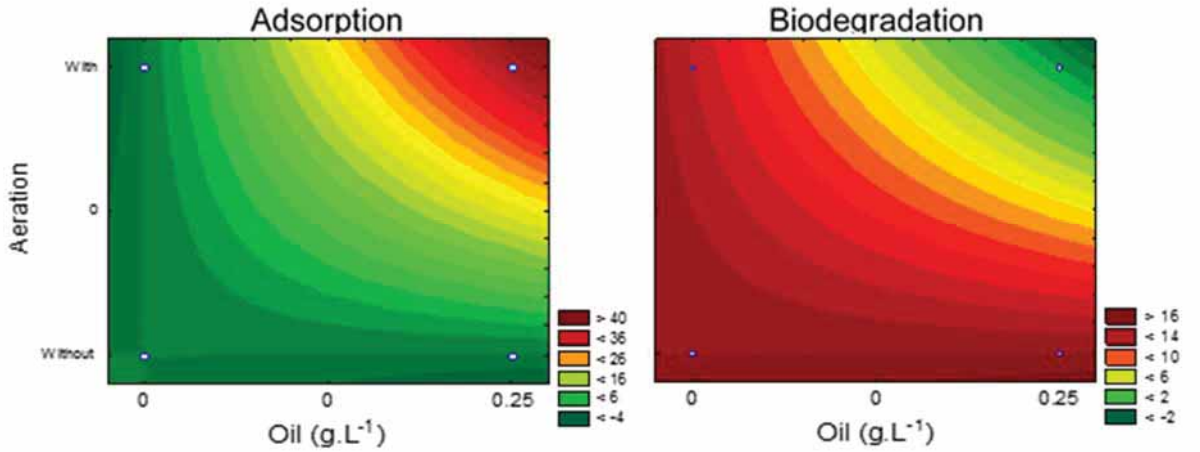


FIGURE 4. Adsorption and Biodegradation efficiency of the total LAS in different condition of the oil concentration and oxygenation

The higher total LAS adsorption was 38% and occurred with 0.25 g oil.L^{-1} and with oxygenation. In this condition the biodegradation was lower. However, adsorption inhibited biodegradation. C10 and C13 were also more adsorbed and less biodegraded in these condition, proving these conditions favored the adsorption and inhibited the biodegradation.

Higher total LAS biodegradation occurred without oxygenation and no depended on oil concentration, both oil concentration tested were 15%. With oxygenation, total LAS biodegradation efficiency was 13% in 0 g oil.L^{-1} and 0% in 0.25 g.L^{-1}. Each homologue were high degraded in different condition and can be observed in **Table 4**.

TABLE 4. Biodegradation efficiency of the total LAS and Homologues

Biodegradation Efficiency		Oxygenation	Oil (g.L^{-1})
Total LAS	Homologue		
13%	C10 – 14% **C11 – 88%** C12 – 63% C13 – 0%	With	0
15%	**C10 – 20%** **C11 – 22 %** C12 – 18% C13 – 0%	Without	0
15%	**C10 – 36%** C11 – 0% C12 – 0% **C13 – 36%**	Without	0.25

LAS biodegradation in anaerobic reactors was altered by oil concentration variation and contact between LAS and oxygen previously anaerobic reactor. These fator interaction can favored homologues adsorption to the detriment of biodegradation. To know the LAS solution composition and influent composition and concentration help to operate the WTP increasing total LAS removal efficiency..

CONCLUSION

Increasing oil concentration caused increase all homologues adsorption in sludge and decrease C10, C11 and C12 biodegradation. C11 and C12 were homologues with higher adsorption, 56 and 44%, respectively. More adsorption efficiency occurred when less biodegradation occurred. C13 homologue adsorption was the lower than the other homologues and only one to be degraded when oil concentration increase.
Oxygenation process caused adsorption increase of the C10 (13%) and C13 (28%) and adsorption decrease of the C11 (19%) and C12 (7%). C12 biodegradation was the only one to be enhanced by oxygenation (23%). Higher degradation occurred when lower adsorption occurred.
In different condition could occur high LAS removal (47%), because of the factors interaction. High total LAS biodegradation occurred: (i) 13% efficiency in 0 g oil.L^{-1} and with oxygenation; (ii) 15% efficiency in 0 g oil.L^{-1} and without oxygenation; and (iii) 15% efficiency in 0.25 g oil.L^{-1} and without oxygenation.

ACKNOWLEDGMENTS

The authors would like to thank the following: DETEN Quimica S.A (Bahia, Brazil), for providing the LAS samples and for their analytical and instrumental support for the Laboratory of Environmental Sanitation (LSA-UFPE) in the Federal University of Pernambuco; the Brazilian agencies FACEPE, FINEP and CNPq, for providing support to the LSA-UFPE via grants and scholarships.

REFERENCES

1. HERA, Environmental Risk Assessment. LAS - Linear Alkylbenzene Sulphonate. (CAS No. 68411-30-3), (2013).
2. Mungray A. K., Kumar P. Fate of linear alkylbenzene sulfonates in environment: A review. Int. Biodeterior. Biodegrad. 65 (2009) 981-987.
3. Karahan O. Inhibition effect of linear alkybenzene sulphonates on the biodegradation mechanisms of activated sludge. Bioresour. Technol. 101 (2010) 92-97.
4. Jiménez L., Breen A., Thomas N., Federle T. W., Sayler G. S. Mineralization of Linear Alkylbenzene Sulfonate by four-Member Aerobic Bacterial Consortium. Applied and Environmental Microbiology 57 (1991) 1566-1569.
5. Scott M. J., Jones M. N. Review The biodegradation of surfactants in environment. Biochim. Biophys. Acta. 1508 (2000), 235-251.
6. Lara-Martín P. A., Gómez-Parra A., Sanz J. L., Gonzalez-Mazo E. Anaerobic Pathway of Linear Alkylbenzene Sulfonates (LAS)in Sulfate-Reducing Marine Sediments. Environ. Sci. Technol. 44 (2010) 1670-1676.

7. Cook, A. M.; Laue, H.; Junker, F. Review microbial desulfonation. FEMS Microbiol. Rev. 22 (1999) 399-419.
8. Boll M., Fuchs G., Heider J. Anaerobic oxidation of aromatic compounds and hydrocarbons. Curr. Opin. Chem. Biol. 6 (2002) 604-611.
9. Díaz E., Jiménez J. I., Nogales J. Aerobic degradation of aromatic compounds. Curr. Opin. Biotechnol. 24 (2013), 431-442.
10. García M. T., Campos E., Ribosa I., Latorre A., Sánchez-Leal J., Anaerobic digestion of linear alkyl benzene sulfonate: Biodegradation kinetics and metabolite analysis. Chemosphere. 60 (2005) 1636-1643.
11. Yang K., Zhu L., Xing B. Sorption of sodium dodecylbenzene sulfonate by montmorillonite. Environ. Pollut. 145 (2007) 571-576.
12. Westall J. C., Chen H., Zhang W., Brownawell B. J. Sorption of Linear alkylbenzene sulfonates on sediment Materials. Environ. Sci. Technol. 33 (1999) 3110-3118.
13. Souza L.F.C., Gavazza S., Florencio L., Kato M. T. Factors enhancing the anaerobic degradation of LAS. World congress on anaerobic digestion, Santiago de compostela, Spain, (2013).
14. Khleifat K. M. Biodegradation of linear alkylbenzene sulfonate by a two-member facultative anaerobic bacterial consortium. Enzyme Microb. Technol. 39 (2006) 1030-1035
15. Eniola K. I. T. Effect of additional carbon source on biodegradation of Linear alkylbenzene sulfonate by LAS-utilizing bacteria. J. Xenobiotics 1 (2011) 6-8.
16. Okada D. Y., Delforno T. P., Esteves A. S., Sakamoto I. K., Duarte I. C. S., Varesche M. B. A. Optimization of linear alkylbenzene sulfonate (LAS) degradation in UASB reactors by varying bioavailability of LAS, hydraulic retention time and specific organic load rate. Bioresour. Technol. 128 (2013) 125-133.
17. APHA, AWWA, WEF *Standard Methods for the Examination of Water and Wastewater*, 22nd Edition (2012)
18. Paria S., Khilar K. C. A review on experimental studies of surfactant adsorption at the hydrophilic solid –water interface. Adv. Colloid Interface Sci. 110 (2004) 75-95.

CHAPTER 7.27 SISTEMA DE CULTIVO HIDROPÓNICO PARA EL APROVECHAMIENTO DE EFLUENTES

Luiza F. C. Souza, Maria E. Souza, Claudio E. S. Oliveira*

Associação Caruaruense de Ensino Superior e Técnico – ASCES, Av. Portugal, Nº 584, Caruaru - PE, Brasil.

RESUMEN

El agua es un elemento esencial para la supervivencia de los seres vivos. Su escasez y mala distribución es una preocupación. El objetivo fue evaluar la viabilidad de la utilización del agua de lavado de ropa en un sistema hidropónico para el cultivo de lechuga (Lactuca sativa L.). El sistema fue hecho con materiales sencillos, botellas de plástico y caballetes de madera, y ubicado en una casa. Los dos tipos de muestras se ensayaron como sigue: agua con nutrientes y agua con detergente y el suavizante de telas. La cuantificación de los principales nutrientes se hizo en cada tipo de muestra. El sistema se hizo funcionar dos veces durante 22 días cada uno. Después del período de 22 días, entre las plantas supervivientes, no hubo diferencia significativa en el tamaño de las hojas de 2,6 ± 0,2 cm y 2,5 ± 0,8 cm, y hipocódilo, 2,2 ± 0,9cm y 2,6 ± 0,8 cm, de regadío con agua y nutrientes y agua + detergente y el suavizante de telas, respectivamente. En relación con el tamaño de la raíz, las plantas regadas con agua + detergente y suavizante de telas fueron mayores que con agua y nutrientes en un porcentaje de 200%. Otro aspecto diferente es el número de hojas que se encuentra en cada planta, cerca de 4 ± 1 y 32 ± 20, en el sistema de riego de agua y nutrientes y agua con detergente y suavizante. En este trabajo se puede observar que el agua + detergente y el suavizante de telas resultantes la máquina de lavado tiene un potencial para ser utilizado en el cultivo de la lechuga hidropónica.

Palabras claves: Aguas residuales, hidroponía, reúso.

INTRODUCCIÓN

El agua es esencial para la supervivencia humana, sin importar el tiempo, el lugar o la cultura. Sus usos incluyen actividades nobles y no nobles[1]. Entre las actividades nobles importantes son las que tienen contacto directo con la piel, tales como el baño, y que implica la ingestión, por ejemplo, en la preparación de alimentos, en este caso la agua tiene que ser de una calidad excelente, bajas concentraciones de ciertos elementos, y ausencia de patógenos[2]. El agua utilizada en la agricultura, el comercio, la industria y por la población se obtienen a través de la captación de los recursos hídricos o de agua de lluvia. Otra forma de obtener agua es a través de captación de agua de lluvia por canaletas en los techos, y almacenados en tanques. Este tipo de captación es ampliamente utilizado en las zonas rurales, donde no hay obras de suministro de agua.

---

*Author for correspondence: claudiooliveira@asces.edu.br

Sin embargo, esta forma de obtención de agua depende de la lluvia, que varía en cada región. Se sabe que la distribución de agua es desigual, provocando que la escasez de este recurso[3].

Después de ser utilizado en muchas actividades, el agua comienza a mostrar diferentes características, que son las aguas residuales, que se pueden clasificar en función de su carga contaminante, aguas grises y negras. Las aguas grises provienen de las duchas, lavabos y lavadoras. Estos tipos de aguas residuales son ricos en jabones, sólidos en suspensión y tienen pequeñas cantidades de bacterias. El agua negra, a su vez provienen de las cocinas y sanitarios y tienen grandes cantidades de materia orgánica y bacterias[4]. El tratamiento de aguas residuales, tanto gris y negras es de importancia fundamental en la planificación y la gestión sostenible de los recursos hídricos, lo que permite la reducción de su impacto sobre el medio ambiente y la reutilización de las aguas tratadas en diversas actividades de la industria, la agricultura y sectores urbanos. El sector agrícola es el mayor consumidor de agua entre los diversos sectores de utilización de este recurso[5]. La reutilización del agua es vital para la sostenibilidad de este recurso que es agotable. La reutilización del agua debería estar presente en todas las áreas que utilizan este proceso natural como una fuente vital[6]. Actualmente hay cuatro factores que contribuyen a la aplicabilidad de la reutilización : a) la protección del medio ambiente, b) el aumento del costo de los tratamientos, c) el aumento de la disminución de la disponibilidad de agua y d) el valor del precio del agua cruda[7]. El objetivo de este trabajo es evaluar y comparar el desarrollo de los vegetales cultivados en sistema hidropónico, compuesto de agua con detergente y el suavizante de telas y las plantas tradicionales de riego con sistema de agua potable.



FIGURA 1. Semillas de lechuga (a) y la germinación de la esponja (b)

MATERIALES Y MÉTODOS

La investigación se basó en un estudio de tipo descriptivo, explicativo y enfoque cualitativo. Fue necesario construir un pequeño sistema hidropónico usando botellas de PET, para el cultivo de la lechuga. Este método se utiliza en cultivos hidropónicos. El objetivo fue verificar si los efluentes que contienen surfactantes pueden ser reutilizados para el riego de pequeños huertos familiares. Por lo tanto, este trabajo fue un estudio preliminar para ver si el agua de las lavadoras podría utilizarse para estos mismos fines. En este trabajo fueran hechas pruebas del sistema hidropónico en dos etapas.

La primera se colocaron las plántulas de lechuga y regadas con agua potable, más nutrientes (H_2O + N) y la otra se colocaron nuevas plántulas, se regaron con una mezcla de agua dulce, jabón líquido y suavizante de telas. Para ambos sistemas se utilizaron semillas de lechuga Cristina (*Lactuca sativa L.*) y esponja de espuma (**Figura 1**).

En cada esponja se hicieron agujeros y cada agujero se colocaron cuatro semillas. La esponja que contiene las semillas se colocó en un recipiente con agua del grifo para germinar (**Figura 2**).

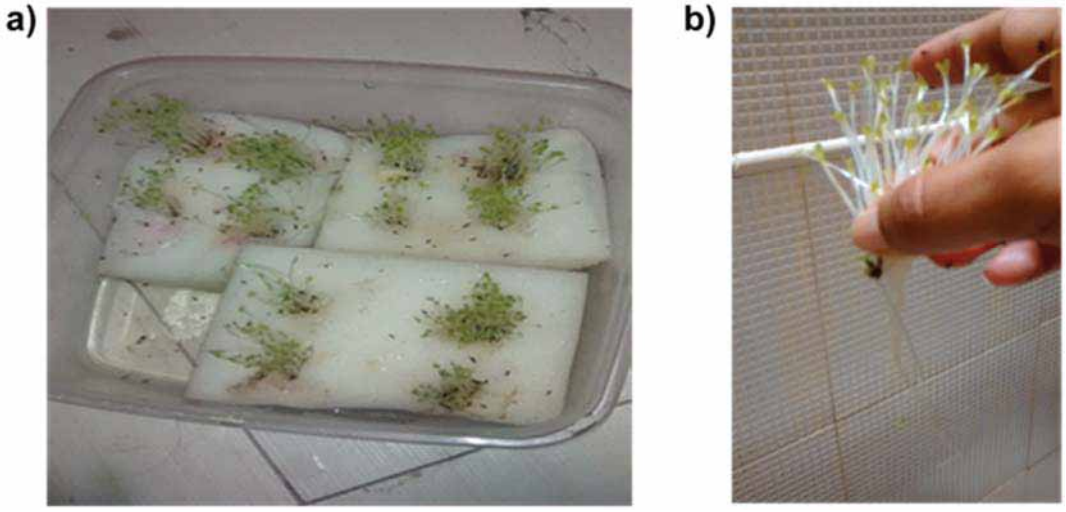


FIGURA 2. La germinación (a) y las plántulas transferidas para el sistema (b)

El sistema consistía en un depósito de 20 litros, junto con un grifo, con una trampa de debajo de ella para controlar el flujo. Esta trampa se adjunta en la parte inferior de una serie de 6 botellas de PET de 500 ml de capacidad. Las botellas se conectan en serie y había un corte en el lado de cada botella para la instalación de un vaso de plástico con la paja de coco y plántulas de lechuga (**Figura 3**).

El reservorio del sistema hidropónico fue pintado de negro; las botellas de plástico tienen un pequeño corte en el lado y se colocarán en posición horizontal, con el lado cortado hacia arriba. Otro corte en el fondo de la botella para interconectar (**Figura 4**).

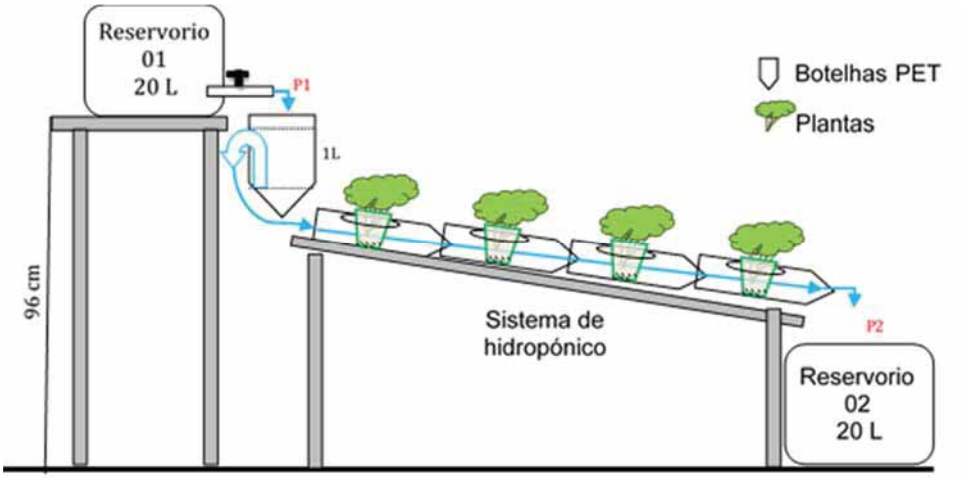


FIGURA 3. Diagrama de sistema de cultivo hidropónico de puntos de recogida de efluentes y lavadora durante el monitoreo: P1 y P2, afluente y el sistema de efluentes.

De esta manera ellas estaban vinculadas en serie. Las botellas fueran conectadas y se colocaron con una inclinación de 3,8%, porcentaje menor que el indicado en la literatura, 5 a 8%[8]. Un tambor de plástico de cinco galones almacena el afluente del sistema. Este se colocó a una altura de 96 cm del suelo, uno grifo fue instalado en el lado del tambor, 3 cm de la parte inferior y través de esto se reguló el flujo en el sistema. La literatura recomienda un flujo de 1 litro por cada 30 minutos[8]. Por lo tanto, el volumen de depósito de 20 litros, fue suficiente para alimentar el sistema durante aproximadamente 10 horas. El agua residual sintética se preparó diluyendo 10 g de detergente para la ropa y el suavizante de tejido en 10 ml en 20 L de agua del grifo. Los productos utilizados fueron adquiridos en tiendas, detergente en polvo 1 kg de suavizante de ropa de 500mL, semillas de lechuga, 100 g de nutrientes y se disolvieron en 20 litros de agua. En la figura 3 son dispuestos los productos y las semillas utilizados.

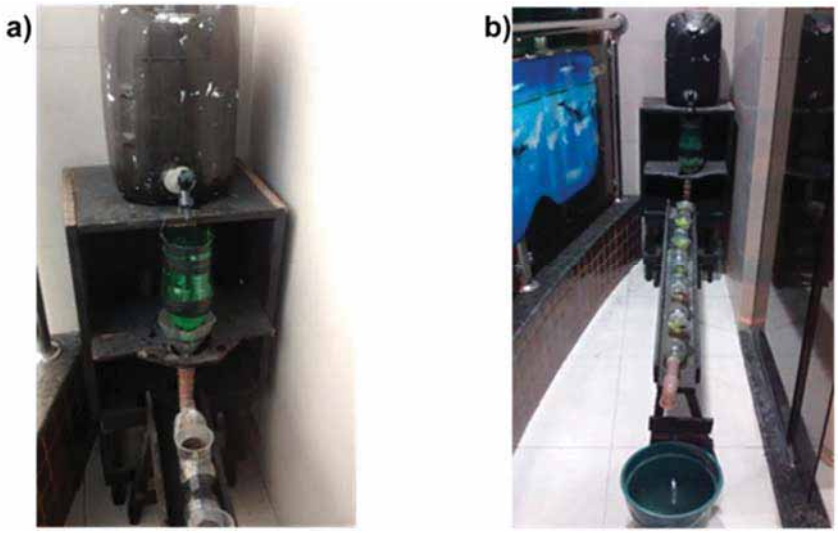


Figura 4. Fotografía del sistema hidropónico con el reservorio y sinfón (a) y el sistema completo para el cultivo (b)

El sistema fue evaluado comparando el crecimiento de las plantas regadas con agua y nutrientes y también con el ablandador de agua y jabón. Después de 21 días se midieron las plantas para evaluar su desarrollo para cada tipo de riego, el número de plántulas que sobrevivieron, a la cantidad de hojas por planta, el tamaño de la raíz y el tamaño de cada tallo.

RESULTADOS Y DISCUSIÓN

Caracterización de muestras. Los resultados del análisis físico-químico con diferentes tipos de residuos utilizados en este trabajo se muestran en la **Tabla 1**. El agua con nutrientes se utilizó como control, agua con detergente y el suavizante de telas como una prueba primaria de la reutilización de agua de la máquina y el agua de la lavadora para ver si las concentraciones de nutrientes serían apropiadas.

TABLA 1. Los resultados promedio y desviación estándar de análisis físico- químico del agua con nutrientes, agua con detergente y suavizante de telas y el agua de máquina

Análisis	Unidad	Agua + nutrientes	Agua + jabón + suavizante	Agua da máquina
pH	-	6±1	10	7,21±0,03
Carbono Inorgánico	mg C-CO_2/L	11±7	57±88	47±1
Carbono orgánico	mg C/L	29±17	377±325	86±64
Nitrato	mg NO_3^-/L	5±6	14	10
Nitrogenito Amónica	mg NH_4^+/L	-	-	6±5
Nitrogenito total	mg N-NTK/L	249±124	83±129	9±5
Orto- fosfato	mg PO_4^{-2}/L	101	< 1	< 1
Clorito	mg Cl^-/L	162±23	280	240±45
Fluoruro	mg F^-/L	2	< 1	1±1
Sulfato	mg SO_4^{-2}/L	98±62	92±94	205±157

El pH de las muestras se distingue entre sí. El valor pH del agua con nutrientes mostró una tendencia ácida que van desde 5 a 7. El pH del agua con el detergente y el suavizante fue básico, y se esperaba este comportamiento ya que la composición de jabones y suavizantes tienen compuestos que elevan su pH. El agua que salía de la máquina de lavado mostró un pH neutro. La literatura citada el pH óptimo para el cultivo de la lechuga debe estar entre el intervalo de 5,5 y 6,5. Si el pH está por debajo de 5 y por encima de 7, es necesario realizar la corrección con bases o ácidos[9]. En agua con nutrientes y agua con detergente y el suavizante de telas, la concentración de nitrógeno total fue 249 y 83 mg/l, respectivamente. El nitrógeno es importante porque su presencia favorece la formación de pigmentos verdes. La concentración de cloruros en las muestras de agua con nutrientes, agua con detergente y el suavizante de telas, y el efluente de la máquina fue de 162, 280 y 240 mgCl/l, respectivamente. Ambos son por encima de la concentración máxima sugerida por la literatura. En segundo lugar[10]. Los

valores de sulfato que se encuentran en las muestras de agua con nutrientes, agua con detergente y el suavizante de telas, y el efluente de la máquina eran 98 mg/l, 92 mg/l y 205 mg/l, respectivamente. Todos los valores fueron muy superiores a los valores óptimos que son de 0,4 a la 0,55 g/l y 0,53 a 2,4[10].

Análisis de crecimiento de las plantas. Para comparar el rendimiento del sistema de cultivo hidropónico con el riego de agua y nutrientes y el agua con el detergente y el suavizante de telas, las mediciones se hicieron de las diversas partes de las pantas, longitud de la raíz, hoja y tallo. El número de plantas que sobrevivieron el sistema y el número de hojas en cada planta y de plántulas fueron cuantificadas. Los resultados se muestran en la **Tabla 2**.

TABLA 2. Resultados Promedio y desviación estándar comparativo de las muestras cultivadas

	Agua + Nutrientes	**Agua + Jabón y Suavizante**
Tamaño de la raíz	1,5 ± 0,2 cm	3 ± 1 cm
Número de hojas	4 ± 1 cm	32 ± 20 cm
Tamaño de las da hojas	2,6 ± 0,2 cm	2,5 ± 0,8 cm
Tamaño del tallo	2,2 ± 0,9 cm	2,6 ± 0,8 cm
Número de plantas que supervivientes	3 unidades	6 unidades

La comparación de las características de los vegetales cultivados con los dos tipos de agua y con el mismo tiempo de ciclo de crecimiento, se observó que las plantas cultivadas con agua con jabón y suavizante de telas tenían un mejor resultado. Las 6 plántulas colocadas en el sistema de riego con agua y nutrientes, y el agua con el detergente y el suavizante de telas, sobrevivieron 3 y 6 respectivamente durante 22 días de cultivo. En la **Figura 5a** y **5b** se puede observar con 22 días de cultivo el sistema con agua y nutrientes y agua con jabón, respectivamente.

Las plantas en ambos sistemas muestran el mismo tamaño, pero el número de hojas en el sistema de cultivo con agua y jabón fue 800 % más alto que el sistema cultivado de agua y nutrientes. El tamaño de las plantas y las hojas eran similares: 2,5 ± 0,8 ± 2,6 cm y 0,2 cm. Sin embargo, el coeficiente de variación fue de 63 % y 25 %, respectivamente. La raíz ha desarrollado mejor en el sistema de riego con agua, jabón y suavizante de telas y tenía una longitud media de 3 ± 1 cm, mientras la raíz con riego de agua con nutrientes tenía una longitud media de 1,5 ± 0,2 cm. En la **Figura 6a** y **6b** se puede observar una plántula para cada sistema, irrigada con agua y nutrientes, y el agua y el detergente y el suavizante de telas, respectivamente.

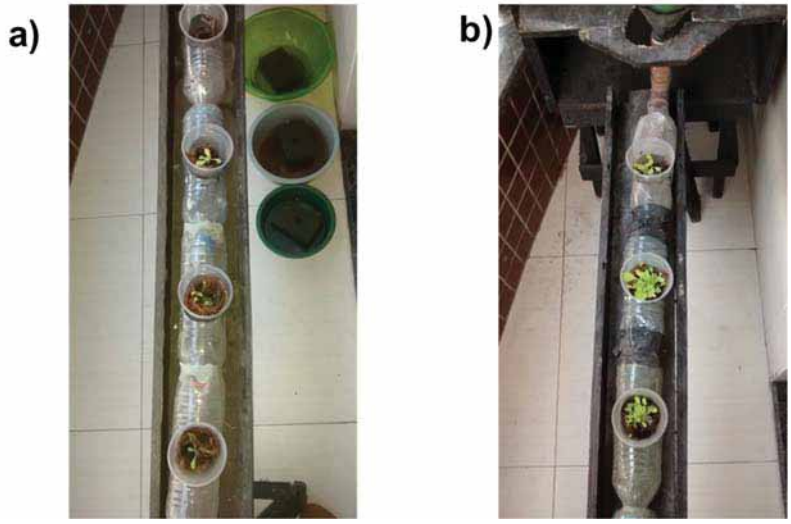


FIGURA 5. Fotografía del sistema de hidroponía después de 22 días de cultivo con nutrientes y agua (A) y con agua, jabón y suavizante (b)

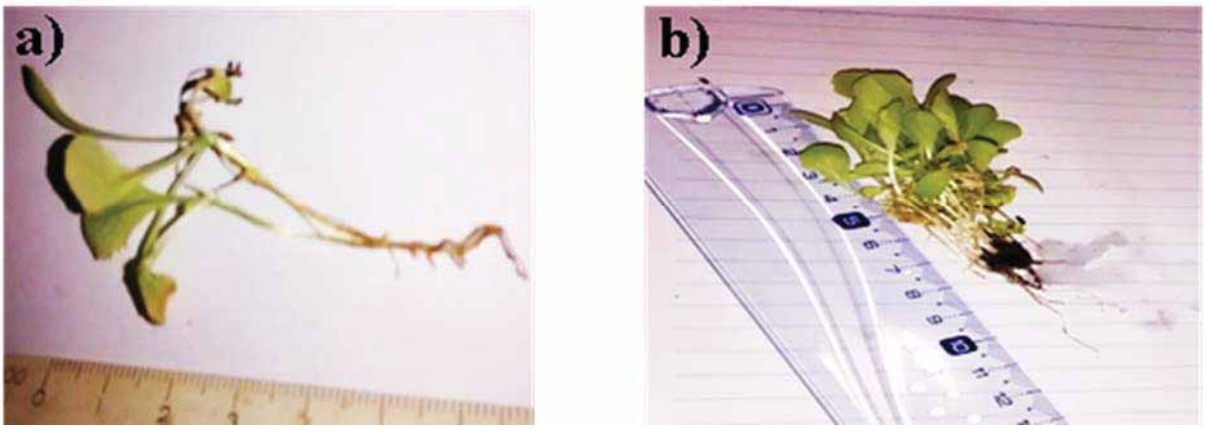


FIGURA 6. Plántulas regadas por el sistema de cultivo hidropónico con agua y nutrientes (a) y con agua, jabón y suavizantes (b), ambos con 22 días de cultivo

A través de este estudio se puede ver que el agua con jabón e suavizante tiene un alto potencial para el uso en el sistema de cultivo hidropónico. A través del análisis físico-químico señaló la falta de ciertos nutrientes, sin embargo, las plántulas regadas con estas aguas tenían un desarrollo satisfactorio.

CONCLUSIÓN

Con el desarrollo de esta investigación se puede verificar que:

- El agua con nutrientes mostraron mejor con presencia de todos los nutrientes necesarios para el desarrollo de la planta.
- El agua con jabón y suavizante de efluentes y la máquina mostró un alto potencial para su reutilización en el sistema de cultivo hidropónico. Ellos estaban presentes

varios nutrientes necesarios para el desarrollo de la planta y en la concentración adecuada. Sin embargo, la falta de algunos compuestos hace uso de esta limitado.

- El desarrollo de un sistema de cultivo hidropónico en casa fue posible, ocupando poco espacio en una zona soleada de la residencia. El volumen generado en una lavadora sería suficiente para abastecer el sistema con el correcto desarrollo de la planta.
- En comparación con el desarrollo de la planta fue diferente en cada tipo de riego. En ambos sistemas, las plantas mostraron longitudes de los tallos similares de aproximadamente 2,4 ± 0,3 cm. Pero con agua y jabón la cantidad de hojas fue de 800% más altas que las plantas regadas con agua y nutrientes.

Este estudio tuvo como objetivo evaluar la posibilidad de utilizar el efluente de la lavadora para su reutilización en el sistema hidropónico pequeño de hortalizas. A través de los datos observados en este estudio se pudieron verificar que el detergente y el suavizante de telas no afectaron el desarrollo de las plantas.

REFERENCIAS

1. Telles D. D.; *A água e o Meio Ambiente. Ciclo ambiental da água: da chuva á gestão*. 1ªed, (2013)
2. Bazzarella B. B. Caracterização e aproveitamento de água cinza para uso não potável em edificações. 2005. dissertação (Pós-Graduação em Engenharia Ambiental) – Centro Tecnologia Universidade Federal do Espírito Santo, Espirito Santo, 2005.165p.
3. Costa R. H. P. G. *Reuso da Água. Ciclo ambiental da água :da chuva á gestão*. 1ªed, (2013)
4. Souza E. F. *Sistema de reuso de água na corporação da polícia militar do bairro de Cambuci*, São Paulo, Dissertação (Graduação Engenharia Civil). Universidade Anhembi MORUMBI. 2008
5. Barroso L. B., Wolff D. B. *Reuso de esgoto sanitário na irrigação de culturas agrícolas.* (2011).
6. BRASIL. Consumo Sustentável: Manual de educação. Brasília: Consumers International/MMA/MEC/IDEC, 2005. 160 p.
7. Telles D. D., Gois J. S. *Usos da Água e Suas Características. Ciclo ambiental da água da chuva á gestão*. 1ªed, (2013)
8. Hidrogood, *Cartilha básica de orientação de cultivo hidropônico.* 4ª ed, (2010).
9. Gomes R. F., Silva, J. P.; Silva, V. D.; Farias, T. P. B.; Monteiro, G. C. L.; Souza, G. T.; Gusmão. S. A. L. *Produção hidropônica de hortaliças na Amazônia* (2012).
10. Rios, E.C.S.V.; Uso de Águas Amarelas Como Fonte Alternativa de Nutriente em Cultivo Hidroponico da Alface, Dissertação do Programa de Pós-graduação em Engenharia Ambiental, Universidade Federal do Espirito Santo,2008.

CHAPTER 7.28 PRODUCCIÓN DE LÍPIDOS EMPLEANDO UNA MICROALGA AISLADA DE TIERRA BLANCA, VERACRUZ Y AGUA RESIDUAL DE TILAPIA

Ana Line Vázquez-Larios *(1); Paula Natalia Robledo-Narváez (1); Luis Alfredo Ortega-Clemente (2) and Elvira Ríos-Leal (3)

(1) Instituto Tecnológico Superior de Tierra Blanca, Avenida Veracruz S/n esquina Héroes de Puebla Colonia Pemex, Tierra Blanca Veracruz, México
(2) Instituto Tecnológico de Boca del Río, Carr. Veracruz-Cordoba Km. 12, Boca del Río, Veracruz. México.
(3) Centro de Investigación y de Estudios Avanzados del Instituto Politécnico Nacional, Av. Instituto Politécnico Nacional 2508, Col. San Pedro Zacatenco, Delegación Gustavo A. Madero, CD MX.

RESUMEN

Se considera que los ácidos grasos provenientes de la biomasa microalgal tienen el potencial de ser utilizados como materia prima para la producción de biocombustibles como el biodiesel o para suplementos alimenticios. Algunas especies de microalgas son notables debido a su composición química de proteína, carbohidratos y lípidos (ácidos grasos). Los objetivos de este trabajo fueron i) aislar una microalga de Tierra Blanca, Veracruz y ii) Evaluar la producción de lípidos en Medio Basal Bold (MBB) y agua residual de Tilapia con la microalga aislada (MCA) y *Chlorella vulgaris*. Las microalgas se inocularon en fotobiorreactores tubulares de vidrio con un volumen de operación de 3 L con MBB y agua residual de Tilapia a una concentración inicial de $1.0X10^6$ células mL^{-1} a 20 ± 0.78 °C e iluminación continua con LED. La concentración de biomasa en la fase exponencial en MBB para MCA y *Chlorella vulgaris* fue 0.2237 y 0.5174 g L^{-1} respectivamente, empleando agua residual de Tilapia, la concentración de biomasa fue 0.2360 y 0.2541 g L^{-1} para MCA y *Chlorella vulgaris,* respectivamente. Para la fase estacionaria la concentración de biomasa en MBB para MCA y *Chlorella vulgaris* fue de 0.5267 y 0.6767 g L^{-1}, para el agua residual de Tilapia fue de 0.3105 y 0.5176 g L^{-1}, respectivamente. Se obtuvo la mayoría del contenido de lípidos en la fase exponencial para agua residual de Tilapia (MCA con 35% y *Chlorella vulgaris* con 52%) en comparación con las cultivadas en MBB (MCA con 32% y *Chlorella vulgaris* con 32%). Estos valores presentan un gran potencial de la MCA y *Chlorella vulgaris* como alternativa para la producción de lípidos a partir de la depuración de los nutrientes contenidos en el agua residual de Tilapia, con remociones de 83, 87 y 91 % de NO_3, NO_2 y PO_4 respectivamente para *Chlorella vulgaris* y 95, 31 y 68 % de NO_3, NO_2 y PO_4 respectivamente para MCA.

Palabras clave: agua residual, microalgas, lípidos

---

*Author for correspondence: paurobnar@gmail.com

INTRODUCCIÓN

Durante el proceso de levante y engorde de tilapia se producen efluentes que aportan contaminación por nutrientes (fósforo y nitrógeno), sólidos, materia orgánica y patógenos a los cuerpos receptores[1,2]. Tales efluentes no son aptos para su reutilización en piscicultura, ni para vertimiento directo a cuerpos receptores, razón por la cual es necesario el tratamiento de los mismos[3]. Diversas tecnologías se han utilizado en el tratamiento de efluentes de tilapia: osmosis[4], recirculación y biofiltración en sistemas acuapónicos[5], sedimentación convencional y reactor aerobio de lecho fluidizado[6], humedales de flujo subsuperficial[7] y plantas acuáticas[8,9].

Las microalgas se han convertido en un potencial recurso sustentable de biomasa debido a su neutralidad hacia el medioambiente[10,11]. En comparación con las plantas terrestres, las microalgas presentan una tasa de crecimiento más rápido[12], y la eficiencia de fotosíntesis puede superar el 10%, siendo este de 10-50 veces mayor que las plantas terrestres[13,14]. Bajo condiciones ambientales desfavorables, las microalgas son capaces de acumular grandes cantidades de lípidos[15,16]. Otra ventaja de la microalgas es su capacidad de remover nitrógeno y fosforo de aguas residuales. Estos nutrientes pueden incorporarse dentro de biomasa celular de las algas y simultáneamente depurar el agua residual[17-20]. El cultivo de algas en agua residual ofrece ventajas de tratamiento y simultáneamente la producción de biomasa para la obtención de diferentes productos. Los objetivos de este trabajo fueron i) aislar una microalga de Tierra Blanca, Veracruz y ii) Evaluar la producción de lípidos en Medio Basal Bold (MBB) y agua residual de Tilapia con la microalga aislada (MCA) y *Chlorella vulgaris*.

MATERIALES Y MÉTODOS

Aislamiento de la microalga. La muestra fue recolectada de la piscina de tortugas de la UMA del Instituto Tecnológico Superior de Tierra Blanca, Tierra Blanca, Veracruz, México (18°26′10.849″N96°20′35.907″O). La muestra fue distribuida en placas Petri con Medio Basal Bold (MBB) con los siguientes nutrientes (L^{-1}): KH_2PO_4, 175 mg; $CaCl_2 \cdot 2H_2O$, 25 mg; $MgSO_4 \cdot 7H_2O$, 75 mg; $NaNO_3$, 250 mg; K_2HPO_4, 75 mg; NaCl, 25 mg; H_3BO_3, 11.42 mg; Na_2HCO_3, 100 mg; 1 mL de la solución de micronutrientes ($ZnSO_4 \cdot 7H_2O$, 8.82 g L^{-1}; $MnCl_2 \cdot 4H_2O$, 1.44 g L^{-1}; MoO_3, 0.71 g L^{-1}; $CuSO_4 \cdot 5H_2O$, 1.57 g L^{-1}; $CoCl_2$, 0.35 g L^{-1}); 1 mL de la solución 1 (Na_2EDTA, 50 g L^{-1}; KOH, 3.1 g L^{-1}); 1 mL de la solución 2 ($FeSO_4$, 4.98 g L^{-1}; H_2SO_4, 1 mL L^{-1}) (Barsanti & Gualtieri, 2006) y 1.5 % de agar. La colonia obtenida después de subcultivos secuenciales fue transferida a nuevas placas con MBB hasta obtener el cultivo puro de la microalga. Las placas se mantuvieron a una temperatura de 20 °C, bajo iluminación continua por 15 d.

Chlorella vulgaris se obtuvo de la colección del Departamento de Acuicultura del Centro de Investigación Científica y de Educación Superior de Enseñanza (CICESE). Las cepas se mantuvieron en 500 mL de MBB a 20 °C bajo una intensidad de 3000 luxes por 24 h y aireación continua.

Agua residual de Tilapia. El agua residual de Tilapia fue recolectada de un estanque de cultivo de Tilapia, en el Instituto Tecnológico de Boca del Río, Veracruz, México. El agua residual fue filtrada a través de una columna equipada con una malla de 100 µm, algodón y fibra de poliéster para remover la materia orgánica y fitoplancton presente en el agua residual. La composición fisicoquímica del agua residual para los ensayos se muestra en la **Tabla 1**.

TABLA 1. Parámetros del agua residual de Tilapia

Parámetro	
$N\text{-}NH_4$	0.20 mg L^{-1}
NO_3	104 mg L^{-1}
NO_2	0.02 mg L^{-1}
PO_4	1.36 mg L^{-1}
pH	6.44

Diseño experimental. El diseño experimental, consistió en evaluar el efecto de tipo de microalga (MCA y *Chlorella vulgaris*) y tipo de medio de cultivo (MBB y Agua residual de Tilapia) sobre la producción de ácidos grasos. El cultivo se realizó en fotobiorreactores de vidrio con un volumen efectivo de 4 L y un volumen de operación de 3 L, acoplados a un sistema de aireación e iluminación LED. La concentración inicial de microalgas fue $1x10^6$ células mL^{-1} para MBB y Agua residual de Tilapia, respectivamente. Los reactores fueron operados bajo iluminación continua (3000 luxes), a 20 ± 0.78 °C y aireación continua. Se retiraron 250 mL de los cultivos en fase exponencial y estacionaria para evaluar la composición lipídica de cada una las microalgas.

Métodos analíticos. El conteo celular se realzo diariamente por conteo mediante un hematocitómetro[21]. Los lípidos totales fueron determinados por el método descrito por Halim *et al*., 2012[22], el contenido de ácidos grasos fue obtenido por derivatización y cromatografía de gases (Perkin Elmer, Model Autosystem, Flame ionization) como se describe en Ferrer-Álvarez *et al*., 2015[23]. Los análisis de nitrato, nitrito, amonio y fosfato fueron realizados mediante un equipo HANNA Multiparameter (Model HI83099).

RESULTADOS Y DISCUSIÓN

La concentración de biomasa en fase exponencial en MBB y agua residual de Tilapia con la MCA y *Chlorella vulgaris* se muestra en la **Figura 1**. La concentración de biomasa en la fase exponencial en MBB para MCA y *Chlorella vulgaris* fue 0.2237 y 0.5174 g L^{-1} respectivamente, empleando agua residual de Tilapia, la concentración de biomasa fue 0.2360 y 0.2541 g L^{-1} para MCA y *Chlorella vulgaris,* respectivamente. Para la fase estacionaria la concentración de biomasa en MBB para MCA y *Chlorella vulgaris* fue de 0.5267 y 0.6767 g L^{-1}, para el agua residual de Tilapia fue de 0.3105 y 0.5176 g L^{-1}, respectivamente.

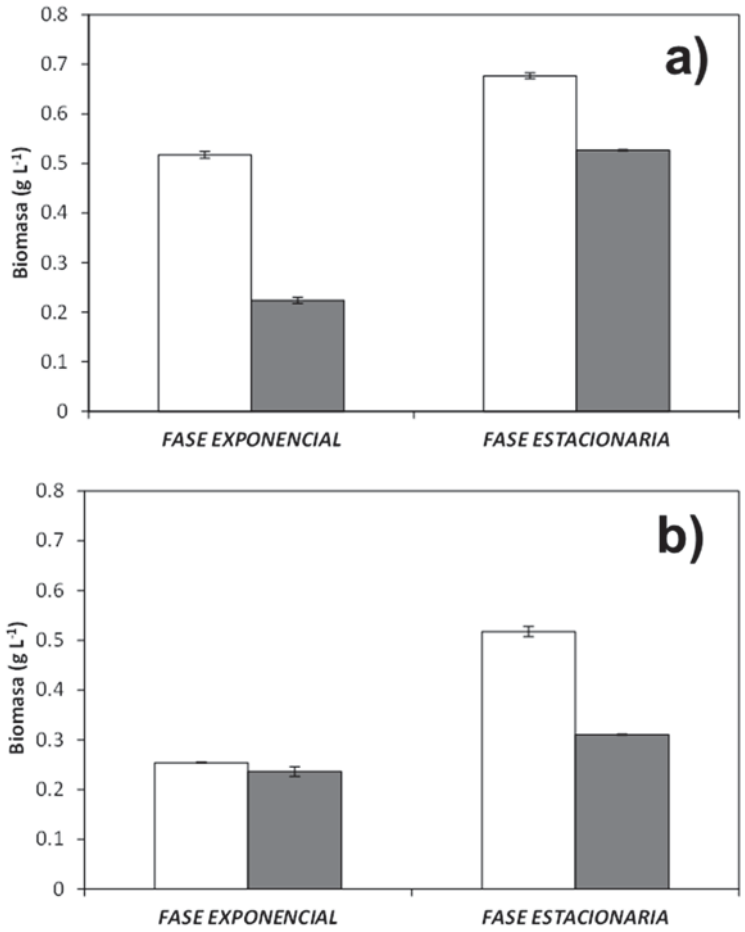


FIGURA 1. Concentración de biomasa en fase exponencial y estacionaria para *Cholrella vulgaris* (□) y microalga aislada (■): *a)* Medio Basal Bold y *b)* agua residual de Tilapia

Las microalgas *Chlorella vulgarias* y la MCA mostraron un incremento en la concentración de biomasa en la fase estacionaria y los valores son similares a lo reportado por Li *et al*., 2015.

Producción de lípidos. El contenido de lípidos de *Chlorella vulgaris* y MCA se muestra en la **Tabla 2.** Para *Chlorella vulgaris* y la microalga aislada mostraron mayores valores del 52 y 40 % de lípidos, respectivamente, aplicando agua residual de Tilapia, estos valores son mayores a lo reportado por Tale *et al*., (2014)[24] y Feng *et al.,* (2011). Tale *et al*. (2014)[24] aplicaron agua residual para la producción de lípido en *Monoraphidium sp*. KMN5 del 20 % y 34 % para MMB. Feng *et al.,* (2011) aplicaron *Chlorella vulgaris* para la producción de lípidos con el tratamiento de agua residual sintética, obtuvieron hasta 42 % de lípidos. Estos resultados muestran el potencial de aplicar agua residual de Tilapia para la producción de lípidos (Tale *et al*., 2014)[24].

TABLA 2. Contenido de lípidos de de *Chlorella vulgaris* y de la microalga aislada

Medio	Microalga	Contenido de lípidos (%)	
		Fase exponencial	Fase estacionaria
Medio Basal Bold	*Chlorella vulgaris*	32±2.16	36±3.56
	Microalga aislada (MCA)	32±0.32	20±0.05
Agua residual de Tilapia	*Chlorella vulgaris*	52±0.97	40±8.58
	Microalga aislada (MCA)	35±4.25	33±4.78

Crecimiento de las microalgas en agua residual de Tilapia. Los resultados indican que los fosfatos y nitratos son consumidos por el metabolismo de las microalgas e incorporados en la biomasa. Tanto el nitrógeno como el fosforo son los componentes principales del agua residual, que podrían apoyar el crecimiento de algas. El presente trabajo muestra valores altos de remoción del 83, 87 y 91 % para nitratos, nitritos y fosfatos para *Chlorella vulgaris*. Para la MCA se obtienen valores de 96, 31 y 68% para nitratos, nitritos y fosfatos, respectivamente (**Tabla 3**). Los valores de remoción son similares a lo reportado por Feng *et al*., quienes reportaron remociones del 96 % de fosfatos por *Chlorella vulgaris* y agua residual sintética.

Tabla 3. Remoción de nutrientes del agua residual de Tilapia

Parámetros	***Remoción (%)***	
	Chorella vulgaris	***Microalga aislada***
NO_3^-	83	96
NH_4^+	25	20
NO_2^-	87	31
PO_4^-	91	68

CONCLUSIÓN

Se obtuvo la mayoría del contenido de lípidos en la fase exponencial para agua residual de Tilapia (MCA con 35% y *Chlorella vulgaris* con 52%) en comparación con las cultivadas en MBB (MCA con 32% y *Chlorella vulgaris* con 32%). Estos valores presentan un gran potencial de la MCA y *Chlorella vulgaris* como alternativa para la producción de lípidos a partir de la simultanea depuración de los nutrientes contenidos en el agua residual de Tilapia, con remociones de 83, 87 y 91 % de NO_3, NO_2 y PO_4 respectivamente para *Chlorella vulgaris* y 95, 31 y 68 % de NO_3, NO_2 y PO_4 respectivamente para MCA

AGRADECIMIENTOS

Se agradece al apoyo técnico del IQ Gustavo Gerardo Medina Mendoza de Central Analítica del Departamento de Biotecnología y Bioingeniería del CINVESTAV-I.P.N., así como al CONACYT por la beca posdoctoral de la Dra. Ana Line Vázquez-Larios.

REFERENCIAS

1. Sánchez, I. A., Matsumoto, T. Hydrodynamic characterization and performance evaluation of an aerobic three phase airlift fluidized bed reactor in a recirculation aquaculture system for Nile Tilapia production. Aquacultural Engineering. 47 (2012) 16-26.
2. Van Rijn J. Waste treatment in recirculating aquaculture systems. Aquacultural Engineering, 53 (2013) 49– 56.
3. Chaux F. G., Caicedo B. J.R. Fernandez M. J. E. Treatment of fish farm effluents (red tilapia) in ponds with *Azolla pinnata*. Biotecnología en el Sector Agropecuario y Agroindustrial 11 (2013) 46-56.
4. Liu, C.C.The Development of a Renewable-Energy- Driven-Reverse osmosis system for Water Desalination and Aquaculture Production. Journal of Integrative Agriculture, 12 (2013) 1357-1362.
5. Campos R., Alonso A., Ávalos D., Asiain A., Reta, J.L. Caracterización fisicoquímica de un efluente salobre de tilapia en acuaponia. Revista Mexicana de Ciencias Agrícolas. 5 (2013) 939-950.
6. Sánchez, I.A., Matsumoto, T. Ammonia removal in a water recirculating system for tilapia. Revista Colombiana de Ciencias Pecuarias, 24 (2001) 263-261.
7. Zachritz, W., Hanson A., Sauceda J., Fitzsimmons K. Evaluation of submerged surface flow (SSF) constructed wetlands for recirculating tilapia production systems. Aquacultural Engineering. 39 (2008) 26-23.
8. Redding T., Tood S., Midlen, A.The Treatment of Aquaculture Wastewaters: A Botanical Approach. Journal of Environmental Management, 50 (1997) 283- 289.
9. Henry-Silva G., Camargo A. Efficiency of aquatic macrophytes to treat Nile tilapia pond effluents. Scientia Agricola. 63 (2006) 433- 438.
10. Karemore A., Pal R., Sen R. Strategic enhancement of algal biomass and lipid in Chlorococcum infusionum as bioenergy feedstock. Algal Res. 2 (2013)113–121.
11. Amaro H.M., Guedes A.C., Malcata F. Advances and perspectives in using microalgae to produce biodiesel. Appl Energy. 88 (2011) 3402–10.
12. Li Y., Horsman M., Wu N., Lan C.Q., Dubois-Calero N. Biofuels from microalgae. Biotechnol Prog. 24 (2008) 9815–20.
13. Rosenberg J.N., Mathias A., Korth K., Betenbaugh M.J., Oyler, G.A. Microalgal biomass production and carbon dioxide sequestration from an integrated ethanol biorefinery in Iowa: a technical appraisal and economic feasibility evaluation. Biomass Bioenergy. 35 (2011)3865–76.
14. Khan S.A., Rashmi, Hussain MZ, Prasad S, Banerjee UC. Prospects of biodiesel production from microalgae in India. Renew Sust Energy Rev.13 (2009) 2361–2372.
15. Richmond A. Open systems for the mass production of photoautotrophic microalgae outdoors: physiological principles. J Appl Phycol. 4 (1992) 281–6.
16. Anandarajah K, Mahendraperumal G, Sommerfeld M, Hu Q. (2012). Characterization of microalga Nannochloropsis sp. mutants for improved production of biofuels. Appl Energy. 96 (2012) 371–7.
17. Rawat I., Ranjith, Kumar R., Mutanda T., Bux, F. Dual role of microalgae: phycoremediation of domestic wastewater and biomass production for sustainable biofuels production. Appl Energy. 88 (2011) 3411–24.

18. McGinn P.J., Dickinson K.E., Bhatti S., Frigon J.C., Guiot S.R., O'Leary S.J.B. Integration of microalgae cultivation with industrial waste remediation for biofuel and bioenergy production: opportunities and limitations. Photosynth Res. 109 (2011)231–47.
19. Takagi M., Karseno, Yoshida T. Effect of salt concentration on intracellular accumulation of lipids and triacylglyceride in marine microalgae *Dunaliella cells*. J Biosci Bioeng.101 (2006) 223–226.
20. Daroch M., Geng S., Wang G. Recent advances in liquid biofuel production from algal feedstocks. Appl Energy. 102 (2013)1371–1381.
21. Pica-Granados Y., Ronco A., Díaz, M.C. Método de enumeración celular basado en el uso de hemocitómetro Neubauer. In: Castillo, G. (Eds.). Ensayos toxicológicos y métodos de evaluación de calidad de aguas. Estandarización, intercalibración, resultados y aplicaciones. México: IMTA: 2004 54-63.
22. Halim R., Michael D., Paul K., Webley A. Extraction of oil from microalgae for biodisel production: A review. Biotechnol. Adv. 30 (2012) 709-732.
23. Ferrer-Álvarez, Y.I.; Ortega-Clemente L.A.; Pérez-Legaspi, I.A.; Hernández-Vergara, M.P.; Robledo-Narváez, P.N.; Ros-Leal, E.R.; Poggi-Varaldo, H.M. Growth of Chlorella vulgaris and Nannochloris oculata in effluents of Tilapia farming for the production of fatty acids with potential in biofuels. African Journal of Biotechnology. 14 (2015) 1710-1717.
24. Tale M., Ghosh S., Kapadnis B., Kale S. (2014). Isolation and characterization of microalgae for biodiesel production from Nisargruna biogas plant effluent. Bioresource Technology.169 (2014) 328–335.
25. Barsanti L., Gualtieri, P. Algae – Anatomy, Biochemistry, and Biotechnology CRC Press, Taylor and Francis Group, Boca Raton, FL (2006) 222
26. Li, L.;Cuia J, Liua Q., Dinga Y., Liu J. Screening and phylogenetic analysis of lipid-rich microalgae. Algal Research. 11 (2015) 9 381–386.

CHAPTER 7.29 NITRIFICATION OF INDUSTRIAL NUCLEAR EFFLUENT USING WHOLE BACTERIAL CELL IMMOBILIZATION

M. Venturini *(1); D. Camporotondi (1); P. Silva Paulo (1); G. Curutchet (2) and R. Pizarro (3)

(1) Biominería y Biotecnología Ambiental, Centro Atómico Ezeiza, Comisión Nacional de Energía Atómica, Presbítero González y Aragón 15, Buenos Aires, Argentina
(2) I3A UNSAM Campus Miguelete, 25 de Mayo y Francia, Buenos Aires, Argentina
(3) Radiobiología, Centro Atómico Constituyentes, Comisión Nacional de Energía Atómica, Av. Gral. Paz 1499, Buenos Aires, Argentina

ABSTRACT

In the nuclear industry, ammonia-derived compounds are used in the processes of manufacture of uranium concentrates (known as “yellow cake”) which are used as raw material to obtain nuclear fuels. For this reason, the effluent of this process contains high concentration of ammonium, and consequently, high levels of uranium. Therefore, these effluents must be treated to diminish the concentrations of NH_4 (4g/l $N\text{-}NH_4^+$) and U (300ppm UO_2^{+2}) in order to fulfill local environmental laws. Ammonium is a very soluble ion and it is difficult to precipitate, meaning, it is not easy to eliminate. The uranium has several oxidation states and this depends on the leachant composition and subsequent precipitating conditions; the soluble forms is uranyl ion (UO_2^{+2}).
In this work, we studied and applied the nitrification process, by an autotrophic aerobic oxidation bacterial community, to oxidize the ammonium to nitrate. Due to the complexation and the long time taken to generate the appropriate amount of biomass, the key point in this process is the bacterial cells immobilization to a solid support, to avoid biomass loss and also to enhance the performance in kinetic and effectiveness terms. Hence, we worked with copolymeric hydrogels previously developed, which were obtained by gamma irradiation of 2-hydroxyethyl methacrylate. These hydrogels were inoculated with the bacterial community and then visualized by electronic microscopy and also kinetically compared. The elastic properties of this material avoided deformations in time, and also prevented the development of anaerobic zones in the internal zone, though inside the hydrogel anaerobic environment was denoted by accumulation of nitrate, which did not appeared in studies without solid supports.
The study was performed at laboratory scale of 5 liters of effluent during 100 days, with an ammonium concentration reduction of 90% (initial value: 4000ppm). The kinetic rate of consumption was 350mg/l.day. The treatment was also evaluated in terms of external parameters (rO_2 and CO_3^- consumption), which are stoichiometric reactant in the nitrification process. Obtained results showed to be a viable process for the treatment of effluents from nuclear industry. The uranyl ions at the end of process were not detected.

Keyword: hydrogels, nitrification, nuclear waste.

---

*Author for correspondence: venturini@cae.cnea.gov.ar

INTRODUCTION

The process of production of uranium concentrates begins with filtration and extraction from the ores, obtaining a uranyl nitrate solution, which in the next step reacts with ammonia, carbon dioxide and water, resulting in the precipitation of ammonium diuranate (ADU). Later on, ADU is washed and filtered for the following conversion to produce UO_2. The effluent obtained from this process consists in a solution with great amount of ammonia (7g $N\text{-}NH_4^+$), nitrate (4g/l $N\text{-}NO_3^-$), methanol and UO_2^{2+} (300ppm, Dioxitek S.A.). This solution must be treated to fulfil local environmental laws.

Remediation of effluents with high nitrogen concentration is performed by different kinds of treatments, which could be chemical, physical or biological. Regarding the physicochemical processes that are now in use for sanitation, they have the disadvantage of requiring high energy consumption for the particular case of nuclear industry effluents, because there are several stages involved: distillation-condensation, coagulation and flocculation (Condorcherm)[1]. On the other hand, biological processes of nitrification linked up to the conventional techniques could be a solid and cheaper way to remove nitrogen derived compounds, with denitrification and a final stage with activated sludge, to allow the reutilization of water in nuclear industry. Within these technologies, new configurations for biological removal have been proposed during the last few years, for example, low aeration systems to produce a shunt in total oxidation of ammonium, leading to nitrite ions (SHARON); the simultaneous nitrification – denitrification (SND); and the utilization of anaerobic bacterial cells which oxidize the ammonium[2]. The advantages of these processes lay on less energy consumption due to less aeration-agitation needed and also less residence time. Nevertheless, since the effluent comes from the nuclear industry, there are high concentrations of nitrate ions and methanol, which leads to a pretreatment to denitrify and get rid of methanol and nitrate. This is the reason why in the nuclear industry, conventional nitrification and the denitrification were always chosen for remediation of effluents.

Furthermore, moving bed biofilm reactors (MBBR) have been stablished as a robust, flexible and compact technology. Bacterial supports are useful materials to determine the stability of the process and to enhance the performance. This kind of technologies is already commercialized and adjusted to specific kind of effluent and microorganism, for example Kaldnes[3]. Moreover, regarding polymer synthesis, ionizing radiation offers to control polymerization and copolymerization with the desired characteristics. We designed 2-hydroxyethyl methacrylate (HEMA) polymers and HEMA-acrylamide copolymers in order to obtain a material with OH^- and NH_2^+ groups in the surface, which are elastic, biocompatible and resistant to collisions in bioreactors.

We studied kinetic parameters from the isolated microorganisms, such as growth rate (μ), NH_4^+ consumption, and NO_3^- production, during 100 days in 250mL flasks. Inhibition for high ammonium concentration, nitrite ion concentration and concentration of effluent were also studied. Later on, at 5lt scale, pO_2 was measured and O_2 consumption was determined by a static method (respirometry), widely used[4], and a dynamic method with continuous aeration[5], in order to evaluate the process on-line and monitor the system.

With all the parameters previously calculated, we designed a semicontinuous assay, beginning with $SO_4(NH_4)_2$ recovery by air stripping, at pH= with CO_3Na_2, reducing the ammonium concentration from 7 to 2,5 $N\text{-}NH_4^+$ g/l, and mobilizing the uranium. Then,

nitrification at 10-15% v/v and denitrification were performed. Ammonium was reduced in 98%, uranium was not detected at the end of the process, and the energy saving was superior in comparison with the actual technology used. Irradiated HEMA polymer showed to be a better option kinetically and much cheaper than those technologies commercialized nowadays.

MATERIALS AND METHODS

Bacterial cultures: Bacteria strains were isolated from NO_3NH_4 fertilized soil and cultivated in selective mediums during 15 days at 25ºC [(6)].

Hydrogels: HEMA monomer was irradiated at 30kGy, at 4kGh/h irradiation rate. Swelling dynamic and equilibrium were determined by Cuggino methodology[7]. Swelling rate (qw) was determined gravimetrically at different times using the equation 1;

$$qw = mh / ms \quad (1)$$

and during the equilibrium

$$qw = me / ms \quad (2)$$

where *mh* is the swelled hydrogel mass at each time, *me* is the hydrogel mass during the equilibrium, and *ms* is the dry hydrogel mass.

Analytic quantifications: ammonium, nitrite and nitrate concentrations were determined spectrophotometrically by normalized methods[8]. Uranium was determined by spectrophotometrically DBM method.

Growth kinetic: An approximated working range was determined to stablish bacterial growth as a function of initial subtracts: Y x/s= biomass produced per mole of subtract. Monod equations and Lineweber-Burk linearization were used. In this work, concentrations between 25 mg/l to 2100 mg/l of $N\text{-}NH_4^+$ were tested, and compared to $N\text{-}NH_4^+$ consumption, $Umax$, maximum growth, (d-1), and Ks substrate saturation constant (g/l).

Inhibition by nitrite ion: Haldene model was used for linearization according to the expression in the equation 3 [(9)]:

$$\mu = \mu max \left(\frac{S(N-NH4)}{(Ks+S)+\left(1+\left(\frac{HNO\,2}{Ki}\right)\right)} \right) \quad linearized\ by\ \frac{1}{\mu} = \frac{1.HNO2}{\mu max} + \frac{1}{\mu max} \quad (3)$$

Inhibition by effluent: different effluent concentrations were tested with 10% v/v of initial inoculum of 10^6cells/mL, and 5, 10, 15 and 20 %v/v of effluent.

Respirometry: Oxygen uptake rate (OUR) was evaluated as static method, and Weismman method for dynamic studies, linearized in order to calculate Ks and $Rmáx$ with the equation 4 [10].

$$(NH3o) - \frac{NH3}{ln\frac{NH3o}{NH3}} = \frac{(RBao * time - Ks\,Bao)}{\left(ln\frac{NH3o}{NH3}\right)} \quad (4)$$

Semicontinuous studies and biomass adhesion: with isolated cultures, adhesion capacity of microorganisms to hydrogel was studied. Tests were performed in duplicate, adding ammonium sulfate (s), and a solution of HCO_3^- 1M in order to maintain pH between 6,5 and 8.

Air stripping: Inside a 10cm diameter column of 1L (column1), air was forced to pass at pH=10 (with CO_3Na_2). Distilled product was collected in a similar column with sulfuric acid 0,1M (column 2). Remaining solution in column 1 was then treated by nitrification.

5L scale tests: Sartorius bioreactor was used, with pH and pO_2 Mettler-Toledo electrodes. pH was maintained at 7,2 by the addition of CO_3Na_2 1M. Biofilm was obtained in a synthetic culture medium, and then, once it was grown, effluent was added semicontinuously at 10 to 15 %v/v concentration, which was previously treated by air stripping. Carbonate consumption as a function of time was measured, and correlated to substrate consumption (ammonium), and mentioned later as TAN (Total Ammonium Nitrogen). CO_3^{2-}/N-NH_4^+ yield was calculated, per CO_3^{-2} mole consumed, 1 mole of N-NH3 is consumed by bacterial cells. The same procedure was follow to calculate SKON (semisaturation constant for oxidized nitrogen).

Microscopy: Microphotographs were obtained using an environmental scanning electron microscope (ESEM) FEI Quanta 200, EDAX DX4. Biofilms were treated with glutaraldehyde solution, dehydrated with mixtures of ethanol/acetone, and metalized with gold.

RESULTS AND DISCUSSION

Figure 1 shows velocity obtained by nitrification with 10%v/v inoculum. Initial concentration of ammonium was changed during time, from 240mg/l to 1400 mg/l N-NH_4^+. Lag phase was considered. In all cases, there was insoluble $CaCO_3$ present, in order to maintain pH around 8.

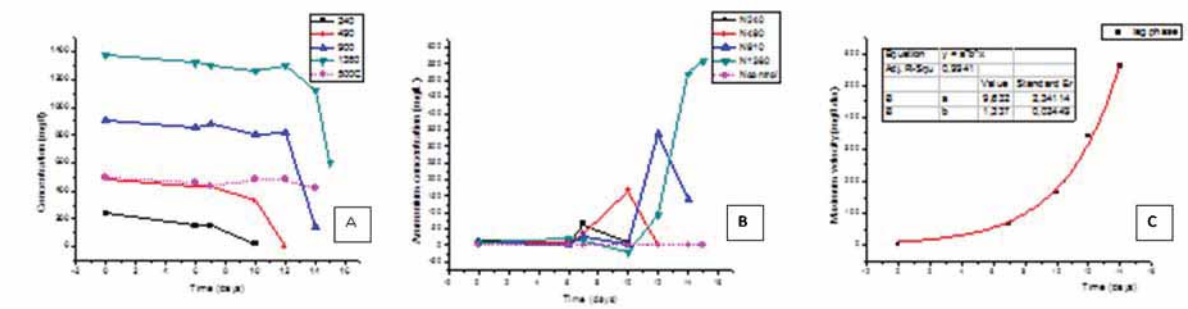


FIGURE 1. (A) Effect of initial concentration of ammonium during lag phase; (B) Velocity evolution in time as a function of substrate addition and (C) Maximum velocity as a function of initial substrate and time

Figure 1A represents N-NH_4^+ consumption as a function of time. Rose line represents the negative control (absence of microorganisms). With increasing initial ammonium concentrations, lag phase is increased, due to the time taken to be metabolized.

Figure 1B shows the incremental velocity consumption of initial ammonium, reaching the maximum value in 6 days for the inferior concentration, and 15 days for the maximum concentration of ammonium. Kinetic oxidation of ammonium shows that velocities obtained were higher, so evaluating the general process (initial – final as a function of time), they are similar. This could be explained by the characteristic behavior of autotrophic cultures.

Figure 1C represents the correlation between the velocity and NH_4^+, which validate the results by getting higher nitrification rates with increasing the age of the cultures (exponential behavior). This is why we should initiate the treatment with high bacterial cells concentrations, and also immobilized.

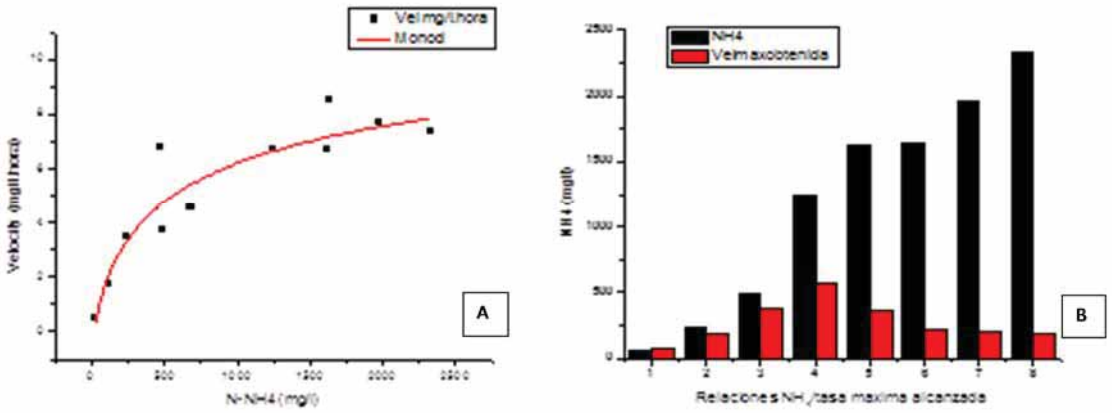


FIGURE 2. A: Initial velocity method as a function of initial N-NH_4^+. B: Velocity as a function of initial substrate. Red bars represent maximum velocity obtained with total nitrification, and black bars represent initial concentrations

Maximun velocity obtained was $279 \pm 27\ \frac{mg\ NH3}{l.day}$. and Ks constant was $Ks = 6{,}02 \pm 0{,}7\ \frac{mg\ NH3}{l}$. These parameters correspond to this particular culture, moreover the values can change because it's a mixed culture affected by changes in environmental and adaptive factors. On the other hand, while initial concentration increases over 1400 mg/l, non-ionized NH_3 begins to show a toxic effect due to diffusion through plasmatic membrane.

Inhibition by nitrite ion: This phenomenon is due to non-ionized species (HNO_2), and the kinetic of reaction corresponds to non-competitive inhibition. The constant of inhibition, Ki, calculated was $Ki = 1{,}25\ \frac{mg}{l}$, twice as much as calculated by S.Park[11], and 50% more than Carrera Muyo[9].

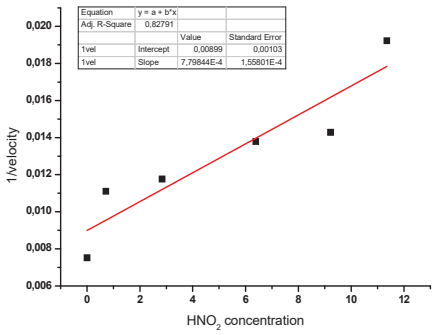


FIGURE 3. Non-competitive inhibition. 1/velocity as a function of HNO_2 concentration. Ki=1.25mg/l

Inhibition by effluent: Organic matter concentration was studied, due to high COD (Chemical oxygen demand) obtained for the effluent 900 mg/l. Ammonium was added at different concentrations in order to determine possible inhibition. **Figure 4** shows no inhibition till10%, though from 15% NH_4^+ inhibition starts to almost be complete at 20%. Tests where concentrations were higher than 20% showed similar inhibition, but an increase in pH that could be explained trough heterotrophic metabolism by CO_2 production and anoxic denitrification.

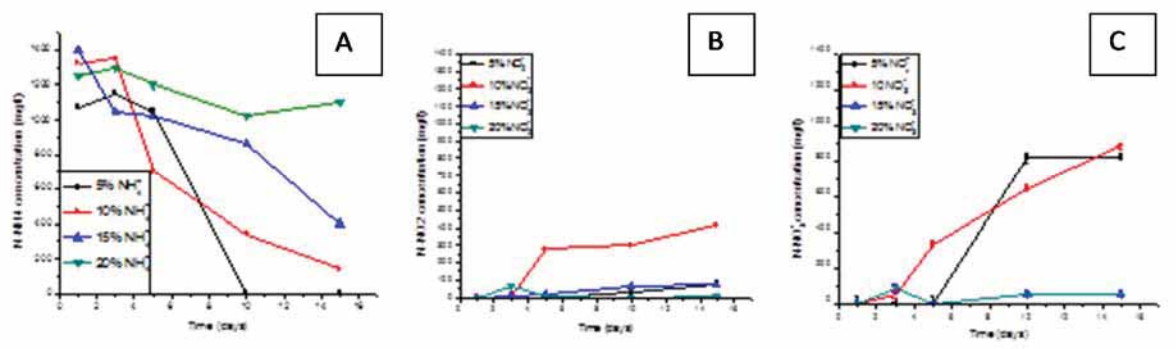


FIGURE 4. (A) Toxicity evaluation for ammonium; (B) Toxicity evaluation for nitrite ion and (C) Toxicity evaluation for nitrate ion

Semicontinuous studies: In this work, we studied HEMA biocompatibility with increasing concentrations of acrylamide and irregular geometry. **Figure 5** shows test with (Biofilm 1 and 2) and without (Planktonic 1 and 2) hydrogels, where the first ones show less nitrate accumulation at the end of the process, in comparison to free microorganisms. These tests were done in Erlenmeyer flasks with orbital agitation, where oxygen is dissolved by simple diffusion and there is no pO_2 limitation. Low oxygen concentrations could be explained by the formation of anaerobic zones where denitrification takes place. First, consortium presented partial nitrification characteristics (nitrite oxidation). However, as time passed, total nitrification showed up (total oxidation to nitrate). Biofilm age is an essential point in this process, due to positive influence in nitrite oxidation at the beginning and nitrate at the end.

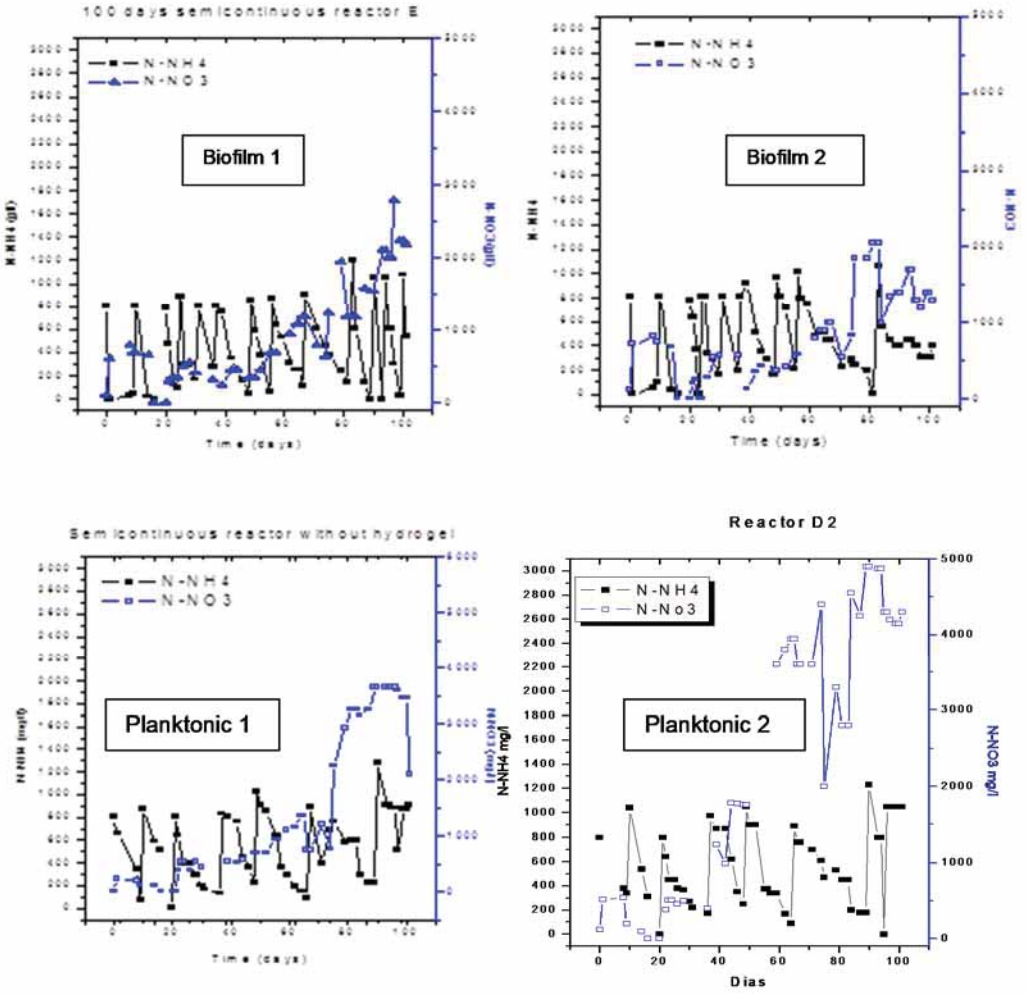
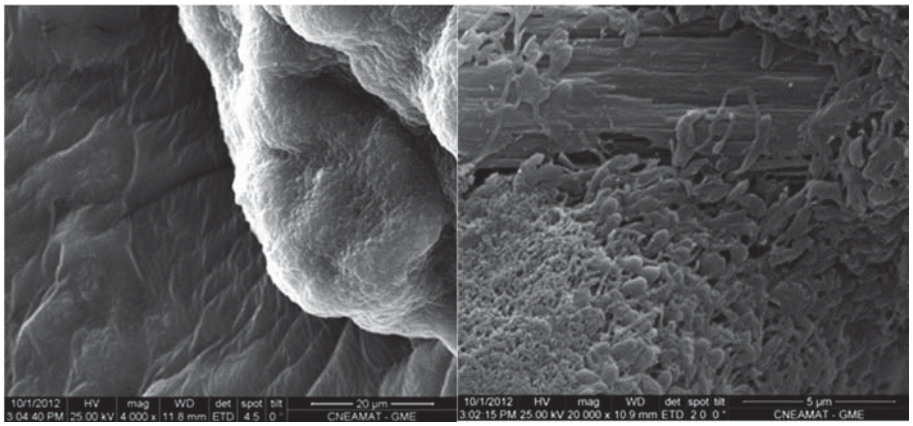


FIGURE 5. Semicontinuous nitrification during 100 days. Upper figures with hydrogel, lower ones without hydrogel

Analysis by microscopy: **Microphotograph 1** shows biofilm adhesion. On the left, we can see biofilm in contact with the hydrogel, leading to think biocompatibility is happening, though it was thought this was not possible because of BAO growth inhibition by organic matter. No significant differences were found between pure HEMA and copolymerized HEMA.



MICROPHOTOGRAPH 1. On the left, 4000X magnification; HEMA (dark grey) and biofilm (clear grey). On the right, Biofilm, 20.000X magnification

Respirometry: **Figure 6** shows respirometry results. In 6A, the on-lime control method was used and in 6B, OUR technique was applied. In the dynamic test, slope value was -2,8mg/L, equivalent to 0,0875 mmole/L.hour. In the second method, similar values were obtained. For semicontinuous bioreactor studies, since there were no differences, dynamic method was chosen to be used.

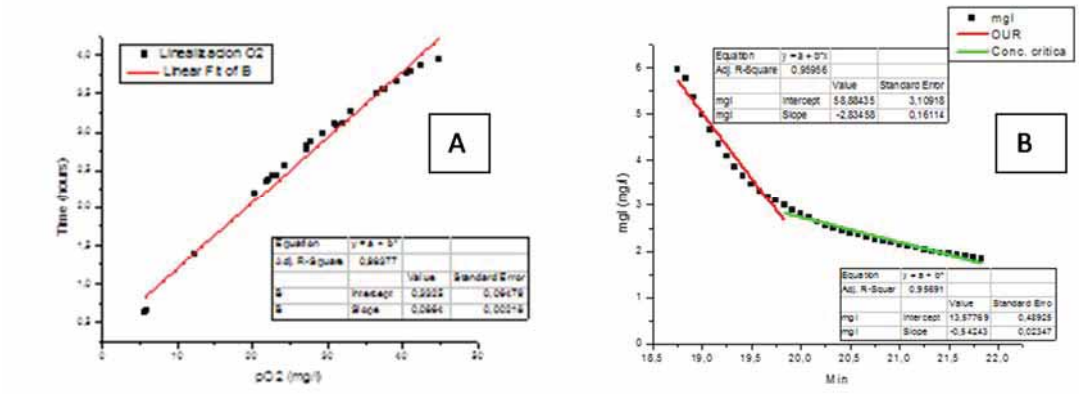


FIGURE 6. Respirometry. On-line control method

Bioreactor studies: Scale-up studies were performed under aeration and pH controlled conditions, during consecutives cycles, starting with ideal conditions to real effluent conditions. Na_2CO_3 1M balance showed 97mL consumption and 500mg of $N\text{-}NH_4^+$, which correspond to 25mmole of Na_2CO_3 and 35mmole of $N\text{-}NH_4^+$. Considering the previously calculated value of 0,085mmole/L.h, for oxygen consumption it was obtained 4mmole per cycle. Stoichiometrically, 2mole of O_2 are consumed per mole of $N\text{-}NH_4^+$

oxidized to nitrate[12]. The difference could be explained considering that not all the amount of ammonium is oxidized to nitrate, where at least 1mole of oxygen is left to other metabolic reactions in the heterotrophic microorganisms. On the right, it can be seen the increase in carbonate consumption and pO_2 rising till 100%, at the same time that $N\text{-}NH_4^+$ decreases (red line).

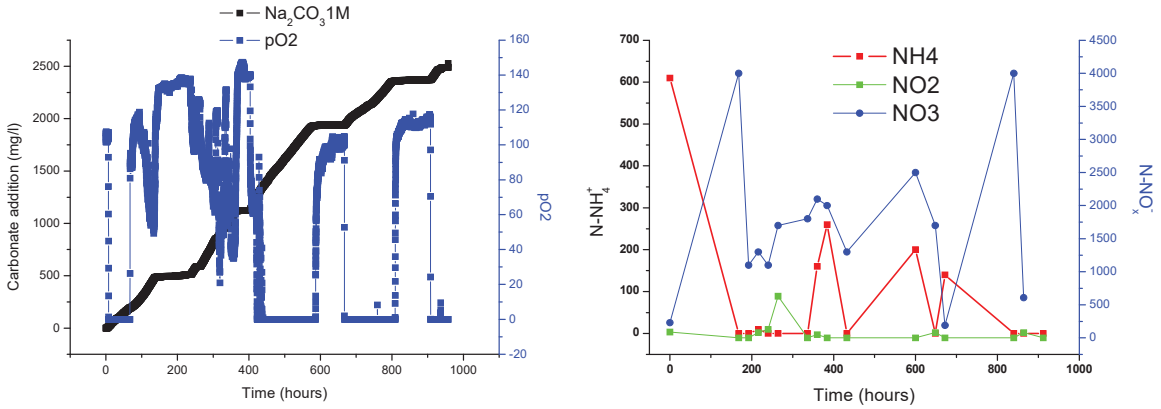


FIGURE 7. Semi continuous nitrifying test, during 1000 hours, with effluent

The first cycle started with a pH of 7,8, and high nitrification rates were obtained. However, during the 3rd cycle (not shown), nitrification stopped around 400hs, where phosphate limitation was studied but no deficiencies were found. At the same time, nitrite accumulation was found, inhibiting the process, so we proceed to repeat the cycle at pH=7,2. In this case, the process succeeded during 1000h, with no nitrite accumulation.

Regarding uranium presence, no inhibition was found during the nitrification process at the dilution rates studied (10-15%v/v). Also, no significant uranium concentrations were found at the end of the process that could be explained by the passive mechanism of biosorption, meaning teichoic acids in bacterial ligands interact with dead cells and possibly also with uranium, leading to its biosorption. However, during the process, uranium (VI) is complexed at pH=7,2 with carbonate, obtaining $UO_2(CO_3)^{4-}$, which has an electrostatic repulsion with bacterial ligands. It is known that carbonate is widely used as eluent[2], but this is contradictory with found results. Low uranium concentrations at the end of the bioreactor could be explained, then, by adsorption of the complex in the anionic amine part of the acrylamide[12] in the hydrogel. Moreover, phosphohydrolases secreted in acid and neutral environments, with a great variety of phosphodiesters represent a known mechanism of resistance to metals and possible uranium immobilization.

CONCLUSION

The bacterial consortium showed an acceptable lower rate of conversion of ammonium to nitrate. Copolymeric acrylamide-HEMA hydrogels showed great biocompatibility and a positive influence in kinetics, allowing removing remaining nitrate.
Nitrification as a treatment for nuclear industry effluents showed positive results regarding better performance to adaptation to effluent environment, at 15% concentration, during a considerate period of time and in 4L scale, which could be scaled-up to pilot scale.
Oxygen consumption and carbonate addition were two positive tools to control the process on-line. In terms of efficiency, more than 98% of conversion of ammonium to nitrate through bacterial catalysis was obtained. Maximum removal rate observed was 300mg/l.day of $N\text{-}NH_4^+$.
On the other hand, initial concentration of 300ppm of uranium was not detected at the end of the process, but other methodologies should be applied to confirm these results. Moreover, the mechanism of uranium removal by immobilization should be studied in order to recover and re-use it.
In terms of economic costs, the synthesis of HEMA by gamma-irradiation is low-cost and more accessible than already commercialized products for cell immobilization, which leads to a reduction in denitrification times due to observed simultaneous denitrification from 1000 days of treatment. Nevertheless, ammonium removal was successful in terms of energy consumption in comparison to other technologies in use, like Condorchem process, and sub-products of commercial value could be obtained.

REFERENCES

1. «Tratamiento de aguas residuales y emisiones atmosféricas». 2016. Accedido junio 20. http://condorchem.com/es/.
2. «ANAMMOX® - PAQUES». 2016. Accedido junio 20. http://es.paques.nl/productos/featured/anammox.A.C.Q. Ladeira *, C.A. Morais. 2005. «Uranium recovery from industrial effluent by ion exchange—column experiment». Minerals Engineering, 1337-40.
3. «ANITA Mox | AnoxKaldnesTM MBBR». 2016. Accedido junio 20. http://technomaps.veoliawatertechnologies.com/anita/en/anita_mox.htm.
4. Ramirez-Vargas, R., A. Ordaz, M. Carrión, I. Y. Hernández-Paniagua, y F. Thalasso. 2012. «Comparison of Static and Dynamic Respirometry for the Determination of Stoichiometric and Kinetic Parameters of a Nitrifying Process». Biodegradation 24 (5): 675-84. doi:10.1007/s10532-012-9615-0.
5. Gustavo Ciudad. s. f. «NITRIFICACION VIA NITRITOEN REACTORES DE DISCOS ROTATORIOS BAJO DOS MODALIDADES DE OPERACIÓN: CONTINUA Y SECUENCIADA». TESIS DOCTORAL 2007. U. DE LA FRONTERA, CHILE. http://www.doctoradorrnn.ufro.cl/index.php?option=com_docman&task=doc_download&gid=8.
6. Kassem A. and Nampierini. 2002. Methods in applied soil microbiology and biochemistry. Academic Press. Capitulo 4.
7. JC Cuggino. 2008. «1. Síntesis de para su posible aplicación en la liberación de drogas controladas, , 16 - 17 Octubre 2008». 2o Encuentro de Jóvenes Investigadores en Ciencia y Tecnología de Materiales – Posadas – Misiones.

https://www.google.com.ar/search?q=1.%09S%C3%ADntesis+de+para+su+posible+aplicaci%C3%B3n+en+la+liberaci%C3%B3n+de+drogas+controladas,+,++16+-+17++Octubre+2008&ie=utf-8&oe=utf-8&gws_rd=cr&ei=uyekVLjSJIGUNpCcg9AD#q=%09S%C3%ADntesis+de+para+su+posible+aplicaci%C3%B3n+en+la+liberaci%C3%B3n+de+drogas+controladas%2C+%2C++16+-+17++Octubre+2008.

8. Diaz, de Santos. 2002. «Métodos normalizados para el análisis de aguas potables y residuales».
9. Carrera, Julián, Irene Jubany, Lorena Carvallo, Rolando Chamy, y Javier Lafuente. 2004. «Kinetic models for nitrification inhibition by ammonium and nitrite in a suspended and an immobilised biomass systems». Process Biochemistry 39 (9): 1159-65. doi:10.1016/S0032-9592(03)00214-0.
10. G. Gustavo Ciudad, Arne Werner, *Cristian Bornhard. 2006. «DETERMINACIÓN DE PARÁMETROS CINÉTICOS DURANTE LA NITRIFICACIÓN MEDIANTE ENSAYOS DE RESPIROMETRÍA Y TITULACIÓN». Universidad de La Frontera, Dpto. Ingeniería Química. http://www.ingenieroambiental.com/4014/ciudad54.pdf.
11. Metcalf and Eddy. 2003. Wastewater Engineering: Treatment AND Reuse. McGraw Hill International Editions. New York (2003).
12. MAHMOUD WAZNE, GEORGE P. KORFIATIS, AND, y XIAOGUANG MENG. 2003. «Carbonate Effects on Hexavalent Uranium Adsorption by Iron Oxyhydroxide *», n.o Environ. Sci. Technol. 2003, 37,: 3619-24.
13. Park, Seongjun, y Wookeun Bae. 2009. «Modeling kinetics of ammonium oxidation and nitrite oxidation under simultaneous inhibition by free ammonia and free nitrous acid». Process Biochemistry 44 (6): 631-40. doi:10.1016/j.procbio.2009.02.002.

CHAPTER 7.30 COMBINATION OF PHOTOCATALYSIS AND BIOLOGICAL OXIDATION FOR THE DEGRADATION OF PHARMACEUTICALS IN WATER

A. Manassero (1); K. A. Villón (2); O. M. Alfano (1) and **M. L. Satuf ***(1)

(1) INTEC (UNL-CONICET), Ruta Nacional Nº 168, Paraje "El Pozo", Santa Fe, Argentina
(2) FBCB (UNL), Santa Fe, Argentina

ABSTRACT

Many pharmaceutical compounds are incompletely removed by conventional processes in wastewater treatment plants, and they are released into natural waters. These compounds are suspected to cause toxic effects on living organisms even at very low concentrations. Because of their continuous input and accumulation in the environment, they are considered as persistent micropollutants. Particularly, clofibric acid (CA), the active metabolite of the lipid regulator clofibrate, is hardly biodegradable and it has been detected in surface waters. Chemical oxidation by photocatalysis can be employed as a pre-treatment step to enhance the biodegradability of wastewaters containing CA, which could then be treated by a biological process with lower costs. This study focuses on the degradation of CA by using a combined treatment of immobilized TiO_2 photocatalysis and biological oxidation.

Photocatalytic experiments were carried out in a fixed-bed reactor filled with TiO_2-coated glass rings. The reactor was cylindrical with two flat, borosilicate glass windows. It operates in a closed recirculating circuit driven by a peristaltic pump. Illumination was provided by two sets of four black light UV lamps, placed on both sides of the reactor. The catalyst (TiO_2 P25 from Evonik) was immobilized on the glass rings (5 mm x 5 mm) by the dip-coating technique. Experiments were carried out employing rings with 1, 2 and 3 catalyst coatings, and different levels of irradiation (100%, 77%, and 37%). Each run lasted 6 hours. Along the treatment, the concentration of CA and its main intermediate, 4-chlorophenol (4-CP), were measured by HPLC. The biodegradability of the samples collected at different stages of the photocatalytic process was evaluated by means of the ratio BOD_5/COD (5-days biochemical oxygen demand/chemical oxygen demand). Biological oxidation was carried out in a laboratory-scale reactor operated in a batch mode. This reactor was mounted on an orbital shaker and it was inoculated with freeze dried bacteria, taken from a commercial consortium called Bi-Chem SM 700 of Sybrom Chemical. Along the biological treatment, the toxicity of the samples and the concentration of 4-CP were assessed. Toxicity was evaluated by means of the Microtox® acute toxicity test.

The highest degradation rate of CA in the photocatalytic reactor was obtained with rings with 3 catalyst coatings and 100 % irradiation level. After 6 h of treatment, CA was fully degraded, but the main intermediate 4-CP still remained in the solution. The BOD_5/COD ratio of the sample was enhanced from 0.2 to 0.7, indicating that this effluent could be

---

*Author for correspondence: mlsatuf@santafe-conicet.gov.ar

subjected to a consecutive biological treatment. After 7 days of biological oxidation, the complete removal of 4-CP was achieved, and the toxicity of the sample was significantly reduced, as evidenced in the decrease from 75% to 22% of the inhibition of the bioluminescence of Vibrio fischeri (Microtox® test).

Keywords: biological treatment, fixed bed reactor, pharmaceuticals, photocatalysis

INTRODUCTION

In the last years, pharmaceuticals have been detected in the aqueous environment. These compounds have been observed in surface water, ground water, sewage effluents and even in drinking water. Pharmaceutical compounds can reach the aquatic environment through various sources such as pharmaceutical industry effluents, hospital wastewaters, and excretion from humans and livestock.

Clofibric acid (CA), the primary metabolite of clofibrate, is a drug commonly used to reduce cholesterol levels in blood and it is one of the most persistent drug residues detected in the aquatic environment worldwide[1].

In many cases, conventional wastewater treatment plants are unable to completely remove pharmaceuticals from water streams; therefore, alternative processes are needed. Advanced oxidation processes (AOPs) have demonstrated to be effective in the removal of pharmaceuticals even at low concentrations. AOPs are based on the production of hydroxyl radicals (·OH), highly oxidant species with low selectivity, able to degrade a wide variety of organic pollutants. Among AOPs, heterogeneous photocatalysis has proven to be an effective method to degrade such compounds in water[2-4].

Photocatalysis employing TiO_2 particles in suspension requires a subsequent filtration step to remove the catalyst from water, increasing the treatment costs. Immobilization of the photocatalyst over inert supports is an alternative to overcome this limitation[5,6]. Additionally, the complete mineralization of organic pollutants by photocatalysis in a single-treatment process could be expensive due to operational costs. To solve this disadvantage, photocatalysis can be employed as a pre-treatment to enhance the biodegradability of wastewaters containing CA, which could then be treated by a biological process with lower costs[7,8].

The aim of this work was to evaluate the degradation of the pharmaceutical clofibric acid with a combined treatment of TiO_2 photocatalysis and biological oxidation. Photocatalysis was carried out in a fixed-bed reactor where glass rings were used as support for the catalyst. Experiments were performed by varying the initial pH of the solution, the irradiation intensity, and the number of TiO_2 coatings on the glass rings. Also, the biodegradability of the treated solution was evaluated. 4-chlorophenol (4-CP) was the main organic intermediate detected after photocatalysis. This is a highly toxic and persistent compound. Therefore, in a second stage, a biological treatment was applied to evaluate the removal of 4-CP. Along the biological treatment, the toxicity of the samples were assessed by means of the Microtox® acute toxicity test.

MATERIALS AND METHODS

Experimental set-up and procedure

Photocatalytic degradation: The photocatalytic degradation of CA was carried out in a cylindrical reactor made of stainless steel, with an inner wall of Teflon, and two circular, borosilicate glass windows. The reactor has a length of 4 cm and an internal diameter of 8.6 cm. Radiant energy was supplied by two sets of four lamps each (TL 4W/08 Black Light UVA lamps from Philips) placed vertically inside metal boxes on both sides of the reactor. The wavelength emission range of the lamps was comprised between 350 nm and 400 nm, with a peak near 365 nm. The reactor was operated in a recirculation batch mode, as shown in **Figure 1**. The storing tank was fitted with a sampling valve, a gas inlet for oxygen supply, and a water-circulating jacket to ensure isothermal conditions during the reaction time. A peristaltic pump (Masterflex) was employed to recirculate the suspension in the system.

The reactor was filled with a total of 115 borosilicate glass rings. The diameter and length of the rings was 5 mm.

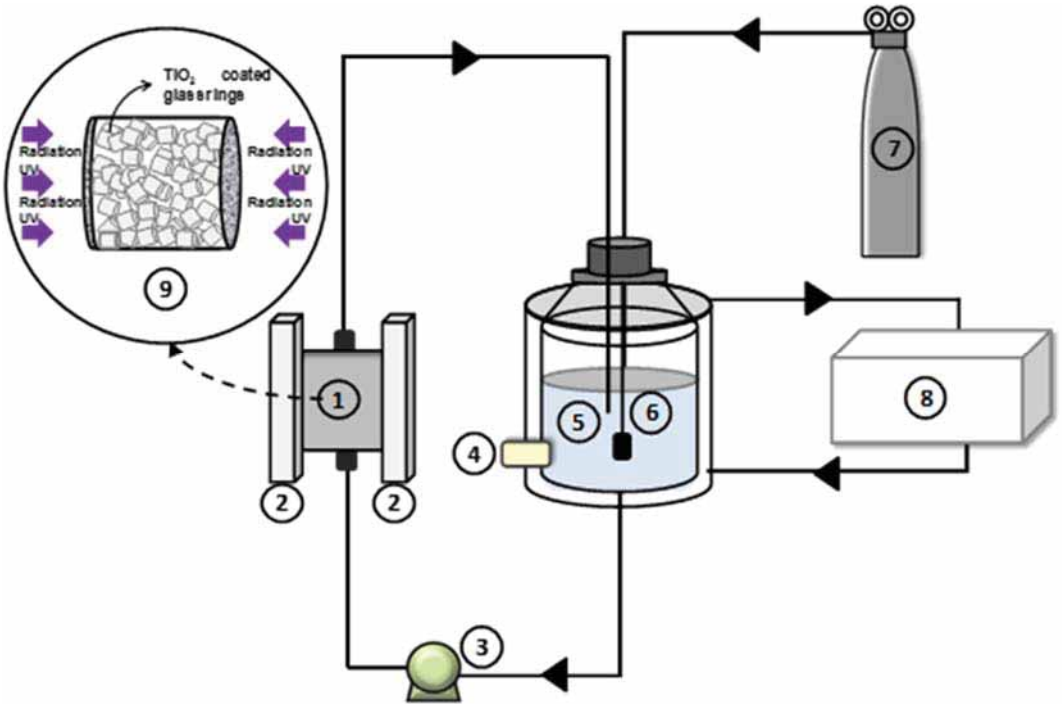


FIGURE 1. Experimental set-up of the photocatalytic reactor: 1- Reactor, 2- Lamps, 3- Pump, 4- Sampling valve, 5- Tank, 6- Thermometer, 7- Oxygen, 8- Thermostatic bath, 9- Fixed-bed reactor

In a typical experiment, the CA solution was prepared by dissolving 20 mg of CA in 1000 mL of ultrapure water. Before starting each experimental run, the reactor was filled up with the TiO_2-coated rings. Then, the CA solution was placed in the tank and it was recirculated in the system by the peristaltic pump at a flow rate of 1.5 L min^{-1} for 2 h to achieve the adsorption equilibrium between TiO_2 and CA. In the meantime, the solution

was saturated with pure oxygen by intense bubbling and the lamps were turned on in order to stabilize the photon emission. Shutters, placed between the lamps and the windows, were employed to prevent the arrival of radiation at the reactor. Once the system was stabilized, the first sample (t = 0) was taken and the shutters were removed to start the photocatalytic reaction. Samples were obtained from the tank every hour during 6 h.

The dip-coating technique was employed to obtain the TiO_2-coated rings. The rings were dipped into a suspension of 150 g L^{-1} of TiO_2 (TiO_2 Aeroxide P25, Evonik Degussa GmbH, Germany) at room temperature, and extracted at a constant withdrawal speed of 3 cm min^{-1}. After the coating, the rings were dried at 110ºC for 24 h and finally calcined at 500ºC for 2 h with a heating rate of 5ºC min^{-1}. This procedure was repeated to obtain rings with different numbers of TiO_2 coatings[9].

Experiments were performed at different initial pHs, number of coatings on the glass rings, and incident radiation levels reaching the reactor windows. Additional experiments were carried out to evaluate the direct photolysis of the pollutant and the inactivation of the catalyst coatings. **Table 1** presents the experimental conditions adopted.

TABLE 1. **Experimental conditions adopted in photocatalytic experiments**

Condition	Value
CA concentration	9.30×10^{-8} mol cm^{-3} (20 mg L^{-1})
pH	2; 5 (natural) and 10
Number of TiO_2 coatings	1, 2 and 3
Level of irradiation	37, 77 and 100 %

The natural pH of a 20 mg L^{-1} CA solution in water was 5. To obtain solutions of pH 2 and 10, appropriate volumes of HCl or NaOH solutions were added, respectively. The level of incident radiation was modified by using optical neutral filters placed between the lamps and the reactor windows.

Once the best condition for CA degradation was determined, a run that lasted 12 h was carried out to evaluate the biodegradability of the solution.

Biological oxidation: The biological oxidation was carried out in a batch, laboratory-scale reactor employing suspended microorganisms. The reactor was mounted inside a fume hood on an orbital shaker in order to ensure homogeneous suspension of microorganisms throughout the experiments. Oxygen was provided by means of a diffuser connected to an aeration pump. **Figure 2** shows a schematic representation of the experimental setup.

A commercial bacterial consortium called Bi-Chem SM 700 of Sybrom Chemical was employed. Prior to start each biological assay, the bacterial consortium was acclimated for a period of 48 hours in a culture medium that was prepared by dissolving the components detailed in **Table 2** in a total volume of 600 mL of distilled water. Once the acclimation phase ended, the biomass was recovered by vacuum filtration and it was resuspended in the effluent obtained from the photocatalytic reactor. The following physicochemical parameters were kept constant during the experimental runs: temperature: 25 ºC, pH: 6–7, dissolved oxygen (DO): 8-9 ppm, agitation: 165 rpm.

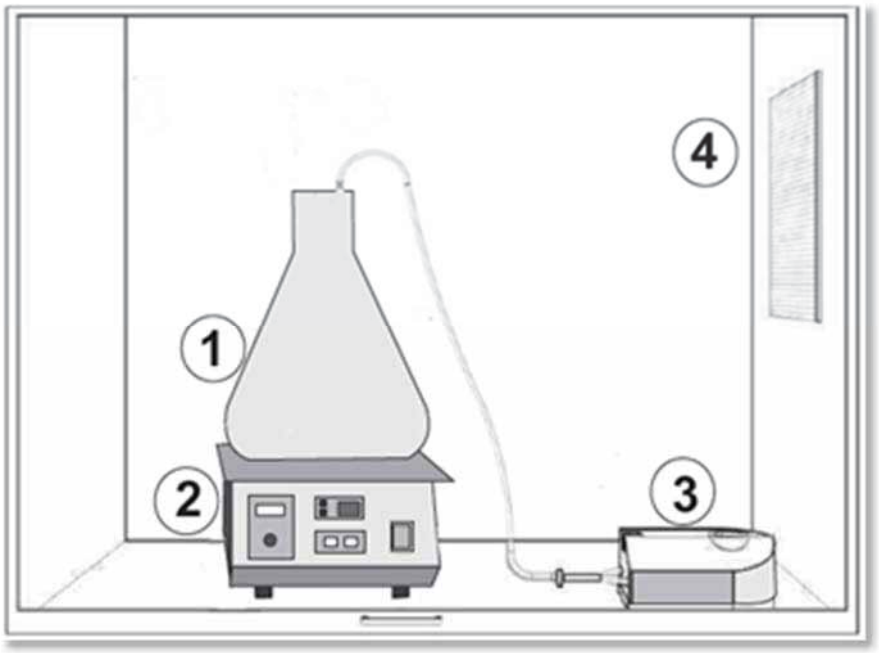


FIGURE 2. Experimental set-up of the biological reactor: 1- Reactor, 2- Orbital shaker, 3- Aeration pump, 4- Fume hood

Analytical methods. HPLC with a UV detector was employed to quantify CA and 4-CP concentrations (Waters chromatograph provided with a RP C-18 column XTerra®). The eluent was a binary mixture of acidified water (containing 0.1% v/v phosphoric acid) and acetonitrile (50:50) pumped at a flow rate of 1 mL min^{-1}. UV detection of CA and 4-CP was performed at 227 nm[10]. The mineralization of the CA was evaluated by analyzing the total organic carbon (TOC), using a Shimadzu TOC-5000 A analyzer.

The biodegradability of the samples was evaluated by the ratio BOD_5/COD (5-days biochemical oxygen demand to chemical oxygen demand). The respirometric method (Velp Scientifica BOD System) with PolySeed® inoculums (Interlab®) was employed to measure the BOD_5. COD was evaluated by a colorimetric method.

The toxicity was assessed by the acute toxicity test with *V. Fischeri* using a Microtox® 500 Analyzer.

TABLE 2. Composition of the culture medium

Component	Concentration (mg L^{-1})
Glucose	1500
$MgSO_4.7H_2O$	2000
KH_2PO_4	2000
Salts of different composition	2000
Inoculum	4000

RESULTS AND DISCUSSION

Photocatalytic degradation

Direct photolysis: In the presence of radiation but without TiO_2-coated rings, no detectable changes in the concentration of CA were observed in the system.

Effect of pH on CA degradation: The conversion of CA after 6 hours of irradiation, obtained under different initial pH values, is shown in **Figure 3.** The highest conversion was observed at pH 5. Thus, natural pH has been selected as the initial condition in the successive experiments. At pH 10, the reaction rate decreases significantly. This behavior could be attributed to the fact that, at alkaline pH, both CA and catalyst are negatively charged and adsorption is discouraged.

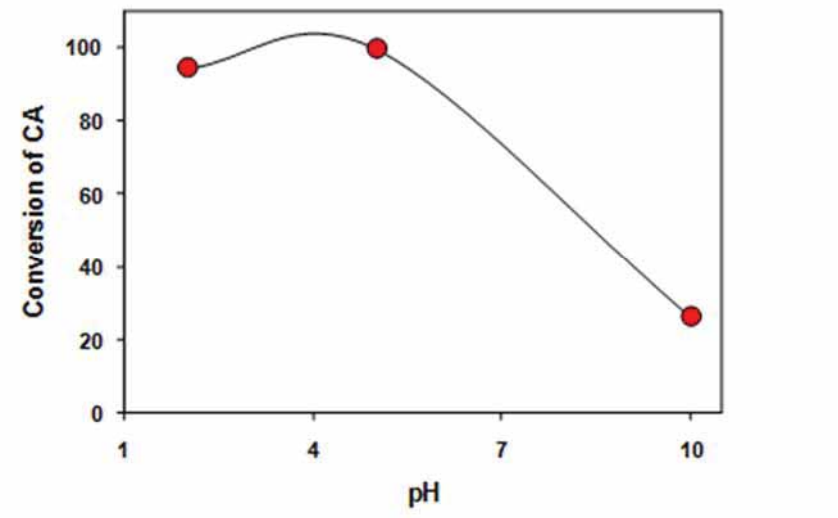


FIGURE 3. Effect of pH on the degradation of CA

Effect of the number of TiO_2 coatings on CA degradation: The conversion and mineralization of CA obtained after 6 h of treatment, for different number of catalyst coatings, are shown in **Figure 4**. As can be observed, CA degradation increased with the number of coatings, yielding a conversion of 74.1%, 89.8% and 99.5% for 1, 2 and 3 coatings, respectively. It is important to note that, in the most favorable condition (3 coatings), CA was fully degraded but complete mineralization was not achieved after 6 h of irradiation. This situation points out the presence of organic intermediates in the samples after the treatment. The organic intermediates identified were 4-chlorophenol (4-CP) and benzoquinone (BQ). **Figure 5** shows the concentration of CA, TOC, 4-CP and BQ corresponding to the experiment carried out with rings with 3 TiO_2 coatings. The intermediate compound BQ was not quantified in the successive experiences because its concentration never reached significant levels.

Because the best conversion of CA was obtained with the rings with 3 TiO_2 coatings, this condition was selected for the following experiences.

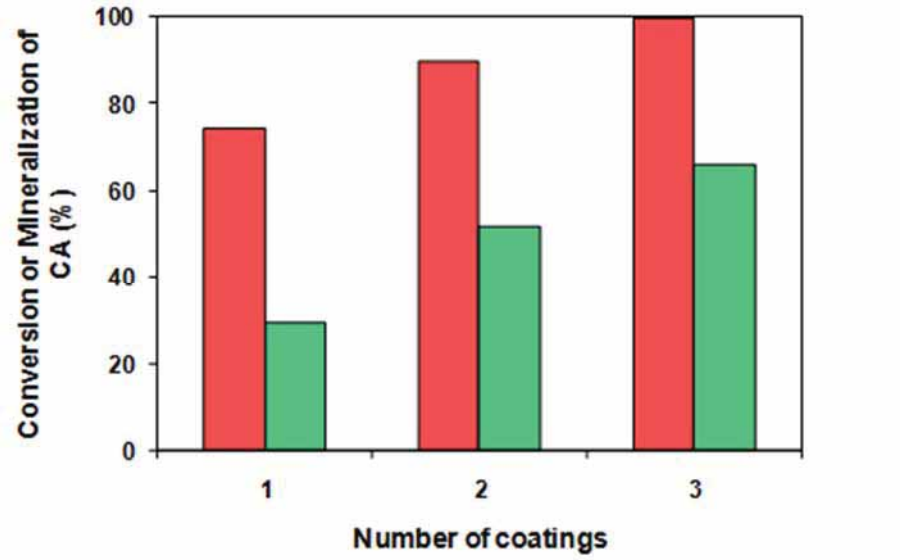


FIGURE 4. Conversion (■) and mineralization (■) of CA for different numbers of TiO_2 coatings and 100% of irradiation level.

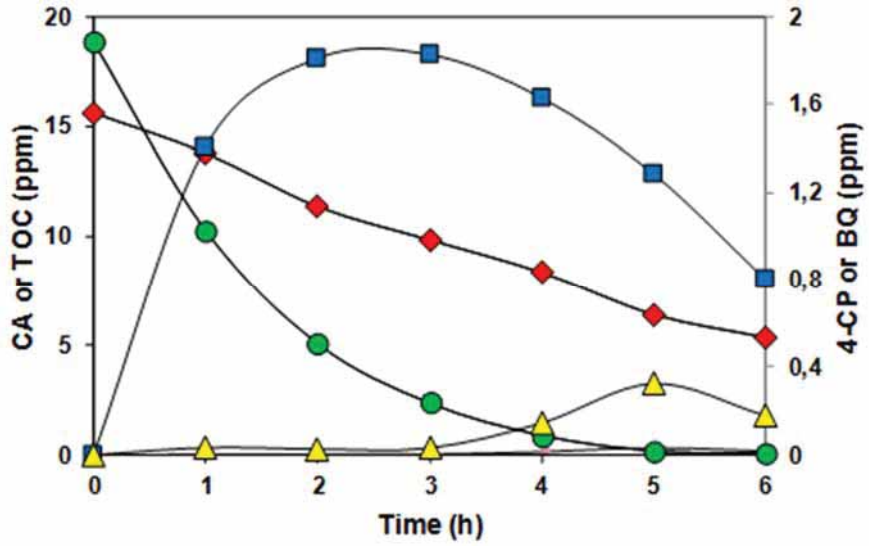


FIGURE 5. Evolution of the concentration of CA (●), 4-CP (■), BQ (▲) and TOC (◆) in the photocatalytic run employing rings with 3 coatings.

Effect of the level of incident radiation on CA degradation: As can be observed in **Figure 6**, the conversion of CA increased with the level of incident radiation. Conversion of CA obtained after 6 hours of reaction was 74.8%, 94.6% and 99.5% for 37, 77 and 100% of incident radiation, respectively.

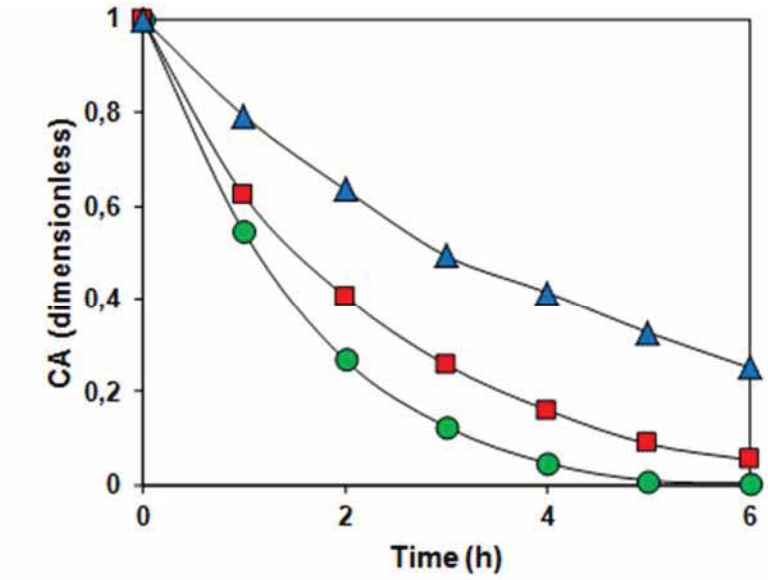


FIGURE 6. Photocatalytic degradation of CA (dimensionless) using glass rings with 3 TiO_2 coatings under different levels of irradiation. (●) 100% of irradiation, (■) 77% of irradiation and (▲) 37% of irradiation

Catalyst deactivation: To evaluate the possible loss of activity of the catalyst, four experiments were performed by reusing the glass rings with 3 TiO_2 coatings. The final conversion of CA obtained after 6 hours of irradiation was similar in all the experiences. These results show that the coated rings could be reused at least 4 times without appreciable loss of activity.

Evaluation of the biodegradability: Based on the previous results, optimal conditions were chosen to carry out an experiment to assess the evolution of the biodegradability of the CA solution photocatalytically treated. These conditions are detailed in **Table 3**.

TABLE 3. Optimal conditions obtained in the photocatalytic experiments

Condition	Value
pH	5 (natural)
Number of coatings	3
Level of irradiation	100 %

The ratio of BOD_5/COD is normally employed to express the biodegradability of wastewaters. When the ratio BOD_5/COD is higher than 0.3, the sample can be considered biodegradable, whereas ratio values lower than 0.3 indicate that the sample is hardly biodegradable[11]. The initial BOD_5/COD ratio of the CA solution was 0.21. After 6 h of photocatalytic treatment, the BOD_5/COD ratio was increased to 0.69, indicating a notable enhancement of the biodegradability. Therefore, it would be feasible to employ a biological treatment to remove the remaining organic compounds from this stage.

Longer periods of irradiation did not significantly enhance the BOD_5/COD ratio. **Table 4** presents the values of BOD_5, COD and TOC of the samples at different times of the photocatalytic treatment.

TABLE 4. Evolution of TOC and BOD_5/COD at different times of the CA solution photocatalytically treated

Time (h)	BOD_5 (mg/L O_2)	COD (mg/L O_2)	TOC (ppm)	BOD_5/COD
0	8	37.34	13.32	0.21
3	10	34.52	8.43	0.29
6	14	20.27	6.26	0.69

Biological treatment

Biological oxidation: The effluent obtained from the photocatalytic reactor was subjected to biological oxidation. The toxicity and the concentration of the intermediate compound 4-CP were measured every day, along 9 days. As observed in **Figure 6**, at the beginning of the experiment, the solution causes an inhibititory effect on the bioluminescence of *V. fischeri* of almost 80 %. By the end of the biological oxidation, inhibition represents only 20%. Additionally, in the seventh day of treatment, the intermediate 4-CP was completely removed.

These results demonstrate that the biological treatment significantly reduced the toxicity of the photocatalytic effluent, probably by removing the toxic reaction intermediate, 4-CP.

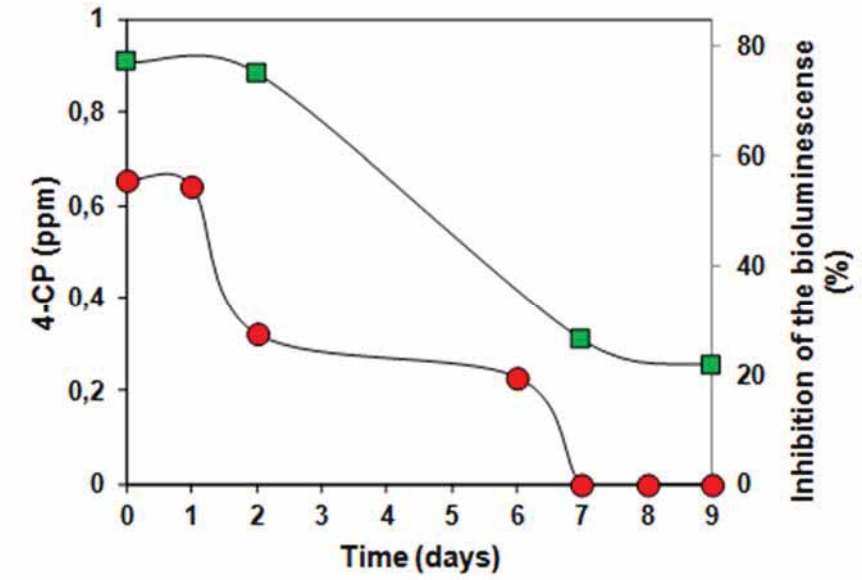


FIGURE 6. Temporal evolution of the 4-CP concentration (●) and percentage of inhibition of the natural bioluminescence of *Vibrio fischeri* (■) during the biological oxidation

CONCLUSION

A solution of the pharmaceutical clofibric acid was successfully degraded by photocatalysis in a fixed-bed reactor filled with TiO_2-coated glass rings. Complete degradation of CA, but not mineralization, was achieved after 6 h of treatment using rings with the highest number of catalyst coatings and the highest level of irradiation assayed (3 coatings and 100% of irradiation level). Additionally, the BOD_5/DOC ratio was increased from 0.21 to 0.69, indicating that photocatalysis notably enhances the biodegradability of CA solutions. The main organic intermediate produced in the photocatalytic treatment (4-CP) was removed by subsequent biological oxidation. Moreover, the toxicity of the sample was significantly reduced at the end of the biological treatment.

ACKNOWLEDGMENTS

The authors are grateful to Universidad Nacional del Litoral (UNL), Consejo Nacional de Investigaciones Científicas y Técnicas (CONICET), and Agencia Nacional de Promoción Científica y Tecnológica (ANPCyT) for financial support.

REFERENCES

1. Rosal R., Gonzalo M. S., Rodríguez, A., García-Calvo, E. Ozonation of clofibric acid catalyzed by titanium dioxide. J. Hazard. Mater. 169 (2009) 411-418.
2. Giraldo A., Peñuela G., Torres-Palma R., Pino N., Palominos R., Mansilla H. Degradation of the antibiotic oxolinic acid by photocatalysis with TiO_2 in suspension. Water Res. 44 (2010) 5158-5167.
3. Martínez C., Canle M., Fernández M., Santaballa J., Faria J. Kinetics and mechanism of aqueous degradation of carbamazepine by heterogeneous photocatalysis using nanocrystalline TiO_2, ZnO and multi-walled carbon nanotubes–anatase composites. Appl. Catal. B Environ. 102 (2011) 563-571.
4. De la Cruz N., Dantas R., Giménez J., Esplugas S. Photolysis and TiO_2 photocatalysis of the pharmaceutical propranolol: Solar and artificial light. Appl. Catal. B Environ. 130-131 (2013) 249-256.
5. Manassero A., Zacarías S. M., Satuf M. L., Alfano O. M. Intrinsic kinetics of clofibric acid photocatalytic degradation in a fixed-film reactor. Chem. Eng. J. 283 (2016) 1384-1391.
6. Manassero A., Satuf M. L., Alfano O. M. Photocatalytic degradation of an emerging pollutant by TiO_2-coated glass rings: a kinetic study. Environ. Sci. Pollut. Res. DOI 10.1007/s11356-016-6855-2
7. Yahiat S., Fourcade F., Brosillon S., Amrane A. Removal of antibiotics by an integrated process coupling photocatalysis and biological treatment- Case of tetracycline and tylosin. Int. Biodeter. Biodegr. 65 (2011) 997-1003.
8. Chen Ch-Y., Kuo J-T., Yang H-A., Chung Y-Ch. A coupled biological and photocatalysis pretreatment system for the removal of crystal from wastewater. Chemosphere 92 (2013) 696-701.
9. van Grieken R., Marugán J., Sordo C., Martínez P., Pablos C. Photocatalytic inactivation of bacteria in water using suspended and immobilized silver-TiO_2. Appl. Catal. B-Environ. 93 (2009) 112-118.

10. Dordio A. V., Candeias A. J. E., Pinto A.P., Teixeira da Costa C., Palace Carvalho A.J. Preliminary media screening for application in the removal of clofibric acid, carbamazepine and ibuprofen by SSF-constructed wetlands. Ecol. Eng. 35 (2009) 290-302.
11. Al- Momani F., Touraud E., Degorce-Dumas J.R., Roussy J., Thomas O. Biodegradability enhancement of textile dyes and textile wastewater by VUV photolysis. J. Photoch. Photobio. A 153 (2002) 191-197.

CHAPTER 7.31 A HYBRID ELECTROOXIDATION/ELECTROCOAGULATION SYSTEM USING Ti/ PbO_2-Al/Fe ELECTRODES FOR CRYSTAL VIOLET DYE REMOVAL

Celestino García-Gómez (1,2); Eneydi Urias (1); Pablo Gortáres-Moroyoqui *(1) and Ruth Gabriela Ulloa-Mercado (1)

(1) Departamento de Biotecnología y Ciencias Alimentarias, Instituto Tecnológico de Sonora, 5 de Febrero, 818 sur. C. P. 85000 Obregón, Sonora, México.
(2) Facultad de Agronomía, Universidad Autónoma de Nuevo León, Francisco Villa S/N, C.P. 66050, General Escobedo, Nuevo León, México.

ABSTRACT

An electrochemical reactor was used to remove crystal violet (CV) by electrooxidation and electrocoagulation process simultaneously. Response surface methodology based on central composite design was used to optimize various operating parameters of the hybrid electrocochemical process for the treatment of industrial effluent. The effects of three independent parameters such as electrolysis time (X_1), recirculation flow rate (X_2), and current intensity (X_3) on CV removal and energy consumption were investigated. A quadratic model was used to predict the CV removal and energy consumption in different conditions. In order to achieve the maximum CV removal and minimum energy consumption, the optimum conditions were obtained by mathematical and statistical methods. The results showed that maximum CV removal efficiency could be achieved at optimum conditions of electrolysis time (X_1)= 20 min, recirculation flow rate (X_2)= 125 $mL \cdot min^{-1}$ with current intensity (X_3)= 0.5 A. In conclusion, hybrid electroxidation process could be applied successfully for removing pollutants from effluent.

Keywords: CCD, electrocoagulation, electrooxidation, removal.

INTRODUCTION

Waterways polluted with dyes from industrial activities have become a problem since the dyes can cause life-threatening diseases and induce abnormal variations in the aquatic ecosystem[1]. The discharge of dyes, even at small concentrations, may be toxic and difficult to remove due to their complex structure[2]. Thus, treatment of coloured wastewater is a major concern for the scientific community.

Triphenylmethane dye compounds, for example crystal violet (CV) a synthetic basic cationic dye, are largely applied in the textile, leather, paper, cosmetic, and food industries. Furthermore, CV is used as a dermatological agent, veterinary medicine, additive to poultry feed to inhibit propagation of harmful bacteria[3,4].

CV in wastewater cause colouration inducing a severe risk to aquatic life, because of the color in water bodies reduces penetration of sunlight to the lower layers. In drinking water, CV constitutes a potential human health hazard, due to this cationic dye can

---

*Author for correspondence: pablo.gortares@itson.edu.mx

easily interact with negatively charged cells membrane surfaces, and be introduced into cells and be concentrated in cytoplasm[5]. This compund is characterized by their low biodegradability and it is estimated that about 20% of the dye remains in the effluents during the industrial process[6].

Biological treatments are been the most feasible option for removing organic pollutants. Nevertheless, these options cannot be used to textile wastewaters due to the toxicity of dyes against the microorganisms used in the treatments[7]. Methods based on the generation and use of hydroxyl radical (•OH) are called Advanced Oxidation Processes (AOPs). Several technologies as UV/O_3, H_2O_2/UV, H_2O_2/O_3, Fenton's reagent, photo-Fenton, and TiO_2 photocatalysis have been successfully evaluated for removal of organic compounds in water[8]. The existence of ionic compounds in water generate conductivity, benefitting wastewater treatment technologies based on electrochemical procedures. Electrochemical systems are promising and versatile alternatives that have the possibility to replace or complete already existing processes becoming ideal tools for addressing environmental problems[9]. Principal reagents used are electrons, which are clean and is not necessary an extra reagent. Electrocoagulation (EC) is a process of destabilizing of suspended, emulsified, or dissolved contaminants in a liquid medium by introducing an electric potential[10]. Meanwhile, in the electrooxidation (EO) process, the organic pollutants are destroyed by direct or indirect oxidation process. In the direct anodic oxidation, the molecules are adsorbed on the anode surface and destroyed by the anodic electron transfer reaction. In indirect oxidation, strong oxidants such as hydrogen peroxide, hypochlorite/chlorine, and ozone are electrochemically produced, destroying the pollutants in the bulk solution[11]. In both processes, the performance of the treatment depends of the current intensity, the time of electrolysis, the anode/cathode electrodes, and flow rates [12]

The objective of this study was to develop a single hybrid system combining the electrooxidation and electrocoagulation using Ti/PbO_2 and Al/Fe electrodes capable to remove CV dye. Different operational conditions of current intensity, electrolysis time, and flow rate were analyzed for optimization by response surface methodology (RSM) based on central composite design (CCD) model.

MATERIALS AND METHODS

Chemicals. All the reagents used for the present study are reagent grade. Crystal violet dye obtained from Sigma–Aldrich was used without further purification. The synthetic effluent was prepared from CV dye dissolved in distiller water. $NaSO_4$ at 400 $mg \cdot L^{-1}$ was used as a supporting electrolyte to increase the conductivity of the solution.

Electrooxidation/electrocoagulation hybrid process. The electrooxidation/electrocoagulation (EO/EC) experiments were carried out in an up-flow mode. The electrochemical reactor flow cell model used for the study is shown in **Figure 1**. Electrochemical experiments were carried out using iron (Fe) and titanium (Ti) as cathode and lead oxide-coated titanium substrate (Ti/PbO_2) and aluminum (Al) as anode. The operation volume was 550 mL, electrodes of 15 cm height and 2 mm thickness were used. At the top edge of the electrodes, provisions were made for power supply. Electrodes were connected to 3 A and 0–30 V regulated power supply. A

peristaltic pump was connected using silicone rubber tubes for a batch recycling operation.

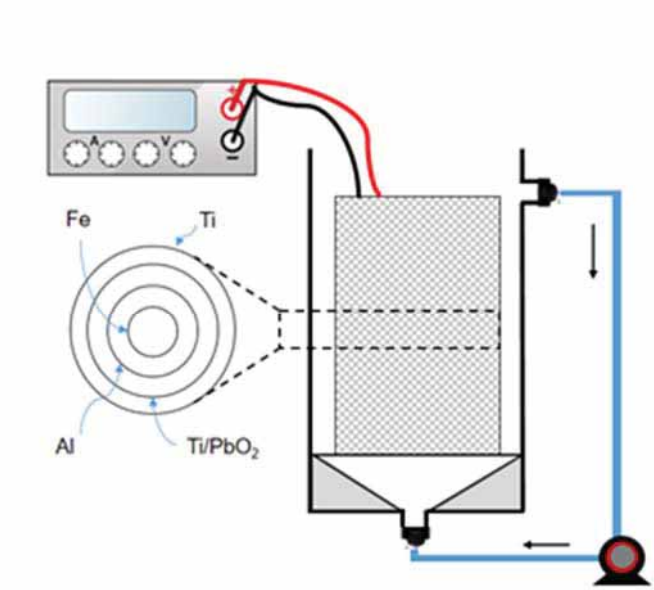


FIGURE 1. Schematic of electroxidation–electrocoagulation (EO/EC) hybrid system

Design of experiments (DOE). The response surface methodology (RSM) is used for process optimization. This is appropriate for fitting a second order polynomial response with a minimum number of runs. Therefore, an attempt has been made by using Software Design Expert 7.0 (State-Ease Inc., USA) for the DOE, statistical analysis of data, development of regression models and optimization of EO/EC process conditions with the factorial experimental design of central composite design (CCD). Experiments for CV removal were optimized using RSM which was applied to describe the correlation between experimental factors (independent variable) and observed results (responses). RSM was used to assess the optimum values of the three factors (current density, electrolysis time, and flow rate) by which desirable efficiencies of the two responses (CV removal and energy consumption) could be obtained. The experimental data obtained from the CCD model can be represented by equation 1.

$$\mathrm{Y} = b_0 + \sum_{i=1}^{k} b_i X_j + \sum_{i=1}^{k} b_{ii} X^2 + \sum_{j} \sum_{i=1}^{k} b_{ij} X_i X_j + e_i \quad (1)$$

Where, Y is the predicted response; k is the number of patterns; X_i and X_j are the coded variables; b_0 is constant; b_i is the linear coefficient; b_{ii} is the regression coefficient for squared effects, b_{ij} is the interaction coefficient; i and j are the index numbers for factor; and e_i is the residual error.

CCD with three input variables consists of 20 experiments with 8 orthogonal two levels full factorial design points (coded as ±1), 6 axial points (or star point coded as ± α

= 1.682) and 6 replications of the central points to provide an estimation of the experimental error variance. The actual values of process variables and their variation limits were selected based on the values obtained in preliminary experiments and coded as shown in **Table 1**. Analysis of variance (ANOVA) was applied to the data obtained from CCD. The R^2 coefficient represents the fitness of polynomial models. The p-value of every single term in the model given in **Eq. (1)** was predicted at a 95% confidence level. 3D surface plots predict the response as a function of two chosen factors.

TABLE 1. Coded and actual values of the variables of the design of experiments for the hybrid EO/EC process

Independent variables	Factor	Levels				
		-α	**-1**	**0**	**+1**	**+α**
Electrolysis time (min)	X_1	13.18	20	30	40	46.82
Recirculation flow rate ($mL \cdot min^{-1}$)	X_2	155.27	188	236	284	316.73
Current intensity (A)	X_3	0.33	0.5	0.75	1	1.17

α=axial points

Analytical methods. Initial concentration of CV of 10 mg L^{-1} was chosen for experimentation. The dye concentration was measured using a UV/Vis spectrophotometer (Cintra 10e, USA) at a wave- length corresponding to the maximum absorbance of the dye (λ_{max} =590 nm). The color removal efficiency, CV (%), was calculated using:

$$CV(\%) = \frac{A_O - A_i}{A_O} * 100 \quad (2)$$

A_O and A_i are the absorbance values of the dye solution before and after treatment, respectively.

The power consumption was calculated as:

$$E = \frac{VIt}{V_t} \quad (3)$$

Where, V is cell voltage (V), I is applied current (A), t is electrolysis time (hour) and V_t is the volume of work (m^3). The total power consumption is expressed in terms of kWh m^{-3} for the process based on the volume of the treated volume.

RESULTS AND DISCUSSION

Statistical analysis. **Table 2** shows the run number, experimental conditions, response, CV removal percentage, and power consumption with the predicted values. Based on this experimental design results, the regression equations with coded variables obtained for describing the CV removal using EO/EC processes suggested a second-order polynomial equation with interaction terms an empirical relationship. The final equations in terms of coded factors can be presented as follows:

$$CV\ removal\ (\%) = +57.88 + 9.44X_1 - 1.68X_2 + 3.06X_3 - 1.70X_1X_2 + 1.71X_1X_3 + 3.0X_2X_3 + 3.66X_1^2 - 1.60X_2^2 - 0.65X_3^2 \quad (4)$$

$$Energy\ consumption, (kWh\ m^{-3}) = +1.89 + 0.64X_1 - 0.023X_2 + 0.91X_3 - 0.044X_1X_2 + 0.27X_1X_3 + 0.013X_2X_3 + 0.028X_1^2 - 0.0085X_2^2 + 0.0.91X_3^2 \quad (5)$$

The obtained CCD experimental data was analyzed by two different tests, namely the sequential model sum of squares and model summary statistics in order to obtain effective regression models among various models such as linear, interactive, quadratic and cubic. The results are shown in the **Tables 3** and **4** for the COD removal percentage and power consumption. According to **Tables 3** and **4**, it was found that the quadratic models exhibited higher R^2, adjusted R^2 and predicted R^2, when compared to the other models. The cubic model was found to be aliased and cannot be used for further modeling of experimental data. A model is aliased means that not enough experiments have been run to independently estimate all the terms for that model. Whenever, there are fewer independent points in the design than there are terms in the model, some parameters cannot be estimated independently. A model is aliased means that model is inappropriate for further investigation. The sequatial model sum of squares. showed that the p-values were lower than 0.0591 for the quadratic and linear models. Therefore, both of these could be used for further study. However, the model summary statistics showed that after excluding the cubic model which was aliased, the quadratic model was found to have the maximum “adjusted R^2” and “predicted R^2” values. Similarly, the analysis was carried out for power consumption and the results are given in **Table 4**. Therefore, the quadratic model was chosen to describe the effects of process variables on the treatment of CV using the EO/EC hybrid process.

TABLE 2. Experimental design matrix and response based on the experimental runs and predicted values on CV removal (%) and Energy consumption proposed by CCD design

X_1 (min)	X_2 (mL·min^{-1})	X_3 (A)	Removal efficiency (%)		Energy Consumption (kWh·m^{-3})	
			Actual	Predicted	Actual	Predicted
15.00	120.91	0.75	59.07	56.18	1.91	1.90
6.59	131.00	0.75	45.32	52.36	0.87	0.89
15.00	131.00	0.33	50.14	54.57	0.64	0.62
15.00	131.00	1.17	64.81	64.87	3.67	3.68
15.00	131.00	0.75	58.00	57.88	1.98	1.89
10.00	137.00	1.00	59.64	55.52	2.06	2.03
15.00	131.00	0.75	58.25	57.88	1.94	1.89
23.41	131.00	0.75	86.65	84.11	3.09	3.05
15.00	131.00	0.75	58.91	57.88	1.74	1.89
20.00	125.00	1.00	70.94	75.18	3.94	3.87
10.00	125.00	0.50	54.40	52.78	0.73	0.71
20.00	125.00	0.50	70.70	71.64	1.45	1.54
15.00	141.09	0.75	43.10	50.53	1.84	1.83
10.00	137.00	0.50	54.24	46.82	0.71	0.73
15.00	131.00	0.75	58.65	57.88	1.84	1.89
20.00	137.00	1.00	75.99	74.42	3.70	3.77
10.00	125.00	1.00	50.74	49.48	1.97	1.97
15.00	131.00	0.75	57.47	57.88	1.88	1.89
15.00	131.00	0.75	56.75	57.88	1.98	1.89
20.00	137.00	0.50	60.82	58.88	1.42	1.38

The significance and adequacy of the model were tested by analysis of variance (ANOVA). The F-test of the regression models produced very low p-values (<0.0001), indicating that both models were highly significance. The determination coefficients (R^2) of the models indicated that 87.81% and 99.66% of the total variability could be explained by the models for the CV removal and Energy consumption, respectively. Adequacy check of the proposed model is an important part of the analytical procedure. Good adequacy ensures that the approximating model provides an adequate approximation to avoid poor or misleading results. The comparison between the experimental and predicted value from the model is given in **Table 2** and **Figure 2a** and **2b**. It was observed that the model predictions matched the experimental values and the data points lay close to the diagonal line**.**

TABLE 3. Sequential model sum of squares and model summary statistics for percentage CV removal

Sequential model sum of squares Source						
Source	**Sum of squares**	**df**	**Mean square**	**F value**	**p-value**	**Prob > F**
Mean vs Total	71352.26	1	71352.26			
Linear vs Mean	1383.98	3	461.33	12.00	0.0002	Suggested
2FI vs Linear	118.32	3	39.44	1.03	0.4107	
Quadratic vs 2FI	253.03	3	84.34	3.46	0.0591	Suggested
Cubic vs Quadratic	189.70	4	47.43	5.27	0.0363	Aliased
Residual	54.04	6	9.01			
Total	73351.33	20	3667.57			
Model summary statistics						
Source	Std. Dev.	R-Squared	Adjusted R-Squared	Predicted R-Squared	PRESS	
Linear	6.20	0.6923	0.6346	0.4421	1115.30	Suggested
2FI	6.18	0.7515	0.6368	0.1621	1675.06	
Quadratic	4.94	0.8781	0.7683	0.0814	1836.43	Suggested
Cubic	3.00	0.9730	0.9144	-4.6127	11220.11	Aliased

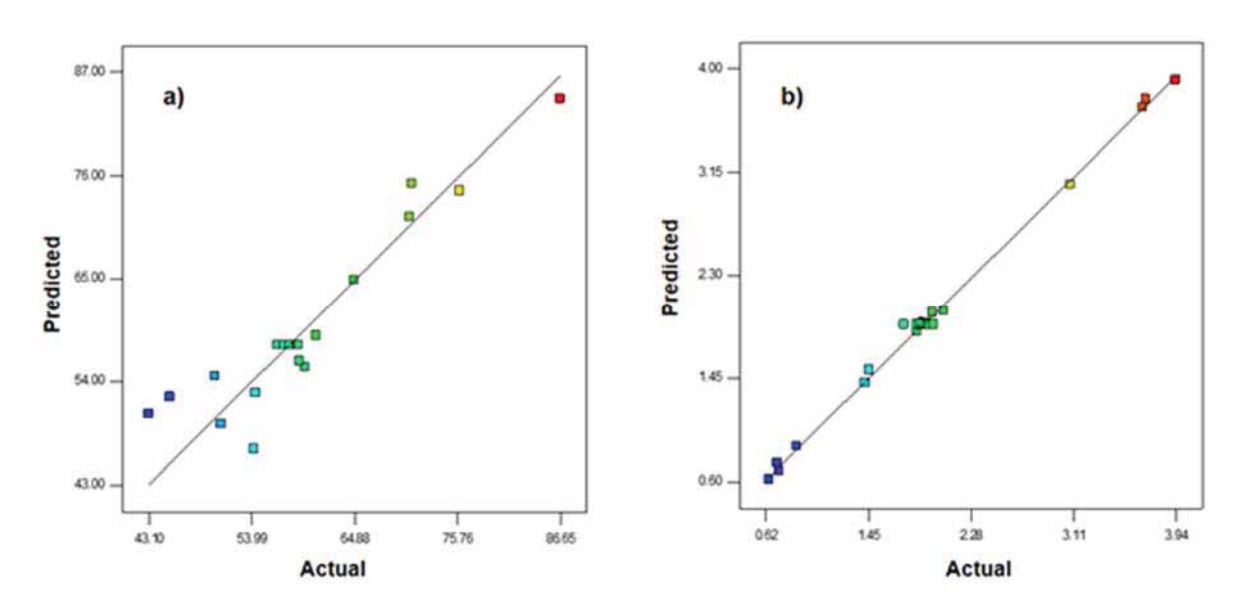


FIGURE 2.The actual and predicted response plot of (a) CV removal y (b) energy consumption

TABLE 4. Sequential model sum of squares and model summary statistics for energy consumption

Sequential model sum of squares Source						
Source	**Sum of squares**	**df**	**Mean square**	**F value**	**p-value**	**Prob > F**
Mean vs Total	77.45	1	77.45			
Linear vs Mean	16.97	3	5.66	113.91	< 0.0001	
2FI vs Linear	0.60	3	0.20	13.67	0.0003	
Quadratic vs 2FI	0.13	3	0.044	7.19	0.0074	Suggested
Cubic vs Quadratic	0.017	4	0.004	0.56	0.6987	Aliased
Residual	0.044	6	0.007			
Total	95.22	20	4.76			
Model summary statistics						
Source	Std. Dev.	R-Squared	Adjusted R-Squared	Predicted R-Squared	PRESS	
Linear	0.22	0.9553	0.9469	0.9198	1.42	
2FI	0.12	0.9892	0.9843	0.9762	0.42	
Quadratic	0.078	0.9966	0.9935	0.9881	0.21	Suggested
Cubic	0.086	0.9975	0.9922	0.9908	0.16	Aliased

The residuals indicated how well the model satisfied the assumptions of ANOVA, whereas the internally studentized residuals measured the standard deviations separating the actual and predicted values. The data were also analyzed to check the normality of the residuals. Results are shown **Figure 3a** and **3b** in which the normal% probability plots of the studentized residuals for (a) CV removal and (b) energy consumption using the EO/EC hybrid process are indicated. A normal probability plot indicates whether the residuals follow a normal distribution, in which the points will form a straight line. Some scatters are expected even with normalized data[13]. It can therefore be concluded from **Figure 3a** and **3b** that the data is normally distributed.

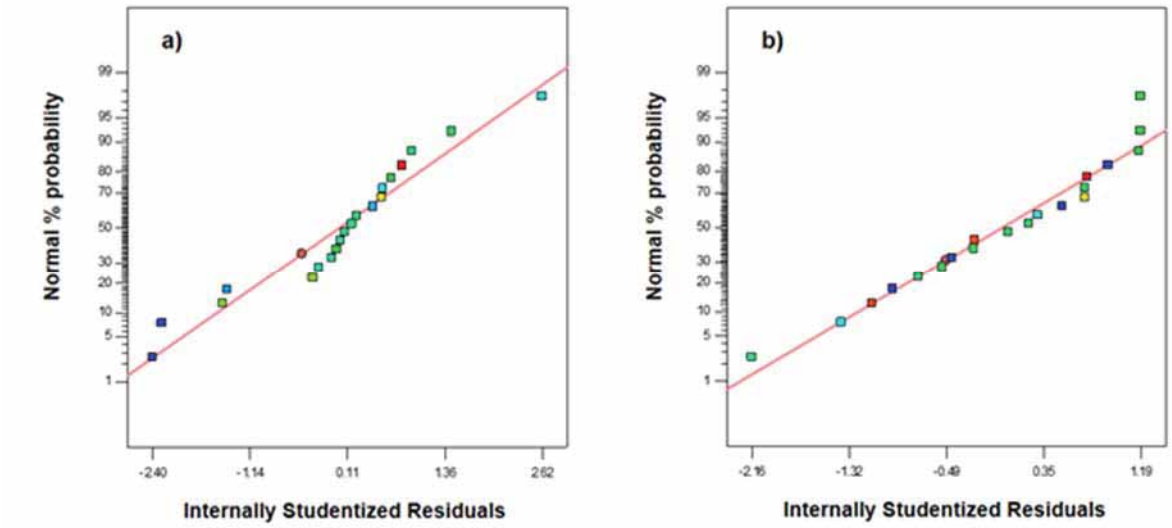


FIGURE 3. The normal% probability and external studentized residuals for CV removal y b) energy consumption

Electrolysis time and Current intensity are the most important parameters for controlling the reaction rate in the hybrid electrochemical processes. The combined effect of electrolysis time (X_1) and current intensity (X_3) on CV removal efficiency and energy consumption were carried out by varying X_1 from 13.18 to 46.82 min under different X_3 from 0.66 to 2.34 A. The results are plotted in **Figure 4a** and **4b** in which shows that the CV removal efficiency was increased with an increase in current intensity and electrolysis time, meanwhile, to lower electrolysis time a change in the current intensity is negligible. Energy consumption also increased with increasing current intensity at any recirculation flow rate. This might be due to potential increase in the cell potential with increase in current intensity, which directly affected the power consumption of the hybrid electrochemical process. In terms of operating cost, the hybrid electrochemical process must operate at limiting current intensity.

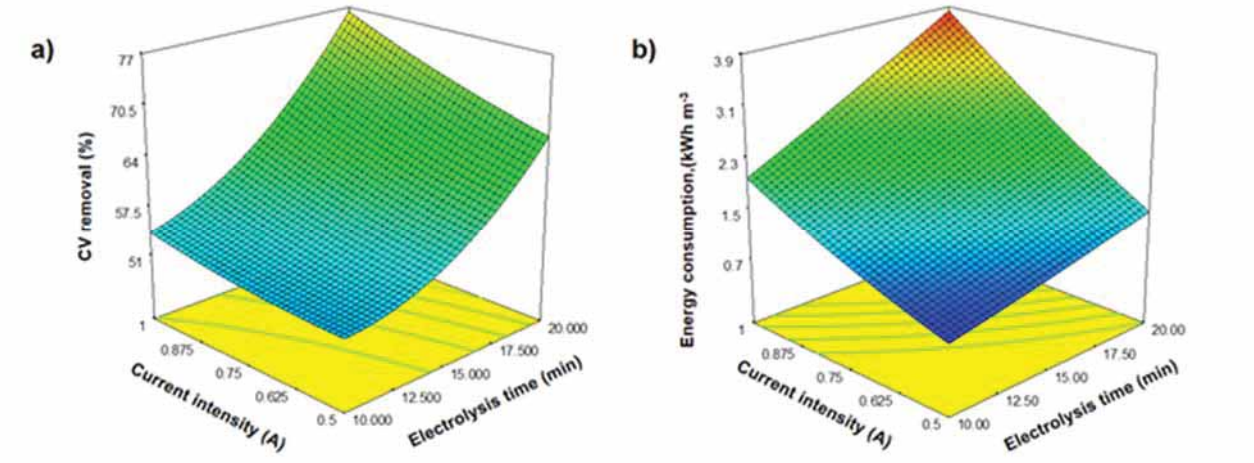


FIGURE 4. Response surface plots for the effects of current intensity and electrolysis time on (a) % CV removal and (b) energy consumption

Optimization. One of the main objectives of this investigation is to obtain the optimal conditions for the removal of CV and energy consumption from synthetic wastewater using a hybrid electrochemical process. The results were optimized using the regression equation of RSM based on the CCD. In the optimization of electrolysis time (X_1), recirculation flow rate (X_2), and current intensity (X_3) were selected as within range, the response CV removal (Y_1) was maximized and energy consumption (Y_2) was minimized. Under these optimum of experimental conditions such as electrolysis time (X_1)= 20 min, recirculation flow rate (X_2)= 125 mL·min^{-1} with current intensity (X_3)= 0.5 A and the percentage removal of CV and energy consumption was found to be 71.63% and 1.51 kWh m^{-3}, respectively which are validated by conducting additional experiments under the above optimal conditions. A mean value of 70.89% for CV removal and 1.49 kWh m^{-3} for energy consumption were obtained from the experimental, which is in close agreement with the predicted values obtained. The good correlation between these actual and predicted results indicate that the reliability of central composite design incorporate desirability function method and it could be effectively used to optimize the hybrid electrochemical process parameters.

CONCLUSION

In this work, CV was treated by a hybrid electrooxidation/electrocoagulation processes. A comparison among these processes in terms of percentage removal and energy consumption was performed. Based on the experimental results, an empirical relationship between the response and independent variables was obtained and expressed by the second-order polynomial equation. The effects of the experimental parameters on the percentage CV removal and energy consumption of the distillery wastewater was established by the response surface predicted by the model. The analysis of variance showed a high coefficient of determination value, thus ensuring a satisfactory adjustment of the second-order regression model with the experimental data.

REFERENCES

1. Gupta V.K., Mittal A. Adsorptive removal and recovery of azo dye erichrome black T, Toxicol. Environ. Chem. 92 (10) (2010) 1813–1823.
2. Mahmoodi N.M., Equilibrium, kinetic and thermodynamic of dye removal using alginate from binary system. J. Chem. Eng. Data 56 (2011) 2802–2811.
3. Mittal A., Mittal J., Malviya A., Kaur D., Gupta V.K. Adsorption of hazardous dye crystal violet from wastewater by waste materials. J. Colloid Interface Sci. 343 (2010) 463–473.
4. Eiichi I., Ogawa T., Yatome T.C., Horisu H. Behavior of activated sludge with dyes. Bull. Environ. Contam. Toxicol. 35 (1985) 729–734.
5. Li S. Removal of crystal violet from aqueous solution by sorption into semi-interpenetrated networks hydrogels constituted of poly (acrylic acid–acrylamide–methacrylate) and amylase. Bioresour. Technol. 101 (2010) 2197–2202.
6. Huang J., Huang K., Liu S., Wang A., Yan C. Adsorption of rhodamine B and methyl orange on a hypercrosslinked polymeric adsorbent in aqueous solution. Colloids Surf. A. 330 (2008) 55–61.

7. Robinson T., McMullan G., Marchant R., Nigam P. Remediation of dyes in textile effluent: a critical review on current treatment technologies with a proposed alternative. Bioresour. Technol. 77 (2001) 247–255.
8. Ribeiro A. R., Nunes O. C., Pereira M. F.R., Silva A.M.T. An overview on the advanced oxidation processes applied for the treatment of water pollutants defined in the recently launched Directive 2013/39/EU. Environment International. 75, (2015) 33–51.
9. Särkkä H., Vepsäläinen M., Sillanpää M. Natural organic matter (NOM) removal by electrochemical methods — A review. Journal of Electroanalytical Chemistry. 755 15 (2015) 100-108.
10. Khandegar V., Saroha A. K. Electrocoagulation for the treatment of textile industry effluent – A review. Journal of Environmental Management. 128, 15, (2013) 949-963.
11. Särkkä H., Vepsäläinen M., Sillanpää M. Recent developments of electro-oxidation in water treatment- A review. Journal of Electroanalytical Chemistry. 754 (2015) 46-56.
12. Peralta-Hernandez J.M., Mendez-Tovar M., Guerra-Sanchez R., Martinez-Huitle C.A., Nava J.L. A brief review on environmental application of boron doped diamond electrodes as a new way for electrochemical incineration of synthetic dyes. Int. J. Electrochem. 2012 (2012) 1–18.
13. Khataee A.R., Zarei M., Moradkhannejhad L. Application of response surface methodology for optimization of azo dye removal by oxalate catalyzed photoelectro-Fenton process using carbon nanotube-PTFE cathode. Desalination. 258 (2010) 112–119.

CHAPTER 7.32 EFFECT OF AERATION REGIME ON DISCOLORATION AND BREAKDOWN OF AROMATIC AMINES FROM AZO DYE TREATMENT

O. F. Menezes *(1); R. Brito (1); M. G. Carvalho (1, 2); M. T. Kato (1); **L. Florêncio** (1) and S. Gavazza (1)

(1) Federal University of Pernambuco, Av. Acadêmico Hélio Ramos, s/n, Recife, Brazil
(2) Federal Institute of Piauí, Av. Pedro Freitas, s/n, Teresina, Brazil

ABSTRACT

Azo dyes are the most widespread pigments in the textile industry. Their discharge into water bodies limits photosynthesis. Azo bonds are better broken anaerobically, thus resulting in aromatic amines as by-products. These compounds are sometimes more toxic than the parent dyes and are better degraded aerobically. In this paper we evaluated the efficacy of anaerobic and micro-aerated (continuous and intermittent) environments on the removal of a tetra-azo dye and its toxic by-products, from synthetic textile wastewater.

The experimental set-up consisted of three independent sequencing batch reactors (R1, R2 and R3) working with distinct anaerobic-aerobic cycles. Acrylic cylindrical reactors were essayed, at mesophilic conditions (37 ± 1 °C), with a working volume of 5 L and 50% of volume exchange. Anaerobic sludge from a pilot scale UASB reactor treating real textile wastewater was used as inoculum. The synthetic effluent was composed of macro- and micro-nutrients solution, NaCl (1 g L^{-1}), tetra-azo dye Direct Black 22 (65 mg L^{-1}; DB22, $C_{44}H_{32}N_{13}Na_3O_{11}S_3$; C. I. 35435; CAS 6473-13-8) and ethanol (1200 mg O_2 L^{-1} as Chemical Oxygen Demand). In each reactor, the cycle time was 24 h, distributed in: filling (15 min), reaction (23 h), settling (30 min) and drawling (15 min). The reaction time in R1 was completely anaerobic. R2 combined anaerobic (12 h) and aerobic (11 h) conditions in the reaction time, while in R3 the reaction time was composed of 12 h of anaerobic reaction, followed by 11 hours of intermittent aeration (30 min of micro-aeration every 2 h). An air flow of 0.30 ± 0.05 L min^{-1} was distributed in R2 and R3 during the aeration phases.

The reactors were operated for 107 days. At apparent steady state conditions, the average of color removal efficiency was 81.4, 74.5 and 76.3%, respectively for R1, R2 and R3. The corresponding COD removal efficiencies were 76.4, 79.5 and 81.4%, respectively. UV-Vis spectrophotometer scan showed accumulation of aromatic amines in R1. R2 and R3 were able to remove these compounds. Thus, intermittent aeration stood out as an energy saving alternative for discoloration and toxicity removal face to continuous aeration.

During a typical cycle of each reactor, it was performed temporal profiles of COD, color, aromatic amines, dissolved oxygen and oxi-reduction potential (ORP). An ORP average of -430, -475 and -448 mV was detected in R1, and during the anaerobic stages of R2, and R3, respectively. In micro-aerated phase, R2 showed maximum ORP of

---

*Author for correspondence: osmar.fonseca@ufpe.br

24 mV, while in R3 it ranged from -4 in micro-aeration peaks to -445 mV in anaerobic intervals. Color removal efficiencies during the anaerobic phase in R2 (83.4 %) and R3 (86.5 %) suggests higher DB22 removal than the indicated by monitoring the final effluent. Increased post-aeration absorbance may be due to autoxidation of aromatic amines, not reflecting the removal of the parent azo dye.

Keywords: anaerobic-aerobic treatment, aromatic amines, azo dye Direct Black 22, micro-aeration, textile wastewater

INTRODUCTION

In the textile industry, the fixation of dyes to fabrics occurs only partially, generating effluents with high color. When these effluents are discharged into water bodies, photosynthesis may be inhibited reducing the water oxygenation. This usually affects the fauna and flora severely. The main pigments used in the textile industry are azo dyes. These compounds are featured by the presence of azo bonds (-N=N-). Their anaerobic degradation in the environment generates byproducts sometimes more toxic than the original dyes[1, 2].

Physico-chemical treatments are widely used for the treatment of textile effluents. However, some drawbacks are described from this technology application: high cost, chemical sludge generation, low efficiency and little versatility. On the other hand, in comparison, biological treatments are lower cost, environmental friendlier and promote compounds degradation[3].

The breakdown of azo bonds decreases the color of the effluent. Especially for azo dyes with high molecular weight, the cleavage of azo bonds occurs in anaerobic environment by the action of non-specific enzymes (azoreductases). The dye acts as an electron acceptor in the degradation of organic matter. Aromatic amines are formed after reduction of the azo bonds. Such compounds are colorless, although highly toxic. The amines are likely to aerobic degradation by acting as carbon source[1, 3].

Hybrid microbial communities, which are subjected to aerobic and anaerobic cycles, are able to reduce azo bonds and break down the aromatic amines[4]. Thus it is possible to perform the treatment in a single compartment under the two conditions over time. The tolerance of mixed anaerobic cultures to oxygen was previously described[5]. In addition, it was observed that small amounts of oxygen are enough to mineralize the aromatic compounds. Under these circumstances, the aerobic environment is named microaerophilic[4, 6].

Considering this background, the aim of this article was to analyze the effect of micro-aeration regime in anaerobic-microaerophilic reactors on the degradation of the tetra-azo dye Direct Black 22. Processes with intermittent, continuous and no aeration were compared about discoloration and removal of toxic compounds from a synthetic textile effluent.

MATERIALS AND METHODS

The experimental set-up consisted of three independent sequencing batch reactors (R1 R2 and R3) working with distinct anaerobic-aerobic cycles. The reactors had cylindrical shape and were made of acrylic with a working volume of 5 L. The replacement volume was 50 %. The reactors were operated at mesophilic temperature of 37 ± 1 °C.

In each reactor, the cycle time was 24 h distributed in: filling (15 min), reacting 23 h), settling (30 min) and drawling (15 min). The reaction time in R1 was completely anaerobic. R2 combined anaerobic stage and 11 h of microaerophilic stage in the reaction time. R3 operated similarly to R2, with intermittent air supply (30 min every 2 h) in the 11 h of the microaerophilic stage.

Sludge from a pilot scale UASB reactor treating real textile wastewater was used as inoculum. Its concentration in the mixed liquor was 2.5 gVSS L^{-1} in all reactors. The reactors were operated without sludge discharge. Systems with longer sludge ages are better for azo dye treatment[1]. Although small amounts of biomass were eventually discharged with effluent, they were not quantified. Substrate-biomass contact was ensured by mixing using magnetic stirrers (Quimis, Q-241, 2006) during the reaction phase.

Circular aerators made of micro-perforated rubber (Resun, Air Curtain, 2015), displaced at the bottom of R2 and R3, were responsible for sparging an air flow of 0.30 ± 0.05 L min^{-1}, producing few fine bubbles. Timers (Clip, CLB-40, 2015) were used to control the power supply of the aerator (Jad, Air-Pump S-2000, 2015) in R2 and R3.

The azo dye used in the treatment was Direct Black 22 (DB22; $C_{44}H_{32}N_{13}Na_3O_{11}S_3$; molecular weight: 1083.97 g mol^{-1}), which is a tetra-azo dye (**Figure 1**). The dye (initial concentration of 65 mg L^{-1} in the mixed liquor) was supplied from a dye stock solution (15 g L^{-1}), periodically (every 15 days) prepared and stored at 4 ± 2 ºC. Dye solubilization followed manufacturer's recommendations: dissolution in deionized water; pH adjustment to 11.00 ± 0.05 with 40% NaOH; heating at 80 ± 10 ° C during 1 h; return to room temperature; and pH adjustment to 7.00 ± 0.05 with 40% HCl.

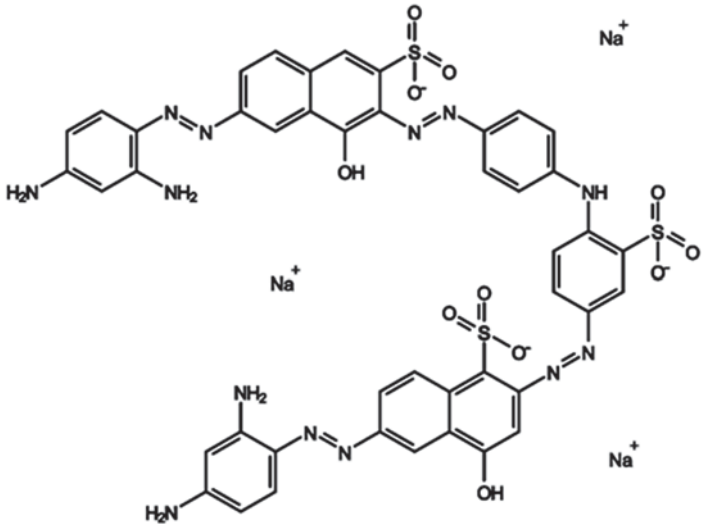


FIGURE 1. Direct Black 22 azo dye structure (CAS 6473-13-8)

Synthetic effluent was composed of: DB22 (65 mg L^{-1}), ethanol as electron donor (1200 mg L^{-1} of Chemical Oxygen Demand - COD), NaCl (1000 mg L^{-1}), NH_4Cl (280 mg L^{-1}), K_2HPO_4 (252 mg L^{-1}), $MgSO_4.7H_2O$ (100 mg L^{-1}), $CaCl_2$ (7 mg L^{-1}), micronutrients solution[7] (1 mL L^{-1}) and $NaHCO_3$ as buffer (1200 mg L^{-1}). It was produced once a week and stored at 4 ± 2 ºC.

The parameters measured merely for control were: pH, dissolved oxygen (DO), salinity, redox potential and alkalinity. These parameters and COD were analyzed in accordance with Standard Methods for the Examination of Water and Wastewater[8]. Absorbance at 476 nm, the wavelength of maximum absorbance for DB22, was monitored as an indicative of DB22 concentration. Aromatic amines were analyzed qualitatively as described before[9]. Spectrophotometric analyses were performed on a spectrophotometer Hitachi U-2910. Samples for COD and spectrophotometric analyses were centrifuged at 3000 rpm for 15 min.

All parameters were analyzed three times a week during the period of biomass adaptation and once a week during steady state conditions. After steady state has been reached, temporal profiles of COD, color, aromatic amines and redox potential were performed throughout a typical cycle of each reactor.

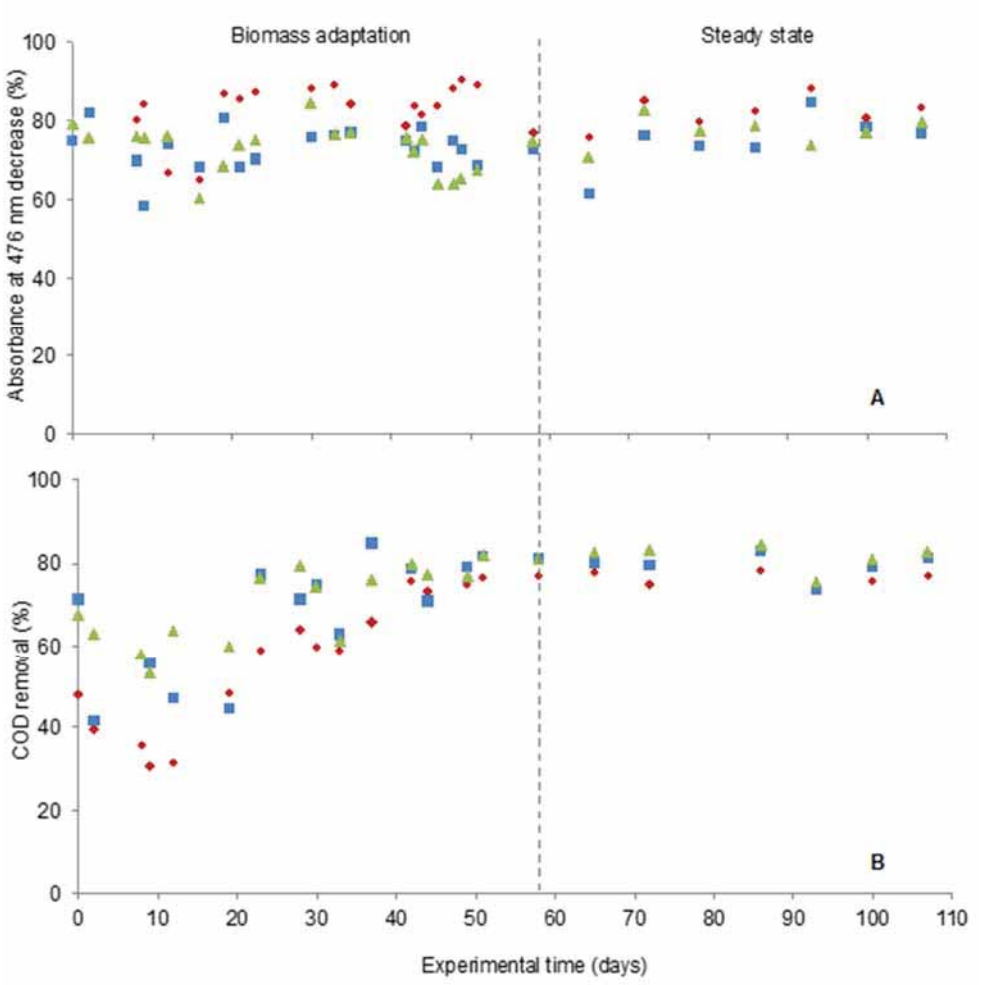


FIGURE 2. Performance of R1 (red diamond), R2 (blue square) and R3 (green triangle) for (A) dye and (B) COD removal efficiencies during the operational period

RESULTS AND DISCUSSION

Results for dye behavior (measured as ABS at 476nm) and COD removal efficiency from the three reactors operation (107 days) indicate that apparent steady state conditions were established after 57 days of operation. At this state, COD removal was 76.4 ± 1.4% for R1, 79.5 ± 3.0% for R2 and 81.4 ± 2.8% for R3. Absorbance at 476 nm decreases were 81.4 ± 4.1% for R1, 74.5 ± 6.6% for R2 and 76.8 ± 3.6% for R3. The standard deviations of the measures were lower than the precision of the methods. Therefore, the reactors were considered stable.

Temporal profiles of oxi-reduction potential (ORP), dye (ABS at 476 nm) and COD of a typical cycle at steady state are shown in **Figure 3**. The ORP behavior followed the expected for the three reactors. R1 values of ORP were kept consistent with the reductive discoloration of DB22 (-434 ± 18 mV). During the anaerobic phase, R2 (-475 ± 54 mV) and R3 (-448 ± 54 mV) behaved similarly to R1. Once micro-aerated stage was initiated, the ORP of R2 and R3 automatically increased. Bacterial community in R2 consumed all oxygen supplied in the first 7h (cycle time of 19h) of the micro-aerated stage, which duration was 11h (data not shown). Then, the oxygen started to accumulate in the mixed liquor and the ORP reached the positive range, remaining close to 0, from 19h to 24h of cycle time.

The ORP in R3 varied between the values found for R2 (-91 ± 134 mV), during the 30 minutes of micro-aeration, and those for R1 (-440 ± 5 mV), during the remaining 1.5 h off aeration. Thus, the intermittent aeration fulfilled the aim of bringing the reactor from a reducing environment to a microaerophilic environment and vice versa in short time intervals (**Figure 3A**). When the aeration was discontinued, oxygen consumption by the bacterial community was fast enough to return R3 to similar reducing conditions found for R1.

The COD consumption in R1 and in the anaerobic phases of R2 and R3 was slower than in aerated phases of R2 and R3 (**Figure 3C**). At the point in which the oxygen started to accumulate in the mixed liquor, R2 and R3 showed no significant degradation of COD. At this moment, the bacterial community had used all easily degradable organic matter and the residual COD corresponded to aerobic-recalcitrant compounds.

COD remained constant in the anaerobic intervals of the intermittent micro-aerated stage of R3 (from cycle time of 12h). Possible reductions of recalcitrant compounds in these intervals did not lead to mineralization, resulting in no increment in COD removal efficiency (**Figure 3C** – green triangle). On the other hand, the anaerobic degradation of ethanol in R3 may have been interrupted due to the aerobic consumption of volatile organic acids.

Figure 3 also shows a decrease in ABS at 476 nm in the three reactors, related to DB22 removal. DB22 removal in all reactors causes an accumulation of aromatic amines (**Figure 4**). In R1 (anaerobic reaction time) the aromatic amines, detected at wavelength range of 200-300nm, accumulated (**Figure 4A**). Despite its effluent was further clarified it was, probably, more toxic than R2 and R3 effluents'. On the other hand, aromatic amines that accumulated in the anaerobic phases of R2 and R3 were partially removed in the micro-aerated stages of the reaction time (**Figure 4B** and **4C**). The degradation of these compounds in general represents a significant decrease of the effluent toxicity and a lower environmental impact[10].

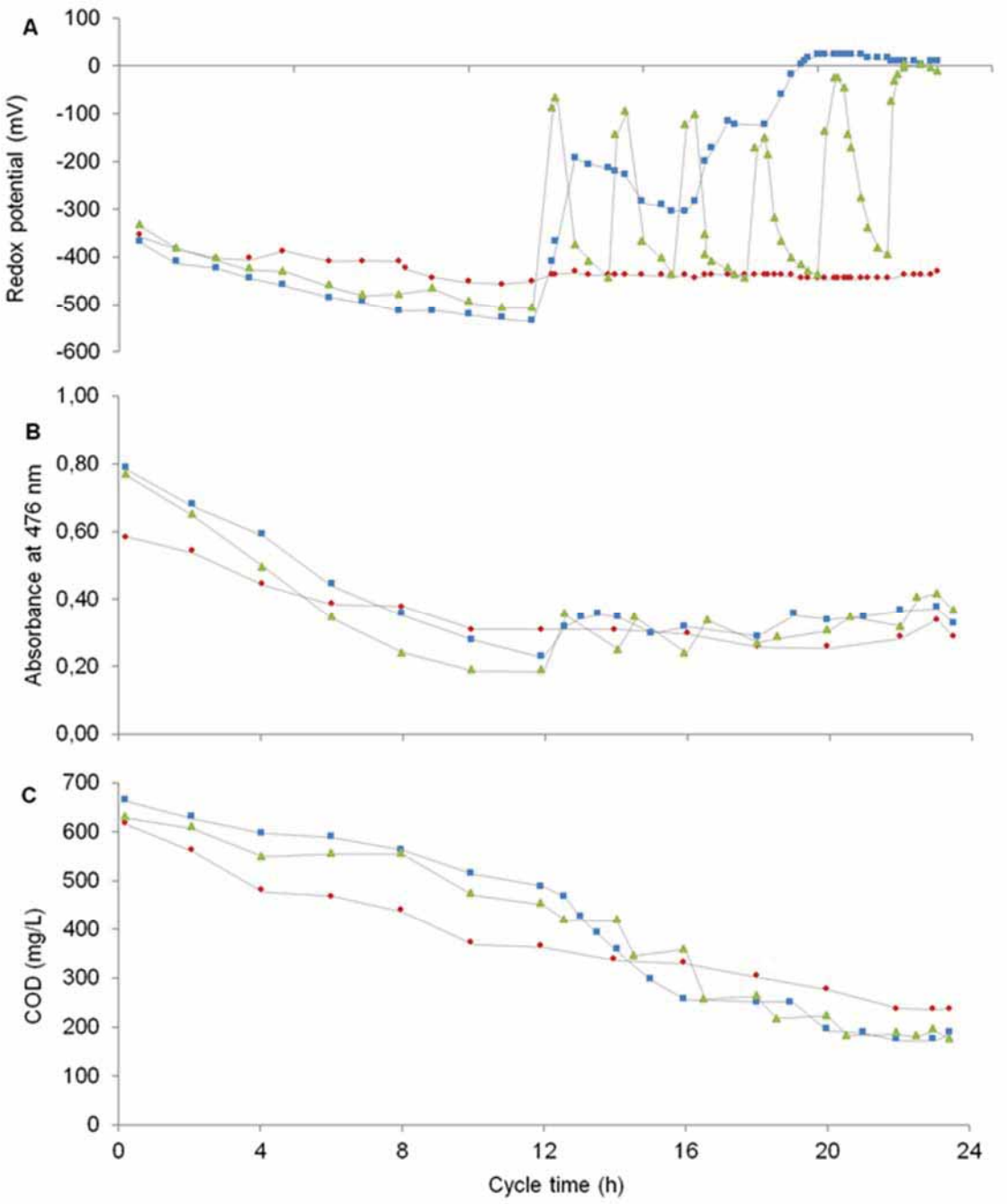


FIGURE 3. Redox potential (A), Absorbance at 476 nm (B) and COD concentration (C) during a typical cycle time in R1 (red diamond), R2 (blue square) and R3 (green triangle)

R3, with intermittent aeration, did not have an operational performance significantly different of R2, with continuous aeration. However, R3 is slightly more efficient in dye removing than R2, whereas both presented equivalent aromatic amines removal. Thus, intermittent aeration has proved to be a technically and economically viable alternative, such as continuous aeration. Only small amounts of oxygen were necessary and their injection could be given intermittently, ensuring energy savings.

Despite the satisfactory performance of R2 and R3, it was observed that rising redox potential caused absorbance increases at 476 nm. The effluent clarified after 12 h of anaerobic reaction acquired a dark red color in both reactors in the first few minutes of aeration. The increase is related to autoxidation of the aromatic amines. Once in the presence of oxygen, some aromatic amines react and form polymers[11, 12]. The autoxidation is often faster than the aerobic degradation of compounds[13]. The formed polymers cause color absorption in the visible range, increasing the absorbance at 476 nm. Therefore, the final color of the R2 and R3 effluents was not an indicative of actual removal of DB22 during the cycle.

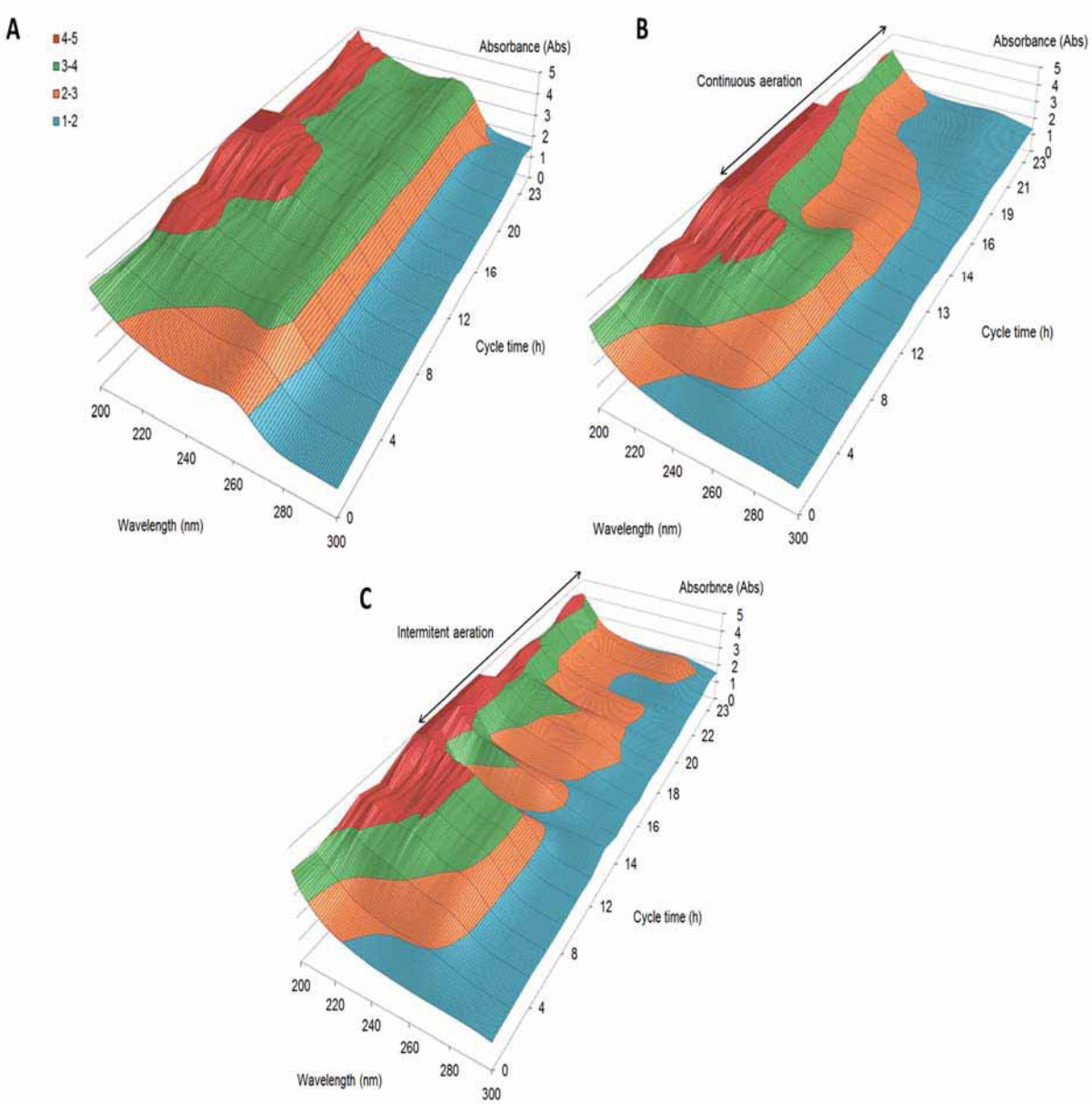


FIGURE 4. Absorbance in the range of aromatic compounds (200 - 300 nm) during a typical cycle time in R1 (A), R2 (B) and R3 (C)

Products from the autoxidation of aromatic amines are recalcitrant to aerobic treatment[14]. However, R3 repetitively ranged between anaerobic and aerobic environments. It was observed that the polymers generated in an aeration peak were once again reduced to amines in anaerobic environment, as shown in **Figure 4C**. In the next aeration peak, the amines were autoxidized and the absorbance at 476 nm increased, as in **Figure 3C**. Thus, such compounds have undergone a futile cycle and were not degraded by the combination of anaerobic-aerobic processes in R3.

CONCLUSION

The biomass of the three reactors was adapted after 57 days of operation. The anaerobic process produced more clarified effluent than hybrid processes, however with a greater toxicity. Intermittent aeration had similar results to continuous aeration, performing as an energy saving process.

The anaerobic discoloration of a textile effluent is not an irreversible process[12]. Once released in the middle, the aromatic amines of the effluent can undergo autoxidation and increase color, although it does not reach the original color of the affluent. In addition, oxygen removed amines by two processes in aerated reactors: mineralization of the compounds (permanent removal) and autoxidation (formation of recalcitrant compounds). Application of advanced oxidation processes in mineralization of the formed polymers was recommended before[13]. The next steps involve the identification of the aromatic amines, the evaluation of their recalcitrance to aerobic treatment and their autoxidation potential.

ACKNOWLEDGMENTS

The authors are grateful to CNPq and FACEPE for their financial support.

REFERENCES

1. Van der Zee FP, Villaverde S (2005) Combined anaerobic-aerobic treatment of azo dyes - A short review of bioreactor studies. Water Res 39:1425–1440.
2. dos Santos AB, Cervantes FJ, van Lier JB (2007) Review paper on current technologies for decolourisation of textile wastewaters: Perspectives for anaerobic biotechnology. Bioresour Technol 98:2369–2385.
3. Khan R, Bhawana P, Fulekar MH (2013) Microbial decolorization and degradation of synthetic dyes: A review. Rev Environ Sci Biotechnol 12:75–97.
4. Field JA, Stams AJM, Kato M, Schraa G (1995) Enhanced biodegradation of aromatic pollutants in cocultures of anaerobic and aerobic bacterial consortia. Antonie Van Leeuwenhoek 67:47–77.
5. Kato MT, Field JA, Lettinga G (1997) Anaerobe tolerance to oxygen and the potentials of anaerobic and aerobic cocultures for wastewater treatment. Brazilian Journal of Chemical Engineerin 14:1-12.
6. Naresh Kumar A, Nagendranatha Reddy C, Venkata Mohan S (2015) Biomineralization of azo dye bearing wastewater in periodic discontinuous batch reactor: Effect of microaerophilic conditions on treatment efficiency. Bioresour Technol 188:56–64.
7. Florencio L, Jeniček P, Field JA, Lettinga G (1993) Effect of cobalt on the anaerobic degradation of methanol. J Ferment Bioeng 75:368–374.

8. American Public Health Association, American Water Works Association, and Water Environment Federation (2005) Standard methods for the examination of water and wastewater. American Public Health Association, Washington, DC.
9. Pinheiro HM, Touraud E, Thomas O (2004) Aromatic amines from azo dye reduction: Status review with emphasis on direct UV spectrophotometric detection in textile industry wastewaters. Dye Pigment 61:121–139.
10. Amaral FM, Kato MT, Florêncio L, Gavazza S (2014) Color, organic matter and sulfate removal from textile effluents by anaerobic and aerobic processes. Bioresour Technol 163:364–369.
11. Tan NCG, Prenafeta-Bold FX, Opsteeg JL, et al (1999) Biodegradation of azo dyes in cocultures of anaerobic granular sludge with aerobic aromatic amine degrading enrichment cultures. Appl Microbiol Biotechnol 51:865–871.
12. Kudlich M, Hetheridge MJ, Knackmuss HJ, Stolz A (1999) Autoxidation reactions of different aromatic o-aminohydroxynaphthalenes that are formed during the anaerobic reduction of sulfonated azo dyes. Environ Sci Technol 33:896–901.
13. Jonstrup M, Kumar N, Murto M, Mattiasson B (2011) Sequential anaerobic-aerobic treatment of azo dyes: Decolourisation and amine degradability. Desalination 280:339–346.
14. Coughlin MF, Kinkle BK, Bishop PL (2002) Degradation of acid orange 7 in an aerobic biofilm. Chemosphere 46:11–19.

CHAPTER 7.33 BIODEGRADABILITY OF PARACETAMOL IN ANAEROBIC CONDITIONS

C. Nepomuceno (1); K. K. Barros *(1) and L. De Souza (2)

(1) Federal University of Pernambuco, Academic Centre of Wasteland, Technology Centre, Environmental Engineering Laboratory, Highway BR-104, Km 59, s/n – Nova Caruaru, Caruaru City, Brazil
(2) Caruaruense Association of Higher and Technical Education - ASCES, Portugal Avenue, N° 585, Caruaru City, Brazil

ABSTRACT

Production and consumption of pharmaceuticals generate wastes that are discharged or excreted in environmental. Occurrence of pharmaceutical and their metabolites in freshwaters may cause adverse effects on wildlife and humans. Analgesics and antipyretics are on the list of most eaten drugs in Brazil. Currently, the eating of paracetamol has increased in Brazil due to the epidemic of Dengue, Chikungunya fever, and Zika virus, because this drug is recommended for the treatment of those diseases. The experiment was planned for evaluating the biodegradability of paracetamol, under anaerobic conditions, using Specific Methanogenic Anaerobic test. The test reactors were inoculated with a solution containing 761 $mg.L^{-1}$ of paracetamol. The results showed that the removal of COD reached 87 ± 3%, but only 16 ± 1% of initial COD was converted to methane in the test reactors. This way, possibly the degradation of paracetamol did not occur by the methanogenesis route and the absence of a nutrient source and the high concentration of paracetamol used in this experiment can have induced the microbial auto-oxidation and toxicity to the anaerobic microorganisms.

Keywords: biodegradation, methane yield, paracetamol, specific methanogenic activity

INTRODUCTION

Production and consumption of pharmaceuticals generate wastes that are discharged in environmental and can contaminate several natural ecosystems. In freshwaters, the occurrence of pharmaceutical wastes is related to the discharge of wastewaters. A large fraction of pharmaceuticals presents in water is composed of anti-inflammatory and analgesic drugs, which are rapidly excreted in urine. Other form of contamination it is the uncontrolled discard of tablets out-dated in the sewages by population that has contributed to increase unchanged form of those pharmaceuticals in sewages[1]. This way, due to possible adverse effects on wildlife and humans, degradation and removal of pharmaceuticals and their metabolites during wastewater treatment is an increasingly important task[2].

Analgesics and antipyretics are on the list of most eaten drugs in Brazil. Paracetamol, which chemical formula is $C_8H_9NO_2$, is a pharmaceutical compound with analgesic and antipyretic properties, but without anti-inflammatory properties clinically significant. It

---

*Author for correspondence: keniakellybarros@gmail.com

acts by inhibiting the synthesis of prostaglandins, cellular mediators responsible for the appearance of pain, and reducing the fever. Currently, the eating of paracetamol has increased in Brazil due the epidemic of Dengue, Chikungunya fever, and Zika virus, because this drug is recommended for the treatment of those diseases.

The paracetamol molecule is quite complex, presenting several functional groups, as for example, Carbonyl group (C = O) that, together with the nitrogen, classifies the paracetamol compost as an amine; hydroxyl group (O – H), an aromatic structure (benzene ring) and nitrile (– CN) (**Figure 1**). When metabolized, paracetamol undergoes deacetylation generating a primary amine, which is combined with arachidonic acid to form the N-arachidonoyl phenol amine, considered an endogenous cannabinoid. Moreover, in the liver, it is metabolized to the sulfate and glucuronide conjugates and later excreted in the urine. Hence, the source of paracetamol pollution in surface water has been mainly domestic sewages[1].

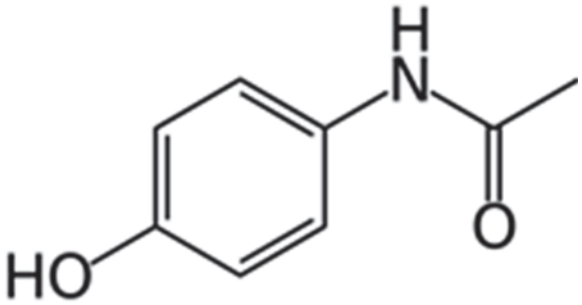


FIGURE 1. Chemical structure of paracetamol[3]

Anaerobic digestion is considered a good alternative to treat domestic and industrial wastewaters, because of its advantages over the aerobic treatment, as for example low sludge production, low energy requirements and biogas yield. However, some microorganisms involved in the anaerobic digestion are sensitive to a wide range of compounds can inhibit the anaerobic digestion and cause upset or failure of anaerobic treatment systems[4, 5].

In the last years, both anaerobic and aerobic treatment systems have been used to treat pharmaceutical wastewaters[6]. However, there are still doubts on anaerobic treatment efficiency and process reliability, since many residues may contain substances that are toxic to methanogenic microorganisms[7]. For this reason, the treatment of effluents containing pharmaceutical compounds has become a difficult task due the wide variety of chemicals present in pharmaceutical compounds[8].

Removal mechanisms of pharmaceuticals present in effluents are biodegradation, abiotic transformations and adsorption to the biomass or suspended solids. Some pharmaceutical compounds are fairly removed in biological treatment via the sludge adsorption, due to their non-polar nature[9, 10].

With respect to the studies of biodegradability and toxicity of pharmaceutical composts, both continuous and batch-feed techniques have been used to evaluate those phenomena[7]. Among those techniques, highlights the Specific Methanogenic Activity tests (SMA test).

Specific Methanogenic Activity tests are used to assess the methane yield maximum rate and the biomass activity in reactors. The activity of microbial groups involved in the anaerobic digestion process can be measured by the kinetics of a known amount of substrate consumed or methane produced[11]. The knowledge of SMA test of a sludge allows estimating the maximum organic load to be applied in the anaerobic reactor without causing risks of imbalance of anaerobic processes[12].

The objective of this experiment was to evaluate the biodegradability of paracetamol in anaerobic conditions, by performing the Specific Methanogenic Activity Test (SMA test).

MATERIALS AND METHODS

The specific methanogenic activity test (SMA test)[11] was carried out in the Environmental Engineering Laboratory (LEA). The LEA is located in the Academic Centre of the Wasteland of Federal University of Pernambuco, in Caruaru city.

The reactors used were borosilicate bottles, with total volume of 535 mL and working volume of 508 mL. Five reactors were used to realize this experiment. Each reactor was loaded with 388 mL of a paracetamol solution, with concentration equal to 761 ± 6 $mg.L^{-1}$, as only carbon source, 102 mL of nutrient solution (201 $g.L^{-1}$)[13] and 14 mL of anaerobic sludge (28 $g.L^{-1}$), sampled from an industrial WWTP.

TABLE 1. Nutrient concentrations in macro and micronutrient solutions[13]

Macronutrients	Units	Concentrations
NH_4Cl	$g.L^{-1}$	0.280
K_2HPO_4	$g.L^{-1}$	0.252
$MgSO_4.7H_2O$	$g.L^{-1}$	0.100
$CaCl_2.2H_2O$	$g.L^{-1}$	0.007
Yeast extract	$g.L^{-1}$	0.100
Bicarbonate	$g.L^{-1}$	5.000
Micronutrients	**Units**	**Concentrations**
$FeCl_2.4H_2O$	$mg.L^{-1}$	2.000
$ZnCl_2$	$mg.L^{-1}$	0.050
$MnCl_2.4H_2O$	$mg.L^{-1}$	0.500
$NiCl_2.6H_2O$	$mg.L^{-1}$	0.142
$NaSeO_3.5H_2O$	$mg.L^{-1}$	0.164
H_2BO_3	$mg.L^{-1}$	0.050
$CuCl_2.2H_2O$	$mg.L^{-1}$	0.038
$CoCl_2.6H_2O$	$mg.L^{-1}$	2.000
$AlCl_3.6H_2O$	$mg.L^{-1}$	0.090
$(NH_4)_6.Mo_7O_{24}.4H_2O$	$mg.L^{-1}$	0.050
EDTA	$mg.L^{-1}$	1.000
HCl	$mL.L^{-1}$	1.000

Three reactors were operated with paracetamol (test) and two reactors were operated without paracetamol (control). The control reactors were used just to check the cell matter decomposition by auto-oxidation. The SMA test was realized at an average temperature equal to 28.8 ± 0.7 ºC and lasted 95 days. The initial average COD of the substrates inoculated in the test reactors were 1160 ± 96 mg $O_2.L^{-1}$. The volatile total solids concentration of anaerobic industrial sludge was 7.3 ± 0.2 g $VTS.L^{-1}$.

The nutrient solution contained macro and micronutrients and was rich in proteins, lipids and carbohydrates. To compose the nutrient solution, 1.0 mL of a micronutrient solution was added in the macronutrient solution. The concentrations of nutrients contained in macro and micronutrient solutions are described in **Table 1**.

Before start the SMA test, the industrial sludge went through a period of 6 days of acclimatization, in contact with 5 mL of a volatile organic acids solution (300 $mg.L^{-1}$). This solution was composed by butyric acid, propionic acid and acetic acid, in the proportion of 100:100:100 $g.L^{-1}$, respectively. Before starting the acclimatization process, the pH of the solution of organic acids was neutralized by adding NaOH (1.0 N). At the end of this period, the reactors were inoculated with the acclimatized sludge.

The parameters used to evaluate the biodegradability of paracetamol were: COD, methane yield, pH, and volatile total solids (VTS). The parameters COD and pH were determined weekly. The methane yield was measured daily. Volatile total solids in sludge were determined at the beginning and end of experiment.

The method used to determine the parameters COD and pH are described on Standard Methods for the Examination on Water and Wastewaters[14]. The methane was measured by volumetric method of methane direct measuring. In this method, the increased pressure of the gas in collector flasks induces the displacement of NaOH contained into the collector flasks. The volume of methane produced during the test was measured by weighing the collector flasks containing the displaced NaOH. The experimental apparatus is described in the **Figure 2**.

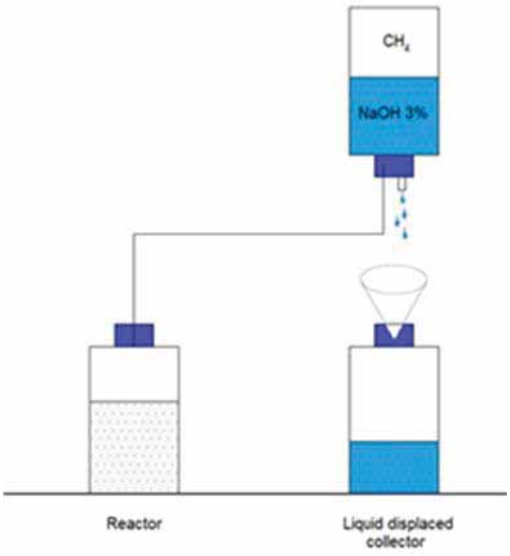


FIGURE 2. Experimental apparatus

The methane yield was calculated in units of degraded COD, using the following relation: 394 mL of CH_4 equivalent to 1.0 g of degraded COD. To evaluate the descriptive statistic of results was used the software Statistic 8.0.

RESULTS AND DISCUSSION

The anaerobic digestion process is quite sensitive to environmental variations, any change in the process causes imbalance among the bacterial populations affecting the performance and speed of the anaerobic digestion. The main environmental factors that should be analysed constantly are temperature, pH, organic matter composition, feed rate and inorganic composition of substrate.

At beginning of this experiment, the values of pH were equals to 9.20 ± 0.00 and 9.10 ± 0.02, in the control and test reactors, respectively. The values of pH remained above the neutral pH limit during, approximately, 15 days. After this period, the values of pH decreased and remained equals to 7.20 ± 0.00 (control) and 7.50 ± 0.05 (test) until at the end of experiment.

Values of pH above the neutrality can provoke toxicity by ammonia. Ammonia is an essential nutrient for the growth of microorganisms involved in anaerobic digestion, as well as acting as an inhibitor at high concentrations[15]. The fermentation of nitrogen-containing materials releases ammonia-nitrogen which exists largely as the ionized form (NH_4^+), but it depends strongly on pH, and consequently the toxic unionized form (NH_3) increases with increasing pH[4].

In 18 days of experiment, the test reactors presented a change in the tonality of effluent (reddish colour) and sludge with disperse aspect presenting some suspended solids. On the other hand, the colours of control reactors stayed the unchanged (Figure 3). After detecting these colour changes, analysis were carried out to monitor the occurrence of colour change. Nevertheless, there was not colour change after the 18th day, and the values of colour remained equals to 2750 ± 00 mg Pt Co.L^{-1}.

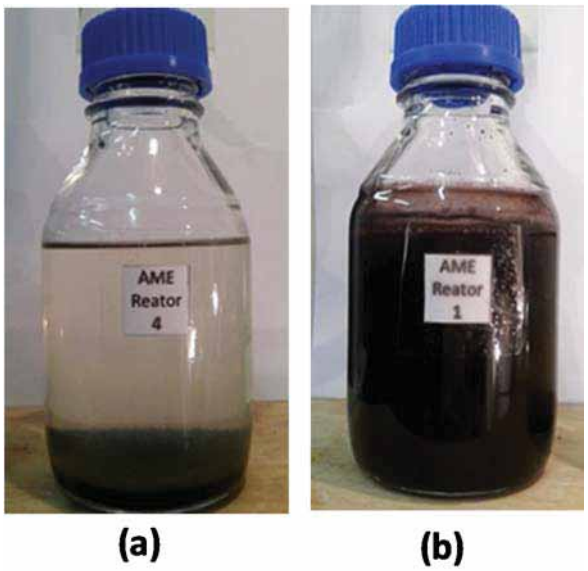


FIGURE 3. Contents of reactors after 18th day. Control (a) and test (b).

In a first moment, those results could indicate a possible oxidation of ion Fe^{2+}, due the reddish colour. It is possible to have a reaction of oxidation of Fe by oxidizing anaerobic bacteria of Fe. Oxidation of iron in anaerobic environments can be carried out both by chemotrophic bacteria as phototrophic bacteria. In anoxic environments, anaerobic organisms that oxidize the iron associate the oxidation of Fe to reduction of NO_3^- , producing NO_2^- or nitrogen gas[16]. However, it is necessary deepen more the studies on the oxidation of Fe^{2+} in the anaerobic digestion of paracetamol. This way, the colour change, probably, occurred due to chemical composition of drug in study that, in addition to its main component (paracetamol), this drug contains other substances (e. g. stearic acid, hypromellose, macrogol and povidone) could have caused some kind of toxicity at the microorganisms involved in the anaerobic digestion or could have induced the paracetamol degradation to another degradation route different from methanogenesis route.

About the biodegradability, the results showed that there was COD removal in the test and control reactors (**Figure 4**). However, in the control reactors, it was observed an increasing of the COD values. These values can be results of sludge mineralization and its subsequent degradation.

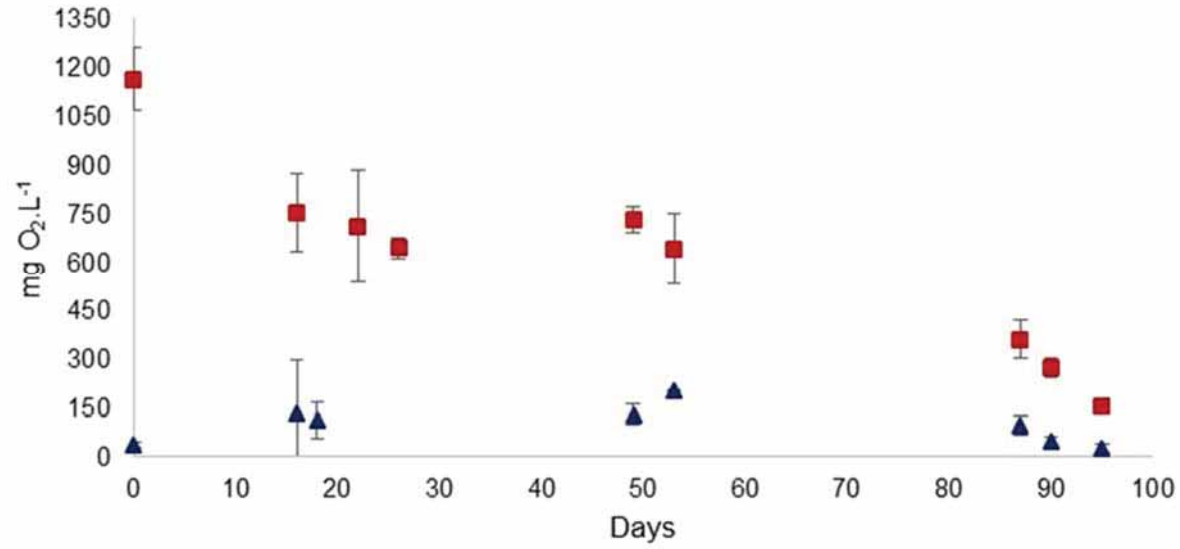


FIGURE 4. COD concentrations. (■) COD Test and (▲) COD Control.

Anaerobic treatments are good alternatives for the removal of pharmaceutical compounds present in industrial wastewaters and domestic sewage, because they are able to support persistent wastes and with high COD loads[17].

The chronic impact of antibiotic tetracycline on the biodegradation of substrate under anaerobic conditions was evaluated in an experiment that used an anaerobic sequencing batch reactor fed with a synthetic substrate contenting doses of tetracycline between 1.65 and 8.5 $mg.L^{-1}$. The results showed that the COD removal reached efficiency above 90%. Nevertheless, when the tetracycline dose increased to 8.5 $mg.L^{-1}$, the COD removal efficient decrease to just 9%[18]. In other research, it was related that anaerobic treatment was suitable for pharmaceutical industry wastewater with concentration of up 40 $mg.L^{-1}$ of sulfamethoxazole. However, higher levels of

sulfamethoxazole exerted toxic effects on the microbial community under anaerobic conditions, causing the inhibition of substrate/COD utilization and biogas generation, leading to a total collapse of the reactor[19].

The inhibitory effect of the antibiotic chlortetracycline chlorhydrate on the anaerobic digestion process, using SMA test, was evaluated and the results found showed that concentrations greater than 50 $mg.L^{-1}$ caused a decreasing of methane production[20]. Concentrations of pentachlorophenol (PCP) between 1.0 and 2.5 $mg.L^{-1}$ inhibited methanogens and acetogens in granular anaerobic sludge. This fact showed that co-substrates must be supplied since the PCP cannot be used as the only carbon source to developed anaerobic granules[21].

The high paracetamol concentration (761 mg $O_2.L^{-1}$) used in this experiment can have caused some kind of inhibition to the more sensitive organisms involved in anaerobic digestion. Some chemicals and/or substances released after the degradation of paracetamol, probably, were not consumed by anaerobic organisms, resulting in a decrease in methane yield and their death. Even so, in 95 days, the COD decreased from 1160 ± 96 mg $O_2.L^{-1}$ to 152 ± 23 mg $O_2.L^{-1}$, corresponding to a removal of 87 ± 3%. Nevertheless, only 16 ± 1% of initial COD was converted to methane (COD equal to 187 ± 72 mg $O_2.L^{-1}$), in the test reactors. So, it is probably this high removal efficient of COD has been caused by the microbial auto-oxidation.

Auto-oxidation is a phenomenon in which microorganisms obtain energy through the decomposition of cell material, when they are already inactive. Biogas yield is an inherent complement of COD removal under anaerobic conditions. In this experiment, as added a low amount of organic matter in control reactors, the methane yield was considered equivalent to the microbial auto-oxidation. Thus, to better represent the methane yield in test reactors, the values of the methane yield recorded in test reactors were subtracted from the values of methane yield recorded in control reactors. This way, the real values of methane yield equivalents to the paracetamol biodegradation could be calculated. The results found indicate that the mineralization of organic matter present in the paracetamol was not equivalent to production of methane, and the methane produced in both reactors may be due to microbial auto-oxidation (Figure 5).

To confirm the occurrence of the sludge mineralization, at the end of the experiment, it was determined the concentration VTS contained in the sludge. The final average concentration found was equal to 6.1 ± 40 g $VTS.L^{-1}$. Thus, there was a reduction of, nearly, 17% in the VTS concentration, since the VTS initial concentration was 7.3 ± 0.2 g $VTS.L^{-1}$.

During the treatment, in UABS reactors, of the wastewater generated by the coffee fruit processing, there was a decrease in the VTS of anaerobic sludge, corresponding to 57% of initial concentration of VTS. This occurred because the affluent organic load was not sufficient to feed the active biomass, causing the auto-oxidation process. The decrease of VTS concentration in anaerobic sludge caused by auto-oxidation damaged the anaerobic digestion process and, consequently, the biogas yield[22]. However, the occurrence of auto-oxidation may be due the presence of inactive microorganisms.

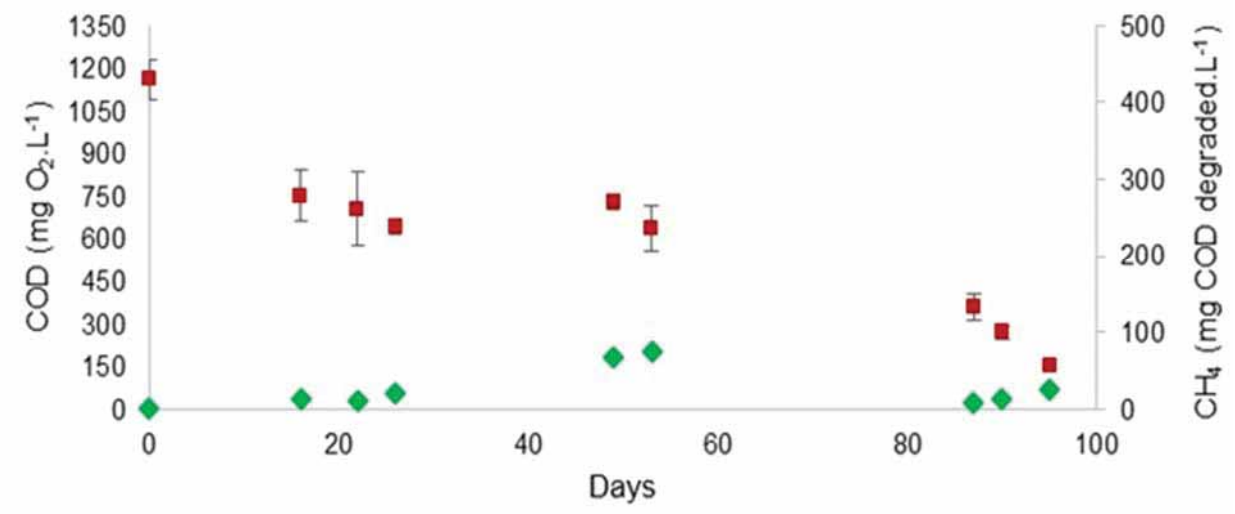


Figure 5. Biodegradability test. (■) COD Test and (◆) methane converted to degraded COD

The maximum methane yield was 176 ± 79 mL. The values of methane yield, in units of degraded COD, registered in the test reactors were similar to the values observed in the control reactors (Figure 6). With regards the SMA, the average values found in this experiment were 5.8 ± 1.3 mg COD-CH_4.(g VSS.d)$^{-1}$, in test reactors, and 6.1 ± 1.1 gCOD-CH_4.(g VSS.d)$^{-1}$, in control reactors.

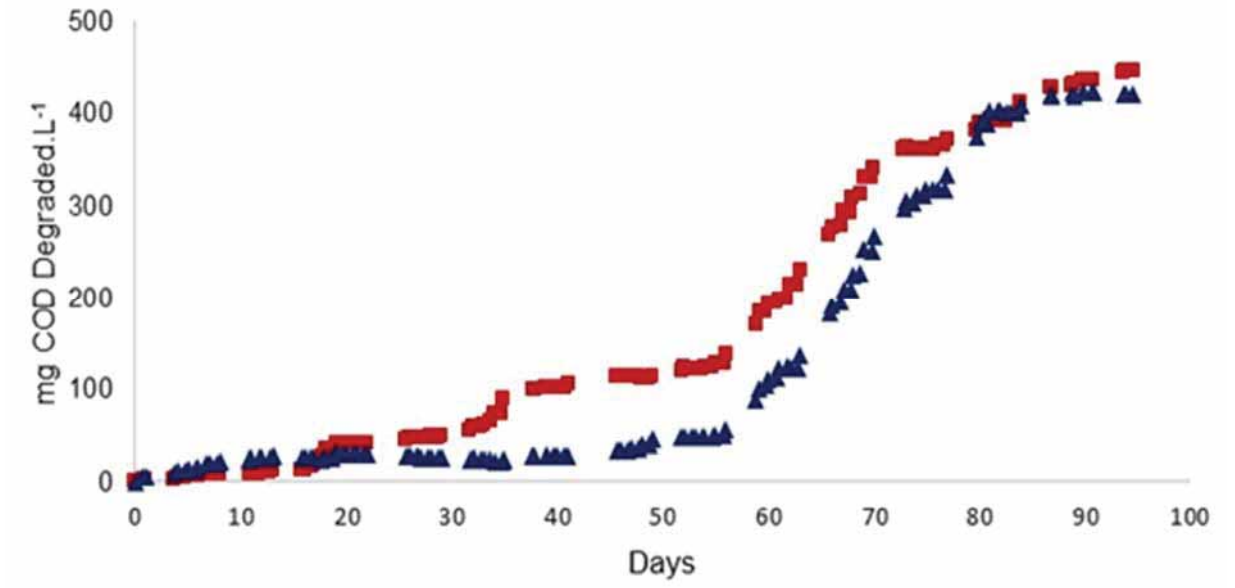


FIGURE 6. Methane converted to degraded COD. (■) Test and (▲) Control

CONCLUSION

The degradation of paracetamol did not occur by the methanogenesis route because there was not an equivalence between values of degraded COD and the values of methane yield in mg COD degraded per litre. The absence of an organic substrate as nutrient source and the high concentration of paracetamol used in this experiment can have induced the microbial auto-oxidation and toxicity to the anaerobic microorganisms. But, to confirm the microbial auto-oxidation, it is recommended to use technical of detection of inactive organisms by DNA-based or PCR assays. It is plausible that the presence of paracetamol strongly influenced the performance of the microorganisms involved in the anaerobic digestion process, which was evident through biodegradability and SMA tests.

ACKNOWLEDGMENTS

The authors would like to thank all the professors, technical and students involved with this experience and to the Academic Centre of Wasteland of Federal University of Pernambuco by laboratorial structure.

REFERENCES

1. Ziylan, A., Ince, N. H. The occurrence and fate of anti-inflammatory and analgesic pharmaceuticals in sewage and fresh water: treatability by conventional and non-conventional processes. Journal of Hazardous Materials 187 (2011) 24-36.
2. Maletz, S., Floehr, T., Beier, S., Klümper, C., Brouwer, A., Behnisch, P., Higley, E., Giesy, J. P., Hecker, M., Gebhardt, W., Linnemann, V., Pinnekamp, J., Hollert, H. In vitro characterization of the effectiveness of enhanced sewage treatment processes to eliminate endocrine activity of hospital effluents. Water Research 47 (2013) 1545-1557.
3. ANVISA. Fundação Oswaldo Cruz. Farmacopeia Brasileira, Volume 2, 5ª Edição, Brasília, Brasil, 2010.
4. Chen, J. L., Ortiz, R., Steele, T. W. J., Stuckey, D. C. Toxicants inhibiting anaerobic digestion: A review. Biotechnology Advances 32 (2014) 1523–1534.
5. Puyol, D., Sanz, J. L., Rodriguez, J. J., Mohedano, A. F. Inhibition of methanogenesis by chlorophenols: a kinetic approach. New Biotechnology 30 1 (2012) 51-61.
6. Ng, W. J., Miranda, G. S. Y., Sivadas, M. Biological treatment of a pharmaceutical wastewater. Biological Wastes 29 (1989) 299-311.
7. Owen, W. F., Stuckey, D. C., Healy Jr., J. B., Young, L. Y., Mccarty, P. L. Bioassay for monitoring biochemical methane potential and anaerobic toxicity. Water Research 13 (1979) 485-492.
8. Chang, C.Y., Chang, J. S., Vigneswaran, S., Kandasamy, J. Pharmaceutical wastewater treatment by membrane bioreactor process – a case study in southern Taiwan. Desalination 234(2008) 393 – 401.
9. Martin, J., Camacho-Muñoz, D., Santos, J. L., Aparício, I., Alonso, E. Occurrence of pharmaceutical compounds in wastewater and sludge from wastewater treatment plants: Removal and ecotoxicological impact of wastewater discharges and sludge disposal. Journal of Hazardous Materials 239-240 (2012) 40-47.

10. Sipma, J., Osuna, B., Collado, N., Monclús, H., Ferrero, G., Comas, J., Rodriguez-Roda, I. Comparison of removal of pharmaceuticals in MBR and activated sludge systems. Desalination 250 (2010)653 – 659.
11. Aquino, S. F., Chernicharo, C. A. L., Foresti, E., Dos Santos, M. L. F., Monteggia, L. O. Metodologias para determinação de atividade metanogênica específica (AME) em lodos anaeróbios. Engenharia Sanitária e Ambiental 12 2 (2007) 192-201.
12. Le Hyaric, R., Chardin, C., Benbelkacem, H., Bollon, J., Bayard, R., Escudié, R., Buffuère, P. Influence of substrate concentration and moisture content on the specific methanogenic activity of dry mesophilic municipal solid waste digestate spiked with proprionate. Bioresource Technology 102 (2011) 822-827.
13. Florencio, M. L. The fate of methanol in anaerobic bioreactors. 137 P. Tese (Ph.D) – Wageningen Agricultural University – Wageningen. Holanda, 1994.
14. APHA; AWWA; WPCF. Standard Methods for the Examination of Water and Wastewater, 21ª ed. Washington D.C, 2005.
15. Koster. I. W., Lettinga, G. The influence of ammonium–nitrogen on the specific activity on pelletized methanogenic sludge. Agric. Waste 9 (1984) 205–16.
16. Madigan, M. T., Markinto, J. M. Bender, K. S., Buckley, D. H., Stahl, D. A. Microbiologia de Brock. 14ª edição. Artmed. Porto Alegre, Brasil, 2016.
17. Oktem, Y., Ince, O., Sallis, P., Donnelly, T., Kasapigi, I., Ince, B. Anaerobic treatment of a chemical synthesis-based pharmaceutical wastewater in a hybrid upflow anaerobic sludge blanket reactor. Bioresource Technology 995, (2008) 1089-1096.
18. Ceteciogly, Z., Ince, B., Gros, M., Rodrigues-Mozaz, S., Barceló, D., Orhon, D., Ince, O. Chronic impact of tetracycline on the biodegradation of an organic substrate mixture under anaerobic conditions. Water Research 47 (2013) 2959–2969.
19. Ceteciogly, Z., Ince, B., Gros, M., Rodrigues-Mozaz, S., Barceló, D., Ince, O., Orhon, D. Biodegradation and reversible inhibitory impact of sulfamethoxazole on the utilization of volatile fatty acids during anaerobic treatment of pharmaceutical industry wastewater. Science of the Total Environment 536 (2015) 667–674.
20. Cetecioglu, Z., Ince, B., Orhon, D., Ince, O. Acute inhibitory impact of antimicrobials on acetoclastic methanogenic activity. Bioresource Technology 114, (2012) 109-116.
21. Wu, W. W., Bhatnagar, L., Zeikus, J. G. Performance of anaerobic granules for degradation of pentachlorophenol. Applied and Environmental Microbiology 59 2 (1993) 389-397.
22. Da Silva, J. F., Campos, C. M. M., Pereira, E. L., Da Silva, V. G. Avaliação microscópica da endogenia microbiana em reatores concêntricos, tratando água residuária do processamento dos frutos do cafeeiro por via úmida. Acta Scientiarium Technology 33 2 (2011) 129-135.

CHAPTER 7.34 INFLUENCE OF TOILET PAPER IN THE ANAEROBIC DIGESTION OF WASTEWATER

D.P.P. Gomes (1); M. L. Figueiras (1); R. B. Pires (1); S. Gavazza (2) and M. S. Santos *(1)

(1) Federal University of Pernambuco – Technology Center, Rodovia BR-104, Km 59, s/n - Nova Caruaru, Caruaru, Brasil.
(2) Federal University of Pernambuco – Civil Engineering Department, Recife, Brasil.

ABSTRACT

There is a worldwide trend to use the sewage system as the final destination of waste ranging from pharmaceuticals, personal materials, diapers, sanitary napkins and toilet paper, and the flushing of the latter, a very common practice in developed world. However, it is known that the toilet paper affects the sewage system from pipes to the treatment plant. Little research has been carried out considering the influence of toilet paper in conventional wastewater treatment plants. In this sense, this work aims to evaluate the influence of toilet paper in the anaerobic digestion of wastewater. Therefore, two laboratory scale UASB reactors were installed: the first one treating a mixture (toilet paper added to synthetic wastewater) and the second one treating synthetic wastewater only. The experiment had two phases, according to the toilet paper concentration added to the synthetic wastewater: Phase I (PI) - one double sheet of toilet paper per liter of synthetic sewage; and Phase II (PII) - two double sheets per liter of synthetic wastewater. The UASB reactor fed with synthetic wastewater with toilet paper (R1) had slight reduction of average raw/filtered chemical oxygen demand removal efficiency (79/76% in PI and 75/70% in PII), compared to R2 (83/82%). R1 had high average removal efficiency for volatile suspended solids, ranging from 94% (PI) to 96% (PII), and R2 had 88%. The average removal efficiency for total suspended solids was 52% (PI) and 64% for R1, and 19% for R2. Methane production was 498 mg COD L^{-1} (PI) and 848 mg COD L^{-1} (PII) for R1 and 186 mg COD L^{-1} for R2, showing increased biogas production due to the addition of toilet paper. In general, the UASB reactor showed ability to withstand the organic load and solids increase after toilet paper additions with an increase in biogas generation. Anyway, flushing toilet paper in the sewage system should cause impacts from the pipes to the treatment plants. However, the improvement of biogas generation in a wastewater plant due to toilet paper addition seems to be viable and more environmental friendly than its disposition in a landfill.

Keywords: biogas, toilet paper, UASB, wastewater

---

*Author for correspondence: smachados@hotmail.com

Regarding the influence of toilet paper in the treatment of domestic sewage, few studies have been conducted and the results are still preliminary. However, it is known the hydrolysis of cellulose is considered the limiting step in anaerobic digesters fed with a high cellulose content[1].

In countries like Japan, Netherlands and United States, which have a proper sewage collection system, a large content of suspended solids and organic matter from the wastewater treated in sewage treatment plants is due to the release of toilet [2,3,4,5].

In Brazil, the universalization of sanitation leads to the implementation of new sewage systems and / or the expansion of the olds. Hence, it is necessary to investigate the possible influence of these new materials in the efficiency of sewage treatment plants, especially in anaerobic reactors, technology often used in tropical countries. The anaerobic technology has the ability to treat high organic content wastewater, generating energy from biogas and producing smaller amount of sludge, compared to aerobic treatment systems [6,7].

In this context, the use UASB (Upflow Anaerobic Sludge Blanket) reactors has a wide acceptance in Brazil, mainly due to the low costs and good removal of organic matter [8,9]. Despite the treatment capacity for high organic content wastewater, the UASB reactors can be affected by the presence of certain substances and / or materials with reduction of its removal efficiency.

Given the above, this study aims to evaluate the influence of toilet paper in wastewater treatment in UASB reactors.

MATERIALS AND METHODS

Two UASB reactors (useful volume - 8 L) were installed and fed with synthetic domestic wastewater + toilet paper (R1), and with synthetic domestic wastewater (R2). Figure 1 shows the dimensions and the reactors configuration. The hydraulic retention time (HRT) was 24 hours, based in high cellulose content of the wastewater[10]. Each reactor was inoculated with sludge from an anaerobic treatment plant of a brewery (average biochemical methane potential (BMP) - 0.1041 g COD CH_4 g^{-1} VSS d^{-1}). The synthetic domestic wastewater was prepared in the laboratory, according with Torres[11] recommendation.

In Phase I (PI), R1 was fed with the addition of one double sheet of white toilet paper (11.5 x 10 cm^2) per liter of the synthetic domestic wastewater used, which was based on Eren and Karadagli [12] recommendation, and resulted in 0.42 g toilet paper per liter. In Phase II (PII), R1 was fed with two double sheet of white toilet paper per liter of synthetic domestic wastewater (0.81 g toilet paper per liter). The increased load was based on studies that support the use of 12 sheets per day of toilet paper per person in England[13] and associated with the 6 L of water flushed in a common toilet in Brazil. R2 had no phase changes.

The toilet paper sheets underwent hydrolysis before entering the reactor, in order to reduce the total suspended solids. Each toilet paper sheet was triturated, dissolved with water (Phase I – 1 sheet L^{-1}; Phase II – 2 sheets L^{-1}) and mixed for 24 hours, with a 1000 rpm mixer. After this period, the ingredients for preparation of synthetic wastewater[11] were added to this mixture. Before feeding the reactors, both wastewaters

(with toilet paper addition for R1 and without for R2) were stored in a refrigerator and warmed in a thermic immersion bath (40° C).

The monitoring period was 79 days (PI) and 30 days (PII), and the parameters were: pH, Chemical Oxygen Demand (COD) (Raw and filtered), solid content, alkalinity, volatile fatty acids (VFA) and glucose, every 3 days. Glucose was measured by Anthrone method[14].

The produced biogas was measured by liquid displacement in a 3% NaOH solution (w/v) for quantifying the methane content[15].

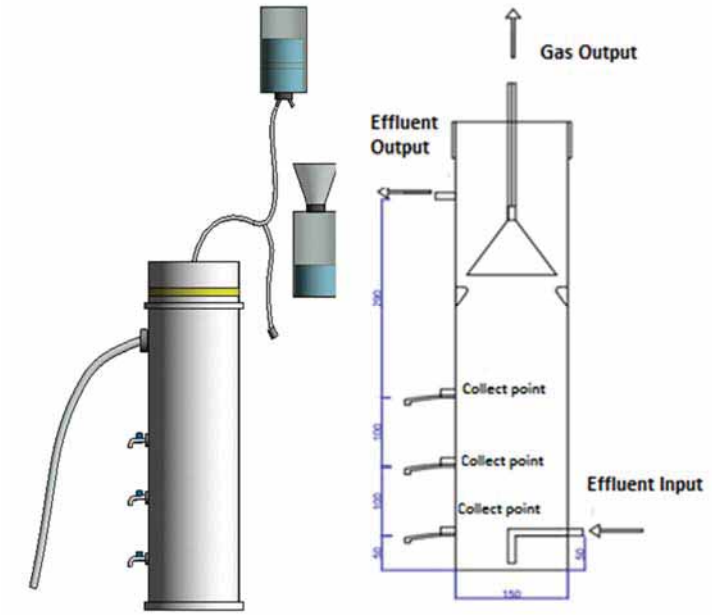


FIGURE 1. Reactor illustrations (dimension units in mm)

RESULTS AND DISCUSSION

Table 1 contains the average results for physical-chemical parameters of the influent and effluent from R1 and R2 reactors.

The effluent average total alkalinity of R1 was 451 and 345 mg $CaCO_3$ L^{-1} in PI and PII respectively. Despite the reduction in total alkalinity due to increased organic load, R1 had buffer capacity enough to maintain balance. The effluent average total alkalinity of R2 remained in 472 mg $CaCO_3$ L^{-1}.

The average VFA of R1 was 25 and 34 mg L^{-1} in PI and PII, respectively. A research carried out in Thailand showed VFA increase (especially acetic acid) proportionally to the addition of toilet paper, leading to acidification of anaerobic reactors[16]. The cited behavior was not observed in the present work.

The addition of two sheets of toilet paper in PII did not significantly influence the COD removal efficiency (79% in PI and 75% in PII - **Figure 2**), especially when we considered that Organic Loading Rate (OLR) was increased from 0,97 (PI) to 1,59 $kgCOD.m^{-3}.d^{-1}$ (PII). It is also important to consider that the control reactor (R2) had an average of raw COD removal efficiency of 83%. Then, the loose of COD removal efficiency from the toilet paper addition was not relevant.

TABLE 1. Results from the characterization of the wastewater (average values)

Parameter	Unit	R1 (PI)		R1 (PII)		R2	
		Influent	Effluent	Influent	Effluent	Influent	Effluent
COD_{R*}	mg L^{-1}	972 ± 65	200 ±15	1587± 46	396 ± 20	518 ± 15	85 ± 6
COD_{F*}		484 ± 31	118± 15	634 ± 38	192 ± 14	349 ± 19	64 ± 7
TSS**		440 ± 56	35 ± 7	678 ± 43	40 ± 6	66 ± 6	11 ± 2
VSS**		395 ± 57	25 ± 7	622 ± 49	20 ± 6	54 ± 6	6 ± 3
FSS**		45 ± 4	10 ± 2	61 ± 2	22 ± 2	12 ± 2	4 ± 1
VFA		-	25 ± 8	-	34 ± 3	46 ± 8	25 ± 5
TA	mg $CaCO_3$ L^{-1}	290 ± 26	435 ± 71	263 ± 15	345 ± 77	286 ± 28	472 ± 26
PA		225 ± 22	384 ± 71	201 ± 13	293 ±70	225 ± 22	428 ± 22
pH	-	8.6 ± 0.7	7.8 ± 0.3	8.7 ± 0.3	7.9 ± 0.3	8.4 ± 0.6	8.0 ± 0.3

*R – Raw and F - Filtered
** Solid content – TSS (total suspended solids), VSS (volatile suspended solids) and FSS (fixed suspended solids)

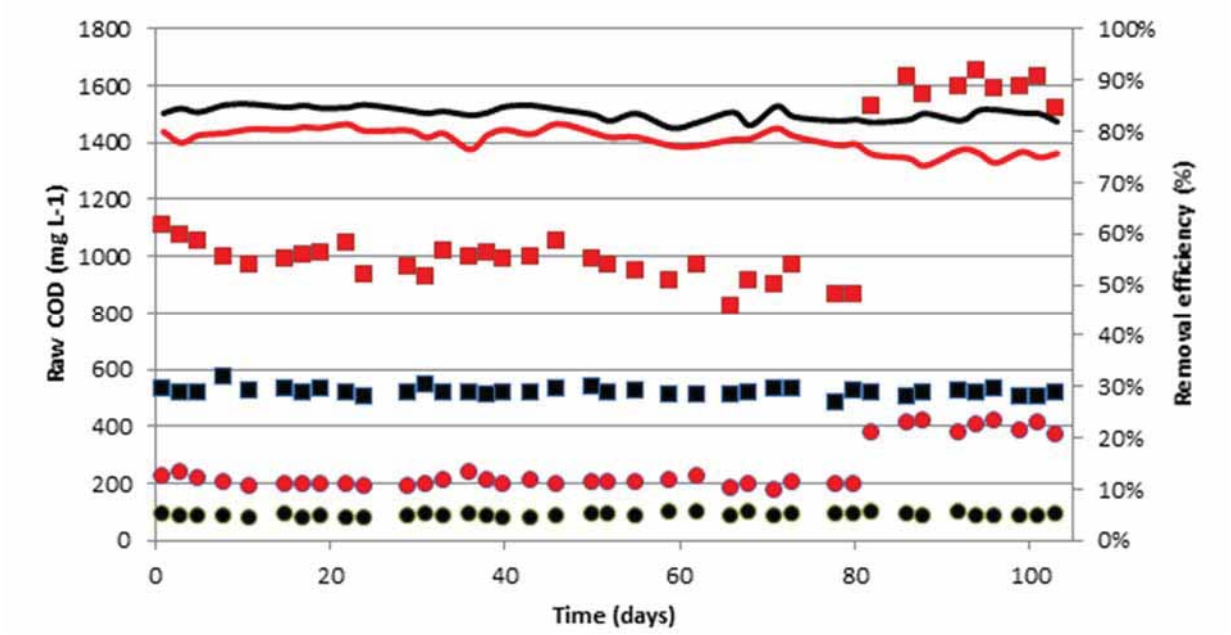


FIGURE 2. Raw chemical oxygen demand: (■) R1 - influent wastewater; (●) R1 – effluent wastewater; (■) R2 – influent wastewater; (●) R2 – effluent wastewater

However, when we considered the filtered COD removal efficiency decreased (from 76% in PI to 70% in PII – **Figure 3**) R1 starts to decrease the behavior from the addition of two sheets (filtered COD removal efficiency of 82% in R2).

The difference between raw COD and COD filtered, with higher values for the first one, is due to the retention of cellulose fibers from the toilet paper. The cellulose fibers, sized between 1.0 and 1.2 mm[17], are retained on the membrane used for filtration even after prehydrolysis.

The removal efficiencies achieved in this study are consistent with the literature: in India, an UASB reactor (real scale) treating paper mill effluent with OLR of 5.75 kg COD m^{-3} d^{-1} and HRT of 20h had COD removal efficiency ranging from 80 to 93%[18]; in Brazil, an UASB reactor (laboratory scale) treating effluent from bleaching of cellulose pulp, with COD ranging from 800 to 1400 mg L^{-1}, had removal efficiency ranging from 79 to 82%[10].

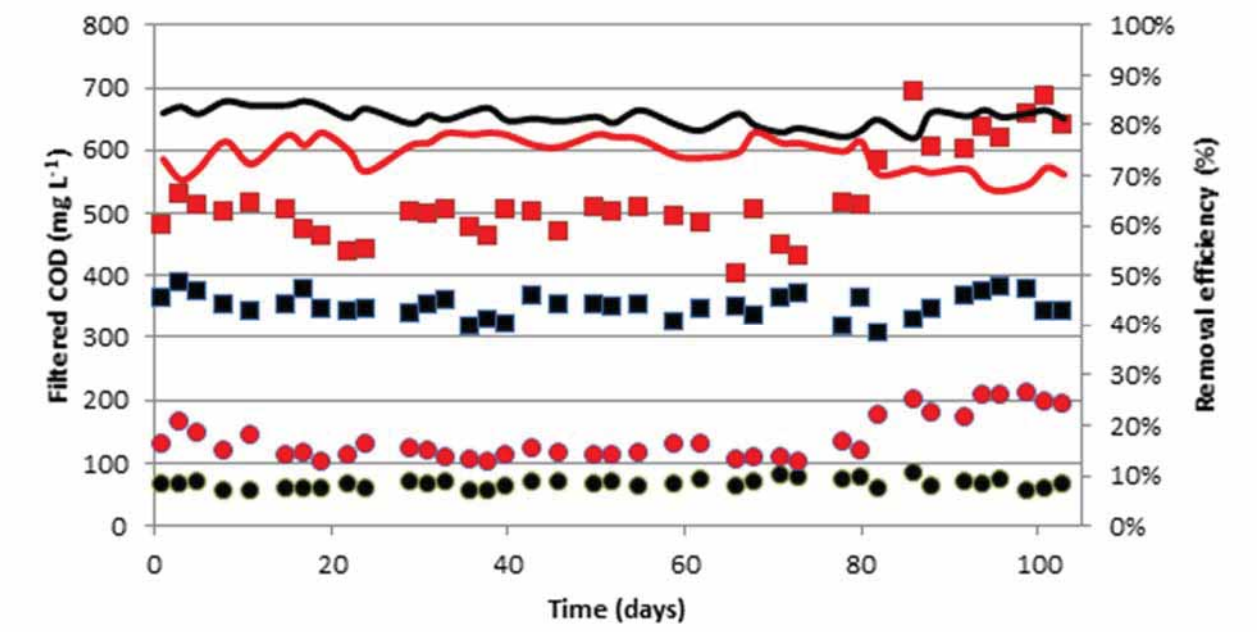


FIGURE 3. Filtered chemical oxygen demand: (■) R1 - influent wastewater; (●) R1 – effluent wastewater; (■) R2 – influent wastewater; (●) R2 – effluent wastewater

The VSS average efficiency removal for R1 was 94% and 96% respectively in PI and PII, and 88% for R2 (**Figure 4**). The high VSS influent values in R1 probably are due to cellulose fibers. A research carried out in a wastewater treatment plant in the Netherlands pointed out that cellulose from toilet paper accounted for 30-50% of the VSS in raw sewage[17]. Despite the increase of VSS in PI and PII, R1 had small reduction in removal efficiency compared to R2.

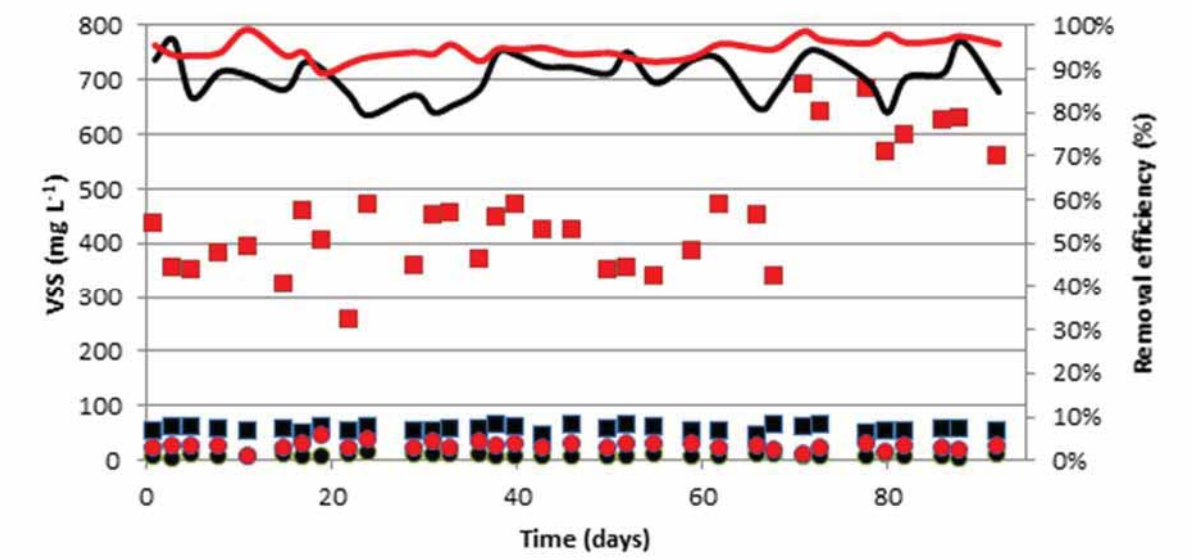


FIGURE 4. Volatile suspended solids: (■) R1 - influent wastewater; (●) R1 – effluent wastewater; (■) R2 – influent wastewater; (●) R2 – effluent wastewater

TSS average efficiency removal for R1 was 52% and 64% respectively in PI and PII, and 19% for R2 (**Figure 5**). The high TSS removal efficiency in R1 may be related to adsorption into sludge of high molecular weight molecules like the cellulose from toilet paper as well as extracellular polymeric substances that are responsible for the immobilization of anaerobic sludge and/or the reinforcement of the grains[20].

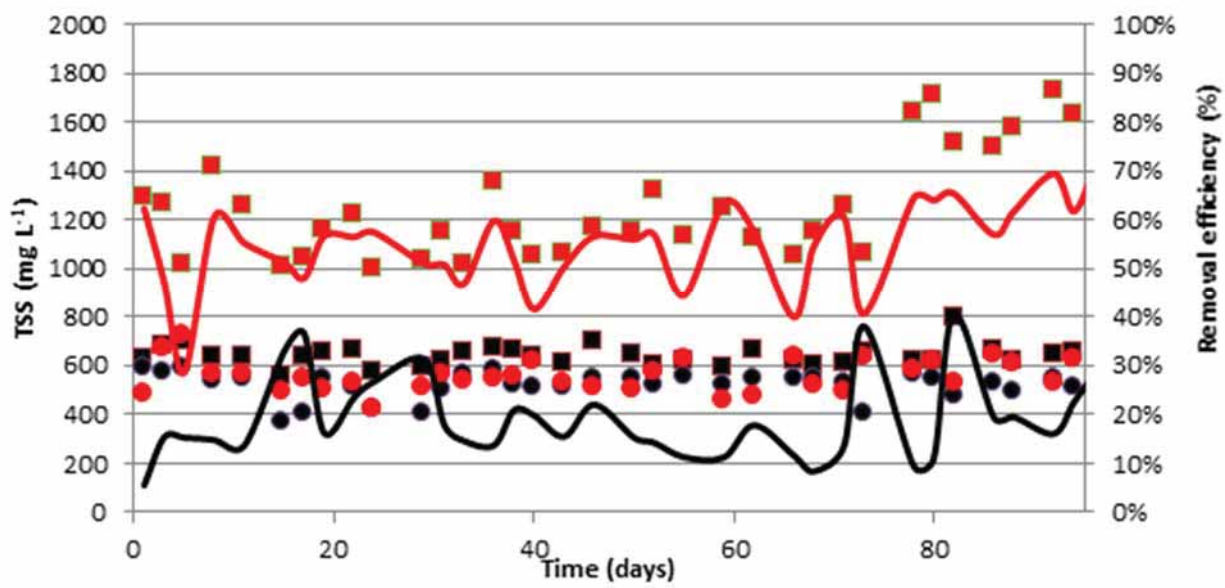


FIGURE 5. Volatile suspended solids: (■) R1 - influent wastewater; (●) R1 – effluent wastewater; (■) R2 – influent wastewater; (●) R2 – effluent wastewater

Average influent glucose in R1 was 499 and 927 mg COD L^{-1} in PI and PII, respectively, and 92 mg COD L^{-1} in R2.

The Anthrone method quantifies polysaccharides as starch or cellulose in the form of glucose. The method was used to relate the glucose content from different toilet paper amounts to cellulose degradation over time, in Thailand[8].

Average methane content in R1 was 498 and 848 mg COD L_{-1} in PI and PII, respectively; and 186 mg COD L^{-1} in R2. **Figure 6** displays glucose content and methane content.

Under normal conditions of temperature and pressure, the 100 mg COD removed corresponds to 350 mL of CH_4[21]. The 1000 mg COD removed corresponded to 254 mL (PI) and 280 mL (PII) in R1, which indicates the use of removed COD as source of energy for the growth of organisms. In general, the introduction of toilet paper in R1 increased methane production.

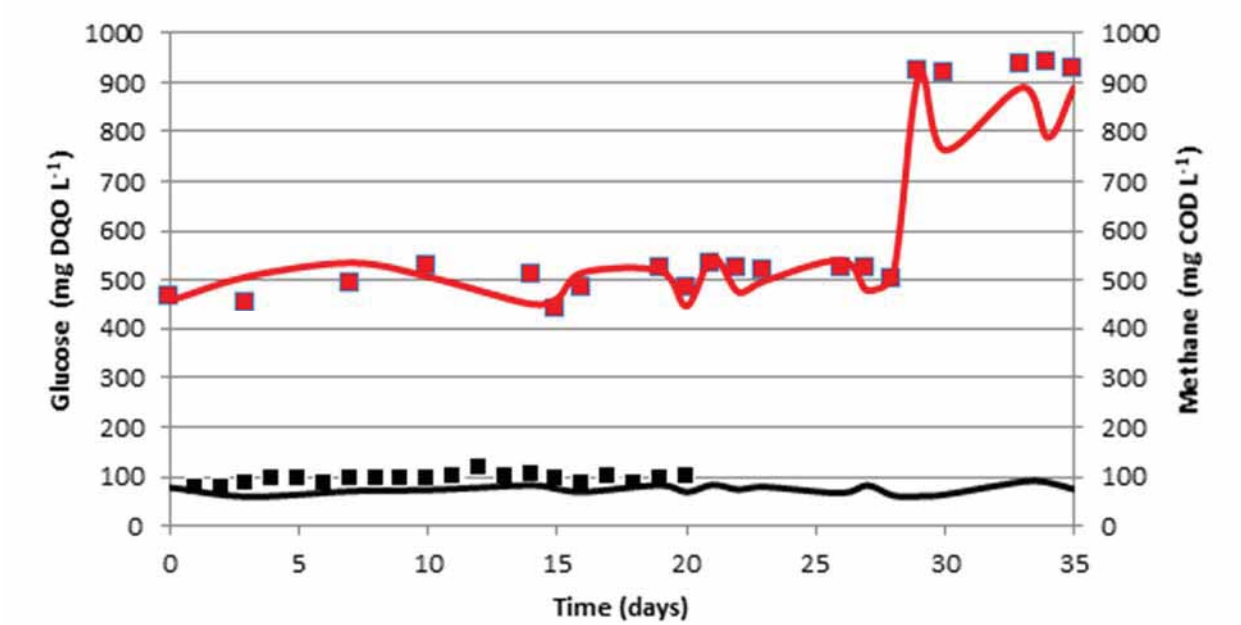


FIGURE 6. Glucose content and methane production (from X (PI) to Y (PII) day): (■) R1 influent glucose; (-) R1 – methane production; (■) R2 – influent glucose; (-) R2 – methane production

CONCLUSION

The addition of toilet paper in domestic sewage resulted in organic load (COD) and solids content increase, especially volatile solids. These solids from cellulose fibers were noticed especially during the COD measurement, due to the difference between the raw COD (972 and 1587 mg L^{-1}) and filtered COD (484 and 634 mg L^{-1}), in PI and PII, respectively, even after hydrolysis of the toilet paper. The presence of cellulose fibers from toilet paper reduced slightly the average COD removal efficiencies: 79% (Raw COD – PI), 75% (Raw COD – PII), 76% (Filtered COD – PI) and 70% (Filtered COD –

PII). R1 also had high average removal efficiency for volatile suspended solids, ranging from 94% (PI) to 96% (PII).
The breaking of toilet paper pulp can be a carbon source for microorganisms, increasing the production of biogas in UASB reactor. The generated energy can be used in the treatment plant itself and its excesses can be sold, increasing the technical and economic viability of the plant. However, parameters such as suspended solids, alkalinity, acid production, among others should be appropriately monitored in order to prevent possible failure.
In general, the UASB reactor showed ability to withstand the organic load and solid content increase after toilet paper additions.

ACKNOWLEDGMENTS

The authors would like to thank CAPES Fundation (Comissão de Aperfeiçoamento de Pessoal do Nível Superior), Propesq (Pró-reitoria de Pesquisa), FINEP (Financiadora de Estudos e Projetos) and CNPq (Conselho Nacional de Desenvolvimento Científico) for the scholarship awarded to the first author.

REFERENCES

1. SUTO, M.; TOMITA, F. Induction and catabolite repression mechanisms of cellulase in fungi. J Biosci Bioeng, v. 92, n. 4, p. 305-311, 2001.
2. CHERNICHARO, C. A. L. Princípios do tratamento biológico de águas residuárias: reatores anaeróbios. 2. ed. Belo Horizonte: Departamento de Engenharia Sanitária e Ambiental - UFMG, 380 p., 2007.
3. CHINNARAJ, S.; VENKOBA RAO, G. Implementation of an UASB Anaerobic Digester at Bagasse-Based Pulp and Paper Industry. Biomass and Bioenergy, v. 30, n.3, p. 273-277, 2006
4. EREN, B.; KARADAGLI, F. Physical disintegration of toilet papers in wastewater systems: experimental analysis and mathematical modelling. Environmental Science & Technology, v.46, n. 5, p. 2870-2876,2012.
5. HONDA, S.; MIYATA, N.; IWAHORI, K. Recovery of biomass celulose from waste sewage sludge. Journal Mater Cycles Waste Manag, v. 4, p. 46-50, 2002
6. GHASHIMI, D.S.M. TAO, Y. ; DE KREUK, M.; ABBAS, B.; ZANDVOORT, M.H.; VAN LIER, J. B. Digester performance and microbial community changes in thermophilic and mesophilic sequencing batch reactors fed with the fine sieved fraction of municipal sewage, Water Research , p.1-11, 2015, b
7. LEITÃO, R.; HAANDEL, A.V.; ZEEMAN, G; LETTINGA, G., The effects of operational and environmental variations on anaerobic wastewater treatment system: A review, Bioresource Technology, v. 97, n. 9, p.1105-1118, 2006.
8. LIN, H.; LIAO, B.; Q, CHEN, J.; GAO, W.;WANG, L.;WANG, F.;LU, X. New insights into membrane fouling in a submerged anaerobic membrane bioreactor based on characterization of cake sludge and bulk sludge. Bioresource Technology., v. 102, n. 3, p.2373–2379, 2011
9. MAHMOUD, N.; ZEEMAN, G.; GIJZEN H.; LETTINGA G. Solids removal in upflow anaerobic reactors, a review. Bioresource Technology, v. 9, p 1-9, 2003b.
10. BUZZINI, A. P; PIRES, E. C. Evaluation of a upflow anaerobic sludge blanket reactor with partial recirculation of effluent used to treat wastewaters from pulp and paper plants. Bioresource Technology, v. 98, n. 9, p.1838-1848, 2007.

11. TORRES, P. (1992). Desempenho de um Reator Anaeróbio de Manta de Lodo (UASB) de Bancada no Tratamento de Substrato Sintético Simulando Esgotos Sanitários. São Carlos, SP. Dissertação (Mestrado) - Escola de Engenharia de São Carlos, Universidade de São Paulo.
12. EREN, B.; KARADAGLI, F. Physical disintegration of toilet papers in wastewater systems: experimental analysis and mathematical modelling. Environmental Science & Technology, v.46, n. 5, p. 2870-2876,2012.
13. ALMEIDA, M.C.; BUTLER, D.; FRIEDLER, E., At-source domestic wastewater quality, Urban Water, v. 1, n. 1, p. 49-55, 1999.
14. YEMM, E.W.; WILLIS, A.J. The estimation of carbohydrates in plant extracts by anthrone. Biochemical Journal, London, v.57, n.3, p.508-514, 1954.
15. AMORIM, S.M.;Avaliação da interferência de diferentes doadores de elétronse Mediadores Redox sobre a remoção anaeróbia de cor em efluentes têxteis. 2010. Dissertação (Mestrado). Programa de Pós-Graduação em Engenharia Civil, Universidade Federal de Pernambuco, Recife, 2010.
16. GIRI, R. R.; TAKEUCHI, J.; OZAKI, H. Biodegradation of domestic wastewater under the simulated conditions of Thailand. Water and Environment Journal, v. 20, n. 3, p. 169-176, 2006
17. RUIKEN, C. J; BREUER G; KLAVERSMA, E; SANTIAGO, T.; VANLOOSDRECHT, M. C. M; Sieving wastewater – Cellulose recovery, economic and energy evaluation. Water Research, v. 47, n. 1, p. 43-48, 2013.
18. CHINNARAJ, S.; VENKOBA RAO, G. Implementation of an UASB Anaerobic Digester at Bagasse-Based Pulp and Paper Industry. Biomass and Bioenergy, v. 30, n.3, p. 273-277, 2006
19. BUZZINI, A. P; PIRES, E. C. Evaluation of a upflow anaerobic sludge blanket reactor with partial recirculation of effluent used to treat wastewaters from pulp and paper plants. Bioresource Technology, v. 98, n. 9, p.1838-1848, 2007.
20. MAHMOUD, N.; ZEEMAN, G.; GIJZEN H.; LETTINGA G. Solids removal in upflow anaerobic reactors, a review. Bioresource Technology, v. 9, p 1-9, 2003b.
21. ANGELIDAKI, I.; SANDERS, W. Assessment of the anaerobic biodegradability of macropollutants. Rev Environ Sci Biotechnol, vol. 3, p.117–129, 2004.

CHAPTER 7.35 FENTON OXIDATIVE PROCESS EVALUATION IN THE TREATMENT OF SYNTHETIC TEXTILE EFFLUENT CONTAINING DYE DIRECT BLACK 22

M.A.P. Kelm *(1); D. S. Figueiroa (1) and N.P.S. Lopes (1)

(1) Associação Caruaruense de Ensino Superior, Av. Portugal, N°584, Caruaru, Brazil

ABSTRACT

Advanced oxidation processes have the potential to transform many substances with difficult elimination in biodegradable substances or even easily eliminated substances by conventional physical and chemical processes, through reactions that generate active oxidizing species, such as hydroxyl free radicals (●OH). Hydrogen peroxide is the generating source more common of these radicals. This work evaluated the performance of the oxidative process advanced Fenton in the treatment of synthetic textile effluent containing direct dye Black 22. Through factorial planning 2^3 with four repetitions in central points, introducing as control variables concentration of H_2O_2 (18 mmol/L, 90 mmol/L) and Fe^{2+} concentration (5 mmol/L, 10 mmol/L) and mixing time (30 min, 60 min) , with pH 3 ±0,2. Tests were done in batch under constant mechanical agitation. As output variables, were analyzed color, turbidity, COD and H_2O_2. In some tests there was reduction true color and turbidity up to ninety percent. COD reduction presented values between thirty-eight and sixty-eight percent. Significance analysis was performed from the effects of the studied factors on each output variable. For color and turbidity removal, the best condition of the factorial design is the one that brings the $[Fe^{2+}]$ = 5 mmol/L, $[H_2O_2]$ = 18 mmol/L and 60 minutes mixing time. The major drawback observed during the process was the waste formation and yellow coloring due to iron oxides.

Keywords: advanced oxidation process, azo dyes, effluent treatment, textile industry.

INTRODUCTION

The stages of textile production make large volumes of wastewater. These are mainly characterized by the presence of organic pollutants and dyes that give the same color, and sources of environmental contamination. The toxicity of textile effluents becomes more relevant when dyes are often used based on heavy metals, sulfur, azo dyes, and other compounds such as surfactants, aromatic solvents, sulfates, among others[1,2,3,4].

The Advanced Oxidation Processes (AOPs) are an alternative for the treatment of this type of effluent. The POAs have the potential to transform many substances difficult to eliminate in biodegradable substances or those easily removed by conventional chemical processes[5].

---

*Author for correspondence: miguel.kelm@outlook.com

Fenton reaction is utilized for oxidation of contaminants and effluent treatment[4]. It is caused by the formation of hydroxyl radicals from the redox hydrogen peroxide (H2O2) catalyzed by divalent iron ions[6]. The process can be represented by the chemical equation (1):

$$Fe^{2+} + H_2O_2 \rightarrow Fe^{3+} + \bullet OH + OH^- \quad (1)$$

Ferric ions present in the reaction are excellent coagulants, which makes Fenton perform dual function in treatment[7]. The oxidative potential of this process to treat effluents is connected to its simplicity, since the reaction occurs at ambient temperature and pressure[8].

It is reported by various authors the importance of pH on the efficiency of the Fenton reaction. The optimum pH for the process is about 3. The first step is the technique of pH adjustment, followed by reaction, neutralization and coagulation / precipitation[9].

MATERIALS AND METHODS

Factorial Design. The study was organized by a factorial design 2^3 with four central points, a total of 12 tests, introducing as control variables concentration of Fe^{2+}, H_2O_2 and mixing time. **Table 1** and **2** report, respectively, the values of minimum, maximum, and the center point of each factor assessed and configuration of the executed tests. As response variables, the factorial design evaluated the removal of color, turbidity and COD, as such as the consumption of hydrogen peroxide.

TABLE 1. Parameters studied in factorial design

Parameter	-1	0	+1
[Fe^{2+}] mmol/L	5	7,5	10
[H_2O_2] mmol/L	18	54	90
Mixing time (min)	30	45	60

TABLE 2. Matrix factorial design

Test	[Fe^{2+}](mmol/L)	[H_2O_2](mmol/L)	Mixing Time (min)
1	-1	-1	-1
2	+1	-1	-1
3	-1	+1	-1
4	+1	+1	-1
5	-1	-1	+1
6	+1	-1	+1
7	-1	+1	+1
8	+1	+1	+1
9	0	0	0
10	0	0	0
11	0	0	0
12	0	0	0

Color, turbidity and COD have been determined following the methodologies described by APHA (2005)[10] and Kato et al (2014)[11]. Hydrogen peroxide was quantified at the end of the reaction, following the methodology proposed by Jung et al.

Preparation of synthetic textile effluent. The synthetic textile effluent produced was composed according to the **Table 3**, as methodology by Mo et al. Azo dye Direct Black 22 (**Figure 1**) was used in the synthetic textile effluent produced as the azo dyes are the most used in textile processing[1].

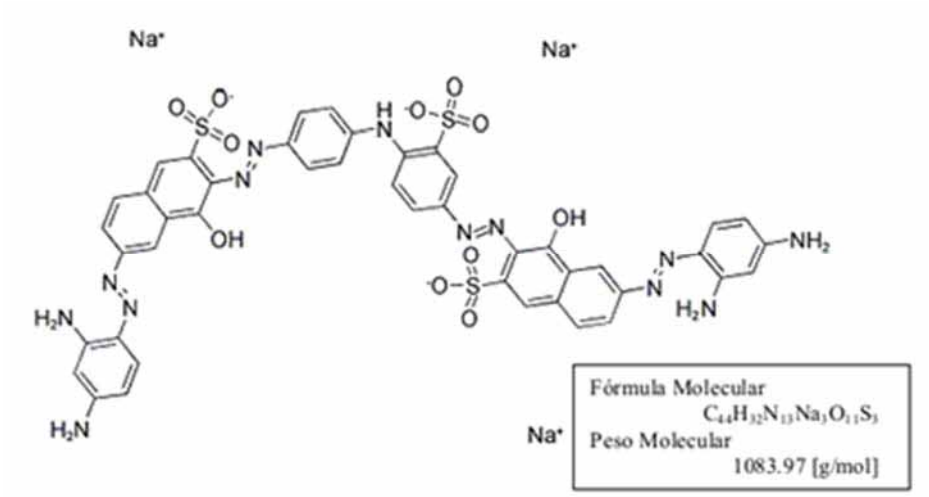


FIGURE 1. Chemical structure Direct Black 22. The dye has four links azo (-N=N-)

Before use it in the treatment process, the solution of this dye was hydrolyzed according to the methodology used by Santos (2012), raising the pH to 11 with NaOH, heating the colored solution at 80 ° C for 1 hour and, after cooling, neutralizing it to pH about 7 with HCl. Commercial starch (Maizena) added to represent the step of sizing / desizing beneficiation process was also conditioned to better solubilization in water, and the mixture heated at 90 ° C for thirty minutes according to the methodology of Santos (2012). Concentration of starch in the composition of the textile effluent was estimated for COD value of approximately 1800 mg O_2/L, the amount was determined by the ratio of 1.00g of a commercial starch to 1188 mg O_2/L value obtained by the author. It was characterized color, turbidity and chemical oxygen demand of the textile synthetic sewage before treatment.

TABLE 3. Composition of the textile synthetic effluent

Components	Concentration (g/L)
Direct Black 22	0,100
Starch	1,50
NaCl	0,250
$NaSO_4$	0,750

Fenton Process. As shown in **Figure 2**, Fenton reactor was assembled from a 500 mL beaker and a mechanical stirrer. Tests were performed in a batch system at room temperature (25.5 ° C). Transferred to 100 ml of this effluent to the reactor and added with 100 ml of iron sulfate (II) solution as a source of Fe^{2+}. then the pH of the mixture was adjusted to a value of 3. Under constant stirring, was added slowly to the reactor 100 mL of hydrogen peroxide solution. At the end of the addition of the peroxide, it was clocked the time of mixing of the substance. After fenton process, treated effluent was characterized by color, turbidity, COD and residual peroxide.

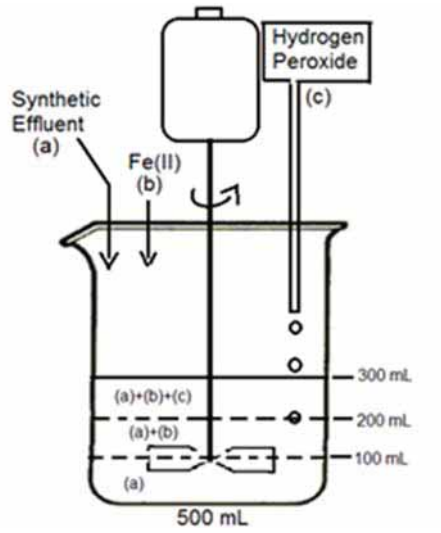


FIGURE 2. Fenton Reactor

RESULTS AND DISCUSSION

More than one condition caused high levels of response variables, including the conditions of lower concentration of reagents and mixing in short time.

In Test Nº. 7, the removal of the original color reached 92%. In tests 1 and 5, where the time and peroxide concentration varied, there was obtained 91% removal. Martins et al. (2011), making use of the Fenton process for treating synthetic textile effluent obtained true maximum color removal of 86% at pH 3 as $[H_2O_2]$ = 1500mgL-1, $[Fe^{2+}]$ = $75mgL^{-1}$ and time 120 min. Andrade et al. (2015) reached removal of 95% of the dye mixture (orange Indosol 2 GL 250, Shiny Red Foron E-2BL 200 and Yellow Optisal 2 RL) at pH 4 with $[H_2O_2]$ = 60mgL-1, $[Fe^{2+}]$ = 50 mgL-1 and reaction time of 62 minutes. Amaral (2015), evaluated the removal of azo dyes in a conventional UASB reactor and UASB reactor with micro-aeration, color removal was obtained in 78% ± 10 and 80 ± 12% in 1.9% saline conditions. The color reduction by Fenton is considered satisfactory, with superior results to that obtained with the UASB and lower than that obtained by Fenton with other types of dyes.

Figure 3 provides a visual comparison between the simulated textile effluent, after Fenton the crude effluent and the filtrate. The reddish crude treated, justified by the presence of oxidized iron generated by the studied treatment process.

The use of the Fenton process achieved satisfactory removal turbidity values (between 86% and 94%). It was noted that the values were lower at higher concentrations of Fe^{2+}. Salgado et al. (2009), using 60 mg of $FeSO_4$ and 0,750 mL concentrated H_2O_2 to 100 mL reaction volume and 30 minutes reaction time could remove of 93.8% in the real textile effluent turbidity.

The COD removal of the tests showed values between 39 and 65%. Martins et al. (2011), with the provisos $[H_2O_2]$ = 1500mgL^{-1}, $[Fe^{2+}]$ = 75mgL^{-1} and time of 120 min, removed 65%. Salgado et al. (2009), using 60 mg of $FeSO_4$ and H_2O_2 0,750mL concentrated to 100 mL reaction volume and time 30 minutes reaction, achieved 50% reduction of COD in real textile effluent, having saved the result as satisfactory and demonstrated that there was formation of side products due to partial mineralization of organic compounds present in the effluent. Andrade et al. (2015) reached 75% of the COD removing the dye mixture under the same conditions for removal of color.

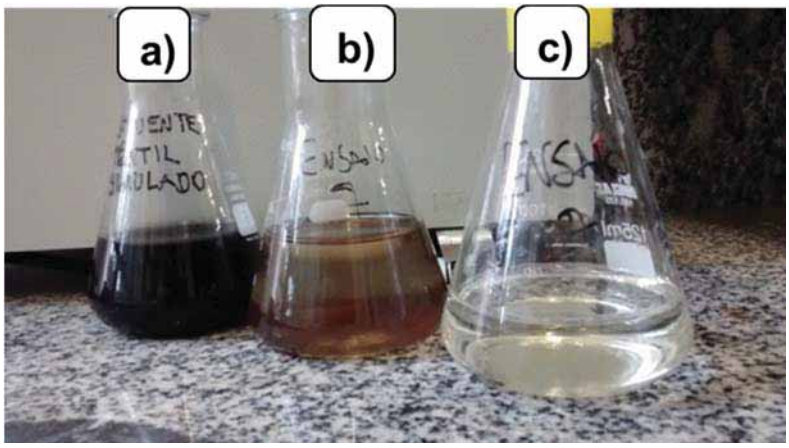


FIGURE 3. Visual comparison between the synthetic effluent (a), after Fenton effluent (b), and after fenton filtered with qualitative filter (c).

Effect Estimates. To color removal, the main factors are the concentration of Fe^{2+}, the concentration of H_2O_2, and the interaction between the two, as shown in **Table 4**, regarding the estimated effects.

TABLE 4. Effect estimates of the factors studied on color removal

Factor	Effect	SE Pure Error	t(3)	p
intercep.	84,4	0,9	98	0,000002
(1) [Fe2+]	-16	2	-8	0,005
(2) [H2O2]	-14	2	-7	0,007
(3) Temp (min)	2	2	0,8	0,5
1by2	-13	2	-6	0,009
1by3	-0,7	2	-0,3	0,8
2by3	-0,2	2	-0,1	0,9
1*2*3	-2	2	-0,9	0,4

According to **Table 4**, increased concentrations of iron and peroxide decreases the removal of color at 16 and 14%, respectively. **Figure 3** reports the removal of the original color interacting with the concentration of Fe^{2+} and H_2O_2. Negative effects of the color parameter, as indicated by table 10 is observed.

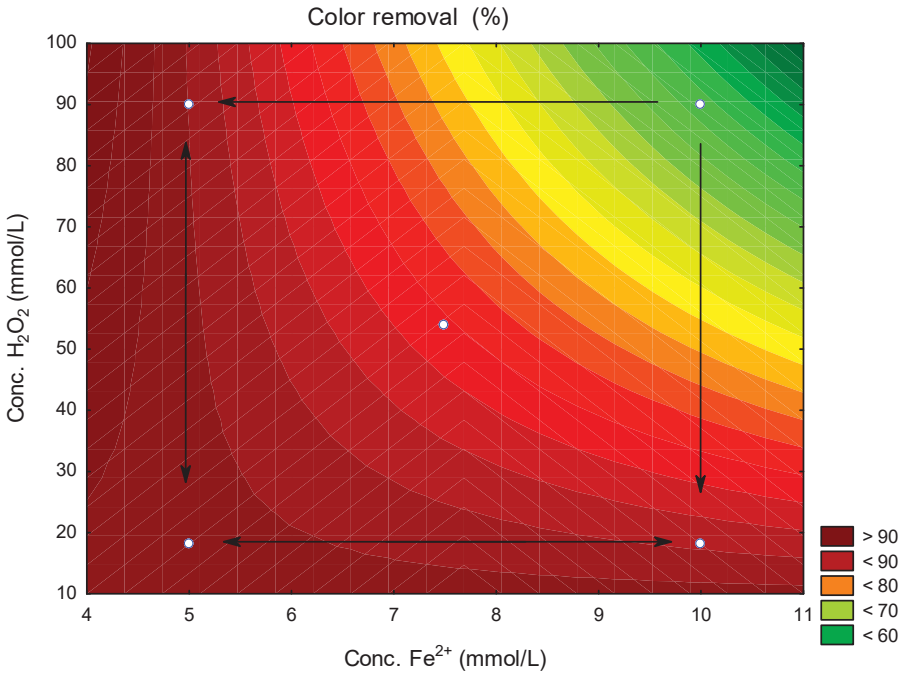


FIGURE 4. Effect of concentration of Fenton reagents on color removal

Observing the **Figure 4**, it is concluded that at low concentrations of H_2O_2, the variation in the concentration of iron (II) did not significantly effect the removal of the color. However at high concentrations of peroxide, the concentration of Fe^{2+} decreases the removal of the color. It is also possible to see that at low values of [Fe^{2+}], the change [H_2O_2] is not significant. However, the opposite is true for high concentrations of iron (II).

TABLE 5. Estimated effects of the factors studied on H_2O_2 consumption

Factors	Effect	SE Pure Error	t(3)	p
intercep.	79,8	0,7	113,9	0,000001
(1) [Fe^{2+}]	20	2	12	0,001
(2) [H_2O_2]	-6	2	-3	0,04
(3) Mixing time (min)	7	2	4	0,03
1by2	10	2	6	0,01
1by3	-3	2	-2	0,1
2by3	11	2	6	0,008
1*2*3	-8	2	-5	0,02

Consumption of hydrogen peroxide is indicative of the occurrence of the Fenton reaction. Therefore, inserting it as the response variable, it was possible to assess which factors studied have effect on the yield of the reaction.

According to the estimated effects, shown in **Table 5**, all the analyzed factors were significant for the consumption of H_2O_2, except the interaction between Fe^{2+} concentration and time. Increased iron (II) and the mixing increases the consumption of H_2O_2 in 20 and 7% respectively and the increase in [H_2O_2] 6% reduces consumption.

The graphic shown in **Figure 5** lists the concentration of the Fenton reagents and the consumption of hydrogen peroxide, represented by the color variation. It is observed that with increasing hydrogen peroxide concentration under Fe^{2+} concentration constant, there was a negative effect. However, with the increase of Fe^{2+}, there is a positive effect on the consumption of peroxide. Interaction between the two factors has a positive effect on the consumption of peroxide.

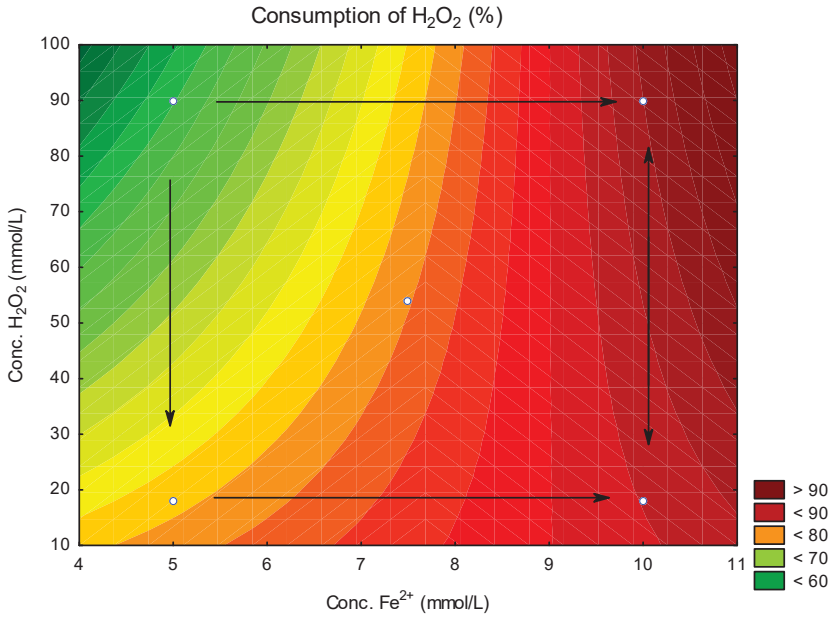


Figure 5. Effect of concentration of reagents on the consumption of hydrogen peroxide

The **Figure 6** shows the interaction between time and the concentration of H_2O_2 which is possible to see that the interaction between these variables favor the process. It was noted, however, that due to the instability of the indicator complexing titanium oxysulfate IV in the presence of small quantities of residual peroxide, complexing suffer interference from external factors such as light. This fact is attributed to the low percentage of peroxide consumption at low levels [H_2O_2] and high mixing, as shown on the left side of the graphic. The titanium oxalate methodology was inaccurate for low residual peroxide levels.

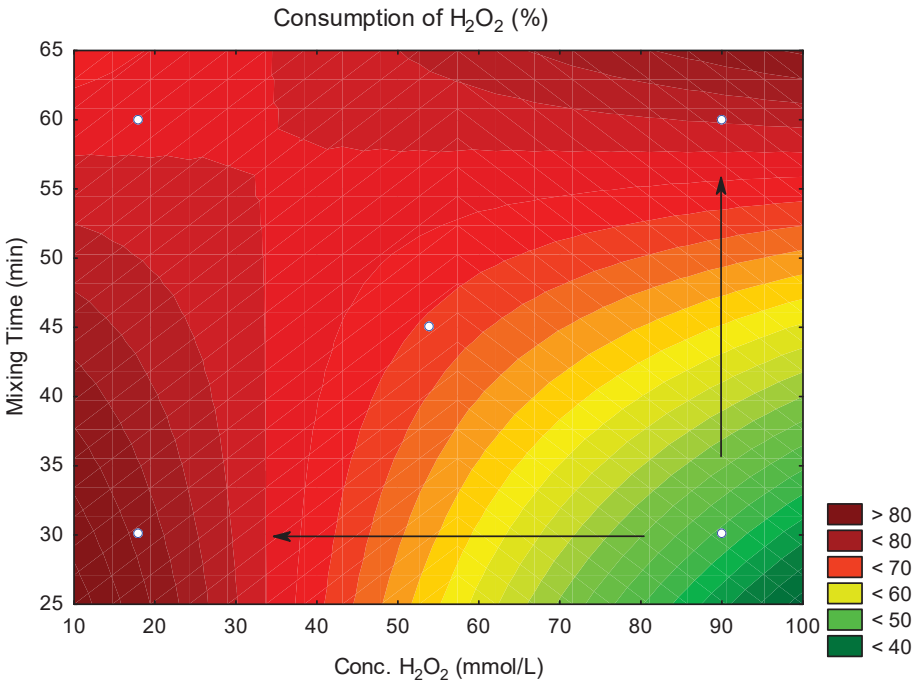


FIGURE 6. Effect of time and H_2O_2 concentration on the consumption of H_2O_2

No parameter of the factorial design showed significant effect for turbidity removal and COD.

CONCLUSION

The application of the Fenton oxidative process on a laboratory scale proved efficient in removing color and turbidity, over 90%, using smaller concentrations of reactants. The COD removal in the experiments obtained average values, which did not attend, for example, the current technical standard in Pernambuco (CPRH NT 2,001 / 2003), is necessary to evaluate the association of Fenton with other techniques to optimize the degradation of organic matter, as the set UV / H_2O_2 / Fe^{2+} (photo-Fenton) and O_3 / H_2O_2 / Fe^{2+} (ozone / Fenton). According to statistical analysis, some control variables damaged, independently, the process was the case of the concentration of Fe^{2+}, which in higher values, negatively influenced the removal of color. In the case of response peroxide consumption variable, it was observed that the concentration of Fe^{2+} influenced their percentages positively, causing the free radicals generated by the peroxide to be almost entirely consumed during the oxidation of Fe^{2+} ions to Fe^{3+}. The interaction between Fe^{2+} concentration and the response time does not affect any variable.
According to the results of the response variables, the best condition is the factorial design which brings the [Fe^{2+}] = 5 mmol / L, [H_2O_2] = 18 mmol / L and mixing of the substance in 60 minutes (test 5). In this configuration, the Fenton process better results removal of the original color and turbidity. The removal of chemical oxygen demand reached maximum values for the intermediate condition.

ACKNOWLEDGMENTS

The authors would like to thank the Laboratory of Environmental Engineering (LEA) and the Laboratory of Environmental Sanitation (LSA), both of the Federal University of Pernambuco.

REFERENCES

1. Marcelino. D.M.S. Evaluation of color removal, organic matter and sulphate of textile effluent through sequential biological reactors, Academic Center of Agreste, Federal University of Pernambuco, Caruaru, Brazil. 2013.
2. Vasconcelos, J.C.F. Textile effluent treatment using gamma radiation, Technology and Geosciences Center, Federal University of Pernambuco, Recife, Brazil, 2011.
3. AMARAL, F.M. Evaluation of color organic matter removal and textile effluent sulfate by anaerobic process followed by aerobic. Technology and Geosciences Center, Federal University of Pernambuco, Recife, Brazil. 2011.
4. Salgado, B.C.B.; Nogueira, M.I.C; Rodrigues, K.A.; Sampaio; G.M.M.S.; Buarque, H.L.B.; Araújo, R.S. Decolorization of synthetic and laundry wastewater containing indigo and azo dyes by the Fenton, photolytic and UV/ H_2O_2. Eng. Sanit Ambient, v. 14, p.1-8, 2009.
5. Hassemer, M.E.N. Photochemical oxidation - UV/H_2O_2 - for degradation of pollutants in effluents from textile industry. Department of sanitary and environmental engineering, Federal University of Santa Catarina, Florianópolis, Brazil, 2006.
6. Gewehr, A. G.; Silva, J.S.; Almeida, D.B.; Fleck, E.; Cybis, L.F.A. Application of the response surface methodology for landfill leached treatment using fenton process. Brazilian Association of Hydric Resources, Bento Gonçalves, Brazil, 2013.
7. Tosato Junior, J.C.; Halasz, M.R.T. Treatment of textile effluent using physical-chemical processes and advanced oxidative. In: International Workshop in Advanced Cleaner Production. 3., 2011, São Paulo, Brazil.
8. Fioreze, M; Santos, E.P; Schmachtenberg, N. Oxidative processes: Fundamentals and advanced environmental application. Electronic magazine in management, education and Digital Technology – REGET, Santa Maria,Brazil, v. 18, n. 1, abr. 2014.
9. Machado, L.L. Use of carbon composite/Fe_2O_3 and pyrite as catalysts of the peroxidation of textile effluents. , Federal University of Santa Catarina, Florianópolis, 2007.
10. APHA. Standard methods for the examination of water and wastewater. 21.ed. Washington: American Public Health Association, 2005.
11. Kato, M.T., Souza, L.F.C.; Moraes, J.; Campos, J.; Fonseca, R.M.; Gavazza, S.; Florencio, L.. Manual of procedures of the laboratory of environmental sanitation.1 ed. Olinda: Livro Rápido, 2014, 156 p.
12. Jung, Y.H.; Kim, H.K.; Park, H.M.; Park, Y.C.; Park, K.; Seo, J.M.; Kim, K.H. Mimicking the Fenton reaction-induced wood decay by fungi for pretreatment of lignocellulose. Bioresource Technology, v. 179, p. 467-472, 2014.
13. Mo, J.; Hwang, J.E.; Jegal, J.; Kim, J . Pretreatment of a Dyeing Wastewater Using Chemical Coagulants. Dyes and Pigments, v. 72, p. 240-245, 2007.
14. Santos, B.R.T. Effect of different electron donors and of changes in sulphate concentration on reductive decoloration of dye Direct Black 22. Technology and Geosciences Center, Federal University of Pernambuco, Recife, Brazil. 2011.

15. Martins, L.M.; Silva, C.E.; Moita Neto, J.M.; Lima, A.S.; Moreira, R.F.P.M. Application of Fenton, photo-Fenton and UV/H_2O_2 in treating synthetic textile wastewater containing the dye Black Biozol UC. Eng. Sanit. Ambient, v. 16, p. 261-270, 2011.
16. Andrade, P.M.; Carvalho, M.A.F.; Miranda, A.S.; Marques, H.R.; Campos, S.R.; Brito, N.N. Remediation of textile dyes mixtures using TiO_2/VIS photocatalysis and Fenton Fe^{2+}/H_2O_2. Brazilian Journal of Biosystems Engineering, v. 9 (4), p. 328-338, 2015.
17. Amaral, F.M. Removal of azo dyes in anaerobic/aerobic reactor system and in UASB reactor with micro-aeration. Technology and Geosciences Center, Federal University of Pernambuco, Recife, Brazil, 2015.

Section 8.
Control and Modelling of Environmental Processes

Page

Chapter 8.1 Water bodies modification caused by effluents with paracetamol 789
N.M.C. Araújo; D. A. Silva; M. J. Silva Júnior; K. K. Barros and L. F. C. Souza

Chapter 8.2 Development of an anaerobic digestion system to determine biogas energy potential 798
H. Numpaque López; B. Criollo; C. L. Díaz; J. D. Alvarado and C. Mendoza

Chapter 8.3 Pesticide trapping in fractal porosity of clays 808
T. Woignier; F. Clostre and M. Lesueur- Jannoyer

CHAPTER 8.1 WATER BODIES MODIFICATION CAUSED BY EFFLUENTS WITH PARACETAMOL

N.M.C. Araújo (1); D. A. Silva (1); M. J. Silva Júnior (1); K. K. Barros (2) and L. F. C. Souza *(1)

(1) University Center of Tabosa de Almeida – ASCES-UNITA. Portugal Avenue, nº. 585. Caruaru City, Brazil
(2) Federal University of Pernambuco, Westland Academic Centre, Technology Centre. Highway BR-104, Km 59, s/n – Nova Caruaru. Caruaru City, Brazil

ABSTRACT

In Brazil, the consumptions of pharmaceutical products have been produced large amounts of solids and liquid residues. One of the major disposal sites of this type of material is in the wastewater, around 20%, including remnants of drugs and patients excretion. Therefore, drugs residue and their metabolites have been found in sewage and natural water, in various parts of the world. Among consumptions drugs, the paracetamol has been used in large scale in Brazil, due to the epidemics of Dengue, Chikungunya fever and Zika. Moreover, the paracetamol non-consumed is discharded in environmental and it can cause diverse impacts to aquatic organisms.
In this experiment, the paracetamol contamination potential was evaluated by characterization of effluents containing drugs composed of paracetamol. Effluent solution was produced by dilution of tablets containing paracetamol, and the final concentration was 750 $mg.L^{-1}$. This solution was prepared 6 times with different manufacturers. The parameters analyzed were: pH, turbidity, electrical conductivity, sulphate, alkalinity, total nitrogen and Chemical Oxygen Demand (COD).
Paracetamol solution presented an acidic character (pH = 5 ± 1) and was slightly soluble in water, causing turbidity and electrical conductivity ranging from 8 to 47 NTU and from 4 to 26 $\mu S.cm^{-1}$, respectively. The average sulphate, chloride, nitrogen and color concentration were 4 ± 2 $mgSO_4.L^{-1}$, 9 ± 7 $mgCl^{-}.L^{-1}$, < 1 mg $N\text{-}NTK.L^{-1}$ and 84 ± 69 $mgCo\text{-}Pt.L^{-1}$, respectively. In relation to the organic load, COD and BOD average values were equal to 1574 ± 93 and < 1 mg $O_2.L^{-1}$, respectively. Almost all the parameter results are in agreement with the effluent discharge standard on water bodies in Brazil, even without treatment. Only in one manufacturer, the pH average was 4.4 ± 0.1, lower than the acceptable (5 to 9). In the same resolution, BOD is the reference parameter for contamination by organic matter. In all solution, BOD was lower than 1 mg $O_2.L^{-1}$, accepted value. However, COD values were high than BOD, indicating recalcitrant property, remain in the environment for long periods. Those results showed a paracetamol solution with concentration equal to 750 mg L^{-1} was considered recalcitrant, acid and, consequently, presents high potential of contamination.

Keywords: drugs, environmental characteristics, pollution

---

*Author for correspondence: luizas@gmail.com

INTRODUCTION

Pharmaceutical compounds have been frequently found in raw and treated domestic effluents, water bodies and drink water[1,2]. Because of this, detailed studies on toxicity, degradability and environment impacts of pharmaceuticals compounds need to be performed. According Peake et al.[3], several problems can occur in environment due to pharmaceutical compounds discharge, loss of diversity biological is an example. In natural ecosystems, there are several types of species, one more sensitive than others. Pharmaceutical compounds can cause quick and extensive ultimate destruction of species and their genetic diversity. Changing ecosystem balance can be caused by destruction of only one species, resulting in chemical, physical and biological changes of the water bodies[4]. The scarcity of natural waters with high quality for human consumption has been caused by the contamination of water bodies and inadequate management of hydrographic basins through discharge of untreated effluents and solid residue in environment and contamination and lack of planning of land use[5,6].

Environment is considered contaminated when there are compounds or organisms capable to cause disease. Aquatic organisms can bioaccumulate compounds or be sick by ingesting contaminated water. Humans can be infected by ingesting contaminated water or contaminated aquatic organisms[7]. Environment may be contaminated by pharmaceutical compounds through the incorrect disposal of medicines and industrial residue, excretion of intact pharmacos and their metabolites, and the lack of adequate sewage treatment for these types of compounds. About 50 to 90% of the intact pharmaceutical compounds from ingested medicines are excreted through urine or faeces. Simultaneously, population usually disposal expired and remains medications in sinks, toilets and domestic garbage. In Brasil, sewage collection network only covers about 57% of Brasilian homes and appropriate sewage treatment systems are lower than this percentage[2,8].

All these factors have been contributed to water bodies and soil contamination by pharmaceuticals compounds, and because of the low concentrations, the active principles are difficult to be detected, identified and quantified, although these concentrations cause serious problems. Technological advancement has allowed to increase the precision and accuracy of analytical methods, expanding the number of possible compounds to be detected. This advance has allowed the study of these compounds[9]. The other compounds founded in medications, known as adjuvants, cause less toxicity than the active principle, however, can alter physical and chemiscal caracteristics of wáter as pH, turbidity, salinity, organic load, etc.

Consumption of medication without control is growing in Brazil every year, through self-medication, which is a common practice in all social classes. Free access to medicine causes a consumption of inappropriate medications generating leftovers and residues[10]. In Brazil, there is no limitations on amount of laboratories to made medicines. Each one have its own medicine formulation, which are similar to each other, but are not equal. The sort of adjuvants and their concentration were the main difference. Because of this, each medicine with the same active principle and the same concentration is different when made from different laboratory. Paracetamol is the current most consumed drug in Brazil. It is an analgesic and antipyretic consumed by adults and children, free sale with and without medical prescription. According Liberal[11],

paracetamol is cited among the most consumed drugs in the self-medication. It is used for mild pain and fever relief also being recommended by the Brazilian Health Ministry in assisting dengue, zika and chikungunya treatments. After administration, a significant portion of drugs, 90% is excreted by humans through the urine, approximately at 24 hours[12].

Costa and Costa[8] described the pollution caused by medicines residues and affirmed to be unnoticed but dangerous, because in small concentrations, changes in the cells can be observated, becoming a threat to the environment and public health. Because of this, the aim of this work was to evaluate the main changes in the physical-chemical characteristics of water from water bodies that could be caused by disposal of medicines consisting of paracetamol. and check for differences between paracetamol medicines produced by different laboratories.

MATERIALS AND METHODS

Three paracetamol medicines produced by three different laboratories were analyzed, L1, L2 and L3, because of the composition of medicines made of each laboratory are different. The laboratories were selected by the higher consumption by the population. Medicines were purchased in drugstores.

For realization of all selected parameters, 2 L sample were prepared. One tablet of 750 mg. g^{-1} was dissolved in 1 L of deionized water. Three authentic replicas for each laboratory were prepared, totaling 9 samples (**Figure 1**).

pH (potenciometric), turbidity (turbidimetric), conductivity (electric), sulfate (gravimetric), alkalinity (potenciometric), and total ammonia nitrogen (titrimetric), Biochemical Oxygen Demand (BOD - manometric), Chemical Oxygen Demand (COD - colorimetric), total and suspended solids (gravimetric) were parameters analyzed following the Standard Methods[13] and laboratory manual[14].

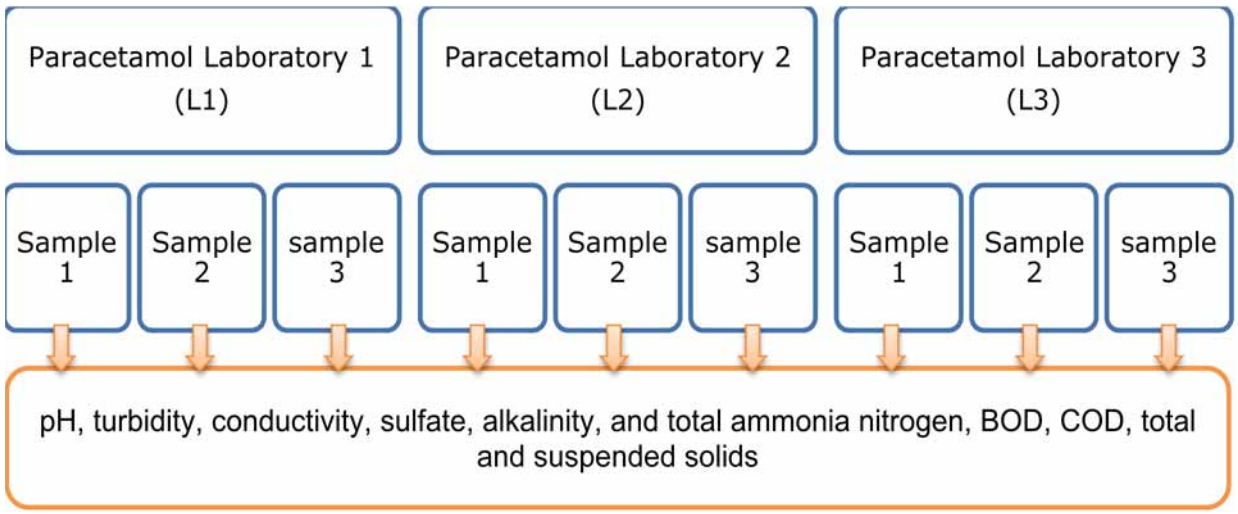


FIGURE 1. Evaluation of samples of paracetamol medicines from different laboratories

RESULTS AND DISCUSSION

Among the studied parameters, the water characteristics alterations were observed. These alterations make it impossible to discharge in water bodies and in the soil. The values of each parameters allowed to discharge in water bodies were determined by legislation. In Brazil, the legislation CONAMA 357/2005[15] and CONAMA 430/2011[16] determine the characteristic to maintain the water bodies quality and the characteristics of the effluent to discharge in water bodies, respectively.

Average pH of each analyzed laboratory were 4.9±0.3 (L1), 6.7±0.2 (L2) and 4.4±0.1 (L3), demonstrating an acid character, which may cause pH reduction of the water body, aquatic life damage and efficiency reduction both biological and physical-chemical treatment systems. The pH of the water after to add each medicine, L1, L2 or L3, was different, thus each medicine can cause different impact. In **Figure 2** average value of each laboratory can be observed.

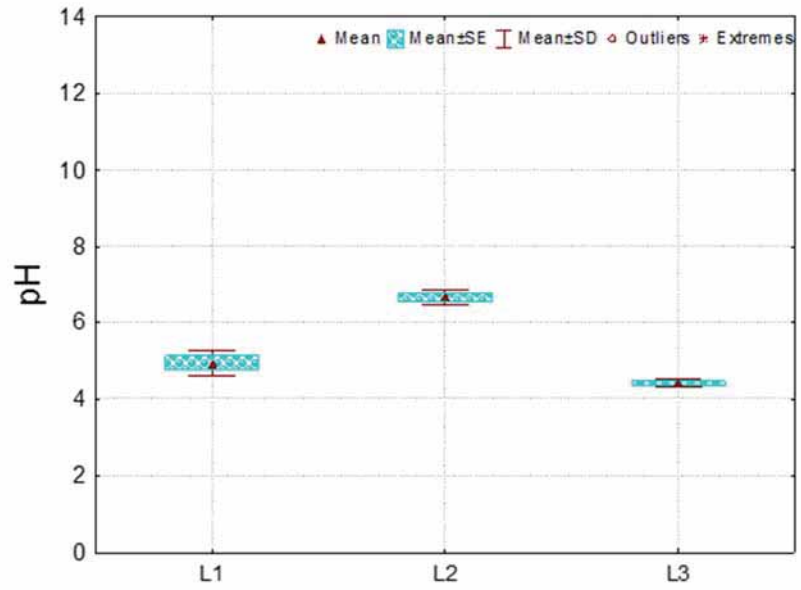


FIGURE 2. Box-plot of the pH of each laboratory

Conductivity average values of L1 and L3 were similar, 6 ± 2 μs.cm^{-1} and 7.4 ± 0.8 μs.cm^{-1}, respectively, but, in L1 sample, values varied more than in L3. Drug produced by L2 generated a solution with higher conductivity than L1 and L3, 21 ± 3 μs.cm^{-1}. In **Figure 3**, average values of conductivity can be observed.

The conductivity measures indirectly salts concentration and salinity. When this solid concentration changes, the conductivity changes too [17]. Than, in sample L2 the suspended solids concentration is higher than in L1 and L3, indicating more insoluble particles in medicine L2. Morrison et al.[18] analyzed the conductivity of raw sewage, treated effluent and water quality of Keiskamma River in South Africa. They observed 36% decrease of conductivity after treatment plant, from 1,08 μS.cm^{-1} to 0,69 μS.cm^{-1}, influent to effluent, respectively. In Keiskamma, the average conductivity of the water

was 0,24 μS.cm^{-1}. The conductivity of the medicine samples tested in this study were higher than the Morrison et al.'s influent, showing high impact potential of this residues.

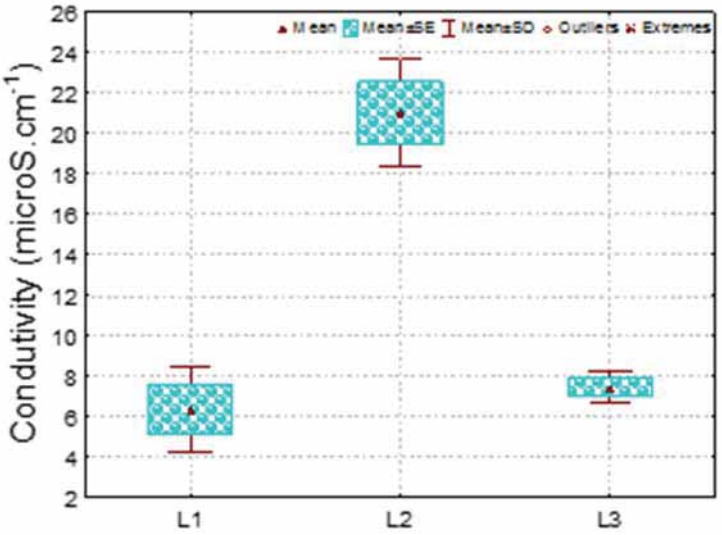


FIGURE 3. Box-plot of the condutivity of each laboratory

In L2, turvibidy average was higher than L1 and L3, around 39 ± 7 NTU. Adjuvants used in medicine formulation by L2 were poorly soluble in water, thereby caused turbidity, obstructing light way through the solution. Solutions with high turbidity, discharged into water bodies may reduce the water oxygenation by the inhibition of photosynthesis by algae. Average turbidity of L1 and L3 were 11 ± 3 NTU and 13 ± 2 NTU. The values of the L1 and L3 are lower than the values allowed by Brasilian laws[16], in Class 1 river to 40 NTU and Class 2, 3 and 4 rivers to 100 NTU. The values of the L2 is out of the range to class 1. Average turbidity values are in **Figure 4.**

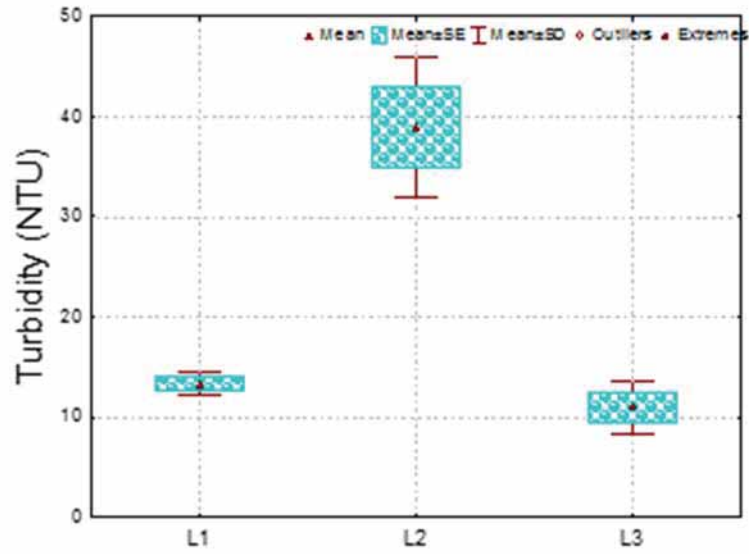


FIGURE 4. Box-plot of the turbidity of each laboratory

Sulfate concentration in each laboratory was lower than 10 $mg.L^{-1}$. These values are not considered pollutants, because of the Brasilian Laws allows the discharge of effluents with up to 250 $mg.L^{-1}$. If the environment is aerobic, sulfate is converted in sulfuric acid, which is highly reactive and can decrease the pH. If the environment is anaerobic, sulfate is converted in gas hydrogen sulfide which has strong odor of rotten eggs. Average sulfate concentration in L2 is higher tan L1 and L3 (**Figure 5**), but lower than the allowed.

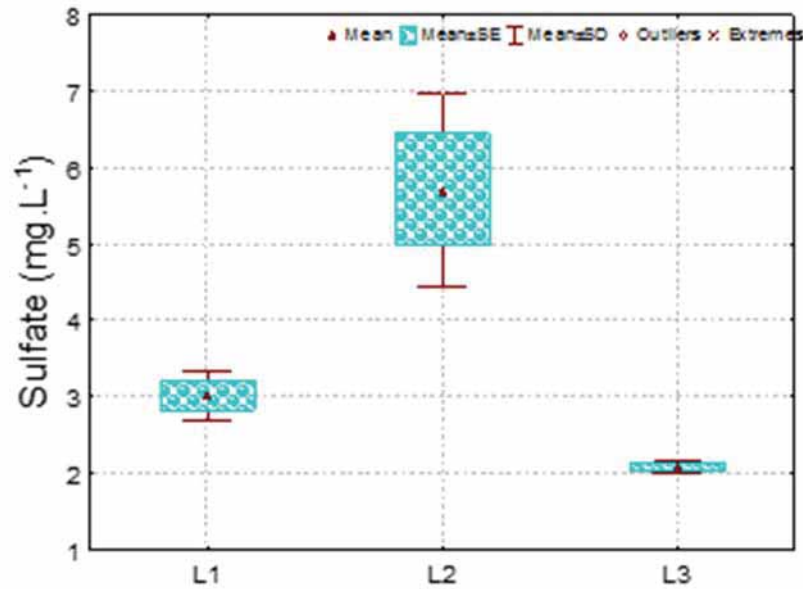


FIGURE 5. Box-plot of the sulfate of each laboratory

None of the samples exhibited buffering capacity, i.e., concentration of the compounds responsible for alkalinity were very low and was not detected by the utilized methods. Organic and amoniacal nitrogen concentration were also low and undetectable by the method used. Disposal of compounds rich in nitrogen can cause eutrophication.

Average raw COD values of L1, L2 and L3 were 1,314 ± 51 mg $O_2.L^{-1}$, 1,305 ± 134 mg $O_2.L^{-1}$ and 1,358 ± 21 mg $O_2.L^{-1}$, respectively (**Figure 6**). These COD values are higher than the average COD of the domestic effluents, which range from 300 to 800 mg $O_2.L^{-1,}$ values up to 1500 are considered strong sewage[19,20]. Filtered COD value is similar to raw COD, indicating the most of organic matter is soluble.

Organic compounds are consumption by microorganisms and if they are aerobic, dissolved oxygen will be consumed in water bodies. Decreasing dissolved oxygen in water, aerobic aquatic organisms are damaged. But organic compound degradation depends on the kind of molecule, toxicity, environment conditions and biodiversity. Pharmaceuticals compounds generally are complex and need specials conditions and specifics species of microorganisms. In this study, one liter of each sample needs around 1,300 mg O_2 dissolved in water river to be transformed by microorganisms in carbonic gas, but in 25ºC only 9 mg O_2 remains dissolved in liquid phase. Then, a long stretch of river is necessary to reduce the pollutant organic load.

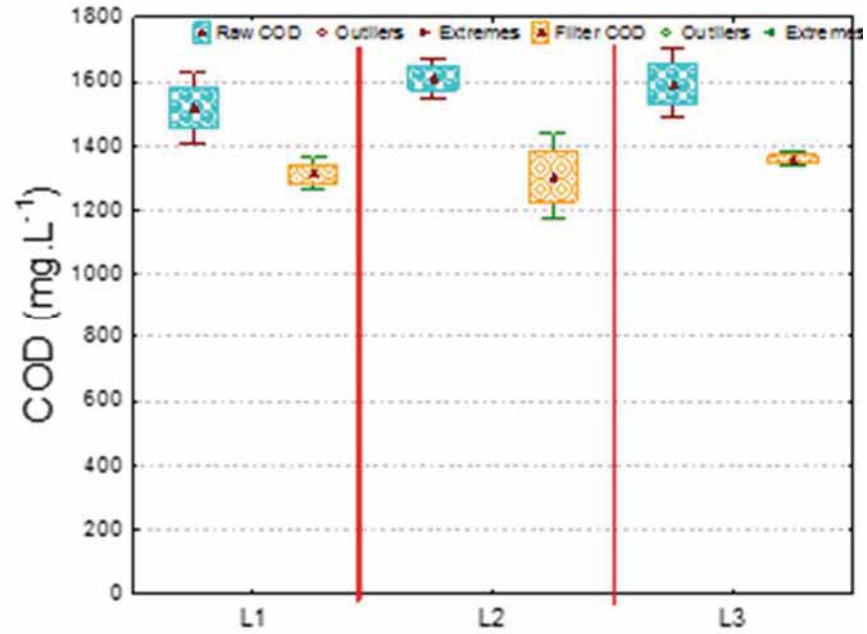


FIGURE 1. Box-plot of the raw and filtered COD of each laboratory

General analysis of the compounds present in the samples was performed through the analysis of solids. In **Figure 7**, solid concentration can be observed. Total solids are sum of dissolved and suspended solids. Most of the solids are organic confirming the results of the COD in all laboratorios.

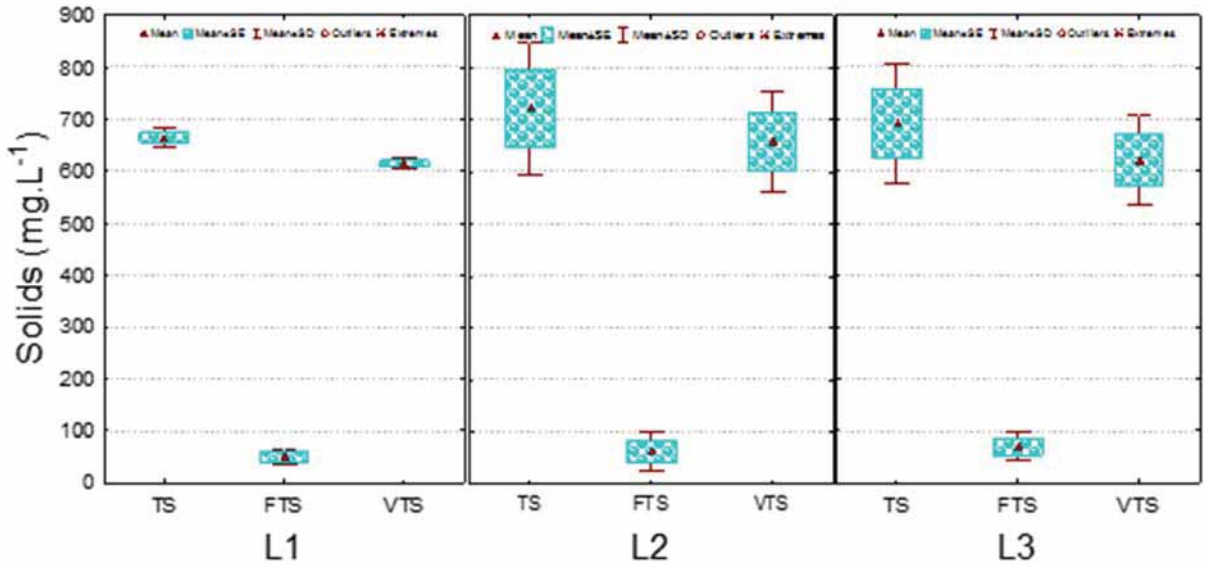


FIGURE *7*. Total solids (TS), Fixed Total solids (FTS) and Volatile Total solids (VTS) in each laboratory.

As previously mentioned, in all laboratories, the organic fraction is greater than inorganic. Evaluating the size of the particles, the organic compounds were dissolved, only a small fraction was suspended. None of the laboratories had suspended fixed solids. Volatile suspended solids concentration were higher in L2 than L1 and L3, but volatile disolved solids concentration in L2 was lower than in L1 and L3 (**Figure 8**).

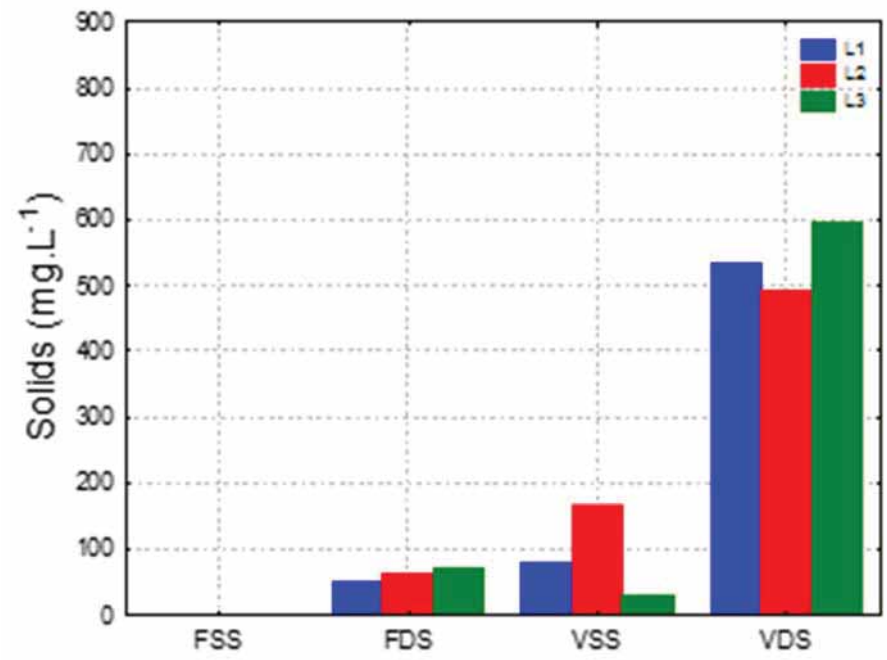


FIGURE 8. Size of volatile and fixed particles in each laboratory. FSS – Fixed Suspended Solids, FDS – Fixed issolved solids, VSS – volatile suspended solids and VDS – Volatile dissolved solids

CONCLUSION

Medicines composed of paracetamol can cause changes in pH, conductivity, turbidity and COD of the water bodies. pH decrease and turbidity, conductivity and COD increase are the main physico-chemical changes in the environment. These drugs did not change the alkalinity, sulfate and nitrogen concentration and nitrogen. Most tablets are formed by volatile dissolved solids Therefore, toxic effects, oxygen depletion and acidification of the médium are expected.
Different laboratories can create formulations that cause greater damage to the environment, so the drugs paracetamol base are not similar.

REFERENCES

1. Daughton C. Pharmaceuticals and the Environment (PiE): Evolution and impact of the published literature revealed by bibliometric analysis, Sci. Tot. Environ. 562 (2016) 391-426.
2. Billa D. M., Dezotti M. Fármacos no meio ambiente. Quim Nova, 26 (2003) 523-530.

3. Peake B., Braund R., Tong A. Y. C., Tremblay L. A. *Impact of pharmaceuticals on the environment.* 2016
4. Katsou E., Alvarino T., Malamis S., Suarez S., Frison N., Omil F., Fatone F. Effects of selected pharmaceuticals on nitrogen and phosphorus removal bioprocesses. Chemical Engineering Journal 295 (2016) 509-517
5. Butkovski A., Hernandez Leal H., Rijnaarts H. H. M., Zeeman G. Fate of pharmaceuticals in full-scale source separated sanitation system. Water Research 85 (2015) 384-392.
6. Taylor D., Senac T. Human pharmaceutical products in the environment - The "problem" in perspective. Chemosphere 115 (2014) 95-99
7. Puckowski A., Mioduszewska K., Lukaszewicz P., Borecka M., Caban M., Maszkowska J., Stepnowski P. Bioaccumulation and analytics of pharmaceutical residues in the environment: A review. Journal of Pharmaceutical and Biomedical Analysis 127 (2015) 232-255.
8. Costa A. S., Costa, M. S. *POLUENTES FARMACÊUTICOS: a poluição silenciosa. 1nd edition*, 2011.
9. Gaffney V. J., Cardoso V. V., Rodrigues A., Ferreira E., Benoliel M. J., Almeida C. M. M. Análise de fármacos em águas por SPE-UPLC-ESI-MS/MS. Quim Nova 37 (2014) 138-149.
10. Beck C., Camara M. R. G. da, Zapparoli I. D. Medidas Mitigadoras para a Indústria de Fármacos Comarca de Londrina – PR, Brasil: Impacto ambiental do despejo de resíduos em corpos hídricos. Brasil, 2011.
11. Liberal, J. P. M. Desenvolvimento e caracterização de comprimidos matriciais de dupla camada contendo paracetamol*,* Dissertation of Master Degree. Faculty of Pharmacy. University of Porto **(**2008) 112 p.
12. Lienert, J., Gudel, K., Escher, B.I. Screening method for ecotoxicological hazard assess-ment of 42 pharmaceuticals considering human metabolism and excretory routes. Environ. Sci. Technol. 41, (2007) 4471–4478.
13. APHA, AWWA, WEF *Standard Methods For The Examination of Water and Wastewater*. *22nd edition*, 2012.
14. Kato, M. T., Souza, L.F.C.; Morais, J. C., Campos, J. S. P., Fonseca, R. M.; Gavazza, S., Florencio, L*. Manual de procedimentos do laboratório de saneamento ambiental*. Livro Rápido, 2014.
15. CONAMA, Dispões sobre a classificação dos corpos de água e diretrizes ambientais para o seu enquadramento, bem como estabelece as condições e padrões de lançamento de efluentes, e dá outras providências, Resolução n° 357. Brasil, 2005.
16. CONAMA, Dispões sobre as condições e padrões de lançamento de efluentes, Resolução n° 430. Brasil, 2011.
17. Silva A. E.P.,Angelis C. F., Machado L. A. T. Influência da precipitação na qualidade da água do Rio Purus. Simposio Brasileiro de Sensoriamento Remoto, 13, Anais..., Florianopolis, (2007) 3577-3584.
18. Morrison G., Fatoki O. S., Persson L., Ekberg A. Assessment of the impact of point source pollution from the Keiskammahoek Sewage Treatment Plant on the Keiskamma River – pH, electrical conductivity, oxygen-demanding substance (COD) and nutrients. Water SA 27 (2001) 475-480.
19. Halalsheh M.,Sawajneh Z.,Zu'bi M., Zeeman G., Lier J., Fayyad M., Lettinga G. Treatment of strong domestic sewage in a 96 m^3 UASB reactor operated at ambient temperatures: two-stage versus single-stage reactor. Bioresource Technology 96 (2005) 577-585.
20. Von Sperling, M. *Introdução à qualidade das águas e ao tratamento de esgotos. 3nd edition*, Departamento de Engenharia Sanitária e Ambiental. UFMG, 2005.

CHAPTER 8.2 DEVELOPMENT OF AN ANAEROBIC DIGESTION SYSTEM TO DETERMINE BIOGAS ENERGY POTENTIAL

H. Numpaque López *(1); B. Criollo (1); C. L. Díaz (1); J. D. Alvarado (1) and C. Mendoza (1)

(1) Universidad de Cundinamarca, Dg 18 N° 20 29, Nº, Fusagasugá, Colombia.

ABSTRACT

The generation of organic solid waste (OSW) has increased among other reasons, as a result of population growth and the lack of alternatives for ehandling and management. In Colombia, 2.2% of the OSW is burnt in open air, or is taken without prior treatment to open dumps (7.6%) or landfill (90.2%)[1]. Under these circumstances, the degradation of organic matter in the absence of oxygen produces leachate and biogas (CH_4 and CO_2) which can pollute groundwater sources and release greenhouse gases into the atmosphere. An alternative OSW management is the use of anaerobic biological degradation processes that have high capacity of degradation of waste with high organic carbon content, transforming OSW into biogas, with low production of leachate[2]. However, the generation of biogas and bioenergy potential depends on factors such as temperature, pH and substrate composition. In this investigation, a control system for temperature and pH Batch bioreactor type was developed. A process of anaerobic digestion of OSW was carried out to identify the impact of temperature, pH and substrate composition in the generation of biogas with high methane content. Four different substrates were used: carrot peel 100%, potato peel 100%, beet peel 100% and mix peels: carrot 20% - potato 20% - beet 20% - vegetables (cucumber and spinach) 20% - fruits (papaya and tamarillo) 20%. The bacterial inoculum consisted of pig manure slurry. Different temperature ranges (mesophilic 40° C and thermophilic 50°C) were worked. Characterization of pH, volatile fatty acids and chemical oxygen demand of each substrate was performed. In addition, the quality of the biogas generated in terms of volume concentration of methane (CH4) and carbon dioxide (CO2) and its heat capacity was evaluated. It was determined that for processing OSW into biogas with a mesophilic temperature range and with a pH varying between 6.5 and 7.5 after 28 days' maximum production of biogas, 19 L carrot peel was obtained. With the substrate beet peel, lower biogas production (4 L) is presented but with a greater volume of methane (34%). Subsequently, when the system is controlled at 40 °C and pH 7, the biogas was obtained with a volumetric methane concentration to 70% and calorific potential 684kcal*m^{-3}, with the substrate compound by mixing peels. With this research, the influence of temperature, pH and substrate composition on the quality of biogas generated was demonstrated.

Keywords: Anaerobic digestion, PID temperature control, organic substrate, methane.

---

*Author for correspondence: hnumpaque@mail.unicundi.edu.co

INTRODUCTION

The problem of municipal solid waste (MSW) has been increasing as a result of rapid population growth and lack of alternatives for the proper handling and management of them. Colombia produces about 27,500 tons/day of solid waste (SW), which 65% is organic waste[3], mainly from food[4]. 90.2% of MSW is stored in landfills, while 7.6% and 2.2% respectively are deposited and burned outdoors, which has generated a negative impact on economic and environmental terms.

Currently, there are different laws on municipal solid waste (MSW) management as integral waste management plants, where as many as possible is recycled. In this way, the environmental impact has been mitigated. However, this solution does not apply to the OSW, because usually, these are disposed in landfills where they decompose naturally generating leachate and greenhouse gases, which adversely impact the environment.

At Universidad de Cundinamarca, GITEINCO research group, has decided to provide solutions to this problem by developing the research project "Evaluation of the biogas energy potential produced by anaerobic digestion of organic fraction of OSW". The purpose of this project is to study the effect of temperature and composition of organic matter in the quality and biogas energy potential produced by anaerobic digestion of OSW.

This research was conducted in three phases. In the initial phase anaerobic batch type bioreactor was developed, with a capacity of five liters and their respective instrumentation modules, which allowed quantify the temperature, pH, and the volume concentration of methane (CH_4) into the reactor. Subsequently, a system to control temperature and pH was developed, in order to promote the growth of the bacterial population that decomposes matter into the reactor to generate biogas. During the second phase, four organic substrates were subjected to anaerobic digestion process under different temperatures. This allowed us to evaluate the impact that has the substrate composition and temperature on the quality of biogas. In the last phase, the calorific potential of biogas generated by each of the four substrates was determined. This is achieved by developing a prototype heater Junker and the calorimetric method[5].

MATERIALS AND METHODS

Bioreactor. To establish the incidence of temperature and composition of the substrate on the quality of biogas, an anaerobic bioreactor type Batch was built based on the model structure defined by Chae[6]. This bioreactor has a system to control the temperature and pH in the substrate, with an effective volume of 5 liters. **Figure 1** shows the diagram of the reactor used and the location of the measurement devices.

Online Measurements. Temperature control into the reactor was effected by a thermal jacket and an electric heater using a PID controller which allowed the temperature set at 40° C (mesophilic regime) or 50°C (thermophilic regime). The pH was measured and controlled in the feed tank. For this, a pH sensor industrial model-12 and LPI-pH transmitter were used (Intech Instruments Ltd, New Zealand). To set the pH between 6.5

and 7.5, hydrochloric acid (0.1N) and sodium hydroxide (0.1N) were dosed via peristaltic pumps and a fuzzy controller[7]. Biogas quality is established based on the volume concentration of methane. To measure this variable, a IR15TT-R infrared gas sensor (e2V, England) was used. This sensor operates on the principle of non-dispersive infrared (NDIR) absorption[8,9].

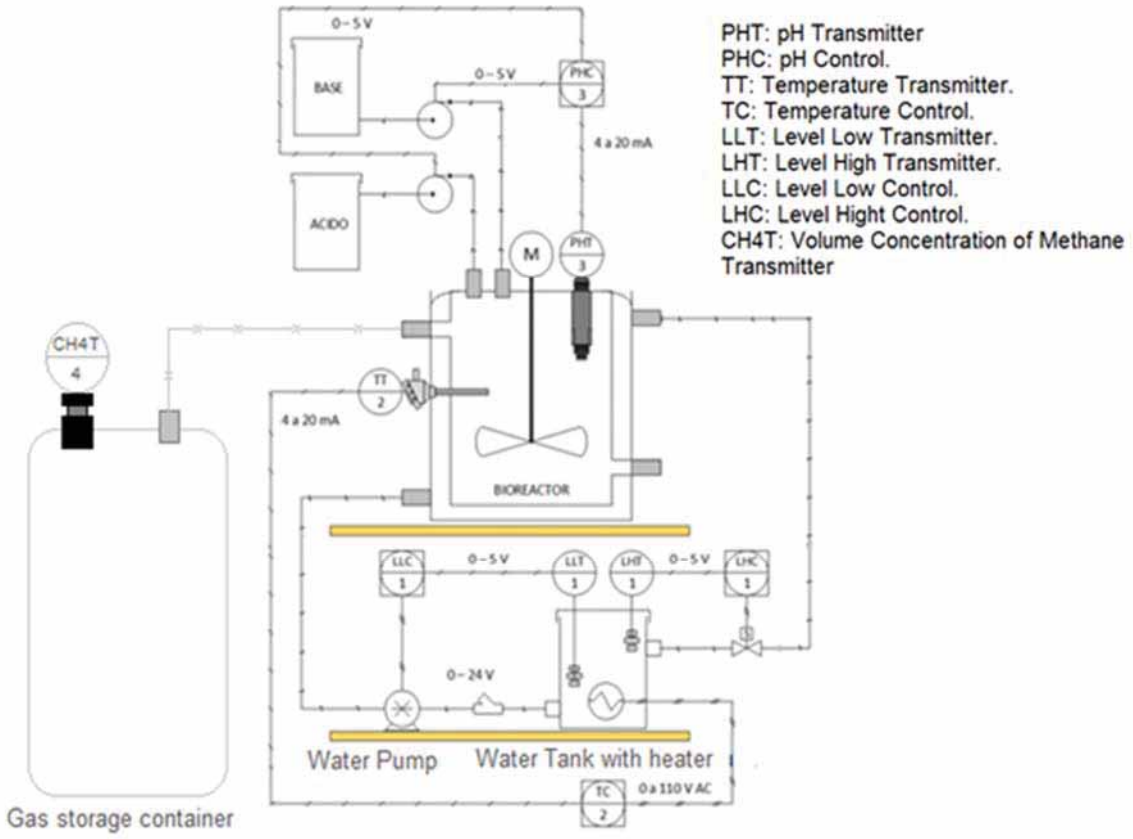


FIGURE 1. Diagram of Anaerobic bioreactor designed

Measurements offline. The volatile fatty acid (FVA) concentration, according to the methodology of "Standard Methods", based on tritation[10]. A solution of 0.1N hydrochloric acid was prepared. A 30 ml sample of organic material was centrifuged for 15 minutes at 6000 rpm. Subsequently 20 ml of supernatant were taken, it was titrated with 0.1N HCl to stabilize the pH at 4.3. The volume of HCl used in titration (VHCl) was recorded. Then, the ratio of FVA was calculated by the equation 1.

$$\mathrm{FVA}_{\mathrm{mg/L}} = \frac{(\mathrm{VHCl}) * \mathrm{N} * 5000}{\mathrm{VS}} \qquad (1)$$

Where:

VHCl= Volume (ml) HCl used for pH 4.3
N= Normality HCl
VS= Volume (ml) of sample supernatant

Measurement of biogas calorific power (BCP). To establish the BCP, a Junker calorimeter was constructed, based on the model proposed by Martina[5]. The calorimeter burns five liters of gas, to heat 1 L water contained in a volumetric flask. **Figure 2** represents the general diagram of the calorimeter designed.

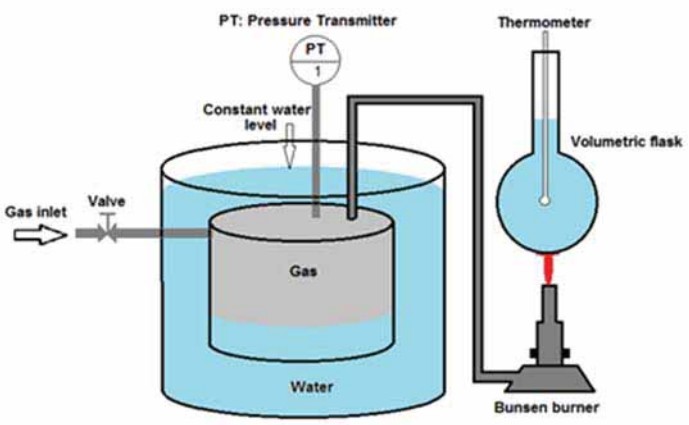


FIGURE 2. Diagram of Junker calorimeter designed to measure the gas calorific power

BCP was determined by the calorimetric method. 5L of biogas contained in the calorimeter were burned. Subsequently, under the same conditions of temperature and pressure, 5L of propane were burned. 5L of each gas were used to heat 1000 ml of water, contained in a volumetric flask. a constant distance of 2 cm was maintained between the flask and the Bunsen burner (**Figure 2**). According to the specific heat of water (Cp_{H2O}), the variation in water temperature (ΔT) obtained with each gas (propane or biogas), the masses of both gases (m), the density of both gases (d) and propane gas heating value (PCP), the calorific power of biogas (BCP) was calculated according to the diagram in **Figure 3**.

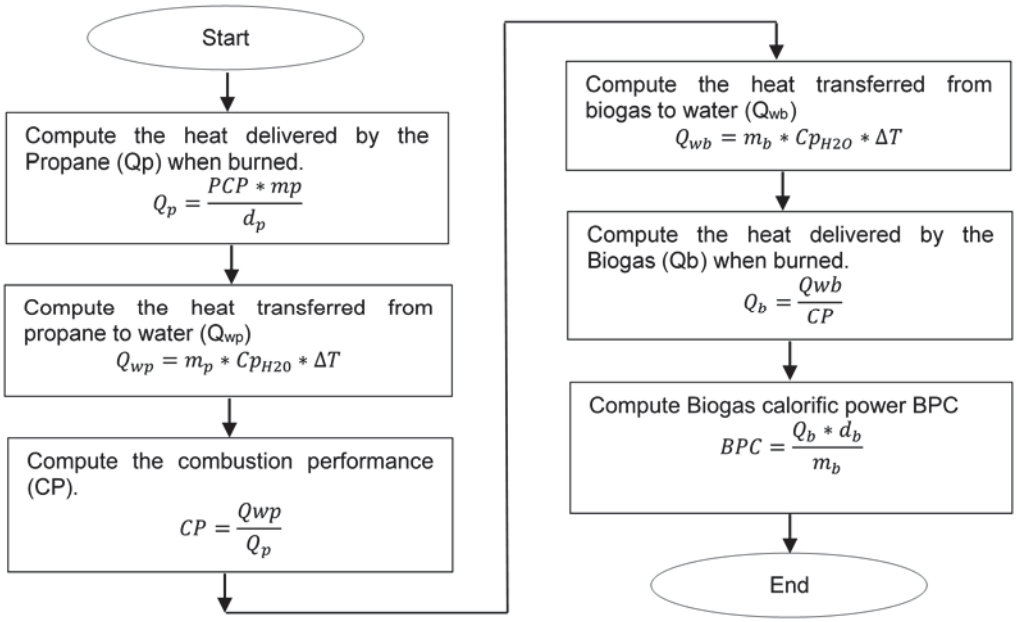


FIGURE 3. Procedure for determining the PCB, with propane as the reference gas

Description of experiment. In the batch reactor described above they were subjected to anaerobic digestion process four substrates of different organic matter. The incidence of temperature, pH and substrate composition on the quality of the biogas production and its calorific power was determined. Biogas quality was evaluated in terms of the volume concentration of methane (CH_4) and Carbon Dioxide (CO_2), because the quality of biogas mainly depends on the presence of these gases[11,12]. Substrate samples evaluated in this experiment were mainly composed of carrot peels, potato peels, beet peels, vegetables (cucumbers and spinach) and peel fruits (papaya and tamarillo). The proportions of these substrates are similar to those generated as waste in restaurants in Fusagasugá - Colombia (**Table 1**).

TABLE 1. Composition of organic matter used in the experiment

Sample	Composition	Weight (g)	percentage (%)
1	Carrot peels	400	100
2	Potato peels	400	100
3	Beet peels	400	100
	Potato peels	100	25
	Carrot peels	100	25
4	Vegetables (cucumber, spinach, beet)	100	25
	Peel fruits (papaya and tamarillo)	100	25

To facilitate hydrolysis process each sample was subjected to a blending process, obtaining a size of less than 2mm particle. After, each of the samples were prepared by mixing 400 g of Fraction Total Solid Waste (FTSW) and 1200 ml of distilled water. As inoculum, 200 g of pig manure slurry were used. They were from a digester located on the farm at Universidad de Cundinamarca. Each sample was loaded in the reactor. These samples showed a concentration of 33% total solids weight of them to decide the organic matter, relative to the total weight of the load. In this experiment, the particle size and mixture ratio 1: 3 between the substrate and water, took into account the criterion Komemoto[13].

The pH of each sample placed in each reactor was measured with a digital pH meter, registering values of 4.74, 4.17, 4.4 and 6.8 respectively. To avoid destabilization of the process by the accumulation of volatile fatty acids (VFA) and formation of inhibitory compounds is necessary to maintain an optimal pH between 6.5 and 7.5[14]. To achieve this optimum pH, it was necessary to stabilize the first three samples at pH 7.0.

Once loaded the reactor, this was sealed tightly and stirring at a constant 120 rpm, it was maintained for five minutes every 24 hours.

RESULTS AND DISCUSSION

The performance of control systems developed temperature and pH were tested experimentally to regulate the temperature and pH of the substrate deposited in the bioreactor. To work in mesophilic conditions, initially bioreactor temperature was stabilized at 35°C, and then the temperature change at 50°C and 40°C (**Figure 4**). To

work in the thermophilic range, temperature took 10 minutes to go from 35°C to 50°C, while working in the mesophilic temperature took 30 minutes to stabilize at 40°C.

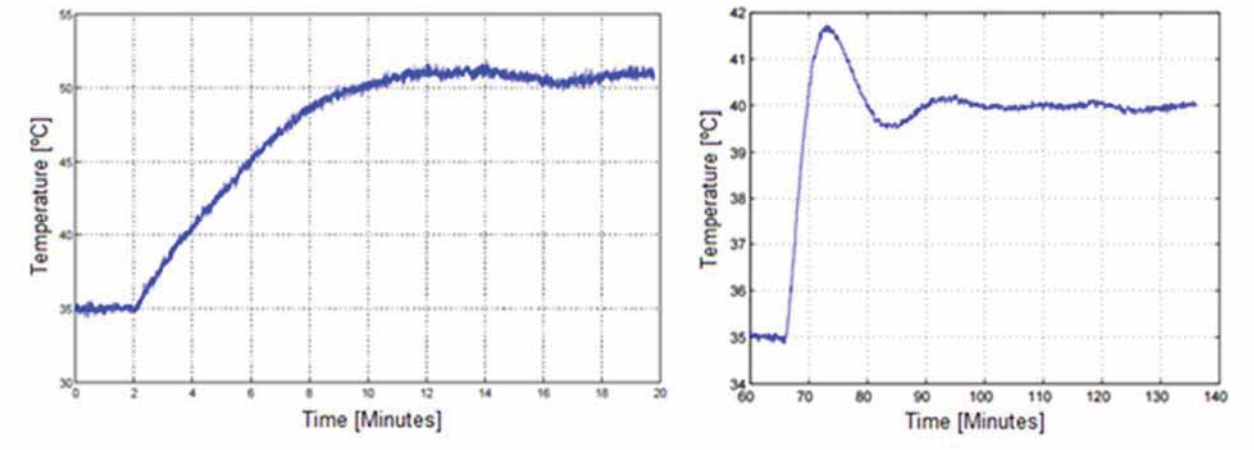


FIGURE 4. Temperature control performance at 50 ° C and 40 ° C.

The behavior of volatile fatty acids (VFA) for the first three samples are presented in **Figure 5**. **Figure 6** shows production of biogas daily accumulated for the three samples operating at a temperature of 40°C.

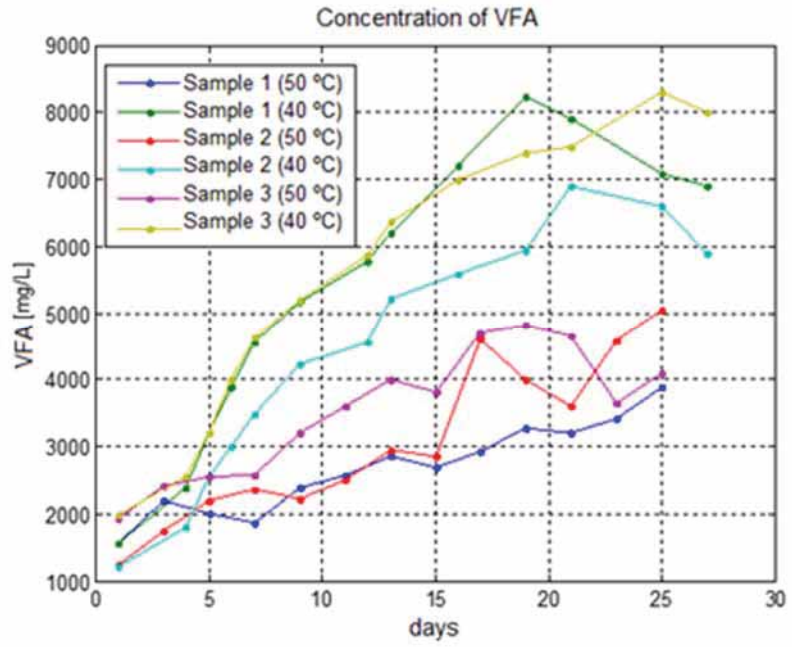


FIGURE 5. VFA concentration for samples 1, 2 and 3 respectively, working at temperatures of 50 ° C and 40 ° C.

In **Figure 5** it shows that VFA production significantly varied by conditions of temperature and substrate characteristics. In the substrate of sample 1 it shows that the concentration of FVA is greater at 40°C with a maximum output of 8.25 $g*l^{-1}$ in day 19.

Then FVA production starts to decrease. The composition of the substrate also played an important role in the production of FVA. Substrates with high protein and fat generated a greater amount of biogas. In this case, the substrate carrot peels (sample 1) had the best performance for the best production FVA and biogas generation as shown in **Figure 6**.

However, it was shown that biogas production was not directly proportional to its quality. Sample 1 (carrot peels) produced throughout the process about 20 L of biogas with a methane concentration of 7.2%, while sample 3 (peels beet) produced approximately 5 L of biogas with a methane concentration of 34%. The results of methane concentrations for samples 1, 2, and 3 are summarized in **Table 2**.

TABLE 2. **Volume concentrations of the components of biogas**

Organic matter	Volumetric concentration of methane gas (CH_4)	Volumetric concentration of carbon dioxide (CO_2)
Sample 1	7.2 %	92.8%
Sample 2	13.8 %	86.2%
Sample 3	34%	66%

In the thermophilic range (50°C) not significant production of biogas was obtained. This was mainly due to the growth trend of the FVA (shown in **Figure 5**), indicating that the process of anaerobic digestion entered inhibition state. In the thermophilic range variables temperature and pH are critical and changes of ± 1°C can lead to the growth process is inhibited bacterial population, generating, for this reason, pH drops and increased FVA.

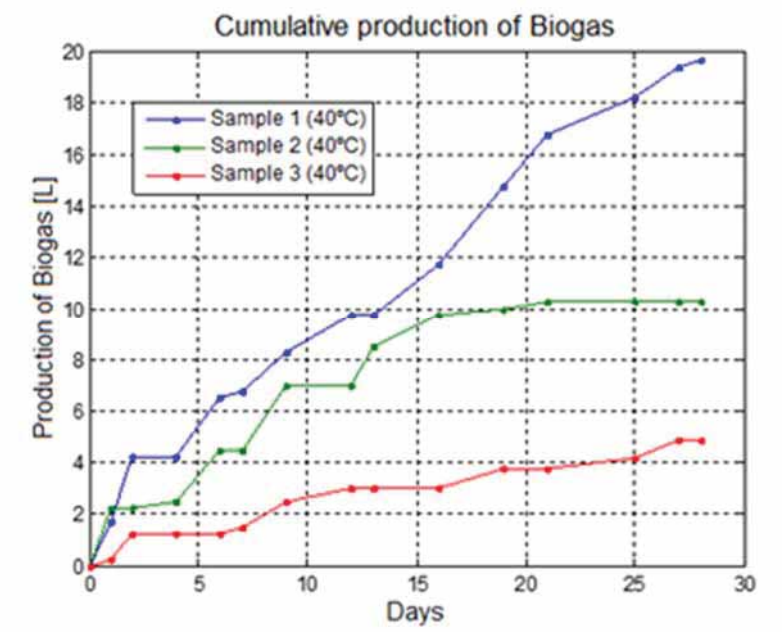


FIGURE 6. Cumulative daily production of biogas, for substrates 1,2, and 3 working in mesophilic regime

Figure 7 shows the behavior of pH and temperature for the substrate 4. **Figure 8** shows the behavior of the quality of the biogas generated. During the days 4, 15 and 23, a disturbance was induced in the process temperature, adjusting around 33°C. However, it was observed that these days the system achievement bioreactor maintain the pH around 7.0 preventing destabilization process. Moreover, the temperature variation generated a decrease in the concentration of methane gas. The most obvious effect was observed on day 15, when the volumetric methane concentration step of 34% to 18%, presenting a factor of 16% drop in volume. Once the control temperature reached to stabilize the system, a recovery trend of concentrations of CH_4 and CO_2 was observed. On day 23 of the experiment, the CH4 concentration reached a value of 34.2% present at the time of the temperature drop. This phenomenon is consistent with the results obtained by Lindofer et al[15] and Ruge and Hernandez[16], who developed a transition temperature in mesophilic conditions and thermophilic to assess the effect on the production of methane biogas, which decreased considerably by varying the temperature of anaerobic digestion. This phenomenon is due to changes in temperature affect the bacterial activity and population and decreasing FVA. However, the biogas production showed a tendency to be restored to the value before change in temperature in the digestion process.

The biogas calorific power (BCP) obtained from the sample 4 was 6847kcal*m^{-3} while for samples 2 and 3 working at 40°C was 750 kcal*m^{-3} and 2570 kcal*m^{-3} respectively. It could not be determined Biogas calorific power (BCP) in sample 1, because the concentration of methane in the biogas was very low for combustion.

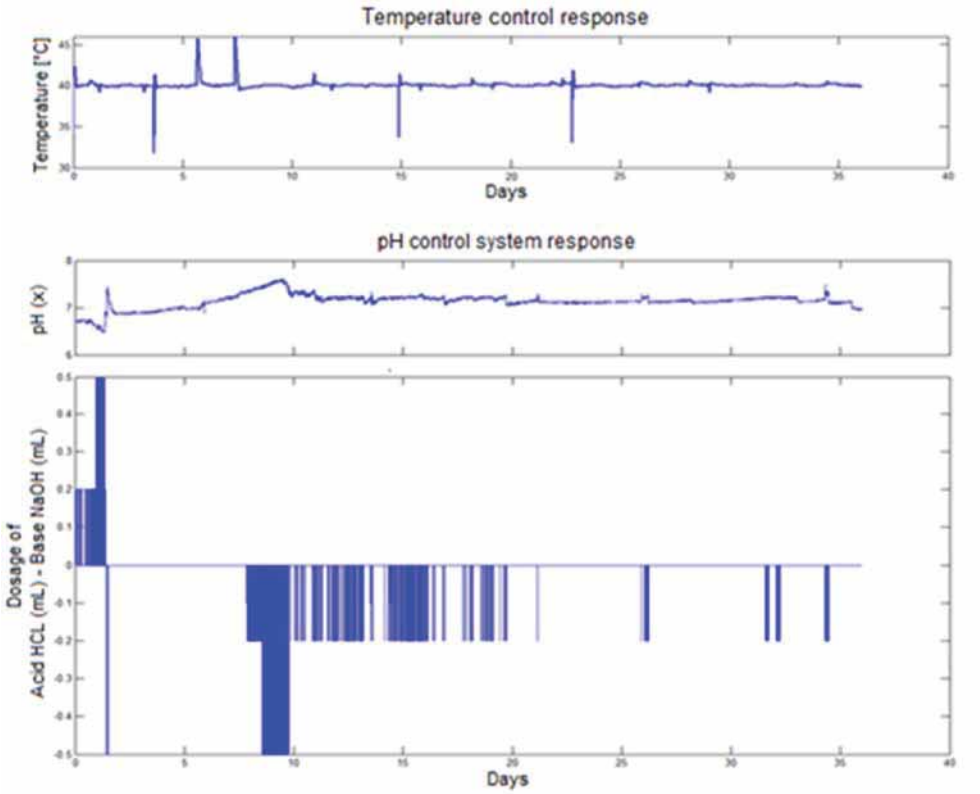


FIGURE 7. Temperature and pH behavior in simple 4

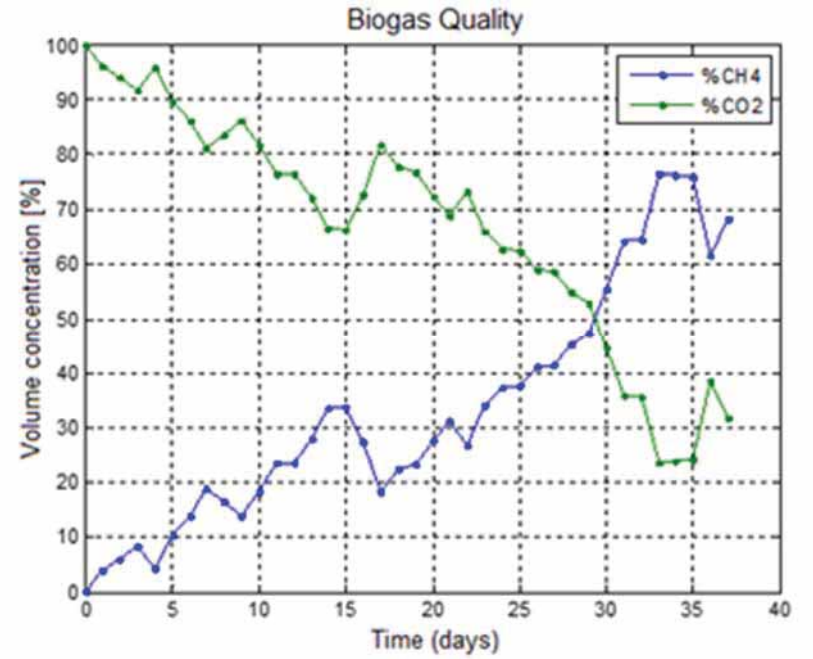


FIGURE 8. Quality Biogas generated with sample 4

CONCLUSION

The temperature has a fundamental role in the transformation of organic waste into biogas during the phases of Acetogenesis and methanogenesis, in anaerobic digestion process. According to the results it is concluded that mesophilic condition (20° C≤ T ≤45°) high production of biogas is obtained. This is because the temperature has a high influence on the specific growth rate of bacterial populations that consume mainly volatile fatty acids (FAV), as acetate, to transform it into biogas. However, it is concluded that the quality of biogas depends on the volumetric concentration of methane. A higher concentration of methane, higher purity and calorific power will have biogas. It is considered good quality biogas production when the volume concentration of methane is between 50% and 70%. In the thermophilic range, ie temperatures being 45 ° C and 70 ° C, the production of methane is generated in less time, but the process can be destabilizing if there are variations of ± 1°C in temperature and pH, causing a decline in the quantity and quality of biogas.

ACKNOWLEDGEMENTS

The authors thank the people in charge of managing electronic laboratories and chemical engineering from the Universidad de Cundinamarca, for the support provided for the loan of equipment that allowed the bioreactor build and develop the electronic control circuits and instrumentation.

REFERENCES

1. CONPES. Lineamientos y estrategias para fortalecer el servicio público de aseo en el marco de la gestión integral de residuos sólidos. Documento CONPES 3530. Consejo Nacional de Política Económica y Social. Departamento Nacional de Planeación. República de Colombia. 2008.
2. Lettinga G. The anaerobic treatment approach towards a more sustainable and robust environmental protection. Water Science and Technology. 2005. 52 (1-2): 1-11
3. Jaramillo H., Zapata Márquez, L.M. Aprovechamiento de los residuos sólidos orgánicos en Colombia. Medellín: Monografía Universidad de Antioquia. 2011.
4. Marmolejo, L., Torres, P., Oviedo, E., Bedoya, D. Flujo de residuos: Elemento base para la sostenibilidad del aprovechamiento de residuos sólidos municipales. Ingeniería y Competitividad. 2009: 79-93.
5. Martina, P. Biogas e Isobutano: Análisis comparativo de una propiedad termodinámica. Universidad Nacional del Nordeste. Comunicaciones Científicas y Ttecnológicas. 2000: 35-38.
6. Chae, K., Jang, A., Yim ,S., Kim, I. The effects of digestion temperature and temperature shock on the biogas yields from the mesophilic anaerobic digestion of swine manure. Bioresour Technol. 2008.
7. Liu, C.F., Yuan, X., Zeng, G., Li, W., Li. J. Prediction of methane yield at optimum pH for anaerobic digestion of organic fraction of municipal solid waste. Bioresourse Technology. 2008: 882-888.
8. SGX Sensortech (IS). Infrared Sensor Application Note 4 Design of Electronics for Infrared Gas Sensors. 2009.
9. e2v technologies (UK). Infrared Sensor Application Note 2 Signal Processing for Infrared Gas Sensors. 2010
10. American Public Health Association & American Water Works Association. Standard methods for the examination of water and wastewater: selected analytical methods approved and cited by the United States Environmental Protection Agency. American Public Health Association. 1981.
11. Mandal, T. Determination of the Quality of Biogas by Flame Temperature Measurement. Energy Conversion & Management. 1999 (40): 1225 - 1228
12. Sambo, A., Garba. B., Danshehu, B. Effect of some operating parameters on Biogas production rate. Renowable Energy. 1995: 343-344.
13. Komemoto, K., Lim, Y. G., Nagao, N., Onoue, Y., Niwa, C., Toda, T. Effect of temperature on VFA's and biogas production in anaerobic solubilization of food waste. Waste management. 2009. 29(12): 2950-2955.
14. Liu, C. F., Yuan, X. Z., Zeng, G. M., Li, W. W., & Li, J. Prediction of methane yield at optimum pH for anaerobic digestion of organic fraction of municipal solid waste. Bioresource Technology. 2008. 99(4): 882-888.
15. Lindorfer H , Waltenberger R , Köllner K , Braun R , Kirchmayr R. New data on temperature optimum and temperature changes in energy crop digesters. Bioresource Technology. 2008. 99(15):7011-7019.
16. Ruge I, Hernández H. Control difuso basado en microcontrolador para la producción de biogás en digestión anaerobia tipo Batch de fracción orgánica de residuos sólidos. Gerenc. Tecnol. Inform. 2011. 10 (28): 73 - 85

CHAPTER 8.3 PESTICIDE TRAPPING IN FRACTAL POROSITY OF CLAYS

T. Woignier *(1,2); F. Clostre (3) and M. Lesueur- Jannoyer (3)

(1) Aix Marseille Univ, Univ Avignon, CNRS, IRD, IMBE, Marseille, France.
(2) IRD - Campus Agro Environnemental Caraïbes, Le Lamentin, Martinique, France
(3) Cirad, UPR fonctionnement agro écologique et performances des systèmes de culture horticoles, UR HortSys, F97232, Le Lamentin, Martinique.

ABSTRACT

Young volcanic soils (andosols) contain amorphous nanoclays (allophane) which present unique structures and porous properties compared to crystalline clays: large pore size distribution and mesoporosity, a high specific surface area and a tortuous (fractal) structure. The aim of the work was to study the influence of the nanoclay microstructure and mesoporosity on the pesticide retention in soils.
Our experimental results show that the allophane microstructure favors pollutants accumulation and trapping. These soils are more polluted than the other kinds of tropical soils but release less pollutants to water and plants. The allophane soils contains up to 10 times more pesticide depending on the allophane content but the pesticides release in water is 5 times less than in non allophane soils. We put forth the importance of the mesoporous microstructure of the allophane nanoclay and the associated tortuous porosity for pollutant trapping. We propose that the poor pollutant accessibility in allophane aggregate could explain the lower pollutant release in environment. Transport properties (permeability and diffusion). strongly decrease with the allophane content and the low transport properties explain the high concentrations and trapping of pollutants allophane nanoclays.

Keywords: allophane clay, chlordecone, fractal structure, pesticide trapping

INTRODUCTION

Andosols contain clay (allophane) that presents unique structures and physical properties compared to crystalline clays. Allophane is an amorphous alumino silicate, the unit cell of which appears as spheroids with diameter between 3 and 5 nm forming aggregates with a fractal structure[1,2,3].

Chlordecone (CLD) is an organochlorine pesticide. This neurotoxic and carcinogenic molecule[4] still persists in the soil and contaminates crops and water resources[5,6] thus leading to human exposition through food. Allophanic volcanic soils (andosols) are generally more polluted than the other kinds of tropical soils (nitisols, ferrisols) but recent data have shown that they release less pesticide to environment[7,8]. The present study hypothesizes that the peculiar properties of allophane and specially the porous

---

*Author for correspondence: thierry.woignier@imbe.fr

microstructure favor pollutants accumulation in soils. The purpose of this work is to: 1) study the pesticides sequestration properties of allophane by transfer experiments; 2) show the influence of allophane concentration on porous features of soils; 3) put forth the importance of the fractal microstructure, the associated tortuous interface and large specific surface area for pollutant trapping; 4). finally we discuss the synergy between soil organic matter and allophane porous microstructure on the pollutant retention in soils.

MATERIALS AND METHODS

We sampled several allophanic soils and for comparison non allophanic soils containing halloysite clays in Martinique (14°40 N, 61°00 W) in the vicinity of the Mount Pelée volcano. These different kinds of soils are representative of the main polluted soils found in French West Indies[7]. The allophanic content was measured by ICP-AES (Inductively Coupled Plasma Atomic Emission Spectroscopy), method of Mizota and van Reewijk[9].

The crystalline and amorphous structure was studied by X-rays diffraction (Cu Kα) and the presence of allophane was characterized by Infrared Spectroscopy. Physical fractionation by sieving in water was done after soil dispersion in water and hexametaphosphate. We isolated by size three different organo mineral fractions: < 50 µm size, 50-200 µm size and > 200 µm size. Three replicates of each fraction were prepared.

Leaching experiment was performed through water extraction such as evaluating soil solution contamination by CLD. Micro-columns containing 5 g of soil were prepared with seven replicates for andosol and eight replicates for nitisol. Leaching with 12.5 ml of nanopure water was slightly forced by gentle centrifugation (500 g) directly in the micro-columns. After percolation through the soil columns, water CLD concentrations were determined by SPME/GC-MS.The soil to water transfer coefficient (WTC) is the ratio of the pesticide concentration in lixiviates to the pesticide concentration in soil expressed in $\mu g.L^{-1}$ / $\mu g.kg^{-1}$ of dry soil)

The specific surface area (SSA) of the sample was calculated from the adsorption curve and the BET equation by N_2 adsorption-desorption curves. The pore volume was calculated from the bulk density and the solid density measured by He pycnometry for the different kinds of soils (2.5 $g.cm^{-3}$ for the allophanic soils and 2.66 $g.cm^{-3}$ for the halloysite soils[10].

The fractal features of the allophane aggregates were characterized by SAXS experiments. The data from the SAXS experiments provided three types of information on the fractal geometry: the maximum size of the fractal clusters *(L)*, the size of the primary particles (*a*) which built the cluster, and the fractal dimension *(Df)* which characterized the spatial arrangement in the cluster[11]. The transmission electron micrographs were obtained with a Transmission Electron Microscope JEOL Type 1200 EX (100 kV). The scanning electron microsgraphs were obtained with a Cambridge stereo scan 360 scanning electron microscope.

All statistical analyses were performed using XL STAT 2012.6.08. ANOVA and Tukey Honestly Significant Difference tests ($p<0.05$) were used to compare means of transfer (WTC and PTC) for the different soil types and to assess the difference of CLD content in the different soil fractions for each soil type. The linear regressions and ANOVA were

used to assess the equation of the linear models, their goodness of fit and the significance of the explanatory variable.

RESULTS AND DISCUSSION

Through the leaching experiment we evaluated the contamination of the soil solution by chlordecone. The transfer of chlordecone to water (WTC, **Table 1**) was twice lower in allophane clay (andosol) than halloysite clay (nitisol). The WTC were significantly different for the two soils ($P<0.0001$). The comparatively low chlordecone concentration in andosol lixiviates was the consequence of the trapping microstructure of allophane clays present in andosols, which we discuss later.

TABLE 1. Transfer of chlordecone to water: the soil to water transfer coefficient (WTC) is the ratio of the pesticide concentration in lixiviates to the pesticide concentration in soil expressed in $\mu g.L^{-1}$ / $\mu g.kg^{-1}$ of dry soil). Differences between clay types were tested by ANOVA (p= 0.05)

Soil and clay type	Soil contamination range (in mg CLD kg^{-1} dry soil)	WTC	
		Mean	Standard deviation
Andosol (allophane)	3.4-6.7	2.33	0.66
Nitisol (halloysite)	0.5-0.91	4.68	1.07

These results obtained in leaching experiments, we compared the transfer coefficient of the pesticide from soil to plant (PTC, **Table 2**) for the two same types of soil. We observed a highly significant difference between the two types of soil ($P < 0.0001$): transfer from andosol is lesser than from nitisol (**Table 2**) with a ratio close to 2.

Moreover the concentration of chlordecone in allophanic soils was several times higher than in halloysite soils (**Table 1** and **2**).These experiments show that 1) allophanic soils are generally more contaminated than halloysite soils and 2) allophanic soils release less pollutant to water and plants than halloysite soils. In the literature, one explanation for this retention effect is the high organic content of andosols combined with the high affinity of the pesticide for soil organic matter[7]. However, soil organic matter cannot solely explain the lower pollutant transfer coefficients in allophanic soils and microstructural features must be accounted for. We will show the influence of the clay microstructure on the accumulation and retention of pesticide in soils.

Allophanic soils. Andosols comprise weathering products such as allophane originating from the lixiviation of volcanic materials. Allophane are referred as X-rays amorphous materials.

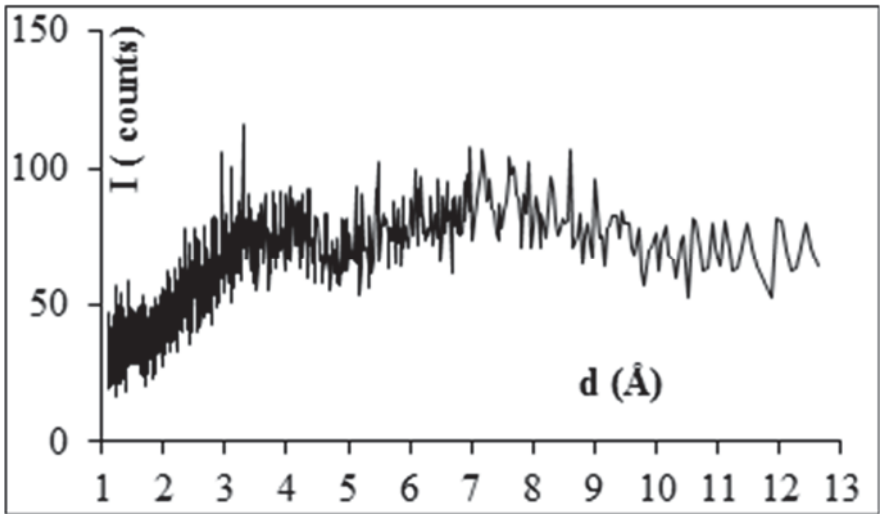


FIGURE 1. X-rays typical diffractogram of allophanic samples. Counts *versus* lattice spacing d (Å)

Figure 1 shows a typical X-rays spectrum that we obtained on the studied andosols, the general trend of this spectrum is a clear evidence of bulges of the base line between 2 and 7 Å, attributed to non-crystalline solids, allophane. The X-ray diffraction spectrum (not shown) for nitisols showed peaks at 4.45 and 7.4 Å that were attributed to the clay halloysite An interesting method to reveal the occurrence of allophane is the infrared spectroscopy (FTIR). In the literature, it has been shown that characteristic bands like 506, 577 and a shoulder at 970 cm^{-1} are the signature of allophane[12]. These bands are also accompanied by a broad band in the –OH stretching region (around 3500-3700 cm^{-1}). **Figure 2** shows the typical FTIR spectrum recorded for the studied andosols. The spectrum reveals the shoulder at 970 cm^{-1} (Si-O stretching), the bands in the range 500-600 cm^{-1} and broad band in the –OH stretching region, characteristics of allophane

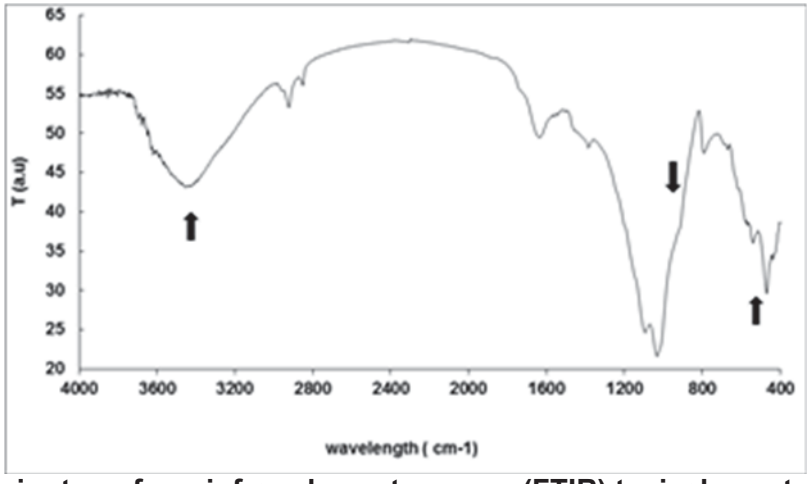


FIGURE 2. Fourier transform infrared spectroscopy (FTIR) typical spectra of allophanic samples. Transmittance is expressed in arbitrary units *versus* wavelength in cm^{-1}

Wada[3] describes the allophane particles as follows: the unit cell appears as spheroids with diameter between 3 and 5 nm. **Figure 3** shows the structure of amorphous clay in comparison with halloysite. The plate-like particles of phyllosilicate clay like halloysite are 300-1000 nm in size (**Figure 3a**). In comparison, the scanning electron micrograph confirms the spongy structure of allophane clay with aggregates around 100 nm (**Figure 3b**). The allophane aggregates are highly porous in the range of the mesoporosity.

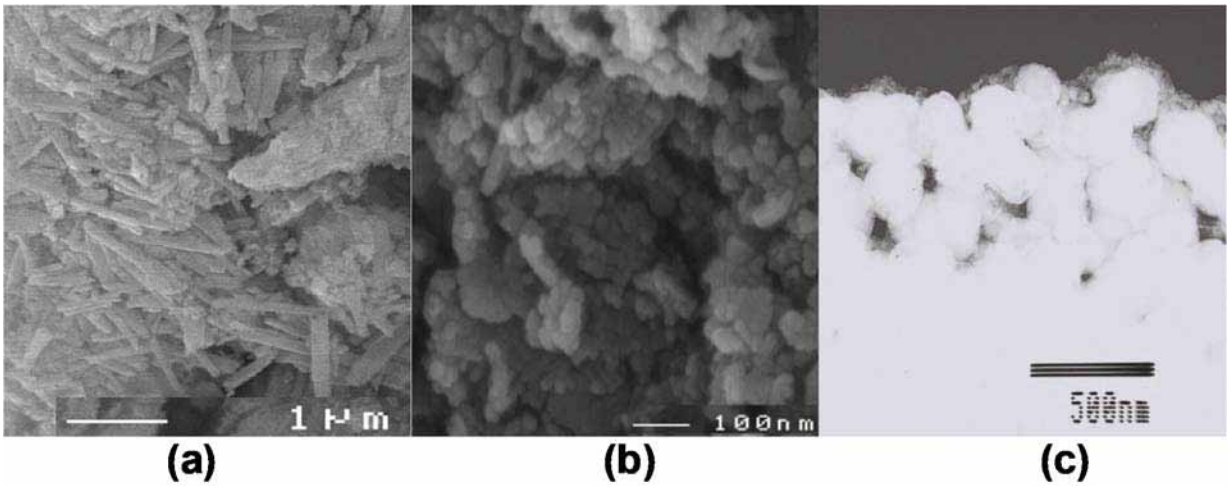


FIGURE 3. (a) Scanning electronic micrographs of phyllosilicate clay; (b) **s**canning electronic micrographs of allophane clay and (c) transmission electron micrographs of allophane clay.

From the transmission electron microscopy (**Figure 3c**) we see that the morphology of the allophane aggregates is peculiar. Allophane has a very open structure made up of aggregated small particles that form clusters of around 10-20 nm. The clusters can stick together and form larger and larger aggregates up to L ~ 200 nm in size (**Figure 3c**). This hierarchical aggregation is characteristic of a fractal microstructure.

Light and X-rays scattering data demonstrate that allophane aggregates have fractal geometry and can be described as clusters formed by aggregation of small particles with a hierarchical structure[1-3]. The fractal dimension found in the literature is close to 1.8[1] measured by light scattering and close to 2.5 measured by SAXS (2). In conclusion, allophane aggregates have peculiar morphological features: large pore volume and water content, a broad pore size distribution, a high specific surface area and a fractal structure.

Influence of allophane clay on soil pore properties. In this part of the study, we will show that the peculiar microstructure of allophane clay has an influence on the soil porous properties. The pore volume *Vp* and the specific surface area *S* were well correlated to the allophane contents. We found that S ($m^2.g^{-1}$) = 43.39+4.99 allophane (%) ($P<0.0001$ and $r^2=0.87$) and *Vp* ($cm^3.g^{-1}$) = 0.58+0.059 allophane (%) ($P<0.0001$ and $r^2=0.79$). The specific surface area could be as high as 200 $m^2.g^{-1}$ and the pore volume close to 2 $cm^3.g^{-1}$.Large specific surface area is generally the signature of an important meso-porosity contribution.

The literature[1-3] describes the allophane aggregates structure as fractal in the range of a few nm up to almost 100 nm. Our data show that the fractal dimension is close to 2.5 and the particles size (*a*) extracted from the scattering spectra is constant (in the range 4-5 nm). The *Df* constant means that the aggregation mechanism is quite the same, whatever the allophane concentration. We show that the maximum size of the fractal aggregate (*L)* increases with the allophane concentration. The new sets of data demonstrates that *L* is positively correlated to the allophane content *L* (nm) = 6.65+1.95 allophane (%) (P< 0.0001 and r^2=0.82).When particles stick together to form clusters they also create voids, i.e. pores, inside the clusters. These clusters stick together to form larger porous clusters with larger pores and so on, up to *L* the maximum size of the fractal aggregates. This kind of aggregation process leads to a microstructure with a high tortuosity and the extent of the tortuous structure, i.e. the extent of the fractal clusters (*L*), increases with allophane content. The allophane aggregate microstructure resembles a labyrinth at the nm scale. This description suggests that the accessibility in the allophane microstructure decreases when the size of the labyrinth increases. This hypothesis is discussed in the following sections.

Influence of allophane content on the CLD retention. Recently it has been shown that the CLD content in soils increases with the allophane concentration[8]. **Table 1** confirms that andosols are more generally contaminated that nitisols.

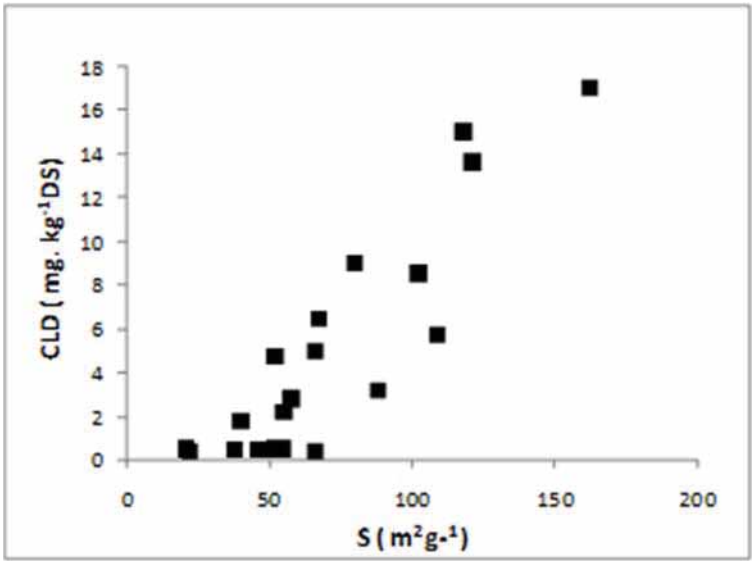


FIGURE 4. CLD concentration *versus* specific surface area *S*

It is reasonable to hypothesize that the ability for a soil to retain chemical species could be related to the soil structure and pore features (arrangement of particles and aggregates, pore volume, tortuosity). Numerous examples cited in the litterature show that allophane have been used for adsorption, retention and trapping purpose[13-15]. For pesticides, there is a need to establish relationship between the retention mechanism and such physical parameters in allophanic soils. The **Figure 4** and **5** shows that the CLD concentration is positively correlated with the soil specific surface area *S*: *CLD* =

0.13 *S* - 4.36 ($P < 0.0001$ and $r^2=0.80$) and with the pore volume *CLD* = 9.56 *Vp* - 4.11 ($P < 0.0001$ and $r^2=0.78$).

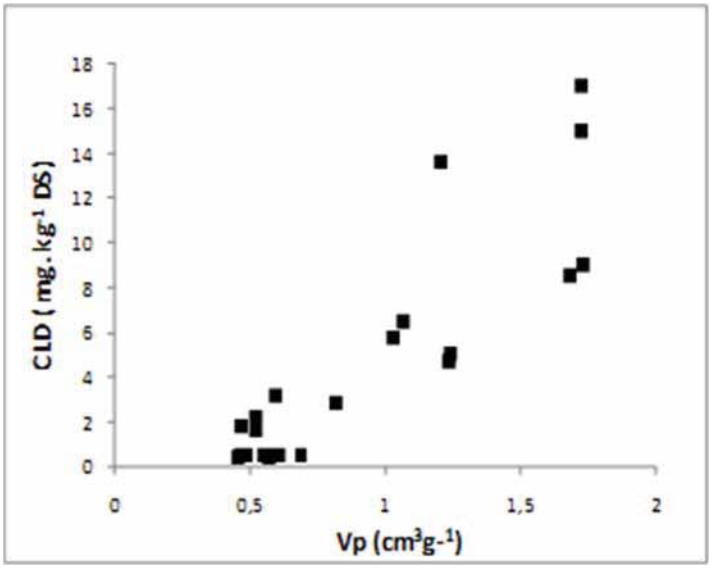


FIGURE 5. CLD concentration *versus p*ore volume *Vp*

To put forth the importance of the allophanic microstructure we fractionated different andosols (allophane) and nitisols (halloysite) and analysed the CLD content in the three size classes obtained: > 200 µm (class a), 50 to 200 µm (class b) and < 50 µm (class c).

TABLE 2. CLD concentration in the different size class a, b and c for AS and NAS soils samples. Values are means of 3 samples ± standard error of the mean. Differences between fractions were tested by ANOVA. Different letters in the same row indicate significant differences (Tukey test, p = 0.05)

	CLD content (in mg CLD kg^{-1} dry soil)						ANOVA Pr> F
Soil type	**fraction a**		**fraction b**		**fraction c**		
Allophane	1.16 ± 0.39	a	2.14 ± 0.26	a	10.25 ± 4.2	b	0.007
Halloysite	0.66±0.11	a	0.99± 0.17	l	0.95± 0.07	a,b	0.031

Table 2 shows the CLD concentration in mg CLD kg^{-1}DS (dry soil) for the different soils samples. For halloysite soil samples, the CLD concentrations are close, between 0.66-0.99 mg kg^{-1} dry soil, for a, b and c fractions. However in the case of the allophane soils samples, the CLD concentration strongly increases for the class c richer in allophane, CLD concentration being 8.8-fold higher than the a fraction, these differences being highly significant (p=0.007). This higher CLD content in the c class is due to its richness in allophane aggregates.

To confirm the effect of the allophane microstructure on the pesticide trapping; we plotted the evolution of the soil pesticide contamination versus the extent of the clay fractal structure i.e. the size of the clusters *(L)*. These data (**Figure 6**) shows a

significant positive correlation: CLD = 0.47 *L* - 6.40 (with P<0.0001 and r^2=0.71) between the CLD soil contamination and the size of the fractal allophane aggregates. These results emphasize the role of the clay micro-porosity features (*S, V_p* and *L*) in trapping CLD. The retention mechanism is developed in the next section.

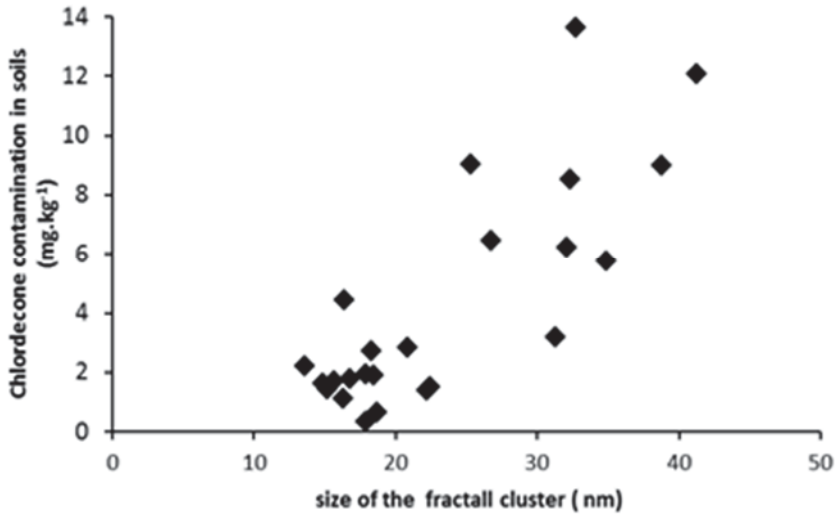


FIGURE 6. CLD concentration *versus* fractal aggregate extent *L*

Trapping mechanism in allophane micro structure. The observed characteristics of allophane: high specific surface area and pore volume, and fractal features correspond to a highly tortuous microstructure and small mesopores. The fractal structure of allophane aggregates is typically in the range 5–100 nm and we may hypothesize that the accessibility inside the aggregates is reduced. Indeed, for example, the trapping inside allophane aggregates is sought to contribute to the protective effect of allophane on biodegradation of soil organic matter, the later becoming inaccessible to microorganisms and enzymes[16-18]. It is generally admitted that CLD is poorly biodegradable especially in environmental conditions explaining its persistence in soils (7). The CLD poor biodegradability is attributed to its peculiar chemical structure (bishomocubane “cage”) and the high steric hindrance caused by the ten chlorine atoms. However, Dolfing et al[19] showed recently that there were no thermodynamic reasons why chlordecone-respiring or -fermenting organisms should not exist. There is some evidence that methanogenic bacteria (*Methanosarcina thermophila*)[20] can dechlorinate CLD and open the bishomocubane “cage”. So chlordecone biodegradation is not impossible but at least very restricted in these clays. We can thus invoke the mesopore protection mechanism proposed for organic matter[16-18] to explain the high CLD content in allophanic soils.

Organo-mineral complexes like allophane form small aggregates with pores in the mesopore scale (2–50 nm) and with high organic matter loadings: 75 to 90% of the soil organic matter found in the pores is in the 10–1000 nm size range[17].Such aggregate pore widths are far below the cut-off for accessibility by bacteria, which is considered to 2 µm. Furthermore, enzymes can penetrate micropores and small mesopores but with difficulty, Zimmerman et al [20] showed that the enzyme activity was 3–40 times lower in mesoporous silica or alumina than that observed for nonporous minerals. The fractal

aggregates in allophane clay likely signs tortuous diffusion pathways. In a previous work[21], numerical simulations on porous structures have shown that permeability in allophane soils is strongly affected by the allophane content. The permeability at the scale of allophane aggregate has been calculated to be low (40 nm^2) in these tortuous pore networks. The value of the effective diffusion coefficient (for Cs^+ ion) in allophane was estimated to $10^{-16} m^2.s^{-1}$, six orders of magnitude smaller than the diffusion coefficient in aqueous solution[22].Thus allophane aggregate structure might be highly porous but has a low permeability and diffusion coefficient; fluids and chemical species migrate with difficulty inside the fractal structure. In addition, the fractal pore structure imposes a range of pore sizes including small as well as large ones. As an allophane aggregate increases in size, the tortuous diffusion pathway will become blocked by pore throats that prevent chemical or biological species passage. The fractal structure of the pore networks may, therefore, retard the enzyme diffusion to the adsorbed CLD and affect the degradation by microorganisms. The high CLD retention capacity is the result of different kinds of mechanism: 1) the high chemical affinity of CLD for organic matter would stabilize the pesticide in the mesoporosity. 2) Microorganisms supposed to be able to degrade the pesticide have a size higher than the allophane aggregates. 3) The low transport properties in allophane aggregate could explain the lesser chlordecone release in environment, crops and water resource. The synergy between organic matter content in allophane and tortuous microstructure prevent CLD from degradation when trapped inside the mesopore network.

CONCLUSION

This study confirms that there are clear correlations between the soil pesticide content and clay microstructure. The pore structure of the allophane aggregates at nano-scale also favors the pesticide retention. It is suggested that chlordecone storage in allophanic soils could be the result of the low permeability and diffusion coefficient of the fractal allophane aggregate.

The high pesticide content in allophanic soils is likely the result of a synergy between the high affinity with the organic matter and the poor accessibility of pesticides into the mesopore structure. Future research for chlordecone degrading microorganisms and other bioremediation tools to clean up polluted soils should take into account the poor chlordecone accessibility.

Pesticide trapping in allophane fractal porosity has two fold implications: on one hand, the allophanic soils are more contaminated than phyllosilicate soils; on the other hand, allophanic clays are poorer secondary contaminant sources thus reducing the risk for pesticide diffusion in the environment. Reducing the environment contamination is clearly useful and should be preserved. This implies that the fragile allophane microstructure should not be destroyed by strong drying which leads to large shrinkage and collapse of the clay porosity.

REFERENCES

1. Adachi Y, Karube J (1999) Application of a scaling law to the analysis of allophane aggregates. Colloids Surf Physicochem Eng Aspects 151 (1-2):43-47
2. Chevallier T, Woignier T, Toucet J, Blanchart E, Dieudonné P (2008) Fractal structure in natural gels: effect on carbon sequestration in volcanic soils. J Sol-Gel Sci Technol 48 (1):231-238. doi:10.1007/s10971-008-1795-z
3. Wada K (1985) The distinctive properties of Andosol. Advances in soil science, pp 173-229
4. Dallaire R, Muckle G, Rouget F, Kadhel P, Bataille H, Guldner L, Seurin S, Chajès V, Monfort C, Boucher O, Pierre Thomé J, Jacobson SW, Multigner L, Cordier S (2012) Cognitive, visual, and motor development of 7-month-old Guadeloupean infants exposed to chlordecone. Environ Res 118 (0):79-85. doi:10.1016/j.envres.2012.07.006
5. Coat S, Monti D, Legendre P, Bouchon C, Massat F, Lepoint G (2011) Organochlorine pollution in tropical rivers (Guadeloupe): role of ecological factors in food web bioaccumulation. Environ Pollut 159 (6):1692-1701. doi:10.1016/j.envpol.2011.02.036
6. Levillain J, Cattan P, Colin F, Voltz M, Cabidoche Y-M (2012) Analysis of environmental and farming factors of soil contamination by a persistent organic pollutant, chlordecone, in a banana production area of French West Indies. Agric, Ecosyst Environ 159 (0):123-132. doi:10.1016/j.agee.2012.07.005
7. Cabidoche YM, Achard R, Cattan P, Clermont-Dauphin C, Massat F, Sansoulet J (2009) Long-term pollution by chlordecone of tropical volcanic soils in the French West Indies: a simple leaching model accounts for current residue. Environ Pollut 157 (5):1697-1705. doi:10.1016/j.envpol.2008.12.015
8. Cabidoche YM, Lesueur-Jannoyer M (2012) Contamination of Harvested Organs in Root Crops Grown on Chlordecone-Polluted Soils. Pedosphere 22 (4):562-571. doi:10.1016/s1002-0160(12)60041-1
9. Mizota C, Van Reewijk LP (1989) Clay mineralogy and chemistry of soils formed in volcanic material in diverse climatic regions. Soil Monograph n°2. International Soil Reference and Information Center, Wageningen
10. Dorel M, Roger-Estrade J, Manichon H, Delvaux B (2000) Porosity and soil water properties of Caribbean volcanic ash soils. Soil Use Manage 16 (2):133-140
11. Teixeira J (1988) Small angle scattering by fractal systems. J Appl Crystallogr 21:781-785
12. Denaix L, Lamy I, Bottero JY (1999) Structure and affinity towards Cd2+, Cu2+, Pb2+ of synthetic colloidal amorphous aluminosilicates and their precursors. Colloids Surf Physicochem Eng Aspects 158 (3):315-325.
13. Garrido-Ramirez EG, Sivaiah MV, Barrault J, Valange S, Theng BKG, Ureta-Zañartu MS, Mora MdlL (2012) Catalytic wet peroxide oxidation of phenol over iron or copper oxide-supported allophane clay materials: Influence of catalyst SiO2/Al2O3 ratio. Microporous Mesoporous Mater 162 (0):189-198.
14. Nishikiori H, Shindoh J, Takahashi N, Takagi T, Tanaka N, Fujii T (2009) Adsorption of benzene derivatives on allophane. Appl Clay Sci 43 (2):160-163.
15. Reinert L, Ohashi F, Kehal M, Bantignies J-L, Goze-Bac C, Duclaux L (2011) Characterization and boron adsorption of hydrothermally synthesised allophanes. Appl Clay Sci 54 (3–4):274-280.
16. Mayer LM, Schick LL, Hardy KR, Wagai R, McCarthy J (2004) Organic matter in small mesopores in sediments and soils. Geochim Cosmochim Acta 68 (19):3863-3872. d
17. McCarthy JF, Ilavsky J, Jastrow JD, Mayer LM, Perfect E, Zhuang J (2008) Protection of organic carbon in soil microaggregates via restructuring of aggregate porosity and filling of pores with accumulating organic matter. Geochim Cosmochim Acta 72 (19):4725-4744.

18. Zimmerman AR, Goyne KW, Chorover J, Komarneni S, Brantley SL (2004) Mineral mesopore effects on nitrogenous organic matter adsorption. Org Geochem 35 (3):355-375.
19. Dolfing J, Novak I, Archelas A, Macarie H (2012) Gibbs free energy of formation of chlordecone and potential degradation products: implications for remediation strategies and environmental fate. Environ Sci Technol 46 (15):8131-8139.
20. Jablonski PE, Pheasant DJ, Ferry JG (1996) Conversion of Kepone by Methanosarcina thermophila. FEMS Microbiol Lett 139 (2–3):169-173.
21. Woignier T, Primera J, Hashmy A (2006) Application of the DLCA model to natural gels : the allophanic soils. J Sol-Gel Sci Technol 40 (2-3):201-207.
22. Mon J, Deng Y, Flury M, Harsh JB (2005) Cesium incorporation and diffusion in cancrinite, sodalite, zeolite, and allophane. Microporous Mesoporous Mater 86 (1–3):277-286.

Section 9.
Environmental Chemistry

Page

Chapter 9.1 Estudio cinético y degradación del triclosán y triclocarbán en suelos agrícolas enmendados con compost 821
Julio César Benítez-Villalba; Noemí Dorival-García; Francisco Paulo Ferreira-Benítez; Samuel Cantarero; Bartolomé Oliver-Rodríguez and José Luis Vílchez

Chapter 9.2 Identificación de fuentes de emisión de pm10 asociadas a los metales presentes en las épocas de lluvia y estiaje en la región Tula-Tepeji, Hidalgo 834
G. Martínez-Reséndiz; R. I. Beltrán-Hernández; A. Ramírez-Reyes; C. Solís Rosales; J. Miranda; S. A. Medina-Moreno and C. A. Lucho-Constantino

Chapter 9.3 Quercetin as metabolic mediator in the phenanthrene phytoremoval process by *Cyperus laxus* 847
G. Calva Calva; N. A. Rivera Casado; O. Gómez Guzmán and J. Pérez Vargas

Chapter 9.4 Germinación, crecimiento y morfología de *Cyperus laxus* crecido in vitro con hidrocarburos 859
G. Calva Calva; N. A. Rivera Casado; O. Gómez Guzmán and J. Pérez Vargas

CHAPTER 9.1 ESTUDIO CINÉTICO Y DEGRADACIÓN DEL TRICLOSÁN Y TRICLOCARBÁN EN SUELOS AGRÍCOLAS ENMENDADOS CON COMPOST

Julio César Benítez-Villalba *(1); Noemí Dorival-García (2); Francisco Paulo Ferreira-Benítez (1); Samuel Cantarero (2); Bartolomé Oliver-Rodríguez (2) and José Luis Vílchez (2)

(1) Facultad de Ciencias Exactas y Naturales, Universidad Nacional de Asunción, Campus Universitario, San Lorenzo, Paraguay.
(2) Grupo de Investigación de Química Analítica y Ciencias de la Vida, Departamento de Química Analítica, Campus de Fuentenueva, Universidad de Granada, E-18071 Granada, España.

RESUMEN

En este trabajo se realizó un estudio cinético, degradación en suelo y compost proveniente de lodos de depuradora y mezcla de ambas matrices. Se utilizó la técnica de extracción por ultrasonido (USE) para separar los analitos de las matrices involucradas y fueron detectados y cuantificado mediante Cromatografía de Líquidos de Ultra Presión (UPLC) acoplada a Espectrometría de Masas en Tandem (MS/MS, QqQ). El tratamiento consistió en añadir los contaminantes de forma manual y regar las parcelas con agua de pozo. Se fijaron dos condiciones diferentes Parcela 1 (P1) suelo con los contaminantes puros aplicados directamente al suelo, Parcela 2 (P2) suelo emendadas con compost y contaminada con Triclosán (TCS) y Triclocarbán (TCB). Se evaluó la cinética de degradación de la P1 y P2 a profundidades (2, 10, 20, 30, 60 cm) a lo largo del tiempo (0, 15 y 30 días), se observó que se ajustaron a una cinética exponencial de primer orden ($C=Co\cdot e^{-k.t}$). En la P1 el TCS era retenido y degradado en la superficie (2 cm) con un tiempo de vida media ($t_{1/2}$) 214.6 h, mientras que el TCB se detecta en los primeros 50 cm. En la P2 el TCS también desaparece por completo en esta zona con un ($t_{1/2}$) de 146.5 h y al igual que en la P2 el TCB lixivia hasta los 50 cm. Como conclusión general, se observa que los tiempos de vida media son mayores en las condiciones experimentales de la parcela P1. Desde el punto de vista medio ambiental el enmendado de los suelos agrícolas con compost es muy beneficioso por que aporta materia orgánica, hecho que favorece el crecimiento de microorganismos que provoca una aceleración en la biodegradación de los componentes estudiados e impidiendo su lixiviación a mayores profundidades.

Palabras clave: biodegradación, compost, cromatografía, matriz.

---

*Author for correspondence: julio81benitez@gmail.com

INTRODUCCIÓN

Una de las mejores alternativas, desde un punto de vista ambiental, para la eliminación de los lodos de desecho de EDAR urbanas es el reciclado a través de su uso en agricultura en el enmendado de suelos como abono, bien de forma directa (después de un tratamiento simple) o tras ser sometidos a un proceso adecuado de compostaje. Sin embargo, estos lodos, pueden representar una de las principales rutas por la que numerosos contaminantes orgánicos potencialmente peligrosos reingresan al medio ambiente[1-3].

En este sentido, existen numerosos aspectos que requieren especial atención para que puedan ser aplicados con suficiente garantía. En primer lugar, es necesario conocer con exactitud la magnitud de su contaminación química, por la posible presencia de numerosas sustancias químicas de origen antropogénicas, así como la variabilidad espacial y temporal de su distribución. En segundo lugar, se desconocen las condiciones de operación óptimas para su eliminación total durante los procesos de compostaje y su evolución en los suelos agrícolas una vez enmendados con dicho material. En tercer lugar, se desconocen los diferentes mecanismos a través de los cuales pueden ser eliminados definitivamente, y las rutas posibles de reingreso y/o permanencia en el medio ambiente, y mucho menos los factores que pueden promover y/o estimular los procesos biológicos a nivel del suelo, que son los que al fin y al cabo pueden asegurar la eliminación definitiva de estas sustancias[4-6].

En los últimos años se ha generado una nueva preocupación en relación a un grupo más extenso de compuestos orgánicos, los llamados “contaminantes emergentes”, de los que se conoce muy poco sobre su persistencia, evolución en aguas y en suelos agrícolas, su comportamiento durante los procesos de depurado de aguas residuales, mecanismos de degradación, transferencia a la cadena trófica, y efectos adversos sobre los ecosistemas y la salud humana. Esta evidencia justifica el temor de algunos países, con respecto al reciclado de los lodos de desecho en agricultura, especialmente a nivel de la industria alimentaria. El control de estas sustancias se ha ido desarrollando a medida que avanza el conocimiento científico sobre ellas[7].

Esta problemática muestra la necesidad de investigación científica, a nivel químico, biológico, microbiológico, toxicológico y ecológico, con objeto de completar la información ya existente en relación a los contaminantes orgánicos regulados, incluyendo los “contaminantes emergentes”[8].

Los compuestos seleccionados para este estudio son el triclosán y triclocarbán; el triclosán, 5-cloro-2-(2,4-dicloro-fenoxi) fenol, se utiliza desde hace más de 40 años como agente antimicrobiano en desodorantes, jabones, cremas y, especialmente, en productos de higiene dental. Es un antiséptico utilizado en productos hospitalarios y productos de consumo (colutorios, desodorantes, dentífricos). Su mecanismo de acción no es muy conocido, pero parece que difunde a través de la membrana citoplasma bacteriana e interfiere su metabolismo lípidico[9,10]. En las dosis de uso normales actúa como bactericida, y en dosis menores tiene efecto bacteriostático[11,12].

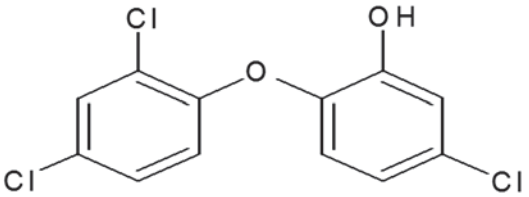


FIGURA 1. Estructura Química del TCS

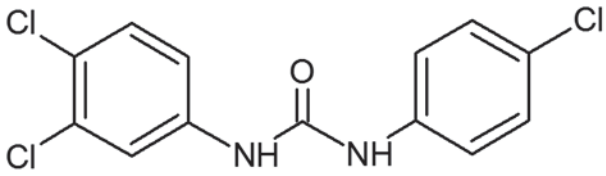


FIGURA 2. Estructura Química del TCB

El triclocarbán, N-(4-clorofenil)-N'-(3,4-diclorofenil) urea, se usa desde 1957 como agente antimicrobiano en numerosos productos de cuidado personal, especialmente jabones, a niveles de hasta el 1.5 % (p/p)[13-16].

Existen dudas sobre los posibles efectos negativos del TCS y TCB sobre la salud humana y animal. El estudio llevado a cabo por Veldhoen en 2007 concluye que una dosis reducida de TCS puede actuar como disruptores endocrinos en animales[17]. El hallazgo hace sospechar que podría tener el mismo efecto en los seres humanos[18].

En este trabajo se ha llevado a cabo un estudio cinético y degradación en suelo agrícola contaminadas con compost procedente de lodos de depuradora. Utilizando la técnica de extracción por ultrasonido para extraer los analitos objeto de estudio de las matrices involucradas utilizando para su cuantificación la Cromatografía de Líquidos de Ultra Presión (UPLC) acoplada a Espectrometría de Masas en Tandem (MS/MS, QqQ).

MATERIALES Y MÉTODOS

***Productos químicos y reactivos*.** Se utilizaron reactivos de grado analítico. Los patrones de Triclosán y Triclocarbán y el patrón interno Ácido Meclofenámico (AMC) fueron suministrados por la casa comercial Sigma-Aldrich (St. Louis, MO). Las soluciones de TCS y TCB (200 $mg.mL^{-1}$) se prepararon en metanol mensualmente y se almacenaban a -20 °C. Las soluciones estándar, mezclas de estos compuestos junto con el patrón interno se prepararon en metanol o en la fase móvil inmediatamente antes de su uso. Estos estándares se almacenaban a 4°C y se preparaban semanalmente. Todas las soluciones se almacenaron en botellas de vidrio oscuro. El agua y metanol que se utilizaron para la preparación de la fase móvil fueron de grado LC-MS suministradas por Fluka (St. Louis, MO, EE.UU.). El amoníaco (> 25%), acetonitrilo, y acetato de etilo se adquirieron de Merck (Darmstadt, Alemania). El agua (18,2 MΩ cm) se purificó por un sistema Millipore Milli-Q (Bedford, MA, ESTADOS UNIDOS).

Instrumentación y software. Para la recolección de la muestras de compost se emplearon palas convencionales y para las muestras de suelos un muestreador de calado (superficiales) y una barrena helicoidal para mayores profundidades. La temperatura y humedad del suelo fueron controladas a las diferentes profundidades del suelo estudiadas, de forma continua, mediante una sonda AquaCheck. El trabajo experimental se desarrolló utilizando una sonda de ultrasonidos Digital Sonifier S450D (BRANSON). Un cromatógrafo Waters Acquity UPLC™ acoplado a espectrómetro de masas triple cuadrupolo Waters H-Class-Xevo TQS™. La separación de los compuestos se obtuvo con una columna ACQUITY UPLC BEH™ C_{18} (1,7 µm; 2,1 mm ×

50 mm) (Waters). Una fuente de ionización ionización por electroespray Z-spray™ ESI para la detección del analitos. El software utilizado para la detección e integración de los picos fue el MassLynx V.4.1 SCN.803 programa de gestión y tratamiento de los datos obtenidos por el cromatógrafo Waters Acquity UPLC™ H-Class - Xevo TQS™. Un Vortex (Yellow line, Wilmington, NC, USA), una centrifuga Hettich Zentrifugen, universal 32 (Tuttlingen, Alemania). Para el tratamiento estadístico se utilizó un software Statgraphics Plus versión 5.0 (Manugistics, Rockville, MD, EE.UU., 2000). Paquetes Microsoft® Office: Word®, Excel® y PowerPoint® 2007.

Desarrollo Experimental

Estudio de campo (TCS y TCB). Este estudio se realizó con el objetivo de evaluar el comportamiento de los analitos (TCS y TCB) en un determinado ambiente natural, donde los contaminantes pueden ser aportados por diferentes vías. En todos los experimentos llevados a cabo se hizo uso de la irrigación forzada.

Descripción de las Parcelas Experimentales. El estudio de campo se llevó a cabo en una parcela experimental que está situada en la Huerta de Santa María en la Vega de Granada – España. En el suelo agrícola no se ha utilizado ningún tipo de pesticida, herbicida o insecticida en los últimos 10 años con el objetivo de no alterar la microbiota del suelo[19]. Las muestras de compost fabricado a partir de lodos de depuradora que fueron utilizados para este ensayo, fueron recolectadas en la empresa compostadora "Biomasa del Guadalquivir" situada en Santa Fe (Granada).

Se prepararon una serie de subparcelas de 4 m^2 (2 x 2 m) para cada ensayo separadas por tasquibas de 30 centímetros de espesor. Se procedió a la limpieza de la vegetación existente para evitar posibles interferencias en los mecanismos de adsorción- desorción, la degradación de los compuestos en estudio, o la interferencia sobre alguna variable general como el índice de evaporación del agua. Se fijaron dos condiciones diferentes, Parcela 1 (P1) con los contaminantes puros aplicados directamente al suelo. Parcela 2 (P2) Enmendada con compost y contaminada con TCS y TCB.

La contaminación tanto de la parcela compostada como de la no compostada se realizó adicionando 1 $g.L^{-1}$ de cada compuesto en un volumen de 120 litros de agua de pozo. Una vez dopada, durante todo el periodo de experimentación se llevaron a cabo sucesivamente dos operaciones, una de muestreo y otra de riego. La toma de muestra se realizó a siete profundidades (superficie, 10, 20, 30, 40, 50 y 60 centímetros) a lo largo del tiempo (0, 15 y 30 días). Durante la primera semana la toma de muestra fue diaria, ya que estudios previos realizados habían demostrado que durante este espacio de tiempo se producía la caída exponencial de la concentración, aportando información de gran importancia sobre el comportamiento del compuesto.

Tratamiento de la muestra. Cada una de las muestras tomadas se sometió a las siguientes etapas para asegurar su correcto análisis en el laboratorio. Adición de formaldehido 1 % (m/v), para evitar el crecimiento microbiano en las muestras. Secado y tratamiento de las muestras, en bandejas de plástico y al sol a temperatura ambiente. Una vez secas se molturaron con un mortero de hierro y se tamizaron con ayuda de una malla de 2 mm. Posteriormente se introdujeron en una bolsa de plástico y se llevaron al laboratorio donde permanecieron a una temperatura de 4ºC hasta su análisis. Una vez en el laboratorio, las muestras de suelo fueron analizadas. Para este ensayo se realizaron en total 12 tomas de muestra a diferentes tiempos.

Se optimizaron las diferentes variables que ejercen una mayor influencia en el rendimiento de las distintas técnicas de extracción empleadas. El valor óptimo para cada variable fue determinado a través del porcentaje de recuperación de la extracción de muestras dopadas con los compuestos (100 µg g^{-1}). A la vista de los resultados globales obtenidos, se seleccionó la técnica de ultrasonidos para el análisis de las muestras por su mayor simplicidad y menor coste. En la **Tabla 1** se muestran los parámetros óptimos para cada contaminante cuando se empleó esta técnica de extracción.

TABLA 1. Parámetros óptimos del análisis mediante USE

	USE
Peso de la muestra	0.5 g
Disolvente de extracción	Metanol
Volumen de disolvente	15 mL
Tiempo de ultrasonidos	25 minutos
Ciclos de extracción	1
Potencia de ultrasonido	75%
Tiempo de centrifugado	30 min a 5000 r.p.m.(3634 xg)
Evaporación	Bajo corriente de N_2
Volumen de redisolución	1 mL

Análisis mediante UPLC-MS/MS. La determinación de la cantidad de los compuestos degradados se realizó mediante la técnica de UPLC-MS/MS, empleando las condiciones descritas en la **Tabla 2.** Se muestran los parámetros optimizados para la separación cromatográficas y la detección mediante espectrometría de masas. Una vez optimizadas estas variables se seleccionaron las dos transiciones en el espectrómetro (cuantificación e identificación) óptimas para la determinación de cada molécula. En la **Tabla 3** se muestran las transiciones seleccionadas.

TABLA 2. Valores óptimos de las condiciones cromatográficas

Fase estacionaria	ACQUITY UPLC® BEH C18 (2.1 x 100 mm) 1.7µm		
Fase móvil	A: Agua (0.025 % amoniaco) B: Metanol (0.025 % amoniaco)		
Modalidad: Gradiente	Tiempo (min)	A %	B %
	0.0	40	60
	6.0	0	100
	6.5	0	100
	6.6	40	60
	10.0	40	60
Flujo	0.3 mL min^{-1}		
Volumen de inyección	4 µL		
Temperatura del horno	40°C		
Detección	ESI-MS/MS		

TABLA 3. Parámetros del espectrómetro de masas para el TCS y TCB

Analito	Transición	CV / CE	Transición	CV / CE	Modo
TCS	287.0→ 141.8	22/32	287.0→ 160.8	22/40	ESI(-)
TCB	313.1→ 150.9	2/14	313.1→ 126.2	2/14	ESI(-)
AMC	294.2→ 258.0	2/16	294.2→ 213.9	2/20	ESI(-)

CV: Voltaje del cono; **CE:** Energía de colisión

RESULTADOS Y DISCUSIÓN

Determinación de la concentración del analito Parcela 1. En la **Tabla 4** y **5** se muestran las concentraciones de cada analito en las muestras de suelo contaminadas.

TABLA 4. Concentraciones de TCS en el tratamiento en la parcela 1

Concentración de TCS (µg kg $suelo^{-1}$)						
Muestra	**Toma 1**	**Toma 2**	**Toma 3**	**Toma 4**	**Toma 5**	**Toma 6**
	5 h	**29 h**	**53 h**	**77 h**	**125 h**	**173.5 h**
2 cm (sup)	16.6	12.2	11.8	10.8	9.7	8.7
Muestra	**Toma 7**	**Toma 8**	**Toma 9**	**Toma 10**	**Toma 11**	**Toma 12**
	245 h	**341 h**	**405.5 h**	**505.5 h**	**673.5 h**	**845.5 h**
2 cm (sup)	6.7	5.4	4.4	3.0	1.3	1.0

TABLA 5. Concentraciones de TCB en el tratamiento en la parcela 1

Concentración de TCB (µg kg suelo^{-1})						
Muestra	**Toma 1**	**Toma 2**	**Toma 3**	**Toma 4**	**Toma 5**	**Toma 6**
	5 h	**29 h**	**53 h**	**77 h**	**125 h**	**173.5 h**
2 cm (sup)	2.6	2.1	1.6	0.9	0.6	0.4
10 cm	5.9	4.1	3.8	2.7	1.2	0.9
20 cm	3.2	2.3	1.7	1.2	0.9	0.8
30 cm	44.7	44.5	40.1	32.1	27.5	24.2
40 cm	1.2	1.1	0.9	0.7	0.7	0.6
50 cm	1.1	0.9	0.8	0.8	0.7	0.6
Muestra	**Toma 7**	**Toma 8**	**Toma 9**	**Toma 10**	**Toma 11**	**Toma 12**
	245 h	**341 h**	**405.5 h**	**505.5 h**	**673.5 h**	**845.5 h**
2 cm (sup)	0.2	0.1	0.1	0.08		
10 cm	0.7	0.6	0.5	0.52	0.19	
20 cm	0.6	0.5	0.5	0.42	0.40	0.26
30 cm	17.6	16.5	13.9	12.74	11.10	10.16
40 cm	0.4	0.4	0.4	0.38	0.29	0.19
50 cm	0.5	0.5	0.4	0.34	0.34	

Cinéticas de Desaparición de los Compuestos en el Suelo (Parcela 1). La variación de las concentraciones de todos los contaminantes estudiados en el suelo agrícola contaminado, a las distintas profundidades, como consecuencia de los procesos adsorción-desorción, transporte y degradación, permite deducir que el proceso de desaparición de los compuestos, en cada uno de los puntos de toma de muestra, sigue una cinética de primer orden. Este modelo se rige por la siguiente ecuación $C = C_o \cdot e^{-kt}$, donde, C representa la concentración de analito (µg kg suelo^{-1}) a un tiempo determinado t (min), C_o es la concentración inicial del analito (µg kg suelo^{-1}) y k es una constante cinética (h^{-1}). En la **Figura 3** y **4** se representan los ajustes obtenidos para los distintos analitos estudiados.

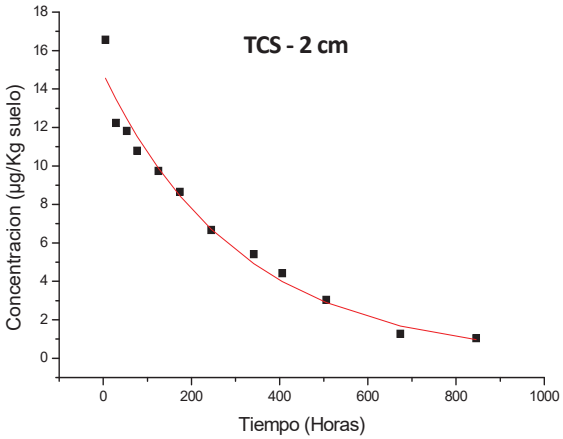


FIGURA 3. Cinética de desaparición del TCS en la superficie (2 cm)

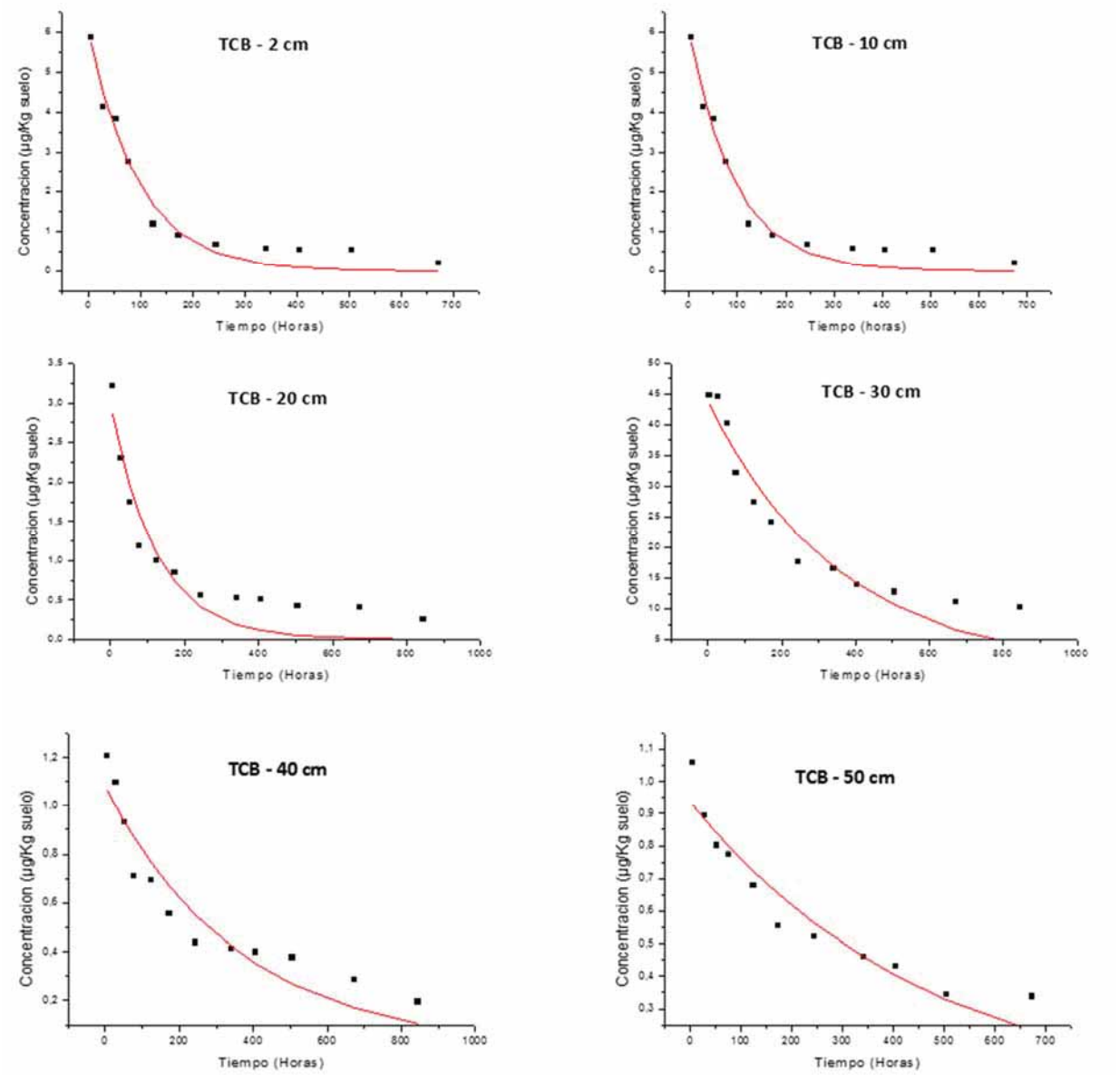


FIGURA 4. Cinética de desaparición del TCB a diferentes profundidades

Los datos mostrados en las figuras, se ajustan, en todos los casos, a la ecuación exponencial de primer orden anteriormente citada ($C= C_0.e^{-kt}$). A partir de los datos, se obtuvieron los correspondientes valores de la constante de desaparición del compuesto (k), el tiempo de vida media en cada zona del suelo ($t_{1/2}$) y coeficiente de determinación (R^2). En la **Tabla 6** se muestran los valores obtenidos para estos parámetros.

TABLA 6. Parámetros del ajuste para el TCS en superficie

k (h^{-1})	$3.2 \cdot 10^{-3}$
C_0	14.8
$t_{1/2}$	214.6
$\%R^2$	97.2

Al igual que en otros casos, el TCS se adsorbe y desaparece en la superficie no lixiviando a mayores profundidades. La degradación del TCS en el suelo fue relativamente rápida con los tiempos de vida media 214.6 h. (**Tabla 7**)

TABLA 7. Parámetros del ajuste TCB a distintas profundidades

	Superficie	**10 cm**	**20 cm**	**30 cm**	**40 cm**	**50 cm**
k (h^{-1})	$1.2 \cdot 10^{-2}$	$1.0 \cdot 10^{-2}$	$8.1 \cdot 10^{-3}$	$2.8 \cdot 10^{-3}$	$2.7 \cdot 10^{-3}$	$2.1 \cdot 10^{-3}$
C_0	2.8	6.1	2.9	43.8	1.1	0.9
$t_{1/2}$	57.6	66.2	85.8	247.5	252.0	333.2
$\%R^2$	98.9	96.9	88.9	92.8	89.5	91.9

Por último, el TCB se detecta en los primeros 50 cm, no lixiviando a la mayor profundidad de 60 cm. La desaparición del compuesto fue rápida con tiempos de vida media comprendidos entre las 57.6 h en la capa superficial a las 333.2 h a los 50 cm de profundidad.

Además y como era de esperar, debido a los fenómenos de degradación y lixiviación principalmente, al establecer la relación entre las constantes obtenidas, se constata que la velocidad de desaparición del compuesto es mayor cuanto más cerca de la superficie se encuentra el analito, de forma que $k_{sup} > k_{10\ cm} > k_{20\ cm} > k_{30\ cm} > k_{40\ cm}$. La explicación radica en que parte del compuesto se degrada y otra parte migra por arrastre con el agua hacia puntos inferiores tras cada uno de los regados.

Determinación de la concentración del analito Parcela 2. Finalizado el estudio en la parcela 1 (suelo con los analitos puros), se repitió el proceso de la misma forma, pero en este caso empleando una parcela que previamente había sido enmendada con compost procedente de lodo de depuradora (parcela 2) tal y como se describió con anterioridad. En la **Tabla 8** y **9** se muestran los datos de concentración obtenidos en los análisis de las diferentes muestras tomadas a las distintas profundidades.

TABLA 8. Concentración de TCS en el tratamiento en la parcela 2

Concentración de TCS (µg kg suelo^{-1})						
	Toma 1	**Toma 2**	**Toma 3**	**Toma 4**	**Toma 5**	**Toma 6**
	5 h	29 h	53 h	77 h	125 h	173.5 h
2 cm (sup)	24.6	19.8	16.7	11.3	9.5	8.7
	Toma 7	**Toma 8**	**Toma 9**	**Toma 10**	**Toma 11**	**Toma 12**
	245 h	341 h	405.5 h	505.5 h	673.5 h	845.5 h
2 cm (sup)	6.3	5.8	3.8	0.9	0.4	

TABLA 9. Concentración de TCB en el tratamiento en la parcela 2

	Concentración de TCB (µg kg suelo^{-1})					
	Toma 1	**Toma 2**	**Toma 3**	**Toma 4**	**Toma 5**	**Toma 6**
	5 h	29 h	53 h	77 h	125 h	173.5 h
2 cm (sup)	1.8	1.4	0.9	0.7	0.6	0.6
10 cm	3.0	2.2	1.9	1.2	0.8	0.8
20 cm	4.6	4.4	3.7	2.7	1.9	1.3
30 cm	0.9	0.9	0.7	0.6	0.6	0.4
40 cm	0.9	0.8	0.8	0.7	0.7	0.7
	Toma 7	**Toma 8**	**Toma 9**	**Toma 10**	**Toma 11**	**Toma 12**
	245 h	341 h	405.5 h	505.5 h	673.5 h	845.5 h
2 cm (sup)	0.4	0.2	0.2	0.1	0.1	
10 cm	0.8	0.5	0.4	0.3	0.1	0.1
20 cm	1.1	0.8	0.7	0.6	0.5	0.3
30 cm	0.3	0.1	0.1	0.1	0.1	0.1
40 cm	0.6	0.4	0.2	0.1	0.1	0.1

Los resultados mostrados en las tablas demuestran que al igual que en el caso del estudio realizado en la primera parcela, el TCS es retenido en la superficie (2 cm), degradándose completamente en este punto. Por último, el TCB, aparece hasta profundidades de hasta 40 cm.

Cinéticas de Degradación de los Compuestos en Suelos Enmendados con Compost (Parcela 2). Al igual que en el caso del primer experimento llevado a cabo en la parcela 1, la observación de la variación de las concentraciones con el tiempo, a las distintas profundidades (**Figura 5** y **6**), permite vaticinar una cinética de primer orden para todos casos estudiados ($C = C_0 \cdot e^{-kt}$).

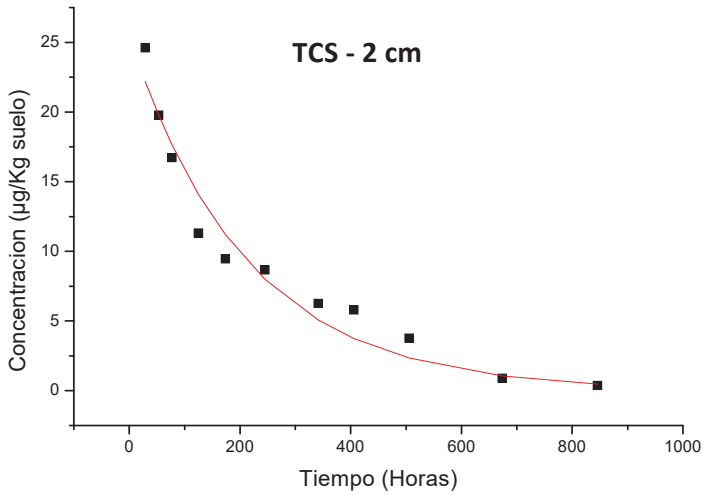


FIGURA 5. Cinética de desaparición del TCS en superficie (2 cm)

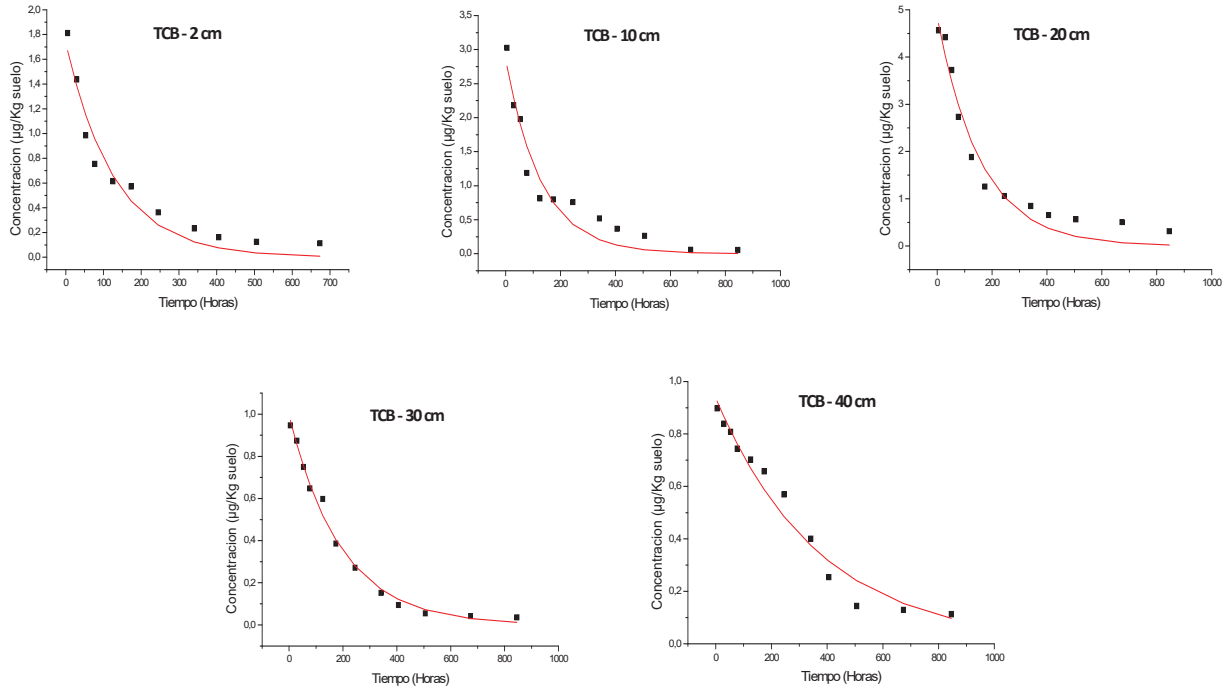


FIGURA 6. Cinética de desaparición de la TCB a las diferentes profundidades

A continuación, partiendo de los datos de concentración obtenidos para cada profundidad, se obtuvieron los parámetros correspondientes de la ecuación exponencial de primer orden $C = C_0 \cdot e^{-kt}$ (**Tabla 10** y **11**), es decir, los valores de la constante de desaparición del compuesto (k), el tiempo de vida medio ($t_{1/2}$) y el coeficiente de determinación (R^2). La siguiente tabla muestra los valores obtenidos.

TABLA 10. Parámetros del ajuste para el TCS en superficie

k (h^{-1})	$4.7 \cdot 10^{-3}$	**$t_{1/2}$**	146.5
C_0	25.4	**%R^2**	95.7

TABLA 11. Parámetros del para el TCB a distintas profundidades

	Superficie	**10 cm**	**20 cm**	**30 cm**	**40 cm**	**50 cm**
k (h^{-1})	$7.7 \cdot 10^{-3}$	$7.7 \cdot 10^{-3}$	$6.3 \cdot 10^{-3}$	$5.2 \cdot 10^{-3}$	$2.7 \cdot 10^{-3}$	$2.3 \cdot 10^{-3}$
C_0	1.7	2.9	4.9	0.9	0.9	52.4
$t_{1/2}$	89.7	89.9	109.8	133.3	257.7	297.5
%R^2	95.0	93.4	96.0	99.2	96.9	95.5

En todos los casos, el comportamiento es similar al observado en la parcela 1, aunque con ciertas diferencias que desarrollaremos a continuación.

Comparación del Comportamiento de los Contaminantes en Suelo y en Suelo Enmendado con Compost. Durante este estudio comparativo de la cinética de degradación de estos compuestos en suelos y suelos enmendados con compost se

demuestra que, los analitos estudiados en las diferentes condiciones, tienen un comportamiento similar, ajustándose en todos los casos a una cinética de primer orden. En la **Tabla 12** se comparan los tiempos de vida media de cada uno de los compuestos estudiados a las distintas profundidades, en ambos estudios.

TABLA 12. Comparación del comportamiento del TCS y TCB en el suelo y suelo enmendado con compost

	$t_{1/2}$	
Profundidades	**TCS**	**TCB**
2cm (sup)	P 1 >P 2	P 1 >P 2
10 cm		P 1 >P 2
20 cm		P 1 >P 2
30 cm		P 1 >P 2
40 cm		P 1 >P 2
50 cm		P 1 >P 2
60 cm		P 1 >P 2

El tiempo de vida media en dos casos es superior para las condiciones de la P1. En el caso del TCS, se puede observar que sólo se absorbe y degrada en la superficie en ambas condiciones, mostrando que el tiempo de vida medio es mayor en las condiciones de la P1. Finalmente, en el caso del TCB, se aprecia que el compuesto aparece hasta la máxima profundidad estudiada (60 cm), pudiendo incluso lixiviar a mayores profundidades. En todos los casos el tiempo de vida media fue mayor bajo las condiciones de la parcela P1.

CONCLUSION

Como conclusión general, se observa que, en la mayoría de los compuestos, los tiempos de vida media son mayores en las condiciones experimentales de la parcela P1. Desde el punto de vista medio ambiental el enmendado de los suelos agrícolas con compost es muy beneficioso por que aporta materia orgánica, hecho que favorece el crecimiento de microorganismos y provoca un aumento tanto en la retención de los analitos impidiendo su lixiviación a mayores profundidades, así como la aceleración en el fenómeno de la biodegradación de estos contaminantes emergentes que en dosis reducida pueden actuar como disruptores endocrinos en animales e incluso seres humanos.

REFERENCIAS

1. Doughton, C.G., Ternes, T.A. Pharmaceuticals and personal care products in the Environment: Agents of subtle change. Environmental Health Perspectives 107 (1999) 907-938.
2. Fent, K., Weston, A.A., Caminada, D. Ecotoxicology of human pharmaceuticals. Aquatic Toxicology 76 (2006) 122-159.

3. Jemba, P.K. Excretion and ecotoxicity of pharmaceutical and personal care products in the environment. Ecotoxicology and Environment 63 (2006) 113-130.
4. Petrovic, M., Hernando, M.D., Díaz-Cruz, M.S., Barceló, D. Liquid chromatography-tandem mass spectrometry for the analysis of pharmaceutical residues in environmental samples: A Review. Journal of Chromatography A 1067 (2005) 1-14.
5. Díaz-Cruz, M.S., Barceló, D. Determination of antimicrobial residues and metabolites in the aquatic environment by liquid chromatography tandem mass spectrometry. Analytical and Bioanalytical Chemistry 386 (2006) 973-985.
6. Temes, T., Joss, A. Human pharmaceuticals, hormones and fragrances: the micropollutant challenge for urban water management. Water 21 (2006) 121-148.
7. Kinney, C.A., Furlong, E., Zaugg, S., Burkhardt, M., Werner, S., Chahill, S., Jorgensen, G. Survey of organic wastewater contaminants in biosolids destined for land Application. Environmental Science and Technology 40 (2006) 7207-7215.
8. European Commission. European workshop on the impact of endocrine disruptors on human health and wildlife. Report Eur 17549, Environment and Climate Research Programme, DG XII. Weybridge (1996) 1-125.
9. Singer, H., Muller, S., Tixier, C. Pillonel L. TCS: occurrence and fate of a widely used biocide in the aquatic environment: field measurements in wastewater treatment plants, surface waters, and lake sediments. Environmental Science and Technology 36 (2002) 4998-5004.
10. Jones, R., Jampani, H.B., Newman, J.L., Lee, A.S. TCS: A review of effectiveness and safety in health care settings. American Journal of Infection Control 28 (2000) 184-196.
11. Veldhoen, N., Skirrow R.C., Osachoff, H., Wigmore, H., Clapson, D.J., Gunderson, M.P., Van Aggelen, G., Helbing, C.C. The bactericidal agent TCS modulates thyroid hormone-associated gene expression and disrupts postembryonic anuran development. Aquatic Toxicology 80 (2006) 217-227.
12. Veldhoen, N., Skirrow R.C., Osachoff, H., Wigmore, H., Clapson, D.J., Gunderson, M.P., Van Aggelen, G., Helbing, C.C. Corrigendum to “The bactericidal agent TCS modulates thyroid hormone-associated gene expression and disrupts postembryonic anuran development”. Aquatic Toxicology 83 (2007) 648-651.
13. Council of the European communities, Directive 76/768/EEC of 27 July 1976 on the approximation of the laws of the Menber States relating to cosmetic product (1976).
14. Scientific committee on consumer products, opinion on triclocarban for other uses than as a preservative (2005) 101-202.
15. TCB consortium, high production volume (HPV) chemical challenge program data availability and screening level assessment for TCB. Report 201-14186A, 2002.
16. European Commission, joint research centre, Institute for Health and Consumer Protection, available at: http://esis.jrc.ec.europa.eu/, accessed on: December 2011.
17. Veldhoen, N., Skirrow R.C., Osachoff, H., Wigmore, H., Clapson, D.J., Gunderson, M.P., Van Aggelen, G., Helbing, C.C. The bactericidal agent TCS modulates thyroid hormoneassociated gene expression and disrupts postembryonic anuran development. Aquatic Toxicology 80 (2006) 217-227.
18. Veldhoen, N., Skirrow R.C., Osachoff, H., Wigmore, H., Clapson, D.J., Gunderson, M.P., Van Aggelen, G., Helbing, C.C. Corrigendum to “The bactericidal agent TCS modulates thyroid hormone-associated gene expression and disrupts postembryonic anuran development”. Aquatic Toxicology 83 (2007) 648-651.
19. Kinney, C. A., Furlong, E. T., Zaugg, S. D., Burkhardt, M. R., Werner, S. L., Cahill, J. D., Jorgensen, G. R. Survey of organic wastewater contaminants in biosolids destined for land application. Environmental Science and Technology 40 (2006) 7207-7215.

CHAPTER 9.2 IDENTIFICACIÓN DE FUENTES DE EMISIÓN DE PM_{10} ASOCIADAS A LOS METALES PRESENTES EN LAS ÉPOCAS DE LLUVIA Y ESTIAJE EN LA REGIÓN TULA-TEPEJI, HIDALGO

G. Martínez-Reséndiz *(1,2); R. I. Beltrán-Hernández (1); A. Ramírez-Reyes (2); C. Solís Rosales (3); J. Miranda (3); S. A. Medina-Moreno (1) and C. A. Lucho-Constantino (1,2)

(1) Centro de Investigaciones Químicas, Universidad Autónoma del Estado de Hidalgo, Carr. Pachuca-Tulancingo km. 4.5. Mineral de la Reforma, Hidalgo, México.
(2) Programa de Ingeniería en Biotecnología, Universidad Politécnica de Pachuca, Carretera Pachuca-Cd. Sahagún. Km. 20. Zempoala, Hidalgo. C.P. 42184.
(3) Instituto de Física, Universidad Nacional Autónoma de México. México, D.F. C.P. 01000.

ABSTRACT

Deteriorating air quality is easily perceived, especially in cities with a high industrial development. The Tula-Tepeji region, in Hidalgo State, Mexico, is a critical area due to the emission of 500 thousand tons/year air pollutants emitted by the activity of the petrochemical, power generation, cement and lime, textile, among others industries. The aim of this study was to determine the concentration of elements associated with PM_{10} and identify possible emissions sources in the municipalities of Atitalaquia, Atotonilco de Tula and Tepeji del Rio, Hidalgo, during the months of June to December 2007. They were collected 42 Nucleopore filters for each sampling site using low-volume equipment (Minivolt-Airmetrics). Element analysis of Ca, Cl, Cr, Cu, Fe, K, Mn, Ni, Pb, S, Ti, V, Zn was determined PM_{10} using PIXE method. PM_{10} concentrations showed a similar dynamic in Atitalaquia and Atotonilco de Tula, in which exceeded at least 6 and 13 times respectively, the maximum allowable limit of PM_{10} according to NOM-025-SSA1-1993. Calcium and sulfur as the major elements in PM_{10} with concentrations between 10142 ± 6160 and 2647 ± 1901 ngm^{-3}, respectively. By other hand, the lead considered criteria air pollutant was presented at concentrations up to 32 ngm^{-3}, inside of limit of current regulations. The rest of the elements range between 587±299 and 13 ngm^{-3}. During the dry season (October to December) were observed increased concentrations of metals in Atitalaquia and Atotonilco de Tula. Factor analysis with Varimax rotation showed that the possible sources of emission of the elements studied were mainly burning coal and oil, soil dust, motor vehicles, construction industry / cement and smelting iron Steel.

Palabras clave: contaminación del aire, fuentes emisoras, zona crítica.

---

*Author for correspondence: luchouaeh@gmail.com

INTRODUCCIÓN

La contaminación atmosférica en las grandes ciudades, se encuentra estrechamente relacionado con su esquema de desarrollo económico, crecimiento de la población y las actividades industriales. Todo esto, provoca una clara tendencia al deterioro de la calidad del aire de estas ciudades y zonas conurbadas, convirtiéndose en un problema cada vez más crítico[1]. En la mayor parte de las ciudades con esta problemática, es común observar la disminución de la visibilidad debido a la presencia de contaminantes atmosféricos. Estos contaminantes se encuentran clasificados por sus características físicas y químicas, sus fuentes de producción o emisión y sus efectos a la salud de la población, que se resumen en la disminución de la capacidad pulmonar, asma, el incremento de la morbilidad y la mortalidad entre otros[2.] La mayoría de los estudios plantean que el mayor impacto sobre la salud es causado por las partículas de carbono elemental, compuestos orgánicos y determinados elementos como: arsénico, cadmio, hierro, zinc, cromo, cobre, aluminio, vanadio, níquel y plomo[3,4].

De acuerdo a la OMS la contaminación presente en una ciudad se determina a través de los denominados contaminantes primarios, ya que están presentes con mayor frecuencia, sus efectos son más conocidos y su acción se refleja a corto plazo[5]. El avance de las técnicas analíticas ha llegado al punto de que es posible detectar aproximadamente 25 elementos presentes en el material particulado[6]. Es importante establecer las fuentes de emisión de elementos traza presentes en el material, ya que se consideran nocivos al mezclarse con el aire respirable como lo son el plomo, mercurio y cadmio. Estos en encuentran principalmente asociados a la incineración de aguas residuales/hospitales, la industria, entre otras. Los elementos traza se han convertido en un tema actual, tanto en el campo ambiental como en el de salud pública. Los daños que causan son tan severos y en ocasiones tan ausentes de síntomas, que las autoridades ambientales y de salud de todo el mundo ponen mucha atención en minimizar la exposición de la población (en particular de la población infantil) a estos elementos tóxicos.

Algunas investigaciones han aportado información importante sobre el comportamiento que las partículas tienen durante un ciclo anual, tanto en temporada de secas como de lluvias, así como en meses de mayor incidencia de contaminación por otros factores[7,8,9]. De esta manera, se ha detectado que el conocer las fluctuaciones en las concentraciones, así como la distribución del material particulado en la atmósfera es un tema de investigación que hay que tomar en cuenta dentro de toda la perspectiva de la contaminación. Durante la época de estiaje se presenta la temporada invernal más crítica respecto a la contaminación atmosférica, por lo que en este período existe coincidencia de enfermedades respiratorias y el aumento de los niveles de contaminación.

La región norte de la Zona Metropolitana de la Ciudad de México (ZMCM) se caracteriza por ser un área en la que confluyen además de una enorme zona industrial y un alto movimiento vehicular, lo que ocasiona que se registren altos índices de contaminación tanto de gases como de material particulado, además del aporte de estos contaminantes hacia el sur por acción de los vientos[10]. La Norma Oficial Mexicana NOM-043-ECOL 1993, clasifica como una zona critica de contaminación atmosférica a la Zona industrial Tula-Vito-Apasco debido a que en esta región se encuentran

asentadas diferentes fuentes emisoras de contaminantes atmosféricos como: el aprovechamiento de materiales pétreos (cal y cemento), industria petroquímica, generación de electricidad, alimentaria, industrias de transformación y maquiladoras entre otras[11].

La finalidad de este estudio fue determinar la concentración de elementos asociados a PM_{10} en los municipios de Atitalaquia, Atotonilco de Tula y Tepeji del Río, Hidalgo, en dos estaciones del año, con la finalidad de identificar las posibles fuentes de emisión de estos contaminantes.

MATERIALES Y MÉTODOS

Descripción del área de estudio. El muestreo de material particulado se llevó a cabo en tres municipios situados en el corredor industrial Tula-Tepeji en el estado de Hidalgo: Atitalaquia (N 20º 03.609´, WO 99º 13.317´), Atotonilco de Tula (N 20º 00.696´, WO 99º 13. 289´) y Tepeji del Río (N 20º 35.280´, WO 99º 20. 325´) durante dos estaciones del año del 2007: época de lluvia (Junio-Septiembre) y estiaje (Octubre-Diciembre).

Monitoreo de PM_{10}. Las partículas PM_{10} se colectaron con un equipo de bajo volumen (Minivol Airmetrics) por periodos de 24 h, utilizando un flujo volumétrico de 5 L min^{-1}, conforme a los métodos IO-2.1 y IO-3.1[12]. Para la colección del material particulado se emplearon filtros de policarbonato (Nucleopore) de 47 mm de diámetro y 0.4 µm de tamaño de poro; los cuales se acondicionaron previamente al muestreo durante 48h bajo condiciones constantes de humedad relativa (47%±5%) y temperatura (22º±2). De igual manera se eliminó la carga electrostática con ayuda de una fuente de ^{210}Po (“Staticmaster” modelo IC200R).

Los filtros recolectados se almacenaron en un ambiente completamente aislado de cualquier factor que afectara sus características, bajo estas condiciones se determinó la concentración de PM_{10} por medio de métodos gravimétricos en una micro balanza (Ohaus modelo GA200D) con una sensibilidad y resolución de 10 □g.

Determinación de elementos traza. El análisis de elementos (Si, S, Cl, K, Ca, Ti, V, Cr, Mn, Fe, Ni, Cu, Zn, Sr, Hg y Pb) se determinó por medio del método PIXE, utilizando un acelerador de partículas con protones de 2-4 MeV de energía en el Instituto de Física de la UNAM[12,13,14].

Análisis estadístico. Se realizó un análisis multivariante de Componentes Principales (ACP) con rotación Varimax, como modelo de receptores, para identificar las fuentes de emisión de 14 metales presentes en PM_{10}, en las épocas de lluvia y estiaje de los sitios de estudio. El análisis de ACP se realizó utilizando el software SPSS versión 21.

RESULTADOS Y DISCUSIÓN

Material particulado PM₁₀. En el municipio de Atitalaquia, las concentraciones de PM_{10} durante la época de estiaje (octubre-diciembre, 2007) presentaron las concentraciones más altas (156 □g m^{-3}) de la zona de estudio (**Figura 1B**). De acuerdo a lo establecido por la NOM-025-SSA1-1993 para exposición aguda, en este sitio se excedió siete veces el valor máximo permisible de 75 □g m^{-3} (promedio de 24 h). Por otra parte, durante la época de lluvia las concentraciones de PM_{10} en los filtros, fueron menores a lo observado durante la época de estiaje, excediéndose el límite máximo permisible de PM_{10} en 3 ocasiones (**Figura 1A**). En el sitio de Atotonilco de Tula, las concentraciones de PM_{10} en la época de estiaje excedieron 11 veces el límite máximo permisible por la NOM-025-SSA1-1993 (**Figura 2B**). Aunque las concentraciones de material particulado en época de lluvia son más bajas en comparación a la época de estiaje, la concentración de PM_{10} excedieron 3 veces el límite establecido por la normatividad mexicana (**Figura 2A**). En el caso de Tepeji del Río, se monitoreo la época de estiaje donde las concentraciones más altas de PM_{10} fue de 96 g m^{-3} (**Figura 3**). Este valor excede el límite máximo permisible de la NOM-025-SSA1-1993, promedio 24 h.

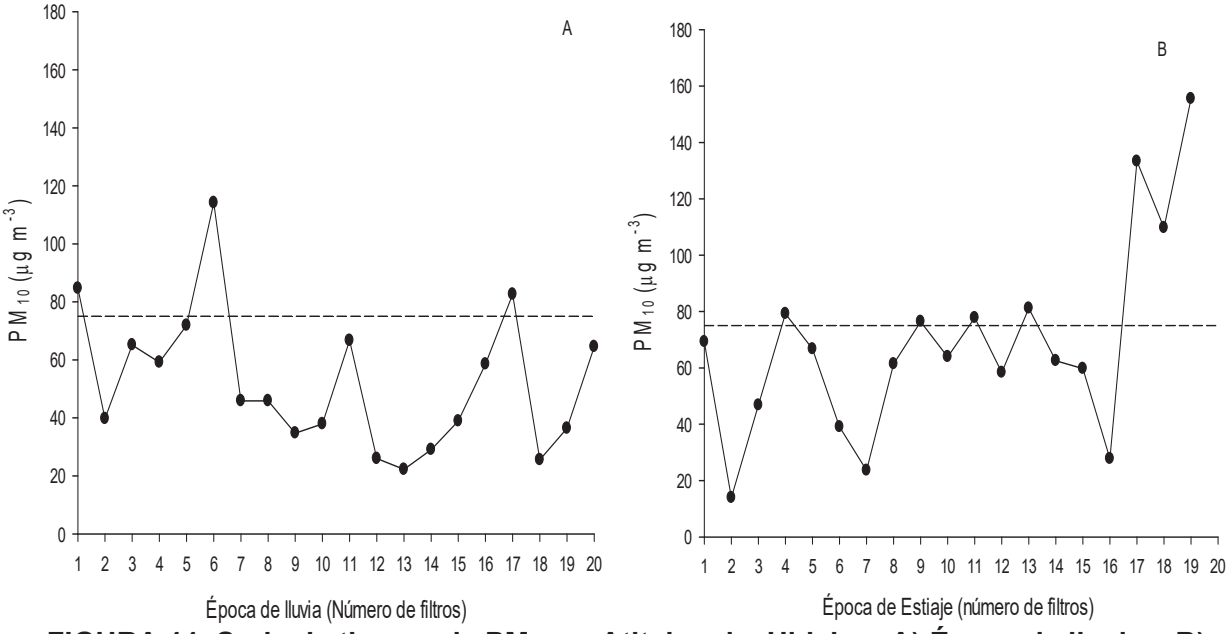


FIGURA 11. Serie de tiempo de PM_{10} en Atitalaquia, Hidalgo. A) Época de lluvia y B) estiaje

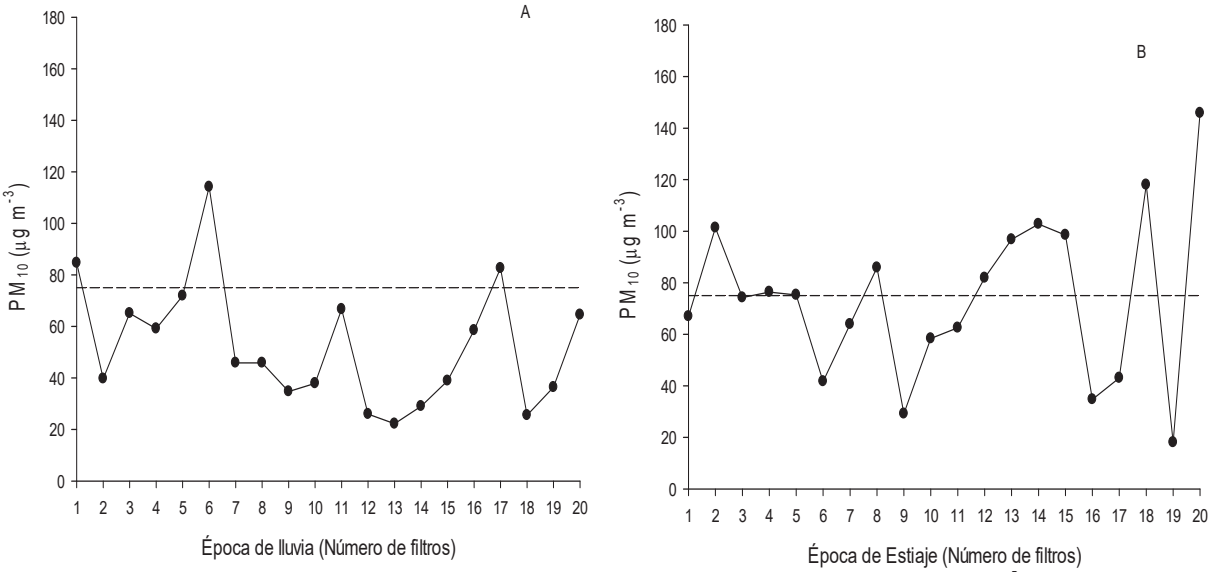


FIGURA 12. Serie de tiempo de PM_{10} en Atotonilco de Tula, Hidalgo. A) Época de lluvia y B) estiaje

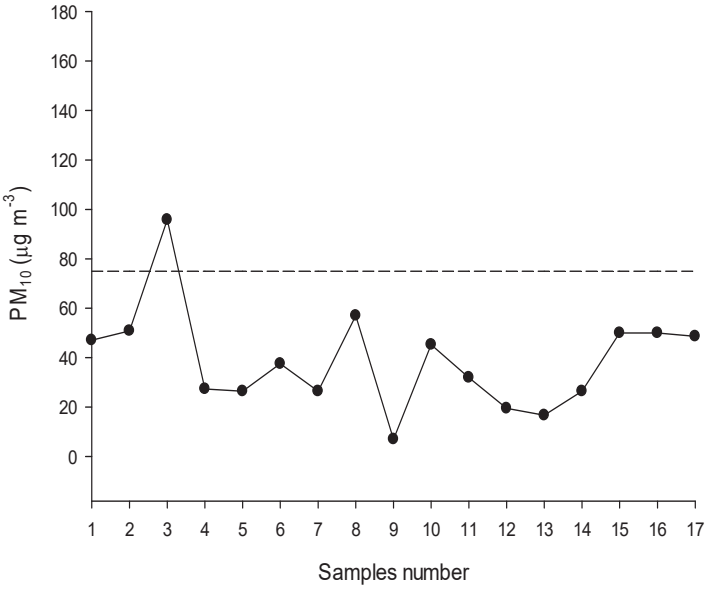


FIGURA 13. Serie de tiempo de PM_{10} en la época de estiaje en Tepeji del Río, Hidalgo

***Determinación de elementos época de lluvia y estiaje en los sitios de estudio*.** En el sitio de Atitalaquia, las mayores concentraciones de los elementos en el material particulado durante la época de lluvia fueron Ca>Si>S>Fe>K>Cl. Las concentraciones de estos elementos corresponden al 98.44% (12,133 ng m^{-3}) de la masa total de PM_{10} determinado en esta época. En la época de estiaje, tanto los elementos presentes (Ca>Si>S>K>Fe>Cl), como la concentración de los elementos en el material particulado fue similar a la época de lluvia (98.59%; 19,267 ng m^{-3}). Para ambos periodos los

elementos con las concentraciones más elevadas fueron Ca, Si y S, estos tres elementos constituyen el 89.40% de la composición de PM_{10} en época de lluvia y con el 89.10% en época de estiaje.

El elemento con mayor concentración presente en las dos épocas del año fue el Ca, con una concentración de 5332±4152 ng m^{-3} en la época de lluvia, aumentando la concentración en el material particulado en un 92.89% en la época de estiaje (10,285 ng m^{-3}±4757). El Ca es un elemento que se encuentra asociado a diferentes fuentes de emisión como polvo del suelo, combustión del carbón y la industria de la construcción/cemento[15]. Otros elementos mayoritarios presentes en PM_{10} fueron el Si y el S. Durante la época de lluvia las concentraciones fueron menores (3624±2149 y 2062±911 ng m^{-3}, respectivamente) en comparación con la época de estiaje (3919±1807 y 3208±1904 ng m^{-3}, respectivamente). El Si y S aumentaron su concentración en el material particulado en la época de estiaje en 8.14 y 55.58%, respectivamente. Estos elementos son emitidos principalmente por tres fuentes como el polvo del suelo, la combustión del carbón y los motores de vehículos[15].

TABLA 1. Concentración de elementos en PM_{10} en los sitios de estudio

Sitio	**Atitalaquia**		**Atotonilco de Tula**		**Tepeji del Río**
Época	Lluvia	Estiaje	Lluvia	Estiaje	Estiaje
Elemento	ng m^{-3}				
Ca	5332	10285	7520	12764	3228
Cl	275	292	349	503	300
Cr	17	16	13	49	11
Cu	16	23	13	16	73
Fe	478	702	477	596	426
K	361	860	812	879	420
Mn	12	18	12	23	13
Ni	8	20	9	25	24
Pb	32	28	22	35	32
S	2062	3208	1915	3343	2790
Si	3624	3919	4063	2799	2343
Ti	59	66	59	49	42
V	34	60	35	92	120
Zn	17	44	20	41	36

Por otra parte, la combustión del carbón, los motores de vehículos y el smog son fuentes emisoras de Fe, K y Cl, estos elementos se encuentran presentes en concentraciones medias en el material particulado. El K fue el elemento que presentó el

mayor incremento en su concentración (138.23%) en la época de estiaje, en comparación con la época de lluvia. Por otra parte, elementos como el Ti, Zn y Mn presentaron concentraciones bajas en el periodo de lluvia. Las principales fuentes de emisión de estos tres elementos son: el polvo del suelo, la combustión del carbón, los motores de vehículos, y la incineración en general (**Tabla 1**). Otros elementos como el V, Cu y Ni presentaron el mismo comportamiento que la mayoría de los elementos evaluados. La industria y la combustión del petróleo son las principales fuentes de emisión de estos elementos [15]. En el caso del Pb y Cr las concentraciones en PM_{10} fueron ligeramente más altas en periodo de lluvia (32±22 y 17±22 ng m^{-3}, respectivamente) en comparación a la época de estiaje (28±19 y 16±7 ng m^{-3}, respectivamente).

En el municipio de Atotonilco de Tula, durante la época de lluvia y estiaje los elementos Ca>Si>S>Fe>K>Cl fueron los elementos mayoritarios en ambas épocas de estudio. Para los dos periodos de muestreo, el Ca, Si y S fueron los elementos mayoritarios aportando un 88.12% del total de los elementos evaluados en la época de lluvia y con un 89.19% para la época de estiaje. Además el Ca presentó las concentraciones más elevadas en ambas épocas de estudio (**Tabla 1**), aportando el 49.09% de los elementos reportados en la época de lluvia y el 60.17% de la época de estiaje.

Los elementos K, Fe y Cl mostraron concentraciones medias en el material particulado en ambas épocas de estudio. Sin embargo, estos elementos incrementaron las concentraciones en PM_{10} en 8.25, 24.95 y 44.13% respectivamente, en la época de estiaje. Este comportamiento fue similar al observado en las determinaciones de estos elementos en el sitio de Atitalaquia. Por otra parte, los elementos como el V, Pb, Zn, Cu, Cr, Mn y Ni muestran concentraciones bajas, pero con incrementos altos en la época de estiaje de 162.86, 59.09, 105.00, 23.98, 276.92, 91.67 y 177.78% respectivamente, en comparación a la época de lluvia (ver **Tabla 1**).

Sin embargo, los elementos Si y Ti presentaron concentraciones más altas en época de lluvia (4063±2141 y 59±40 ng m^{-3}, respectivamente) en comparación a la época de estiaje (2799±1414 y 49±36 ng m^{-3} respectivamente). Estos elementos se asocian principalmente a las fuentes de polvo del suelo, la combustión del carbón, motores de vehículos y la incineración.

En el sitio de Tepeji del Río los elementos con mayores concentraciones en PM_{10} fueron Ca>S>Si>Fe>K>Cl>V contribuyendo con el 97.65% (9628 ng m^{-3}) de los elementos evaluados. Al igual que los sitios de Atitalaquia y Atotonilco de Tula, el Ca, S y Si son los elementos mayoritarios, aportando un 84.80% de los elementos presentes en el material particulado. El Ca fue el elemento con las más altas concentraciones de los elementos en la época de estiaje (3228±1844 ng m^{-3}, 32.74% de la masa total). Cabe mencionar que la concentración de este elemento en este sitio de estudio, fue menor que las concentraciones encontradas en los sitios de Atotonilco y Atitalaquia, en estos dos sitios de estudio existen varias empresas que explotan materiales pétreos, como la cal y el cemento. De igual manera, elementos como el S y el Si se encuentran presentes en concentraciones altas ( ). Por otra parte, los elementos minoritarios como el Cu, Ti, Zn, Pb, Ni, Mn, Cr contribuyendo apenas con el 3.32% (232 ng m^{-3}) del total de los elementos analizados.

Identificación de posibles fuentes emisoras por medio de análisis de componentes principales. La identificación de las posibles fuentes de emisión de elementos presentes en la fracción gruesa PM_{10}, se realizó por medio de un ACP con rotación Varimax, que correlacionó a los elementos presentes en el material particulado de los sitios de estudio, en nuevas variables llamadas factores, los cuales resultan ser, las posibles fuentes de emisión de los metales en la zona de estudio.

Atitalaquia. En el caso de la época de estiaje, se identificaron las posibles fuentes de emisión en 4 factores (F), que explican en conjunto el 86.63% de la varianza de los elementos en estudio. El Factor (F1) representó el 23.07% de la varianza total (**Tabla 2**). Para el F1, las asociaciones se presentan entre los elementos como el Si, Ti y Fe, los cuales están asociados a fuentes como el polvo del suelo, así como el Si y Fe, los cuales son emitidos por la combustión del carbón, por otra parte, los elementos Si, Fe y Zn se encuentran asociados a los motores de vehículos y el Zn y Ti a la incineración en general.

TABLA 2. Análisis factorial con Rotación Varimax de los elementos presentes en PM_{10} en Atitalaquia durante la época de estiaje

Parámetro	Factor 1	Factor 2	Factor 3	Factor 4	Factor 5
Autovalores iníciales	3.000	2.916	2.422	1.490	1.433
% varianza	23.077	22.431	18.633	11.464	11.026
% Varianza acumulada	23.077	45.508	64.141	75.605	86.631
	Autovalores iníciales				
PM_{10}	**0.741**	0.423	-0.267	-0.230	-0.213
Si	**0.522**	0.137	-0.275	0.368	**0.528**
S	0.099	**0.572**	-0.308	-0.375	**0.503**
Cl	0.028	0.320	-0.086	**0.850**	0.117
K	0.164	**0.941**	-0.006	0.205	0.090
Ca	0.312	**0.832**	0.111	0.118	0.115
Ti	**0.909**	0.053	0.242	0.067	0.155
Fe	**0.821**	**0.482**	-0.060	-0.035	0.074
Ni	**0.504**	0.189	**-0.511**	**-0.506**	-0.003
Zn	**0.533**	**0.639**	0.395	0.288	0.056
Pb	0.006	0.099	0.148	0.084	**0.883**
Mn	-0.019	0.141	**0.900**	0.090	-0.034
Cr	0.070	-0.033	**0.922**	-0.151	0.089

Con un 22.43% de la varianza total explicada, el Ca, K, Zn y Fe en el Factor 2 (F2) presentaron asociaciones con fuentes de emisión como el polvo del suelo y la combustión del petróleo y motores de vehículos (S, Fe y Zn) (**Tabla 2**). Por otra parte, el Factor 3 (F3) presentó asociaciones con la industria en general (Cr) y la fundición del hierro (Mn y Cr). El elemento Ni, presentó correlaciones negativas en este factor, por lo que no se asocia a una fuente de emisión específica. En el Factor 4 (F4, 11.46% de la

varianza total), la presencia de Cl en el material particulado se encuentra correlacionado con la incineración de residuos de hospitales o residuos sólidos. En el caso del Factor 5 (F5, 11.02% de la varianza total), los elementos Si, S y Pb se asocian principalmente a la emisión generada por los motores de vehículos o quema de combustibles fósiles.

En la época de lluvia, el ACP mostró cuatro factores, los cuales explican el 81.12% de la varianza total de los datos. El F1 con el 25.21% de la varianza total se asoció a varias fuentes de emisión del PM_{10} como el polvo del suelo (Ti y K), la combustión del carbón (S y K) y motores de vehículos (S, Ti y Zn). Por otra parte, el F2, con 24.24% de la varianza total) se asoció principalmente con el polvo del suelo e industria de la construcción/cemento (Ca, Ti y Fe) (**Tabla 3**). Este mismo factor, también presentó asociaciones con otras fuentes como, la combustión del carbón, motores de vehículos, la industria en general, la fundición (Fe) y la incineración (Ti). El F3, con 18.86% de la varianza total) presentó asociaciones con la industria en general (V) y la combustión del petróleo (V y Ni). Finalmente, el F4, con 12.79% de la varianza total, muestra una correlación del Pb y K asociada a la combustión de motores de vehículos (**Tabla 3**).

TABLA 3. Análisis factorial con Rotación Varimax de los elementos presentes en PM_{10} en Atitalaquia durante la época de lluvia

Parámetro	Factor 1	Factor 2	Factor 3	Factor 4
Autovalores iníciales	2.774	2.667	2.075	1.408
% varianza	25.214	24.247	18.863	12.796
% Varianza acumulada	25.214	49.461	68.324	81.120
Autovalores iníciales				
PM_{10}	**0.693**	**0.566**	-0.059	0.236
Si	0.293	0.424	0.314	**-0.482**
S	**0.749**	-0.003	0.186	0.165
K	**0.649**	0.196	0.304	**0.562**
Ca	0.042	**0.919**	0.176	0.191
Ti	**0.579**	**0.552**	0.228	-0.022
V	0.215	0.098	**0.908**	0.295
Fe	0.157	**0.956**	0.050	-0.048
Ni	0.148	0.143	**0.927**	0.014
Zn	**0.885**	0.137	0.143	-0.191
Pb	0.110	0.133	0.236	**0.783**

Atotonilco de Tula. El ACP de los elementos presentes en el material particulado en la época de lluvia mostraron cuatro factores, los cuales explican el 82.39% de la varianza total los datos experimentales (**Tabla 4**). En el F1 (26.91% de la varianza), los elementos Cr, Mn y Pb mostraron una fuerte correlación con actividades como la combustión del carbón, los motores de vehículos, la incineración y la fundición. Los

elementos Si, Cl, Ti, Cr y Fe se encuentran correlacionados en el F2 (26.74% de la varianza total) (**Tabla 4**). Estos elementos se encuentran asociados a la emisión de fuentes como el polvo del suelo (Si, Ti y Fe), los motores de vehículos (Si y Fe), la fundición de hierro/acero (Cr y Fe), la industria de la construcción/cemento (Fe) y la incineración (Cl). Los elementos S y Ni se encuentran correlacionados con el material particulado en el F3 (18.45% de la varianza total).

TABLA 4. **Análisis factorial con Rotación Varimax de elementos presentes en PM_{10} Atotonilco de Tula durante la época de estiaje**

Parámetro	Factor 1	Factor 2	Factor 3	Factor 4
Autovalores iníciales	2.961	2.942	2.030	1.131
% varianza	26.915	26.744	18.457	10.283
% Varianza acumulada	26.915	53.660	72.116	82.399
	Autovalores iníciales			
PM_{10}	-0.107	0.375	**0.667**	-0.323
Si	-0.053	**0.936**	0.179	0.069
S	0.078	0.410	**0.702**	0.087
Cl	-0.111	**0.684**	0.367	-0.236
Ti	0.204	**0.704**	-0.283	0.260
Cr	**0.986**	**0.058**	-0.082	-0.066
Mn	**0.986**	0.027	-0.070	-0.049
Fe	0.118	**0.868**	0.221	0.128
Ni	0.063	-0.093	**0.854**	0.186
Cu	-0.121	0.164	0.099	**0.913**
Pb	**0.954**	0.024	0.216	0.007

Estos elementos se encuentran asociados generalmente a fuentes como la combustión del petróleo, el cual es utilizado para la generación de energía y en la refinación de la gasolina que se produce en la región Tula-Tepeji. Por otra parte, la fuerte correlación del Cu en el F4 (10.28% de la varianza total) podría estar asociado con la industria en general.

Las asociaciones de elementos presentes en la época de lluvia se encuentran agrupados en cuatro factores, que explican el 72.18% de la varianza de los datos experimentales (**Tabla 5**). En el F1 los elementos como el K, Ca, Ti, Fe y Pb se encuentran correlacionados con PM_{10}. Los elementos como el K, Ca, Ti y Fe se asocian a fuentes como el polvo del suelo y la industria de la construcción/cemento (Ca y Fe). Otra fuente identificada como la combustión del carbón emite elementos como el K, Ca y Fe. De igual manera el Fe y Pb se asocian a otras fuentes como los motores de vehículos, un caso particular, es el Pb, que se asocia a fuentes como la incineración y la fundición en general.

Los elementos Cr, Cl, Pb y Mn presentes en el F2 (con 19.59% de la varianza total), se asocian con el proceso de la incineración en genera y los procesos de fundición e industria en general. Los elementos S, Ni y Cu en el F3 se asocian a fuentes como la industria en general, la combustión del petróleo y la industria de la construcción/cemento, este factor contribuye con el 13.20% de la varianza total. Los motores de vehículos (Si y Cl) y la incineración (Cl), son las fuentes identificadas dentro del F4 con 12.75% de la varianza total.

TABLA 5. **Análisis factorial con Rotación Varimax de elementos presentes en PM_{10} Atotonilco de Tula durante la época de lluvia**

Parámetro	Factor 1	Factor 2	Factor 3	Factor 4
Autovalores iníciales	3.728	2.743	1.848	1.786
% varianza	26.629	19.593	13.203	12.756
% Varianza acumulada	26.629	46.222	59.424	72.180
Autovalores iníciales				
PM_{10}	**0.774**	0.048	0.031	0.278
Si	0.185	0.135	0.097	**0.881**
S	-1.68E-5	-0.030	**0.813**	0.152
Cl	-0.205	-**0.559**	-0.347	**0.550**
K	**0.645**	-0.421	-0.220	-0.215
Ca	**0.900**	0.057	-0.127	0.149
Ti	**0.821**	0.224	0.062	0.040
Cr	-0.193	**0.836**	-0.089	0.273
Mn	-0.009	**0.944**	-0.001	-0.090
Fe	**0.866**	-0.187	0.198	0.118
Ni	0.003	0.015	**0.836**	-0.157
Cu	-0.046	-0.354	**0.458**	-0.453
Zn	0.315	0.002	-0.043	0.442
Pb	**0.513**	**0.655**	0.177	0.118

Tepeji del Rio. El ACP en la época de estiaje presentó 5 factores que explican el 85.23% de la varianza acumulada (**Tabla 6**). El F1 se asoció a varias fuentes, ya que los elementos Cr, Mn y Pb, son emitidos por la combustión del carbón, los motores de vehículos, la incineración y la industria en general. En el caso del F2 los elementos presentes como el Si, Ca, Ti y Fe se encuentran asociados a la industria de la construcción/cemento. Por otra parte, los elementos como el Ni y Cu presentes en el F3, se emiten principalmente por motores de vehículos, incineración y combustión del petróleo. En los últimos dos factores, los elementos S, Ca y Zn en el F4 se asoció a la industria construcción/cemento y el Cu en el F5 a la industria en general.

TABLA 6. **Análisis factorial (Rotación Varimax) de elementos presentes en la fracción gruesa de Tepeji del Río época de estiaje**

Parámetro	Factor 1	Factor 2	Factor 3	Factor 4	Factor 5
Autovalores iníciales	2.971	2.847	2.254	1.775	1.234
% varianza	22.853	21.896	17.342	13.655	9.941
% Varianza acumulada	22.853	44.749	62.091	75.747	85.238
			Autovalores iníciales		
PM_{10}	-0.076	0.296	**0.835**	0.161	-0.196
Si	-0.039	**0.891**	0.194	0.239	0.123
S	0.159	0.273	0.463	**0.534**	0.408
Ca	-0.035	**0.543**	0.193	**0.676**	0.041
Ti	0.149	**0.803**	-0.083	-0.312	0.044
Cr	**0.977**	0.081	-0.079	-0.101	-0.096
Mn	**0.978**	0.048	-0.088	-0.088	-0.071
Fe	0.068	**0.890**	0.215	0.135	0.137
Ni	0.100	-0.168	**0.757**	0.147	0.334
Zn	0.161	0.101	0.107	**-0.808**	0.219
Pb	**0.966**	0.010	0.130	0.043	0.065
Cu	-0.134	0.210	-0.057	-0.150	**0.890**
Cl	0.109	-0.259	**-0.772**	0.343	0.147

CONCLUSION

Durante el año de 2007, las concentraciones de PM_{10} en los sitios de A y AT sobrepasaron los límites de la normatividad mexicana entre un 43 y 52% de los días monitoreados en la época de estiaje. Durante la época de lluvia en ambos sitios, sólo se excedió este límite máximo permisible en un 15% para los sitios antes mencionados.
En la zona de estudio, las fuentes emisoras de material particulado fueron la combustión del petróleo y del carbón, industria de la construcción/cemento, así como motores de vehículos, la incineración y la fundición de metales.

AGRADECIMIENTOS

A PROMEP por el financiamiento de este proyecto (UPPPACH-PTC-028), al COEDEH, por su colaboración en los muestreos llevados cabo en este proyecto y al personal de los Centros de Salud Urbano del Municipio de Atitalaquia, Atotonilco de Tula y Tula Tepeji, Hidalgo por su invaluable apoyo para la realización de este proyecto.

REFERENCIAS

1. Diario Oficial de la Federación. (2005). Modificación a la Norma Oficial Mexicana NOM-025-SSA1-1993, Salud ambiental. Criterios para evaluar la calidad del aire ambiente, con respecto a material partículado. Valor de concentración máxima de material partículado para partículas suspendidas totales PST, partículas menores de 10 micrómetros PM10 y partículas menores de 2.5 micrómetros PM2.5 en el aire ambiente como medida de protección a la salud de la población.
2. Miranda, J., Barrera V.A., Espinosa A.A., Galindo O.S., and Meinguer J. (2005). PIXE analysis of atmospheric aerosols in Mexico City. X-Ray Spectrum 34, 315.
3. Wichmann-Fiebig M. (2005). Contaminación atmosférica: modelos de dispersión de contaminantes atmosféricos. Control de la contaminación ambiental. Pp
4. WHO. Health aspects of air pollution with particulate matter, ozone and nitrogen dioxide. World Health Organization, Ginebra, (2003).
5. Quijano-Parra A., (1999) Promedios geométricos de material partículado fracción respirable (PM10) y detección de metales en el aire de Bucaramanga-(Colombia). Bistua 2, 24.
6. Aldape F., Flores M.J. (2004). Source apportionment of fine airborne particulate matter collected in the Mexico City metropolitan area. International Journal of PIXE 14, 147-160.Quijano-Parra A., (1999) Promedios geométricos de material partículado fracción respirable (PM10) y detección de metales en el aire de Bucaramanga-(Colombia). Bistua 2, 24.
7. González-Lozano, M, C., Cerezo-Moreno A., González-Macías, C. y Coria-Zalazar C. (1999). Comportamiento de las partículas suspendidas y polen en la atmósfera de la región norte de la Zona Metropolitana de la Ciudad de México. Revista de la Sociedad Química de México 43, 156.
8. Aldape F. y Flores M.J. (2005). Elemental composition and source identification of $PM_{2.5}$ particles collected in downtown Mexico City. International Journal of PIXE 15, 266-269.
9. Manchado A., Velázquez H., García N., García C., Acosta L., Córdova A. y Linares M. (2007). Metales en PM10 y su dispersión en una zona de alto tráfico vehicular. Interciencia 32, 314-316.
10. González-Lozano, M.C., Cerezo-Moreno A., González-Macías, M., C. y Coria-Zalazar C. (1999). Comportamiento de las partículas suspendidas y polen en la atmósfera de la región norte de la Zona Metropolitana de la Ciudad de México. Revista de la Sociedad Química de México 43, 156.
11. Periódico Oficial Hidalgo, 2002. Ordenamiento Ecológico Territorial de la Región Tula-Tepeji. Publicado el 17 de Julio de 2002.
12. EPA, 1999: Method IO-3.1. Compendium of methods for Inorganic Air Pollutants, Office of Research and Development, United States Environmental Protection Agency, OHIO.
13. Pérez, Z.G., Hernández, P.I., Ramos A.M., Guibert G.R., Molina E.E., Martínez, M.V., Fernández A.A., Aldape U.F., Flores M.J.(2009). Use of PIXE analysis to study urban atmospheric aerosols from downtown Havana City. Nucleus, 46, 27-33.
14. Skov, H., Wahlin, P., Christensen, J., Heidam, N.Z y Petersen, D. (2006). Measurements of elements, sulphate and SO2 in Nuuk Greenland. Atmospheric Environment, 40(25), 4775-4781.
15. Vallius, M., Lanki, T., Tiittanen, P., Koistinen, K., Ruuskanen, J. y Pekkanen, J. (2003). Source apportionment of urban ambient $PM_{2.5}$ in two succesive measurement campaigns in Helsinki, Finland. Atmospheric Environment. 37:615-623.

CHAPTER 9.3 QUERCETIN AS METABOLIC MEDIATOR IN THE PHENANTHRENE PHYTOREMOVAL PROCESS BY *CYPERUS LAXUS*

G. Calva Calva *(1); N. A. Rivera Casado (1); O. Gómez Guzmán (1) and J. Pérez Vargas (2)

(1) CINVESTAV-IPN, Av. IPN 2508, Ciudad de México, México
(2) Tecnológico de Estudios Superiores de Ecatepec, Av. Tecnológico S/N, Estado de México, México

ABSTRACT

Cyperus laxus is a plant species previously stated with potential for phytoremediation owing to it produces phenolics and lipids which can chemically condense with hydrocarbons to produce hydrocarbon-phenolics and hydrocarbon-lipids conjugated molecules. In this work*, in vitro* experiments revealed that this plant species do produce particular lipidic and unknown phenolics compounds as a strategic mechanism for removal of phenanthrene (FNN). Seeds of *C laxus* were germinated at Murashige and Skoog medium added with FNN (0–280 mM). The fatty acid (FA) and the phenolic profile in extracts from the underground and aerial plant tissue were performed by GC-MS and HPLC/UV-VIS respectively. From the FA analysis, common FA compounds (C14-C24) were detected, but an unusual increment up to 200%-400% of the C16-C18 FA content was observed in plants cultivated in presence of FNN regarding to non-contaminated plants. Besides, from the phenolic profile several flavonoids were detected; however, quercetin (QTN) was identified as the main phenolic compound. Interestingly, an increment of the long chain (≥C20) and odd-chains with uncommon unsaturation FA, as well as the presence of FNN and some of its oxidation metabolites, free or conjugated with lipids or phenolics, spatially with QTN, were detected distributed through all the plant tissue and in the medium culture. In addition, observations from the plant morphology, specifically of the foliar tissue, showed that notable changes at membrane and cell wall level were produced. These results revealed that this hydrocarbon was really uptake by the plant tissue, after which the hydrocarbon is catabolized through the plant metabolic mediators (QTN) usage. The role of QTN as metabolic-mediator as a plant strategy during FNN removal, is discussed.

Keywords: *Cyperus* seedlings, fatty acids, flavonoid, Phytoremediation.

INTRODUCCIÓN

Las actividades antropogénicas y los cambios hidrológicos naturales han ocasionado la contaminación por petróleo crudo de grandes extensiones de tierra en el estado de Tabasco, México.[1] Estudios previos revelaron que en los suelos de esos sitios prevalece la presencia de hidrocarburos poliaromáticos (HPA), compuestos recalcitrantes, tóxicos y carcinogénicos debido a su bajo nivel de biodisponibilidad y

---

*Author for correspondence: gcalva@cinvestav.mx; djperezvargas@hotmail.com

biodegradabilidad [1, 2] Aunque para la recuperación de sitios similares contaminados con hidrocarburos se han reportado diversas tecnologías, una de las estrategias más recientes es la oxidación de los hidrocarburos mediante la participación de diversos compuestos orgánicos denominados mediadores (M). Estos suelen ser moléculas pequeñas capaces de acarrear electrones que después de haber sido oxidadas por agentes oxidantes naturales o por enzimas (E) son liberadas al medio ambiente para oxidar al xenobiótico (X).[3] De esta manera, el mecanismo de formación del complejo enzima-mediador-xenobiótico (EMX) o mediador - xenobiótico (MX) estará supeditado a los potenciales de óxido reducción de cada una de las fases de la reacción. Por lo anterior, nuestro grupo de investigación ha propuesto el uso de mediadores metabólicos detectados en plantas y de hongos como una alternativa más eficiente, barata y compatible con el medio ambiente durante la oxidación de HPA.[4] Ejemplo de estos mediadores pudieran considerarse las moléculas semi-oxidadas de fenilpropanoides o flavonoides que por sus características químicas pueden formar radicales libres inestables, los cuales se ha reportado que tienden a oxidar a otras moléculas para neutralizar sus cargas electrónicas radicales. [5-7]

Por otro lado, estudios previos sobre el perfil de compuestos fenólicos de una planta pionera crecida en sitios contaminados con hasta 325 000 ppm de hidrocarburos totales del petróleo (HTP) en Tabasco (*Cyperus laxus*), evidenciaron que durante el proceso de fitorremediación a nivel invernadero, la composición y cantidad de compuestos fenólicos se modificó produciendo un incremento en la cantidad de flavonoides. También se observó la presencia de compuestos resultado de conjugaciones entre HPA con fenoles en los tejidos de los órganos principales de esta planta, sugiriendo interacciones químicas y/o enzimáticas entre el xenobiótico y los metabolitos vegetales.[4] Adicionalmente, se demostró que la presencia de hidrocarburo en el suelo afecta drásticamente la composición lipídica de los órganos de *C. laxus*, promoviendo la síntesis de moléculas de ácidos grasos mayores a C20 e insaturadas, sugiriendo que la remoción de HPA en un sistema de fitorremediación también depende de los cambios en la composición de lípidos en la célula. Adicionalmente, también se reportó un incremento en las actividades enzimáticas oxidativas del peroxidasa, fenoloxidasa y catecol oxidasa en el tejido de *C. laxus*, principalmente en raíz y cormo.[4, 8]

Lo anterior sugiere que el complejo EMX pudiera están involucrado en los procesos de fitorremoción de hidrocarburos y que éste pudiera verse favorecido por los cambios en la composición lipídica de las células vegetales. Aunque el mecanismo de remoción de HPA depende de la capacidad metabólica de cada especie vegetal, no se tiene suficiente información acerca de la interacción entre los compuestos estructurales de la planta y los compuestos xenobióticos durante el proceso de fitorremoción. Por lo que el objetivo de este trabajo, fue evidenciar la presencia de moléculas antioxidantes del tipo flavonoide que pudieran estar participando en la formación de complejos EMX para promover la remoción de hidrocarburo a partir del suelo contaminado. Para ello se analizó el perfil de compuestos fenólicos de los órganos de *C. laxus* y se evaluó el cambios en la composición lipídica de los órganos de la planta. Al final se plantea la estrategia metabólica de *Cyperus laxus* para efectuar la fitorremediación de HPA cuando es crecido en sistemas *in vitro* bajo presencia de fenantreno (FNN) como HPA modelo.

MATERIALES Y MÉTODOS

Cultivos in vitro de Cyperus laxus. Se colectaron semillas de *C. laxus pI* de plantas crecidas en invernadero. Previa desinfestación (etanol 70%- NaHClO 5%) las semillas se dejaron en agua desionizada durante 12h. Las semillas desinfestadas se colocaron en medio MS semisólido (4.3g/L de MS basal, 30 g/L de sacarosa, 1 g/L de vitaminas y 1.8 g/L de Gelrite).

Adición y cuantificación de FNN. Se preparó y esterilizó por filtración una solución stock de fenantreno en acetona. Se incorporó en caliente a 25 mL de medio MS previamente esterilizado obteniendo concentraciones finales de 0, 5, 15, 30 y 50 g/L (0, 28, 84, 168, 280 mM). El FNN residual se obtuvo mediante extracciones con acetato de etilo/agua (1:1). La concentración de FNN se cuantificó por HPLC en una columna PRODIGY ODS2.

Transesterificación directa de compuestos lipídicos en tejido vegetal. A partir de tejido de raíz (R), cormo (C) y Hoja (H) de *C. laxus* se realizó la transesterificación directa.[9] La identificación y cuantificación de ácidos grasos se llevó a cabo por CG y GC/MS mediante la comparación con los tiempos de retención con el estándar SUPELCO 37 FAME MIX.

Extracción primaria de metabolitos. A partir de la materia vegetal tanto de invernadero como in vitro previamente molida en presencia de nitrógeno líquido y se pesó una muestra y se realizó una primera extracción con metanol:cloroformo (1:1) para obtener la fracción acuosa y la fracción orgánica. Para ello fue necesaria la adición de agua desionizada hasta observar la separación de fases.

Extracción de compuestos fenólicos. A partir de la fracción metanólica de la extracción primaria de metabolitos se tomaron 200 µL para su inyección en HPLC utilizando una columna PRODIGY ODS2 fase reversa (C18, 25 cm x 4.6 mm; 5µm; HPLC UV-visible Thermo Separation). La elución se desarrolló utilizando como solvente A ácido trifluoroacético (TFA) 50µM y como solvente B acetonitrilo HPLC. Los tiempos de retención de algunos flavonoides que se usaron como referencia son: QTN, 34.1 min; QTRN, 23.4 min; CRY, 38.95 min; MAY, 23.06 min; LUT, 32.9 min; RUT, 16.58 min.

Reacciones enzimáticas in vitro para la formación del complejo EMX. Los reacciones se realizaron en viales de vidrio de 1.5 mL con 500µL de mezcla de reacción (0.1M de Buffer de Potasio pH 6.0, 1% acetonitrilo grado HPLC, 350µM de SDS 1%, 50 µM de FNN, 300µM de QTN 0.000187 U/ µL de peroxidasa de rábano). La concentración de H_2O_2 varío de 0 - 30000 µM dependiendo del experimento. Las condiciones de incubación fueron a 37°C/180rpm.

Extracción de metabolitos de las reacciones enzimáticas in vitro. Se realizaron 3 extracciones con 750 µL de cloroformo. Se juntaron las fases orgánicas y se llevaron a sequedad a 40°C. Para su inyección en HPLC se resuspendieron en 1 mL de

dimetilformamida:acetona (1:1). Mientras que para la inyección de la fase acuosa (≈400 µL) se le adicionó 100 µL de metanol.

Identificación y cuantificación parcial de metabolitos en las reacciones enzimáticas in vitro. Se utilizó una columna PRODIGY ODS2 fase reversa (C18, 25 cm x 4.6 mm; 5µm; HPLC UV-visible Thermo Separation). La elución se desarrolla utilizando como solvente A acetonitrilo HPLC y como solvente B TFA 1mM con el siguiente gradiente: de 0-4 min 0%B; de 4-5 min 35%; de 5-8 min 35%B; de 9-13 min 20%B y de 15-18 min 80%B. El análisis se lleva a cabo utilizando el software PC1000/HPLC y Chromeleon 7.

RESULTADOS Y DISCUSIÓN

Perfil de compuestos fenólicos en tejido de C. laxus crecido in vitro. En el caso de la plantas en los control sin FNN (R0 y H0), el perfil de compuestos fenólicos de raíz-cormo y hoja evidenció la presencia de metabolitos como ácidos benzoicos del tipo hidroxi-metoxi; flavonoides principalmente quercetina (QTN) y quercetrina (QTRN) y compuestos con estructuras parecidas a los HPA como el acenaftileno (ACNFTY) (**Figura 1**), aunque estos últimos en un porcentaje muy bajo, por lo que su presencia pudiera estar relacionada con substancias naturales como los reguladores de crecimiento vegetal o metabolitos secundarios propios de las plantas.

Como puede verse, la diferencia entre el perfil de fenoles en las plantas crecidas en ausencia de fenantreno fue principalmente el tipo de ácido benzoico presente: mientras en los órganos subterráneos (R) dominó el alcohol vainillínico (HMBOH), en el follaje (H) dominó el ácido vainillínico y el ácido protocatecóico. Sin embargo, en los órganos de las plantas crecidas en presencia de FNN, tanto en R como en H, fue notable la presencia de fenoles del grupo de los flavonoides, como la QTRN y QTN; los cuales por análisis espectral UV produjeron una correlación del 74-92% con compuestos de referencia. Como se observa, la presencia del hidrocarburo afectó substancialmente el perfil de compuestos fenólicos. Por ejemplo, en H de las plantas control (FNN =0) se detectaron cantidades pequeñas compuestos que son presuntamente conjugados naftaleno-ácido protocatecóico (NAF-PTC) y Fluoranteno-Alcohol vainillínico (FLT-HMBOH); sin embargo, en H de las plantas crecidas en presencia de FNN se detectó una variedad de compuestos conjugados mucho mayor y a concentraciones mayores. Entre estos posibles conjugados figuran: NAF-DMBA, FNN-pHBA, i123P-ConOH, ACNFTY-VN, FL-QTN, FLT-SLA, ACNF-DMBA, NAF-ConOH. Estos resultados indican que la presencia de FNN promueve la síntesis de QTN y QTRN tanto en H como R, favoreciendo la formación de conjugados entre estos flavonoides con el hidrocarburo. Por consiguiente, soportan la hipótesis de que la formación de este tipo de reacciones de conjugación entre los metabolitos de origen vegetal y los hidrocarburos poliaromáticos es un mecanismo que pudiera estar involucrado en los procesos metabólicos de remoción de este tipo de xenobióticos por *Cyperus laxus*.

Perfil de ácidos grasos en órganos de C. laxus cultivados in vitro en presencia de FNN. La presencia de FNN también afectó la cantidad y tipo de ácido graso presente en los órganos principales de la planta indicando cambios importantes a nivel de

metabolismo primario de los lípidos (**Figura 2**). En todos los órganos (raíz, cormo y hoja) de las plantas en presencia de FNN se observó un incremento en la cantidad de ácidos grasos de C14- C24, tanto saturados como insaturados y con hasta tres insaturaciones con respecto a las plantas sin FNN (barras C0 en **Figura 2**). En raíz, la presencia de FNN no afectó el contenido de la mayoría de los ácidos grasos comunes (AGC) C16:0, C18:0, C18:1, C18:2; sin embargo se observó un incremento notorio de C18:3n3 en los tratamientos con 15 y 50 g de FNN/L. En hoja, el FNN produjo un efecto similar al de raíz, sin embargo se observó un decremento en el contenido de C18:1 con respecto al tratamiento sin FNN. En contraste con lo observado en raíz y hoja, en cormo fue notable la disminución en la cantidad de AGC específicos (C14-C18), aunque como en los otros órganos, en presencia de FNN se observó la aparición de ácidos grasos de cadenas mayores a C20 no observados en ausencia de FNN. Este efecto fue notorio principalmente para cormo y hoja, mientras que para raíz fue notorio sólo para los ácidos C20:3n3 y C24:0. En resumen, se observaron incrementos considerables en la cantidad de ácidos grasos en tejido de raíz y hoja (**Tabla 1**), con un aumento considerable en el contenido de ácidos grasos de C20-C24 en todos los órganos de la planta (**Figura 2**). Estos resultados en combinación con lo reportado previamente para plantas de *Cyperus laxus* crecidas en sistemas de fitorremediación a nivel de invernadero,[8] sugieren que bajo la presencia de HPA, *C. laxus* es capaz de dirigir los flujos metabólicos hacía la producción ácidos grasos que podrían ser parte de estructuras celulares que tiene por objeto el salvaguardar la integridad vegetal, como es la membrana, la cutina, la suberina y las ceras, produciendo así cambios a nivel bioquímico y fisiológico de la planta. Estos cambios metabólicos, según los principios de ingeniería metabólica, podrían estar autorregulados a través de nódulos metabólicos flexibles o puntos de bifurcación involucrados en la compleja arquitectura bioquímica de la planta.[10]

TR(min)	R0	R15	R30	R50	HC	H 15	H30	H50
2.6	QTN 80	QTN 90		QTN 92		QTN 93	QTN 89	QTN 36
3.4	QTRN 79		QTN 81	QTRN 78	QTRN 78	QTRN 78	QTRN 79	QTRN 79
4.6			LUT 74	FL/QTRN 83/82				
5.1						QTN 84		
6.0						NAF/DMBA 86/87		NAF/VA 82/88
7.6	[illegible]			[illegible]	[illegible]		NAF/DMBA 89/83	NAF/DMBA 89/82
13.2	QTN 78						CRY 77	
14.3					QTN 89		QTN 82	
14.9	FLT/ConOH 70/89							
16.7								
17.1								
19.7					ANT/FNN 61/51			
21.7								
23.5							FL/QTN 80/80	
24.6							ACNFTY/VA 55/55	
31.9							I123P/PTC 78/87	
33.5	CRY 79							
34.7	FLT/ACNFTY 65/60					QTRN 84		
35.9				QTRN 75			FNN/PHBA 94/73	I123P/PTC 77/79
36.1								LUT/QTRN 80/77
38.3				CRY 92			ACNF/ACNFTY 73/64	
40.4	QTN 73	RUT/QTN 77/81	RUT/QTN 75/78					
40.8		FL/QTN 83/75						
41.3		ANT/FNN 73/74						
42.5	ACNFTY/NAF 77/34							
45.9	NAF/DMBA 72							
48.8		ACNFTY/VA 63/61	ACNF/ACNFTY 57/38					
49.4	ACNF/ACNFTY 60/45	ACNFT/VA 62/56	ACNF/ACNFTY 65/44	I123P/PTC 50				
50.2		FNN 99	FNN 99	FNN 99		FNN 99		
51.4		ANT/FNN 87/61		ANT/ pHBA 90/14	FLT/VN 66/81			
52.6						FLT/VN 65/80		QTN 69
53.7		ACNFTY/VA 64/64						
55.1				FLT/VN 65/79				
56.4			QTN 67					
59.9	QTN 74							
60.3	QTN 67							
61.5	QTN 59							
69.2	BaA/Phtoz 62/81							
71.7								

FIGURA 1. Perfil de compuestos fenólicos en la parte subterránea (R = raíz-cormo) y aéreo follaje (H) de C. laxus crecidas in vitro en medio MS adicionado con 0-50 g FNN/L. Se expresa el o los compuestos identificados al tiempo de retención correspondiente (TR). El número al interior de cada cuadro indica el % de correlación espectral UV respecto a los estándares. NAF = naftaleno; FL=fluoreno; FLT=fluoranteno, ACNFTY= acenaftileno, ANT=antraceno; FNN=fenantreno, i123P=indeno-1,2,3-perileno; BaA=venzo(a)antraceno; QTN=quercetina; QTRN= quercetrina, LUT=luteína; CRY=crisina, DMBA=ácido dimetoxibenzóico; pHBA= ácido p-hidroxibenzóico; PTC=ácido protocatecoico; ConOH=alcohol coniferílico; VA= ácido vainillínico; VN=vainillín amina

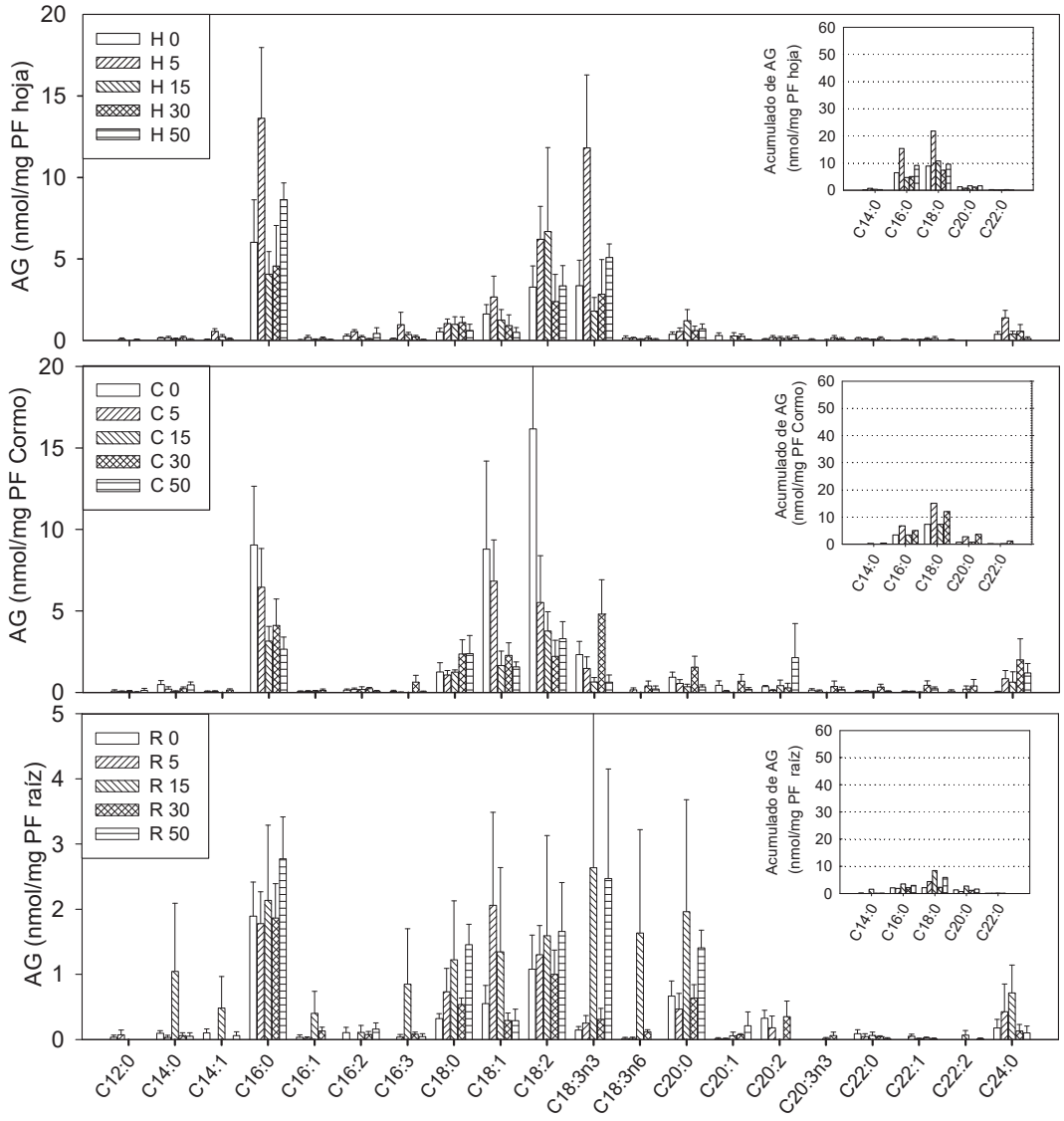


FIGURA 2. Perfil de ácidos grasos en raíz, Cormo y hoja de Cyperus laxus cultivado in vitro en medio MS adicionado con 0-50 g/L de FNN

Sobrevivencia y fenología de C. laxus en presencia de FNN. Por otro lado, la sobrevivencia de las plantas y su contenido de clorofila también se vieron afectados por la presencia de FNN. Después de 7, 14 y 21 días de cultivo con 30 g/L y 50 g/L, de 15 g/L, y de 5 g/L de FNN exógeno respectivamente, se observó claramente el proceso de clorosis por el amarillamiento del tejido foliar causado por la falta de clorofila en las hojas. *C. laxus* tampoco presentó cambios fenológicos antes de 21 días de tratamiento a concentraciones de FNN hasta mil veces superiores a las reportadas como tóxicas para *Arabidopsis*. Esto sugiere que esta *Cyperaceae* posee características metabólicas específicas que le permite sobrevivir a la presencia de FNN; lo que pudiera estar relacionado con la cantidad de FNN y la parte de la planta donde es llevado y procesado el xenobiótico. En este estudio se observó mayor acumulación de FNN en raíz respecto a los demás órganos (**Tabla 1**), y en general, aunque los valores de

contenido del hidrocarburo en los tejidos mostraron una relación un poco errática respecto a la cantidad de FNN exógeno, el contenido se incrementó en los diferentes órganos al aumentar la cantidad de hidrocarburo exógeno. Así, los datos más elevados de acumulación y de remoción se obtuvieron en los tratamientos con 30 g de FNN exógeno/L de medio de cultivo.

TABLA 1. Fenantreno residual, contenido de ácidos grasos (mg/g FW) y contenido de FNN (g/Kg) en los órganos de plantas *Cyperus* después de 21 días de cultivo

FNN (g/L)	FA/FNN en Tejido	**RAIZ**	**CORMO**	**HOJA**
Adicionado (0)	Sat/Insat	1.31	0.44	0.81
Removido (0)	In (%)	43.25	69.29	55.32
	Total (mg/g FW)	**1.71±0.11**	**11.55±1.04**	**4.82±0.37**
	FNN (g/Kg)	n.d	n.d	n.d
Adicionado (5)	Sat/Insat	0.52	0.54	0.71
Removido (1.65)	In (%)	65.96	64.93	58.58
	Total (mg/g FW)	**4.61±0.36**	**8.35±0.54**	**11.67±0.93**
	FNN (g/Kg)	1.00 ± 0.81	0.54 ± 0.53	0.60 ± 0.17
Adicionado (15)	Sat/Insat	0.61	0.82	0.55
Removido (6)	In (%)	62.12	54.82	64.68
	Total (mg/g FW)	**5.35±0.24**	**3.59±0.26**	**6.38±0.43**
	FNN (g/ Kg)	3.14 ± 1.85	0.39 ± 0.36	0.39 ± 0.29
Adicionado (30)	Sat/Insat	0.06	0.70	0.28
Removido (20.9)	In (%)	94.14	58.95	77.83
	Total (mg/g FW)	**17.66±3.07**	**7.32±0.34**	**11.17±1.17**
	FNN (g/ Kg)	5.20 ± 2.93	0.75 ± 0.02	0.75 ± 0.07
Adicionado (50)	Sat/Insat	0.33	0.32	0.74
Removido (5.2)	In (%)	75.03	75.85	57.42
	Total (mg/g FW)	**6.83±0.75**	**12.90±0.88**	**7.74±0.55**
	FNN (g/ Kg)	4.30 ± 1.02	0.87 ± 0.77	1.34 ± 0.05

Transformación enzimática de FNN: investigación de la formación de complejos Enzima-Mediador-Xenobiótico (EMX). Como parte del mecanismo de remoción de FNN por *Cyperus*, en esta sección se evaluó la participación del flavonoide QTN en el proceso de oxidación del FNN en sistemas de reacciones enzimáticas *in vitro*. Como enzima modelo se utilizó una peroxidasa debido a que existen reportes donde se sabe que ésta enzima está presente en todos los órganos de las plantas y que previamente se encontró que en *C. laxus* incrementa su actividad cuando se cultiva en presencia de hidrocarburos recalcitrantes del petróleo.[4] Debe mencionarse que en esos estudios se estableció que para la oxidación de HPA la concentración de H_2O_2 (H) fue un parámetro fundamental para la actividad de la enzima, lo cual se estableció en base a reportes sobre la concentración natural de H_2O_2 en tejido vegetal, que corresponde a de 0.6 a 10 µmol/g de peso fresco de tejido. [11] Durante los estudios para evaluar la cinética de oxidación de FNN en presencia de QTN, se observó una remoción de FNN de hasta el 50% en 24h de reacción a una velocidad de desaparición durante las primeras 5h de 0.047 µM de FNN/min. Interesantemente, el comportamiento de la curva de remoción de FNN después de 6.7 horas fue similar en presencia (POX +) y ausencia (POX-) de enzima. Después de 24h de reacción la cantidad remanente de QTN fue estimada en un 41%, siendo éste el primer reporte donde se evaluó la variación de la concentración de un mediador en sistemas enzimático de oxidación de xenobióticos mediante la formación del complejo EMX.

Dado que los resultados de arriba sugieren que el H_2O_2 podría haber llegado a concentraciones limitantes para la reacción, se decidió evaluar el efecto de los niveles de este compuesto sobre velocidad de la reacción (**Tabla 2**). Los resultados mostraron que a concentraciones de hasta 3 mM de H_2O_2, o en el intervalo de 0.1-10 de la elación H_2O_2/QTN, se obtuvo la mejor velocidad remoción. El cambio en la velocidad de transformación del FNN en función de la concentración de H_2O_2 muestra que la presencia de H_2O_2 por debajo de 3 mM, afecta positivamente la transformación de FNN llegando a valores de velocidad de desaparición de 0.02 µM FNN/min. Interesantemente, en ausencia de enzima (E^-) la velocidad de desaparición de FNN a concentraciones bajas de peróxido muestra valores similares a los máximos alcanzados en la mezcla de reacción completa y disminuye gradualmente con el aumento de H_2O_2; sin embargo, en ausencia del mediador QTN (M^-), la velocidad se incrementó o se mantuvo casi constante a concentraciones de H_2O_2 menores a 30 mM. Este comportamiento sugiere que en presencia de cantidades pequeñas de peróxido (menores a 3 µM de H_2O_2, o una relación H_2O_2/QTN < 0.01), la QTN podría estarse oxidando parcialmente a formas químicas capaces de promover la oxidación de FNN sin la participación de la enzima. Esto implicaría que en la mezcla completa (EMXH) la E podría utilizar el peróxido preferentemente para oxidar QTN, pero en ausencia de QTN la enzima puede dirige su actividad oxidativa hacia el FNN. En resumen, estos resultados sugieren que para la transformación de FNN en presencia de un mediador metabólico como la QTN, no es necesaria la participación de la enzima, ya que tan solo la presencia del peróxido de hidrógeno (H) puede promover la oxidación del mediador y éste a su vez la oxidación del hidrocarburo (X). En otras palabras, en el sistema experimental utilizado la transformación del FNN depende de la presencia del mediador (quercetina) o de la enzima, no de los dos. Así, en congruencia con lo sugerido en la literatura para otros sistemas, se sugiere que el H_2O_2 puede actuar como sustrato para

la enzima o como generador de radicales libres de quercetina mediante la interacción con las especies reactivas de oxígeno.[12, 13]

De lo anterior se puede proponer que la transformación química del FNN en ausencia de enzimas se puede llevar a cabo de acuerdo a la reacción (1).

$$2QTN + H_2O_2 \overset{k1}{\rightarrow} 2QTN_{rad} + FNN \overset{k2}{\rightarrow} (FNN - QTN) \overset{k3}{\rightarrow} FNN_{ox} + QTN_{ox} \quad (1)$$

donde:

si k1 ≤ k2 no será posible detectar el radical de QTN y,
si k1 > k2 sí se podrá detectar QTNrad

Por lo que la velocidad de oxidación de FNN (k3) estará regulada por la oxidación de QTN y generación de radicales (k1). En este punto, la oxidación de QTN también podría llevarse a cabo por las especies reactivas de oxígeno: radical hidroxilo ($HO^{\cdot}$) y radical superóxido ($O_2^{\cdot-}$). [14]

TABLA 2. Velocidad de desaparición del FNN en función de la concentración de H_2O_2 (0-720min de reacción)

[H2O2]	[H2O2 / QTN]	V [µMFNN/min]			
µM		EMXH	E-MXH	EMXH	E-MXH
3	0.01	-0.011	-0.022	-0.016	-0.018
30	0.1	-0.025	-0.021	-0.017	-0.014
300	1	-0.016	-0.016	-0.033	-0.002
3000	10	-0.022	-0.009	-0.023	-0.013
30000	100	-0.012	-0.014	-0.013	-0.016

Este razonamiento se ve reflejado en los resultados mediante el análisis estequiométrico de la reacción: para 300µM de QTN y 30µM de H_2O_2 se obtendría el 100% de transformación de FNN con la oxidación de la QTN total. Sin embargo, dado la cantidad residual de QTN libre, se sugiere que el peróxido no actúa directamente sobre el mediador, lo que disminuye la producción de QTNrad y por lo tanto la oxidación de FNN. Mientras que la oxidación del resto de QTN se pudo haber llevado a cabo por la presencia de moléculas QTNrad, que promueven la generación QTNox mediante la acción de otra molécula QTNrad. Es importante considerar que de acuerdo a algunos autores, [15, 16] k2 será variable y que dependerá del tipo de radical libre formado y de la rapidez de formación de moléculas estables del mediador (quercetina-quinona).

CONCLUSION

Como respuesta a la presencia de fenantreno en el medio de cultivo, *C. laxus* es capaz de sintetizar moléculas antioxidantes como QTN, además de presentar modificaciones en la cantidad y composición de compuestos lipídicos. De acuerdo al proceso de detoxificación de HPA por células vegetales propuesto por [17], se ha establecido como primer paso una serie de reacciones de óxido-reducción del xenobiótico (fase I) para posteriormente poder ser incorporadas a la célula vegetal y conjugarse con metabolitos vegetales intracelulares (fase II). Es justamente durante la Fase I donde la participación de los complejos EMXH y MXH pudieran estar favoreciendo la oxidación del hidrocarburo y por lo tanto disminuyendo su hidrofobicidad. Por lo anterior, los resultados de este trabajo sugieren que la síntesis de ácidos grasos de cadenas >C20 en los órganos vegetales involucradas en la síntesis de estructuras celulares como ceras, cutina y suberina pudieran favorecer la adsorción del FNN. De esta manera, una vez que el FNN se ha acercado a la célula vegetal, las peroxidasas u otras enzimas oxidativas localizadas a nivel de pared, membrana o extracelulares, ejercen su actividad utilizando el H_2O_2 u alguna forma de oxígeno activa presente en el medido circundante para activar oxidativamente a los fenoles o flavonoides del tipo QTN sintetizados como resultado del estrés por la presencia del hidrocarburo. Esto debería generar la formación de radicales libres capaces de iniciar la oxidación del FNN u otros HPA. Alternativamente, los fenoles o flavonoides podrían ser oxidados directamente por el H_2O_2 o alguna forma reactiva de oxígeno para formar radicales libres que promuevan la posterior oxidación de los hidrocarburos.

ACKNOWLEDGMENTS

This work was supported by the Consejo Nacional de Ciencia y Tecnología (CONACyT Mexico: 211085-5-29307B). The first author, Noemí Araceli Rivera Casado, acknowledges a doctoral fellowship from CONACyT.

REFERENCES

1. Palma Cruz, F., F.J. Esparza Garcia, J.J. Peña Cabriales, R. Ferrera Cerrato,H. Poggi Varaldo. Changes in the number of plant species in sites from Tabasco, México, chronically polluted with oil. in The First International Meeting on Environmental Biotechnology and Engineering. CINVESTAV IPN; 2004:
2. Semple, K.T., K.J. Doick, K.C. Jones, P. Burauel, A. Craven, *et al.*, Defining Bioavailability and Bioaccessibility of Contaminated Soil and Sediments is complicated. Environ. Sci. Technol. 2004; 38: 228A-231A.
3. Baiocco, P., A.M. Barreca, M. Fabbrini, C. Galli,P. Gentili, Promoting laccase activity towards non-phenolic substrates: a mechanistic investigation with some laccase-mediator systems. Organic Biomolecular Chemistry. 2003; 1: 191-197.
4. Rivera-Casado, N.A., M.C. Montes-Horcasitas, F.J. Esparza-Garcia, A. Ariza-Castolo, O. Gómez-Guzmán, *et al.*, Fitotratamiento de suelos impactados por derrames de petróleo: interacción entre hidrocarburos poliaromáticos, fenoles y enzimas oxidativas. CENIC. Ciencias Químicas. 2010; 41: 1-11.

5. Torres-Duarte, C., R. Roman, R. Tinoco,R. Vazquez-Duhalt, Halogenated pesticide transformation by a laccase-mediator system. Chemosphere. 2009; 77(5): 687-692.
6. Torres-Duarte, C., R. Roman, R. Tinoco,R. Vazquez-Duhalt, Halogenated pesticide transformation by a laccase-mediator system. Chemosphere. 2009; 77(5): 687-92.
7. Veitch, N.C., Horseradish peroxidase: a modern view of a classic enzyme. Phytochemistry. 2004; 65: 249-259.
8. Rivera Casado, N.A., M.d.C. Montes Horcasitas, R. Rodríguez Vázquez, F.J. Esparza García,A. Ariza Castolo. Changes in fatty acid composition of C. laxus in a phytotreatment system of petroleum-contaminated soil. in Second International Symposium on Bioremediation and Sustainable Environmental Technologies. Columbus OH 2013:
9. Burja, A.M., R.E. Armenta, H. Radianingtyas,C.J. Barrow, Evaluation of Fatty Acid Extraction Methods for *Thraustochytrium* sp. ONC-T18. J. Agric. Food Chem. 2007; 55: 4795-4801.
10. Stephanopoulos, G.N., A.A. Aristidou,J. Nielsen, Metabolic Engineering. Principles and Methodologies.Vol., San Diego: 1998:193-196
11. Cheeseman, J.M., Hydrogen peroxide concentrations in leaves under natural conditions. Journal of Experimental Botany. 2006; 57(10): 2435-2444.
12. Hernandez, C.E.L.R., D.S. Werberich,E. D'Elia, Electroenzymatic oxidation of polyaromatic hydrocarbons using chemical redox mediators in organic media. Electrochemistry Communications. 2008; 10(1): 108-112.
13. Yamasaki, H., Y. Sakihama,N. Ikehara, Flavonoid-Peroxidase Reaction as a Detoxification Mechanism of Plant Cells against H2O2. Plant Physiology. 1997; 115(4): 1405-1412.
14. Dhaouadi, Z., M. Nsangou, N. Garrab, E.H. Anouar, K. Marakchi*, et al.*, DFT study of the reaction of quercetin with and radicals. Journal of Molecular Structure: THEOCHEM. 2009; 904(1–3): 35-42.
15. Zhou, A.,O.A. Sadik, Comparative Analysis of Quercetin Oxidation by Electrochemical, Enzymatic, Autoxidation, and Free Radical Generation Techniques: A Mechanistic Study. Journal of Agricultural and Food Chemistry. 2008; 56(24): 12081-12091.
16. Awad, H.M., M.G. Boersma, J. Vervoort,I.M.C.M. Rietjens, Peroxidase-catalyzed formation of quercetin quinone methide-glutathione adducts. Archives of Biochemistry and Biophysics. 2000; 378(2): 224-233.
17. Coleman, J.O.D., M.M.A. Blake-Kalff,T.G.E. Davies, Detoxification of xenobiotics by plants: chemical modification and vacuolar compartmentation. Trends in Plant Science. 1997; 2: 144-151.

CHAPTER 9.4 GERMINACIÓN, CRECIMIENTO Y MORFOLOGÍA DE *Cyperus laxus* CRECIDO *IN VITRO* CON HIDROCARBUROS

G. Calva Calva *(1); N. A. Rivera Casado (1); O. Gómez Guzmán (1) and J. Pérez Vargas (2) *

(1) CINVESTAV-IPN, Av. IPN 2508, Ciudad de México, México.
(2) Tecnológico de Estudios Superiores de Ecatepec, Av. Tecnológico S/N, Estado de México, México.

RESUMEN

Cyperus laxus es una planta invasora y pionera en sitios intemperizados de la zona tropical de Tabasco, México, después de haber sido impactados derrames de petróleo crudo. Estudios previos sobre fitorremediación de los suelos de esos sitios con varias especies vegetales autóctonas de esos sitios impactados demostraron que esta especie puede eliminar grandes cantidades de hidrocarburos de petróleo (> 300.000 ppm), incluyendo hidrocarburos poliaromáticos (PAH). El efecto de los hidrocarburos sobre la germinación y la fisiología de esta especie, así como el mecanismo utilizado por esta especie para la remoción de estos compuestos, especialmente en ausencia de microorganismos, no se ha investigado. Así, el objetivo del presente trabajo fue investigar el efecto del antraceno (ANT), fenantreno (FNN) y queroseno (K) sobre la germinación, crecimiento, y cambios morfológicos de esta planta cuando se crece en condiciones asépticas en cultivos *in vitro*. El desarrollo experimental demostró que los cambios fisiológicos de las plantas fueron evidentes a los 35 días, concomitantemente con una alta velocidad de toma de hidrocarburos a partir del medio de cultivo. Los resultados revelaron que solamente el K en cantidades superiores a 3g/L afectó drásticamente la frecuencia de germinación; sin embargo, después de tres semanas en los tratamientos con FNN se observó un claro aumento en el grosor y morfología de las hojas, formando espirales con curvaturas de hasta 180°. Interesantemente, el perfil de compuestos fenólicos en hoja y raíz de plantas crecidas con fenantreno mostraron la presencia de fenantreno y varios de sus productos metabólicos. La comparación de las propiedades espectrales de esos metabolitos con los homólogos producidos por hongos filamentosos durante la degradación de este hidrocarburo sugiere que además esta planta debe absorber y translocar los hidrocarburos además de degradarlo en todos los tejidos de la de la planta.

Palabras clave: *Cyperaceae*, fenantreno, germinación, metabolitos secundarios

---

*Author for correspondence: gcalva@cinvestav.mx; djperezvargas@hotmail.com

INTRODUCCION

La fitorremediación es un conjunto de procesos biotecnológicos a base de plantas para la remoción, contención o transformación de contaminantes[1,2]. Por ejemplo, *Cyperus laxus* es una especie vegetal pionera de sitios del estado de Tabasco, intemperizados después de haber sido contaminados por derrames de petróleo crudo[3], la cual es capaz de crecer en suelos con grandes cantidades de hidrocarburos de petróleo (>300,000 ppm) y que ha demostrado tener un gran potencial en procesos de fitorremediación[4,5]**.**

Los hidrocarburos de petróleo, en especial los aromáticos y poliaromáticos, son uno de los contaminantes con mayor preocupación debido a su naturaleza carcinogénica y a que son la fuente principal de muchos problemas ambientales de este siglo. Los más utilizados como modelo para estudios de fitorremediación están el fenantreno (FNN), antraceno (ANT) y los contenidos en el queroseno (K). Estos se ha utilizado por sus características físico-químicas y potencial carcinogénico aunque el queroseno se caracteriza por ser una mezcla compleja que incluye compuestos tanto aromáticos como alifáticos[6,7].

En trabajos previos, nuestro grupo de investigación ha reportado que los metabolitos secundarios producidos por *Cyperus laxus* pueden actuar como mediadores metabólicos en el proceso de fitorremediación de suelos intemperizados de sitios de Tabasco con alto contenido de hidrocarburos después de haber sido impactados por derrames de petróleo crudo[8]. Durante esos estudios se encontró que puede haber interacciones químicas y bioquímica entre los metabolitos y enzimas de la planta con la formación de complejos metabolito-xenobiótico durante el proceso de remoción[9,5]. Sin embargo, el conocimiento sobre estas interacciones aun es escaso. Así mismo, se desconocen los mecanismos que utiliza la planta para la degradación o trasformación de estos contaminantes. En seguimiento a estos estudios en este trabajo se presentan los resultados de los cambio en la fisiología, sobrevivencia y cambio en el perfil de compuestos fenólicos, de plantas de *Cyperus laxus* crecidas en sistemas asépticos *in vitro* pero en presencia de hidrocarburos y en total ausencia de microorganismos. Se evalúa el efecto sobre el crecimiento y sobrevivencia de la planta, desde la germinación de semillas en presencia del hidrocarburo.

MATERIALES Y MÉTODOS

Material vegetal. Se usaron semillas de plantas crecidas en invernadero sobre suelo procedente de sitios intemperizados de Tabasco después de 10-50 años de haber sido impactados crónicamente por derrames de petróleo crudo y conteniendo hasta 350,000 ppm de hidrocarburos totales.

Desinfestación de semillas. Las semillas se embeben en agua por 12 horas, con la finalidad de rehidratar y eliminar material flotante. La desinfestación se realizó dentro de una campana de flujo laminar y con material en condiciones de esterilidad. Se realizaron tres lavados con agua destilada y desionizada estéril a las semillas y se sumergieron en etanol al 70% por 20 segundos. Se repitió el proceso de lavado y

después se sumergió en hipoclorito de sodio al 5% de cloro activo por 20 minutos. Se repiten los lavados y se reposan en agua desionizada estéril para su posterior uso.

Geminación. Se agregaron 20 mL de medio MS[10] en placas Petri. Para los tratamientos con hidrocarburos se adicionaron al medio aun líquido la cantidad necesaria de soluciones stock de ANT Y FNN en diclorometano para llegar a concentraciones mM de 0.01, 0.1, 0.7, 1, 3, 5 y 10, con los respectivos controles que incluyen sólo solvente (0 mM) y las de K las concentraciones fueron g/L. Sobre el medio gelificado se colocan las semillas desinfestadas y se sella la caja para su cultivo en oscuridad por 7 días. Posteriormente se exponen a la luz para que continúe el crecimiento de las plántulas generadas por la germinación. En este tiempo se estima la frecuencia de germinación y se sigue monitoreando este factor por 35 días. El valor de la frecuencia de germinación se obtuvo contando las semillas germinadas y las semillas totales a los 7 días. La sobrevivencia se evalúo hasta los 50 días dejando a la planta en contacto con el hidrocarburo.

***Extracción y análisis de compuestos fenólicos*.** Se realizó a partir del método reportado por Martínez-Juárez *et al*[11] con las plántulas de cada semana de todas las concentraciones para los 3 hidrocarburos. Se separó raíz-bulbo y hoja (**Figura 1**) y se determinó peso fresco para posteriormente triturarlas por separado y con N_2 líquido. Se realizó la extracción con cloroformo: metanol (1:1) por triplicado. La fase metanólica acuosa se evaporó con una corriente de N_2 gaseoso y resuspendió en metanol-agua (1:1). La fase de cloroformo se evaporó y se resuspendió en hexano-etanol (1:1). El análisis de los fenoles de cada fracción se realizó por HPLC-UV.

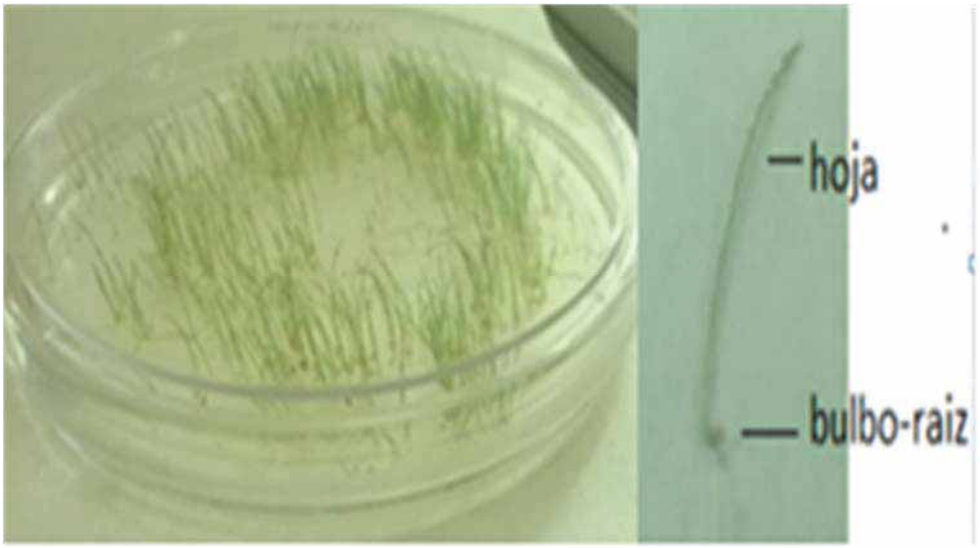


FIGURA 1. Semillas germinadas de *Cyperus laxus* y sus órganos fundamentales

RESULTADOS Y DISCUSIÓN

Efecto de la concentración de hidrocarburos sobre la germinación de semillas. Se determinó el efecto fitotóxico de los hidrocarburos sobre la germinación de semillas de *Cyperus laxus*. El proceso de germinación se consideró completo cuando la cubierta de la semilla se rompe completamente y emerge la radícula y el cotiledón (**Figura 2**) según lo reportado por Amadi *et al*[12] (1993) y por Maila & Cloete[13]. Tanto en ausencia como en presencia de hidrocarburos la germinación se observó claramente después 7 días de incubación en oscuridad (**Figura 2**).

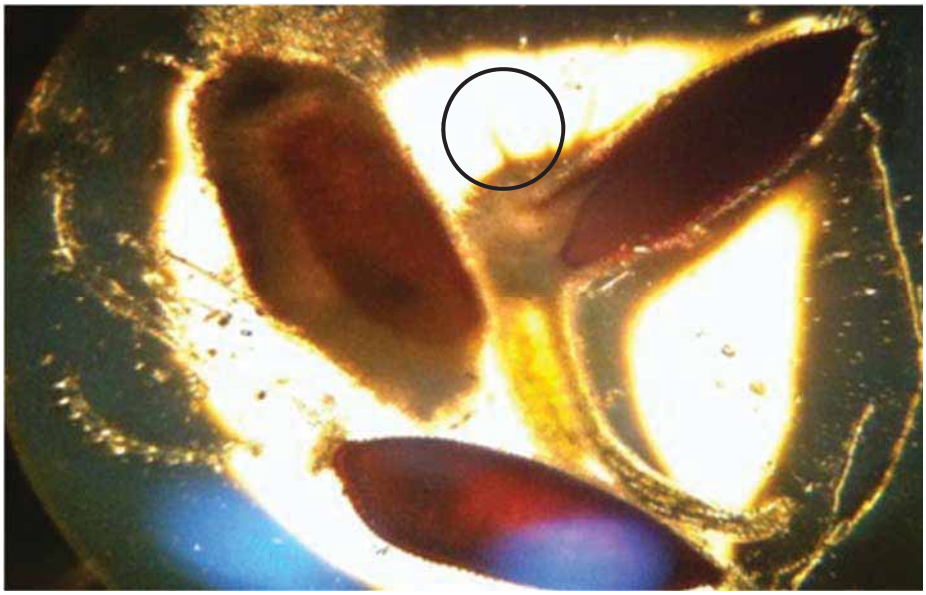


FIGURA 2. Microfotografía (40X) de semillas de C*yperus laxus* germinadas después de 7 días de incubación en oscuridad

El fenantreno y antraceno afectaron poco la frecuencia de germinación a las concentraciones utilizadas, sin embargo en presencia de queroseno la germinación fue inhibida a partir de los 3 g/l (**Figura 3**). La diferencia del K con los otros hidrocarburos utilizados, es la presencia en K de compuestos alifáticos lineales presentes en el K, lo que sugiere que estos son los que podrían estar promoviendo la inhibición de la germinación en presencia de esta mezcla de hidrocarburos. Este efecto probablemente se deba a que los compuestos alifáticos penetren más fácilmente la semilla impidiendo y/o reduciendo el intercambio de agua y nutrientes en el medio necesarios para la germinación. Estos resultados concuerdan con reportes que sugieren que debido a que la mayoría de los xenobióticos son lipofílicos y pueden ser absorbidos y/o acumulados a niveles tóxicos por tejidos vegetales de especies que llevan a cabo mecanismos de detoxificación a través de dos procesos secuenciales: transformación química y compartamentalización[12]. Al respecto, en ese estudio se propone que la inhibición de la germinación está relacionada con las propiedades hidrofóbicas de los hidrocarburos, así mismo aunque el medio sea rico en nutrientes, será imposible para la semilla tomarlos y poder finalizar el proceso de la germinación.

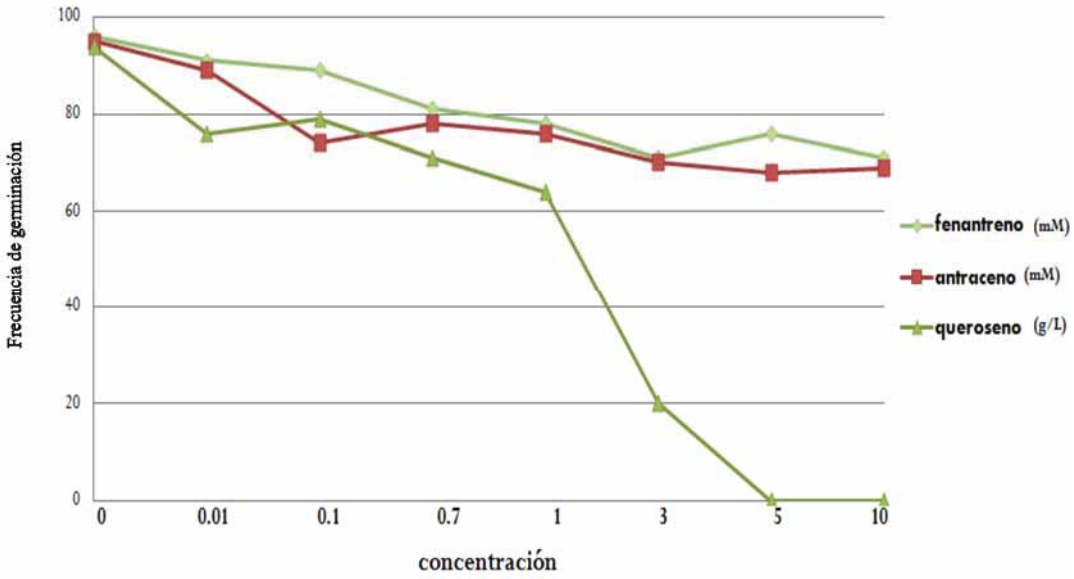


FIGURA 3. Efecto de la concentración de hidrocarburos (mM para antraceno y fenantreno y g/L para queroseno)) sobre la frecuencia de germinación de semillas de *C. laxus*

Efecto de la concentración de hidrocarburos sobre el crecimiento de C. laxus. La influencia del tipo y concentración de hidrocarburos sobre el crecimiento y morfología de las plantas se determinó evaluando los cambios en tamaño y geotropismo de las partes aéreas y sumergidas por 35 días de cultivo *in vitro* (**Figura 4**). En ausencia de hidrocarburos y después de dos semanas, las plantas mostraron la orientación de crecimiento geotrópico común, es decir las partes aéreas eran erguidas con orientación ageotrópica y las raíces sumergidas con orientación geotrópica (**Figura 4A**). Sin embargo, en presencia de hidrocarburos se observaron cambios morfológicos importantes, especialmente con FNN, donde las partes aéreas cambiaron su geotropismo a un crecimiento ageotrópico paralelo al medio de cultivo (**Figura 4B**). Además, a partir de 0.7 mM de FNN y después de 21 días de cultivo, se detectó un claro incremento en el espesor de las hojas acompañado de la formación de una singular curvatura acairelada de hasta 180°, en ocasiones resultando en la presencia de hojas en forma de espirales (**Figura 4C**). Debe enfatizarse que este cambio morfológico respecto al geotropismo y espesor de las hojas se acentuó después de la tercera semana, pero el cambio en la dirección de crecimiento geotrópico a un crecimiento paralelo al medio de cultivo se detectó poco después de la germinación. Interesantemente, los tratamientos con ANT no causaron cambios apreciables en el espesor y forma de las hojas en comparación con el control, pero el crecimiento de las plantas también fue ageotrópico paralelo al medio de cultivo similar al observado con FNN (**Figura 4B**). En contraste, el K no promovió cambios ni la morfología de las hojas ni en la orientación en el crecimiento, mostrando plantas con características similares a las del control (**Figura 4A**). Estos resultados con K pueden ser debidos a que esta mezcla contiene principalmente hidrocarburos alifáticos (>80%) y sólo una pequeña cantidad de aromáticos (<20%), por lo que el contenido de FNN u otros HPA en los tratamientos de este experimento probablemente no fue suficiente para ejercer un efecto significativo sobre la fisiología, anatomía y morfología de las plantas.



FIGURA 4. *Cyperus laxus* después de 21 días de cultivo en ausencia de hidrocarburos (A) y en presencia de 0.7 mM de FNN (B, C). Obsérvese el típico crecimiento geotrópico en A y la formación de hojas espirales en B y C

Efecto de los hidrocarburos sobre el perfil de compuestos fenólicos. El perfil de compuestos fenólicos contenidos en los extractos metanólicos-acuosos de hoja y bulbo-raíz de plantas crecidas en ausencia de hidrocarburos mostró la presencia de diversos fenilpropanoides y flavonoides libres (**Figura 5A**). En presencia de 0.7 mM de FNN, además de estos compuestos en forma libre también se observaron conjugados (picos a y b en la **Figura 5A**), que por su menor tiempo de retención y conservación del espectro UV del FNN (pico e) fueron putativamente identificados como conjugados del FNN con el ácido benzoico (FNN-dimetoxibenzoato, pico a) y con el p-hidroxibenzoico (FNN-p-hidroxibenzoato, pico b). Interesantemente, en la fase orgánica (cloroformo) de estos extractos (**Figura 5B**) se observaron señales claras de FNN libre (picos e), lo que sugiere que el sistema vegetal tomó y trasladó el hidrocarburo hacia los órganos fundamentales. Así mismo se detectó la presencia de dos compuestos espectralmente parecidos a metabolitos que han sido reportados para la degradación del FNN por hongos filamentosos (Sutherland et al., 1991), lo que sugiere que *Cyperus* podría estar siguiendo alguna ruta de degradación de FNN similar a la de esos hongos filamentosos.

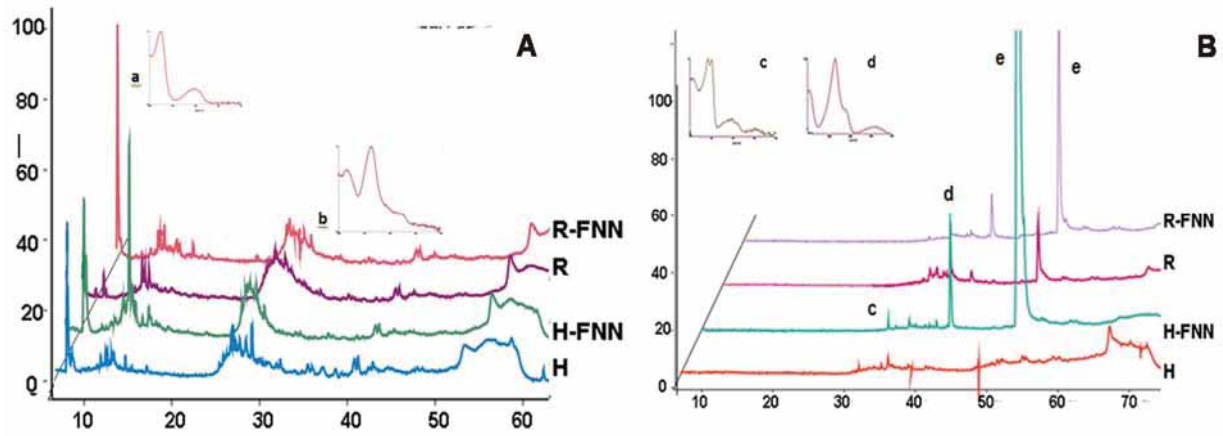


FIGURA 5. Perfil de compuestos contenidos en la fase metanólica (220nm) (A) y de cloroformo (250) (B) de extractos de hoja (H) y bulbo-raíz (R) de plantas de *Cyperus laxus* crecidas en 0.7 mM de FNN

Efecto de los hidrocarburos sobre la sobrevivencia de Cyperus laxus. Al evaluar sensorialmente la sobrevivencia a través de la presencia de clorofila se observó que después de 35-40 días las plantas se iban tornando cloróticas y después de 50 días de cultivo las hojas de las plantas en todos tratamientos habían perdido completamente el color verde característico de la presencia de clorofila (**Figura 6**).



FIGURA 6. Hojas cloróticas después de 50 días.

Remoción de hidrocarburos. Finalmente, la remoción de FNN en el tratamiento con 0.7 mM, donde se detectó la presencia de sus metabolitos y conjugados, fue del 80% (0.56 mM) mientras que para el tiramiento con 10 mM fue del 70% (0.7 mM). La disminución en la tasa de remoción puede ser debida a que a 10 mM el FNN afectó más severamente la germinación (**Figura 3**), morfología (**Figura 4**) y el crecimiento de las plantas; sin embargo, también pudo ser debido a la cantidad de semillas germinadas en cada placa.

CONCLUSION

Considerando las características toxicológicas de FNN, ANT y K, compuestos altamente recalcitrantes que por años han sido un gran problema de contaminación, *Cyperus laxus* demostró tener la capacidad de resistir altas concentraciones de estos hidrocarburos cuando se cultiva asépticamente *in vitro* en comparación con otras especies vegetales. De estos compuestos, la presencia de FNN afectó severamente la morfología a nivel de hoja y probablemente la fisiología de este y otros órganos. Sólo el queroseno afectó severamente la germinación. El perfil de compuestos fenólicos fue dependiente del hidrocarburo y de su concentración, similar a las observaciones previas de que la cantidad y tipo de hidrocarburo afectan no solo el metabolismo de esta planta a nivel fisiológico, sino también la biosíntesis y perfil de fenoles que pueden actuar como intermediarios metabólicos en el proceso de fitorremoción. En los órganos de plantas crecidas con FNN, se detectó la presencia de fenoles conjugados con hidrocarburos y los hidrocarburos libres así como metabolitos putativamente productos de la degradación de este hidrocarburo, lo que soporta la hipótesis de que esta planta es capaz de tomar este compuesto del medio de cultivo y trasladarlo a los órganos de la planta. Un efecto a largo plazo de la presencia de los hidrocarburos fue la perdida de la clorofila.

AGRADECIMIENTOS

El primer autor agradece al laboratorio de Ingeniería metabólica del departamento de biotecnología y bioingeniería de CINVESTAV por el apoyo constante para realizar este trabajo.

REFERENCIAS

1. Salt, D.E., Smith, R.D., Raskin, I., Phytoremediation. Ann. Rev. Plant Physiol. Plant Mol. Biol. 1998. 49, 643–668.
2. Gunther, T., Kirsche, B., Fritsche, W. Potential of plant–microbe-interactions for in situ bioremediation of hydrocarbon- contaminated soils. In: Wise, D.L., Trantolo, D.J., Cichon, E.J., Inyang, H.I., Stottmeister, U. (Eds.), Bioremediation of Contaminated Soils. Marcel Dekker, USA, 2000. pp. 285–293.
3. Palma Cruz Felipe J., Esparza García Fernando, Poggi Varaldo Héctor M., Rodríguez Vázquez Refugio, Peña Cabriales José J., Ferrera Cerrato Ronald, Pérez Vargas Josefina, Calva Calva Graciano Changes in the number of plant species in sites from Tabasco, México, chronically polluted with oil. The first International meeting on environmental biotechnology and engineering. Institut de Recherche Pour le Developpement/CINVESTAV Eds. Sept., 6-8.. México D. F., México. 2004. CD, Paper IMEBE 152.
4. Rivera C. Relación entre el perfil de compuestos fenólicos e hidrocarburos poliaromáticos con la actividad de enzimas oxidativas de la rizósfera de Cyperus laxus crecidos en suelos de sitios impactados por derrames de petróleo crudo. (2009). pp 15-18.
5. Rivera Casado N. A., Montes Horcasitasa M. C., Rodríguez Vázquez R., Esparza García F. J., Pérez Vargas J., Ariza Castolo A., Ferrera-Cerrato R., Gómez Guzmán O., Calva Calva G. (2015). Fatty acid profile of Cyperus laxus from a phytoremediation system of soils from aged oil spill impacted sites. PLOS ONE (2014). ISSN: 1932-6203(Electronic) DOI http://www.editorialmanager.com/pone/
6. Guerrero-Zuñiga L.A, Rodriguez-Dorantes A.M. Efecto de la presencia de fenantreno sobre la expresión de proteínas y la actividad enzimática de *Cyperus hermaphroditus.* Polibotanica, 2009. 27:103-130.
7. Ritchie G.D., Still R.K., Ross J., Beckkedal V.Y.M., Bobb J.A., Arfsten P.D. Biological and health effects of exposure to kerosene-based jet fuels and performance additives. J. Toxicology and Environ. Health. 2003. Part B. 6:357-451.
8. Rivera Casado N.A., Rodríguez-Vázquez R., Montes-Horcasitas M.C., Pérez-Várgas J., Gómez-Guzmán O., Calva-Calva G. *Hidrocarburos Aromaticos y Fenilpropanoides Presentes en la Rizosfera de Plantas de Cyperus laxus Crecido en Suelos Contaminados con Hidrocarburos*. Tecnocultura, 2008, 20: p. 4-15.
9. Rivera Casado, N.A., Montes-Horcasitas, M.C., Esparza-Garcia, F.J., Ariza-Castolo, A., Gómez Guzmán, O., Pérez-Vargas, J., Calva-Calva, G. Fitotratamiento de suelos impactados por derrames de petróleo: interacción entre hidrocarburos poliaromáticos, fenoles y enzimas oxidativas. Revista CENIC. Ciencias Químicas, Magazine Article. 2010, 41:1-11
10. Murashige T., Skoog FA revised medium for rapid growth and bioassays with tobacco tissue cultures. Physiol. Plant. 1962, 15(3):473-497.
11. Martínez-Juárez, V. M., N. Ochoa-Alejo, E. Lozoya-Gloria, M. L. Villarreal-Ortega, A. Ariza-Castolo, F. J. Esparza-Garcia, G. Calva-Calva. Specific synthesis of 5,5'-dicapsaicin by cell suspension

cultures of capsicum annuum var. annuum (chili Jalapeno chigol) and their soluble and NaCl-extracted cell wall protein fractions. J Agric Food Chem. 2004, 52(4), p. 972-9.

12. Amadi A, Dickson A.A y Mate G.O. Remediation of soil: effect of organic and inorganic nutrient supplement in the performance of maize (*Zea mays L).* Water Air Soil Poll, 1993, 66,59-76.
13. Maila M.P., Cloete T.E. Germination of *Lepidium sativum* as a method to evaluate polycyclic hydrocarbons (PAHs) removal from contaminated soil. International Biodeterioration and Biodegradation, 2002, 50:107-113.

Section 10.
Environmental Education, Environmental Toxicology and Environmental Health

Page

Chapter 10.1 The effects of environmental education at the medicine discharge in Caruaru City-Pe, Brazil
Emanuele D. Guerra; Janielle S. Matos; Ângela M. C. Andrade; Cláudio E. Oliveira; Risonildo P. Cordeiro and Luiza F. C. Souza 870

Chapter 10.2 Generation and quantification of domestic solid waste in the origin
E. M. Silva Rodríguez; F. J. Manriquez Rojas; M. Quezada Cruz and B. Camacho Pérez 880

Chapter 10.3 Expresión de biomarcadores en tillandsia usneoides como respuesta a la exposición prolongada a metales atmosféricos
G. Martínez-Reséndiz; C. A. Lucho-Constantino; G. A. Vázquez-Rodríguez; C. Coronel-Olivares and R. I. Beltrán-Hernández 888

Chapter 10.4 Parasitic contamination of public places in urban and rural environments in the slovak republic
N. Sasáková; I. Papajová; J. Pipiková; F. Tóth and J. Venglovský 899

CHAPTER 10.1 THE EFFECTS OF ENVIRONMENTAL EDUCATION AT THE MEDICINE DISCHARGE IN CARUARU CITY-PE, BRAZIL

Emanuele D. Guerra (1); Janielle S. Matos (1); Ângela M. C. Andrade (1); Cláudio E. Oliveira (1); Risonildo P. Cordeiro (1) and Luiza F. C. Souza *(1)

(1) University center of Tabosa de Almeida – ASCES-UNITA, Av. Portugal, 584, Bairro Universitário- Caruaru - PE – Brasil

ABSTRACT

Contaminants compounds and their impact on the environment studies have been conducted for the environment and public health preservation. Wastewater treatment and the recovery of contaminated areas by chemicals and medicines have been a challenge for environmental professionals. The improper medicines discharge can alter the environment properties and affect the human health. In Brazil, the large-scale production of medicines began in 1999, promoting the economic development and medicine overconsumption by population without health professional prescription. Knowledge about the environmental impacts produced by each waste can cause changes in the society habits reducing or preventing pollution. The environmental education has been considered the best strategy to interact with the population and to disseminate information. Therefore, this study aimed to evaluate the environmental education to reduce the inappropriate medicines discharge in the environment by the population of the Caruaru City in Northeastern Brazil.

This project was developed in University Center of Tabosa de Almeida (ASCES-UNITA) in four phases. First, a questionnaire was applied to the population of several neighborhoods of Caruaru city, before conducting environmental education. It was realized between November 2014 and July 2015. Interviewed education level and age were obtained during the interviews; where and how the medicines were obtained, and discharged by interviewed were registered and their knowledge about the environmental impact of medicines were analyzed. After that, lectures and training were realized to explain, for the population and students, the correct way to medicines discharge and associated benefits. Than, two medicine collectors were installed on June 2015 in ASCES-UNITA and, finally, the medicine residue was monitored.

The Caruaru's population were 347,088 habitants in 2015, and 1,271 habitants were interviewed. The most used destination was the common trash, around 88%, by people between 16 and 75 years and regardless of educational level. Only 1.3% interviewed performed proper discharge without environment education, i.e. return the medicines residue to health units. They were between 15 and 45 years old. People over 75 years used to use all the medicine without leftovers. Most of interviewed people, 51%, did not know medicine problems on the environment and 78% never received information about this subject. In first (June 2015) and last (December 2015) month of medicine collector monitoring, the amount of medicine collected was 7 and 152 units per week, respectively, meaning a significant increase in correct medicine discharge.

---

*Author for correspondence: Luizas@gmail.com

This occurred because of the environmental education. In this period, nine lectures, six trainings and twelve games in schools, physical therapy clinics and college campus were realized. In this project the importance of environmental education was observed, reducing improper medicine discharge by increasing of public awareness about its environmental risks.

Keywords: environmental education, discharge, medicines, solids residue.

INTRODUCTION

New technologies development and pharmacologically active substances discovery, with few collaterals effects, have triggered medicine consumption increase by the population. Thereby, medicine industries earn billions, encouraging new medicines production and no concern with medicine residue discharge and treatment of the waste produced by production process or by consumers.

Self-medicine practice was usually performed by population, causing increase of inadequate consumption of medicines to treat many kind of diseases or exaggerated consumption amounts. Leftover medicines are stored in home or in commercial or health establishment, and after expiration date they are discharged. Water bodies and ground contamination can be avoiding if right discharge forms are informed or supported by industries.

In Brazil, around 10 to 28 thousand tons of medicines are discharged annually[4]. Incorrect discharge of medicine can cause serious environment contamination, the effects several affect the human health and alter the environment balance. These substances can persist in environment due to complex molecules and their hard degradation, causing pollution. These medicines are discharged in domestic trash or in toilet and they are composed by toxic substances or simple substance that can become toxic after interacted with other. These compounds can be accumulated in organisms, saturating enzymes systems and become toxic[5]. Final destination and medicine inactivation are the challenge of the professionals due to complexity and diversity of molecules, formulation composition and low concentrations of toxic substances.

Pharmaceutical medicines are composed by different kind of substances as dyes, acidulants, complexing agents, diluents, preservatives, dispersants, among others. Incorrect discharge of medicines, in sinks, toilet and domestic trash, for example, (I) affect the water bodies when untreated sewage is discharged, because of 50 to 90% of ingested medicines are excreted intact by animals[1] and 10 to 50% are medicines metabolites and no degraded medicines and metabolites in raw and treated sewage[2]; (ii) affect the ground, when the solids residue are buried or sent to landfills, medicines can reduce ground productivity, or making it infertile; and (iii) affect the air by volatile compounds or by dispersal solids particles and aerosols. For exemple bacterium *Xanthomonas campestris pv. passiflorae Per*. causes problems in culture of passionflower, the transmission this bacterium is made by the wind, rains, contaminated seedlings, insects, harvesting boxes, tools and utensils, machines and contaminated seed orchards[3].

Many kind of medicines have been detected in surface, underground and potable water and in soil after sludge of the WTP application. According Carvalho et al.[6], presence of medicines in environment can induce bacterial resistance, i. e., increasing medicine resistance of some bacteria species and decreasing medicine effectiveness in infections treatment. Metabolism and behavior modification in aquatic organisms were also observed by those authors, resulting in aquatic population imbalance. Infected organisms can be ingested by humans and can contaminate them.

Public awareness about environment and health impacts caused by improper medicine disposal can reduce this practice and the water and soil pollution. Therefore, environmental education is one of the best strategy to change the public behavior, to inform population about the right practice to use, store and discharge and to explain the health risks. Incorrect discharge of medicine have been done by all classes of the population, regardless of education, social class and age. However, they are fundamental to the success of mitigating actions for the proper disposal of this residue[7]. Mitigation proposals must be taught to people for environmental education.

Extension project “Medicine Discharge in Environment” has been developed in ASCES-UNITA since November 2014 to decrease the environment impacts of the medicine by Caruaru populations, Brazil northeastern, is the main goal. This project has been guide correct form to medicine discharge through environment education. In this study, the evaluation of the environmental education impact in reducing the inappropriate medicine disposal, thereby reducing environmental contamination by this sort of residue, was the main aim. For this, the public perception about the environment and health damage caused by the incorrect medicine disposal, the usual forms of disposal this residue by this population, as well as the monitoring of a medicine collector during the environmental education activities were evaluated.

MATERIALS AND METHODS

Medicine discharge in environment project was developed in four phases as show the flowchart of **Figure 1**.

In Phase 1, one kind of questionnaire was applied in Caruaru’s neighborhoods from november 2014 to july 2015, by interviews. Where, when and how the medicines were obtained, stored and discharged and population knowledge about the environment and health impacts caused by medicines were analyzed by this questionnaire. Some private information about the interviewed were registered, as age and education level. The interviewed selection was random, approaching people in the street, fairs, bus stop and in colleges. During questionnaire application, the population did not receive guidance or lectures about the subjective for achieve real results of population behavior. Know the actual situation of the medicine discharge, the interviewed characteristics and their knowledge about this subjective were the aim of this phase.

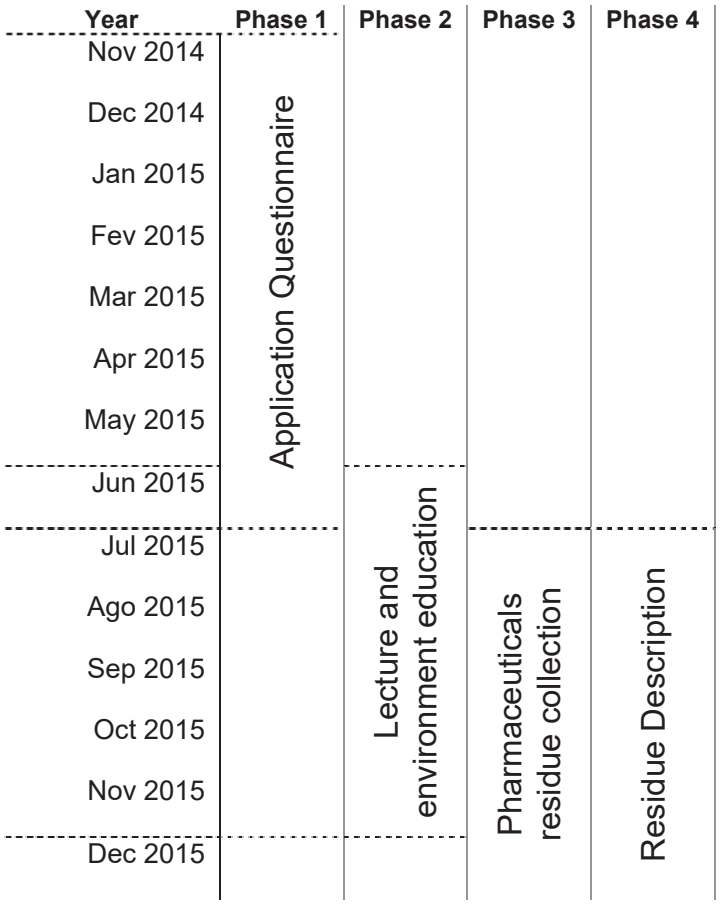


FIGURE 1. Chronology of the project development

In Phase 2, trainings, speeches, lectures, games and researches were realized to explain the right way and benefits to discharge of medicines. Children, young, older, graduated and undergraduated participated in this phase. Because of the different kind of public, different educations activities were realized. This project was realized in a University center that had many kind of health clinics and had promoted educations actions in schools and fairs. Lectures were taught by students involved in this project, in clinical school, in high school, in this university center socio-educational activities, all of them in Caruaru city. This phase has been realized since June 2015.

In Phase 3, two medicine collectors were installed in July 2015, in Campus University and the residues discharged have been monitored since July 2015. Folders with collectors location and how to discharge the medicines were distributed to students, staff and visitors during the education activities. In phase 4 Materials were collected once a week by students of the project, about 20 undergraduate students of environmental engineering, pharmacy and industrial engineering. Materials collected were separated by pharmaceutical forms (solid, semi-solid and liquid) and type of material (glass, plastic, paper and metal); then were weighed and finally all information (concentration, expiration date, manufacturer, active ingredients, etc.) were noted. In **Figure 2**, photographs of each phase of the research conducted by students are shown.



FIGURE 2. Application questionnaire, lectures and environmental education, collection and residue description, respectively

RESULTS AND DISCUSSION

In phase 1, 1,271 people were interviewed. Most of the interviewed, 88%, usually throw out the leftovers of medicines and the out of date in domestic trash can. Toilet was the second place most used to discharge medicines by Caruaru population. Only a small proportion of the interviewees return the leftovers to hospitals or to health agents. Similar results were obtained by Vaz et al.[8] in Federal District Brazil, 78% disposal medicines in domestic trash and 13% in toilet. They mentioned less than 1% of return to health agents or clinics. In **Figure 3**, the main discharge places used by population to discharge the leftovers of medicines are showed.

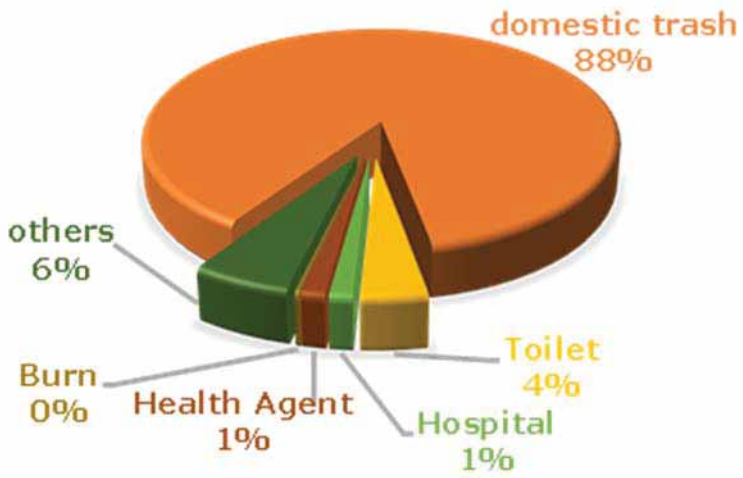


FIGURE 3. Disposal sites of pharmaceutical material often used by the Caruaru population

In Brazil, the responsibility to discharge the solids residues in correct place is shared by all producers and is established by National Policy on Solids Residues (Law nº 12.305/10)[9]. Solids residues are collected at the door of the houses by employees of residue collection company. All collected residues must be separated and each type of residue must be taken to a landfill or recycling sites as recommended by the law. However, domestic residues are not properly separated by population, organic and recycling residues are collected mixed and final disposal has been held in dumps.

In 2010, Brazilian law nº 12.305/10 determined landfills as correct way of final disposal of solids residue, and stipulated a deadline for adequacy of old dumps. Under current conditions in Brazil, final disposal of solid waste in dumps has no soil preparation to prevent groundwater contamination by leachate. Brazilian controlled landfills have inadequate systems to remove pharmaceutical compounds although satisfactory organic matter removal.

Solid residues are classified in dangerous (class I) and not dangerous, inert and not inert, (class II) by Brazilian Norm - NBR 10.004/2004[10], and health solids residues are classified as dangerous. Only 2% of 149.000 tons of domestic and commercial residues daily generated in Brazil were solid residue and 10 to 25% needed special attention[11].

Adequate transportation and treatment of this residue, in northeastern Brazil, were realized by specialized private company contracted by state and municipal governments or private companies generating dangerous residue[12]. Specialized company collects dangerous residues in hospital, laboratories, industries, etc. and do not collect domestic residue. Because of this, medicines discharged by population in own trash, do not receive adequate final destination and treatment. The most part of this kind of residue are disposed in landfill and dumps, without adequate compounds inactivation, causing impacts in ground, in groundwater and air.

Pharmaceuticals materials discharged in toilet, corresponding the 4%, go directly to sewage. In Caruaru, only 40% of produced sewage are collected and 20% are treated. Treated and untreated sewage are discharged in water bodies that cross the city as Ipojuca River and Capibaribe River. Water of these rivers is used for human consumption, livestock and agriculture by rural population. Medicine discharge in domestic trash and in toilet can cause serious health and environment problems, mainly because the inadequate final destination of solid residues and sewage treatment.

The main respondents' ages were between 15 and 45 years. People up to 75 years usually consume complete medications, due to chronic diseases. This information shows how important exact amount of medicines dispensation is, avoiding leftovers and guides effective ways to promote environment education. Reduction of solids residues production can occur by environment education according Brazilian National Council of Environment and it is encouraged by this organ[13]. This preventive action is considered less expensive than corrective action in reducing pollution and health problems.

According Alvarenga and Nicoletti[14], medicine discharge is realized in domestic trash because of unfamiliarity informations about the right form of discharge this kind of residue. About 63% of respondents have no knowledge about the problems caused by incorrect discharge of medicines in environment. Howerver, 37% of the interviewed responded to know problems caused by incorrect discharge of medicine, but do not know the correct form to discharge (**Figure 4**).

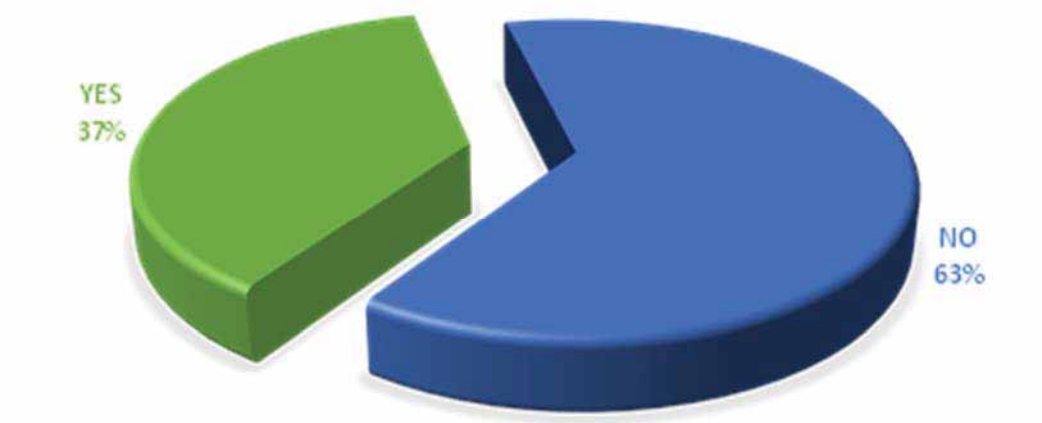


FIGURE 4. Population knowledge about environment problems causeds by incorrect medicine dischage

Alvarenga and Nicoletti[14] affirm that legislation is created to guide, standardize, setting boundaries, rights and obligations of commerce and industries and does not include population. Population conduct towards the correct practices of pharmaceutical disposal is not published in the legislation, meaning that only companies generate residue and pollute the environment. The most of respondents (78%) affirmed to have no knowledge about the correct forms of pharmaceutical disposal. Among the respondents, health and environment students and professionals participated and they may have contributed to the percentage (22%) that knew these practices.

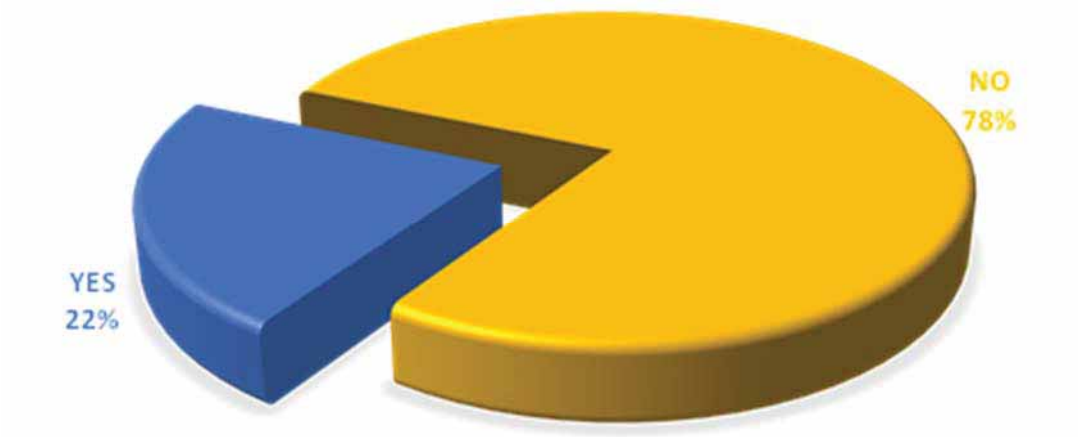


FIGURE 5. Population knowledge about correct medicine dischage

Incentive programs to correct medicine discharge and installation of medicine collectors can be performed by hospitals, health clinicals, drugstores, industries and Colleges. Howerver, legislation encourages these practices, but does not specify how they should be implemented and does not require people to participate[15].

After questionnaire aplication, nine lectures, six trainings and twelve games about right medicine discharge and their environment impacts were realized by ASCES-UNITA Students. Socio-educational activities were performed in schools, college, clinics and in the streets with all ages people (**Figure 6**).



FIGURE 6. Lectures and trainnings

Medicine collectors were monitoring from June 2015 to December 2015. The medicine amount discharged increased because of the environment education activities, from 7 to 150 units per week. The amount of medicine disposed in December was lower than in October. This was due to collectors are installed within the University center, and the flow of students decreases in this period. Cumulative and monthly amounts of collected medicines can be seen in the graph of the **Figure 7**.

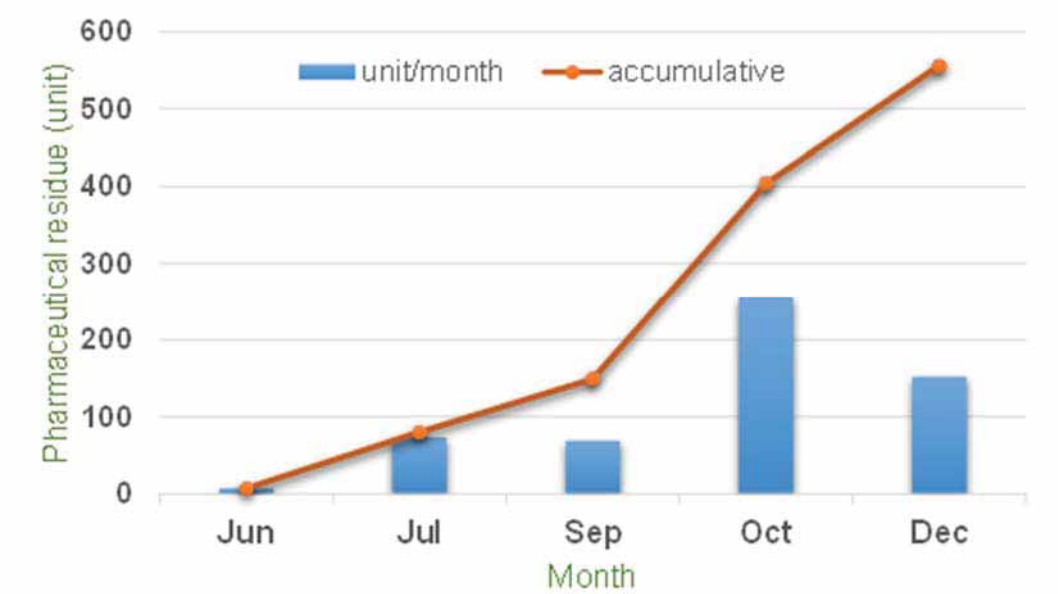


FIGURE 7. Cumulative and monthly amounts of collected medicines

Population have been contributed in water and ground contamination by phamaceuticasl products, as medicines and packages. This has been occurred due to Brazilian legislation emphasize commercial activities, population has not been received information or trainning to correct pharmaceutical products discharge and their environment impacts. Through this project, people's behavior could be modified, increasing residue collection, by environmental education. The most appropriate activities for environmental education were chosen based on the responses of the population in the questionnaire.

According Layrargues[16], nature recovery is not enough for their protection. This old model must be associated to new perspectives of environmental education, making

people more informed about environment issues. Main causes of incorrect discharge of medicines is the population without information[17].

This project installed two collectors in ASCES-Unity and the material collected was discharged with health and chemical university residue. Because of this, no collector has been installed outside the university center and educations activities were realized mainly inside the University. To enlarge the amount of collectors, it is necessary to partner with health units and companies. However, it is important to realize educational activities with different age groups, disseminating information and enhancing the quality of life.

CONCLUSION

Increasing medicine production and consumption by population generates huge concern as stimulate acquisition without prescription, increasing consumption of inadequate medicines, increasing the remains of medicines, increasing residue. Without information at the time of purchase, population discharged in incorrect way the medicines. In Caruaru, the population discharged the leftover medicines in wrong way, domestic trash (88%) and toilet (4%). Only 1.3 % returned to hospital and health agents. The most of responders of questionnaire did not know correct way to discharge medicines (63%) and their environment and health impacts (78%).

The most of interviewed had no knowledge about the environment problems caused by medicines and because of this discharged them in wrong location. Environment education is a satisfactory strategy to guide and inform population about problems that medicines can cause in environment and health if they were discharged in wrong place and how to disposal this kind of residue without serious impacts. After lectures, trainings and games, quantity of medicine collected in medicine collectors increased, proving the effectiveness of educational activities.

REFERENCES

1. Vida e saúde. Atenção na hora de descartar seus medicamentos. 2008. Disponível em: http://www.ecodesenvolvimento.org.br/conteudo/voceecod/descarte-de-remedios-o-que-fazer. Acessado em: 28/05/2016.
2. Zuccato E., Castioglioni S., Fanelli R. Identification of the pharmaceuticals for human use contaminating the Italian aquatic environment. Hazard Mat. 122 (2005) 205-209.
3. Bergamin A., Kimati H., Amorim L. Manual de Fitopatologia. Princípios e Conceitos. 1 (1995).
4. ANVISA Agência Nacional de Vigilância Sanitária. Disponível em: http://www.anvisa.gov.br/medicamentos/glossario/glossario_p.htm. Acessado em: 28/05/2016.
5. Maher J. F. Alterações Farmacocinéticas na Insuficiência Renal e na Diálise. Farmacologia em Terapia Intensiva. (1993) 29-50.
6. Carvalho E., Viviani E., Ferreira E., Mucini L., Santos C. Aspectos legais e toxicológicos do descarte de medicamentos. Rev. Bras. Toxicol. 22 (2009) 1-8.
7. Gasparini J. C., Gasparini A. R., Frigieri M. C. Estudo do descarte de medicamentos e consciência ambiental no município de Catanduva-SP. Ciência e Tecnologia. 2 (2010) 38-51.
8. Vaz, K. V.; Freitas, M. M.; Cirqueira,J. Z. Investigation about ways of discarding expired medicaments. Cenarium Pharmacêutico, v. 4, 2011.

9. BRASIL. Política Nacional de Resíduos Sólidos. Lei nº 12.305/10, 2 de agosto de 2010. Portal da Legislação. 2010. Disponível em: http://www.mma.gov.br/port/conama/legiabre.cfm?codlegi=636. Acessado em: 01/07/2016.
10. BRASIL. Resíduos Sólidos – Classificação. Portaria nº 1469/2000. ABNT NBR 10.004. 2004. Disponível em: http://www.videverde.com.br/docs/NBR-n-10004-2004.pdf. Acessado em: 02/07/2016.
11. BRASIL. Dispõe sobre o tratamento e a disposição final dos resíduos dos serviços de saúde e dá outras providências. Resolução CONAMA nº 358/2005, 29 de abril de 2005. Portal da Legislação. 2005. Disponível em: http://www.mma.gov.br/port/conama/legiabre.cfm?codlegi=462. Acessado em: 02/07/2016.
12. BRASIL. A ANVISA determina novos procedimentos para o tratamento dos resíduos gerados na área de saúde, da produção até o destino final. Revista Cidades do Brasil, Ed. 52, 2004
13. BRASIL. Dispõe sobre a Política Nacional do Meio Ambiente, seus fins e mecanismos de formulação e aplicação, e dá outras providências. Lei nº 6938/1981, de 31 de agosto de 1981. Portal da Legislação. 1981. Disponível em: http://www.mma.gov.br/port/conama/legiabre.cfm?codlegi=313. Acessado em: 03/07/2016.
14. Alvarenga L. S. V., Nicoletti M. A**.** Descarte Doméstico de Medicamentos e Algumas Considerações sobre o Impacto Ambiental decorrente. Revista Saúde. 4 (2010) 34-39.
15. Hoppe T. R. G., Araújo L. E. B. Contaminação do Meio Ambiente pelo Descarte Inadequado de Medicamentos Vencidos ou não Utilizados. REMOA/UFSM. 6 (2012) 1248–1262.
16. Layrargues P. P. Educação ambiental com responsabilidade social. MMA. 13 (2004) 50-156.
17. Morais S., Latini R. O. Descarte inadequado de medicamentos: apresentação de informações para produção de cartilhas educativas. Disponível em: http:// www3.izabelahendrix.edu.br/ojs/index.php/aic/article/view/862/687. Acessado em: 28/06/2016.

CHAPTER 10.2 GENERATION AND QUANTIFICATION OF DOMESTIC SOLID WASTE IN THE ORIGIN

E. M. Silva Rodríguez (1); F. J. Manriquez Rojas *(1); M. Quezada Cruz (1) and B. Camacho Pérez (1)

(1) Universidad Tecnológica de Tecámac, Carretera Federal México Pachuca Km. 37.5, Tecámac, México.

ABSTRACT

The increase in population, industrialization and the economic development in countries affect consumer patterns of societies, these three patterns modify the amount and variety of solid waste. The problem of waste is that most of it is treated as trash. In Mexico, landfills are used as garbage dumps, some of them are controlled and some others are not. These places are land for disposal of municipal solid waste (MSW). However, being the waste collection and transport operations managed by authorities, most municipalities do not have regulations in this issue; handling and storage centers are minimal, so as the generation and composition studies. Materials and energy resources are squandered. This study considered a social sample of five municipalities in the State of Mexico, consisted of surveys and training to participating families. After that, densities of each kind of waste were determined and quantified by measuring weight and volume. Also, characterization of generated waste was determined for the sample housing. Social, cultural and economic characteristics of these municipalities are similar. In each house from two to eight people live, four in average. Waste separation is carried out in only 44% of housing. In 68% of housing, waste is placed on the collection truck which is, eventually, placed in controlled or uncontrolled landfills. There is no data about the amount of recovered waste during the journey from the housing to the landfill. The aim of this work was to obtain data of quantities and characteristics of the waste generated at the source. Regarding quantification, it was found that the average total mass generated was 0.392Kg / person / day. The relation in weight of waste generation: organic / inorganic was 1.02. In the characterization of inorganic waste, cardboard, paper, plastic and pet were quantified. It corresponds to 36% of the total weight generated. For a sustainable management and disposal of MSW is essential to know its quantity and features; in society terms, it is essential to be aware about prevention and separation from the origin, to propose effective plans for recovering materials and to regulate rules for collection, transport, selection and disposal services, either for government or private instances.

Keywords: solid waste from the origin, waste characterization, waste quantification.

---

*Author for correspondence: ibqjavier@yahoo.com.mx

INTRODUCTION

In the world, on average, 1.3 billion tons of solid waste per year are produced. In Latin America and the Caribbean 160 million tons / year are produced, with a range of 0.11 to 5.5 kg / person / day, depending on the level of the incomes[1]. In the European Union the generation per capita is estimated in 2014 was 474 kg, of which 28% was placed in landfills, 27% incinerated, 27% recycled, 16% composted or digested and the rest was not managed[2]. In Mexico 42 million tons of waste were generated in 2012, nationwide, of which over 50% is inorganic. The estimated national generation volume increased 28% from 1997 to 2008. It turns from 29.3 to 37.6 million tons. The per capita generation increased from 0.84 to 0.97 kg in the same period. The recycling rate is low, 3.8% in 2008[3].

Mexico faces environmental and political changes. Similar to other Latin American countries, there are not consolidated public health systems; therefore, solid waste management is unsustainable. The country concentrates its urban areas, 70% of the population, in just ten cities. Having this situation; environmental, technical, administrative, economic and social goals are being discussed according to the National Development Plan 2013 - 2018[4]. In the national population, 12.8% live in the State of Mexico and from this amount 11% is concentrated in Ecatepec; this municipality, like most municipalities in the State of Mexico, has a poor urban planning with the consequent lack of garbage collection services, network transport, recreational areas, public lighting nor an appropriate sewerage network[5].

In the State of Mexico 8,284,985 kg / day of MSW are produced. These kilograms correspond to 9.6% which is generated at national level. Regarding the National Infrastructure for waste disposal, it is found that the number of landfills increased from 30 in 1995 to 260 in 2012; consequently, the total storage capacity increased from 5.95 to 27.98 million tons. There are 16 landfills[6] in the state of Mexico. The municipalities of Acolman, Coacalco de Berriozabal, Tecamac and Zumpango are some nearby municipalities. For them, there is a controlled landfill in Ecatepec, a municipal landfill in Tecamac and a private landfill which receives industrial waste and MSW from, at the least, other five municipalities. Apart from these, there are also uncontrolled disposal sites. Although in INEGI[7] the daily MSW generated tons by each municipality are reported, there is no corresponding information in Ecatepec of which has the largest number of inhabitants. It is reported less MSW generation than in Coacalco. There is not available information of the amount of MSW that is generated in the two out of the five municipalities, Tecámac and Acolman (**Figure 1**).

Waste transport in these municipalities, from the origin to final disposal, is handled by the Department of Public Services that gives concessions to collectors who are economically dependent on the sale of waste to recycling companies. They start the selection since the moment that they have the waste in the transport unit. The garbage is placed, in the best case, in a public or private landfill. If the low rates of economic valorization are added to this practice, a minimal recovery of materials is caused; either for reuse or for their energy content. From the 123 municipalities in the State there are just 43 collection centers in 12 municipalities, there have been studies on waste generation in five of these municipalities and there have been studies Composition[7] in only four of them.

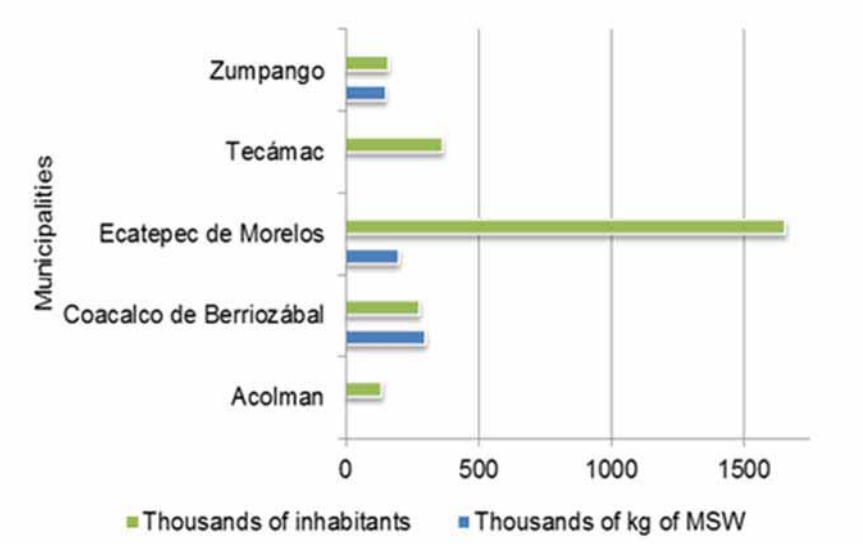


FIGURE 1. Daily average waste collected by municipality

Over the past 40 years the global waste management has improved by going from putting them in landfills to recycling, composting or incinerating them in order to minimize the extraction or production of virgin material and the production of chemical fertilizers and heat [8]. When the quantities and characteristics of waste are known, management options and treatment of MSW can be assessed in domestic, municipal or state level. Studies of generation, disposition and characteristics of the MSW allow knowing strategies to improve the handling, transportation and disposal. This paper presents a study of quantification and composition of waste from the origin.

MATERIALS AND METHODS

A study to collect data such as number and proportion of types of solid waste from the source; i. e. recent generated waste by housing, was carried out. Also, surveys were applied and participating families were trained for the separation of organic and inorganic waste. Tecnico Superior Universitario en Química students, from UTTec, contributed in the measurement of volume and weight of the waste generated in each house so as to the classification and the weighting of inorganic waste. The study was conducted in the period January - June 2015, a total of 180 days; 145 families participated in five municipalities of the State of Mexico.

Characteristics of the population of the studied municipalities. The municipalities of Acolman, Coacalco de Berriozábal, Ecatepec de Morelos, Tecamac and Zumpango are part of the metropolitan area of the Valley of Mexico (**Figure 2**); they are at 2250 meters above sea level having a total land area of 659 km^2. The population in these municipalities is 17.1% of the total in the State of Mexico. Ecatepec has the highest population density; 10.91%, the municipal average number of persons per housing is from 3.7 to 4.3, Coacalco is the municipality with the lowest indicator of poverty and lack of basic services; 22.4% and 0.2% respectively. Zumpango has the highest poverty rate; 49.8%, and Acolman has the highest percentage of basic services lack, 21.9% [9].



FIGURE 2. Metropolitan Area of Mexico

Surveys and training. Surveys were conducted to housewives so that they could learn about the handling and disposal of waste generated in their homes. They were asked for their participation and solid waste management training was given to them, the training guided them to two things: to distinguish organic and inorganic waste and to handle the corresponding separation of them. At least two labeled containers for waste separation (organic and inorganic) were supplied to each house. In the organic waste container, food waste (peels, stems, leaves) and prepared food were deposited; in the inorganic waste container, paper, plastics of different materials, pet, glass, tetra pack containers, metal (tinplate and aluminum) and textiles were put. Construction waste, batteries or any others who are not part of those already mentioned were not considered.

Measuring procedure. Data collection was divided into four stages, i) measuring of the volumes of the containers, ii) weighting ten waste samples in the filled containers, for determining the densities of the two types of waste, iii) classifying and weighting organic waste to obtain the fraction of each material and iv) quantifying the number of containers generated in 180 days. For weighting, spring balance of 1 and 12 kg were used. **Table 1** describes the equations used.

TABLE 1. Equations used in obtaining data

Determination	Equations
Volume (cylinder)	$V = At * h$
Volume (square)	$V = Base * h$
Density	$\rho = \frac{\text{Mass of one type of waste}}{\text{Container volume}}$
Total mass generated	$Mass = \rho\ waste * \text{Container volume} * \text{Total containers}$
Mass fraction	$\%\ \text{Fraction} = \frac{\text{Weight individually residue}}{\text{Total weight of inorganic waste}} * 100$
Generation per person per day	$\text{Waste generation per capita} = \frac{\text{Weight of waste generated per household}}{\text{Total persons in housing} * \text{Total generation Days}}$

RESULTS AND DISCUSSION

From the surveys. The survey responses indicate that in only 44% of the participating housing separate waste into organic and inorganic; common containers where waste is deposited are polyethylene bags, plastic cans, common containers (metal or sack) or separation container (**Figure 3**); the percent of houses that have a common or with separations containers is minimal, this is exclusive for a set of houses in private street or in apartments (houses studied corresponding to 25%). 68% of people dispose their waste (separated or not) through the garbage truck; 30% reuses organic waste as pet food and deposits inorganic waste in the garbage truck, 1% burns it, or 1% throws it into dumps near their homes (**Figure 4**). The garbage truck may or may not take the waste to a collection center or directly to a controlled landfill or an uncontrolled site. In Mexico, authorities are working so that only landfills could be used for the disposal waste. In 1995, 70% of waste was placed in uncontrolled sites and only 20% in landfills, those numbers changed to 20% and 60 % respectively by 2005[10].

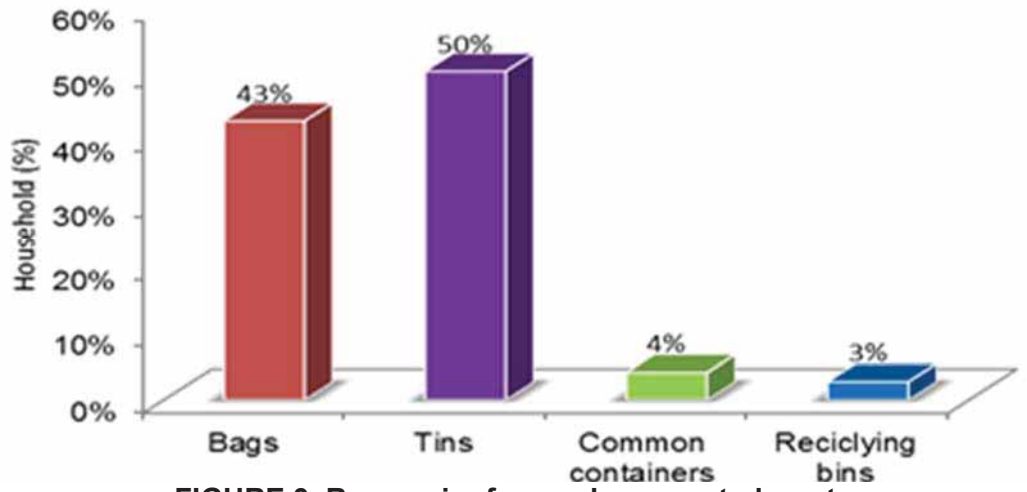


FIGURE 3. Reservoirs for newly generated waste

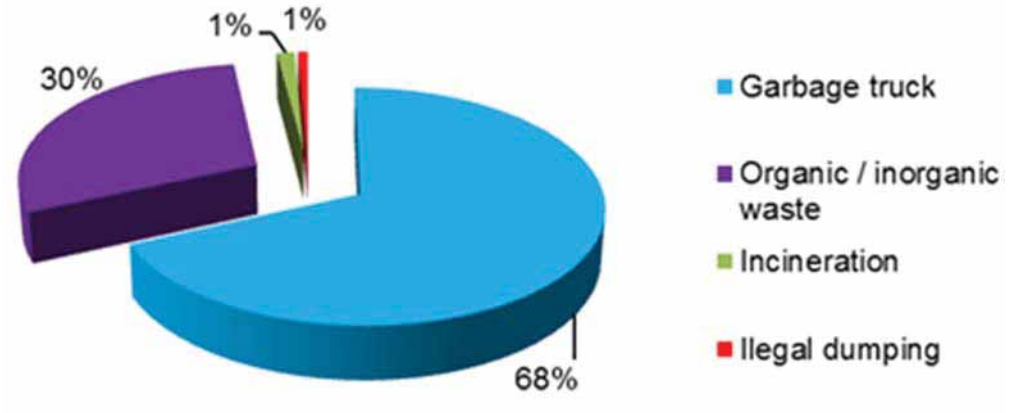


FIGURE 4. Forms of waste disposal

Measurement. The densities obtained in the origin were 288 kg / m^3 and 88 kg / m^3 for organic and inorganic solid waste respectively. The inorganic waste occupies four more times volume than organic and inorganic / organic ratio is 1: 1.02 by weight (**Figure 5**). In Murugaian y Sulaiman[11] a density of 311.73 kg / m3 is reported and Saldaña[12] 261.04 kg / m3 for RSM, on the arrival to a landfill. The density of the waste is different because of the characteristics such as: composition, compaction and leaching effect. Furthermore, the composition mainly depends on the socioeconomic status of communities.

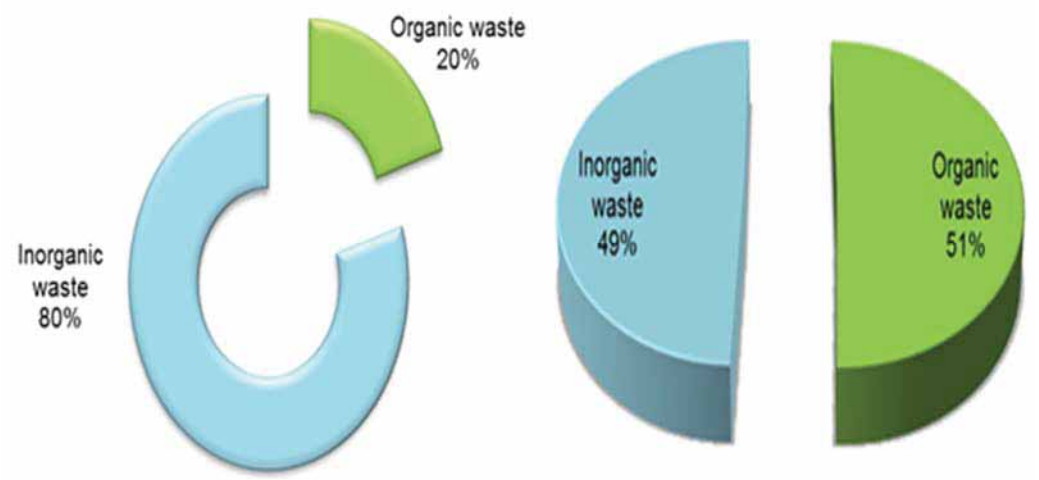


FIGURE 5. Ratio of organic and inorganic waste generated at the source

The generation of waste in the origin was 0.392 kg / person / day. This data is lower than the one reported by SEDESOL[13] (0.97 kg / person / day national average) and similar to the one reported by Castillo[14] (0.384 kg / person / day). This data varies because MSW studies include waste from business, schools and thoroughfares. In national statistics, it is reported that 53% of organic waste corresponds to the national average[15]; this percent is higher compared with the findings in this study. The total volume of solid waste in the origin was 3.5 x 10^{-3} m^3 per capita per day.

Organic waste which is generated in the origin includes cardboard, paper, plastic, glass, metal, tetra-pack and others like textiles and Styrofoam; all consumer products and their packaging. 0.2 kg of organic waste is produced per person per day. cardboard, paper, plastic and pet, with 0.14 kg per capita per day are the inorganic waste that is more produced; on average 52 g, among glass, metal, tetra-pack and others, are generated per person per day (**Figure 6**).

There is a hierarchical organization of waste which has options such as: reduction from the origin, reuse, composting and biodegradation, recycling, incineration with recovery of energy and disposal in a landfill[16]. Knowing the reason of waste generation and its characteristics can improve the sustainable waste management.

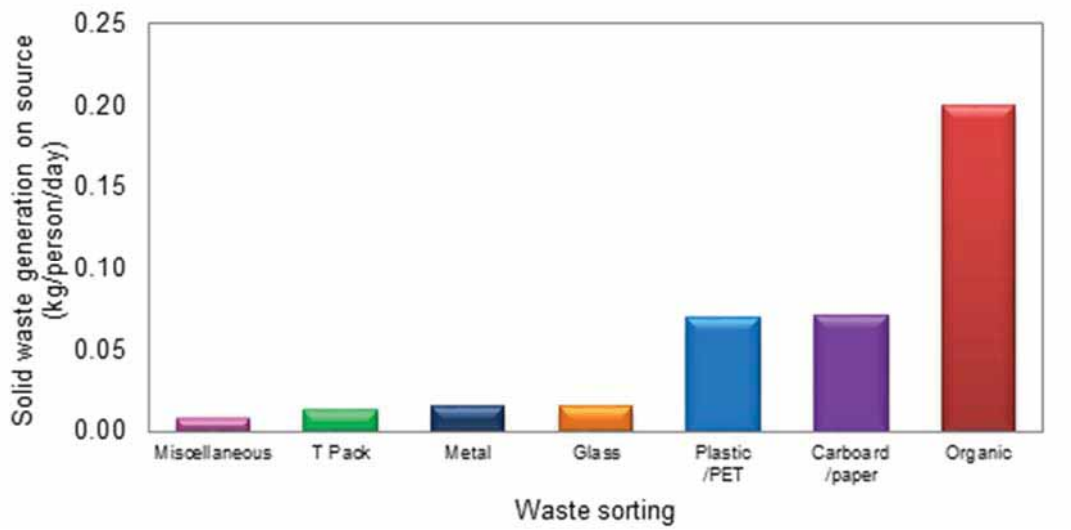


FIGURE 6. Fractions of waste at source

Inorganic waste volumes can be reduced with the selection of waste in the origin; therefore, selective collection allows a greater recovery of materials such as plastic, cardboard, paper and pet. The transport of organic waste, which are the highest density, to composting centers in strategic locations, reduces costs and are given a beneficial use; once composted they can be used as fertilizer for public gardens, orchards or family gardens.

CONCLUSION

MSW generation is increasing with the growing density of population in the Valley of Mexico. The amount of organic and inorganic waste is similar in weight, 51 and 49% respectively; 36% of the total waste corresponds to plastic, cardboard, paper and pet, all of them potentially recyclable, with commercial value. Consumerism, socioeconomic status and lifestyles affect the characteristics of the waste generated in the source. Moreover, the lacks of waste separation culture and nonregulated policies lead to an ineffective management of MSW, leaving waste disposal in landfill as the main destination.

The environmental benefit can be obtained with basic practices such as recycling inorganic waste or compost organic waste. It is a job for all sectors of society.

REFERENCES

1. Hoornweg D. y Bhada-Tata P. What a waste. A global review of solid waste management. The World Bank, 2012.
2. European Commission. Environment – Waste, 2016. Encontrado en http://ec.europa.eu/environment/waste/index.htm
3. SEMARNAT. Base de datos estadísticos. Secretaria de Medio ambiente y Recursos Naturales, 2012. Encontrado en http://www.semarnat.gob.mx/temas/estadisticas-ambientales/badesniar
4. DOF. Programa Sectorial de Medio Ambiente y Recursos Naturales 2013-2018 (PROMARNAT). Diario Oficial de la Federación, 2013.

5. H. Ayuntamiento de Ecatepec de Morelos 2013 - 2015. Cuaderno de Información Estadística y Geográfica Municipal No. 1.Sistema Municipal de Información estadística y geográfica, 2015.
6. SEMARNAT. El Medio Ambiente en México, Residuos Sólidos Urbanos, 2014. Encontrado en http://apps1.semarnat.gob.mx/dgeia/informe_resumen14/07_residuos/7_1_2.html
7. INEGI. Instituto Nacional de Estadística y Geografía. Residuos sólidos urbanos. Censo Nacional de Gobiernos Nacionales y Municipales, 2011.
8. Ekvall, T., Assefa, G., Bjorklund, A., Eriksson, O., Finnveden, G. What life cycle assessment does and does not do in assessments of waste management. Waste Management 27, (2007) 989–996.
9. CONEVAL. Informe anual sobre la situación de pobreza y rezago social de los municipios de Acolman, Coacalco, Ecatepec, Tecámac y Zumpango. Consejo Nacional de Evaluación de la política de Desarrollo Social. Secretaría de Desarrollo Social, 2012.
10. SEDESOL. Secretaría de Desarrollo Social. Dirección General de Equipamiento e Infraestructura en Zonas Urbano-Marginadas. México, 2009.
11. Murugaian P. T. y Sulaiman H. Generation and composition of Municipal Solid Waste (MSW) in Muscat, Sultanate of Oman. Procedia APCBEE. 10 (2014) 96-102.
12. Saldaña D.C., Hernández R.I., Messina F.S. y Pérez P.J. Caracterización física de los residuos sólidos urbanos y el valor agregado de los materiales recuperables en el vertedero el Iztete, de Tepic-Nayarit, México. Revista Internacional de Contaminación Ambiental. 29 (2013) 23-32
13. SEDESOL. Secretaria de Desarrollo Social. Dirección General de Equipamiento e Infraestructura en Zonas Urbano-Marginadas, 2013
14. Castillo G. E. y De medina S. L. Generación y composición de residuos sólidos domésticos en localidades urbanas pequeñas en el estado de Veracruz, México. Revista Internacional de Contaminación Ambiental. 30 (2014) 81-90.
15. SEMARNAT. Secretaria de Medio Ambiente y Recursos Naturales. Programa Nacional para la prevención y gestión integral de residuos 2009-2012. Diario Oficial de la Federación, 2009.
16. INE. Instituto Nacional de Ecología. Manejo Integral de los residuos sólidos, 2007. Encontrado en http://www2.inecc.gob.mx/publicaciones/libros/133/manejo.html.

CHAPTER 10.3 EXPRESIÓN DE BIOMARCADORES EN *Tillandsia usneoides* COMO RESPUESTA A LA EXPOSICIÓN PROLONGADA A METALES ATMOSFÉRICOS

G. Martínez-Reséndiz (1); C. A. Lucho-Constantino (1); G. A. Vázquez-Rodríguez (1); C. Coronel-Olivares (1) and R. I. Beltrán-Hernández *(1)

(1) Universidad Autónoma del Estado de Hidalgo, Chemical Research Center, Carr. Pachuca-Tulancingo km. 4.5. Mineral de la Reforma, Hidalgo, México.

RESUMEN

El objetivo de este trabajo fue evaluar la idoneidad de algunos biomarcadores en *Tillandsia usneoides* como respuesta a contaminantes atmosféricos. El estudio se llevó a cabo en dos municipios del estado de Hidalgo, México: Tlaxcoapan, sitio receptor de la contaminación atmosférica producida en el corredor industrial Tula-Vito-Apasco, y Actopan, sitio control sin actividad industrial. En ambos sitios se realizó un biomonitoreo activo con *T. usneoides* de febrero a octubre de 2012. Al inicio y al final del experimento se midieron los siguientes biomarcadores de efecto en *T. usneoides*: superóxido dismutasa (SOD), peroxidasa (POD), nitrato reductasa (NR), proteínas totales, ácido ascórbico y clorofilas. Además, se cuantificaron los metales Ca, Cu, Cd, Fe, Mg, Mn, Ni, Pb y Zn en el biomonitor como biomarcadores de exposición. La significancia estadística de las diferencias encontradas se determinó aplicando un ANOVA; la asociación lineal entre los biomarcadores de efecto y los de exposición se evaluó mediante correlaciones de Pearson. Los biomarcadores de efecto que presentaron cambios significativos después de la exposición fueron: clorofilas, proteínas totales, POD, NR y ácido ascórbico. Los biomarcadores anteriores también mostraron correlaciones con los metales Ca, Cu, Mg, Mn, Pb y Zn. Los metales principalmente retenidos por *T. usneoides* fueron Ca y Pb, seguidos por Cu, Mg y Zn. Las concentraciones de Fe y Mn permanecieron prácticamente constantes, mientras que las de Ni y Cd se encontraron por debajo del límite de detección. De acuerdo con los resultados, *T. usenoides* responde a la presencia de Pb y Ca en un amplio rango de concentraciones por lo que estos metales podrían ser empleados como biomarcadores de exposición. Por otra parte, las clorofilas, proteínas totales, POD, NR y ácido ascórbico podrían ser útiles como biomarcadores de efecto en *T. usneoides*.

Keywords: active biomonitoring, environmental biomarkers, *Tillandsia usneoides*.

---

*Author for correspondence: icelabeltran@yahoo.com.mx

INTRODUCCIÓN

En el campo de las ciencias ambientales, los biomarcadores son expresiones bioquímicas, celulares, fisiológicas o comportamentales que se manifiestan en un organismo como respuesta a la exposición a uno o más contaminantes[1]. Los estudios sobre biomarcadores en los diferentes compartimentos terrestres han ido en aumento, debido a que proporcionan información sobre el impacto de determinados contaminantes en los seres vivos[2].

Las plantas han sido ampliamente utilizadas como biomonitores de la calidad atmosférica y en los últimos años también se han comenzado a evaluar biomarcadores en ellas. Esta información toxicológica complementa la que provee el monitoreo físico convencional[3]. Por
ello, la observación de la contaminación del aire mediante el uso de biomonitores se surgiere como una alternativa potencialmente útil, eficaz y económica para determinar la presencia de contaminantes, su ruta destino y sus efectos en los seres vivos. Esto es especialmente relevante para el monitoreo de áreas extensas.

Las plantas superiores funcionan como biomonitores de contaminación por metales atmosféricos debido a que pueden acumularlos, lo que a su vez puede ocasionarles efectos a nivel bioquímico: como la activación de algunas enzimas que tienen como objetivo evitar la oxidación de las células del organismo, y así prolongar su vida.

T. usenoides es una planta epífita, la cual ha sido propuesta por Markert et al.[4] como un biomonitor para el estudio de aerosoles atmosféricos. El análisis por medio de microscopía electrónica de barrido sugiere que los contaminantes asociados con las partículas son absorbidos por las hojas de la superficie, las escalas y el tallo de *T. usneoides*[5].

Debido a las características anteriores y a su amplia distribución geográfica, *T. usenoides* ha sido empleada en diversas partes del mundo como modelo biológico para la medición de contaminantes atmosféricos como elementos químicos[6]. Sin embargo, no existen estudios de la expresión de biomarcadores de efecto en esta especie, tales como actividad enzimática (superóxido dismutasa (SOD), peroxidasa (POD), nitrato reductasa (NR), proteínas totales, ácido ascórbico (AA) y clorofilas, como respuesta a la presencia de los contaminantes atmosféricos.

Con base en lo expuesto anteriormente, se realizó este trabajo cuyo objetivo fue evaluar la expresión de algunos biomarcadores en *Tillandsia usneoides* como una respuesta a los contaminantes atmosféricos.

MATERIALES Y MÉTODOS

Sitios de estudio. Para realizar el biomonitoreo activo se colectaron ejemplares de *T. usenoides* en la comunidad Bella Vista, Hgo., (20°59’28.86” N, 98°58’29.00”), la cual es zona rural con 297 habitantes, sin actividad industrial que se localiza fuera de los 25 km del área de influencia de la pluma de dispersión de contaminantes del sitio emisor: el corredor industrial Tula-Vito-Apasco (TVA). En este corredor se ubican tres parques industriales, que generan más del 90% de las emisiones de PM_{10}, $PM_{2.5}$, SO_2, CO, NO_x y NH_3 en el estado de Hidalgo, las cuales se dispersan en un radio de

aproximadamente 25 km[7]. Los ejemplares colectados se trasplantaron en el sitio receptor: Tlaxcoapan, Hgo., (20°05'43" N, 99°13'12"O), ciudad agrícola, ubicada a 7 km lineales al noreste del corredor industrial TVA[8,9]. También se expusieron muestras de *T. usneoides* en el sitio control: Actopan, Hgo. (20° 16' 12" N, 98° 57' 42" O), ciudad con poco desarrollo urbano, circulación automovilística escasa y sin actividad industrial, localizada a 35 y 42 km lineales al sureste, respectivamente, de Tlaxcoapan y del corredor industrial TVA[10], lo que la ubica fuera del área de influencia de la pluma contaminante.

Preparación de material vegetal. Los ejemplares colectados de *T. usenoides* se lavaron con agua de la llave, para quitar el polvo que las cubría y se dejaron secar al aire. Después se tomó una muestra, se enjuagó con agua destilada y se eliminó el exceso de agua para determinar los valores iniciales de los biomarcadores de efecto (clorofilas, proteína total, ácido ascórbico y actividades enzimáticas: SOD, POD y NR) y de los elementos químicos (Ca, Cu, Cd, Fe, Mg, Mn, Ni, Pb y Zn) como biomarcadores de exposición. El resto del material colectado fue expuesto en los sitios receptor y control durante 8 meses (de febrero a octubre de 2012). Después de la exposición se analizaron nuevamente ambos grupos de biomarcadores en las muestras. Todas las determinaciones se realizaron por sextuplicado.

Determinación de los biomarcadores de exposición: elementos químicos. Se realizó la digestión ácida de 0.2 g de muestra de acuerdo al método EPA 3052[11], y después se cuantificó el contenido de metales por espectrofotometría de absorción atómica (Varian, Spectra AA-800, Australia). Los elementos analizados en el biomonitor fueron: Ca, Cu, Cd, Fe, Mg, Mn, Ni, Pb y Zn.

Determinación de biomarcadores de efecto en T. usenoides. Para el análisis de las clorofilas a y b, se pesaron 0.2 g de muestra fresca y se analizaron de acuerdo al procedimiento descrito por Menéndez[12]. Para el resto de las determinaciones biológicas se obtuvo un extracto de la siguiente manera: se pesaron 0.2 g de *T. usenoides*, y se maceraron con 6 mL de solución tampón 50 mM de Tris-HCl (pH 7.5). La suspensión se centrifugó a 12 000 rpm durante 15 min. El extracto se conservó en un baño de hielo para mantener las condiciones ideales (3°C) para cada una de las determinaciones siguientes. Las proteínas totales se cuantificaron tratando 500 µL del extracto de cada muestra con un volumen igual del reactivo de Bradford de acuerdo al protocolo de Bradford[13]. La actividad peroxidasa (POD) se determinó siguiendo el procedimiento propuesto por Putter[14] y Malik y Singh[15]. Las actividades superóxido dismutasa (SOD) y nitrato reductasa (NR) y el contenido de ácido ascórbico se determinaron conforme a los métodos descritos por Sadasivam y Manickam[16].

RESULTADOS Y DISCUSIÓN

Determinación de biomarcadores de exposición: elementos químicos. En la **Figura 1a** se puede observar que la concentración de Pb al inicio del experimento fue menor al límite de detección, mientras que al final sí fue detectable y significativamente diferente ($p < 0.05$) entre los sitios: 2.5 mg kg^{-1} en el sitio control (Actopan) y 73.7 mg kg^{-1} en el sitio receptor (Tlaxoapan). Los datos anteriores confirman la utilidad que tiene *T. usenoides* como biomonitor de Pb en la atmósfera, dado el amplio rango de concentraciones en que lo puede retener. Calvario-Rivera[17] y Martínez-Carrillo et al.[18] encontraron este mismo comportamiento de *T. usenoides* con respecto al Pb.

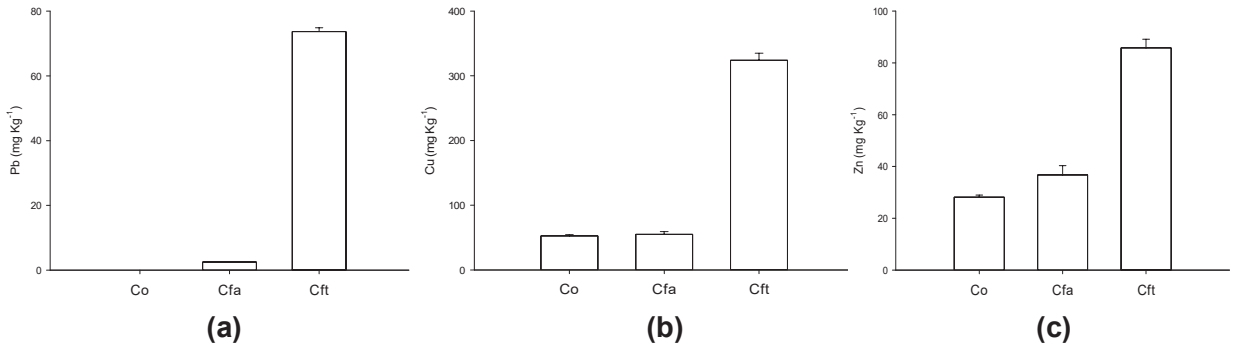


FIGURA 1. Concentración de Pb (a), Cu (b) y Zn (c) en el biomonitor. Co: concentración inicial, Cfa y Cft: concentración final en Actopan y Tlaxcoapan, respectivamente

En el caso del Cu, la concentración final en Actopan (55.08 mg kg^{-1}) fue muy similar a la inicial (52.5 mg kg^{-1}), en tanto que en Tlaxcoapan hubo un aumento significativo con respecto a las dos concentraciones anteriores (324.18 mg kg^{-1}, $p < 0.05$) (**Figura 1b**). Al igual que en el caso del Pb, es evidente que *T. usenoides* responde a la presencia de Cu en un amplio rango de concentraciones.

El Zn se comportó de manera similar al Cu: en Actopan, al final del experimento, hubo un ligero incremento con respecto a la concentración inicial en el biomonitor (de 28.13 a 36.73 mg·kg^{-1}), a diferencia de Tlaxcoapan donde la concentración final fue igual a 85.79 mg·kg^{-1} (**Figura 1c**). Según indican los resultados de Pb, Cu y Zn en *T. usneoides* el contenido de estos elementos es significativamente mayor en Tlaxcoapan, el sitio receptor.Entre las fuentes emisoras de estos metales, en los sitios de estudio se encuentran: fuentes generadoras de energía (Pb) tráfico vehicular (Pb y Cu) ,actividad agrícola (Cu y Zn) y fundidoras de metales (Cu y Zn).

En la **Figura 2a** se observa que el Mg también presentó un incremento significativo en ambos sitios al final de la exposición. Sin embargo, a diferencia de los metales anteriores, la mayor concentración se detectó en Actopan: 3.5 veces mayor que la inicial (1383.37 mg·kg^{-1}) mientras que en Tlaxcoapan fue solo 2.5 veces mayor. El Mg fue uno de los elementos que el biomonitor retuvo en grandes concentraciones.

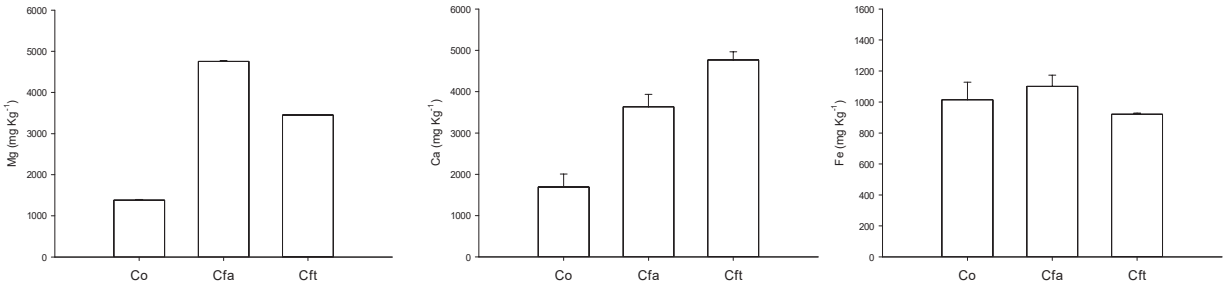


FIGURA 2. Concentración de Mg (a), Ca (b) y Fe (c) en el biomonitor. Co: concentración inicial, Cfa y Cft: concentración final en Actopan y Tlaxcoapan, respectivamente

El Ca fue el elemento que *T. usneoides* retuvo en mayor concentración. En la **Figura 2b** se puede apreciar la diferencia entre la concentración inicial (1692.07 $mg \cdot kg^{-1}$) y las finales (3364.13 y 4768.50 $mg \cdot kg^{-1}$, en Actopan y Tlaxcoapan, respectivamente), las cuales fueron significativamente diferentes entre sí ($p < 0.05$). De acuerdo con Owega et al.[19] la mayoría de las plantas no tienen sistemas excretores para eliminar el exceso de Ca y la pared celular y la vacuola representan grandes sumideros de este elemento. Lo anterior, así como la retención de material particulado en los tricomas de *T. usneoides* podría explicar las concentraciones de Ca encontradas en el biomonitor. Otros investigadores, como Calvario-Rivera[17] y Zambrano et al.[20] han encontrado en *T. usneoides* y en *T. recurvata*, respectivamente, concentraciones de Ca, similares a las reportadas en este estudio. La abundancia de Ca y Mg en el biomonitor podría explicarse por la actividad de las empresas productoras de cal y cemento en los parques del corredor industrial TVA.

Por otra parte, el Fe no presentó variaciones significativas como se observa en la **Figura 2c**: la concentración inicial fue de 1014.15±114.15 mg kg^{-1} y después de la exposición incrementó ligeramente en Actopan (1100.86±72.86 mg kg-1) mientras que en Tlaxcoapan disminuyó (921.74±7.18 mg kg^{-1}).

La concentración de Mn permaneció prácticamente constante, de 609.26 mg kg^{-1} al inicio disminuyó a 589.10 mg kg^{-1} y 595.40 mg kg^{-1} en Actopan y Tlaxcoapan, respectivamente, después de la exposición. Roholla et al.[21] encontraron que la acumulación de Mn en las plantas tiende a disminuir por la asimilación de Mg y Ca, los cuales fueron elementos mayoritarios en los tejidos del biomonitor. Esta podría ser una causa del ligero descenso que se observó en este estudio.

Las concentraciones de Ni y Cd en el biomonitor se encontraron por debajo del límite de detección.

Determinación de biomarcadores de efecto en T. usenoides

Clorofilas a y b. En ambos sitios de estudio se observó un aumento significativo ($p< 0.05$) en la producción de clorofila *a* al final del experimento. En el sitio control (Actopan) el incremento fue del 39%, mientras que en el sitio receptor (Tlaxcoapan) fue del 15% (**Figura 3a**). El contenido final de clorofila *b* también fue significativamente mayor al final

de la exposición en ambos sitios, 31% en Actopan y 19% en Tlaxcoapan ($p < 0.05$, **Figura 3b**). Este aumento en la producción de clorofilas puede explicarse por el acondicionamiento que se les dio a las plantas antes de la exposición y por la forma en que fueron expuestas. Debido a que las plantas se lavaron antes de exponerlas se eliminó una cantidad considerable de polvo, proveniente de las vialidades no pavimentadas del sitio basal. En diversos estudios se ha comprobado que el polvo interfiere con el proceso de fotosíntesis al reducir la cantidad de luz que recibe la planta y también al alterar el proceso de difusión de gases[22,23]. La cantidad de radiación solar que recibe una planta es un factor determinante en su actividad fotosintética; incluso, en una misma planta las partes más expuestas a la luz solar tienen una tasa fotosintética mayor que las que están en semisombra[24]. Generalmente *T. usneoides* crece en los árboles semiprotegida de la luz solar, en cambio en el experimento, las muestras se expusieron formando una cortina, de manera que toda la planta recibía luz solar.

Por la diferencia observada en las concentraciones de clorofilas *a* y *b* en los sitios de estudio, podría pensarse que el biomonitor expuesto en Tlaxcoapan experimentó algún tipo de estrés que afectó su actividad fotosintética. Dado que las condiciones climáticas son similares en ambos sitios, se descartaron como un factor que pudiera explicar estas diferencias. Por otra parte, se sabe que algunos contaminantes, como los metales, pueden alterar la fotosíntesis[24,25]. De los metales evaluados en este experimento, las concentraciones finales de Ca, Cu, Pb y Zn en el biomonitor expuesto en Tlaxcoapan fueron significativamente mayores que las iniciales y que las encontradas en Actopan, lo que podría sugerir un posible efecto adverso de estos metales sobre la fotosíntesis. Sin embargo, el análisis de correlaciones de Pearson no apoyó esta idea, ya que las correlaciones encontradas entre los metales antes mencionados y las clorofilas fueron positivas. Únicamente se encontraron correlaciones negativas de la clorofila *b* con el Fe ($r = -0.980$, $p < 0.01$) y con el Mn ($r = -0.940$, $p < 0.01$), ambos micronutrientes, con concentraciones similares en los biomonitores de los dos sitios.

Proteínas totales. Al final del experimento el contenido de proteínas disminuyó prácticamente en la misma proporción en ambos sitios (17% en Actopan y 16% en Tlaxcoapan) (**Figura 3c**). Algunos contaminantes, como los metales, pueden provocar un mal plegamiento de las estructuras de las proteínas, o bien inducir la formación de especies reactivas de oxígeno, que a su vez provocan la desnaturalización de las proteínas[26]. En Actopan se encontró una correlación negativa entre el contenido de proteínas y las concentraciones de Pb, Mg y Ca en el biomonitor ($r = -0.814$, -0.817 y -0.869, respectivamente, $p \leq 0.05$). En Tlaxcoapan las correlaciones encontradas entre la concentración de proteínas y los metales anteriores presentaron valores de r entre -0.745 y -0.759; sin embargo, no fueron significativas. Con base en los datos anteriores, podría pensarse que el Pb, Mg y Ca afectaron directa o indirectamente la producción de proteínas. Cabe mencionar que Ca y Mg actúan como cofactores de algunas proteínas con actividad enzimática[27]. Sin embargo, la correlación negativa que presentaron con las proteínas en este trabajo pudo deberse a las concentraciones tan elevadas en que se encontraron estos metales en el biomonitor.

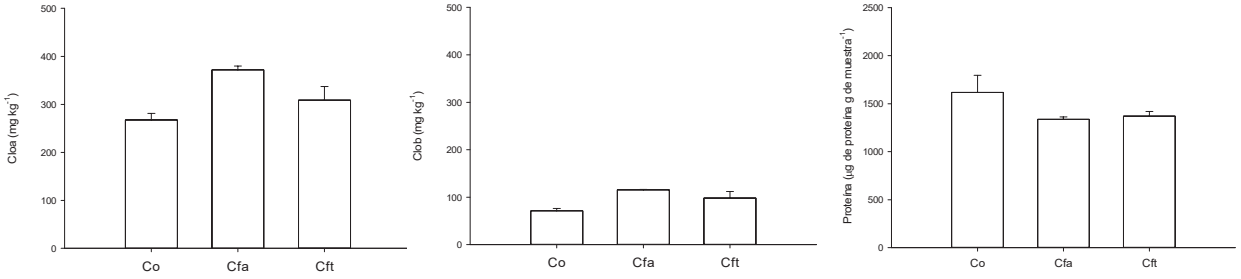


FIGURA 3. Concentración de clorofila *a* (a), clorofila *b* (b) y proteínas totales (c) en el biomonitor. Co: concentración inicial, Cfa y Cft: concentración final en Actopan y Tlaxcoapan, respectivamente

Actividad peroxidasa (POD). En Actopan, la actividad POD no presentó cambios significativos (2.22±1.30 μmol min g de muestra^{-1}) con respecto a la actividad inicial (2.35 μmol min g de muestra^{-1}). En Tlaxcoapan, por el contrario, esta actividad fue seis veces mayor (12.98 μmol min g de muestra^{-1}) y significativamente diferente con respecto a la inicial y a la de Actopan ($p < 0.05$, 20) (**Figura 4a**). Las POD, junto con la SOD y la ferritina, son los antioxidantes primarios que protegen a los organismos del estrés oxidativo. Entre los contaminantes atmosféricos que pueden causar este tipo de estrés se encuentran los NO_x, SO_2, O_3 y metales[28].

El incremento de la actividad POD en Tlaxcoapan se correlacionó positivamente con los contenidos de Ca, Cu, Mg, Pb y Zn en el biomonitor ($0.738 \leq r \leq 0.764$). Sin embargo, estas correlaciones no resultaron significativas. La única correlación significativa que se encontró fue con la actividad SOD ($r = -0.911$, $p < 0.05$). Los datos anteriores indican que el incremento de los metales antes mencionados en el biomonitor podría ser un factor estresante que incentiva la actividad POD, pero no así la actividad SOD. Esto último se discutirá más adelante.

***Superóxido dismutasa (SOD*).** La actividad SOD fue prácticamente la misma al inicio que al final del experimento (9.12±0.06 a 10.00±0.00 U g^{-1}). El comportamiento observado de la actividad SOD ha sido reportado en otros estudios. Li[29] (2003) encontró que la actividad SOD no variaba, en las hojas de *Ficus microcarpa*, en función de la concentración de contaminantes atmosféricos. En abetos rojos[30], bajo condiciones de laboratorio y en plantas de calabaza[31], la actividad SOD tampoco varió con la exposición a aire contaminado.

Nitrato reductasa (NR). En este experimento la actividad de la NR disminuyó ligeramente en el biomonitor expuesto en Actopan con respecto a la inicial (0.010 mol min g^{-1}); no así en Tlaxcoapan, donde se cuantificó una actividad 2.2 veces mayor que la inicial (**Figura 4b**). La NR es una enzima que se encuentra en la mayoría de las plantas superiores y es un regulador clave en la asimilación de nitrato[32]. Es válido suponer que existió una concentración suficiente de NO_x para inducir la acción de la NR en el biomonitor, de acuerdo al mecanismo que se comenta a continuación. Los NO_x, por encontrarse en forma gaseosa, entran a las plantas por medio de los estomas; una vez en el interior se disuelven en el agua intracelular trasformándose en NO^{3-}, sustrato

inductor de la NR. También es posible que los NO_x se depositen sobre la superficie foliar, en donde reaccionan con el agua para formar NO^{3-} que pueden ser asimilados por la planta[33].

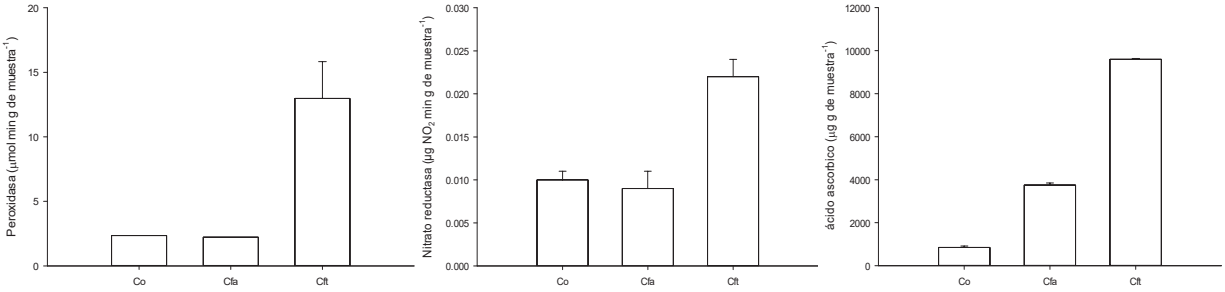


FIGURA 4. Concentración de POD (a), NR (b) y de ácido ascórbico (c) en el biomonitor. Co: concentración inicial, Cfa y Cft: concentración final en Actopan y Tlaxcoapan, respectivamente

Ácido ascórbico. En la **Figura 4c** se observa que el contenido de ácido ascórbico se incrementó significativamente en las muestras expuestas en Tlaxcoapan (9605 µg g^{-1}) con respecto a las de Actopan (3747 µg g^{-1}) y al estado inicial (848 µg g^{-1}) ($p < 0.05$). El contenido final en Actopan también fue significativamente mayor al inicial ($p < 0.05$). Un aumento en el contenido de ácido ascórbico es indicativo de la presencia de contaminantes, debido a que actúa como antioxidante para contrarrestar los efectos de los mismos. El ácido ascórbico protege a las macromoléculas del daño oxidativo que pueden causar las especies reactivas de oxígeno (ROS, por sus siglas en inglés), que se producen como respuesta a la presencia de contaminantes[34]. En este experimento, la producción de ácido ascórbico en Tlaxcoapan se correlacionó positivamente ($p \leq 0.01$) con las concentraciones de Ca ($r = 0.995$), Cu ($r = 0.998$), Pb, Zn y Mg ($r = 0.999$) y negativamente con las de Fe y Mn, también en el biomonitor ($r = -0.957$ y -0.997, respectivamente, $p \leq 0.01$).

En Actopan, la producción del ácido ascórbico se correlacionó positivamente con la actividad SOD y las concentraciones de Pb, Mg y Ca ($r = 0.987$, 0.994, 0.994 y 0.979, respectivamente, $p \leq 0.01$). Los datos anteriores parecen indicar que la producción de ácido ascórbico en *T. usenoides* se incrementó como respuesta a la presencia de Ca, Cu, Fe, Mn y Pb en las concentraciones encontradas en los sitios de estudio.

CONCLUSION

Los resultados mostraron que Tlaxcoapan sí es un sitio receptor de contaminantes generados en el corredor industrial TVA. Por otra parte, Actopan también presentó concentraciones importantes de algunos contaminantes, contrario a lo que se esperaría de un sitio control, por lo que sería interesante determinar el origen de la contaminación en este sitio.

En cuanto al biomonitor, se corroboró la efectividad de *T. usenoides* para reflejar cambios en la concentración de algunos elementos atmosféricos en un amplio. Se

confirmó la capacidad de acumulación de Ca y Pb de *T. usenoides*, lo que hace de estos dos elementos buenos biomarcadores de exposición en este biomonitor. En los que respecta a los biomarcadores de efecto, las clorofilas, el ácido ascórbico y la actividad POD podrían ser empleados como tales en este biomonitor.

También se encontró que los metales que se correlacionaron con la producción de las clorofilas, el ácido ascórbico y la actividad POD, fueron Pb, Ca, Fe, Mn, Mg y Cu. Dado lo anterior, sería interesante confirmar si la actividad POD se ve afectada a determinadas concentraciones de los elementos de estudio con los que presentó correlaciones negativas, principalmente Pb y Ca serían de interés, el primero por su carácter tóxico y el segundo por su abundancia en la zona de estudio.

AGRADECIMIENTOS

Los autores agradecen a la Quím. Argelia Vega por las facilidades otorgadas para la realización de este estudio. Asi como al CONACyT, por el financiamiento otorgado para la realización de esta investigación a través de proyecto Clave 106559 y la beca No. 325984, proporcionada a la M.B. Georgina Martínez Reséndiz para sus estudios de doctorado y por

REFERENCIAS

1. Dailianis, S. (2010). Environmental impact of anthropogenic activities: the use of mussels as a reliable tool for monitoring marine pollution. In: McGevin L. (Ed.) Mussels: Anatomy, Habitat and Environmental Impact. *Nova Science Publishers*. Patras, Greece. (2010).
2. Jemec, A., Drobne, D., Tišler, T., Sepčić, K. Biochemical biomarkers in environmental studies-lessons learnt from enzymes catalase, glutathione *S*-transferase and cholinesterase in two crustacean species*. Environmental Sci. Poll. Res. 25* (2009). 1-11.
3. Mena-Ulecia, K., Guanche-Gallardo, D., Hernández-Hernández, H. Marcadores de estrés oxidativo en raíces de *Allium* cepa L. expuestas a las aguas contaminadas del río Cojímar. *Revista CENIC Ciencias Biológicas*. 41 (2010) 189-193.
4. Markert, B.A., Breure, A.M., Zechmeister H.G. Definitions, strategies and principles for bioindication/biomonitoring of the environment. In: Markert, B.A., Breure, A.M. Zechmeister, H.G. (Eds) Bioindicators and Biomonitors. Oxford*.* (2003).
5. Carbone, S., N'siala, M.S., Gatti, A., Capitani, F., Vianello, G., Antisari, L. Exposure of *Tillandsia usneoides* at silver nanoparticles. *Brno, Czech Republic*. 10 (2012) 23-25.
6. Martínez-Reséndiz, G., Lucho-Constantino, C.A., Vázquez-Rodríguez, G.A., Coronel-Olivares, C., Beltrán-Hernández, R.I. *Tillandsia usneoides* as biomonitor of air pollution. AARJM. 2(6) (2015) 262-285
7. SEMARNAT, Secretaría de Medio Ambiente y Recursos Naturales. Inventario de emisiones de la Región Tula-Tepejl, 2005. (2009).
8. De Foy, B., Fast, D.J., Paech, J.S., Phillips, D., Walters, T.J., Coulter, L.R., Martin, J.T., Pekour, S.M., Shaw, J.W., Kastendeuch, P.P., Marley, A.N., Retama, A., Molina, T.L. Basin scale wind transport during the MILAGRO field campaign and comparison to climatology using cluster analysis. *Atmos. Chem. Phys. Discuss.* 7 (2007) 13035-13076.
9. Rivera, C., Sosa, G., Höhrnschimmel, H., De Foy, B., Johansson, M., Galle, B. Tula industrial complex (Mexico) emission of SO_2 and NO_2 during the MCMA 2006 field campaign using a Mini-DOAS system. *Atmos. Chem. Phys. Discuss.* 9 (2009) 5153-5176.

10. Enciclopedia de los Municipios de México (2005): Instituto Nacional para el Federalismo y el Desarrollo Municipal, Gobierno del Estado de Hidalgo. Retrieved from: http://www.inafed.gob.mx/work/enciclopedia/EMM13hidalgo/municipios/13003a.html.
11. EPA. Method 3052 Microwave assisted acid digestion of siliceous and organically based matrices. Environmental Protection Agency. (1996). Retrieved from: www.caslab.com/EPA-Methods/PDF/EPAMethod-3052.pdf
12. Menéndez, M. Manual de procedimientos analíticos para muestras ambientales. 7004UY Determinación de clorofila a, b y c1+c2 y Feopigmentos de clorofila a (feofitina a) encontrados en fitoplancton de agua dulce y marina. Método espectrofotométrico de extracción con acetona. DINAMA. (2009) 1-9.
13. Bradford, M.M. A rapid and sensitive method for the quantitation of microgram quantities of protein utilizing the principle of protein-dye binding. *Anal Biochem*. 72 (1976) 248-254.
14. Putter, J. In: Methods of Enzymatic Analysis 2 (Ed. Bergmeyer) Academic Press New York, (1991).
15. Malick, C.P. y Singh, M.B. Plant enzymology and histoenzymology. Kalyani Publishers New Delhi. (1980).
16. Sadasivam, S. Manickam, A. Biochemical Methods. India, New Age International. (1996). p 56.
17. Calvario-Rivera C.I. Monitoreo y biomonitoreo de elementos atmosféricos en la región de Tula-Tepeji empleando *Tillandsia usneoides* L. Tesis de doctorado. Pachuca, Hidalgo, México: Universidad Autónoma del Estado de Hidalgo. (2012).
18. Martínez-Carrillo, M.A., Solís, C., Andrade, E., Isaac-Olivé, K., Rocha, M., Murillo, G., Beltrán-Hernández, R.I., Lucho-Constantino, C.A. PIXE analysis of *Tillandsia usneoides* for air pollution studies at an industrial zone in Central Mexico. *Microchem. J*. 21 (2010) 1-15.
19. Owega, S., Evans, G. J., Jervis, R. E., Tsai, J., Kremer, E., & Tan, P. V. LAMS, Laser Ablation/Ionization Mass Spectrometry for Aerosol Characterization and Source Apportioning. Biomonitoring of atmospheric pollution (with emphasis on trace elements)-*BioMAP II*. (2003) 77.
20. Zambrano G.A., Medina, C.A., Rojas, López, V.D., Chang, M.L, Sosa, I.G. Distribution and sources of bioaccumulative air pollutants at Mezquital Valley, Mexico, as reflected by the atmospheric plant *Tillandsia recurvata* L. *Atmospheric Chemestry Physics*. 9 (2009) 6479-6494.
21. Roholla, M. S., Shahsavari, M., Rezaei, M. A general overview on manganese (Mn) importance for crops production. Australian Journal of Basic and Applied Sciences. (2011) 1799-1803.
22. Thawale, P.R., Satheesh, B.S., Wakode, R.R., Singh, S.K., Kumar, S., Juwarkar, A.A. Biochemical changes in plant leaves as a biomarker of pollution due to anthropogenic activity. Environmental Monitoring and Assessment. 177 (2011) 527-35.
23. Thompson, J.R., Mueller, P.W., Flückiger†, W., Rutter, A.J. The effect of dust on photosynthesis and its significance for roadside plants. Environmental Pollution Series A, Ecological and Biological. 34 (1984) 171-190.
24. Azcón-Bieto, R., Pardo, A., Gómez-Casanovas, N., Irigoyen, J. J., Sánchez-Díaz, M. Respuestas de la fotosíntesis y la respiración en un medio ambiente variable. En: Reigosa, M. J., Pedro, B. N. y Sánchez, M. A. (Eds.) La Ecofisiología Vegetal. Una Ciencia de Síntesis. Thomson. Madrid. (2003) p. 873-900.
25. Dazy, M., Masfaraud, J.F., Férard, J.F. Induction of oxidative stress biomarkers associated with heavy metal stress in *Fontinalis antipyretica* Hedw. *Chemosphere*. 75 (2009) 297-302.
26. Shaw, B. P., Sahu, S.K. y Mishra, R. K. Heavy metals induced oxidative damage in terrestrial plants. Heavy metals stress in plants. M. N. V. Prasad. Hyderabad, Springer (2004) 46.
27. Goday A., Pagés, M. Proteínas de respuesta al estrés hídrico. In: Reigosa, M. J., Pedrol, B. N. y Sánchez, M. A. (Eds.) La Ecofisiología Vegetal. Una Ciencia de Síntesis. Thomson. Madrid. (2004).

28. Pukacka, S., Pukacki, M.P. Seasonal changes in antioxidant level of Scots pine (*Pinus sylvestris* L.) needles exposed to industrial pollution. I. Ascorbate and thiol content. *Acta Physiologiae Plantarum*. 22 (2000) 451-456.
29. Li, H.M. Peroxidase and superoxide dismutase activities in fig Leaves in response to ambient air pollution in a subtropical city. *Archives of Environmental Contamination and Toxicology*. 45 (2003) 168-176.
30. Nast, W., Mortensen, L., Fischer, K. Fitting, I. Effects of air pollutants on the growth and antioxidative system of Norway spruce exposed in open-top chambers. *Environmental Pollution*. 80 (1993) 85-90.
31. Ranieri, A., Schenone, G., Lencioni, L., Soldatini, G.F. Detoxificant enzymes in pumpkin grown in polluted ambient air. *Journal of Environmental Quality*. 23 (1994) 360-364.
32. Campbell, W.H. Nitrate reductase and its role in nitrate assimilation in plants. *What´s new in plants phisiology*. 74 (1988) 214-219.
33. Rosas, P.I., Álvarez, C.D.E. Revisión y sistematización de la literatura nacional e internacional sobre los impactos de la contaminación del aire en cultivos agrícolas y forestales. Informe. Instituto Nacional de Ecología, 2009.
34. Bahl, A., Kahl, G. Air pollutant stress changes the steady-state transcript levels of three photosynthesis genes. *Environmental Pollution*. 88 (1995) 57-65.

CHAPTER 10.4 PARASITIC CONTAMINATION OF PUBLIC PLACES IN URBAN AND RURAL ENVIRONMENTS IN THE SLOVAK REPUBLIC

N. Sasáková *(1); I. Papajová (2); J. Pipiková (2); F. Tóth (2) and J. Venglovský (1)

(1) University of Veterinary Medicine and Pharmacy in Košice, Komenského 73, 041 81 Košice, Slovak Republic
(2) Institute of Parasitology of the Slovak Academy of Sciences, Hlinkova 3, 040 01 Košice, Slovak Republic

ABSTRACT

The present study was carried out to ascertain the presence of parasitic germs in dog's faeces collected at random from the public places in urban and rural localities in the eastern Slovakia. Out of 504 dog's excrements from public places, 28.4 % of them were found positive for the presence of the propagative stages of endoparasites. 8 species of intestinal endoparasites were detected in samples, dominated by *T. canis* eggs. Particularly, dogs from the big towns showed lower prevalence than dogs from smaller towns and villages. High prevalence of *Toxocara* spp. eggs and eggs of other intestinal helminths in dogs pointed to the contamination of the environment, in which animals move. Therefore, contamination of sand samples from the sandpits were also monitored. Out of 211 sandpits, parasite eggs were detected in 9.9 % of them. The unfenced sandpits were found to be more contaminated than fenced sandpits. Based on our resalts we can conclude that environment contaminated with eggs of endoparasites might pose the potential risk for spread of parasitosis among animals, but also in human population.

Keywords: dogs, endoparasites, environment, public places.

INTRODUCTION

The increasing densities of dog populations in urban and rural aglomeration and the close relationship of people with their animals provide the benefits to human beings. Besides these benefits, large populations of untreated owned animals or stray dogs and cats present a continuous reservoir of infection, contamination of the environment with parasitic germs and potential sources of infection to humans and other paratenic hosts.

Dogs are associated with more than 60 zoonotic parasites. These animals pose a serious zoonotic risk as they have the potential of to transmit zoonotic parasites through contamination of the environment with parasite eggs and oocysts in excrements[1]. Endoparasitic germs are highly resistant in outdoor environment and can survive in the environment for a long time and represent a risk factor for animals and also for the human population. Since the public places have free access to pet and stray animals, they potentially act as a source of contamination. Pets are brought to such public places for defeacation, thereby contaminating the soil.

---

*Author for correspondence: nada.sasakova@uvlf.sk

The present study was carried out to ascertain the presence of parasitic germs in dog's faeces collected at random from the public health importance places in urban and rural localities in the east part of Slovak Republic.

MATERIALS AND METHODS

Dog's faecal samples from towns (Košice Region - Košice, Trebišov, Veľké Kapušany; Prešov Region - Prešov, Snina, Levoča) and villages (Dlhé Stráže, Dravce, Valaliky) in eastern Slovakia were examined for the presence of parasitic germs. A total of 504 faecal samples of unknown dogs were collected at random from the different public places which are of public health importants (public parks, playgrounds, sandpits, sidewalks, road sides). 434 samples of dog's excrements were examined from the urban (Košice - 158, Trebišov - 64, Veľké Kapušany - 31, Prešov - 100, Snina - 23, Levoča - 58) and 70 samples from the rural (Valaliky - 37, Dlhé Stráže - 17, Dravce - 16) localities. After collection, faecal samples were stored at 4°C and examined for the presence of propagative stages of endoparasites. A flotation method with the Shaeter's flotation solution (specific gravity 1.3 $g.ml^{-1}$) was used for coprological examination. For the detection of *Giardia* oocysts, the Faust flotation solution (specific gravity 1.18 $g.ml^{-1}$) was used.

Sand samples collected from 211 children sandpits in order to identify the presence of parasite eggs in the environment were investigated. Out of them, 136 sandpits were from Košice, 6 from Valaliky, 24 from Veľké Kapušany, 30 from Prešov and 15 from Snina. The sandpits were classified as fenced and unfenced. The sand samples were investigated according to Kazacos[2]. Samples were examined under the light microscope.

RESULTS AND DISCUSSION

Dog's ownership in cities as well as in the countryside creates a continuing increasing trend. The problem of large towns is a high density of dog's faeces and thus high environmental burden. Dog's excrements in the grass, public parks, playgrounds, sandpits, sidewalks, road sides present not only aesthetic problems, but it is also problem of hygiene and epidemiology. Therefore, the possibility of soil contamination at different public places which are of public health importants with propagative stages of intestinal endoparasites in the Slovak Republic was monitored.

A total of 504 dog's faecal samples were examined and 143 were positive for the presence of the propagative stages of endoparasites. In the examined samples, 8 different species of intestinal parasites were detected. Toxocara *canis* eggs, *Trichuris* spp. eggs, eggs from the family Ancylostomatidae, *Taenia* type eggs, eggs of *Toxascaris leonina*, *Capillaria* spp., *Diphylidium caninum* and coccidia oocysts were present. Dog's faecal samples were divided into two groups according to their collection point - urban or rural localities. The differences of parasite eggs presence between urban and rural ecosystems were not recovered.

434 dog's faecal samples were collected from public places in towns and 27.9 % of examined samples were found positive for the presence of parasite germs. The occurrence of parasitic species in the excrements from the public places in selected towns is summarised in Table 1. In Košice Region, the highest prevalence of

endoparasite was found in towns Trebišov and Veľké Kapušany. The highest prevalence of intestinal parasites in dog's faeces from public areas in Prešov Region was found in Snina (**Table 1**).

TABLE 1. Occurence of dog's endoparasites in excrements from the public places in the urban localities in the eastern Slovakia

	Košice Region			Prešov Region		
	Košice (n-158) (%)	Trebišov (n-64) (%)	Veľké Kapušany (n-31) (%)	Prešov (n-100) (%)	Snina (n-23) (%)	Levoča (n-58) (%)
Toxocara canis	13.3	28.1	41.9	10.0	17.4	3.5
Toxascaris leonina	2.5	7.8	25.8	3.0	0	1.7
***Trichuris* spp.**	7.0	32.8	32.3	2.0	0	1.7
family Ancylostomatidae	2.5	22.0	45.2	5.0	21.8	3.5
***Capillaria* spp.**	0	0	19.4	0	0	0
Dipilidium caninum	0	0	0	0	0	1.7
family Taeniidae	0	0	0	0	0	24.1
coccidia oocysts	0	0	0	0	0	0
Total prevalence	24.1	57.8	61.3	18.0	39.1	32.8

n - number of examined samples

Only 70 dog's excrements were examined from studied villages and 3 different species (eggs from the family Taeniidae, T. canis and eggs from the family Ancylostomatidae) were detected (**Table 2**). Particularly, dogs from the big towns (Košice and Prešov) showed lower prevalence than dogs from smaller towns (Trebišov, Veľké Kapušany, Snina, Levoča) and villages (Valaliky, Dlhé Stráže, Dravce).

TABLE 2. Occurence of dog's endoparasites in excrements from the public places in the rural localities in the eastern Slovakia

	Košice Region	Prešov Region	
	Valaliky (n-37) (%)	Dlhé Stráže (n-17) (%)	Dravce (n-16) (%)
Toxocara canis	18.9	11.8	0
Toxascaris leonina	0	0	0
***Trichuris* spp.**	0	0	0
family Ancylostomatidae	16.2	0	0
***Capillaria* spp.**	0	0	0
Dipilidium caninum	0	0	0
family Taeniidae	0	0	29.4
coccidia oocysts	0	0	0
Total prevalence	32.4	41.2	18.8

n - number of examined samples

Several factors can influenced these differences. In fact, dogs from small towns and rural agglomerations are usually at high risk of infection being frequently outdoors in their gardens or in large green areas and the majority of them are not being in the care of a veterinarian. This is probably also due to free movement of dogs in the environment contaminated with faeces of wild animals and consumption of small mammals or wastes from dead and killed wild-boars[3]. In the studied rural localities and towns Trebišov, Veľké Kapušany and Levoča, there are also segregated Roma settlements with poor hygiene, bad socioeconomic status and lack of veterinary care for household animals. The animals from these localities have free movement without restriction and they can contaminate public places with excrements.

Among the recovered parasite species in dog's excrements, *T. canis* and Ancylostomatidae are considered of great public health significance[4,5]. High prevalence of *Toxocara* spp. eggs and eggs of other intestinal helminths in dog populations pointed to the contamination of the environment, in which animals move. Therefore contamination of sand samples from the sandpits were also monitored. Out of 211 sandpits, parasite eggs were detected in 9.9 % of them. The unfenced sandpits were found to be more contaminated than fenced sandpits (**Table 3**).

TABLE 3. Occurence of endoparasites germs in sandpits in the eastern Slovakia

	Košice (n/p)	Valaliky (n/p)	Veľké Kapušany (n/p)	Prešov (n/p)	Snina (n/p)
fenced	50/0	4/0	9/0	0/0	5/0
unfenced	86/10	2/2	15/5	30/4	10/0
total	136/10	6/2	24/5	30/4	15/0

n - number of examined samples, p - number of positive samples

Only *Toxocara* spp. eggs were detected in examined sandpits in Košice and Valaliky. In Veľké Kapušany, eggs from the family Ancylostomatidae, *Toxocara* spp. and *Trichuris* spp. eggs were present in 5 positive sandpits. The eggs of *Toxocara* spp. and eggs from the familly Ancylostomatidae were recovered in sandpits from Prešov. In Snina, no eggs were found in any of the investigated sandpits in Snina. Above mentioned parasites occured occasionally in examined sandpits. Animal faeces were not found in any of the sandpits. Our results correspond with those of other authors. In Slovak Republic, the prevalence of *Toxocara* spp. in sandpits ranged from 6.8 % to 28.3 %[6-8].

CONCLUSION

The results of the present study show that public places in studied urban and rural localities in the eastern Slovakia pose the main area for risk of human exposure eggs. Soil contamination is prevalent in peridomestic environments and is exacerbated by poverty, poor hygiene and the risk of contact with infected animals. In conclusion, intestinal parasites do represent a silent hazard not only for other animals, but also for the general public health.

ACKNOWLEDGMENTS

The study was supported by the Project VEGA No. 2/0140/13.

REFERENCES

1. Schär, F., Inpankaew, T., Traub, R. J., Khieu, V., Dalsgaard, A., Chimnoi, W., Chhoun, Ch., Sok, D., Marti, H., Muth, S., Odermatt, P. The prevalence and diversity of intestinal parasitic infections in humans and domestic animals in a rural Cambodian village. Parasitol. Int. 63 (2014) 597-603.
2. Kazacos, K. R. Improved method for recovering ascarid and other helminth eggs from soil associated with epizootics and during survey studies. Am. J. Vet. Res. 44 (1983) 896-900.
3. Antolová, D., Reiterová, K., Dubinský, P. The role of wild boars (*Sus scrofa*) in circulation of trichinelosis, toxascarosis and ascariosis in the Slovak Republic. Helminthologia 43 (2006) 92-97.
4. Lee, A. C., Schantz, P. M., Kazacos, K. R., Montgomery, S. P., Bowman, D. D. Epidemiologic and zoonotic aspects of ascarid infections in dogs and cats. Trends Parasitol., 26 (2010) 155-161.
5. Riggio, F., Mannella, R., Ariti, G., Perrucci, S. Intestinal and lung parasites in owned dogs and cats from central Italy. Vet. Parasitol. 193 (2013) 78-84.
6. Szabová, E., Juriš, P., Miterpáková, M., Antolová, D., Papajová, I., Šefčíková, H. Prevalence of important zoonotic parasites in dog populations from the Slovak Republic. Helminthologia 44 (2007) 170–176.
7. Ondriska, F., Mačuhová, K., Melicherová, J., Reiterová, K., Valentová, D., Beladičová, V., Halgoš, J. Toxocariasis in urban environment of western Slovakia. Helminthologia, 50 (2013) 261–268.

Section 11.
Environmental Engineering

Page

Chapter 11.1 Environmental considerations of underground water wells in La Rioja - Argentina 906
V. Calbo; O. J. Furlong; E. J. Marchevsky and M. Torres Deluigi

Chapter 11.2 The effect of substrate/inoculums ratio on the kinetics of methane production in swine wastewater anaerobic digestion 917
Verónica Córdoba; Mónica Fernández and Estela Santalla

Chapter 11.3 Compostaje del digestato producido en un reactor de hidrólisis anaerobia de lecho escurrido 929
R. Espinosa; G. Saucedo and O. Monroy

Chapter 11.4 Design of a bioretention cell for mitigating the effects of urban runoff in xeric climates 940
G. A. Vázquez-Rodríguez; J. E. Ortiz-Hernández; L. Lizárraga-Mendiola; C. Coronel-Olivares; R. I. Beltrán-Hernández; C. A. Lucho-Constantino and M. R. González-Sandoval

Chapter 11.5 Desempeño de suelos para uso pecuario construidos con geotextiles y material granulado 948
M. Vitón; J. Gasulla; M. Prieto and D. Crespo

Chapter 11.6 Airborne bacterial spore's inactivation with uv radiation over tio2 coated glass rings 956
M. L. Satuf; S. M. Zacarías; M.E. Visuara and O. M. Alfano

Chapter 11.7 Inactivation of *Aspergillus niger* with photocatalytic paints 965
S. M. Zacarías; R. Schumacher; F. Salvadores; O. M. Alfano and M. M. Ballari

CHAPTER 11.1 ENVIRONMENTAL CONSIDERATIONS OF UNDERGROUND WATER WELLS IN LA RIOJA - ARGENTINA

V. Calbo *(1,2); O. J. Furlong (3,4); E. J. Marchevsky (3) and M. Torres Deluigi (4)

(1) GAIA, Grupo de Actividades Interdisciplinarias Ambientales, UTN Facultad Regional La Rioja. San Nicolás de Bari Este 1100, CP 5300 La Rioja, Argentina.
(2) CENIIT, Centro de Investigación e Innovación Tecnológica, Universidad Nacional de La Rioja. Luis Vernet 1130, CP 5300, La Rioja, Argentina.
(3) CONICET, Argentina.
(4) Departamento de Física, Universidad Nacional de San Luis, Ejército de los Andes 950, CP 5700, San Luis, Argentina.

ABSTRACT

Recently, underground water studies were carried out in La Rioja within the framework of agreements with the World Bank. In these studies, two environmental issues to be considered were identified: the water quality against the rapid corrosion of pumping facilities in the capital city of La Rioja, and the disposal of waste from the reverse osmosis plants that are used to treat underground brackish water in some of the province departments.

Regarding the first issue, an already concluded study detected that the premature deterioration of the pumping facilities is due to the MIC (Microbiologically Induced Corrosion) phenomenon. Some signs of the MIC phenomenon in a well during its operation are the decrease of flow without a decrease in the phreatic level, and the alteration of the water organoleptic quality. Another sign appears during maintenance, in which the obstruction and embedding of filters and pressure pipes can be observed. These aforementioned signs are present in La Rioja.

In order to confirm the MIC phenomenon and propose the necessary corrective measures, microbiological and optical microscopy studies were performed. Complementarily, scanning electron microscopy tests were performed as well.

The microbiological cultures grown in liquid and solid media showed the presence of aerobic ferrobacteria (iron bacteria) and anaerobic sulfate-reducing bacteria, which is consistent with the MIC phenomenon.

During this phenomenon, bacteria accelerate the metal corrosion of the facilities. The rusted and dissolved metal precipitates as bacterial metabolites in the form of biominerals. These biominerals have the same chemical composition as the iron minerals but a peculiar structure. The scanning electron microscopy performed on the embedded samples detected the organic morphology of the mineral, and the energy dispersive spectrometer detected the spectrum of iron oxides.

The MIC phenomenon is confirmed, so that corrective and preventive measures are required, since it is possible that the bacteria are nonnative and reach the aquifers by contamination. These bacteria produce endospores when their environment is adversely altered, and reactivate when the conditions become adequate once again.

---

*Author for correspondence: vicentecalbo@yahoo.com.ar, ojfurlong@unsl.edu.ar

The spores can contaminate the drilling equipment, which in turn, can inoculate them in another aquifer.
Regarding the second issue, it is still under study. A priori, two alternatives are being considered for the disposal of the brackish water: natural evaporation in the case of facilities with low capacity, and the disposal in deep wells or very salty waters in the case of facilities with higher capacity.

Keywords: environment, La Rioja, underground, water.

INTRODUCTION

Underground water is a renewable resource whose utilization involves an investment for the perforation and equipment of the well, and the use of energy for its extraction. Underground water is used when surface water, which has a lower cost since it only requires its capture and conduction, is not available with enough quality or amount.

The province of La Rioja does not count with permanent water courses, and therefore livestock breeding mainly relies on harvesting of rainwater during the summer season and its subsequent storage in dams. Furthermore, the water for agriculture, industry and drinking water supply mainly comes from underground sources.

Recent studies performed by the IPALaR (Instituto Provincial del Agua de La Rioja, “La Rioja Water Provincial Institute”) within the framework of the National Bank, posed two issues to evaluate: a) the need of determining if the Microbiologically Induced Corrosion (MIC) phenomenon is the cause of the premature aging of the wells of the capital of La Rioja, and its implications regarding the population health; and b) disposal of the reject water from reverse osmosis plants in localities within the province[1].

Presented in this work are the results of the studies performed on the first issue, MIC phenomenon, while the second is still under investigation.

The study of the MIC phenomenon dates back to 1898, when bacteria that attack and precipitate iron were characterized as chemoautotrophs[2], determining that they obtained energy by the oxidation of Fe^{2+} to Fe^{3+}. Afterwards, two functional groups were defined: metallo-oxidizing bacteria, which attack and precipitate the metal, and metallo-precipitating non-oxidizing bacteria[3]. These are currently known as iron bacteria or ferrobacteria, although strictly speaking, they also oxidize and precipitate manganese. These bacteria are aerobic, mesophilic and develop in environments with a pH between 6.5-9.

After the ferrobacteria, sulfate-reducing bacteria (SRB) were detected, which generate the non-assimilatory reduction of sulfate and use this compound as final electron acceptor. The energy required for their metabolism is generated during these redox reactions, and the final result is the formation of sulphides. There are two domains associated with this process, Bacteria and Archaea; both microorganisms are encompassed within the SRB[4]. The SRB are obligate anaerobic bacteria; the adequate pH for their development is in the range of 6.5-8.5; they are mesophilic or slightly thermophilic; and they can be complete- or incomplete-oxidizing bacteria[5].

During the middle of the 20th century, these bacteria were associated with the premature aging of underground water pumping installations. In Argentina, the problem

was detected at the end of the last century in the provinces of Río Negro, Santa Cruz, Mendoza, Entre Ríos, La Pampa and Buenos Aires[6]. More recently, the province of Catamarca was added to this list, and as a result of the present work, this problem is also confirmed in La Rioja.

Bacteria in general, including the ones associated with the MIC phenomenon, can be planktonic (they develop suspended in a liquid medium) or sessile (they develop their cycle adhered to a surface), or present both behaviors. The bacteria associated to the MIC phenomenon are mainly sessile, but the resulting detachments acquire a planktonic behavior until they find another suitable surface to colonize, and this presents one of the possible pathways of contamination of other installations. The sessile bacteria form a layer on such surfaces called biofilm, which is formed in stages and is a structure within which the cells are scattered, and where most of the organic carbon is retained as an extracellular polymeric substance that acts as a protecting coating and a potential reserve of nutrients for the bacteria that live there[7].

The aerobic iron bacteria and the anaerobic SRB consume the material through different but complementary mechanisms, leading to its thinning or perforation. Another negative effect is the biofouling, which consists on the sedimentation and cementation of the bacteria metabolic products. Over time, each bacteria produces a specific sediment that increases its thickness layer after layer. When the surface affected corresponds to the inner side of a pipe (conductions) or holes (filters), the fouling or biofouling leads to an obstruction that eventually turns the installations inoperative. These effects are shown in **Figure 1**.



FIGURE 1: Effects of the MIC phenomenon (Left: layer corrosion, Right: biofouling)

The negative impacts of these problems are social due to the temporary shortages of drinking water, in particular in the capital city of La Rioja, and economic due to the cost of a more frequent maintenance/replacement of the installations. The problem is also critical since it involves a phenomenon susceptible to propagation (contamination)[8].

MATERIALS AND METHODS

The suspicion of the presence of the MIC phenomenon is due to signs or manifestations observed during the exploitation of some wells, mainly the decrease of the water flow rates without a decrease of the phreatic level, and changes in the water organoleptic quality.

During maintenance operations, in particular due to the replacement of the pump, the pipeline surface was observed. These observations revealed the presence of nodules, crusts, dark colors under brownish foulings, and perforations by pitting or scaling.

In order to confirm the presence of MIC microorganisms, combined bacteriological and microscopy techniques were used in the laboratory.

Bacteria involved in the MIC phenomenon correspond to several species and genders; therefore, diverse solutions and culture media (liquid and solid) were used, and an approximated composition of the bacterial consortium was determined through the combination of the results obtained. Different aliquots were subjected to a series of cultures in glass jars and test tubes, for which enriched and differential culture broths were used. **Figure 2** shows the sampling and inoculation procedures.



FIGURE 2: Sampling and inoculation. (a) Sampling, (b) Sample, (c) Inoculation, (d) SRB+

The inoculated culture media were incubated at 35 and 45°C. Subsequently, their morphological analysis was performed and monitored by Gram staining.

The first results obtained from the seeded media showed the presence of a few Gram-positive and coagulase-negative cocci, and some Gram-positive bacilli with endospores. In addition, many pleomorphic and heterotrophic Gram-negative bacilli. The culture media incubated at 45°C did not show any bacterial development, so that the present bacteria are mesophilic or slightly thermophilic.

In the media with Gram-positive bacteria inhibitors, a slow development of pleomorphic Gram-negative bacilli was observed. These did not ferment glucose nor lactose, and developed in aerobic conditions, so that it was discarded them being enterobacteria. Other Gram-negative prospered in special liquid and solid media for the development of SRB (with lactate, different mineral salts and sulfur) in anaerobic conditions. **Table 1** summarizes the results observed with the different solid media.

TABLE 1: Inoculations performed in solid media and observed developments

Solid media	Cocci +	Bacilli +	Bacilli -
Nutrient Agar enriched with thioglycolate	+	+	+
Blood Agar	+	+	+
Chocolate Agar	+	+	+
MacConkey	-	+	-
Levine	Not seeded	+	-
CLED	Not seeded	+	-
TSI	Not seeded	Not seeded	-
E.M.B.	Not seeded	Not seeded	-

In addition, optical microscopy and morphological analysis of petri dish cultures were performed.

Complementarily, scanning electron microscopy (SEM) studies were carried out on the samples. This was done in a LEO 1450-VP microscope (see **Figure 3**) from the Laboratory of Electron Microscopy and Microanalysis (LABMEM) of the National University of San Luis (UNSL), Argentina. The SEM allows obtaining high-resolution images of the shape of objects down to the nanometer range, and also counts with analytical capabilities by means of EDS (Energy-Dispersive X-Ray Spectroscopy), which provides information on the chemical composition of solid samples[9].



FIGURE 3: Scanning Electron Microscope. 1) WDS spectrometer, 2) EDS spectrometer, 3) Backscattered electron detector, 4) Secondary electron detector, 5) Electron gun, and 6) Chamber

RESULTS AND DISCUSSION

The preliminary evaluation of the observed signs indicated the probable presence of the MIC phenomenon in the underground water wells of the capital city of La Rioja. The operating life of the pumping installations is relatively short, and in numerous occasions during the maintenance operations, effects of this phenomenon were observed, such as corrosion, pitting and obstruction of the pipelines.

The laboratory cultures of the foulings turn out positive for both, ferrobacteria (**Figure 4**) as well as SRB.

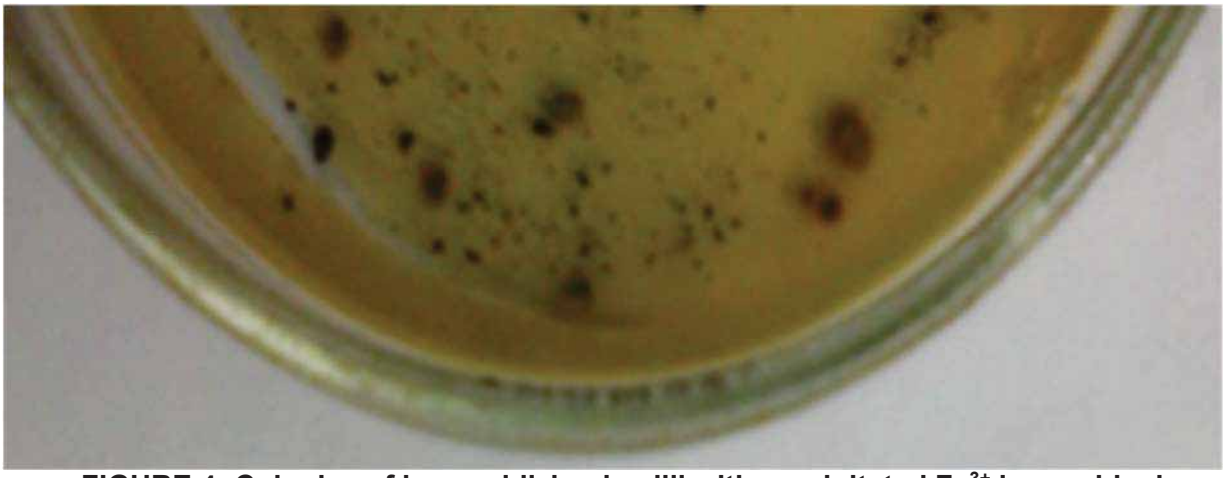


FIGURE 4: Colonies of iron-oxidizing bacilli with precipitated Fe^{3+} in aerobiosis

The optical microscopy allowed to directly observe these microorganisms and confirmed their sporulation capacity (**Figure 5**). The endospores are a latent form of life that allows these microorganism to survive if the environmental conditions become hostile; when the conditions become adequate once again they restart their cycle.

The foulings´ samples were also analyzed by SEM, and the obtained micrographs showed the peculiar shape of the foulings resulting from the iron bioprecipitation.

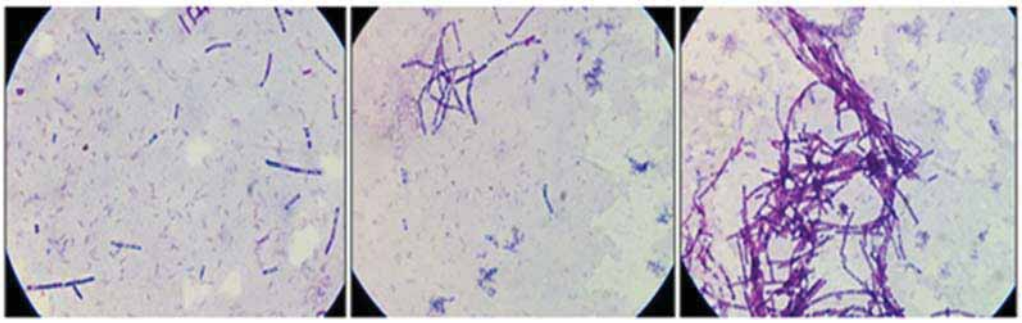


FIGURE 5: Endospores formation

The foulings present different coloration according to the pipeline side being analyzed. The outer side presents an ochre color, while the inner side is dark brown or black (**Figure 6**). This is due to the different metabolites that compose them. The outer

side corresponds to ferrobacteria metabolites and are composed of iron oxides, whose chemical formula is similar to iron minerals but present a peculiar shape.



FIGURE 6: Color of the foulings (Left: Ferrobacteria, Right: SRB)

It can be observed that the SRB have acted on the inner side of the pipe. Aerobic niches are formed there, where the aerobic ferrobacteria consume oxygen and form impermeable layers that inhibit the oxygen from reaching the interior of the biofilm. The SRB metabolites are iron sulphides.

It should be noted that, from the chemical point of view, the MIC is the same as the chemical corrosion, where the bacteria act as a catalytic agent that accelerate the chemistry kinetics. The difference lies on the morphology of the precipitates. The theoretical chemical reactions that explain this phenomenon are[6]:

Reactions of the ferrobacteria in aerobiosis:

$Me \rightarrow Me^{++} + 2e^-$ (Dissolution of the metal – Anodic reaction)

$O_2 + H_2O + 4e- \rightarrow 4OH^-$ (Electron capture – Cathodic reaction)

$3Me^{2+} + 6OH^- \rightarrow 3Me(OH)_2$ (Precipitation of insoluble products – Metabolites)

Reactions in the corrosion by SRB in anaerobiosis:

$4Fe \rightarrow 4Fe^{+2} + 8e^-$ (Anodic reaction)

$8H_2O \rightarrow 8H^+ + 8OH^-$ (Water dissociation)

$8H^+ + 8e^- \rightarrow 4H^2$ (Cathodic reaction)

$4H_2 + SO4^{-2} \rightarrow S^{-2} + 4H_2O$ (Bacterial cathodic depolarization)

$Fe^{+2} + S^{-2} \rightarrow FeS$ (Corrosion product)

$3Fe^{+2} + 6OH^- \rightarrow 3Fe(OH)_2$ (Corrosion product)

The Eh corresponding to the chemical reactions in the presence of ferrobacteria are in the range of 0-200 mV, while in the case of SRB are between 0 and -100 mV.

The SEM and microanalysis are consistent with the previous results. The micrographs show the morphology of the mineral metabolites (**Figure 7**), and the EDS spectra confirm the different metabolites corresponding to both, ferrobacteria as well as SRB (**Figure 8a** and **8b**, respectively). In the second case, sulfur is observed in addition to oxygen and iron.

The bacteria responsible for the CIM phenomenon can be indigenous or nonnative. In the second case, they could have entered the aquifer through water courses or nature's own mechanisms, or by anthropic action[10].

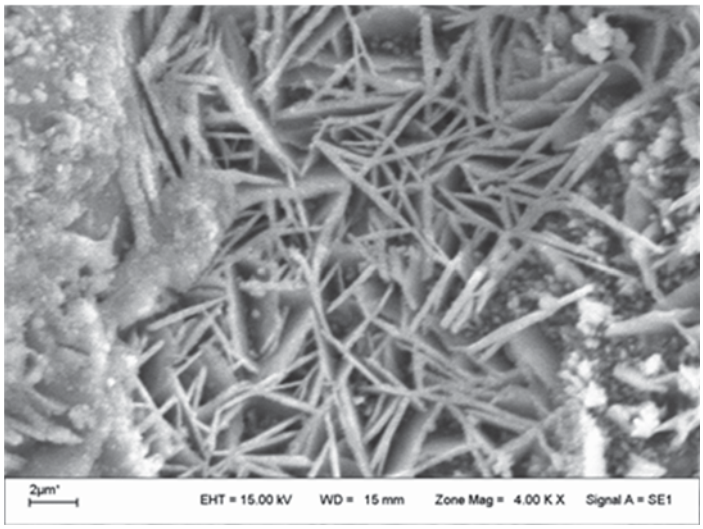


FIGURE 7: Micrograph of MIC phenomenon metabolites

In addition, it should be taken into account the possibility that, under the presence of indigenous bacteria, other bacteria (or their endospores) are introduced from the exterior adhered to metallic materials such as drills, pipes, pumps, etc. In this case, indigenous bacteria coexist with nonnative ones.

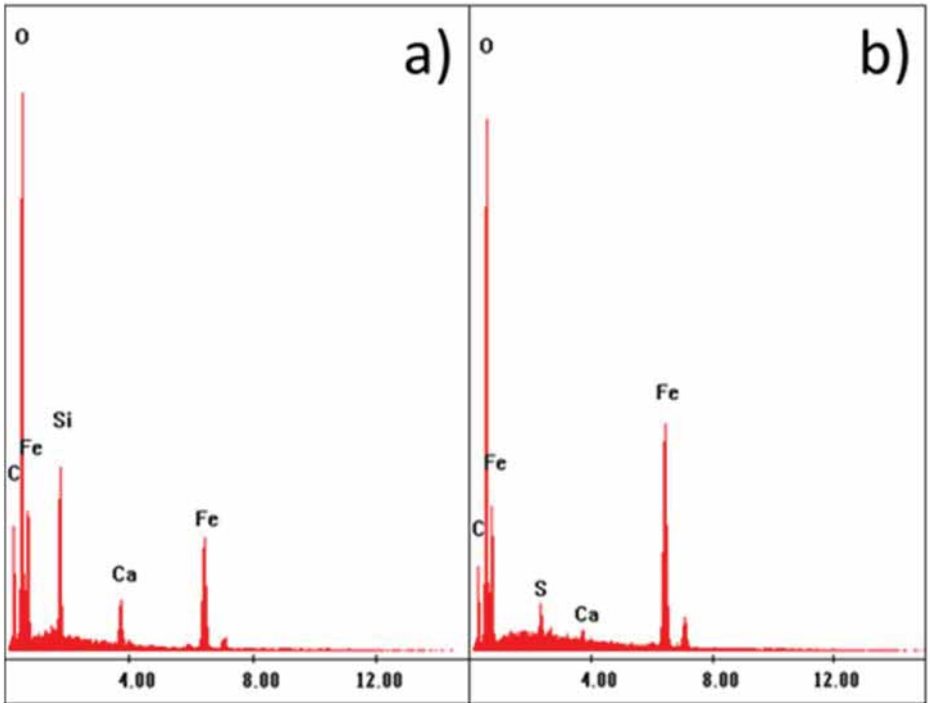


FIGURE 8: EDS spectra of the fouldings. a) outer side and b) inner side

The bacteria detected can present planktonic behavior or can be detached in the mucilage and migrate through the aquifer in the flow direction until finding a surface to adhere, such as the case of the tubing of another well, which would result in indigenous bacteria. They can also colonize the cast iron distribution networks or reach domestic and/or industrial installations.

The MIC phenomenon bacteria are non-pathogenic; however, they can affect the water quality causing gastrointestinal disorders. They are controlled by the chlorination of the water.

CONCLUSION

The MIC phenomenon has been confirmed in the underground water wells of La Rioja. It was initially detected through the evaluation of the observed signs. The bacteriological studies performed confirm the presence of both types of bacteria of the MIC phenomenon, ferrobacteria and SRB. It can also be concluded that there are mesophilic and slightly thermophilic bacteria among them, and that in several cases, it is found that they have sporulation capabilities. These data are important due to that they confirm the propagation risk by spores, and that the installations are susceptible to be thermally treated (pasteurization).

SEM studies were also performed on the pipelines surface samples and the fouldings, ratifying the presence of these microorganisms.

The MIC phenomena is foreseen as more serious or sever, since it can be present by anthropic propagation or by indigenous presence in other aquifers of the province. The bacteria associated to the phenomenon are not considered pathogenic, and therefore no analyses are performed for their detection and can go unnoticed.

A set of actions is proposed to reduce the impact in the medium-term and extend the service life of the underground water installations, as well as to prevent the propagation towards other installations. In addition to the costs reduction, this will also lower the inconveniences faced by the city inhabitants when the service is restricted due to maintenance operations and the replacement of pipelines and pumps.

In order to control the MIC phenomenon and avoid its propagation, it is recommended to:

- Keep a detailed log of the operations of each well.
- Periodically monitor with video probe inside the pressure pipes of the wells (**Figure 9**).
- Disinfect with hypochlorite all the equipment and tools of the perforation before making a well.
- Clean the sludge pump from previous residues and chlorinate the circuits of the perforation equipment.
- Treat the perforation sludges for their reuse as well as for their disposal.
- Treat the water that will be used for the preparation of the sludge in order to achieve sterility.
- Chlorinate the tools of the drill rig by immersing them in sodium or calcium hypochlorite solution, or to treat them thermally, and ensure the sterility of the gravel, casings and filters that are used in the termination of the well.

- Disinfect with vapor or hypochlorite solution the drill yards during the perforation execution as well as their maintenance, since contaminated detachments remain in them (**Figure 9**).
- Treat the new pumps, pipes and cables with hypochlorite solution before their installation.
- Treat the repaired pumps before introducing them into the perforation, especially if they are different from the original ones.
- Test other materials in tubings, such PVC, galvanized steel, etc.
- Compile a mandatory protocol for drilling companies (local and from other provinces).
- Compile information material for all the operators so that they become aware of the problem and its causes.



FIGURE 9: Video probe (left); drill yard (right)

REFERENCES

1. IPALAR Annual Report, 2014.
2. WINOGRADSKY S.J., *Eisenbacterien a ls anorgoxidanten Zentralblat für Bakternologie. Parasietenkunde und Infektions franhtheiten*. Abt., 1922,57,1-21.
3. CULLIMORE D.R., MCCANN A. E., *The Identification, Cultivation and control of Iron Bacteria in Ground Water*, Aquatic Microbiology: Shinner F. A., Shewa J. M. eds. Academic Press. Inc. New York, 1977
4. MÜYZER G., STAMS A.J.M., *The ecology and biotechnology of sulphate-reducing bacteria*. Nat. Rev. Microbiol. 2008.
5. WIDDEL F., *Microbiology and ecology of sulphate and sulphur reducing bacteria. Biology of anaerobic microorganisms*. Zehnder A.J.B., (Ed). Wiley Interscience, New York, USA. 1988, 469-586.
6. GARIBOGLIO M.A., SMITH S.A., *Corrosión e incrustación de microbiológica en sistemas de captación y conducción agua. Aspectos teóricos y aplicados*, Consejo Federal de Inversiones CFI. Buenos Aires, 1993.
7. CULLIMORE D.R*., Think Tank on Biofilms and Biofouling in Wells and Groundwater Systems*, Regina Water Research Institute, University of Regina, *Ed*. *IPSCO 1986.*
8. CALBO V. *Cooperación de Bacterias aeróbicas y anaeróbicas en la corrosión de perforaciones de agua subterránea***.** Terceras Jornadas de Vinculación y Transferencia Científica y Tecnológica de La Rioja, 2015

9. GOLDSTEIN J., NEWBURY D.E., JOY D.C., LYMAN C.E., ECHLIN P., LIFSHIN E., SAWYER L., MICHAEL J.R., *Scanning Electron Microscopy and X-ray Microanalysis*, 3rd ed., Springer, 2003.
10. DRISCOLL F.G., *Groundwater and Wells*, Johnson Filtration System Inc. 2nd ed., St. Paul, Minnesota, 1986.

CHAPTER 11.2 THE EFFECT OF SUBSTRATE/INOCULUMS RATIO ON THE KINETICS OF METHANE PRODUCTION IN SWINE WASTEWATER ANAEROBIC DIGESTION

Verónica Córdoba *(1)**;** Mónica Fernández (1) and Estela Santalla (1)

(1) Facultad de Ingeniería UNICEN. Av. Del Valle 5737. B7400 JWI Olavarría

ABSTRACT

Methane production from swine wastewater was evaluated by using sewage sludge as inoculums in three SIR (A: 1/1, B: 3/1, C: 6/1), with the objective to identify the ratio that optimizes the performance of the process. Duplicated batch bioreactors of 1 L capacity under mesophilic conditions were used to carry out the experience. The highest biogas yield was observed in A treatment (554±75 mL/g VS) followed by B (394±25 mL/g VS) and C (466±7 mL/g VS). Cumulative methane production decreased from (382±22) to (232±5 ml/g SV) when SIR increased from 1/1 to 6/1. Modified Gompertz equation was used to model the experimental cumulative methane yield. The effect of the SIR was analyzed based on the kinetic parameters methane production potential, maximum methane production rate and lag-phase time. The obtained results showed that Gompertz equation adjusted adequately the experimental data (R^2>0.99). The best performance in terms of the kinetic parameters was obtained for treatment A however treatment B could still ensure a stable process. The use of higher inoculums concentration generated 469.2% higher methane production rate and required 77.2% lower adaptation time (lag-phase) in the SIR range employed. When higher SIR is used (e.g.14/1, previous work) it could be observed that Gompertz equation also adjusted adequately the experimental data (R^2>0.99) although the lag-phase time did not remain in a linear relationship with SIR but exponential above SIR=6/1. These results demonstrated that when low amount of inoculums was used, the adaption time of microorganisms resulted much higher than expected delaying the methane production, extending the processing time needed to achieve adequate methane production.

Keywords: Inoculums, kinetics, methane production, swine wastewater.

INTRODUCTION

One of the most important current challenges is to find a solution to the pollution caused by waste and wastewater of industrial and agricultural activities and to satisfy the growing demand of energy[1]. The livestock sector has suffered big changes as a result of economic fluctuations, especially in developing countries. Livestock production, especially pigs and poultry, is becoming more intensive and more concentrated geographically[2]. The high concentration of animals per area is one of the main causes of

---

*Author for correspondence: vcordoba@fio.unicen.edu.ar

the increase of the amount of waste, characterized by its high organic matter content and inorganic nutrients concentration. Its inappropriate treatment has generated environmental problems on soil, water and air, such as odor generation, attraction of rodents, insects, release of pathogens agents, release of gases such as methane and ammonia, as well as nutrients such nitrogen and phosphorus, saturating thereby ability of systems to absorb these componentes[3]. Anaerobic digestion (AD) tend to solve partially this problem through the availability of renewable energy source based on the use of the methane generated[4]. However, the estimation of net energy to be produce through this process is a complex task due to the wide range of factors that affect methane production[5].

Between livestock waste, swine wastewater is considered an appropriate substrate to generate methane under AD due to its high water contents, high buffering capacity and a wide variety of nutrients needed for anaerobic bacteria[6]. However, it is also a complex substrate that contains undissolved and dissolved organic matter such as polysacharides, lipids, proteins and volatile fatty acids (VFA)[7,8] that interact during AD process in a complex system.

In an anaerobic reactor, methane is produced only by methanogenic bacteria[9]. These can be found among others, in the intestinal track of animals[10] and therefore they stay in swine wastewater. However, those bacteria were not adequate to achieve a good and steady performance for methane production in a short time, as could be demonstrated by Córdoba et al., (2016)[12] when used fresh liquid swine manure as substrate in AD without inoculum, where long process times were recorded. This result agreed with those reported by Llabrés-Luengo and Mata-Alvarez, (1987)[13], which indicated that if a digester is started without inoculum, intermediate compounds can accumulate and inhibit the bacterial activity. As a function of these results, the use of an inoculum is critical, where the quality and quantity of it is a key factor that determines the length of the start-up and operation in a steady state of the reactor[9].

Different types of inoculums have been used in AD under mesophilic conditions. Córdoba et al (2016)[12] used stabilized swine manure, sewage sludge and bovine rumen fluid as inoculums in AD of fresh swine wastewater and results showed that inoculation improved the productivity in the AD process in terms of biogas and methane productions. However, between them, sewage sludge and stabilized liquid swine manure showed better capacity than rumen to improve methane production. One of the problems founded in that research was that the low inoculum concentration used resulted in a long processing time. Based on these results, it is necessary to determine the most suitable concentration of inoculum in order to obtain high methane production in a short time. The inoculum concentration in an anaerobic reactor can be expressed as a function of a parameter called substrate to inoculum ratio (SIR).

Several investigations have been conducted in order to determine the best SIR; in general it has been found that there is a strong dependence between the physical-chemical characteristic of inoculums and substrates on methane production. Neves et al., (2004)[14] used four SIR in the range 0.5 to 2.3 and two types of sludge inoculum (granular and suspended) in the AD of kitchen waste finding that granular inoculum prevents acidification of the reactors throughout the range of SIR studied, but in the case of suspended sludge acidification was only prevented with the lower SIR. Chynoweth et al., (1993)[15] found out that the decrease in SIR may be necessary for recalcitrant

substrates suggesting a ratio of 0.5 to 1. Liu et al., (2009)[16] showed that the SIR significantly affected the biogas production in AD of food and green waste. Whilst, Chynoweth et al., (1999)[3] reported that careful attention should be paid to SIR when batch reactors are used.

The objective of the present study is to identify the optimal SIR that increases the methane production of AD of swine wastewater. Experimental data of methane production will be adjusted to a non linel model to obtain the kinetics parameters of the process with the purpose of identifying the condition that ensure a stable methane production.

MATERIALS AND METHODS

Substrate and Inoculum used for anaerobic digestion assay. The substrate used was liquid fresh swine wastewater collected from a piggery the same day that was produced and previous to the discharge in a covered lagoon.

Sewage sludge obtained from the local wastewater treatment plant was used as inoculum. In order to ensure the degradation of the easily degradable organic matter that could be still present in the inoculum, it was maintained in a batch reactor at mesophilic conditions at 35°C ±1 until use[12].

Experimental design. Three treatment in duplicated were carried out in a batch laboratory-scale experiment, using the SIR of 1/1, 3/1 and 6/1. Samples were prepared by mixing S and I in the proportions showed in **Table 1**. The mixtures were prepared using the same volume of substrate and adding the volume of inoculums until achieves the selected SIR. No water was added to the digester due to the total solids content of the substrate resulted in less than 10% assuring wet anaerobic digestion[17].

TABLE 1. Experimental design

Treatment	Volume (mL)		SIR
	S	I	g VS S/g VS I
A	250	533.3	1/1
B	250	177.8	3/1
C	250	88.9	6/1

Bioreactors of 1000 mL capacity were filled with each one of the mixtures and were kept in a thermostatic water bath at 35°C according to Córdoba et al (2016)[12]. Experiment was daily monitored during 80 days and stopped when methane production rate decrease under 0.5%.

***Physical and chemical analysis of substrates and inoculum*.** The parameters analyzed for the characterization of S and I were total solids (% TS), volatile solid (% VS), chemical oxygen demand (COD, mg/L), total ammonium nitrogen (TAN, mg/L), pH and total alkalinity (TA, mg/L). All these parameters were performed through APHA

methods[18]. For each treatment, the percentage of VS was measured at the beginning and at the end of the experiment.

Biogas analysis. Volume of biogas (mL) was evaluated in all the samples by volume displacement according to Córdoba et al (2016)[12]. The quality of biogas was evaluated by its methane percentage. Measurements were done periodically (at least daily) using a portable Landgem GA2000 instrument with infrared cells to measure methane and carbon dioxide (maximum error ±0.5%), and electrochemical cell for oxygen content (maximum error ±1.0%). Calibration was done with certified standard type gas mixture 60-40 (CH_4-CO_2) from AGA (Certification Number 165342).

In order to identify the biogas and methane productions exclusively produced from S, it was conducted a blank with I. The methane production of the blank was therefore subtracted from the methane production of the mixture samples[19].

Kinetics of the methane generation. Kinetic studies of anaerobic digestion models can provide useful information for the analysis, design and operation of a fermentation process[7,20]. First-order kinetic models are the simplest models applied to the AD of complex substrates as they provide a simple basis for comparing steady process performance under practical conditions. The cumulative methane production in a batch of high-solids digestion can be described by the Gompertz equation[21,22]. This is a non-linear regression used in the simulation of methane and hydrogen productions for several systems such as granular sludge[23,24], co-digestion of swine manure and food waste [25], among other. The following equation describes the Gompertz equation:

$$M(t)= P exp[-exp(R/P)(\lambda-t)e+1)] \quad (1)$$

where M is the methane cumulative production (mL/g VS) at time t (d); λ is the lag-phase time (d); P is the methane production potential or maximum methane production (mL/g VS); R is the maximum methane production rate (mL/g VS/d) and e is a mathematical constant (2.718).

The experimental data of the cumulative methane production was non-linearly fitted by applying the Equation 1 by using Statgraphics Centurion XVI (v.16.2.04).

Statistical analysis. Statistical analysis of the results was performed using t-Student at 95.0 % confidence level through Statgraphics Centurion XVI (v.16.2.04). Data was expressed as mean value (±) the standard deviation of replicates (n = 2). ANOVA test was performed to determine the significance of mean values. Fisher's least significant difference (Fisher's LSD) was calculated at α = 0.05. Statistical methods were performed by using Statgraphics Centurion XVI (v.16.2.04).

RESULTS AND DISCUSSION

Table 2 shows the characterization of S and I through the parameters evaluated. As can be observed I has lower percentage of TS than S indicating higher water content; meanwhile, swine wastewater exhibits a high organic matter concentration than I, which

can be seen through VS (4.60%) and COD (56109 mg/L) parameters. TA is another parameter that is usually assessed in AD, since is an indication of the system buffer capacity. Several authors[26,27] reported that values of TA higher than 3000 mg/L assure the stability of the process. Sewage sludge used as inoculum showed a value of TA lower than the substrate (6285 mg $CaCO_3$/L). While TAN concentration (1959 mg NH_4^+-N/L) in S should not be a risk regarding the range between 3000 and 5000 mg/L suggested by Drosg, (2013)[28] that could be cause of inhibition.

TABLE 2. Physic-chemical characterization of inoculums, substrate and mixtures

Parameter	Inoculum	Substrate	Treatment (SIR)		
	Sewage Sludge	Swine wastewater	A (1/1)	B (3/1)	C (6/1)
%TS	3.65±0.04	5.57±0.66	4.22±0,22[a]	4.69±0,34[a]	4.96±0,42[a]
%VS (w.b.)	2.16±0.05	4.60±0.66	3.56±0,75[a]	4.68±0,33[a]	4.95±0,49[a]
pH	7.32	6.15	7.13	6.70	6.50
TA, (mg $CaCO_3$/L)	2357±1	6285±112	3736±222[a]	4957±118[b]	5687±158[c]
COD, (mg/L)	44708±3794	56109±3794	48201±1643[a]	52043±2799[a]	55886±3293[a]
TAN,(mg $N\text{-}NH_4^+$/L)	350±6	1959±50	836±12[a]	1182±16[b]	1515±1[c]

Values are means of replicates ± standard deviation. Values with the same letter in the same row have no significant differences (p>0.05) according to LSD´s test.

Table 2 also shows the characterization of each mixture based on the different treatments analyzed, which differ in the concentration of inoculum used. The results show that non-significant differences were found between treatments (p>0.05) in COD, TS and VS values. pH value of all treatment resulted in the adequate range suggested for the methanogenic bacteria growth[9]. TA and TAN values decreased with the increase of inoculum added to the system as a result of lower values of these parameters in it; although they remained in the suggested range that assure stability of the process.

Biogas and Methane Production. The highest biogas production was observed in A treatment (554 ±75 mL biogas/g VS) followed by C (466±7 mL/g VS) and B (394±25 mL/g VS) with no significant differences between treatment (p=0.0875). Otherwise, methane production decreased in a broader range from A (382±22) to C (232±5), where treatment A is significantly different to the others treatments (p= 0,0033). Both biogas and methane production are shown in **Figure 1**. These results are in agreement with those reported by Feng et al., (2013)[30] who compared AD of vinegar residue with sludge as inoculum in six SIR (1 to 6); they founded that the higher inoculum concentration, the higher methane production. It was reported that methane production increased 25% when SIR decreased from 6 to 1; in thisstudy, the observed increase resulted f 64.5% for the same SIR raise. Therefore, as can be observed from these results, higher

amount of inoculum not only promoted higher methane yield, but also increased biogas quality in terms of methane concentration (49.8% in C, 61.2% in B and 69.8% in A).

Organic matter removal varied from 38.8% up to 61.5% for the different treatments. The lower VS removal was observed in treatment C (38.8±0.1%), explained through the lower amount of inoculum added to the reactor, resulting also in lower methane production.

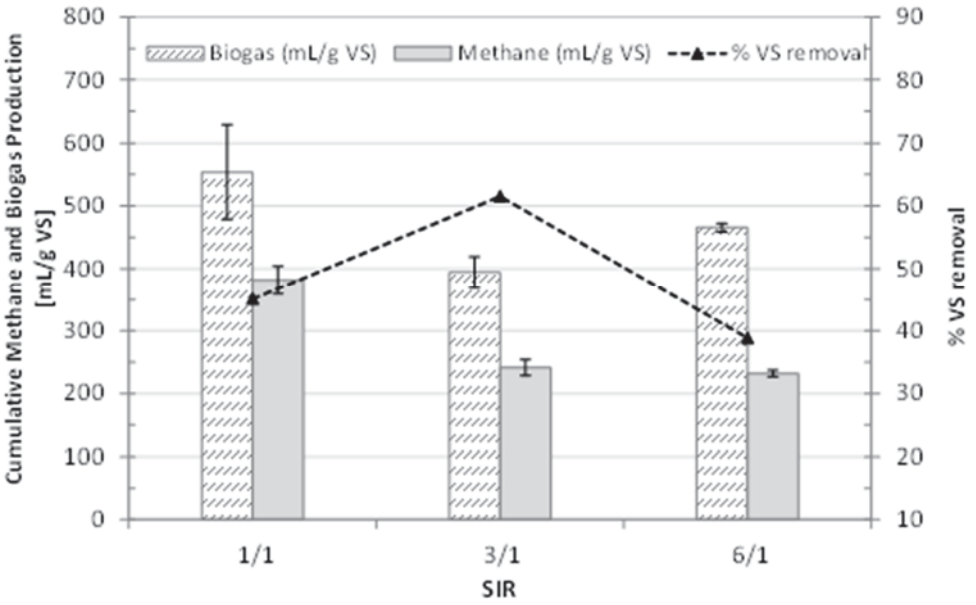


FIGURE 1. Cumulative methane and biogas yield and % of VS removal

Cumulative methane production obtained for the S/I ratio of 1/1 (382±22 ml/g SV) and organic matter removal (45.1±3.7% SV) obtained for the S/I ratio of 1/1, were both are in the order of the values reported by other researchers. In this sense, Chynoweth et al., (1999)[3] reported a final methane production in the range 320 to 480 mL/g VS with and an organic matter removal of between 40 to and 60% in VS when studied swine wastewater. Moller et al., (2004)[31], meanwhile, reported a values of 350 mL/g VS in mesophilic AD, however, they indicated that this value depended strongly on the pretreatment and digestibility conditions of the substrate. They also reported a value of 516 mL/g VS for the theoretical methane production estimated based on the average chemical composition of the substrate;, this value resulted is 35% higher than the value found by this experience in the present study for S/I ratio of 1/1, increasing this difference to 122% when it is compared with the value obtained with by the S/I ratio of 6/1.

Kinetics analysis of methane production. In order to verify the variation of kinetics parameters in a wider SIR range, experimental values obtained in a previous research[12] when swine wastewater was treated anaerobically with sewage sludge as inoculum in a SIR of 14/1 (named treatment D) were jointly analyzed with the results of treatments A, B and C of the present study.

A technological parameter known as Technical Digestion Time (T_{80}) defined as the required time to produce 80% of the maximum methane production was evaluated to analyze the performance of the process[32]. T_{80}, as an indicator of the methane production rate is shown for each treatment in **Figure 2**. As can be observed this parameter is affected by the SIR; the higher the SIR, the higher T_{80} (p=0.0001). By increasing the SIR from 1 to 3, T_{80} increased in 101% which represent the highest increase, while, T_{80} increased 62% when the SIR increased 100% (3/1 to 6/1). For other biomass it has been found a similar behavior. For vinegar residue Feng et al., (2013)[30] reported values of T_{80} from 28 (SIR=1) to 60 (SIR=6), which represented an increase of 114%.

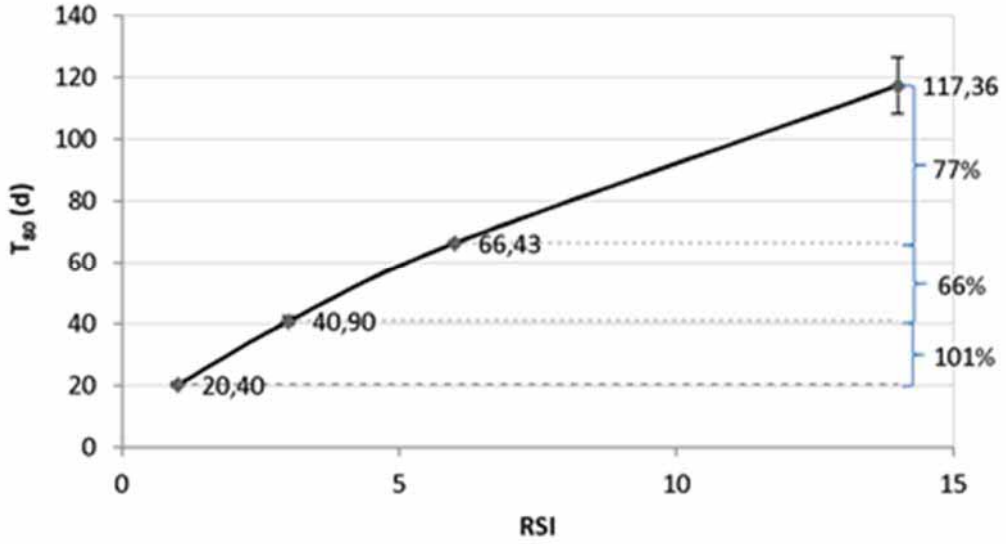


FIGURE 2. Technical digestion time of methane production from AD of swine wastewater with sewage sludge as inoculums

Kinetics modelling of methane yield. Methane production kinetics was analyzed through the Gompertz equation in order to identify the swine wastewater kinetic parameters for the different SIR studied. It can be observed from **Figure 3a** that experimental data from all treatments adjusted adequately to Gompertz equation since the correlation coefficients (R^2) resulted higher than 99%. **Table 3** details the experimental and calculated values of the parameters P, R and λ and their statistics. **Figure 3b**, shows the experimental data obtained for treatment DSIR. According to Cordoba et al (2016)[12], when low concentration of inoculums is used it can be identified two stages of methane production: the first one is the result of the methanogenic bacteria provided by the substrate itself and the second one due to bacteria provided by the inoculums. Based on this, the experimental data were fitted to a double Gompertz equation, which gives kinetics information of the two stages; however, for comparison purposes with the treatments A, B and C of the present study, only the second stage data from experiment D were analyzed (**Table 3**).

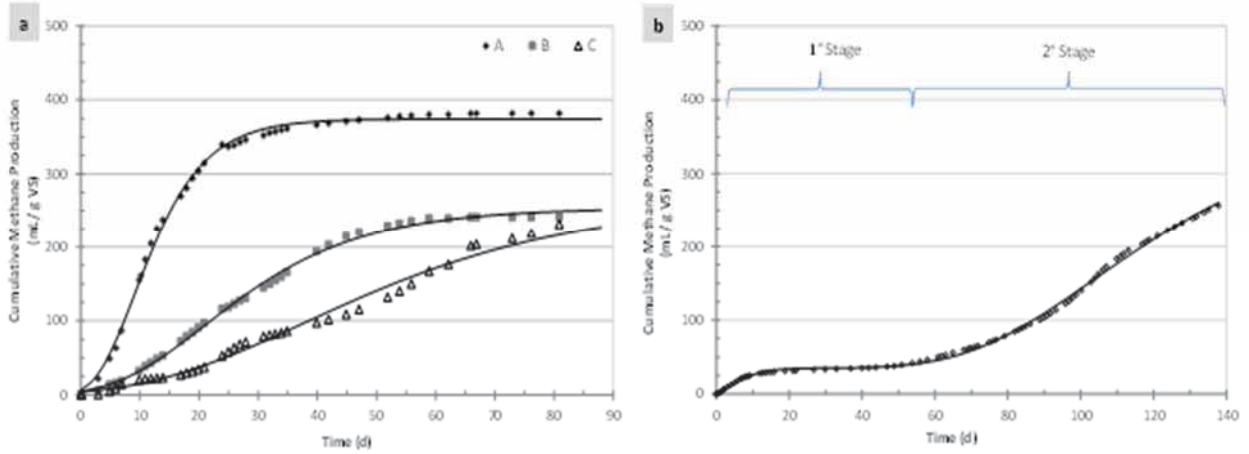


FIGURE 3. Cumulative methane yield and fitted Gompertz equation

The highest methane production potential P was obtained for A treatment, decreasing as the SIR increases; however, no statistical differences were found between treatments. Comparisons between predicted and measured values for treatments A and B showed differences of 2.0 and 5.2 % respectively, while in C the difference was 13.8 % and for treatment D the difference was of 28.6%. The higher differences founded in methane production for the last two treatments could be explained on the lower methane production rate observed when higher SIR were used.

TABLE 3. Estimated regression parameters from the non-linear Gompertz equation

SIR	Methane Production		Error %	R^2	Kinetics Parameters	
	Experimental (mL/g VS)	P (mL/g VS)			R (mL/g VS d)	λ (d)
A (1/1)*	382[a]	374.3[a]	2.0%	99.71	20.9[b]	2.6[a]
B (3/1)*	241[b]	253.7[a]	-5.2%	99.71	6.2[a]	5.8[ab]
C (6/1)*	232[b]	263.9[a]	-13.8%	99.02	3.7[a]	11.3[b]
D (14/1)**	256[b]	329.9[a]	-28.6%	99.81	3.5[a]	68.9[c]
p value+	0.0033	0.0579			0.0010	0.0000

*values correspond to 80 days of AD process

**Adjustment of experimental data from the second stage of the cumulated methane production to Gompertz´s equation

+Values with the same letter indicate no significant differences at 95% of confidence.

The variation of the Gompertz kinetics parameters (R and λ), over the range of the SIR analyzed is shown in **Figure 4**.

According to Swinnen et al. (2004)[33], the lag phase (λ) is a phenomenon inherent to microbial kinetics affected among other by the amount of inoculums used. On this basis, it was expected an increase in the lag phase with the decrease of the amount of inoculums used. For treatment A (1/1), the lag phase was 2.67±0.22 days, which indicates a good methanogenic activity of the inoculums as methane production started quickly after inoculation, growing at an exponentially rate (R^2=0.9882) with the

increasing of the SIR as shown in **Figure 4** for the whole range. Considering the range of SIR between 1 and 6 (treatments A, B and C) a linear regression was the best relationship between λ and SIR, while when the whole range of SIR is considered (including treatment D), the experimental results demonstrated that the linear regression would underestimate the final value of the lag phase in 62.9%.These results indicated that when a low inoculum concentration is used, the lag phase could be much higher than expected.

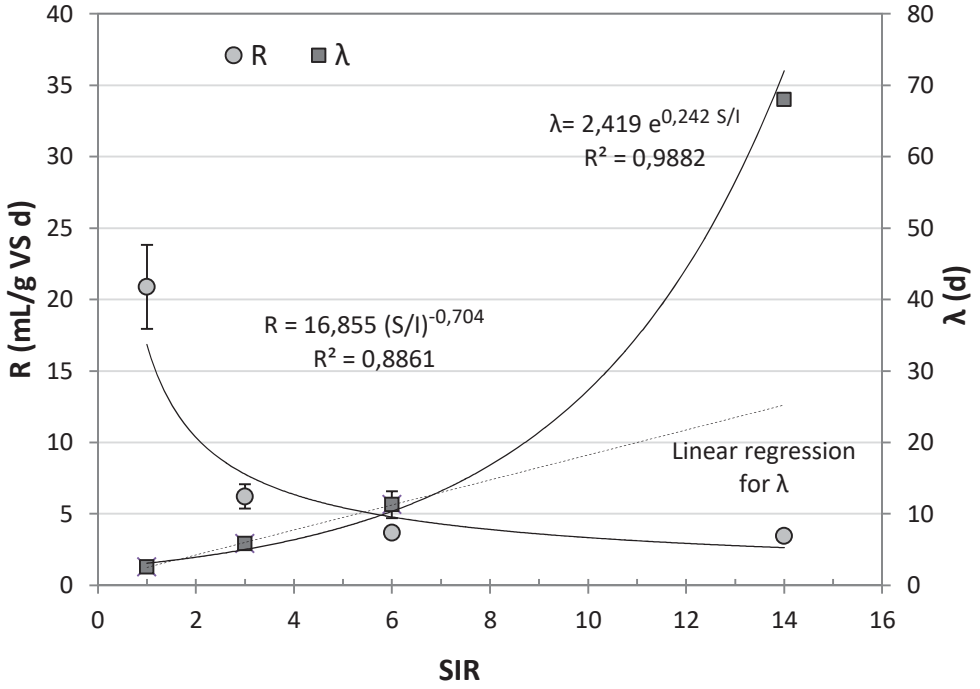


FIGURE 4. Methane production rate (R) and lag phase (λ) for the SIRs studied

Regarding the methane production rate R, a negative potential relationship with SIR was observed (**Figure 4**). This is a result of some degree of inhibition of the process, which reduces methane generation rate as increases the concentration of substrate in the reactor. The largest reduction (70.2%) was observed between SIR 1/1 and 3/1; for higher SIR the increase in the amount of substrate did not significantly affect this parameter since the decreases only differed 1.1% (from SIR 1/1 to SIR 6/1 the decrease was 82.4%, while for the SIR 1/1 to SIR 14/1 1 the decrease was 83.5%. The results of R for SIR higher than 1/1 showed no significant differences (at 95% confidence) as can be observed for B, C and D treatments (**Table 3**). Shorter lag phases and therefore faster adaptation to the process as well as higher methane production rate resulted indicators of higher methanogenic activity promoted by a high inoculum concentration.

CONCLUSION

Methane production from mesophilic AD of swine wastewater was evaluated by using sewage sludge as inoculum in three SIR (1/1; 3/1; 6/1). It was evaluated the performance of the process in terms of the methane production and identification of kinetic parameters of the process.
Results showed that higher amount of inoculum not only promoted higher biogas and methane production, but also increased methane concentration in biogas.
The non linear Gompertz model adequately adjusted the experimental data highlighting differences in data kinetics according to the SIR. The best performance in terms of the kinetic parameters was obtained for treatment A however treatment B could still ensure a stable process. The use of higher inoculums concentration generated higher methane production rate (R) requiring lower adaptation time (lag-phase) in the SIR range employed. When higher SIR is used (e.g.14/1, previous work) the lag-phase time did not remain in a linear relationship with SIR but exponential above SIR=6/1. These results demonstrated that when a low amount of inoculums was used, the adaption time of microorganisms resulted much higher than expected delaying the methane production, extending the processing time needed to achieve adequate methane production.

ACKNOWLEDGMENTS

This research was made possible by the support of the Argentine National Council of Scientific and Technical Research (CONICET) and the National University of the Center of Buenos Aires Province UNCPBA. Authors would also thanks to the local Cooperative of Electricity of Olavarría for the supply of the sewage sludge used in this study.

REFERENCES

1. Budiyono, Widiasa, I. N., Johari, S. & Sunarso. Influence of inoculum content on performance of anaerobic reactors for treating cattle manure using rumen fluid inoculum. Int. J. Eng. Technol. 1, 109–116 (2009).
2. FAO - Organización de las Naciones Unidas para la Agricultura y la Alimentación. El estado mundial de la agricultura y la alimentación. (2009). at <http://www.fao.org/catalog/inter-s.htm>
3. Chynoweth, D. P., Wilkie, A. C. & Owens, J. M. Anaerobic processing of piggery waste: a review. in ASAE Annu. Int. Meet. 1–38 (1998).
4. Triolo, J. M., Ward, A. J., Pedersen, L. & Sommer, S. G. in Biomass Now – Sustain. Growth Use 307–326 (InTech, 2013). doi:http://dx.doi.org/10.5772/54424
5. Mateescu, C. & Constantinescu, I. Comparative analysis of inoculum biomass for biogas potential in the anaerobic digestion. Sci. Bull. 73 (2011) 99–104.
6. Campos, E., Palatsi, J. & Flotats, X. Co-digestion of pig slurry and organic waste from food industry. in II Int. Symp. Anaerob. Dig. SOLID WASTE (1999)192–195.
7. Angelidaki, I., Ellegaard, L. & Ahring, B. K. A Mathematical Model for Dynamic Simulation of Anaerobic Digestion of Complex Substrates: Focusing on Ammonia Inhibition. Biotechnol. Bioeng. 42 (1993) 159–166.
8. Campos Pozuelo, A. E. Optimización de la digestión anaerobia de purines de cerdo mediante codigestión con residuos orgánicos de la industria agroalimentaria. (2001). at <www.tdx.cat/bitstream/handle/10803/8229/Tecp1de1.pdf?sequence=1>

9. Gerardi, M. H. The microbiology of anaerobic digesters. (John Wiley & Sons, Inc., Hoboken, New Jersey, 2003).
10. Zeikus, J. G. The Biology of Methanogenic Bacteria. Bacteriol. Rev. 41 (1977) 514–541.
11. Córdoba, V., Fernández, M. & Santalla, E. Ensayo batch de co-digestión anaeróbica en purines de cerdo. III Congr. Int. Ambient. y Energías Renov. (2013) 484–494.
12. Córdoba, V., Fernández, M. & Santalla, E. The Effect of Different Inoculums on Anaerobic Digestion of Swine Wastewater. J. Environ. Chem. Eng. 4 (2016) 115–122.
13. Llabrés-Luengo, P. & Mata-Alvarez, J. Kinetic study of the anaerobic digestion of straw-pig manure mixtures. Biomass 14 (1987) 129–142.
14. Neves, L., Oliveira, R. & Alves, M. M. Influence of inoculum activity on the bio-methanization of a kitchen waste under different waste/inoculum ratios. Process Biochem. 39 (2004) 2019–2024.
15. Chynoweth, D. P., Turick, C. E., Owens, J. M., Jerger, D. E. & Peck, M. W. Biochemical methane potential of biomass and waste feedstocks. Biomass and Bioenergy 5 (1993) 95–111.
16. Liu, G., Zhang, R., El-Mashad, H. M. & Dong, R. Effect of feed to inoculum ratios on biogas yields of food and green wastes. Bioresour. Technol. 100 (2009) 5103–8.
17. Bolzonella, D., Innocenti, L., Pavan, P., Traverso, P. & Cecchi, F. Semi-dry thermophilic anaerobic digestion of the organic fraction of municipal solid waste: focusing on the start-up phase. Bioresour. Technol. 86 (2003) 123–129.
18. APHA. APHA: Standard Methods for the Examination of Water and Wastewater. 20th ed. Washington, DC. (American Public Health Association, 1999).
19. Hansen, T. L. et al. Method for determination of methane potentials of solid organic waste. Waste Manag. 24 (2004) 393–400.
20. Mu, Y., Wang, G. & Yu, H.-Q. Kinetic modeling of batch hydrogen production process by mixed anaerobic cultures. Bioresour. Technol. 97 (2006) 1302–7.
21. Lay, J., Li, Y., Noike, T., Endo, J. & Ishimoto, S. Analysis of environmental factors affecting methane production from high-solids organic waste. Water Sci. Technol. 36 (1997) 493–500.
22. Lay, J., Li, Y. & Noike, T. Influences of pH and moisture content on the methane production in high-solids sludge digestion. Water Res. 31 (1997) 1518–1524.
23. Lin, C. & Shei, S. Heavy metal effects on fermentative hydrogen production using natural mixed microflora. Int. J. Hydrogen Energy 33 (2008) 587–593.
24. Li, C. & Fang, H. H. P. Inhibition of heavy metals on fermentative hydrogen production by granular sludge. Chemosphere 67 (2007) 668–673.
25. Shin, J. et al. Predicting Methane Production Potential of Anaerobic Co-digestion of Swine Manure and Food Waste. Environ. Eng. Resour. 13 (2008) 93–97.
26. Molina, F., Ruiz-Filippi, G., Garcia, C., Lema, J. M. & Roca, E. Pilot-Scale Validation of a New Sensor for On-Line Analysis of Volatile Fatty Acids and Alkalinity in Anaerobic Wastewater Treatment Plants. Environ. Eng. Sci. 26 (2009) 641–649.
27. Voß, E., Weichgrebe, D. & Rosenwinkel, K. H. FOS/TAC-Deduction, Methods, Application and Significance. in Int. Konf. Biogas Sci. (2009) 2–4.
28. Drosg, B. Process monitoring in biogas plants. (IEA Bioenergy, 2013). at <http://www.iea-biogas.net/files/daten-redaktion/download/Technical Brochures/Technical Brochure process_montoring.pdf>
29. Raposo, F., Banks, C. J., Siegert, I., Heaven, S. & Borja, R. Influence of inoculum to substrate ratio on the biochemical methane potential of maize in batch tests. Process Biochem. 41 (2006) 1444–1450.
30. Feng, L. et al. Biochemical Methane Potential (BMP) of Vinegar Residue and the Influence of Feed to Inoculum Ratios on Biogas Production. BioResource 8 (2013) 2487–2498.
31. Moller, H. B., Sommer, S. G. & Ahring, B. K. Methane productivity of manure, straw and solid

fractions of manure. Biomass and Bioenergy 26 (2004) 485–495.
32. Cheng, X. & Zhong, C. Effects of Feed to Inoculum Ratio, Co-digestion, and Pretreatment on Biogas Production from Anaerobic Digestion of Cotton Stalk. Energy & Fuels 28 (2014) 3157–3166.
33. Swinnen, I. a M., Bernaerts, K., Dens, E. J. J., Geeraerd, a. H. & Van Impe, J. F. Predictive modelling of the microbial lag phase: a review. Int. J. Food Microbiol. 94 (2004) 137–59.

CHAPTER 11.3. COMPOSTAJE DEL DIGESTATO PRODUCIDO EN UN REACTOR DE HIDRÓLISIS ANAEROBIA DE LECHO ESCURRIDO

R. Espinosa *(1); G. Saucedo (1) and O. Monroy (1)

(1) Departamento de Biotecnología, UAM-I, Av. San Rafael Atlixco 189, Col. Vicentina, 09340 Iztapalapa., Ciudad de México.

RESUMEN

A partir de la hidrólisis de la fracción orgánica de los residuos sólidos urbanos (FORSU) en un reactor de hidrólisis anaerobia de lecho escurrido (RHALE) se obtienen: un lixiviado rico en materia orgánica soluble que se destina a la producción de metano en un reactor de lecho de lodos anaerobios[1] y un residuo sólido, llamado digestato, que requiere ser acondicionado como biosólido, es decir, un abono orgánico libre de olores, con un adecuado balance de C:N, con pH neutro y capaz de retener humedad.

La relación C:N de la materia orgánica a compostear se debe encontrar en un rango de 25-35[2]. Por debajo de este rango se acumula NH_4^+ que con valores altos de pH se disocia en NH_3[3], mientras que con valores superiores de relación C:N se tiene un proceso deficiente debido a la baja disponibilidad de nitrógeno para la sintesis enzimática[4]. Dada la baja C:N del digestato (16.13 ± 2.79) es necesario acondicionarlo mezclándolo con materia orgánica de bajo contenido en nitrógeno. Para facilitar la aereación es necesario agregar un material que aumente la porosidad de la masa en composteo y permita el paso del aire evitando la generación de zonas anaerobias.

Para determinar las mezclas que permitan obtener la zona de operación de mayor degradación de materia orgánica se realizó un experimento basado en un diseño de mezclas simplex centroide acoplado con la metodología de superficie de respuesta con diez tratamientos (proporciones distintas de digestato, FORSU y aserrín) con 9 días de composteo. Los datos experimentales fueron ajustados al modelo de Scheffé para construir un modelo de degradacion de materia orgánica en función de las fracciones en base seca de los componentes. Se encontró que la zona de mayor degradación de materia esta compuesta por proporciones de mezcla con 0.28-0.42, 0.48-0.62, 0.10-0.12 para FORSU, digestato y aserrín respectivamente. Dos mezclas dentro de la zona de operación y una fuera se probaron en un reactor de 95.4 L diseñado y construido para medir la producción de CO_2, degradación de materia orgánica y temperatura. Se hicieron tres corridas con 35.25, 22.8 y 20 kg de digestato siguiendo el proceso hasta su terminación en 12 días.

Se concluyó que trabajando con mezclas ubicadas en la zona de operación determinada es posible degradar hasta 35% de materia y el biosolido producido puede ser utilizado como mejorador de suelos, mientras que fuera de la zona de operación la eficiencia de degradación de materia orgánica es menor al 10%. La tasa de producción de CO_2 a partir de los 12 días es menor a 2.5 $gCO_2h^{-1}Kg_{MSI}^{-1}$ (donde MSI es materia seca inicial) indicando estabilidad en el biosólido.

---

*Author for correspondence: esru88@gmail.com

Palabras claves: compostaje, digestato, diseño de mezclas simplex-centroide.

INTRODUCCIÓN

En la Ciudad de México se generan diariamente aproximadamente 6,715 T de la fracción orgánica de residuos sólidos urbanos (FORSU), siendo 1,690 T confinados en plantas de compostaje (Texcoco y en las delegaciones Álvaro Obregón, Cuajimalpa, Iztapalapa, Milpa Alta y Xochimilco) y el resto en rellenos sanitarios (La Cañada, Cuautitlán, El Milagro, Tepotzotlán y Cuautla)[5].

La acumulación de FORSU como consecuencia del desarrollo económico y del aumento poblacional, tiene consecuencias ambientales que repercuten en la salud humana y en los ecosistemas[6]. Dentro de los principales efectos se encuentran:

- Generación de contaminantes y de gases de efecto invernadero.
- Contaminación de los suelos y cuerpos de agua.
- La transformación de los residuos sólidos y su contacto con el agua producen lixiviados que pueden contaminar mantos acuíferos.
- Proliferación de fauna nociva y transmisora de enfermedades.

Una alternativa para el aprovechamiento y disposición de la FORSU es la producción de biosólidos (para el uso en agricultura como acondicionadores de suelo) mediante el tratamiento combinado por digestión anaerobia y compostaje[7], hasta llegar al compost que es un producto estable que evita la erosión, aumenta la permeabilidad y mantiene la humedad del suelo. Biológicamente mejora la capacidad de absorción de nitrógeno y de los componentes de la tierra, debido a la presencia de colonias microbianas como los saprófitos que confieren al suelo resistencia a la colonización por patógenos[8].

La digestión anaerobia es un proceso de reducción de la materia, donde el carbono orgánico es transformado en biogás (principalmente metano y dióxido de carbono) y un semisólido parcialmente estabilizado (digestato). Este proceso es realizado de manera simbiótica por diferentes grupos de bacterias[9].

El digestato presenta una relación C:N baja (16.13 ± 2.79) y humedad superior al 85%, su composición depende del sustrato alimentado en la digestión anaerobia y de las condiciones de operación (temperatura y tiempo de retención)[10]. Principalmente está compuesto por biopolímeros, moléculas del tipo esteroide y lignina, considerados como los precursores de ácidos húmicos[11].

El compostaje es un proceso aerobio en el que el carbono orgánico es transformado en CO_2; asimilado por las comunidades microbianas; y parte es transformado en humus. El nitrógeno orgánico es mineralizado a NH_4^+ y NO_3^-, los cuales son asimilados por los microorganismos o son empleados para la síntesis de ácidos húmicos[12]. Las sustancias húmicas están formadas por materia orgánica sin organización celular que presenta un aspecto amorfo, macromolecular y polimérico. Se clasifican de acuerdo a su solubilidad en huminas, ácidos fúlvicos y ácidos húmicos[13].

Para que un material pueda ser sometido a este proceso debe tener humedad entre 50-70%[14] y una relación C:N entre 25-35[2]. para evitar la generación de amoniaco o tener un proceso lento[3]. Existen materiales que se agregan al sustrato para incrementar los espacios vacíos y alcanzar una mejor circulación del aire, o bien, aumentar la cantidad de compuestos orgánicos fácilmente asimilables e incrementar la C:N de la mezcla[15].

La finalidad de este trabajo es compostear un digestato complementando sus propiedades con materiales que permitan la producción de biosólidos que puedan ser utilizados como compost para viveros y sustitutos de tierra para macetas, áreas verdes urbanas y reforestación.

MATERIALES Y MÉTODOS

Materiales para el diseño de mezclas. En esta etapa se utilizaron como unidades experimentales frascos de vidrio con capacidad de 1.4 L provistos de una tapa de hule acoplada a dos tubos para la entrada y salida de gases, en la parte inferior se colocó una malla de acero para retener la mezcla. Cada unidad experimental se alimentó con 650-740 g de una mezcla de digestato, FORSU y aserrín, trabajando a una temperatura controlada de 35 °C mediante un recirculador Perkin Elmer Polystat 12104-00. El aire fue suministrado a un flujo de 0.5 L min^{-1} Kg_{MSI} $^{-1}$, siendo alimentado desde la parte inferior. El tiempo de operación fue de 9 días. Este experimento se realizó dos veces trabajando con lotes diferentes de digestato y de FORSU y se utilizó como iniciador un compost proveniente de la planta Bordo Poniente representando el 5 % de la mezcla total.

Reactor de compostaje. Se diseñó y construyó un reactor de agitación horizontal de 95.4 L (longitud = 60 cm, diámetro = 45 cm) en acero al carbón galvanizado (**Figura 1**). Fue montado sobre una báscula con capacidad de 300 kg para monitorear la pérdida de peso diariamente. Dos termopares tipo *J* son introducidos en tubos perforados (1) para monitorear la temperatura interna del proceso Uno de los costados es desmontable para facilitar la recolección del producto (2). En la parte inferior hay una salida para la recuperación de lixiviados. Cuenta con agitadores de turbina de palas (3) montadas sobre un eje para agitar manualmente (4).

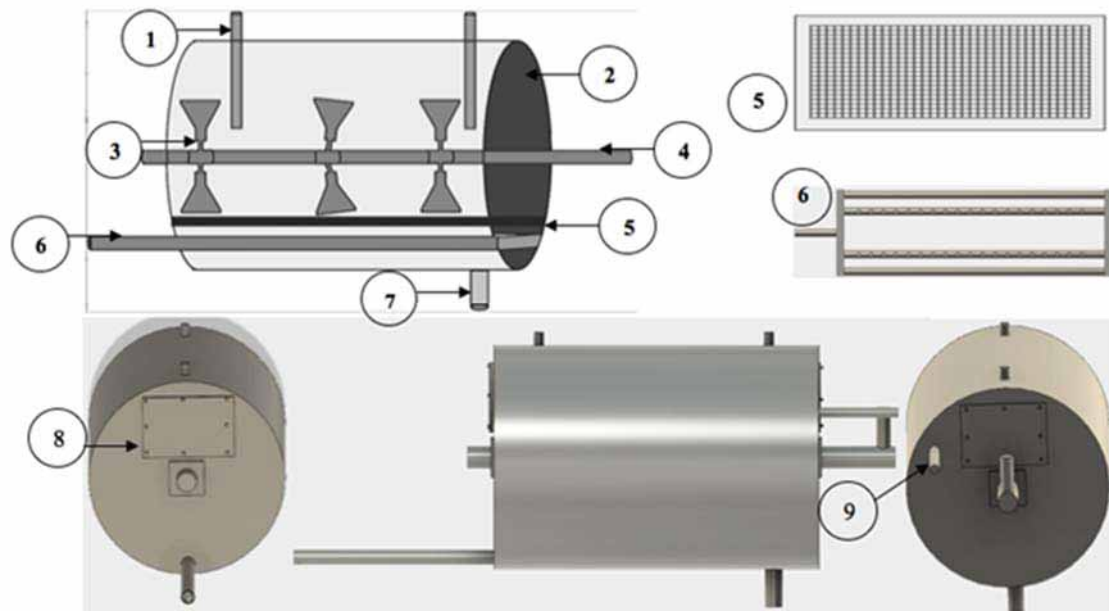


FIGURA 1. Reactor de compostaje visto desde distintos ángulos

La mezcla es retenida sobre una malla de acero (5). En la parte inferior se encuentra el distribuidor de aire (6). La extracción de lixiviados se efectúa por una válvula ubicada en la parte inferior (7). En ambos lados cuenta con tapas de 20 x 15 cm por donde se extraen las muestras (8). La salida de gases se ubica en la parte superior en un costado del reactor (9).

Contenido de carbono y nitrógeno. La determinación de carbono y nitrógeno se realizó en un analizador elemental Series II 2400 CHNS/O (Perkin Elmer, Boston, USA). La calibración se realizó con un estándar de acetanilida (C_8H_9NO). La muestra fresca fue colocada sobre una charola de aluminio y secada en una estufa a 60 °C, una vez seca fue molida para reducir el tamaño de partícula. Por último se tamizó a malla 100 y se pesaron entre 2 y 3 mg en capsulas de estaño en una microbalanza de alta precisión. Los resultados se expresaron en porcentaje (%) de cada elemento referido a la materia seca de la muestra.

pH. 5 g de muestra fueron adicionados a 10 mL de agua destilada y se agitaron durante 30 min. Se dejó reposar la suspensión durante 15 min. Posteriormente se calibró el potenciómetro HANNA HI 255 y se inició la medición de las muestras lavando el electrodo con agua destilada antes de cada lectura. Se registró el pH al momento en que la lectura se estabilizó.

Contenido de humedad y materia seca. La determinación de humedad se realizó de la forma siguiente: La muestra húmeda (P_0) fue pesada en un crisol de porcelana previamente tarado (T) en una balanza de precisión. Posteriormente se sometieron a secado a 105 °C hasta obtener peso constante. La muestra fue enfriada en el desecador para después ser pesada (P_f). El porcentaje de humedad ($\%H$) y porcentaje de materia seca ($\%MS$) fueron determinados según las siguientes ecuaciones:

$$\%H = \frac{P_0 - P_f}{P_o - T} \tag{1}$$

$$\%MS = 100 - \%H \tag{2}$$

Materia orgánica. La muestra seca (P_o) fue colocada en la estufa durante 60 min a 550 ± 25 ºC, después el crisol caliente fue puesto en un desecador hasta que se enfrió, para ser pesado en la balanza (P_f). La determinación de porcentaje de MO se realizó a partir de la siguiente expresión:

$$\%MO = \frac{P_0 - P_f}{P_o} \tag{3}$$

Temperatura. La temperatura se midió a través de dos termopares tipo J y la temperatura externa con un termistor interno acoplado al módulo de adquisición de

datos. Las lecturas se recopilaron automáticamente cada 20 min mediante la interfaz de adquisición de datos myPCLab® marca NOVUS.

Medición de CO_2. El efluente de gases se hizo pasar a través de una columna empacada con sílica-gel para deshidratarlo, antes de llegar a un detector infrarrojo de CO_2 (%). Las mediciones se realizaron cada 20 min y los resultados se expresan como g CO_2 $h^{-1}g_{MSI}^{-1}$. Estos datos se integraron para obtener la producción total de CO_2.(g). Los datos de CO_2 (%) son transformados mediante la siguiente expresión que determina la tasa de formación de CO_2:

$$\frac{dCO_2}{dt} = \frac{(\%CO_2) \times f \times a \times 273.15 \times b}{Kg_{MSI} \times 22.4 \times T_{externa}} = \frac{gCO_2}{hKg_{MSI}} \quad (4)$$

Donde:

$\frac{dCO_2}{dt}$ = tasa instantánea de producción de CO_2 (g CO_2 h^{-1} Kg^{-1}_{MSI})
$\%CO_2$ = CO_2 en la salida del reactor (%)
f = Flujo en la sálida del reactor (L h^{-1})
a = Factor de corrección de la presión atmosférica a la altura de la Ciudad de México/P atmosférica en condiciones estándar de los gases (0.7697).
b = Peso molécular del CO_2 (44 g mol^{-1})
Kg_{MSI} = Materia seca inicial (Kg)
22.4 = Volumen normal de un gas a 1atmosfera de presión y a 273.15 K (Lmol-1)

Índice de germinación. Un volumen de 50 mL de agua destilada se adicionó a 5 g de compost fresco y se agitó durante 1 h y se filtró. Una alícuota de 5 ml de esta suspensión se colocó en cajas Petri conteniendo dos piezas de papel filtro. Un total de 20 semillas de rábano (Raphanus sativus) fueron distribuidas sobre el papel filtro e incubadas a la oscuridad a 33±2 ºC durante 48 h. Agua destilada fue empleada como control del tratamiento. El procedimiento se realizó por triplicado para cada muestra. Se midió la longitud de las raíces y la tasa de germinación. El índice de germinación (*IG*) se calculó de la siguiente manera:

$$IG(\%) = \frac{Semillas\ germinadas\ x\ longitud\ de\ la\ raíz\ del\ tratamiento\ (mm)}{Semillas\ germinadas\ x\ longitud\ de\ la\ raíz\ del\ control\ (mm)} x100 \quad (5)$$

RESULTADOS Y DISCUSIÓN

En la **Tabla 1** se muestran los resultados del análisis elemental. Dado que el valor de la relación C/N reportada para el proceso de compostaje se encuentra en un rango de 25-35 y conforme a las características de los componentes de la mezcla se eligieron diez tratamientos, dando mezclas con relación C:N cercanas a esta condición (**Tabla 2**).

TABLA 1. Análisis elemental de los componentes empleados

Componente	C	H	N	Relación C:N
Digestato	43 ± 5.9	7 ± 1.14	3 ± 0.39	16.13 ± 2.79
FORSU	42.28 ± 2.73	6.42 ± 1.24	1.87 ± 5.083	23.23 ± 2.66
Aserrín	45.44 ± 2.96	5.98 ± 0.17	2 ± 0.08	77.18

TABLA 2. Relación C:N y eficiencias de degradación de materia de los 10 tratamientos del diseño de mezclas simplex centroide

Tratamiento	1	2	3	4	5	6	7	8	9	10
Relación C:N	24.1	38.9	25.6	32.2	31.5	24.85	27.95	28.00	27.4	29.7
Eficiencia (%)	13.83 13.10	9.53 21.20	18.54 34.11	17.33 35.46	13.53 17.22	27.66 38.23	18.47 17.44	19.92 18.93	24.36 33.38	2.31 0.77

Del diseño de mezclas simplex centroide se obtuvieron las eficiencias de degradación de materia (**Tabla 2**) las cuales fueron ajustadas al modelo polinomial Scheffé mediante el software IBM SPSS statistics 18. El modelo tuvo un coeficiente de correlación de 0.85, lo que indica que representa significativamente la eficiencia de degradación de materia en función de las fracciones de los componentes de la mezcla en base seca.

$$E = -193.884F - 2.293D + 379.59A + 539.71FD + 54.132FA - 815.05AD \quad (6)$$

Donde:

E: Eficiencia de degradación de materia orgánica

F: Fracción de FORSU; *D*: Fracción de digestato; *A*: Fracción de aserrín

A partir del modelo se construyó una gráfica de contornos para ubicar la zona de operación donde ocurre la mayor degradación de materia orgánica (**Figura 2**). Esta zona de operación está compuesta por los siguientes rangos de fracciones: 0.48-0.62 para digestato, 0.28-0.42 para FORSU y 0.1-0.12 para aserrín.

El aserrín como agente de carga con fracciones superiores a 0.12 en las mezclas estudiadas disminuye la eficiencia de degradación de materia, lo anterior ha sido atribuido a una baja tasa degradación, permaneciendo la mayor parte al final[16].

En cuanto al digestato, una fracción de 0.62 corresponde a la máxima mineralización dentro de la zona de operación. A diferencia de otros trabajos[17,18 y 19] donde se utilizan digestatos provenientes de la etapa metanogénica que contienen compuestos de difícil degradación, el digestato de esta investigación al ser un producto de la etapa de acidogénesis de la digestión anaerobia se encuentra parcialmente degradado, y por lo tanto rico en compuestos de fácil asimilación, como consecuencia la eficiencia de degradación de materia se ve favorecida al tener una mezcla cuya fracción de digestato sea dominante.

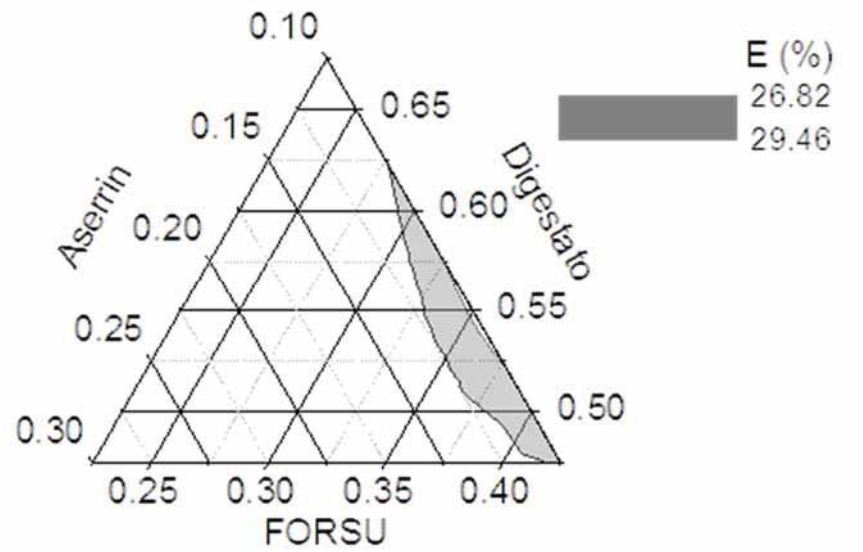


FIGURA 2. Gráfico ternario donde se muestra la zona de operación

La FORSU fue utilizada como un material complementario con el objetivo de proporcionar a la mezcla compuestos fácilmente asimilables y que permitiera que las bacterias en la etapa inicial tuvieran el sustrato suficiente para reproducirse y alcanzar la temperatura termófila (mayor a 45ºC) en los primeros días de proceso. No obstante los resultados indican que este componente presentó compuestos ,menos asimilables que el digestato, obteniendo una fracción de 0.48 como la máxima dentro de la zona de operación.

Se realizarón tres corridas a nivel planta piloto durante 12 días, solo la primera estuvo ubicada fuera de la zona de operación (D = 0.53, F =0.28 y A = 0.19) alimentando el reactor con 35.25 Kg, dado que se observó compactación en la mezcla, se decidío operar las siguientes pruebas con una cantidad menor de material. En el segundo ensayo se alimentó al reactor con 22.8 Kg y ubicado dentro del área de operación (D = 0.62, F =0.28 y A = 0.10). Finalmente la tercera prueba ubicada también dentro de la zona de operación (D = 0.53, F =0.36 y A = 0.11) se ensayó con 20 Kg de material. Al termino de los experimentos el producto obtenido tuvo un aspecto oscuro y no presentó olor desagradable.

TABLA 3. Características de las mezclas utilizadas en las pruebas a nivel planta piloto

Prueba	Humedad (%)		pH		Materia seca (Kg)		Materia orgánica (%)		Relación C:N
	inicial	Final	Inicial	Final	Inicial	Final	Inicial	Final	Final
1*	79	71	4.5	7.6	7.66	6.86	90	85	-
2	82	82	4.6	7.7	3.54	2.29	93	79	13.58
3	83	79	4.9	7.5	3.81	3.03	85	70	15.18

*Valores obtenidos después de 17 días de proceso

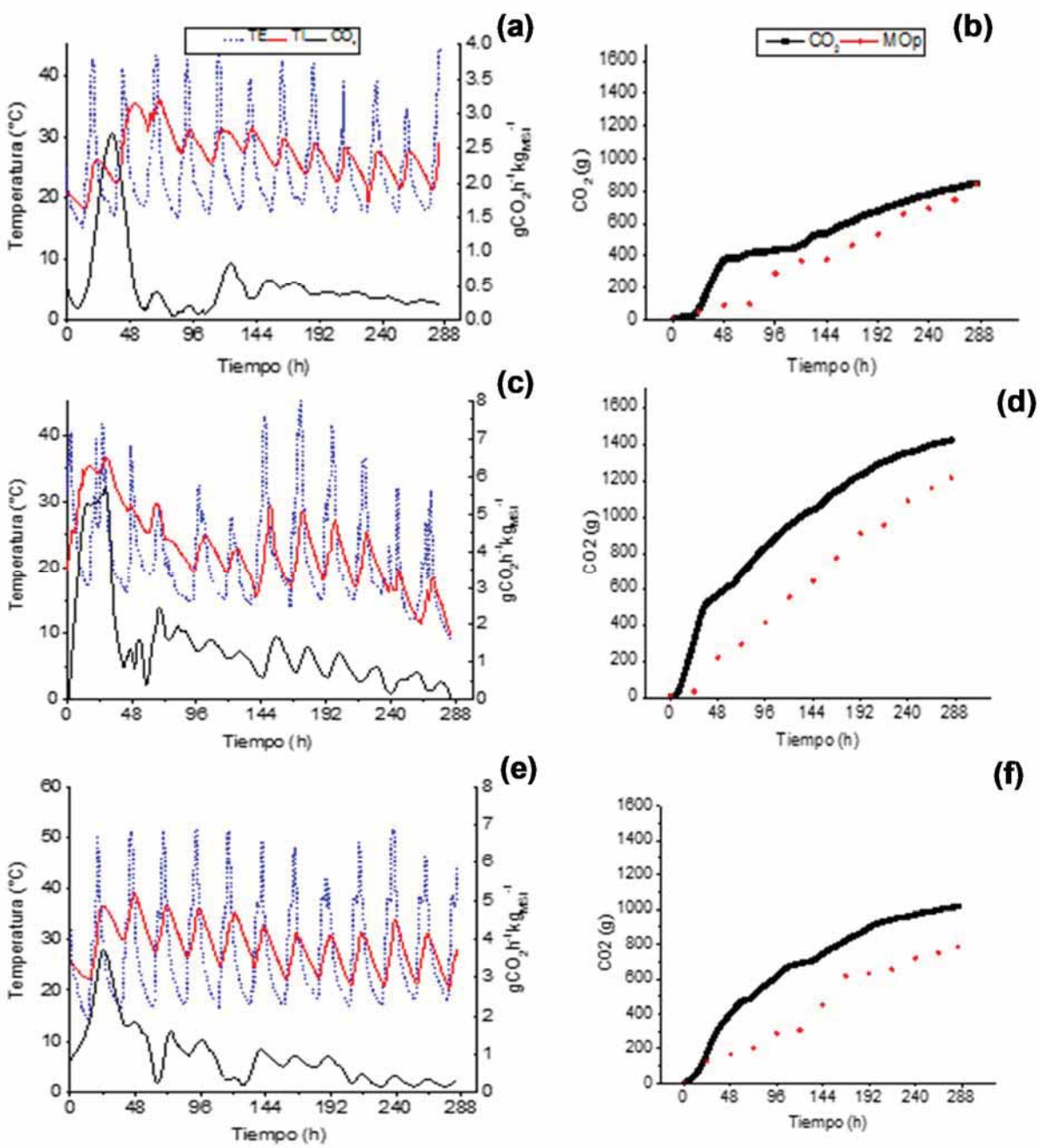


FIGURA 3. Evolución de temperatura, producción de CO_2 y pérdida de materia orgánica en el compostaje de digestato, FORSU y aserrín de pino. Prueba 1(a y b), prueba 2 (c y d) y prueba 3 (e y f). Las líneas punteadas de color azul corresponden a la temperatura externa, las líneas rojas a la temperatura interna y las de color negro representan las tasas de producción de CO_2. Del lado derecho los puntos rojos se refieren a la materia orgánica pérdida y las líneas de color negro al acumulado de CO_2.

De las pruebas realizadas las mezclas 2 y 3 presentaron la mayor eficiencia de pérdida de materia seca (35.5% y 20.4, respectivamente), un valor esperado con base en los resultados obtendos de la zona de operación. Por otro lado la prueba 1 al

encontrarse en un punto lejano al de la zona de operación tuvo un porcentaje de degradación bajo (8.8%).

Los valores de pH en los tres casos partieron de valores ácidos y en el transcurso del proceso con la producción de compuestos de carácter básico llegaron a alcanzar un valor cercano a la neutralidad.

Conforme a lo observado en el transcurso del proceso en el primer dia se obtiene la mayor tasa de producción de CO_2 (**Figura 3**), siendo la segunda prueba (**Figuras 3b** y **3c**) donde se registro una mayor producción de CO_2 (400.85 g CO_2/Kg_{MSI}). En la prueba 1 se obtuvo una baja producción de CO_2 dado que se encuentra en un punto lejos de la zona de operación, donde con fraccciones de aserrín superiores a 0.12 se obtienen bajas eficiencias de degradación.

A lo largo del proceso se observan oscilaciones en la temperatura, donde los valores mas altos corresponden a lecturas tomadas durante el día, mientras que los valores mas bajos se tomaron en el transcurso de la noche. Se ha reportado que en un reactor de 100 L es posible alcanzar temperaturas superiores a los 70 °C, siempre y cuando el aislamiento del sistema sea garantizado[20]. En ninguna de las pruebas se logró alcanzar la temperatura termófila probablemente porque el material biodegradable no fue el suficiente[21] además de existir perdidas importantes de calor hacia el ambiente.

A partir de las 192 h puede observarse que la actividad metabólica disminuye notablemente mostrando una tasa de producción de CO_2 (2.5 $gCO_2h^{-1}Kg_{MSI}^{-1}$) baja y una temperatura con un valor mínimo muy cercano al de la temperatura externa del reactor, indicando una baja actividad metabólica.

En cuanto a los resultados obtenidos para el indice de germinación los compost de las pruebas 1 y 2 podrían utilizarse en viveros y como sustitutos de tierra para macetas (IG>85%), mientras que la prueba 3 se encuentra en el limite (IG=84%), por lo que podría ser empleada en reforestación de acuerdo a la NADF-020-AMBT-2011.

Como parte de la aplicación del compost producido se propuso utilizarlo como fertilizante en árboles. Se seleccionaron fresnos de hoja ancha (*Fraxinus excelsior*). En la **Figura 4** se muestran fotografías del desarrollo de las plantas. Se puede apreciar que en ambos casos hay un crecimiento favorable sin indicios de fitotoxicidad, lo que comprueba el uso del compost producido como fertilizante.



FIGURA 4. Fresnos cultivados empleando el compost producido como sustituto de tierra para macetas

CONCLUSION

Se obtuvo un biosólido de C:N de 13.6 y 15.2, humedad del 80% con una mezcla de componentes consideradas en una zona de operación donde se obtienen las mejores eficiencias de degradación de materia orgánica del proceso (35%) en función de las fracciones en base seca de digestato (0.48-0.62), FORSU(0.28-0.42) y aserrín (0.1-0.12).
El biosólido se obtiene en 12 días de reacción con un gasto de aire de 0.5 $Lmin^{-1}Kg_{MSI}^{-1}$ para lograr se logró obtener una reducción de 35% de la masa inicial.
A pesar de no alcanzar la temperatura termófila, el producto final no presentó mal olor, ni fitotoxicidad, tuvo un pH adecuado, por lo que puede ser utilizado para el crecimiento de plantas.

AGRADECIMIENTOS

Para la realización de la investigación se contó con el apoyo del CONACyT a través de la beca 570209.

REFERENCIAS

1. Rodríguez, R. I., Rodríguez, S., Monroy O. y Ramírez, F. (2015). Effect of organic loading rate on the performance of two-stage anaerobic digestion of the organic fraction of municipal solid waste (OFMSW). Water science and technology 72.3. http://doi.org/10.2166/wst.2015.223
2. Lopez, W. (2010). Estudio del uso de residuos industriales no peligrosos a través del proceso de compostaje y su aplicación para el cultivo de maíz y frijol (Maestría). Instituto Politecnico Nacional.(32-33).
3. Jiang, T., Schuchardt, F., Li, G., Guo, R., & Zhao, Y. (2011). Effect of C / N ratio, aeration rate and moisture content on ammonia and greenhouse gas emission during the composting. Journal of Environmental Sciences, 23(10), 1754–1760. http://doi.org/10.1016/S1001-0742(10)60591-8
4. Bueno Marquez, P., Diaz Blanco, M. J., Cabrera, F. (2008). Factores que afectan al proceso de compostaje. En: Compostaje, (eds) Moreno Casco, J. y Moral Herrero, R. Mundi-Prensa, pp. 111-140.
5. Flores, A., Rodríguez, C., Solares, V. (2012). Informe de la situación del medio ambiente en México, compendio
6. de estadísticas ambientales indicadores clave y de desempeño ambiental. Secretaría de Medio Ambiente y Recursos Naturales (SEMARNAT), México DF.
7. Semarnat. Bases para Legislar la Prevención y Gestión Integral de Residuos. México. 2006.
8. Bibby, K., Viau, E., & Peccia, J. (2010). Pyrosequencing of the 16S rRNA gene to reveal bacterial pathogen diversity in biosolids. Water Research, 44(14), 4252–4260. http://doi.org/10.1 016/j.watres.2010.05.039
9. Sharma VK, Canditelli M, Fortuna F, Cornacchia G (1997). Processing of urban and agro-industrial residues by aerobic 0.45-0.625 ing: review. Energy Convers Manag;38:453–78.
10. Ziemiński, K., & Frąc, M. (03 de 2012). Methane fermentation process as anaerobic digestion of biomass: Transformations, stages and microorganisms. *African Journal of Biotechnology*, 11(18), 4126-4130.

11. Sheets, J. P., Yang, L., Ge, X., Wang, Z., & Li, Y. (2015). Beyond land application: Emerging technologies for the treatment and reuse of anaerobically digested agricultural and food waste. Waste Management, 44, 94-115.
12. Tambone, F., Scaglia, B., Imporzano, G. D., Schievano, A., Orzi, V., Salati, S., & Adani, F. (2010). Chemosphere Assessing amendment and fertilizing properties of digestates from anaerobic digestion through a comparative study with digested sludge and compost. Chemosphere, 81(5), 577–583. http://doi.org/10.1016/j.chemosphere.2010.08.034
13. Kuo S, Ortiz-Escobar ME, Hue NV, Hummel RL (2004) Composting and compost utilization for agronomic and container crops. Recent Res Devel Environ Biol 1:451–513.
14. Melo, L. L. (2006). Análisis y caracterización de ácidos fúlvicos y su interacción con algunos metales pesados. Trabajo de Investigación. Instituto de Ciencias Básicas e Ingeniería, Pachuca de Soto, Hidalgo.
15. Hubbe, M. A., Nazhad, M., & Sánchez, C. (2010). Composting As A Way To Convert Cellulosic Biomass And Organic Waste Into High-Value Soil Amendments: A Review. 5(4), 2808-2854
16. Haug, T. R (1993). The Practical Handbook of Compost Engineering. Lewis Publishers: Boca Raton.
17. Banegas, V., Moreno, J. L., Moreno, J. I., Garcia, C., Leon, G., & Hernandez, T. (2007). Composting anaerobic and aerobic sewage sludges using two proportions of sawdust. Waste Management, 27(10), 1317-1327.
18. Tambone, F., Scaglia, B., Imporzano, G. D., Schievano, A., Orzi, V., Salati, S., & Adani, F. (2010). Chemosphere Assessing amendment and fertilizing properties of digestates from anaerobic digestion through a comparative study with digested sludge and compost. Chemosphere, 81(5), 577–583. http://doi.org/10.1016/j.chemosphere.2010.08.034
19. Koening, B. (2014). Comparison of Compost Efficiency of Digestate to Undigested Organic Waste from a Dry Anaerobic Digester. University of Wisconsin System, Environmental Research and Innovartion center.
20. Bustamante MA, Restrepo AP, Albuquerque JA, Pérez-Murcia MD, Paredes C, Moral R, et al. Recycling of anaerobic digestates by composting: effect of the bulking agent used. J Clean Prod 2013; 47: v6,1–9.
21. Franke-whittle, I. H., Confalonieri, A., Insam, H., Schlegelmilch, M., & Körner, I. (2014). Changes in the microbial communities during co-composting of digestates. Waste Management, 34(3), 632–641. http://doi.org/10.1016/j.wasman.2013.12.009
22. Phillip, E. A. (2010). The Design and Construction of a Pilot-Scale Compost Reactor for the Study of Gas Emissions from Compost under Different Physical Conditions (Doctoral dissertation, McGill University).

CHAPTER 11.4. DESIGN OF A BIORETENTION CELL FOR MITIGATING THE EFFECTS OF URBAN RUNOFF IN XERIC CLIMATES

G. A. Vázquez-Rodríguez *(1); J. E. Ortiz-Hernández (1); L. Lizárraga-Mendiola (2); C. Coronel-Olivares (1); R. I. Beltrán-Hernández (1); C. A. Lucho-Constantino (1) and M. R. González-Sandoval (1)

(1) Área Académica de Química, Universidad Autónoma del Estado de Hidalgo, Carretera Pachuca-Tulancingo Km. 4.5, Mineral de la Reforma, Hidalgo, México.
(2) Área Académica de Ingeniería, Universidad Autónoma del Estado de Hidalgo.

ABSTRACT

Paved surfaces modify the urban water cycles because their imperviousness alter the natural drainage pathways and diminish aquifer recharge. Consequently, urban runoff increases, as well as the occurrence of peak flows and floodings. Bioretention cells are technologies commonly implemented in temperate regions (with annual rainfall higher than 500 mm) to mitigate the negative effects of urban runoff and to improve its quality. However, they are not widely employed in xeric climates (with annual rainfall lower than 500 mm) yet, that is why the purpose of this study was to adapt the conventional bioretention design to the constraints imposed by these climates. We proposed and constructed a bioretention pilot with gravel, zeolite and hydrogel as filtering materials, and covered with decorative marble and a succulent assemblage. The vegetative cover survived well throughout the study period (160 days), probably due to the hydrogel. A global water balance showed that the pilot could bioretain (*i.e.*, to evapotranspirate and to accumulate water in the system) 47.35% of the total water entries, which is similar to the bibliography reports. The microbial pollution removal capacity of the pilot was measured with a synthetic urban runoff ($6.72x10^7$ CFU/100 mL) as equal to 15%. Although this value was low, it represents only the extreme rainfall conditions used in the test. Consequently, the performance of the system has still to be evaluated concerning other pollutants and under moderate-to-low rainfall conditions. Finally, a full-scale bioretention design was proposed specifically for our university campus, which has to be constructed and validated for real-world xeric conditions. It is our view that the construction of low-impact technologies like bioretention cells could mitigate the impact of impervious surfaces and optimize water management in urban areas of xeric regions.

Keywords: aquifer recharge, imperviousness, rain gardens, stormwater.

---

*Author for correspondence: g.a.vazquezr@gmail.com

Urban runoff (UR) has been acknowledged as one of the most important nonpoint pollution sources in continental and coastal water bodies, and its control has been identified as key to protect the quality of aquatic ecosystems worldwide[2]. The pollutants found in UR include organic matter, nutrients, heavy metals, pathogens, oil and grease, persistent organic compounds, and emerging pollutants. However, UR is now considered as a potential source of municipal supply in many water scarce regions, as is the case in the most part of Mexico.

Bioretention cells are being gradually implemented around the world to mitigate the negative consequences of urban runoff and to improve its quality[3]. These systems, also called *rain gardens*, are ground depressions filled with filtering material (as gravel or sand) and covered with vegetation. The bioretention cells allow the temporal retention of urban runoff, thereby mitigating peak flows and floodings, as well as its physical, chemical and biological treatment. Besides, they are attractive and easily integrated into the urban landscape, and require only a minimal amount of maintenance. Bioretention cells are not widely employed in xeric climates yet, even though floodings and peak flows are also common in cities located in these regions[4]. However, it is necessary to adapt the conventional bioretention design to the constraints imposed by xeric climates, noticeably concerning the structure of the vegetative cover.

To this end, the aim of this work was to design a bioretention cell to be constructed in a xeric zone. Firstly, a bioretention pilot was designed to stand the short, but often intense, rain periods of the Central Highlands of Mexico, which are followed by prolonged dry spells. The hydrological performance of the pilot and its capacity for removing microbial pollution was assessed. Secondly, we designed and sized a full-scale bioretention cell able to mitigate the effects of urban runoff in our university campus.

MATERIALS AND METHODS

Configuration of the bioretention pilot. Bench-scale testing was conducted in a bioretention box of 40.8 L with 1632 cm^2 of surface area and 25 cm of depth (**Figures 1-2**). As filtering media, the following materials were used (from the top to the bottom of the pilot): decorative marble (ϕ_{max}: 23 mm), clinoptilolite zeolite (ϕ_{max}: 5 mm, CEC: 367.6 meq/100 g), polyacrylamide hydrogel (80 g_w/g), pumice gravel (ϕ_{max}: 13 mm) and coarse gravel (ϕ_{max}: 15 mm). The hydrogel was added to the filtering material to increase the water holding capacity of the system and the resistance of the vegetative cover to the long dry periods of the study zone. As vegetative cover, we used several succulent plants, which show a distinct ability to store water in their organs and then to withstand extended periods of drought. They have demonstrated to tolerate the extreme conditions typically found in rooftops, and consequently they are widely used in green roofs[5].

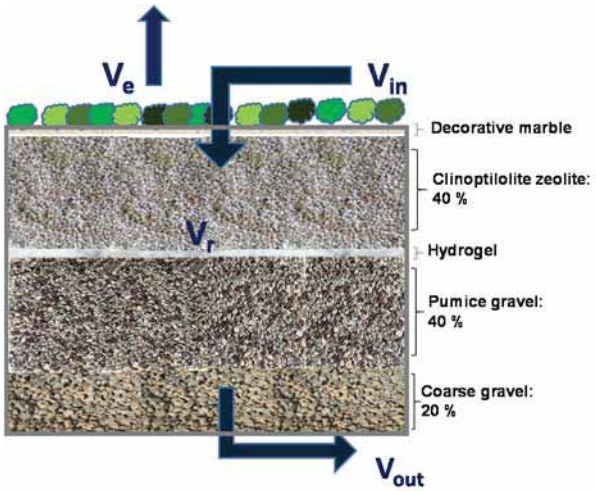


FIGURE 1. Stratification of the filtering materials of the bioretention pilot. V_{in}, V_{out} and V_r correspond to the volume of water entering, leaving and being stored in the pilot, respectively. V_e is the volume of water lost by evapotranspiration



FIGURE 2. Vegetative cover of the bioretention pilot
1: *Opuntia senilis;* 2: *Tradescantia* sp.; 3: *Cylindropuntia imbricata;* 4: *Agave americana;* 5: *Myrtillocactus geometrizans;* 6: *Aloe sp.;* 7: *Echeveria sp.;* 8: *Crassula perforata;* 9: *Sedum sp.;* 10: *Stenocereus dumortieri;* 11: *Tradescantia sp.;* 12: *Echeveria sp.;* 13: *Stenocereus peruvianus;* 14: *Gasteria sp.;* 15: *Agave sp.*

Evaluation of the hydrological performance of the bioretention pilot. The bioretention box was placed outdoors and its operation was evaluated during 160 days, from September 2014 to February 2015. The pilot was mostly rain-fed but it received also synthetic urban runoff (SUR) to evaluate the removal of microbiological pollution.

The precipitation data provided by the National Meteorological Center (corresponding to the aforementioned period) and all the inputs of SUR were used to calculate the total volume of water entering to the pilot (V_i). All volume of water recovered at the outlet of the system was recorded and used to calculate V_{out}. The sum of the water accumulated in the system (V_r) and the water lost by evapotranspiration (V_e) is the bio-retained water, and it was calculated by subtracting V_{out} from V_i.

Evaluation of the removal of microbiological pollution. To this end, a synthetic urban runoff (SUR) consisting in a suspension of *Escherichia coli* ($6.72x10^7$ CFU/100 mL) in an isotonic saline solution (0.85% of NaCl w/v) was employed. SUR was fed at a rate of 30.64 mm during 10 min, which correspond to an extreme rain event according to a previous historical review[6]. The cell count at the inlet and at the outlet of the bioretention system was carried out by culture on eosin methylene blue solid agar (Beckton Dickinson, U.S.A.). The plates were incubated at 37°C for 48 hours.

Study zone and climate conditions. The university campus is located in the municipality of Mineral de la Reforma, Hidalgo, Mexico, between the coordinates 20°05'47'' NE and 98°42'37'' WL (**Figure 3**). It is a semi-arid zone with a mean temperature of 14.6°C and an annual rainfall of 377 mm. The rainy season lasts from May to September[7].



FIGURE 3. Location of the study area (in red)

From an analysis of the direction of the runoff and the topography of the micro watershed, the study area was divided into five sub-basins. We identified the sub-basin 1 (Sb-1) as key to mitigate the impacts of peak flows and consequently it was chosen to accommodate the bioretention cell (**Figure 4**). Sb-1 is situated in the most elevated zone of the study area and represents the major source of the runoff in the micro watershed because it covers a substantial part of the micro watershed surface (38.4%, corresponding to 113,565.4 m^2). The maximal length of the runoff path (L) is 614 m, with a 1.47% slope (S).



FIGURE 4. Study area (delimited by green lines), sub-basin1 (Sb-1; delimited by red lines) and proposed location of the bioretention cell (in yellow)

Hydrological design variables. The Kirpich equation[8] was used to estimate the concentration time (*Tc*) of the runoff from its origin point to its outlet point (Equation 1):

$$Tc = 0.0663\left[\frac{L}{\sqrt{S}}\right]^{0.77} \quad (1)$$

Where:
Tc = concentration time [h]
L = maximal length of the runoff path [m]
S = slope [dimensionless]

The rainfall intensity (*i*) was calculated from the design rainfall (*P*) and the concentration time of the runoff (*Tc*) (Equation 2):

$$i = \frac{P}{Tc} \quad (2)$$

Where:
i = rainfall intensity [mm/h]
P = design rainfall [mm]

The peak runoff (at 5 min, 10 min, 15 min, 30 min, 1 h, 24 h) was calculated from the Rational Method[9] (Equation 3):

$$Q = (Rc)x(i)x(A) \quad (3)$$

Where:
Q = peak runoff [m^3/s]
Rc = runoff coefficient (0.8 for asphalt)
i = rainfall intensity [m/s]
A = drainage area [m^2]

RESULTS AND DISCUSSION

Evaluation of the hydrological performance of the bioretention pilot. The evaluation of this variable is often based on the reduction (as percentage) of the water entries (V_{in}). A typical volume reduction in a bioretention system varies between 40 and 50%, but it can reach 100%[4]. The **Figure 5** shows the global mass balance of the study pilot, *i.e.*, evaluated at the end of the 160-day period. It is worth to note that its global hydrological performance is comparable to the literature reports. However, when individual rainfall events are considered, the volume reduction was highly variable. For some rainfall events, all of them preceded by dry periods long enough, volume reductions higher than 90% could be achieved. At the opposite, the lowest volume reductions were measured for closely spaced rainfall events.

Evaluation of the removal of microbiological pollution. A mass balance of *E. coli* was also made to evaluate the microbial removal capacity of the pilot, which was found as equal to 15%. This removal capacity can be considered low according to the literature data; for instance, *E. coli* removals between 48 and 97% were reported for several bioretention units, where the highest value corresponds to an unvegetated control unit[10]. In the same study, it was stated that the performance of a bioretention cell will fluctuate widely during its first year of operation. After this period, the porosity of the filtering material is likely to diminish, leading to a higher microbial removal capacity. Then, the low removal measured in our unit could reflect this lack of settlement and further compacting of the filtering media.

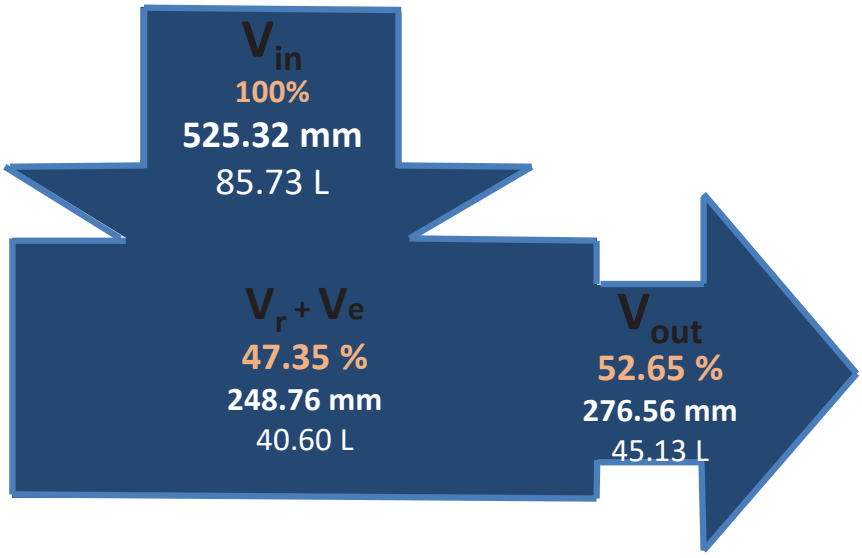


FIGURE 5. Global water balance of the bioretention cell

Hydrological design. The hydrological variables calculated, as well as the constants used to calculate them, are presented in **Table 1**.

TABLE 1. Description of the hydrological variables

Drainage area (A) = 113,565.4 m^2	Runoff coefficient (Rc) = 0.8
Runoff length (L) = 614 m	Rainfall intensity (i, m/s) = 2.3 x 10^{-7}
Slope (S) = 1.47	Concentration time (Tc, min) = 5
Peak runoff (Q) = 5.8 x 10^{-5} m^3/s	

For our campus, we propose a bioretention cell with a 50 m^2 (5 m x 10 m) surface and a depth of 1.8 m, accompanied with a solids interceptor at the inlet and a storage tank of treated urban runoff at the outlet. The proposed system has the same stratification of the filtering media than the bioretention pilot studied. The vegetative cover should be also similar to the succulent assemblage used in the pilot. However, preference will be given to the most massive plants of the assemblage, as *Agave* sp., *Aloe* sp. or *Opuntia* sp., which possess strong aerial parts and are more prone to withstand real-world conditions than, for instance, *Sedum* sp. The longitudinal section of the design is shown in **Figure 6**.

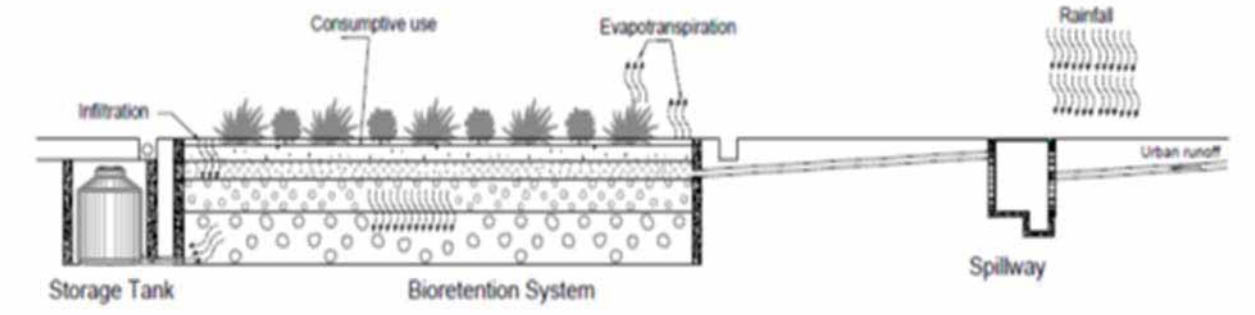


FIGURE 6. Detail of the full-scale bioretention system proposed

CONCLUSION

We proposed and constructed a bioretention pilot adapted to the particular conditions of xeric climates. The vegetative cover, based on succulent plants, survived well throughout the study period (160 days), probably due to the hydrogel present as filtering material. A global water balance showed that the pilot could bioretain (*i.e.*, to evapotranspirate and to accumulate water in the system) a water fraction similar to that reported in the bibliography. Although the microbial pollution removal was low under the extreme rainfall conditions of the test, the performance of the system has still to be evaluated concerning other pollutants and under moderate-to-low rainfall conditions. Finally, a full-scale bioretention design was proposed specifically for our university campus, which has to be constructed and validated for real-world xeric conditions.

ACKNOWLEDGMENTS

The authors acknowledge the financial support from the 2015-2016 Annual Research Program (PAI from its Spanish acronym) of the Universidad Autónoma del Estado de Hidalgo. Special thanks are given to Dr. Carlos Bigurra for his help with the architectural plan of the bioretention cell.

REFERENCES

1. United Nations, *World Urbanization Prospects: The 2014 Revision*, Department of Economic and Social Affairs, Population Division (ST/ESA/SER.A/366), New York, U. S. A., 2015.
2. Petrucci G., Gromaire M.C., Shorshani M.F., Chebbo G. Nonpoint source pollution of urban stormwater runoff: a methodology for source analysis. Environ. Sci. Pollut. Res. 21 (2014) 10225-10242.
3. Hunt W.F., Lord B., Loh B., Sia A. Plant *Selection for Bioretention Systems and Stormwater Treatment Practices*, SpringerBriefs in Water Science and Technology. DOI: 10.1007/978-981-287-245-6_1.
4. Steffen, J. R. Bioretention hydrologic performance in a semiarid climate. Ph. D. Dissertation, The University of Utah, 2012.
5. Dvorak B., Volder A. Green roof vegetation for North American ecoregions: a literature review. Landscape Urban Plan. 96 (2010) 197-213.
6. SMN Precipitation data for Pachuca weather station, 1951-2010. Servicio Meteorológico Nacional, Mexico, 2010. http://smn.cna.gob.mx/index.php?option=com_content&view=article&id=42&Itemid=75.
7. Lizárraga-Mendiola L., Vázquez-Rodríguez G., Blanco-Piñón A., Rangel-Martínez Y., González-Sandoval M. Estimating the Rainwater Potential per Household in an Urban Area: Case Study in Central Mexico. Water 7 (2015) 4622-4637.
8. Qin, H.P., Li, Z.X., Fu, G. The effects of low impact development on urban flooding under different rainfall characteristics. J. Environ. Manage. 129 (2013) 577-585.
9. Liaw C.H., Tsai Y.L., Cheng M.S. Low-impact development: an innovative alternative approach to stormwater management. J. Marine Sci. Technol. 8 (2000)41-49.
10. Kim M.H., Sung C.Y., Li M.H., Chu K.H. Bioretention for stormwater quality improvement in Texas: Removal effectiveness of *Escherichia coli*. Sep. Purif. Technol. 84 (2012) 120-124.

CHAPTER 11.5. DESEMPEÑO DE SUELOS PARA USO PECUARIO CONSTRUIDOS CON GEOTEXTILES Y MATERIAL GRANULADO

M. Vitón *(1); J. Gasulla (2); M. Prieto (1) and D. Crespo (1)

(1) CNIA INTA Castelar, De los Reseros S/N, Hurlingham, Argentina.
(2) CNIA INTA-CONICET Castelar, De los Reseros S/N, Hurlingham, Argentina.

RESUMEN

El objetivo del trabajo fue comparar los perfiles hidráulicos, el contenido de nitrógeno (N) y materia orgánica (MO), empleando diferentes combinaciones de geotextiles y material granulado como alternativa al uso de suelos nativos en superficies de uso pecuario. Se construyeron columnas de pruebas, con válvulas en el extremo inferior, medio y superior para recolectar los líquidos lixiviados (VL), filtrados (VF) y escurridos (VE), respectivamente. Se utilizaron diferentes densidades de geotextiles, distintos espesores y diámetros de material granulado (grava). La columna A (CA) fue construida con geotextil no tejido (densidad de 125 g/m^2), 50 mm de espesor de grava tipo 1 y 100 mm de espesor de grava tipo 2. La Columna B (CB) fue construida con geotextil no tejido (densidad 250 g/m^2), igual espesor de grava tipo 1 que la columna anterior y 50 mm de grava tipo 2. La columna control (CC) se construyó con capas de suelo compactado de 150 mm de espesor. A cada columna se agregó estiércol bovino y se aplicó una lluvia mediante un simulador de lluvia. Se determinó para cada columna los valores de VL; VF, VE, MO, N y la resistencia a la penetración (RP) de los materiales. Los resultados mostraron que el valor VF fue similar en CA y CB, aproximadamente de 90% del volumen total. Para la columna CA, el parámetro VL fue del 12%, sin embargo el parámetro en la columna CB fue nulo. El VE fue del 44%, reteniéndose el volumen restante de lluvia en la capa superior del suelo en la columna CC, pero en las columnas con geotextiles no se detectó dicha variable. Se demostró que hubo retención de la MO del estiércol agregado del 60% y del 85% para los VF de CA y CB, respectivamente y del 0.8% en el VE del CC. En cuanto al parámetro estudiado N, en el CC mostró en el VE un contenido 10 veces superior al contenido determinado en los VF de CA y CB. En la columna control se observó una disminución del 35% de la RP, mientras que en las columnas con geotextiles no se encontró una disminución. Como conclusión global, ambas columnas construidas con geotextil y material granulado eliminan el VE, retienen un porcentaje mayor de MO y N, y presentan una RT mayor que los suelos compactados (CC). Los materiales de la CB mostraron ser más eficientes en el VL del agua de lluvia.

Palabras claves: barros, ganados, geotextiles, material granulado.

---

*Author for correspondence: mauro.viton@inta.gob.ar

INTRODUCCIÓN

Muchas prácticas pecuarias hacen uso de superficies confinadas y/o de tránsito. Comúnmente estas áreas tienen altas densidades de población animal y pueden ser fuentes de contaminación de aguas superficiales y subterráneas. El escurrido y el lixiviado que percola a través de la columna de suelo son una fuente rica de nutrientes tales como fosforo y nitrógeno. Además, las áreas con alta densidad y tráfico animal pueden generar barros durante épocas de lluvia intensa, lo que dificulta el movimiento de maquinaria, afecta el desempeño de los animales y su alimentación[1,2] y contribuye a la erosión del suelo y a la degradación del ambiente.

El acarreo y distribución del alimento usando maquinaria agrícola sobre suelo no protegido puede producir ahuellamiento y posterior formación de barro por acumulación de agua. Dicha generación de barro incrementa el stress animal y provoca una gran variedad de problemas sanitarios, incluyendo enfermedades bacterianas y protozoarias.

El barro además puede provocar que el suelo se mueva fuera de los sitios de explotación como escurrido. Cuando ocurre la erosión, la capa fértil se pierde. A pesar de que esta capa es la de mayor valor agronómico, puede actuar como contaminante físico de cursos de agua por acción de la erosión. Adicionalmente puede arrastrar patógenos, contaminantes y nutrientes junto con las partículas de suelo.

El tratamiento de superficies usadas puede disminuir la creación de barro, creando un área de fácil mantenimiento y reduciendo la cantidad de alimento desperdiciado y requerido por el ganado.

Los suelos construidos con combinaciones de geotextiles y material granulado (grava) ofrecen una alternativa de bajo costo a los materiales hormigonados para la provisión de superficies para tráfico animal y de maquinaria, y para zonas de alimentación y estadía. Estas superficies se han utilizado exitosamente en diversas operaciones pecuarias. Los geotextiles se pueden utilizar para muchas aplicaciones en estas operaciones, incluyendo filtración, separación, drenaje, control de la erosión, control de sedimentos, y refuerzo estructural. Esencialmente, los geotextiles están diseñados para separar materiales de distinta granulometría, tales como roca y tierra. Por ejemplo, cuando se usa para estabilizar un camino agrícola o para tráfico pesado, la tela geotextil crea una separación entre la interfaz de roca y suelo, proveyendo integridad estructural y extendiendo la vida útil de la superficie. A su vez, el uso de la tela geotextil, proporciona refuerzo al distribuir las cargas que ejercen las pezuñas o ruedas sobre un área mayor. El uso de este sistema de bajo costo crea una estructura de larga duración y conserva los recursos naturales mediante la reducción de la erosión.

Se debe tener especial consideración en su uso en las zonas donde se almacene o deposite estiércol animal y el suelo bajo o adyacente al geotextil sea permeable. Debido a que la trama del geotextil mejora el drenaje, puede existir una posibilidad de movimiento del estiércol, nutrientes y bacterias hacia el suelo situado alrededor y, posiblemente, hacia cursos de agua adyacentes.

Estudios realizados con estiércol animal muestran ciertos fenómenos de oclusión en algunos tipos de geotextil en contacto directo con el estiércol[3], indicando la potencial transformación de los geotextiles en barreras de protección para recursos hídricos subterráneos. Singh *et al.* (2003)[4] estudiaron el efecto de diferentes combinaciones de

geotextiles y grava (150-200mm de fondo) sobre la tasa de infiltración vertical y la contaminación por estiércol bovino. Dichos investigadores encontraron que la concentración de sólidos totales (ST) y demanda química de oxigeno (DQO) se redujo en un 90%, pero este valor se redujo al aumentar las precipitaciones y la carga acumulada.

Estudios previos mostraron que el impacto ambiental producido por DQO, Nitrógeno total y ST se podría reducir en el transporte vertical a través de una superficie construida con geotextiles y material granulado, lo que facilitaría el tratamiento posterior mediante humedales[5]. El suelo subyacente podría resultar menos contaminado si se usase una capa doble de geotextil. La capa superior podría promover el drenaje mientras que la capa inferior podría tener un efecto de barrera protegiendo el suelo subyacente, previniendo el lixiviado y depósito de nutrientes y la contaminación de aguas subterráneas.

En el estudio realizado por Singh et al. (2008)[4], el foco se puso sobre el escurrido y el lixiviado en respuesta a al diseño de la superficie, aplicación de estiércol y precipitación pluviométrica, donde el líquido lixiviado y drenado se trataron como un único factor.

El objetivo general del presente trabajo fue la identificación de la combinación geotextil/material granulado que tenga el mejor perfil de retención de nutrientes cuando es sometida a una precipitación severa. Los objetivos específicos fueron determinar si una combinación geotextil/material granulado otorga una protección aceptable al suelo subyacente; identificar la combinación que ofrece el mejor drenaje (menor volumen de escurrido cuando se expone a cargas de estiércol y precipitaciones); determinar el perfil de generación de barro (volumen de líquido de lluvia retenido versus volumen de líquido evacuado) y los cambios físicos ocurridos en las combinaciones ensayadas.

MATERIALES Y MÉTODOS

Materiales de prueba. Se usaron, en este ensayo, dos tipos de geotextiles no tejidos agujados de filamentos de PET. Los geotextiles A y B poseen una apertura aparente de poro (AOS) de 0.15 mm y 0.13 mm y densidad de 150 y 200 gr/m2 respectivamente. Antes de comenzar los ensayos se comprobó la densidad de los geotextiles A y B pesando cinco rectángulos de 0.05x0.05 m de geotextil recortados de los rollos de cada variedad. El espesor de los geotextiles A y B se midió con calibres tipo Vernier (**Tabla 1**).

TABLA 1. Propiedades físicas de los geotextiles

Propiedades	Geotextil A	Geotextil B	Unidades
Espesor	1.2±0.05	1,5±0.1	mm
Densidad	145±5	200±3	gr/m2 (ASTM D 5261)
AOS (apertura aparente de poro)	0.15	0.13	mm (ASTM 4751)
Permeabilidad normal	0.42	0.40	cm/s (ASTM 4491)

El estiércol se obtuvo del campo de cría experimental del CICVyA del CNIA INTA Castelar. Sobre esta muestra se analizaron los siguientes parámetros: solidos totales (%ST), cenizas (% cenizas), materia orgánica (%MO) y contenido de nitrógeno total por Kjeldhal (NTK) (**Tabla 2**).

TABLA 2. Caracterización del estiércol

Propiedades	Estiércol
%ST	15.7 ±0.6
% Cenizas	30.49 ±1.3
%MO	69.5 ±1.2
%NTK	0.09 ±0.03

Dispositivos de prueba. Las columnas de pruebas se construyeron con tubería de PVC de 160 mm de diámetro externo y 147 mm de diámetro externo, y 750 mm de altura (**Figura 1**), según el modelo establecido por Barrington *et al* para ensayar la colmatación de geotextiles no tejidos con efluentes líquidos.

Las secciones de geotextiles a ensayar se sostienen entre dos bridas aseguradas con tuercas sobre una sección de 150 mm de suelo compactado separado mediante una geogrilla de un lecho de piedra.

Los puertos de extracción de muestras se encuentran a nivel fondo para recolectar los líquidos lixiviados (VL), a nivel medio por encima de la sección de geotextil para colectar los líquidos filtrados (VF), y a nivel superior para colectar los líquidos escurridos (VE).

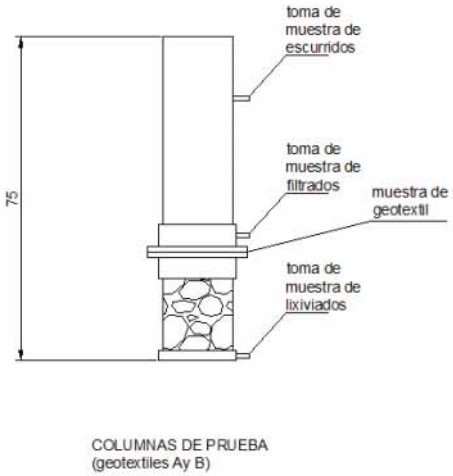


FIGURA 1. Esquema de columnas de prueba

Las columnas de pruebas correspondientes a los testigos (**Figura 2**) no disponen de bridas para sostener los geotextiles, ni puerto de extracción de VF.

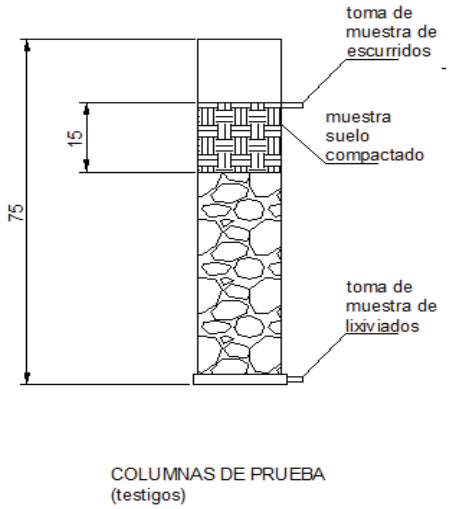


FIGURA 2. Columna de prueba para testigos

Para simular el efecto de la lluvia se utilizó un simulador de lluvia desarrollado por el Instituto de Suelos del CNIA. El mismo posee una estructura de hierro y chapa de 50 cm por 50 cm de base (0.25m^2) y 1.5m de altura. La estructura se ensambla con pequeños bulones que permiten su armado en zonas planas y en pendiente. La zona de medición está protegida del viento por cuatro paños de film plástico que se adhieren a la estructura mediante un tejido de velcro. En la parte superior se apoya la placa de goteo, de acrílico, en cuya base están insertados los 169 goteros construidos con la parte central de un cable coaxial.

Esta placa es provista de agua desde un reservorio recargable, de acrílico transparente graduado en mm de lluvia. Los goteros presentan una cobertura de plástico que permite la formación de una gota de agua de entre 4.7 a 5.1 mm de diámetro.

Método de Prueba. Se construyeron columnas para probar diferentes densidades de geotextiles, distintos espesores y diámetros de material granulado (grava). La **Tabla 3** muestra las características de las columnas de prueba fabricadas.

TABLA 3. Características de las columnas de prueba

	Columna A (CA)	Columna B (CB)	Columna A (CC)
Geotextil no tejido	Geotextil A	Geotextil B	-
Grava tipo 1 (20-40 mm de diámetro)	50mm de espesor	50 mm de espesor	-
Grava tipo 2 (2-8 mm de diámetro)	100mm de espesor	50 mm de espesor	-
Suelo compactado	-	-	150mm

Se realizaron 9 réplicas por cada combinación. A cada una de las columnas, se agregaron 20 g de estiércol bovino, equivalente a 6 cabezas de ganado durante cuatro horas en un corral (MWPS-18, 2000).

Las columnas se emplazaron en la zona de medición del simulador de lluvias y se sometieron a un evento pluviométrico de intensidad y duración severa (120 mm-60 minutos), recogiéndose los líquidos filtrados, escurridos y lixiviados de cada columna testeada. Una vez concluida la etapa de prueba bajo descarga pluviométrica, se testearon los cambios en la resistencia a la penetración en cada columna.

Recolección y muestreo de filtrados, escurridos y lixiviados. La medición de los volúmenes y el muestreo de los líquidos filtrados, escurridos y lixiviados se realizaron dentro de los 60 minutos del evento pluviométrico. Los volúmenes de líquidos filtrados, lixiviados y escurridos se midieron usando vasos de precipitado de 5000 ml de capacidad, separándose fracciones de 1000 ml para su análisis.

Métodos analíticos. Para la determinación de solidos totales (%ST) y cenizas (%cenizas) en el estiércol, líquido filtrado, escurrido y lixiviado se utilizaron las técnicas estándar de secado en estufa e incineración en horno. El contenido de materia orgánica (%MO) es la diferencia entre el contenido de solidos totales (%ST) y el contenido de cenizas (%cenizas).

Se analizaron además muestras representativas de líquidos filtrados, escurridos y lixiviados para determinar la concentración de nitrógeno total por Kjeldhal (NTK).

Parámetros de estimación.

Reducción de masa. El coeficiente de retención de masa (MRE) es una aplicación de la conservación de la masa de un analito ***j***, por ejemplo, los sólidos medidos y nutrientes vegetales, restantes en un suelo al final de cada evento pluviométrico. Es un parámetro acumulativo a través de la extensión del tiempo de duración de la lluvia y está representado por la siguiente ecuación:

$$MREpl = \frac{MijS}{Mfjev}\ x\ 100 \qquad (1)$$

Dónde:

MijS= masa inicial de un analito ***j*** agregada al suelo previamente al evento pluviométrico.

Mfjev= masa evacuada de un constituyente j al final del evento pluviométrico.

Reducción de concentración. La reducción de concentración (influente a efluente) es otro parámetro para evaluar la eficiencia de remoción de un analito ***j*** a través de la combinación geotextil/material granulado o suelo. La reducción de concentración promedio de un analito ***j*** (CRj) puede expresarse como:

$$CRj = \frac{(CINj - COUTj)}{CINj}\ x\ 100 \qquad (2)$$

Donde:
CINj es la concentración del analito agregada a la columna (influente)
COUTj es la concentración del analito en el líquido evacuado (efluente).

RESULTADOS Y DISCUSIÓN

Escurridos. El VE (volumen de escurrido) de la columna CC correspondió al 44% del volumen de líquido agregado como lluvia, mientras que CA y CB no registraron VE.

El VE de CC mostró una CR (reducción de concentración) de NTK de 99.3% y una MRE (retención másica promedio) de 0.31%; por otro lado, la MRE de MO arrojo resultados negativos y el CR de MO fue de 72%.

Filtrados. El VF (volumen de filtrado) para CA y CB fue de 88% y 87 %, respectivamente, del volumen total de lluvia agregado por sección de superficie en ambas combinaciones. La CC no mostro VF alguno.

Para el contenido de NTK en el filtrado, la columna CA mostro una CR promedio de 80% y CB de 78% respecto a la concentración de NTK en el estiércol agregado. La CR del VF de CA y CB referido a la concentración de NTK del VE de CC fue del 79 y 73%, respectivamente. La MRE de NTK para CA fue de 57% y para CB de 49%.
Para MO, CA y CB mostraron una CR de 88% y 81%, CC, por otro lado mostro valores negativos. La MRE para MO de CA fue de 66%, de CB 73% y CC arrojo resultados negativos.
Lixiviados. El VL (volumen de lixiviado) observado en CA correspondió al 12% del volumen de lluvia agregado, mientras que CB y CC no demostraron VL alguno.

Cambios físicos. Se observó, luego del ensayo, una disminución del 35% en la resistencia a la penetración de las columnas testigo (CC), las columnas CA y CB no mostraron cambios apreciables.

TABLA 4. Cambios en la resistencia a la penetración (kg/m^2)

Columna	Previo ensayo	Posterior a ensayo
CA	2.8 ±0.5	2.8±0.6
CB	2.4 ±0.3	2.4±0.3
CC	2.1 ±0.1	1.67±0.18

CONCLUSION

La combinación CB ofrece una mayor protección al suelo subyacente al no permitir la generación de lixiviados por tener un geotextil con densidad mayor y AOS más pequeño. Los resultados arrojados permiten concluir que las superficies construidas con geotextiles pesados (CB), con menor espesor de material granulado, reducen la ocurrencia de lixiviados, en comparación a las construidas con geotextiles más livianos (CA).

Ambas combinaciones se mostraron eficientes en la eliminación del escurrido superficial y mostraron una gran similitud en la eficacia de reducción de barros.
CA presentó un mejor perfil de retención de NTK y MO que CB, pudiendo esto deberse al mayor espesor de la capa de material granulado sobre el geotextil.
Ambas combinaciones no mostraron alteraciones en su resistencia a la penetración.
Los resultados muestran que las combinaciones de geotextiles y material granulado no solo tienen una función de reducción de barros y mejora del drenaje para áreas con alto tránsito y permanencia de animales, sino también funciones de filtrado y retención de nutrientes, así como protección de suelos.

AGRADECIMIENTOS

Agradecemos al Ing. Javier Herrera de Maccaferri Argentina y a la Ing Victoria Ormaisteguy por su inestimable colaboracion y experiencia.

REFERENCIAS

1. Riskowski, G. L., & DeShazer, J.A. Work requirement for beef cattle to walk through mud. Transaction of ASAE, 19(1). (1976)., 141-144.
2. Degen, A. A., & Young, B.A. (1993). Rate of heat production and temperature of steers exposed to simulated mud and rain conditions. Canadian Journal of Science, 73,207-210.
3. Barrington, S.F., El Moueddeb, K., Jazestani, J. and Dussault, M., The Clogging of Nonwoven Geotextiles With Cattle Manure Slurries",Geosynthetics International, Vol. 5, No. 3 (1998), pp. 309-325.
4. Singh, A., Bicudo, J.R., & Workman, S.R. (2008). Runoffand drainage water quality from geotextile and gravel pads used in livestock feeding and loafing areas. Bioresource Technology (2003). 99, 3224-3232.
5. Von Wachenfelt, H. Treatment of manure contaminated rainwater from outdoor yards in a constructed wetland (in Swedish with English summary). Special Report 245, Swedish University of Agricultural Sciences, Department of Agricultural Biosystems and Technology. 95.
6.
7. Van Santvoort, G.P.T.M, "Geotextiles and Geomembranes in Civil Engineering", Prentice Hall, Englewood Cliffs, New Jersey, USA (1994), 595 p..
8. ASAE, 1999. ASAE Standards, Manure Production and Characteristics, 46th ed. St. Joseph, MI.
9. Goode, G.L. Seepage quality from geotextile and gravel pads used in heavy livestock traffic areas. MS Thesis, Department of Biosystems and Agricultural Engineering, University of Kentucky, Lexington, KY (2003), p. 95.
10. MWPS-18, Manure characteristics. Manure Management System Series, Section 1, MidWest Plan Service, Iowa State University, Ames, (2000). IA, p. 23.

CHAPTER 11.6. AIRBORNE BACTERIAL SPORES INACTIVATION WITH UV RADIATION OVER TiO_2 COATED GLASS RINGS

M. L. Satuf *(1,3); S. M. Zacarías (1,2); M.E. Visuara (2) and O. M. Alfano (1,3)

(1) INTEC (UNL-CONICET), Ruta Nacional Nº 168, Paraje "El Pozo", Santa Fe, Argentina
(2) FBCB (UNL), Ruta Nacional Nº 168, Ciudad Universitaria UNL, Santa Fe, Argentina
(3) FICH (UNL), Ruta Nacional Nº 168, Ciudad Universitaria UNL, Santa Fe, Argentina

ABSTRACT

Bioaerosols containing viruses, bacteria, and fungi can be responsible for infectious diseases, toxic reactions, and allergic responses. Therefore, research on disinfection technologies to control bioaerosols in air constitutes an area of great scientific interest. Heterogeneous photocatalysis is a potential alternative to mitigate the problem of air contamination indoors, mainly to inactivate resistant forms of microorganisms such as bacterial spores. In this study, the photocatalytic inactivation of *Bacillus subtilis* (strain ATCC 6633) spores over TiO_2-coated rings is evaluated.
Borosilicate glass rings (5 mm diam × 10 mm length) were coated with 1, 2 and 3 layers of TiO_2 P-25 (Evonik) by the “dip-coating” technique. The coated rings were nebulized with a suspension of spores employing a 6 jet "Collison" type nebulizer (BGI Instruments), and then exposed to UV-A radiation for 12 hours. UV lamps of different irradiation power were employed in separate assays. Bacterial inactivation was followed by analyzing the concentration of viable bacteria every 4 hours. Experimental results were fitted with the exponential equation $N=N_0 \exp(-kt)$, where N (CFU cm^{-2}) is the concentration of viable bacteria per unit area of support, N_0 (CFU cm^{-2}) is the initial bacterial concentration, k (h^{-1}) is the apparent kinetic inactivation constant, and t (h) is the irradiation time. CFU stands for colony forming units.
After 12 h of irradiation significant reduction of the spores’ viability was observed along the treatment. An increase in the UV-A irradiance or in the TiO_2 content increases the absorption of energy by the catalyst and, therefore, the availability of reactive oxygen species able to damage the spores structure. It is worth noting that the spores’ viability over glass rings without catalyst showed no changes in the presence of UV-A radiation.

Keywords: bacterial spores, inactivation, photocatalysis, titanium dioxide.

INTRODUCTION

Pollution of indoor air by pathogenic microorganisms represents a major problem in modern societies, where people spend most of their time indoors. Bioaerosols, containing viruses, bacteria, and fungi, can be responsible for infectious diseases, toxic reactions, and allergic responses.[1]

---

*Author for correspondence: mlsatuf@santafe-conicet.gov.ar

Photocatalysis with TiO_2 has many advantages over conventional technologies to remove microorganisms from air. Mainly, it can effectively destroy biological species, it does not produce hazardous by-products, and it can be operated under ambient conditions of temperature and pressure.

Photocatalytic air purification devices should assure the inactivation of all pathogenic microorganisms transported by air as bioaerosols. Therefore, studies on the inactivation of resistant forms of microorganisms, such as bacterial and fungal spores, are mandatory.

Specifically, spores of *Bacillus* species are much more resistant to adverse environmental conditions and inactivation technologies than vegetative cells and can therefore be employed as biological indicators to evaluate disinfection processes.

The present work evaluates the photocatalytic inactivation of *Bacillus subtilis* spores employing glass rings as support for the catalyst. This material would be used to fill up a photocatalytic reactor for air purification. Bacterial spores were nebulized over the glass rings with different number of TiO_2 coatings and then irradiated with artificial UV-A light. The nebulization of the spores simulates the real condition of bioaerosols in contact with a photocatalytic purification device.

MATERIALS AND METHODS

Experimental Setup. The photocatalytic experiments were carried out in an experimental setup consisting of a UV radiation emitting system, an irradiation compartment, and a support to hold the coated glass rings with the spore samples during irradiation (**Figure 1**).

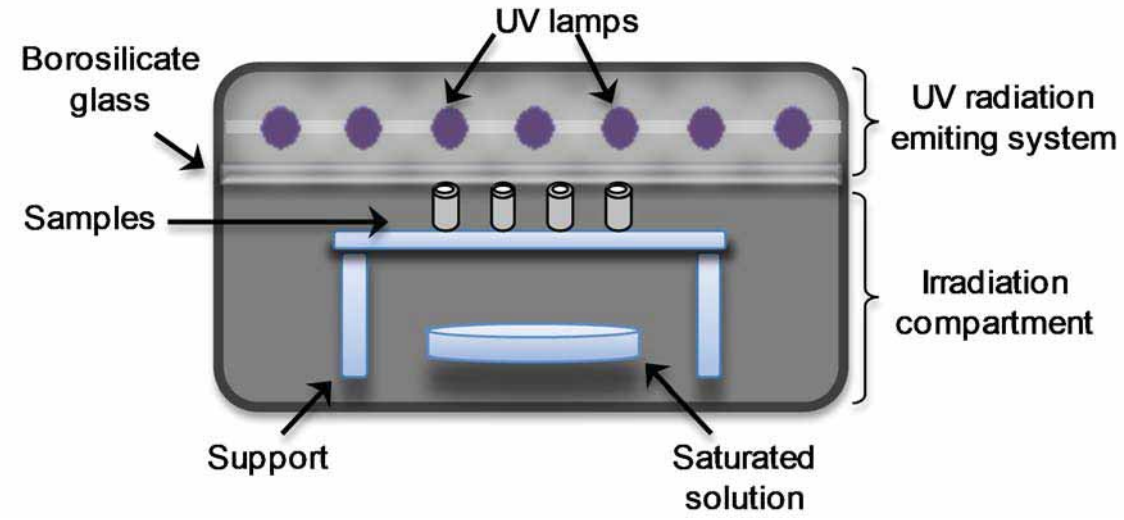


FIGURE 1. Experimental setup

A borosilicate glass plate separates the UV emitting system from the irradiation compartment. The UV emitting system consists of a set of seven tubular fluorescent lamps held by a metallic rectangular box above the irradiation compartment in a horizontal parallel arrangement. UV lamps of different irradiation power were employed

in separate assays. The emission of the lamps was comprised between 300 and 400 nm, with a maximum at 365 nm (UV-A). The power output spectra of the two types of lamps employed in the experiments are shown in **Figure 2** (recorded with a USB 2000 UV/VIS ES miniature fiber optic spectrometer, Ocean Optics). More details about the experimental setup can be found elsewhere.[2]

Inside the irradiation compartment, local measurements of the radiation flux incident at different positions on a plane were made using a radiometer (ILT 1700, International Light Technologies). Only the most illuminated surface, placed at the central zone of the irradiation compartment, was employed for the experiments. The average incident net radiation flux obtained was 1.76 mW cm^{-2} (Yarlux 8W/BLB) and 7.47 mW cm^{-2} (Philips Actinic BL TL 8W). The measurement of the incident radiation flux was performed by placing the radiometer below the borosilicate glass that separates the lamps from the irradiation compartment; therefore, the value obtained takes into account the absorption of the aforementioned borosilicate glass.

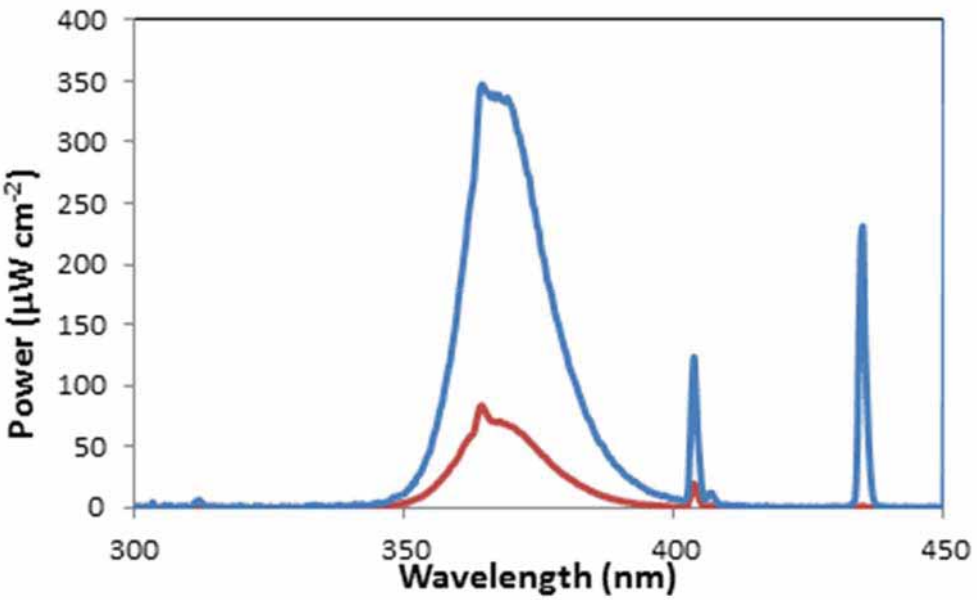


FIGURE 2. Spectral distribution of the incident radiation
Red line: Yarlux 8W/BLB. Blue line: Philips Actinic BL TL 8W

Photocatalytic rings with spore samples were held vertically in the central zone of the irradiation compartment. A saturated solution of ammonium sulfate was included in the irradiation compartment to secure an atmosphere with high and constant relative humidity, necessary to obtain sustainable TiO_2 photocatalytic activity. Throughout the experiments, the relative humidity and temperature inside the irradiation compartment were kept constant at 70% and 40 °C, respectively. A thermohygrometer (Oakton Thermohygrometer Kit) was employed to measure these variables.

Photocatalyst Preparation. The photocatalytic inactivation of *Bacillus subtilis* spores was assayed over TiO_2 coatings. A suspension of 150 g L^{-1} of TiO_2 (TiO_2 Aeroxide P25,

Evonik Degussa GmbH, Germany) in ultrapure water (Osmoion Ultrapure Water, Apema) at a pH value of 1.5 (adjusted with HNO_3) was used.[3]

Preparation and coating of photocatalytic rings. Before TiO_2 immobilization, the borosilicate glass rings were washed with a solution containing 20 g of potassium hydroxide, 250 mL of isopropyl alcohol, and 250 mL of ultrapure water. The rings remained in contact with the washing solution for 24 h and then for 2 h under sonication (Ultrasonik 300). Afterward, they were heated for 8 h at 500 °C to remove any trace of organic material that might still remain on the surface. The size of the rings was 0.5 cm (diameter) × 0.9 cm (length). TiO_2 immobilization on the glass rings was achieved by the dip-coating technique, with a withdrawal speed of 3 cm min^{-1} at room temperature (25 °C). Then, the rings were dried in an oven at 110 °C for 24 h and then heated at 500 °C for 2 h at a heating rate of 5 °C min^{-1}. This procedure was repeated to obtain rings with more coatings.

Characterization of photocatalytic rings. *The* thicknesses of the TiO_2 films were calculated from SEM images acquired by a Scanning Electron Microscope (JEOL, JSM-35C) equipped with an acquisition system of digital images (SemAfore). The mass of TiO_2 immobilized on the glass rings was determined by weight difference of a significant number of rings.

Spore formation and collection. The model microorganism was *Bacillus subtilis* (ATCC 6633 strain). Following the technique proposed by Shehata and Collins,[4] suspensions of spores in distilled water were prepared. To do this, a Roux bottle containing a sporulation medium, consisting of nutritive agar (Merck Chemicals) with 0.05% $MnSO_4$ and 0.05% $MgSO_4$, was inoculated and incubated at 30 °C for a 10-day period. Then, the spores and vegetative cells obtained were recovered by washing the surface of the sporulation medium with sterile saline solution. After this step, the spores recovered were centrifuged three times at 3500 rpm for 15 min with the same buffer. The suspension was kept at 30 °C for 48−72 h to induce vegetative cell lysis. Then, the vegetative cells and the spores were washed again according to the instructions outlined above. This procedure was repeated three times to wash the cells. The spores were finally suspended in sterile distilled water and stored at 4 °C.

Inactivation experiments. To ensure the absence of vegetative cells before carrying out the irradiation experiments, the spore suspension was held for 10 min at 80 °C.

The deposition of the microorganisms over the rings was carried out in a sterile cabin, employing a 6 jet "Collison" type nebulizer (CN25 MRE Modified, BGI Instruments), which generates droplets containing *B. subtilis* spores. The spores' suspension was nebulized during 10 minutes over the TiO_2-coated rings (**Figure 3**). Then, the rings were dried at 25 ºC in a sterile environment. Afterward, these rings were placed in the irradiation compartment and exposed to UV-A radiation for different time periods (4, 8 or 12 h). The initial concentration of spores over the coated rings was 1×10^5 CFU cm^{-2}.

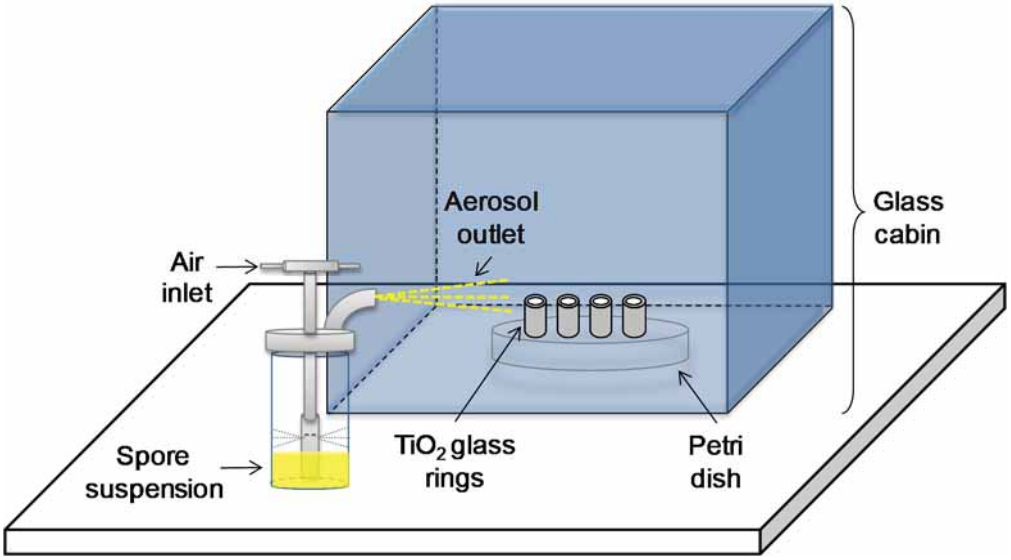


FIGURE 3. Nebulization of spores over the glass rings

To perform the counting of viable spores after irradiation, each ring was placed in a tube with 10 mL of sterile extraction solution (0.1% peptone in distilled water with 0.01% of Tween 80), stirred in vortex for 2 min, and then sonicated for 15 min. Finally, aliquots of 1 mL of the resulting suspension were spread onto nutrient agar plates (Merck Chemicals), incubated at 30 ºC for 48 h, and the colony forming units counted. Appropriate dilutions were made to count 30-40 colonies per plate. The tests were repeated twice for each experimental condition studied, and the counting of the viable spores was made in duplicate.

The decay of viable spores as a function of the irradiation time was fitted with the exponential equation:

$$N = N_0 \, e^{-kt} \qquad (1)$$

where N (CFU cm^{-2}) is the remaining viable bacterial concentration per unit area of support, N_0 (CFU cm^{-2}) is the initial bacterial concentration, k (h^{-1}) is the apparent kinetic constant, and t (h) is the irradiation time.

Two control experiments were carried out. One was conducted in the dark with TiO_2-coated rings, and the second one was conducted with radiation but employing uncoated glass rings.

RESULTS AND DISCUSSION

Characterization of photocatalytic rings. Glass rings before and after the TiO_2 deposition are shown in **Figure 4**. The thicknesses of the TiO_2 films were calculated from SEM images. **Figure 5** shows a SEM image of the cross section of a glass support with 3 coatings of TiO_2.



FIGURE 4. Glass rings before and after dip coating procedure

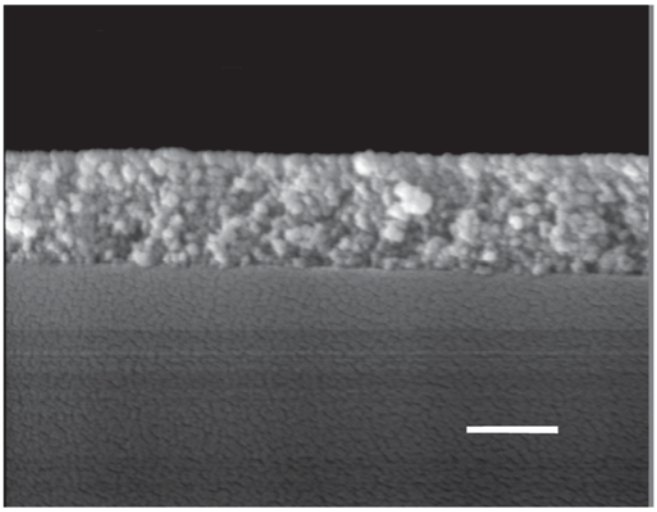


FIGURE 5. SEM image of the support with 3 coatings of TiO_2 (white bar = 1 μm)

The mass of TiO_2 immobilized on the glass rings was determined by weight difference of a significant number of rings. In **Table 1**, the average thickness of the TiO_2 films and the amount of TiO_2 immobilized on the glass supports are reported.

As expected, a proportional increase of the film thickness and of the TiO_2 content was obtained by increasing the number of coatings.

TABLE 1. Film thickness and mass of catalyst immobilized over the glass rings

Number of TiO_2 coatings	Film thickness (μm)	Mass of TiO_2 (mg cm^{-2})
1	0.35	0.28
2	0.69	0.54
3	1.15	0.86

Photocatalytic spore inactivation. **Figure 6** shows the experimental values of viable spore concentration (dimensionless) as a function of the irradiation time, obtained with the rings with 1, 2 and 3 TiO_2 coatings, under the two irradiation conditions assayed. The corresponding fitting curves are also depicted in the figure.

Table 2 presents the estimated values of the apparent kinetic constant k with the 99% confidence interval, and the orders of magnitude reduction of the initial concentration of viable bacteria after 12 h of irradiation.

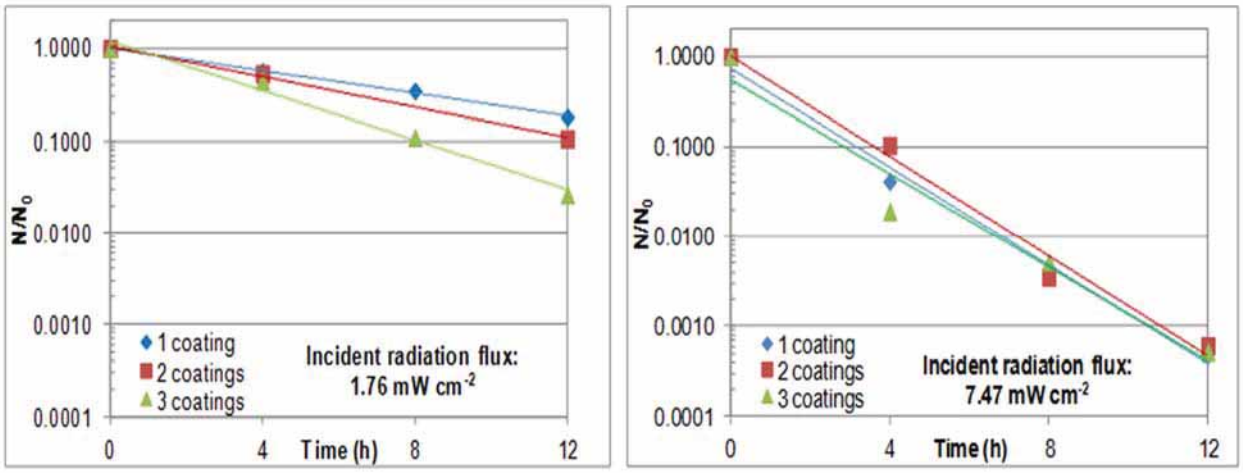


Figure 6. Viable spore concentration vs irradiation time over 1, 2 and 3 layers of TiO_2 coated glass rings and two different irradiations fluxes. Experimental values (◇, □, Δ) and fitting (——).

It is worth mentioning that the spores viability over glass rings without catalyst showed no changes in the presence of UV-A radiation (data not shown), ruling out the possibility of photochemical inactivation of the spores under the operating conditions used. Additionally, no changes in the survival of the spores were observed when the TiO_2 coated rings were stored in the dark.

TABLE 2. Apparent kinetic constants

Incident radiation flux				
TiO_2 coatings	1.76 mW cm^{-2}		7.47 mW cm^{-2}	
	k [h^{-1}]	OMR*	k [h^{-1}]	OMR*
1	0.14 ± 0,01	0.74	0.59 ± 0.06	3.31
2	0.18 ± 0,02	0.97	0.68 ± 0.03	3.39
3	0.31 ± 0,02	1.58	0.62 ± 0.04	3.29
*OMR: Orders of Magnitude Reduction				

When *B. subtilis* spores were irradiated over TiO_2 films, their viability decreased significantly and the inactivation extent increased with the irradiation time. It is generally accepted that the photocatalytic inactivation of microoganisms is mainly due to interaction with highly reactive oxygen species, particularly hydroxyl radicals, produced when the catalyst absorbs UV radiation. Hydroxyl radicals are able to damage the spore structure, finally leading to inactivation.

When the coated rings were exposed to 1.76 mW cm^{-2}, the inactivation rate increased with the TiO_2 loading. UV-A photons activate the TiO_2, promoting charge separation and formation of •OH radicals. More catalyst produces more radicals, leading to an increase in the inactivation rate. With 3 coatings, the inactivation kinetic constant doubles the value obtained with 1 coating.

Under the highest irradiation level, greater inactivation was obtained. More than 3 orders of magnitude reduction of the initial concentration of spores was achieved after 12 h of irradiation. However, no significant differences between 1, 2 or 3 coatings were observed. Apparently, a maximum inactivation rate has already been achieved with 1 coating. At high UV irradiance, more catalyst could generate an excessive production of hydroxyl radicals in the catalytic film, leading to the formation of hydroperoxyl radicals, which are less effective for bacteria inactivation.[5] Therefore, more TiO_2 content does not produce greater inactivation.

CONCLUSION

Considerable decrease in the viability of the resistant form of *B. subtilis* has been achieved by photocatalysis, and the inactivation extent increased with the irradiation time.

Regarding the effect of the mass of TiO_2 immobilized over the glass rings, under low irradiation levels, an appreciable increase in the inactivation rate by increasing the TiO_2 content is observed.

Concerning the effect of the irradiation level, experimental results show that higher radiation fluxes enhance spore inactivation.

Therefore, an increase in the UV-A irradiance or in the TiO_2 content increases the absorption of energy by the catalyst and, therefore, the availability of reactive oxygen species able to damage the spores structure.

Glass rings coated with TiO_2 have shown to be promising fillings for air purification photocatalytic reactors.

ACKNOWLEDGMENTS

The authors are grateful to Universidad Nacional del Litoral (UNL), Consejo Nacional de Investigaciones Científicas y Técnicas (CONICET), and Agencia Nacional de Promoción Científica y Tecnológica (ANPCyT) for the financial support. They also thank Antonio C. Negro for his help during the experimental work.

REFERENCES

1. Lee B.U. Life Comes from the Air: A Short Review on Bioaerosol Control. Aerosol Air Qual. Res. 11 (2011) 921–927.
2. Zacarías S. M., Satuf M. L., Vaccari M. C., Alfano O. M. Photocatalytic inactivation of airborne bacterial spores using TiO_2 films with silver deposits. Chem. Eng. J. 266 (2015) 133–140.
3. Van Grieken R., Marugán J., Sordo C., Pablos C. Comparison of the photocatalytic disinfection of E. coli suspensions in slurry, wall and fixed-bed reactors. Catal. Today. 144 (2009) 48.
4. Shehata T. E., Collins E. B. Sporulation and heat resistance of psychrophilic strains of Bacillus. J. Dairy Sci. 55 (1972) 1405.
5. Caballero L., Whitehead K. A., Allen N. S., Verran J. Inactivation of *Escherichia coli* on immobilized TiO2 using fluorescent light. J. Photochem Photobiol A: Chem. 202 (2009) 92–98.

CHAPTER 11.7. INACTIVATION OF *ASPERGILLUS NIGER* WITH PHOTOCATALYTIC PAINTS

S. M. Zacarías (1,2); R. Schumacher (2); F. Salvadores (1); O. M. Alfano (1) and M. M. Ballari *(1,2)

(1) INTEC (Universidad Nacional del Litoral - CONICET), Ruta Nacional Nº 168, Paraje "El Pozo", Santa Fe, Argentina
(2) Facultad de Bioquímica y Ciencias Biológicas, Universidad Nacional del Litoral, Ruta Nacional Nº 168, Ciudad Universitaria, Santa Fe, Argentina

ABSTRACT

The environmental fungi inactivation employing photocatalytic paints was assessed for different illumination conditions. The paint was formulated with a modified carbon doped TiO_2 active under visible radiation. However, the inactivation of *Aspergillus niger* by the photocatalytic oxidation of the TiO_2 present in the paint was not distinguishable working with visible light. The latter was concluded after testing several non-photoactive blanks under visible light, in which a fungi inactivation comparable to the photocatalytic paint was achieved. Nevertheless, better control of the microorganism growth by the photocatalytic process was observed for the experiments carried out under UV light, when the photocatalytic paint could inactivate more *Aspergillus niger* conidia than the tested blanks. In addition, a commercial antifungal paint was evaluated in order to compare the efficiency of the photocatalytic material with the actual mold control method applying fungicide compounds.

Keywords: inactivation, fungi, paint, photocatalysis.

INTRODUCTION

Diverse microorganisms are transported as bioaerosols being a health risk for people living in indoor environments. A particular but very common problem is the fungus or mold growth in environments without ventilation and with high relative humidity[1]. The exposure to these microorganisms is associated to the development of asthma and allergy, among others respiratory problems[2]. Additionally, the fungus development on walls can be a deterioration cause of these surfaces. Nowadays, there are different wall paints or paint additives with antifungal properties employing chemical fungicides. However, some of these antifungal compounds at certain concentrations are dangerous for humans and the environment[3].

The heterogeneous photocatalysis is an efficient method for the chemical and biological purification of water and air. The antimicrobial power of this technology was widely studied employing UV radiation, but less investigated applying visible light as the energy source[4-8]. In these works the inactivation of virus, bacteria and fungus was assessed. One of the most studied environmental and non-pathogen molds in

---

*Author for correspondence: ballari@santafe-conicet.gov.ar

photocatalytic works is the *Aspergillus niger* principally under UV-A and UV-C radiation[4,9-16]. However, working with a conidia suspension of *Aspergillus niger* over a photocatalytic surface no growth inhibition was found after a short time exposure under visible light[4]. On the other hand, positive results were found working with photocatalytic coated visible fluorescent lamps for the *Aspergillus niger* conidia reduction in air phase[7, 8].

An increasingly common application of heterogeneous photocatalysis is the combination of titanium dioxide (TiO_2) with different building materials[17,18] which gives self-cleaning and air- purification properties. In previous works in our group, a photocatalytic paint containing a commercial carbon doped TiO_2 with photoactivity in the visible light spectrum was formulated. This paint was tested for a frequent indoor air organic volatile compound, acetaldehyde, observing satisfactory results when the samples were irradiated with fluorescent visible light lamps[19].

The bactericidal effect of photocatalytic paints or coatings under visible light was studied in some works[20,21]. However, the environmental fungi control applying photocatalytic paints was only approached employing UV radiation and observing the growth inhibition of the vegetative form of *Aspergillus niger* on the photocatalytic surface[22] or using indoor lighting but also measuring the vegetative colony diameters after different irradiated exposition time[23].

In the present work, the evaluation of environmental fungus inactivation employing the designed photocatalytic paint with a commercially available carbon doped TiO_2 is carried out. Different types of illumination (UVA and visible light) were applied and *Aspergillus niger* was selected as the model microorganism. The fungus conidia inactivation is assessed, unlike other works with photocatalytic paints where only the growth inhibition of the vegetative structure was studied. In this way, the reduction evaluation of the dispersion propagule of *Aspergillus niger* that can disseminate more mold colonies on surfaces is carried out. In addition, normal or non-photoactive surfaces were prepared as the blanks of the photocatalytic process and a commercial antifungal paint with a chemical fungicide agent was evaluated as well. The obtained experimental results were theoretically analyzed through the exponential regression of Colony Forming Units (CFU) along time, and the calculation of the apparent photonic efficiency.

MATERIALS AND METHODS

Tested paints. Photocatalytic paint composed of water (30%), modified carbon doped TiO_2 Kronos vlp 7000 (18%), $CaCO_3$ (18%), styrene-acrylic resin (33%) and dispersing agent (1%) was developed. Also, a normal paint was prepared with the same composition but replacing the photocatalytic TiO_2 by the pigment rutile TiO_2 (Kronos 2360).

In addition, an "antifungal" latex paint and a normal indoor paint both commercially available were also analyzed. It is worth noting that the paint composition of the antifungal paint is not declared by the manufacturer.

Paint deposition. Borosilicate glass plates of 2 cm × 2 cm were used as support to immobilize the paints. Before paint immobilization, the glass plates were cleaned-up with soap and water, and then immersed in a solution containing 20 g of potassium

hydroxide, 250 mL of isopropyl alcohol, and 250 mL of ultrapure water. The plates were kept in contact with the washing solution for 24 h and then for 2 h under sonication.

The ‘‘dip-coating’’ technique was employed to obtain the photocatalytic films over the glass plates. This method basically consists of immersing the glass to be coated in the paint, and then withdrawing it at a controlled speed. The plates were withdrawn from the paint at a speed of 3 cm min^{-1}, and then dried at 25ºC for 24 h. The quantity of the different deposited paints on the glass plates was determined by weight difference of a large number of plates.

Model microorganism. *Aspergillus niger* (ATCC 16404) conidia were used as model microorganism for the inactivation assays. This microorganism was selected because it represents the typical environmental fungi present in contaminated indoors; it is an innocuous microorganism and it is one of the most studied in papers about the photocatalytic inactivation of microorganisms in air[4,9-16].

Microorganism culture. *Aspergillus niger* (ATCC 16404) was revived from conservation beads, where the strain was adsorbed, in malt extract broth and incubated for 72 h at 28ºC. Then, it was inoculated on Potato Dextrose Agar (PDA, Merck Chemicals) plate for 7 days at 28ºC. Next, 10 mL of sterile saline solution (0.9%) was used to suspend the conidia that were scraped from the surface culture of PDA. The viable conidia were counted using the surface plate count technique with PDA incubated for 48 h at 28ºC. Also, the obtained conidia suspension was observed under an optical microscope to exclude the presence of vegetative mycelium in the suspension. Finally, the suspension was stored at 4ºC until 6 months.

Experimental setup. The photocatalytic experiments were carried out in an experimental setup consisting of a radiation emitting system, an irradiation compartment, and a support to hold the coated glass plates with the paint samples during irradiation (**Figure 1**). A borosilicate glass separates the emitting system from the irradiation compartment. The radiation emitting system consists of a set of seven tubular fluorescent lamps T5 of 8W held by a metallic rectangular box above the irradiation compartment in a horizontal parallel arrangement. Two kinds of fluorescent lamps were employed: white visible light lamps (360 - 720 nm) and UV black-light (310 - 400 nm). Inside the irradiation compartment, local measurements of the radiation flux incident at different positions on a plane were performed using a radiometer (ILT 1700, International Light Technologies) equipped with visible and UV light sensors for each type of lamp, respectively. More details of the employed experimental setup can be found in Zacarías et al. (2012)[24].

The photocatalytic plates coated with the paint samples were held horizontally in the central zone of the irradiation compartment, where the radiation flux was almost uniform. A saturated solution of magnesium nitrate hexahydrate was included in the irradiation compartment to secure an atmosphere with a constant relative humidity, necessary to obtain sustainable TiO_2 photocatalytic activity. Throughout the experiments, the relative humidity and temperature inside the irradiation compartment were kept constant at 30ºC and 50% RH. A thermohygrometer was employed to measure these variables.

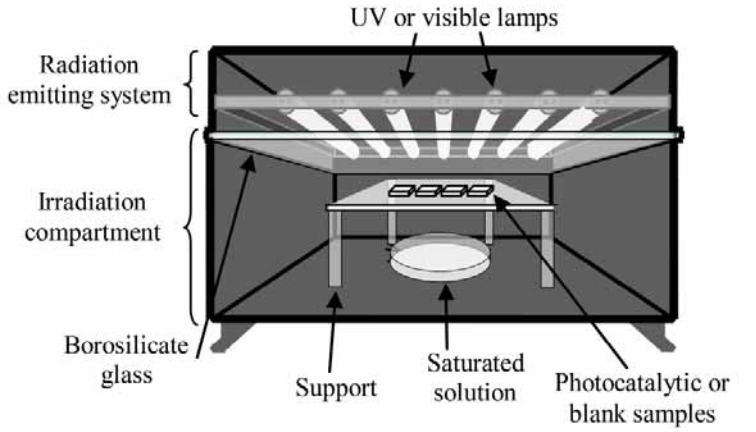


FIGURE 1. Experimental setup[24]

Microorganism destruction test. The inactivation of *Aspergillus niger* conidia was evaluated over the previously described paints: the developed photocatalytic paint, a homemade non active paint, a commercial normal indoor paint, and a commercial "antifungal" latex type paint. Before starting every inactivation assay, 10 µL aliquots of the conidia suspension of approximately 5.0×10^7 CFU mL^{-1} were spread over the coated plates covering an area of 1.5 cm × 1.5 cm. After that, the plates were maintained at 25ºC to dry the samples. Then, the dry plates were placed in the irradiation compartment and exposed to visible or UV radiation for different time periods. Irradiation assays were performed with dry conidia to represent the environmental conditions in which they are disseminated by air. After the programmed irradiation time for each sample, the photocatalytic plates were removed and the remaining viable conidia were counted. The same procedure was performed for the samples kept for the same period of time without radiation (in the dark at 30ºC and 50% RH).

To perform the counting of viable conidia, each irradiated plate was placed in a tube with 10 mL of sterile extraction solution (0.1% peptone in distilled water). Then, the sample was gently scraped with a sterile spatula to separate the conidia from the surface of the plate. Subsequently, the tube with the plate, the spatula and the extraction solution were stirred for 5 min. Finally, aliquots of 0.1 mL of the resulting suspension were spread over the surface of PDA plates, incubated at 28ºC for 48 h, and the Colony Forming Units (CFU) counted. The tests were repeated twice for each studied experimental condition, and the counting of the viable conidia of each repetition was made in duplicate.

Theoretical analysis of the experimental results. The decay of viable conidia as a function of the irradiation time was fitted with the following exponential equation[25]:

$$N = N_0 e^{-kt} \quad (1)$$

where N (CFU mL^{-1}) is the conidia concentration at time t, N_0 (CFU mL^{-1}) the initial conidia concentration, k (day^{-1}) an apparent kinetic constant, and t (day) the irradiation time.

In order to compare the microbiologic inactivation by the formulated photocatalytic paint with others photocatalytic studies, the apparent photonic efficiency η_{app} for the photocatalytic process can be calculated by[24]:

$$\eta_{app} = \frac{\left[\left(\frac{dN}{dt}\right)_{Photocatal.paint,t=0} - \left(\frac{dN}{dt}\right)_{Blank,t=0}\right] V_{aliq}}{q_w A} = \frac{\left[(N_0k)_{Photocatal.paint} - (N_0k)_{Blank}\right] V_{aliq}}{q_w A} \quad (2)$$

where N_0k [CFU mL^{-1} day^{-1}] is the observed initial inactivation rate $\left(\frac{dN}{dt}\right)_{t=0}$ for the photocatalytic paint and blank samples, respectively; V_{aliq} [mL] is the conidia suspension aliquot volume deposited on an area A [cm^2] of the coated glass plates; and q_w [photon cm^{-2} day^{-1}] is the irradiance flux on the paint samples.

RESULTS AND DISCUSSION

Characterization of paint depositions. An average of 2.29 mg cm^{-2} for the mass of photocatalytic paint per unit area deposited on the plates was obtained. On the other hand, when the "antifungal" commercial paint was used, the mass per unit area with the same coating technique was 8.50 mg cm^{-2}. **Table 1** shows the average deposited weight for all tested paints.

TABLE 1. Average specific load on the glass plates of the different tested paints

Sample	mg cm^{-2}
Photocatalytic paint	2.29
Rutile paint	2.58
Antifungal paint	8.50
Commercial paint	10.19

Radiation flux measurement. Using the radiometer, the incident radiation flux measurements were performed at different positions on the irradiation compartment. Only the most illuminated surface, placed at the central zone of the irradiated camera, was employed for the experiments. A value of 6.91 mW cm^{-2} for the visible irradiation condition between 400-1064 nm was obtained. For the fungus inactivation tests employing ultraviolet light, a value of 1.78 mW cm^{-2} for the radiation flux between 300-400 nm was measured.

Microorganism inactivation results. During the preliminary tests made for one to three days, a non-significant fungus inactivation was observed. Therefore, with the exception of the UV irradiation experiments, longer tests of a week of duration were performed for every prepared sample. **Table 2** summarizes the tested paints, the experimental

conditions and the kinetic parameters resulting from the exponential fitting with Eq. (1) of the experimental data.

After 7 days, over an 80% of conidia reduction was obtained when the photocatalytic paint samples were exposed to visible radiation. On the other hand, when the same samples were kept in the darkness at 30ºC and 30% of relative humidity, conidia abatement was not observed for the same period of time. These results are shown in **Figure 2**, where the error bars represent the 99% confidence interval of the experimental data. In addition, the exponential regression of the *Aspergillus niger* CFU versus time can be observed in **Figure 2**, obtaining k = 0.227 days^{-1} for the irradiated condition (see **Table 2**).

TABLE 2. Summary of the performed tests and the exponential regression results

Sample	Illumination	k [day^{-1}]	N_0 [CFU mL^{-1}]	R^2
Photocatalytic paint	Visible	0.227 ±0.011	$2.437\times10^7\pm0.566\times10^6$	0.976
Photocatalytic paint	UV	1.347±0.069	$3.931\times10^7\pm0.995\times10^6$	0.988
Rutile paint	Visible	0.299±0.033	$4.329\times10^7\pm1.652\times10^6$	0.967
Rutile paint	UV	0.687±0.039	$4.615\times10^7\pm1.231\times10^6$	0.972
Commercial paint	Visible	0.260±0.032	$3.813\times10^7\pm1.435\times10^6$	0.964
Glass	Visible	0.297±0.019	$1.887\times10^7\pm0.566\times10^6$	0.994
Antifungal paint	Dark	0.223±0.032	$2.444\times10^7\pm1.805\times10^6$	0.907
Antifungal paint	Visible	0.244±0.026	$3.213\times10^7\pm1.872\times10^6$	0.938

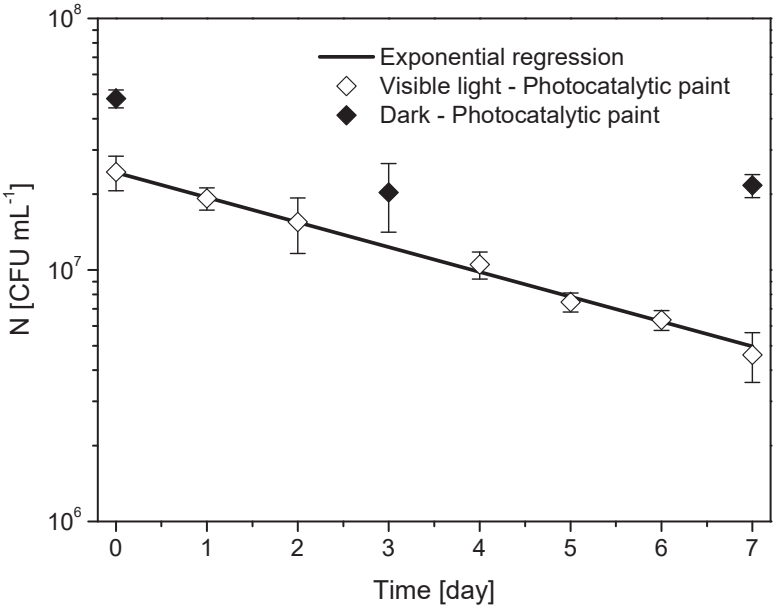


FIGURE 2. *Aspergillus niger* inactivation on photocatalytic paint under visible light and dark conditions

Optical micrographs of the conidia on the photocatalytic surface under illuminated and dark conditions at different times are shown in **Figure 3**. The conidia were losing their characteristic pigmentation and spherical shape when the paint samples were irradiated.

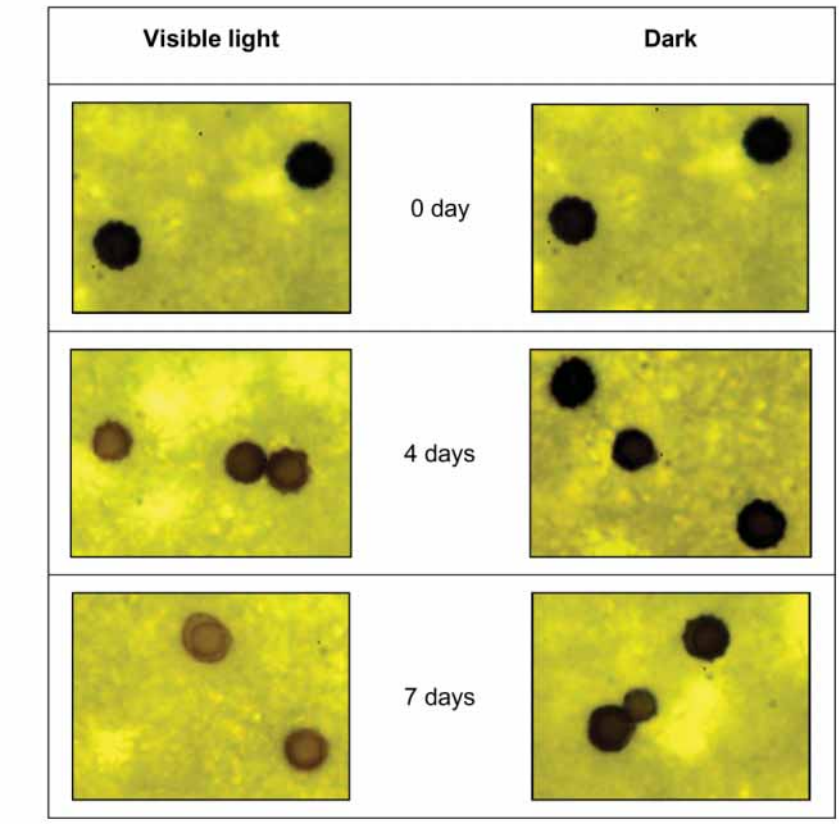


FIGURE 3. Optical micrographs of the *Aspergillus niger* conidia on the photocatalytic paint under visible light and dark conditions

One could conclude from these first results that the formulated photocatalytic paint is efficient to inactive *Aspergillus niger* in indoor environments with visible light exposure. However, an additional analysis is required when the blank tests employing different non active surfaces are carried out. Three different samples were used as the fungus inactivation blank: a rutile TiO_2 pigment paint prepared in our laboratory, a commercial indoor paint, and an uncoated glass. The inactivation results for the rutile paint under visible light and in the darkness are shown in **Figure 4**. Approximately, the same inactivation kinetic constant “k” from the exponential regression is obtained for the photocatalytic paint and the named rutile paint (**Table 2**). Moreover, similar results were obtained for the rest of the tested blanks, indicating no difference between the designed photocatalytic paint and others surfaces regarding the fungus growth control under visible light.

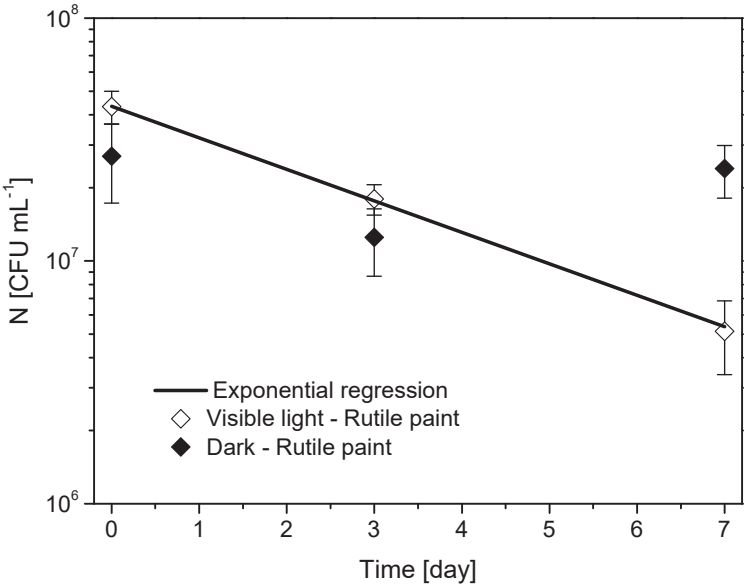


FIGURE 4. *Aspergillus niger* inactivation on normal paint with rutile TiO_2 pigment under visible light and dark conditions

Subsequently, UV tests were performed in order to find greater photocatalytic activity of the developed paint for the *Aspergillus niger* inactivation. In **Figure 5** these results are shown employing the called rutile paint and the photocatalytic paint. For both paints, the fungus inactivation is faster than those results employing visible radiation. However, the developed photocatalytic paint presents an inactivation constant "k" which is almost twice the constant of rutile paint due to a stronger photocatalytic oxidation process under the UV radiation. In addition, when UV radiation was applied, the same fungus abatement of the visible light exposure of 7 days was obtained in just 1.5 days.

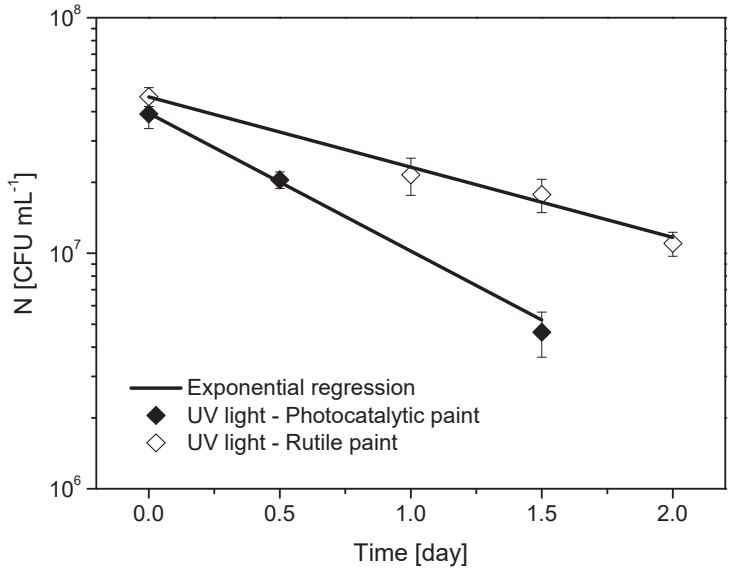


FIGURE 5. *Aspergillus niger* inactivation on photocatalytic paint and normal paint under UV light

The calculated apparent photonic efficiency taking into account only the photocatalytic inactivation of the fungi conidia under UV radiation was 7.7 $\times 10^{-14}$ CFU photon^{-1}. This value is comparable to the apparent efficiency of about 2×10^{-14} CFU photon^{-1} calculated by Zacarías et al. (2012)[24] for bacteria spore inactivation, employing Degussa P25 TiO_2 under UV irradiation. However, the calculated inactivation efficiency for *Aspergillus niger* in this work is significantly lower than the reported one for vegetative bacteria in aqueous system[26] of about 1×10^{-11} CFU photon^{-1}. On the other hand, it is worth to mention that the calculation of the apparent efficiency was not performed for the visible radiation because the initial inactivation rate for the photocatalytic and blank samples are almost the same.

Finally, an antifungal commercial paint containing a fungicide agent was tested (**Figure 6**). After 7 days, the same inactivation rate for both conditions of visible irradiation and darkness was observed, showing that this type of paint is working without illumination as well. Nevertheless, the antifungal paint shows almost the same performance of the photocatalytic paint and the others non-photoactive surfaces under visible light.

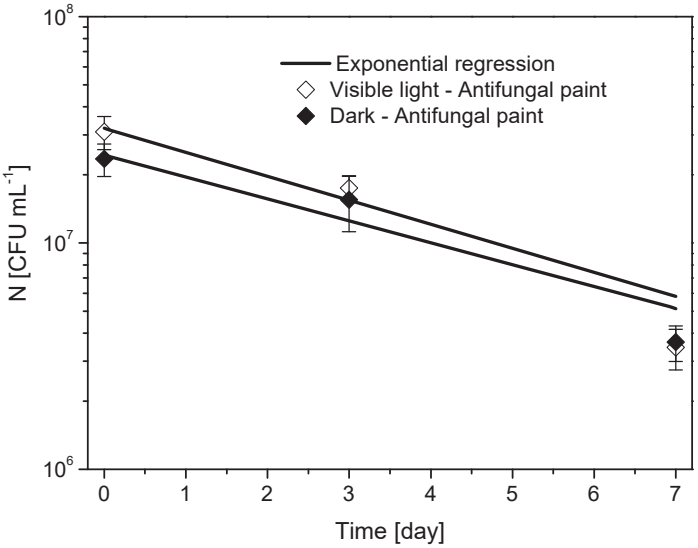


FIGURE 6. *Aspergillus niger* inactivation on commercial antifungal paint under visible light and dark conditions

CONCLUSION

The inactivation of environmental fungal conidia using *Aspergillus niger* conidia as the model microorganism and applying a developed photocatalytic paint was studied under different illumination conditions of UV and visible light. Therefore, the dissemination agent that can generate more growth mold in surfaces and affect the people health could be controlled.

Significant conidia abatement was obtained for both radiation exposure, but principally applying UV light. The tested photocatalytic paint under visible light was even able to equal the fungus inactivation of a commercial antifungal paint with the disadvantage of employing sometimes harmful fungicides in its formulation. However, under conditions of

visible radiation the photocatalytic effect of the modified carbon doped TiO_2 in the paint was undistinguishable because similar inactivation levels of the *Aspergillus niger* were achieved when non-photoactive paints and surfaces were tested as the blanks. On the other hand, a greater environmental mold inactivation capacity by the photocatalytic paint was achieved when UV light was used as the photocatalyst activator. The photocatalytic oxidation power of the designed paint has been improved only when it was irradiated with UV light. Based on these results, a promising technology for microorganism control over photocatalytic coated surfaces can be expected for UV irradiated conditions, without the application of dangerous and toxic chemical fungicide in the paint. For forthcoming works new paint formulations using visible light photocatalysts and others indoor environmental conditions will be assessed to prove the fungicide effect of this photocatalytic building material under visible radiation.

ACKNOWLEDGMENTS

The authors are grateful to Universidad Nacional del Litoral (UNL), Consejo Nacional de Investigaciones Científicas y Técnicas (CONICET), and Agencia Nacional de Promoción Científica y Tecnológica (ANPCyT) for financial support. We also thank Antonio C. Negro for his valuable help during the experimental work, and Dr. María Lucila Satuf for her helpful advice.

REFERENCES

1. Sivasubramani S.K., Niemeier T.T., Reponen T., Grinshpun S.A. Assessment of the aerosolization potential for fungal spores in moldy homes. Indoor Air 14(6) (2004) 405-12.
2. Richardson G., Eick S., Jones R. How is the indoor environment related to asthma?: Literature review. J. Adv. Nurs. 52(3) (2005) 328–39.
3. Kappock P.S., Glaser J.K., Cornish A. Protecting paints: Zinc pyrithione could replace conventional fungicide/algaecides blends. European Coatings Journal 4 (2005) 144-149.
4. Mitoraj D., Janczyk A., Strus M., Kisch H., Stochel G., Heczko P.B., Macyk W. Visible light inactivation of bacteria and fungi by modified titanium dioxide. Photochem. Photobiol. Sci. 6 (2007) 642–648.
5. Liou J.W., Chang H.H. Bactericidal effects and mechanisms of visible light-responsive titanium dioxide photocatalysts on pathogenic bacteria. Arch. Immunol. Ther. Exp. 60 (2012) 267-275.
6. Caballero L., Whitehead K.A., Allen N.S., Verran J. Inactivation of *Escherichia coli* on immobilized TiO_2 using fluorescent light. J. Photochem. Photobiol. A 202 (2009) 92-98.
7. Chuaybamroong P., Thunyasirinon C., Supothina S., Sribenjalux P., Wu C-Y. Performance of photocatalytic lamps on reduction of culturable airborne microorganism concentration. Chemosphere 83 (2011) 730-735.
8. Sungkajuntranon K., Sribenjalux P., Supothina S., Chuaybamroong P. Effect of binders on airborne microorganism inactivation using TiO_2 photocatalytic fluorescent lamps. J. Photochem. Photobiol. B 138 (2014) 160-171.
9. Chen F., Yang X., Wu Q. Photocatalytic oxidation of *Escherischia coli*, *Aspergillus niger*, and formaldehyde under different ultraviolet irradiation conditions. Environ. Sci. Technol. 43 (2009) 4606-4611.
10. Chen F., Yang X., Wu Q. Antifungal capability of TiO_2 coated film on moist wood. Build. Environ. 44 (2009) 1088-1093.

11. Pigeot-Remy S., Reala P., Simoneta F., Hernandez C., Vallet C., Lazzaronie J.C., Vacherd S., Guillard C. Inactivation of *Aspergillus niger* spores from indoor air by photocatalytic filters. Appl. Catal. B Environ. 134-135 (2013) 167-173.
12. Vohra A., Goswami D.Y., Deshpande D.A., Block S.S. Enhanced photocatalytic disinfection of indoor air. Appl. Catal. B Environ. 65 (2006) 57–65.
13. Wolfrum E.J., Huang J., Blake D.M., Maness P., Huang Z., Fiest J., Jacoby W.A. Photocatalytic oxidation of bacteria, bacterial and fungal spores, and model biofilm components to carbon dioxide on titanium dioxide coated surfaces. Environ. Sci. Technol. 36 (2002) 3412-3419.
14. Chuaybamroong P., Chotigawin R., Supothina S., Sribenjalux P., Larpkiattaworn S., Wu C-Y. Efficacy of photocatalytic HEPA filter on microorganism removal. Indoor Air 20 (2010) 246-254.
15. Muranyi P., Schraml C., Wunderlich J. Antimicrobial efficiency of titanium dioxide-coated surfaces. J. Appl. Microbiol. 108 (2010) 1966-1973.
16. Bai W., Krishna V., Wang J., Moudgil B., Koopman B. Enhancement of nano titanium dioxide photocatalysis in transparent coatings by polyhydroxy fullerene. Appl. Catal. B Environ. 125 (2012) 128-135.
17. Ballari M.M., Brouwers H.J.H. Full scale demonstration of air-purifying pavement. J. Hazard. Mater. 254-255(1) (2013) 406-414.
18. Chen J., Poon C-S. Photocatalytic construction and building materials: from fundamentals to applications. Build. Environ. 44 (2009) 1899-1906.
19. Salvadores F., Alfano O.M., Ballari M.M. Formulation and assessment of indoor photocatalytic paints active under visible light. In: Ried A, Esplugas S (Eds) Ozone and Advanced Oxidation Leading-edge Science and Technologies, Proceedings of IOA World Congress 2015, Barcelona, Spain (2015) pp 13.3-1-13.3-6.
20. Caballero L., Whitehead K.A., Allen N.S., Verran J. Photoinactivation of *Escherichia coli* on acrylic paint formulations using fluorescent light. Dyes Pigments 86 (2010) 56-62.
21. Zuccheri T., Colonna M., Stefanini I., Santini C., Di Gioia D. Bactericidal activity of aqueous acrylic paint dispersion for wooden substrates based on TiO_2 nanoparticles activated by fluorescent light. Materials 6 (2013) 3270-3283.
22. Vučetić S.B., Rudić O.L., Markov S.L. Bera O.J., Vidaković A.M., Sever Skapin A.S., Ranogajec J.G. Antifungal efficiency assessment of the TiO_2 coating on façade paints. Environ. Sci. Pollut. Res. 21 (2014)11228-11237.
23. Markowska-Szczupak A., Ulfig K., Grzmil B., Morawski A.W. A preliminary study on antifungal effect of TiO_2-based paints in natural indoor light. Pol. J. Chem. Technol. 12(4) (2010) 53-57.
24. Zacarías S.M., Satuf M.L., Vaccari M.C., Alfano O.M. Efficiency evaluation of different TiO_2 coatings on the photocatalytic inactivation of airborne bacterial spores. Ind. Eng. Chem. Res. 51 (2012)13599-13608.
25. Horie Y., David D.A., Taya M., Tone S. Effects of light intensity and titanium dioxide concentration on photocatalytic sterilization rates of microbial cells. Ind. Eng. Chem. Res. 11 (1996) 3920-3926.
26. Marugán J., van Grieken R., Sordo C., Cruz C. Kinetics of the photocatalytic disinfection of *Escherichia coli* suspensions. Appl. Catal. B Environ. 82 (2008) 27-36.

Section 12.
Environmental Nanotechnology

	Page
Chapter 12.1 An overview on microbial fuel cell technology for soil remediation K. B. Sánchez-López; C. G. Mar-Pineda; H. M. Poggi-Varaldo; M. García-Rocha; J. G. Cabañas-Moreno; O. Solorza-Feria; D. Bahena-Uribe; B. Camacho-Pérez; N. Rinderknecht-Seijas	978
Chapter 12.2 Sustainable iron based bionano-bioparticles from a dehalogenating microbial consortium allows remediation of water polluted with PCE L. Breton-Deval and H. M. Poggi-Varaldo	1007
Chapter 12.3 Hybrid material from nalidixic acid ions and ZnAl layered double hydroxide used as ecological pesticide E. Morales-Irigoyen; Y. Gómez y Gómez; J. L. Flores-Moreno and M. O. Franco-Hernández	1015
Chapter 12.4 Efectividad de las micro/nanopartículas de quitosano obtenidas de residuos pesqueros en la adsorción de cromo hexavalente J. B. Dima and N. Zaritzky	1020

CHAPTER 12.1 AN OVERVIEW ON MICROBIAL FUEL CELL TECHNOLOGY FOR SOIL REMEDIATION

K. B. Sánchez-López (1); C. G. Mar-Pineda (2); H. M. Poggi-Varaldo*(1,2); M. García-Rocha (1); J. G. Cabañas-Moreno (1); O. Solorza-Feria (1); D. Bahena-Uribe (1); B. Camacho-Pérez (3); N. Rinderknecht-Seijas (4)

(1) Centro de Investigación y de Estudios Avanzados del I.P.N., Nanoscience and Nanotechnology Program, Mexico City, Mexico
(2) Centro de Investigación y de Estudios Avanzados del I.P.N., Dept. Biotechnology & Bioengineering, Environmental Biotechnology and Renewable Energies Group, P.O.Box 14-740, Ciudad de México (D.F.), 07000, Mexico
(3) Technological University of Tecamac, Tecámac, State of México, Mexico
(4) ESIQIE-IPN, Campus Zacatenco, Mexico City, Mexico

ABSTRACT

The development of new technologies such as those represented by bioelectrochemical devices, i.e., microbial fuel cells (*MFCs*), is crucial for the remediation of soils contaminated with toxic and recalcitrant pollutants. A great variety of pollutants such as organic chlorinated compounds, pesticides, petroleum hydrocarbons, dyes and other recalcitrant contaminants have been successfully treated in *MFCs*. On the other hand, research on remediation of soils contaminated with emerging pollutants that affect human health using *MFC* is still scarce. It has been reported that the use of co-substrates may affect or benefit the process; the most used co-substrates to oxidise difficult compounds as azo dyes, ethanol, pyruvate, acetate, among others, are glucose and other carbohydrates. Notwithstanding, hydrocarbon remediation does not usually need co-substrates. *MFC* configurations show that there are two main types of arrangements: *in situ* cells (anodes buried in the solid matrix) and the more conventional *ad situ* cells (two and one chamber ones). In spite of the possible lower costs of the first type of configuration, the latter offers a better process control and higher treatment rates. Regarding the *ad situ* type, it was shown that placing the anode horizontally can optimise the process. The *ad situ MFC* approach can treat a wide range of soils, from sandy to very “heavy” soils (high contents of both clay and organic matter) as research of our own Group has shown. Therefore, *MFC* remediation could be more advantageous than the very popular *in situ* remediation that is limited by low hydraulic conductivity and low permeability of soils.

Keywords: Contaminated soils, contaminated water, microbial fuel cell, remediation

---

* Author for correspondence; r4cepe@yahoo.com

INTRODUCTION

Environmental pollution is a serious threat to human health. Contaminated soils often are used to grow food crops without adequate controls and remediation, causing several damages to the human health and the environment.

Microbial fuel cells (*MFCs*) are an innovative proposal that is friendly to the environment. It can biodegrade pollutants in soils and waters besides providing electricity generation. *MFC*s emerge as a synthesis of Biotechnology (bioreactors, biocatalysts) and Electrochemistry (fuel and electrolysis cells)[1]. In such cells, the microorganisms can transfer or receive electrons extracellularly to a solid electrode such as the anode or cathode, depending on the cell configuration and type. The electrons collected by the anode are transported externally (via wires/circuit) to the cathode where they typically meet an electron acceptor (O_2) and protons effecting the oxygen reduction reaction and closing the circuit with the concomitant power generation. This type of degradation is possible with terminal electron acceptors such as oxygen, nitrate, sulphate or metal oxides. In the *MFC* technology, typically atmospheric oxygen acts as electron acceptor which is transferred by the electrodes in a simpler and less expensive manner.

An application of the *MFC* is in the form of soil/sediment microbial fuel cells (*SMFCs*) where the natural potential gradient created between the sediment and the upper aqueous phase generates the oxidation of organic compounds and the consequent release of electrons, which flows from the anode to the cathode through an external circuit[2]. Direct application of *SMFCs* allows generation of electric power which has diverse applications where the expected *in situ* generation of electricity may have small appliances. Currently, the *SMFCs* has obtained an average of sustainable energy of 10-100 mW per square meter of anodic electrode footprint area (*EFA*)[2]; these energy levels show that the energy produced is not enough to provide the necessary electricity for applications that require higher inputs of energy, and therefore, with the current level of technology, it cannot be used primarily as a power generation system.

However, although the technology is not feasible for the exclusive production of electricity, *SMFC* and *BES* still exhibit important and diverse applications. In previous studies, three explanations of why the *MFC* could stimulate refractory removal efficiencies of organic pollutants have been discussed: *(i)* anaerobic microorganisms, through their accelerated metabolism, produce electrons which are received by the anode[3,4]; *(ii)* one way to change the cell metabolism is altering the permeability of the cytoplasmic membrane by changing the electric field in the chamber leading to increased transport of extracellular substances to inside[5]; *(iii)* using the electric field can stimulate microorganisms to produce certain enzymes involved in organic removal reactions[6,7].

The main objective of this review is to give a critical overview of the advances made so far using the soil or sediment *MFC*s, covering the issues: *(i)* Types of pollutants in soils and sediments treated with *BES*; *(ii)* Influence of co-substrate on *MFC* performance; *(iii)* Cell configurations; *(iv)* Types of soils treated in *MFC*s and similar devices; *(v)* Type of inoculum; *(vi)* Combination of other technologies for remediation with microbial fuel cells, and *(vii)* Perspectives and conclusion. The scope of this review is to address the *MFC* focused on soil remediation; we do not consider the *MFC* either

for water remediation or where it requires energy in their operation mode such as microbial electrolysis cells.

TYPES OF POLLUTANTS IN SOILS AND SEDIMENTS TREATED WITH BIOLECTROCHEMICAL SYSTEMS

In Nature various anaerobic reactions occur and are considered of great importance since they are responsible for degrading organic pollutants. Such reactions are driven by microorganisms that can degrade various organic compounds in either anoxic or aerobic conditions[8]. An important family of such pollutants consists of polycyclic aromatic hydrocarbons (*PAH*). These are produced in the incomplete combustion of fossil fuels, wood, and other organic substances[9,10]. These compounds are differently generated and are of public concern since they are potentially carcinogenic and mutagenic in living beings. Their properties such as moderate to high molecular weight and aromatic ring structure (with fused rings)[11], as well as their low water solubility, absorption coefficient, high octane-to-water partition coefficient, recalcitrant quality, limited volatility, etc. cause them to accumulate in natural environments and trophic chains, and their accumulation has toxic effects[12]. Remediation techniques for soils contaminated with hydrocarbons and other pollutants such as biological, chemical and electrochemical treatments[13,14,15,16,17] are available and are being developed either *in situ* or *ex situ*. One of the drawbacks to accelerate degradation is that the *PAHs* have low bioavailability because of their complex nature and their adsoprtion onto the organic matter and clay of sediments and soils[11,18,19,20,21]. The work done by microorganisms to degrade these contaminants is critical either aerobically or anaerobically[22,23], but unfortunately the natural attenuation rate is very slow[24]. Deficiency of efficient electron acceptors can be an obstacle to the extent and kinetics of biodegradation of contaminants in sediments. One factor that could stimulate microbial activity is biostimulation with electron acceptors such as oxygen[10,25,26]. It is well known that aerobic biodegradation can provide higher rates of degradation than anaerobic biodegradation, but the main obstacle is that transport of O_2 to the microbes could result expensive and cumbersome[20,27], but it has the advantage that homogenizes the distribution of nutrients in the sediment suspension through aeration[28]. It has been reported the anoxic degradation of contaminants such as PAHs in sediments, where other than O_2 electron acceptors (nitrates, sulfates or oxides of Fe^{3+}) are available in the interface sediment-water and used by microbes[27,29,30,31].

Unfortunately certain contaminants are not easily degraded in waterlogged soils or sediments due to the lack of the aforementioned electron acceptors that can induce anaerobic oxidation of pollutants. On the other hand, oxygen can also react with reduced species such as Fe^{2+}, and its implementation is more difficult (energy requirements related to aeration or air injection, low O_2 solubility in water, etc.), but still widely used because it is well known that the aerobic degradation of organic contaminants can be faster than anaerobic degradation, although much more expensive[8].

As it was mentioned above, it has been shown that there are electron acceptors, *i.e.*, sulfate and nitrate, that give good results in the microbial degradation of *PAHs*[27,29]: Yet, *ex situ* treatment of sediments on the surface may cause problems due to the soluble nature of these acceptors, which tend to spread/migrate some distance from the point of

application[27]. Fortunately, it was reported that oxides of Fe^{3+} might be in insoluble form in polluted sediments and thus can affect the degradation of PAHs[31,32]. More studies are needed to find the effects of Fe^{3+} on the degradation of pollutants based on the matrix. So far, it has been demonstrated that amorphous ferric hydroxide has no significant effect on the biodegradation of *PAHs* in mangrove sediments[4].

It has been shown that *PAHs* are easier to degrade when their molecular weight is lower and there[16]. It has also been reported that the anaerobic degradation of aromatic compounds starts at the saturated ring which results in the formation of cis-dihydro diol[27].

In search of new alternatives for bioremediation, *SMFC* has been proposed for application in bioremediation of organic matter and pollutants in soils and contaminated sediments[10,33,34]. The *SMFC's* anode can act as a major recipient of low electron potential and as a continuous electron sink[10,35]. On the other hand, it has been proposed that an electrode poised at a sufficiently low potential can serve as an electron donor and simultaneously can be applied to induce microbial reduction of nitrate[36], uranium[37], and chlorinated solvents[38,39]. There are reports on the use of an external potential in the *MFC* system to treat chlorinated solvents[40], azo dyes[41], nitrobenzene[42], chlorides[40], etc. Research is under way to improve the design of these systems and eventually their scale-up for field applicatons[43].

Morris *et al.*[35] and Morris & Jin[44] found that it is possible to enhance anaerobic biodegradation of some contaminants using microorganisms by providing an acceptor of electrons in the solid state as in the case of the anode in an *MFC*. Importantly, in the release of electrons by the biodegradation of organic compounds in an *MFC* not only electricity is produced, but a variety of side chemical or biochemical reactions can occur as well that would help in removing pollutants. Due to the great variety of contaminants, each *MFC* responds differently depending on their actual operating conditions and matrix characteristics. In contrast to the use of poised MFC for removing pollutants reported above, the generation of *in situ* potential system in a *MFC* applied to the elimination of phenol[3], color, carbohydrates[45], the *COD* of complex chemical wastewater[17], proteins[45], lindane[34] and nitrate[46] has been reported. Interestingly, there are also experiments on the removal of polybrominated diphenyl ethers (*PBDEs*), which are difficult to be biodegraded in more conventional biological treatment processes. It is possible that some enzymes involved in the dechlorination of polychlorinated biphenyls (*PCB*) could be associated to the transformation and degradation of *PBDEs* because *PCB* and *PBDE* have similar chemical structures.

Earlier studies showed that microbial communities able to degrade *PBDEs* might be affected by environmental conditions, being the genera *Geobacter*, *Pseudomonas* and *Shewenalla* anodic bacteria involved in the pollutant degradation. There is some evidence that some bacteria can slowly reduce the brominated organic compounds to decabromodiphenyl ether (*BDE-209*)[47].

Cao *et al.*[7] worked with soil microbial fuel cells (MFCs) for remediation of topsoil polluted with hexachlorobenzene (HCB), which is a toxic organic pesticide. HCB removal efficiencies in the three tested systems (soil MFCs, open circuit control group, and non-inoculated with anaerobic sludge) were 71.1, 52.5, and 38.9%, respectively. The highest surface area power density was 77.5 mW/m^2 when the cells were loaded with an external resistance of 1000 ohms. It was found that HCB was degraded following the

route of reductive dechlorination pathway. It seems that removals of HCB in the cells was promoted by electrogenic bacteria that supplied more electrons to increase the metabolic reactions rates of anaerobic bacteria. They also found that when contaminants are adsorbed on the anode surface, they are more easily degraded using electron transfer reactions. This process was coined as direct anodic oxidation (*DAO*). In the *MFC* released protons and electrons can combine with water to generate hydroxyl radicals ($*OH^-$) plus hydrogen. The $*OH^-$ can be adsorbed on to the anode resulting in the oxidation of pollutants through *DAO*. Moreover, the indirect anodic oxidation (*IAO*) where free radicals destabilise the molecule results in a resonance mechanism and leads to the formation of intermediate compounds which are unstable in the aqueous phase will also discover these reactions to be continuous cause free radicals are attached and detached from the anode surface intermittently to promote degradation.

The activity generated by the introduction of a bioelectrochemical electrode[10,18] and an associated bioelectrocatalyst can give better results for the removal of polynuclear aromatic hydrocarbons (*PAH*)[48].

Recently, studies on improving *MFC*s performance have focused on the identification and enrichment of electrochemically active bacteria (*EAB*)[49,50,51]. *EAB* are capable of catalyzing the oxidation of pollutants and other electron donors at the anode, and extracellularly transfer the electrons to the anode, hence the electrons travel through an external circuit to the cathode electrode which serves to reduce the O_2 (obtained from the environment) to H_2O or another suitable electron acceptor that closes the bioelectrochemical circuit. Also, other researchers have examined the adaptation of wireless sensors to monitor pollutant online and remote[52]. In the search for improvements in *MFC* the range of contaminants that can be treated with such devices has been expanded, Zhang *et al*.[10] showed that toluene and benzene can be degraded using a graphite electrode as the electron acceptor. Later, results on degradation of using phenol[8], methyl benzoate, petroleum hydrocarbons[35] and *PAHs*[53] in *MFC*s have also been reported.

It has been found valuable information for each group of contaminants, using *SMFC* for organic compounds with high polarity (e.g. alkanoates, azo dyes sulfonic or phthalates). On the other hand, their degradation occurs when incorporating nitrate to systems treating compounds with low polarity (e.g., *PAH*s, polybrominated diphenyl ethers) showing high removal of homologous compounds to benzene. Yet, this approach should be taken with catuion because the use of nitrate might lead to risky forms of N in aquatic environments. Comparable results were obtained with reduced iron based microbial extracellular electron transfer. In contaminated environments, various complex methods are recommended to increase the success probability[54].

In the environmental community there is the perception that bioremediation does not end with the removal of the original pollutant(s). That is the reason why bioremediation studies should be accompanied by ecotoxicity studies to verify that the natural environment has been recovered[55,56] recognised that ecotoxicology could provide a better understanding of the ecological assessment and remediation to make the right decisions to amend the situation with success[53].

INFLUENCE OF CO-SUBSTRATE ON *MFC* PERFORMANCE

In several studies the addition of co-substrates has shown to improve the performance of *MFC*. It is known that for the substrate oxidation at the anode or, the reduction or oxidation of a compound to take place within or outside a microorganism, are indispensable activation energies which generate a decrease in potential, which are considered in the lower range current densities that are important for understanding the *MFC*[57].

Also, the presence and interactions of various microbial strains can generate several parallel metabolic reactions, and that leads to high energy losses that cause activation or also known as electron loss, due to the competition of such pathways.

That is the reason why a good selection and availability of carbon source to be used for the anode biocatalyst is important to maintain the performance. It is known that transfer injection should not limit the substrate to the anode, since it can lead to decreased concentration or mass transfer[65], this requires lower diffusion gradients solutions[53]. **Table 2** displays a compilation of works that used co-substrates in *MFCs*.

When acetate is used as a fermentable substrate, high coulomic efficiences (*CE*) can be achived (70% or higher). *CE* is the percentage of electrons that are recovered or the total ratio of coulombs transferred to soil anode[66]. Huang *et al*.[8] noted that the total chemical oxygen demand (*TCOD*) from the floor in a closed *MFC* with a 42.25 and 35.01 g/L, a *CE* circuit of 3.7%, lower than the obtained in *SMFC* was reached. *CE* might be negatively affected by the following reasons: *(i)* electrons are transferred from the substrate to other electron acceptors in the ground electrode such as sulphate; *(ii)* the microorganisms that cannot use the electrode as electron acceptor were likely to use the substrate for fermentation and methanogenesis that is, competing metabolisms that impairs the harvest of electric charge and power in the *BES*. Comparison of *COD* and phenol removals in *MFC* closed circuit, open circuit *MFC* and *MFC using* not waterlogged soil indicated that other respiratory processes were carried out simultaneously; *(iii)* the internal resistance of the device can also account for a significant part of the reduction of the *CE*[66].

Furthermore, it has been shown that supplementing biosolids as organic matter addition may generate higher power and increase the degradation of total petroleum hydrocarbons (*TPH*)[8]. In other studies, the addition of co-substrates or electron donors helped PBDE biodebromination[47].

Moreover, during the biodegradation of *PAHs* it was found that increasing substrate concentration, higher *PAH* degradation rates were reached compared to lower concentrations of substrate were added. Biodegradation was affected by the mass transfer of the contaminant and the subsequent metabolism of the biocatalyst, where the effect of changes in substrate injection can lead to pollutant degradation and energy production[48]. There may be a slowdown mechanism that occurs in the second stage where the depleted carbon source such as acetate could act as co-substrate to stop promoting the degradation of *PAHs*[64].

TABLE 1. Contaminated soils and sediments treated in *MFC*

Matrix	Pollutant	Inoculum	pH	Removal (%)	Reference
Seawater sediments	Benzoate or toluene	*Metallireducens Geobacter*			10
Sediment	Organic material		7.23	3.4	58
Waterlogged soil	Phenol		7.85	90.1%	8
Freshwater sediments	Two graphite electrodes		7.8.	99.47 ± 0.15 y 94.79 ± 0.63	47
Oil sludge	Petroleum	Anaerobic sewage sludge	7		48
Saline soils	Petroleum hydrocarbon		6.8 a 7.1	42	59
Lake sediment					60
Soil fluvisol	Acetonitrile and dibenzothiophene			50	53
Saline soils	Petroleum hydrocarbon		8.26	20 a 72	54
NR	Polybrominated diphenyl ethers (PBDES)			58.9	47
Freshwater sediments	Methane production			36	61
Sandy loam	Diesel		6.71 ± 0.03	72.4	52
Soil 1.99 mS / cm	Petroleum		8.3	15.3 ± 0.2	62
	Phenanthrene and benzene	Anaerobic sludge inoculum was initially set		95	63
River sediments	Heavy metals (Cu, Hg, Cd, Cr, Zn, As), polycyclic aromatic hydrocarbons (PAHS) and polybrominated diphenyl ether (PBDE Ethers)			22.1	19
Vegetable soil	Hexachlorobenzene (HCB)		6.71	71.14	7
Surface sediments	Pyrene	Macrophyte treatments		87.18 ± 5.62 y 76.40 ± 6.93	64
Clay soil	Lindane and organic matter	Inoculum of sulphate reduction acclimated to lindane	7.2	78 and 76	34

Furthermore, it has been observed that the power generated by the bacteria produces a great quantity of electrons when there are available co-substrates as sodium acetate. Certain electrons are transported from anode to cathode to produce electricity and the

remaining are for reductive dechlorination of the contaminant *HCB*[7], similarly to the use of glucose, formic acid or acetic acid as co-substrates for anaerobically biodegrading *HCB*, the latter acts as a terminal electron acceptor. The reduction was performed by the electrons obtained from the co-substrates, demonstrating that increased electron quantities promote the degradation of refractory co-substrates using organic compounds. These results were consistent with those reported by Sun *et al.*[67] and Cao *et al.*[7].

In another work, root exudates of plants were reported to be used by the electrochemically active bacteria. There was an interaction with the anode, the main fatty acids formate, acetate, citrate and malate[19], expanding the menu of co-substrates used in in *SMFC*.

It was suggested that the addition of co-substrates to the *MFC* does not generally inhibit the uptake of pollutant by the microbial communities. It is thought that co-substrate stimulate the joint biodegradation joint of the two substrates, because anaerobic versatile adapted communities contain enzymes which can degrade contaminants and co-substrate. However, there are few reports that mention that competitive inhibition between pollutant and co-substrate can occurs[63].

CELL CONFIGURATION

A number of electrochemical and biological factors were found to influence the performance of *MFC*, particularly those aspects like the cell architecture and configuration, as well as other variables (pH, conductivity, external load, type of substrate, temperature, *inter alia*[66].

Although *SMFCs* are appropriate for bioremediation in an open system, to some extent, its ability to generate electricity and the efficiency of removal of contaminants has been severely limited because of several factors: *(i)* the complications inherent to the assemblage (or arrangement) of the anode and cathode; *(ii)* the large distance between electrodes, resulting in a high internal resistance; *(iii)* the low solubility of O_2 in the water layer in contact with the cathode; *(iv)* electrode fouling by organisms or chemicals present in the water column[58].

There are reports of different designs of *MFC* such as the U-tube one, that increased cell performance by 120% compared to the control in studies on biodegradation of oil hydrocarbons around the anode at a distance of <1 cm with a trial period of 25 days[59].

The cell configuration is limitless and has also been implemented with anodes incorporating multiple layers of contaminated soil, using three anodes in the *SMFC* and activated carbon as the cathode material in experiments with saline soil contaminated with *PAHs* and n-alkanes. This configuration increased the rate of degradation compared to the offline control[69]. It was observed a gradual increase in the soil pH associated with decreasing distance to the aerated cathode. The authors ascribed this increase to the accumulation of OH^- and / or generated bicarbonate by the biodegradation of contaminants cathode, where the alkaline environment could have increased the bioavailability of hydrocarbon and thereby increase electricity production with parallel pollutant degradation. It worth highlighting that some increase in soil pH can lead to metal ions (such as Ca^{2+} and Mg^{2+}) to precipitate and restrict cation transport, thus negatively affecting cell performance.

TABLE 2. Co-substrates used in the treatment of soils in microbial fuel cells or similar

Matrix	Co-substrate	Pollutant	Type cameras and cell electrodes	Removal (%)	Reference
Seawater sediments		Benzoate or toluene	Two graphite electrodes		10
Sediment		Organic material	Airy tubular cathode *MFC* (TAC-*MFC*) with a structure of cathode assembly cloth (CCA)	3.4	58
Waterlogged soil		Phenol	Graphite electrode	90.1	8
Freshwater sediments	Phenanthrene and pyrene	Two graphite electrodes	Cylindrical stainless steel electrodes	99.47 ± 0.15 y 94.79 ± 0.63	47
Oil sludge	Domestic wastewater	Petroleum	Graphite plates		48
Saline soils		Petroleum hydrocarbon	*MFC* U-tube air cathode. Carbon mesh electrodes	42	59
Lake sediment	Acetate		Non-conductive polycarbonate plate with sandwich electrodes.		60
Soil fluvisol	Sodium acetate	Acetonitrile and dibenzothiophene	Merc-remediating, multi microbial cells	50	53
Saline soils		Petroleum hydrocarbon	Three anode layers inserted in parallel on the floor and aerated cathode, the anodes were carbon mesh	20 a 72	54
NR	Lactate	Polybrominated diphenyl ethers (PBDES)	Dual camera	58.9	47
Freshwater Sediments	Acetate	Methane production	Plain carbon graphite electrodes	36	61
Sandy loam		Diesel	Granulated graphite anode (GGA) and the other an anode biochar (BCA). The aerated cathode consisted of stainless steel mesh.	72.4	52
Soil		Petroleum	Aerated cathode consisted of stainless steel mesh; mesh anode was made of carbon.	15.3 ± 0.2	62
	Riboflavin and anthraquinone -2-sulfonate (AQS) feed lot	Phenanthrene and benzene	2 cameras	95	63
River sediments		Heavy metals (Cu, Hg, Cd, Cr, Zn, As), polycyclic aromatic hydrocarbons (PAHS) and polybrominated diphenyl ether (PBDE Ethers)	Five pieces of plain graphite plate anode copper wires. Graphite cathode foam.	22.1	19
Vegetable soil	CH_3COONa	Hexachlorobenzene (HCB)	Electrodes granular activated carbon (GAC)	71.14	7
Surface sediments		Pyrene	Graphite felt electrodes	87.18 ± 5.62 y 76.40 ± 6.93,	68
Clay soil	Sucrose: sodium acetate: lactate	Lindane and organic matter	One camera, the anodes were graphite discs whereas the cathodes were of Toray carbon cloth, the cathodes were in contact with atmospheric air	78 and 76	34

Other studies with granulated graphite and biochar evaluating its effectiveness to be used as anode materials because they are inexpensive and easy implementation in *BES* column type for soil remediation. Biochar is fairly new considering some reports about it,

however, it has been studied as a soil additive and sequestration of pollutants but there is the perception that its commercial availability is limited[52].

A cell that used a magnesium electrode modified with chitin particles gave a high maximum power density of 1878 ± 982 mW/m^2, compared with a graphite electrode also modified with chitin particles (maximum power density of 1.9 ± 0.6 mW/m^2). Yet, it was was observed that the main process of power production in the magnesium-anode was generated by a phenomenon of magnesium corrosion[70] which detracts from the soundness of this approach.

Another change in the configuration of the electrodes is that the cells equipped with aerobic/aerated cathode *MFC* were arranged horizontally (*HA*) or arranged vertically (*VA*). Comparison studies on *TPH* removal from soils of such arrangements[62] showed that the *HA* performed compared than *VA.*

Currently, there is an area of research focusing on approaches to control the redox mediators in cells, which concentrates on the mechanisms used by electrochemically active bacteria to carry out the transfer of electrons to the anode. It is perceived that the application of exogenous redox mediators can improve the electron transfer thus increasing electrochemical performance. The context is complex, since there are several factors to consider and elucidate, such as the relationship of the redox mediator with the oxidation of the substrate, the anode potential, the toxicity as mediator and its permeable cell membrane to transport the molecules of the redox mediator. Also, it is worth noting (as it was mentioned above) that by supplementing NaCl to the elecrolytes, the salinity increases and thereby conductivity of the anolyte also increase thaus leading to a lower internal resistance within the *MFC*. Yet, this approach might negatively affect cell performance because of possible negative effects of high salinity on bacterial physiology[63].

There are other factors involved in the generation of electricity as the presence of various organic materials such as humic acids in sediments, which may not be usable for the production of energy, since these may reduce the amount of electricity[19].

Some research points out to benefits of the application of *MFC* in soils and cell architecture. It is sustained that the approach causes less damage to the soil structure, causing minor damage to the microbial communities when using a simple configuration and minimal consumption of energy[7].

Besides, it has been sought to reduce costs in the construction of *MFC* by replacing conventional membranes separators (that are usually very expensive) by other low cost separators. Song *et al.*[71] compared cells equipped with a proton exchange membrane (*PEM*), a cation exchange membrane (*CEM*), and polypropylene felt (*PP*) for effluent treatment (not soil). Ethanolamine (*ETA*) was used as a pollutant and a carbon source in a single air-cathode *MFC*. The cell equipped with *PP* exhibited the highest COD removal (94%) along with an ammonium removal of 52%. Yet, power generation was reduced. Overall, there was a greater degradation of *ETA* at lower costs than the conventional configuration. On the other hand, *CEM* had the highest power density of 584 mW/m^2 at a current density of 0.15 mA/cm^2 whereas the coulombic efficiencies were 25.1, 23.7, and 10.5% for the cells equipped with *PEM*, *CEM*, and *PP*, respectively.

TYPES OF SOIL TREATED IN MICROBIAL FUEL CELLS AND SIMILAR DEVICES

In order to develop MFC technologies and broaden their applications to soil remediation it must be taken into account that the actual soil moisture is <60%, the sediment is > 90% or soil of paddy rice 70-80%[59]. First, remediation of contaminated soils and sediments are different from polluted water and wastewater remediation in that remediation is more difficult because most contaminants are hydrophobic and typically adsorbed onto the solid matrix (either soil or sediment). Second, studies about *MFC* technologies in water and sediment have been carried out, but they are not being tested in actual, full scale soil setups, with the exception of rhizo-deposits of *MFC*. On the other hand, studies on actual soils are very scarce or nonexistent..

In situ MFCs have been tested for cold marine sediments. These devices produce energy with bioactalysts that consisted of anodophlici anaerobic-repiring bacteria (*ARB*) native to the sediments. On the other extreme, overlying water promotes aerobic marine cathodic reaction. Strains belonging to *Geobacteraceae* have been identified as dominant and active microbes in these experiments[66].

Wang and Ren[59] carried out experiments in SMFC with soil was polluted with alkanes. The soil showed a salinity gradient related to its water content. They observed that the conductivity was related to the distance from the anode. In a soil with 33% of moisture, at a distance <1 cm around the anode, the conductivity increased with decreasing water content up to 13.4 mS/cm. In the soil at 2-3 cm around the anode the conductivity decreased to 7.32 mS/cm. As a result of the study it was observed that n-alkanes at a distance of <1 cm were degraded by 79%, unlike that those found at a distance of 1-2 cm and 2-3 cm where alkane removals were relatively lower (67 and 75%, respectively). The control units exhibited alkane removal of 66%.

Wang *et al*.[72] showed that although aqueous *MFC* generate higher power densities than *MFC* in soils, the latter can be effective for the bioremediation of soils polluted with petroleum hydrocarbons whenever cell configuration is changed to the U-tube model. Cathode aerated biostimulation accompanied with good removal results at a distance from anode <1 cm. in another study, it was confirmed that *PAH*s and n-alkanes may be degraded in soil implementing this configuration[59].

Another important issue is soil texture. Soils with fine texture and relatively high organic matter contents are thought to be more difficult to remediate than those of coarse texture and low organic matter concentration. In this regard, Camacho-Perez *et al.*[34] successfully remediated a soil that was polluted with lindane using a *SMFC* at room temperature. The soil exhibited a clayish texture and the organic matter content was very high (8%) for a mineral soil.

To improve the performance of the *MFC* other variables have been tested such as salinity. Adelaja *et al.*[63] worked with different concentrations of salinity and improved electrochemical parameters as well as biodegradation performance using a salinity up to 1.5% w/v were observed. However, electrochemical parameters and pollutant biodegradagion decreased 35 times and 4 times respectively by increasing salinity to 2.5% w/v.

The effect of varying the temperature has been also the subject of some research. It was observed that the degradation rates and the maximum power density increased twice at 40 °C compared with 30 °C, however, it went sharply down four times when he

was brought to 50 °C. Interestingly, production of electricity increased 30 times when riboflavin was added[63].

TYPE OF INOCULUM

In bioremediation a range of live microorganisms with different characteristics are typically used to reduce or eliminate environmental pollutants. There are strategies or tools such as acclimation, bioaugmentation (seeding or inoculation), and biostimulation (supplementing the cultures with nutrients or specific substances) that can be utilized for fostering the degradation of pollutants by microorganisms. In many occasions microbial consortia must be acclimated to the contaminant before being used as inoculum.

For instance, efficient degradation of *PAHs* was achieved using bioaugmentation[59]. In some cases the bioaugmentation process harmed the microorganisms by decreasing their viability during and after inoculation likely due to soil native bacteria competition with foreign microorganisms (seeded), etc. Lately, microorganisms from contaminated soil have been used along with biostimulation, that is, addition of nutrients (C, N, and P), electron acceptors (such as nitrate, hydrogen peroxide, sulphate), and other substances (vitamins, for example) that resulted in an increase of the rate of degradation of the contaminants. This technology was shown to be very efficient to bioremediate soils polluted with oil hydrocarbons. When necessary this strategy can be accompanied by acclimation and bioaugmentation. Camacho-Perez *et al.*[34] work is an example of using a combination of acclimation and bioaugmentation of inoculum in a *SMFC.* They acclimated a sulphate reducting culture to lindane in a mesophilic, complete mix sulphate-reducing lab scale reactor. Inocula from this bioreactor were used to seed (bioaugment) the *SMFC*. The *SMFC* was batch-operated *for* 30 days at room temperature and a lindane removal extent of 78% and organic matter removal of 76% were observed. Removals of lindane in control slurry bireactors that worked with native soil microflora were significantly lower.

In the *MFC* anaerobic microorganisms usually oxidise both the organic matter and organic contaminants[8]. There are studies that elucidate have focused on the elucidation of the mechanisms involved in the transfer of electrons within the *MFC*, which are divided into two groups: *(i)* the use of microbial organelles such as nanowires or pilli, and cytochromes in the bacterial membrane, or *(ii)* the use of recalcitrant organic electron shuttles (mediators) as Flavin. Natural humic materials are also being tested as mediators.

It is important to know the scale transfer mechanisms that are held for the measurements that are carried out in the field. There are models proposed by Revil *et al*.[73] where microscale electron aggregation transfer is observed (it may be between cells and cells or from aquifer precipitates) to generate macroscopic dipoles. The soil bacterial consortia can act as an anode. Molecular biology studies have demonstrated that the source of electrons is not only organic contaminants but also other compounds (sometimes inorganic such as ammonia) related to chemoautotrophs mechanisms (for example, NH_3 oxidation by strains of ammonia-oxidizing β –*Proteobacteria, Nitrosolobus spp*).

The *Geobacteraceae* family, frequently found in *MFC,* has been isolated from biofilms formed on the electrodes *MFC* of marine sediments, as well as in mesophilic *MFC*[66].

Strains from that family have often been identified as anaerobic dominant and active anode-respiring bacteria (*ARB*); more studies are needed in order to know their temperature range and to determine their adaptation and communities changes in mixed cultures setups.

COMBINATION OF OTHER TECHNOLOGIES FOR REMEDIATION WITH MICROBIAL FUEL CELLS

The *MFC* has mainly been studied for two main purposes, the energy production and remediation of contaminated soils and sediments. The combination of *MFC* with other technologies has been conducted primarily to those two goals but new studies on *MFC* and other technologies have also emerged for different purposes.

MFC for power generation. For power generation there are different reports where the conductivity of the soil through simultaneous technology for *in situ* formation of colloidal silica had been carried out. As the *MFC* productivity is affected by the structure, moisture and salt concentration of the soil, with the formation of these colloids the mobility of the ions increased and the soil resistance decreased, so power generation increased 10 times according to Dominguez-Garay *et al.*[74]. This technology is recommended for soils with low conductivity and high organic material content.

Other studies focused on power generation with technology wetlands and *MFC* demonstrate power generation on a large scale, between two species *Spartina anglica* salt marsh and *Phragmites australis* peat soil, of 18 and 1.3mW/m^2 respectively in each plant growth area. *Spartina anglica* reached a power output at the anode of 2900 mW/m^3, the potential current generation for *S. anglica* is 210 to 480 mA/m^2 and for *P. australis* is from 150 to 860 mA/m^2 [(75)]. However, a water layer intermediate in the sediment of S*MFC* to increase the flow of electrons and organic matter to improve the maximum power and the maximum current density at the anode has been used[76].

Much research has focused on improving the electrodes of S*MFC*, such as adding iron sheets in the wet sediment, where three tests (1) "S*MFC*-GF-iron" where graphite felt was used as anode and iron sheets outside the circuit, (2) "S*MFC*-iron" where iron sheets were serving as anode and graphite felt serves as anode without addition of iron, and (3) "S*MFC*-GF". The results obtained in S*MFC*-iron with maximum power density of 170 mW/m^2, S*MFC*-GF-iron 63 mW/m^2, against S*MFC*-GF with 37 mW/m^2, the flow of electrons is awarded in S*MFC*-iron by electrochemical corrosion same of iron giving a voltage of 652 mV, for iron S*MFC*-GF-380 mV as a result of increased microbial activity reductive of iron and S*MFC*-GF 259 mV. On the siding removal efficiency loss on ignition (LOI) for S*MFC*-GF was 32.1% to S*MFC*-iron 23.1% and the highest, S*MFC*-GF-iron, with 39.1%[68]. Efforts are focused on improving the cathode, seeking greater concentration of oxygen reduction reactions, such as the application of *MFC* with algae producing more dissolved oxygen in the cathode serving as biocathode, giving a maximum power density of 46.148 mW/m^2 and doubling the power output[77]. Another study of algae in the cathode area is the one carried out by Wang *et al.*[78], coupled with a layer of nanotubes as a catalyst in the cathode of graphite felt, where 38 mW/m^2 of power generation were obtained.

***Nanotechnological electrodes in MFC*.** To improve the *MFC*, recent studies are betting the combination with nanotechnology at the cathode. One of these studies used stainless steel as electrodes, where electrophoretic deposition of carbon nanotubes multi-walled was made; the control was stainless steel without nanotubes, which turned the maximum power density to 31.6 mW/m^2 which was 3.2 times higher than its control. However, for the cathode was not detected a significant increase[79]. A similar study by Zhu *et al.*[80] used carbon nanotubes on graphite felt cathode. They tested different conditions of electrophoretic deposition, giving 215 ± 9.9 mW/m^2 of maximum power density. With this, the electrophoretic activity improved and the microbial biomass increased.

Another study concerned to improve the output power, the cathode was made of nanosheets of polyaniline-graphene, and the electrode rounded with graphite felt which acts as cathode. With this modification a voltage of 640 mV was obtained and the power density was 99 mW/m^2 [(81)]. However, in the relentless pursuit of improvements to cathode materials, technologies with a high cost such as nano-decoration of the electrode has been tested (carbon paper with Au nanoparticles) achieving a maximum power density of 374.9 $mW/m^{2.}$ Regarding the removal of COD, it had no improvement; in fact, the control removed the COD faster than the *MFC* with nano-modification, however, both came into a complete removal. It was also observed that the microbial diversity related to the density of nanoparticles is promoted, although the way it influences is still unknown[82].

Concerning the combination of nanotechnology and *MFC* for improved degradation of the toxic pollutants in soils and sediments by adding suitable nanoparticles (*NP*s) to either the anodic or cathodic chambers in order to improve removal efficiencies little has been made so far[83]. Not surprisingly, there is more research on this combination applied to the treatment of contaminated waters and wastewaters[84,85].

Regarding the combination of nanoparticle and bioelectrochemical remediation of soils, an important avenue of research opens regarding the use of greener methods for *NP* fabrication. One promising approach that deserves further research and evaluation is the *NP* fabrication that uses vegetable extracts. Plant extracts or liquors (root, stem, leaves, bark, fruit materials) are known to contain complex organic substances (such as tannins and flavonoids) with some reducing power. Metallic solutions ($FeCl_3$, $AgNO_3$, etc.) in contact with such liquors can lead to the formation of metallic or mixed metallic-metal oxide *NP*s that could be supplemented to *SMFC f*or enhancing the removal of toxic pollutants in soils and sediments[83,86,87].

In fact, there is a considerable body of research on the fabrication of *NP*s using plant extracts for a variety of applications (water remediation, health, etc.). **Table 3** shows a compilation of results published in the open literature on this method of “green” *NP*s fabrication. However, it should be highlighted that in spite of such a great amount of papers published on these methods, there are no reports on the yields of *NP*s. Moreover, information on application to soil remediation is scarce. Green synthesis of nanoparticles (*NP*s) has received great attention because, in principle, it seems that it could be more economic and generate less toxic compounds than conventional synthesis methods. Mar-Pineda et al.[83] evaluated the fabrication or synthesis of iron-based NPs using ethanol extracts of *Eysenhardtia polystachya* (Palo Azul for its

Spanish, common name). They tested normal environmental conditions and inert conditions (N_2 atmosphere) synthesis procedures. The salt $FeCl_3 \cdot 6H_2O$ was the precursor for the synthesis at two concentrations, namely 0.10 and 0.16 M. Yields of the NPs synthesis using ethanol extracts under normal environmental conditions (*a*) and inert conditions (*i*) were very low, 0.18 and 0.16%, respectively (basis iron in *NP*/iron in salt). The *NP*s obtained were elongated structures with an average length of 40.4 nm and an average diameter of 2.33 nm. Energy dispersive spectroscopy coupled to scanning electron microscopy analysis confirmed the presence of oxygen in the *NP*s that was ascribed to magnetite (Fe_3O_4) by infrared spectroscopy analysis coupled to Fourier Transform. Analysis of the spent liquors from *NP*s synthesis showed that pH was as low as 1.82. Electrical conductivity was high (14.25 mS cm^{-1}) these values being 3 and 4.75 times higher, respectively, than the values allowed for industrial wastewater discharges in Mexico. In addition, the spent liquors showed an average Chemical Oxygen Demand of 326 400 mg L^{-1}, which far exceeds the maximum allowed value of the discharge limit of this parameter. It was concluded that further and systemic evaluation of these synthesis methods before claiming that the *NP* fabrication based on vegetal extracts is green.

Benthic Microbial Fuel Cells. Salvin *et al.*[111] conducted a study with MFC for energy production in mangroves, taking advantage of the *in situ* salinity and microbial characteristics of such environmental niches. The devices were constructed with inexpensive material (PVC) and were operated for 10 days. A power density of 30 mW/m^2 was obtained and a voltage of 453 mV was reached. The main characteristic of this study is that no external elements were added, only nutrients from the environment and mangrove were used.

In another study with these devices[112], types of electrode materials were evaluated, such as an activated carbon cathode, which was used with 20% in weight of polytetrafluoroethylene; granular activated carbon and nanofibers and carbon brush activated carbon anodes were used. The results showed that the carbon brush had a volumetric power 1810 mW/m^3, the carbon nanofibers were 1250 mW/m^3 with voltages of 500 and 600 mV respectively, unlike granular activated carbon which had not so good results giving a power density of 400 mW/m^3 and 450 mV, the voltage and current correlation showed a sharp decline.

It should be noted that both the brush and the nanofibers are fragile and have low mechanical strength which translates into high costs of maintenance and poor durability.In contrast, granular activated carbon has high mechanical strength and durability, notwithstanding it is advisable in long processes.

Now, research focuses on improving the graphite anode coated with manganese oxide/multiwall carbon nanotubes, which proposes a mechanism of synergy in the transfer of electrons of Mn ions and redox reactions between the interface biofilm and the anode, resulting in a maximum output power of 109.1 mW/m^2 and maximum constant current of 1.2 mA[113]. Regarding this type of studies, it is very important to determine whether the cathode area and processes or the corresponding anodic ones are the electron transfer bottleneck in the *MFC*, in order to focus the efforts on optimizing the materials, surface size and texture, etc., of the significant electrode.

TABLE 3. Fabrication of nanoparticles using vegetal extracts.

Common name	Scientific name	Part of the plant used	Precursor salt	Characteristicof the NP	Use	Ref.
Absinthe	*Artemisia absinthium*	Leaf	Silver nitrate ($AgNO_3$)	AgNPs with different shapes in a range of 5 to 20 nm	Antibacterial, antioxidant and cytotoxic activities	88
Pricklypear cactus	*Opuntia ficus-indica*	Leaf	Cloroauric acid ($HAuCl_4$)	Gold NPs with different shapes of 10 to 20 nm in size	Biomedicine, optics and electronics	89
Indian banyan	*Ficus benghalensis*	Bark	Silver nitrate ($AgNO_3$)	Spherical Silver NPs with a size of 40 nm	Antimicrobial activity and antiproliferative response against osteosarcoma	90
Neem	*Azadirachta indica*	Bark	Silver nitrate ($AgNO_3$)	Spherical Silver NPs with an average size of 50 nm		
Cuachalalate	*Amphipterygium adstringens*	Bark	Silver nitrate ($AgNO_3$)	Spherical Silver NPs with a size of 3 nm	Bactericidal and antimycotic activities against oral microbes	91
Liquorice	*Glycyrrhiza glabra*	Root	Silver nitrate ($AgNO_3$)	Spherical Silver NPs with a size of 9 nm		
Cardus marianus	*Silybum marianum L.*	Seed	Iron chloride ($FeCl_3{\cdot}6H_2O$) and Copper chloride ($CuCl_2{\cdot}2H_2O$)	Cu/Fe3O4 NPs with a range of 8.5 to 60 nm	Catalyst for the reduction of nitroarenes	92
Pomelo fruit	*Citrus maxima*	Peel	Iron chloride ($FeCl_3{\cdot}6H_2O$)	Zero Valent Iron NPs in a range of 10 to 100 nm	Treatment of Cr(VI) solutions.	93
Banana	*Musa × paradisiaca*	Peel	Silver nitrate ($AgNO_3$)	Spherical Silver NPs with an average size of 27.9 nm	Antibacterial Activity	94 95
Caterpillar tree	*Plumeria alba*	Flower	Silver nitrate ($AgNO_3$)	Spherical Silver NPs with an average size of 36.19 nm	Catalytic and various biological activities	96
Cape Jasmine	*Gardenia jasminoides*	Leaf	Iron sulphate ($FeSO_4$)	Hexagonal Iron NPs with an average size of 32 nm	Antibacterial Activity	97

TABLE 3. Fabrication of nanoparticles using vegetal extracts (*Continued*).

Common name	Scientific name	Part of the plant used	Precursor salt	Characteristic of the NP	Use	Ref.
Henna	*Lausonia mermis*	Leaf	Iron sulphate ($FeSO_4$)	Hexagonal Iron NPs with an average size of 21 nm	Antibacterial Activity	97
Eucalyptus	*Eucalyptus*	Leaf	Iron sulphate ($FeSO_4$)	Amorphus Iron Nps with an average size of 57.6 ± 17.4 nm	N.D.	98
European black elderberry	*Sambucus nigra*	Fruit	Silver nitrate ($AgNO_3$)	Spherical AgNPs in a range of 20 to 80 nm	Anti-inflammatory activity	99
Elephant apple	*Feronia elephantum*	Leaf	Silver nitrate ($AgNO_3$)	AgNPs with different shapes with an average size of 32 nm	Adulticidal properties against filariasis, malaria, and dengue vector mosquitoes	100
Barley	*Hordeum vulgare*	Leaf	Iron chloride ($FeCl_3 \cdot 6H_2O$)	Amorphus Iron NPs with an average size of 30 nm	Fenton catalyses	101
Common sorrel	*Rumex acetosa*	Leaf	Iron chloride ($FeCl_3 \cdot 6H_2O$)	Amorphus Iron NPs with an average size of 40 nm	Biomedicine	101
Sweet flag	*Acorus calamus*	Rhizomne	Silver nitrate ($AgNO_3$)	AgNPs with different shapes with an average size of 31.83 nm	Antibacterial activity	102
Black tea	*Camellia sinensis cultivar Hunan Xiangbolu*	Leaf	Iron sulphate ($FeSO_4$)		Degradation of malachite	103
Oolong tea	*Camellia sinensis cultivar Chin Shin*	Leaf	Iron sulphate ($FeSO_4$)	Spherical Iron NPs AgNPs in a range of 40 to 80 nm	Degradation of malachite	103
Green tea	*Camellia sinensis*	Leaf	Iron sulphate ($FeSO_4$)		Degradation of bromothymol blue and malachite	103 104
Sweet wormwood	*Artemisia annua*	Leaf	Silver nitrate ($AgNO_3$)	N.D.	Antimicrobial, antioxidant	105

TABLE 3. Fabrication of nanoparticles using vegetal extracts (*Continued*).

Common name	Scientific name	Part of the plant used	Precursor salt	Characteristic of the NP	Use	Ref.
Broomweed	*Sida acuta*	Leaf	Silver nitrate ($AgNO_3$)	N.D.	Antimicrobial, antioxidant and corrosion inhibition	105
Jiwanti	*Leptadenia reticulata*	Leaf	Silver nitrate ($AgNO_3$)	Spherical AgNPs in a range of 50 to 70 nm	Biomedical and pharmaceutical applications	106
Mondell Pine	*Pinus eldarica*	Bark	Silver nitrate ($AgNO_3$)	Spherical AgNPs in a range of 10 to 40 nm	Biomedical, pharmaceutical and other applications	107
Bastard oleaster	*Elaeagnus latifolia*	Leaf	Silver nitrate ($AgNO_3$)	AgNPs in a range of 30 to 50 nm	Pharmacological and electronical industries	108
Wormwood	*Artemisia capillaris*	Aerial parts	Silver nitrate ($AgNO_3$)	AgNPs in a range of 26 to 30 nm	Antibacterial activities	109
Sweet Cinnamon	*Cinnamon zeylanicum*	Bark	Silver nitrate ($AgNO_3$)	Spherical AgNPs in a range of 31 to 40 nm	Bactericidal activity	110

MFC for decontaminating soil or sediments. On the other hand, there are studies in hybrid technologies focused on decontaminating soil or sediments. Doherty et al.[114] (**Figure 1**), explain the union of the *MFC* and constructed wetlands (*CW*s) based on the on microbial activity to degrade pollutants. This union was named *CW-MFC*, focused on remediated sewage water, which states that removal of COD is about 64-95% and power density is about 1.84-44.6 mW/m^2 in the wet zone, note that the power density increases relatively to the COD load but to some range of 50 mg/L to 250 mg/L with a density power of 44.63 mW/m^2 to 250 mg/L since it has been shown that at concentrations of 500 mg/L and 1,000 mg/L average power densities of 33.7 mW/m^2 and 21.33 mW/m^2 were obtained respectively, showing the fall of the curve. This was expected because high concentrations of COD propitiate a possible higher concentration of organic matter at the cathode and the need of oxygen to degrade generates a reduced concentration of oxygen available for oxidation reactions at the cathode resulting in lower density power. One answer to this problem is the introduction of the cathode in the plant roots as it is known that the roots release oxygen mainly on the day increasing the

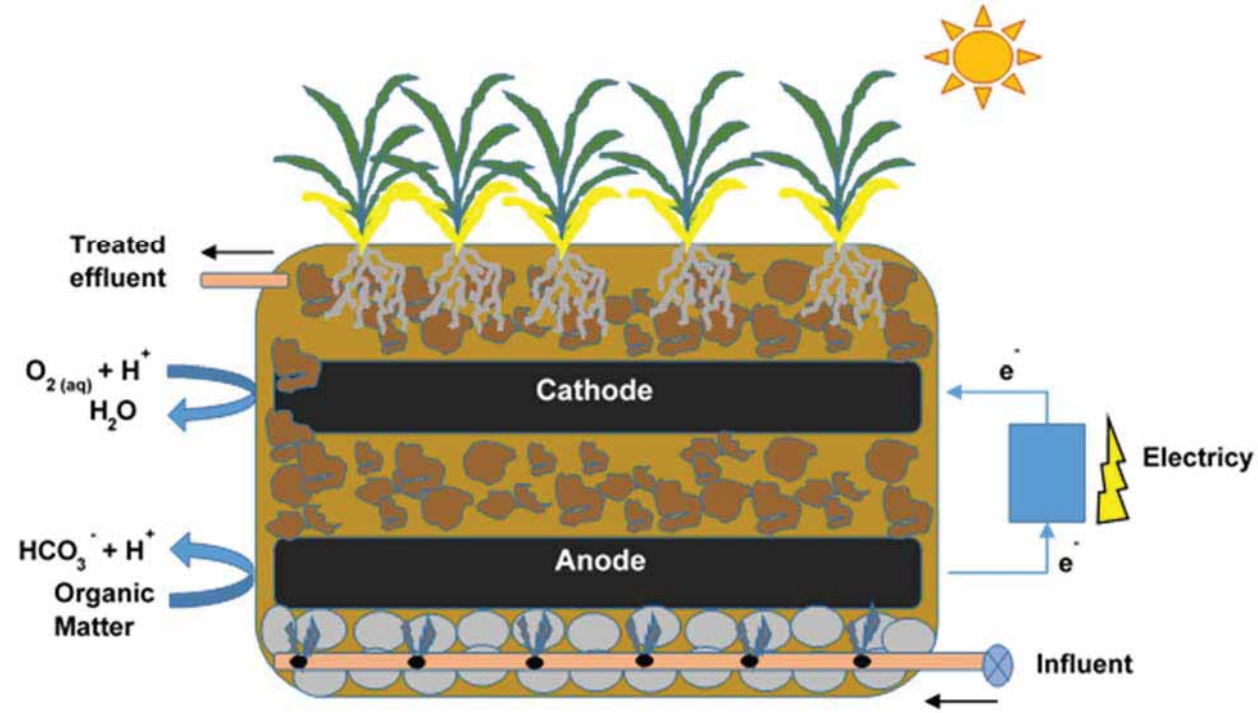


FIGURE 1. Scheme of the combination of constructed wetland and microbial fuel cell for remediation of wastewater. Modified from Doherty *et al.*[114].

oxygen concentration in the anode available for reduction reactions improving device performance at higher concentrations of COD. With this union of technologies as biofilm formation in the anode and cathode, it leads to an increasing redox potential.

Other studies focused on bioremediation of petroleum hydrocarbons by adding sand to the *MFC* with the intention of improving mass transport. This resulted in increased transport which facilitates the dynamism of oxygen and protons in a matrix, increasing the porosity from 44.5% to 51.3%. Its ohmic resistance decreased 46% but the hydrocarbon degradation increased 268%[115].

Research has been conducted to *MFC* in combination with ferric hydroxide to enhance biodegradation of contaminants such as phenanthrene and pyrene, which are found in freshwater sediments. Three experiments were carried out. The first experiment included the addition of amorphous ferric hydroxide sediments, the second was with the use of an *SMFC* and the third was the fusion of the two technologies. At 240 days of operation higher extents of removal of phenanthrene and pyrene were obtained (up to 99 and 94% respectively) in the three experiments where both technologies were combined. Results of only *SMFC* and only Fe $(OH)_3$ were much lower.

The combination of technologies increases the potential degradation of contaminants under anaerobic conditions while humification of organic matter in sediment was stimulated, which could adsorb residual *PAHs* and reduce their bioavailability. Sequestering of *PAHs* in sediments along with microbial degradation could increase *PAHs* removal[116].

Microbial electrochemical snorkel. New models of cells such as the Microbial Electrochemical Snorkel (MES) have been built and operated at lab scale[117]. This type of device is an evolution of *MFC* in the sense that the same electrode serves as an anode at one end (anaerobic) and as a cathode on the other end (aerobic) with resistance minimization. The main objective was not to produce energy, rather to remediate sediments. The authors applied this device to remediate sediments contaminated with petroleum hydrocarbons. Removal of these pollutants ranged from 12 to 21%. However, more research is needed to analyse configurations suitable for the application.

MFC for growth and maintenance of plants. Finally, new applications are now born, such as S*MFC* with other technologies as its main objective is the growth and maintenance of plants along with macrophytes, the latter to promote water quality. In the experiment was evaluated a closed circuit, an open circuit and control plants without S*MFC*. Survival rate of plants of 103.7% in closed circuit and 107.4% in open circuit were obtained, but only 18.5% of the plants survived without S*MFC*. Sequencing analysis showed greater abundance in reducing iron in a closed circuit and stimulation of plant growth in an open circuit. On the part of macrophytes, *Potamogeton malaianus* showed a significant increase in the survival rate and biomass content[118]. Another study indicated that a combination of macrophytes with *SMFC* had an increase in pyrene degradation of sediment compared to the exclusive use of *SMFC*. Stages of plant development seemed to dictate a relationship with pollutant degradation while it is treated with macrophytes. The root exudates of a plant depend on the development of the environmental factors and their physiological state, showing lower rates of bleeding at the seedling stage. Elimination of pyrene from the sediment was associated with variations in the production of root exudates[116].

PERSPECTIVES AND CONCLUSION

A great variety of pollutants such as organic chlorinated compounds, pesticides, petroleum hydrocarbons, dyes and other recalcitrant contaminants have been successfully treated in *MFCs*. On the other hand, research on remediation of soils contaminated with emerging pollutants that affect human health using *MFC* is still scarce. It has been reported that the use of co-substrates may affect or benefit the process; the most used co-substrates to oxidise difficult compounds as azo dyes, ethanol, pyruvate, acetate, among others, are glucose and other carbohydrates. Notwithstanding, hydrocarbon remediation does not usually need co-substrates. *MFC* configurations show that there are two main types of arrangements: *in situ* cells (anodes buried in the solid matrix) and the more conventional *ad situ* cells (two and one chamber ones). In spite of the possible lower costs of the first type of configuration, the latter offers a better process control and higher treatment rates. Regarding the *ad situ* type, it was shown that placing the anode horizontally can optimise the process. The *ad situ MFC* approach can treat a wide range of soils, from sandy to very “heavy” soils (high contents of both clay and organic matter) as research of our own Group has shown. Therefore, *MFC* remediation could be more advantageous than the very popular *in situ* remediation that is limited by low hydraulic conductivity and low permeability of soils.

In the early stages of starting benthic microbial fuel cells (*BMFC*) appeared to be a very effective bioremediation option with several potential benefits, providing accelerated decontamination, as self-sustaining operation, relatively simple implementation, combined control and environmental welfare. Currently, the *MFCs* have unique characteristics regarding their configuration and operation, generating reasons to be subjected to different application challenges. This technology has created a whole field of research which is considered to lead to more sustainable and more controlled applications at the same time. It is environmentally friendly and effective in cleaning soils and contaminated sediments. The continuous generation of evidence shows the capability of *MFC* to increase the efficiency of bioremediation of contaminated sites. However, more studies are needed to implement *MFC* laboratory scale in solving real problems in the field; there are gaps where knowledge is insufficient and lead to delays in implementation, there are even some issues and phenomena that have not been identified yet.

The *SMFC* is a very promising technology for bioremediation of contaminants in soils and sediments. Yet, typical results of power production are in the low side of range reported for remediation of liquid matrices. Mass transfer, possibly mixing, to keep high values of specific electrode area, enrichment of biocatalysts in electrochemically active bacteria to foster electron transfer to/from electrodes, seem to be very important issues in *SMFC*, even more crucial than in *MFC* treating effluents.

In spite of the increasing number of *MFC* technology applications to remediation of waters and sediments/soils, there is still the need to focus R&D on full scale demonstrations. So far, applications were reduced to lab or bench scale devices. There is a need to improve design, engineering, monitoring and evaluation, along with combining efforts of several disciplines to (microbiology, molecular biology analysis of biocatalysts in relation to process performance, nanotechnology applied to materials of electrodes and membranes, etc.) in order to achieve sound full scale *SMFC*s.

ACKNOWLEDGEMENTS

The authors wish to thank CONACYT (Mexico) for a graduate scholarship to KBS-L as well as S.N.I. (Mexico) for partial support to CGM-P. HMP-V also acknowledges CONACYT for the Infrastructure Project 188281.

REFERENCES

1. Hérnandez-Correa, E.; Poggi-Varaldo, H.M.; Ponce-Noyola, M.T.; Romero-Cedillo, L.; Rios-Leal, E.; Solorza-Feria, O. 2017. "Production of Value-Added products and Commodities by Electrofermentation and its Integration to Biorefineries. Battelle, Fourth International Symposium on Bioremediation and Sustainable Environmental Technologies. Miami, FL, USA.
2. De Schamphelaire, L., K. Rabaey, P. Boeckx, N. Boon, and W. Verstraete. 2008. "Outlook for benefits of sediment microbial fuel cells with two bio-electrodes." Microbial Biotechnology. 1(6): 446-462.
3. Luo, H., G. Liu, R. Zhang, and S. Jin. 2009. "Phenol degradation in microbial fuel cells." Chemical Engineering Journal. 147(2): 259-264.

4. Li, J., G. Liu, R. Zhang, Y. Luo, C. Zhang, and M. Li. 2010. "Electricity generation by two types of microbial fuel cells using nitrobenzene as the anodic or cathodic reactants." Bioresource technology. 101(11): 4013-4020.
5. Rittmann, B.E., and P.L. Mc-Carty (Eds.). 2001. Environmental Biotechnology: principles and applications. McGraw-Hill. NY.
6. Pitts, K.E., P.S. Dobbin, F. Reyes-Ramirez, A.J. Thomson, D.J. Richardson, and H.E. Seward. 2003. "Characterization of the Shewanella oneidensis MR-1 decaheme cytochrome MtrA expression in Escherichia coli confers the ability to reduce soluble Fe (III) chelates." Journal of Biological Chemistry. 278(30): 27758-27765.
7. Cao, X., H.L. Song, C.Y. Yu, and X.N. Li. 2015. "Simultaneous degradation of toxic refractory organic pesticide and bioelectricity generation using a soil microbial fuel cell." Bioresource Technology. 189: 87-93.
8. Huang, D.Y., S.G. Zhou, Q. Chen, B. Zhao, Y. Yuan, and L. Zhuang. 2011. "Enhanced anaerobic degradation of organic pollutants in a soil microbial fuel cell." Chemical engineering journal. 172(2): 647-653.

9. Perel, L.W. 2010. "Review: in situ and bioremediation of organic pollutants in aquatic sediments." Journal of hazardous materials. 177(1): 81-89.
10. Zhang, T., S.M. Gannon, K.P. Nevin, A.E. Franks, and D.R. Lovley. 2010. "Stimulating the anaerobic degradation of aromatic hydrocarbons in contaminated sediments by providing an electrode as the electron acceptor." Environmental microbiology. 12(4): 1011-1020.
11. Mohan, S.V., T. Kisa, T. Ohkuma, R.A. Kanaly, and Y. Shimizu. 2006. "Bioremediation technologies for the treatment of PAH-contaminated soil and strategies to enhance process efficiency." Reviews in Environmental Science and Bio/Technology. 5(4): 347-374.
12. Hellou, J. and Leonard, J. 2004. “Polycyclic aromatic hydrocarbons bioaccumulation and biotransformation products in trout exposed through food pellets”. Polycyclic Aromatic Compounds. 24: 697–712.
13. Mishra, S., J. Jyot, R.C. Kuhad, and B. Lal. 2001. "Evaluation of inoculum addition to stimulating in situ bioremediation of oily-sludge-contaminated soil." Applied and environmental microbiology. 67(4): 1675-1681.
14. Launen, L.A., V.H. Buggs, M.E. Eastep, R.C. Enriquez, J.W. Leonard, M.J. Blaylock, J.W. Huang, and M.M. Häggblom. 2002. "Bioremediation of polyaromatic hydrocarbon-contaminated sediments in aerated bioslurry reactors." Bioremediation Journal. 6(2): 125-141.
15. Pizzul, L., M.P. Castillo, and J. Stenström. 2006. "Characterization of selected actinomycetes degrading polyaromatic hydrocarbons in liquid culture and spiked soil." World Journal of Microbiology and Biotechnology. 22(7): 745-752.
16. Santos, E.C., R.J.S. Jacques, F.M. Bento, R.M.C. Peralba, P.A. Selbach, E.L.S. Sá, and F.A.O. Camargo. 2008. "Anthracene biodegradation and surface activity by an iron-stimulated Pseudomonas sp." Bioresource technology. 99(7): 2644-2649.
17. Mohan, S.V., B.P. Reddy, and P.N. Sarma. 2009. "Ex situ slurry phase bioremediation of chrysene contaminated soil with the function of metabolic function: process evaluation by data enveloping analysis (DEA) and Taguchi design of experimental methodology (DOE)." Bioresource technology. 100(1): 164-172.
18. Mohan, S.V., and K. Chandrasekhar. 2011. "Self-induced bio-potential and graphite electron accepting conditions enhances petroleum sludge degradation in bio-electrochemical system with simultaneous power generation." Bioresource technology. 102(20): 9532-9541.

19. Yang, Y., Z. Lu, X. Lin, C. Xia, G. Sun, Y. Lian, and M. Xu. 2015. "Enhancing the bioremediation by harvesting electricity from the heavily contaminated sediments." Bioresource technology. 179: 615-618.
20. Haritash, A.K., and C.P. Kaushik. 2009. "Biodegradation aspects of polycyclic aromatic hydrocarbons (PAHs): a review." Journal of hazardous materials. 169(1): 1-15.
21. Johnsen, A.R., Karlson, U. 2003. “Evaluation of bacterial strategies to promote the bioavailability of polycyclic aromatic hydrocarbons”. Applied Microbiology and Biotechnology. 63(4): 452-459.
22. Hale, S.E., P. Meynet, R.J. Davenport, D.M. Jones, and D. Werner. 2010. "Changes in polycyclic aromatic hydrocarbon availability in River Tyne sediment following bioremediation treatments or activated carbon amendment." Water research. 44(15): 4529-4536.
23. Li, X., P. Li, X. Lin, C. Zhang, Q. Li, and Z. Gong. 2008. "Biodegradation of aged polycyclic aromatic hydrocarbons (PAHs) by microbial consortia in soil and slurry phases." Journal of hazardous materials. 150(1): 21-26.
24. Yu, K.S.H., Wong, A.H.Y., Yau, K.W.Y., Wong, Y.S. and Tam, N.F.Y. 2005. “Natural attenuation, biostimulation and bioaugmentation on biodegradation of polycyclic aromatic hydrocarbons (PAHs) in mangrove sediments”. 4th International Conference on Marine Pollution and Ecotoxicology. 51(8-12): 1071-1077.
25. Margesin, R., and F. Schinner. 2001. "Bioremediation (natural attenuation and biostimulation) of diesel-oil-contaminated soil in an alpine glacier skiing area." Applied and Environmental Microbiology. 67(7): 3127-3133.
26. Saison, C., C. Perrin-Ganier, M. Schiavon, and J.L. Morel. 2004. "Effect of cropping and tillage on the dissipation of PAH contamination in soil." Environmental Pollution. 130(2): 275-285.
27. Coates, J.D., R.T. Anderson, J.C. Woodward, E.J.P. Phillips, and D.R. Lovley. 1996. "Anaerobic hydrocarbon degradation in petroleum-contaminated harbour sediments under sulfate-reducing and artificially imposed iron-reducing conditions." Environmental Science & Technology. 30(9): 2784-2789.
28. Lu, X.Y., T. Zhang, and H.H.P. Fang. 2011. "Bacteria-mediated PAH degradation in soil and sediment." Applied microbiology and biotechnology. 89(5): 1357-1371.
29. Lovley, D.R., J.C. Woodward, and F.H. Chapelle. 1994. "Stimulated anoxic biodégradation of aromatic hydrocarbons using Fe (in) ligands." Nature. 370: 128-131.
30. Mihelcic, J.R., and R.G. Luthy. 1988. "Degradation of polycyclic aromatic hydrocarbon compounds under various redox conditions in soil-water systems." Applied and Environmental Microbiology. 54(5): 1182-1187.
31. Li, Z., and B.A. Wrenn. 2004. "Effects of ferric hydroxide on the anaerobic biodegradation kinetics and toxicity of vegetable oil in freshwater sediments." Water research. 38(18): 3859-3868.
32. Lovley, D.R., and E.J.P. Phillips. 1987. "Rapid assay for microbially reducible ferric iron in aquatic sediments." Applied and Environmental Microbiology. 53(7): 1536-1540.
33. Song, T.S., Z.S. Yan, Z.W. Zhao, and H.L. Jiang. 2010. "Removal of organic matter in freshwater sediment by microbial fuel cells at various external resistances." Journal of chemical technology and biotechnology. 85(11): 1489-1493.
34. Camacho-Pérez, B., E. Ríos-Leal, O. Solorza-Feria, P.A. Vazquez-Landaverde, J. Barrera-Cortés, M.T. Ponce-Noyola, J. Garcia-Mena, N. Rinderknecht-Seijas, and H.M. Poggi-Varaldo. 2013. "Performance of an electrobiochemical slurry reactor for the treatment of a soil contaminated with lindane." Journal of New Materials for Electrochemical Systems. 16(3): 217-228.
35. Morris, J.M., S. Jin, B. Crimi, and A. Pruden. 2009. "Microbial fuel cell in enhancing anaerobic biodegradation of diesel." Chemical Engineering Journal. 146(2): 161-167.
36. Gregory, K.B., D.R. Bond, and D.R. Lovley. 2004. "Graphite electrodes as electron donors for anaerobic respiration." Environmental microbiology. 6(6): 596-604.

37. Gregory, K.B., and D.R. Lovley. 2005. "Remediation and recovery of uranium from contaminated subsurface environments with electrodes." Environmental science & technology. 39(22): 8943-8947.
38. Aulenta, F., P. Reale, A. Canosa, S. Rossetti, S. Panero, and M. Majone. 2010. "Characterization of an electro-active biocathode capable of dechlorinating trichloroethene and cis-dichloroethene to ethene." Biosensors and Bioelectronics. 25(7): 1796-1802.
39. Strycharz, S.M., T.L. Woodard, J.P. Johnson, K.P. Nevin, R.A. Sanford, F.E. Löffler, and D.R. Lovley. 2008. "Graphite electrode as a sole electron donor for reductive dechlorination of tetrachlorethene by Geobacter lovleyi." Applied and environmental microbiology. 74(19): 5943-5947.
40. Aulenta, F., A. Canosa, M. Majone, S. Panero, P. Reale, and S. Rossetti. 2008. "Trichloroethene dechlorination and H_2 evolution are alternative biological pathways of electric charge utilization by a dechlorinating culture in a bioelectrochemical system." Environmental Science & Technology. 42(16): 6185-6190.
41. Mu, Y., R.A. Rozendal, K. Rabaey, and J. Keller. 2009a. "Nitrobenzene removal in bioelectrochemical systems." Environmental science & technology. 43(22): 8690-8695.
42. Mu, Y., K. Rabaey, R.A. Rozendal, Z. Yuan, and J. Keller. 2009b. "Decolorization of azo dyes in bioelectrochemical systems. "Environmental science & technology. 43(13): 5137-5143.
43. Williams.K.H., K.P. Nevin, A.E. Franks, P.E. Long, D.R. Lovley. 2010. "An electrode-based approach for monitoring *in situ* microbial activity during subsurface bioremediation." Environmental Science and Technology. 44:47–54.
44. Morris, J.M., and S. Jin. 2007. "Feasibility of using microbial fuel cell technology for bioremediation of hydrocarbons in groundwater." Journal of Environmental Science and Health, Part A. 43(1): 18-23.
45. Mohan, S.V., G. Mohanakrishna, G. Velvizhi, V. Lalit Babu, and P.N. Sarma. 2010. "Bio-catalyzed electrochemical treatment of real field dairy wastewater with simultaneous power generation." Biochemical Engineering Journal. 51(1): 32-39.
46. Clauwaert, P., K. Rabaey, P. Aelterman, L. De Schamphelaire, T.H. Pham, P. Boeckx, N. Boon, and W. Verstraete. 2007. "Biological denitrification in microbial fuel cells." Environmental science & technology. 41(9): 3354-3360.
47. Yang, Y., M. Xu, Z. He, J. Guo, G. Sun, and J. Zhou. 2013. "Microbial electricity generation enhances decabromodiphenyl ether (BDE-209) degradation." PloS one. 8(8): e70686.
48. Chandrasekhar, K., and S.V. Mohan. 2012. "Bio-electrochemical remediation of real field petroleum sludge as an electron donor with simultaneous power generation facilitates biotransformation of PAH: effect of substrate concentration." Bioresource technology. 110: 517-525.
49. Poggi-Varaldo, H.M.; Martinez, A.O.; Vazquez-Larios, A.L.; Rindernknecht-Seijas, N.F.; Vazquez, G.V. and Solorza-Feria, O. 2009. “Application of biocathodes and enrichment strategies as promising alternative for enhanced bioelectricity generation in microbial fuel cells”. New Biotechnology. 25(1): S252-S252.
50. Ortega-Martinez, A.C.; Vázquez-Larios, A.L.; Juarez-Lopez, K.; Solorza-Feria, O. and Poggi-Varaldo, H.M. 2010. “A review of biocathodes and enrichment strategies of electrochemically active bacteria for enhanced bioelectricity generation in microbial fuel cells”. Journal of Biotechnology. 150(1): S144-S145.
51. Sathish-Kumar, K., Solorza-Feria, O., Tapia-Ramírez, J., Rinderkenech-Seijas, N. and Poggi-Varaldo, H.M. 2013. “Electrochemical and chemical enrichment methods of a sodic–saline inoculum for microbial fuel cells”. International Journal of Hydrogen Energy. 150(28): 12600-12609

52. Lu, L., H. Yazdi, S. Jin, Y. Zuo, P.H. Fallgren, and Z.J. Ren. 2014. "Enhanced bioremediation of hydrocarbon-contaminated soil using pilot-scale bioelectrochemical systems." Journal of hazardous materials. 274: 8-15.
53. Rodrigo, J., K. Boltes, and A. Esteve-Nuñez. 2014. "Microbial-electrochemical bioremediation and detoxification of dibenzothiophene-polluted soil." Chemosphere. 101: 61-65.
54. Xia, C., M. Xu, J. Liu, J. Guo, and Y. Yang. 2015. "Sediment microbial fuel cell prefers to degrade organic chemicals with higher polarity." Bioresource technology. 190: 420-423.
55. Hamdi, H., S. Benzarti, L. Manusadžianas, I. Aoyama, and N. Jedidi. 2007. "Bioaugmentation and biostimulation effects on PAH dissipation and soil ecotoxicity under controlled conditions." Soil Biology and Biochemistry. 39(8): 1926-1935.
56. Hankard, P.K., C. Svendsen, J. Wright, C. Wienberg, S.K. Fishwick, D.J. Spurgeon, and J.M. Weeks. 2004. "Biological assessment of contaminated land using earthworm biomarkers in support of chemical analysis." Science of the total environment. 330(1): 9-20.
57. Logan, B.E. 2009. “Exoelectrogenic bacteria that power microbial fuel cells”. Nature Reviews Microbiology. 7: 375-381.
58. Yuan, Y., S. Zhou, and L. Zhuang. 2010. "A new approach to in situ sediment remediation based on air-cathode microbial fuel cells." Journal of Soils and Sediments. 10(7): 1427-1433.
59. Wang, H., and Z.J. Ren. 2013. "A comprehensive review of microbial electrochemical systems as a platform technology." Biotechnology advances. 31(8): 1796-1807.
60. Zhang, Y., and I. Angelidaki. 2012. "Self-stacked submersible microbial fuel cell (SS*MFC*) for improved remote power generation from lake sediments." Biosensors and Bioelectronics. 35(1): 265-270.
61. Ueno, Y., and Y. Kitajima. 2012. "Suppression of methane gas emission from sediment using a bioelectrochemical system." Environmental Engineering & Management Journal (EEMJ). 11(10): 1833-1837.
62. Zhang, Y., X. Wang, X. Li, L. Cheng, L. Wan, and Q. Zhou. 2015b. "Horizontal arrangement of anodes of microbial fuel cells enhances remediation of petroleum hydrocarbon-contaminated soil." Environmental Science and Pollution Research. 22(3): 2335-2341.
63. Adelaja, O., T. Keshavarz, and G. Kyazze. 2015. "The effect of salinity, redox mediators and temperature on anaerobic biodegradation of petroleum hydrocarbons in microbial fuel cells." Journal of Hazardous Materials. 283: 211-217.
64. Yan, Z., H. Jiang, H. Cai, Y. Zhou, and L.R. Krumholz. 2015. "Complex Interactions Between the Macrophyte Acorus Calamus and Microbial Fuel Cells During Pyrene and Benzo [a] Pyrene Degradation in Sediments." Scientific reports. 5:1-11.
65. Rinaldi, A., B. Mecheri, V. Garavaglia, S. Licoccia, P.D. Nardo, and E. Traversa. 2008. "Engineering materials and biology to boost the performance of microbial fuel cells: a critical review." Energy & Environmental Science. 1(4): 417-429.
66. Michie, I.S., J.R. Kim, R.M. Dinsdale, A.J. Guwy, and G.C. Premier. 2011. "The influence of psychrophilic and mesophilic start-up temperature on microbial fuel cell system performance." Energy & Environmental Science. 4(3): 1011-1019.
67. Sun, J., Y.Y. Hu, Z. Bi, and Y.Q. Cao. 2009. "Simultaneous decolorization of azo dye and bioelectricity generation using a microfiltration membrane air-cathode single-chamber microbial fuel cell." Bioresource Technology. 100(13): 3185-3192.
68. Zhang, H., D. Zhu, T.S. Song, P. Ouyang, and J. Xie. 2015a. "Effects of the presence of sheet iron in freshwater sediment on the performance of a sediment microbial fuel cell." International Journal of Hydrogen Energy. 40(46): 16566-16571.

69. Li, X., X. Wang, Y. Zhang, L. Cheng, J. Liu, F. Li, B. Gao, and Q. Zhou. 2014. "Extended petroleum hydrocarbon bioremediation in saline soil using Pt-free multianodes microbial fuel cells." RSC Advances. 4(104): 59803-59808.
70. Jung, S.P., M.H. Yoon, S.M. Lee, S.E. Oh, H. Kang, and J.K. Yang. 2014. "Power generation and anode bacterial community compositions of sediment fuel cells differing in anode materials and carbon sources." Int. J. Electrochem. Sci. *9*: 315-326.
71. Song, Y.H., B.M. An, J.W. Shin, and J.Y. Park. 2015. "Ethanolamine degradation and energy recovery using a single air-cathode microbial fuel cell with various separators." International Biodeterioration & Biodegradation. 102: 392-397.
72. Wang, X., Z. Cai, Q. Zhou, Z. Zhang, and C. Chen. 2012. "Bioelectrochemical stimulation of petroleum hydrocarbon degradation in saline soil using U-tube microbial fuel cells." Biotechnology and Bioengineering. 109(2): 426-433.
73. Revil, A., C.A. Mendonça, E.A. Atekwana, B. Kulessa, S.S. Hubbard, and K.J. Bohlen. 2010. "Understanding biogeobatteries: Where geophysics meets microbiology." *Journal of Geophysical Research*: Biogeosciences. 115(G1).
74. Domínguez-Garay, A., A. Berná, I. Ortiz-Bernad, and A. Esteve-Núñez. 2013. "Silica colloid formation enhances performance of sediment microbial fuel cells in a low conductivity soil." Environmental science & technology. 47(4): 2117-2122.
75. Wetser, K., J. Liu, C. Buisman, and D. Strik. 2015. "Plant microbial fuel cell applied in wetlands: Spatial, temporal and potential electricity generation of Spartina anglica salt marshes and Phragmites australis peat soils." Biomass and Bioenergy. 83: 543-550.
76. Lee, Y.S., J. An, B. Kim, H.J. Park, J. Kim, and I.S.Chang. 2015. "Increased Power in Sediment Microbial Fuel Cell: Facilitated Mass Transfer via a Water-Layer Anode Embedded in Sediment." *PloS one.* 10(12).
77. Najafgholi, Z., and M. Rahimnejad. 2016. "Improvement of sediment microbial fuel cell performance by application of sun light and biocathode." Korean Journal of Chemical Engineering 33(1): 154-158.
78. Wang, D.B., T.S. Song, T. Guo, Q. Zeng, and J. Xie. 2014. "Electricity generation from sediment microbial fuel cells with algae-assisted cathodes." International Journal of Hydrogen Energy. 39(25): 13224-13230.
79. Song, T.S., X.Y. Wu, and C.C. Zhou. 2013. "Electrophoretic deposition of multi-walled carbon nanotube on a stainless steel electrode for use in sediment microbial fuel cells." Applied biochemistry and biotechnology. 170(5): 1241-1250.
80. Zhu, D., D.B. Wang, T.S. Song, T. Guo, P. Ouyang, P. Wei, and J. Xie. 2015. "Effect of carbon nanotube modified cathode by electrophoretic deposition method on the performance of sediment microbial fuel cells." *Biotechnology letters*. 37(1): 101-107.
81. Ren, Y., D. Pan, X. Li, F. Fu, Y. Zhao, and X. Wang. 2013. "Effect of polyaniline-graphene nanosheets modified cathode on the performance of sediment microbial fuel cell." Journal of Chemical Technology and Biotechnology. 88(10): 1946-1950.
82. Alatraktchi, F.A.A., Y. Zhang, and I. Angelidaki. 2014. "Nanomodification of the electrodes in a microbial fuel cell: Impact of nanoparticle density on electricity production and microbial community." Applied Energy. 116: 216-222.
83. Mar-Pineda, C.G., Flores-Ortiz, O., Hernández-Vera, R. and Poggi-Varaldo H.M. 2017. “How Green is the Green Synthesis of Iron Nanoparticles using *Eysenhardtia polystachya*”. Fourth International Symposium on Bioremediation and Sustainable Environmental Technologies. Miami, FL, USA.
84. Du, Z., Li, H. and Gu, T. 2007. “A state of the art review on microbial fuel cells: A promising
85. technology for wastewater treatment and bioenergy”. Biotechnology Advances. 25: 464-482.

86. Liu, X.W., Sun, X.F., Huang, Y.X., Sheng, G.P., Zhou, K., Zeng, R.J., Dong, F., Wang, S.G., Xu, A.W., Tong, Z.H. and Yu, H.Q. 2010. “Nano-structured manganese oxide as a cathodic catalyst for enhanced oxygen reduction in a microbial fuel cell fed with a synthetic wastewater”. Water Research. 44(18): 5298-5305.
87. Mar-Pineda, C.G. 2016. “Remediación de suelos con tecnologías combinadas”. Thesis CINVESTAV and Technological University of Tecamac, Mexico.
88. Flores-Ortiz, O. 2016. “Caracterización y tratamiento de licores residuales provenientes de la síntesis de nanopartículas a partir de extractos vegetales”. Advance Report B.S. Thesis CINVESTAV and ENCB-IPN, Mexico.
89. Ali, M., Kim, B., Belfield, K., Norman, D., Brennan, M., and Ali, G. S. 2016. “Green synthesis and characterization of silver nanoparticles using Artemisia absinthium aqueous extract — A comprehensive study”. Materials Science and Engineering C. 58: 359-365.
90. Álvarez, R. A., Cortez-Valadez, M., Neira-Bueno, L., Britto-Hurtado, R., Rocha-Rocha, O., Delgado-Beleño, Y., Martínez-Nuñez, C.E. and Serrano-Corrales, L.I. 2016. “Vibrational properties of gold nanoparticles obtained by green synthesis”. Physica E. 84: 191-195.
91. Nayak, D., Ashe, S., Rauta, P. R., Kumari, M., and Nayak, B. 2016. “Bark extractmediated green synthesis of silver nanoparticles: Evaluation of antimicrobial activity and antiproliferative response against osteosarcoma”. Materials Science and Engineering C. 58: 44-52.
92. Rodríguez-Luis, O.E., Hernandez-Delgadillo, R., Sánchez-Nájera, R.I., Martínez-Castañón, G., Niño-Martínez, N., Sánchez-Navarro, M.C., Ruiz, F. and Cabral-Romero, C. 2016. “Green Synthesis of Silver Nanoparticles and Their Bactericidal and Antimycotic Activities against Oral Microbes”. Journal of Nanotechnology. 2016: 1-10.
93. Sajadi, S. M., Nasrollahzadeh, M., and Maham, M. 2016. “Aqueous extract from seeds of Silybum marianum L. as a green material for preparation of the Cu/Fe3O4 nanoparticles: A magnetically recoverable and reusable catalyst for the reduction of nitroarenes”. Journal of Colloid and Interface Science. 469: 93-98.
94. Wei, Y., Fang, Z., Zheng, L., Tan, L., and Tsang, E. P. 2016. “Green synthesis of Fe nanoparticles using *Citrus maxima* peels aqueous extracts”. Materias Letters. 185: 384–386.
95. Ibrahim, H. 2015. “Green synthesis and characterization of silver nanoparticles using banana peel extract and their antimicrobial activity against representative microorganisms”. Journal of Radiation Research and Applied Sciences. 8: 265–275.
96. Bankar, A., Joshi, B., Kumar, A. and Zinjarde, S. “Banana peel extract mediated novel route for the synthesis of silver nanoparticles”. Colloids and Surfaces A: Physicochemical and Engineering Aspects. 368(1-3): 58-63.
97. Mata, R., Nakkala, J. R., & Sadras, S. R. 2015. “Catalytic and biological activities of green silver nanoparticles synthesized from *Plumeria alba* (frangipani) flower extract”. Materials Science and Engineering: C. 51: 216-225.
98. Naseem, T., and Farrukh, M. A. 2015. “Antibacterial Activity of Green Synthesis of Iron Nanoparticles Using *Lawsonia inermis* and *Gardenia jasminoides* Leaves Extract”. Journal of Chemistry. 2015: 1-7.
99. Zhuang, Z., Huang, L., Wang, F., and Chen, Z. 2015. “Effects of cyclodextrin on the morphology and reactivity of iron-basednanoparticles using Eucalyptus leaf extract”. Industrial Crops and Products. 69: 308-313.
100. David, L., Moldovan, B., Vulcu, A., Olenic, L., Perde-Schrepler, M., Fischer-Fodor, E., Florea, A., Crisan, M., Chiorean, I., Clichici, S. and Filip, G.A. 2014. “Green synthesis, characterization and anti-inflammatory activity of silver nanoparticles using European black elderberry fruits extract”. Colloids and Surfacs B: Biointerfaces. 122: 767-777.

101. Veerakumar, K., and Govindarajan, M. 2014. “Adulticidal properties of synthesized silver nanoparticles using leaf extracts of *Feronia elephantum* (Rutaceae) against filariasis, malaria, and dengue vector mosquitoes”. Parasitology Research. 113: 4085-4096.
102. Makarov, V. V., Makarova, S. S., Love, A. J., Sinitsyna, O. V., Dudnik, A. O., Yaminsky, I. V., Taliansky, M.E. and Kalinina, N.O. 2014. “Biosynthesis of Stable Iron Oxide Nanoparticles in Aqueous Extracts of *Hordeum vulgare* and *Rumex acetosa* Plants”. Langmuir. 30: 5982-5988.
103. Nakkala, J. R., Mata, R., Gupta, A. K., and Sadras, S. R. 2014. “Biological activities of green silver nanoparticles synthesized with *Acorous calamus* rhizome extract”. European Journal of Medicinal Chemistry. 85: 784-794.
104. Huang, L., Weng, X., Chen, Z., Megharaj, M., and Naidu, R. 2014. “Green synthesis of iron nanoparticles by various tea extracts: Comparative study of the reactivity”. Spectrochimica Acta Part A: Molecular and Biomolecular Spectroscopy. 130: 295-301.
105. Hoag, G.E., Collins, J.B., Holcomb, J.L., Hoag, J.R., Nadagouda, M.N. and Varma, R.S. 2009. “Degradation of bromothymol blue by ‘greener’ nano-scale zero-valent iron synthesized using tea polyphenols”. Journal of Materials Chemistry. 19: 8671-8677.
106. Johnson, A., Obot, I., and Ukpong, U. 2014. “Green synthesis of silver nanoparticles using *Artemisia annua* and *Sida acuta* leaves extract and their antimicrobial, antioxidant and corrosion inhibition potentials”. Journal of Materials and Environmental Science. 5(3): 899-906.
107. Swamy, M. K., Sudipta, K., Jayanta, K., and Balasubramanya, S. 2014. “The green synthesis, characterization, and evaluation of the biological activities of silver nanoparticles synthesized from *Leptadenia reticulata* leaf extract”. Applied Nanoscience. 5(1): 73-81.
108. Iravani, S., and Zolfaghari, B. 2013. “Green synthesis of silver nanoparticles using *Pinus eldarica* bark extract”. BioMed Research International. 2013: 1-5.
109. Phanjom, P., Sultana, A., Sarma, H., Ramchiary, J., Goswami, K., and Baishya, P. 2012. “Plant-mediated synthesis of silver nanoparticles using *Elaeagnus latifolia* leaf extract”. Digest Journal of Nanomaterials and Biostructures. 7(3): 1117-1123.
110. Park, Y., Noh, H. J., Kim, H.S., Kim, Y.J., Choi, J.S., Kim, C.K., Kim, Y.S. and Cho, S. 2012. “*Artemisia capillaris* extracts as a green factory for the synthesis of silver nanoparticles with antibacterial activities”. Journal of Nanoscience and Nanotechnology. 12: 7087-7095.
111. Sathishkumar, M., Sneha, K., Won, S., Cho, C.W., Kim, S., and Yun, Y.S. 2009. “*Cinnamon zeylanicum* bark extract and powder mediated green synthesis of nano-crystalline silver particles and its bactericidal activity”. Colloids and Surfaces B: Biointerfaces. 73: 332-338.
112. Salvin, P., O. Ondel, C. Roos, and F. Robert. 2015. "Energy harvest with mangrove benthic microbial fuel cells." International Journal of Energy Research. 39(4): 543-556.
113. Karra, U., E. Muto, R. Umaz, M. Kölln, C. Santoro, L. Wang, and B. Li. 2014. "Performance evaluation of activated carbon-based electrodes with novel power management system for long-term benthic microbial fuel cells." International Journal of Hydrogen Energy. 39(36): 21847-21856.
114. Fu, Y., Yu J., Zhang, Y., and Meng, Y. 2014. "Graphite coated with manganese oxide/multiwall carbon nanotubes composites as anodes in marine benthic microbial fuel cells." Applied Surface Science. 317: 84-89.
115. Doherty, L., Y. Zhao, X. Zhao, Y. Hu, X. Hao, L. Xu, and R. Liu. 2015. "A review of a recently emerged technology: Constructed wetland–Microbial fuel cells." Water research. 85: 38-45.
116. Li, X., X. Wang, Z.J. Ren, Y. Zhang, N. Li, and Q. Zhou. 2015. "Sand amendment enhances bioelectrochemical remediation of petroleum hydrocarbon contaminated soil." Chemosphere. 141: 62-70.
117. Yan Z.S., N. Song, H.Y. Cai, J.H. Tay, H.L. Jiang. 2012. "Enhanced degradation of phenanthrene and pyrene in freshwater sediments by combined employment of sediment microbial fuel cell and amorphous ferric hydroxide." Journal of hazardous materials. 199:217-225.

118. Viggi, C.C., E. Presta, M. Bellagamba, S. Kaciulis, S.K. Balijepalli, G. Zanaroli, M.P. Papini, S. Rossetti, and F. Aulenta. 2015. "The “Oil-Spill Snorkel”: an innovative bioelectrochemical approach to accelerate hydrocarbons biodegradation in marine sediments." *Frontiers in microbiology*. 6.
119. Zhou, Y.L., H.F. Wu, Z.S. Yan, H.Y. Cai, and H.L. Jiang. 2016. "The enhanced survival of submerged macrophyte Potamogeton malaianus by sediment microbial fuel cells." Ecological Engineering. 87: 254-262.

CHAPTER 12.2 SUSTAINABLE IRON BASED BIONANO-BIOPARTICLES FROM A DEHALOGENATING MICROBIAL CONSORTIUM ALLOWS REMEDIATION OF WATER POLLUTED WITH PCE

L. Breton-Deval (1) and H. M. Poggi-Varaldo *(1)

(1) Environmental Biotechnology and Renewable Energies Group, Department of Biotechnology and Bioengineering, Centro de Investigación y Estudios Avanzados del IPN, P.O.Box 14-740, Ciudad de México D.F.,07000, México

ABSTRACT

The purposes of this research were *(i)* to synthesize nanoparticles (*NPs)* using a biological-based method using bioparticles from anaerobic fluidized bed reactors, *(ii)* to evaluate the effect of the precursor salt used (either $Fe(NO_3)_3$ or $FeCl_3$) on *NP*s characteristics, and *(iii)* to evaluate the removal/degradation of *PCE* by these *NPs*. Bioparticles from anaerobic fluidized bed reactors were used as departing support for *NPs* synthesis. The consortium could successfully synthesize magnetite *NPs* without using expensive and hazardous chemical reducing agents. The diameter of *NPs* was 5 – 60 nm. Samples from the method that used the $Fe(NO_3)_3$ showed aggregates while the other *NP*s from the precursor iron chloride exhibited smaller size. The removal of *PCE* was more efficient for *NP*s formed from the chloride salt, after 4 days the removal was 99%. On the other hand, the *NPs* biosynthesized with Fe $(NO_3)_3$ removed 93% of *PCE*. Control units containing bioparticles with dehalogenating consortium but no *NPs* could just remove 38%. In general, the main *PCE* metabolite found was *TCE*, although at low concentrations. This suggested that *NP*s had a high dehalogenating efficiency. We conclude that the dehalogenating consortium is capable of synthesizing *NPs* that can effectively degrade *PCE*, second, the *NPs* obtained from $FeCl_3$ precursor exhibited smaller diameter and increased rates and extents of pollutant removal. Finally, our biosynthesis route for magnetite *NPs* implies significant savings in chemical reagents as well as energy in contrast to the typical chemical techniques for magnetite *NPs* fabrication

Keywords: biosynthesis, bio-nano bio particles, nanoparticles, PCE treatment

INTRODUCTION

Perchloroethylene (*PCE*) is a chlorinated organic compound (*COC*) mainly used in dry cleaning industry, in metal cleaning operations. It has been widely used due to its no flammability, easiness to reuse and its strong solvent capacity[1].

---

*Author for correspondence: erikairigoyen@hotmail.com

However, it has been considered as a potentially toxic and carcinogen compound[2]. Moreover, daughter products of *PCE* reductive dechlorination, such as trichloroethylene (*TCE*), dichloroethylene (*DCE*) and vinyl chloride (*VC*) show higher toxicity than *PCE* itself[3].

In addition, *PCE* is the most reported organo-chlorinated contaminant in groundwater, where it forms a dense phase at the bottom of the aquifer. Due to its low solubility is difficult to remove, representing a sustained release source of the contaminant and a risk for the health and the environment[4]. Therefore, the search of successful technologies that allow the efficient removal of these chlorinated compounds continues.

Several works have been carried out with the aim of removing *PCE* and their metabolites using iron nanoparticles (*NPs*)[5-7]. Iron is the material most used in the treatment of *COCs* compounds due to its low cost, abundance, ease, and reactivity[8]. The iron can serve as a fixed source of electrons for the reductive dehalogenation of *PCE*[9-11]. The *NP* size have a high surface area to mass ratio, making them more reactive compared to the conventional iron. However, the application of nano iron still faces challenges, such as the longevity, iron *NPs* could be very reactive; they quickly oxidize and lose their reductive power. Other challenge is the transport through aquifer. The *NPs* tend to agglomerate and form aggregates, resulting in a decrease in the activity and mobility of the particles[12].

There are different ways to synthesize *NPs*, namely, chemically, physical and biological methods. Regarding the latter some research has focused on the synthesis of *NPs* using specific microbes with promising results[13,14].

The metals can act as nutrients for the microorganism or enzymatic cofactors; they are essential for some cellular process. However, high concentrations of some metals could be toxic[15-17]. The microorganisms have two different methods for capturing metal cations. One of them is inespecific whereas the second mechanism is very specific and uses the *ATP* hydrolysis as energy plus the chemiosmotic gradient[18]. Over the years microorganisms have developed strategies to tolerate the detrimental effects of high concentrations of metals such as synthesizing cellular components that capture ions by neutralizing its toxicity, using enzymes that are able to reduce metals, and with membrane transporters that expel harmful components out of the microbial cell. Synthesis of nanoparticles by microorganisms is based on the process that develops the metal resistant genes of the microorganism exposed to metals[19].

During this research the microbial consortium cellular machinery was used to reduce the metal cation and form *NP*s. We hypothesized that the *in situ* biosynthesis of *NPs* by the consortium would allow a prompt use of the *NPs* for effective dehalogenation of *PCE.* The microbial consortium, in turn, was grown on core activated carbon particles, that is, they originally formed bioparticles nearly 1.5 to 2 mm diameter. Therefore, the purposes of this research were *(i)* to synthesize active *NPs* using a biological-based method using bioparticles from anaerobic fluidized bed reactors as support and agent, *(ii)* to evaluate the effect of the precursor salt used (either $Fe(NO_3)_3$ or $FeCl_3$) on *NP*s characteristics, and *(iii)* to evaluate the removal/degradation of *PCE* by these *NPs*.

MATERIALS AND METHODS

Bioparticles. The bioparticles were the anaerobic consortium grown on the activated carbon particles that are inside the methanogenic fluidized bed bioreactors (*MFBB*) with an iron filings filter (HFBB) for more details about HFBB checked Breton-Deval *et al.* (2016)[20]. Initially, the MFBB were seeded with digestates from a mesophilic, solid substrate methanogenic anaerobic digester. The characteristics of the initial mesophilic inoculum were pH 7.4 ± 0.06; total volatile organic acids concentration (VOA) 3912 (± 541) mg COD/Kg_{wmr}; 23.14 ± 0.72 %TS; 11.03 ± 0.35 % VS, 0.83 NL CH_4 $(L_r.d)^{-1}$ methane productivity I_{CH4}. A portion of the contents of the seed reactor was loaded to the *HFBB* plus activated carbon to create the bioparticles of ca. 1.5 – 2 mm diameter.

Synthesis of bio nano bioparticles. The synthesis of *NP*s was carried out using the bioparticles[5,21,22]. Two different precursor salts of iron were tested $FeCl_3$ o $Fe(NO_3)_3$ at two different concentrations 0.15 and 0.25 M. That is, the experiment was a 2x2 factorial design. The media were prepared as follows: $((NH_4)_2HPO_4)$ (0.89 mg/L) plus MeOH (3mL/L) as electron donor solution was carefully added to a either $FeCl_3$ or $Fe(NO_3)_3$ salt (0.25 or 0.15 M final concentration in the medium) stirring few minutes; pH was adjusted to a value of 5. This solution was added to serum bottles of 60 mL capacity that were previously loaded with 5 g of bioparticles sampled previously from an anaerobic fluidized bed bioreactor.

Batch PCE degradation. A batch experiment was implemented in order to test two different types of precursor salts, either $FeCl_3$ or $Fe(NO_3)_3$. Serum bottles of 60 mL capacity fitted with Teflon septa were used. The batch units were loaded with 5 g of bioparticles sampled from a HFBB, plus 5 mL/L methanol, and 0.15 or 0.25 M precursor salts, either $FeCl_3$ or $Fe(NO_3)_3$. For the degradation tests, *PCE* (80 mg/L) was added at the end of 3 days of incubation at 28°C. All experiments were performed by triplicate.

Control experiments were carried out to evaluate pollutant removal due to abiotic losses such as evaporation and adsorption. The controls were: *(i)* only bioparticles without metallic salt, *(ii)* the metallic salts without bioparticles, *(iii) PCE* without salts and without bioparticles.

Characterization of nanoparticles. The morphology of bio-nanoparticles was determined by scanning electron microscopy (*SEM*) using a microscope HRSEM-AURIGA 3916 and the chemical composition was measured by energy dispersive spectrum (*EDS*) detector coupled to *SEM*. X-ray diffraction (*XRD*) was performed in order to determine the crystal structure and crystallinity of the Fe/Pd *NPs*. The *XRD* patterns were measured in a Rigaku D/Max B system with a Cu Kα 1 (λ = 1.541 A) radiation source.

Analyses. *PCE* and chlorinated intermediates in the aqueous phase were analyzed by headspace chromatography in Perkin-Elmer chromatograph equipped with a flame ionization detector, Perkin Elmer Elite-624 Series Capillary Columns. Injector and detector temperatures were 200°C and 250°C, respectively. The temperature program

of the column was as follows: start at 40°C, followed by an increase of 6°C/min up to 119°C. Nitrogen was the carrier gas, at 18 psig.

RESULTS AND DISCUSSION

The consortium could synthesize spherical particles with both kind of salts $FeCl_3$ or $Fe(NO_3)_3$. The *XRD* study showed that reflections in the diagram were identified to belong to iron oxide Fe_3O_4 and iron. However, the formation of iron in some samples was also noted. The analysis showed that *NPs* were of magnetite; however, it is difficult to know if fresh particles were different because fresh *NPs* could instantly start to reduce the *PCE*. The *EDS* confirm previous results; spectrum contains peaks of C, O, and Fe. The C signals are attributed mainly to the carbon of the bioparticles. The atomic percentages as obtained by *EDS* quantification were 46.3% C, 24.5 % Fe, 12.5% O. The SEM images show spherical forms between 10 to 60 nm in the treatments with 0.25 M of $FeCl_3$ or $Fe(NO_3)_3$ (**Figure 1a** and **b**). However, the images of the treatments with 0.15 M of of $FeCl_3$ or $Fe(NO_3)_3$ form irregular clusters (**Figure 1c** and **d**).

Most of the research has dealt with the biosynthetisis magnetite nanoparticles using with pure cultures: Bharde *et al.* (2005)[23] biosynthesized (extracelluar) magnetite NPs with an average particle size around 30 nm using *Actinobacter spp.*

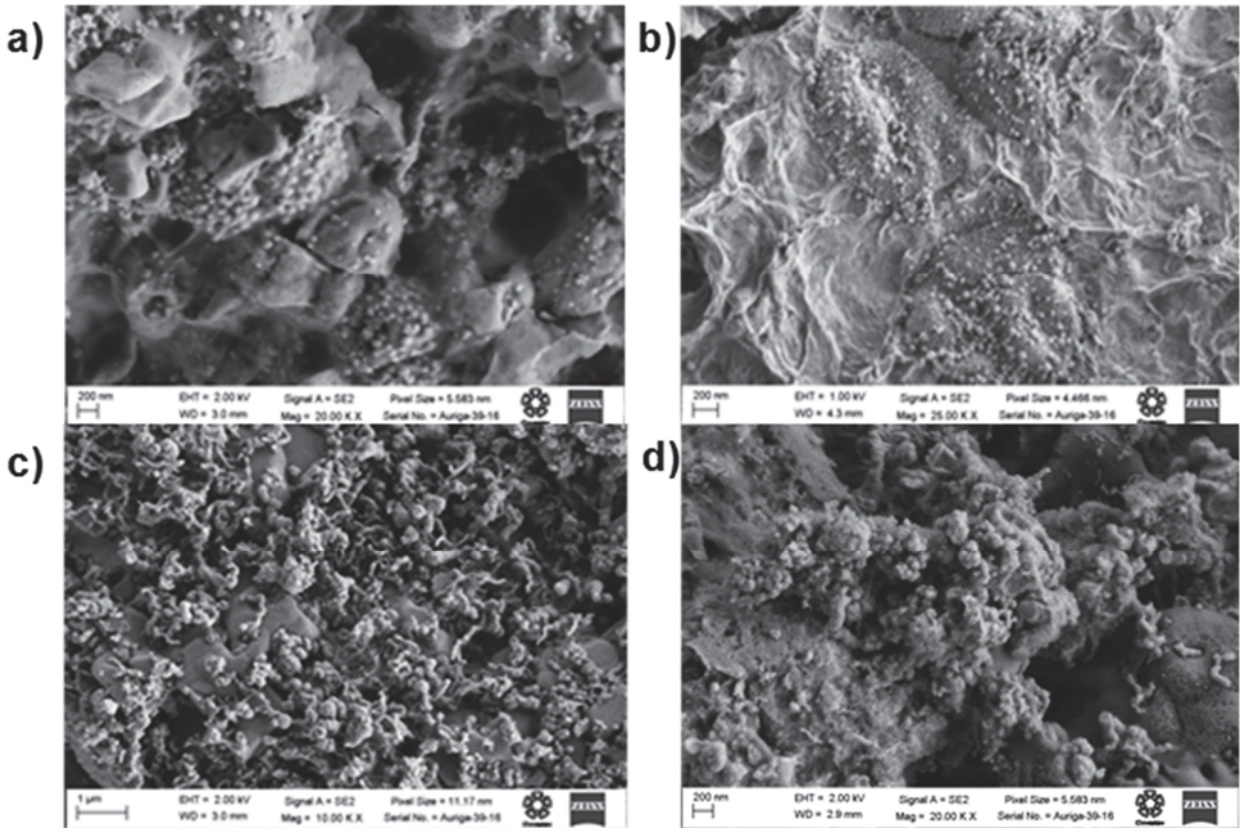


FIGURE 1. Michrograph by scanning electron microscopy where (a) is the view of the surface of bioparticle that used 0.25 M of $FeCl_3$ as precursor salt, (b) used 0.25 M of $Fe(NO_3)_3$, (c) used 0.15 M of $FeCl_3$ and (d) used 0.15 M of $Fe(NO_3)_3$.

Roh *et al.* 2007[25] used *Thermoanaerobacter ethanolicus* and *Shewanella loiha* for extracellular biosynthesis of magnetite NPs with average size of 35 nm for both.

To the best of our knowledge, this is the first time that an anaerobic consortium is used for biosynthesis of NPs that decorated the surface of the bioparticles. This is very important because waters polluted with PCE and alike are not aseptic; these waters carry a microflora that could displace the pure cultures that produce the NPs, thus impairing the success of the whole process. The microbes that grow on the bioparticles subjected to the bioreductive processes are more resistant to microbial contamination as well as other deleterious events that can occur in biological wastewater treatment.

The results revealed that when the precursor salt concentration was 0.15 M, *NP*s formed irregular clusters and not spherical, discrete particles. It is likely that the salt concentration was not sufficient for a sound bacterial attack (reduction), or the *NP*s were too small and some agglomeration occurred. Other researchers have observed a relationship between the concentrations of salt added to the bacteria and the particle size. Gericke and Pinches[24], 2006 found that if the precursor salt ($AuCl_4^-$) was above 500 mgL^{-1} the particle sizes increased and continued increasing when the salt concentration was increased. This is not desirable, since it is known that smaller particles are more reactive with PCE and other pollutants. Furthermore, high concentrations of precursor salts could be toxic to the microbes, either pure strains or microbial consortia. In this regard, it seems that the adequate salt concentration is subjected to a trade-off.

The removal of *PCE* was more efficient in the treatment that used $FeCl_3$ as precursor salt; after 4 days the removal was 99.12 ± 0.44 % (**Figure 2**). The *NPs* biosynthesized with $Fe(NO_3)_3$ removed 93.01 ± 0.16 % of *PCE*. On the other hand, the control units containing bioparticles with the dehalogenating consortium but not *NPs* or precursors salts could remove 38% ± 1.5 and present metabolites as *TCE*, *DCE,* and *VC*. The control units with only precursor salts but no bioparticles removed just 4.58 ± 1.34 % with $Fe(NO_3)_3$ and 8.16 ± 1.84% with $FeCl_3$.

The treatments with a concentration of 0.15 M of precursor salts showed removals of 48 ± 1.8% using $Fe(NO_3)_3$ and 45 ± 0.78% using $FeCl_3$. It is likely that the *PCE* removal of the latter is the synergism of the consortium plus the salt. There have been past efforts to use the bio-nanoparticles for treating chlorinated pollutants: Baxter-Plant *et al.,* 2003 used the sulphate reducing bacteria's *Desulfovibrio desulfuricans* and *Desulfovibrio vulgaris* to synthesize Pd NPs to treat chlorophenol and polychlorinated biphenyl compounds. They found that the Pd nanodecorated cells of *D. desulfuricans* and *D. vulgaris* were more effective treatment to reduce Pd(II) to Pd (0) than chemicals, and most importantly, the reductive dehalogenation of the *COC*s was successful.

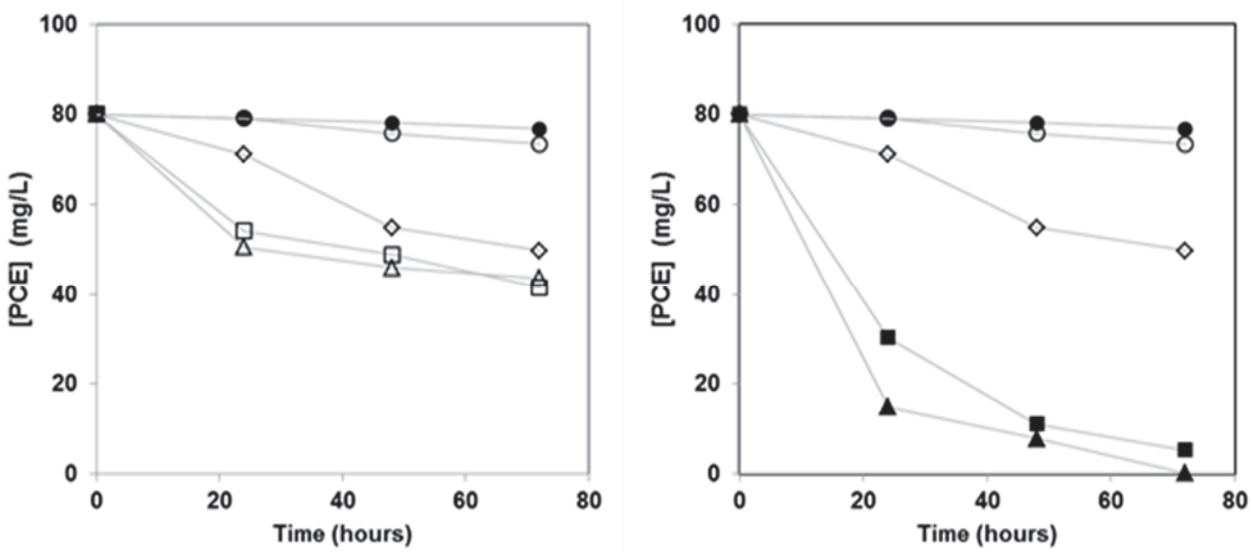


FIGURE 2. Batch degradation of *PCE*. Keys: black circles, control with $FeCl_3$; white circles, control with $Fe(NO_3)_3$; white diamonds, is the treatment with the bioparticles; white squares, is the treatment with bionanobioparticles formed with 0.15 M $Fe(NO_3)_3$ as precursor; white triangles bionanobioparticles formed with 0.15 M $FeCl_3$; black squares is the treatment with bionanobioparticles formed with 0.25 M $Fe(NO_3)_3$ as precursor; white triangles, is the treatment with bionanobioparticles formed with 0.25 M $FeCl_3$ as precursor

CONCLUSION

First, we conclude that the biological synthesis of *NP*s on the surface of bioparticles sampled from anaerobic fluidized bed bioreactors lead to magnetite *NP*s with a high capability for degrading *PCE*.
Second, the bionanobioparticles formed in this way and obtained with the precursor salt $FeCl_3$ exhibited smaller diameter and increased rates and extents of pollutant removal. Abiotic removals were negligible; the high *PCE* removals were mainly effected by the bionanobioparticles. Biological removals (plain bioparticles) were moderate.
Finally, our biosynthesis route for obtaining magnetite *NPs* implies significant savings in chemical reagents (several of them expensive and hazardous) as well as energy compared to typical chemical techniques for *NPs* fabrication.

ACKNOWLEDGMENTS

The authors wish to thank Mr. Alvaro Ángeles Pascual, M. en I., Dr. Daniel Bahena Uribe, Dr. Jorge Roque De La Puente of LANE, CINVESTAV, for excellent technical help and advice on the synthesis and characterization of *NPs*; Mr. Rafael Hernández-Vera for his help with batch tests and lab management; Mr Gustavo Medina for his assistance with the technique of analysis of *PCE* and its metabolites. CONACYT granted a graduate fellowship to LMB-D and an Infrastructure Project 188281 to HMP-V.

REFERENCES

1. Albino J, Nambi I (2009) Effect of biosurfactants on the aqueous solubility of *PCE* and *TCE*. Journal of Environmental Science and Health. 44(14):1565-1573
2. Aschengrau A, Rogers S, Ozonoff D (2003) Perchloroethylene contaminated drinking water and the risk of breast cancer : additional results from Cape Cod, Massachusetts, USA. Environmental Health Perspectives 111 (2): 167-175.
3. EPA (2002) National Primary Drinking Water Standards. Office of Water (4606M); EPA 816-F-03-016; www.epa.gov/safewater.
4. Shin M, Choi H, Kim D, Baek K. (2008). Effect of surfactant on reductive dechlorination of trichloroethylene by zero-valent iron. Desalination 223:299-307.
5. Breton-Deval L, Poggi-Varaldo H.M., Rios-Leal E., Juarez K. (2013) Evaluation of bioreactors performance for pump and treat bioremediation of high concentrations of *PCE*. Chapter C-33 In: Darlington R, Sirabian M (Editors). *Bioremediation and Sustainable Environmental Technologies-2013*. Battelle Press, Columbus. Book in CD-ROM. ISBN 978-0-9819730-7-4
6. Song H, Carraway E, Kim Y (2005) Synthesis of nano-sized iron for reductive dechlorination. Environ. Eng. Res. 10 (4): 174-180
7. Wei J, Xu X, Liu Y (2004) Kinetics and mechanism of dechlorination of chlorophenol by nanoscale Pd/Fe. Chem. Res. Chinese U. 20 (1):71-76.
8. Cross K.M., Lu Y., Zheng T., Zhan J., McPherson G.L., John V.T. (2014). Water decontamination using iron and iron oxide nanoparticles. In: Street, Sustich, Duncan and Savage. *Nanotechnology Applications for Clean Water*, 2nd Edition, Elsevier Inc., New York, USA.
9. Wu L., Ritchie S.M.C. (2006). Removal of trichloroethylene from water by cellulose acetate supported bimetallic Ni/Fe nanoparticles. Chemosphere 63: 285-292.
10. Xiu Z, Jin Z, Li T, Mahendra S, Lowry G, Alvarez P (2010) Effects of nano-scale zero valent iron particles on a mixed culture dechlorinating trichloroethylene. Bioresource Technology 101:1141-1146
11. Zhou L, Thanh TL, Gong J, Kim JH, Kim EJ, Chang YS (2014). Carboxymethyl cellulose coating decreases toxicity and oxidizing capacity of nanoscale zerovalent iron. Chemosphere 104: 155-161.
12. Phenrat, T., Saleh N., Sirk K., Tilton RD., Lowry GV. (2007). Aggregation and sedimentation of aqueous nanoscale zerovalent iron dispersions. Enviromental Science and Technology. 41: 284-290.
13. Hennebel T. De Corte S., Verstraete W., Boon N. (2012). Microbial production and environmental applications of Pd nanoparticles for treatment of halogenated compounds. Current Opinion in Biotechnology 23:555-561.
14. Hulkoti N.I., Taranath T.C. (2014). Biosynthesis of nanoparticles using microbes – A review. Colloids and Surfaces B: Biointerfaces 121:474-483.
15. Suarez P., Reyes R. (2002). La incorporacon de metales pesados en las bacterias y su importancia para el ambiente. Interciencia 27(4):160-4
16. Gonzales A.G., Pokrovsky O.S., Jimenez-Villacorta F., Shirokova L.S., Santana-Casiano J.M., Gonzalez-Davila M., Emnova E.E. (2014) Chemical Geology 372:32-45.
17. Marrero-Coto J., Diaz-Valdivia A., Coto-Perez O. (2010). Mecanismos moleculares de resistencia a metales pesados en las bacterias y sus aplicaciones en la biorremediación. Revista CENICA Ciencias Biologicas 41(1):67-78.
18. Eisele T.C. Gabby K.L (2014). Review of reductive leaching of iron by anaerobic bacteria. Mineral processing & extractive metal 35:75-104.

19. Kaushik N., Thakkar M.S., Snehit S., Mhatre M.S. Rasesh Y., Parikh M.S. (2010) Biological synthesis of metallic nanoparticles. Nanomedicine: Nanotechnology, Biology and Medicine 6:257-262.
20. Breton-Deval L. Solorza-Feria O., Rios-Leal E., Poggi-Varaldo H.M. (2016). Dechlorination of *PCE* with nanoscale particles of zero valent iron and palladium. In: R.R. Sirabian and R. Darlington. Bioremediation and Sustainable Environmental Technologies-2013. Battelle Press, Columbus, OH, USA. ISBN 978-0-9819730-7-4.
21. Herrera-Lopez D, García-Mena J, Poggi-Varaldo HM. (2007). The addition of zero-valent iron to batch bioreactors with simultaneous electron acceptors: influence on removal of high concentrations of perchloroethylene. In: Gavaskar AR, Silver CF (Editors). *In Situ and On-Site Bioremediation-2007,* Battelle Press, Columbus, OH, ISBN 978-1-57477-161-9.
22. Moreno-Medina C, Bretón-Deval L, Ríos-Leal E, Barrera-Cortés, Rinderknecht-Seijas N, Poggi-Varaldo HM. (2011). Incremento de la solubilización de percloroetileno con un tensoactivo no iónico. Interciencia 36:224-228.
23. Bharde A., Wani A., Shouche Y., Pattayil A., Bhagavatula L., Sastry M. (2005) Bacterial aerobic synthesis of nanocrystalline magnetite Journal of the American Chemical Society:9326-7
24. Gericke, M., Pinches A. (2006). Biological synthesis of metal nanoparticles. Hydrometallurgy 83, 132-140.
25. Roh, Y., Jang, H.D., Suh, Y. (2007) Microbial synthesis of magnetite and Mn-substituted magnetite nanoparticles: influence of bacteria and incubation temperature. J. Nanosci. Nanotechnol 7, 3938-3943

CHAPTER 12.3 HYBRID MATERIAL FROM NALIDIXIC ACID IONS AND ZnAl LAYERED DOUBLE HYDROXIDE USED AS ECOLOGICAL PESTICIDE

E. Morales-Irigoyen *(1); Y. Gómez y Gómez (1); J. L. Flores-Moreno (2) and M. O. Franco-Hernández (1)

(1) Instituto Politécnico Nacional, Unidad Profesional Interdisciplinaria UPIBI-IPN, Avenida Acueducto s/n, Col. Ticomán, C.P. 07340, Ciudad de México, México.
(2) Universidad Autónoma Metropolitana, Avenida San Pablo 180, Colonia Reynosa Tamaulipas C.P. 02200, Ciudad de México, México.

ABSTRACT

A reconstruction method was used to prepare a ZnAl-NAD composite from ZnAl-NO_3 layered double hydroxide (LDH) as inorganic matrix (IM) and nalidixic acid (NAD) ions as biologically active molecule (BAM). The X-ray and FTIR results confirmed that the intercalation of NAD anions into the interlplanar space of inorganic layered matrix. However, this nanohybrid contains NAD ions and mixed oxides ZnAl (O), which were not exchanged. Antibacterial properties were evaluated against *Escherichia coli* and *Pectobacterium carotovorum* strains by disk diffusion method. ZnAl-NO_3 matrix resulted to be inactive against two bacteria, in contrast to NAD sodium salt (pure drug), which generated inhibition halos significantly larger than generated by ZnAl-NAD. These results clearly indicated that a biocide effect was caused by NAD ions. For this, nanohybrid ZnAl-NAD was an ecological alternative to chemical agents used commonly.

Keywords: Hybrid-material, layered-double-hydroxide, nalidixic-acid, pesticide.

INTRODUCTION

Phytopathogens as *Pectobacterium carotovorum* that induces soft rot disease in several crops as potatoes, lettuce, tomatoes and carrots, not only causes post-harvest economic losses also causes an agressive agricultural practices arising from the need to control this and other plant diseases. The dangerous agricultural practices are based on the use of higly toxic chemical agents and pesticides synthesised form large spectrum antibiotics solutions administered in excessive and inappropriate doses resulting in negative effects such as pathogens resistance and damages in human health and environment.

In this sense, and accord to sustainable agriculture, many efforts have been aiming to development new materials that reduce the enviromental negative impact. For this, a synthesis of hybrid materials based on association or intercalation of biologically active molecules (drugs or antibiotics with a particular biocide action) into layered double

---

*Author for correspondence: erikairigoyen@hotmail.com

hydroxides (LDH) or hydrotalcite like compounds represented by the formula $[M^{2+}_{1-x}M^{3+}_{x}(OH)_2]A^{n-}_{\frac{x}{n}} \cdot mH_2O$[1] is a promising alternative.

Intercalation process into a matrix is an option to protect these biologically active molecules sensible to thermal degradation and hydrolysis process. The matrix-antibiotic complex might reduce the probability for leaching, induced by irrigation or rain, due to the matrix water insolubility.

In addition, this complex it functions as a controlled release system increasing the selectivity of bioactive compound and minimizing the final concentration of antibiotic applied on soil and crops.

By the above, an ecological agriculture practice could be possible using nanohybrid composite as pesticide friendly with environment. Therefore, the objective of this work was to evaluate nanohybrid material ZnAl-NAD synthesized from layered double hidroxide (LDH) as supports of biologically active molecules like nalidixic acid (NAD), to be used as alternative of toxic pesticides commonly used against phytopathogenic strain *Pectobacterium carotovorum*.

MATERIALS AND METHODS

Biological material. Two Gram (-) strains were used, a phytopathogenic strain *Pectobacterium carotovorum* and *Escherichia coli* as control. Strains were supplied by UPIBI-IPN and ENCB-IPN, respectively.

Synthesis of hybrid material. The pristine inorganic matrix ZnAl-NO_3 layered double hydroxide (LDH) was synthetized by the urea hydrolysis method[2].

The hybrid material ZnAl-NAD was prepared by reconstruction taking advantage of the memory effect property, using a previously LDH calcined at 500 °C mixed with NAD sodium salt solution during 7 days at 25°C and argon atmosphere to avoid reconstruction carbonate anions in the interlplanar space.

Material characterization. Infrared spectroscopy (FTIR) analyses, in the 4000 - 400 cm $^{-1}$ region, were performed in Perkin-Elmer® GX spectrometer.

The X-ray patterns are collected with Rigaku® diffractometer using CuKα source (λ=1.542 A) at 40 KV, 35 mA and scan range 2°- 80° (2θ) degrees.

Antibacterial activity. Antibacterial activity was determined by a disk diffusion method[3], using sterile disks (6 mm of diameter) impregnated at 0.025 μg_{solid}/disk as final concentration of inorganic matrix suspension, BAM (acid nalidixic in a sodium salt) or nanohybrid suspension.

Statistical analysis. Data of inhibition zone reported in mm were analyzed by analysis of variance (ANOVA) and Duncan's tests ($p \leq 0.05$) using a software SAS® system version 9.0[(4)].

RESULTS AND DISCUSSION

Material characterization. The FTIR spectrum for inorganic matrix is shown in **Figure 1a**. A band centered at 3438 cm^{-1} attributable of the OH^- groups of water hosted in the interlaminar region and exhibited an intense band at 1381 cm^{-1} attributable to NO_3^- asymmetrical stretching vibration.

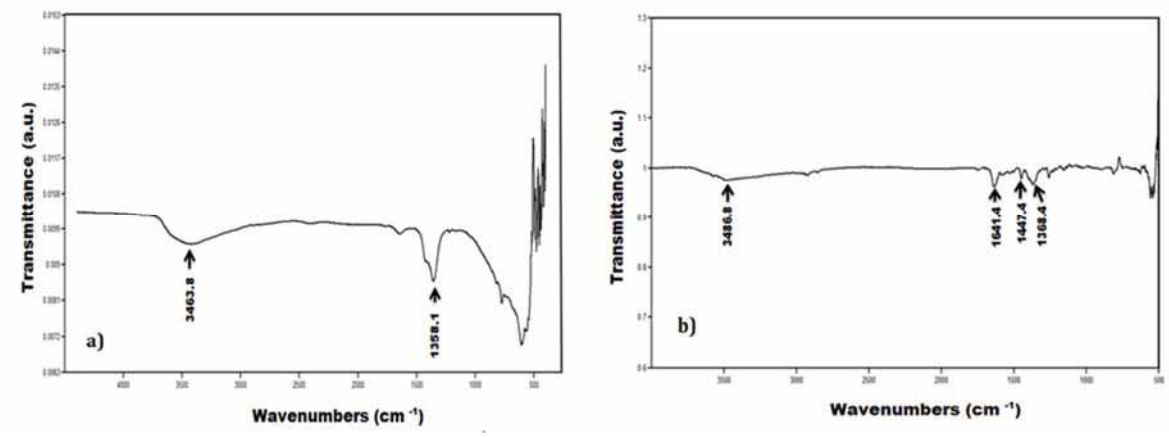


FIGURE 1. (a) FTIR spectrum of the inorganic matrix; (b) FTIR spectrum of the nanohybrid

In **Figure 1b**, the nanohybrid spectrum show two bands at 1638.2 cm^{-1} and 1447.44 cm^{-1} corresponding to asymmetrical and symmetrical stretching vibrations of the C=O group of the aromatic rings, respectively; while the band at 1368.4 cm^{-1} was assigned to the symmetric stretch of the $–COO^-$ group[5-7].

X-ray diffraction pattern of inorganic matrix is shown in **Figure 2**. In the inorganic matrix diffraction pattern, the characteristic diffraction of peaks corresponding a typical of layered double hydroxides at 9.96 (2θ) were observed, confirming the presence of nitrate ion into the interlplanar space, before the intercalation process.

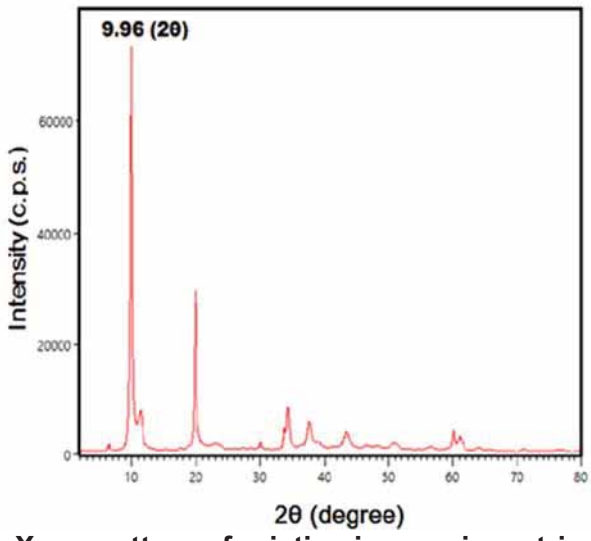


FIGURE 2. X-ray pattern of pristine inorganic matrix with NO_3^- ions

In the **Figure 3** was observed the X-ray pattern corresponded to nanohybrid material. The inorganic matrix (IM) recovered the original layered structure after intercalation process (memory effect property) but with NAD ions in the interlayer space instead of the initial nitrate ions. However, a partial intercalation was observed due the presence of diffraction peaks at 31.83, 34.47 and 36.44 ° (2θ) attributable with mixed oxides ZnAl (O).

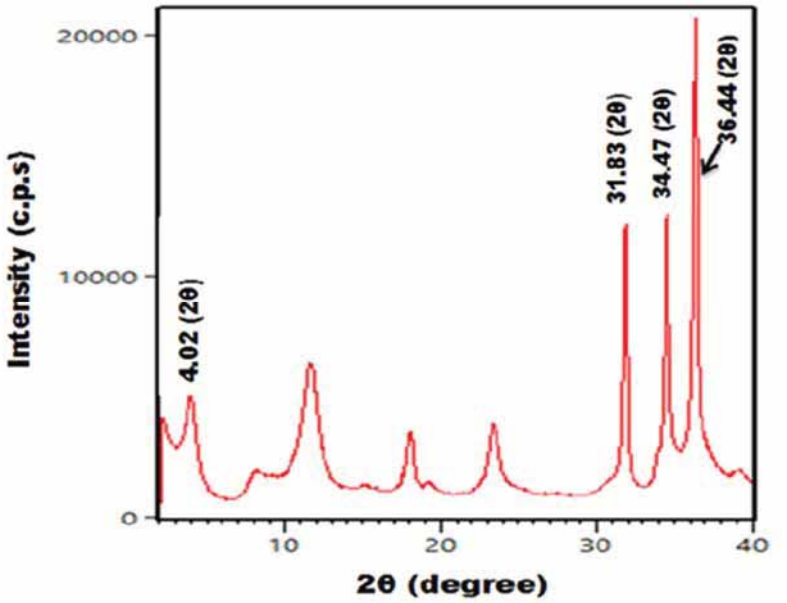


FIGURE 3. X-ray pattern of nanohybrid material

The initial d-spacing value (d_{003}) of inorganic matrix with initial nitrate ion was 8.88 Å (2θ= 9.96°) and after intercalation of the nalidixic acid anions this d_{003} spacing increased to 21.93 Å (2θ = 4.02°). This shifting to angles smaller is attributable to the presence of the molecules larger (nalidixic acid) than initial molecule (nitrate ions) in the interlplanar space, indicating that a successful intercalation of NAD ions into an inorganic matrix.

Antibacterial activity. In the **Table 1**, the inhibition zone (IZ) generated by inorganic matrix (IM), biologically active molecule (BAM) and nanohybrid (NH) was shown. Inorganic matrix was inactive against two strains; this biocide effect was attributable to nalidixic acid ions since the inorganic matrix was inactive. This indicated effective release of NAD ions from inorganic matrix. The pure NAD (pure antibiotic) generated inhibition zones significantly larger than nanohybrid, this for two strains. However, the intercalation of BAM into inorganic matrixes to generated new materials as ZnAl-NAD complex is an alternative to protect the BAM against degradation process as thermal decomposition. Other advantage is the protection of NAD (water soluble) to leaching due to insolubility of inorganic matrix conferring protection to rain and/or irrigation.

Table 1. Inhibition zone (IZ) generated by inorganic matrix (IM), biologically active molecule (BAM) and nanohybrid (NH)

	Inhibition zone (mm)		
STRAIN	**IM**	**BAM**	**NH**
Escherichia coli	0^{c}	34.5 ± 1.0^{a}	21.0 ± 0.1^{b}
P. carotovorum	0^{c}	38.0 ± 0.8^{a}	26.2 ± 0.5^{b}

Results are presented as diameter inhibition zone in mm ± standard deviation (n=4).
0 indicates no inhibition zone.
^{a,b,c} IZ (mm) with same letter in the same row are not significantly different by strain (Duncan, $p \leq 0.05$, n = 4).

CONCLUSION

The synthesis of ZnAl-NAD using an inorganic matrix hosting a NAD as biologically active molecule was successful.
These results indicated that the biocide effect was caused by NAD ions from ZnAl-NAD complex, due to inorganic matrix was inactive.
Nanohybrid ZnAl-NAD was an ecological alternative to chemical agents used commonly.

ACKNOWLEDGMENTS

Special thanks to Secretaría de Investigación y Posgrado from Instituto Politécnico Nacional (SIP-IPN) for projects support 20140278, 20150288 and 20160123 codes. Thanks to Centro de Nanociencias y Micro y Nanotecnologías from Instituto Politécnico Nacional (CNMM-IPN) for technical support. E. E. M-I received grant-aided support from Consejo Nacional de Ciencia y Tecnología (CONACyT), México.

REFERENCES

1. S. Miyata, “Physico-Chemical Properties of Synthetic Hydrotalcites in Relation to Composition,” Clays Clay Miner., vol. 28, no. 1, pp. 50–56, 1980.
2. A. Inayat, M. Klumpp, and W. Schwieger, “The urea method for the direct synthesis of ZnAl layered double hydroxides with nitrate as the interlayer anion,” Appl. Clay Sci., vol. 51, no. 4, pp. 452–459, Mar. 2011.
3. S. J. T. M. Bauer AW, Kirby WM, “Antibiotic susceptibility testing by a standardized single disk method,” Am J Clin Pathol, vol. 45, no. 4, pp. 493–6, 1966.
4. U. SAS Institute Inc., Cary, NC, “Software Version 9.00 (TS M0),” 2009.
5. N. B. Behrens, G. M. Diaz, and D. M. L. Goodgame, “Metal complexes of the antibiotic nalidixic acid,” Inorganica Chim. Acta, vol. 125, no. 1, pp. 21–26, Sep. 1986.
6. S. Gunasekaran, R. K. Natarajan, R. Rathikha, and D. Syamala, “Vibrational spectra and normal coordinate analysis of nalidixic acid,” vol. 43, no. July, pp. 503–508, 2005.
7. U. Neugebauer, A. Szeghalmi, M. Schmitt, W. Kiefer, J. Popp, and U. Holzgrabe, “Vibrational spectroscopic characterization of fluoroquinolones.,” Spectrochim. Acta. A. Mol. Biomol. Spectrosc., vol. 61, no. 7, pp. 1505–17, May 2005

CHAPTER 12.4 EFECTIVIDAD DE LAS MICRO/NANOPARTÍCULAS DE QUITOSANO OBTENIDAS DE RESIDUOS PESQUEROS EN LA ADSORCIÓN DE CROMO HEXAVALENTE

J. B. Dima (1,2) and **N. Zaritzky ***(1,3)

(1) Centro de Investigación y Desarrollo en Criotecnología de Alimentos (CIDCA -CONICET- UNLP). Calle 47 y 116 La Plata (1900) Argentina
(2) Centro Nacional Patagónico (CECIMAR- CENPAT -CONICET). Puerto Madryn, Chubut, Argentina
(3) Depto de Ingeniería Química, Facultad de Ingeniería. Universidad Nacional de La Plata. Argentina

RESUMEN

El procesamiento de crustáceos en la ciudad de Puerto Madryn genera residuos sólidos, exoesqueletos, que son descartados en basurales constituyendo un contaminante ambiental para la región. El quitosano (QS) es un polisacárido lineal que se obtiene por desacetilación parcial de la quitina, componente principal de estos exoesqueletos. Por sus propiedades funcionales y fisicoquímicas, el quitosano presenta aplicaciones muy variadas, entre ellas la capacidad de adsorber metales. En una primera etapa se obtuvo quitina a partir de desechos de exoesqueletos de langostinos los cuales fueron despigmentados, descalcificados y desproteinizados. Para la obtención de quitosano, la quitina fue desacetilada con NaOH al 50%, determinándose su peso molecular y el grado de desacetilación (método potenciométrico y FTIR). El rendimiento en quitina fue de 24.1%; el grado de desacetilación del quitosano obtenido fue del 90.2% y su peso molecular de $2x10^5$Da. Debido a la baja estabilidad del quitosano a bajos pH, se sintetizaron micro/nano partículas de quitosano (MQS) por gelificación iónica utilizando tripolifosfato de sodio como agente reticulante. Se determinó el efecto de las concentraciones relativas de los reactivos empleados en el potencial Z y en el tamaño de las partículas. Para una relación de QS-TPP de 1,25mg/ml y 1,50mg/ml se observaron tamaños de partículas menores a 140nm.
Las partículas de quitosano y las micro/nanopartículas se aplicaron para la remoción de Cr(VI), altamente tóxico y cancerígeno. La concentración de cromo total se determinó por espectroscopía de absorción atómica. Se obtuvieron experimentalmente las isotermas de adsorción de Cr(VI) en QS y MQS y las cinéticas correspondientes. Se analizaron los efectos del pH, el tiempo de contacto. Además, se determinó el estado de oxidación del metal adsorbido. Tanto QS como MQS mostraron una buena eficiencia en la adsorción de Cr (VI), la cual varió significativamente en función del pH del medio; el equilibrio se alcanzó después de1h de contacto para el QS y 3h para las MQS. Al igual que en la adsorción, el porcentaje de desorción vario con el pH del medio y el tiempo de contacto; el mismo fue mayor para QS que para MQS, sin embargo, los análisis de oxidación mostraron que el 66% cromo desorbido por las MQS fue cromo trivalente. El quitosano y las micropartículas de quitosano fueron efectivas para la remoción del C(VI), las MQS mejoraron la adsorción del metal a bajos pH y

---

*Author for correspondence: zaritzkynoemi@gmail.com

disminuyeron el grado de toxicidad del mismo. El aprovechamiento de los desechos de exoesqueletos de crustáceos patagónicos constituye un tema importante en la revalorización económica de residuos para la región. Por otro lado, el desarrollo de nuevos sistemas permitirá realizar aportes originales en la obtención de productos que contribuyan al desarrollo de tecnologías ligadas al medio ambiente.

Palabras claves: micro/nanopartículas de quitosano, remoción Cr (VI), residuos pesqueros

INTRODUCCIÓN

Los desembarcos de crustáceos en Argentina representan varios miles de toneladas anuales siendo la ciudad de Puerto Madryn (Patagonia-Argentina) uno de los principales puertos de desembarco[1]. La mayor captura corresponde a langostinos, seguido por centolla, camarón y cangrejos. Durante su procesamiento, para el aprovechamiento del músculo comestible, se generan residuos sólidos de difícil disposición (exoesqueletos), que se acumulan en basurales constituyendo un contaminante ambiental. El exosqueleto descartado depende de la especie; en la industrialización de la carne del langostino, éste representa entre un 35% y 50% de su peso total. Esta biomasa desechable tiene una composición rica en quitina, de la que se obtienen derivados de gran interés como el quitosano, polisacárido catiónico natural, biodegradable y biocompatible de variadas aplicaciones industriales. El quitosano (QS) puede prepararse en escamas, en polvo, disuelto en líquido o formando micropartículas (MQS), en función de su utilización. En los últimos años las MQS están siendo investigadas en diferentes áreas científico-tecnológicas: como portadoras de agroquímicos, fármacos, etc[2,3], como agente antibacteriano[4] o como adsorbente de metales[5], etc.

Los metales pueden provenir de efluentes urbanos o industriales. El uso de cromato y dicromato tiene muchas aplicaciones industriales, tales como la industria textil, la galvanoplastia, curtido de cuero, pinturas, pigmentos y metalurgia[6]. El Cr(VI) es un metal tóxico para los seres humanos, ya que es cancerígeno y se debe remover de las aguas residuales antes de ser descargadas. En Argentina las normas de descarga de aguas residuales establecen un límite máximo permisible de 0,2mg/L en los cursos de agua superficiales. El proceso de adsorción es considerado una de las técnicas más adecuadas para su eliminación, debido a sus ventajas como la alta eficiencia y menor costo[7]. Es así, que se ha estudiado la adsorción en biopolímeros entre los que se encuentra el quitosano, que se obtiene del residuo generado por la industria procesadora de crustáceos. El mismo ha demostrado remover eficazmente metales como cobre, mercurio y plomo, entre otros. Sin embargo, el QS resulta inestable a bajos pH[5]; las modificaciones químicas son adecuadas para evitar su disolución en medios ácidos; de esta manera, las cadenas de quitosano pueden ser químicamente reticuladas con tripolisfosfato de sodio (TPP) y conducir amatricesestables[8].

El objetivo del presente trabajo fue: a) desarrollar micropartículas de quitosano, utilizando la técnica de gelificación iónica, a partir del quitosano extraído de residuos de exosqueletos de langostinos y caracterizarlo fisicoquímicamente; b) determinar el

tamaño y distribución de las partículas obtenidas; c) evaluar la eficacia de las MQS en la adsorción de Cr(VI).

MATERIALES Y MÉTODOS

Obtención y caracterización de quitosano de exoesqueleto de langostino. Se recolectaron exoesqueletos de las plantas elaboradoras de langostino patagónico (*P.mulleri*) en Puerto Madryn (Chubut, Argentina). Los mismos se secaron y molieron, luego se descalcificaron con HCl 1,5M y por último, se desproteinizaron con NaOH al 4,5%. El producto obtenido se lavó con abundante agua destilada, se secó en estufa por 24h obteniéndose quitina. Posteriormente, la quitina fue tratada con NaOH al 50% a 120ºC, luego filtrada y lavada con abundante agua destilada, se secó en estufa por 24h y se obtuvo quitosano (QS)[9].El QS obtenido se caracterizó según su grado de desacetilación y peso molecular viscosimétrico. El grado de desacetilación se determinó por valoración potenciométrica utilizando la técnica original descripta por Broussignac[10] y por espectroscopía infrarroja (FTIR)(Equipo Bruker IFS 66); en este último se usó el método de correlación propuesto por Brugnerotto et al[11] de acuerdo a la ecuación 1:

$$DD(\%) = 100-[31,92*(A(1320cm^{-1})/A(1420cm^{-1})) -12,20] \quad (1)$$

donde $A(1320cm^{-1})$ y $A(1420cm^{-1})$ son las absorbancias de los picos del espectro IR.

La evaluación del peso molecular viscosimétrico (Mv) del QS se llevó a cabo mediante la técnica de viscosimetría capilar utilizando un viscosímetro de Ostwald y la ecuación de Mark-Houwink-Kuhn-Sakurada (MHKS) donde [η] es la viscosidad intrínseca y k, a parámetros de la ecuación.

$$[\eta] = k\, Mv^{a} \quad (2)$$

Producción de micro/nanopartículas de quitosano reticuladas con tripolifosfato. Debido a la toxicidad del glutaraldehído y otras moléculas orgánicas utilizadas en la síntesis de geles con uniones covalentes, se propuso la utilización de la técnica de gelificación iónica que utiliza TPP como agente reticulante. Las MQS se prepararon tomando como base el procedimiento reportado por Calvo et al[8]. En primer lugar, se realizaron diversas pruebas con el fin de obtener el tamaño deseado de las partículas en suspensión, variando la concentración y volúmenes relativos de las soluciones de QS y TPP bajo agitación magnética constante y a temperatura ambiente. Las micropartículas se recolectaron por centrifugación a 10000rpm durante 20m. El tamaño de la partícula se determinó por espectroscopía de correlación de fotones utilizando un equipo Delsa™NanoC Instrument (BeckmanCoulter) y por observación en un microscopio electrónico de barrido (SEM) Philips X-L 30.

Aplicación de QS y MQS en la remoción de cromo hexavalente. Se estudió la capacidad de adsorción del QS y las MQS para eliminar el Cr(VI) de aguas residuales. Los experimentos de adsorción se realizaron bajo diferentes condiciones de: concentración inicial de Cr(VI) (50 a 400mg/L), tiempos de contacto (30min, 1h, 2h, 3h),

y pH (2-6). Los experimentos de adsorción se llevaron a cabo utilizando 80mg de QS y 40mg de MQS en 50ml de volumen de Cr(VI).Los experimentos se llevaron a cabo en ensayos batch a 25ºC, bajo agitación constante. Las concentraciones finales deCr(VI) se determinaron por espectrometría de absorción atómica de llama (Instrumental Laboratorio IL457). La capacidad de adsorción de Cr(VI) en condiciones de equilibrio se calculó según la siguiente ecuación:

$$Qe = \frac{(Ci - Ceq)}{w} V \qquad (3)$$

donde: Qe(mg/g) es la cantidad de iones metálicos adsorbidos, Ci y Ceq son las concentraciones de metal(mg/l) en la solución a tiempo cero y después del equilibrio, V(L) es el volumen de la solución y w es la masa(g) del adsorbente.

Para la descripción matemática de las relaciones de equilibrio de los iones de Cr(VI)en QS y MQS se utilizaron las isotermas de Langmuir, Freundlich y Temkin. Los análisis cinéticos se determinaron usando los modelos de pseudo primer y segundo orden y la ecuación de Elovich. Los parámetros de operación fueron: T=25°C, pH=4 y pH=2, tiempo=3h.

Estudios de desorción para determinar el estado de oxidación de las especies de cromo adsorbido. Con el fin de determinar el estado de oxidación de los iones de cromo adsorbidos en QS y MQS se llevaron a cabo experimentos de desorción a temperatura ambiente según lo propuesto por Baneshwari et al[12]. La concentración de Cr(VI)resultante en la solución desorbentese determinó mediante análisis espectrofotométrico por la reacción del Cr(VI) con 1,5-difenilcarbazida en solución fuertemente ácida[13]. El complejo coloreado se midió a 540 nm usando un espectrofotómetro Hewlett-Packard HP 8452a. La concentración de Cr(III) se calculó a partir de la diferencia entre las concentraciones de Cr(VI) y Cr total. Para determinar la concentración total de Cr [Cr (III) + Cr (VI)], la solución de desorción se oxidó primero a Cr(VI) con persulfato de amonio 98%, en condición ácida a 100°C, utilizando $AgNO_3$ como catalizador. Las concentraciones totales de cromo también se determinaron por espectroscopia de absorción atómica de llama para verificar los resultados.

RESULTADOS Y DISCUSIÓN

Caracterización del quitosano obtenido. El rendimiento y propiedades del quitosano varían de acuerdo a la materia prima (exoesqueleto de origen) y al tratamiento empleado para su obtención. El rendimiento en quitina en función del peso del material triturado fue de 24,9%. El quitosano representó el 76,8% de la quitina inicial. El grado de desacetilación fue de 90,2% (por la técnica potenciométrica) y de 88,6% (por FTIR) (**Figura 1**). El peso molecular viscosimétrico se determinó a partir de la Ec. (2) de MKHS utilizando los parámetros hallados por Rinaudo[14]; K=0,074 y a=0,80 donde Mv resultó de $2,39x10^5$ Da.

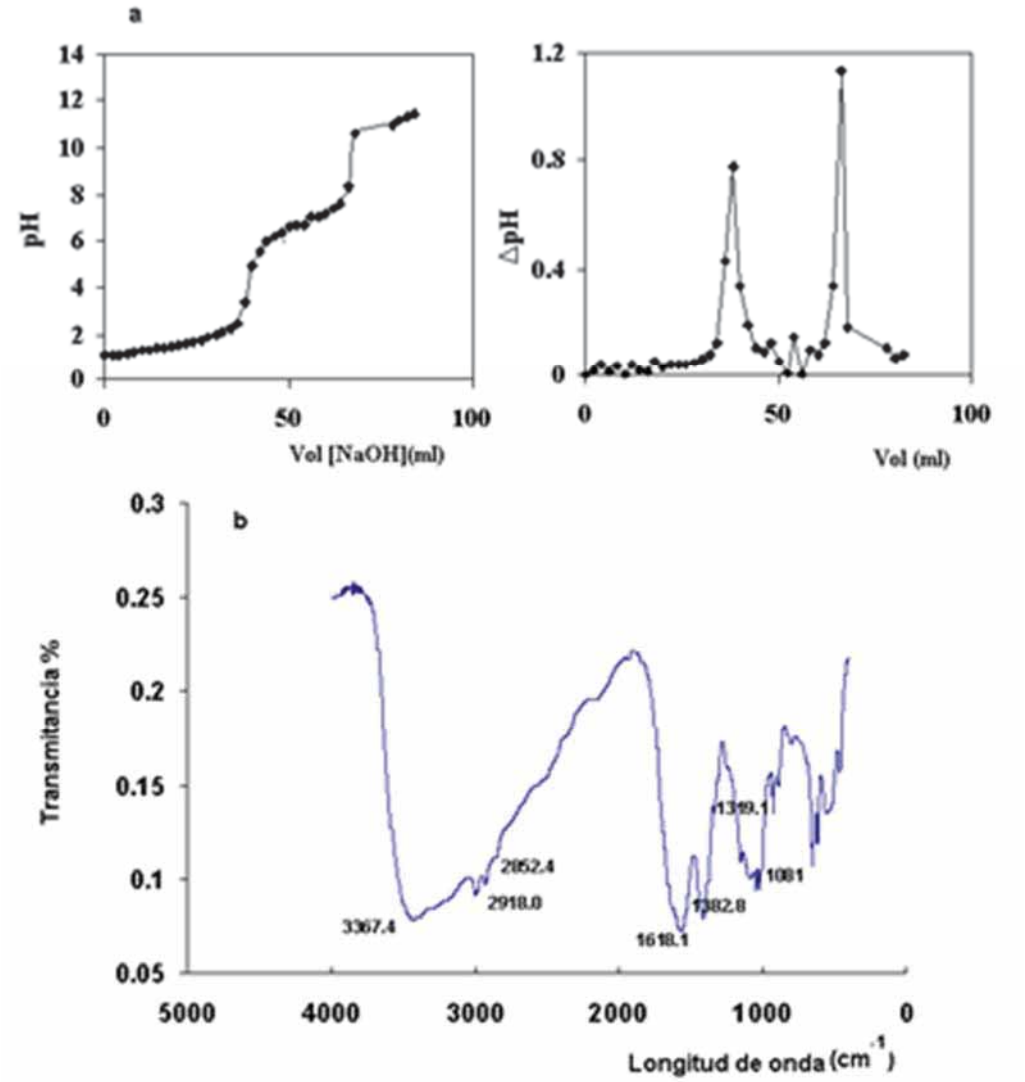


FIGURA 1. Determinación del grado de desacetilación del quitosano obtenido por: a) técnica potenciométrica b) FTIR

Resultados de la obtención y caracterización de las MQS reticuladas con TPP. Se identificaron visualmente cuatro sistemas diferentes: solución clara, suspensión opalescente clara, suspensión opalescente y agregados. Las suspensiones opalescentes corresponden a la presencia de micropartículas (**Figura 2**). Las MQS se formaron espontáneamente, en una suspensión estable, tras la incorporación de una solución de TPP de concentración 1-1.5g/L a una solución ácida 1.25g/L de QS, en proporción volumétrica 1:3

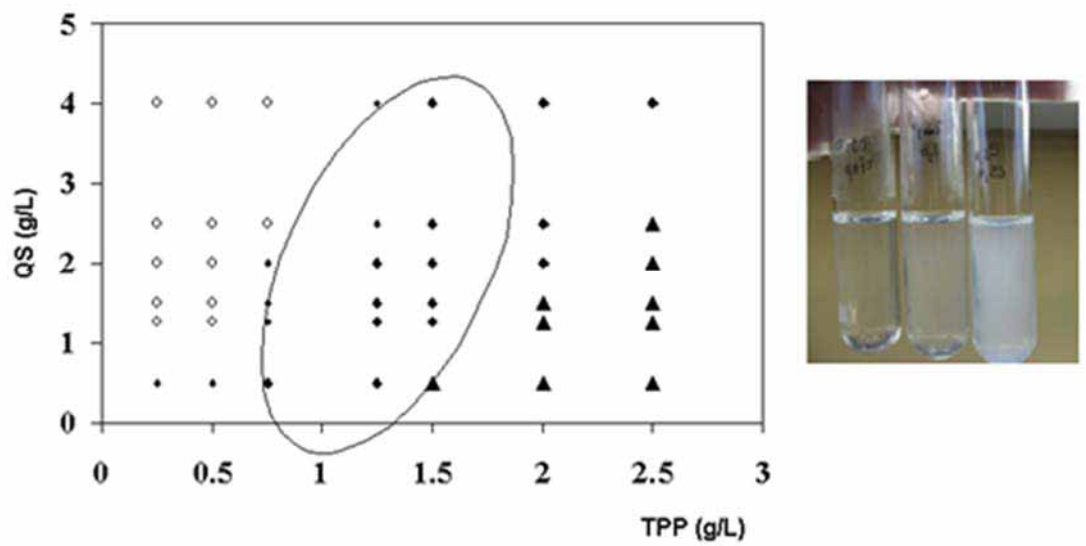


FIGURA 2. (◇) Solución clara, (•) Solución levemente opalescente, (◆) Solución opalescente y (▲) Agregados

El tamaño medio de las MQS obtenidas para ese rango de concentraciones relativas fue de 101nm (P_{10}=88nm; P_{90}=145nm) y con una distribución de tamaño estrecha (polidispersidad<1). El tamaño de las MQS determinado por el equipo Coulter Beckman (**Figura 3a**) coincidió con el observado por microscopía SEM (**Figura 3b**) encontrándose en el rango de las nanopartículas[15].

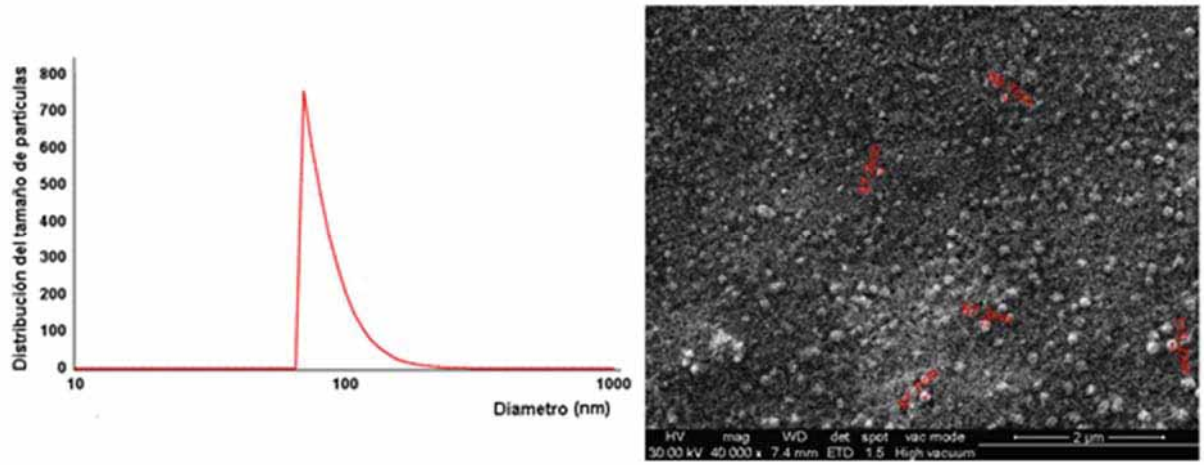


FIGURA 3. Distribución del tamaño de las micropartículas de quitosano y micrografía SEM para una relación QS-TPP 1.25-1.5g/L, pH=4

La potencial zeta (PZ) la distribución y tamaño de partícula en función de la concentración de TPP añadido, se observa en la **Figura 4**. En la **Figura 4c**, la línea llena representa el PZ para QS en AcH (0,125%) versus el agregado de diferentes concentraciones de TPP. Por otro lado, la línea punteada muestra el PZ de las partículas obtenidas con diferentes concentraciones de TPP, centrifugadas y re-suspendidas en agua, para eliminar exceso de QS o TPP que pudiera tener la

suspensión original. La potencial zeta de las MQS disminuyó con la cantidad de TPP añadido. Cuando el TPP aniónico se utiliza como agente reticulante del QS con carga positiva, el PZ de las MQS dispersas en solución acuosa disminuye. Por lo tanto, cuanto menor es la fracción de TPP presente en las partículas mayor es el PZ[16]. La interacción entre el TPP y el QS da lugar a partículas cuyo comportamiento electrocinético puede modularse tanto a través de las condiciones propias de la formación de las MQS (como el agregado de TPP) como modificando las condiciones del medio de síntesis (presencia o ausencia de ácido o QS en exceso). Es importante notar que el proceso de lavado de las MQS es esencial a la hora de diseñar un sistema para aplicaciones basadas en estas partículas. Por ejemplo, si se pretende utilizar a las MQS como adsorbentes de contaminantes, las especies remanentes de la síntesis deben eliminarse cuidadosamente previo a la preparación de sistemas batch o columnas.

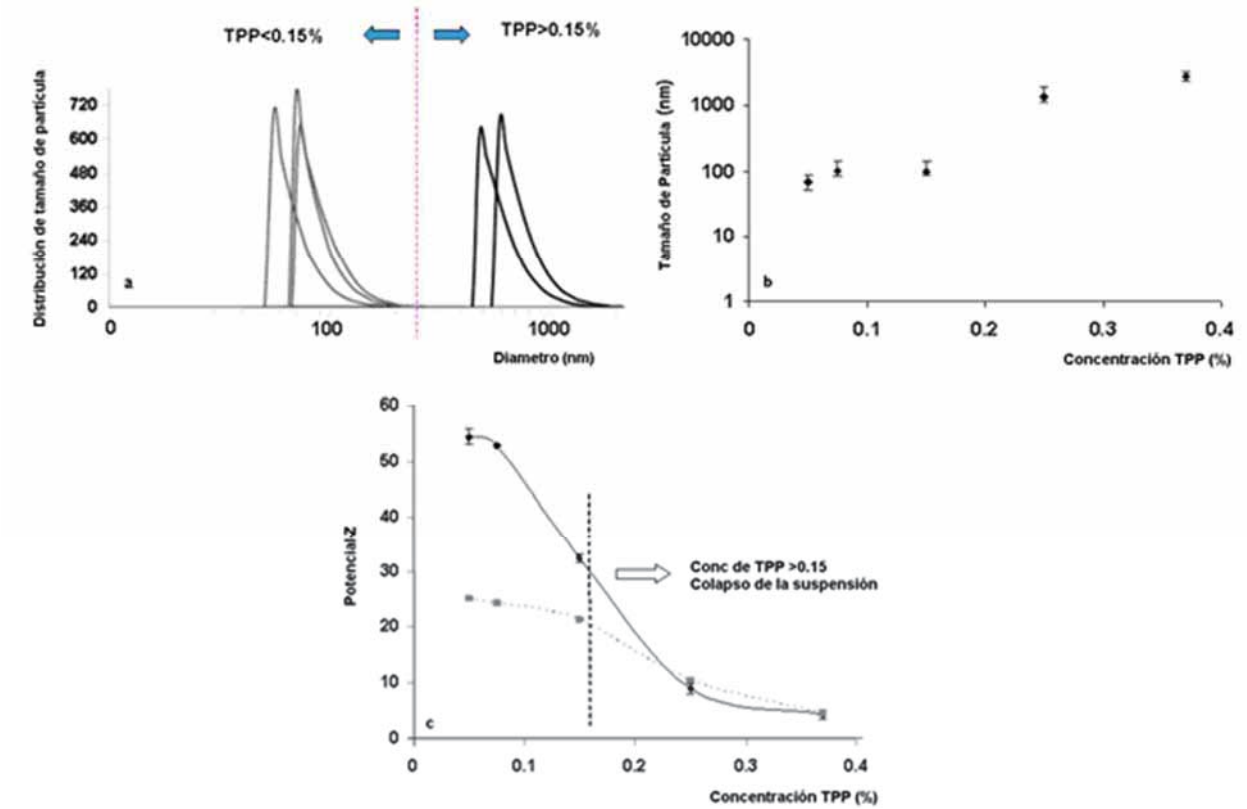


FIGURA 4. Efecto del porcentaje de TPP añadido en: a) Distribución de tamaños de partícula, b) tamaño medio de partícula y c) Potencial Z en solución original (línea llena) y en solución acuosa (línea punteada)

Resultados de la remoción de Cr(VI) sobre QS y MQS. La **Figura 5** muestra el efecto simultáneo de la concentración de Cr(VI) inicial y el pH sobre el porcentaje de remoción de Cr(VI) para QS y MQS y el tiempo de adsorción de equilibrio para cada sistema. El pH del medio posee un efecto considerable en la remoción de Cr(VI); cuando el pH disminuyó de 4 a 2 la remoción se redujo en un 29% para QS(Fig.5a) y aumentó en un 80% para MQS(Fig. 5b). Los datos de equilibrio se analizaron utilizando las expresiones de las isotermas de Langmuir, Freundlich, y Temkin[6].

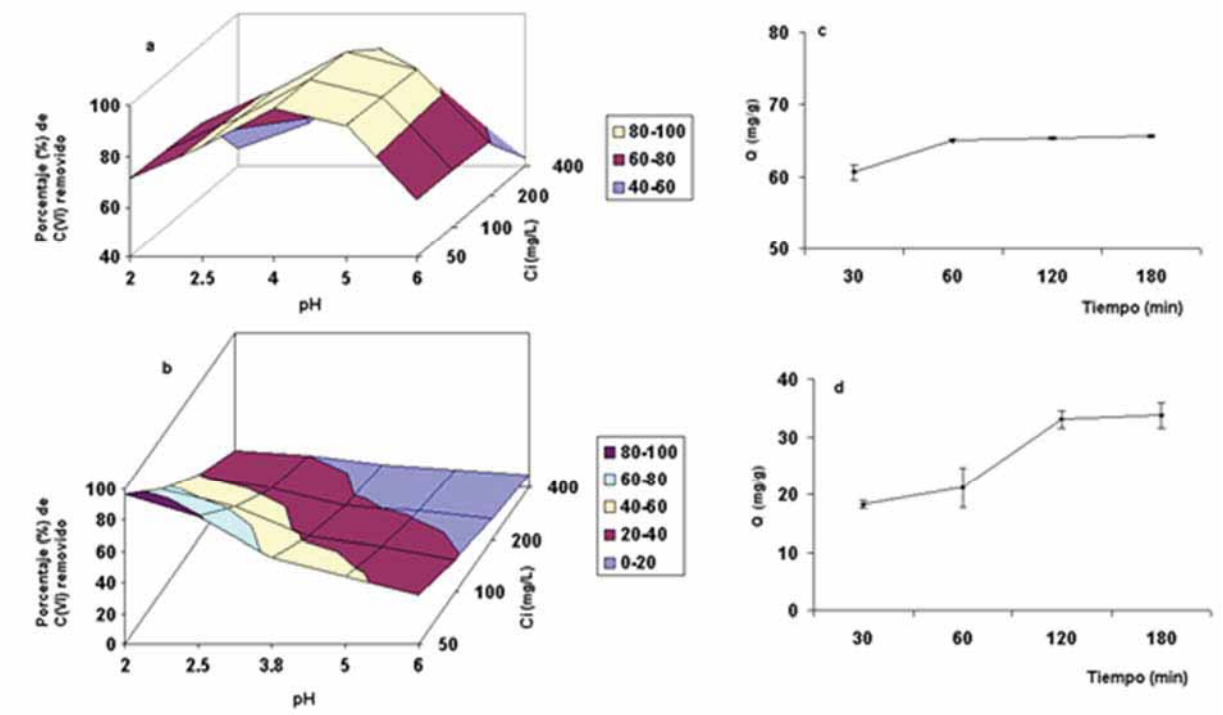


FIGURA 5. Efecto simultáneo de la concentración de Cr(VI) inicial y el pH sobre el porcentaje de remoción de Cr(VI) para QS(a) y MQS (b). Tiempo de contacto necesario para la remoción de Cr(VI) para QS(c) y MQS(d)

La isoterma de Langmuir está dada por la ecuación:

$$\frac{Ceq}{Qe} = \frac{Ceq}{Qm} + \frac{1}{K_L Qm} \qquad (4)$$

donde Qe es la cantidad adsorbida por unidad de adsorbente en el equilibrio (mg/g); Ceq la concentración de equilibrio del adsorbato después de la adsorción (mg/L), K_L la cte de Langmuir(g/L) y Qm la máxima capacidad de adsorción en la monocapa (mg/g).

La isoterma de Freundlich es una ecuación empírica que supone que el proceso de adsorción tiene lugar en superficies heterogéneas. Se puede definir como:

$$\ln Qe = \ln K_f + (1/n)\ln Ceq \qquad (5)$$

donde K_f es la cte de Freundlich (mg/g) y n el factor de heterogeneidad relacionado a la intensidad de adsorción.

La isoterma de Temkin en su forma lineal está dada por la ecuación:

$$Qe = B_t \ln(K_t) + B_t \ln(Ceq) \qquad (6)$$

La isoterma de Temkin asume que el calor de adsorción de las moléculas en la capa disminuye linealmente con la cobertura dada por las interacciones adsorbente-adsorbato. Bt, se relaciona con el calor de adsorción y K_T es la constante de unión de equilibrio.

Los parámetros obtenidos de las ecuaciones de adsorción se muestran en la Tabla 1. El modelo de Langmuir fue el que mejor se ajustó a los datos experimentales, lo que indica la naturaleza homogénea del adsorbente.

TABLA 1. Parámetros de las isotermas de equilibrio para Cr (VI) adsorbido en quitosano (QS) y micro/nanopartículas de quitosano (MQS)

	Langmuir			**Freundlich**			**Temkin**		
	Qm (mg/g)	**K_L (l/mg)**	**R^2**	**1/n**	**K_f (mg/g)**	**R^2**	***B_t***	***Kt* (l/mg)**	**R^2**
QS a pH=4	250	0.018	0.999	0.43	44.70	0.941	45.01	2.76	0.997
MQS a pH=4	68.9	0.014	0.990	0.36	7.02	0.983	13.95	1.76	0.989
MQS a pH=2	124	0.086	0.990	0.12	60.42	0.977	22.55	1.46	0.939

Por otro lado, se requiere de un análisis cinético para obtener la velocidad de adsorción y la etapa limitante del mecanismo de transporte, que se utiliza en el diseño del proceso. Las ecuaciones cinéticas de pseudo-primer orden, pseudo-segundo orden y la ecuaciónElovich[6] se ajustaron a los datos experimentales.
El modelo cinético de pseudo primer orden, conduce a la siguiente ecuación:

$$\ln\left(\frac{Qe}{Qe-Q}\right)=k_1 t \qquad (7)$$

donde Q es la cantidad de metal adsorbido en el momento t(mg/g), Qe es la cantidad de metal adsorbido en el t de equilibrio(mg/g) y K_1 es la constante de velocidad (min^{-1}):
La cinética de pseudo- segundo orden, se representa en forma integrada por:

$$\frac{t}{Q}=\frac{1}{k_2 Qe^2}+\frac{1}{Qe}t \qquad (8)$$

donde k_2 es la constante de velocidad de pseudo segundo orden.

La ecuación de Elovich, se expresa como:

$$Q=\beta\ln(\alpha\beta)+\beta\ln t \qquad (9)$$

donde Q es la cantidad de metal adsorbido en un tiempo t, α es la velocidad de adsorción inicial (mg $g^{-1}h^{-1}$), y β es la constante de Elovich.

Los parámetros cinéticos obtenidos se muestran en la Tabla 2. El modelo cinético de pseudo segundo orden fue el que mejor ajustó a los datos experimentales.

TABLA 2. Parámetros cinéticos para Cr(VI) adsorbido en quitosano y micropartículas de quitosano

	Pseudo-Primer Orden		Pseudo-Segundo Orden		Elovich		
	$k_1(h^{-1})$	R^2	k_2 (g/mgh)	R^2	β (g/mg)	α (mg/gh)	R^2
QS	2.71	0.871	0.76	0.999	0.37	$6.0x10^{10}$	0.750
MQS	1.94	0.932	0.078	0.946	0.10	116.8	0.877

Resultados del estado de oxidación del cromo adsorbido. La medición del estado de oxidación de las especies de cromo adsorbidas indicó que cuando se utilizó QS como material adsorbente del Cr(VI), en el proceso de desorción no se detectó presencia de Cr (III), es decir el cromo adsorbido permanecía como Cr (VI).Por el contrario, utilizando quitosano reticulado (MQS), más del 60% del cromo adsorbido se redujo a Cr(III) que no es tóxico; por lo tanto las MQS reducen Cr(VI) a Cr(III). Estos resultados son muy importantes desde el punto de vista toxicológico. El estudio del mecanismo de reducción de las MQS debe ser estudiados en profundidad para futuras aplicaciones.

CONCLUSION

Se estudió el uso de biopolímeros como el quitosano y quitosano reticulado (micro/nanopartículas) en la efectividad de remoción del cromo (VI) altamente tóxico y cancerígeno. Para ello, se obtuvo quitina y quitosano de exoesqueletos proveniente de desechos de la industria pesquera del langostino patagónico (*P. muelleri*). Se determinaron los rendimientos del proceso y se lo caracterizó según su grado de desacetilación y peso molecular Los valores obtenidos se encontraron dentro de los reportados para ser considerado quitosano. Por otro lado, dada la inestabilidad del QS a bajo pH, se sintetizaron micropartículas de quitosano utilizando tripolifosfato de sodio como agente reticulante. El tamaño medio de partícula fue de 101nm para una relación de QS-TPP de 1,25g/L-1,5g/L.

Se realizaron estudios de adsorción de Cr(VI) en QS y MQS bajo diferentes condiciones de pH, tiempo de contacto, y concentración Cr(VI) inicial. Asimismo, se evalúo el estado de oxidación del cromo adsorbido. La cantidad de cromo adsorbido varió notablemente con el pH de la solución inicial. La isoterma de equilibrio de Langmuir y el modelo cinético de pseudo-segundo orden proporcionó la mejor correlación de los datos experimentales. El presente trabajo demostró el QS y las MQS fueron efectivas para la remoción del Cr(VI), aunque las nanopartículas mejoraron la adsorción del metal a bajos pH (<3), disminuyendo adicionalmente la toxicidad del sistema acuoso, ya que el cromo adsorbido sobre MQS era, en un porcentaje mayor al 60%, cromo (III). El aprovechamiento de los desechos de exoesqueletos de crustáceos patagónicos constituye un tema importante en la revalorización económica de residuos para la región. Por otro lado el desarrollo de nanopartículas permitirá realizar aportes originales

en la obtención de productos que contribuyan al desarrollo de tecnologías ligadas al medio ambiente.

AGRADECIMIENTOS

Centro Nacional Patagónico (CENPAT- CONICET), Centro de Investigación y Desarrollo en Criotecnología de Alimentos (CIDCA, UNLP-CONICET), Universidad Nacional de La Plata, Agencia de Promoción Científica y Tecnológica (ANPCYT), a la Universidad Nacional de Córdoba y la Empresa “Altamare” SA de Puerto Madryn.

REFERENCIAS

1. Ministerio de Agricultura, Ganadería y Pesca (Minagri 2014)
2. Rodríguez Hamamura, N., Valderrama Negrón, A., Alarcón Cavero, H., & López Milla, A. Preparación de partículas de quitosano reticuladas con tripolifosfato y modificadas con polietilenglicol. *Revista de la Sociedad Química del Perú*, *76*(4), (2010) 336-354.
3. Hussain, M. R., Devi, R. R., &Maji, T. K. Controlled release of urea from chitosan microspheres prepared by emulsification and cross-linking method. Iranian Polym Journal, *21*(8), (2012) 473-479.
4. Wei, D., Sun, W., Qian, W., Ye, Y., & Ma, X. The synthesis of chitosan-based silver nanoparticles and their antibacterial activity. *Carbohydr Res*, *344*(17), (2009) 2375-2382.
5. Laus, R., Costa, T. G., Szpoganicz, B., &Fávere, V. T. Adsorption and desorption of Cu (II), Cd (II) and Pb (II) ions using chitosan crosslinked with epichlorohydrin-triphosphate as the adsorbent. J Hazard Mater, 183(1), (2010) 233-241.
6. Hena, S. Removal of chromium hexavalent ion from aqueous solutions using biopolymer chitosan coated with poly 3-methyl thiophene polymer. J Hazard Mate*r*, *181*(1), (2010) 474-479.
7. Yu K., Ho J., McCandlish E., Buckley B., Patel R., Li Z., Shapley N.C.Copper ion adsorption by chitosan nanoparticles and alginate microparticles for water purification applications. Colloid. Surface A. (2013) 425: 31-41.
8. Calvo, P., Remunan-Lopez, C., Vila-Jato, J. L., & Alonso, M. J. Novel hydrophilic chitosan-polyethylene oxide nanoparticles as protein carriers. J ApplPolymSci, 63(1), (1997) 125-132.
9. Dima, J. B., Sequeiros, C., &Zaritzky, N. E. Hexavalent chromium removal in contaminated water using reticulated chitosan micro/nanoparticles from seafood processing wastes. Chemosphere, 141,(2015) 100-111.
10. Brugnerotto, J., Lizardi, J., Goycoolea, F. M., Argüelles-Monal, W., Desbrieres, J., &Rinaudo, M. An infrared investigation in relation with chitin and chitosan characterization. Polymer, *42*(8), (2001) 3569-3580.
11. Broussignac, P. Chitosan: a natural polymer not well known by the industry. Chim. Ind. Genie Chim, 99(9), (1968) 1241-1247.
12. Bhuvaneshwarl, S., Sruthi D., Sivasubramanian V., Kanthimathy K. Regeneration of chitosan after heavy metal sorption. J. Scientific and Ind. Research, JSIR , 71 ,(2012) 266-269.
13. Clescerl L.S., Greenberg A.E., Eaton A.D. 1999. Standard Methods for the Examination of Water and Wastewater. Method 3500 Chromium Colorimetric Method
14. Rinaudo, M. Chitin and chitosan: properties and applications. Progpolymsci, 31(7), (2006) 603-632.
15. Qu X., Alvarez P.J., Li Q. Applications of nanotechnology in water and wastewater treatment. Water Res. 47(12), (2013)3931-3946.
16. Qi L., Xu Z. Lead sorption from aqueous solutions on chitosan microparticles. Colloid Surf A. 251(1), (2004) 183-190.